BRITISH JOURNAL OF

APPLIED PHYSICS

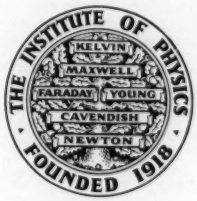

EDITOR

H. R. LANG

PH.D., A.R.C.S., F.INST.P.

Secretary of The Institute of Physics

VOLUME 3

LONDON

THE INSTITUTE OF PHYSICS

32
R44

BRITISH JOURNAL OF APPLIED PHYSICS

ADVISORY COMMITTEE, 1951–52

Representing The Institute of Physics

W. E. CURTIS, D.SC., A.R.C.S., D.I.C., F.INST.P., F.R.S., *President*

E. R. DAVIES, O.B.E., B.SC., F.INST.P., *Honorary Treasurer*

B. P. DUDDING, M.B.E., A.R.C.S., PH.D., F.INST.P., *Honorary Secretary*

T. E. ALLIBONE, D.SC., PH.D., M.I.E.E., F.INST.P., F.R.S., *Vice-President*

E. G. COX, D.SC., F.R.I.C., F.INST.P., *Vice-President*

B. M. CROWTHER, M.A., PH.D., F.INST.P.

N. L. HARRIS, B.SC., F.INST.P.

W. J. MEREDITH, M.SC., F.INST.P., *Member of Board*

E. W. H. SELWYN, B.SC., A.R.C.S., D.I.C., F.INST.P., *Member of Board*

S. WHITEHEAD, M.A., PH.D., M.I.E.E., F.INST.P., *Vice-President*

Representing the Institute's Branches, Groups, and the Participating Societies

E. M. CROOK, M.SC., PH.D., A.R.I.C., A.INST.P., *Representing the Electron Microscopy Group*

A. E. DE BARR, B.SC., F.INST.P., *Representing the X-ray Analysis Group*

J. S. FORREST, M.A., D.SC., M.I.E.E., F.INST.P., *Representing the Royal Meteorological Society*

E. K. FRANKL, M.A., *Representing the Stress Analysis Group*

A. G. GAYDON, D.SC., PH.D., A.R.C.S., D.I.C., A.INST.P., *Representing the Physical Society*

P. L. KIRBY, M.SC., A.INST.P., *Representing the North Eastern Branch*

F. LLEWELLYN JONES, M.A., D.PHIL., F.INST.P., *Representing the South Wales Branch*

D. PARKINSON, D.SC., PH.D., F.INST.P., *Representing the Midland Branch*

F. Y. POYNTON, M.SC., F.INST.P., *Representing the Education Group*

J. S. RANKIN, B.SC., PH.D., M.I.MECH.E., F.INST.P., *Representing the Scottish Branch*

S. RODDA, B.SC., F.INST.P., *Representing the Electronics Group*

R. SCHNURMANN, M.SC., DR.RET.NAT., F.INST.P., *Representing the Manchester and District Branch*

W. S. STILES, O.B.E., PH.D., D.SC., *Representing the Physical Society*

L. R. G. TRELOAR, B.SC., PH.D., F.INST.P., *Representing the London Branch and also the Faraday Society*

E. VAN SOMEREN, B.SC., F.INST.P., *Representing the Industrial Spectroscopy Group*

C. W. WILSON, M.SC., PH.D., F.INST.P., *Representing the British Institute of Radiology*

W. J. WILTSHIRE, G.M., B.A., F.INST.P., *Representing the Industrial Radiology Group*

CONTENTS OF VOLUME 3

JANUARY 1952

Original contributions: PAGE

A physical investigation of heat production in human tissues when exposed to microwaves. By H. F. Cook . 1
On the problem of focusing diffracted X-rays on an oblique flat film. By F. Buckens 7
Grain density fluctuations in photographic emulsions. By P. E. Hodgson 11
An experimental investigation of the diffusion of electrolytic hydrogen through metals. By H. R. Heath . 13
Compilation of the propagation constants of an inhomogeneously-filled waveguide. By Ll. G. Chambers . 19
Numerical ray-tracing in electron lenses. By J. C. Burfoot 22

Special report:

Summarized proceedings of a conference on electron microscopy—St. Andrews, June 1951. By D. G. Drummond and G. Liebmann 25

Correspondence:

Differential methods of vacuum leak detection. From G. Nief 29
Isotope catalogue on punched cards. From J. M. A. Lenihan 29
Theory of stresses in glass butt seals. From N. L. Svensson; M. Zaid; H. Rawson 30

FEBRUARY 1952

Special article:

Microwaves in medical and biological research. By J. E. Roberts and H. F. Cook 33

Original contributions:

Characteristics of the hot cathode electron microscope gun. By M. E. Haine and P. A. Einstein . . 40
Radioassay of potassium in solid samples. By O. J. Russell 47
The study of the thermal behaviour of structures by electrical analogy. By G. Burnand 50
The modulation characteristic of cathode-ray tubes in television. By R. B. Mackenzie 54

Correspondence:

Three dimensional electrical potential analyser. From V. E. Gough; S. C. Redshaw 58
The thermal conductivity of liquid oxygen. From S. Prosad 58

New books 60

Notes and comments 64

MARCH 1952

Special article:

The relaxation method in stress analysis. By D. G. Christopherson 65

Original contributions:

The elasticity and strength of paper and other fibrous materials. By H. L. Cox 72
Temperature distribution with simultaneous platten and dielectric heating. By H. M. Nelson 79
Helmholtz resonators in the acoustic treatment of broadcasting studios. By C. L. S. Gilford . . . 86
Transit time oscillations in triodes. By O. H. Critchley and M. R. Gavin 92
A method of designing a compensated solenoid giving approximately uniform field. By T. A. Heddle . 95
Some measurements of the total emissivity of metals and pure refractory oxides and the variation of emissivity with temperature. By A. H. Sully, E. A. Brandes and R. B. Waterhouse 97

New books 102

Notes and comments 104

APRIL 1952

Special report:

Summarized proceedings of a conference on stress analysis, Liverpool, 1951. By E. K. Frankl 105

Original contributions:

Liquid films formed by means of rotating disks. By B. E. Dixon, A. A. W. Russell and J. E. L. Swallow . 115
The elastic constants of piezoelectric crystals. By R. F. S. Hearmon 120
A radio-frequency power supply system for high voltage accelerators. By P. A. Davenport 124
Pool surface and cathode spot temperature of mercury cathodes as a problem in heat conduction. By H. v. Bertele 127

New books 132

Notes and comments 136

MAY 1952

Special report:

Report of conferences on electron microscopy—Washington and Philadelphia 1951. By V. E. Cosslett . . 137

Original contributions:

Time-resolved spectroscopy of spark discharges. By F. Tsui 139
A graphical treatment of the tone reproduction problem in television systems. By R. B. Mackenzie . . 141
Mechanical strength of piezoelectric crystals. By R. Bechmann and P. L. Parsons 147
The bending and twisting of anisotropic plates. By R. F. S. Hearmon and E. H. Adams 150
The two-dimensional magnetic or electric field inside a semi-infinite slot terminated by a semi-circular cylinder. By N. Davy and N. H. Langton 156
Measurement of die pressures in wire drawing by photoelastic methods. By P. M. Cook and J. G. Wistreich 159

New books 166

Notes and comments 168

JUNE 1952

Special article: PAGE

Recent research on radio-luminescence. By G. F. J. Garlick 169

Original contributions:

A method for the electron and optical microscopic examination of identical areas. By E. D. Hyam and J. Nutting 173

Errors in stress determination at the free boundaries of "frozen stress" photoelastic models. By V. M. Hickson 176

The application of molecular resonance to microwave frequency stabilization. By H. R. L. Lamont and E. M. Hickin 182

The atomization of liquid in a flat spray. By R. G. Dorman 189

The rheology of plastic dispersions. By P. A. Briscoe, W. J. Dunning and R. C. Seymour 193

The solution of temperature distribution problems by computation and electrical analogy. By J. C. Williams 197

Permanent magnets for spectrographs and nuclear physical research. By D. Hadfield and D. L. Mawson . 199

Correspondence:

Aerial prospecting and the absorption of γ-radiation. From J. F. Steljes; D. H. Peirson and E. Franklin . 203

New books 204

JULY 1952

Special article:

The method of dimensions. By E. W. H. Selwyn . 209

Original contributions:

Radiation intensity from high energy accelerators. By J. D. Lawson 214

An improved apparatus for the differential thermal analysis of minerals. By J. J. Theron 216

Conduction of heat in tissue supplied with blood. By J. C. Jaeger 221

The saturation curve at high ionization intensity. By J. W. Boag and T. Wilson 222

A method of studying the formation of cracks in a material subjected to stress. By R. Jones 229

A castable polyester resin for photoelastic work. By B. Sugarman, G. O. Moxley and I. A. Marshall . 233

New books 238

Notes and comments 240

AUGUST 1952

Special article:

The physics of transistors. By E. Billig 241

Original contributions:

A comparison of the dielectric behaviour of pure water and human blood at microwave frequencies. By H. F. Cook 249

The spectrophotometry of light sources. By S. T. Henderson and M. B. Halstead 255

Frictional and elastic properties of high polymeric materials. By B. Lincoln 260

The use of polarized light for the examination of etched metal crystals and their orientation. By P. Dunsmuir 264

The viscosity of suspensions of rigid spheres. By R. Roscoe 267

New books 270

Notes and comments 272

SEPTEMBER 1952

Special reports: PAGE

Summarized proceedings of the fourth industrial physics conference—Glasgow, June 1952. By W. Rheinallt Thomas 273

Summarized proceedings of a conference on structures of silicate minerals—London, November 1951. By K. Robinson and E. R. S. Shaw 277

Original contributions:

The measurement of velocities for solid-fluid flow in a pipe. By C. Jones and G. Hermges 283

The effect of frequency on the behaviour of rubber under cyclical deformation. By D. M. Davies . . . 285

The ignition of wood by radiation. By D. I. Lawson and D. L. Simms 288

The properties of semi-conducting ceramic glaze. By D. H. Lucas 293

Heat flow in an infinite medium heated by a sphere. By H. Goldenberg and C. J. Tranter 296

Some mechanical and adhesive properties of indium. By A. C. Moore and D. Tabor 299

New books 301

Notes and comments 304

OCTOBER 1952

Special report:

Summarized proceedings of a conference on X-ray analysis—Edinburgh, April 1952. By C. A. Beevers and A. E. De Barr 305

Original contributions:

On two problems in potential theory and their application to the design of magnetic recording heads for digital computers. By A. D. Booth 307

A quick method of distortion measurement in nuclear emulsions. By J. V. Major 309

Production and separation of small glass spheres. By W. Paul and R. V. Jones 311

A study of the oil-film formation in gears by electrical resistance measurements. By T. B. Lane and J. R. Hughes 315

An improved technique for high-speed photography. By D. A. Senior and C. O. J. Grove-Palmer . . . 318

Electrical measurement of the cathode temperature of diodes. By D. A. Bell, J. C. Cluley and H. O. Berktay 322

Secondary electron emission from barium oxide. By J. Woods and D. A. Wright 323

An ultrasonic phase lag method for measuring the thickness of rubber. By P. Hatfield 326

The development of a multi-flash camera and its application to the study of liquid jets. By M. A. Mahrous . 329

Correspondence:

A note on the measurement of damping in vibrating rods. From G. G. Parfitt 332

Calculation of the propagation constants of an inhomogeneously-filled waveguide. From J. A. Bradshaw; Ll. G. Chambers 332

Pool surface and cathode spot temperature of mercury cathodes as a problem in heat conduction. From R. Tucker; H. v. Bertele 333

New books 333

Notes and comments 336

NOVEMBER 1952

Special report: PAGE

Summarized proceedings of a conference on microwave physics—Oxford, July 1952. By D. A. WRIGHT . . 337

Special article:

Secondary processes active in the electrical breakdown of gases. By L. B. LOEB 341

Original contributions:

Effect of vertical divergence on the displacement and breadth of X-ray powder diffraction lines. By J. N. EASTABROOK 349

Some problems in the analysis of steels by X-ray fluorescence. By E. GILLAM and H. T. HEAL 353

Current densities of free-moving cathode spots on mercury. By H. v. BERTELE 358

A similarity theorem in electrical contacts. By P. M. DAVIDSON 361

Correspondence:

Transit time oscillations in triodes. From I. A. HARRIS; M. R. GAVIN 363

New books 364

Notes and comments 368

DECEMBER 1952

Special report: PAGE

Summarized proceedings of the third international spectroscopy colloquium—Hoddesdon, September 1952. By D. M. SMITH 369

Original contributions:

A method for measuring the potential of a current-carrying electrode. By A. G. MILLIGAN 372

Second-order transition points in high polymers. By K. L. FLOYD 373

The use of extrapolation techniques with electrical network analogue solutions. By R. CULVER 376

Stability and accuracy of numerical solutions of the heat flow equation. By P. H. PRICE and M. R. SLACK . 379

The production of specimen mounting grids for the electron microscope. By C. E. CHALLICE and C. D. SUTTON 384

Absorption and scattering of radiation by water sprays of large drops. By P. H. THOMAS 385

Correspondence:

Ignition of wood by radiation. From H. P. STOUT; D. I. LAWSON and D. L. SIMMS 394

New books 396

Notes and comments 399

Index to Volume 3 401

INDEX TO VOLUME 3

SUBJECTS

Accelerators
  high energy, Radiation intensity from 214
  high voltage, A radio-frequency power supply system for 124
Acoustic treatment of broadcasting studios, Helmholtz resonators in the 86
Advances in physics 64
Analogue solutions, electrical network, The use of extrapolation techniques with 376
Analogy
  electrical, The solution of temperature distribution problems by computation and 197
  electrical, The study of the thermal behaviour of structures by 50
Analyser, Three dimensional electrical potential 58
Analysis
  stress, Summarized proceedings of a conference on, Liverpool, 1951 105
  stress, The relaxation method in 65
Anisotropic plates, The bending and twisting of 150
Anniversary of the discovery of X-ray diffraction, Fortieth 304
Apparatus, An improved, for the differential thermal analysis of minerals 216
Ash and clinker in industry, Conference on 336
Atomic
  energy, Instrumentation and 168
  energy research reports 400
Atomization of liquid in a flat spray, The 189
Australian Radiophysics Laboratory, The 399
Award, City and Guilds of London Institute Insignia 399

Barium oxide, Secondary electron emission from 323
Bessel functions, Tables of the 400
Blood
  Conduction of heat in tissue supplied with 221
  human, A comparison of the dielectric behaviour of pure water and, at microwave frequencies 249
Books, New
  Absorptions—Spektralanalyse 239
  Advanced
    five-figure mathematical tables 206
    practical physics for students 398
    treatise on physical chemistry, An, Vol. II 63
  Allgemeine metallkunde 335
  Applied
    atomic energy 133
    mechanics for engineers 60
    nuclear physics 61
    research in the United States 334
  Auger Effect, The 397
  Automatic and manual control 303
  Basic electrotechnics 134
  Bibliography of interlingual scientific and technical dictionaries 208
  Bibliographical survey of flow orifices and parallel-throated nozzles, A 271
  Careers in physics 270
  Chambers's dictionary of scientists 63
  Cloud chamber photographs of the cosmic radiation 397
  Colour
    cinematography 166
    in theory and practice 396
  Conduction of electricity through gases, The 208
  Corrosion testing procedures 303
  Currents and fields in electrical engineering 303
  Cybernetique, La—theorie du signal et de l'information 133

Books, New (*continued*)
  Department of Scientific and Industrial Research—Report for the year 1949–50 61
    Report for the year 1950–51 334
  Dictionary of mathematical sciences. Vol. 1: German–English 239
  Dimensional analysis 334
  Electrical phenomena at interfaces 239
  Electromagnetic waves 204
  Electronic and ionic impact phenomena 302
  Elements of thermodynamics and statistical mechanics 238
  Encyclopedia on cathode-ray oscilloscopes and their uses 204
  Engineering metrology 270
  Exercises in experimental physics 367
  F.B.I. register of British manufacturers—1951–2 208
  Ferromagnetism 132
  Fifty years of British Standards 1901–1951 167
  Fouriersynthese von Kristallen 335
  Fundamentals
    of automatic control 103
    of electronics 206
    of technical electricity 302, *correspondence on* 366
  General
    astronomy 207
    homogeneous co-ordinates in space of three dimensions 60
  Gyroscope through the ages, The 271
  Hardness of metals, The 135
  Heat and thermodynamics 270
  Illumination of photographic darkrooms, The 167
  Internal ballistics 60
  International Conference on Science Abstracting (Final Report) 102
  Interpretation of X-ray diffraction photographs, The 167
  Introduction
    to acoustics, An 365
    to applied mathematics, An 207
    to electronic circuits, An 271
    to statistical method 63
    to the theory of control in mechanical engineering, An 61
  Jubilee book of the National Physical Laboratory 62
  Lightning protection 396
  Low temperature physics—Four lectures 335
  Magnetic and electrical methods of non-destructive testing 166
  Magnetische werkstoffe 396
  Mass spectrometry 364
  Mathematical engineering analysis 135
  Mathematics, queen and servant of science 302
  Mechanical properties of cheese and butter, The 335
  Mechanics and properties of matter 367
  Methods of algebraic geometry. Vol. 2 335
  Modern magnetism 166
  Oxide-coated
    cathode, The. Vol. I 62
    cathode. Vol. II 301
  Phase microscopy. (Principles and applications) 365
  Physics as a career 238
  Physical properties of glass 366
  Practical
    electron microscopy 301
    manual of rubber hardness testing, A 103
  Preparation of programs for an electronic digital computer, The 205
  Principles
    of air navigation, The 62

Books, New (*continued*)
Principles (*continued*)
of lighting 239
of the control and stability of aircraft, The 365
Proceedings of the International Conference on Low Temperature Physics—Oxford 1951 239
Progress in biophysics and biophysical chemistry. Vol. 2 238
in metal physics. Vol. 3 398
Quantum mechanics of particles and wave fields 205
Radiation monitoring in atomic defence 206
Radio
Vol. 1 366
astronomy 271
Recent developments in rheology, Some 165
Report
of the Department of Scientific and Industrial Research for the year 1949–50 61
on interlingual scientific and technical dictionaries 208
Reports
on progress of physics. Vol. XIV, 1951 102
on progress in physics, Vol. XV, 1952 397
Rubber technology 207
Sensations, The, their functions, processes and mechanisms 335
Servomechanisms and regulating system design. Vol. 1 134
Sound insulation and room acoustics 206
Space—Time—Matter 63
Steels in modern industry 208
Surface
chemistry 103
chemistry of solids, The 133
Systèmes asservis, Les 134
Tensor analysis 238
Textbook
of electrochemistry, Vol. II 205
of physics, Vol. 2. Heat 271
Théorie des images optiques, La 61
Theory
and design of valve oscillators 135
of mechanics 367
of relativity, The 333
Thermal properties of buildings 302
Tungsten 303
Ultrasonics 207
Wavelength tables of sensitive lines 167
Bowen Trust Fund 399
Breakdown, electrical, of gases, Secondary processes active in the 341

Camera, a multi-flash, The development of, and its application to the study of liquid jets 329
Cards, punched, Isotope catalogue on 29
Career, Physics as a 136
Catalogue, Isotope, on punched cards 29
Cathode
electron microscope gun, hot, Characteristics of the 40
spot temperature of mercury cathodes as a problem in heat conduction, Pool surface and 333
spots, free-moving, on mercury, Current densities of 358
temperature of diodes, Electrical measurement of the 322
Cathodes, mercury, Pool surface and cathode spot temperature of, as a problem in heat conduction 127, 333
Ceramic glaze, semi-conducting, The properties of 293
Charts, Overhead-line 336
City and Guilds of London Institute Insignia Award 399
Clinker in industry, Conference on ash and 336
Colloquium, Third International Spectroscopy, Hoddesdon, September 1952 136
Summarized proceedings of 369
Commission on glass, The international 304
Computation and electrical analogy, The solution of temperature distribution problems by 197
Computors, digital, On two problems in potential theory and their application to the design of magnetic recording heads for digital computers 307
Conduction, heat, Pool surface and cathode spot temperature of mercury cathodes as a problem in 333
Conference
Fourth, on Industrial Physics 136
fourth industrial physics, Glasgow, June 1952, Summarized proceedings of the 273
International, on the theory and applications of photography 399
on ash and clinker in industry 336
on electron microscopy—St. Andrews, June 1951, Summarized proceedings of a 25
on electron microscopy—Washington and Philadelphia 1951, Report of 137
on microwave physics—Oxford, July 1952, Summarized proceedings of a 337
on stress analysis, Liverpool, 1951, Summarized proceedings of 105
on structures of silicate minerals—London, November 1951, Summarized proceedings of a 277
on Textile Physics, Autumn 240
on X-ray analysis—Edinburgh, April 1952, Summarized proceedings of a 305, 368
Congress on rheology, Second international 336
Constants, propagation, of an inhomogeneously-filled waveguide, Calculation of the 332
Contacts, electrical, A similarity theorem in 361
Conveyor belts, non-inflammable, The use of polyvinyl chloride in the manufacture of 400
Cracks in a material subjected to stress, A method of studying the formation of 229
Crystals
etched metal, and their orientation, The use of polarized light for the examination of 264
piezoelectric, Mechanical strength of 147
piezoelectric, The elastic constants of 120
Current densities of free-moving cathode spots on mercury 358

Damping in vibrating rods, A note on the measurement of 332
Debye–Scherrer patterns, Counter spectrometers for the investigation of 104
Densities, Current, of free-moving cathode spots on mercury 358
Die pressures, Measurement of, in wire drawing by photoelastic methods 159
Dielectric
behaviour of pure water and human blood at microwave frequencies, A comparison of the 249
heating, Temperature distribution with simultaneous platten and 79
Diffraction lines, X-ray powder, Effect of vertical divergence on the displacement and breadth of 349
Diffusion of electrolytic hydrogen through metals, An experimental investigation of the 13
Dimensions, The method of 209, 368
Diodes, Electrical measurement of the cathode temperature of 322
Discharges, spark, Time-resolved spectroscopy of 139
Distortion measurement in nuclear emulsions, A quick method of 309
Duddell Medal, Award of the 399

Education of physicists, The scientific 168, 336
Elastic constants of piezoelectric crystals, The 120
Elasticity and strength of paper and other fibrous materials, The 72
Electric field, The two-dimensional magnetic or, inside a semi-infinite slot terminated by a semi-circular cylinder 156
Electrical
contacts, A similarity theorem in 361
breakdown of gases, Secondary processes active in the 341
measurement of the cathode temperature of diodes 322
network analogue solutions, The use of extrapolation techniques with 376

Electrical (*continued*)
resistance measurements, A study of the oil-film formation in gears by 315
Electrode, current-carrying, A method for measuring the potential of a 372
Electron
and optical microscopic examination of identical areas, A method for the 173
lenses, Numerical ray-tracing in 22
microscope gun, hot cathode, Characteristics of the 40
microscope, The production of specimen mounting grids for the 384
microscopy, Proposed school in 104
microscopy, Report of conferences on—Washington and Philadelphia 1951 137
microscopy, Summarized proceedings of a conference on—St. Andrews, June 1951 25
Electronics symposium and exhibition 240
Emission from barium oxide, Secondary electron 323
Emissivity
of metals and pure refractory oxides, Some measurements of the total, and the variation of emissivity with temperature 97
Energy
accelerators, high, Radiation intensity from 214
atomic, Instrumentation and 168
Exhibition
Electronics symposium and 240
Ramsay's centenary 336
Extrapolation techniques, The use of, with electrical network analogue solutions 376

Field
approximately uniform, A method of designing a compensated solenoid giving 95
The two-dimensional magnetic or electric, inside a semi-infinite slot terminated by a semi-circular cylinder 156
Films, Liquid, formed by means of rotating disks 115, 168
Flow
Heat, in an infinite medium heated by a sphere 296
solid-fluid, The measurement of velocities for, in a pipe 283
Fluorescence, X-ray, Some problems in the analysis of steels by 353
Focusing diffracted X-rays on an oblique flat film, On the problem of 7
Frequency, The effect of, on the behaviour of rubber under cyclical deformation 285
Fuel research 400

Gamma-ray sources for radiography 64
Gases, electrical breakdown of, Secondary processes active in the 341
Glass
butt seals, Theory of stresses in 30
spheres, small, Production and separation of 311
The international commission on 304
Glaze, semi-conducting ceramic, The properties of 293
Grain density fluctuations in photographic emulsions 11
Grids, specimen mounting, The production of, for the electron microscope 384

Heat
Conduction of, in tissue supplied with blood 221
conduction, Pool surface and cathode spot temperature of mercury cathodes as a problem in 127, 333
flow equation, Stability and accuracy of numerical solutions of the 379
flow in an infinite medium heated by a sphere 296
production in human tissues when exposed to microwaves, A physical investigation of 1, 64
Helmholtz resonators in the acoustic treatment of broadcasting studios 86
High-speed photography, Recently developed techniques in 368
Hydrogen, electrolytic, the diffusion of, through metals, An experimental investigation of 13

Identical areas, A method for the electron and optical microscopic examination of 173
Ignition of wood by radiation, The 288, 394
Indium, Some mechanical and adhesive properties of 299
Industrial
Physics, Fourth Conference on 136
physics conference—Glasgow, June 1952, Summarized proceedings of the fourth 273
Institute of Physics, The, Elections to 64, 136, 240, 272, 368
Instrumentation and atomic energy 168
Instruments, scientific, Safe transit of 168
Ionization intensity, high, The saturation curve at 222
Isotope catalogue on punched cards 29

Japanese Applied Mechanics Institute Reports 304
Jets, liquid, The development of a multi-flash camera and its application to the study of 329
Journal of the mechanics and physics of solids 368

Laboratory and workshop notes, A further volume of 64
Leak detection, vacuum, Differential methods of 29
Lenses, electron, Numerical ray-tracing in 22
Light
polarized, The use of, for the examination of etched metal crystals and their orientation 264
Science of 104
sources, The spectrophotometry of 255
Liquid
films formed by means of rotating disks 115, 168
The atomization of, in a flat spray 189

Magnetic
recording heads for digital computers, On two problems in potential theory and their application to the design of 307
The two-dimensional, or electric field inside a semi-infinite slot terminated by a semi-circular cylinder 156
Magnets, Permanent, for spectrographs and nuclear physical research 199
Measurement of die pressures in wire drawing by photoelastic methods 159
Measurements of the total emissivity of metals and pure refractory oxides and the variation of emissivity with temperature, Some 97
Mechanics and physics of solids, Journal of the 368
Medal, Duddell, Award of the 399
Mercury
cathodes, Pool surface and cathode spot temperature of, as a problem in heat conduction 127
Current densities of free-moving cathode spots on 358
Metals and pure refractory oxides, Some measurements of the total emissivity of, and the variation of emissivity with temperature 97
Method
An ultrasonic phase lag, for measuring the thickness of rubber 326
for measuring the potential of a current-carrying electrode, A 372
for the electron and optical microscopic examination of identical areas, A 173
in stress analysis, The relaxation 65
of designing a compensated solenoid giving approximately uniform field, A 95
of dimensions, The 209, 368
of distortion measurement in nuclear emulsions, A quick 309
of studying the formation of cracks in a material subjected to stress, A 229
Methods, Differential, of vacuum leak detection 29
Microscope
electron, The production of specimen mounting grids for the 384
gun, hot cathode electron, Characteristics of the 40
Microscopic, electron and optical, examination of identical areas, A method for the 173

Microscopy
electron, Proposed school in 104
electron, Report of conferences on—Washington and Philadelphia 1951 137
electron, Summarized proceedings of a conference on—St. Andrews, June 1951 25
Microwave
frequencies, A comparison of the dielectric behaviour of pure water and human blood at 249
frequency stabilization, The application of molecular resonance to 182
physics, Summarized proceedings of a conference on—Oxford, July 1952 337
Microwaves
A physical investigation of heat production in human tissues when exposed to 1, 64
in medical and biological research 33
Minerals, silicate, Summarized proceedings of a conference on structures of, London, November 1951 277
Modulation characteristic of cathode-ray tubes in television, The 54, 104
Molecular resonance, The application of, to microwave frequency stabilization 182

Nuclear
emulsions, A quick method of distortion measurement in 309
physics, Argentinian publications on 104
physical research, Permanent magnets for spectrographs and 199

Oil-film formation in gears by electrical resistance measurements, A study of the 315
Optical microscopic examination of identical areas, A method for the electron and 173
Oscillations in triodes, Transit time 92, 363
Oxygen, liquid, The thermal conductivity of 58

Paper and other fibrous materials, The elasticity and strength of 72
Papers, Notes on the preparation of 104, 168, 336
Photoelastic
methods, Measurement of die pressures in wire drawing by 159
models, "frozen stress," Errors in stress determination at the free boundaries of 176
work, A castable polyester resin for 233
Photographic emulsions, Grain density fluctuations in 11
Photography
An improved technique for high-speed 318
high-speed, Recently developed techniques in 368
International conference on the theory and applications of 399
Physicists, The scientific education of 168, 336
Physics
as a career 136
conference, fourth industrial—Glasgow, June 1952, Summarized proceedings of the 273
Industrial, Fourth Conference on 136
microwave, Summarized proceedings of a conference on—Oxford, July 1952 337
nuclear, Argentinian publications on 104
of solids, Journal of the mechanics and 368
of transistors, The 241
textile, Autumn Conference on 240
Piezoelectric
crystals, Mechanical strength of 147
crystals, The elastic constants of 120
Plastic dispersions, The rheology of 193
Plates, anisotropic, The bending and twisting of 150
Platten and dielectric heating, Temperature distribution with simultaneous 79
Polyester resin, A castable, for photoelastic work 233
Polyethylene, The stretching and relaxing of 64
Polymeric materials, high, Frictional and elastic properties of 260
Polymers, high, Second-order transition points in 373
Polyvinyl chloride in the manufacture on non-inflammable conveyor belts, The use of 400
Pool surface and cathode spot temperature of mercury cathodes as a problem in heat conduction 333
Potassium in solid samples, Radioassay of 47
Potential
of a current-carrying electrode, A method for measuring the 372
theory, On two problems in, and their application to the design of magnetic recording heads for digital computers 307
Power supply system, A radio-frequency, for high voltage accelerators 124
Preparation of papers, Notes on the 104, 168, 336
Prizes for original contributions published in this Journal 399
Propagation
constants of an inhomogeneously-filled waveguide, Calculation of the 19, 332
Properties
Frictional and elastic, of high polymeric materials 255
of indium, Some mechanical and adhesive 299
of semi-conducting ceramic glaze, The 293
Prospecting, Aerial, and the absorption of gamma-radiation 203

Radiation
Absorption and scattering of, by water sprays of large drops 385
The ignition of wood by 288, 394
intensity from high energy accelerators 214
Radioassay of potassium in solid samples 47
Radiography, Gamma-ray sources for 64
Radio-luminescence, Recent research on 169
Radiophysics Laboratory, The Australian 399
Ramsay's centenary exhibition 336
Refractory oxides, pure, Some measurements of the total emissivity of metals and, and the variation of emissivity with temperature 97
Relaxing of polyethylene, The stretching and 64
Reports
Atomic energy research 400
Japanese Applied Mechanics Institute 304
Resin, A castable polyester, for photoelastic work 233
Resistance measurements, electrical, A study of the oil-film formation in gears by 315
Resonance, molecular, The application of, to microwave frequency stabilization 182
Resonators, Helmholtz, in the acoustic treatment of broadcasting studios 86
Rheology
of plastic dispersions, The 193
Second international congress on 336
Rubber
under cyclical deformation, The effect of frequency on the behaviour of 285
the thickness of, An ultrasonic phase lag method for measuring 326

Saturation curve at high ionization intensity, The 222
Seals, glass butt, Theory of stresses in 30
Short-circuit testing, Comparison between British and American standards for 304
Solenoid, compensated, A method of designing a, giving approximately uniform field 95
Solids, Journal of the mechanics and physics of 368
Specimen mounting grids, The production of, for the electron microscope 384
Spectrographs and nuclear physical research, Permanent magnets for 199
Spectrometers, Counter, for the investigation of Debye–Scherrer patterns 104
Spectrophotometry of light sources, The 255
Spectroscopy
of spark discharges, Time-resolved 139
Colloquium—Hoddesdon, September 1952, Third International 136, 369
Spray, flat, The atomization of liquid in a 189
Sprays, water, of large drops, Absorption and scattering of radiation by 385

Stabilization, microwave frequency, The application of molecular resonance to 182
Standards for short-circuit testing, Comparison between British and American 304
Steels, Some problems in the analysis of, by X-ray fluorescence 353
Strength
  Mechanical, of piezoelectric crystals 147
  of paper and other fibrous materials, The elasticity and 72
Stress
  analysis, Summarized proceedings of a conference on, Liverpool, 1951 105
  A method of studying the formation of cracks in a material subjected to 229
  analysis, The relaxation method in 65
  determination at the free boundaries of "frozen stress" photoelastic models, Errors in 176
Stresses in glass butt seals, Theory of 30
Stretching and relaxing of polyethylene, The 64
Structures
  of silicate minerals, Summarized proceedings of a conference on—London, November 1951 277
  The study of the thermal behaviour of, by electrical analogy 50
Symposium and exhibition, Electronics 240

Tables of the Bessel functions 400
Television
  systems, A graphical treatment of the tone reproduction problem in 141
  The modulation characteristic of cathode-ray tubes in 54, 104
Temperature
  distribution with simultaneous platten and dielectric heating 79
  distribution problems, The solution of, by computation and electrical analogy 197
  cathode, of diodes, Electrical measurement of the 322
  the variation of emissivity with, Some measurements of the total emissivity of metals and pure refractory oxides and 97
  Pool surface and cathode spot, of mercury cathodes as a problem in heat conduction 127, 333
Textile Physics, Autumn Conference on 240
Theorem in electrical contacts, A similarity 361
Thermal
  analysis of minerals, differential, An improved apparatus for the 216
Thermal (*continued*)
  behaviour of structures by electrical analogy, The study of the 50
  conductivity of liquid oxygen, The 58
Tissue supplied with blood, Conduction of heat in 221
Tissues, human, when exposed to microwaves, A physical investigation of heat production in 1, 64
Tone reproduction problem in television systems, A graphical treatment of the 141
Transistors, The physics of 241
Transit
  of scientific instruments, Safe 168
  time oscillations in triodes 363
Transition points in high polymers, Second-order 409
Triodes, Transit time oscillations in 92, 363

Ultrasonic phase lag method for measuring the thickness of rubber, An 326

Vacuum leak detection, Differential methods of 29
Velocities for solid-fluid flow in a pipe, The measurement of 283
Viscosity of suspensions of rigid spheres, The 267

Water
  pure, and human blood, A comparison of the dielectric behaviour of, at microwave frequencies 249
  sprays of large drops, Absorption and scattering of radiation by 385
Waveguide
  an inhomogeneously-filled, Calculation of the propagation constants of 19, 332
Wood, The ignition of, by radiation 288, 394
Workshop notes, A further volume of laboratory and 64

X-ray
  analysis, Summarized proceedings of a conference on—Edinburgh, April 1952 305, 368
  diffraction, Fortieth anniversary of the discovery of 304
  fluorescence, Some problems in the analysis of steels by 353
  powder diffraction lines, Effect of vertical divergence on the displacement and breadth of 349
X-rays, diffracted, On the problem of focusing, on an oblique flat film 7

AUTHORS

Adams, E. H., *see under* Hearmon, R. F. S.

Bechmann, R., and P. L. Parsons, Mechanical strength of piezoelectric crystals 147
Beevers, C. A., and A. E. De Barr, Summarized proceedings of a conference on X-ray analysis—Edinburgh, April 1952 305, 368
Bell, D. A., J. C. Cluley and H. O. Berktay, Electrical measurement of the cathode temperature of diodes 322
Berktay, H. O., *see under* Bell, D. A.
Billig, E., The physics of transistors 241
Boag, J. W., and T. Wilson, The saturation curve at high ionization intensity 222
Booth, A. D., On two problems in potential theory and their application to the design of magnetic recording heads for digital computors 307
Bradshaw, J. A., Calculation of the propagation constants of an inhomogeneously-filled waveguide *Correspondence* 332
Brandes, E. A., *see under* Sully, A. H.
Briscoe, P. A., W. J. Dunning and R. C. Seymour, The rheology of plastic dispersions 193
Buckens, F., On the problem of focusing diffracted X-rays on an oblique flat film 7
Burfoot, J. C., Numerical ray-tracing in electron lenses 22
Burnand, G., The study of the thermal behaviour of structures by electrical analogy 50

Challice, C. E., and C. D. Sutton, The production of specimen mounting grids for the electron microscope 384
Chambers, Ll. G., Compilation of the propagation constants of an inhomogeneously-filled waveguide 19, 332
Christopherson, D. G., The relaxation method in stress analysis 65
Cluley, J. C., *see under* Bell, D. A.
Cook, H. F., A physical investigation of heat production in human tissues when exposed to microwaves 1, 64. A comparison of the dielectric behaviour of pure water and human blood at microwave frequencies 249. *See also under* Roberts, J. E.
Cook, P. M., and J. G. Wistreich, Measurement of die pressures in wire drawing by photoelastic methods 159
Cosslett, V., Report of conferences on electron microscopy—Washington and Philadelphia, 1951 137
Cox, H. L., The elasticity and strength of paper and other fibrous materials 72
Critchley, O. H., and M. R. Gavin, Transit time oscillations in triodes 92
Culver, R., The use of extrapolation techniques with electrical network analogue solutions 376

Davenport, P. A., A radio-frequency power supply system for high voltage accelerators 124
Davidson, P. M., A similarity theorem in electrical contacts 361
Davies, D. M., The effect of frequency on the behaviour of rubber under cyclical deformation 285
Davy, N., and N. H. Langton, The two-dimensional magnetic or electric field inside a semi-infinite slot terminated by a semi-circular cylinder 156
De Barr, A. E., *see under* Beevers, C. A.
Dixon, B. E., A. A. W. Russell and J. E. L. Swallow, Liquid films formed by means of rotating disks 115, 168
Dorman, R. G., The atomization of liquid in a flat spray 189
Drummond, D. G. and G. Liebmann, Summarized proceedings of a conference on electron microscopy—St. Andrews, June 1951 25
Dunning, W. J., *see under* Briscoe, P. A.
Dunsmuir, P., The use of polarized light for the examination of etched metal crystals and their orientation 264

Eastabrook, J. N., Effect of vertical divergence on the displacement and breadth of X-ray powder diffraction lines 349
Einstein, P. A., *see under* Haine, M. E.

Floyd, K. L., Second-order transition points in high polymers 373
Frankl, E. K., Summarized proceedings of a conference on stress analysis, Liverpool, 1951 105
Franklin, E., *see under* Peirson, D. H.

Garlick, G. F. J., Recent research on radio-luminescence 169
Gavin, M. R., Transit time oscillations in triodes *Correspondence* 363. *See also under* Critchley, O. H.
Gilford, C. L. S., Helmholtz resonators in the acoustic treatment of broadcasting studios 86
Gillam, E., and H. T. Heal, Some problems in the analysis of steels by X-ray fluorescence 353
Goldenberg, H., and C. J. Tranter, Heat flow in an infinite medium heated by a sphere 296
Gough, V. E. Three dimensional electrical potential analyser *Correspondence* 58
Grove-Palmer, C. O. J., *see under* Senior, D. A.

Hadfield, D., and D. L. Mawson, Permanent magnets for spectrographs and nuclear physical research 199
Haine, M. E., and P. A. Einstein, Characteristics of the hot cathode electron microscope gun 40
Halstead, M. B., *see under* Henderson, S. T.
Harris, I. A., Transit time oscillations in triodes *Correspondence* 363
Hatfield, P., An ultrasonic phase lag method for measuring the thickness of rubber 326
Heal, H. T., *see under* Gillam, E.
Hearmon, R. F. S., The elastic constants of piezoelectric crystals 120
Hearmon, R. F. S., and E. H. Adams, The bending and twisting of anisotropic plates 150
Heath, H. R., An experimental investigation of the diffusion of electrolytic hydrogen through metals 13
Heddle, T. A., A method of designing a compensated solenoid giving approximately uniform field 95
Henderson, S. T., and M. B. Halstead, The spectrophotometry of light sources 255
Hermges, G., *see under* Jones, C.
Hickin, E. M., *see under* Lamont, H. R. L.
Hickson, V. M., Errors in stress determination at the free boundaries of "frozen stress" photoelastic models 176
Hodgson, P. E., Grain density fluctuations in photographic emulsions 11
Horsley, R. A., and H. A. Nancarrow, The stretching and relaxing of polyethylene 64
Hughes, J. R., *see under* Lane, T. B.
Hyam, E. D., and J. Nutting, A method for the electron and optical microscopic examination of identical areas 173

Jaeger, J. C., Conduction of heat in tissue supplied with blood 221
Jones, C., and G. Hermges, The measurement of velocities for solid-fluid flow in a pipe 283
Jones, R., A method of studying the formation of cracks in a material subjected to stress 229
Jones, R. V., *see under* Paul, W.

Lamont, H. R. L., and E. M. Hickin, The application of molecular resonance to microwave frequency stabilization 182
Lane, T. B., and J. R. Hughes, A study of the oil-film formation in gears by electrical resistance measurements 315
Langton, N. H., *see under* Davy, N.
Lawson, D. I., and D. L. Simms, Ignition of wood by radiation 288, 394
Lawson, J. D., Radiation intensity from high energy accelerators 214
Lenihan, J. M. A., Isotope catalogue on punched cards *Correspondence* 29
Liebmann, G., *see under* Drummond, D. G.

Lincoln, B., Frictional and elastic properties of high polymeric materials 260
Loeb, L. B., Secondary processes active in the electrical breakdown of gases 341
Lucas, D. H., The properties of semi-conducting ceramic glaze 293

Mackenzie, R. B., The modulation characteristic of cathode-ray tubes in television 54, 104. A graphical treatment of the tone reproduction problem in television systems 141
Mahrous, M. A., The development of a multi-flash camera and its application to the study of liquid jets 329
Major, J. V., A quick method of distortion measurement in nuclear emulsions 309
Marshall, I. A., *see under* Sugarman, B.
Mawson, D. L., *see under* Hadfield, D.
Milligan, A. G., A method for measuring the potential of a current-carrying electrode 372
Moore, A. C., and D. Tabor, Some mechanical and adhesive properties of indium 299
Moxley, G. O., *see under* Sugarman, B.

Nancarrow, H. A., *see under* Horsley, R. A.
Nelson, H. M., Temperature distribution with simultaneous platten and dielectric heating 79
Nief, G., Differential methods of vacuum leak detection *Correspondence* 29
Nutting, J., *see under* Hyam, E. D.

Parfitt, G. G., A note on the measurement of damping in vibrating rods *Correspondence* 332
Parsons, P. L., *see under* Bechmann, R.
Peirson, D. H., and E. Franklin, Aerial prospecting and the absorption of γ-radiation *Correspondence* 203
Paul, W., and R. V. Jones, Production and separation of small glass spheres 311
Price, P. H., and M. R. Slack, Stability and accuracy of numerical solutions of the heat flow equation 379
Prosad, S., The thermal conductivity of liquid oxygen 58

Rawson, H., Theory of stresses in glass butt seals *Correspondence* 30
Redshaw, S. C., Three dimensional electrical potential analyser *Correspondence* 58
Roberts, J. E., and H. F. Cook, Microwaves in medical and biological research 33
Robinson, K., and E. R. S. Shaw, Summarized proceedings of a conference on structures of silicate minerals—London, November 1951 277
Roscoe, R., The viscosity of suspensions of rigid spheres 267
Russell, A. A. W., *see under* Dixon, B. E.
Russell, O. J., Radioassay of potassium in solid samples 47

Selwyn, E. W. H., The method of dimensions 209, 368
Senior, D. A., and C. O. J. Grove-Palmer, An improved technique for high-speed photography 318
Seymour, R. C., *see under* Briscoe, P. A.
Shaw, E. R. S., *see under* Robinson, K.
Simms, D. L., *see under* Lawson, D. I.
Slack, M. R., *see under* Price, P. H.
Smith, D. M., Summarized proceedings of the third international spectroscopy colloquium—Hoddesdon, September 1952 369
Steljes, J. F., Aerial prospecting and the absorption of γ-radiation *Correspondence* 203
Stout, H. P., Ignition of wood by radiation *Correspondence* 394
Sugarman, B., G. O. Moxley and I. A. Marshall, A castable polyester resin for photoelastic work 233
Sully, A. H., E. A. Brandes and R. B. Waterhouse, Some measurements of the total emissivity of metals and pure refractory oxides and the variation of emissivity with temperature 97
Sutton, C. D., *see under* Challice, C. E.
Svensson, N. L., Theory of stresses in glass butt seals *Correspondence* 30
Swallow, J. E. L., *see under* Dixon, B. E.

Tabor, D., *see under* Moore, A. C.
Theron, J. J., An improved apparatus for the differential thermal analysis of minerals 216
Thomas, P. H., Absorption and scattering of radiation by water sprays of large drops 385
Thomas, W. Rheinallt, Summarized proceedings of the fourth industrial physics conference—Glasgow, June 1952 273
Tranter, C. J., *see under* Goldenberg, H.
Tsui, F., Time-resolved spectroscopy of spark discharges 139
Tucker, R., Pool surface and cathode spot temperature of mercury cathodes as a problem in heat conduction *Correspondence* 333

v. Bertele, H., Pool surface and cathode spot temperature of mercury cathodes as a problem in heat conduction 127, 333. Current densities of free-moving cathode spots on mercury 358

Waterhouse, R. B., *see under* Sully, A. H.
Williams, J. C., The solution of temperature distribution problems by computation and electrical analogy 197
Wilson, T., *see under* Boag, J. W.
Wistreich, J. G., *see under* Cook, P. M.
Woods, J., and D. A. Wright, Secondary electron emission from barium oxide 323
Wright, D. A., Summarized proceedings of a conference on microwave physics—Oxford, July 1952 337. *See also under* Woods, J.

Zaid, M., Theory of stresses in glass butt seals *Correspondence* 30

PRINTED IN GREAT BRITAIN BY UNWIN BROTHERS LIMITED, WOKING AND LONDON

BLANK
PAGE

A physical investigation of heat production in human tissues when exposed to microwaves

By H. F. Cook, B.Sc., Ph.D., A.M.I.E.E., F.Inst.P., Department of Physics Applied to Medicine, The Middlesex Hospital Medical School, London

[*Paper first received* 24 *May*, 1951, *and in final form* 18 *June*, 1951]

Experimental investigations of temperature rises produced in parts of the human body during exposure to microwaves of 10 and 9·4 cm wavelength are described. Application of linear heat flow theory shows that the experimental skin temperature rise in the initial stages of a microwave exposure is consistent with a thermal conductivity for tissues of 0·005 cal cm^{-1} sec^{-1} $°C^{-1}$. With occlusion of the blood supply to the irradiated region the conductivity remains at this value until the pain threshold is reached. With no occlusion, increase in blood supply due to heating causes the effective conductivity to rise during exposure, but the theory becomes inapplicable as soon as heat flow is non-linear. Comparison is made of theoretical and experimental subcutaneous and muscle temperatures after microwave exposure and the differences explained. The influence of wavelength variation and air-cooling of the skin are discussed.

A preliminary report of investigations of the effects of microwaves on humans and animals has already been published.[1] This paper will be concerned mainly with the thermal analysis of some of the results reported previously and of some obtained more recently. The application of conduction theory has been found to provide information regarding the thermal conductivity of human tissues whilst exposed to microwaves, and to comparison between the experimental and theoretical temperature distribution at a depth.

A brief description follows of the experimental arrangements by which the results to be discussed were obtained.

OUTLINE OF THE EXPERIMENTAL ARRANGEMENT

Arrangement using a pulsed source of microwaves of 10 cm wavelength. Pulsed radiation from a type 277 Naval radar set was transmitted by rectangular waveguide (7·62 × 2·54 cm) to the apparatus shown diagrammatically in Fig. 1. The part of the body to be

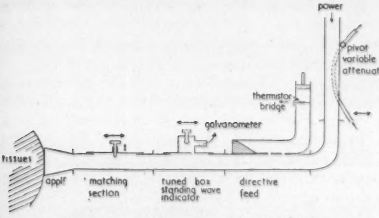

Fig. 1. Diagrammatic section of rectangular waveguide apparatus used at 10 cm wavelength

irradiated was placed in contact with the aperture of the wave-guide applicator and, at low power, a match was quickly achieved by adjusting the mismatch unit until the output from the directive feed was decreased to zero. The feed-through wattmeter (also acting as a standing wave indicator), previously calibrated against a water load, then enabled the water attenuator to be adjusted until the level of power required for the irradiation was obtained.

The free-space wavelength of the radiation was 10 cm, the pulse length 0·6 μsec, and repetition frequency 500 c/s. Average power, rather than that in the pulse, is the factor determining heat production and the results were related to this throughout. Two applicator sizes were available, 7·6 × 7·0 cm, and 3·8 × 2·5 cm, both rectangular. The smaller aperture was provided by a short length of wave-guide of this size filled with Perspex to allow progressive wave propagation. The field strength variation across the aperture was determined by the mode of propagation, H_{01}. There was thus a sine law variation of field strength across the longer axis, no variation with position occurring in the direction at right-angles.

Arrangement using a continuous wave source at 9·4 cm wavelength. Equipment was designed (in collaboration with T. J. Buchanan) for clinical applications, employing a continuous wave magnetron kindly lent by the General Electric Co. Ltd. Power from the source was fed by cable to either of the rectangular applicators described above or to a cylindrical H_{11} waveguide, the aperture of which provided, by means of interchangeable diaphragms, two applicator field sizes of 7 cm and 3·2 cm diameter respectively.

The power transmitted into tissues terminating the wave-guide applicators was a function of the magnetron current. Previous calibration with a water calorimeter thus enabled the power to be estimated from the magnetron current.

Thermometric arrangements. Temperatures were measured with thermocouples connected to a suitable galvanometer and previously calibrated. For the skin temperature measurement it was found possible to use a junction of fine copper and Constantan wires stretched across the aperture in contact with the skin and at right-angles to the electric field vector, the junction being at the centre of the field. No field pick-up effects were observed with powers several times higher than those used for tissue heating. The big advantage of this technique was that skin temperature variation could be recorded during the exposure.

Subcutaneous and muscle temperatures were measured with a steel hypodermic needle, at the point of which was a junction with an insulated copper wire running inside the needle. Measurements at various depths were made as quickly as possible after exposure. Since temperatures at each depth were measured at different times after exposure, corrections have been made to allow for differences in cooling at each depth.

Accuracy. The accuracy of power measurement was worst for low powers, where the limits of error were estimated to be $\pm 5\%$. These limits decreased progressively as the power increased. Skin temperature rises were thought to be quite accurate, to about $\pm 0{\cdot}1^\circ$ C, but tissue temperature rises suffered wider error limits. This was due mainly to some uncertainty in the cooling corrections applied, but possible errors arising from heat conduction along the steel needle have also to be considered. The work of Mendelssohn and Rossiter[2] would appear to suggest that the latter are negligible. It is thought that tissue temperature rises are accurate to $\pm 0{\cdot}3^\circ$ C.

DISTRIBUTION OF POWER IN THE MICROWAVE BEAMS

Dielectric constant measurements on human skin, fat, muscle and bone, reported elsewhere,[3] have enabled the absorption coefficients of these tissues for microwaves of various wavelengths to be evaluated. The power distribution in a plane perpendicular to the electric field

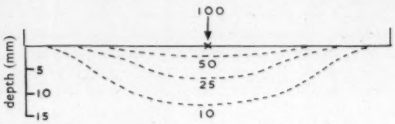

Fig. 2. Isopower curves in saline phantom

Principal plane perpendicular to electric field; $7{\cdot}6 \times 7{\cdot}0$ cm aperture; $\lambda = 10{\cdot}0$ cm.

and containing the central axis of the microwave beam was then measured experimentally by means of a probe moving in a saline solution. The salt concentration and temperature of this were adjusted to have an absorption coefficient equal to that for human muscle at 37° C for wavelengths of 10 cm and 9·4 cm. To illustrate the results obtained, Fig. 2 shows isopower curves in such a phantom when microwaves of 10 cm wavelength from the $7{\cdot}6$ cm $\times$ $7{\cdot}0$ cm applicator were applied. The actual power distribution in the human arm or thigh would differ somewhat from that shown since wave propagation would be modified by the presence of the skin and subcutaneous fat layers, which have dielecric constants and absorption coefficients different from those of muscle.

The power distribution in the plane of the aperture and transverse to the beam axis is shown in Fig. 3 for

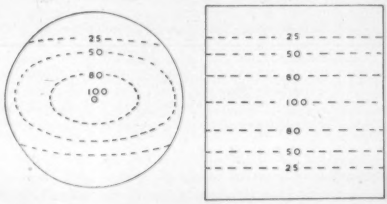

Fig. 3. Theoretical power distribution in plane of the apertures

7 cm diameter circle and $7{\cdot}6 \times 7{\cdot}0$ cm rectangle

the cases of rectangular and circular apertures. These distributions have been derived from the theoretical electric field patterns in the plane of the aperture. They can be taken as representing approximately the power distribution at the skin surface when tissues are irradiated.

SOME OF THE EXPERIMENTAL RESULTS ON HUMANS

Male volunteers were used, the inner forearm and anterior thigh being irradiated. Investigations of the variation of skin temperature with power and time were made, some representative results being shown in Figs. 4, 5 and 6. In all cases the temperatures shown are those at the central point of the exposed area. Differences between individuals were not unexpected but, in the main, these were small.

Investigations of the temperatures in the subcutaneous and muscle tissues along the central axis of a microwave beam were also carried out in collaboration with A. C. Boyle and others. A typical set of results for a male thigh are shown in Fig. 7 where the temperatures all relate to 30 sec after the termination of the exposure times shown against the curves.

DISCUSSION

The conditions under which the above experimental results were obtained approximate to those of a semi-infinite solid with internal heat generation. The case of

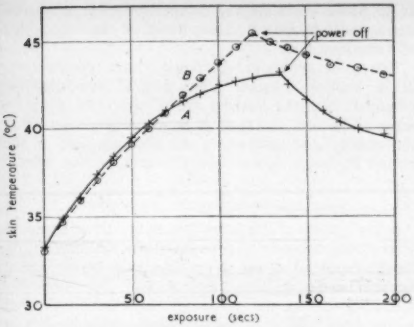

Fig. 4. Skin temperature *v.* exposure

Curve *A*—normal blood supply.
Curve *B*—with occlusion of blood supply.
Forearm; 7·6 × 7·0 cm rectangle; $\lambda = 10{\cdot}0$ cm; power = 17 W; room temperature = 20° C.

the semi-infinite solid in which the rate of heat production depends on depth according to $A_0 e^{-\alpha x}$, and where the surface at $x = 0$ is held at zero temperature, has been dealt with by Carslaw and Jaeger.[4] In the present case it can be assumed that heat flow into the irradiated tissues only need be considered. That into the terminating material of the microwave applicators (cork or Perspex) will be assumed negligible in comparison, since these materials have conductivities much lower than that of human tissues.

An extension of the case treated by Carslaw and Jaeger to cover the present condition where the temperature at $x = 0$ is allowed to rise is due to A. J. Vendrik (unpublished work). The relation derived, using the notation of Carslaw and Jaeger, is:—

$$v_x = a + bx + \left(2b + \frac{2A_0}{K}\right) \cdot \sqrt{(kt)} \cdot ierfc\left[\frac{x}{2\sqrt{(kt)}}\right] + \frac{A_0}{2\alpha^2 K} \exp(\alpha^2 kt - \alpha x) \cdot erfc\left[-\frac{x}{2\sqrt{(kt)}} + \alpha\sqrt{(kt)}\right] + \frac{A_0}{2\alpha^2 K} \exp(\alpha^2 kt + \alpha x) \cdot erfc\left[+\frac{x}{2\sqrt{(kt)}} + \alpha\sqrt{(kt)}\right] - \frac{A_0}{\alpha^2 K} \exp(-\alpha x)$$

where

v_x = temperature at time t and at depth x.
a = initial temperature at $x = 0$.
b = temperature gradient.
A_0 = heat developed per unit time per unit volume at $x = 0$.
α = energy absorption coefficient.
K = thermal conductivity.
$k = K/$(density × specific heat).

Use of this relation in conjunction with experimental results has enabled the thermal conductivity of the irradiated tissues to be calculated.

Skin temperatures during exposure to microwaves

Of the experimental results of skin temperature rises, those shown in Fig. 4 were obtained under conditions which approximate most closely to the semi-infinite solid. They also show the marked effect of occlusion of the blood supply.

To apply the theory to the experimental case it is necessary to relate the microwave power with A_0, to choose the correct value of α and to know the initial temperature gradient, b. It is also necessary to allow for the transverse power density variation across the irradiated area.

Taking the central block of tissues of cross-section, 4 × 7 cm, it was found experimentally that the average temperature of the skin after irradiation over this area was 0·9 of that measured at the central point. It was also found from the known power density variation that if W is the power in watts crossing the whole cross-section of the applicator, the average power density in the central section, 4 × 7 cm was 0·030 W. It can then be shown that the average value of A_0 for this case is given by:

$$A_0 = 0{\cdot}00723 W\alpha \text{ cal sec}^{-1} \text{ cm}^{-3}$$

The absorption of energy in the central block of tissues, 4 × 7 cm, can be shown, by analysis of the isopower curves of Fig. 2, to approximate closely to that for a plane-wave if a 10% increase in the plane-wave absorption coefficient is made. A theoretical study of plane-wave propagation in human tissues (to be described elsewhere) has shown that, in the present case of the forearm, the effective plane-wave absorption coefficient is not much lower than that for muscle, the influence of the thin skin and fat layers being small. The dielectric constant measurements already mentioned have shown that the value of this absorption coefficient for muscle at a wavelength of 10 cm is approximately 1·5. Hence this value for α was used in the thermal analysis since the two effects above tend to cancel each other.

The temperature gradient, b, was not measured in this case, but was taken as 2° C per cm, a figure appropriate to the prevailing room temperature. The specific heat and density of the tissues of the forearm were both assumed to be unity in their respective units.

It was then found that curve *B* (with occlusion) of Fig. 4 agreed well with a theoretical one calculated using the above data and a thermal conductivity, independent of exposure time, of 0·005 cal cm^{-1} sec^{-1} °C^{-1}. This figure fits well into the range of values of conductivity (10^{-3} to 10^{-2}) quoted in the literature for normal tissues, and shows that, with occlusion of the blood supply, the heat production caused by microwave irradiation has little effect on the thermal conductivity.

Curve *A* of Fig. 4 was analysed similarly and showed

that the effective thermal conductivity of the tissues rises to high values as the exposure proceeds. The temperature rise in the first 30 sec is consistent with $K = 0{\cdot}005$, but the temperature reached after 2 min can only be explained by assuming that the average conductivity operative over this period was increased to $0{\cdot}015$, the instantaneous value of K operative at this time being even higher. This increase can be related to the known enhancement of blood circulation and must be allowed for in theoretical calculations of tissue temperatures obtained when the human body is exposed to any thermogenic agent. The loss of heat from the irradiated region by means of transference by blood flow to non-irradiated regions becomes so large at longer exposures as to make worthless any comparison of experimental results with theoretical values based on the assumption of linear heat flow.

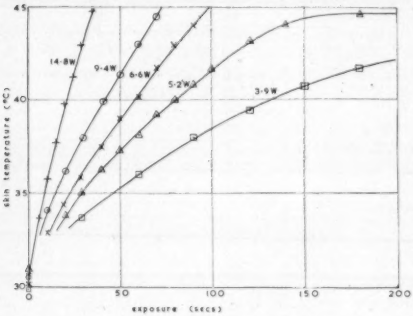

Fig. 5. Skin temperature *v.* exposure

Forearm; $3{\cdot}8 \times 2{\cdot}5$ cm aperture; $\lambda = 10{\cdot}0$ cm; room temperature = 19° C.

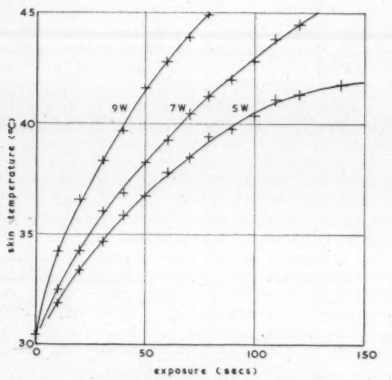

Fig. 6. Skin temperature *v.* exposure

Anterior thigh; 7 cm circular aperture; $\lambda = 9{\cdot}4$ cm; room temperature = 17° C.

The results shown in Figs. 5 and 6 have been analysed in a similar manner. The thermal conductivities obtained from the analysis are of the same order as those above, but the analysis is less accurate owing to the smaller area involved in the one case, and to the greater transverse power density variation in the other.

Subcutaneous and muscle temperatures

It is of interest to compare experimental tissue temperatures after irradiation with temperatures calculated from Vendrik's relation. Fig. 8 provides such a comparison for the irradiation conditions stated. To obtain the theoretical curves the values of the effective thermal conductivity derived in the preceding section have been used in the calculations. The experimental curves in this case are based on the mean results obtained using three individuals, the temperatures being corrected to refer to the time the exposures terminated.

Reasonable agreement is obtained between experiment and theory for these relatively short exposure times. Attempts to obtain agreement in the case of longer exposure times fail, however, even assuming K to increase considerably. Thus, it can be concluded that the flow of heat in irradiated tissues is approximately linear during the initial stages of exposure, but is no longer so when the exposure is prolonged. This is due, presumably, to a progressive increase in vasodilation and lateral heat transference out of the irradiated zone during exposure.

Interesting features of the experimental curves of temperature as a function of depth are the trough and peak in the curves, not apparent in the theoretical ones. These can be correlated with the existence of a layer of fatty tissue interposed between skin and muscle tissues. Adipose tissue has a dielectric constant and loss much lower than those of skin and muscle. It will be shown in another paper that the combined effect of the lower energy absorption in the fatty tissue layer and the multiple reflexion of radiation at the tissue interfaces is to modify the shape of the temperature-depth curve from that of the theoretical one in homogeneous muscle (Fig. 8) to that of the experimental curves shown in Figs. 7 and 8. The effect depends on the thickness of the fat layer. The results presented here refer to thighs where this thickness is approximately 6 mm.

Influence of wavelength on temperature rises of skin and subcutaneous tissues

The effect of a change in wavelength (and hence absorption coefficient) on temperature rise can be calculated. It can be shown readily that the transmitted intensity of radiation required to produce any given skin temperature rise after prolonged exposure is inversely proportional to the absorption coefficient. Thus, the

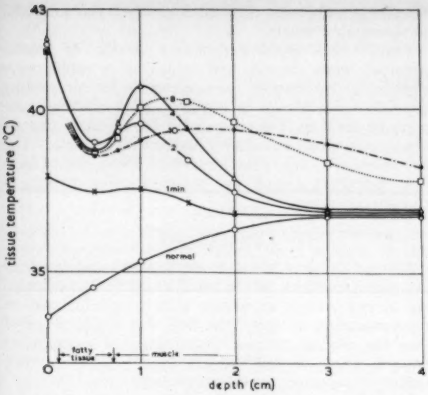

Fig. 7. Tissue temperature *v.* depth 30 sec after exposure times shown

Anterior thigh; central axis of field 3·8 = 2·5 cm; $\lambda = 10{\cdot}0$ cm; power = 3 W; room temperature = 25° C.

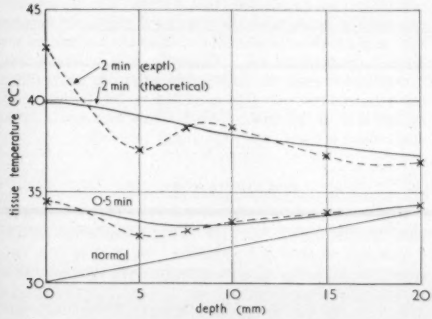

Fig. 8. Tissue temperature *v.* depth

Full lines: theoretical for plane wave in muscle; $\lambda = 10{\cdot}0$ cm; 0·42 W cm−2.

Broken lines: experimental for central axis of beam from aperture 3·8 × 2·5 cm in tissues of anterior thigh; $\lambda = 10{\cdot}0$ cm; 2·5 W.

transmitted intensity of infra-red radiation (from a therapeutic heat lamp) and of 1·25 cm microwaves ($\alpha = 15$ in both cases), which can be tolerated by the human body without pain, is 1/10th of the tolerated intensity of 10 cm microwaves ($\alpha = 1{\cdot}5$).

Use of the theoretical relation (based on linear heat flow) to determine the effect of a change of wavelength on temperature variation with depth in irradiated tissues must be confined to cases where the exposure time is short enough for the linear heat flow condition to be satisfied approximately. Fig. 9 shows the theoretical temperature distribution in superficial skin and muscle tissues (negligibly thin fatty layer) after a 2 min exposure to microwaves of different wavelengths. Although the absorption coefficient decreases from 15 at 1·25 cm wavelength to 1·5 at 10 cm wavelength, the relatively high thermal conductivity has the effect of decreasing considerably the differences in temperature gradient which might be expected from such a difference in absorption coefficient. For wavelengths longer than 10 cm the absorption coefficient falls very slowly with increasing wavelength, and the temperature variation with depth will differ little from that shown for 10 cm wavelength.

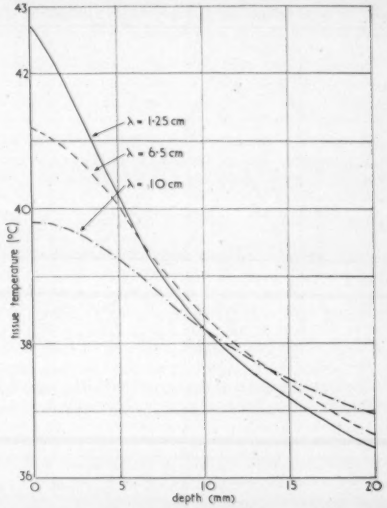

Fig. 9. Theoretical tissue temperatures for plane wave propagation in muscle after 2 min exposure at different wavelengths

Initial skin temperature = 30° C; initial temperature gradient = 2° C cm−1; thermal conductivity = 0·015 cal cm−1 sec−1 °C−1; 0·42 W cm−2.

Since the reflexion coefficients of tissue interfaces (skin-fatty tissue, fat-muscle, muscle-bone) are relatively constant in the microwave region,[3] the magnitude of the effect of the presence of fatty tissue and bone in modifying the temperature variation with depth should be approximately independent of wavelength.

The influence of heat losses to the region $x < 0$

Where tissues are exposed to radiation under conditions such that heat is lost to the region $x < 0$ (by

radiation, convection and vaporization) the preceding theory and arguments may no longer hold. Such conditions obtain in therapeutic practice where an air space intervenes between the exposed region of the body and the microwave applicator.

If the loss of heat at the surface to the region $x < 0$ is at a high rate, the surface temperature does not rise and the theoretical variation of temperature rise with depth would be of the type shown in Fig. 10. However, with room conditions normally encountered the loss of heat to the region $x < 0$ is relatively small, the skin temperature rises, and the temperature gradient is considerably reduced. Another factor contributing to the reduction of the temperature gradient is vasodilatation. In experiments on animals under air-cooling conditions (carried out in collaboration with A. C. Boyle and D. L. Wolfe) no evidence has yet been obtained of the existence, during exposure, of temperatures at depths below the skin in excess of those of the skin, in anatomical regions well supplied with blood.

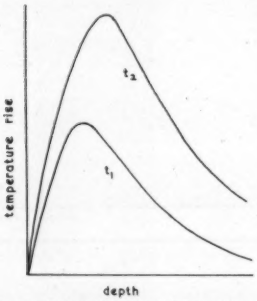

Fig. 10. Form of the theoretical temperature rise variation with depth in homogeneous tissues exposed under conditions where the surface temperature is held constant ($t_1 < t_2$)

A positive temperature gradient in tissues exposed in the presence of air-cooling can be found experimentally a short time after the termination of exposure, but when allowance is made for the rate of cooling at the surface being greater than at a depth during temperature measurements, it is found that the corrected gradient is approximately zero. This suggests that, in practice, the loss of heat to the region $x < 0$ under normal air conditions is not sufficiently great to cause any large qualitative change from the results found when the exposed tissues are in contact with a poor thermal conductor.

In other experiments with gelatine phantoms, exposed under air cooling conditions to 10 cm microwaves, the temperature gradient (corrected for cooling during temperature measurements after exposure) was found to be positive only when the surface at $x = 0$ was subjected to strong air currents.

Clark[5] has given preliminary details of results obtained when the eye and testicle of a rabbit were exposed to microwaves, presumably under air cooling conditions. Evidence is obtained of a positive temperature gradient in the eye and it is suggested that the absence of blood circulation makes this possible. The experiments with gelatine mentioned above would indicate that Clark's result was obtained under strong air-cooling conditions.

CONCLUSIONS

Human tissues exposed to microwaves undergo temperature rises which, in the initial stages of the exposure, are in approximate agreement with those calculated on the assumption of linear heat flow if it is also assumed that the effective thermal conductivity of tissues rises from a value of $0{\cdot}005$ cal cm^{-1} sec^{-1} °C^{-1} to much higher values as the exposure proceeds.

However, the divergence of the experimental case from the theoretical one of the semi-infinite solid with linear heat flow becomes too great for comparison to be made as soon as capillary dilatation due to heating becomes significant.

It can be concluded that, when the microwave exposure is made with the irradiated region in contact with a poor thermal conductor, the skin undergoes the highest temperature rise. However, it is possible that, if exposure is made in the presence of strong air cooling, the temperature rise at depths below the surface may exceed that of the skin. This is likely to occur only in anatomical regions devoid of blood circulation.

ACKNOWLEDGMENTS

It gives pleasure to acknowledge the author's indebtedness to Dr. A. J. Vendrik, whose assistance in the theoretical work was invaluable. He was also a collaborator in some of the experimental work on skin temperature measurements.

Thanks are also due to the Director of Radio Equipment, Admiralty and to The General Electric Co. Ltd. for the loan of apparatus.

REFERENCES

(1) Boyle, A. C., Cook, H. F., and Buchanan, T. J. *Brit. J. Phys. Med.*, **13**, p. 2 (1950).
(2) Mendelssohn, K., and Rossiter, R. J. *Quart. J. of Exp. Physiol.*, **32**, p. 301 (1944).
(3) Cook, H. F. *Brit. J. Appl. Phys.*, **2**, p. 295 (1951).
(4) Carslaw, H. S., and Jaeger, J. C. *Conduction of Heat in Solids* (London: Oxford University Press, 1947).
(5) Clark, J. W. *Proc. Instn. Radio Engrs.*, **38**, p. 1028 (1950).

On the problem of focusing diffracted X-rays on an oblique flat film

By F. Buckens, Dr.Ing., University of Louvain, Belgium

[*Paper first received* 25 *June*, 1951]

A geometrical treatment of focusing in the X-ray back-reflexion method is given. The form of the irradiated surface, the breadth of the emitting source, and the size and location of the limiting diaphragm are considered. A theory of "secondary focusing" is suggested, with experimental support. The idea can be used for effecting focusing on both sides of an oblique flat film.

The purpose of this paper is to discuss some general aspects of focusing conditions and to describe a method of "secondary focusing" which, when properly applied, should be of some help in the measurement of superficial strains by the so-called "X-ray back-reflexion method."

In this method a monochromatic X-ray beam i (Fig. 1) is used, which is diffracted along r with an inclination $\epsilon = \pi - 2\theta$ by those micro-crystals of the tested metallic agglomerate, whose recticular planes, making an angle θ with the incident beam, have the spacing d given by the Bragg relation

$$d = n\lambda/2 \sin \theta \qquad (1)$$

λ being the wave-length of the incident X-rays, and n an integer.

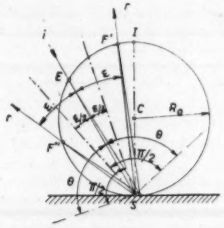

Fig. 1

Owing to the large number of micro-crystals, those satisfying equation (1) give, for the same value of n, a continuous distribution of diffracted rays along a conical surface around the incident beam. (Except for coarse-grained materials; these are characterized by a pattern of discrete spots on the Debye-Scherrer photograph.) The incident beam is collimated, but cannot be made very small in diameter if diffracted rays are to be easily observed and recorded.

Diffraction thus takes place at a small but definite area on the specimen. Let us assume that incident rays are emitted from the point E (Fig. 1). It is known that diffracted rays from the spot S focus on a sphere of radius R_0, tangent at the irradiated area on S and passing through the emitting centre E (for, in any plane containing i, the circle passing through E and tangent at S to the irradiated surface is the locus of vertices of equal angles ϵ, whose sides converge to two fixed points on that circle, the centre E and the focus). For an irradiated area of finite size the point S is taken at its "centre."

The locus of the foci on the sphere is given by its intersection with the conical surface of opening 2ϵ around the incident beam i. It is at these points that photographic or photometric records of the position of the diffracted rays should give the best definition.

Experience shows that a diaphragm fulfils the role of a centre of emission E; as will be shown below, the principal influence in this connexion is the breadth of the actual emitting source. Instead of a pin-hole, one can use a narrow slit parallel to the tangent plane at S, with the result that the sharpest lines will be obtained at the points F' and F'' (Fig. 1) of the meridian plane normal to the irradiated surface at S and passing through E and S.

The quality of the definition at F' and F'', for a given spot S, depends on the form of the surface at this point. It will be most favourable if this surface has at S principal radii of curvature which are both equal to R_0, the radius of the sphere (Fig. 1). At least the radius of curvature in the considered meridian plane should equal R_0.

In the following, consideration is given to the location of the foci F in this "principal" plane E, S, F', F''.

GEOMETRICAL CONSIDERATIONS

There are, in the principal meridian plane, three factors which control focusing when the X-rays are incident obliquely: (1) the form of the irradiated surface and the angle of incidence α; (2) the finite breadth of the emitting source; (3) the effect of the diaphragm.

In order to simplify discussion of the first two factors, it will be supposed that the diaphragm, if any, lies on the surface of the material, and merely defines the area of the irradiated spot.

(1) *Form of the irradiated surface.* If, as is often the case, the macroscopic surface of the material is plane, the loci of the points F' and F'' for various angles of incidence α are parabolas (Fig. 2). If d be the distance of E from the plane, the equation of the straight line SF is

$$y = x \tan (\alpha - \epsilon) + d \tan \alpha \qquad (2)$$

or, putting $u = \tan \alpha$, $v = \tan \epsilon$,

$$y(1 + uv) = x(u - v) + ud(1 + uv) \qquad (3)$$

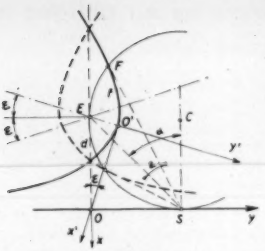

Fig. 2

The envelope of SF for various values of α, or u, is obtained by eliminating u between equation (3) and

$$yv = x + (1 + 2uv)d \tag{4}$$

Its equation becomes

$$y^2v^2 + x^2 - 2xyv + 2x(1 + v^2)d + d^2 = 0 \tag{5}$$

The transformation to new axes x' and y' (Fig. 2) gives

$$x'^2 + 2y'd \sin \epsilon = 0 \tag{6}$$

which shows that the parabola equation (5) has its focus in E and its axis ($O'y'$) inclined at ϵ to the plane surface.

More generally let R be the radius of curvature of the surface line at the point S (Fig. 3); the position of F, contact point of SF with its envelope, can be found by determining the instantaneous centre of rotation I of the rigid angle ESF, whose side ES must pass through the fixed point E, and whose vertex S describes the circular arc s, Fig. 3.

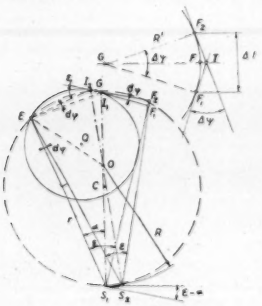

Fig. 3

It is readily seen that this construction is equivalent to Fig. 1, the points E, S, F, I lying on the same circle. Let f measure the length of the arcs described by F on the envelope.

It will be shown that the sharpness of focus in F for the given position of E with respect to S can be characterized by the ratio

$$ds/df = \lim_{S_2 \to S_1} (S_1S_2/F_1F_2) \tag{7}$$

Now
$$df = d(\overline{SF}) + ds \sin (\epsilon - \alpha) \tag{8}$$

with
$$\overline{SF} = r \cos (\epsilon - \alpha)/\cos \alpha$$

Calling c the constant distance EO (Fig. 3), we have

$$c^2 = R^2 + r^2 - 2Rr \cos \alpha$$

so that

$$d\alpha = (dr/\sin \alpha)(\cos \alpha / r - 1/R) = ds(\cos \alpha / r - 1/R)$$

In this manner, from equation (8),

$$ds/df = \cos \alpha/[2 \sin \epsilon \, (1 - r/2R \cos \alpha)] \tag{9}$$

The centre of curvature G of the envelope f lies on a circle passing through E, I_1 and I_2. The radius of curvature is:

$$R' = df/d\phi = rdf/\cos \alpha \, ds$$
$$= 2r \sin \epsilon \, (1 - r/2R \cos \alpha)/\cos^2 \alpha \tag{10}$$

The best concentration of the diffracted rays is found when $ds/df = \infty$ (or $R' = 0$), that is, ϵ being greater than zero,

$$r = 2R \cos \alpha \tag{11}$$

and in this case the centre of curvature O coincides with the centre C of the circle ES_1S_2F (Fig. 3).

If the surface of the material is plane, we have $R = \infty$, and

$$ds/df = \cos \alpha / 2 \sin \epsilon \tag{12}$$

For monochromatic rays, and ideal micro-crystals in which boundary effects are absent, the breadth of the pencil at F normal to the diffracted beam would be (Fig. 3)

$$b_S = \overline{FT} = R'[1/\cos (\tfrac{1}{2}\Delta\phi) - 1] = R'(\Delta\phi)^2/8 = \Delta f \Delta\phi/8$$

or
$$b_S = r(\Delta\phi)^2/8 \cos \alpha \, (ds/df) \tag{13}$$

assuming that the emitting source is a point. For a given angle $\Delta\phi$, b_S increases with Δf. The more interesting factor is Δf, however, since it gives a tolerance in the location of the film, the breadth b_S, as will be shown, usually having only a minor influence on the actual divergence of the diffracted pencil.

(2) *Finite size of the emitting source.* In Fig. 4 let $E_1E_2 = e$ be the actual breadth of the emitting source, measured normally to the incident beam. It is readily seen that, normal to the diffracted beam, the "focus" spreads out by an amount

$$b_E = \overline{SF}e/r = e \cos (\alpha - \epsilon)/\cos \alpha \tag{14}$$

and in these circumstances the breadth of the focused pencil would be

$$b = b_S + b_E \qquad (15)$$

Usually the term b_S is small compared with b_E. Assuming the surface of the material to be plane and

$$r = 50 \text{ mm}, \epsilon = 18°, \alpha = 45°, \Delta\phi = 3/50 = 0{\cdot}06, \text{ and } e = 0{\cdot}5 \text{ mm}$$

one finds $ds/df = 1{\cdot}1$, $R' = 61{\cdot}8$ mm, $\Delta f = 3{\cdot}71$ mm, and $b_S = \sin\epsilon \,.\, r(\Delta\phi)^2/4\cos^2\alpha = 0{\cdot}0278$ mm,

while $b_E = 0{\cdot}629$ mm.

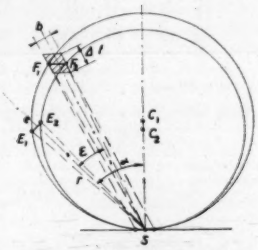

Fig. 4

It is only when the radius of curvature R is much smaller than the distance r, for example of the order of $0{\cdot}05\ r$, that b_S can become as important as b_E, assuming usual values for e. A case in point is the measurement of stress concentrations in grooves.

To sum up, it is seen that, owing to the finite sizes of both the irradiated spot S and the source E, the focus is spread out over a finite area, indicated in Fig. 4 by a shaded parallelogram.

(3) *Effect of a diaphragm.* The diaphragm, whose aperture is taken to be $D_I D_{II}$ in Fig. 5, defines an angle of irradiation for every centre of emission along E_1E_2.

Determining the foci (F_1', F_1'') and (F_2', F_2'') for the extreme points E_1 and E_2, one obtains the loci $F_1'F_2'$ and $F_1''F_2''$ (exaggerated in Fig. 5 and taken as approximately a straight line), which define the radially extended areas of depth $\Delta f_E = (df/ds)\Delta s_E$, where

$$\Delta s_E = \overline{D_I D_{II}} r_E/(r_E - r_D) \qquad (16)$$

and df/ds is given by equation (11) or (12).

Considering the diaphragm as a new centre of emission, similarly (F_I', F_I'') and (F_{II}', F_{II}'') are obtained corresponding to D_I and D_{II}. For example, one can regard a pin-hole as a sequence of centres spread out along $D_I D_{II}$, giving rise to the segments $F_I'F_{II}''$ and $F_I''F_{II}'$. Around these small areas of depth $\Delta f_D = (df/ds)\ \Delta s_D$ can be defined, with

$$\Delta s_D = \overline{E_1E_2} r_D/(r_E - r_D) \qquad (17)$$

The shaded areas of Fig. 5 indicate positions where photography (or photometry) should give the most favourable definition, and this seems to be confirmed by experience.

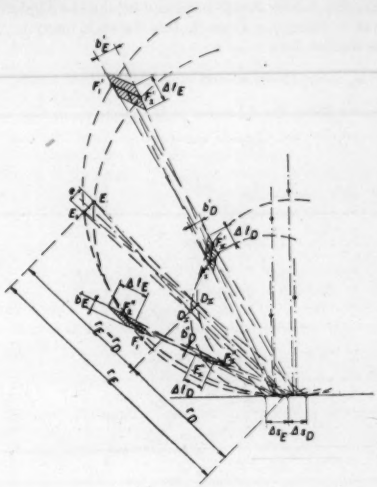

Fig. 5

EXPERIMENTAL ASPECTS

Usually in the X-ray back-reflexion method a flat cassette is located at right angles to the direction of the incident beam. With this arrangement, in order to measure the angle ϵ, it is essential to know the distance between the film and the point S. This is made possible by direct calibration using a thin coating of silver (or gold, etc.) powder whose diffraction angles, $\epsilon_n = \pi - 2\theta_n$, are known.

The problem is to obtain good focusing conditions for F' and F'' (Fig. 1) at the same time, these conditions to hold both for the given material and for the calibration metal. Normal incidence ($\alpha = 0°$) does not present much difficulty, but for oblique incidence (usually $\alpha = 45°$) good focusing can usually be obtained at one side of the beam ES only. It is noteworthy, however, that, on the same side of ES, excellent focusing conditions can be obtained simultaneously for one reflexion from the material being examined, and for two different reflexions from the silver powder (Fig. 6).

If a cobalt target is used as X-ray source, the "reflecting" crystal planes (310) of iron give $\epsilon = 18{\cdot}8°$, whereas for silver the planes (420) give $\epsilon_1 = 23{\cdot}5°$, and the planes (331) $\epsilon_2 = 34{\cdot}8°$.

Considering the diaphragm D as the effective X-ray

source, it happens that, for an oblique incidence of $\alpha = 45°$, the corresponding points F' may be located approximately along the same normal n to the incident beam (Fig. 6). The normal n gives the desired position of the film, which should be placed behind the diaphragm D, at a distance a from it, this distance being in any case smaller than

$$a_m = \tfrac{1}{2} r_D(1/\cos\alpha - 1) = 0{\cdot}207 r_D, \text{ for } \alpha = 45°,$$

$r_D/\cos\alpha$ being the diameter of the circle c_D in Fig. 6.

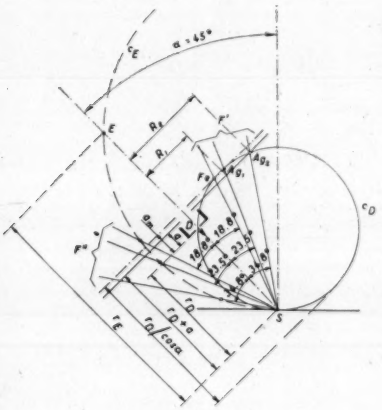

Fig. 6

Fig. 7 is a reproduction of a photograph taken at a short distance $r_D + a \simeq 51$ mm, for the purpose of recording simultaneously the two silver reflexions referred to above. In this way the distance $(r_D + a)$ can be determined from the separation $(R_2 - R_1)$. The photograph is interesting because of the high definition of the reflexion for iron on the side opposite to F'. This appears to be due to what could be called a "secondary" focusing effect, involving those rays emitted by the cobalt target which are not affected by the diaphragm D, as explained above. A "primary" slit or diaphragm at E, Fig. 6, should produce a similar result.

In any case the circle c_E, passing through the points F''_E and tangent in S to the irradiated spot, cuts the line SD at the point E, and the position of E would probably correspond approximately with the cobalt target. Accordingly, it was found that an increase of

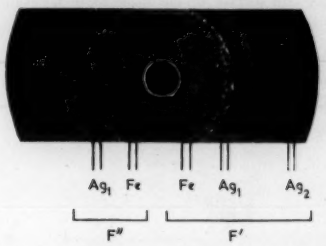

Fig. 7. Back reflexion photograph corresponding to Fig. 6

Aperture of diaphragm	0·6 mm dia
Exposure time	35 min
Distances—r_D	44·2 mm
a	6·8 mm

the aperture of the diaphragm D, although causing the reflexions F' to become very slightly blurred (larger b'_D, see Fig. 5 and equation (14)), gave a greater intensity of the reflexion F''_E for iron (larger Δf_E, nearly no change in b''_E, which depends on Δs_E).

It would seem that a systematic use of secondary focusing should, when a satisfactory compromise is reached, make possible improved focusing of obliquely incident beams on flat films. The problem is to choose r_D and $(r_E - r_D)$ in such a way as to make F'_D and F''_E lie on the same normal n to the incident beam.

From Fig. 6,

$$r_D + a = (r_D/\cos\alpha)\cos(\alpha - \epsilon)\cos\epsilon$$
$$= (r_E/\cos\alpha)\cos(\alpha + \epsilon)\cos\epsilon$$

whence
$$r_D \cos(\alpha - \epsilon) = r_E \cos(\alpha + \epsilon) \quad (18)$$

$$r_D = \tfrac{1}{2}(r_E - r_D)(\cot\alpha \cot\epsilon - 1) \quad (19)$$

$$a = (r_D/\cos\alpha)\sin(\alpha - \epsilon)\sin\epsilon \quad (20)$$

These formulae do not depend on the specific materials used here, and should remain valid, for example, when employing a copper target for aluminium, etc., provided proper values of ϵ are used.

Grain density fluctuations in photographic emulsions

P. E. HODGSON, Ph.D., B.Sc., A.R.C.S., D.I.C., Imperial College of Science and Technology, London, S.W.7

[*Paper received* 24 *May* 1951]

The fluctuations of the number of grains in successive sections of tracks produced by charged particles in nuclear research emulsions have been investigated. It is shown that the observed departures from the expected Poisson distribution can be attributed to close pairs of grains remaining unresolved, and that the standard deviation of a grain count is about three-quarters of the square root of the total number of grains counted.

The method of grain counting is extensively used to estimate the rate of energy loss of charged particles traversing nuclear research emulsions. It is therefore of importance to know the accuracy with which the grain density is determined by a count along a given section of track. It is generally assumed that the distribution follows Poisson's Law so that the standard deviation of the counts along successive sections of track is equal to the square root of the mean number of grains per section. The purpose of this investigation is to find the applicability of Poisson's Law to the problem, and to account for any deviations from it.

Grain-counts were made along a number of tracks formed by energetic particles in Ilford G5 emulsion. Such tracks were chosen so that the change in rate of energy loss from one end of the track to the other was very small. Small changes of grain density occurred, however, due to variations of development, especially when the particle traversed the emulsion from the top to the bottom. The tracks chosen were of low grain density, so that blocks of grains were rare, but, where they occurred, they were counted as two or three grains according to their length.

The results of a typical grain-count along a track of 13 300 microns is shown in Fig. 1. The track was divided into one thousand 13·3 micron sections, and the number of grains in each counted, the mean number per section being 3·45. The solid histogram shows the experimental results, while the straight line shows the Poisson distribution with the same mean.

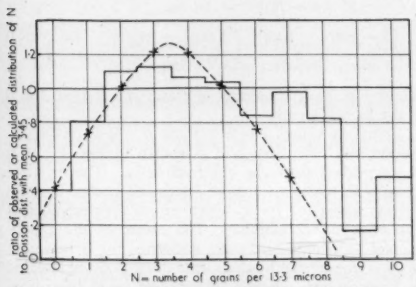

Fig. 1. Typical grain density fluctuation. The histogram shows the experimental results

----- calculated with $\mu = 0{\cdot}325$, $a = 0{\cdot}8$.
——— Poisson distribution with mean 3·45.

Rather surprisingly, the experimental distribution is sharper than the Poisson. The probability that the experimental results occur as a random fluctuation on a Poisson distribution was found by the χ^2-test to be negligibly small.

The experimental distribution has a standard deviation $\sigma = 1{\cdot}66$. The standard deviation expected if the grains have a Poisson distribution is the square root of the mean number of grains per section, viz. $\sqrt{N} = \sqrt{3{\cdot}45} = 1{\cdot}86$.

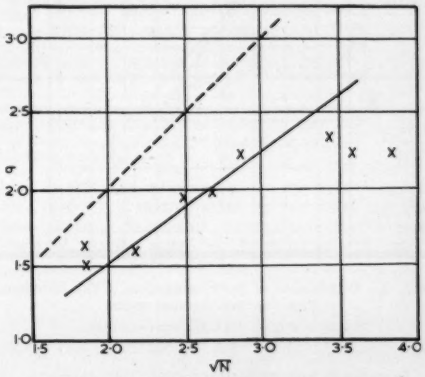

Fig. 2. Observed and expected standard deviations

----- expected standard deviation on Poisson's Law.
——— $\sigma = 0{\cdot}75\sqrt{N}$. × observed.

These measurements were repeated for several more tracks, and the values of observed and expected standard deviations are plotted in Fig. 2. It is found that the observed standard deviation is about three-quarters of the expected.

There are several possible explanations of a deviation of the observed distribution from that given by Poisson. These include variation of the energy of the particle from one end of its track to the other, experimental errors, and emulsion and developing inhomogeneities.

But all these causes lead to a broadening of the distribution and not to a sharpening as observed.

This effect has also been observed independently by L. Jauneau, who suggests that it may be due to the development of one grain lowering the concentration of developer in its vicinity, and consequently reducing the probability of development of an adjacent grain. This would give the observed effect, but it does not seem likely that this is the whole explanation owing to the long development times of nuclear emulsions.

Another possibility, which does not exclude the above, is that if two grains are separated by a distance less than a (say), they will be unresolved and counted as one. This effect will also sharpen the observed distribution.

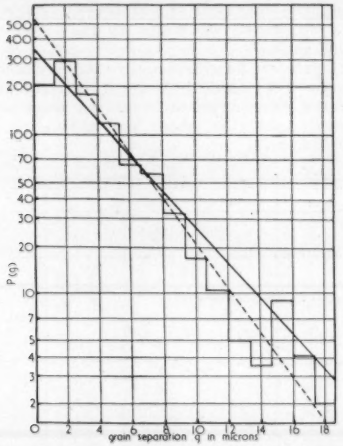

Fig. 3. Distribution of grain separations. The histogram shows the experimental results
——— $P'(g)dg = 1\,000\mu' \exp(-\mu' g)dg$.
- - - - - fitted for $g > 1{\cdot}33$ microns.

In order to investigate this further, the separations of one thousand consecutive grains along a track were measured. The distribution of g, where g is the grain separation measured from the centre of one grain to the centre of the next, is given in Fig. 3, and shows a marked deficiency of small grain separations, which agrees with the above loss hypothesis. If μ is the true grain density along the track, it may easily be shown that, if the distribution of grains follows Poisson's Law, then the distribution of g is given by

$$P(g)dg = \alpha\mu \exp(-\mu g)dg \qquad (1)$$

where α is the true number of grains, including those lost.

If the small separations lost are assumed to be all less than $1{\cdot}33$ microns, then μ can be estimated by fitting the experimental results for the 795 separations longer than this by the best curve of the above form. This was done by the method of least squares, and the best curve found to be

$$P(g)dg = 406 \exp(-0{\cdot}325g)dg \qquad (2)$$

The distribution

$$P'(g)dg = 1\,000\mu' \exp(-\mu' g)dg \quad (\mu' = 0{\cdot}259)$$

calculated from the observed grain density μ' is also shown for comparison in Fig. 3, and disagrees with the experimental results.

Comparing (1) and (2), we have $\mu = 0{\cdot}325$ $\alpha\mu = 406$. The latter relation, together with the expression

$$\int_{1{\cdot}33}^{\infty} \alpha\mu \exp(-\mu g)dg = 795$$

$$\text{i.e. } \alpha \exp(-1{\cdot}33\mu) = 795$$

can be used to find another value of μ, viz. $\mu = 0{\cdot}329$. A third estimate of μ can be made from the number of sections with no grains, which is independent of any loss mechanism. This gives $\exp(-13{\cdot}3\mu) = 0{\cdot}013$ whence $\mu = 0{\cdot}326$. These three values are in good agreement.

The problem of estimating the true grain density from the observed is similar to that of estimating the number of particles μ entering a counter of dead time a from the observed number of counts μ'. Blackman and Michiels* have examined the latter problem and have derived the relation

$$\text{Efficiency} = \frac{\mu'}{\mu} = \frac{1}{1+\mu a}$$

Applying this formula to the grain densities, we obtain $a \simeq 0{\cdot}8$ micron. It can be shown that, if the true grains have a Poisson distribution, then, neglecting certain second order effects, the observed grain density distribution is given by

$$P(N) = \sum_{y=N}^{\infty} \frac{(\mu d)^y \exp(-\mu d)}{y(y-N)!(N-1)!} \times$$
$$\left[1 - \exp(-ya/d)\right]^{y-N}\left[\exp(-ya/d)\right]^{N-1} \text{ for } N > 0$$
$$= \exp(-\mu d) \quad \text{for } N = 0$$

where y is the true number of grains in a section, and d is the section length.

Using the values $\mu = 0{\cdot}325$ and $a = 0{\cdot}8$, this distribution was calculated and is shown in Fig. 1. It is more peaked than the observed curve. This is quite consistent, owing to a small systematic change in grain density along the track, which causes a broadening of the observed distribution. The excess of the experimental distribution over the calculated for large values of N is due to one blocked scale division being counted as three grains, whereas in fact this could have been produced by only two grains.

* Blackman, M., and Michiels, J. L. *Proc. Phys. Soc.*, **60**, p. 549 (1948).

It seems therefore that the hypothesis made can satisfactorily account for the observations. The assumption of a sharp cut-off is clearly only an approximation to the truth. In fact, the probability of observing a pair of grains as two distinct grains rises from zero at $g = 0$ to unity at $g \sim 1$. The value found for a, 0·8 micron, is rather larger than might be expected, being the same as the mean grain diameter. This may indicate the existence of some other effect, such as that suggested by Jauneau.

From this investigation into grain density fluctuations it is concluded that the distribution of the observed grains along the track of a charged particle does not follow Poisson's Law. This may be understood if the distribution of true grains does follow this law, but close pairs of grains are unresolved, causing the observed number of grains to be less than the true number. The standard deviation of a grain count was found to be about three-quarters of the square root of the number of grains counted. This effect is of importance if an accurate estimate of the grain count error, or of the true number of grains developed, is required.

ACKNOWLEDGMENT

I should like to express my thanks to Professor Sir George Thomson, Mr. S. Lattimore and Mr. R. Elston for many valuable discussions.

An experimental investigation of the diffusion of electrolytic hydrogen through metals

By H. R. HEATH, Ph.D., A.Inst.P., Battersea Polytechnic, London, S.W.11

[*Paper first received* 1 *June*, 1951, *and in final form* 5 *July*, 1951]

Experiments have been made to test whether hydrogen produced electrolytically on one side of a metal plate will diffuse through the plate. The Shakespear katharometer was used to detect and measure the diffused gas. The metals examined were iron, nickel, cobalt, copper, zinc, silver, palladium, platinum, and lead. Only in the case of iron and palladium was any diffusion observed. Measurements were made with iron showing how the amount of diffused gas varied with time, and how the rate of steady diffusion varied with the thickness of the plate. The variation of the rate of diffusion with the electrolysing current density was observed for plates of iron and palladium. The results agree well with those of other observers for large values of the current density, but show that a threshold value of current density does not exist and that for low values of current density the rate of diffusion is approximately proportional to it. The diffused gas appears to be in the ordinary molecular state. A simple theory which explains the general character of the experimental results is given.

It has long been known that hydrogen produced electrolytically or chemically at an iron surface is not all evolved from the surface, but some diffuses into the metal. Thus if an iron tube is immersed in sulphuric acid, some of the hydrogen produced passes through the iron and appears on the inside of the tube. Now while the problem of diffusion of ordinary hydrogen through many metals at high temperatures has received much careful attention from various experimenters, especially by Smithells and Ransley,[1] the problem of diffusion of electrolytic hydrogen seems to have been less extensively studied. In spite of the practical importance of this type of diffusion, no systematic survey seems to have been made, and hence an examination has been made by a series of simple experiments.

A valuable general summary of work dealing with the diffusion of gases through metals has been given by Smithells.[2]

EXPERIMENTAL

The apparatus (Fig. 1) consisted of a glass tube G which was used as an electrolytic cell, with a 1% solution of sulphuric acid as electrolyte, a platinum plate A as anode and the experimental plate C as cathode. The experimental plate C was fixed on the end of the glass tube by means of sealing wax, and was itself mounted on a brass cap B also by means of wax. The cap was fixed on to a Shakespear katharometer K,[3] a lead washer L making a gas-tight joint. Inlet and outlet

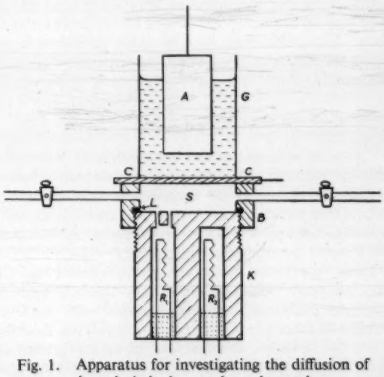

Fig. 1. Apparatus for investigating the diffusion of electrolytic hydrogen through metals

tubes with taps were fitted into the cap B so that any gas desired could be introduced into the space S which was in communication with the open cell R_1 of the katharometer by the diffusion holes in the copper block. Normally this space contained air and the katharometer circuit was balanced under these conditions, so that the zero reading of the bridge galvanometer corresponded with air in the open cell R_1. A light gas such as hydrogen has greater thermal conductivity than air so that if any hydrogen appears in the space S, it will diffuse into the open cell of the katharometer, increase the heat conduction from the spiral, and so lower its temperature and resistance. The spiral in the closed cell R_2 is not affected by the gas in S and hence the bridge is thrown out of balance, producing a deflexion on the galvanometer. The circuit was calibrated for mixtures of hydrogen and air so that the concentration of hydrogen in air corresponding to any galvanometer reading was known.

On electrolysing the solution in G, hydrogen is produced at the upper surface of plate C and if any of this hydrogen diffuses through the plate and emerges into S, its presence will be detected. By means of the calibration curve, the increase in the concentration of hydrogen in the hydrogen-air mixture in S could be followed directly and the rate in cubic centimetres of gas at N.T.P. diffusing through unit area of plate could thus be calculated. The rapidity, simplicity, and accuracy of this method of gas analysis allows the diffusion process to be followed continuously so that initial effects may be observed and also very small rates of diffusion can be measured.

Experiments were made at room temperature only and with electrolysing current densities up to 0·22 A/cm^2 of the metal plate. The plates were carefully cleaned before testing by rubbing with fine emery paper, and washing in very dilute nitric acid and finally in distilled water. Low current densities only were used so that there was no appreciable warming of the solution or the plate. The small variations in room temperature produced no appreciable effect on the experimental results obtained.

RESULTS

Survey of different metals. Experiments were made with the apparatus described using plates of a number of different metals as the cathode C of the electrolytic cell. The procedure was to carry out electrolysis with a current density of 0·2 A/cm^2 for a period of one hour, and observe the bridge galvanometer.

These experiments confirmed previous results showing that hydrogen would diffuse readily through iron and steel and palladium, and these metals were used in a number of subsequent investigations which are described later. No diffusion was observed, however, through any of the other plates examined, details of which are given in the following table:

Metal	*Thickness*
aluminium	0·03 mm
nickel	0·05
cobalt	0·38
copper	0·03
zinc	0·08
silver	0·05
tin	0·05
platinum	0·06
lead	0·15

The iron used throughout was obtained from ordinary soft "tin-plate" by removal of the tin. Its typical carbon content would be 0·5%. It was in an annealed condition.

Charpy and Bonnerot[4] were also unable to detect any diffusion through copper, but indirect evidence that hydrogen may enter aluminium during the process of pickling has been obtained by Sutton and Taylor.[5] The accuracy of the gas analysis with the katharometer is sufficient to ensure that if any diffusion at all occurred in the case of the metals mentioned above, it must be less than 10^{-3} of the effect for iron and palladium. Thus it seems that iron and palladium have some special property at ordinary temperatures.

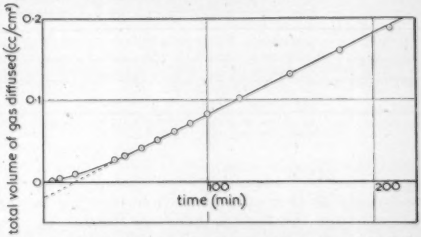

Fig. 2. Variation of total volume of hydrogen diffused through an iron plate with time

The graph shown in Fig. 2 gives the total volume of hydrogen which diffused through 1 sq cm of an iron plate of thickness 0·08 mm, using a current density of 0·0106 A/cm^2, plotted against time. The zero represents the instant when electrolysis was begun. The amount of hydrogen produced by electrolysis is $2{\cdot}5\times10^{-3}$ c.c./sec. which shows that the amount passing through the plate, when a steady state is reached, is about 1 part in 83 of the total amount produced. Hydrogen produced by chemical action also diffuses through iron. In these experiments, tests made with no electrolysing current showed this was negligible. In the initial period of about 40 min the rate of diffusion is increasing gradually to a final steady maximum after which the graph becomes accurately linear. Diffusion will not become steady until the plate itself has absorbed hydrogen to saturation value after which the amount leaving the plate is equal to the amount entering. The significance of the "foot" in this type of curve has been discussed by Barrer.[6]

Composite plates. As hydrogen will diffuse through iron and palladium but not through the other metals examined, it is of interest to examine the behaviour of a composite plate consisting of layers of either iron or palladium and of a metal which will not allow diffusion of hydrogen.

The composite plate most easily made is one consisting of a layer of iron tinned on one side, and such a plate of total thickness 0·2 mm was mounted as the cathode *C* in the apparatus shown in Fig. 1 with iron on the upper side and tin on the lower side. Electrolytic hydrogen was then produced on the upper side, and in order to be detected by the katharometer, it would have to diffuse through the layer of tin. No hydrogen diffused through into the space *S*.

A similar experiment was made with a plate having tin on the upper side and iron on the lower side, and another experiment with a plate consisting of a layer of tin between two layers of iron. In neither case was any diffusion of hydrogen observed, suggesting that hydrogen is incapable of penetrating the space lattices of metals other than iron and palladium at room temperature.

Variation of the rate of diffusion with thickness. For the diffusion of ordinary hydrogen through iron at high temperatures, the experiments of Lewkonja and Baukloh[7] have shown that the rate of diffusion is inversely proportional to the thickness of the plate. This is not necessarily true in the case of electrolytic hydrogen and no experimental evidence for it has been obtained, although the law is sometimes assumed in the calculation of diffusion rates so that results can be stated for a plate of standard thickness.

Accordingly, experiments were made on a piece of iron plate, observing the steady rate of diffusion with different thicknesses of metal, using a constant electrolysing current of density 0·222 A/cm². The same piece of plate was used throughout, beginning with a thickness of 1·6 mm. It was rolled down in convenient stages to a thickness of 0·2 mm, observing the steady rate of diffusion at each stage. Precautions were taken to get the metal into the same condition for each reading, as the rate of diffusion is known to depend on the condition of the metal and the surfaces. The plate was therefore always annealed by maintaining it at dull red heat for two minutes and cooling it slowly. The plate was afterwards cleaned with fine emery paper and washed by rubbing with cotton wool soaked in very dilute nitric acid. Nitric acid has the effect of etching the surfaces and thus to some extent increasing the surface area, but as this process was carried out for each determination, the surfaces would always be in about the same state. Plates of thickness less than 0·2 mm were not used owing to the increasing percentage error involved in the measurement of thickness and the variation over the plate.

The result of this experiment is shown in Fig. 3. The left-hand curve shows the variation with thickness and the right hand one the variation with the reciprocal of thickness, which would be a straight line through the origin if the rate of diffusion were inversely proportional to thickness. It has a linear character for thicknesses less than 0·7 mm, but the straight linear portion does not pass through the origin. If this linearity were maintained, no diffusion could occur through plates of thickness greater than about 0·9 mm, but a deviation

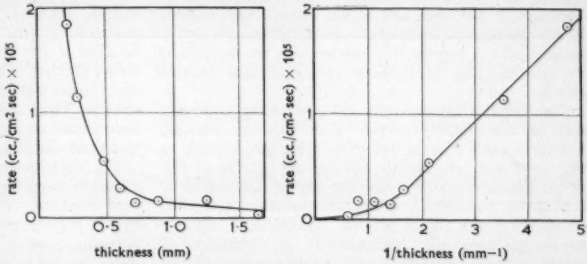

Fig. 3. Variation of the rate of diffusion with the thickness of an iron plate

from the straight line occurs so that there is a small rate of diffusion for greater thicknesses, but the rate of diffusion is relatively very small. It is not very surprising that the simple law of inverse proportionality is not followed in this case as the process cannot be regarded as one of simple diffusion. It involves not only diffusion inside the metal but surface processes on both sides of the plate, similar to those involved in diffusion at high temperatures.[8]

The experimental results of this work are given as observed rates in cubic centimetres of gas at N.T.P. per second for a plate of area 1 cm² the thickness being stated for each experimental plate, since the procedure of reducing observations to fit a plate of standard thickness assuming the law of inverse proportionality, is evidently not justifiable.

The nature of the diffused gas. Attempts have already been made to investigate the nature of the diffused gas. Hulubei[9] has reported that hydrogen ions are formed when hydrogen diffuses through heated palladium if an electric field is applied to the exit side. More recent experiments by Stansfield[10] have, however, shown that hydrogen which had diffused through palladium at high temperatures, carried no charge. In the present experiments it has been found in the case of electrolytic hydrogen, that passing an electric current of 1 A across the cathode plate at right angles to the direction of gas flow produced no effect on the rate of diffusion. The

gas when it leaves the plate might, however, consist, at least in part, of monatomic hydrogen.

Many tests have been made using nitrogen in the space S (Fig. 1) instead of air, and in all cases the observed rate of diffusion of hydrogen is the same as with air, showing that the presence of oxygen has no bearing on the results obtained. Two further experiments have been made to test for the presence of monatomic hydrogen, using the apparatus shown in Fig. 1.

In the first, the space S (Fig. 1) and the open cell of the katharometer were filled with cylinder hydrogen, the taps shut and the bridge rebalanced so that zero reading of the bridge galvanometer corresponded to hydrogen in the open cell of the katharometer. Now if any monatomic hydrogen emerges from the lower surface of the experimental plate (iron or palladium) its presence will be detected owing to one of two effects.

The thermal conductivity of monatomic hydrogen will be considerably greater than that of diatomic hydrogen and hence, if any monatomic gas appears in the space S it will rapidly diffuse into the open cell of the katharometer, increase the rate of conduction of heat from the spiral, reduce its resistance and thus throw the bridge out of balance, producing a deflexion on the galvanometer. Alternatively, recombination of atoms to form molecules in the neighbourhood of the spiral might produce a rise in its temperature and a corresponding rise in its resistance, thus producing a deflexion on the galvanometer in the opposite direction. Since the diffusion holes of the katharometer were very close to the underside of the plate and the diffusion of monatomic hydrogen would be very rapid, this method would probably have detected a very small proportion of monatomic hydrogen in ordinary hydrogen. No effect at all was observed.

The following experiment might also be a test as to whether the gas which has diffused through the metal is entirely in the ordinary molecular state. Two sheets of palladium (each 0·03 mm thick) were placed in contact and the edges sealed together with wax. For practically the whole of the area, therefore, the two sheets were separated by a very small air gap. This "double plate" was now arranged as the cathode C of the electrolytic cell (Fig. 1) and electrolytic hydrogen produced at the upper surface of the first plate. Diffusion undoubtedly occurred through the first plate, but no hydrogen could be detected in the space S, showing that hydrogen could not diffuse through the second sheet of palladium. This suggests that the hydrogen in the small space between the two sheets is in the ordinary molecular state.

These observations indicate that in these experiments the gas cannot escape from a metal surface except in the molecular state.

Variation of the rate of diffusion with the electrolysing current density. It was shown by Bodenstein[11] that the experimental results for R, the rate of diffusion of electrolytic hydrogen through iron, were well represented by an equation of the form

$$R = k\, I^{\frac{1}{2}}$$

where I is the electrolysing current density. Borelius and Lindblom[12] discovered, however, that a better representation was given by

$$R = k(I^{\frac{1}{2}} - I_t^{\frac{1}{2}})$$

where I_t is a temperature dependent threshold value of the electrolysing current density, i.e. no diffusion at all is possible until $I > I_t$. This representation was deduced from observations made with large values of the current density. Barrer[6] has also obtained a linear relation between R and $I^{\frac{1}{2}}$ for large values of I for palladium. His graphs indicate a departure from linearity at low values of I so that instead of a threshold value, the curves are bent round so as to pass through the origin, but no experimental evidence for this is shown. Thus it appears that no experimental test has been made of the existence of the threshold value by using sufficiently small currents.

The present method enables very low rates of diffusion to be observed very much more easily than any method used previously. The apparatus used is as shown in Fig. 1, the electrolysing current being measured by an ammeter in series. The high sensitivity of the katharometer to the presence of hydrogen in air or nitrogen combined with the use of thin metal plates, enabled measurements of diffusion to be made with electrolysing currents of a much lower order of magnitude than had hitherto been attempted.

Experiments were made on palladium, iron, and mild steel, observing the rate of diffusion and the current density. A sufficient time for the rate of diffusion to become quite steady was allowed before each reading. In Fig. 4 is shown the steady rate of diffusion plotted

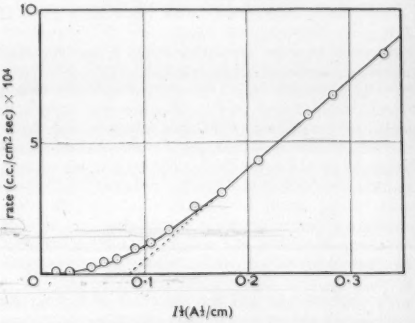

Fig. 4. Variation of the rate of diffusion through palladium (specimen 1) with the square root of the electrolysing current density

against $I^{\frac{1}{2}}$ for a palladium plate (specimen 1) of thickness 0·030 mm. For values of $I^{\frac{1}{2}} > 0{\cdot}18$ A$^{\frac{1}{2}}$/cm, the curve conforms well to the law suggested by Borelius and Lindblom, corresponding to a value of $I_i^{\frac{1}{2}} = 0{\cdot}085$, as shown by the dotted line. The real curve shows that a threshold value does not exist, and diffusion of hydrogen was observed using a current density of less than 0·001 A/cm^2. The shape of the lower part of the curve shown in Fig. 4 suggests that for very small currents, the rate of diffusion will depend on some higher power of I. Fig. 5 shows the first 9 points on a graph of R against I and indicates that the rate of diffusion is approximately proportional to current density at sufficiently low values.

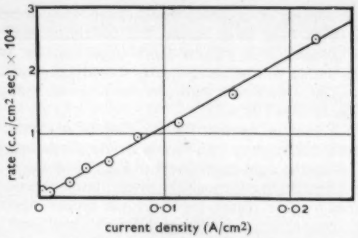

Fig. 5. Variation of the rate of diffusion through palladium (specimen 1) with electrolysing current density, for small current densities

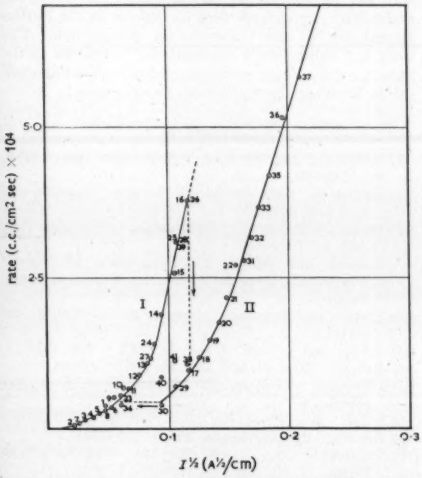

Fig. 6. Variation of the rate of diffusion through palladium (specimen 2) with the square root of the electrolysing current density

A more detailed investigation was subsequently made on a second sheet of palladium (specimen 2) of thickness 0·025 mm. The results are shown in Fig. 6 as a graph of R against $I^{\frac{1}{2}}$ for the purpose of comparison with Fig. 4. The points are numbered to show the order in which they were observed and no measurement was made until R was quite steady. The curve consists of two parts. Low points lie on curve I, high points on curve II. Over a small range of values in between, points have been obtained which seem to lie on either curve. Barrer[6] has shown that diffusion of hydrogen through palladium depends to a marked extent on the surface condition of the plate, and the two curves I and II may be associated with different conditions of the surface.

The rate of diffusion at low values of I is again approximately proportional to I, but a logarithmic plot indicates that

$$R = kI^{4/3}$$

gives a better fit with experimental results in this case.

Iron and mild steel plates have also been examined in similar tests. Fig. 7 shows a graph of R against $I^{\frac{1}{2}}$ for an annealed mild steel plate of thickness 0·20 mm. This

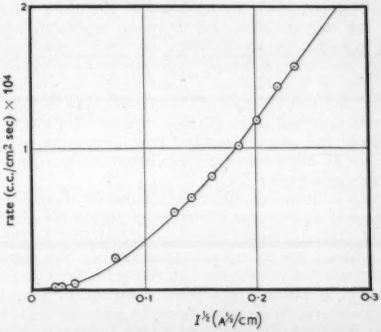

Fig. 7. Variation of the rate of diffusion through mild steel with the square root of the electrolysing current density

plate was one supplied by the Steel Company of South Wales who gave the following composition:—

carbon	0·05%
sulphur	0·03
phosphorus	0·015
manganese	0·30
nickel	0·07
copper	0·10
tin	0·01
remainder iron	

The linear relationship at high values of the current density and the departure from it at low values are again evident.

Since the amount of gas produced at the surface of any experimental cathode will be directly proportional to the current density, there is a close analogy between this case and the case of diffusion of ordinary hydrogen through metals at high temperatures, gas pressure in the latter case corresponding to current density in the former. The law

$$R = kp^{\frac{1}{2}}$$

was first proposed. Then the idea of a threshold pressure was put forward in the equation

$$R = k(p^{\frac{1}{2}} - p_i^{\frac{1}{2}})$$

Finally Smithells and Ransley[1] have shown that a threshold does not exist, the departure from the square root law being similar to that now observed in the case of electrolytic hydrogen.

DISCUSSION

Wang[8] has explained the diffusion of diatomic gases through metals at high temperatures assuming certain surface processes. The same general argument is now applied to the case of electrolytic hydrogen.

The processes which are assumed to take place are: (1) hydrogen atoms are produced on the upper surface of the cathode plate and form an adsorbed layer; (2) from this layer some atoms are able to combine in pairs and form molecular hydrogen which escapes as bubbles in the electrolyte; other atoms pass into the metal and pass through to the opposite side to form a second adsorbed layer; (3) the combination of atoms in pairs in this second adsorbed layer allows the gas to escape as molecular hydrogen which appears in the katharometer cell.

With a current density I the number of atoms being deposited on unit area of the upper surface per second is AI. When a steady state has been reached let there be n_1 atoms per cm^2 on the upper surface. The chance of a single atom combining with another to form a molecule will be directly proportional to the concentration of other atoms in the neighbourhood, i.e. proportional to n_1. Thus the number of atoms which escape from 1 cm^2 of surface in unit time is proportional to n_1^2, say equal to Bn_1^2. The number which diffuse into the metal is

$$n = AI - Bn_1^2$$

The flow into the metal may also be written as the difference between the number passing from the adsorbed layer into the metal and the number returning from just inside the metal to the adsorbed layer. If ν_1 represents the concentration just inside the metal

$$n = Cn_1 - D\nu_1$$

It is assumed that the diffusion of gas atoms inside the metal will take the form

$$n = \frac{E}{x}(\nu_1 - \nu_2)$$

where x is the thickness of the metal and ν_2 the concentration of gas atoms just inside the lower surface.

The net flow from the metal to the lower adsorbed layer will be

$$n = D\nu_2 - Cn_2$$

and finally the rate of escape of atoms from the layer into the katharometer cell will be

$$n = Bn_2^2$$

Eliminating $n_1\, n_2\, \nu_1\, \nu_2$ from these equations gives

$$n^2\left(\frac{Dx}{E} + 2\right)^2 + n^{3/2}\frac{2C}{\sqrt{B}}\left(\frac{Dx}{E} + 2\right) + n\frac{2C^2}{B} = \frac{C^2A}{B}I$$

For a plate of constant thickness n^2 will be nearly linear with I for large values, but the terms involving lower powers of n will be more important for small values and n will be more nearly directly proportional to I. This agrees well with the experimental results in Figs. 4, 5, 6, and 7.

For a constant current the variation of n with x will evidently not be given by a simple inverse proportionality law. Thus the right-hand graph of Fig. 3 is not expected to be a straight line through the origin; but it approaches linearity for thin plates, for which the process approximates more closely to ordinary diffusion conditions.

ACKNOWLEDGMENT

The problem was suggested to me by Dr. T. L. Ibbs who has throughout shown an interest in the work; preliminary experiments were carried out in the Physics Department of the University of Birmingham. The work was subsequently extended and developed at the Battersea Polytechnic and I am indebted to the Principal, Dr. R. W. West, for the facilities he has granted.

REFERENCES

(1) Smithells and Ransley. *Proc. Roy. Soc.*, **A150**, p. 172 (1935).
(2) Smithells. *Gases and Metals* (London: Chapman and Hall Ltd., 1937).
(3) Daynes, with a note by Shakespear. *Proc. Roy. Soc.* **A97**, p. 273 (1920).
Daynes, *Gas Analysis by Measurement of Thermal Conductivity* (London: Cambridge University Press, 1933).
(4) Charpy and Bonnerot. *Comptes Rendus*, **154**, p. 592 (1912).
(5) Sutton and Taylor. *J. Inst. Met.*, **55**, p. 149 (1934).
(6) Barrer. *Trans. Faraday Soc.*, **36**, p. 1235 (1940).
(7) Lewkonja and Baukloh. *Z. Metallk.*, **25**, p. 309 (1933).
(8) Wang. *Proc. Camb. Phil. Soc.*, 1936, **32**, p. 657 (1936).
(9) Hulubei. *Comptes Rendus*, **199**, p. 199 (1934).
(10) Stansfield. *Proc. Camb. Phil. Soc.*, 1938, **34**, p. 120 (1938).
(11) Bodenstein. *Z. Electrochem.*, **28**, p. 517 (1922).
(12) Borelius and Lindblom. *Ann. Physik Lpz.*, **82**, p. 201 (1927).

Compilation of the propagation constants of an inhomogeneously-filled waveguide

By Ll. G. Chambers, M.Sc., A.Inst.P., Royal Naval Scientific Service

[*Paper received* 8 *August*, 1951]

Use is made of the Rayleigh-Ritz method of finding frequencies of vibration of a mechanical system, for finding the propagation constants of an inhomogeneously-filled waveguide.

INTRODUCTION

The use of the Rayleigh–Ritz method to determine the "eigenfrequencies" of mechanical systems is well known. This method can also be used to determine the propagation or attenuation constants of the various modes existing in an inhomogeneously filled waveguide. It is thought that this application of the method is new and it will be illustrated by a simple example. First of all, however, it is necessary to consider certain general properties of a conservative system with a finite number of degrees of freedom.

Suppose that the generalized co-ordinates are q_r. The kinetic energy is of the form

$$T = \tfrac{1}{2}\Sigma\Sigma A_{rs}\dot{q}_r\dot{q}_s$$

and the potential energy of the form

$$V = \tfrac{1}{2}\Sigma\Sigma B_{rs}q_rq_s$$

Suppose now that we write

$$q_r = c_r \cos(\omega t + \epsilon_r),$$

ω being one of the "eigenfrequencies" of the system.

The equation of conservation of energy gives us that $T + V = K$, i.e.

$$\Sigma\Sigma\begin{bmatrix} A_{rs}\omega^2c_rc_s \sin(\omega t + \epsilon_r)\sin(\omega t + \epsilon_s) \\ + B_{rs}c_rc_s \cos(\omega t + \epsilon_r)\cos(\omega t + \epsilon_s) \end{bmatrix} = 2K$$

Now, $\sin(\omega t + \epsilon_r)\sin(\omega t + \epsilon_s)$
$= \cos(\epsilon_r - \epsilon_s) - \cos(\omega t + \epsilon_r)\cos(\omega t + \epsilon_s)$

Hence, the energy equation assumes the form

$$\Sigma\Sigma\begin{bmatrix} c_rc_sA_{rs}\omega^2\cos(\epsilon_r - \epsilon_s) + c_rc_s \\ (B_{rs} - \omega^2A_{rs})\cos(\omega t + \epsilon_r)\cos(\omega t + \epsilon_s) \end{bmatrix} = 2K$$

Now K is independent of t, and so is the first term on the left-hand side.

It follows that

$$\Sigma\Sigma c_rc_s(B_{rs} - \omega^2A_{rs}) = 0$$

Now supposing that it is required to find the eigenfrequencies, we proceed as follows: The Lagrangian function is $L = T - V$, and the equations of motion are given by

$$\frac{d}{dt}\left(\frac{\partial L}{\partial \dot{q}_r}\right) - \frac{\partial L}{\partial q_r} = 0$$

or

$$\sum_s(A_{rs}\ddot{q}_s + B_{rs}q_s) = 0$$

And if we put $q_s = c_s\cos(\omega t + \epsilon_s)$. This set of equations becomes

$$\sum_s(B_{rs} - \omega^2A_{rs})q_s = 0$$

and so ω must satisfy

$$|B_{rs} - \omega^2A_{rs}| = 0$$

Thus, the "eigenvalues" ϕ of the equation

$$\sum_r\sum_s(B_{rs} - \phi A_{rs})c_rc_s = 0$$

are given by the determinantal equation for ϕ

$$|B_{rs} - \phi A_{rs}| = 0$$

There are, in fact, as many "eigenvalues" as there are degrees of freedom (excluding degenerate cases, when two of the roots may coalesce).

If the eigenvalues ϕ are negative, there is an exponential decay instead of a free vibration. (This will not occur in a physically realizable system, because T and V are both positive definite forms.)

"LEAST SQUARES" APPROXIMATION

Suppose that we have a complete orthogonal set of functions

$$\psi_0, \psi_1, \ldots, \psi_r, \ldots$$

Then, over R, the range over which the complete orthogonal property holds, we may write any reasonable function $F(x)$ in the form*

$$F(x) = \sum_{r=0}^{\infty} f_r\psi_r(x), \quad f_r = \int_R F(x)\psi_r(x)g(x)dx$$

In the "least squares" sense, the best approximation to $F(x)$, using only $\psi_0, \ldots, \psi_n$, is given by[1]

$$F_n(x) = \sum_{r=0}^{n} f_r\psi_r(x)$$

Now quantities which do not depend in detail on $F(x)$ are approximated to by taking $F_n(x)$ instead of $F(x)$. It is by utilizing this concept that the Rayleigh–Ritz

* It has been assumed here that we have a complete normalized orthogonal set with weighting function $g(x)$, such that

$$\int_R \psi_r(x)\psi_s(x)g(x)dx = \delta_{rs}$$

where

$$\delta_{rs} = 1, r = s,$$
$$= 0, r \neq s$$

method has been applied with success to find the eigenfrequencies of various structures.[2] It is clear that, if the $f_r(x)$ separately satisfy any boundary conditions which may be imposed on $f(x)$, even though they do not satisfy the differential equations governing the system, it will be helpful, and the approximation will more nearly represent the nature of the generating function.

It may also be remarked that similar considerations apply to more than one dimension, e.g. for 3 dimensions one writes

$$f(x, y, z) = \sum_r f_r\psi_r(x, y, z)$$

where the ψ_r are taken in some suitable order.

INHOMOGENEOUSLY-FILLED WAVEGUIDES

Suppose we have a waveguide, which is filled partially with some (non-lossy) dielectric, the cross-section being uniform. Following on the remarks in the last section, we approximate to the field distribution in any mode, by a partial sum of the various modes which would exist were the waveguide homogeneously filled. These possess the advantage pointed out above of satisfying the boundary conditions on the walls of the waveguide. We proceed as follows:—

Any component of a wave being propagated down a waveguide can be written in the form

$$\chi = \chi_0 \exp\left[-i(\omega t - hz)\right]$$

where χ_0 is a real quantity which gives the field distribution across the waveguide.

We may write in general, for a field of the form

$$\vec{H} = \vec{H}_0 \exp(-i\omega t),\ \vec{E} = \vec{E}_0 \exp(-i\omega t)$$

$$\vec{\nabla} \cdot \vec{S^*} = -\tfrac{1}{2}\sigma|\vec{E}|^2 + i\omega\tfrac{1}{2}(\mu|\vec{H}|^2 - \epsilon|\vec{E}|^2)$$

where $\vec{S^*}$ is the complex Poynting vector[3] (p. 137). Now consider the quantity

$$\int_{z_0,\,c}^{z_0+2\pi/h} \vec{\nabla} \cdot \vec{S^*} d\tau = \int \vec{S^*} \cdot d\vec{A}$$

where c is the cross-section of the waveguide and h is the propagation constant, z_0 being arbitrary and A being the surface area bounding the volume considered.

Now this quantity is zero because $\vec{S^*}$ vanishes on the walls of the waveguide, and $\vec{S^*}$ is periodic along the waveguide. Also σ is zero, because we are assuming non-lossy dielectrics and so we have

$$\int_{z_0,\,c}^{z_0+2\pi/h} (\mu|\vec{H}|^2 - \epsilon|\vec{E}|^2) d\tau = 0$$

Now in order to explain the method, it will be convenient to consider *T–M* modes. It will be seen that the method applies equally well to other kinds of modes. For *T–M* fields the various field components may be defined in terms of an electric polarization potential Π as indicated on page 350 of reference (3).

$$E_1 = \frac{1}{h_1}\frac{\partial^2\Pi}{\partial z \partial u_1},\ E_2 = \frac{1}{h_2}\frac{\partial^2\Pi}{\partial z \partial u_2}$$

$$E_z = -\frac{1}{h_1 h_2}\left[\frac{\partial}{\partial u_1}\left(\frac{h_2}{h_1}\frac{\partial\Pi}{\partial u_1}\right) + \frac{\partial}{\partial u_2}\left(\frac{h_1}{h_2}\frac{\partial\Pi}{\partial u_2}\right)\right]$$

$$H_1 = \epsilon\frac{1}{h_2}\frac{\partial^2\Pi}{\partial t \partial u_2},\ H_2 = -\epsilon\frac{1}{h_1}\frac{\partial^2\Pi}{\partial t \partial u_1},\ H_z = 0$$

where the element of length is given by

$$ds^2 = h_1^2 du_1^2 + h_2^2 du_2^2 + dz^2$$

Now Π and all the field components are of the form

$$\chi = \chi_0 \exp\left[-i(\omega t - hz)\right]$$

We drop the exponential factor and Π satisfies

$$\frac{1}{h_1 h_2}\left[\frac{\partial}{\partial u_1}\left(\frac{h_2}{h_1}\frac{\partial\Pi}{\partial u_1}\right) + \frac{\partial}{\partial u_2}\left(\frac{h_1}{h_2}\frac{\partial\Pi}{\partial u_2}\right)\right] + (k^2 - h^2)\Pi = 0$$

We approximate to

$$\Pi(u_1, u_2) \text{ by } \Pi_N(u_1, u_2) = \sum_{r=0}^{N} \pi_r\gamma_r(u_1, u_2)$$

where the $\gamma_r(u_1, u_2)$ are the modes which would exist were the waveguide homogeneously filled. As pointed out previously Π_N will not satisfy the differential equation of Π, but the field derived from it by the processes indicated approximates the true fields. It is clear that the energy equation gives rise to an equation of the form

$$\sum_{r=0}^{N}\sum_{s=0}^{N}(A_{rs} + B_{rs}h^2 + C_{rs}\omega^2)\pi_r\pi_s = 0$$

Now this gives rise, in the manner indicated previously to a determinantal equation

$$|A_{rs} + B_{rs}h^2 + C_{rs}\omega^2| = 0$$

which gives the various approximate value of ω^2 for a given h^2. Alternatively, we may consider this determinantal equation to determine the values of h^2 in terms of ω^2. In this case, negative values of h^2 must be admitted. Positive values of h^2 correspond to a propagated mode, and negative values correspond to an evanescent mode. (We note that the value of h^2 does not depend in detail upon the field configuration and so it is possible to get a satisfactory result with very few terms in the expansion.)

DISCUSSION

The example discussed briefly in the appendix indicates the amount of approximation necessary to get a reasonable result. The particular problem concerned has an exact solution, but the utility of the solution lies in cases where an exact solution is impossible, and can be used for a waveguide of arbitrary cross-section with an

arbitrary amount of dielectric filling, provided that the relevant field distributions are known for the waveguide when empty. It will be noticed that it has been assumed that the dielectric has been assumed loss free. This has been done for simplicity, as lossy dielectrics can be accounted for by replacing ϵ by $(\epsilon + \sigma/i\omega)$. This will mean that h^2 will be complex, as might be expected, involving an attenuation of all the modes in the guide. It may also be remarked that the method still holds when μ is variable, although this case is unlikely to occur in present practice.

The numerical solution of the determinantal equation when $N > 3$ creates certain difficulties, but because the quantities that we are concerned with do not depend in detail on the shape of the field, this difficulty is not critical as it is not often necessary to proceed beyond $N = 3$. The error involved in stopping short at finite N is given for an example in the appendix.

Furthermore, the properties of the dielectric are not usually repeatable, and so a result for λ/λ_g which is accurate to within 2% is good enough, any further accuracy not being physically meaningful.

It may be remarked that a similar method could be used for the sonic case, if one had a sound wave propagated down a pipe filled with materials with different elastic properties.

ACKNOWLEDGMENT

This paper is published with the approval of the Lords Commissioners of the Admiralty, but the responsibility for any statements of fact or opinions expressed rests solely with the author.

REFERENCES

(1) SOMMERFIELD, A. *Partial Differential Equations of Mathematical Physics* (New York: Academic Press Inc.).

(2) ROLLO, W. T., and CHAMBERS, LL. G. *Phil. Mag. Ser.* 7, **38**, p. 609 (1947).

(3) STRATTON, J. A. *Electromagnetic Theory* (New York: McGraw-Hill Book Co., Inc.).

(4) MONTGOMERY, DICKE and PURCELL. *Principles of Microwave Circuits* (New York: McGraw-Hill Book Co., Inc.).

APPENDIX

We will consider, as an example, a problem which can be solved exactly, that of a waveguide $0 < y < a$, filled with dielectric (ϵ) in $0 < y < c = a/2$, and with dielectric ϵ_0 in $c < y < a$. We have, dropping the "exp $[-i(\omega t - hz)]$" factor

$$E_x = \sum_{n=1}^{\infty} A_n \sin(n\pi y/a), \quad E_y = E_z = 0$$

$$H_x = 0$$

$$H_y = -\frac{ih}{i\omega_n} \sum_{1}^{\infty} A_n \sin(n\pi y/a)$$

$$H_z = -\frac{1}{i\omega_n} \sum_{1}^{\infty} A_n (n\pi/a) \cos(n\pi y/a)$$

(In this particular case it is not necessary to use Π). On substituting in the energy equation

$$\int_{z_0,\,c}^{z_0+2\pi/h} (\mu|\vec{H}|^2 - \epsilon|\vec{E}|^2)d\tau = 0$$

we obtain

$$\sum_{r=1}^{N}\sum_{s=1}^{N} A_r A_s \left[\delta_{rs}\left(\frac{h^2a^2}{\pi^2} + rs\right) - \frac{k_0^2 a^2}{\pi^2} X_{rs}\right] = 0$$

$$X_{rs} = [\epsilon/\epsilon_0 + (-1)^{r+s}]\left[\frac{\sin(r-s)\pi/2}{(r-s)\pi} - \frac{\sin(r+s)\pi/2}{(r+s)\pi}\right]$$

We note that the $\sin(n\pi y/a)$ are the modes for a homogeneously-filled waveguide.

We will assume that $\lambda = a$. For the waveguide without any dielectric this is such that $\lambda_g = 2\lambda/\sqrt{3}$ for the first mode and the second mode is just evanescent.

We also take $\epsilon/\epsilon_0 = 2{\cdot}45$.

It is found that using the partial approximations

$$E_{xN} = \sum_{n=1}^{N} A_n \sin(n\pi y/a)$$

the successive values of λ/λ_g are

N	λ/λ_g	
1	1·2145	4 decimal places having been used throughout.
2	1·3497	
3	1·3546	

Now this problem can be solved exactly by the method indicated in[4] (p. 387), and yields the result

$$\lambda/\lambda_g = 1{\cdot}3585$$

(The value of dielectric constant used is merely that which has been used for the calculations of Fig. 11.11 of [4], and does not have any particular significance.)

The error in λ/λ_g for the various approximations is as follows:

N	1	2	3
% error	10·6	0·7	0·3

Numerical ray-tracing in electron lenses

By J. C. BURFOOT, M.A., A.Inst.P., Cavendish Laboratory, Cambridge

[*Paper first received* 24 *May*, 1951, *and in final form* 6 *July*, 1951]

For the solution of the paraxial ray equation, a very simple step-by-step method is given, using a procedure due to Fox and Goodwin for equations of the type $d^2y/dx^2 = f(x)y$. The accuracy of the method can be increased to any desired extent without increasing the complexity. All sources of inaccuracy except those present in the given field data can thus be avoided, and the aberration integrals can be accurately evaluated. If required, an approximate solution may be obtained initially, which is easily modified later for better accuracy, without redundancy of the early work. Graded intervals are easily introduced. A worked example is given for a strong electrostatic lens.

In the course of an investigation which required accurate numerical ray-tracing through an electron lens (in which the potential distribution was known) a method has been developed for the step-by-step integration of the ray equations, which does not seem to have been used before.

The accuracy of ray-tracing is limited initially by the accuracy of the potential distribution data, but if we suppose this limitation to be removed or unimportant, the limit is set by the numerical methods used for the ray-tracing. High accuracy in the computation of trajectories will be required if one is interested in the aberrations occurring in the image plane, and speed will be required if a number of determinations is to be made; for example, for different positions of the object plane, different object points within that plane, and different initial directions of the track. Speed usually implies simplicity, and unfortunately the requirements of accuracy and simplicity in numerical methods are to a certain extent mutually exclusive.

Aberrations may be evaluated by integration of the general ray equations[1–4] and comparison of several rays. Alternatively, in systems of rotational symmetry, one may integrate the "paraxial ray equation"[5–11] and substitute the results in certain well-known aberration integrals.[12, 13] The former class is wider in application, but inevitably less simple. It must be used if one is interested in aberrations of fifth order and beyond. In either class, the integration of the ray equation is carried out in steps through the lens, using, for example, a Taylor series in the path co-ordinate, or some similar procedure. Methods may be characterized by the nature of this process, some using only a few terms of the series, or a few finite differences. Some methods can be extended to make use of more terms in order to increase accuracy, usually with a corresponding increase in complexity. There seems to be room for fast methods in which the accuracy of this integration process may be increased as far as desired without any loss of simplicity. One can then arrange that only the field data influence the accuracy of the ray-tracing.

THE RAY-TRACING METHOD

The paraxial ray equation for the motion of the electrons is

$$r''\Phi + \tfrac{1}{2}r'\Phi' + \tfrac{1}{4}r\left(\Phi'' + \frac{eH^2}{2mc^2}\right) = 0 \qquad (1)$$

where
- the z axis is the axis of rotational symmetry;
- $r(z)$ is the off-axis distance of a track;
- $\Phi(z)$, $H(z)$ are the electrostatic potential and the magnetic field on the axis, in terms of which the whole distribution may be described;
- and primes denote differentiation with respect to z.

If we use the variable introduced by Picht,[14] $R \equiv r\Phi^{\frac{1}{4}}$, equation (1) becomes

$$R'' = -TR \qquad (2)$$

where

$$T \equiv \frac{3}{16}\left(\frac{\Phi'}{\Phi}\right)^2 + \frac{eH^2}{8mc^2\Phi} \qquad (3)$$

Apart from its simpler form, this offers the advantages that the curvature of R is everywhere less than that of r, so that the path integration can be restricted to a smaller range (see example appended), and that calculation of Φ'' from Φ is no longer necessary. Errors in Φ affect Φ'' much more than they do Φ', and have very little effect on $\Phi^{\frac{1}{4}}$.

Fox and Goodwin[15] have given a method for the numerical solution of equations of the type

$$y'' = fy \qquad (4)$$

where f is any function of the independent variable x. They show that equation (4) may be represented in terms of central differences by the three-point recurrence formula

$$(1 - \tfrac{1}{12}h^2f_1)y_1 = (2 + \tfrac{5}{6}h^2f_0)y_0 - (1 - \tfrac{1}{12}h^2f_{-1})y_{-1} + \Delta \qquad (5)$$

where

$$\Delta = -\tfrac{1}{240}\delta^6 + \tfrac{13}{15120}\delta^8 - \tfrac{17}{1008000}\delta^{10} + \tfrac{1}{297000}\delta^{12} - \ldots \qquad (6)$$

In this equation h is the tabulation interval, the subscripts -1, 0, 1, indicate any three successive points, and δ^s is the sth central difference at the point indicated by 0. Neglecting Δ and with the two y-values at the beginning of the z range as "boundary conditions," they solve the equation step-by-step throughout the range of x. They calculate Δ from these approximate results and repeat the process, using this value of Δ in the equation, continuing until two runs provide the same solution, to the accuracy required. They point out that the use of such

finite difference equations is not new, but that the idea of carrying out a complete run at each degree of approximation has advantages over the more usual method of satisfying the complete expression (5) at each step. Thus it is not necessary to guess differences and adjust them retrospectively, as in some methods. Also higher differences are not needed in the early stages, and may be calculated later if increased accuracy is required. In this case, no part of the previous work becomes redundant. For a similar reason, the retention of guard figures does not imply an appreciable increase in the work.

Applying equation (5) to equation (2), we have

$$a_1 R_1 = b_0 R_0 - a_{-1} R_{-1} + \Delta \qquad (7)$$

where
$$\left.\begin{aligned} a &= 1 + \left[\frac{1}{64}\left(\frac{\Phi'}{\Phi}\right)^2 + \frac{eH^2}{96mc^2\Phi}\right]h^2 \\ b &= 2 - \left[\frac{1}{64}\left(\frac{\Phi'}{\Phi}\right)^2 + \frac{eH^2}{96mc^2\Phi}\right]10h^2 \end{aligned}\right\} \qquad (8)$$

a and b may be tabulated at once for the lens, and used for all rays which are to be traced. It will be seen that Δ is small, its leading term being in δ^6, so that the convergence is good. (The writer has never found more than two runs necessary in his applications of the method.) It has the advantage, in common with similar iterative processes, such as Relaxation, that both accidental errors and accumulated inaccuracies are automatically detected and rectified at the next run.

ILLUSTRATION

A simple example is appended to illustrate the simplicity of the method. Φ is taken from an expression of Regenstreif[16] for the potential distribution in a three-aperture unipotential lens similar to one studied by Bruck and Romani.[17] Regenstreif's expression has been differentiated to give Φ'. If we take $h = 1$, we have

$$\left.\begin{aligned} a &= 1 + \frac{1}{64}\left(\frac{\Phi'}{\Phi}\right)^2 \\ b &= 2 - \frac{10}{64}\left(\frac{\Phi'}{\Phi}\right)^2 \end{aligned}\right\} \qquad (9)$$

For the purpose of illustration, it has been assumed that the dimensions of the diaphragms are known to an order higher than quoted (e.g. $d_0 + e = 12{\cdot}690$ units). This is equivalent to knowing Φ to five figures. Then a and b are known to eight figures over important portions of the lens, and up to fifteen figures at other parts. The runs have been worked to eight figures, and quoted to six, as a guard against building-up errors, though this is pessimistic at the beginning of the trace. With an ordinary electric desk-calculating-machine, several runs will be made in an hour. Unless a National accounting machine is available, the differencing will take longer, and it may be quicker to use the expression $\delta^6 = -20y_0 + 15(y_{-1} + y_1) - 6(y_{-2} + y_2) + (y_{-3} + y_3)$. The corresponding coefficients for δ^8, δ^{10}, δ^{12}, if required, are

+ 70	− 56	+ 28	− 8	+ 1		
− 252	+ 210	− 120	+ 45	− 10	+ 1	
+ 924	− 792	+ 495	− 220	+ 66	− 12	+ 1

The ray traced leaves the axis at the object at $z = -20$. Choice of the second initial value, at $z = -19$, is arbitrary, since multiples of this simple solution are also solutions. It has here been chosen to make r' unity at $z = -20$, so that the results could be directly used in the aberration formulae. Equation (7) gives R at $z = -18$ from these two values, and so on throughout the lens. With the addition of the other trace which is necessary, it was found that the spherical aberration constant could be calculated to a probable five figures, certainly reliable to four. In some cases, substitution of the paraxial approximation in the integrals may further limit this accuracy, but this limit may be removed if so required by using the expressions for the general plane, adding the aberrations to r as a correction, and repeating the process. For a strong lens such as this, relativistic correction would be necessary[10] at voltages normally used in electron microscopy. Furthermore, Φ will not often be known to five figures, but the illustration shows that a, b, which represent the field data in the computations, have much greater accuracy.

In the example, h has been chosen so that only the first two terms of Δ are required to keep the error less than the last digit quoted; thus its calculation is not arduous. In cases where high accuracy is not required, the rapid convergence of the method means that fewer steps need be used. It should be noticed that Δ corresponds to the position indicated by the suffix 0. The table shows that the Δ arising from the second run $R(2)$, is the same as that from $R(1)$, so that $R(3)$ would present no further change. r is therefore obtained from $R(2)$. R has a constant slope beyond $z = 18$, and crosses the axis again at $z = 2\,290$. Constant slope for r occurs much later. It will be seen that $R(2)$ does not differ from $R(1)$ by more than $0{\cdot}005\%$ even at $z = 19$. Thus where only approximate paraxial solutions are required, it will often be possible, even with a larger h, to stop at $R(1)$, omitting Δ entirely.

In other methods, the work has sometimes been repeated with h halved in order to estimate the errors due to the neglected terms.[18, 19] This is not necessary here, since we do not neglect any terms which affect significant digits. The choice of h is made such that the differences converge reasonably quickly. If more figures are required, a smaller h will be used. The differences in Δ are of such high order that the disappearance of its terms into the region of insignificance is extremely sensitive to this decrease of h. Graded intervals will frequently be desirable, and are very easily handled in this method. In the example given, r'' increases to more than $0{\cdot}1$ in the central region, so that a finer interval

z	Φ	a	b	$R(1)$	$\Delta.10^4$	$R(2)$	$\Delta.10^4$	r
− 20	99·105929	1·0000000	2·0000000	0				0
− 19	99·086041	1·0000000	2·0000000	3·15519				1·00005
− 18	99·036834	1·0000000	1·9999999	6·31038				2·00035
− 17	98·930018	1·0000000	1·9999996	9·46557				3·00134
− 16	98·704160	1·0000002	1·9999983	12·6208				4·00407
− 15	98·218092	1·0000008	1·9999920	15·7759				5·01125
− 14	97·146992	1·0000040	1·9999604	18·9308				6·02993
− 13	94·871581	1·0000169	1·9998307	22·0846				7·07630
− 12	90·793267	1·0000473	1·9995271	25·2334				8·17454
− 11	85·096856	1·0000846	1·9991535	28·3675				9·33992
− 10	78·498869	1·0001188	1·9988120	31·4727				10·5735
− 9	71·531956	1·0001516	1·9984839	34·5328				11·8743
− 8	64·469610	1·0001871	1·9981291	37·5298				13·2446
− 7	57·463788	1·0002278	1·9977223	40·4422				14·6888
− 6	50·632842	1·0002738	1·9972620	43·2435				16·2111
− 5	44·107973	1·0003206	1·9967938	45·9026				17·8118
− 4	38·065515	1·0003535	1·9964651	48·3855				19·4797
− 3	32·754549	1·0003412	1·9965882	50·6654	+ 1		+ 1	21·1784
− 2	28·511166	1·0002462	1·9975376	52·7423	+ 4	52·7424	+ 4	22·8248
− 1	25·729410	1·0000874	1·9991265	54·6673	− 1	54·6680	− 1	24·2731
0	24·754899	1·0000000	2·0000000	56·5315	− 7	56·5327	− 7	25·3445
1	25·729410	1·0000874	1·9991265	58·3859	− 1	58·3868	− 1	25·9243
2	28·511166	1·0002462	1·9975376	60·1745	+ 4	60·1750	+ 4	26·0413
3	32·754549	1·0003412	1·9965882	61·7887	+ 2	61·7891	+ 2	25·8282
4	38·065515	1·0003535	1·9964651	63·1549		63·1555		25·4260
5	44·107973	1·0003206	1·9967938	64·2562		64·2570		24·9340
6	50·632842	1·0002738	1·9972620	65·1114		65·1123		24·4093
7	57·463788	1·0002278	1·9977223	65·7527		65·7538		23·8821
8	64·469610	1·0001871	1·9981291	66·2140		66·2152		23·3679
9	71·531956	1·0001516	1·9984839	66·5264		66·5277		22·8759
10	78·498869	1·0001188	1·9988120	66·7176		66·7191		22·4148
11	85·096856	1·0000846	1·9991535	66·8138		66·8154		21·9988
12	90·793267	1·0000473	1·9995271	66·8423		66·8441		21·6546
13	94·871581	1·0000169	1·9998307	66·8325		66·8344		21·4149
14	97·146992	1·0000040	1·9999604	66·8079		66·8099		21·2806
15	98·218092	1·0000008	1·9999920	66·7795		66·7816		21·2134
16	98·704160	1·0000002	1·9999983	66·7502		66·7525		21·1780
17	98·930018	1·0000000	1·9999996	66·7209		66·7233		21·1566
18	99·036834	1·0000000	1·9999999	66·6914		66·6940		21·1416
19	99·086041	1·0000000	2·0000000	66·6620		66·6647		21·1297

might be used here. Most of the contribution to the aberration integrals comes from this region.

In certain circumstances it may be possible to reduce the work even further by using only one term of Δ in the early runs, or by adding extra guard figures only in the last run. Computers will readily find many such modifications suited to particular cases.

REFERENCES

(1) GODDARD, L. S. *Proc. Phys. Soc., Lond.*, **56**, p. 372 (1944).

(2) GODDARD, L. S., and KLEMPERER, O. *Proc. Phys. Soc., Lond.*, **56**, p. 378 (1944).

(3) MOTZ, H., and KLANFER, L. *Proc. Phys. Soc., Lond.*, **58**, p. 30 (1946).

(4) LIEBMANN, G. *Proc. Phys. Soc., Lond.*, **62B**, p. 753 (1949).

(5) MALOFF, I. G., and EPSTEIN, D. W. *Proc. Inst. Radio Engrs.*, **22**, p. 1386 (1934).

(6) GANS, R. *Z. techn. Phys.*, **18**, p. 41 (1937).

(7) RECKNAGEL, A. *Z. Phys.*, **104**, p. 381 (1937).

(8) DOSSE, J. *Z. Phys.*, **117**, p. 722 (1941).

(9) SPANGENBERG, K., and FIELD, L. M. *Proc. Inst. Radio Engrs.*, **30**, p. 138 (1942).

(10) RAMBERG, E. G. *J. Appl. Phys.*, **13**, p. 582 (1942).

(11) COSSLETT, .V E. *Introduction to Electron Optics*, p. 37 (London: Oxford University Press, 1946).

(12) GLASER, W. *Z. Phys.*, **83**, p. 104 (1933).

(13) SCHERZER, O. *Z. Phys.*, **101**, p. 593 (1936).

(14) PICHT, J. *Ann. Phys., Lpz.*, **15**, p. 926 (1932).

(15) FOX, L., and GOODWIN, E. T. *Proc. Camb. Phil. Soc.*, **45**, p. 373 (1949).

(16) REGENSTREIF, E. *C.R. Acad. Sci., Paris*, **229**, p. 1311 (1949).

(17) BRUCK, H., and ROMANI, L. *Cah. de Phys.*, **24**, p. 15 (1944), Lens VIII.

(18) DUNCAN, W. J. *Phil. Mag.*, **39**, p. 493 (1948).

(19) FOX, L. *Phil. Trans. A.*, **242**, p. 345 (1950), Part D.

SPECIAL REPORT

Summarized proceedings of a conference on electron microscopy —St. Andrews, June 1951

The Electron Microscopy Group of the Institute of Physics held a conference in the University of St. Andrews, Scotland, on 19 and 20 June, 1951. On the first day the three symposia held were on the recent experiences in the cutting and further treatment of thin sections for biological and histological investigations, on the critical testing of instrument performance, and on replica techniques. These were followed by an instructional film in which the principles and application of the electron microscope were demonstrated, and by a few short original papers. The second day was entirely devoted to the reading and discussion of papers. A notable feature of the conference was the opportunity for many informal discussions between small groups of people interested in special subjects. The symposia, papers and the discussions are summarized in this report.

In opening the session on section cutting and related histological techniques, MR. M. S. C. BIRBECK (Chester Beatty Research Institute) proceeded to discuss some of the modifications in histological technique arising from the requirement that sections for electron microscopy must be much thinner than those for optical microscopy. The embedding medium must be harder, and "ester wax," which combines hardness at room temperature with a fairly low melting point, is recommended. Mr. Birbeck has not been concerned with detail near the ultimate resolution limit of the electron microscope and has been content with sections of 0·4 μ, and occasionally 0·2 μ, giving a resolution of 0·1 μ or rather better; an ordinary safety razor blade (expendable) has proved satisfactory for this, when backed by a water bath (with a trace of alcohol) on to which the sections float. DR. C. E. CHALLICE (National Institute for Medical Research), who opened the discussion on this paper, has on the other hand been interested in viruses in tissues, and sections not thicker than 0·2 μ are required in order to show structures of 10 to 20 mμ. Safety razor blades are unsatisfactory for this and a microtome knife with a fixed back, sharpened by Hillier's method,[1] is preferred. Dr. Challice also finds pure diethylene glycol distearate better than the unpurified "ester wax" and recommends cutting in a cold room (+ 4° C) which not only reduces compression of the sections but retards rusting of the knife blade by the water bath. For harder tissues he finds a double embedding[2] desirable, using 8–12% celloidin followed by diethylene glycol distearate. PROF. L. H. BRETSCHNEIDER (University of Utrecht) (whose paper was read by Ir. J. B. Le Poole), in cutting sections of 0·2 μ, uses an embedding medium consisting of equal parts of paraffin, beeswax and carnauba wax and works in a cold room (0°–4° C). He emphasizes that temperature equilibrium is essential; it is not sufficient to cool the knife or the specimen or both.

In dealing with fixation of tissues MR. BIRBECK said that most of the usual fixatives, though satisfactory for detail in the optical microscope's range, cause fine precipitation of proteins and give spurious structures in the electron microscope size range; exceptions are formaldehyde, potassium dichromate and osmium tetroxide ("osmic acid"). For electron microscope work the most satisfactory fixatives are plain 2% osmic acid or Altmann's mixture (2% osmic acid + 5% potassium dichromate). On the other hand, Dr. Bernhard of the Paris Cancer Research Institute has used chromic acid and Prof. Bretschneider recommends Champy's or Regaud's mixtures. The disadvantage of osmic acid is its low penetration into tissues, but this is of little consequence in electron microscope work where the blocks of tissue used are no bigger than $\frac{1}{16}$ in cube.

The subsequent treatment of the sections varies with different workers: Mr. Birbeck has found it possible to sublime the embedding ester wax in the electron beam, but Dr. Challice prefers to remove the wax by independent heating *in vacuo* before exposure to the beam. Prof. Bretschneider removes his embedding medium by solution in xylene.

It is clear from the papers read at this meeting, as well as from DR. LIEBMANN'S report of the recent Hamburg meeting, that the actual cutting of thin sections is no longer a serious problem but that the difficulties are in the preparative and subsequent treatments. Several workers use the Rocker microtome by the Cambridge Instrument Co. Ltd., modified to cut 0·2 μ sections, while on the continent a rocker-type microtome, with carefully balanced forces, designed by Kellenberger and made by Trüb-Täuber and Co. AG. of Zurich, will cut to 0·05 μ, and another sliding type designed by Mölbert and Beyersdorfer and made by F. Jung of Heidelberg will cut to 0·1 μ.

The session on replica techniques, opened by DR. A. F. BROWN reading an introductory paper for DR. J. NUTTING (Department of Metallurgy, University of Cambridge) was, as is too often the case, confined to replica methods for metallurgical purposes. Nutting considers that only now, after ten years, is the electron microscope beginning to give results of genuine value to metallurgists. The early aluminium oxide replicas[3] gave beautiful pictures of high resolution (grain size 30 Å), but their importance was limited to aluminium and its alloys, and attempts to form and strip oxide films from other metals have given results of doubtful metallurgical significance because of the severe chemical and thermal treatment accorded to the specimen. Tsou and Nutting have, however, recently developed an oxide replica process for iron and steel which avoids heating the specimen and has advantages over plastic film replicas, particularly for structures involving small particles of secondary phase, though its resolution is only 200 Å—no better than that of plastic film replicas.

For general use in everyday metallurgy the plastic (Formvar) replica is adequate for most purposes, and though its grain size of 200 Å prevents the full use of the resolving power of the electron microscope, detail well below the optical limit can be studied. Using the dry-stripping technique[4] favoured by Nutting, electron microscope results can be obtained more quickly and easily than optical results under the high power. Comparison of electron and optical micrograms is made possible by a method, developed by E. D. Hyam, of taking dry-stripped replicas from an area which has been observed and selected under the optical microscope and this has shown that, at least for structures which can

be resolved by the light microscope, these replicas are completely reliable.

For improved resolution of detail, preshadowing of the prepared metal surface may be used, though in the discussion following this paper sharp differences of view emerged as to whether it was possible to strip the shadowing metal from a perfectly clean metal specimen or only from a slightly greasy one or vice versa.

Polymerization of a plastic monomer in contact with the surface to be studied, to form a soluble intermediate replica,[5] is a method of general application capable of giving resolution better than 50 Å, but is a much longer process than dry-stripping.

In discussion Ir. J. B. Le Poole (Technical University, Delft) referred to two-stage replicas made by evaporating silver on to the specimen and then silicon monoxide on to the silver intermediate cast; this he claimed has a grain of atomic dimensions and gives maximum resolution.

Dr. G. L. J. Bailey (British Non-Ferrous Metals Research Association) opened the discussion on Dr. Nutting's paper and suggested that the biggest problem before the electron microscopist in this field is to persuade the metallurgist to accept his results. In this connexion he cited instances of electron micrograms having proved trustworthy when the conventional optical methods had given misleading results.

In a copper–nickel–iron alloy containing 5% nickel and 1% iron the optical metallographers found considerably more of a second phase than appeared in the electron micrograms, but a re-examination using optical phase-contrast confirmed the electron optical observations; pitting in the specimen had given a spurious appearance of a second phase in the first optical pictures. Differences in the colour of protective films formed on a similar alloy (5% nickel, 1·3% iron) exposed to aerated sea-water were traced to a transformation occurring at 600° C, which could not be detected either by optical microscopy or by X-ray diffraction, but which did show up in the electron micrograms as well as in a change of magnetic properties.

Dr. Bailey was in full agreement with Dr. Nutting that Formvar replicas have produced more valuable metallurgical results than any other method, but he prefers the wet-stripping methods since the films can be made thinner and give better quality micrograms than the dry stripping method.

Dr. A. F. Brown (Cavendish Laboratory, University of Cambridge) drew attention to the fact that, because of the great depth of focus of the electron microscope and the smallness of the field of view, it is unnecessary to polish metal specimens as carefully as is required for light microscopy, nor need the surface be flat. Local structure less than 1 μ is quite interpretable though detail greater in extent than this may be unreliable when the surface is rough.[6]

In the more general sessions of the conference three further papers on metallurgical subjects were read. Mr. A. W. Agar and Mr. R. S. M. Revell (Metropolitan Vickers Electrical Co. Ltd.) have worked on ferrous specimens and obtained consistent and reliable pictures of the major structures but somewhat erratic fine detail. Mottled areas appear, particularly on the ferrite grains, which suggest incipient precipitation and appear to change with ageing. More extended work, however, makes it unlikely that the appearance is truly connected with ageing, nor is it due to defects of the Formvar replica since a preshadowed specimen confirms the observations; it is suggested that the effect is to be attributed to the etching process—though it is observed both with nital and picral etchants.

A paper by Dr. J. F. Brown and Mr. D. Clark (Imperial Chemical Industries Ltd., Billingham) was interesting as an example of the use of electron diffraction to identify materials observed in the electron microscope. The work was on 25/20 and 18/8 chromium-nickel steels containing some sigma phase together with chromium carbide. These latter could be isolated from the steel by electrolysis and examined in the electron microscope as separate particles whose appearance could be correlated with structures shown by replicas of the steel surface. Crystallographic data for single particles were obtained from their electron diffraction patterns. The basis of interpretation of the replicas in this case is thereby broadened and strengthened.

Mr. J. Trotter (National Physical Laboratory) also read a paper on nitrides in α-iron in which he suggests that two intermediate nitride phases have been observed in addition to the well-known Fe_4N phase. The correlation of this work with that of Radavich and Wert[7] was discussed.

Some fascinating results on crystal growth were shown by Dr. I. M. Dawson and Dr. V. Vand[8] (Chemistry Department, University of Glasgow). Calculation shows that the formation of the nucleus of a new molecular layer on a flat crystal face may require much more energy than is available under supersaturation conditions, though extension of a molecular layer from a step edge of molecular height is relatively easy. Growth will therefore take place more readily if the necessity for formation of fresh nuclei can be avoided and this is the case if growth takes place from a spiral dislocation. The pictures show that a crystal face of *n* hexatriacontane ($C_{36}H_{74}$) may indeed grow outwards in the form of a shallow spiral ramp. To obtain the pictures, crystals were grown from solution on to collodion film and were then shadowed with palladium and examined directly; some points of general interest to electron microscopists emerged from this work. Gold–manganin as a shadowing metal failed because it is mobile on the paraffin surface in the electron beam; palladium is better on such hydrogen-rich material. The effects of the electron beam on these and similar low melting point crystals gave rise to some discussion. Chemical structure seems to be at least as important as melting point in determining whether a given material will withstand bombardment by electrons. Thus though a paraffin which melts at 74° C is unaffected, an aromatic hydrocarbon melting at 200° C may polymerize in the beam. The graphitization which occurs on electron bombardment is not instantaneous and, in fact, the paraffin crystals continue to give their characteristic electron diffraction pattern for about five minutes before this degenerates into diffuse rings.

Mr. G. A. Bassett (Research Laboratories, General Electric Co. Ltd.) has observed another curious type of growth in the form of fine uniform filaments. The spongy silica produced by the decomposition of furnace bricks containing zirconium silicate is shown to consist of filaments ranging between 100 Å and 600 Å in diameter, any one filament being of very uniform diameter. The X-ray diffraction pattern is that of vitreous silica. A similar form of growth (with filaments 0·3 μ wide by 0·3 mm long) is found in silicon prepared from the vapour phase by the reaction of $SiCl_4$ with zinc. Silica condensing in the neighbourhood of quartz blowing operations, on the other hand, forms chains of particles instead of uniform threads.

Unexpected behaviour of siliceous material in the electron beam was reported by MR. S. F. WARD (British Cotton Industry Research Association) in connexion with the use of the diatom *Synedra fulgens* for magnification calibration of an electron microscope. Careful measurements show that this diatom shrinks by 5 to 10% on first exposure to the beam, but that thereafter its dimensions remain stable. The work also shows that the coefficient of variation of the interval spacings in a diatom of this species may be as much as 9% so that for accurate magnification measurements the optical calibration must be over the identical region used in the electron microscope measurements.

Developments in methods of particle counting based on work by Williams and Backus[9] were described by MR. H. L. NIXON (Rothamsted Experimental Station). A known concentration of standard, easily recognizable particles, is added to the unknown particle suspension and the mixture sprayed on to the microscope mounts and dried. The contents of each separate droplet form a patch of deposit in which the number of standard particles gives the original volume of the drop and then the number of unknown particles gives the concentration of the original suspension. MR. NIXON uses tomato bushy stunt virus as his standard particles (diameter 280 Å) instead of the polystyrene latex (diameter 2 950 Å) used by Williams and Backus, and keeps the droplet traces down to 2–3 μ in diameter. It is then possible to photograph each whole trace at a magnification sufficient to distinguish between the bushy stunt virus and any other particles in the size range 100–500 Å, and the smallness of the standard particle allows of its use in sufficient numbers to give adequate statistical accuracy without the necessity of counting large numbers of droplet traces.

DRS. C. E. CHALLICE and A. S. MCFARLANE (National Institute for Medical Research) have also used the spraying technique in work with vaccinia virus, though not in this case for counting purposes but because examination of the whole contents of a droplet helps to avoid unconscious subjective selection of the material in a field. The work was on the effect of sodium chloride on the purification of vaccinia. More than four or five washings in buffer solution produced no further improvement in purification of vaccinia, and if this preparation was flocculated slowly with molar sodium chloride the virus deposit was almost perfectly clean and sharp as seen in the electron microscope. If, however, the salt treatment was applied after insufficient washing, a fine granular deposit became attached to the virus particles and could not be separated from them, though the virus bodies themselves appeared sharper in the electron micrograms. It is believed that slowness of flocculation is the primary factor responsible for the separation of the virus from its closely associated protein.

An account of electron microscope work in the Department of Biomolecular Structure in the University of Leeds was presented by DR. R. REED. Studies on the structure of human influenza virus have been carried out in collaboration with DR. L. HOYLE of the General Hospital, Northampton. Ether treatment of the influenza virus bodies results in a loosening of structure with the production of many smaller particles which are separable into two groups, one showing antigenic activity and the other agglutination properties. The stages of this reaction have been followed in the electron microscope and the particle sizes determined. A possible mode of reproduction of the virus was discussed, the replicating units being considered as small protein macromolecules which later aggregate to form the virus elementary body.

Another research described by Dr. Reed was on the fibrous components of the human skin and was carried out in conjunction with the Leeds Medical School and the Rheumatism Research Unit in Manchester. Slides were shown illustrating changes in the collagen and elastic tissue fibrils in a range of pathological conditions. Histological and X-ray diffraction studies of subcutaneous lesions in rheumatoid arthritis were correlated with the electron microscope findings which showed normal collagen fibrils in the regions of normal tissue, degradation of the collagen in the intermediate regions, and only tissue debris in the badly diseased regions. Preliminary findings concerning the action of A.C.T.H. and cortisone on the fibrinoid regions of the diseased tissue were also mentioned; A.C.T.H. does not appear to repair the collagen, but it seems possible that cortisone may produce some restoration.

DR. I. M. DAWSON and DR. H. STERN (Chemistry Department, University of Glasgow) have made electron microscope studies of the cell walls of bacteria. *Staphylococcus aureous* treated with cetyl-trimethyl-ammonium bromide (C.T.A.B.) appears to lose the cell wall which can be discerned in electron micrograms of untreated organisms. Cell wall material was, however, isolated by shaking a buffered suspension of the organisms with glass beads to rupture the cells and then separating the contents by centrifugation; it was found to be resistant to C.T.A.B. as well as ribonuclease, pepsin and trypsin. It is suggested that the cell wall is of polysaccharide and not protein material. The apparent disappearance of the wall of the intact cells in C.T.A.B. is explained as due to swelling of the cytoplasm into intimate contact with the cell wall so that the latter is no longer separately distinguishable. DR. V. E. COSSLETT (Cavendish Laboratory, Cambridge) reported similar observations on *B. coli*.

In connexion with work on life histories of bacteria whose life cycles range over several days or weeks (e.g. mycobacterium tuberculosis or pleuropneumonia) it is necessary, before inoculation, to sterilize the film-covered electron microscope grids on which the organisms are to be grown, and MR. R. W. HORNE (Cavendish Laboratory, Cambridge) has found that exposure to ultra-violet radiation for 15 minutes (intensity unspecified) is the most effective way of doing this. Sterilization by heat fails because it destroys the thin supporting film.

The structure of another type of spermatozoon has been described by DRS. J. B. DLUGOSZ and J. W. HARROLD (University College, Dundee). This is the sperm of the spider beetle *Ptinus tectus* and is shown to develop from a circular chromatid to a filamentous mature form which has neither a head nor a nucleus. The chromosome material migrates, from the compact nucleus of the early spermatid, in the form of discrete bodies which are distributed along the central axis in the mature sperm. This is surrounded by a helical membrane which consists of twenty-two fibres of which two possess striated sheaths.

DR. H. J. WOODS with MR. S. M. MUKHERJEE and MR. J. SIKORSKI (Textile Physics Laboratory, University of Leeds) have followed up the work of Rånby and Ribi[10] by treating cellulosic textile fibres with concentrated sulphuric acid and have followed the change from fibrillar to particulate disintegration. Specially sharply defined particles were obtained from cotton, ramie and jute cellulose, the ultimate bodies from all the fibres being very similar, of the form of elongated tablets. Each fibre gave a characteristic size of tablet the

thicknesses ranging from 20 to 40 Å and the widths from 80 to 160 Å.

Films of these particles prepared by evaporating the colloidal solution on to glass show preferential orientation of the (101) planes parallel to the surface (X-ray data); the densities of such films are higher than those of the native fibres, as would be expected if the treatment had selectively removed non-crystalline cellulose to leave the more resistant crystalline particles. Mercerized fibres gave similar tablet-shaped particles.

When preparing electron microscope specimens from the colloidal solutions it was found unnecessary to resort to Ribi and Rånby's technique of coating the supporting film with beryllium to prevent aggregation of the particles during deposition.[11]

The session on critical testing of instrument performance was opened with a lecture by MR. M. E. HAINE (Research Laboratory, Associated Electrical Industries Ltd.). The resolution achieved in practice is rather worse than that given by the theoretical limit due to spherical aberration. Low resolution may often be due to some coarse and easily detected defects, like stage drift, bending of the instrument column, or electrostatic charges. Removal of these more obvious faults may still leave a lack of resolution, and Mr. Haine gave a list of possible causes, and the means of their detection. For example, a.c. stray fields near the instrument can be measured with a search coil, connected to an oscilloscope; astigmatism can be detected by observing ZnO crystals, or if less prominent, by the observation of the Fresnel pattern near the focus, as used by Hillier[12] and others. These tests can all be applied to ordinary instruments with resolving powers down to about 30 Å. For the most exacting requirements, the Fresnel fringe test with coherent illumination as described by Haine and Mulvey,[13] can be applied. This method determines the practical resolving power in the absence of lens aberrations and is sensitive beyond the limit given by the aberrations.

The discussion was opened by IR. LE POOLE, who mentioned his method of locating charged-up areas by imaging them on to the observation screen. Lens current and h.t. variations can be determined from the change in the electron diffraction pattern. Astigmatism is often caused by the specimen (e.g. SiO films). Further contributions to the discussion came from DRS. COSSLETT and CHALLICE, who stressed the requirement of simplified controls, MR. HALMA, and IR. VAN DORSTEN, who uses a radiation counter to check which parts of the instrument wall are hit by the electron beam.

DR. H. J. WOODS and MR. J. SIKORSKI (Textile Physics Laboratory, University of Leeds) read a short paper on the filament life in the type E.M.3 instrument, by Metropolitan Vickers Electrical Co. Ltd. They found an average life of 15 working hours (at 75 kV), but filament life appears very dependent on the experience of the operator. With experienced operators filaments last sometimes for 30 to 60 hours.

IR. J. B. LE POOLE and IR. A. C. VAN DORSTEN (Philips Laboratories) described a short focal length objective. From consideration of the limiting case of the field between pole tips excited just above saturation, the pole tips being perforated by very small holes to let the electron beam pass through, they found that an objective of 0·8 mm focal length (at 80 kV) should be possible. Experiments with soft iron pole pieces confirmed this, giving the predicted focal length. Slightly more favourable dimensions can be obtained with CoFe pole pieces. The advantage of such a short focal length objective is its low chromatic aberration, which reduces the requirement for voltage and current stabilization. In the discussion, DR. G. LIEBMANN (Research Laboratory, Associated Electrical Industries Ltd.) mentioned that he had investigated the magnetic "pinhole" lenses represented by the small perforations of the pole tips, and had found that the aberrations introduced through these are not negligible.

DR. G. LIEBMANN then read a report on the papers and discussions of the Hamburg meeting of the German Society for Electron Microscopy, which he had attended on behalf of the Institute of Physics Group; this report has since been published.[14]

A paper on the performance of high voltage electron guns, as used in electron microscopes, was read by MESSRS. M. E. HAINE and P. A. EINSTEIN (Research Laboratory, Associated Electrical Industries Ltd.). Although the performance of electron guns has been studied by many authors, no previous attempts had been made to relate the gun performance to the theoretical limiting value predicted by thermodynamics. In this paper it was shown that for a wide range of electrode geometries the theoretical limit of brightness, as predicted by D. Langmuir, can be achieved if suitable bias voltages for the shield electrode are chosen. The geometry of the gun is only important in determining the most economical working conditions, i.e. lowest total current for maximum brightness. Space charge was found to be of little significance.

DR. G. LIEBMANN read a paper on magnetic projector lenses, which was an extension of the work previously reported at the Paris conference. The focal length of all symmetrical projector lenses can be represented by one single curve. All lenses can be operated at a point where they are free from radial distortion; spiral distortion, however, cannot be avoided unless image rotation is also eliminated. Calculations agree well with Ruska's measured data. Certain results of use in practical lens design were combined in a design chart from which the relevant design or operational parameters can be read directly.

DR. C. E. CHALLICE described a modification of the projector lens of the RCA "B" type electron microscope, which turns the two-stage instrument in effect into a three-stage one, by replacing the standard pole pieces of the projector lens by a double gap pole piece insert. In this way the usable range of magnifications can be greatly increased, being now 2 500× to 25 000× without appreciable distortion.

A similar modification was carried out by DR. J. F. BROWN and MR. D. CLARK (Imperial Chemical Industries Ltd., Billingham) on their type E.M.2 instrument by the Metropolitan Vickers Electrical Co. Ltd. They added a further excitation coil and replaced the existing pole piece insert by a double gap insert, adding also a diffraction diaphragm.

DR. G. L. ROGERS (University College, Dundee) gave a talk on "The elements of diffraction microscopy." He reviewed the principles of Gabors proposals, and pointed out that each "hologram" can be considered a zone plate. Thus a definite focal length $\pm f$ can be ascribed to each hologram, $1/f = (1/v - 1/u)$, where u and v are the distances of source and object from the photographic plate. It follows that the "reconstruction" of the image of the original could be carried out without using lenses at all. While the position of the image is given by the above value of f, its magnification is $u_1(u_2 - v_2)/(u_1 - v_1)u_2$, where suffix 1 refers to the taking of

the "hologram," and suffix 2 to the "reconstruction." The image position is determined by f, whereas the magnification of the "reconstruction" follows from geometrical considerations.

D. G. DRUMMOND
G. LIEBMANN

REFERENCES

(1) HILLIER, J. *Rev. Sci. Instrum.*, **22**, p. 185 (1951).
(2) PEASE, D. C., and BAKER, R. F. *Proc. Soc. Exp. Biol. and Med.*, **67**, p. 470 (1948).
(3) MAHL, H. *Metallwirtsch.*, **19**, p. 1082 (1940).
(4) SCHAEFFER, V. J. *Science*, **97**, p. 188 (1943).
(5) BROWN, A. F., and JONES, W. M. *Nature, Lond.*, **159**, p. 635 (1947).
(6) BUJNOV, N. N., and LERINMAN, R. M. *Dokl. Akad. Nauk, U.S.S.R.*, **74**, pp. 707 and 929 (1950).
(7) RADAVICH, J., and WERT, C. *J. Appl. Phys.*, **22**, p. 367 (1951).
(8) DAWSON, I. M., and VAND, V. *Proc. Roy. Soc.* (*A*), **206**, p. 555 (1951); *Nature, Lond.*, **167**, p. 476 (1951).
(9) WILLIAMS, R. C., and BACKUS, R. C. *J. Amer. Chem. Soc.*, **71**, p. 4052 (1949).
(10) RÅNBY, B. G., and RIBI, E. *Experientia*, **6**, p. 12 (1950).
RÅNBY, B. G. *Acta Chem. Scand.*, **3**, p. 649 (1949).
(11) RIBI, E., and RÅNBY, B. G. *Experientia*, **6**, p. 27 (1950).
(12) HILLIER, J., and RAMBERG, E. G. *J. Appl. Phys.*, **18**, p. 588 (1947).
(13) HAINE, M. E., and MULVEY, T. *Proc. Int. Congress Electron Microscopy, Paris*, Sept. 1950.
(14) LIEBMANN, G. *Nature, Lond.*, **168**, p. 70 (1951).

Correspondence

Differential methods of vacuum leak detection

In your August 1951 issue, Messrs. Blears and Leck described their technique for leak detection in which a manometer reading is obtained which depends on the composition of the gas in the continually pumped vessel under test. The sensitivity of the method is limited by the background fluctuation of the manometer readings. If a gas having a different sensitivity in the gauge is substituted for air, in the neighbourhood of a leak, this substitution will affect the pressure indication. This allows leak detection by addition or subtraction methods.

A somewhat different subtraction method has been used in these laboratories. Our manometer consists of a single ionization gauge protected by a liquid air trap. The only requisite for the gas used in testing for leaks is that it should have a negligible vapour pressure at liquid air temperature; if this condition is fulfilled, the presence of the gas is detected by a lowering of the pressure reading, independent of its nature. We chose carbon dioxide on account of its ready availability, non-inflammability and relative non-toxicity.

The four main causes of fluctuations in the manometer reading are as follows: (*a*) Variations in pumping speed, which can be damped out by placing between the evacuated system and the pump a short length of tubing, of low intrinsic pumping speed compared to that of the pump. This method is also used by Messrs. Blears and Leck. (*b*) The rate of gas evolution from the walls of the system is not necessarily constant, but as the indication of the trapped ionization gauge is independent of the evolution of condensable vapours, the fluctuations of the manometer readings correspond only to that of the residual permanent gas pressure which will generally be low enough not to be disturbing. (*c*) Pressure variation may be caused by the unsteadiness in the rate of flow of larger leaks. (*d*) Fluctuations in the emission from the gauge cathode will cause small variations in the readings, even when the grid current is stabilized by an electronic device.

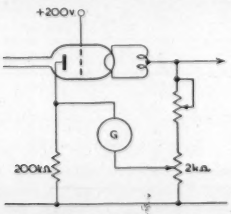

Current for differential vacuum leak detection

The circuit shown in the accompanying figure provides an increase in stabilization by use of a null method. Part of the cathode current serves to balance the plate current of the gauge. So long as the pressure remains constant, the fraction of the cathode current necessary to keep the circuit balanced is largely independent of total cathode emission. Thus the sensitivity of the meter reading is practically independent of the pressure. We used a galvanometer giving a 1 mm deflexion for a current of 10^{-9} A.

The main differences between the technique of Messrs. Blears and Leck and ours can be summarized as follows: Their method provides compensation for fluctuations described above (*a*), (*c*) and (*d*), whereas ours provides compensation for items (*a*), (*b*) and (*c*).

While, in our opinion, the extent to which item (*d*) in their method or item (*b*) in ours is successfully dealt with is debatable, we have consistently obtained the following results: The smallest pressure variation that we can observe is 2×10^{-8} mm of mercury when the residual pressure is 5×10^{-5} mm of mercury. The maximum ratio (total leak flow)/(flow of studied leak) at which a leak can still be detected is 2 500. In a system of moderate volume (about 1 litre), pumped out at the speed of about 100 c.c./sec, a leak of 0·01 mm³/h is readily detected.

Commissariat à l'Energie Atomique — G. NIEF
Laboratoire de Chimie-Physique
Fontenay-aux-Roses, Seine.

Isotope catalogue on punched cards

It has been found useful here to transfer the information contained in recent isotope catalogues to a set of punched cards. Each nuclear species is represented by a card with 84 small holes. A ticket punch is used to remove small pieces of card between the holes and the edges and a simple code enables the essential properties of the nucleus to be represented in this way. Sorting the cards, to find nuclei with some particular set of properties, is quickly done with a knitting needle.

Cards suitable for this application are now available from the Copeland-Chatterson Company, Stroud, Gloucestershire.

Western Infirmary, — J. M. A. LENIHAN
Glasgow.

Theory of stresses in glass butt seals

In his paper in your June 1951 issue Mr. Rawson has considered that the misfit between the two tubes at the temperature T_2 can be eliminated by the application of a ring of radial forces as shown in his Fig. 3. This idea is satisfactory (as will be shown below) only when the elastic properties of the two tube materials are the same. When the two materials have different elastic properties (e.g. glass-metal butt seals) the ring of radial forces is not sufficient to ensure continuity of the mean radius line.

Mr. Rawson's theory can be extended by considering a more general system of forces consisting of the radial force P per unit length together with a ring of bending couples M_0 per unit length as shown in the accompanying figure.

Timoshenko* has shown that for a tube loaded in this manner, the deflexion is given by the equation

$$\eta = \frac{e^{-\beta x}}{2\beta^3 D}[P\cos\beta x - \beta M_0(\cos\beta x - \sin\beta x)] \qquad (1)$$

where β is now defined as

$$\beta = \left(\frac{Et}{4DR^2}\right)^{\frac{1}{4}} = \left[\frac{3(1-\sigma^2)}{R^2t^2}\right]^{\frac{1}{4}}$$

and D = flexural rigidity

$$= \frac{Et^3}{12(1-\sigma^2)}$$

and the notation otherwise is the same as that used by Mr. Rawson.

The correction referred to above lies in the use of D to replace EI and also in the definition of β.

The inward deflexion of tube 2 is

$$\eta_2 = \frac{e^{-\beta_2 x}}{2\beta_2^3 D_2}[P\cos\beta_2 x - \beta_2 M_0(\cos\beta_2 x - \sin\beta_2 x)] \qquad (2)$$

and for tube 1 is

$$\eta_1 = -\frac{e^{-\beta_1 x}}{2\beta_1^3 D_1}[P\cos\beta_1 x + \beta_1 M_0(\cos\beta_1 x - \sin\beta_1 x)] \qquad (3)$$

where again x is positive when moving away from the joint in both directions. For the continuity of the mean radius line, then:

$$\left.\begin{aligned} -(\eta_1)_{x=0} + (\eta_2)_{x=0} &= R\delta \\ \text{and} \quad \left(\frac{d\eta_1}{dx}\right)_{x=0} + \left(\frac{d\eta_2}{dx}\right)_{x=0} &= 0 \end{aligned}\right\} \qquad (4)$$

Substituting equations (2) and (3) in the equation (4) leads to the solutions

$$M_0 = \frac{2R\delta\beta_1^3\beta_2^3 D_1 D_2(\beta_1^3 D_1 - \beta_2^3 D_2)}{2(\beta_1 D_1 + \beta_2 D_2)(\beta_1^3 D_1 + \beta_2^3 D_2) - (\beta_1^3 D_1 - \beta_2^3 D_2)^2} \qquad (5)$$

$$P = \frac{4R\delta\beta_1^3\beta_2^3 D_1 D_2(\beta_1 D_1 + \beta_2 D_2)}{2(\beta_1 D_1 + \beta_2 D_2)(\beta_1^3 D_1 + \beta_2^3 D_2) - (\beta_1^3 D_1 - \beta_2^3 D_2)^2} \qquad (6)$$

If the elastic properties of the two tubes are the same then

$$\sigma_1 = \sigma_2;\ E_1 = E_2$$

and this leads to

$$\beta_1 = \beta_2;\ D_1 = D_2$$

then equations (5) and (6) become

$$M_0 = 0$$
$$P = R\delta\beta^3 D$$

which is equivalent to that obtained by Mr. Rawson when D replaces EI.

It should be noted that M_0 will not be zero in cases where the elastic properties of the two tubes are different and when the two tubes are of different wall thickness.

The values of the bending moments are then

$$M_1 = -D_1\frac{d^2\eta_1}{dx^2} = -\frac{e^{-\beta_1 x}}{\beta_1} \times [P\sin\beta_1 x + \beta_1 M_0(\sin\beta_1 x + \cos\beta_1 x)] \qquad (7)$$

$$M_2 = -D_2\frac{d^2\eta_2}{dx^2} = \frac{e^{-\beta_2 x}}{\beta_2} \times [P\sin\beta_2 x - \beta_2 M_0(\sin\beta_2 x + \cos\beta_2 x)] \qquad (8)$$

which become the same as Rawson's equations (14) when the elastic properties are the same.

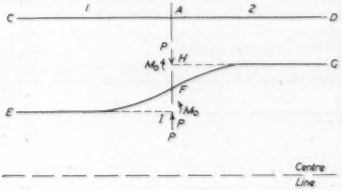

Movement of centre line of glass butt seal with change of temperature

The shearing forces are given by

$$F_1 = \frac{dM_1}{dx} = e^{-\beta_1 x}[P(\sin\beta_1 x - \cos\beta_1 x) + 2\beta_1 M_0\sin\beta_1 x] \qquad (9)$$

$$F_2 = \frac{dM_2}{dx} = -e^{-\beta_2 x}[P(\sin\beta_2 x - \cos\beta_2 x) - 2\beta_2 M_0\sin\beta_2 x] \qquad (10)$$

which become Rawson's equations (15) for the same elastic properties.

The hoop stresses are (for the cases considered in the experiments)

$$P_0 = \frac{E\eta}{R} = \frac{E}{R}\frac{Pe^{-\beta x}\cos\beta x}{2\beta^3 D} = \frac{E\delta}{2}e^{-\beta x}\cos\beta x \qquad (11)$$

Then the retardation

$$R_e = \pm\, Ct E\delta e^{-\beta x}\cos\beta x \qquad (12)$$

which is the same as Rawson's equation (17).

It is to be noted that the value of β in my equation (12) is different from Mr. Rawson's. In fact the value of β found here is $\sqrt[4]{0{\cdot}91} = 0{\cdot}977$ times that used previously. This

* Timoshenko, S. *Strength of Materials*, Pt. II, p. 166 (New York: D. Van Nostrand Co. Inc., 1946).

means that the experimental points should be displaced slightly to the left whilst the theoretical curve is not altered.

Aeronautical Research Laboratories, Melbourne, Australia. N. L. SVENSSON

I make the following comments on the paper by Mr. H. Rawson which appeared in your June 1951 issue. His equations (8) and (9) should be changed to read

$$\eta_2 = \frac{e^{-\beta_2 x}}{2\beta_2^3 D_2}[P_0 \cos \beta_2 x - \beta_2 M_0(\cos \beta_2 x - \sin \beta_2 x)] \quad (1)$$

$$\eta_1 = \frac{e^{-\beta_1 x_1}}{2\beta_1^3 D_1}[P_0 \cos \beta_1 x_1 - \beta_1 M_0(\cos \beta_1 x_1 - \sin \beta_1 x_1)] \quad (2)$$

The reason for the use of D rather than EI lies in the fact that warping is prevented in the tube, whereas it is not in the strip on elastic foundation. It should be cautioned that in the general case of $D_2 \neq D_1$, the use of $M_0 = 0$ is not correct. The value of M_0 is obtained from the satisfaction of the boundary condition

$$\left.\frac{d\eta_2}{dx}\right]_{x=0} = \left.\frac{d\eta_1}{dx_1}\right]_{x_1=0} \quad (3)$$

i.e.
$$\theta_1 = -\frac{d\eta_1}{dx_1}, \quad \theta_2 = -\frac{d\eta_2}{dx}$$

$$\theta_1 = \theta_2 \text{ at } x_1 = x = 0$$

It will be noted in Mr. Rawson's paper, if after D is substituted for EI and the misprint $P_0^{-\beta x}$ is corrected to read $Pe^{-\beta x}$ in both equations with the proper subscripts of "1" or "2" in β and D wherever they appear,t hen $d\eta_2/dx \neq d\eta_1/dx_1$ and this violates the condition for continuity of slope. Only for the special case of $D_1 = D_2$ will $M_0 = 0$ and the equations (8) and (9) be correct (Fig. 1.)

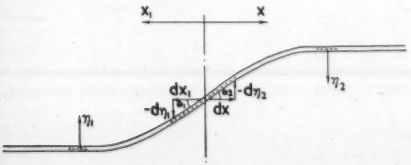

Fig. 1

If we add the author's boundary condition of

$$[\eta_1 + \eta_2]_{x_1=x=0} = R\delta \quad (4)$$

then from equations (1), (2), (3) and (4) above we can evaluate P_0, M_0 as a function of β_1, D_1, β_2, D_2, R.

Now, in connexion with replacing EI by D we must also take w = unity, throughout. Thus

$$\beta = (K/4D)^{\frac{1}{4}}, \text{ where } K = Et/R^2 \quad (5)$$

or
$$\beta = \left(\frac{Et}{4DR^2}\right)^{\frac{1}{4}} = \left[\frac{3(1-\nu^2)}{R^2t^2}\right]^{\frac{1}{4}} \quad (6)$$

where the proper subscripts are to be used in equations (5) and (6). These values for β and K should be used in place of those given by the author. It might be noted from the original paper that

$$\beta = [3/R^2t^2]_{\frac{1}{4}} \quad (7)$$

so that the factor of $(1 - \nu^2)$ represents the effect of preventing the strip from warping.

The above analysis will still reduce to Rawson's equation (12) for the special case of $D_1 = D_2$.

To evaluate M we need only use

$$M = -D\frac{d^2\eta}{dx^2} \quad (8)$$

where the D replaces EI, and the value of η is now taken from equations (1) and (2) above. To evaluate the shear F, once again these values of η should be used.

Thus the author has solved correctly the case where $D_1 = D_2$, given by his equation (12). All other results given by his equations (8) to (14) and the equations for F_1, F_2 are no longer valid.

The following errors should also be corrected. In equation (6) write I instead of T, equations (8) and (9) should be corrected as already noted, and in equation (9) write E_1 instead of E_2 and β_1 instead of β.

The section on three component seals neglects the moment M_0. It also fails to consider that the centre section is of finite length. Hence considerable doubt is to be cast on the results in this section.

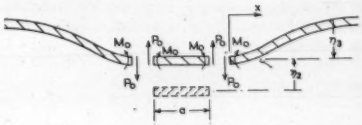

Fig. 2

One method of analysis would be to assume the centre section so short that it will not bend, as in Fig. 2. Here M_0 can be neglected in the centre seal, for which

$$\eta_2 = \frac{(2P_0)R^2}{Eta} \quad (9)$$

Since $D_3 = D_1$, $E_3 = E_1$, then

$$\eta_1 = \eta_3 = \frac{e^{-\beta_3 x}}{2\beta_3^3 D_3}[P_0 \cos \beta_3 x - \beta_3 M_0(\cos \beta_3 x - \sin \beta_3 x)] \quad (10)$$

The boundary conditions will be

$$[\eta_2 + \eta_3]_{x=0} = R\delta \quad (11)$$

$$\left[\frac{d\eta_3}{dx}\right]_{x=0} = 0 \quad (12)$$

As a special case it will be noted that as $a \to 0$ we need have $P_0 = 0$ from equation (9). From the boundary condition $[d\eta_3/dx]_{x=0} = 0$, it is seen that also $M_0 = 0$. Thus $\eta_1 = \eta_3 = 0$, $\eta_2 = R\delta$. This indicates, as shown in Fig. 3, that for a zero length spacer the tube will not be deflected, which is to be expected.

Since Mr. Rawson neglects three basic quantities in his derivation, his results cannot be exact. First, he neglects the possibility of having a moment, M_0. Second, he neglects the

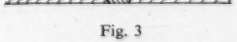

Fig. 3

condition of continuity of slope at the joint. Third, he does not consider that the centre piece is finite and in evaluating CL he has overlooked the term $e^{\beta x}(A \cos \beta x + B \sin \beta x)$; where only if $x \to \infty$ will $A, B \to 0$.

From the method suggested here in equations (9) to (12), the problem can be completely determined for small a. For large a one would have to consider the bending of the centre seal, which can be done as suggested above.

In either example it should not be felt that the "hoop stress" is merely the p_0 given by the author. A second component that gives no P_r resultant must be added. This is the stress that prevents warping and its value will be $\pm 6\nu M/t^2$, and is really caused by a moment νM acting on the circumference.

Sperry Gyroscope Company, M. ZAID
Great Neck,
Long Island,
New York.

I thank Mr. Svensson for his contribution, which widens the scope of my theory. I quite agree with the remarks he makes and his calculations. However, it is not a very serious matter if one neglects the effect of the bending moments, M_0, in glass-metal seals. If one considers a Kovar-glass seal having a diameter of 20 mm and a wall thickness of 1 mm, Mr. Svensson's equations give a value for the hoop stress in the glass at the joint about 15% higher than the value given by my equations. This difference is not very important when one remembers first that the determination of δ, the differential free contraction, can rarely be accurately carried out, and secondly that the values of the breaking strength of glass is such an indeterminate quantity that one has to use a large factor of safety in designing glass-metal seals.

In reply to Dr. Zaid I wish first to call attention to my reply to Mr. Svensson. I do not agree with Dr. Zaid's remarks concerning the section of my paper dealing with three component seals. I tried to make it clear in that section of the paper that I was only considering glass–glass seals. This being so, $D_1 = D_2 = D_3$ and there is, then, no need to introduce bending moment terms to maintain continuity of slope at the joints. I intentionally limited my considerations to an all-glass seal so that I could deal with a composite tube in which all three parts have the same Young's modulus. This makes it possible to use the principle of superposition and so avoid the difficulty caused by the finite length of the central tube. The good agreement between my theoretical curves and my experimental results shows that it is unlikely that my method of dealing with the problem of three component seals is seriously in error.

I agree with Dr. Zaid's list of errors that appeared in print.

Research Laboratories, H. RAWSON
The British Thomson-Houston Co. Ltd.,
Rugby.

Journal of Scientific Instruments

Contents of the January issue

ORIGINAL CONTRIBUTIONS

An electronic digital recording machine—the SETAR. By N. T. Welford.

A two fluxmeter method of measuring ferromagnetic hysteresis loss. By H. Aspden.

The design of mobile electronic laboratories. By P. H. Parkin.

A new type of α-particle bench monitor. By R. D. Connor.

An apparatus for the measurement of small differential expansions and its use for the study of fused silica. By R. W. Douglas and J. O. Isard.

The development of Ilford G5 emulsion with ID19 developer. By A. J. Herz.

A modified Budenberg pressure balance. By J. F. Pearse.

A servo-mechanical apparatus for the investigation of the properties of visco-elastic materials. By L. J. Hastewell and F. J. U. Ritson.

Internal standard flame photometry. By E. G. Walsh.

A note on the temperature coefficients of running voltage of glow-discharge tubes. By F. A. Benson and H. Bache.

LABORATORY AND WORKSHOP NOTES

The ionization gauge—two modifications. By J. H. Burrow and E. W. J. Mitchell.

The construction and properties of light pith levers. By C. P. Luck.

A fluorescent screen mounting for X-ray goniometers. By A. L. Mackay.

NEW INSTRUMENTS, MATERIALS AND TOOLS

Infra-red spectrophotometer with cathode-ray tube representation—Safety Pipette—Telepipette—Universal water baths.

CORRESPONDENCE

British Instrument Industries Exhibition—London, 1951. From M. W. Thring.

MANUFACTURERS' PUBLICATIONS

British Journal of Applied Physics

Original Contributions accepted for publication in future issues of this Journal

Errors in stress determination at the free boundaries of "frozen stress" photo-elastic models. By V. M. Hickson.

Pool surface and spot temperature of mercury cathodes as a problem in heat conduction. By H. von Bertele.

Liquid films formed by means of rotating disks. By B. E. Dixon, A. A. W. Russell and J. E. L. Swallow.

A radio-frequency power supply system for high voltage accelerators. By P. A. Davenport.

A graphical treatment of the tone reproduction problem in television systems. By R. B. Mackenzie.

A castable polyester resin for photoelastic work. By B. Sugarman, G. O. Moxley and I. A. Marshall.

The application of molecular resonance to microwave frequency stabilization. By H. R. L. Lamont and E. M. Hickin.

The two-dimensional magnetic or electric field inside a semi-infinite slot terminated by a semi-circular cyclinder. By N. Davy and N. H. Langton.

Time-resolved spectroscopy of spark discharges. By F. Twiss.

The elastic constants of piezoelectric crystals. By R. F. S. Hearmon.

The bending and twisting of anisotropic plates. By R. F. S. Hearmon and E. H. Adams.

Mechanical strength of piezoelectric crystals. By R. Bechmann and P. L. Parsons.

Permanent magnets for spectrographs and nuclear physical research. By D. Hadfield and D. L. Mawson.

THIS JOURNAL is produced monthly by The Institute of Physics, in London. It deals with all branches of applied physics (including theory and technique). All rights reserved. Responsibility for the statements contained herein attaches only to the writers.

EDITORIAL MATTER. Communications concerning editorial matter should be addressed to the Editor, The Institute of Physics, 47 Belgrave Square, London, S.W.1. (*Telephone:* Sloane 9806.) Prospective authors are invited to prepare their scripts in accordance with the *Notes on the Preparation of Contributions*. (Price 2*s*. 6*d*. including postage.)

ADVERTISEMENTS. Communications concerning advertisements should be addressed to the agents, Messrs. Walter Judd Ltd., 47 Gresham Street, London, E.C.2. (*Telephone:* Monarch 7644.)

SUBSCRIPTION RATES. A new volume commences each January, and annual subscriptions will only be accepted for complete volumes of the monthly parts (January–December). The charge is £4 per volume ($11.50 U.S.A.), including index (post paid), payable in advance. Single parts, so far as available, may be purchased at 8*s*. each ($1.15 U.S.A.), post paid, cash with order. Orders should be sent to The Institute of Physics, 47 Belgrave Square, London, S.W.1, or to any Bookseller.

SPECIAL ARTICLE

Microwaves in medical and biological research

By J. E. Roberts, D.Sc., F.Inst.P., and H. F. Cook, Ph.D., F.Inst.P., Department of Physics Applied to Medicine, The Middlesex Hospital, London, W.1

Recent work on the absorption of microwave radiation in the frequency range 10^9 c/s to 3×10^{10} c/s is reviewed, with particular reference to materials of biological interest. The relative importance of ionic conduction, dipolar relaxation, particularly of water molecules, and resonance is discussed briefly. Conventional methods for dielectric constant and loss measurements at microwave frequencies can be adapted for use with biological materials and a number of such modifications is described. The results of investigations into the dielectric properties of water, the most abundant biological material, proteins and a variety of body tissues are outlined and discussed in terms of established dielectric theory. High power microwave generators have been used to study tissue heating, the heating pattern comparing favourably with predictions from the radiation propagation constants and the thermal properties of the materials. A few experiments on the effects of microwaves on animal tumours and on viruses are described.

INTRODUCTION

Electromagnetic radiation has been used as a therapeutic agent in medicine for many centuries, and long before their nature was understood heating by infra-red rays and the curious beneficial effects of solar ultra-violet were well appreciated. In more recent times, extensions of the known electromagnetic spectrum seem to have led inevitably to a study of the biological effects of the radiations and the possibilities of their use in medicine. The discovery of X-rays and its immediate consequences produced new tools, not only for the diagnosis and treatment of disease, but for fundamental studies of both animate and inanimate matter. On the other hand, although the results are not so spectacular, the use of high frequency currents in the "radio" range of frequencies, where localized or general body heating is required, is an accepted feature in the practice of physiotherapy.

Developments during the 1939–45 war opened up a largely neglected range of the spectrum when pulsed and continuous wave sources of radiations between 1 and 50 cm wavelength were produced for use in radar. During the war many speculative inquiries came to hospital departments concerning the possible physiological ill effects of these radiations on operators. Observers who investigated this problem, Daily,[1] Follis,[2] and Lidman and Cohen,[3] found no evidence of a biological effect other than that due to heat production. Hence no serious ill effects of microwave radiation were envisaged. On the contrary, it was considered that microwave radiation might prove a useful thermogenic agent in the practice of physiotherapy if the problems of dosage measurement and method of application to patients could be solved. Physical investigations have been carried out with this object in view. Concurrently, the search for any specific action of intense microwave fields on micro-organisms, virus particles, and other biological molecules has been commenced.

The ready availability of stable low-power sources of microwaves gave impetus to the study of the behaviour of dielectrics at these frequencies and of molecular relaxation processes. Investigations of the dielectric properties at microwave frequencies of biological materials have been included in this field, although, in an embryonic state, useful information regarding relaxation processes and molecular structure in living tissues and protein solutions has already been obtained. The propagation constants of human tissues, as determined from dielectric constant measurements, have been of great value in connexion with studies of microwave propagation in the human body.

ABSORPTION BY BIOLOGICAL MATERIALS IN THE MICROWAVE REGION

In a review such as this it will be of value briefly to outline the relative importance of the different processes which may give rise to the absorption of energy from microwave radiation propagated in biological materials.

From the point of view of microwave propagation, most materials of biological interest can be regarded as "lossy" dielectrics which are frequently macroscopically or microscopically heterogeneous. The processes by which dielectric loss occurs and thereby energy is transferred to the medium depend obviously on the nature of the material and the frequency range of radiations in use. Electronic conduction does not enter into the question, but ionic conductivity, resonance and molecular relaxation are all possibilities.

In general, ionic conductivity is frequency independent up to frequencies higher than those considered here. However, in heterogeneous materials such as animal tissues and cell suspensions, specific ionic conductivity increases with increasing frequency up to the region of 10^8 c/s. This effect is due to intracellular fluids being separated from the extracellular fluid by thin non-conducting membranes. Cell contents are thus shielded from low-frequency fields, but are able to provide increasing contributions to dielectric loss as the frequency rises. At microwave frequencies the effect of the cell membranes becomes negligible and the specific ionic conductivity of a cell suspension can be assumed constant in the microwave region at a value higher than obtains

at lower frequencies. This is exemplified below in the case of whole blood.

It is interesting to speculate on the possibilities of resonance absorption in the microwave region by molecules which make up living matter and the consequent possibilities of specific biological actions which may be used diagnostically or therapeutically. Although, in the opinion of some authorities, resonance absorption at microwave frequencies is a possible process of absorption by large biological molecules, it is likely that the practical importance of such absorption in therapeutic applications would be very small, though it would be of great interest from the point of view of molecular structure. With one or two possible exceptions, evidence of such absorption at microwave frequencies is as yet lacking.

The third process to be considered is the relaxation of dipolar molecules or groups. The relaxation times of proteins in aqueous solution are in the region of 10^{-7} sec, giving maximum energy absorption per cycle in the ordinary radio-frequency range (10^6 c/s). Water, on the other hand, shows anomalous dispersion in the range 10^9 to 10^{11} c/s so that it is strongly absorbent in the microwave region. Since water is a major constituent of all living biological material, its relaxation plays a prominent part in absorption processes. Up to the present, significant absorption by dipole orientation of other constituent molecules or groups in such materials has not been demonstrated.

Summarizing, it can be said that: (*a*) ionic conductivity in biological materials is frequency independent in the microwave region, and provides an energy loss per cycle inversely proportional to frequency; (*b*) energy loss per cycle due to water relaxation increases with frequency through the microwave region and becomes maximal at frequencies (depending on temperature) in the region of 2×10^{10} c/s; and (*c*) significant microwave absorption by resonance processes or by dipole orientation in molecules other than water has not yet been found.

An example of the relative importance of ionic conductivity and water relaxation can be given in the case of human muscular tissue. The ratio of the contributions to dielectric loss by ionic conductivity and water relaxation decreases from 14 at 10^9 c/s (free-space wavelength = 30 cm) to 0·05 at 3×10^{10} c/s (free-space wavelength = 1 cm), with equal contributions at approximately 4×10^9 c/s. The combined effect on the linear energy absorption coefficient for plane waves propagated in human muscle is to cause this coefficient to increase slowly with frequency from 10^9 c/s to 3×10^9 c/s, and then much more rapidly as the frequency increases above 3×10^9 c/s.

TECHNIQUES FOR DIELECTRIC CONSTANT MEASUREMENTS

In the study of absorption processes the fundamental problem reduces to the measurement over a wide frequency range of a complex dielectric constant, $\epsilon' - j\epsilon''$, where the loss tangent, ϵ''/ϵ', may be comparatively large. The experimental problem involves the adaptation of existing methods to the peculiarities of the media under consideration.

Methods of measurement of the dielectric constant of conventional dielectrics at microwave frequencies are based on well-known relationships (see, for example, von Hippel and Breckenridge,[4] or Jackson[5]) between the dielectric constant and other parameters. Redheffer[6] has provided a valuable survey and summary of thirty existing methods. In principle, any of these methods could be used to determine the dielectric constant and loss of materials of biological interest. However, the high dielectric constant and loss of most biological substances, together with their other peculiar properties, limit the choice of method.

Experience has shown that, to achieve the highest accuracy, methods of choice are those in which measurements are made in the material itself. Thus direct measurements of α (the attenuation coefficient) and β (the phase constant) for progressive or stationary waves in the material (contained in coaxial line or wave-guide) lead to the calculation of the complex dielectric constant from its relationship with the propagation constant, $\alpha + j\beta$.

Buchanan[7] has recently devised null methods used successfully for accurate measurements of both α and β in liquid or solid materials of biological interest at frequencies near 10^{10} and $2{\cdot}4 \times 10^{10}$ c/s. In one method, one output from an oscillator feeds via wave-guide to a liquid cell and another to a cut-off attenuator. The outputs of both feed the arms of a hybrid tee from which the combined signal goes to a wave-guide mixer. Using a receiver as detector, phase and magnitude balance of the two signals is obtained at as many consecutive wavelengths in the cell as possible. Accurate measurements of α and β are thus obtained. A modification of this method using a probe at two fixed points in a sample of material in a short-circuited wave-guide section can be used for both liquid and solid specimens with a wide range of loss characteristics. A method described by Collie and others[8] has provided accurate results for the dielectric constant of water and ionic solutions. This method involves direct measurement of α in two specimen-filled wave-guides, the dimensions of which are chosen to be just above, and just below, cut-off. The method has also been used recently for measurements on protein solutions.[9]

For measurements on liquid biological materials[10] at frequencies in the range $1{\cdot}5 \times 10^9$ to 5×10^9 c/s it has been found convenient to use a method which is the coaxial version of a twin-line method employed for investigations on water and ionic solutions by Knerr[11] and Cooper.[12] In this method, the signal strength in an air-filled section of line is dependent on the position of a movable short-circuiting plunger in an adjacent specimen-filled section. Observations of plunger position and the corresponding signal strength when the latter passes through minimum and maximum values provide directly the propagation constant of the wave in the specimen.

England[13,14] has reported the use of the Roberts and von Hippel method for measurement of the microwave dielectric constant of human tissue specimens. In this method the standing wave set up in an air-filled section of wave-guide or coaxial line terminated by a specimen-filled short-circuited section is measured. England employed different sets of wave-guide apparatus for each frequency used and found it convenient to use half-wavelength distrene transformers between the specimen and air-filled sections. Cook[15] has also investigated the dielectric behaviour of human tissues at microwave frequencies by means of the Roberts and von Hippel method. In these studies one coaxial line apparatus served for measurements on a single specimen over a range of frequency from $1{\cdot}5 \times 10^9$ to 5×10^9 c/s. A feature of this adaptation was the use of a slotted Distrene-filled line in place of the usual air-filled slotted section. This overcame difficulties regarding the formation of a plane dielectric interface (involving some compression when soft tissues are concerned) without introducing complications arising from the need to cover in a single apparatus a wide frequency range.

For low loss materials, such as fatty acid esters and glycerides, much work has been done by the Roberts and von Hippel method using conventional air-filled slotted sections of wave-guide and coaxial line in which to make standing wave measurements. Resonant cavity methods are not suitable for dielectric measurements on high loss biological materials. However, Bayley[16] has employed a coaxial line resonator method for investigations of the dielectric properties of solid crystalline proteins over a frequency range centred near 3×10^9 c/s (7·3 cm to 15·3 cm wavelength). This method was chosen by Bayley because solid proteins have low dielectric loss and are only available in small quantities.

DIELECTRIC PROPERTIES OF WATER AT MICROWAVE FREQUENCIES

By far the most abundant and probably the most important biological material is water. Any biophysical study, therefore, in the microwave region should be preceded by an investigation of the dielectric properties of water at these frequencies. A considerable amount of work on these lines has been carried out but, unfortunately, many early investigators used damped waves, and techniques used more recently have not always been conducive to accuracy. Collie, Hasted and Ritson,[8] however, have published a comprehensive series of experimental results of considerable accuracy on water between wavelengths 1 cm and 10 cm (3×10^{10} and 3×10^9 c/s) and at various temperatures. More recently Cook,[10] using quite different techniques, has confirmed the results. Some examples of the values of the complex dielectric constant are shown in Tables 1 and 2.

In analysing these results, it can be assumed that the only effect contributing to the loss is orientation polarization, ionic conductivity and resonance being effectively absent. On this assumption, the results can be studied in terms of Debye's[17] theory of dispersion in polar liquids, from which the relaxation time of the process concerned can be derived. Some values of the relaxation time so derived are shown in Table 3.

Table 1. *Dielectric constants for water at different wavelengths at 20° C*

Wavelength (cm)	ϵ'	ϵ''
10·00	77·7	13·0
6·48	74·0	18·8
3·195	61·5	31·6
1·262	31·0	35·7

Table 2. *Dielectric constants for water at 3·195 cm*

Temperature (° C)	ϵ'	ϵ''
0	(43·4)	(41·1)
5	49·6	39·2
10	54·4	37·1
20	61·5	31·6
30	64·8	25·6
40	65·5	20·9
50	64·6	17·0

Table 3. *Relaxation time for dipolar orientation in water*

Temperature (° C)	*Cook*[10]	*Collie and others*[8]
0	$1{\cdot}78 \times 10^{-11}$ sec	$1{\cdot}77 \times 10^{-11}$ sec
10	1·28	1·27
20	0·93	0·96
30	0·72	0·74
40	0·60	0·59
50	0·50	0·48

Single values are given in Table 3 but, as pointed out by Cook, the experimental results are equally consistent with the existence of a small spread of relaxation times in water. Such a small distribution of relaxation times can be invoked to link the experimental microwave and long infra-red dielectric constants without introducing any additional dispersion process between the two parts of the spectrum.

Further analysis indicates that the relaxation process in water is closely linked with the rupture and formation of hydrogen bonds. Large increases in the relaxation time of water have been shown[18,19] to take place in mixtures of water with dioxan, a substance with which water forms hydrogen bonds. The influence on the water relaxation time of hydrogen and other types of intermolecular bonding between the water and other molecules and groups (particularly those of biological interest) is being investigated further by Hasted, Haggis and Buchanan.

DIELECTRIC PROPERTIES OF BODY TISSUES AT MICROWAVE FREQUENCIES

The use in medicine for therapeutic tissue heating of condenser field methods has led to a number of studies of the dielectric properties of animal tissues in the "radio" range of wavelengths from 3 to 20 m and beyond (see, for example, Rajewsky[20] and Iwase[21]). In the microwave region, much less information is available (England and Sharples,[13] England,[14] Cook[15,22]). Dielectric measurements in this range on blood, the

tissue with the best known structure, are of particular interest. Typical results[10] for whole human blood are shown in Fig. 1 together with comparable results for pure water at the same temperature.

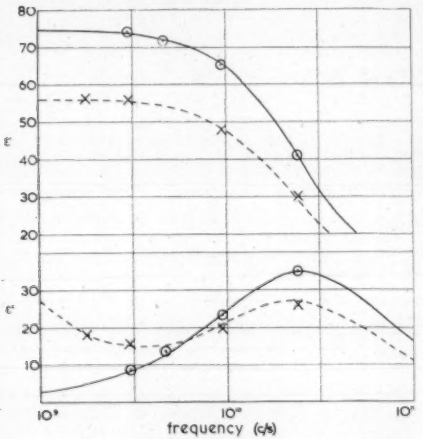

Fig. 1. Variation with frequency of ϵ' and ϵ'' for pure water and whole human blood at 35° C

Experimental points: ○ = water; × = blood.
Theoretical: Full curves—water;
broken curves—blood.
(From reference 10.)

Comparison indicates that the dispersion region of ϵ' for blood is the same as that for water and is due to the orientation polarization of the water molecules present in the blood. Variations in ϵ'', however, suggest that there is another contribution to the dielectric loss in addition to the water molecule relaxation. As the relaxation time of protein molecules is in the region of 10^{-7} sec, it is safe to assume that this relaxation makes a negligible contribution in the microwave region. The additional loss is, therefore, that due to ionic conduction. It has been reported[22] that the blood results satisfy the Debye dispersion equations if an additional term allowing for ionic conductivity is included. It has also been shown[10] that the microwave ionic conductivity and dielectric constant, ϵ', of whole blood are consistent with Danzer's[23] extension of Wagner's[24] dispersion theory for inhomogeneous dielectrics. This theory explains approximately the large drop in ϵ' (from about 5 000 at low frequencies to about 56 at microwave frequencies), and the attendent increase in specific conductivity as the frequency increases. Wagner's theory leads to dispersion equations of the same form as the Debye equations, with a time constant (relaxation time) related to cell membrane and intracellular fluid constants.

Further analysis of the results has also yielded estimates for human erythrocytes of intracellular haemoglobin hydration and the ionic conductivity of the intracellular fluid. This is probably the first experimental determination of haemoglobin hydration in human erythrocyte contents without destruction of the cells. The estimates of hydration and ionic conductivity depend very much on the validity of theories for inhomogeneous media. That of Fricke[25] has been used in this case and has given results in accord with expectations.

Turning now to solid human tissues, England[13, 14] has made dielectric measurements on specimens of skin, fat, bone, and some tumour tissues at 10·0, 3·2 and 1·27 cm free-space wavelengths. Cook[15] has also investigated various types of normal and pathological human tissues at wavelengths between 6 and 17 cm. Results obtained at 10·07 cm wavelength are shown in Table 4.

Table 4. *Dielectric constants of human tissues*

Wavelength, 10·07 cm; temperature, 37° C

	ϵ'	ϵ''
Skin		
(*a*) Breast	40·0	12·3
(*b*) Sole of foot	42·4	13·1
(*c*) Near faecal fistula	51·1	15·2
Muscle		
(*a*) Pectoralis major	50·0	17·1
(*b*) Soleus	51·0	18·0
Fatty tissues		
(*a*) Breast (normal)	3·94	0·87
(*b*) Breast (fibrosed by X-rays)	14·7	3·95
(*c*) Abdominal wall	4·92	1·46
(*d*) Near faecal fistula	7·0	1·75
Bone		
Mid-tibia	8·35	1·32

The properties of skin and muscle may be interpreted in very much the same way as those of blood, namely in terms of water molecule relaxation and of ionic conductivity. As before, the dispersion effects of inhomogeneity appear to be negligible at microwave frequencies. The microwave results have been shown to be in accord with estimates of dielectric constant and loss calculated from the known chemical composition of these tissues, approximate protein hydration and extra-cellular fluid volume.

Fatty tissues and bone present a much more difficult problem. In general the fluid contents are lower than for skin and muscle and vary quite considerably from one specimen to another. Furthermore, it seems possible that dispersion in the microwave region due to inhomogeneity is superimposed on that caused by water relaxation in the case of these tissues.

It is interesting to note that in this series of observations the two specimens of pathological tissues, taken from near a fistula and from a fibrosed breast, show different dielectric properties from the corresponding normal. This is almost certainly due to a difference in water content.

DIELECTRIC PROPERTIES OF PROTEIN SOLUTIONS AND SOLID PROTEINS

Measurements made in the conventional radio-frequency range show that relaxation of protein molecules in aqueous solution occurs in the region of 10^6 to 10^7 c/s and that the dielectric constant, ϵ', falls to a steady value, ϵ^*, at frequencies lower than those of microwaves. The contributions to the dielectric constant and loss of such solutions from protein orientation polarization are, therefore, negligible at microwave frequencies. In physiological processes, however, the hydration of protein molecules in aqueous solution is of considerable importance. Hasted, Ritson and Collie[26] have shown that microwave measurements on ionic solutions can give estimates of the hydration of ions and recently Haggis, Hasted and Buchanan[9] have extended this idea to protein solutions. Measured dielectric constants of bovine serum albumin solutions satisfy the Debye equations with relaxation times as for water and with values of ϵ^* decreasing with increasing concentration. This decrement is interpreted as being due to the binding of a proportion of the water molecules to the protein in such a way as to prevent them contributing to ϵ^*. The experimental results of Haggis and others lead to a hydration of $0{\cdot}15 \pm 0{\cdot}1$ gram water/gram protein and suggest an elongated form of molecule. This figure is lower than that generally accepted, but it takes account only of non-relaxing water molecules and some of the molecules bound to the protein surface may be able to make a contribution to ϵ^*. Similar investigations have been carried out with methaemoglobin. Further work on other proteins and particularly on smaller molecules such as amino acids is now being carried out with a view to more detailed interpretation of protein structure and hydration.

Investigations of the dielectric properties of some solid crystalline proteins, amino acids and peptides have recently been reported by Bayley.[16] All the materials studied showed dispersion in the microwave region, possibly due to relaxation of polar groups or a resonance. However, Bayley remarks that it is not certain to what extent the dispersion is due to sorbed water.

TISSUE HEATING BY MICROWAVES

As long ago as 1890, d'Arsonval demonstrated that when currents of frequencies greater than 10 000 c/s were passed through the human body, there was no muscular contraction, but heating of the tissues resulted. Since that time, tissue heating by high-frequency currents has been a routine procedure in physiotherapy. In the early 1930's the development of valves capable of oscillating at high powers in the 30 Mc/s range led to the use of induction and condenser field heating at these frequencies.

With the introduction of the cavity magnetron, extending the frequency range to 3 000 Mc/s and over, the investigation of the clinical possibilities of these radiations followed naturally. The early development of these investigations was largely due to Krusen and his collaborators.[27, 28] In this work the generator consisted of an air-cooled continuous wave magnetron from which the energy (free-space wavelength 12 cm) was fed by a coaxial cable to a director system. The latter, in most cases, consisted of a dipole with a reflector in the form of a hemisphere from 4 to 6 inches in diameter. During irradiation the director is placed a few centimetres away from the skin surface, and skin and subcutaneous temperatures are measured by means of thermocouples immediately after switching off. With this arrangement, as with earlier forms of high-frequency heating, dosage measurement, in the accepted sense of the estimation of absorbed energy at points in the tissues, is almost impossible. This is largely due to the difficulties in predicting the propagation pattern of the radiation and the effects of surface reflection. Control is exercised in terms of the power output of the generator, the director-skin distance and the time of exposure, with the patient's sensation acting as a limiting factor. Using generator powers of the order of 50 to 100 W the American workers carried out extensive investigations on the temperature rises produced in animals and humans and on the effects of the irradiation on blood circulation.

A considerable advance towards the solution of the physical problems of microwave therapy is reported by Boyle and others,[29] and Cook.[30] In their original arrangement, pulsed radiation from a radar set is transmitted directly by way of rectangular wave-guide to applicators (wave-guide flare, etc.) in contact with the tissues. The introduction of a mismatch unit ensures that all energy passing through the guide enters the tissues. This energy can be measured by means of a calibrated wattmeter, thus providing a physically sound dosage system. Owing to the utilization of all the transmitted energy in this method, powers required for therapeutic heating are much lower than when the applicator or director is used at a distance from the skin. A further advantage of the contact applicator method is that, by placing a fine wire thermojunction across the aperture, at right angles to the electric field vector, there is no direct heating of the couple due to field pick-up and so skin temperatures can be measured during exposures.

Recently in the writers' laboratory, a mobile continuous wave apparatus has been constructed, in which the microwave power at 9·4 cm wavelength is fed by way of a flexible coaxial cable to interchangeable rectangular and circular wave-guide applicators. This makes a very suitable arrangement for clinical trials of microwave heating (Fig. 2).

The results published by Cook[30] show that with an input power of the order of 0·5 W per cm^2 the skin temperature rises by about 10° C and then remains constant. At higher powers, pain and burning intervene before the constant level is reached. Cooling is mainly due to blood circulation. This is demonstrated by occluding the circulation during exposure when the skin temperature rises almost linearly to the maximum tolerable level.

The variation of temperature with tissue depth is complicated by the differences in the dielectric properties of

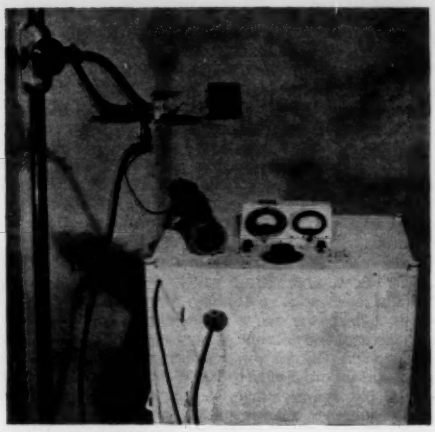

Fig. 2. Continuous wave set ($\lambda = 9{\cdot}4$ cm) for therapeutic applications, with power output up to 50 W

the tissue layers. This is illustrated in Fig. 3 by one curve taken from Cook's results. The curve refers to the application of 3 watts for 2 minutes over an area of 10 cm^2 on a human thigh. The effect of the presence of a 6 mm layer of fat of lower dielectric loss than skin and muscle is clearly shown in the trough of the curve.

For the purpose of microwave propagation, the tissues may be regarded as a series of layers of homogeneous material with different dielectric constants and reflection coefficients. Using the dielectric measurements described earlier it is then possible to calculate the electric field distribution in the tissues along the radiation beam axis. The energy absorption at any point is then proportional to $(\text{field})^2 \times \epsilon''$ and so relative temperature rises can be estimated. The result of such a calculation for the particular example of the human thigh mentioned above is shown in Fig. 3. Heat flow is ignored in the calculation, but its effect would be expected to smooth the theoretical curve to the shape of that observed experimentally. Recently,[30] a more detailed analysis has been made of the experimental results of tissue heating by microwaves in terms of absorbed energy distribution and of linear heat flow in the irradiated region. For short exposures the skin temperature rises observed lead to a thermal conductivity of tissues of 0·005 cal cm^{-1} sec^{-1} $°C^{-1}$, a figure in fair agreement with normally accepted values. If the exposure is prolonged the effective tissue conductivity increases rapidly, indicating the induction by the heating of increased blood flow and hence the removal of heat by the blood to neighbouring tissues.

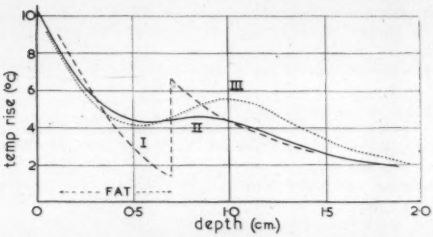

Fig. 3. Variation of tissue temperature with depth in human thigh after 10 cm microwave exposure

Curve I—calculated (neglecting heat flow).
II—experimental, after 2 min exposure.
III—experimental, after 4 min exposure.

RESONANT ABSORPTION IN THE MICROWAVE REGION

In common with other parts of the electromagnetic spectrum, the idea of specific biological action in the radio wave range has long seemed attractive. Many claims to such specific action and therapeutic usefulness of high frequency currents corresponding to wavelengths in the 5–100 m range have been made. Although few workers interpreted the term "specific action" precisely, the phenomenon sought was essentially that of resonance absorption by vital biological molecules. Thus, if sufficiently strong, it was hoped that such absorption could lead to the inactivation of disease-producing organisms or molecules in vivo at a particular frequency, without causing a large general rise in temperature of the treated tissues.

Claims made by other workers for specific action at different frequencies were investigated by Curtis, Dickens and Evans,[31] who showed that all the observed effects could be attributed to general tissue heating by ionic conduction currents.

The fundamental approach in the search for resonant absorptions is by dielectric constant measurements using low radiation power levels. A report by Dryden and Jackson,[32] suggesting a possible resonant absorption in the microwave region by methyl palmitate, led to dielectric studies of this fatty acid ester with a view to extension to the more biologically-important glycerides. An investigation on methyl palmitate in the microwave region, using a number of frequencies greater than was used by Dryden and Jackson and covering a wide temperature range, was reported by Cook and Buchanan.[33] Their results are summarized in Fig. 4. The plateau in the ϵ' curve round about 4×10^9 c/s, where ϵ'' is a maximum, suggests a resonance absorption mechanism. This suggestion is supported by the fact that the frequency of the absorption peak is independent of temperature and that the plateau in the ϵ' curve persists at low temperatures. On the other hand, the variation of the peak loss with temperature is the opposite to that which would be expected from resonance alone. It has been suggested that the results might be due to both a relaxation and a resonant absorption process occurring together in the microwave region. Further work on other fatty acid esters and related compounds is being carried on by Buchanan and will be reported in due course.

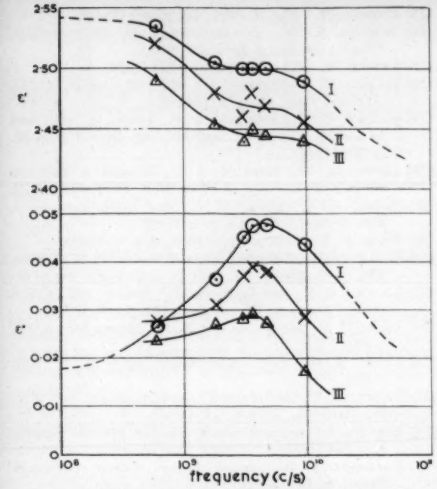

Fig. 4. Variation of the dielectric constant, $\epsilon' - j\epsilon''$, of methyl palmitate with frequency and temperature
Curve I: 22° C; Curve II: 0° C; Curve III: −20° C.

BIOLOGICAL EFFECTS OF MICROWAVES

All work on the biological effects of microwaves so far reported can be explained on the basis of general heat production in the extra- and intra-cellular fluids of tissues, or in the suspension medium of biologically-active agents when these have been irradiated in vitro.

For example, the irreversible biological changes produced in animals by various American workers occurred only when the tissue temperatures exceeded a critical level. The same changes could presumably be produced by other thermogenic agents, and point to no specific action of microwaves.

In some preliminary experiments Boyle and others[29] irradiated about 9 cm² of an animal's leg at 8 W for 5 min. No general effects on the animal were observed, but the limb became rigid, swollen and discoloured at the site of application. Post-mortem coagulation necrosis was observed in the subcutaneous tissues, an effect which would be expected from any heating process. Clark[34] has summarized and analysed a number of other observations on intense microwave heating of living tissues. He demonstrates the serious tissue damage which can be caused, particularly in organs such as the eye lens and the testes, which have small blood and nerve supplies. One of the dangers suggested by Clark is that with radiations of the order of 10 cm wavelength, a positive temperature gradient may be set up in the tissues, the deeper structures being at a higher temperature than the skin with its warning mechanism of pain. It has, however, been pointed out[30] that this should only occur under very exceptional conditions in which the skin is vigorously cooled by external means. Under all normal conditions of irradiation no tissue is subject to a greater temperature rise than the skin and this in general will not tolerate a temperature of more than 45° C.

A few attempts have been made to destroy malignant tumours in animals by means of microwave heating. Superficial tumours in mice have been irradiated (10 cm microwaves) using a modification of the wave-guide contact applicator described previously. Regression of tumours has been observed, presumbly due to coagulation following the heating. England[37] has obtained similar results when irradiating small rat tumours with 3 cm microwaves. Insufficient evidence has been obtained to estimate the future possibilities of this process.

De Seguin and others[35] have reported the biological effects of microwaves of 21 cm wavelength. The effects on microbes in vitro, tissue cultures and laboratory animals were all found to be due to general heating.

An attempt to destroy a virus by specific microwave absorption is reported by Epstein and Cook.[36] In one series of experiments small quantities of material containing the virus of the Rous fowl sarcoma were placed between mica sheets, mounted in a wave-guide and irradiated with 10 cm microwaves. During irradiation the temperature was allowed to rise freely. Under these conditions absorption of energy by dipolar orientation and ionic conduction in the medium surrounding the virus particles will be very high and will result in considerable temperature rises. After irradiation the virus material was found to be incapable of producing tumours, its activity having been destroyed by the heating. In a second series the specimens were maintained at −70° C by means of solid carbon dioxide. At this temperature absorption by ionic conduction and dipolar orientation in the medium or in the virus itself is negligible. Epstein and Cook found no evidence of inactivation of the virus under these conditions, indicating that in the frequency range used there is no specific resonant absorption.

The results up to the present of irradiations of biological materials by microwaves at relatively high power may be summarized thus: (*a*) no evidence has yet been produced of any specific biological effects other than heating due to ionic conductivity and dipole orientation; (*b*) heating of tissues takes place to an extent depending on the nature and depth of the tissues, but under all normal conditions the greatest temperature rise is in the skin which serves as a warning mechanism of possible ill effects.

REFERENCES

(1) DAILY, L. E. *Navy Med. Bull., Washington*, **41**, p. 1052 (1943).
(2) FOLLIS, R. H. *Amer. J. Physiol.*, **147**, p. 281 (1946).
(3) LIDMAN, B. I., and COHEN, D. *Air Surgeons' Bull.*, **2**, p. 448 (1945).
(4) VON HIPPEL, A., and BRECKENRIDGE, R. G. *N.D.R.C. Report*, 14–122 (1943).
(5) JACKSON, W. *Trans Faraday Soc.*, **42A**, p. 91 (1946).

(6) REDHEFFER, R. M. *Technique of Microwave Measurements*, Chapter 10 (New York: McGraw-Hill Book Co., Inc., 1947).
(7) BUCHANAN, T. J. In preparation.
(8) COLLIE, C. H., RITSON, D. M., and HASTED, J. B. *Proc. Phys. Soc.*, **60**, p. 145 (1948).
(9) HAGGIS, G. H., BUCHANAN, T. J., and HASTED, J. B. *Nature*, **167**, p. 607 (1951).
(10) COOK, H. F. Thesis, University of London (1951).
(11) KNERR, H. W. *Phys. Rev.*, **52**, p. 1054 (1937).
(12) COOPER, R. *J. Instn Elect. Engrs*, **93**, Pt. III, p. 69 (1946).
(13) ENGLAND, T. S., and SHARPLES, N. A. *Nature*, **163**, p. 487 (1949).
(14) ENGLAND, T. S. *Nature*, **166**, p. 480 (1950).
(15) COOK, H. F. *Brit. J. Appl. Phys.* **2**, p. 295 (1951).
(16) BAYLEY, S. T. *Trans Faraday Soc.*, **47**, p. 509 (1951).
(17) DEBYE, P. *Polar Molecules* (New York: The Chemical Catalog Co. Inc., 1929).
(18) HASTED, J. B., HAGGIS, G., and HUTTON, P. *Trans Faraday Soc.*, **47**, p. 577 (1951).
(19) COOK, H. F. *Trans Faraday Soc.*, **47**, p. 751 (1951).
(20) RAJEWSKY, B. *Radiology*, **31**, p. 697 (1938).
(21) IWASE, Y. *Theory and Application of High Frequency Phenomena* (edited by Y. Asami), p. 21 (Hokkaido University, Japan, 1950).
(22) COOK, H. F. *Nature*, **168**, p. 247 (1951).
(23) DANZER, H. *Ann. d. Phys.*, **20**, p. 463 (1934).
(24) WAGNER, K. W. *Die Isolierstoffe der Electrotechnik*, Chap. 1 (Berlin: J. Springer, 1924).
(25) FRICKE, H. *Phys. Rev.*, **24**, p. 575 (1924).
(26) HASTED, J. B., RITSON, D. M., and COLLIE, C. H. *J. Chem. Phys.*, **16**, p. 1 (1948).
(27) KRUSEN, F. H., HERRICK, J. F., LEDEN, U. M., and WAKIM, K. G. *Proc. Staff Meeting, Mayo Clinic*, **22**, p. 209 (1947).
(28) LEDEN, U. M., HERRICK, J. F., WAKIM, J. G., and KRUSEN, F. H. *Brit. J. Phys. Med.*, **10**, p. 177 (1947).
(29) BOYLE, A. C., COOK, H. F., and BUCHANAN, T. J. *Brit. J. Phys. Med.*, **13**, p. 2 (1950).
(30) COOK, H. F. *Brit. J. Appl. Phys.*, **3**, p. 1 (1952).
(31) CURTIS, W. E., DICKENS, F., and EVANS, S. F. *Nature*, **138**, p. 63 (1936).
(32) DRYDEN, J. S., and JACKSON, W. *Nature*, **162**, p. 656 (1948); JACKSON, W. *Nature*, **164**, p. 486 (1949).
(33) COOK, H. F., and BUCHANAN, T. J. *Nature*, **165**, p. 358 (1950).
(34) CLARK, J. W. *Proc. Instn Radio Engrs*, **38**, p. 1028 (1950).
(35) DE SEGUIN, L., CASTELAIN, G., and PELLETIER, M. *Rev. Sci. Paris*, No. 3294, p. 335 (1948).
(36) EPSTEIN, M. A., and COOK, H. F. *Brit. J. Cancer*, **5**, p. 244 (1951).
(37) ENGLAND, T. S. *British Empire Cancer Campaign Report*, p. 180 (1950).

ORIGINAL CONTRIBUTIONS

Characteristics of the hot cathode electron microscope gun

By M. E. HAINE, M.Sc., A.Inst.P., A.M.I.E.E., and P. A. EINSTEIN, M.Sc., Grad.I.E.E.,
Associated Electrical Industries Research Laboratory, Aldermaston, Berkshire

[*Paper received* 15 *August*, 1951]

Experiments have been carried out on hot cathode, high-voltage three-electrode electron guns. The brightness has been measured and found under optimum operating conditions to approach closely the value expected from the theoretical considerations developed by Langmuir. The effect of varying geometry over a fairly wide range is shown to be of secondary importance, except in as far as it influences the bias conditions and current efficiency. The mechanism of electron beam formation is discussed briefly.

The type of electron gun used on the electron microscope and, in some cases, other instruments such as the electron diffraction camera and high-speed cathode-ray oscillograph, consists (Fig. 1) of a tungsten hairpin filament as cathode, a modulator electrode or cathode shield, and an anode with a central hole to allow the beam to leave the gun. The electrodes are mounted coaxially and the shield is usually biased negatively with respect to the cathode, the anode/cathode voltage ranging from 20 kV to 100 kV or more.

The performance of this type of gun has been discussed by several authors. Hillier and Baker[1] described some peculiarities of the focused spot which occur under certain operating conditions. Ellis[2] analysed the gun performance by an approximate trajectory tracing method and showed that an image of the cathode would be formed between cathode and anode. Von Borries[3] described the measured properties of the electron microscope gun, giving curves of the performance in terms of various geometrical parameters. Modifications of the electron gun geometry to give a real instead of virtual focus were described by Bricka and Bruck,[4] Steigerwald,[5] Renaud,[6] and Ehrenberg and Spear.[7, 8] Only Bricka and Bruck have attempted to relate the brightness given by the virtual and real focus types of gun to Langmuir's[9]* theoretical limiting value; unfortunately, their experimental results are somewhat restricted and appear to be in error owing to the aperture used in the

* *Note added in proof:*

A paper by J. Dosse† has recently come to our attention in which the author attempts to correlate measured brightness with the theoretical value. Conclusions similar to ours in limited respects are reached but for a different type of electron gun.

† *Z. Phys.*, **115**, pp. 530–56 (1940).

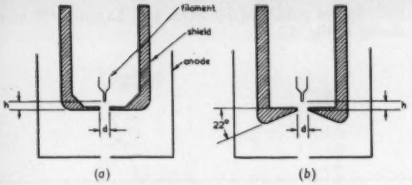

Fig. 1. Schematic drawing of high-voltage electron gun showing two shapes of cathode shield used

measurement of beam angle being too large in relation to other dimensions of their apparatus.

The object of the investigation described in the present paper was to obtain performance data for the high-voltage electron gun over a wide range of operating conditions and to relate the measured brightness to the theoretical maximum. It was found that the forms of the performance characteristics were very little affected by geometry and that for optimum operating conditions any geometry within wide limits gave a brightness very close to the theoretical value.

THEORETICAL PERFORMANCE

List of symbols.

- α total beam angle (radians).
- β brightness (amperes per cm^2 per unit solid angle).
- β_{max} maximum brightness.
- β_T theoretical brightness.
- d shield aperture diameter (inches).
- d_c source diameter (inches $\times 10^{-3}$).
- e electronic charge, e.s.u.
- ϕ_B bias potential (volts).
- ϕ_e most probable emission velocity (volts) in Maxwellian distribution at cathode.
- ϕ_0 final accelerating potential (volts).
- h filament height (inches).
- I_B total beam current (microamps).
- k Boltzmann's constant.
- T absolute temperature of cathode (° K).
- ρ_c specific emission at cathode (amperes per cm^2).

In most applications of electron guns the factors of interest are the current density per unit solid angle ("brightness") and the focused spot size. The maximum possible brightness was given by Langmuir[9] as

$$\beta_T = \frac{\rho_c e\phi_0}{\pi kT} = \frac{\rho_c \phi_0}{\pi \phi_e}$$

For constant values of ρ_c, ϕ_0 and ϕ_e, the maximum possible brightness is invariant and independent of the optical system employed. This invariance precludes the possibility of controlling the brightness by variation of magnification. The optics of any focusing system following the gun are determined only by practical requirements such as the required spot size and illuminating beam angle.

EXPERIMENTAL

Measurements of gun performance were taken on the apparatus shown schematically in Fig. 2. The experimental electron gun comprised a disk-type insulator capable of being operated up to 100 kV, and an arrangement allowing ready interchange of the electrodes. Adjustments to the filament for centring and height control could be made through insulating rods while the apparatus was running. Below the gun was a magnetic lens of magnification $\times 5$ in which a beam defining aperture could be inserted, and centred from outside

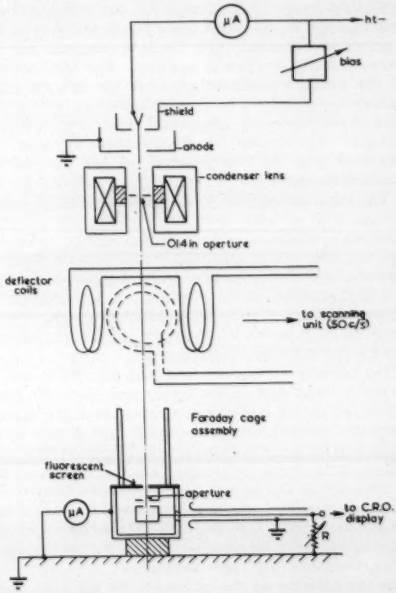

Fig. 2. Schematic diagram of experimental apparatus for investigating the characteristics of hot cathode electron guns

during operation. Following the lens was a Faraday cage containing a small aperture for the measurement of the beam current density. The beam was swept across this aperture by a magnetic deflecting system consisting of two pairs of coils at right-angles energized from a Selsyn unit with 50 c/s sinusoidal current. This arrangement allowed a rotation of the sweep to investigate the symmetry of the beam. The current entering the Faraday cage passed to earth through a resistor; the voltage drop across this was amplified by a variable gain amplifier and finally displayed on a cathode-ray oscilloscope against a 50 c/s sinusoidal time base, giving a trace (on a linear scale) of the current density distribution across the electron beam. The oscilloscope trace was

recorded, using a 35 mm camera, and subsequently analysed. It was found essential to take precautions against the loss of collected current by secondary emission, which could amount to 30%. This loss could not easily be prevented by biasing of the collector electrode as the energy of a large fraction of the secondary electrons is relatively high. A sufficiently high collection efficiency was, however, obtained by making the collector electrode a hollow cylinder having an entry aperture as small as possible. Means were provided for centring the various components of the apparatus.

The distribution of current density/unit solid angle in a focused image of the source (i.e. the minimum beam cross-section in the image space of the accelerating lens system) was obtained with the lens energized and the beam defining aperture in position. The axial position of the source was determined from the lens current, a calibration of current versus object distance having been carried out previously using a real object irradiated from the gun. The angular distribution across the beam was obtained with the lens switched off and the defining aperture removed.

The electrical supplies to the gun consisted of a high voltage unit, variable up to 100 kV and measured by a generating voltmeter, a 1 000 V bias supply, calibrated and variable, and an insulated accumulator to heat the filament, the heater current being adjustable by continuously variable series resistors. A d.c. supply for filament heating was chosen in preference to 50 c/s a.c., since the latter causes a high degree of beam modulation due to filament temperature ripple.

The brightness β was obtained from the current density in the focused spot at the screen and the solid angle subtended by the beam defining aperture at the screen. Since the defining aperture selected only a very small fraction of the beam from the gun the brightness measured is termed the "peak brightness," i.e. that corresponding to the peak of the approximately Gaussian distribution across the beam. Later on reference will be made to the maximum brightness; by this is understood the maximum value of the peak brightness obtained by varying some other parameter (e.g. bias voltage).

In the experiments the brightness for the fixed small aperture angle (5×10^{-3}), the source size, the total beam angle (at "half-height"), and the position of the source were measured for each gun geometry as a function of bias. These data were recorded for varying filament heights, and at each height for several filament temperatures. All of this was repeated for different shield aperture diameters, and for the two shapes of the shield electrode shown in Fig. 1.

The cathode temperature is of great importance since the brightness and cathode life are critically dependent upon it. A disappearing filament optical pyrometer was used to measure the cathode temperature. The accuracy of the latter measurements was checked with the aid of demountable cylindrical diode having two guard rings. The saturated current density obtained from samples of the wire used for the gun filaments was measured as a function of temperature. Good agreement was found with figures published by Jones and Langmuir[10] as is shown in Fig. 3.

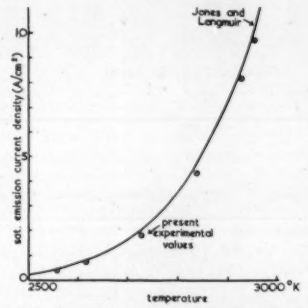

Fig. 3. Specific emission from tungsten wire according to present authors compared with results by Jones and Langmuir

Fig. 4 shows graphically a series of results for one electrode system (d = constant) for varying filament height. Three sets of curves show the brightness β, the total beam current I_B, and the beam angle α and source diameter d_c plotted against bias. At constant filament height and temperature, brightness increases quickly with decreasing bias from zero at "cut-off bias," to a maximum value, and thereafter falls slowly as the bias is further reduced. At the same time the total beam current increases rapidly. The total beam angle near "cut-off" is fairly constant, but rises rapidly for smaller bias as the bias is reduced. The source diameter is very nearly constant. The variations follow the same trends over a wide range of filament height. The maximum value of brightness is independent of filament height except at the extreme ends of the range depicted. The source diameter is also quite independent of filament temperature as is the beam angle at lower temperatures. The beam angle, however, increases with temperature at the higher temperatures (2 700–2 900° K). At constant bias and geometry as the filament temperature is raised the total beam current increases at first in proportion to the expected increase in cathode current density (ρ_c). Later the relationship becomes less than proportional, as is shown in Fig. 5(a). A similar relation holds between brightness and cathode current density. The falling off in the ratios of total current to specific emission (ρ_c), and the increase in the total beam angle as high temperatures and therefore high specific emission are reached indicate the onset of space charge effects. Over the proportional part of the temperature range the maximum brightness obtained equals the theoretical value (Fig. 5b).

Although filament height has little effect on the form of the gun characteristics, it considerably modifies the bias voltage for "cut-off" (Fig. 6), and the total current flowing at maximum brightness. Fig. 7 shows the

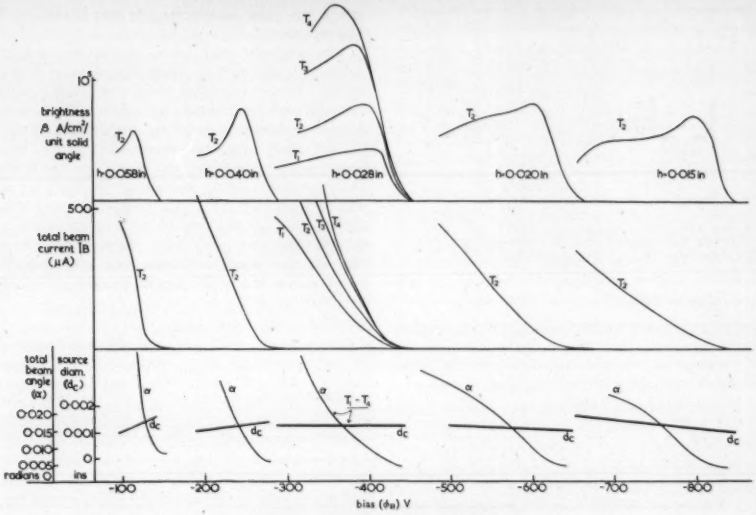

Fig. 4. Electron gun characteristics

Flat shield, $d = 0{\cdot}070$ in, $\phi_0 = 50$ kV, $T_1 = 2\,585°$ K, $T_2 = 2\,650°$ K, $T_3 = 2\,720°$ K, $T_4 = 2\,800°$ K.

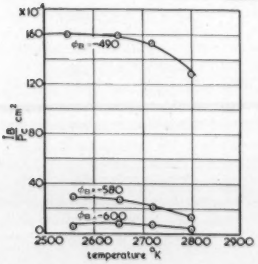

Fig. 5(*a*). Beam current/cathode current density ratio versus filament temperature at different values of bias

Flat shield, $\phi_0 = 50$ kV, $d = 0{\cdot}050$ in, $h = 0{\cdot}009$ in.

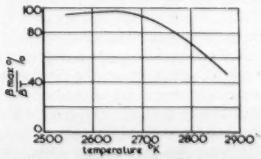

Fig. 5(*b*). Brightness efficiency versus filament temperature at optimum bias

Flat shield, $\phi_0 = 50$ kV, $d = 0{\cdot}050$ in, $h = 0{\cdot}009$ in.

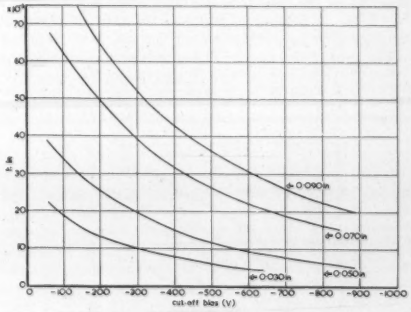

Fig. 6. Variation of cut-off bias with filament height for various shield hole diameters

$\phi_0 = 50$ kV.

variation of total current at maximum brightness with filament height for different values of cathode shield aperture diameter. For high current efficiency (ratio of maximum brightness to total current) a small height and small aperture diameter are necessary.

In Fig. 8 is shown the variation in axial position of the source (as seen from the condenser lens) with beam current, for different cathode heights. Within the limits of accuracy of the measurement of source position

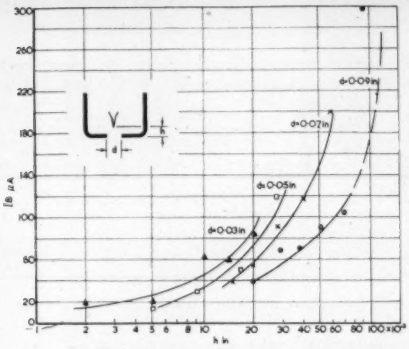

Fig. 7. Variation of total current for maximum brightness with filament height for various shield hole diameters

($T = 2\,650$ K.)

($\pm$ 1 mm) the source lies near the cathode close to "cut-off," moving towards the anode as the beam current is increased by reduction of the bias voltage. The dotted line (Fig. 8) refers to the re-entrant cathode shield (Fig. 1*b*) (used in the Metropolitan-Vickers types E.M.2 and E.M.3 electron microscopes) with the filament protruding 0·010 in through the shield aperture. The position of the source in this case reaches the anode at low bias. A separate experiment showed that this latter arrangement gave a current of 500 μA in a 70 μ half-width spot at the anode. This current and focused spot size is the same as obtained in the Ehrenberg–Spear[7] type of gun.

The intensity distribution across the focused spot never departed very far from Gaussian in these experiments. It was only when the gun was operated at a very low bias and low filament temperature that the multiple images reported by previous authors[1] were observed. On the other hand, the angular distribution of current density across the beam was of a Gaussian nature only at low beam current, becoming "hollow" as the bias was reduced. Fig. 9 shows successive traces illustrating the variation of the current density distribution across the electron beam with bias. Experiment also showed that the maximum brightness was proportional to the anode voltage in accordance with Langmuir's calculations.

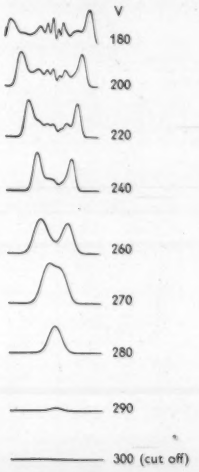

Fig. 9. Oscillograms showing distribution of current density in beam angle at different values of ϕ_B

$d = 0{\cdot}050$ in, $h = 0{\cdot}025$ in.

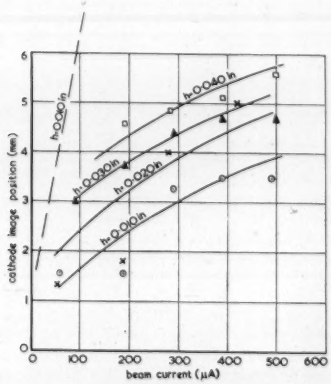

Fig. 8. Variation of cathode image position with beam current for various heights

——————— flat shield.
— — — — — — — re-entrant shield.
$d = 0{\cdot}050$ in, $\phi_0 = 50$ kV, T = const.

EFFECT OF FILAMENT MISALINEMENT

Misalinement of the filament tip in the shield causes a tilt of the beam leaving the gun. Bias, filament temperature and anode voltage have little effect on the tilt angle so produced, nor is there a change in brightness of the beam leaving the gun. The effect of tilt can be quite serious in an electron microscope, for instance, as the beam may fail to pass through the condenser aperture. Measurements show that a lateral shift of 0·001 in of the filament tip produces a tilt of the order of 0·002 radian. A practically simple method for the correction of tilt consists in moving the gun anode with respect to the cathode and cathode shield. The electrostatic pinhole lens formed by the anode aperture provides a correcting tilt which remains constant for all accelerating voltages.

DISCUSSION OF RESULTS

The most significant property deduced from the experimental results is that the high-voltage electron gun is capable of giving a brightness equal to the theoretical value. The maximum brightness is, therefore, dependent only on the cathode emission current density and the temperature. The maximum brightness begins to fall below the theoretical value at high temperatures, but at least up to the maximum practical operating temperature the deficiency is only small. It is practically possible, therefore, to obtain a brightness approaching $2{\cdot}5 \times 10^5$ A/cm^2 per unit solid angle at voltages between 50 and 100 kV. Such a figure is at least an order of magnitude greater than normally used in the electron microscope and would allow visual observation of objects at magnifications up to 250 000 times, if the objects would withstand this intensity (250 kW/cm^2 if all the energy were absorbed).

Variation of the geometry of the electron gun within wide limits has no other significant effect than to vary the current efficiency and the value of the bias required. From a practical point of view the use of high current efficiency is advantageous in requiring a lower total beam current and thus reducing the loading of the d.c. power unit, and the electrical smoothing required. However, high current efficiency entails a low total beam angle and requires more accurate gun alinement to ensure that the beam falls symmetrically on to the condenser aperture.

A comparison of the form of gun characteristics with those described by von Borries[3] shows a general agreement, though there are also certain discrepancies. Von Borries shows curves of brightness versus bias voltage, in which the brightness rises as the bias is increased from zero. The curve flattens off but does not fall again as in the experiments described here. It is possible that an insufficient range of bias voltage was covered. Von Borries also shows a marked variation in the focused spot size which was not found by the authors. It is possible to make serious errors when measuring the image size visually on a fluorescent screen or photographic plate since these have non-linear characteristics.

SELF-BIASING

There has been some confusion in discussions on electron guns as to the effect of self-biasing (automatic biasing), the bias being obtained from the voltage drop across a resistance connected in series with the h.v. supply. With this type of biasing an electron gun exhibits the property, frequently termed "saturation," whereby the current rises with temperature to a limiting value beyond which increase in temperature produces little increase in beam current. This has been attributed to the gun running into the space charge limited condition. That this is not so is readily seen when this type of bias is replaced by a variable, independent bias; no such effect then takes place. The actual operation of self-bias is illustrated by the curves of Fig. 10; curves *A* show the total gun current plotted against bias for different temperatures. The straight lines have slopes corresponding to various values of the bias resistor. The operating point for a particular value of resistor and temperature is the intersection of the corresponding straight line and the total current curve. The way in which the total current varies with temperature for a fixed bias resistor is illustrated in curves *B*. It is seen that the saturation effect results not from space charge limitation but from the form of the beam current-bias curves.

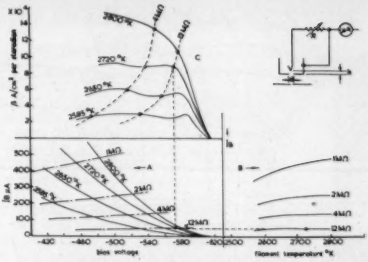

Fig. 10. Diagram illustrating operation of automatic bias
$d = 0{\cdot}050$ in, $h = 0{\cdot}009$ in, $\phi_0 = 50$ kV

The optimum value of bias resistor for a given geometry and temperature can be determined from the curves by drawing a vertical line from the maximum of the brightness curve *C* to intersect the corresponding total current curve *A*. The slope of the line from the zero of coordinates to the intersection corresponds to the required value of the bias resistor. In practice the bias for a given gun is so sensitive to changes in filament height that it is not normally possible to work from the curves in this way, since the height cannot simply be set with adequate accuracy; it is therefore desirable to arrange for the bias resistor to be variable.

THE MECHANISM OF BEAM FORMATION

The effect of bias on the gun performance is to restrict the area of the cathode from which electrons can be emitted. Resistor network[11] plots show that for a given bias the zero equipotential cuts the tip of the cathode in a ring (cf. Fig. 11). Behind this ring the surface field is negative and emission is therefore not possible here. At some value of bias the zero equipotential occurs just in front of or at the cathode tip so that all emission is suppressed, and the gun is "cut-off."

In the case of the high-voltage gun the filament tip is approximately spherical. (It is of importance when carrying out electron trajectory determinations for this type of gun to make allowance for the sphericity of the tip of the hairpin cathode. In separate measurements carried out on a replica of the Ehrenberg–Spear type of gun the beam angle was found to be several times larger than shown by Spear's[9] trajectory plots. The discrepancy almost certainly lies in his assumption of a flat cathode.) The surface field will be a maximum at the tip and fall off to zero at the point of intersection of the zero equipotential. Emission may be expected to become

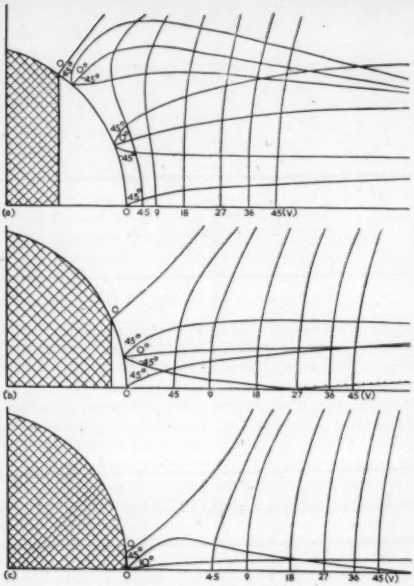

Fig. 11. Potential field and electron trajectory plots near cathode tip

Initial velocity 0·3 V. (*a*) at low bias (beam current = 500 μA); (*b*) at optimum bias (beam current = 100 μA); (*c*) near "cut-off" (beam current = 10 μA).

temperature limited at the tip, but there must always be some area of space charge limited emission close to the ring of intersection of the zero equipotential.

The general performance of the gun will be affected by several factors such as the geometry (particularly near the cathode), limitation of emission, space charge spreading of the beam, and the initial velocities of the electrons. The initial velocities are dependent only on temperature and enter the theoretical expression of brightness which is taken as the comparison standard. The other factors are more or less interdependent, making a full analysis of the mechanism of beam formation difficult.

It is possible to estimate whether the cathode is mainly space charge or temperature limited by measuring the sensitivity of the total current to filament temperature changes. If the cathode is entirely temperature limited, the current should vary in proportion to the specific electron emission as the temperature is raised, and if space charge limited, the relation should be rather less than proportional. Thus it was shown that below a temperature of the order of 2 700° K the beam was not significantly affected by space charge in any part of the bias range.

Since at the lower temperatures space charge cannot be invoked as the agent causing the brightness to fall below the theoretical value at either side of the maximum value, the departure must be explained by some other mechanism which affects one of the fundamental parameters in Langmuir's expression. A pure geometric aberration cannot do this; the explanation must be that the strong chromatic aberration of the accelerating system coupled with the energy spread of the emitted electrons reduces the component of current density from the electrons emitted with high velocity at a large angle with the axis. This effect is that of a chromatic filter, both reducing the current density and also the effective energy spread (ϕ_e), the former to a much greater extent, however. The actual mechanism takes place very close to the cathode, as illustrated in Fig. 11, which shows a series of trajectories (traced graphically).

For the optimum conditions (Fig. 11*b*), the electrons leaving the axis with a given radial velocity enter a more or less uniform field which is well known to produce small aberrations. Nearer to "cut-off" (Fig. 11*c*) the same electrons enter a strongly converging field which deflects them across the axis, whereas electrons leaving with smaller radial velocity enter a more uniform region of the field, and suffer no deflection across the axis. In the case of low bias (Fig. 11*a*) the "off-axis" field is divergent, again giving rise to aberration, though to a lesser extent.

It is of interest to note that for the condition at low bias (Fig. 11*a*) electrons leaving the cathode at some distance from the axis (zonal region) are given an outward radial component of velocity for points not too far from the axis; at points approaching the zero equipotential (marginal region) the electrons emitted with outward radial velocity components run into the strongly convergent field which deflects them across the axis. This is the mechanism which leads to the "hollow-beam" formation.

ACKNOWLEDGMENT

The authors wish to thank Dr. T. E. Allibone, Director of this Laboratory, for permission to publish this paper.

REFERENCES

(1) Hillier, J., and Baker, R. F. *J. Appl. Phys.*, **16**, p. 469 (1945).
(2) Ellis, S. G. *J. Appl. Phys.*, **18**, p. 879 (1947).
(3) von Borries, B. *Optik*, **3**, p. 389 (1948).
(4) Bricka, M., and Bruck, H. *Ann. de Radioelec.*, **3**, p. 339 (1948).
(5) Steigerwald, K. H. *Optik*, **5**, p. 469 (1949).
(6) Renaud, P. *J. de Physique et le Radium*, **11**, p. 619 (1950).
(7) Ehrenberg, W., and Spear, W. E. *Proc. Phys. Soc. B.*, **64**, p. 67 (1951).
(8) Spear, W. E. *Proc. Phys. Soc. B.*, **64**, p. 233 (1951).
(9) Langmuir, D. B. *Proc. Instn Radio Engrs*, **25**, p. 977 (1937).
(10) Jones, H. A., and Langmuir, I. *Gen. Elect. Rev.*, **30**, p. 310 (1927).
(11) Liebmann, G. *Brit. J. Appl. Phys.*, **1**, p. 92 (1950).

Radioassay of potassium in solid samples

By O. J. Russell, B.Sc., A.Inst.P., Norwich, Norfolk

[*Paper first received* 13 *June*, 1950, *and in final form* 6 *February*, 1951]

Powdered samples are assayed for potassium by the use of a Geiger counter designed for liquid samples. With precautions, the statistical accuracy expected in considerations of counting random events is achieved satisfactorily. A pure potassium compound is employed as an "absolute" standard of potassium content, obviating the use of calibrating solutions or synthetic standard mixtures. Full advantage of this is taken by employing a density correction, so that the use of an effectively "infinite" sample thickness, and hence large amounts of sample, is avoided. Unexpectedly, interference was experienced from uranium present in the phosphatic constituents of fertilizer samples tested. It was found possible to correct for this, and obtain satisfactory agreement with chemical determinations. The manipulation of powders instead of preparing solutions has advantages in rapidity for routine commercial or geological examination of many samples. Accuracy and sensitivity depend upon the usual statistical considerations encountered in radioactivity measurements. Good sensitivity and accuracy are attained without long counting periods, and it is considered that further developments are likely.

The chemical determination of potassium is generally a tedious and lengthy proceeding. Attention has been directed to determining natural potassium by the radioactivity of the long-lived K^{40} radio-isotope associated with all natural potassium from mineral, biological and commercial sources. Two methods of estimating potassium in this way have been described by Gaudin and Pannell,[1] and by Barnes and Salley.[2] These papers give justification of the procedure on the grounds of the invariant isotopic constitution of potassium from a variety of sources. Practically, the beta-radiation of 1·35 MeV maximum energy provides the means of detecting and estimating the K^{40} isotope, as 90% of the radiation consists of beta-particles, and these are much more efficiently detected by a Geiger counter than the small amount of gamma-radiation also emitted. The relatively small content of 0·012% of K^{40} in natural potassium enables the total potassium content to be determined through the easily measured beta-radiation.

Absorption effects are well marked with beta-radiation, and this constitutes a practical difficulty in the assay of beta-emitters. Gaudin and Pannell[1] employed a large amount of sample surrounding the counter, so that the thickness was effectively infinite. Barnes and Salley,[2] working with solutions, employed an empirical correction curve to allow for the effect of varying density of solutions.

A first approximation to the self-absorption effects[3, 4] in a thick sample of a beta-emitting substance, shows that the fractional activity $F = (1/\mu g)e^{-\mu g}$, where g is the sample thickness expressed in grams/cm^2, and μ is a constant for a given maximum energy of the beta-radiation. For K^{40} beta-particles, the maximum range (i.e. the thickness of sample effectively "infinite") is approximately 0·60 g/cm^2, but due to the exponential nature of the absorption curve, an addition x of sample so as to increase an initial "thickness" of 0·25 g/cm^2 to any extent whatsoever, can never increase the original counting rate by more than about 30%. The actual sensitivity of detection thus falls off with increasing sample thickness.

In view of the above considerations, the MRC type of solution-holding beta-sensitive Geiger counter, originally produced by Messrs. Alltools Ltd. (now succeeded by Nucleonic and Radiological Developments Ltd.) to the design of N. Veall,[5] seemed ideally suited. In estimating the very feeble "residual" radio-activity to be found in almost every mineral, the writer has found it convenient and simple to "pour" powdered mineral samples into the sample holding space of these tubes in the same way as a liquid sample.

For the present measurements, the large MRC2 counter-tube having a sample volume of about 16 ml was used so as to provide a reasonably high counting rate. In the MRC type of counter, a central thin-walled cylindrical counter having a nominal "thickness" of 0·035 g/cm^2, is surrounded by an integral close-fitting glass skirt, so that an annular sample space is formed between the outer glass skirt and central counting tube. The spacing from tube to skirt is 0·20 cm, so that with a sample density of unity, the sample "thickness" is 0·20 g/cm^2. This gives an optimum sample "thickness" for a large number of beta-emitters of moderate energies. The use of powders having a particle size very much less than the total effective range of the beta-radiation, gives a good approximation to a homogeneous medium, so that the effective or apparent density of the packed powder determines the absorption effects.

To obviate the use of calibrating solutions or known synthetic samples,[1, 2] pure potassium chloride of analytical reagent purity formed an "absolute" standard of potassium concentration, and any pure stable potassium salt would be equally suitable.

The MRC counter was shielded by a cylindrical lead shield 10 cm in diameter, and 3 cm thick, so as to reduce the cosmic-ray background to about 25 counts/min, which is half the normal unshielded background. An iron tube, 1 mm thick, directly surrounded the MRC2 counter-tube, so as to remove any possible radiation from contaminations in the lead, or from possible secondary electrons emitted under cosmic-ray action. Despite this, the background with a distilled water blank filling was slightly lower (27·4 counts/min) than for a completely empty tube (29·5 counts/min), an effect noticed also by Barnes and Salley.[2] The activities in the present work are so high that this difference is

negligible, but self-screening of the cosmic-ray background can be quite important in geological work upon feeble "residual" activities, and in determining traces of potassium.

Counting equipment consisted of a binary scaler by Messrs. Alltools Ltd. having a scaling factor of 1 024 operating from the output of their standard counter unit connected to the MRC2 counter-tube. Counting rates were so low, that coincidence or resolution losses were completely negligible.

Table 1. *Initial standardization*

sample	*observed c/min*	*apparent density*	*corrn. factor*	*corrected count*	*potassium count*
KCl std.	1 844	0·920	1·02	1 881	1 881
KCl std.	1 835	0·961	1·01	1 853	1 853
KCl std.	1 848	0·961	1·01	1 860	1 860
KCl std.	1 827	0·961	1·01	1 846	1 846
KCl std.	1 816	0·961	1·01	1 834	1 834
KCl std.	1 828	0·920	1·02	1 865	1 865
				Mean 1 857	± 0·36%

Samples were "poured" into the sample space of the MRC2 counter-tube, with gentle tapping so as to consolidate the powder, remove air pockets and to ensure a uniform distribution. The tube was always filled to a standard height, and the volume corresponding to this height determined in the usual way with distilled water run in from a burette. Samples varied in physical state from fine free-flowing crystalline powders (pure potassium chloride) needle-like crystals tending to adhere together (impure potassium chloride) to coarse-grained powders (fertilizers) and fine floury powders (apatite). It was found easy to treat all these almost as liquids, and a simple matter to remove all effective traces of a sample by shaking and tapping. In cases of doubt the tube may be washed, by shaking a small quantity of the next sample in the tube and rejecting that portion. After a test on the most active substance (pure potassium chloride), and tapping out the tube, the background count was found to be only one count above normal—a negligible degree of contamination. A counting time of ten minutes was adopted for the samples, and after counting each sample was weighed, so that the apparent density could be calculated. In routine work only the mass of sample would be required for any given volume of sample.

Density corrections for beta-ray absorption have been exhaustively examined and determined by Faul and Sullivan.[6] Fig. 1 gives a curve for K^{40} radiation derived from their data. This curve is taken as standard, but superimposed upon it are points derived from independent papers by Barnes and Salley,[2] N. Veall[5] and the present work, showing very close agreement. Only these subsidiary points are marked. The nearly straight line agrees with the expression quoted previously, which predicts as a first-order approximation that the relationship depends upon the reciprocal of density.

In comparing various samples for potassium content, it is in effect necessary to compare counting rates for

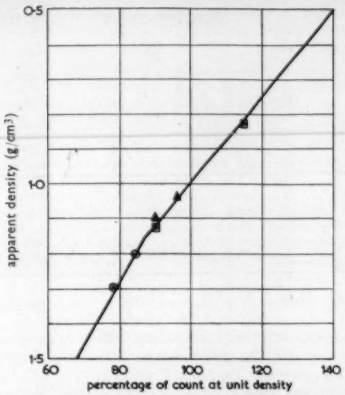

Fig. 1. Normalization curve for a constant percentage of potassium. Derived from Faul and Sullivan, with points derived from other workers superimposed.
○ Barnes and Salley. △ Veall. ⊡ Russell.

equal weights of sample. Therefore in addition to correcting counts to some standard density such as unity, it is necessary also to correct to a constant weight of sample. The corrections both depend upon sample density, and hence the weight of sample filling a given sample space, so they may be combined in a single correction curve. This is shown in Fig. 2, and as the two corrections tend to cancel out, the actual total correction is relatively small. Furthermore the curve shows that for densities greater than unity the correction becomes almost constant, which shows that the "infinite sample" and "non-weighing" technique of Gaudin and Pannell[1] is effective with thicknesses appreciably less than the maximum range of the beta-rays. The small "thickness" (0·030 g/cm²) of the MRC2 counter-tube represents a

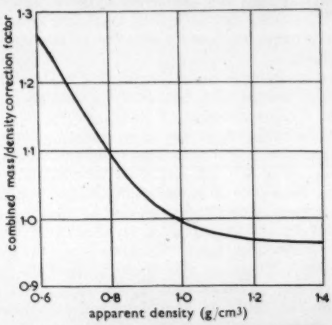

Fig. 2. Factor reducing counts to constant mass at unit density. Combined correction factor for absorption due to sample density and quantity of sample taken.

Table 2. *Analysis of samples*

sample	*observed c/min*	*apparent density*	*corrn. factor*	*density corrected count*	*uranium count*	*potassium count*	*calculated K_2O*	*chemical K_2O*
Impure KCl	1 723	0·914	1·02	1 757	Nil	1 757	59·8%	59·3%
Fert. A	420	0·910	1·02	428	119	309	10·5	10·0
Fert. A	417	0·910	1·02	426	119	307	10·4	10·0
Fert. B	234	0·828	1·065	249	127	122	4·4	4·4
Fert. B	252	0·996	1·00	252	117	125	4·5	4·4
Fert. C	301	0·942	1·01	304	110	194	6·8	6·5
Fert. D	292	0·918	1·02	297	130	167	5·6	5·3
Fert. E	374	0·936	1·01	378	109	269	9·4	9·5

negligible addition to the total absorption, and the curve of Fig. 2 was used to correct observed counting rates.

Calculation of the corrected counting rates for several standard determinations showed excellent agreement. The potassium content (calculated in the analytical convention as potassium oxide) of the impure commercial potassium chloride agreed very well with the chemical figure. However, the fertilizer samples gave results very much higher than the chemical determinations. It was then found that samples of apatite from which superphosphate is made were appreciably radioactive. It is well known that traces of uranium are associated with phosphatic rocks and minerals in small and almost constant amount, it having even been suggested that its constant amount is an indication of the uranium forming part of a complex structure. In view of this, several apatite samples from different dumps and consignments were measured. From the data of Faul and Sullivan[6] the correction curve for uranium radiation, where the uranium is present as an aged mineral, is almost identical with that for potassium. The counting rates were corrected using the correction curve (Fig. 2), and the final results show a surprisingly uniform activity. This activity corresponds[2, 6] to an approximate uranium content of 0·006%, and this uniformity should be further investigated, with more widely varied sources of apatite. All samples examined in the present work were from North Africa. It was then found that superphosphate derived from apatite showed an activity almost exactly that to be expected from the ratios of phosphatic content. It is understood that beyond the addition of a calculated amount of sulphuric acid to apatite, no further processing occurs, so that the superphosphate would presumably retain the original uranium activity, together with the associated decay products.

As phosphate determinations of both soluble (superphosphate) and insoluble (unchanged apatite) phosphates are a straightforward chemical procedure, and these determinations are a normal feature of fertilizer analysis, the available figures were used to determine the activity present in the fertilizer samples due to uranium introduced from the phosphate additions. These figures were then subtracted from the observed sample counting rates, thus giving the true counting rates due to potassium only. The potassium contents calculated from the corrected figures give very good agreement with the chemical figures. The deviations correspond to those to be expected upon statistical considerations, especially as the need to subtract the uranium correction increases the uncertainty over a simple determination of a single counting rate.

The unforeseen need for correction for the presence of a naturally occurring contaminating radio-element does not affect the general utility of radioactive methods of determining potassium. For fertilizer analyses, the question of the constancy of uranium content of phosphatic materials needs investigation before applying the method. In the analysis of commercial products and potassium salts generally it is clear that accuracy appears to be limited only by counting statistics. Statistical considerations cannot be treated here, but the curves of Fig. 3 show the counting times required under the

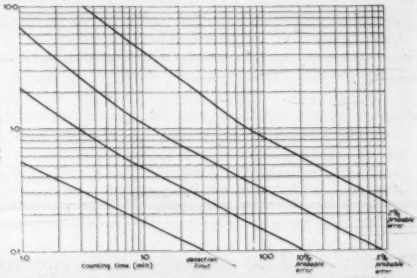

Fig. 3. Relation between counting time and precision for the conditions of tube sensitivity and background holding for the present measurements

experimental conditions of this paper, for varying statistical accuracies. In addition a "minimum detectable" amount of potassium curve shows the concentration of potassium equivalent to an increase equal to five times the probable error of a background determination. Fluctuations of this order occur only once in about a thousand determinations, so that an observed deviation equal or greater represents a practical test of the minimum detectable level of potassium concentration.

It will be seen that amounts down to 0·1% of potassium can be readily determined in a reasonable time, while amounts down to 0·02% can be detected. By various expedients it may be feasible to determine amounts down to about 0·02% and detect amounts of 0·003%. This would mean more sensitive tubes and provision of thicker shielding so as to reduce the cosmic-ray background to a greater extent. In the case of pure

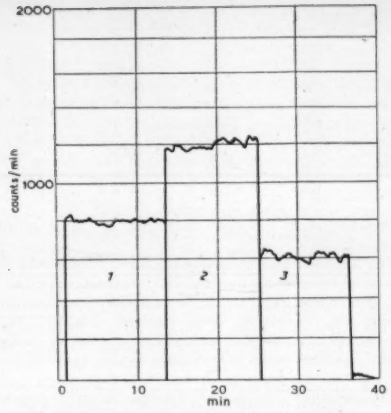

Fig. 4. Recording pure salts against counting rates.
(1) $KClO_3$. (2) KCl. (3) $KMNO_4$.
Reproduction of recording ratemeter chart.

samples of potassium salts, the purity should be checkable to about 0·5% of the actual potassium content. In this connexion, while spectrographic methods for estimating potassium are much more sensitive, the accuracy of the customary spectrographic methods does not increase greatly with concentration, whereas above the minimum detectable concentration, the radioactive method increases in precision with concentration.

A further advance lies in the use of a recording type of ratemeter to record automatically the activity of a number of samples. Despite the random fluctuations of the recording needle, the average position of the needle can be estimated quite closely by estimating the mean height of an extended length of recording, the accuracy corresponding to a count over an equivalent period of time. Using pure samples of potassium chloride, chlorate and permanganate their counting ratios were determined both on a ten-minute recording on a ratemeter and simultaneously on a scaler. The ratio chloride to chlorate from the chart recording was 1·60, and from the scaler figures 1·58 after density corrections. The chloride/permanganate ratios were 2·06 from both chart and scaler. The theoretical values of chloride/chlorate ratio and chloride permanganate are 1·64 and 2·12. Thus ratios of interest chemically can be determined by a radio-active counting method, while chart recording offers advantages in routine potassium determinations.

ACKNOWLEDGMENT

My thanks are due to the Directors of Nucleonic and Radiological Developments, Ltd., for permission to publish details of this work.

REFERENCES

(1) GAUDIN, A. M., and PANNELL, J. *Analyt. Chem.*, **20**, p. 1154 (1948).
(2) BARNES, R. B., and SALLEY, D. J. *Indust. Engng Chem. (Analyt. Ed.)*, **15**, p. 4 (1943).
(3) REID, A. F. *Preparation and Measurement of Isotopic Tracers* (Michigan: J. W. Edwards, 1946).
(4) FLUHARTY, R. G. *Nucleonics*, **2**, No. 5, p. 28 (1948).
(5) VEALL, N. *Brit. J. Radiol.*, **21**, p. 247 (1946).
(6) FAUL, H., and SULLIVAN, G. R. *Nucleonics*, **4**, No. 1, p. 53 (1949).
(7) RUSSELL, O. J. *Electronic Engng*, p. 100 (1948).

The study of the thermal behaviour of structures by electrical analogy

By G. BURNAND, M.Sc., Building Research Station, Garston, Watford, Herts

[*Paper first received* 24 *July*, 1951, *and in final form* 9 *October*, 1951]

The application of the analogy to the study of heating in dwellings, the maximum size of the units of capacity and resistance in the electrical models, and the methods of connecting up the model components are discussed. Electronic equipment for use with electrical models of houses is described briefly. Comparisons with observed temperature data in a room agreed with electrical model results when the model was modified to account for the presence of temperature gradients and hot air streams in the actual room.

In the electrical-thermal analogy the following are equivalent:

Thermal resistance, R_2.	Electrical resistance, R_1.
Thermal capacitance, C_2.	Electrical capacitance (a capacitor with one plate earthed), C_1.
Rate of heat supply, (dH/dt_2).	Electric current, (dQ/dt_1).
Temperature, θ.	Electric potential, V.

If m and n are defined by the following relations:

$$H = mQ \quad (1)$$

$$\theta = nV \quad (2)$$

then from the definitions of resistance and capacitance the following scaling equations may be derived:

$$C_2 = (m/n)C_1 \quad (3)$$

$$R_2 = (n/m)\,(dt_2/dt_1)R_1 \quad (4)$$

The thermal and electrical sets of units need only be consistent in themselves. For thermal units B.Th.U., °F, h, and practical electrical units, if 24 hours of the thermal system is represented by $\frac{1}{10}$ sec in the electrical system, then $(dt_2/dt_1) = 1\,200$. The factor (n/m) is chosen for convenience of model construction.

The analogy has been applied by Linvill and Hess[1] and Paschkis and Baker.[2] The present work follows more closely that of the former workers, except that the electronic equipment is more adaptable, allowing the introduction of outside temperature variation and the simultaneous observation of "temperature" and "heat supply," and an investigation of the accuracy of the method has been attempted.

The advantage of the use of analogous electrical models over full-scale heating trials is one of convenience; the components are easily changed and the time scale is reduced.

THE USE OF DISCRETE ELEMENTS OF RESISTANCE AND CAPACITANCE

Although the exact analogue of a layer of material is an inductionless transmission line, a thin layer of material can be represented by two equal resistances connected in series with a capacitor connected from the junction to earth. For economy in constructing a model it is important to fix the safe upper limit of size of such a "T" circuit. In the case of a sinusoidal potential applied to an infinite series of "T" circuits, with resistance R, and capacitance C, the characteristic impedance differs from that of the corresponding inductionless line by a fractional error of modulus $(\omega RC/8)$, when ωRC is small. For 50 c/s, the error modulus is less than 0·01 when RC is less than 250 $\Omega.\mu$F corresponding to 0·013 cycle. Also the attenuation in n "T" circuits differs from that of the corresponding inductionless line by a fractional error of modulus $(n/24)[\exp\sqrt{(\omega RC/2)}](\omega RC)^{3/2}$, when ωRC is small. For 50 c/s and n less than 10, the error modulus is less than 0·01 when RC is less than 250 $\Omega.\mu$F. The errors in representing a given layer of material, under similar boundary conditions, varies inversely with the square of the number of "T" circuits used. Unsymmetrical RC circuit elements show greater errors. While the errors for these special conditions are only a guide, in practice the presence of pure thermal resistances in the full scale and the surface resistances should reduce the overall errors of the behaviour of the model. For most materials a layer of $\frac{1}{2}$–1 in may be represented by a single "T" circuit.

An experimental check was made with a model of a 9 in brick wall with a constant heating rate instantaneously applied. The temperature curves were practically the same when four or eight "T" circuits were used, although considerable differences occurred when one or two units were used.

REPRESENTING ACTUAL STRUCTURES

Dwelling structures are mainly composed of uniform plane layers of material, and the directions of heat flow are normal to the surfaces. It is convenient to build the model up from models of plane uniform layers, using approximations when necessary. The thermal resistance and capacitance of each layer are calculated from its dimensions, and data of thermal conductivity and specific heat, and the equivalent electrical resistance and capacitance are found. If the layer is too thick to be represented by a single "T" element, the model is built up of a number of "T" elements that are not necessarily similar. A group of capacitors with the correct total capacity is used and they are linked up by resistances of proportionate magnitude; i.e. the total electrical resistance and capacitance R_1 and C_1 are subdivided into elements kR_1 and kC_1 such that $\Sigma k = 1$: it is necessary that $k^2R_1C_1$ should be sufficiently small for each "T" element. The adjustment of separate condensers to specified values is thus avoided. From a stock of fixed capacitors it is easy to select a suitable group within 2% of the correct capacitance. Small toroidal wire-wound rheostats form convenient adjustable resistance units, and are mounted with the capacitors on boards with spring terminals.

THE MODEL OF A ROOM

Since the inner surfaces of a room are exposed to roughly the same conditions, it could be expected that a model of a room could be formed by connecting in parallel units representing the walls, floor, ceiling, etc. This procedure can be justified theoretically if, as in Fig. 1(*a*), the "inner surface"

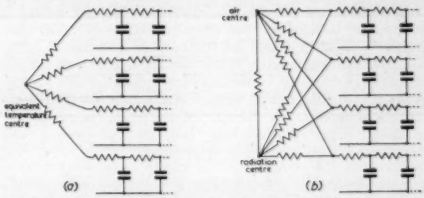

Fig. 1 (*a*) Equivalent temperature method of connecting the model.
(*b*) Connecting the model for the separate indication of air and radiation temperature.

of each unit is connected to a common point through the electrical equivalent of R_S/A, the surface resistance relative to unit area, divided by the area. If a varying current is then applied to the common junction of the "surface resistances," the potential there is proportional to the equivalent temperature in the full-scale room with a similarly varying heat supply.

The model can also be arranged to indicate air and radiation temperatures separately, if the temperature of the bulk of air in the room is uniform. As in Fig. 1(*b*), two resistances are connected to the "inside surface" of each model unit, R_R the equivalent of 1/[(radiation transfer coefficient) × (area)] and R_G, the equivalent of 1/[(convection transfer coefficient) × (area)]. All the R_R resistances are then connected to one common point, which we call the "radiation centre," and all the R_G resistances are connected to another common point, the "air centre." A radiated heat supply is equivalent to a current applied at the "radiation centre," and a convected heat supply is equivalent to a current applied at the "air centre." The potentials at these centres indicate the radiation and air temperatures in the room, respectively. The effect of ventilation is represented by a resistance connected from the air centre to earth.

Radiation from the water vapour and carbon dioxide in the air of the room can be represented approximately by connecting, between the radiation and air centres of the model, the electrical resistance equivalent of the thermal resistance $(1 - e_g)/(h_r e_g A_0)$, where e_g is the emissivity of the air in the room and A_0 is the overall surface area of the room, and h is the radiation transfer coefficient for the surfaces. At 60° F, 60% R.H., in a 12 ft cubical space we find $e_g = 0{\cdot}13$[3] and in this case the radiation exchange between the air and the room surfaces is of the same order as that between the floor and the rest of the room, for similar temperature differences.

THE MODEL OF A HOUSE

It would be possible to construct a model house room by room with separate units for each partition, etc. Since average results for the whole house are usually required, it is possible to represent all the external walls of similar structure by a single model unit, all partitions of similar structure by a single unit and so on. In this way the model is reduced to

manageable size. The units are connected to a common point through their respective surface resistances and an approximate average equivalent temperature, weighted according to the exposed area in each room, is given. The effect of ventilation is represented approximately by connecting a resistance between the equivalent temperature centre and earth.

With a complete house the induced temperature changes caused by the daily external air temperature alternation and solar radiation are of interest. For each external surface, it is necessary to represent the diurnal variation of sol-air temperature, which includes the effect of air temperature variation and solar radiation. This is done by injecting alternating currents of suitable amplitude and phase at the "outer surfaces" of the model units. An additional alternating current applied at the "inside" of the model takes account of direct penetration of solar heat through glazing, and ventilation by air at varying temperature.

DIFFICULTIES IN REPRESENTING ACTUAL CONDITIONS

Firstly, the accuracy of the model depends on the accuracy of data of thermal conductivity and specific heat for building materials. There is some uncertainty in these data because of the porosity of the materials and uncertainty of their water content.

Although the thermal capacitance of fittings and furniture is small and can be accounted for, the effect of shielding of walls and floors is uncertain. The effect has been ignored except with built-in cupboards for which approximate models can be made.

THE ELECTRONIC EQUIPMENT

The equipment can be divided into seven units, as in the block diagram, Fig. 2.

(*a*) the resistance capacitance network constituting the model,
(*b*) a stabilized power supply unit,
(*c*) an oscillator,
(*d*) a wave shaper, a triggered multivibrator,
(*e*) the output stages,
(*f*) a "thermostat," a potential limiting device,
(*g*) a double beam cathode-ray oscillograph.

The repetition frequency of the system is governed by the frequency of the oscillator signal. This is made low, 50 c/s, so that the effect of stray capacitances in the model network is reduced to a minimum. This entails the use of convenient ranges of resistance and capacitance in the model, 500 Ω to 1 MΩ and 0·001–0·5 μF.

The model is fed by the anode currents from the output valves, while the double beam cathode-ray oscillograph indicates the "temperature," i.e. the potential, at a point of the model and the "heat supply," i.e. the current input. The point of the model where the potential is to be observed is

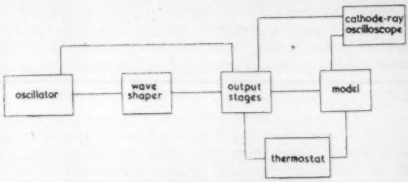

Fig. 2. Block diagram of the equipment

connected to one plate of the cathode-ray oscillograph, and the potential across the cathode resistance of an output valve is applied to the other plate, via a resistance capacitance coupling. Results are obtained as photographs of cathode-ray oscillograph traces, some of which are reproduced in Fig. 3. It is desirable that the output stages operate with high output impedance, and resistances of the order of 10 kΩ are used in the cathode circuits of the output valves which are normally high μ triodes.

CHECKING THE MODEL

Firstly, observations on a model of a 9 in brick wall, for instantaneously applied steady heat flow, were compared with calculations from a mathematical solution and agreement was found within experimental error.

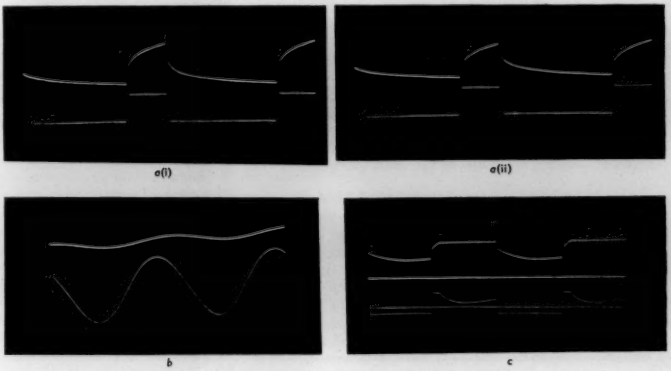

Fig. 3. Photographs from the electrical model

(*a*) Air temperatures for convection heating in the test room of the Heating Laboratory. The upper trace represents air temperature, and the lower the rate of heat supply.
(i) At 5 ft from floor; (ii) at 2 ft 6 in from floor.

(*b*) Infiltration of temperature variation into a high capacity house in winter with no internal heating. The lower trace represents a 10° F, 24 h period sine wave, from which outside temperature variations are derived, after adjustment of amplitude and phase. The upper trace represents the variation of average equivalent temperature in the house.

(*c*) Intermittent heating, 12 h on, 12 h off, with thermostat control, in a high capacity house. The lower traces represent the heat supply rate, the continuous line giving the mean value. The upper trace represents the average equivalent temperature, the continuous line representing the average temperature without heating.

The model was then checked against full-scale heating trials in a test room. Observation of air and equivalent temperature for transient heating of the test room of the Heating Laboratory, the Building Research Station, were available and were used.(4) The model of the room consisted of six units—wall area, ceiling, floor, windows, door, and air capacity—and was first arranged to record equivalent temperature (only eighteen separate capacitors were used in the whole model). The results of the tests are shown in Fig. 4, the curves being scaled to common heat input. The actual equivalent temperature for a radiant source lies above the model curve, while for tubular and convector heaters it lies below the model curve. The former disagreement may be explained by the position of the measuring instrument, a eupatheoscope, in the direct beam of radiation from the fire, but the difference found for the other heaters was not explained at this stage.

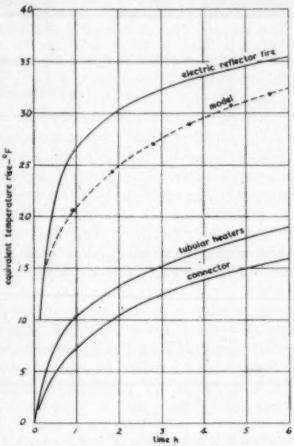

Fig. 4. Equivalent temperature in the Heating Laboratory;(4) heat input, 4·49 kW; ceiling height of test room, 11 ft 6 in.

The model was then modified to indicate air and radiation temperatures separately and a current was applied at the air temperature centre to simulate convection heating. It was found that the model air temperatures were greatly in excess of the actual observations, although the gradients of the temperature curves were similar. The radiation temperature indicated by the model (approximately the mean surface temperature for the test) was much less than the air temperature.

It was soon realized that the air temperature in a convection heated room would be reduced by the presence of hot air currents near the ceiling or walls. It was found that the model could be modified to take account of such air currents, provided that their velocity and temperature excess relative to the main body of air remain constant. It can be shown that the surfaces over which the currents flow receive, in effect, direct heat supplies. These can be represented by currents from additional ganged output valves, but it can be shown that some direct supplies may be simulated by injecting the supply currents at, or observing the potential variation at points in the surface resistances; not more than two separate current sources are then needed.

For the case of tubular heating it was possible to estimate the effective direct heat supplies from heat flow measurements recorded in other experiments.(5) When this distribution of heat supply was represented in the model, good agreement with actual observations was given, both for the room unventilated and for 3 air changes per hour.

It yet remained to obtain agreement for convection heating, and full-scale tests were carried out to provide complete data for a convection heated room. In these tests it was found that the air temperature gradient in the room was considerable, and remained nearly constant after half an hour. The coefficients of heat transfer by convection at the ceiling and wall surface were found to be 1·9 and 1·0 (B.Th.U.) $(ft)^{-2}$ $(h)^{-1}$ $(°F)^{-1}$ respectively. These were much greater than the normal values, due to the comparatively great air flow.

The direct heat supplied for the ceiling and walls was then estimated from the air temperature excesses at 2 in from their surfaces. Thus, relative to the average air temperature (θ_a) at 5 ft from the floor, the direct supply to the ceiling is found to be:

[Air temperature 2 in below ceiling $- \theta_a$] $\times$ [convection coefficient] $= 8{\cdot}4 \times 216 \times 1{\cdot}9 = 3\,440$ (B.Th.U.) $(h)^{-1}$, i.e. about 27% of the total heat input to the room, which was 12 600 (B.Th.U.) $(h)^{-1}$. The direct supplies depend on θ_a and if, as a basis, the temperature at 2 ft 6 in from the floor is chosen, the direct supply to the ceiling becomes 48%. The model results agreed well with the air temperature observations at both 5 ft and 2 ft 6 in from the floor (see Fig. 5.)

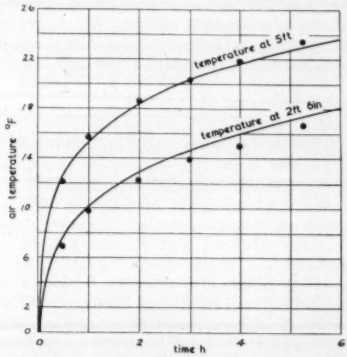

Fig. 5. Temperature curves from the photographs in Fig. 3(*a*), compared with points representing actual air temperature observations; heat input, 3·7 kW; ceiling height of test room, 8 ft 6 in.

CONCLUSION

It is found possible to work conveniently with analogous electrical models to an accuracy surpassing that of the data of the full scale. With them the design of structures can be studied from the point of view of intermittent heating; for instance, a study of intermittent heating conditions in whole houses has been made and has given useful results.

ACKNOWLEDGMENT

The work described in this paper has been carried out as part of the programme of the Building Research Board and the paper is published by permission of the Director of Building Research.

REFERENCES

(1) LINVILL, J. G., and HESS, J. J. *Massachusetts Inst. Technology Thesis* (1945).
(2) PASCHKIS, V., and BAKER, H. D. *Trans Amer. Soc. Mech. Engrs*, **64**, p. 105 (1942).
(3) MCADAMS, W. *Heat Transmission* (New York: McGraw-Hill Publishing Co. Inc., 1942).
(4) DUFTON, A. F. *J. Instn Heat Vent. Engrs*, **14**, p. 103 (1946).
(5) DUFTON, A. F., and MARLEY, W. G. *J. Instn Heat. Vent. Engrs*, **10**, p. 17 (1942).

The modulation characteristic of cathode-ray tubes in television*

By R. B. MACKENZIE, B.Sc.(Eng.), A.M.I.E.E., Research Laboratories, The General Electric Co., Ltd., Wembley, England

[*Paper first received* 19 *March*, 1951, *and in final form* 27 *August*, 1951]

The ambiguity which arises in defining the modulation characteristic of a television cathode-ray tube in terms of gamma is discussed. A method of eliminating this ambiguity is proposed, which is partly empirical, but leads to a simple mathematical treatment. Theoretical and actual characteristics for two different types of tube are compared; the effect of stray light and the variation with luminance of the sensitivity of the human eye are discussed. It is shown that, taking these factors into account, the error arising from the use of values derived by the proposed theoretical treatment instead of actual measured values is likely to be insignificant for many purposes. For greater precision, an extension of the system of definitions is suggested.

A factor of importance in the analysis of tone reproduction properties of a television system is the relationship between luminance (photometric brightness) and modulator volts in the reproducing cathode-ray tube. This relationship is often described in terms of "gamma," by analogy with photographic processes. There is, however, a lack of agreement as to how the gamma of a cathode-ray tube should be defined. The purpose of the present communication is to suggest a means by which the modulation characteristic of a tube used in television may be uniquely defined, to a sufficiently close approximation.

VISUAL RESPONSE CHARACTERISTICS

It is desirable in the first place to consider briefly the relationship between luminosity (apparent or subjective brightness) and luminance (physical or photometric brightness). If maximum picture luminance is assumed to be 15 foot lamberts, and adaptation luminance is estimated at 1 ft.l., the relationship is generally as shown in Fig. 1; one unit of luminosity represents a just distinguishable step. Hopkinson, Stevens and Waldram have given a general discussion of visual response characteristics† and Fig. 1 is taken from their paper.

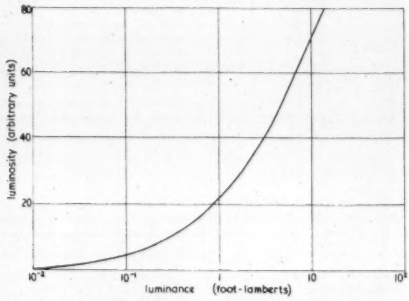

Fig. 1. Curve showing relationship between luminosity and luminance for television viewing (after Hopkinson, Stevens and Waldram)

* Communication No. 472.

† R. G. Hopkinson, W. R. Stevens and J. M. Waldram, *Trans Illum. Engng Soc.*, **6**, p. 37 (1941).

BLACK-OUT POINT

The gamma of a cathode-ray tube is defined generally as the slope of the (log luminance)/(log drive volts) characteristic luminance being measured on a normal television raster. The photographic analogy is, however, imperfect. In defining the cathode-ray tube characteristic an ambiguity arises of a kind which is not met with in photographic practice; i.e., for any given value of luminance the quantity described as drive voltage is dependent on the value of modulator/cathode voltage chosen as the zero or datum point. Conventionally, drive voltage is measured positively from black-out or cut-off voltage; this is variously defined as the voltage at which there is (*a*) no distinguishable luminance (i.e. zero luminosity) on a raster, (*b*) no distinguishable luminance on a spot, (*c*) no measurable luminance, or (*d*) no measurable beam current. According to the criterion adopted, the modulator/cathode potential designated as the black-out value may differ by several volts.

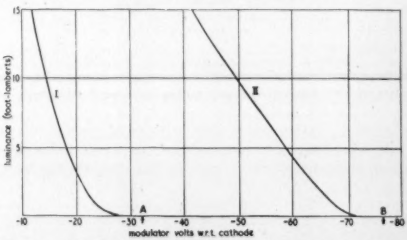

Fig. 2. Cathode-ray tube modulation characteristics. Curve I—Standard electromagnetic tube. Curve II—Special electrostatic tube developed for monitoring purposes. Points *A* and *B* indicate visual black-out points (raster)

Fig. 2 shows actual static characteristics. In Figs. 3 and 4 these curves are re-plotted on logarithmic coordinates. Curve I in each of these figures is derived by measuring drive voltage from the respective black-out points shown in Fig. 1. In Fig. 3 two additional curves (II and III) have been drawn to illustrate the effect when drive voltage is measured from points respectively 2 V negative and 2 V positive with respect to *A* (Fig. 2). The gradients at all points are seen to be considerably altered, and it is evident that to attempt to define the

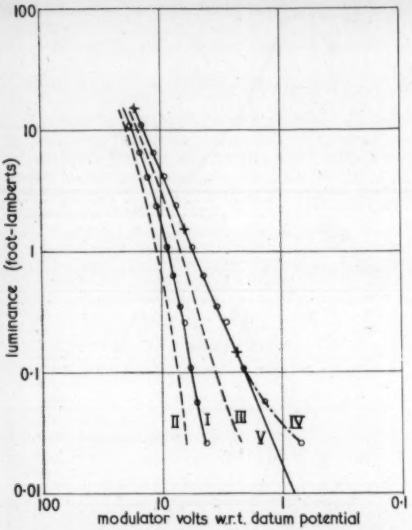

Fig. 3. Modulation characteristics of electromagnetic tube; voltage measured from different datum points

○ experimental points. + key points.

Curve No.	*Datum potential w.r.t. cathode (volts)*	*Curve derived from*
I	−32	Experimental rdgs.
II	−34	Experimental rdgs.
III	−30	Experimental rdgs.
IV	−28·4	Experimental rdgs.
V	−28·4	$\log L = 2{\cdot}4 \log V + \log 0{\cdot}018$

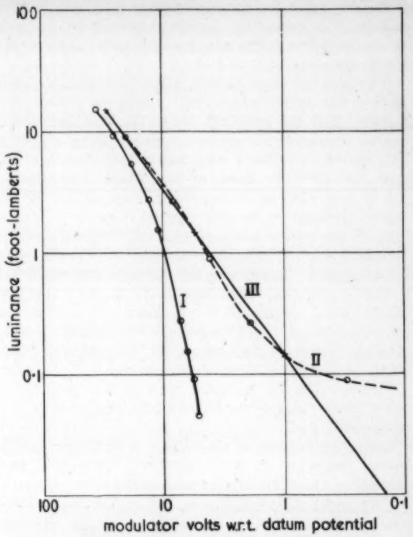

Fig. 4. Modulation characteristics of electrostatic tube; voltage measured from different datum points

○ experimental points. + key points.

Curve No.	*Datum potential w.r.t. cathode (volts)*	*Curve derived from*
I	−77	Experimental rdgs.
II	−71·2	Experimental rdgs.
III	−71·2	$\log L = 1{\cdot}4 \log V + \log 0{\cdot}15$

performance of a tube, or to compare the characteristics of different tubes, by quoting figures either for the gradient at a particular luminance or for an average gradient would be liable to yield misleading results unless the method adopted to determine the black-out voltage were exactly specified.

Even so, reliability of the results obtainable by any of the first three methods is low, in (*a*) or (*b*) because of the greatly decreased sensitivity of the eye at very low luminance, and in (*c*) because of dependence on the sensitivity of the measuring device used. The repetition accuracy of (*d*) is quite good, but it cannot be asserted with confidence that the value of black-out voltage so obtained corresponds to zero luminance, since stray emission or leakage effects, contributing to the measured current but not to screen excitation, may be present.

It is, however, unnecessary to go into the relative merits of methods of determining black-out voltage. It can be shown that the actual value is of no significance in analysing the performance of a television tube, and that the characteristic can be defined quite specifically without reference to any measured black-out voltage. In justification of this statement, it may be pointed out that the minimum value of luminance arising from stray light on the screen of a tube installed in a television set is very unlikely, even if the tube is aluminized, to be less than 1% of the maximum. Assuming limits of 15 and 0·15 ft.l. it can be deduced from Fig. 1 that the minimum intrinsic tube luminance which would be distinguishable when superimposed on a background of 0·15 ft.l. would be about 0·05 ft.l. Further, the law which most closely defines the tube characteristic over the operative range may not be the same as that which would be deduced from a consideration of its behaviour nearer black-out. There is therefore adequate justification for ignoring the lower end of the tube characteristic, and defining the characteristic by virtue of the law to which it most closely approximates over the effective operating range. A means by which this can conveniently be achieved will now be discussed.

PROPOSED METHOD OF DEFINING CHARACTERISTIC

Inspection of Fig. 3, in which the curve III approaches a straight line, suggests the possibility that by choosing

a suitable value for the datum point from which drive voltage V is measured, a close approach to a simple power law relationship between luminance L and voltage V may be obtained.

The problem then resolves itself into one of determining the datum point which results in closest conformity over the operative range between the experimental characteristic, derived from measurements of L and modulator-cathode volts, and a characteristic of the type $L = kV^n$. In terms of logarithmic co-ordinates, this is equivalent to determining the conditions for the closest approach of the experimental values to a straight line. If the determination of what constitutes the closest approach is left to individual judgment there is still room for ambiguity. Therefore a definite criterion, which has a partly empirical basis but leads to a convenient mathematical treatment, is proposed. It is that the experimental curve and the straight line should coincide at three values of luminance, the intermediate value being the geometric mean of the extremes.

Theory. The mathematical basis of this proposal is quite simple, and is as follows (the treatment is not rigorous):

Given, on a curve of the form $y = kx^n$, three points having ordinates, A, B, C such that $A/B = B/C$, and abscissae a, $(a + b)$, $(a + c)$ respectively.

Then, since $A/B = B/C$

$$a/(a + b) = (a + b)/(a + c)$$

which may be simplified to

$$a(c - 2b) = b^2 \quad \text{or} \quad a = b^2/(c - 2b) \qquad (1)$$

Thus, if A, B, C, b and c are known, and an equation of the form $y = kx^n$ is assumed, the value of a necessary to make the three points lie on such a curve can be evaluated in terms of b and c.

Also, since $\log A = \log k + n \log a$

and $\log B = \log k + n \log (a + b)$,

then
$$n = \frac{\log B/A}{\log [(a + b)/a]} \qquad (2)$$

The term $(a + b)/a$, or $(1 + b/a)$, may by substitution from equation (1) be expressed as $[1 + (c - 2b)/b]$ or $(c/b - 1)$. Thus the value of n may be expressed as

$$n = (\log B/A)/\log (c/b - 1) \qquad (3)$$

and can be derived without evaluating a.

If $B/A = C/B = 10$, equation (3) becomes

$$n = 1/\log (c/b - 1) \qquad (4)$$

PRACTICAL APPLICATION

Assume that the tube characteristic can be defined by the power law $L = kV^n$, where V is measured positively from a datum point V' volts negative with respect to cathode. Let the peak working luminance be denoted by $\hat{L}$, and let the modulator/cathode volts corresponding to $\hat{L}$, $\hat{L}/10$ and $\hat{L}/100$ be denoted by d, e, and f respectively (see Fig. 5). Then from equation (4)

$$\lambda = 1/\log \{[(d - f)/(e - f)] - 1\} \qquad (5)$$

For convenience this function is plotted in Fig. 6.

The value of V' can be derived as follows:

From equation (1),

$$f - V' = (e - f)^2/[(d - f) - 2(e - f)] \qquad (6)$$

hence
$$V' = f - [(e - f)^2/(d + f - 2e)] \qquad (7)$$

This may conveniently be described as the virtual black-out voltage, and the quantity V as the virtual drive volts.

The value of k, if required, may be found by

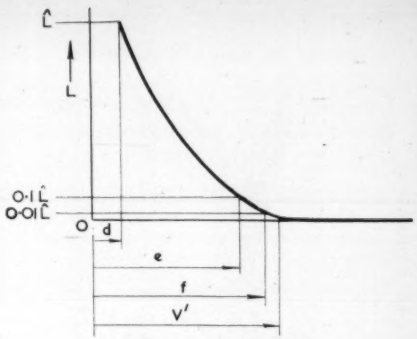

Fig. 5. Curve of λ V, c/b

$c = d - f$; $b = e - f$; $\lambda = 1/\log[(c/b) - 1]$

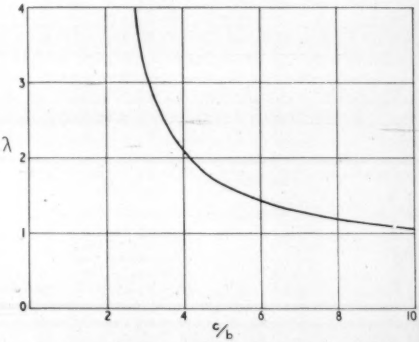

Fig. 6. Curve illustrating practical application of proposed method of defining tube characteristic; curve not drawn to scale

substitution in the equation $L = kV^{\lambda}$, or, more conveniently,

$$\log L = \log k + \lambda \log V \qquad (8)$$

Thus, $\log k = \log (\hat{L}/100) - \lambda \log (f - V') \qquad (9)$

Numerical values for the two tubes of Fig. 2 are shown in the table. The datum potential V' being established, a complete L/V curve may be plotted from the experimental results as indicated by curve IV in Fig. 3 and curve II in Fig. 4. The theoretical curve, corresponding

Numerical values for two cathode-ray tubes

	electromagnetic tube Fig. 3	*electrostatic tube Fig. 4*
$\hat{L}$ (ft.l.)	15	15
d	−11·9	−41·5
e	−22·1	−65·7
f	−26·0	−70·2
$d - f (= c)$	14·1	28·7
$e - f (= b)$	3·9	4·5
c/b	$3 \cdot 6_2$	$6 \cdot 3_8$
λ (from Fig. 6)	2·4	1·4
$f - V' (= a)$ (from equation 6)	2·4	1·0
$V' = f - a$	−28·4	−71·2
k (from equation 9)	0·018	0·15

to the equation $\log L = \log k + \lambda \log V$, is shown by curve V in Fig. 3 and curve III in Fig. 4. A considerable divergence between the experimental and theoretical curves will be noted below about 0·1 ft.l. To put this in true perspective, however, it should be pointed out

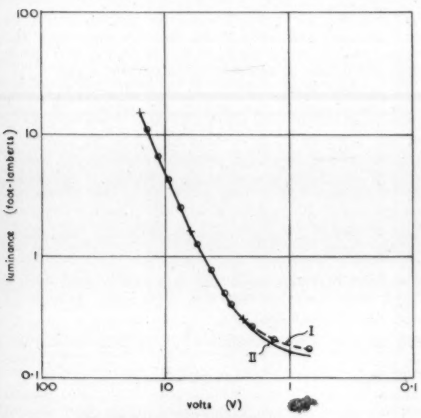

Fig. 7. Dynamic modulation characteristics of electromagnetic tube, with uniform stray luminance of 0·15 ft.l.

○ experimental points. + key points.

Curve No.	*Datum potential w.r.t. cathode (volts)*	*Curve derived from*
I	−28·4	Experimental rdgs.
II	−28·4	$\log L = 2{\cdot}4 \log V + \log 0{\cdot}018$

that, in accordance with the assumption made earlier, a luminance of 0·15 ft.l. due to stray light has to be superimposed on all values in Figs. 3 and 4. Curves obtained by adding these levels to the experimental values and to the theoretical values are shown in Figs. 7

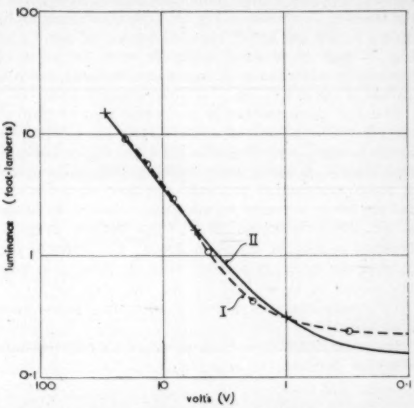

Fig. 8. Dynamic modulation characteristics of electrostatic tube, with uniform stray luminance of 0·15 ft.l.

○ experimental points. + key points.

Curve No.	*Datum potential w.r.t. cathode (volts)*	*Curve derived from*
I	−71·2	Experimental rdgs.
II	−71·2	$\log L = 1{\cdot}4 \log V + \log 0{\cdot}15$

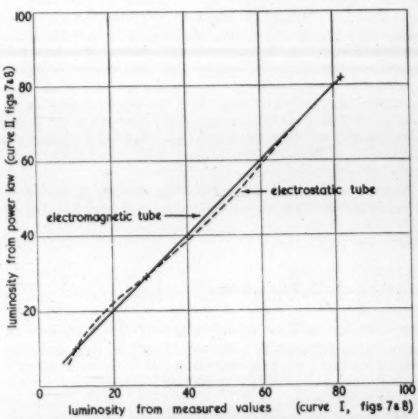

Fig. 9. Curves showing luminosity values based on power law modulation characteristics compared with luminosity based on experimental readings; stray luminance assumed = 0·15 ft.l. in each case

and 8. In Fig. 7 curves I and II are practically indistinguishable except at the lower end.

If now luminance values as read from curves I and II of Figs. 7 and 8 are each converted to luminosity by reference to Fig. 1, and luminosity thus derived from curve II is plotted against luminosity derived from curve I the result is as shown in Fig. 9. The conclusion to be drawn is that the use of curve II instead of curve I of Fig. 7 leads to a quite negligible error in terms of luminosity, while the error introduced by using curve II instead of curve I of Fig. 8 nowhere exceeds 4 units.

The L/V characteristics of a considerable number of tubes have been examined, and in no case has a departure from a power law much greater than that shown in Fig. 4 been found. It would seem therefore that in the study of tone reproduction problems the tube characteristic can for many purposes be adequately defined in terms of the above concepts. For more precise analysis, however, it may be useful to specify the slope of the curve at the three key points. Thus the slope at $\hat{L}$ may be denoted by $h\lambda$, at $\hat{L}/10$ by $m\lambda$, and at $\hat{L}/100$ by $s\lambda$. (This is an adaptation of a form of nomenclature used in photography.)

Since the factor $(e - f)$ in equation (5) represents a difference between two relatively large quantities, high accuracy is called for in the measurement of e and f. The values used in calculating λ should either be averages of a number of readings or should be derived from a luminance/(modulator volts) curve plotted from a large number of points.

CONCLUSION

To sum up, it is suggested that the static characteristic of a television cathode-ray tube can be defined closely enough for most practical purposes by measuring the cathode-modulator voltage at maximum recommended luminance ($\hat{L}$) on a normal raster and at 0·1 and 0·01 of this luminance, and calculating values for λ and for the cathode-modulator voltage corresponding to virtual black-out (V'). From a knowledge of λ, $\hat{L}$, V' and one of the values of d, e, f, it is possible to reconstruct the complete curve of luminance V modulator-cathode volts to a good approximation.

It is possible that greater accuracy could be obtained by an alternative choice of the intermediate key point. Its location does not appear to be critical, however, and the choice of the three points as corresponding to luminances in the ratio 100 : 10 : 1 is thought to be justified by the resultant mathematical simplicity.

Correspondence

Three dimensional electrical potential analyser

In the paper by Professor S. C. Redshaw published in your October 1951 issue it is said (p. 292) that there are nine tiers, whereas Fig. 3 numbers the tiers 0 to 9, making 10. My interpretation is that tier 9 does not exist, it is merely a common point connected to tier 8 by resistances. It is not specifically stated which is the master tier, although presumably it is tier 0, and that this is the top left-hand tier in Fig. 1. If this is so, remembering that the master tier is the one on which the model is to be set up, what is the significance of the object which appears to have a number of leads into the bottom right-hand panel of Fig. 1?

Finally, is it correct to infer that the analyser as described is restricted to the study of three dimensional fields around two dimensional models, as the models are set up on the master tier only?

53 Melrose Avenue, V. E. Gough
Sutton Coldfield, Warwickshire.

The analyser has nine actual tiers, and tier 9 consists of an array of points which may be connected to a common point if desired. An examination of Fig. 3 shows that tier 9 has no tier resistances but is connected to tier 8 by the normal inter-tier resistances.

The master tier is tier 0, and this is the bottom right-hand tier in Fig. 1. The object which can be seen plugged into this tier consists of the model, as described in the first full paragraph on page 293, and in the second paragraph of the section describing the experimental procedure. Starting from the master tier, the tiers follow in order moving upwards on the right-hand side, downwards through the centre and finally upwards on the left-hand side to the auxiliary tier 9, which can be seen mounted on top of the instrument.

The analyser is not restricted to the study of three dimensional fields around two dimensional models. A three dimensional model, with symmetry about a plan normal to the flow, could be set up by using the master tier as a plane of symmetry and then using additional resistances to modify the inter-tier resistances, where the boundary of the model did not coincide with a mesh nodal point. For an unsymmetrical model an intermediate tier, such as tier 4, would have to be selected as the master tier, in which case there would probably be an insufficient number of tiers to obtain undisturbed flow at a distance remote from the model; this could be rectified by fitting additional tiers which could have a coarser mesh separation than that which would be required in the vicinity of the model.

Civil Engineering Department, S. C. Redshaw
The University,
Birmingham, 15.

The thermal conductivity of liquid oxygen

The accurate determination of thermal conductivity of liquids is often difficult and the results obtained by different investigators are often not in agreement. The results obtained by the early workers lacked accuracy due to the use of thick layers of liquid with large temperature difference giving rise to convection currents. Recent improvements in this direction

have utilized thin layers of liquids and small temperature differences. Bridgeman[1] designed an apparatus in which he could use a liquid layer $\frac{1}{64}$ in thick and a temperature difference of 1° F, and obtained fairly accurate data. However, it has been found that it becomes exceedingly difficult to measure accurately the temperature difference with very thin layers of liquids. Bates[2] constructed a well-designed apparatus containing a guard ring. He used thick layers of liquid and showed that one convection effect was negligible. He, however, observed the presence of "surface effect" at the interface of the stationary liquid and metallic surface during the transmission of heat. Hutchinson[3] constructed an apparatus using a "hot wire technique," which in fact was a modification of the method originally used by Goldschmidt.[4] He used a liquid layer of 5 mm thickness and temperature difference of the order of 1° C or less. His results are within 3% of the reliable data found in literature.

The thermal conductivity of liquid oxygen between −207° C and −191° C has been determined by Hammann[5] by the method which was originally used by Jakob and later modified by Meisner. In this method the liquid layer 1·2 cm thick was enclosed between two copper disks, the heat flow being measured from the upper to the lower disk. The temperature difference was measured by differential thermoelements located in the liquid layer. An accuracy of ±1% was claimed.

Recently, investigations were carried out on the heat transfer coefficient (h_m) for condensing oxygen vapour.[6] In this investigation condensation of the vapour was brought about on the outside of a vertical copper tube between 1 and 1·7 atmosphere pressure and the latent heat was absorbed by boiling liquid oxygen inside the tube at atmospheric pressure.

Nusselt[7] deduced a theoretical equation for predicting the heat transfer coefficient for condensing pure saturated vapour on a vertical surface as

$$h_m = 0{\cdot}943\left(\frac{kg\rho^2\lambda}{L\mu\Delta t}\right)^{\frac{1}{4}}$$

where k, ρ, μ and λ are respectively the thermal conductivity, density, viscosity and latent heat of vaporization, g the gravitational constant, L the length of the tube (40 cm) and Δt the temperature difference across the condensing film.

In deducing the equation Nusselt specified a number of conditions relating to the vapour and liquid flow and the temperature distribution in the system. Several workers have reported discrepancies between the experimental and Nusselt values. These discrepancies have been attributed mainly to the divergence of the experimental conditions from Nusselt's assumptions. In the design and operation of the present apparatus[6] every attempt was made to conform to the conditions required by Nusselt's equation. Great care was taken to measure the temperature drop across the condensing film which ranged from 0·082° C to 2·42° C. As the thickness of the condensing film was of the order of a few microns* there was little likelihood of the presence of any convection current in the film.

The values of thermal conductivity (k) of liquid oxygen between −179·6° C and −182° C have been calculated from the heat transfer data using Nusselt's equation and are given in the table. The data is plotted in the figure. The points are fairly scattered as is usually the case with heat-transfer data but they compare favourably with the extrapolated curve of Hammann plotted in the figure (*b*). The mean value of the thermal conductivity between −177·6° C and −182° C is $5{\cdot}05 \times 10^{-4}$ cal per sec per cm² per °C per cm.

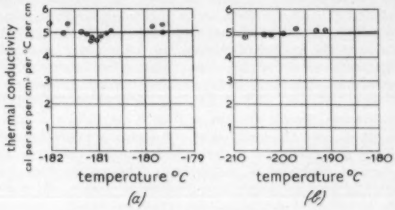

Effect of temperature on thermal conductivity
(*a*) Experimental data (*b*) Hammann's data

condensate film temp. °C	*heat trans. coeff.* (h_m) *gram cal per sec per* °C *per cm²* × 10⁻⁴	*latent heat* (λ) *cal per gram*	*viscosity* (μ) *poise* × 10⁻³	*density gram per c.c.*	*temp. diff.* °C	*thermal cond.* (*k*) *gram cal per sec per cm² per* °C *per cm* × 10⁻⁴
−182·0	1 897	50·7	1·83	1·137	0·082	5·36
−181·7	1 558	50·7	1·82	1·137	0·142	4·93
−181·6	1 666	50·6	1·80	1·136	0·169	5·31
−181·3	1 260	50·6	1·80	1·134	0·346	5·00
−181·3	1 221	50·6	1·80	1·134	0·408	5·06
−181·2	1 126	50·6	1·80	1·134	0·525	4·94
−181·1	1 016	50·5	1·79	1·134	0·687	4·74
−181·1	1 001	50·5	1·79	1·134	0·713	4·68
−181·0	946	50·5	1·78	1·132	0·878	4·64
−180·9	979	50·5	1·77	1·132	0·861	4·82
−180·8	971	50·5	1·76	1·132	0·978	4·97
−180·7	944	50·5	1·76	1·131	1·13	5·02
−179·8	921	50·3	1·74	1·128	1·45	5·27
−179·6	900	50·3	1·72	1·127	1·65	5·32
−179·6	775	50·3	1·72	1·127	2·48	5·01

The values for viscosity obtained by Rudenko[8] were used in these calculations. The data on the latent heat was taken from a recent survey by Bhattacharya and Newitt summarizing earlier work and the data on density was taken from the *International Critical Tables*.[9]

The method employed in the investigation offers a new approach to the method of measurement of thermal conductivity of liquids and can be used to determine disputed and undetermined data. The measurement of thermal conductivity using thin films of liquid of the order of a few microns is a distinct advantage over the other methods. Further, the accuracy with which the temperature drop (Δt) can be measured is unaffected by the thickness of the liquid film.

Industrial Research Laboratory, S. PROSAD
Science College, Patna 5, India.

REFERENCES

(1) BRIDGEMAN. *Proc. Amer. Acad. Arts and Science*, **59**, p. 141 (1923).
(2) BATES. *Ind. Eng. Chem.*, **25**, p. 431 (1933).
(3) HUTCHINSON. *Trans Faraday Soc.*, **41**, p. 87 (1945).
(4) GOLDSCHMIDT. *Physik Z.*, **12**, p. 417 (1911).
(5) HAMMANN. *Ann. Physik*, **32**, p. 593 (1938).
(6) HASELDEN and PROSAD. *Trans Inst. Chem. Eng.*, **27**, p. 195 (1949).
(7) NUSSELT. *Z. Ver. dtsch. Ing.* [*VDI*] **60**, p. 541 (1916).
(8) RUDENKO. *J. Exp. Theor. Phys., USSR*, **9**, p. 1078 (1939).
(9) *International Critical Tables*, Vol. III, p. 20.

* The thickness of the condensing film at the lowest point on the condensing tube for the maximum rate of condensation was calculated according to the equation $x^3 = \frac{3w\mu}{\pi D\rho^2 g}$ where x is the thickness of the film, w is the mass rate of flow of condensate from the lowest point on the condensing surface and D is the outside diameter of the tube and was found to be 16·1 microns.

New books

Applied mechanics for engineers. By SIR CHARLES INGLIS. (London: Cambridge University Press.) Pp. xii + 404. Price 42*s*. net.

As was to be expected from the pen of so distinguished an engineer and teacher as Sir Charles Inglis, this is a stimulating book which should be of real value not only to the student, but also to the teacher of engineering. It is not a textbook in the usual sense of the term. The author states in his introduction that it is based on his lectures to honours engineering classes, and it bears the characteristics which such lectures should possess in that it constitutes a commentary on, and an extension of, the matter contained in the ordinary textbooks rather than an exhaustive treatment of the various branches of the subject. The author does not attempt to go very deeply into theoretical aspects. In most of the branches of mechanics with which he deals he contents himself with a very brief summary of the principles involved and then proceeds to demonstrate the application of the principles to the solution of a number of practical problems. But the summaries given are in general admirable in their clarity and conciseness, the issues are not confused by the citing of a number of "special cases," and there is a directness of outlook which should do much to give the student a clearer conception of the bearing of the principles upon practical problems. The explanations given of the limitations of rigid-body statics in framework problems, of the relation between the principles of energy and momentum, and of the principle of the gyroscope are particularly good. One subject which is not so well treated is the important one of weight and mass. Surely in a book of this calibre the mass of a body merits something better than a definition as "the quantity of matter" which the body contains. The worked examples are noteworthy in that they are almost exclusively taken from actual engineering problems, and that they illustrate the methods of solution of a wide variety of problems, a number of which are of considerable complexity.

The first six chapters of the book deal with statics, mainly in relation to two-dimensional structural problems, and in this section the elementary aspects of the subject are dealt with rather more fully than in any of the others. It includes not only rigid-body statics but also problems on extensible chains and deformable frameworks. There are four chapters on "particle" dynamics, four on the dynamics of a rigid body in two dimensions, four on mechanical vibrations including harmonic analysis, one on friction between solid surfaces and one on gyroscopic motion. Throughout the book the emphasis is on the straightforward solution of practical problems by direct application of fundamental principles. Graphical methods are used whenever they are suitable, and there are several examples of the use of approximations and step-by-step methods. The illustrations given of the use of such methods in problems involving aperiodic vibrations are particularly instructive. The matter of the book is well arranged and presented, the text is fully illustrated with diagrams, and there is an ample supply of exercises at the end of each chapter for the student to work.

This is not a book for the reader who wishes to be spoon-fed, but the serious student who reads it in conjunction with other textbooks will find that it provides a valuable link between the rigorous theory of applied mathematics and the more empirical methods of approach frequently adopted in engineering.

H. T. JESSOP

Internal ballistics. Edited by F. R. W. HUNT. (London: H.M. Stationery Office.) Pp. x + 311. Price 25*s*. net.

This volume summarizes much of the research work on internal ballistics which has been undertaken in this country during the last thirty years. The contributors are mostly past or present members of the Military College of Science and the Armament Research Establishment which ensures the authoritative nature of the book.

The subject matter includes the chemical, thermal and ballistic properties of propellants, the derivation and solution of the various ballistic equations, experimental methods for velocity and pressure measurement and an outline of the application of statistical methods to cordite production and proof. Recent experimental work is briefly reviewed and the special problems of "leaking" guns and the heating of a gun barrel are examined. An extensive bibliography is also appended.

The editors have succeeded in giving within a limited space a comprehensive review of the subject although the treatment is necessarily of a general nature particularly on the experimental side. Probably for the first time the various methods of solution of the ballistic equations are presented with a common notation. No detailed critical comparison of the methods is, however, given.

The textbook is clearly written for the practising ballistician and will provide a valuable background for new entrants to this field of work, particularly in view of the previous paucity of literature openly published in this country. For the general reader, probably most interest will be found in an appreciation of the scope of the work involved, and in such problems as the burning of solid propellants and the heating of a gun barrel.

H. ROE

General homogeneous co-ordinates in space of three dimensions. By E. A. MAXWELL. (London: Cambridge University Press.) Pp. xiv + 169. Price 15*s*. net.

This attractive book is a sequel to Dr. Maxwell's earlier volume on "The methods of plane projective geometry based on the use of general homogeneous co-ordinates," and is intended for students of mathematics in their second year at the university, although some third-year students will not find it too elementary.

The book is concerned with the geometry of projective space as defined by four complex homogeneous co-ordinates. The first chapter deals with the point, the straight line and the plane, and is followed by chapters on the quadric surface and the generators of a quadric surface. Then line co-ordinates are introduced and there are further chapters on the twisted cubic and systems of quadrics. There is a useful chapter on the applications to Euclidean geometry.

All this is lucidly explained and can be followed by those with little knowledge of projective geometry but who are familiar with the co-ordinate geometry of three dimensions.

Dr. Maxwell, however, intends his book to help those who will proceed to further study and to such books as J. A. Todd's *Projective and analytical geometry* in which projective geometry is synthesized with modern matrix algebra. Consequently he devotes his last chapter to an introduction to matrices followed by some applications to the geometry of the main part of the book.

Many readers, other than students of mathematics, who wish to catch a glimpse of modern geometry, will find this account most helpful and illuminating.

J. TOPPING

Report of the Department of Scientific and Industrial Research for the year 1949–50. (London: His Majesty's Stationery Office.) Pp. 214. Price 4*s*. 6*d*. net.

The Advisory Council's Report refers to steps that have been taken to enable it to deal more effectively with the problem of how the resources at the Department's disposal could, subject to the needs of basic research, most effectively be used in relation to the country's economic requirements, and particularly to the improvement of industrial efficiency and productivity. In this connexion, the responsibilities of the Intelligence Division of the Headquarters Office of the Department have been enlarged. The main part of the Report (some 150 pages) gives in summary a review of the work of the 14 Research Establishments of the Department, of the 40 Research Associations which are partly supported by it and the three other bodies receiving grants from the Department; the net expenditure of the Department was just under £4 million. These figures alone give some idea of the wide field and the extent of the Department's work. Five appendices give the lists of various research boards and statistical data.

An introduction to the theory of control in mechanical engineering. By R. H. MACMILLAN. (London: Cambridge University Press.) Pp. xiv + 196. Price 30*s*. net.

Much of the theory and practice of control systems as known to-day has been developed during the last fifteen years although, of course, many of the principles used were known before. The rapid growth of the subject has been accompanied by growth of a vocabulary which tends to make even an elementary discussion of control problems seem very involved to those who have not been in close contact with it. This difficulty does not affect the student so much as the worker in other fields who may wish to pursue further a subject of which he has only a general knowledge, and he may well find that such terms as phase margin, conditional stability or—to take more elementary examples—floating control or transfer function, make the subject appear more difficult than it really is. It is very much to the author's credit that with this book he has enabled the reader to penetrate these defences and to grasp the underlying physical principles of the subject.

The book is written primarily for the mechanical engineer, but the treatment is fundamental and will be appreciated by physicists and others interested in the subject. Indeed there will be many such who, although not concerned directly with the design of control systems, will welcome a treatment enabling a correct approach to the design and use of many types of physical system. It should perhaps be pointed out, however, that the author sets out to teach the principles of the theory of control and not to provide a handbook on the design of control systems. Familiarity with the methods and ideas may be gained by working out the examples given at the end of each chapter.

Although the book deals primarily with the theory of control, Chapter 2 contains a short description of some mechanical control and servo elements and discusses the characteristics of some commonly encountered control systems. Then follow chapters on the operation and performance of servo systems and on servo analysis. The treatment discusses only linear systems but there are short notes on non-linear and discontinuous systems. Up to this stage no more mathematics is required than the ability to solve linear differential equations with constant coefficients but familiarity with operational methods is assumed throughout. In the last two chapters analytical and graphical methods of determining transient solutions are discussed, and stability criteria and the various response loci are considered. There are short appendices on the use of complex numbers and on the Laplace transformation.

The book is beautifully printed and produced and only minor mistakes and ambiguities (such as M for A in Fig. 8.5, omission of X and Y from Fig. 15.1 or acklash for Backlash in the index) have been detected. A. E. DE BARR

La théorie des images optiques. (Paris: Service des Publications du Centre National de la Recherche Scientifique, 1949.) Pp. 322. Price 44*s*. net.

An international conference on The Theory of Optical Images was held in Paris in October 1946, and was intended to be the first of a series of thirty industrial reunions for which generous help had been given by the Rockefeller Foundation. This volume is a collection of forty-six contributions presented at that conference by various authors; some of the accounts are in French and others in English, with one in Italian. The book provides a most useful summary of much of the recent work on optical imagery, as in many instances the articles are themselves condensed accounts of papers published elsewhere, and for which references are given. In some instances, it is true, contributions at the conference are covered by summaries which are all too brief, and the reader must refer to the referenced work for details. Such cases are few, however, and the length of the volume is a tribute to the editors' success in obtaining from the authors accounts of their contributions. Messrs. Maréchal and Lansraux acted as secretaries for the conference, and together with Mme. Anglade edited this volume. Its publication was made possible by assistance from the Centre National de la Recherche Scientifique and from U.N.E.S.C.O.

The subject matter is divided rationally into seven chapters corresponding with sessions of the conference: the first two deal with aberrational theory with papers by T. Smith, van Heel, H. H. Hopkins, Colacevich, Maréchal, Herzberger and Durand, and summaries of contributions by Platzeck and Simon. Chapter 3 covers the application and production of non-spherical surfaces for optical elements, with contributions by Perry, O'Brian, R. E. Hopkins, Herzberger, Missel, Rinia, van Alphen, Bayle and Dourneau. Chapter 4 contains seven articles describing recent work on diffraction theory by H. H. Hopkins, Jacquinot, Boughon, Dossier, Lansraux, Savornin, Desvignes and Toraldo di Francia. In Chapter 5 Zernike, Nijboer, H. H. Hopkins, Maréchal, T. Smith and van Heel deal with diffraction in the presence of aberrations. Chapter 6 is concerned with phase-contrast, with contributions by Zernike (reported by Locquin), Lyot, Flamant, Françon, Kastler and Didelin. Chapter 7 fittingly contains five papers on receptors, visual and photographic, by Arnulf, Françon, Ronchi, Marquet and Tearle.

Misprints and omissions are rather common, but these are generally so obvious that no ambiguity arises. Everyone interested in the subject will find much useful information in this book. Whilst certain of the papers are inevitably mathematical, there is ample interesting material for those who find the mathematical approach too difficult to follow.
K. J. HABELL

Applied nuclear physics. (2nd edition). By E. C. POLLARD and W. L. DAVIDSON. (London: Chapman and Hall.) Pp. vii + 352. Price 40*s*. net.

The first edition of this book appeared in 1942, at a time when nuclear physics was purely an academic subject with

hardly any practical applications. The publication of the book happened to coincide with the advent of the first nuclear reactor, which heralded the atomic age. Apart from the atom bomb, which made nuclear physics a subject of military importance, the possibility of using nuclear energy as a source of power has led to the development of a new branch of technology, nuclear engineering. The large-scale production of radioactive isotopes, and their ever-increasing uses in medicine, biology, chemistry, technology and industry, has brought in a legion of new adepts of applied nuclear science. For a long time Pollard and Davidson's was the only textbook on nuclear physics written in a language intelligible to workers in outside fields, and many a nuclear engineer or isotopist owes his specialized education to this book.

The same developments, however, which gave the book such great value, also spelled its decline, for it soon became obsolete. The aim of the present edition was to bring it up-to-date, and, generally speaking, this has been achieved. The chapters on the detection of nuclear particles and methods of acceleration have been considerably enlarged and modernized, and a new chapter, on nuclear chain reactions, added. Despite, however, the increase of the volume of the book by about 40%, the actual subject of applications of nuclear physics is given little more space than in the first edition, although the material dealing with these problems has been completely re-arranged. The main value of the present edition is, therefore, not as a survey of the various applications of nuclear physics but rather as a lucid and comprehensive exposition of the principles, methods and techniques used in that subject.

In addition to the chapters mentioned above, the book contains chapters dealing with transmutation, radioactivity, techniques in artificial radioactivity and its practical uses, applications of stable isotopes, nuclear fission, nuclear theory and cosmic-rays. Of very great value are the appendices, of which there are eleven; they contain tables of various nuclear data, a very good summary of the elementary pile theory, and discussions on neutron diffraction and cross-sections. In the last appendix several nuclear experiments, which might be suitable for student laboratories, are suggested.

The external appearance of the present edition is of a much higher standard than that of the war-time first edition; both the typography and illustrations are excellent. It is, therefore, the more annoying to find some misprints, both in text and drawings. Some of the proof-reading omissions are only too often met with in second editions. Thus, for example, the mass of Li^7 is given as 7·01818 on page 96, 7·01804 on page 97 and 7·01824 on page 309. The colloquialism of the style is sometimes exasperating and occasionally one has doubts about some of the statements, as for example, about the future role to be played by accelerators (p. 71). Despite, however, these shortcomings, it is a valuable book which should meet the needs of students who begin to study this subject, as well as of the vast group of chemists and engineers who desire to acquire an understanding of the fundamentals of nuclear physics. J. ROTBLAT

The oxide-coated cathode. Vol. I. By Dr. S. WAGENER. (London: Chapman and Hall, Ltd.) Pp. viii + 148. Price 21*s.* net.

Although it is nearly fifty years since Wehnelt made the first experiments which demonstrated the high emission properties of oxide-coated thermionic cathodes, it is only during the past twenty-five years that cathodes of this type have given sufficiently reliable results for the various thermionic devices which now form such an important part of electronic equipment

The importance of the subject and the considerable effort which has been made in all parts of the world to the study of oxide-coated cathodes, particularly those containing barium-strontium and barium-strontium-calcium oxides, may be measured by the numerous papers published in recent years, and this volume by Herrmann and Wagener appears at an opportune time. The book is a translation of an edition which was first published in German. As the authors point out in the preface, "Many of the measures taken during manufacture can only be understood by virtue of their effect on the physical mechanism, while investigation of the physical phenomena must be based on a thorough knowledge of how to make a good cathode." The authors have, therefore, devoted this first volume almost entirely to the manufacture of oxide-coated cathodes.

Following a brief historical introduction, there are two excellent chapters on the processes and techniques involved in the preparation and activation of cathodes. Chapter 4 gives a detailed account of the characteristics of these cathodes, including the more recent results on pulsed emission and the effect of coating and interface resistance which have formed the subject of such intensive study by workers during and since the war.

The volume concludes with a chapter on special cathodes, including those produced by the vapour process—now almost forgotten, but at one time used almost exclusively in receiving valves—thoria cathodes, and cathodes for gas-filled electronic devices and lamps.

The illustrations and diagrams are well produced and there are numerous references to original work in all countries. There is also a useful bibliography of other works on thermionic emission. G. W. WARREN

The principles of air navigation. By E. W. ANDERSON. (London: Methuen and Co. Ltd.) Pp. xiii + 264. Price 25*s.* net.

The author expounds both the science and art of his subject with commendable simplicity. In discussing controversial techniques such as the assessment of information, the author does well to advise the beginner to adopt a formal approach. In this connexion the importance accorded the treatment of errors is to be welcomed.

The specialist—in radio or meteorology, for example—will find his own subject set in true perspective, although summarizing and simplifying results in wording which is occasionally a trifle loose.

Practising navigators will find the presentation novel and stimulating, but the beginner may boggle at the solid geometry, vector resolving and rotating axes he is confronted with so soon after a disarmingly simple introduction to mathematics. The serious student will seek fuller information on various topics and a suitable bibliography would add greatly to the value of the present work. D. E. ADAMS

Jubilee book of the National Physical Laboratory. By JOHN LANGDON-DAVIES. (London: H.M. Stationery Office.) Pp. 104. Price 4*s.* net.

This absorbing little book has been produced to commemorate the completion of fifty years' development of the National Physical Laboratory. It is well written and illustrated and begins with a justification to the non-technical

reader of the importance of the work carried on at the N.P.L. This is followed by a brief sketch of the growth of the present organization, which includes references to some of the leading personalities concerned.

A whole chapter is devoted to the maintenance of the many standards which are the concern of the Laboratory. Then follows an attempt to cover in less than forty small pages the most important aspects of the research that has been and still is being carried on at the N.P.L. The main branches mentioned are fluid flow; materials; instruments; electromagnetic waves and electrons.

The book concludes with two chapters on special investigations and testing and an attempt to forecast intelligently probable future trends in the applications of science to industry.

The point is made that war has been one of the great formative factors in the history of the laboratory. It is to be hoped that the next fifty years will see a development of the work of the N.P.L. comparable with that outlined in this book, but without a similar stimulus.

R. HARESNAPE

Space—Time—Matter. By HERMANN WEYL. (New York: Dover Publications, Inc.) Translated from the German by H. L. BROSE. Pp. xviii + 330. Price $3.95 net.

This is the first American printing of this now well-known book. It is a translation into English of the fourth edition of *Raum—Zeit—Materie*, which was first published in 1921. The translator has adhered as closely as possible to the original, not only as regards the general text, but also in the choice of English equivalents for technical expressions.

Chambers's dictionary of scientists. By A. V. HOWARD, B.Sc. (London: W. and R. Chambers Ltd.) Pp. vi + 250. Price 12*s*. 6*d*. net.

This volume contains some 1 300 "potted" biographies of scientists from Chaldean times to the present. They vary in length from about 50 to 200 words and besides the usual biographical information, brief technical details are given of the man's special contributions to knowledge. Where the assignment of a discovery or invention is controversial, the balance of opinion has been quoted without any attempt to enter the argument for or against. A useful feature of the book is the subject index, which enables the reader to trace those connected with any particular topic. The reproduction of portraits of 70 of the illustrious persons mentioned are on the whole disappointing. The printing of the book is adequate, although the type is rather small.

The author's intention was to provide a handy and accurate reference book for those who have neither the time nor opportunity to consult the larger reference works and to provide them with the central facts about those whose names frequently appear in print. In this, he has succeeded.

H. R. LANG

An advanced treatise on physical chemistry. Vol. II. By J. R. PARTINGTON. (London: Longmans, Green and Co. Ltd.) Pp. xliv + 448. Price 50*s*. net.

Professor J. R. Partington is undertaking an extremely important work in his *Advanced treatise on physical chemistry*. His second volume on *The properties of liquids*, with its clarity of expression, detailed references, neatness of presentation and comprehensive survey, maintains the exceptionally high standard set up in the first volume on *Fundamental principles and the properties of gases*. By present-day standards the price is reasonable.

For such a large text it is remarkably free of typographical errors. The small number which have come to notice are trivial, and the set-up by the publishers deserves the highest praise. The reviewer agrees with the relegation of the parachor to a secondary position. The limits of its value in elucidating chemical constitution are clearly pointed out.

The following remarks are not in the way of criticism, but are suggestions that might be kept in view for later editions. A large amount of space (over thirty pages) has been given to literature abbreviations, symbols and fundamental physico-chemical constants. The reviewer has noticed that many recent books have lists more or less on these lines. Possibly the new joint report on *Symbols, signs and abbreviations*, issued by the Royal and other Societies, might be more generally adopted and the need for their repetition in future texts avoided. With the space saved some sections could be expanded, e.g. the theory of liquids is restricted to six pages and little mention is made of optical properties of liquids, in particular of refractive indices. The mathematical appendices, though brief, are comprehensive, and form an excellent refresher for the worker who has already covered this field. It is doubtful, however, if they would be of much use to a reader not already familiar with it.

Professor Partington in his preface states that special emphasis is given to experimental work. But there is still a place for a text on physico-chemical methods, since practical details in this text are restricted. This holds even though complete reference lists are given to sources and comprehensive lists of experimental results, in tabular form, are included.

J. REILLY

Introduction to statistical method. By B. C. BROOKES and W. F. L. DICK. (London: William Heinemann Ltd.) Pp. 288. Price 21*s*. net. (Part I is available separately.)

This book should fulfil a long-felt need amongst teachers, research workers and technicians in all fields. The introduction stresses the essentially practical nature of statistical techniques, and outlines their development from the early philosophical stages to the modern applications in all walks of life.

The subjects covered include presentation of data and estimation of variability in Part I, and comparison of small sample results, correlation between two variables and an outline of the essentials of experimental design in Part II. The analysis of complex experiments is rightly deemed to be outside the scope of this book, but a regrettable omission from the presentation of data is the simple control chart, which can be of inestimable use in increasing the efficiency of production and the reliability of factory data which are to be subjected to the more advanced statistical techniques.

Good literary explanations, designed to make one think about the principles underlying the methods, are supported where necessary by mathematical proofs at the end of the section, where they do not interfere with the flow of the argument for the non-mathematical reader.

Examples from all fields are used to illustrate the theory, and many useful practical hints are given. Summaries of the main ideas are given at the end of each chapter, and many questions (with answers) are set at the end of each section. Though the book is ideally suited as a textbook for senior schools and technical colleges, it should not be beyond the understanding of those of us who have forgotten most of our mathematics.

JOAN KEEN

Notes and comments

Elections to The Institute of Physics

The following elections have been made by the Board of The Institute of Physics:

Fellows: J. A. Chalmers, J. G. Dawes, A. F. Henson, H. E. Huntley, A. Nemet, B. O. Payne, D. H. Peirson, T. N. Seshadri, W. A. Simmonds, A. Stewart.

Associates: L. Ainsworth, M. D. Armitage, A. N. Barker, M. M. Bluhm, M. S. Bukhari, R. W. Cahn, D. R. Chick, P. Chippindale, H. Cooper, E. L. Deacon, E. R. Drake-Seager, D. R. R. Fair, E. J. Gooding, F. J. Glen Earl, A. J. Goss, J. C. Hammerton, R. Hardy, A. E. Hawkins, G. M. Horn, H. C. Lewis, J. H. McGuire, G. K. Mehta, R. Scott, R. N. Settle, R. V. Sharman, R. B. Sims, C. E. Skinner, C. H. Smith, D. H. Squire, H. P. Stadler, J. Watkins, P. E. Watson, D. P. D. Webb, R. W. H. Wright.

Sixty-eight Graduates, eighty-four Students and six Subscribers were also elected.

Gamma-ray sources for radiography

New sources of gamma-rays now available in this country have not only extended the field in which radiography can be usefully applied but have also permitted considerable improvements to existing techniques. Indeed a wide range of radiography is now possible without X-ray equipment. In order that full advantage should be taken of these new sources The Industrial Radiology Group of The Institute of Physics prepared a memorandum for the convenience of its members, giving technical data about these sources and briefly describing the technique to be used in handling and transporting them. The interest in this circular was so great that it has now been printed and copies are obtainable, price 3s. 6d., from The Institute of Physics, 47, Belgrave Square, London, S.W.1.

A further volume of laboratory and workshop notes

A volume entitled *Further Laboratory and Workshop Notes* contains a second selection of notes prepared mainly from those appearing originally in the *Journal of Scientific Instruments* from 1946 onwards, with the addition of several from the earlier years for which no room was found in the first volume. As before, through the courtesy of the authors, the royalties from the sale of this volume will be placed to the credit of The Institute of Physics' Benevolent Fund. This collection of notes is divided into the following sections: graphs and drawings; optical devices and techniques; devices for liquids and gases; heat, thermometry and furnaces; laboratory and workshop tools, processes and devices; vacuum and pressure techniques and devices; and electrical devices and ancillary equipment and techniques.

This book represents a further fund of practical knowledge which is not readily available and we invite all readers to order at least one copy, if they have not already done so, because we believe that the book will prove most useful to them. We hope too that they will encourage others to order copies so that the amount received by the Benevolent Fund is as large as possible.

The volume can be obtained through any bookseller or from the publisher, Messrs. Edward Arnold and Co., 41, Maddox Street, London, W.1 (price 28s. net).

Advances in physics

We have received the first copy of a new quarterly supplement of the *Philosophical Magazine* entitled *Advances in Physics*, which is being produced under the editorship of Professor N. F. Mott. Its purpose is to publish quickly specialist articles, written by experts for experts, which will review whatever is of current interest in physics. The range of subjects on which articles will be acceptable will be as wide as for the *Philosophical Magazine*; that is to say it will include theoretical and experimental physics and certain branches of applied mechanics; but, in the interest of the reader whose interests are more limited, it is hoped that whenever possible the contributions in each number will be confined to a more restricted field. This first number, for example, deals with some problems in the physics of the solid state, while further issues are planned which will deal with the properties of liquid helium, the theory of dislocations and the science of the upper atmosphere.

The subscription price is £2 15s. 0d., post free, and the price for single parts is 15s. The publishers are Taylor and Francis Ltd., of London.

Errata

In the article *The stretching and relaxing of polyethylene*, by R. A. Horsley and H. A. Nancarrow, published in the December issue, reference (2) *should read* BROWN, A. *J. Appl. Phys.*, **20**, p. 552 (1949).

In the article *A physical investigation of heat production in human tissues when exposed to microwaves*, by H. F. Cook, published in the January issue, the first part of the third term of the equation on page 3 *should read:*

$$\left(2b + \frac{2A_0}{\alpha K}\right) \text{ and not } \left(2b + \frac{2A_0}{K}\right)$$

Journal of Scientific Instruments

Contents of the February issue

ORIGINAL CONTRIBUTIONS

Notes on the design, adjustment and calibration of spectrophotometers. By C. W. B. Normand and R. H. Kay.
A constant stress device adjustable for specimen length. By A. J. Kennedy.
The design of circuits using electro-mechanical devices. By R. A. Brooker.
A universal slit drive mechanism for single beam infra-red spectrometers. By C. G. Cannon.
A bridge circuit for wire resistance strain gauges. By B. V. Hamon.
An interference micrometer for diameter measurement of textile filaments in moisture-controlled atmospheres. By P. Denton.

LABORATORY AND WORKSHOP NOTES

Mercury bulb lift. By O. Kantorowicz.
Correction for false energy in an infra-red spectrometer. By R. A. G. Carrington.
Resilient instrument constraints. By O. Kantorowicz.

CORRESPONDENCE

Anemometers for the Norwegian–British–Swedish Antarctic Expedition 1949–52. From K. Langlo.
The development of thick nuclear research emulsions with amidol-bisulphite developer. From A. J. Herz.

NEW INSTRUMENTS, MATERIALS AND TOOLS

NOTES AND COMMENTS

THIS JOURNAL is produced monthly by The Institute of Physics, in London. It deals with all branches of applied physics (including theory and technique).

All rights reserved. Responsibility for the statements contained herein attaches only to the writers.

EDITORIAL MATTER. Communications concerning editorial matter should be addressed to the Editor, The Institute of Physics, 47 Belgrave Square, London, S.W.1. (*Telephone:* Sloane 9806.) Prospective authors are invited to prepare their scripts in accordance with the *Notes on the Preparation of Contributions*. (Price 2*s.* 6*d.* including postage.)

ADVERTISEMENTS. Communications concerning advertisements should be addressed to the agents, Messrs. Walter Judd Ltd., 47 Gresham Street, London, E.C.2. (*Telephone:* Monarch 7644.)

SUBSCRIPTION RATES. A new volume commences each January, and annual subscriptions will only be accepted for complete volumes of the monthly parts (January–December). The charge is £4 per volume ($11.50 U.S.A.), including index (post paid), payable in advance. Single parts, so far as available, may be purchased at 8*s.* each ($1.15 U.S.A.), post paid, cash with order. Orders should be sent to The Institute of Physics, 47 Belgrave Square, London, S.W.1, or to any Bookseller.

SPECIAL ARTICLE

The relaxation method in stress analysis*

By D. G. CHRISTOPHERSON, O.B.E., Ph.D., Department of Mechanical Engineering, University of Leeds

This paper discusses various proposals which have been made to accelerate the convergence of the relaxation method as applied to the solution of some of the well-known differential equations of physics and engineering. It is shown that a very high accuracy can easily be achieved in simple cases where the differential equation is of the second order.

In the case of the biharmonic (fourth order) equation, which occurs in the analysis of plane stress and plane strain, a method is proposed by which, in suitable cases, a high accuracy can be achieved by employing two second-order equations successively. It is suggested that where this can be done a given accuracy can be achieved with relatively little labour, though it is recognized that the method proposed has only a limited application.

The study of the application of numerical methods to problems of stress analysis has in the past fifty years or so been approached from two quite different directions. On the one hand the mathematician faced with what was in mathematical terms an insoluble differential equation (or simultaneous linear equations with too many variables for formal solution within a reasonable time) has sought for other more rapid means of finding an approximate solution, and on the other the engineer, concerned in the first place usually with complicated frameworks, has rejected the traditional apparatus of analysis, and has sought for assistance in processes of computation, in which imagination or intuition about the way in which the structure would behave, could play as large a part as mathematical ability. The Moment-Distribution method of Hardy–Cross, which is probably the most important contribution to structural engineering on the theoretical side which this century has so far produced, is typical of such an engineer's method; although the arithmetical processes involved have been largely standardized, the method retains the characteristic feature, that the operator can and should at every stage have in his mind's eye the picture of the deformation taking place as the loads are gradually transferred from an imaginary rigid scaffolding to the structure itself. Similarly, the relaxation method, devised by Sir Richard Southwell, was applied first to essentially structural problems, and the original title, now almost forgotten "the method of the systematic relaxation of constraints" drew attention to just this feature of the processes involved.

It is not, however, to the question of stresses in frameworks that attention is drawn in this paper. The greatest successes of the relaxation method have been won in fields remote from structural engineering. But even when the subject under discussion has been an apparently unrelated one, as, for example, the flow of a fluid through an orifice, or the behaviour of magnetic lines of force, the aim has always been to keep in the mind of the operator a mechanical model to which he can refer his judgment and apply his imagination. In these problems, which may be termed the problems of theoretical physics (including elasticity and plasticity), the general outline of the process is usually the same. In mathematical terms it can be stated as follows:

The required quantities can be obtained in terms of a function or functions whose value over the given area is determined by a differential equation and by specified conditions on the boundaries of the area. If the area is then covered by a net or grid, the differential equation can be replaced by finite-difference equations in which the value of the function at the nodes or junctions is given in terms of its value at surrounding nodes. If these equations are then solved by ordinary or by approximate methods the function is determined at the nodal points and hence at all other points by interpolation.

To obtain what might be described as an engineer's view of the same process, a particular problem may be selected. The simplest one, round which much of the discussion of numerical methods has turned, is the problem of the torsion of a uniform prismatical bar of any cross-section. The classical theory of elasticity gives the shear stresses τ_{yz} τ_{xz} in such a cross-section as the gradients $\delta\phi/\delta x$, $\delta\phi/\delta y$ of a function ϕ determined by the equation.

$$\frac{\delta^2\phi}{\delta x^2} + \frac{\delta^2\phi}{\delta y^2} = -2G\theta \text{ (Poisson's equation)} \qquad (1)$$

where ϕ is zero on the boundary, and where θ is the angle of twist per unit length and G the rigidity modulus.

A mechanical analogue to this problem has been available for a long time in the well-known Prandtl soap-film experiment. By simple statics it is easy to show that the transverse displacement of a uniform membrane acted on by a small pressure satisfies equation (1), and thus, by constraining the soap-film round a boundary of the same shape as the cross-section in question, we can observe the form of the deflexion and hence deduce the corresponding stresses in torsion by analogy. To replace the differential equation by its finite-difference equivalent is, in effect, to replace the soap-film by a net, stretched over the area by a uniform tension in all directions, and loaded not by a pressure but by individual small loads applied at each nodal point. Thus the mathematical problem can be reduced to what is essentially a structural problem. The imaginative treatments which have been referred to can now be applied.

Plainly, a good deal of freedom of choice as to the form of the net is available: for example, a triangular mesh, a square mesh, or a square mesh with diagonals (Fig. 1). For the simplest case, the square net, the equilibrium equation governing the displacement w_0 of node 0 surrounded by nodes 1, 2, 3, 4 is:

$$\sum_1^4 w - 4w_0 = +a^2Z \qquad (2)$$

where $Z = -2G\theta$, the r.h.s. of the original equation. The arithmetical problem is then to solve a number, often a large number, of such simple linear equations.

The first attempts to provide a numerical solution for equations of this type in bulk, for example, those by Richardson[1] and Thom and Orr,[2] mostly employed the so-called

* Based on a lecture given to the Stress Analysis Group of The Institute of Physics in Liverpool on 4 April, 1951. The summarized proceedings of this conference will be published in the next issue. Some descriptive material which can be found in other publications has been omitted to make room for some detailed numerical examples.

"iteration" method. Suppose that any trial values have been calculated (or guessed) for w at all the nodal points. Then start at point 0 and correct w_0 by giving it the value necessary to satisfy equation (2) exactly. Then do the same for point 1, satisfying the corresponding equation for w_1. (Notice that since w_1 is now modified equation (2) no longer holds for point 0.) Then proceed to w_2 and so on till all points have been modified. The process is then repeated until the necessary modifications have become small. Of course, many devices can be employed, mostly having the character of an extrapolation, to accelerate the convergence of the method. But the essential feature that the numerical procedure is automatic and gives little scope for choice by the operator is usually retained.

The numerical side of the relaxation method is in fact very different although it bears a superficial resemblance to the iteration technique which has occasionally misled people whose interest was mainly in the fundamental mathematics of the method. The procedure originally employed has been described in a number of papers, one of the earliest being Christopherson and Southwell.[3] A very good practical account has been given recently by Fox[4] and a brief summary must serve here. The first step is the calculation of the "residual loads" F corresponding to any assumed form of deflexion, given for the simple square mesh by the equation:

$$\sum_1^4 w - 4w_0 - a^2Z = F_0 \qquad (3)$$

These "residual loads" are the forces which would have to be imposed on the nodal points of the net in order to make the displacements conform with the initial assumption. If they were zero, the assumed form would coincide with the true solution to the original set of equations. The aim of the operator is to reduce all the residuals to zero. If over some areas of the net there is a general tendency for them to be positive, over these areas the displacements must be increased *en bloc*. Similarly a generally negative tendency in the residuals requires a "block" reduction of the displacements. In some cases, there may be large residual forces on individual points which require displacement on their own. The arithmetic necessary to keep account of the changes in displacements and residual forces is very simple. A modification of 1 unit in value of w_0, for example, produces changes in the residuals as shown on the right of the nodes in Fig. 1(*a*). Block relaxations are equally straight-forward. It is the sign of the experienced "relaxer" that he does few "single-point" relaxations until the final tidying up. Those who have turned their attention to the question of designing a machine to perform the relaxation operation have sometimes suggested that the machine would correct at every stage that node and only that node which had the largest residual force. Although such a machine if made would no doubt work with superhuman accuracy and speed, it would by human standards be a very bad relaxer and would have to go through enormously more numerous operations to arrive at the same result.

Plainly, the time taken by the process depends a great deal on the accuracy of the initial guess, and the procedure known as the "advance to finer nets" was evolved to ensure that the relaxation of a net involving a large number of nodal points was always started from the best possible approximation. The process begins with a very "coarse" net containing very few points, perhaps only one, which can be used as the starting approximation for the next finer net, and so on. Apart from its advantages in shortening the arithmetic this device is of the greatest value in determining the final accuracy achieved.

A very wide range of problems can be investigated by the solution of equations of this type and it is worth while considering in some detail the alternative methods which can be employed. Numerical results can be best achieved sometimes by one method and sometimes by another, depending on the nature of the problem, and in particular on the character of the boundary conditions. This is, of course, a subject on which more than one view is possible. Much depends on whether the problem is one in which the greatest emphasis must be placed on accuracy or one in which a high accuracy is not necessary, and simplicity in the calculations is of prime importance.

The terms which have been neglected in passing from the differential equation (1) to the finite-difference form equation (2) are of order a^4. Both sides of the equation are of order a^2 and thus the error in this transition is of order a^2, where a is the mesh size. Thus if in the original coarse net of one node, the error is about 20%, as it often is, this will mean that we shall obtain an accuracy of about $\frac{1}{4}$% when we have proceeded to a mesh size $\frac{1}{2}$ as large. To fix ideas, consider a problem in which the boundary is a square. The finest net would then require 225 nodes, though for symmetrical boundary conditions the number of *different* nodes would be only 36. It will plainly be an advantage if the answer can be obtained by the consideration of fewer points. There are three distinct ways by which this can be done.

First, there is the method of extrapolation first employed I think by Richardson and Gaunt,[5] though they obtained the various individual solutions by iteration methods. Let us suppose that we have obtained an original "coarse net" solution, and also the next one to it. (For the symmetrical square, these will contain respectively 1 and 3 points.) The error in the original net was 20%, in the next one will be approximately 5%, since a has been halved. Thus if the difference between these nets at the common point was E, we may expect that the remaining error is $\frac{1}{3}E$, and we can make this correction forthwith. We may in some cases be misled by the circumstance that the original net had a spurious accuracy due to two large sources of error cancelling out, but, in general, we can expect that the extrapolated result from a net of side a and one of side $\frac{1}{2}a$ will be as good as or better than the uncorrected result for side $\frac{1}{4}a$. Thus the thirty-six nodes for the square would be reduced to ten (though some additional interpolation would be needed to present the result in a practicable form).

The second method, which we may call the "difference" method has been developed by Fox[6] at the National Physical Laboratory. This method makes use of the calculus of finite differences to improve the accuracy of equations like (2). Let us suppose that the values of w have been determined on a net of moderate size. The error in the original finite-difference expression can be specified in the following way:

$$\sum_1^4 w - 4w_0 - a^2Z = \tfrac{1}{12}(\delta^4_{ox} + \delta^4_{oy}) + \ldots + \text{terms of order } a^6 \qquad (4)$$

where δ^4_{ox}, δ^4_{oy} are the values of the fourth difference of the function w at the point 0 in the directions of x and y respectively. By constructing a difference table from our approximate values of w we can estimate the δ's and thus we can introduce these quantities as new residual loads, and apply the necessary corrections to w, which will, of course, be small. We can then recalculate the difference-table and recorrect, should this be necessary.

The great advantage of Fox's method is that it enables one to specify with precision by a consideration of only a

single net what accuracy has been achieved. For if, let us say, the sixth differences in the table are of magnitude only $\frac{1}{3}\%$, then when the fourth differences have been dealt with no other error remains. In several papers Fox has shown that very great accuracy can be achieved by this procedure. Its disadvantage in my view is this. That the procedure in its entirety cannot be applied to a coarse net, because such a net will not contain sufficient points to enable the higher differences to be calculated, and thus the system of progress from net to net we have described is not available. Further some extrapolation of the higher differences will always be necessary near the boundaries, and it is near the boundaries that the interesting things happen in problems of this sort. From the computational point of view, it will also be necessary to use fairly complicated difference formula in order to compute the necessary boundary gradients. However, the ten-point net referred to in dealing with the extrapolation method for the square is more than sufficient to enable the difference method to be worked in its entirety.

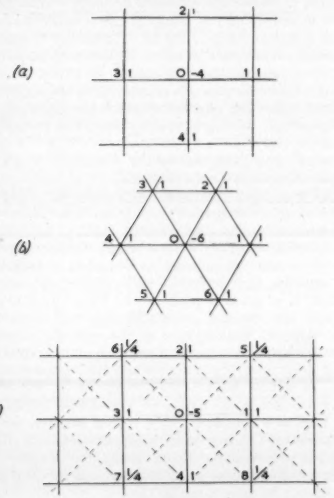

Fig. 1

In the early days of the relaxation method, it was thought that the way to achieve high accuracy was by employing difference equations which involved larger numbers of nodes than the original four. Thus if we replace the square mesh by a "triangular" one, as shown in Fig. 1*b*, the finite-difference approximation to (1) becomes

$$\sum_1^6 w - 6w_0 = \tfrac{3}{2}a^2Z_0 + \tfrac{3}{32}a^4\nabla^2Z_0 + \ldots + 0(a^6) \qquad (5)$$

where the symbol ∇^2 stands for the Laplace operator $\delta^2/\delta x^2 + \delta^2/\delta y^2$, and the term $0(a^6)$ indicates that terms of order a^6 have been neglected. The "relaxation pattern" is almost equally easy to work, and the error is now of order a^4. If we retain the square mesh, but employ a formula involving eight surrounding points instead of four we can make the error of order a^6, but the right-hand side of the equation will involve not only the value of Z and ∇^2Z at the origin, but also the value of ∇^2Z at surrounding points.

$$\sum_1^4 w + \tfrac{1}{4}\sum_5^8 w - 5w_0 = \tfrac{1}{10}a^2Z_0 + \tfrac{7}{40}a^4\nabla^2Z_0 + \tfrac{1}{160}a^6\nabla^4Z_0 - \tfrac{1}{20}a^2\sum_1^4 Z + 0(a^8) \qquad (6)$$

The basic theory underlying this procedure has recently been given by Bickley,[7] and it is my own opinion that this approach where applicable is still the best of the alternative means of accelerating convergence.

The accuracy of this method in a suitable case is best demonstrated by a simple example, the working of which will be described in some detail, since it is felt that the difficulty of the relaxation method to anyone approaching it for the first time is neither in the basic mathematics, nor in actual correcting process itself, but in deciding on the general procedure to be followed.

Take the case of the torsion of a rectangle having width $2b$, length $3b$. The first net in this case will consist of two points, as shown in Fig. 2, and by symmetry the value of ϕ is the same at both of them. The quantity $2G\theta\, b^2$ must be given a numerical value and to take the value 25 600 avoids decimals. Remembering that ϕ is zero on the boundary, equation (6) applied to this net gives

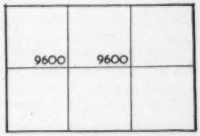

Fig. 2

$$-4\phi = -38\,400;\ \phi = 9\,600 \qquad (7)$$

We must next evolve some starting approximation for the next net shown in Fig. 3. The simplest procedure is to apply equation (2) to the diagonal mesh of points marked with black spots in Fig. 3. The remaining points can then be fitted in by applying equation (2) again. The values shown above the line on the left of the nodes of Fig. 3 have been

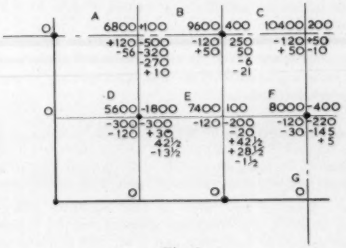

Fig. 3

obtained in this way. On the right are the residuals calculated by the application of equation (6) to these estimates.

In this diagram the following operations have been entered:

(i) a displacement -300 at D to distribute the large residual there,

(ii) a "block" displacement -120 of all points to reduce the mean residual to near zero,

(iii) a block displacement $+50$ at B and C to reduce the mean residual over the central portion to near zero,

(iv) point displacements -56 at A, and -30 at F to remove the remaining large residuals.

At this stage, the residuals have already been reduced to about 2% of their original values on the average, and it will probably be as well to recalculate them and start again. The final result of the relaxation of this net is shown above the lines in Fig. 4. An additional figure has been added to reduce "rounding-off" errors.

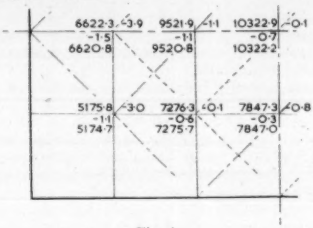

Fig. 4

Even this, however, is not the best that can be done with this net. We can make use of the extrapolation technique referred to above to effect a further improvement. Carrying Bickley's technique a stage further, we find that the largest term neglected on the right-hand side of equation (6) is $(20/8!)a^8(\delta^8\phi/\delta x^4\delta y^4)$. If on the other hand we apply it to the next larger net—that indicated by dotted lines in Fig. 4, as is V_2 larger, and the neglected term is $(320/8!)a^8(\delta^2\phi/\delta x^4\delta y^4)$. If, therefore, taking the values of ϕ given in Fig. 4, we compute residuals for this diagonal net by applying equation (6) in the ordinary way, the value obtained will be about $(300/8!)a^8(\delta^8\phi/\delta x^4\delta y^4)$, and thus the error term in the original solution is known. This error term is shown on the right of the points in Fig. 4. (Only the three central values are obtained directly, the remainder are extrapolated, making use of the fact that $\delta^8\phi/\delta x^4\delta y^4$ satisfies Laplace's equation.) The corrections of ϕ which result are on the left below the line, with the final values of ϕ immediately below. The errors in these values are not likely to exceed 3 units in the last (fifth) figure.

To complete the calculation, we need to estimate the maximum gradient of ϕ, to give maximum stress and the total volume to give the torque. The volume is easily obtained by Bickley's formula.

$$\int_{-a}^{a}\int_{-a}^{a}\phi\,dx\,dy = \frac{a^2}{45}(88\phi_0 + 16\sum_1^4\phi + 7\sum_5^8\phi) - \frac{1}{45}a^6\nabla^4\phi + O(a^8) \qquad (8)$$

for the volume of any block of four squares. Since the gradient required is a boundary gradient, central difference formulae cannot be employed, and if we wish to avoid losing accuracy we must develop a formula based on more than one or two of the specified values of ϕ. By making use of

(1) the known zero value of ϕ anywhere on the boundary,
(2) the governing equation for $\phi(\nabla^2\phi = -25\,600)$,
(3) its values at the points C, F (and the point symmetrical with F), equally spaced at interval $a\ (= \frac{1}{2}b)$,

we obtain the formula

$$720a\left(\frac{\delta\phi}{\delta y}\right) = 1\,222\phi_F - 298\phi_c - 203\cdot25600\frac{a^2}{b^2}$$

Replacing the numerical scale factor 25 600 by a quantity $2G\theta$ which it represents, we obtain

$$\tau_{max} = 0\cdot8477G\theta b$$

and the torque required to produce twist θ is

$$T = 0\cdot19603G\theta(2b)^4)$$

An analytical solution of this problem by means of an infinite series is given by Timoshenko.[8] The values obtained (to three significant figures) agree with those given here.

Plainly in a simple problem of this kind an accuracy far greater than is required in practice can be obtained with very little trouble. The full advantage of the more accurate procedure is only apparent when the solution of greater difficulty is attempted.

There are two objections to all these means of improving accuracy which no mathematical argument can overcome and which in certain cases will be very important. Firstly, if we have a very irregular boundary, a coarse net, with its few boundary points, cannot possibly represent it fairly; there may even be a large oscillation of the boundary between one boundary point and the next. Accordingly, a fine net must be employed and that being so the simplest procedures will be sufficient to ensure the necessary accuracy. How far this argument is sound I do not think there is yet evidence to say. It may be that even when a fine net is necessary to represent the boundary, there may be still a discrepancy between the "fineness" required in the two cases. Secondly, all finite-difference substitution depends essentially on the supposition that in any region the required solution can be represented as a polynomial. If this is untrue, the whole procedure is questionable, and there may be cases in which the simple equations will give numerical results which are as good or better than more complicated methods.

Relaxation or other numerical methods for the solution of Poisson's or Laplace's equation (usually called the "harmonic" problem because in the later case the function calculated is plane-harmonic), are I think now widely employed and no difficulty is usually encountered in obtaining a satisfactory solution rapidly. It is perhaps worth pointing out here that this in itself is of value in problems of plane stress or plane strain where the principal stress difference can be obtained by photo-elasticity and the sum of the principal stresses is then a harmonic function having a known boundary condition.

Next in order of difficulty are the so-called quasi-harmonic problems in which the governing equation is still of the second order, but is no longer of the simple symmetrical form of Laplace's equation. As a typical example we may take the equation which governs torsional stress in a circular shaft whose cross-section varies along the length. The governing equation for the stress-function ϕ in terms of which the stresses can be determined is:

$$\frac{\delta^2\phi}{\delta r^2} - \frac{3}{r}\frac{\delta\phi}{\delta r} + \frac{\delta^2\phi}{\delta z^2} = 0 \qquad (9)$$

with ϕ zero on the axis and ϕ = constant on the surface, where r is the radial coordinate and z the coordinate measured axially. This equation can, of course, be put in finite-difference form and "relaxed" in the usual way. If we do this we find that the net analogue requires that the tension in the strings of the net is now not uniform, but is a function of r so that when a node is displaced the load upon it is not divided equally among the surrounding points; more of it goes in one direction than the other. We can, however, avoid this complication by a trick. Instead of determining ϕ we may elect to determine $\psi = r^{-3/2}\phi$, for which the governing equation is:

$$\frac{\delta^2\psi}{\delta r^2} + \frac{\delta^2\psi}{\delta z^2} - \frac{15}{4r^2}\psi = 0 \qquad (9a)$$

and the simplest finite difference approximation

$$\sum_1^4 \psi - \left(4 + \frac{15a^2}{4r^2}\right)\psi_0 = 0 \qquad (9b)$$

where a is the mesh-size of the net. In the mechanical analogy the net is now uniform, but to each node is attached a small spring which produces a restoring force $15a^2/4r^2\psi$ when the node is displaced a distance ψ.

It is perhaps of interest to examine how the change from (9) to (9*a*) could be justified from three different points of view:

(*a*) from the mathematical point of view we have replaced the awkward operator of (8) by the well-known Laplace operator and, accordingly are at liberty to use its familiar properties;

(*b*) from the arithmetical point of view, we have replaced a numerical equation which had two irregular coefficients by one having only one, and, moreover, this one will become rapidly less important over much of the area as the mesh-size diminishes;

(*c*) from the engineering point of view, we have replaced a model whose behaviour is not easy to envisage by a more straightforward one.

Apparently these points of view differ profoundly, but it may be that they are really only different statements of the same fact.

The quasi-harmonic equations are not on the whole of the first importance in stress-analysis, since the problems to which they refer are fairly specialized. At the next stage, however, we come to the problem which is perhaps the most important of all—the question of the plane stress or plane strain. Given a uniform plate or section having any boundary shape and with any forces imposed on the boundaries in the plane of the plate, it is required to determine the stress condition at all points. Mathematically, this problem is usually expressed in terms of the determination of an Airy function χ given by:

$$\frac{\delta^4\chi}{\delta x^4} + 2\frac{\delta^4\chi}{\delta x^2\delta y^2} + \frac{\delta^4\chi}{\delta y^4} = 0 \qquad (10)$$

the stresses then being given by

$$\sigma_x = \frac{\delta^2\chi}{\delta y^2}; \quad \sigma_y = \frac{\delta^2\chi}{\delta y^2} \quad \tau_{xy} = -\frac{\delta^2\chi}{\delta x\delta y}$$

$\delta\chi/\delta x$ and $\delta\chi/\delta y$ are specified on the boundary in terms of the applied forces.

Here, also, we have a mechanical analogy in the example of the uniform plate supported round a boundary of similar shape and bent by edge moments, and in the general case by loads q per unit area perpendicular to the plane of the plate, the deflexion w is then given by

$$\frac{\delta^4 w}{\delta x^4} + 2\frac{\delta^4 w}{\delta x^2\delta y^2} + \frac{\delta^4 w}{\delta y^4} = \frac{q}{D} \qquad (11)$$

where D represents the flexural stiffness of the plate.

The simplest finite-difference approximation to equation (11) corresponding with equation (2) is:

$$8\sum_1^4 w - 2\sum_5^8 w - \sum_9^{13} w - 20w_0 = -\frac{qa^4}{D} + 0(a^6) \qquad (12)$$

in which subscripts refer to points as numbered in Fig. 5, and this involves thirteen points instead of five, as in the case of the harmonic equation. The corresponding relaxation pattern is shown on the right of the nodes.

Now it has been shown repeatedly that it is perfectly possible to solve this equation by the same straight-forward methods as have been employed on simpler problems. But it is a great deal slower and more difficult. The simple block relaxations which lead one irresistibly to the solution of an

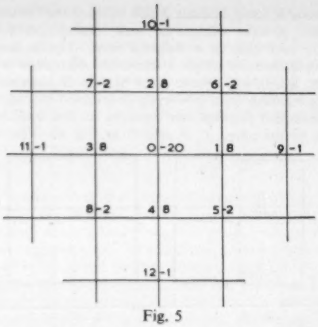

Fig. 5

equation of the second order are no longer available, and although some attempts have been made, notably by Wood at the Building Research Station, to evolve corresponding processes, these are of necessity relatively complicated.

Once again it is possible to express the difficulty in several ways which perhaps amount to the same thing. We can say:

(1) that the equations are "ill-conditioned" that is to say that appreciable errors in the required values of w produce only small consequences in the residual loads F;

(2) accordingly, a small residual load remaining during the relaxation process will be very hard to get rid of by local adjustments. There will be a tendency as soon as it is eliminated for a similar error to pop up elsewhere;

(3) alternatively, we can simply say that it is much less easy to imagine the behaviour of a plate under small loads of various magnitudes and direction than it is to do the same thing for a net.

The difficulty could be avoided if the nature of the boundary condition were different. If the specified quantities on the boundary were w and $\nabla^2 w$, then all would be plain sailing; one would simply write $\nabla^2 w = W$ (say) and solve

$$\nabla^2 W = q/D \text{ with known } W \text{ on the boundary} \qquad (13)$$

and then

$$\nabla^2 w = W \text{ with known } w \text{ on the boundary} \qquad (14)$$

both these steps are of the simplest, and a high accuracy could easily be achieved. But in practice W is usually unknown on the boundary; what we have is w and its gradient normal to the boundary.

To overcome this difficulty, Southwell[9] recently proposed the following procedure. Start by solving equation (12) normally, but only to a very moderate accuracy. Then deduce from this solution by numerical differentiation the value of $\nabla^2 w = W$ on the boundary. A solution of high accuracy can be obtained as described for this W, and for the right boundary values of w. Because of errors in the original solution, the boundary gradients, however, will not be quite as required; a second correcting solution imposed the necessary boundary gradients can then be worked out as before, and if necessary a third. Again a high accuracy is not required, since these second and third solutions are only small modifications on the first.

It happened that I did not see this proposal of Southwell's until after I started preparing this paper. I had in mind a

very similar scheme, but one which avoided the "biharmonic" relaxation process altogether and instead corrected the boundary condition in a different way. Let us consider a very simple case for which a numerical treatment is already available, a uniform square plate of side $2b$ clamped on all four edges loaded by a uniformly distributed load q.

The coarsest possible net consists in this case of three different points only, A, B, and C in Fig. 6. The value of

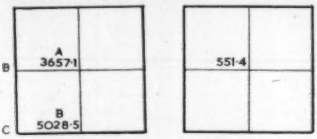

Fig. 6

$W(=W_c)$ at the corner points C is necessarily zero, and thus one equation relating W_A and W_B is obtained by applying equation (6) at the point A.

$$4W_B - 5W_A = \tfrac{3}{2}qb^2 \tag{15}$$

A second equation can be obtained by applying Green's theorem to the plate as a whole.

$$\iint_A W dx dy = \iint_A \frac{\delta^2 w}{\delta x^2} + \frac{\delta^2 w}{\delta y^2}\delta x \delta y = \int_c \frac{\delta w}{\delta \nu} ds = 0 \tag{16}$$

when the last integral is taken round the boundary on which $\delta w/\delta \nu$ is zero everywhere as the plate is clamped. Applying equation (8) again we have

$$88W_A + 64\,W_B = 0 \tag{17}$$

Solving these equations and taking $qb^2 = 25\,600$ for convenience as before we obtain the values of W shown in Fig. 6*a*. To complete this stage, equation (14) in form (6) is then applied again to determine w at the central point, as in Fig. 6*b*.

Proceeding to the next net (Fig. 7), it is convenient to obtain the solution in two stages. In the first instance, we retain the boundary value W_B already determined and calculate remaining W's choosing that value for W_G the new boundary point which ensures that (16) is still satisfied. This solution shown in Fig. 7*a* can be computed direct from equations (6) and (8) without any relaxation. The corresponding values of w can then be easily obtained (Fig. 7*b*).

The original assumption that W_B is correct is, of course, not necessarily exact, and so a second solution is obtained in which the consequence of modifying W_B by an amount Δ is traced (Fig. 8 *a* and *b*). Since the loading q is already accounted for, the right-hand side of equation (6) is taken as zero in this solution.

All that remains is now to combine these solutions in the right proportions. To do so, we apply Green's theorem, not to the plate as a whole, but to the central strip $ABGJ$ (Fig. 7*b*), since $\delta w/\delta \nu$ is zero on the boundaries and on lines of symmetry, we have

$$\iint_{ABGJ} W dx dy = \int_J^G \frac{\delta w}{\delta x} dy \tag{18}$$

A numerical means of evaluating this second integral is therefore required. This can be developed without difficulty. If the notation of Fig. 5 to identify points on each side of the line is used, we find

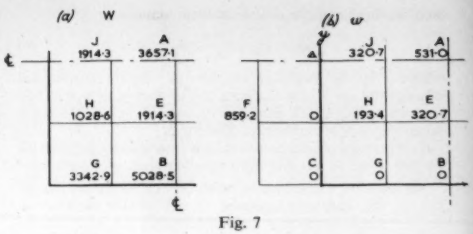

Fig. 7

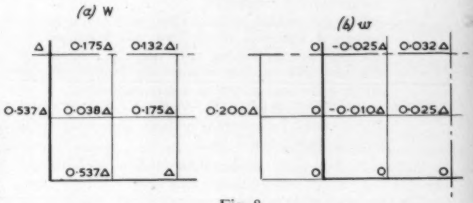

Fig. 8

$$360\int_{-a}^{+a} \frac{\delta w}{\delta x} dy = -120(w_1 - w_3) + 180(w_5 + w_6 - w_7 - w_8) + 60(w_8 - w_{11}) - 92(W_1 - W_3)a^2 - 14(W_5 + W_6 - W_7 - W_8)a^2 + 0(a^6) \tag{19}$$

It might be thought that a more direct approach could be obtained by employing an equation like (19), to express the condition that the boundary gradient is zero, without applying Green's theorem. Such a formula would necessarily involve extrapolation of the known values of w, and W to points outside the boundary of the square, or some equivalent process, and accuracy is almost always lost in extrapolation. (An extrapolation for the value of w at one external point F as shown in Figs. 7*b* and 8*b* is in any case required, and this is obtained by applying equation (6) for a diagonal mesh as shown in Fig. 4 to a square centred at H, but the coefficient of this extrapolated value in equation (19) is small and little inaccuracy will be introduced from this source.

The necessary integrals are found to be, for the first solution (Fig. 7).

$$\left.\begin{aligned} 2\iint_{ABGJ} W dx dy &= -885{\cdot}7 \\ 2\int_J^G \frac{\delta w}{\delta x} dy &= 837{\cdot}96 \end{aligned}\right\} \tag{20}$$

(The reversal of sign is due to the fact that x is taken as positive in the inwards direction.) The fact that these values are not equal is an indication that the assumed value of W_B is not correct. For the correcting solution Fig. 8, we have

$$\left.\begin{aligned} 2\iint_{ABGJ} W dx dy &= 0{\cdot}1514\,\Delta \\ 2\int_J^G \frac{\delta w}{\delta x} dy &= -0{\cdot}0451\,\Delta \end{aligned}\right\} \tag{21}$$

and it is easy to show that the required condition will be met if we superpose solution (2) and solution (1) with $\Delta = 448{\cdot}7$.

The final solution, satisfying all the required conditions is shown in Figs. 9 *a* and *b*.

This result is almost as accurate as that obtained by Fox in his treatment of this problem employing the difference-correction method on a mesh of half the size of that shown in Fig. 9. The method employed here has therefore not only eliminated the difficult biharmonic relaxation pattern, but seems also to have improved the accuracy attained with any given mesh size.

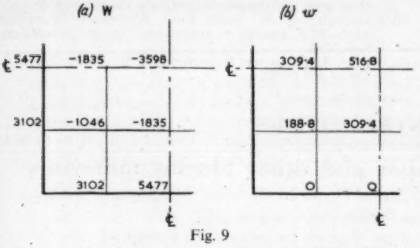

Fig. 9

THE QUESTION OF "IRREGULAR STARS"

The question of the irregular boundary referred to above is tied up with the very similar question of what is to be done when the areas considered are not so well-mannered as to be bounded by straight-lines at right angles or at 60°. Then the central-difference formulae we have referred to will not be immediately applicable near the boundary. The simplest procedure is then as follows:

(1) extend the net to imaginary points outside the field until all the "stars" or clusters of points surrounding the interior nodes are complete;

(2) make use of the net analogue to deduce the values of the required function at exterior points (the equivalent of linear interpolation).

In fact, this very simple procedure leads to errors of order a near the boundary, and is accordingly open to objection on the score of accuracy.

Fox's procedure can, of course, still be applied. Given approximate values of the function its differences can be worked out and known interpolation formulae can be used to determine the necessary exterior values of the function in terms of the specified boundary values. The interpolation formulae are, of course, much less convenient and involve more computation than when the specified values fall conveniently at equal intervals along the line, but the method is not substantially different.

Apparently, the use of more accurate finite-difference formulae of the kind employed in this paper, is rendered almost out of the question by the "irregular stars." Such formulae would become too complicated, but a totally different approach might be worth considering. Let us suppose, for example, that we have in mind a typical plane-stress problem—to find the stresses in a tension specimen of a given outline, like, for example, that shown in Fig. 10. Ordinary procedure would require a very fine mesh at the points A, where we know the stress-concentration will occur, and it is here also that the "irregular stars" will be found.

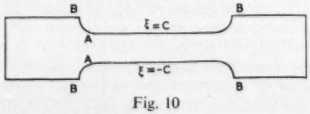

Fig. 10

Suppose, however, we make use of the device of conformal transformation. We can regard this as being simply a change from one set of coordinates, x–y, to another set, ξ–η, and let us suppose that we take the side boundaries of the specimen as $\xi = C$ and $\xi = -C$ and its ends as lines of constant η. Then if we compute ξ, η so that

$$\frac{\delta^2\xi}{\delta x^2} + \frac{\delta^2\xi}{\delta y^2} = \frac{\delta^2\eta}{\delta x^2} + \frac{\delta\eta^2}{\delta y^2} = 0^* \qquad (22)$$

we can transform all the standard equations from x and y to ξ and η, and we shall be left simply with a problem of computation which is essentially that of the rectangular plate, with no irregular stars, in which no difficulty arises. The equations to be solved will not be quite identical, as a factor representing the change in scale from one picture to the other will come in to the governing equation, but this need introduce no essential difficulty. In point of fact, this change of scale is an advantage because it enlarges (and hence makes more accurate) those areas in which the stresses are large and reduces to insignificance the corner areas B, in which there are no stresses. Of course, if we were to determine the values of ξ, η in the x–y plane we should still have to deal with the awkward "irregular stars." My suggestion is the converse—that x, y should be computed in the plane of ξ, η. The boundary condition enabling this to be done is not quite straight-forward, it involves a specified relation between x and y on the boundary, but it seems no more difficult than other boundary conditions which have been successfully coped with in other fields. It is perhaps of interest to remark that if this procedure is adopted the final errors in the process will be expressible exactly in terms of engineering tolerances, i.e. in errors in the physical dimensions of the specimen.

It should be made quite clear that this suggestion is not put forward as being of universal application. In many cases, particularly of multiply-connected areas, it is not possible to transform conformally into a rectangle or other simple shape. I suggest only that there are many problems in which it can be done, and that in these cases, this procedure offers a hope of high accuracy combined with reasonable economy in time of computation.

It seems to me that in a paper addressed to stress-analysts some attempt must be made to assess the place of numerical methods in the general field of stress determination. How do the numerical techniques compare for difficulty, for accuracy, and for speed with experimental techniques? Perhaps it should be said that the fields covered by the two do not entirely coincide. So far as I am aware relaxation has been applied very little to the three-dimensional problems for which stress-freezing has been developed. On the other hand, it has been applied to a very large range of problems, mainly in the field of vibrations, of stability, and of plasticity in which no experimenta lmethod is available except perhaps the direct measurement of strain and displacement by electronic means.

In those fields which computation and experiment have in common, they are not, of course, in competition in any real sense, since to possess two entirely separate methods of doing the same thing is a highly desirable state of affairs. Which of the two is economically of the greatest value is in my view a matter which depends on circumstances. If only a small number of results are required, plainly the numerical method can be employed without the capital expenditure necessary to

* Once ξ has been determined by relaxation, η its harmonic conjugate can be deduced immediately, cf., for example, Gandy and Southwell.[10]

purchase and maintain equipment. Any conceivable type of loading can be computed (some much more easily than others), but there may be practical difficulties in applying some loads to a photo-elastic specimen. On the other hand, where analysis of a large number of roughly similar but complicated specimens is required I have no doubt that time can be saved by the use of the experimental method.

In this paper I have tried to show that although in some of the very difficult problems which have been shown to be within the scope of the relaxation method, the computational work is necessarily very heavy, there are many problems of interest to the stress-analyst in which by an appropriate choice of method on points of detail, results of value can be obtained with relatively very little labour.

REFERENCES

(1) Richardson, L. F. *Philos. Trans. A*, **210**, p. 307 (1910).
(2) Thom, A., and Orr, J. *Proc. Roy. Soc. A*, **131**, p. 30 (1931).
(3) Christopherson, D. G., and Southwell, R. V. *Proc. Roy. Soc. A*, **168**, p. 317 (1938).
(4) Fox, L. *Quart. J. Mech. Appl. Math.*, **1**, p. 253 (1948).
(5) Richardson, L. F., and Gaunt, J. A. *Philos. Trans. A*, **226**, p. 299 (1927).
(6) Fox, L. *Philos. Trans. A*, **242**, p. 345 (1950).
(7) Bickley, W. G. *Quart. J. Mech. Appl. Math.*, **1**, p. 35 (1948).
(8) Timoshenko, S. P. *Theory of Elasticity*, 1st Ed., p. 248 (New York: McGraw-Hill Publishing Co. Inc., 1934).
(9) Southwell, R. V. *Hardy Cross Symposium "Numerical Methods of Analysis in Engineering,"* p. 66 (MacMillan, New York).
(10) Gandy, R. W. G., and Southwell, R. V. *Philos. Trans. A*, **238**, p. 453 (1940).

ORIGINAL CONTRIBUTIONS

The elasticity and strength of paper and other fibrous materials

By H. L. Cox, M.A., F.R.Ae.S., A.M.I.Mech.E., The National Physical Laboratory, Teddington, Middlesex

[*Paper first received* 18 *May*, 1951, *and in final form* 13 *August*, 1951]

An analysis is made of the effect of orientation of the fibres on the stiffness and strength of paper and other fibrous materials. It is shown that these effects may be represented completely by the first few coefficients of the distribution function for the fibres in respect of orientation, the first three Fourier coefficients for a planar matrix and the first fifteen spherical harmonics for a solid medium. For the planar case it is shown that all possible types of elastic behaviour may be represented by composition of four sets of parallel fibres in appropriate ratios. The means of transfer of load from fibre to fibre are considered and it is concluded that the effect of short fibres may be represented merely by use of a reduced value for their modulus of elasticity. The results of the analysis are applied to certain samples of resin bonded fibrous filled materials and moderately good agreement with experimental results is found.

1. INTRODUCTION

The elastic properties and strength of any material depend upon the detail of its structure, and analysis of this structure should enable the strength and stiffness of the whole to be correlated to that of its parts. This paper is concerned with those materials which derive their strength and stiffness wholely or mainly from thin fibres capable of transmitting high loads along their lengths but offering no great resistance to loading transverse to their lengths. The first and main purpose of the note is to consider how the properties of such materials may depend upon the orientation of the fibres. For this purpose the conception of an ideal mat of fibres is first propounded; the characteristic properties of such an ideal mat are then established, and the extent to which these properties may be adjusted by suitably orienting the fibres is explored. The application to practical materials of the conclusions with regard to orientation effects is, of course, affected by the differences between the ideal mat and the actual material. The effect of some of these differences is partially explored and the manner in which the behaviour of the actual material may be modified is demonstrated.

2. THE IDEAL MAT OF FIBRES

The considerations in this paper are based in the first place on the conception of an ideal paper or fabric, consisting of a perfectly homogeneous plane or solid mat of long straight thin fibres oriented either at random or according to some definite law of statistical distribution. Each fibre is assumed to extend in one straight line throughout the whole body of the material and to be loaded only at its ends. The flexural stiffness of a single fibre is assumed to be negligible, so that the fibre can transmit load only in tension, and the loading applied at the edges or free surfaces of the material is assumed to fulfil this condition. If at the loaded edges the fibres are all bonded rigidly together this condition is met automatically without consideration of the details of the applied loading, except that a check is needed to ascertain that no fibre is thrown into compression; and the need for this check may be evaded by assuming that initially the whole mat is subjected to uniform biaxial or triaxial tension so that the initial tensile load (equal in every fibre) is sufficient to annul any compressive component of load afterwards applied, or by assuming that the fibres are otherwise supported so that they can carry compression. All the characteristics of the ideal mat of fibres may be illustrated by a pocket handkerchief stretched between the hands, and the entire lack of stiffness of this model to shear parallel to the warp and weft demonstrates the utility of the ideal mat as a means to represent the effects of fibre orientation.

3. THE PLANAR MAT OF FIBRES

If a planar mat of fibres is subjected to tensile strains e_1 and e_2 in two directions at right angles and to a shear strain ϕ between these directions, the strain of a fibre inclined at angle θ to the direction of e_1 is $e_1 \cos^2\theta + e_2 \sin^2\theta + \phi \cos\theta \sin\theta$, and the load in the fibre will be assumed to be proportional to this strain. Then the contributions of this fibre to the loads in the directions

of e_1 and e_2 respectively are the products of the load in the fibre with $\cos\theta$ and $\sin\theta$ respectively.

The number of fibres at angle θ which intersect lines of unit length perpendicular to the directions of e_1 and e_2 respectively are $f(\theta)\cos\theta$ and $f(\theta)\sin\theta$, where $f(\theta)$ is the "distribution function" which expresses the manner in which the fibres are grouped according to the angle θ; that is, $f(\theta)$ is the number of fibres at angle θ in unit width transverse to their own direction, and we take

$$\int_0^{\pi} f(\theta)d\theta = 1^* \tag{1}$$

Combining these data, the loads per unit width of edge, P_1 in the direction of e_1 on the edge perpendicular to e_1, P_2 in the direction of e_2 on the edge perpendicular to e_2, and Q in the direction of e_1 on the edge perpendicular to e_2 or vice versa are defined as

$$P_1 = K\int_0^{\pi}(e_1\cos^2\theta + e_2\sin^2\theta + \phi\cos\theta\sin\theta)\cos^2\theta f(\theta)d\theta$$

$$P_2 = K\int_0^{\pi}(e_1\cos^2\theta + e_2\sin^2\theta + \phi\cos\theta\sin\theta)\sin^2\theta f(\theta)d\theta$$

$$Q = K\int_0^{\pi}(e_1\cos^2\theta + e_2\sin^2\theta + \phi\cos\theta\sin\theta)\cos\theta\sin\theta f(\theta)d\theta$$

where K is a constant, the product of fibre modulus and density of fibres; or, preferably, if the loads are divided by the density (specific loads), K is the fibre modulus divided by the density of the fibre material.

That is
$$\left.\begin{aligned} P_1 &= c_{11}e_1 + c_{12}e_2 + c_{16}\phi \\ P_2 &= c_{12}e_1 + c_{22}e_2 + c_{26}\phi \end{aligned}\right\} \tag{2}$$
and
$$Q = c_{16}e_1 + c_{26}e_2 + c_{66}\phi \quad\dagger$$

where

$$\left.\begin{aligned} c_{11} &= K\int_0^{\pi}\cos^4\theta f(\theta)d\theta, \\ c_{22} &= K\int_0^{\pi}\sin^4\theta f(\theta)d\theta \\ c_{16} &= K\int_0^{\pi}\cos^3\theta\sin\theta f(\theta)d\theta, \\ c_{26} &= K\int_0^{\pi}\cos\theta\sin^3\theta f(\theta)d\theta \text{ and} \\ c_{12} &= c_{66}\text{(which is one of Cauchy's relations)} \\ &= K\int_0^{\pi}\cos^2\theta\sin^2\theta f(\theta)d\theta \end{aligned}\right\} \tag{3}$$

The functions $\cos^4\theta$, etc., may be re-written in the forms

$$\left.\begin{aligned} \cos^4\theta &= (1/8)(3 + 4\cos 2\theta + \cos 4\theta) \\ \sin^4\theta &= (1/8)(3 - 4\cos 2\theta + \cos 4\theta) \\ \cos^2\theta\sin^2\theta &= (1/8)(1 - \cos 4\theta) \\ \cos^3\theta\sin\theta &= (1/8)(2\sin 2\theta + \sin 4\theta) \\ \cos\theta\sin^3\theta &= (1/8)(2\sin 2\theta - \sin 4\theta) \end{aligned}\right\} \tag{4}$$

and the function $f(\theta)$, which must clearly be periodic, may be expanded in the form

$$\pi f(\theta) = 1 + a_1\cos 2\theta + a_2\cos 4\theta + a_3\cos 6\theta + \ldots + b_1\sin 2\theta + b_2\sin 4\theta + \ldots$$

Therefore by integration the formulae for c_{11}, etc., become

$$\left.\begin{aligned} c_{11} &= \frac{K}{16}(6 + 4a_1 + a_2),\ c_{22} = \frac{K}{16}(6 - 4a_1 + a_2) \\ c_{16} &= \frac{K}{16}(2b_1 + b_2),\ c_{26} = \frac{K}{16}(2b_1 - b_2) \\ \text{and } c_{12} &= c_{66} = \frac{K}{16}(2 - a_2) \end{aligned}\right\} \tag{5}$$

None of the higher order terms in the expansion of $f(\theta)$, such as $a_3\cos 6\theta$, affects the elastic constants. Furthermore, since strains $e_1 e_2$ and ϕ have been specified, the direction $\theta = 0$ may still be chosen arbitrarily. Accordingly this direction may be chosen to eliminate one of the four coefficients $a_1 a_2$, etc., or to satisfy one arbitrary relation between them. However, it is convenient for later application to retain the forms (5) and merely to note that the four constants are derived from three only.

By inverting the formulae (2) in the forms

$$\left.\begin{aligned} e_1 &= S_{11}P_1 + S_{12}P_2 + S_{16}Q \\ e_2 &= S_{12}P_1 + S_{22}P_2 + S_{26}Q \\ \phi &= S_{16}P_1 + S_{26}P_2 + S_{66}Q \end{aligned}\right\} \tag{6}$$

The constants S_{11}, etc., may be expressed in the form

$$\left.\begin{aligned} S_{11} &= [(2 - a_2)(6 - 4a_1 + a_2) - (2b_1 - b_2)^2]/\Delta \\ S_{22} &= [(2 - a_2)(6 + 4a_1 + a_2) - (2b_1 + b_2)^2]/\Delta \\ S_{12} &= -[(2 - a_2)^2 - 4b_1^2 + b_2^2]/\Delta \\ S_{16} &= -4[(2 - 2a_1 + a_2)b_1 + (2 - a_1)b_2]/\Delta \\ S_{26} &= -4[(2 + 2a_1 + a_2)b_1 - (2 + a_1)b_2]/\Delta \\ S_{66} &= 16(2 + a_2 - a_1^2)/\Delta \\ &\text{where} \\ \Delta &= K[(2 + a_2 - a_1^2)(2 - a_2 - b_1^2) - (a_1b_1 - b_2)^2] \end{aligned}\right\} \tag{7}$$

By substituting $(\theta + \alpha)$ for θ in the expansion for $f(\theta)$ and then choosing the direction $\theta = 0$ so that $b_1 = 0$, it may be shown that

$$KS_{11} = [(12 - 2a_1^2 - a_2^2 - b_2^2) - 4a_1(2 - a_2)\cos 2\alpha + 2(a_1^2 - 2a_2)\cos 4\alpha + 4a_1b_2\sin 2\alpha - 4b_2\sin 4\alpha]/[(2 - a_2)(2 + a_2 - a_1^2) - b_2^2] \tag{8}$$

$$KS_{66} = 8[(4 - a_1^2) + (2a_2 - a_1^2)\cos 4\alpha + 2b_2\sin 4\alpha]/[(2 - a_2)(2 + a_2 - a_1^2) - b_2^2] \tag{9}$$

(The denominator Δ is, of course, invariant to change of reference line for θ.)

These formulae (8) and (9) show that the moduli

---

* $\int_0^{\pi} f(\theta)d\theta$ is actually the fibre density, the total number of fibres of unit length per unit of area; but in a homogeneous mat fibre density merely determines the scale of the load-strain relationships and does not affect their type. Therefore for discussion of the effects of fibre orientation we may take $\int_0^{\pi} f(\theta)d\theta = 1$ without loss of generality.

† The suffix 6 is used instead of 3 in order to conform to the notation used in discussion of the three-dimensional case.

$E = 1/S_{11}$ and $G = 1/S_{66}$ are capable of varying with α in a rather complex manner.

If the material were isotropic $a_1a_2b_2$ must all be zero and Young's modulus, $E = 1/S_{11} = K/3$.

Shear modulus, $G = 1/S_{66} = K/8$.

Poisson's ratio, $\sigma = -S_{12}/S_{11} = 1/3$.

and, of course, $E/G \equiv 2(1 + \sigma)$.

4. FIBRE DISTRIBUTIONS REPRESENTED BY SYSTEMS OF PARALLEL FIBRES

So far as the elastic properties of the planar mat of fibres is concerned, the distribution of the fibres is completely represented by the kernel of the distribution function

$$\pi f(\theta) = 1 + a_1 \cos 2\theta + a_2 \cos 4\theta + b_2 \sin 4\theta \quad (10)$$

but this form affords no clue as to the values which the coefficients a_1, a_2 and b_2 may assume. A clearer insight into the structure of the distribution function is afforded by representation of the distribution by systems of parallel fibres.

If all the fibres were parallel to the direction $\theta = \beta$, the distribution function would be

$$\pi f(\theta) = 1 + 2\cos 2(\theta - \beta) + 2\cos 4(\theta - \beta) + 2\cos 6(\theta - \beta) + \ldots \quad (11)$$

and by combining this with the system parallel to the direction $\theta = \pi/2 + \beta$, namely

$$\pi f(\theta) = 1 - 2\cos 2(\theta - \beta) + 2\cos 4(\theta - \beta) - 2\cos 6(\theta - \beta) + \ldots \quad (12)$$

the crossed system composed of equal numbers of fibres in the two directions $\theta = \beta$ and $\theta = \pi/2 + \beta$ is represented by

$$\pi f(\theta) = 1 + 2\cos 4(\theta - \beta) + 2\cos 8(\theta - \beta) + \ldots \quad (13)$$

a result which follows also by substituting $2(\theta - \beta)$ for $(\theta - \beta)$ in (11), so that the distribution previously repeated at intervals of π now repeats at intervals of $\pi/2$.

By taking together X fibres of system (11), with $\beta = 0$, Y fibres of system (12), with $\beta = 0$ (at right angles to the X system), and $Z(= 1 - X - Y)$ fibres of system (13) distributed equally between the direction $\theta = \beta$ and $\theta = \pi/2 + \beta$, the kernel of the complete distribution function becomes:

$$\begin{aligned}\pi f(\theta) &= 1 + 2(X - Y)\cos 2\theta + 2(X + Y)\cos 4\theta + 2Z\cos 4(\theta - \beta) \\ &= 1 + 2(X - Y)\cos 2\theta + 2[1 - Z(1 - \cos 4\beta)]\cos 4\theta + 2Z\sin 4\beta \sin 4\theta \end{aligned} \quad (14)$$

Thus for any fibre distribution which may be representable in this way

$$a_1 = 2(X - Y),\ a_2 = 2[1 - Z(1 - \cos 4\beta)]$$

and

$$b_2 = 2Z \sin 4\beta$$

Then, since X, Y and Z must all lie between 0 and 1, the values of a_1 a_2 and b_2 must also lie between -2 and 2. That the values of a_1, etc., are so restricted, no matter how the fibres are distributed, is at once apparent by generalizing (11) in the form

$$\pi f(\theta) = \Sigma X + 2(\Sigma X \cos 2\beta)\cos 2\theta + \ldots \quad (15)$$

Under the conditions that all X are positive and that $\Sigma X = 1$, it is clear that $|\Sigma X \cos 2\beta| \leqslant 1$; but the formulae imply certain other restrictive relations between the values of a_1, a_2 and b_2. It is uncertain whether these further restrictions apply also irrespective of the detail of the fibre distribution; but it is very probable that they do, and the further argument will be developed on this assumption.

Thus it will be assumed that the elastic properties of any fibre distribution whatsoever may be reproduced by arranging X fibres at $\theta = 0$, Y at $\theta = \pi/2$ and dividing the remainder Z equally between the directions $\theta = \beta$ and $\theta = \pi/2 + \beta$. For this system

$$a_1 = 2(X - Y),\ 2 - a_2 = 2Z(1 - \cos 4\beta)$$

and

$$b_2 = 2Z \sin 4\beta \quad (16)$$

5. ASYMMETRICAL FIBRE DISTRIBUTIONS

The fibre distribution is asymmetrical unless the choice of reference axis which eliminates b_1 also eliminates b_2, that is unless $4\beta = 0$ or π. The principal characteristic of an asymmetrical system is naturally the asymmetry of its properties, and such a system is unlikely to be chosen unless this specific characteristic is required. In such cases, or in cases which may occur naturally, the elastic properties are best discussed in terms of formulae (5), that is in terms of the coefficients c_{11}, etc. Since the values of c_{16} and c_{26} will probably be the subjects of stated requirements, the variations of the moduli E and G with orientation α [formulae (8) and (9)] are then of secondary interest, and it seems unnecessary to attempt to discuss formula (8) in detail. On the other hand, the presence of the term b_2 does not complicate formula (9) so much, and it appears worth while to examine the variation of G with α in the general case.

From formula (9), by rearranging the denominator

$$G = \{(4 - a_1^2)^2 - [(2a_2 - a_1^2)^2 + 4b_2^2]\}/32[(4 - a_1^2) + (2a_2 - a_1^2)\cos 4\alpha + 2b_2 \sin 4\alpha] \quad (17)$$

of which the principal values are

$$G = (1/32)\{4 - a_1^2 \pm [(2a_2 - a_1^2)^2 + 4b_2^2]^{\frac{1}{2}}\} \quad (17a)$$

at $\tan 4\alpha = 2b_2/(2a_2 - a_1^2)$ (the principal directions being inclined at $\pi/4$). Expanding the term $(2a_2 - a_1^2)^2 + 4b_2^2$ and substituting for a_2 and b_2 from (16), this term may be written

$$(4 - a_1^2)^2 - 8Z[4(1 - Z) - a_1^2](1 - \cos 4\beta)$$

where

$$4(1 - Z) = 4(X + Y) > 4(X + Y)^2 > 4(X - Y)^2 > a_1^2$$

Therefore the greatest value of this term is when $\beta = 0$ and is then $(4 - a_1^2)^2$ and its least value is when $\beta = \pi/4$ and is $(4 - a_1^2 - 8Z)^2$. Both these cases are symmetrical arrangements, and it therefore follows (*inter alia*) that the highest possible value of G (see below, Section 6) results from a symmetrical distribution. Moreover, from (17) it is apparent that the presence of b_2 increases the variation of G with α.

Therefore it is reasonable to conclude that asymmetrical distributions offer no advantage in respect of shear modulus. Similar discussion of formula (8) is not feasible because E is a function of both 2α and 4α; but it appears unlikely that any real benefit would result from the use of an asymmetrical distribution.

6. SYMMETRICAL FIBRE DISTRIBUTIONS

When the fibre distribution is symmetrical $\beta = 0$ or $\pi/4$ and $b_2 = 0$; but we may also exclude the case $\beta = 0$, because it merely represents a two-axis system, which can be represented with $\beta = \pi/4$ by writing $X + \frac{1}{2}Z$ for X and $Y + \frac{1}{2}Z$ for Y and 0 for Z.

Therefore

$$a_1 = 2(X - Y), a_2 = 2(1 - 2Z) \quad (18)$$

and without loss of generality we may assume $X > Y$.

Then

$$G = \frac{(2 - a_2)(2 + a_2 - a_1^2)}{8[(4 - a_1^2) + (2a_2 - a_1^2)\cos 4\alpha]} = \frac{Z[4(1 - Z) - a_1^2]}{2[(4 - a_1^2) + (4 - a_1^2 - 8Z)\cos 4\alpha]} \quad (19)$$

and

$$E = (2 - a_2)(2 + a_2 - a_1^2)/[(12 - 2a_1^2 - a_2^2 - 4a_1(2 - a_2)\cos 2\alpha + 2(a_1^2 - 2a_2)\cos 4\alpha] = 2Z[4(1 - Z) - a_1^2]/\{[(4 - a_1^2) + 8Z(1 - Z)] - 8a_1 Z\cos 2\alpha - (4 - a_1^2 - 8Z)\cos 4\alpha\} \quad (20)$$

The two principal values of G are

$$Z/4 \text{ at } \alpha = 0 \quad (21)$$

$$(1/4)[(1 - Z) - (X - Y)^2] \text{ at } \alpha = \pi/4 \quad (22)$$

and the *three* principal values of E are

$$[(1 - Z) - (X - Y)^2]/[(2 - Z) - 2(X - Y)] \text{ at } \alpha = 0 \quad (23)$$

$$Z[(1 - 2Z) - (X - Y)^2]/[(1 + Z)(1 - 2Z) - (X - Y)^2] \text{ at } \alpha = \tfrac{1}{2}\cos^{-1}\frac{(X - Y)Z}{[(X - Y)^2 - 1 + 2Z]} \quad (24)$$

and

$$[(1 - Z) - (X - Y)^2]/[(2 - Z) + 2(X - Y)] \text{ at } \alpha = \pi/2 \quad (25)$$

If $|(X - Y)Z| > |(X - Y)^2 - 1 + 2Z|$, the value of α corresponding to the intermediate principal value of E is imaginary; in that case the value of E at $\alpha = 0$ is the maximum value and the value of E at $\alpha = \pi/2$ is the minimum. On the other hand, when the value of α corresponding to the intermediate principal value of E is real, this principal value is either less than the value of E at $\alpha = \pi/2$ or greater than that at $\alpha = 0$. The necessary and sufficient condition that the true maximum value of E should exceed that at $\alpha = 0$ is

$$X < (1 - Y)(1 - 2Y)/(1 + 2Y) \quad (26)$$

and the similar condition that the true minimum value of E should be less than that at $\alpha = \pi/2$ is

$$Y > (1 - X)(1 - 2X)/(1 + 2X) \quad (27)$$

In Fig. 1 contours of constant E_0, $E_{\pi/2}$, E_{max} and E_{min} are shown plotted on a map representing all possible combinations of X, Y and Z; and Fig. 2 shows contours of constant G_0 and $G_{\pi/4}$. The contours of E_0 and $E_{\pi/2}$ are continuous over the whole field, but the lines (26) and (27) divide the field into three parts and only in the central part do E_0 and $E_{\pi/2}$ represent the true maximum and minimum values of the modulus. When more than half the total number of fibres is arranged at $\pm\pi/4$, the distribution is highly resistant to shear at $\alpha = 0$ or $\pi/2$, but the modulus in these directions is low and the maximum modulus is developed in a direction between $\alpha = 0$ and $\alpha = \pi/4$; this is represented in Fig. 1 by the contours of E_{max} which in the lower region deviate from the contours of E_0. Similarly when a high proportion of the total number of fibres is arranged at $\pi/2$, the arrangement is not strongly resistant to shear and the true minimum modulus is developed in a direction between $\alpha = \pi/4$ and $\alpha = \pi/2$; this is represented in Fig. 1 by the contours of E_{min} which in the upper region deviate from the contours of $E_{\pi/2}$. In the middle region the values of the modulus at all values of α lie between the values of E_0 and $E_{\pi/2}$.

In Fig. 2 the lines of constant Z also represent contours of constant G_0, but the contours of constant $G_{\pi/4}$ are parabolas. At high values of Z, $G_0 > G_{\pi/4}$ and the line defined by $G_0 = G_{\pi/4}$ which is $(X - Y)^2 = 1 - 2Z$ lies wholly in the region in which E_0 and $E_{\pi/2}$ are the true maximum and minimum values of the modulus. All three limiting lines $E_0 = E_{max}$, $E_{\pi/2} = E_{min}$ and $G_0 = G_{\pi/4}$ meet at the common point $2X = 2Y = Z = \frac{1}{2}$, which represent a state of complete isotropy.

One feature of Fig. 1 is that, when $Y = 0, E_0 + 4G_0 = 1$. If the value of G_0 be specified, this condition gives the greatest possible value of $E_0 = 1 - 4G_0$. Although the

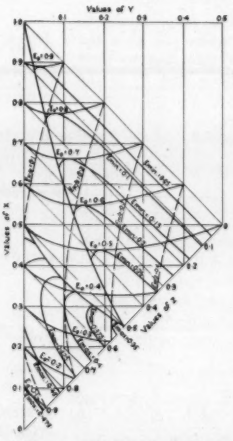

Fig. 1. Effect of fibre orientation on the principal values of Young's modulus

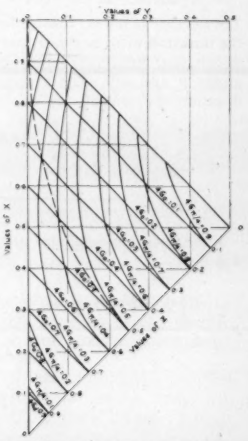

Fig. 2. Effect of fibre orientation on the principal values of shear modulus

corresponding value of $E_{\pi/2}$ is not zero, it may be inconveniently low; by rotating a few fibres from $\alpha = 0$ to $\alpha = 90°$, that is, by increasing Y slightly at the expense of X, the value of $E_{\pi/2}$ may be improved without serious reduction of E_0; moreover, this change improves the value of $G_{\pi/4}$. This is illustrated by the comparison below:

	X	Y	Z	E_0	$E_{\pi/2}$	G_0	$G_{\pi/4}$
Case 1	0·60	0	0·40	0·600	0·086	0·100	0·060
Case 2	0·54	0·06	0·40	0·577	0·144	0·100	0·092

7. THE SOLID MAT OF FIBRES

The case of the solid mat may be treated exactly as in Sections 3 to 6. It may be shown that the 21 elastic constants reduce to 15 by the automatic satisfaction of the Cauchy relations, $c_{12} = c_{66}$, $c_{14} = c_{56}$, etc., and that the elastic constants depend only on the first fifteen of the coefficients of the expansion of the fibre distribution function in spherical harmonics. Furthermore, the last nine of these coefficients affect only the coefficients such as c_{14} which describe the effects of direct stress in causing shear strains and of shear stress in causing direct strains.

However, here attention is restricted to highly symmetrical fibre distribution subjected to direct strains only, since these cases suffice to illustrate the modification of the conclusions drawn for a planar mat when in fact the fibres lie not entirely in one plane.

If a solid mat of fibres be subjected to strains e_1, e_2 and e_3 in three directions at right-angles, a fibre making an angle θ with the direction of e_1 and lying in a plane making an angle ψ with the plane of e_1 and e_2 is subjected to a strain

$$(e_1 \cos^2\theta + e_2 \sin^2\theta \cos^2\psi + e_3 \sin^2\theta \sin^2\psi)$$

The number of fibres crossing unit area perpendicular to the direction of e_1 is $f(\theta, \psi)\cos\theta$, where $f(\theta, \psi)$ is the distribution function of the fibres according to their angles θ and ψ.* The average fibre load P_1 in the direction of e_1 is then

$$P_1 = \frac{\int_0^{2\pi}\int_0^{\pi/2} K(e_1 \cos^2\theta + e_2 \sin^2\theta \cos^2\psi + e_3 \sin^2\theta \sin^2\psi)\cos^2\theta f(\theta, \psi) d\theta d\psi}{\int_0^{2\pi}\int_0^{\pi/2} f(\theta, \psi) d\theta d\psi} \tag{28}$$

If the fibres are orientated at random, $f(\theta, \psi) = \sin\theta$, and then

$$P_1 = \frac{K\int_0^{\pi/2}(e_1 \cos^2\theta + \tfrac{1}{2}e_2 \sin^2\theta + \tfrac{1}{2}e_3 \sin^2\theta)\cos^2\theta \sin\theta d\theta}{\int_0^{\pi/2} \sin\theta d\theta}$$

$$= \frac{K}{5}\left(e_1 + \frac{1}{3}e_2 + \frac{1}{3}e_3\right) \tag{29}$$

and by symmetry the formulae for P_2 and P_3 are similar.

* As in the planar case, we assume that the lateral distribution of fibres is statistically uniform.

It follows that

$$e_1 = \frac{6}{K}\left(P_1 - \frac{1}{4}P_2 - \frac{1}{4}P_3\right)$$

and similarly for e_2 and e_3. In this case, therefore, Young's modulus $= K/6$, Poisson's ratio $= 1/4$ and the shear modulus $= K/15$.

The condition of completely random orientation of fibres in a solid mat is not likely to be realized in a paper, so that it appears worth while to attempt to represent a compromise between the planar and the solid mat. This may be done by assuming $f(\theta, \psi) = \sin\theta$ for $\alpha < \theta < \pi/2$ and $f(\theta, \psi) = 0$ for $\theta < \alpha$. Then using the formula (29) and the corresponding forms for P_2 and P_3 it may be shown that

$$e_1 = \frac{3(15 - 10\cos^2\alpha + 3\cos^4\alpha)}{4K\cos^4\alpha}\left[P_1 - \frac{\cos^2\alpha(5 - 3\cos^2\alpha)}{15 - 10\cos^2\alpha + 3\cos^4\alpha}(P_2 + P_3)\right]$$

and

$$e_2 = \frac{3(85 - 30\cos^2\alpha + 9\cos^4\alpha)}{4K(15 - 10\cos^2\alpha + 3\cos^4\alpha)}\left[P_2 + \frac{5 - 30\cos^2\alpha + 9\cos^4\alpha}{85 - 30\cos^2\alpha + 9\cos^4\alpha}P_3 - \frac{(5 - 3\cos^2\alpha)(15 - 10\cos^2\alpha + 3\cos^4\alpha)}{\cos^2\alpha(85 - 30\cos^2\alpha + 9\cos^4\alpha)}P_1\right] \tag{30}$$

and similarly for e_3 with P_2 and P_3 interchanged.

These formulae reduce correctly to those appropriate to the solid mat of random orientation when $\alpha = 0$ and they also reduce to those for the planar mat when $\alpha = \pi/2$. This is because

$$\frac{P_1}{\cos^2\alpha} = \frac{K}{5}\left[e_1 \cos^2\alpha + \frac{1}{6}(5 - 3\cos^2\alpha)(e_2 + e_3)\right]$$

and P tends to $(K/6)(e_2 + e_3)\cos^2\alpha$, which itself tends to zero as α tends to $\pi/2$.

On the other hand, if P_1 is made identically zero, as α tends to $\pi/2$, e_2 tends to

$$\frac{17}{4E}\left(P_2 + \frac{1}{17}P_3\right),$$

a result substantially different from the form

$$e_2 = \frac{3}{E}\left(P_2 - \frac{1}{3}P_3\right)$$

obtained in Section 3.

The explanation of this apparent discrepancy is that, if the fibres are even to the slightest degree kinked out of the e_2e_3 plane, tensile forces in this plane tend to straighten them; there being no fibres in the direction

normal to the e_2e_3 plane, this straighening is resisted only by the fibres at right-angles to the direction of tension, the ends of which must approach or recede in accordance with the lateral motion in the direction e_1. Since this secondary effect on the fibres at right-angles is a toggle action, it is more than sufficient to counteract the usual contraction appropriate to a true planar mat and to result in lateral *expansion*, i.e. a negative value of Poisson's ratio. At the same time, of course, the Poisson's ratio through the thickness must have a very high positive value (proportional to $\sec^2 \alpha$).

In practice the appropriate value of α may be expected to be well removed from both limits ($\alpha = 0$ and $\alpha = \pi/2$); values of the effective modulus in the plane e_2e_3 and of the two Poisson's ratios (in the plane and through the thickness of the paper) are shown in Fig. 3. It will be seen that the variation of modulus with α is not great, but that the variation of the Poisson's ratios is very considerable.

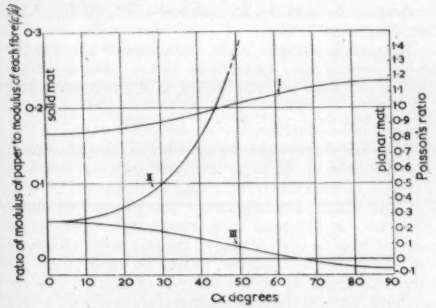

Fig. 3. Variation of elastic properties as structure varies from solid to planar mat

(I) Young's modulus (E^1/E).
(II) Poisson's ratio through thickness of paper.
(III) Poisson's ratio in plane of paper.

The effect of preferred orientation of the fibres in the e_2e_3 plane may readily be superposed, e.g. by using a function $f(\theta, \psi) = \sin\theta \cos^2\psi$ in place of $\sin\theta$ only; but this extension of the analysis along the lines of Sections 3 to 6 is not attempted here.

8. APPLICATION OF THE CONCLUSIONS TO PRACTICAL MATERIALS

In seeking to apply the conclusions of Sections 3 to 7 to actual materials consideration has to be given to the effect of departures from the conditions stated in Section 2; the fibres are not in practice very long and for that reason and for others the distribution of fibres cannot be quite homogeneous. In respect of length it is not unreasonable to assume that individual short fibres are disposed in continuous lines either end to end or with a slight overlap, or that at each point of overlap between fibres three or more are arranged at such angular spacings that the forces at the joint are automatically in balance. Whatever assumption is made in this respect it is still necessary to consider how the loads may be transmitted from one fibre to another. This latter consideration is really the more important one, and a satisfactory representation of the means by which the loads may be transmitted must itself virtually solve the problem of continuity of the fibre structure. The conception developed here is one appropriate to resin-bonded fibrous filled materials, where each fibre may be considered as embedded in the continuous solid medium of the resin. For this case it may be assumed that the resin matrix as a whole is strained homogeneously, but that locally this state of uniform stress and strain is perturbed by the transfer of load to the fibres. If then it be assumed that the lateral stiffness of the fibres is the same as that of the resin matrix it is necessary to discuss only how the load in the direction of the length of the fibre is shared between fibre and matrix in consequence of the greater stiffness of the fibre in this direction.

If a straight fibre of length l is embedded in a solid matrix, and if the whole matrix is subjected to a strain e in the direction of the fibre, the rate of transfer of load from matrix to fibre and vice versa will depend on the relation between the displacement u in the direction of the length of the fibre at distance x from one end and v the displacement of the matrix at the same point, if the fibre were absent. If we assume that $dP/dx = H(u - v)$, where P is the load in the fibre and H is a constant, then since $P = EA(du/dx)$, where A is the area of section of the fibre and E is its modulus of elasticity,* and since $dv/dx = e = \text{constant}$, we have $d^2P/dx^2 = H(P/EA - e)$.

Then $P = EAe + R \sinh \beta x + S \cosh \beta x$, where $\beta = \sqrt{(H/EA)}$ and R and S are constants. Taking into account the end conditions, $P = 0$ at $x = 0$ and at $x = l$, we have finally

$$P = EAe\left[1 - \frac{\cosh \beta(l/2 - x)}{\cosh \beta(l/2)}\right] \tag{31}$$

The mean load in the fibre is then

$$EAe\left[1 - \frac{\tanh (\beta l/2)}{(\beta l/2)}\right] \tag{32}$$

so that its effective modulus is reduced in the ratio

$$1 - \frac{\tanh (\beta l/2)}{(\beta l/2)} \tag{33}$$

If $\beta l/2$ is large, the value of this ratio approaches unity, but if $\beta l/2$ is small, it tends to zero; we have therefore to consider the magnitude of $\frac{1}{2}l\sqrt{(H/EA)}$.

If the fibre has the form of a round rod of radius r_0, $A = \pi r_0^2$; if the mean separation of the fibres normal to their length is r_1, and if the shear modulus of the matrix is G, then

$$H = 2\pi G/\log_e (r_1/r_0) \tag{34}$$

But approximately $2\pi r_0^2/\sqrt{(3)}r_1^2 = \text{relative fibre density} = \text{actual fibre density}/1{\cdot}57$.† Hence $r_0/r_1 =$

* Strictly the excess of its modulus over that of the displaced thread of resin.

† Assuming that the packing of the fibres transversely is roughly hexagonal and taking the density of the (cellulose) fibre as 1·57.

$0{\cdot}42\sqrt{}$(fibre density). For a resin-bonded board of s.g. 1·40 containing 40% resin of s.g. 1·26, the actual fibre density is $1{\cdot}40 - 0{\cdot}4 \times 1{\cdot}26 = 0{\cdot}896$, so that $r_0/r_1 = 0{\cdot}4$ and hence $H = 6{\cdot}85G$, and finally $\frac{1}{2}l(H/EA)^{\frac{1}{2}} = \frac{1}{2}(l/r_0)(6{\cdot}85G/\pi E)^{\frac{1}{2}} =$ about $0{\cdot}12(l/r_0)$ taking $E = 10 \times 10^6$ lb/in^2 and $G = 0{\cdot}25 \times 10^6$ lb/in^2. We may therefore conclude that $\beta l/2$ is of the order $0{\cdot}2(l/d)$, where d is the diameter of the fibre.

Taking $d = 0{\cdot}01$ mm, $\beta l/2$ is approximately $20l$ (l being measured in mm); values of the modulus ratio for various values of l are given below.

l (mm)	0·1	0·2	0·3	0·4	0·5
Modulus ratio	0·518	0·750	0·833	0·875	0·900
l (mm)	1·0	2·0	3·0	4·0	5·0
Modulus ratio	0·950	0·975	0·983	0·988	0·990

Although fibre lengths exceeding 1 mm are included in the above table, it would at first sight appear that the condition that the fibre shall be straight, must restrict the application of the present results to fairly short fibres, say 1 mm or less in length. On the other hand, suppose a long fibre of length l is kinked at each half-millimetre, then each of these sub-lengths except the two end ones may be considered to be "grouted" into the matrix and to be subjected to the same uniform strain as the matrix throughout its length. The two end lengths each 0·5 mm long, being rigidly held at one end and free at the other, are by symmetry equivalent to one fibre 1 mm long with both ends free. Accordingly the mean modulus ratio for the whole fibre is

$$(1/l)(l - 1 + 0{\cdot}95) = 1 - (0{\cdot}05/l)$$

but it will be seen that this ratio is exactly that given by the table. Moreover, this conclusion is independent of the "kink length" assumed, provided that this length exceeds 0·1 mm (or more generally 10 times the fibre diameter). Accordingly it is concluded that the restriction that the fibre shall be straight is unnecessary, and that the results are applicable to all fibre lengths.

The derivation of the value of r_0/r_1 from the value of the fibre density is, of course, far from precise, but at the same time it is clear that $(r_0/r_1)^2$ must vary directly as the fibre density. The resulting dependence of $\beta l/2$ on fibre density is only slight; reduction of the density from 1 to $\frac{1}{2}$ reduces $\beta l/2$ by 15% only. Since the modulus ratio itself varies only slowly with $\beta l/2$, it appears that the error in the estimation of β may seldom be important.

The general conclusion from this section is that transfer of load from fibre to fibre reduces the effective modulus of the fibre material, but that this reduction is important only if the fibre length is less than 100 times the fibre diameter. If the fibre length is about 10 times its diameter the effective modulus may be reduced to about one-half.

Moreover, the reasoning used for the deduction of the effective modulus of short fibres in effect covers the uncertainty in respect of the actual disposition of the fibres. If a succession of fibres were arranged in line with a moderate overlap the adhesion between this group through the resin matrix might be improved, but elsewhere the effective fibre density must be correspondingly reduced, so that the *average* degree of adhesion would not be much affected.

9. ILLUSTRATION OF THE APPLICATION OF THE CONCLUSIONS

For one resin-bonded board made of 60% paper and 40% resin the specific moduli in two directions at right-angles were 1 370 km and 610 km.* The modulus of the resin was about 300 km, so that the moduli of the paper alone were about 2 080 km and 820 km. From formulae (23) and (25) of Section 6, assuming $X + Y = Z = \frac{1}{2}$†, we find $X = 0{\cdot}412$, $Y = 0{\cdot}088$, and the true fibre modulus should exceed 4 480 km by the allowance to be made for imperfect adhesion. Actually in this paper the fibre length was long, so that the appropriate reduction is probably negligible, and the value 4 480 km is close to the modulus for cellulose (10×10^6 lb/in^2 for specific gravity 1·57).

The specific strengths of the resin-bonded board in the two directions were 14 km and 5½ km. The contribution of the resin per unit weight in the two cases may be estimated as $\frac{300}{1\,370} \times 14 = 3{\cdot}1$ km and $\frac{300}{610} \times 5{\cdot}5 = 2{\cdot}7$ km, and these values are certainly of the right order. The strengths of the paper itself are then $(14 - 0{\cdot}4 \times 3{\cdot}1)/0{\cdot}6 = 21{\cdot}3$ km and $(5{\cdot}5 - 0{\cdot}4 \times 2{\cdot}7)/0{\cdot}6 = 7{\cdot}4$ km. These values indicate a fibre strength of about 35–40 km on the basis of a planar mat. The actual strength may be slightly greater because some allowance for non-planar distribution should be made; but the difference indicated by the analysis of Section 7 is far too great, because the toggle action there described would in this case be prevented by the resin.

For any given combination of fibre and resin it is easy to amend Section 7 to include the effect of the resin. This has been done for the combination of 60% fibre and 40% resin, taking the modulus of the resin as 300 km and its Poisson's ratio as 0·40; these are measured values of one sample. The fibre is assumed to be laminated in the form of paper or fabric and the orientation in the plane of lamination is assumed to be random; the orientation out of the plane of lamination is represented by the limiting angle α as in Section 7. The variation of the modulus in the plane of lamination and of the two Poisson's ratios, in this plane and through the thickness, are shown below for values of α from 90° (planar distribution) to 0° (completely random distribution).

Measurements made on one or two samples of fabric-filled, resin-bonded plastics gave values of the two Poisson's ratios of about 0·25 and 0·45, indicating only a slight degree of lamination of the fibres (α = about

* The specific modulus is the modulus divided by the density, and this quantity has the dimensions of a length. If a length of the material equal to $1/n$ of the specific modulus were suspended vertically, the elastic strain at the upper end would be $1/n$.

† Variation of the division between $X + Y$ and Z makes only slight differences.

α	90° (plane)	80	70	60	50	40	30	20	10	0 (solid)
Modulus (km)	1 016	991	917	814	716	650	613	593	584	580
Poisson's ratio: width	0·341	0·331	0·297	0·244	0·201	0·201	0·233	0·270	0·297	0·306
Poisson's ratio: thickness	0·440	0·478	0·584	0·692	0·710	0·616	0·487	0·385	0·325	0·306

30°); the stiffness of these materials was correspondingly low (about 600 km). One sample of sliver-filled material gave values of Poisson's ratio 0·16 and 0·67 and this material had a modulus of about 850 km; but this material had a resin content rather less than 40%. Except for the Poisson's ratio in the plane of lamination, which seems rather low, these values are consistent with a high degree of lamination (α = about 60°) as would be expected from the form of the fibre filling. Unfortunately similar data for paper-filled, resin-bonded materials are not available.

ACKNOWLEDGMENTS

The work described above was carried out in the Engineering Division of the National Physical Laboratory on behalf of the Ministry of Supply. This paper is published by permission of the Director of the Laboratory and with the approval of the Chief Scientist, Ministry of Supply.

Temperature distribution with simultaneous platten and dielectric heating

By H. M. NELSON, B.Sc., A.M.I.E.E., Aeronautical Research Laboratories, Department of Supply, Melbourne, Australia

[*Paper first received* 18 *May*, 1951, *and in final form* 2 *July*, 1951]

The temperature distribution in a solid of infinite area bounded by two parallel planes in which heat is being uniformly generated and the surfaces of which are maintained at an elevated temperature is evaluated for the case in which the solid is initially at a uniform temperature throughout. A comparison is made between platten and combined heating which shows that the heating time can be divided by a factor which depends on the tolerable temperature variation, but which is of the order of 10 for a variation of 19% and 2·5 for a variation of 1·2%. Some consideration is given to the optimum conditions required for the setting of synthetic resins and like materials for which the setting time is a function of the temperature. Practical considerations which restrict the choice of some of the parameters are mentioned.

1. INTRODUCTION

The temperature distribution in a solid of infinite extent bounded by two parallel planes, the temperature of which is initially uniform and the surfaces of which are maintained at this initial temperature while heat is generated uniformly in the solid, has been determined by Brown,[1] Herne[2] and Carslaw and Jaeger.[3] Numerical evaluations have been made by Brown for a particular value of diffusivity.

A configuration of this type is frequently encountered, an example being the heating of materials by dielectric loss. Even when the surfaces are curved the results of the analysis can be applied with reasonable accuracy providing that the radius of curvature is everywhere large compared with the thickness of the slab. The assumed boundary conditions will obtain if the electrodes are cooled or are of high thermal conductivity and mass so that they remain at the initial temperature. Under these conditions the material near the surfaces must remain unheated, the thickness of this unheated layer depending on the heating rate. We shall see below that this layer is very thin when the rate of generation of internal heat is large. In the steady state (i.e. after a very long heating time) the temperature distribution is of parabolic form rising more slowly towards the centre of the slab.

It is clear that for many processes this type of distribution would not be satisfactory and various devices have been suggested and some used in practice to obtain a more uniform temperature; for example Brown and others[4] suggested a combination of hot plate and heating by dielectric loss. Two curves were published which show a "hump" in the temperature distribution curve near the heated plattens and they also claim that there is no combination of fixed plate temperature and heating rate which will result in a completely uniform temperature. The results presented hereinafter substantially confirm this statement.

In processes involving the curing of many thermosetting resins the criterion for a satisfactory result is not necessarily ultimate temperature uniformity, but uniformity of setting, and, as the setting time is a function of temperature, the time-temperature relationship at each layer of the slab must also be considered. The latter part of this paper is devoted to this problem, and there it is shown that the combination of heating by plattens and dielectric loss can lead under suitable conditions to a substantially uniform result.

While it is shown that this heating method can produce a material which is satisfactorily cured, nevertheless the most satisfactory heating system would be one which raised the temperature at all points of the material at the same rate. Among the methods which have been proposed and used to achieve this result may be mentioned: (1) the use of plattens the temperature of which is raised at the same rate as the body of the material; (2) the use of well insulated plattens of low thermal mass; (3) the use of "dummy boards" between the heated material and the unheated press plattens.

All of these methods result in a substantially uniform rate of temperature rise throughout the material, but there may be cases where, owing to the high pressures required, thin electrodes or dummy boards are inadmissible, or where the heat lost in repeated heating and cooling of heavy plattens would lead to excessive manufacturing cost. If this be the case, the findings of the present paper may be of some interest. It will be obvious, however, that the choice of method will be determined not only by technical superiority but by economic factors, the consideration of which is beyond the scope of the present paper.

maintained at temperature θ_1 and it will be assumed that the material is initially at a uniform temperature θ_0 °C. Heat is generated uniformly within the material at a constant rate of H cal cm^{-3} sec^{-1}.

The equation of heat conduction when heat is generated uniformly within the material has been derived for the case of one dimensional heat flow by Herne[2] and Carslaw and Jaeger.[3] The present case differs from that already treated only insofar as the boundary conditions are modified. It has been found that the present boundary conditions can be readily satisfied with little deviation from the method already outlined by these authors.

2. NOTATION

x	distance measured normally from one surface	cm
t	heating time	sec
t_1	heating time for which the temperature at the centre of the material is equal to the surface temperature	sec
t_2	heating time for which temperature maximum and minimum are symmetrically disposed about the surface temperature	sec
t_3	heating time required for the setting of material at constant temperature	sec
b	thickness of material	cm
θ	temperature at distance x from one surface	°C
θ_0	initial temperature of the material	°C
θ_1	elevated temperature at which the surfaces of the material are maintained	°C
θ_2	temperature at which the material cures in unit time	°C
θ_3	constant temperature at which the material is completely cured in time t_3	°C
$\Delta\theta$	maximum deviation of temperature from the surface temperature	°C
H	rate of generation of heat	cal cm^{-3} sec^{-1}
K	thermal conductivity of the material	cal cm^{-2} sec^{-1}
ρ	density of the material	g cm^{-3}
c	specific heat of the material	
ϵ	permittivity of the material	
$\cos\phi$	power factor of the material	
v	voltage gradient in the material	V cm^{-1}
α	fraction of material which is cured after time t	

Quantities derived from the above are:

$a = kt/b^2$	a dimensionless time variable
$k = K/\rho c$	the thermal diffusivity of the material
$\lambda = \epsilon \cos\phi$	the loss factor of the material
$h = Hb^2/\pi^2 K(\theta_1 - \theta_0)$	
$p = 100\,\Delta\theta/(\theta_1 - \theta_0)$	the maximum percentage variation in temperature through the material
h_1 and h_2	specific values of h which lead to the particular types of temperature distribution which are discussed in the text

3. THE HEAT FLOW EQUATION AND ITS SOLUTION

Some simplification of the conditions encountered in practice will be made in order that an explicit mathematical solution can be obtained. Thus, we shall consider the linear flow of heat in material which is bounded by the two parallel planes at $x = 0$ and $x = b$. We shall assume that the material is isotropic and that its relevant physical constants are independent of temperature. The surfaces at $x = 0$ and $x = b$ are

Thus, for the case of one dimensional heat flow in which heat is generated in the material, we can write:

$$\frac{\partial^2\theta}{\partial x^2} - \frac{1}{k}\frac{\partial\theta}{\partial t} = -\frac{H}{K} \qquad (1)$$

the steady solution of which with $\theta = \theta_1$ at $x = 0$ and $x = b$ is:

$$\theta = \theta_1 + \frac{H}{2K}x(b - x) \qquad (2)$$

If in equation (1) we put

$$\theta = u + \theta_1 + \frac{H}{2K}x(b - x) \tag{3}$$

we get: $$\frac{\partial^2 u}{\partial x^2} - \frac{1}{k}\frac{\partial u}{\partial t} = 0,\ t > 0,\ 0 < x < b \tag{4}$$

and this equation has the new boundary conditions:

$$u = 0 \text{ when } x = 0 \text{ and } x = b,\ t > 0$$

and $$u = \theta_0 - \theta_1 - \frac{H}{2k}x(b - x),\ t = 0.$$

The solution of equation (4) yields the transient part of the behaviour of the system, and has been shown by Carslaw and Jaeger to be:

$$u = \sum_{n=1}^{\infty} a_n \sin\frac{n\pi x}{b} e^{-kn^2\pi^2 t/b^2} \tag{5}$$

where the values of a_n depend on the conditions holding at $t = 0$.
Inserting these conditions we have:

$$\theta_0 - \theta_1 - \frac{H}{2K}x(b - x) = \sum_{n=1}^{\infty} a_n \sin\frac{n\pi x}{b},\ 0 > x < b \tag{6}$$

from which the values of a_n are found to be:

$$a_n = 2(\cos n\pi - 1)\left(\frac{Hb^2}{K\pi^3 n^3} + \frac{\theta_1 - \theta_0}{\pi n}\right) \tag{7}$$

From equations (3), (5) and (7) the complete solution of equation (1) with the stated boundary conditions can be written. It is:

$$\theta = \theta_1 + \frac{H}{2K}x(b - x) - 4\frac{Hb^2}{K\pi^3}\sum_{n=1}^{\infty}\left[\frac{e^{-(2n-1)^2\pi^2 kt/b^2}\sin(2n-1)\pi x/b}{(2n-1)^3}\right] - \frac{4}{\pi}(\theta_1 - \theta_0)\sum_{n=1}^{\infty}\left[\frac{e^{-(2n-1)^2\pi^2 kt/b^2}\sin(2n-1)\pi x/b}{2n-1}\right] \tag{8}$$

However, for the purpose of drawing dimensionless curves of temperature distribution with combined platten and dielectric heating, it has been found convenient to put the complete solution in the form:

$$\theta = \theta_1 + (\theta_1 - \theta_0)[hF - G] \tag{9}$$

where

$$F = \frac{4}{\pi}\left[\frac{\pi^3}{8}\left(\frac{x}{b} - \frac{x^2}{b^2}\right) - \sum_{n=1}^{\infty}\frac{e^{-(2n-1)^2\pi^2 kt/b^2}\sin(2n-1)\pi x/b}{(2n-1)^3}\right] \tag{10}$$

$$G = \frac{4}{\pi}\left[\sum_{n=1}^{\infty}\frac{e^{-(2n-1)^2\pi^2 kt/b^2}\sin(2n-1)\pi x/b}{2n-1}\right] \tag{11}$$

and $$h = Hb^2/\pi^2 K(\theta_1 - \theta_0)$$

4. COMPUTATION

The two infinite series are fairly rapidly convergent for values of kt/b^2 greater than 0·01 and four figure accuracy is obtainable at $kt/b^2 = 0{\cdot}01$ with five terms of G and four terms of F. The fact that F is composed of the difference of two terms which approximate to one another as t tends towards zero necessitates the evaluation of the series part of F to a greater accuracy than the G series. In general the computations have been made to a degree of accuracy that is warranted by the graphical method of presenting the results and the inaccuracy has been estimated by noting that, after the first few terms, the series converge slightly more rapidly than a geometrical progression, the remainder of which can be evaluated.

The temperature distributions are clearly symmetrical about the plane $x = 0{\cdot}5b$ and the diagrams have thus been drawn only for the region $0 \leqslant x \leqslant 0{\cdot}5b$.

5. GRAPHICAL REPRESENTATION OF THE RESULTS

In Fig. 1 the values of F have been plotted for a range of values of kt/b^2 from 0·001 to ∞. The temperature resulting from the use of dielectric heating alone with

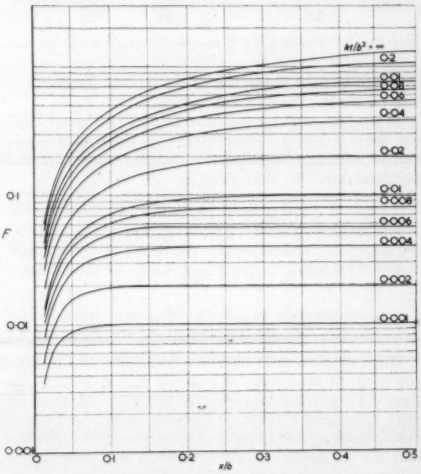

Fig. 1. The function F for kt/b^2 from 0·001 to ∞

the plattens maintained at the initial temperature of the material can be found from these curves, and is given by:

$$\theta = \theta_0 + \frac{Hb^2}{\pi^2 K}F \tag{13}$$

It is clear that as t tends towards infinity, θ assumes the parabolic form

$$\theta = \theta_0 + \frac{H}{2K}(xb - x^2) \tag{14}$$

All the other temperature distribution curves lie below this limit. The height of the parabola ($Hb^2/8K$), that is the maximum temperature which is reached in the material with dielectric heating alone, depends only on

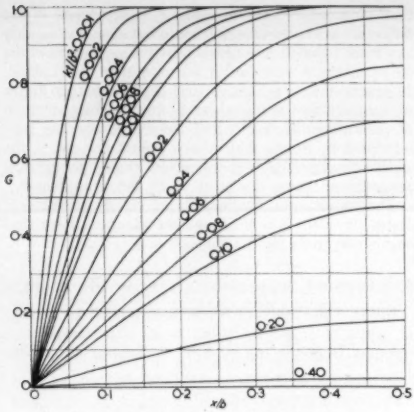

Fig. 2. The function G for kt/b^2 from 0·001 to ∞

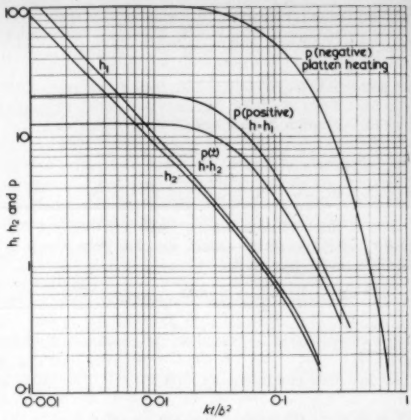

Fig. 3. Values of the factor h required to produce the types of temperature distributions discussed in Sections 6.1 and 6.2. The resulting percentage temperature variations are also shown with a curve for platten heating alone for comparison

the ratio of the heating rate to the thermal conductivity and on the thickness of the material.

The values of G for the same range of values of kt/b^2 are given in Fig. 2. From these the temperature distribution resulting from platten heating alone can be obtained directly. It is given by:

$$\theta = \theta_1 - (\theta_1 - \theta_0)G \qquad (15)$$

The limiting value of θ is θ_1, the surface temperature of the material. That is to say, the whole of the material eventually reaches the same temperature as the plattens.

6. COMBINED PLATTEN AND DIELECTRIC HEATING

Three possible cases will be considered: (1) a process requiring the attainment of a certain minimum temperature; (2) a process requiring the minimum variation of final temperature about a specified mean; and (3) a process such as the setting of synthetic resins in which the time for completion of the process at any point in the material is a function of the thermal history at that point.

6.1. *Temperature distribution with a lower temperature limit*

It is clear that the plattens must be at a temperature at least as high as the lower temperature limit. We shall adjust h so that the temperatures at the surface and the centre are equal to the limit temperature at the end of the heating time. Thus, from equation (9) this condition will obtain after time t_2 for a value of h equal to h_1 given by:

$$\theta_1 = \theta_1 + (\theta_1 - \theta_0)[h_1 F - G]$$
$$\text{for } x/b = 0{\cdot}5 \text{ and } t = t_2 \qquad (16)$$

whence $h_1 = G/F$ for $x/b = 0{\cdot}5$ and $t = t_2$.

h_1 is a function of kt_2/b^2 alone and is plotted in Fig. 3 for values of kt_2/b^2 from 0·001 to 0·2. Corresponding temperature distributions are shown in Fig. 4 for selected values of kt_2/b^2.

The temperature is everywhere greater than the surface temperature and Fig. 3 shows the maximum percentage variation in temperature p for a given value of kt_2/b^2. p is given by:

$$p = 100\,\Delta\theta/(\theta_1 - \theta_0) \qquad (17)$$

where $\Delta\theta$ represents the maximum deviation of temperature from the surface temperature.

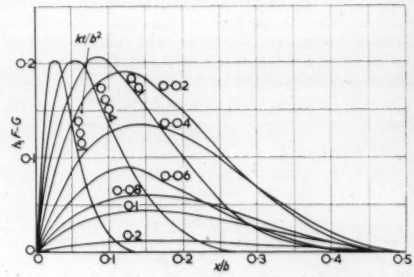

Fig. 4. Temperature distribution with $h = h_1$

We see that for values of kt_2/b^2 up to 0·02 there is a plane near the surface where p is of the order of 20, This "hump" becomes less pronounced and moves towards the centre of the slab as the value of kt_2/b^2 is increased. In Fig. 3 the values of p for platten heating

alone have been shown for comparison and we see that, whereas with combined heating a value of p as low as 20 can be achieved with $kt_2/b^2 = 0{\cdot}001$, platten heating requires a time which is about 200 times as long. When the value of p must be very much less than 20 the advantages of combined heating are less marked. Thus, if $p = 1$, the use of platten heating alone requires a time about 2·3 times that required with a combination of heating methods.

Briefly then: the use of combined heating can result in a large reduction of heating time when a maximum variation of the order of 20% can be tolerated, but when the permissible variation is much lower than this, combined heating is less advantageous. It should also be noted that the greatly reduced heating times, corresponding, for example, to kt_2/b^2 of 0·001, require a large value of h and hence of dielectric heating rate. In a later paragraph it will be shown that there are certain practical limits which restrict the choice of h. Thus, it may not be possible in every case to achieve the greatly reduced heating times which thermal considerations alone predict.

6.2. *Temperature distribution with minimum variation about a mean*

By a series of successive approximations, values h_2 of h have been chosen which result in a symmetrical disposition of the temperature maxima and minima about the surface temperature after a heating time t_3. The values of h_2 are shown in Fig. 3 and are everywhere somewhat lower than the corresponding values of h_1.

The temperature distributions which exist after a heating period with $h = h_2$ are shown in Fig. 5. The maximum values of p occur for small values of kt_3/b^2 and are of the order of $\pm$ 12.

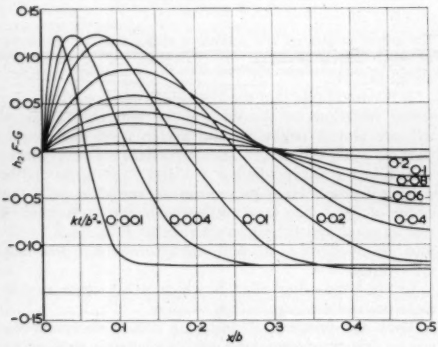

Fig. 5. Temperature distribution with $h = h_2$

The distribution curves exhibit the same general characteristics as were discussed in the previous paragraph, and the previous discussion relating to the reduction of heating time effected by the use of combined heating is broadly applicable to the present case.

6.3. *Conditions for uniform setting of synthetic resins and adhesives*

In the curing of moulding materials or in the glueing of stacks of plywood with synthetic adhesives the form of the heating curve at any plane in the material must also be considered. With most materials of this kind the setting or curing process at any point in the material takes place at a rate which depends on the temperature at that point.

By way of illustration, heating curves for various planes within the material have been plotted in Fig. 6

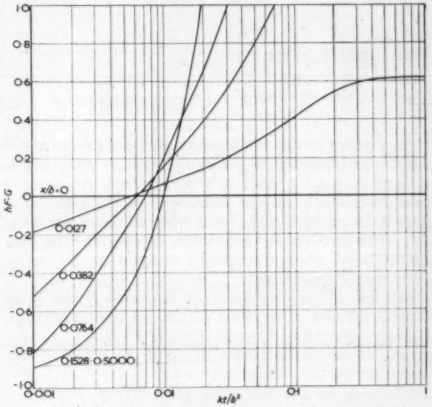

Fig. 6. Heating curves for various planes within the material with $h = 10$

for $h = 10$. The surface ($x/b = 0$) immediately attains the temperature of the plattens, whereas it is some time before the temperature at the centre of the material ($x/b = 0{\cdot}5$) starts to rise. Thus, if the material has a setting rate which increases with temperature, the surfaces which are at platten temperature for the whole of the heating time can be maintained at a temperature less than that to which the centre rises. This is discussed in more detail below.

6.3.1. *A typical time relationship.* Under constant temperature conditions a typical relationship between θ_3 (the temperature at which the material is held) and t_3 (the time required for satisfactory setting) is given by:

$$\theta_3 = \theta_2 - m \ln t_3$$

that is:

$$t_3 = e^{(\theta_2 - \theta_3)/m} \qquad (18)$$

in which m and θ_2 are positive constants, $-m$ being the slope of the θ_3, $\ln t_3$ curve and θ_2 the temperature at which setting is complete in unit time.

We will not concern ourselves with the exact mechanism of the setting process but will assume that a fraction α of the material is satisfactorily cured at time t. α will thus be zero for fresh unheated material and unity when the whole material is satisfactorily set. We will further

assume that the relationship of equation (18) is applicable for unsteady temperature conditions.

That is that:
$$\frac{d\alpha}{dt} = e^{(\theta - \theta_2)/m} \quad (19)$$

6.3.2. *Condition for uniform setting throughout the slab.* If the surfaces of the slab are held at temperature θ_3 then the material at the surface will be completely cured in time t_3 and the material at any other point of the slab will be cured provided that:

$$\int_0^{t_3} \frac{d\alpha}{dt} dt \geqslant 1$$

that is (with $\theta_1 = \theta_3$):

$$\int_0^{t_3} e^{[(\theta_3 - \theta_2) + (\theta_3 - \theta_0)(hF - G)]/m} dt \geqslant 1 \text{ for all values of } x/b \quad (21)$$

It is clear that the optimum condition is the one which makes the integral of equation (21) exactly unity, for an integral of greater than unity corresponds to a state of over-cure, which may be deleterious to the material or impair the strength of the bond when adhesives are being set. The problem is to establish, if possible, the conditions under which the equality of equation (21) can be most nearly approached.

In view of the complexity of functions F and G an explicit solution of equation (21) seems hardly possible. However, graphical representations of F and G at various points in the material are available in terms of the dimensionless time variable $a = kt/b^2$.

Changing the variable of equation (21) we get:

$$\int_0^{kt_3/b^2} e^{[(\theta_3 - \theta_2) + (\theta_3 - \theta_0)(hF - G)]/m} da \geqslant k/b^2$$
for all values of x/b (22)

and a separation of time variable and invariant parts give:

$$\int_0^{kt_3/b^2} e^{(\theta_3 - \theta_0)(hF - G)/m} da \geqslant e^{(\theta_2 - \theta_3)/m} k/b^2$$
for all values of x/b (23)

or on substituting t_3 for $e^{(\theta_2 - \theta_3)/m}$ from equation (18) we get:

$$\int_0^{kt_3/b^2} e^{(\theta_3 - \theta_0)(hF - G)/m} da \geqslant kt_3/b^2 \text{ for all values of } x/b \quad (24)$$

Values of kt/b^2 which satisfy equation (24) with the minimum variation of integrand have been found by graphical integration using the following procedure.

Numerical values which are likely to be experienced in practice are assigned to $(\theta_3 - \theta_0)/m$ and h and sets of the integrand $e^{(\theta_3 - \theta_0)(hF - G)/m}$ for various values of x/b are plotted against the variable a. A typical set is shown in Fig. 7 for $h = 1$ $(\theta_3 - \theta_0)/m = 4$. Values of kt_3'/b^2 which satisfy the relation:

$$\int_0^{kt_3'/b^2} e^{(\theta_3 - \theta_0)(hF - G)/m} da = kt_3'/b^2 \quad x/b = 0{\cdot}5 \quad (25)$$

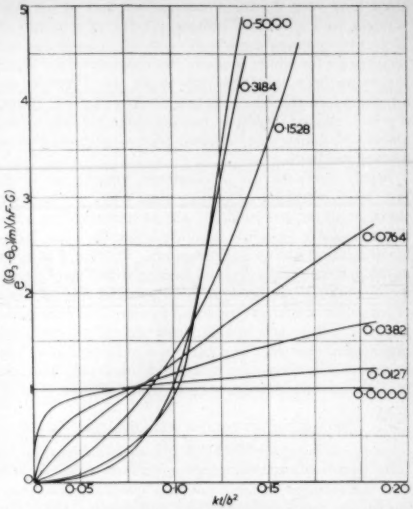

Fig. 7. The integrand as a function of kt/b^2 and x/b for $(\theta_3 - \theta_0)/m = 4$ and $h = 1$

can then be found quite quickly by graphical methods. Evaluations of the integral

$$\int_0^{kt_3'/b^2} e^{(\theta_3 - \theta_0)(hF - G)/m} da$$

for other values of x/b enable a small correction to be applied which gives a set of values of t_3 satisfying equation (24).

It is remarkable that for low values of $(\theta_3 - \theta_0)/m$ and h the variations of the integral for different values of x/b are almost negligible and are in most cases comparable with the errors in integration. The example shown in Fig. 7 for which $h = 1$ and $(\theta_3 - \theta_0)/m = 4$ is a typical case. Here the maximum variation is of the order of 7%. For larger values of h the uniformity is not as good and the variation rises to 17% for $h = 10^{\frac{1}{2}}$ and $(\theta_3 - \theta_0)/m = 4$ and 29% for $h = 10$ and $(\theta_3 - \theta_0)/m = 4$.

In Fig. 8 the values of kt_3/b^2 which satisfy equation (24) have been plotted against $(\theta_3 - \theta_0)/m$.

Thus, the problem of designing a suitable system to ensure that the material is uniformly cured is reduced to that of finding the simultaneous solution of equation (18) which states that

$$t_3 = e^{(\theta_2 - \theta_3)/m}$$

and a relationship of the form:

$$kt_3/b^2 = f[(\theta_3 - \theta_0)/m, h] \quad (26)$$

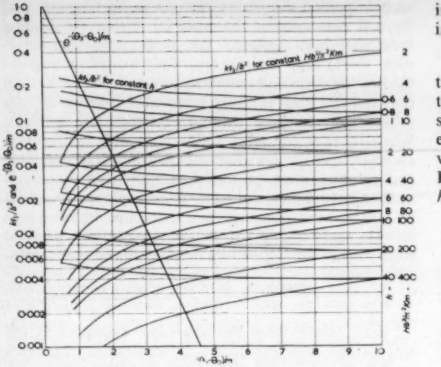

Fig. 8. Optimum values of kt_3/b^2 for uniform setting

Equation (18) may be rewritten as

$$kt_3/b^2 = \left[\frac{k}{b^2}e^{(\theta_2-\theta_0)/m}\right]e^{-(\theta_3-\theta_0)/m} \qquad (27)$$

and when superimposed on Fig. 8 this represents a set of parallel lines with a slope of -1, making an intercept of $+(k/b^2)e^{(\theta_2-\theta_0)/m}$ on the $(\theta_3-\theta_0)/m$ axis. Thus, if the properties of the material (k, θ_2 and m) and the initial temperature and thickness are known, the value of $(k/b^2)e^{(\theta_2-\theta_0)/m}$ can be calculated and set off on the $(\theta_3-\theta_0)/m$ axis. A straight line drawn parallel to the $e^{-(\theta_3-\theta_0)/m}$ line marked on the chart then satisfies equation (27) for the particular condition of the problem and values of $(\theta_3-\theta_0)/m$, and h and the corresponding values of kt_3/b^2 are then determined. The particular operating conditions, i.e. values of $(\theta_3-\theta_0)/m$ and h which are selected in a given case are determined by such factors as the maximum value which can be ascribed to h and the maximum temperature to which the material can be heated at its centre.

6.3.3. *Limitations in the choice of h.* The fact that h is itself a function of $(\theta_3-\theta_0)$ and b introduces a further restriction which must be considered. Equation (12) defines h as the ratio $Hb^2/\pi^2K(\theta_1-\theta_0)$ or with plattens at θ_3° C as $Hb^2/\pi^2K(\theta_3-\theta_0)$, where H is the rate of generation of heat and K is the thermal conductivity. Rewriting (12) we get:

$$h(\theta_3-\theta_0)/m = Hb^2/\pi^2Km \qquad (28)$$

The factors on the right-hand side of equation (28) would be known in a given case, so that the lines of constant Hb^2/π^2Km in Fig. 8 enables a unique choice of $(\theta_3-\theta_0)/m$ and hence kt_3/b^2 to be made.

The value chosen for H might require modification for two reasons. In the first place too high a value for H might lead to an excessive temperature in the centre of the material; this is discussed in the following section and, secondly, an arbitrary choice of H is not possible in view of electrical limitations which will be discussed in Section 7.

6.3.4. *Temperature limits.* The maximum temperature reached in the material at the end of the heating time is of some importance as the material may be unstable above a specified maximum temperature. To enable the maximum temperature to be determined the values of $(hF-G)$ for $x/b = 0{\cdot}5$ have been plotted in Fig. 9 for values of $(\theta_3-\theta_0)/m$ from 0·5 to 10, and h of 1 and 10.

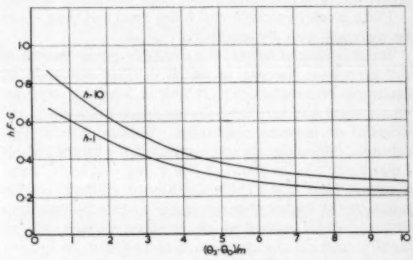

Fig. 9. Temperature at centre after heating time t_3

6.3.5. *General implications.* The foregoing results leading to the graphical representation of Fig. 8 indicate that, in general, thicker slabs of material will require a longer heating time and lower value of platten temperature. The heating time can be reduced by an increase of dielectric heating rates (i.e. of h) and a higher platten temperature, but this results in a less uniform setting of the material.

The effect of continued curing during the cooling period of thick slabs cannot be ignored. In the previous discussion it has been assumed that curing must be complete before the material is removed from the heating fixture or press. There is some danger in the case of thick slabs that the material will be over-cured during the subsequent cooling period. This would not be the case in the treatment of a thick stack of separate sheets which could be separated on removal from the press for rapid cooling. In the case of thick single slabs which must be immediately removed from the heating fixture a compromise would be necessary between the reduction in strength due to over-curing during the cooling period, and that due to reduction of pressure before curing is complete.

If a number of fixtures were available satisfactory results should be obtained by discontinuing the high frequency heating before the centre of the material is fully cured and allowing the centre to cure out while the material is being cooled by conduction to the plattens.

The establishment of optimum conditions for this latter type of operation presents a further problem of considerable interest but one which is outside the scope of the present paper.

7. LIMITATIONS IN THE CHOICE OF H

An arbitrary choice of H based on thermal requirements alone is not possible in practice as the rate of dielectric heating is limited in various ways.

The rate of generation of heat is given by:

$$H = \frac{v^2\omega\lambda}{36\pi} \cdot 10^{-11} \text{ watts cm}^{-3} \quad (29)$$

$$H = \frac{v^2\omega\lambda}{36\pi J} \cdot 10^{-11} \doteqdot 6{\cdot}72v^2\omega\lambda \cdot 10^{-15} \text{ cal cm}^{-3} \text{ sec}^{-1} \quad (30)$$

where all the symbols used have been previously defined.

For a given material λ and K are fixed and thus H can be increased only by increasing v or ω.

But v is limited by: (1) the available power output of the generator, the size of which is often governed by economic considerations; (2) loss in coupling arrangements when λ is very low; (3) voltage breakdown in the material or between electrodes. Without special precautions, difficulties are to be expected if v exceeds about 3 000 V cm^{-1} or vb about 15 000 V and ω cannot exceed a certain limit due to: (1) the loss of efficiency in the generator at higher frequencies—for there is usually a frequency limit beyond which the efficiency falls off very rapidly; and (2) the occurrence of variation in heating rate due to standing waves along the length of the electrodes.

8. CONCLUSION

The foregoing analysis is an attempt to establish design criteria for a dielectric heating system which can be physically realized. Much remains to be done before it can be said that the problem has been more than broached; but it is doubtful whether the time would be usefully spent in extending the present analysis when such important factors as changes in heating rate and thermal constants of the material during the heating cycle have been ignored. An ideal matching arrangement would keep the generator fully loaded throughout the heating cycle and ensure an almost constant heating rate, but this ideal is rarely achieved in practice and the problem of changing thermal constants still remains. When thermal constants which vary with temperature are inserted an explicit solution can no longer be obtained, and recourse must be made to approximate solution methods, the differential analyser or analogue computer for an answer. An analogue computer which would provide rapid answers to this more complex problem might well be the logical step in obtaining further results.

9. ACKNOWLEDGMENTS

I must acknowledge the invaluable assistance of the staff of the Instrumentation Laboratory, Fishermen's Bend, both in criticism of the text and in the computation of the results. I must also thank the Chief Scientist, Department of Supply, Melbourne, and the Manager of the Research Laboratories of The General Electric Co. Ltd., Wembley, Middlesex, where the work was started, for permission to publish the results.

REFERENCES

(1) BROWN, G. H. *Proc. Inst. Radio Engrs.*, **21**, p. 537 (1943).
(2) HERNE, H. *Wireless Eng.*, p. 377 (Aug., 1944).
(3) CARSLAW, H. S., and JAEGAR, J. C. *Conduction of heat in solids*, p. 108. (London: Oxford University Press, 1947.)
(4) BROWN, G. H., HOYLER, C. N., and BIERWIRTH, R. G. *The theory of radio-frequency heating*, p. 248. (New York: Van Nostrand, 1947.)

Helmholtz resonators in the acoustic treatment of broadcasting studios

By C. L. S. GILFORD, M.Sc., F.Inst.P., Research Department, Engineering Division, British Broadcasting Corporation, London

[*Paper first received* 19 *March*, 1951, *and in final form* 8 *November*, 1951]

A theory of the action of Helmholtz resonators as sound absorbers is presented, covering both the isolated resonator and regular arrays. Experiments in reverberation rooms and acoustically treated studios are described and general recommendations for design are given. Regular arrays are preferable to single resonators, openings being made more resistive by covering with a fabric. It is concluded that great variations in design to suit architectural requirements may be made without loss of effectiveness, and the widths of the frequency band over which absorption takes place may be varied between wide limits.

1. INTRODUCTION

The Helmholtz resonator consists of a cavity which has a comparatively narrow neck. An alternating air pressure applied to the opening of the neck will cause the air in the neck to oscillate, the natural frequency of the oscillation being determined by the mass of the air in the neck and the stiffness presented by the air enclosed behind it. Any such oscillation is accompanied by viscous losses, particularly in the neck where the particle velocity is highest, and the Helmholtz resonator therefore acts as a sound absorber, the absorption being greatest at the resonance frequency, at which the particle velocities are highest.

The use of Helmholtz resonators as sound absorbers in architectural acoustics offers great advantages since it is possible to design quite small resonators to absorb efficiently at very low frequencies. They therefore provide an alternative in the extreme low frequency region to bulky and costly porous absorbers on the one hand and, on the other, to wood

panelling, the absorption of which is not amenable to accurate prediction.

Another effect, however, may be present; the rate of energy loss may in some circumstances be so low in relation to the total stored energy in the system that the resonator will have the effect of prolonging the reverberation time of a heavily damped room. It has been suggested[1] that pots embedded in the walls of ancient Scandinavian churches may have served to enhance the traditional ecclesiastical acoustics, not to improve intelligibility of speech by reducing the reverberation time, as had been assumed previously. More recently resonators of this kind have been used in Denmark for lecture halls and broadcasting studios. Although the derivation of the resonance frequency is well known, there is no accepted theory to guide the use of Helmholtz resonators in room acoustics, recent papers having presented analyses and numerical results which cannot be reconciled.

This paper proposes a theory of the behaviour of such resonators as sound absorbers and describes experiments made to verify it. The experiments were limited to frequencies below 200 c/s, as sound of higher frequencies is more conveniently absorbed by porous absorbers. Applications to higher frequencies have been discussed by other authors.

2. THEORY

2.1. *Determination of resonance frequencies.*

The complete series of modes of vibration is best studied by considering the system as two cylindrical pipes, the neck forming one and the cavity the other (cf. Richardson[2]).

Let ρ, η = density and viscosity of air respectively
r, S, l_0 = radius, cross-section and length of neck respectively
l = effective length of neck. For resonators of small neck diameter compared with cross-section of cavity, $l = l_0 + 1{\cdot}7r$
$m = Sl\rho$ = effective mass of air in neck
S', l', U = cross-section, length and volume of cavity
$\omega/2\pi$ = frequency of incident sound
c = velocity of sound in air

Let Z_0, Z_1, and Z_2 be the impedances at the positions shown in Fig. 1.

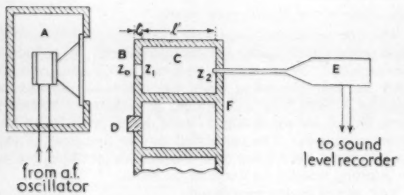

Fig. 1. Arrangement used to obtain response curves
A, loudspeaker; *B*, neck; *C*, cavity; *D*, corked hole; *E*, probe microphone; *F*, block of resonators.

The characteristic acoustic impedance of a tube of cross-section S is $\rho c/S$. We may therefore write the value of Z_1 in two forms as follows:

$$Z_1 = \frac{\frac{i\rho c}{S}\left(Z_0 - \frac{i\rho c}{S}\tan\frac{\omega l}{c}\right)}{Z_0\tan\frac{\omega l}{c} - \frac{i\rho c}{S}} = \frac{\frac{i\rho c}{S'}\left(Z_2 - \frac{i\rho c}{S'}\tan\frac{\omega l'}{c}\right)}{Z_2\tan\frac{\omega l'}{c} - \frac{i\rho c}{S'}} \qquad (1)$$

At resonance Z_0 must be zero (neglecting losses) and since Z_2 is infinite the equations reduce to

$$\tan\frac{\omega l}{c}\tan\frac{\omega l'}{c} = \frac{S}{S'} \qquad (2)$$

The roots of this equation are the values of ω for resonance. In practice, three special cases only are of interest.

Case 1. $\omega l, \omega l' \ll c$.

Here $\omega^2 ll'/c^2 = S/S'$, which has only one positive root, giving

$$f = \frac{\omega}{2\pi} = \frac{c}{2\pi}\sqrt{\frac{S}{lU}} \qquad (3)$$

Case 2. $S = S'$ (stopped pipe).

$$\tan\frac{\omega l}{c}\tan\frac{\omega l'}{c} = 1 \qquad \text{which gives}$$

$$\omega(l + l')/c = (2n + 1)\,\pi/2$$

Whence
$$f = \frac{2n + 1}{4(l + l')}\,c \qquad (4)$$

Case 3. $\omega l \ll c$ (long resonator with short neck).

Here
$$\omega \tan \omega l'/c = cS/lS' \qquad (5)$$

This equation has an infinite series of roots, and graphical solution shows that the first is close to that of Case 1, and the rest approximately equal to those of a pipe of length l' closed at both ends, i.e. $\omega = \pi nc/l'$. The first root is very much lower than any of the subsequent ones; for example, in one of the experimental resonators described below the roots are

$$f = 75,\ 950,\ 1\,900\ \ldots\ \text{c/s}$$

This wide separation has an advantage for the present purpose, since by suitable design the absorption at the higher modes may be made negligible.

2.2. *The Helmholtz resonator as a simple resonant system.*

Resonators satisfying Case 3 may be regarded, over a wide frequency band on either side of the lowest mode, as a simple system with one degree of freedom. The relevant parameters are then

$$\text{acoustic inertance} = m/S^2 = l\rho/S \qquad (6)$$

and
$$\text{acoustic compliance} = U/\rho c^2 \qquad (7)$$

The acoustic resistance has two components, the radiation resistance R_1 and the internal resistance R_2, due to viscous flow in the neck and other sources of loss. The internal resistance is determined solely by the properties of the neck, but the radiation resistance varies according to the nature of the sound-field and the proximity of other resonators. For a single resonator in an infinite wall,[3]

$$R_1 = 2\pi\rho c/\lambda^2 \qquad (8)$$

and for one of an infinite equally spaced two-dimensional array

$$R_1 = \rho c/\sigma \qquad (9)$$

where σ is the area of wall per resonator.

For an open cylindrical neck[3]

$$R_2 = \frac{l}{rS}\sqrt{(2\rho\eta\omega)} \qquad (10)$$

Finally, the "magnification" of the system, Q, is given by

$$Q = \frac{l\rho\omega}{S(R_1 + R_2)} \qquad (11)$$

2.3. *Absorption of sound.*

If the inside of the resonator is rigid and non-porous, the absorption of energy during excitation will occur entirely in the neck. The viscous resistance of the neck, given by equation (10), may be increased by altering the neck dimensions or by covering or filling the neck with a fibrous or porous material.

At resonance frequency the reactance of the resonator is zero and hence the volume flow in the neck is $p/(R_1 + R_2)$, where p is the r.m.s. pressure. The rate of absorption of energy is, therefore, $R_2[p/(R_1 + R_2)]^2$ which attains its maximum value when $R_1 = R_2$. The problem of achieving the greatest possible sound absorption reduces to one of matching the internal resistance of the neck to its radiation resistance. If $R_2 = \mu R_1$, the efficiency of the neck as an absorber compared with the value of $\mu = 1$ is $4\mu/(1 + \mu)^2$.

Two important cases must be examined: that of a single resonator in an isolated position, equation (8), and in a plane array, consisting of a large number of resonators equally spaced over a plane surface, equation (9). The radiation resistances differ greatly in these two cases.

2.3.1. *Single resonator.* In this case, we have $R_2 = 2\pi/c/\lambda^2$ and hence the rate of absorption of the matched condition, where $R_1 = R_2$, is

$$\frac{p^2}{4R_1} = \frac{p^2\lambda^2}{8\pi\rho c}$$

If we equate this to the energy flow in the tube of area A' terminating in the wall surface, we may say that the absorption is equivalent to 100% over an area A' surrounding the neck. This energy flow is given by $(p^2A')/(\rho c)$ and equating this to the absorption gives $A' = \lambda^2/8\pi$.

For any other value of R_2, where $R_2 = \mu R_1$,

$$A' = \frac{\lambda^2}{8\pi} \cdot \frac{4\mu}{(1 + \mu)^2} \tag{12}$$

This quantity A' is the number of absorption units to be added to the denominator of Sabine's expression for reverberation time. Brüel points out[1] that the presence of a wall surrounding the resonator neck will almost double the pressure so that A' has a theoretical upper limit of

$$\frac{\lambda^2}{2\pi} \cdot \frac{4\mu}{(1 + \mu)^2} \tag{13}$$

2.3.2. *Resonator in an array.* Here the radiation resistance is $\rho c/\sigma$ and hence the energy absorbed per second is given by

$$\frac{p^2\sigma}{4\rho c} \cdot \frac{4\mu}{(1 + \mu)^2}$$

Therefore since

$$\frac{p^2A'}{\rho c} = \frac{p^2\sigma}{4\rho c} \cdot \frac{4\mu}{(1 + \mu)^2}$$

$$A' = \frac{\sigma}{4} \cdot \frac{4\mu}{(1 + \mu)^2} \tag{14}$$

If the array is embedded in a wall, so that the pressure is doubled, this becomes

$$A' = \frac{4\sigma\mu}{(1 + \mu)^2} \tag{15}$$

showing that at resonance a maximum absorption coefficient of unity may be obtained over the whole area of the array for $\mu = 1$.

2.4. *The effect of stored energy.*

In a very important paper Rschevkin[4] showed that the simple theory of absorption outlined above was inadequate for application to room acoustics, ignoring as it does the effect of energy storage in the resonator, which may actually increase the reverberation time of the room.

He replaced Sabine's classical formula for reverberation time, $T = 0{\cdot}162 \times 10^{-2}\, V/A$, where V is the volume and A the total absorption of the room, by

$$T_2 = 0{\cdot}162 \times 10^{-2}(V + nV')/(A + nA') \tag{16}$$

where n is the number of resonators, and V' the effective increase in the volume of the room due to the presence of each resonator, which he called the "additional volume." The reverberation time is increased by the resonators if V'/A' is greater than V/A, and decreased if it is less.

The energy density in a room in which a steady sound field is maintained is given by $p_0^2/\rho c^2$, where p_0 is the r.m.s. pressure. At the resonance frequency of the resonator the r.m.s. pressure in the interior of the resonator will be Qp_0 and hence the energy density is $Q^2p_0^2/\rho c^2$. Assuming instantaneous energy exchange between room and resonator, a condition which Rschevkin shows to be satisfied in all practical cases, the resonator will contribute, from the viewpoint of energy storage, an effective additional room volume Q^2U. Hence, we may write

$$V' = Q^2U \tag{17}$$

For high values of Q and small values of μ therefore the increase of volume may result in a considerable increase in the reverberation time of the room.

Though Rschevkin's theoretical treatment for the individual resonator is sufficient to account for the main phenomena, experimental verification is not complete and the effects of interaction between neighbouring resonators are not considered. It was therefore found necessary to make tests to verify the main features of the theory, as it applies to single and combined resonators and to determine the practical limitations associated with the phenomenon.

3. EXPERIMENTAL

3.1. *Experiments on single resonators.*

The first resonators constructed were designed to have the ideal properties of rigidity and low internal loss. Six cylindrical tins each of 2 530 c.c. volume were cast into a concrete block, each tin communicating with the outer air through an opening 3·8 cm long and 4·1 cm in diameter. Sixteen of these blocks, shown in Fig. 2, were made, providing a total of 96 resonators. The calculated natural frequency of each resonator was 144 c/s and other frequencies could be obtained by inserting wooden bushes into the necks.

Two sets of bushes were made:

(*a*) $l_0 = 3{\cdot}8$ cm, $r = 1{\cdot}27$ cm, giving resonator frequency of 105 c/s;

(*b*) $l_0 = 1{\cdot}59$ cm, $r = 1{\cdot}27$ cm, giving resonator frequency of 75 c/s.

A wooden block of six resonators similar to (*b*) was also made.

Measurements of frequency and Q were first made on a single resonator, the others in the same block being corked. A small hole was bored in the back of the resonator cavity and a probe microphone was inserted, as shown in Fig. 1, through the hole into the cavity. The block of resonators was

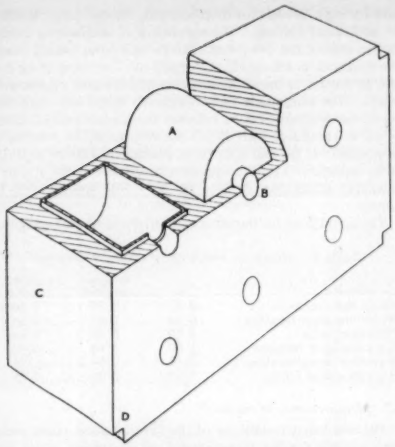

Fig. 2. Experimental block of resonators

A, metal cylinder; *B*, removable wooden bung; *C*, concrete body; *D*, hand grip.

Table 1. *Resistances of resonator necks*

	Q	R_2 measured (g sec^{-1} cm^{-4})	R_2 calculated (g sec^{-1} cm^{-4})	μ (array)	Frequency c/s
144 c/s resonator					
$\sigma = 225$ cm^2					
$R_1 = 3{\cdot}7 \times 10{-}3$					
(g sec−1 cm−4)					
(single resonator)					
Open neck	35–40	$1{\cdot}8 \times 10^{-2}$	$1{\cdot}08 \times 10^{-2}$	0·10	144
One layer bandage	15	4·5	—	0·24	144
Open mesh hessian	13	5·3	—	0·28	—
Two layers bandage	10	6·8	—	0·36	—
Cullum's scrim	10	6·8	—	0·36	—
Rockwool in cavity	9	7·6	—	0·41	—
Fibreglass fabric	8	8·5	—	0·46	140
Three layers bandage	5	13·6	—	0·73	—
Bandage in neck	5	13·6	—	0·73	—
105 c/s resonator					
$\sigma = 225$ cm^2					
$R_1 = 1{\cdot}95 \times 10{-}3$					
(g sec−1 cm−4)					
(single resonator)					
Open neck	18	$5{\cdot}4 \times 10^{-2}$	$3{\cdot}5 \times 10^{-2}$	0·29	—
One layer bandage	8	12·0	—	0·64	—
75 c/s resonator					
$\sigma = 225$ cm^2					
$R_1 = 1{\cdot}28 \times 10{-}3$					
(g sec−1 cm−4)					
(single resonator)					
Open neck	13	$9{\cdot}3 \times 10^{-2}$	$5{\cdot}1 \times 10^{-2}$	0·50	—
One layer bandage	6·5	18·5	—	1·00	—
Two layers bandage	5·5	22	—	1·18	—
Rockwool in cavity	5·5	22	—	1·18	—
Fibreglass fabric	3·5	34	—	1·82	—
Bandage in neck	3·5	34	—	1·82	—
75 c/s wooden resonator $\sigma = 295$ cm^2					
$R_1 = 1{\cdot}28 \times 10{-}3$					
(g sec−1 cm−4)					
(single resonator)					
Open neck	13	$9{\cdot}3 \times 10^{-2}$	$5{\cdot}1 \times 10^{-2}$	0·65	—
One layer bandage	6·5	18·5	—	1·30	—

placed in the open air and energized with tone of slowly varying frequency from a loudspeaker 2 m away. Later experiments were made indoors after it had been found that the reflexions from the walls of the room did not affect the results. The resonance curves obtained were used to calculate Q and hence, by equation (11), the total resistance $R_1 + R_2$.

The results are shown in Table 1. The value of R_2 shown in the second column is found by subtracting a calculated value of R_1 for an isolated resonator from the total resistance $R_1 + R_2$ derived from Q. The third column shows, where appropriate, the value of R_2 calculated from equation (10). The measured values are seen to be somewhat higher than the calculated values, possibly owing to eddy formation. It will also be noticed from the table that the addition of a particular fabric across or within the neck raises the resistance by a factor which is approximately the same for the 75 c/s as for the 144 c/s necks. The resonance frequency was not modified by the addition of the fabrics except where they took the form of wads stuffed into the necks. The fourth column shows the value of μ as defined in Section 2.3, obtained from R_2 in the second column and R_1 for an array as given in equation (9), by division.

3.2. *Absorption measurements.*

Measurements were made in a reverberation chamber having a volume of 28 m^3 (1 000 ft^3), using 84 individual resonators contained in 14 blocks. Control runs were made between experiments with the resonator holes blocked with corks. The same arrangement of resonators in the chamber was maintained throughout the tests. The 144 c/s resonators produced negligible absorption with open necks, but with one layer of bandage over the holes a peak absorption coefficient of 65% was reached at 140 c/s (Fig. 3).

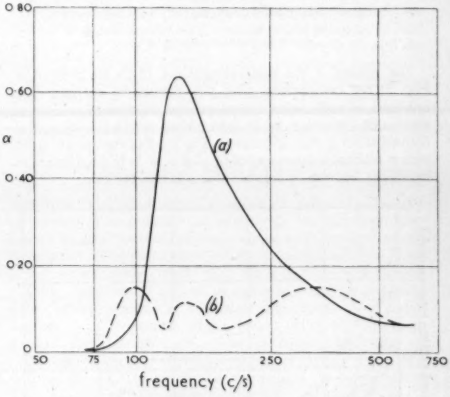

Fig. 3. Absorption coefficient of 144 c/s resonators

Curve (*a*) one layer of bandage, curve (*b*) open necks.

The subsequent work was done with the resonators fitted with the 75 c/s bushes, since these were more uniform in diameter than the holes in the concrete castings. The 75 c/s resonators were tested with open necks, with a wad of bandage inserted in each neck and with one and two layers of bandage across the orifice. The curves so obtained are shown in Fig. 4.

A peak of reverberation time at 75 c/s in the empty room made accurate measurements in this region difficult and many tests had to be made. The wads of bandage were observed to vary greatly in resistance and it was found preferable to use a closely woven glass fabric where high resistances were required.

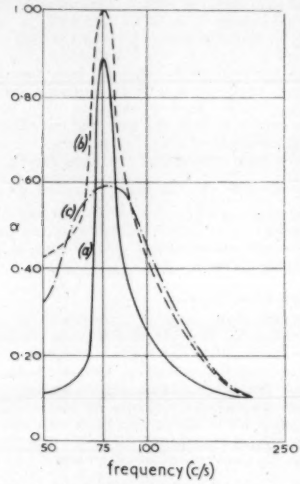

Fig. 4. Absorption coefficient of 75 c/s resonators
Curve (*a*) open necks, curve (*b*) two layers of bandage, curve (*c*) wad of bandage in neck.

The results of the measurements at 75 c/s are plotted in Fig. 5 for comparison with the theoretical curves. The ordinate of each point represents the reverberation time at resonance frequency, while the abscissa shows the value of μ derived from Q measurements. The lowest time was obtained with a resistance corresponding to a μ of 1·18 (two layers of bandage), but the optimum value was not critical.

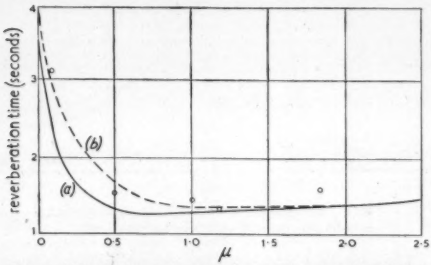

Fig. 5. Calculated and measured reverberation times in tiled room
○ experimental points, curve (*a*) simple theory, curve (*b*) corrected curve allowing for energy storage.

Table 2 shows a comparison between absorption coefficients derived from the measurements by means of equation (15) and Eyring's formula for reverberation, disregarding the effect of additional volume. The agreement is satisfactory except in the case of the 144 c/s resonators with open necks, where the measured coefficient is very much too low, suggesting that energy storage in the resonators may be having an appreciable effect. The magnitude of this effect is consistent with this view, the calculated "extra volume" from equation (17) being 37 m³ as compared with 28 m³, the volume of the reverberation room. If the real absorption coefficient is taken as 0·33, from equation (15), the apparent coefficient from Eyring's formula would be $0{\cdot}33 \times 28/(28 + 37)$ approx. $= 0{\cdot}14$ approx.

The corrections for the other cases in the table are negligible.

Table 2. *Absorption coefficient of resonators in array*

Resonator	μ	*Absorption coefficient calculated*	*Absorption coefficient measured*
144 c/s open neck	0·10	0·33	0·14
144 c/s one layer bandage	0·24	0·62	0·65
75 c/s open neck	0·50	0·90	0·88
75 c/s one layer bandage	1·00	1·00	0·92
75 c/s two layers bandage	1·18	0·99	0·99
75 c/s glasswool fabric	1·82	0·90	0·75

3.3. *Measurements in studios.*

The abnormal conditions of the reverberation room were very suitable for the measurement of absorption, since the ratio of volume to absorption was high and the increase of absorption due to the resonators would be expected to outweigh any possible increase in effective room volume. This condition would not hold in any ordinary room in which the average absorption coefficient of the walls might be as high as 0·2 or more, and accordingly tests were made in three such rooms, one quality listening room and two small talks studios. The same 84 resonators were used, tests being made with holes open, closed and covered with resistive materials.

The listening room had a reverberation time of approximately 0·65 sec at 75 c/s with the resonators blocked. This was reduced by the action of the resonators whether the holes were open, covered with fabric or filled with bandage, corresponding to a range of μ from 0·55 to 2·0. The reductions of reverberation time were in accordance with the values of μ.

The first talks studio had a volume of 43 m³ (1 500 ft³) and a reverberation time of 0·35 sec at 75 c/s, falling to 0·32 sec at 144 c/s. This was treated with 75 c/s resonators open and matched to give $\mu = 1$, with blocked resonators as a control, and 144 c/s resonators with open necks. The 144 c/s open resonators produced a very marked reverberation time increase from 0·32 sec to 0·52 sec at 144 c/s which, by the use of Table 2 and equation (16), may be shown to correspond to an "additional volume" of 28 m³ (1 000 ft³). Traces obtained with a logarithmic high-speed level recorder were linear, indicating that there was rapid exchange of energy between the resonators and the room. Careful listening tests using short pulses of tone, moreover, revealed this peak of reverberation but no tendency for the pitch of neighbouring tones to be modified during decay.

Another striking observation was that the resonators did not appear to "colour" speech from the studio heard over a microphone-loudspeaker listening chain. The increase of reverberation time at 144 c/s corresponds to an additional volume of 27·5 m³ (970 ft³).

The second talks studio was an experimental studio of approximately the same volume as the first with a reverberation time of 0·47 sec at 144 c/s. Fig. 6 shows the effect of 84 resonators with open necks (*b*) and with two layers of bandage (*c*), both tuned to 144 c/s. The increase of

reverberation time in (*b*) corresponds to an additional room volume of 22·5 m³ (790 ft³), a figure close to that obtained in the first studio. As in the first studio this pronounced peak of reverberation had very little effect on the subjective qualities of the room as a talks studio. Indeed, disk recordings made in the studio with the resonator necks open were actually preferred by a majority of observers taking part in controlled listening tests to those made with matched or closed resonators. There was no audible coloration at 144 c/s though it may be that the effect, if present, was insignificant in comparison with a previously existing coloration at 115 c/s due to a structural resonance.

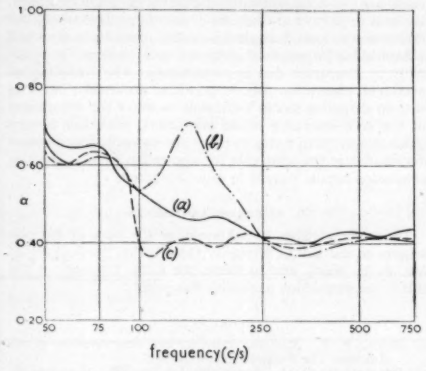

Fig. 6. Reverberation time measurements in second studio
Curve (*a*) necks closed, curve (*b*) necks open $\mu = 0{\cdot}07$, curve (*c*) necks with additional resistance $\mu = 0{\cdot}45$.

Following these observations some subjective tests were made on the influence of resonators of various frequencies in determining speech quality. The tests were made in a dead room and gave differing results according to the spectrum of the voice used.

4. DISCUSSION OF RESULTS

4.1. *Frequency of resonance.*

It was found that measurements of resonance frequency were in exact agreement with calculation. The concrete castings designed for 144 c/s, for example, gave a mean measured figure of 144 c/s with a standard deviation of $\pm 3{\cdot}8$ c/s for individual resonators. This variation corresponds to the observed variation in neck diameter. The 75 c/s bushes gave a smaller standard deviation on account of their greater uniformity. Prediction is therefore sufficiently accurate since these variations are considerably smaller than the bandwidths normally used.

4.2. *Absorption.*

It is not possible to predict the amount of absorption so accurately, since it depends on the nature of the sound-field and the arrangement of the resonators. Table 2 shows a remarkable agreement between calculation and measurement for arrays, the measurements having been carried out in a reverberation room in which, at low frequencies, the sound field consists of plane waves. The values of additional volume quoted in Section 3.3 above, however, imply values of Q, after correction for frequency variation between individual resonators, from 41 to 49, of the same order as that for an open-necked resonator in a hemispherical sound field rather than in a plane-wave field. Further experiments to elucidate this showed that in the reverberation chamber the radiation resistance was substantially unaffected by arrangement. Moreover, if the resonators were tuned to the frequency of the second vertical mode of the room and placed upon the floor, absorption reached a maximum if the neck resistance corresponded to the plane-wave resistance, whether the resonators were grouped together or separated.

It is therefore clear that the performance of a resonator depends upon the nature of the sound field in the room to a very considerable degree, and it is necessary to study the room modes about the resonance frequency before deciding upon the position of the resonator. Alternatively, all practical designs should make provision for varying the neck resistance.

The low Q values of arrayed resonators are in apparent contradiction to the high values of resistance required for maximum absorption. The latter requirement is in agreement with other workers,[5, 6] who find that there is good agreement between the absorption of arrays consisting of perforated panels and the resistance figures measured by the impedance tube method. There are, however, no published values of the resistance of open necks measured when arranged as arrays in ordinary room conditions.

The apparent contradiction arises from the interaction between neighbouring resonators. When the driving sound-field ceases these tend to get into antiphase and act together as dipoles or more complicated combinations in which the resistance presented to each resonator is low compared with that of the room. The individual variations in resonance frequency facilitate this change of regime. The measured Q values for open neck resonators is therefore low. When the neck resistance is artificially raised to achieve maximum absorption of the sound in the room, the resistance presented to each resonator by the neighbouring necks becomes at least as high as the $\rho c/\sigma$ resistance of a plane-wave field, and the tendency to interact is greatly reduced. Maximum absorption is therefore obtained with resistance values suitable for plane-wave conditions. This view has been checked qualitatively by experiments using a large number of bottles which could be arranged in any manner in either the reverberation room or an acoustically treated studio.

The conclusion is that if accurate prediction is desired, a choice must be made between isolated resonators and comparatively large plane arrays in which the value of μ is unity or greater. The question of bandwidth has not been considered in detail as this has been treated fully by Kosten and Zwikker.[5] The bandwidth of an isolated resonator with $\mu = 1$ is extremely small, and these authors recommend μ values between 10 and 40 in order to obtain a sufficient width, thereby reducing the peak absorption to a small fraction. The resistance of an array, being high in comparison with its inertance, gives an absorption band of reasonable width even at values of μ approaching unity, and this width may be increased with only a second-order reduction in peak absorption.

5. PRACTICAL FORMS OF HELMHOLTZ RESONATORS

The experimental resonators described above were designed for the special purposes of quantitative investigation. Where manufacture in large quantities is intended, some simplification is required. Other shapes may be used for architectural reasons, and, to a certain extent, existing parts of the building may be used as the cavities. Simplification and increased

efficiency may be effected by mounting the resonators in a large array, with groups of equally spaced holes having common air spaces. It is desirable in this case not to allow communicating air spaces to extend more than a fraction of a wavelength and, therefore, partitions must be provided at suitable intervals, say every 2–3 ft, in a low-frequency absorbing array. Stiffening members would in any event be required at intervals of this order.

Sound of low frequency may be absorbed by resonators of very small size and depth compared with other types of low frequency absorber. For instance, the volume of the experimental 75 c/s resonators could have been reduced to one-tenth with a suitable adjustment to the neck diameter. A reduction in size can only be made, however, by reducing the width of the frequency band over which effective absorption takes place, so that the advantages of small dimensions are outweighed by the necessity to provide a greater number to absorb over a given range of frequencies. Herein lies the great flexibility of the method, since almost any basic dimensions may be chosen to fit the architectural design of the building.

It is possible also to use the resonator units as sound diffusers. Experimental cylindrical diffusers have been made from fibrous plaster and mounted so that the slit between the edge of each resonator and the wall, in conjunction with the hollow interior, formed a resonator of frequency 80 c/s. Approximate agreement was obtained between the frequency and the theoretical value for a slot resonator given by Pedersen,[7] and with a resistive material in the slot, broad or selective absorption was obtained, the absorption coefficient in the latter case having maximum values up to 100% based on the area of wall covered by the diffuser. Rectangular pilasters or coffering could be used in a similar manner, such shapes also being preferable for other reasons (see Somerville and Ward[8]).

Resonators arranged in rows, having properties intermediate between the isolated resonators and two-dimensional arrays, also lend themselves readily to architectural designs and to prediction. They are being used extensively for a music studio now under construction by the B.B.C.

Reference should also be made to perforated panel resonators for middle and high frequency absorption. These have been treated very completely by several authors, notably Ingerslev[6] and Kosten and Zwikker.[5] The range of absorption may also be extended by adding a layer of rockwool and a perforated cover over the front of an array of low frequency resonators, the rockwool being adjusted in density and thickness to provide the necessary matching of the resonators and to give an overall curve of the required shape.

6. CONCLUSIONS

The experimental work described in this paper establishes that Helmholtz resonators tuned to low frequencies form an extremely flexible method of absorbing sound. The most effective way of using them is to arrange a comparatively large number as a series of plane arrays and to raise the neck resistance to a value rather higher than the radiation resistance. Isolated resonators are capable of very large absorption, but this cannot be used, because this condition results in too small a bandwidth for practical purposes, and involves the possibility of coloration due to re-radiation. The frequency of maximum absorption may be predicted accurately, but it is wise in designing studio treatments to allow for adjustment of the neck resistance of the resonators, since this is very much simpler than trying to make allowance for the pressure distribution in the room over the absorption band. This last conclusion applies equally to other absorbers.

7. ACKNOWLEDGMENTS

The author wishes to acknowledge the help of his colleagues in the B.B.C. Research Department, particularly of Mr. F. L. Ward, and to thank the Chief Engineer of the B.B.C. for permission to publish this paper.

REFERENCES

(1) Brüel, P. V. *Resonant Absorbers and Reverberation*, p. 15. (London: The Physical Society, 1949.)
(2) Richardson, E. G. *Sound*, 4th Ed., p. 234. (London: E. Arnold and Co., 1947.)
(3) Rayleigh, Lord. *Theory of Sound*, **2**, 2nd Ed., p. 319. (London: Macmillan and Co. Ltd., 1929.)
(4) Rschevkin, S. N. *C.R. Acad. Sci. URSS*, **18**, p. 25 (1938.)
(5) Zwikker, C., and Kosten, C. W. *Sound Absorbing Materials*, p. 143 (Amsterdam: Elsevier, 1949.)
(6) Ingerslev, F. *Akustik*, p. 189 (Copenhagen: Teknisk Forlage, 1949.)
(7) Pedersen, P. O. *Lydtekniske Undersøgelser*, p. 194, Ing. Str. No. 5. (Copenhagen: *Akademiet for de Tekniske Videnskaber*, 1940.)
(8) Somerville, T., and Ward, F. L. *Acustica*, **1**, p. 40 (1951).

Transit time oscillations in triodes

By O. H. Critchley, M.Sc., A.R.C.S.,* and M. R. Gavin, M.B.E., D.Sc., F.Inst.P., Department of Physics and Mathematics, College of Technology, Birmingham

[*Paper received* 10 *October*, 1951]

Oscillations which are critically dependent on anode voltage have been obtained over a wavelength range of 6 to 20 cm in disk seal triodes. The oscillations occur when the cathode-grid transit time is about five-quarters of the alternating period. They are closely analogous to the negative resistance oscillations obtained in diodes

1. INTRODUCTION

When an electron moves from the cathode to the anode of a diode under the influence of a steady field, the electron loses potential energy and acquires kinetic energy as expressed by the familiar relationship

$$\tfrac{1}{2}mv^2 = eV \qquad (1)$$

where m, e and v are the mass, charge and velocity of the electron and V is the potential at the instantaneous position of the electron, the cathode potential being taken as zero. If the field is alternating at a frequency sufficiently high for appreciable change to occur during the electron transit from cathode to anode then equation (1) no longer gives the instantaneous kinetic energy of the electron. For example, if the field is increasing during the transit, then the mean value of the field will be less than the value at the time the

* Now with the Engineering Division of the Australian Post Office.

electron reaches the anode. The final kinetic energy will be less than the value corresponding to the potential of the anode when the electron arrives there. Similarly, it is possible for an electron to reach the anode with kinetic energy greater than the value corresponding to the anode potential. In either case the difference between the gain in kinetic energy and the loss of potential energy may be accounted for in terms of the energy of the alternating field. If, on the average for all the electrons, there is an excess of kinetic energy, then this constitutes a drain on the energy of the alternating source. It is usual to express this drain in terms of a resistance in series or in parallel with the source of the alternating field, the value of the resistance being such that it would consume the same amount of power from the source as the electrons. The variation of this resistance with the electron transit time has been investigated by several authors and their results are summarized in the next section.

2. TRANSIT TIME OSCILLATIONS IN DIODES

For a space-charged limited planar diode Llewellyn[1] has shown that the series input resistance R is given by

$$\frac{R}{R_a} = 12\left[\frac{2(1-\cos\theta)-\theta\sin\theta}{\theta^4}\right] \tag{2}$$

where R_a = low-frequency slope resistance
and θ = the transit angle $= 2\pi f T$, where
f = frequency
and T = transit time.

Equation (2) may be written in the form

$$R/R_a = 12F(\theta)/\theta^4 \tag{3}$$

where $$F(\theta) = 2(1-\cos\theta)-\theta\sin\theta \tag{4}$$

For a temperature limited planar diode North[2] has expressed the shunt conductance G, due to electron loading in the form

$$G/G_0 = 2F(\theta)/\theta^2 \tag{5}$$

where G_0 = diode d.c. conductance.

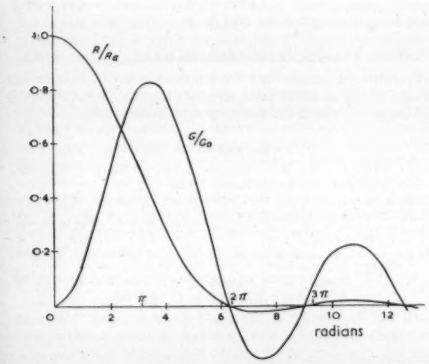

Fig. 1. The variation with transit angle of the a.c. resistance (R/R_a) of a space-charge limited diode and the conductance (G/G_0) of a temperature limited diode

The similarity of expressions (3) and (5) will be noted. They are shown graphically in Fig. 1. The quantities R and G are seen to be negative for transit angles between 2π and about 3π. This means that, in both cases, over this region the electrons are transferring some of their energy to the alternating field. In such circumstances the alternating field, once set up, will increase in value or, in other words, diodes may act as self-oscillators when the electron transit angle from cathode to anode is between 2π and 3π. The optimum condition for oscillation occurs in both cases at a transit angle of about $5\pi/2$ radians, i.e. a transit time of about a period and a quarter.

Experimental confirmation of these effects has been obtained for both temperature limited and space-charge limited diodes. Müller[3] produced a self-oscillator for a wavelength of 1 m using a pair of space-charge limited diodes. Llewellyn and Bowen[4] have obtained oscillations at 10 cm from a diode under both temperature limited and space-charge limited conditions. In all these experiments it was essential to use a very good resonator as the oscillations were very weak.

It is interesting to note that the electronic loading of a pair of transverse deflecting plates[5] such as are used in cathode-ray tubes, may also be expressed as an equivalent shunt conductance in the form

$$G = kF(\theta)/\theta^2 \tag{6}$$

where k is a constant. The transverse system has not been used for the production of oscillations, but equation (6) shows that the maximum value of the negative conductance will occur at a transit time through the deflecting system which is about one and a quarter times the natural period of the oscillatory circuit connected between the deflecting plates.

Anomalous oscillations have been obtained with a number of disk seal triodes over the range of 6 to 20 cm and it is shown below that these occur when the transit time in the cathode-grid space is one and a quarter periods of the oscillation. The oscillations are obtained with a number of valves of the type CV273[6] with a variety of electrode clearances. The circuit is the double concentric line of the common-grid earthed-anode oscillator which is normally used with this type of valve. The oscillations differ from normal oscillations in two main respects. They are very weak and they depend critically on the value of the applied anode voltage.

3. TRANSIT TIME OSCILLATIONS IN TRIODES

The transit time τ of an electron from the cathode to the grid of a triode is given by the equation

$$\tau = d_1/6 \times 10^7\sqrt{V_g} \tag{7}$$

where d_1 = cathode-grid clearance in cm and V_g = effective grid voltage.

When the only applied voltage is V_a to the anode then

$$V_g = \frac{V_a}{\mu}\Big/\left[1+\frac{1}{\mu}\left(1+\frac{4}{3}\frac{d_2}{d_1}\right)\right]$$

where μ = amplification factor and d_2 = grid-anode clearance.

If the transit time bears a definite relation to the period of the high frequency oscillation then equation (7) may be expressed in terms of the wavelength λ as

$$1/\lambda = \sqrt{V_g}/Kd_1 \tag{8}$$

where K is a constant. Thus there should be a linear relationship between $1/\lambda$ and the square root of the effective grid voltage. In Fig. 2 these quantities have been plotted for a series of seven valves and it will be seen that in each case straight lines passing through the origin are obtained.

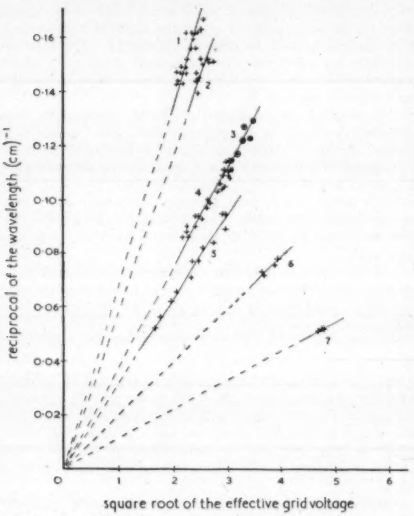

Fig. 2. Relation between the wavelength and voltage for transit time oscillations in seven triodes

The constant K can be determined for each valve from the slope of the line. Particulars of the valves and the values of K are given in the table. It will be seen that K does not vary much for the different valves. Its weighted mean value is 128. No correlation could be established between the wavelength of oscillation and the grid-anode transit time.

Particulars of valves and values of K

Valve	μ	d_1 mm	d_2 mm	Number of observations	K
1	38	0·10	0·39	19	138
2	46	0·13	0·34	10	125
3	40	0·20	0·30	6	123
4	39	0·22	0·30	23	
5	38	0·24	0·53	12	125
6	42	0·41	0·30	6	124
7	39	0·45	1·03	3	153

Weighted mean value of $K = 128$.

4. TRIODE INPUT CONDUCTANCE

In Section 2 it is shown that electronic loading in three different systems may be expressed as a series resistance or shunt conductance in the form

$$G = AF(\theta)/\theta^n \qquad (9)$$

where A is a constant and n has the value 2 or 4. In section 3 it is shown that the triode input conductance has a negative maximum which is closely related to the cathode-grid transit time. It is of interest, therefore, to consider whether the triode conductance obeys the same form as (9) where θ is the cathode-grid transit angle. It is known that for small transit angles G varies as θ^2 and to satisfy this condition it may easily be verified that n must take the value 2. Equation (9) shows that maximum negative conductance would occur when the transit angle is about $5\pi/2$. This condition may be expressed in terms of the wavelength and clearance in a form exactly similar to equation (8) and it is found that K is equal to 128, i.e. the same as the mean experimental value.

The significance of the exact equality of the calculated and experimental values of the constant K must be judged in terms of the accuracy of the measurements and other relevant factors. The wavelengths were measured to an accuracy of better than 1%. The valve clearances, which were measured optically, were consistent to within $\pm 0{\cdot}1$ mm. In the worst case, valve number 1, this represents 10% of d_1. In determining V_g, no allowance was made for contact potentials. These might amount to as much as 0·5 V and could affect the value of K by 5%. Finally, the initial velocities of the electrons have been neglected in calculating transit times. This would be equivalent to an error of about 0·1 V in V_g and should be negligible.

From the above considerations it will be seen that the equality of the two values of K must be, to some extent, a coincidence. However, it is reasonable to conclude that the triode input conductance at high frequencies obeys a similar law to the other devices and that oscillations may be obtained when the cathode-grid transit angle is $5\pi/2$.

As the oscillations are very weak it is unlikely that they would have useful application for generation of power, but they constitute a source of parasitic oscillation which may cause trouble under certain conditions, particularly in a pulsed system where the electron transit time varies over a wide range during the rise and decay of the pulse.

5. ACKNOWLEDGMENT

The authors are pleased to thank the Research Laboratories of the General Electric Company, Limited, for providing the valves on which the measurements were made.

REFERENCES

(1) LLEWELLYN, F. B. *Electron-inertia Effects*. (London: Cambridge University Press, 1941.)
(2) NORTH, D. O. *Proc. Inst. Radio Engrs*, **24**, p. 108 (1936).
(3) MÜLLER, J. *Hochfrequenztech. u. Electroakus.*, **43**, p. 195 (1934).
(4) LLEWELLYN, F. B., and BOWEN, A. E. *Bell Syst. Tech. J.*, **18**, p. 280 (1939).
(5) GAVIN, M. R., and WARREN, G. W. *G.E.C. Journal*, **14**, p. 97 (1946).
(6) BELL, J., GAVIN, M. R., JAMES, E. G., and WARREN, G. W. *J. Instn Elect. Engrs*, **93**, IIIA, p. 833 (1946).

A method of designing a compensated solenoid giving approximately uniform field

By T. A. HEDDLE, B.Sc., A.Inst.P., British Scientific Instrument Research Association, Chislehurst, Kent

[*Paper first received* 4 *September*, 1951, *and in final form* 8 *October*, 1951]

This paper describes a method of calculating the design of a solenoid with any number of compensating end coils to produce an approximately uniform magnetic field along a large portion of the solenoid length. The design of a solenoid with two end coils at each end is given in a numerical example and its estimated performance compared with experimental results.

INTRODUCTION

Methods of obtaining approximately uniform magnetic fields include the use of a solenoid of large length-to-diameter ratio and Helmholtz coils or similar arrangements by Barker[1,2,3] of two, three, or four coils. For some applications these are inconvenient because the length of the solenoid and the diameters of the coils are much larger than the dimensions of the field required. Clark[4] has wound an approximation to a spherical coil with uniform field, but the coil former is complicated by the different internal diameters of the sections and access is restricted.

One might expect that the ideal winding would have a profile somewhat as sketched in Fig. 1, but the practical difficulties of winding such a coil, even if the design calculations could be made readily, suggested that an approximation would be desirable. Lewis[5] has given a design procedure for a solenoid with one additional coil at each end and the method could be extended to a closer approximation to this profile by using more coils. The curves of field variation along the axes of the solenoid and end coils are matched by eye to give approximate compensation when combined. However, a direct calculation is preferred and its mathematica difficulties were solved by the method given below.

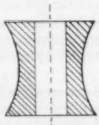

Fig. 1. Ideal profile of solenoid

GENERAL DESCRIPTION

The solenoid consists of a main uniform winding with extra windings added, each uniform in itself and wound directly on the main winding with the same gauge wire, and connected in series.

The calculation gives the number of turns for each end coil to obtain equality of the field strengths at a number of points on the axis. If the number of coils at each end is p, the number of points of equal field strength on the axis is $2p + 2$. The positions of these points may be chosen freely, perhaps to space evenly along the portion of the axis where uniformity is required. The field will vary between these positions to an extent not predictable until the design is complete. The variation can then be calculated, and, if necessary, a closer approximation to the ideal can be obtained by moving the chosen points to more critical positions, or adopting a larger number of end coils, any number of which can be calculated.

THE CALCULATION

At the outset all linear dimensions of the windings are assumed, even those that are to be found. A convenient internal and external diameter and length are chosen and the positions, widths, and depths of the end coils are taken provisionally as suggested by approximating to Fig. 1. Although the depths of the end coils are to be found by the calculation and the winding density of all parts is to be the same, it is convenient in the first place to assume certain winding depths. An expression for the total field strength at each of the chosen points due to all parts of the winding is then obtained, and equating these expressions gives the winding densities that would be needed to make these field strengths equal.

The depths of the windings are then adjusted in proportion to the calculated winding densities and the calculation repeated with these revised depths. This adjustment is based on the fact that to a first approximation the effect of an end coil is dependent on the number of turns and independent of the depth of the winding.

This process of adjustment and recalculation can be repeated as often as required, but it is found that the results rapidly converge on the exact solution. In the example given below only one repetition of the calculation is needed to yield a result within a $\frac{1}{2}$% of the ultimate.

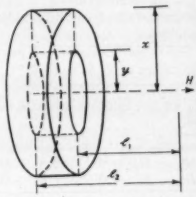

Fig. 2. Uniform circular coil

The calculation is based on the standard formula for the field at a point on the axis of a uniform coil, which can be obtained by integration of Laplace's formula. Thus with reference to Fig. 2:

$$H = K[f(l_2, x) - f(l_1, x)] \text{ where } K = \frac{2\pi nI}{10},$$

and $f(l, x) = l \log_e \left[\frac{x + \sqrt{(x^2 + l^2)}}{y + \sqrt{(y^2 + l^2)}}\right]$, H = field in oersteds, n = winding density in turns per sq cm, I = current in A and all linear dimensions are in cm.

This can be applied to a solenoid with end coils as in Fig. 3 by adding the components due to the different sections.

NUMERICAL EXAMPLE

Initial assumptions. The dimensions given in Fig. 3 are those on which the calculation of a particular solenoid was based. The internal radius of the winding was the external radius ($1\frac{1}{2}$ in) of a tube suitable to house other apparatus. The length was chosen to be a suitable round number approximately one and a half times the length of the uniform field required. The widths of the end coils were chosen so that the extreme coils were just outside the important region of field. The depth of winding at the centre was chosen to be a round number such that, if the solenoid were wound to that depth along its whole length, the field strength required could be obtained at the centre, using a convenient current from a particular d.c. supply. These choices were partly arbitrary, but the results proved their suitability.

Direct calculations. The first stage of the calculation is to

add all components of the axial field at each selected position A, B, C on the axis as shown in Fig. 3. Thus

$$H_A = \Sigma_A K[f(l_2, x) - f(l_1, x)]$$

and similarly for H_B and H_C, where $x = 4{\cdot}81$ for the centre section, $x = x_2$ for the intermediate end coil and $x = x_3$ for the extreme end coil.

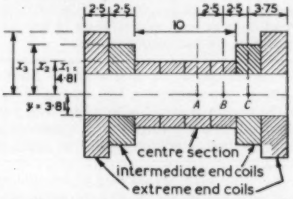

Fig. 3. Particular example of solenoid with end coils

The method of direct solution would continue by treating $H_A = H_B$ and $H_A = H_C$ as simultaneous equations with x_2, x_3 as variables and K = constant. This leads to intractable difficulties which can be avoided by successive approximations as follows.

First approximation. A provisional assumption is made of the values of $x_1 = x_2 = 4{\cdot}81$, $x_3 = 5{\cdot}81$, and K_1, K_2, and K_3 are treated as variables, where $K = K_1$ for the centre section, K_2 for the intermediate end coil and K_3 for the extreme end coil.

Then by five-figure logarithms:

$$H_A - H_B = 0{\cdot}13188\,K_1 - 0{\cdot}07618\,K_2 - 0{\cdot}06312\,K_3 = 0$$
$$H_A - H_C = 0{\cdot}35831\,K_1 - 0{\cdot}14724\,K_2 - 0{\cdot}21728\,K_3 = 0$$

and hence $K_1 = 0{\cdot}92145\,K_3$ and $K_2 = 0{\cdot}76663\,K_3$.

These give the ratios by which the winding depths must be adjusted, as described above, to correspond with $K_1 = K_2 = K_3$ to a first approximation.

$\therefore\ x_1 - y = 0{\cdot}92145$, $x_2 - y = 0{\cdot}76663$, and $x_3 - y = 2{\cdot}0$ as before.

Second approximation. A further approximation is obtained in exactly the same manner by adopting these revised values of x_1, x_2, x_3 and abandoning the equality $K_1 = K_2 = K_3$. Hence:

$$H_A - H_B = 0{\cdot}12338\,K_1 - 0{\cdot}06106\,K_2 - 0{\cdot}06312\,K_3 = 0$$
$$H_A - H_C = 0{\cdot}33354\,K_1 - 0{\cdot}11792\,K_2 - 0{\cdot}21728\,K_3 = 0$$

giving $K_1 = 1{\cdot}0040\,K_3$ and $K_2 = 0{\cdot}99737\,K_3$.

These are within a $\frac{1}{2}\%$ of the ideal $K_1 = K_2 = K_3$, and the adjustment of winding depths gives $x_1 - y = 0{\cdot}92145 \times 1{\cdot}004 = 0{\cdot}925$, $x_2 - y = 0{\cdot}76663 \times 0{\cdot}99737 = 0{\cdot}765$, and $x_3 - y = 2{\cdot}0$. This is considered close enough to the ultimate solution to be the basis of a winding in which the practical errors of winding could swamp any further refinements.

METHOD OF WINDING

In winding the solenoid it is more important to obtain the correct ratios of the numbers of turns than to obtain the exact winding depths calculated. The winding density for the chosen gauge of wire can be found experimentally from the first stage of the winding. Therefore a uniform winding of 5 832 turns in 16 layers was made along the full 20 cm length of the solenoid giving an external radius of 4·6 cm. This is as close to the required value of $x_2 = 4{\cdot}575$ cm as is possible with 26 s.w.g. single silk- and enamel-covered wire. Hence the experimental value of n can be found and the additional turns calculated for the centre section and extreme end coils to obtain the correct ratios with those of the intermediate end coils.

Winding these extra turns of 611 and 1 180 respectively gave an external radius of the centre section of 4·85, compared with $x_1 = 4{\cdot}735$, and of the extreme end coil of 5·98, compared with $x_3 = 5{\cdot}81$. To keep these extra turns in place during the winding, wooden rings were clamped over the uniform layers already wound in the position of the intermediate end coils. The winding space thus left was lined with paper and the turns varnished at each layer so that the rings could later be removed safely.

FINAL PERFORMANCE

The mean field near the centre of the solenoid was found to be 428·5 oersteds/A by measurements with an accurately made single layer search coil in comparison with a standard mutual inductor. The uniformity of the field was explored by another shorter multilayer search coil balanced against a variable mutual inductor when at the centre of the solenoid.

Fig. 4 shows the measured variation in the field compared with the calculated variation, and also the calculated variation of the field of an uncompensated uniform solenoid of the same length, but wound entirely as the centre section. Along the central 13 cm of the axis, the uncompensated variation of $\pm 6\%$ is reduced to $\pm 0{\cdot}35$. Calculation shows that the discrepancy between the calculated and measured variation in the compensated solenoid is due primarily to inaccuracies in the winding as revealed by the differences between the measured and calculated external radii. The winding was done on a hand-fed and hand-cranked machine without additional precautions for uniform winding. Secondarily, a small difference is to be expected on account of the finite size of the search coil compared with the calculation of the field at a number of points. The search coil enclosed a mean volume of approximately $1\frac{1}{2}$ cm diameter by $\frac{3}{4}$ cm length.

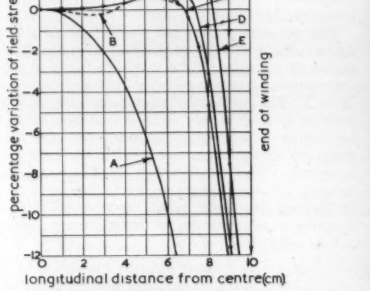

Fig. 4. Field variation of particular compensated and uncompensated solenoids of the same size

Uncompensated solenoid:
A, variation along axis.

Compensated solenoid:
B, calculated variation along axis;
C, measured variation along axis;
D, measured variation parallel to and 1 cm from axis;
E, measured variation parallel to and 2 cm from axis.

Fig. 4 also shows the variation along lines parallel to, but displaced from, the axis. Four equally spaced lines were taken at each distance from the axis and the maximum variation found is shown in the figure. It is seen that a variation of less than $\pm \frac{1}{2}$ % is obtained in a volume of 2 cm diameter and 13 cm length, the overall dimensions of the solenoid being approximately 12 cm diameter and 22 cm length including end cheeks.

The interesting result that $x_2 < x_1$ in this particular case may be due to the position of the point *C*, Fig. 3, and to the small number of end coils.

ACKNOWLEDGMENTS

The author wishes to thank Dr. A. J. Maddock and the Director of the British Scientific Instrument Research Association for supporting the work and the Council of the Association for permission to publish this paper.

REFERENCES

(1) BARKER, J. R. *Brit. J. Appl. Phys.*, **1**, p. 65 (1950).
(2) BARKER, J. R. *J. Sci. Instrum.*, **26**, p. 273 (1949).
(3) BARKER, J. R. *J. Sci. Instrum.*, **27**, p. 197 (1950).
(4) CLARK, J. W. *Rev. Sci. Instrum.*, **9**, p. 320 (1938).
(5) LEWIS, B. *Brit. J. Appl. Phys.*, **1**, p. 238 (1950).

Some measurements of the total emissivity of metals and pure refractory oxides and the variation of emissivity with temperature

By A. H. SULLY, M.Sc., Ph.D., F.I.M., F.Inst.P., E. A. BRANDES, B.Sc., A.R.C.S., F.I.M., and R. B. WATERHOUSE, B.A., A.I.M., Fulmer Research Institute Ltd., Stoke Poges, Bucks

[*Paper first received* 22 *August*, 1951, *and in final form* 2 *October*, 1951]

A method has been described for the rapid determination of the total emissivity of metals and oxides in the temperature range 300–800° C. Values have been obtained for lampblack and polished platinum and also for Nimonic 75, pure nickel, and stainless steel, with various surface conditions. The total emissivities of the pure oxides ceria, zirconia, thoria, magnesia, alumina and fused silica have also been determined. The effect of particle size of the oxides and the variation of emissivity with angle of emission have been studied.

INTRODUCTION

The measurements described in this paper were made in connexion with a wider investigation of the possibility of reducing radiant heat transfer in engines, particularly gas turbine flame tube systems, by applying to metal parts coatings with a low thermal emissivity. This has involved the measurements of the total emissivity at various temperatures of some alloys which are used as engine parts and of certain pure refractory substances which might be used as constituents in radiation-suppressing coatings.

Other workers[1–8] have made measurements of the total emissivity of some metals and refractory oxides, but factors which have an important effect on the emissivity such as the condition of the surface and the size of the refractory particles do not seem previously to have received adequate attention.

The apparatus developed in this work enables the total emissivity of metal surfaces in various conditions and of ceramic materials to be determined quickly over the temperature range 300–800° C, both normally and obliquely to the surface. The apparatus is also constructed so that a direct comparison can be made between the radiation properties of a coated and uncoated piece of metal.

EXPERIMENTAL METHOD

The apparatus consists of a strip of metal heated electrically and capable of being rotated about its long axis without change of temperature. Radiation from the central part of the strip which is at a uniform temperature is allowed to fall via an aperture in an asbestos screen on to a thermopile connected to a galvanometer. For experiments with metals, the strip was the metal under examination; for refractories, a layer of the material was applied to the strip from an aqueous suspension. Firstly, to calibrate the thermopile, the strip mounting was removed and a furnace with uniform internal temperature substituted which had a slit opening of the same dimensions as the strip. Extraneous radiation was prevented from reaching the thermopile by means of a water-cooled screen. The complete apparatus is shown schematically in Fig. 1. This arrangement gave the galvanometer deflexions equivalent to a black body of the temperature of the furnace. The furnace temperature was measured with platinum/platinum 13% rhodium thermocouples. A master couple made from the same batch of wire was calibrated against the melting-points of zinc, antimony, aluminium and silver. The deviation in this case was less than $\pm$ 0·5° C. The couples used in

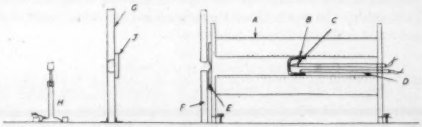

Fig. 1. Diagram of apparatus

A, furnace casing; *B*, graded winding; *C*, platinum/platinum-rhodium thermocouple; *D*, control couple; *E*, standard slit; *F*, water-cooled screen; *G*, Sindanyo screen; *H*, thermopile; *J*, shutter

this work were calibrated against this master couple, the accuracy of measurement being within $\pm$ 0·5° C over the range of temperature investigated. To check this arrangement a curve was plotted of the log of the galvanometer deflexion against the log of the difference of the fourth power of the furnace temperature and the fourth power of thermopile temperature in degrees Kelvin. This yielded a straight line relation. The absorption of radiation, for the wavelengths significant in our measurements, by passage through the air (40 cm path length) was negligible. This was confirmed by calculations based on the figures given by Fowle.[9] Secondly, the total emissivity-temperature relations for certain standard surfaces were determined. These were polished platinum, lampblack, and Nimonic 75 oxidized at 1 200° C. These values were used subsequently as described below. For this the strip was set up in the holder and a platinum/platinum-rhodium thermocouple junction inserted in a small hole drilled in the centre of the back of the strip. The couple wires were only 0·0015 in diameter so that the heat extracted along them could be ignored. In the case of polished platinum and oxidized Ninomic 75 the metals were used plain, but for

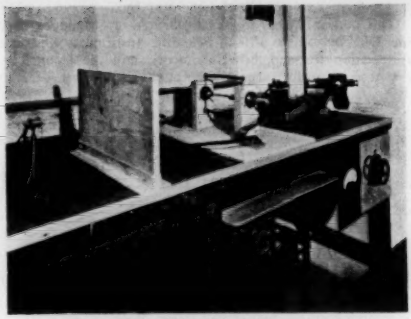

Fig. 2. General view of emissivity apparatus

lampblack a layer was deposited on Nimonic 75. The readings obtained were compared directly with the black body readings previously recorded for the corresponding temperature. Thirdly, the apparatus was used with a strip of oxidized Nimonic 75 coated on one side with the ceramic substance under test, the other side being either the surface oxidized at 1 200° C or coated with lampblack as in the standardization. Readings were then taken of the thermopile galvanometer by exposing first the one side and then the other, the total emissivity being obtained from this ratio together with the value for the standard surface. This arrangement is shown in the photograph, Fig. 2. Lastly, the apparatus was used to measure total emissivity at an angle other than normal to the surface by taking the reading with the strip inclined to the vertical and comparing the value with that expected from the cosine relationship.

THE STANDARD SUBSTANCES

Values for the total emissivity of lampblack and polished platinum between 300 and 900° C are shown in Fig. 3 and for Nimonic 75 oxidized at 1 200° C in Fig. 4. Lampblack and oxidized Nimonic 75 were convenient standards for use in the rapid third method because since they are of high emissivity they give larger galvanometer deflexions and thereby reduce errors. Lampblack, however, could only be used at the lower temperatures since above 550° C it burned off rapidly. The values for platinum were measured with the idea of comparing the method with measurements made by other workers and different methods. The lower part of Fig. 3 shows all the determinations made on polished platinum and Table 1 gives a comparison of the figures from the curve drawn through these points with some of the other available figures. The mean deviation of the experimental determinations from the curve is ± 0·006.

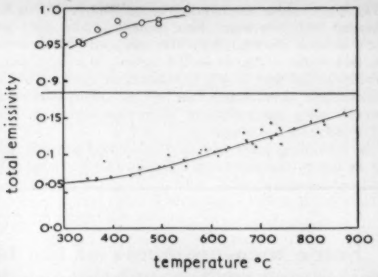

Fig. 3. Total emissivity of lampblack and polished platinum between 300° C and 900° C

○ lampblack ● polished platinum

Table 1. *Total emissivity of polished platinum*

Temperature °C	°K	*Present value from Fig. 3*	*Davisson and Weeks*[5]	*Randolph and Overholser*[3]	*Foote*[8]	*Pirani*[14]
300	573	0·062	0·071	—	0·061	—
400	673	0·070	0·087	0·086	0·070	—
500	773	0·083	0·102	—	0·080	0·118
600	873	0·103	0·116	0·110	0·088	0·110
700	973	0·122	0·130	—	0·097	0·108
800	1 073	0·142	0·144	—	0·106	0·103
900	1 173	0·160	0·156	—	0·114	—

Davisson and Weeks measured the electrical energy input to a platinum wire in a very high vacuum and compared this with the theoretical emission. They measured the temperature by measurement of the electrical resistance of the wire. Randolph and Overholser's figures are obtained by calculation from the electrical resistance. Foote's values were obtained from true and apparent temperature readings, the apparent temperature being measured by a total radiation pyrometer and the true temperature by an optical pyrometer assuming the monochromatic emissivity of platinum to be constant with temperature.

Pirani's method consisted of withdrawing the specimen from a furnace and exposing the cooling, radiating surface to

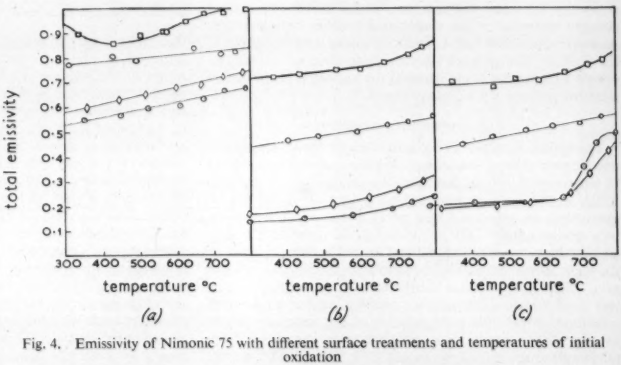

Fig. 4. Emissivity of Nimonic 75 with different surface treatments and temperatures of initial oxidation

□ oxidized at 1 200° C ○ oxidized at 900° C ◇ oxidized at 600° C ○ unoxidized

(*a*) shot blasted (*b*) buffed (*c*) as-rolled

a thermopile. The curve obtained was extrapolated back to zero time and the emissivity values calculated by using established figures for quartz as a standard. These are the only figures which show decreasing values of total emissivity with increasing temperature.

NIMONIC 75, PURE NICKEL AND FIRTH-VICKERS STAYBRIGHT F.D.P. 18% CR 8% NI STAINLESS STEEL WITH VARIOUS SURFACE TREATMENTS

The specimens were prepared in the form of strips and given the appropriate surface treatment. The shot-blasted specimens were blasted with fused alumina. All the specimens were cleaned with carbon tetrachloride. Oxidation was carried out in electric furnaces open to the air, and continued for a sufficient length of time for a steady state to be achieved.

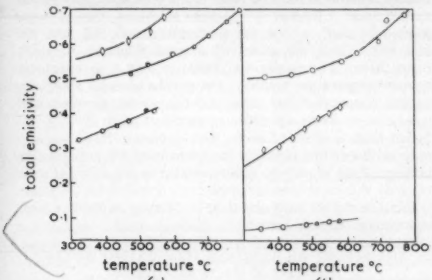

Fig. 5. Emissivity of pure nickel with different surface treatments and temperatures of initial oxidation

○ oxidized at 900° C ◇ oxidized at 600° C ○ unoxidized

(*a*) shot blasted (*b*) buffed

The specimens were set up in the apparatus as described in the previous section, the temperatures again being measured with the small platinum/platinum-rhodium thermocouple. The results for Nimonic 75, pure nickel and 18/8 stainless steel are shown graphically in Figs. 4, 5 and 6 respectively.

The roughening of the surface produced by shot blasting has increased the total emissivity of the polished metal surfaces in the unoxidized condition by a factor varying from 2, in the case of the 18/8 steel, to 5 in the case of pure nickel. This difference is reduced a little after oxidation at 600° C, and is very much less noticeable after oxidation at 900° C and, in the case of Nimonic 75, at 1 200° C. The as-rolled surface of Nimonic 75 is very similar in its emissivity to the polished surface, apart from a rapid oxidation which occurs when the as-rolled specimen is heated above 650° C as indicated by the steep rise of the lower two curves in Fig. 4(*c*). That this rise was irreversible was shown by emissivity measurements made during heating and cooling of the same specimen. This oxidation also occurs in the polished specimen, as indicated by the similarity of the emissivity curves of the polished and as-rolled surfaces after oxidation at 900° C, but the oxidation proceeds at a much slower rate. The as-rolled specimen in the 18/8 steel shows a higher emissivity after oxidation at 600° C than the polished or shot-blasted surface. This may be due to inhomogeneity of the metal surface caused during the rolling process. The polished and shot-blasted specimens of pure nickel have almost identical emissivities after oxidation at 900° C, but oxidation at 600° C produces an unexpected effect. The roughened surface has an emissivity greater than the same surface after oxidation at 900° C. This could be explained by the fact that the film of oxide on the polished specimen is much thinner than on the shot-blasted surface and therefore more transparent to radiation from the underlying metal. (This influence of coating thickness on emissivity is discussed at greater detail below.) The shot-blasted surface, on the other hand, shows the emissivity characteristics of the oxide only. It has been reported[10] that nickel oxide shows a lightening in colour after prolonged heating at temperatures of 800° C, and from observations of oxidized nickel held for long periods at 600 and 900° C it appears that there is an attendant decrease in emissivity at the higher temperature.

PURE OXIDES

The purest samples of ceria and thoria were selected from the available sources of supply by spectrographic examination. The British Aluminium Co. kindly provided samples of pure alumina of various particle size. Pure magnesia was prepared from super purity magnesium. The fused silica specimen was prepared from broken fragments of fused silica laboratory ware which were crushed in a steel mortar

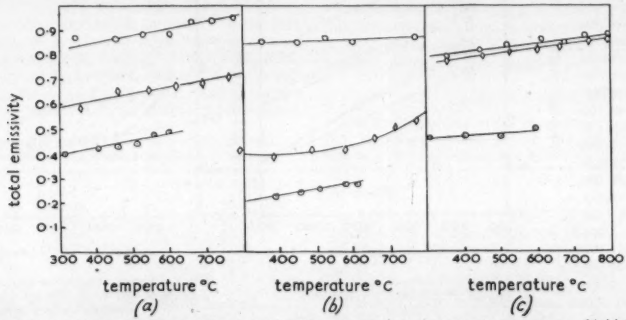

Fig. 6. Emissivity of Vickers F.D P. stainless steel with different surface treatments and temperatures of initial oxidation

○ oxidized at 900° C ◇ oxidized at 600° C ○ unoxidized

(*a*) shot blasted (*b*) buffed (*c*) as-rolled

and then milled in a steel mill with steel balls for 60 h, and the powder treated with 50% hydrochloric acid to remove iron, and washed.

The powders were applied in the form of a water suspension to one side of a weighed oxidized Nimonic 75 strip whose emissivity had been measured by the method described above. The coated strip was dried and weighed and the area of the coating measured, and the weight of oxide per unit area calculated. The strip was placed in the apparatus and readings of the thermopile galvanometer deflexion taken when the coated and the uncoated side of the strip were exposed to

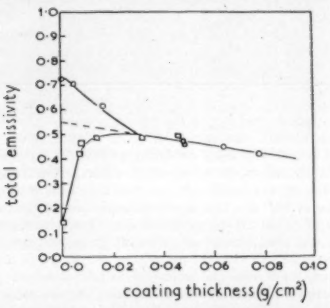

Fig. 7. Variation of the value obtained for total emissivity of ceria at 400° C, using various thicknesses of oxide and different supporting strips

○ oxidized supporting strip □ buffed supporting strip

the thermopile, at various temperatures between 300 and 800° C. The temperature of the strip was determined from a calibration graph prepared from the values of thermopile galvanometer deflexion against temperature obtained during the measurement of the emissivity of the oxidized Nimonic strip. The surface of the oxide coating is at a slightly lower temperature than the strip, but this has been allowed for by the method described below. Determinations of the emissivity of each oxide were made for a range of thicknesses of the coating.

When the emissivity of a particular oxide at a certain temperature is plotted against the thickness of the applied coating a curve of the form shown in Fig. 7 is obtained. It indicates that below a certain limiting thickness the radiation is not wholly characteristic of the oxide coating but radiation from the underlying metal is penetrating the coating. To show this clearly some determinations were made on a buffed Nimonic 75 strip as well as the oxidized strip. In Fig. 7 the points shown as circles were measured on the oxidized strip and can be seen at the low values of thickness departing from the straight line and moving up to the value for oxidized Nimonic 75 while the points shown as squares measured on the buffed strip show the departure in the opposite direction to the value for the buffed metal. This curve is for ceria at 400° C. The value of the limiting thickness is governed by the particle size and such properties as the refractive index of the oxide. The slow decrease in emissivity at thicknesses greater than the limiting thickness is due to the temperature drop through the coating. In order to derive the emissivity of the oxide at this temperature, the straight line portion of the graph above the limiting thickness was extrapolated as indicated by the dotted line in Fig. 7 and the value at zero thickness taken as the true value of the total emissivity at this temperature. Emissivity against thickness curves were plotted for each oxide at the temperatures 400, 500, 600, 700 and 800° C and the emissivity at zero thickness obtained from them. The results are shown in Fig. 8 as emissivity against temperature graphs. The graphs of total emissivity against temperature for ceria, zirconia, thoria, alumina, and magnesia, are linear within the temperature range 300–800° C. Fused silica is almost linear. This departure from linearity may be due to the difficulty in determining the straight line portion of the emissivity against thickness graph in the case of silica, due to its great transparency; the limiting thickness is therefore rather great and there is difficulty in holding such coatings on the strip heater.

THE EFFECT OF PARTICLE SIZE ON THE TOTAL EMISSIVITY OF PURE OXIDES

In order to assess the effect of particle size on the total emissivity of a pure oxide, graded samples of fused alumina were obtained. In the case of two of the samples, particle size figures were given as measured by a sedimentation method. However, these figures were found to disagree with figures obtained by microscopical measurements. This was to be expected since alumina has a basal cleavage and the ground particles therefore tend to be plate-like. The particles lie on the microscope slide with their short dimension parallel to the axis of the microscope, thus the two longer dimensions are

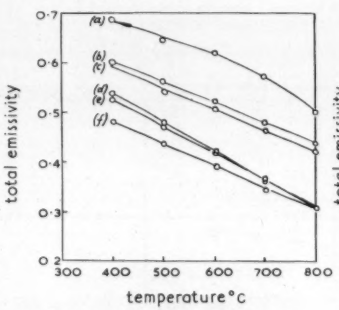

Fig. 8. Total emissivity of some pure oxides at various temperatures corrected for thickness

(*a*) silica (*b*) thoria
(*c*) magnesia (*d*) zirconia
(*e*) ceria (*f*) alumina

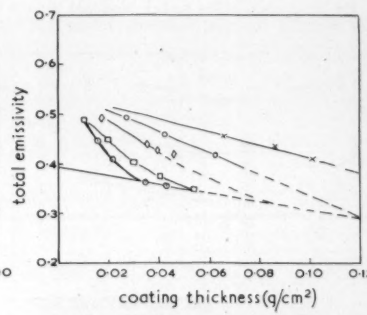

Fig. 9. Values obtained of total emissivity of alumina at 600° C at different thicknesses for various particle sizes

○ 8 μ-particles □ 13 μ-particles
◇ 20 μ-particles ○ 30 μ-particles
× 44 μ-particles

always measured. Sedimentation figures, on the other hand, give the diameter of the sphere whose terminal velocity would be the same as that of the particle in the particular medium employed. Microscopic measurements on 100 grains were made on each of the samples of alumina, and the averages were taken as the particle size of the sample.

The total emissivity of each sample for various thicknesses was determined as described previously. Emissivity against thickness curves were plotted for each sample at the temperature 600° C. These are drawn in Fig. 9.

Unfortunately it was not possible to investigate the variation of emissivity with thickness over a wide range of thickness, as it was found that with particles in the larger size ranges there was a limiting thickness above which it was impossible to keep the coating adhering to the heated strip. With finer grades than those reported cracks developed in the coating which gave false results.

The results given in Fig. 9 suggest that for a given thickness of coating the emissivity decreases as the particle size decreases. It is considered, however, that this is only true below a certain range of thickness. It is to be noted that the values of emissivity for particles of size 8 μ and 13 μ are almost identical for a coating thickness of 0·054 g/cm² and it is not unreasonable to assume that above a limiting thickness of about this value the straight line portion of the emissivity thickness relation is the same for both sizes of particle. It is also thought possible that the curves for the other sizes of particle will merge into the same straight line but at limiting thicknesses which increase with the particle size. This suggests that the limiting thickness is a function of the number of particle air interfaces encountered by the radiation in passing through the coating. If this were so the ratio of limiting thickness to particle size should be a constant.

Values of limiting thickness can be obtained from Fig. 9 for the 8 μ and 13 μ samples, but in the case of the larger particle sizes can only be obtained from undesirably long extrapolations. The ratios of limiting thickness to particle size derived in this way are given in Table 2. The ratio

Table 2. *Ratio of limiting thickness to particle size*

Particle size	*Limiting thickness*		*Limiting thickness divided by particle size*
μ	g/cm²	μ	
7·9	0·0241	178	22·6
12·8	0·0407	302	23·6
20·3	0·0717	531	26·2
29·8	0·1158	858	28·8

increases with particle size, because no correction has been applied to compensate for the fall in emissivity due to the temperature drop through the coating. If the limiting thickness is taken as the points of intersection of the curves with the horizontal line through the extrapolated value of the zero thickness emissivity the values shown in Table 3 are obtained.

Table 3. *Ratio of limiting thickness to particle size after correction for temperature drop*

Particle size	*Limiting thickness*		*Limiting thickness divided by particle size*
μ	g/cm²	μ	
7·9	0·0216	0·160	20·2
12·8	0·0323	239	18·7
20·3	0·0506	375	18·5
29·8	0·0703	521	17·5
44·2	0·1133	840	19·0
			avg. 18·8

The values of the ratio are seen to be fairly constant.

These results suggest that the effects of particle size encountered are incidental in the method which places a layer of material on a heater strip. The true total emissivity of the oxide is independent of particle size and would be that of a large single crystal of the substance. The figures given in Fig. 7 represent these values at the temperatures concerned.

VARIATION OF TOTAL EMISSIVITY WITH ANGLE OF OBSERVATION

It has been reported[7] that Lambert's cosine law is not obeyed by certain materials, notably polished metals, when the radiation emitted by them at elevated temperatures is observed obliquely to the surface. This has been stated to be due to variations in the total emissivity with the angle of emission. The rotatable strip heater described earlier in this paper allows this deviation to be readily determined. Determinations of the total emissivity of polished platinum, oxidized Nimonic 75, oxidized nickel, and pure alumina were made at various angles of emission. In Tables 4 and 5 values of the thermopile galvanometer deflexion D are tabulated against the angle of emission θ. If Lambert's law is obeyed $D/\cos\theta$ or $D/(a\cos\theta + b\sin\theta)$ where the thickness of the strip cannot be neglected (a and b are constants), is a constant.

Table 4. *Variation of emission with angle for polished platinum*

θ *degrees*	D	$D/\cos\theta$	*% deviation from Lambert's law*
0	12·50	12·50	—
40	9·95	12·85	2·8
5C	8·70	13·50	8·0
60	7·35	14·70	17·6
70	6·00	17·60	40·8
80	3·70	21·30	70·5

Table 5. *Variation of emission with angle for oxidized Nimonic 75, oxidized nickel and pure alumina*

θ *degrees*	D	$D/(a\cos\theta + b\sin\theta)$	
0	13·35	39·3	oxidized Nimonic 75
20	12·70	38·3	
40	10·95	38·6	
60	7·84	38·8	
80	3·69	38·8	
0	11·00	33·4	oxidized nickel
20	10·70	32·2	
40	9·10	33·0	
60	6·25	31·9	
80	2·65	28·8	
0	8·15	24·0	pure alumina
60	5·05	25·0	

From these results it is seen that there is a marked deviation from the Lambert cosine law with polished platinum, but that the law is obeyed in the case of oxidized Nimonic 75, oxidized nickel, and pure alumina.

ACKNOWLEDGMENT

The work described in this paper forms part of an investigation sponsored at the Fulmer Research Institute by the Ministry of Supply (National Gas Turbine Establishment) to whom the authors are indebted for permission to publish the results.

REFERENCES

(1) LIEBMANN. *Z. Phys.*, **63**, p. 404 (1930).
(2) PRICE and LOWERY. *J. Iron Steel Inst.*, **149** (1), p. 523 (1944).
(3) RANDOLPH and OVERHOLSER. *Phys. Rev.*, **2** (2), p. 144 (1913).
(4) PIRANI. *J. Sci. Instrum.*, **16**, p. 12 (1939).
(5) DAVISSON and WEEKS. *J. Opt. Soc. Amer.*, **8**, p. 585 (1924).
(6) WILKES. *Heat Insulation.* (John Wiley: New York, 1950.)
(7) BAUER and MOULIN. *C.R. Acad. Sci., Paris*, **150**, p. 167 (1910).
(8) FOOTE. *Bull. Bureau of Stand.*, **11**, p. 607 (1914).
(9) FOWLE. *Smithsonian Inst. Pubs. Misc. Coll.*, **68**, No. 8 (1917).
(10) PRASAD and TENDULKER. *J. Chem. Soc.*, p. 1403 (1931).

New books

International Conference on Science Abstracting (Final Report). (Paris: United Nations Educational Scientific and Cultural Organization.) Pp. 192. Price 12*s*. 3*d*.

The conference of which this is the final report took place in the summer of 1949, and it may be questioned whether anything appearing so long after the event can have much value, except for the archives. Closer inspection, however, shows that it has substantial value as a current reference book, containing as it does somewhere in its pages the pros and cons of practically every argument and opinion, sensible or silly, that is ever mentioned when this subject is discussed; all delegates to any future conference should be made to read this report in full before they are admitted. It is made up in part of extracts from the Preliminary Report prepared before the conference by Dr. Thérèse Grivet, which gave a wide review of current practice with its multiplicity of variations; and attached thereto, chapter by chapter, the discussion at the conference is given practically verbatim. The presentation thus maintains considerably more regularity than did some of the delegates in their contributions, and in one or two of the chapters the contrast between the objective analysis of the Preliminary Report and the dogmatism and irrelevance of the discussion is rather marked. The editing and layout are admirable, and there is a detailed index to all the subjects, authorities and journals mentioned at the conference, including also the name of every speaker.

It cannot truthfully be said that the conference accomplished a great deal, nor that the opinions expressed there were much more than the personal opinions, often contradictory, of so many individuals. The fact is that the problems of science abstracting are rather intractable, and cannot be solved by conferences of this sort, however valuable they may be for gathering opinions. Real progress can only come from the abstracting journals themselves in the long run, and extensive operational research would seem to be the most reliable guide for them in their generally sincere endeavours to serve the scientific community. B. M. CROWTHER

Reports on progress of physics, Vol. XIV, 1951. Edited by A. C. STICKLAND. (London: The Physical Society.) Pp. 411. Price 50*s*.

The present volume consists of eleven contributions. Each of these, following the practice of recent years, comprises a table of contents, an abstract of the report, the report itself and a comprehensive table of references, covering work done in the last few decades. A good deal of compression has been inevitable, which makes for some unevenness in writing and, for the non-specialist, not easy reading. The printing and reproduction of photographs and diagrams follow the high standard set in these reports. In the preface it is stated that it is proposed to publish next year an index of authors and subject matter for Volumes I–XV. This will add considerably to the usefulness of this valuable series of publications. The reports are summarized briefly below.

"Recent advances in ultra-violet absorption spectroscopy" (W. C. Price, King's College, London). This gives a summary, over the last twenty years, of progress in design and construction of equipment and development of technique.

"Anomalous fine structure of hydrogen and singly ionized helium" (W. E. Lamb, Jr., Columbia University). In this report an account is given of the fine structure of the levels $n = 2$ for hydrogen and singly-ionized helium both from the theoretical and experimental aspect. Reference is made to the use of micro-wave methods in which the author and his collaborators have been concerned. The object of the work described was to reveal deviations from the predictions made on the basis of Dirac's theory of these atoms.

"New techniques in optical interferometry" (H. Kuhn, Clarendon Laboratory, Oxford). This is an account of the optical properties of thin films, interference and polarization filters and some new developments in the methods of using Fabry–Pérot etalons. Wavelength standards pure isotope light sources and gauge-testing methods are considered, and a description of the "wave-front shearing interferometer" follows. The various forms of the method of using the multiple beam interference fringes are described and their applications indicated. The report concludes with a description of recent modifications of the methods of interferometry to study gas flow at high speed and recent designs of interference microscopes.

"The diffraction theory of aberrations" (E. Wolf, University of Edinburgh). This report contains a short account of the geometrical treatment of aberrations followed by a brief review of the historic development of the diffraction theory of aberrations. Then follows a fuller account of advances in the theory since 1940. The report is illustrated by numerous isophote diagrams and photographs.

"Spectrum of the airglow and the aurora" (A. B. Meinel, University of Chicago). A discussion of the spectrum of the airglow, twilight glow and aurora and the determination of the heights and temperatures associated with these emissions. A number of outstanding problems are briefly mentioned.

"The microphysics of clouds" (B. J. Mason and F. H. Ludlam, Imperial College). Recent work concerning the microphysical processes connected with cloud formation and precipitation is discussed under the heads: growth of droplets in clouds and fog; ice formation; growth of ice particles and development of precipitation. The report concludes with an account of some of the problems whose solution is urgently desired.

"Angular correlations in nuclear reactions" (M. Deutsch, Massachusetts Institute of Technology). This deals mainly with experiments designed to study nuclear energy states and gives a broad view of the physical problems and experimental methods involved. It discusses the basic physical processes under such heads as conservation of linear momentum, and the laws of interaction between nuclei and emitted or absorbed rays.

"The nuclear interactions of cosmic rays" (G. D. Rochester and W. G. V. Rosser, University of Manchester). The following topics form the main subdivisions of this report: types of nuclear interaction; transition effects of the nucleonic and nuclear components; attenuation of high energy nucleons in the atmosphere and the nucleonic components in the atmosphere and their correlations. Data have been collected for evaporation stars and the recent work on heavy unstable particles discussed. In conclusion, the authors remark on the rapid accumulation of empirical knowledge and the comparative backwardness in the discovery of the basic theoretical principles. They discuss, briefly, the regions in which clarification is beginning to appear and those in which no clear picture has yet emerged, e.g. the mechanism of meson formation and how this is connected with star size.

"Nuclear effects in atomic spectra" (E. W. Foster).

This report is concerned with the results of investigation of hyperfine structure, particularly for isotopes. Recent work on nuclear mass effect in helium is described. Isotope shifts in spectra of heavy elements is dealt with in some detail and a brief description of some magnetic hyperfine structure investigations given. Effects due to finite distribution of nuclear charge and of nuclear magnetic moment are discussed.

"A critical survey of ionospheric temperatures" (N. C. Gerson, Air Force Research Laboratories, Massachusetts). This is an analysis aiming to review and explore the methods of deducing temperatures from ionospheric parameters. In the course of the analysis the author realized that certain deficiencies of theory and experiment must be made good if notable advances are to be made in this field. Among these is the removal of discrepancies between temperatures deduced from aurora band spectra and from other data, lack of knowledge concerning electron collisions with atomic oxygen and various ions, determination of the recombination coefficient at low pressure and its dependence on temperature.

"Some applications of nuclear physics in medicine" (W. V. Mayneord, Department of Physics, Royal Cancer Hospital, London). The main applications lie in the use of artificial radioactive materials and of beams of high energy particles provided by cyclotrons, etc. The social consequences, arising from the development of atomic piles and the danger of atomic warfare, raise problems which urgently require solution. A description of the manufacture of radioactive isotopes is given and a discussion of the use of radioactive phosphorus, iodine, iron and sodium is given. The questions of dosage and the use of high energy quanta and particles and the discussion of protection concludes the volume. J. F. Wood

Fundamentals of automatic control. By G. H. Farrington. (London: Chapman and Hall Ltd.) Pp. xii + 285. Price 30*s.* net.

It is very satisfying that there is now available a book presenting a comprehensive account of the theory of automatic process control. An awkward decision faces any author bold enough to tackle the task, successfully accomplished by Mr. Farrington. He may assume some knowledge of his subject in his readers and restrict his appeal to specialists, or he may start from the beginning. Mr. Farrington has chosen the latter and more difficult course and achieves his purpose with commendable success.

The book deals basically with process control in which field Mr. Farrington's experience is clearly wide, but at appropriate points it makes contact with a wider field embracing electro-mechanical systems. A clear statement of definitions is given in the opening chapters and the reader is referred to "the textbooks" when this is appropriate. Unfortunately for the beginner, however, the textbooks are not specified clearly enough for ready reference to be possible.

The three basic control functions of proportional, derivative and integral are introduced and their effect in combination analysed in terms of polar diagrams for typical process system equations. The utility of electrical analogues in this connexion is pointed out and later a comprehensive example illustrates the precautions and approximations that the use of these analogies involve. The polar diagram method is generalized and use is made in design of a conformal grid of constant frequency and constant damping characteristics applying to the controlled process. The various influences affecting the system are distinguished for the purpose of analysing the system's reaction to them. The treatment of distributed parameter systems and distance-velocity lag effects is to be particularly welcomed.

In all aspects, the work is adequately illustrated by numerical examples which demonstrate Mr. Farrington's facility with his chosen methods of analysis. A brief chapter on multiple control shows how these methods may be extended to systems complicated by containing inner loops. The methods proposed do not appear to be so well suited here as in the more extensively treated single loop case.

During the course of the concluding chapters Mr. Farrington sets down some of his practical conclusions on process system analysis and for the specialist these are the most valuable chapters of the book; Mr. Farrington is clearly more at home on this ground and succeeds most admirably in conveying the importance of matching analysis to the problem. J. H. Westcott

Surface chemistry. By A. E. Alexander. (London: Longmans, Green and Co.) Pp. 70. Price 7*s.* 6*d.*

This little book is intended as a short and elementary treatment of surface chemistry. After an interesting historical survey it discusses the nature of surface films at the air-water and oil-water interface, and the adsorption behaviour at the solid-gas, solid-liquid interface. The final chapter deals with electrical phenomena at interfaces. Apart from a slightly irritating habit of inserting quite important explanations in parentheses, the book is well written and very readable and refers whenever possible to practical applications such as foams, emulsions, lubrication, gas masks and germicides. Professor Alexander, whose own work in colloid science is well known, has packed a surprising amount into seventy pages, and the greater part of the book will be perfectly clear to readers with an elementary knowledge of science. One or two sections, however, e.g. the Gibbs equation, presuppose a rather deeper knowledge of physical chemistry. On the whole, however, this booklet provides a very useful introduction to the subject of surface chemistry. D. Tabor

A practical manual of rubber hardness testing. By A. L. Soden. (London: Maclaren and Sons, Ltd.) Pp. 49. Price 6*s.* 6*d.* net.

Hardness in rubber means resistance to indentation and one might imagine its measurement would be a simple matter, but in fact no other property of rubber has been responsible for the development of such a large and confusing variety of tests. The author of this handbook is a member of the staff of the Research Association of British Rubber Manufacturers, whose present director, Dr. J. R. Scott, has made many contributions to the study of rubber hardness.

Mr. Soden has accomplished very ably his purpose in bringing together the practical details of the various tests and has dealt adequately with the good and bad features of each one in turn. The short section on simple theory might with advantage have been amplified, and it might have been pointed out that the value of the equations relating indentation to stress and Young's modulus rests solely on the fact that reasonably empirical agreement can be obtained only over restricted ranges. Further, it should be noted that the usual definition of Young's modulus is not strictly applicable to rubber because of its non-linear stress-strain relation. Some reference to these matters could well have been included if only to indicate the scope of the work that remains to be done in the fundamentals of the subject. D. Parkinson

Notes and comments

Notes on the preparation of papers

A revised and enlarged edition of the booklet *Notes on the preparation of contributions to the Institute's journals and other publications* is now available. These notes, first issued in 1931, are intended to assist less experienced authors and to serve as a reference book for all who contribute to the Institute's publications. Apart from the special information concerning these publications the notes deal with the preparation, length and cost of publishing papers, the form of script and diagrams required, the setting out of tables and mathematics, and the correction of proofs. A short bibliography of dictionaries and books on writing is included. The appendix contains notes and examples of spellings, symbols and abbreviations, the Greek alphabet (so often unrecognizably written in scripts) and printers' marks for correcting proofs.

In these days of mounting costs it is good to see authors reminded (p. 6) that the cost of a page of this *Journal* is as much as £10, that a typical minor change to a line of type once it is set may be 5*s*. or more and that even such a simple matter as removing a comma costs about 1*s*. 6*d*.

Readers who have earlier editions of these *Notes* are invited to obtain a copy of the new one, since a number of small variations in acceptable spellings and abbreviations, etc., have been made to conform more with new international and other agreements.

Copies of the booklet may be obtained from The Institute of Physics, 47 Belgrave Square, London, S.W.1, price 2*s*. 6*d*. Orders should be accompanied by remittance.

Argentinian publications on nuclear physics

We have received the first two issues of a new series of booklets published by the University of Buenos Aires. They are: *Sobre a teoria das forcas nucleares*, by José Leite Lopes (58 pages), and *Neutrones y positrones*, by Earnesto E. Galloni (88 pages).

Proposed school in electron microscopy

If there is sufficient demand, The Electron Microscopy Group of The Institute of Physics will again hold a school in the principles and practice of electron microscopy. It would comprise lectures, demonstrations and practical work covering the basic theory of the electron microscope and its various accessory techniques, and would be intended primarily for beginners. Opportunities would be arranged for operating and noting the characteristics of several types of instrument.

It is hoped to hold the school at the University of Leeds either this year or early next year, and that accommodation will be found in university hostels. The estimated cost of a two weeks' course, excluding accommodation and travelling expenses, is of the order of £15.

Readers who are interested should inform Dr. R. Reed, Acting Honorary Secretary of The Electron Microscopy Group of The Institute of Physics, Department of Leather Industries, The University, Leeds 2.

Counter spectrometers for the investigation of Debye–Scherrer patterns

The Equipment Sub-Committee of The X-Ray Analysis Group of The Institute of Physics announces that a memorandum comprising notes on the design of counter spectrometers for the investigation of Debye–Scherrer patterns has been prepared for the powder camera and Geiger–Müller counter spectrometer panel. Copies may be obtained (free of charge) from The Institute of Physics, 47 Belgrave Square, London, S.W.1.

Science of light

We have received the first two issues of a new journal entitled *Science of light* which contains reports of the Institute for Optical Research, Tokyo University of Education, 400, 4-chome, Hyakunin-machi, Shinjuku-ku, Tokyo, Japan, and other contributions on suitable subjects. The papers are written in Japanese with English abstracts.

These two issues contain 116 pages and comprise the first volume. In the future volumes the papers will be written in English.

Erratum

In the paper *The modulation characteristic of cathode-ray tubes in television*, by R. B. Mackenzie, published in the February issue, the legends to Figs. 5 and 6 should be transposed.

Journal of Scientific Instruments

Contents of the March issue

ORIGINAL CONTRIBUTIONS

A design for standard resistance coils. By C. R. Barber, A. Gridley and J. A. Hall.
A single channel pulse amplitude analyser for measurement of coincident pulses. By R. Wilson.
Single response thickness-shear mode resonators using circular bevelled plates. By R. Bechmann.
An instrument to measure and compute the mean and standard deviation of the oscillations of a recording arm. By B. Hogley.
A monitor for measuring X-ray beam intensities. By C. M. Hargreaves, E. Prince and W. A. Wooster.
Capillary depression in mercury barometers and manometers. By F. A. Gould and T. Vickers.
Toroidal Geiger counters. By N. G. Trott.
A magnetic thickness gauge of new design. By E. G. Harrison.
A servo-controlled constant-stress rheometer. By E. N. Thrower.
Magnetic focusing with a prolate spheroidal field—details of a β-spectrometer and magnet. By H. O. W. Richardson.

LABORATORY AND WORKSHOP NOTES

A modified thermostatic controller. By E. D. Lacy.
Prevention of excessive supercooling in cryoscopic determinations. By D. C. Spanner.
Cathetometer motion. By O. Kantorowicz and C. W. Couling.
A simple method of observing the constancy of a current. By G. H. F. Seiflow.
Radiography of fabric in tyres. By E. Hughes.
A constant stress creep test apparatus. By A. Latin.
Glassblower's knife. By C. Kantorowicz.

CORRESPONDENCE

Behaviour of platinum/platinum-rhodium thermocouples at high temperatures. From H. J. Svec.
Indicator for non-luminous flames. From W. Summer: C. Atkins and F. A. Lytton.

MANUFACTURERS' PUBLICATIONS

NEW INSTRUMENTS, MATERIALS AND TOOLS

NEW BOOKS

NOTES AND COMMENTS

British Journal of Applied Physics

Original contributions accepted for publication in future issues of this Journal

A method of studying the formation of cracks in a material subjected to stress. By R. Jones.
The atomization of liquid in a flat spray. By R. G. Dorman.
The viscosity of suspensions of rigid spheres. By R. Roscoe.
A method for the electron and light optical microscopic examination of identical areas. By E. D. Hyam and J. Nutting.
The rheology of plastic dispersions. By P. A. Briscoe, W. J. Dunning and R. C. Seymour.
The saturation curve at high ionization intensity. By J. W. Boag and T. Wilson.
An improved apparatus for the differential thermal analysis of minerals. By J. J. Theron.

THIS JOURNAL is produced monthly by The Institute of Physics, in London. It deals with all branches of applied physics (including theory and technique). All rights reserved. Responsibility for the statements contained herein attaches only to the writers.

EDITORIAL MATTER. Communications concerning editorial matter should be addressed to the Editor, The Institute of Physics, 47 Belgrave Square, London, S.W.1. (*Telephone:* Sloane 9806.) Prospective authors are invited to prepare their scripts in accordance with the *Notes on the Preparation of Contributions*. (Price 2*s*. 6*d*. including postage.)

ADVERTISEMENTS. Communications concerning advertisements should be addressed to the agents, Messrs. Walter Judd Ltd., 47 Gresham Street, London, E.C.2. (*Telephone:* Monarch 7644.)

SUBSCRIPTION RATES. A new volume commences each January, and annual subscriptions will only be accepted for complete volumes of the monthly parts (January–December). The charge is £4 per volume ($11.50 U.S.A.), including index (post paid), payable in advance. Single parts, so far as available, may be purchased at 8*s*. each ($1.15 U.S.A.), post paid, cash with order. Orders should be sent to The Institute of Physics, 47 Belgrave Square, London, S.W.1, or to any Bookseller.

SPECIAL REPORT

Summarized proceedings of a conference on stress analysis Liverpool, 1951

The Fifth Annual Conference of the Stress Analysis Group of The Institute of Physics was held in the Mechanical Engineering Department of the University of Liverpool on 4–6 April 1951. Nine papers, dealing with numerical methods, electric resistance strain gauge methods, developments in France, fatigue and photoelastic work, were read, and are summarized in this report.

RELAXATION METHODS

The opening lecture of the conference was delivered by PROFESSOR D. G. CHRISTOPHERSON (University of Leeds) on "Numerical methods in stress analysis, with special reference to the relaxation method."* He outlined the manner in which the application of numerical methods to problems of stress analysis has been approached from two quite different directions. On the one hand, the mathematicians faced with insoluble differential equations have sought for rapid means of finding an approximate solution, on the other the engineer concerned in the first place usually with complicated frameworks has rejected the traditional apparatus of analysis and has sought for assistance in processes of computation in which engineering imagination or intuition could play as large a part as mathematical ability. The speaker then turned to a more detailed consideration of relaxation solutions of problems encountered in the computation of stresses. His paper is being published separately.

FORCES IN POWER LOOMS

MR. R. G. WOLFENDEN (British Cotton Industry Research Association, Shirley Institute, Manchester) read a paper on: "The use of electric resistance strain gauges for the measurement of transient forces in power looms." Most of the problems with which this speaker is concerned involve the determination of the magnitude of forces in certain directions, rather than the determination of stress patterns or of the directions of the principal axes. The forces under consideration are transients lasting from $\frac{1}{20}$ to $\frac{1}{100}$ of a second and repeating every half second. On the other hand, there are some forces which are virtually steady, having a periodicity of about half a second. The forces occurring during the weaving process do not repeat to an accuracy better than about 5–10%, which made 5% the accuracy aimed at in this work.

The speaker described some of the equipment which had been used in this work. The force-time curves were displayed on the screen of a cathode-ray oscillograph (type E800 by Mullard Ltd.), photography of the traces being done by a home-made fixed focus camera on Kodak R.55 recording film. As transients of much less than $\frac{1}{100}$ sec were of no importance the oscillator frequency was chosen to be about 2 200 c/s. The oscillator circuit is shown in Fig. 1. The oscillating valve is a pentode, whose anode is connected back to the grid by a three-stage phase-shift C/R network. A portion of this output is fed from a 500 kΩ potentiometer between anode and earth, on to the grid of a triode whose anode load is a step-down transformer. Such an oscillator works only very feebly, if at all, due to the high attenuation of the C/R circuits. However, the system may be made to oscillate very strongly and with very little distortion by placing a choke of 80 H in the cathode lead. The choke seems to provide cathode coupling between the two valves sufficiently strong to maintain a healthy oscillation at a frequency determined by the constants of the C/R network. Unfortunately, the oscillator is fairly sensitive to supply voltage and will not oscillate when this is less than 350 V, though between 370 and 400 V it gives a satisfactory output which is manually controlled by the potentiometer and indicated by means of the rectifying diode and the microammeter.

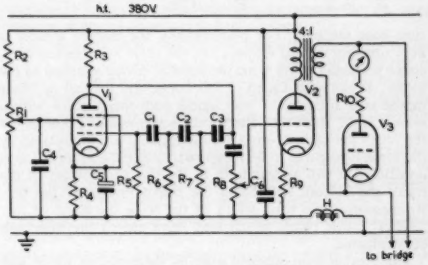

Fig. 1. Oscillator circuit used with resistance strain gauge for the measurement of transient forces

$R_1 = 70$ kΩ, $R_2 = 43$ kΩ, $R_3 = 68$ kΩ, $R_4 = 1$ kΩ, $R_5 = 330$ kΩ, $R_6 = 330$ kΩ, $R_7 = 330$ kΩ, $R_8 = 500$ kΩ, $R_9 = 1$ kΩ, $R_{10} = 10$ kΩ, $C_1 = 60$ μμF, $C_2 = 60$ μμF, $C_3 = 60$ μμF, $C_4 = 1$ μF, $C_5 = 50$ μF, $C_6 = 1$ μF, $V_1 = 6J7$, $V_2 = 6J5$, $V_3 = EA50$, $H = 80$ H

As it was difficult to deal with distortions of wave-form by oscillator design an *m*-derived filter was placed after the bridge. This filter was designed to act as a rejector circuit for the second harmonic which was almost completely eliminated. Another advantage of using such a filter was that if it was placed after the preamplifying valve it removed the noise produced in this valve. Considerable care had to be taken to match the input and output impedances of the filter. For a frequency of 2 000 c/s, the impedance must be about 1 000 Ω, but such a resistance is not suitable as the load of an amplifying pentode and the filter must therefore be preceded by a cathode follower as shown in Fig. 2. This is an impedance changing device which presents to the filter an input of $1/g_m$ of the valve, that is about 400 Ω, while the valve appears to the preamplifier as a very high impedance, about 7 MΩ in our particular example.

The speaker mentioned that due to the vibration and noise in a weaving shed the preamplifying valve had to be seismically and acoustically shielded. This was done by suspending it by four rubber bands inside a box lined with cotton wool. The leads to the valve holder were coils of very fine wire.

The cathode-ray oscillograph has electronic provision for most of the work to be done. When two external contacts operated by the loom are closed and kept closed the spot will make a single sweep of the screen at a speed determined by the

* Published in the March issue of this JOURNAL.

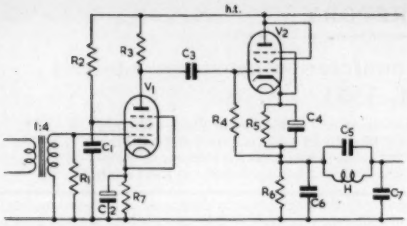

Fig. 2. Amplifier (*left*) and cathode follower and *m*-derived filter placed after bridge used with resistance strain gauge

$R_1 = 25\ k\Omega$ w.w. $C_1 = 0{\cdot}5\ \mu F$ $V_1 = EF37A$
$R_2 = 168\ k\Omega$ $C_2 = 50\ \mu F$ $V_2 = 6J7$
$R_3 = 60\ k\Omega$ w.w. $C_3 = 0{\cdot}1\ \mu F$
$R_4 = 680\ k\Omega$ $C_4 = 50\ \mu F$ $H = 16{\cdot}5$ mH
$R_5 = 1\ k\Omega$ $C_5 = 0{\cdot}079\ \mu F$
$R_6 = 10\ k\Omega$ $C_6 = 0{\cdot}13\ \mu F$
$R_7 = 500\ \Omega$ w.w. $C_7 = 0{\cdot}13\ \mu F$

time-base settings. For photography the camera shutter is kept open for several seconds and the beam suppression used, either manually or by some mechanical device attached to the loom. It has been found in this connexion that an ordinary mouse-trap provides a very good high-speed relay which, once it is on, stays on. Electrical oscillations of 2 000 c/s are fed on to the cathode-ray oscillograph and are modulated by the force-time curve to be measured. Since the modulation is unrectified it will appear both at the top and bottom of the trace, the bottom half being the mirror image of the top. By measuring the total width of the trace the effect of any residual mains ripple which may have passed the filter will be eliminated.

The speaker then outlined some of the problems which had been studied with the aid of this apparatus. In a loom the weft is contained in a package in a shuttle weighing about 12 oz. The shuttle is projected or picked across the warp to lay a weft thread by means of a wooden or metal bar, called the picking stick. It is about 3 ft long, $1\frac{1}{2}$ in wide and $\frac{3}{4}$ in thick, and usually tapered in both directions. Though there are several types of picking mechanism possible, Fig. 3 shows the principle involved. The picking mechanism is virtually a bell crank lever with the picking stick forming the longer arm and the shorter arm carrying the cam follower.

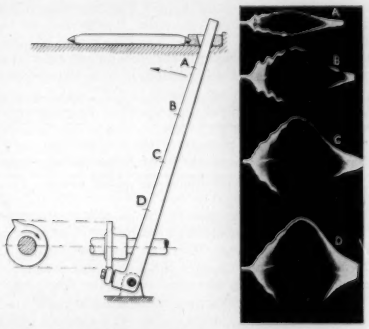

Fig. 3. (*Left*) "Picking" mechanism used in weaving. (*Right*) Strain gauge records corresponding to the points marked *A*, *B*, *C*, *D*

The cam is fixed on one of the main loom shafts. This causes the bar to move forward in its turn to project the shuttle across the loom. The acceleration of the shuttle considerably exceeds 50*g*, which makes the effective mass something between 50 and 100 lb. The aim of the work carried out is to reduce the forces and accelerations of picking so as to be able to reduce the bulk of the mechanism and hence the wear on the parts and the power wasted. One of the steps in this direction is to lighten the picking stick by a suitable design of its shape. Work has been carried out on this problem at the Shirley Institute by placing 1 000 Ω wire resistance gauges (by H. Tinsley and Co. Ltd.) on the side of the stick and connected in series so as to eliminate the bending of the stick in a direction at right angles to the plane of its movement. The traces shown in the right-hand half of Fig. 3 indicate that the section of the picking stick under investigation could be considerably reduced near the top.

Mr. Wolfenden also discussed the problem involved in stopping the shuttle at the end of its travel and the necessity to design an accelerometer which could be carried in the shuttle and which would be capable of withstanding accidental accelerations of up to 1 000*g* while giving a full-scale deflexion for about 500*g* at full sensitivity. An instrument designed to deal with this problem was described. It consists of a mass supported on a cantilever. The deflexion of the cantilever is effectively measured by two small woven resistance strain gauges stuck to each side of the cantilever. The main difficulties encountered with this instrument were the provision of adequate damping and the set-up required for the calibration of the accelerometer.

BRITTLE LACQUERS

Monsieur H. de Leiris (French Naval Research Laboratories) read a paper entitled: "Development of very short gauge-length strain gauge and brittle lacquer techniques in France." M. de Leiris dealt with brittle lacquers first, and distinguished between two techniques, the fusion technique in which the coating is melted and applied hot, and the dissolving technique in which the application to the specimen is carried out cold in the dissolved state. The fusion technique is typified by Dietrich's[1] procedure. In it the base of the brittle coating is unprocessed resin of the purest quality (so-called crystals). In this state the resin is insufficiently brittle and homogeneous. It has therefore to be subjected to prolonged heating in a suitable iron container. The specimen is flame heated to about 80° C and rubbed with a stick of treated resin, so as to obtain a film of 0·1–0·2 mm thickness. When the temperature drops to about 28–30° C the coating is both sufficiently fragile and subjected to contraction stresses capable of causing consistent cracks when small additional strains are caused in the coating.

By treating the raw resin in accordance with a technique developed by Marcel Jean, coatings can be obtained which are particularly consistent as regards spontaneous cracking. The procedure is as follows:

A definite quantity of ferric ammonium sulphate is dissolved in water and then precipitated by means of ammonia. The ferric hydroxide is filtered, well washed in boiling water and incompletely dried at between 30–40° C. Still wet, it is placed in a retort with 100 g of the unprocessed resin and 1 g of sodium peroxide which acts as a catalyst. It is then distilled at a pressure of 30–50 mm of mercury. Under these conditions the temperature of the vapour is easily maintained between 130–150° C. The results obtained with this technique are very nearly independent of factors other than the proportion of iron which has been incorporated. More especially,

the initial condition of the unprocessed resin is unimportant and the same can be said within wide limits of the duration of the treatment. At the usual prevailing temperatures it is advisable to use from 5–10 g ferric ammonium alum for every 200 g of unprocessed resin. It is as well to raise the temperature of the specimen above that suggested by Dietrich to about 120° C and to preheat the stick of lacquer to about 35–40° C to prevent breakage. If a flame is used to spread the lacquer evenly on the specimen, it is important to avoid any overheating which might lead to the formation of resinous oils. Load should only be applied to the specimen after the viscosity of the coating is sufficiently low, i.e. about 40° C. The cracks are easily visible by observation at an angle.

The dissolving technique has been described more frequently than the fusion technique and is better known in this country.[2,3,4,5,6] Details of this method may be found in a paper by C. W. Smith.[4] With this technique cracks can only be produced if the coating has become sufficiently dry. Atmospheric drying has only proved adequate when there has been no change in atmospheric conditions during the drying process, and if the conditions are those for which the coating has been chosen. If the humidity is too high the coating will not crack, and if it is too low, crazy cracking will be caused. For this reason some authors[6] are in favour of drying the coating in an oven. If cracks do not appear when the specimen is loaded, either because the stresses are too small or the coating is insufficiently brittle, the appearance of cracks can be accelerated by cooling. Once the crack pattern has formed it can be observed or photographed as in the fusion technique. Nevertheless, it has proved helpful to use a dye etching agent which both enlarges and tints the cracks.

It is clear that the ways in which the cracks are formed are very similar with both methods of application. In either case the contraction of the coating and the stresses (assumed to be uniform) which are due to it, play a dominant part in the formation of the pattern. This is proved not only by the appearance of crazy cracking in both techniques, when the contraction stresses are too large before application of load to the specimen, but also for the dissolving technique by the possibility of using cooling to bring out a pattern. Without this contraction it would not be possible for the pattern to remain visible once the load on the specimen has been removed. It follows that if the temperature distribution in the specimen is not uniform the distribution of the contraction stresses in the coating may be modified and the controlling effect of the deformations at the surface of the specimen may be more or less affected. If, however, it is possible to eliminate all such temperature variations it has been established that the crack pattern is an effective reproduction of the isostatic pattern.

If reliable quantitative results are to be obtained by such methods two conditions must be fulfilled: the results must be reproducible with an unequivocal correspondence between cause and effect and, secondly, the laws of cracking of the coating must be clearly established. The reproducibility of the crack pattern need only be ensured with regard to the criterion which is taken as a basis for comparing the results obtained. Such criteria are the crack density, the appearance of the first crack and the length of the cracks.

M. de Leiris continued by saying that, generally, a greater crack density corresponds to a greater strain in the specimen. The converse is not true because of a saturation phenomenon described by Smith[4] which limits the minimum distance between cracks to about five times the thickness of the coating. The existence of contraction stresses in the coating is the main factor to be considered compared with which the strains in the specimen represent, after all, only the straw which breaks the camel's back. The density of the cracks will be influenced mainly by local faults in the coating or by any superficial action on the coating such as pressure, friction or cold air currents. Crack density will not therefore furnish a satisfactory criterion.

M. de Leiris said that previous remarks on the accidental initiation of cracks apply also to the appearance of the first crack. The scatter of the results is such that it is impossible to hope for a statistical interpretation of the results as it is impracticable to carry out the required number of tests. The appearance of the first crack must therefore also be abandoned as a criterion.

American authors[7] have suggested that for each step of loading the length of each crack be determined. A pattern of isoentatics is thus sketched which defines the propagation of the cracks with increasing load. Here, the disturbing influence of fortuitous circumstances can, in principle, be considered to have been allowed for statistically by the large number of cracks considered simultaneously.

On the other hand, this method infers that the propagation of any crack is gradual, and that the length of the crack is limited by the conditions existing in the region of the coating into which its extremity has penetrated. It appears that this can be assumed to be correct for a coating obtained by the dissolving technique. It is not true for coatings obtained by the fusion technique. In this type of coating the cracks appear by a mechanism which is similar to brittle failure. Each of the cracks tears off at one of its ends and spreads instantaneously to the other, without any increase of load on the specimen. In so doing the crack may propagate across regions where the surface stresses in the specimen are appreciably smaller than those at the point where the tearing began. This difference of behaviour appears to be related to the existence of more or less regularly distributed bubbles in the lacquer. These may cause initiation of cracks due to the local stress concentrations.

The pattern of the isoentatics appears therefore in the lacquer technique to be sufficiently reproducible to render the method quantitative. It still remains to state the laws of cracking clearly. With reference to the cracking of brittle materials, the criteria of breakdown which first spring to mind are those of maximum stress or maximum strain. This was also the view of Dietrich and Lehr in their original paper.[1] This criterion has certain advantages: firstly, the calibration of the coating can be carried out on a simple specimen, for instance, a prismatic beam in bending; secondly, since the contraction of the coating imposes a definite strain on the lacquer it follows that with this criterion, it is easy to take the effect of temperature into account. In view of the fact, however, that the initiation of a crack corresponds to a separation of its sides, there are reasons to think that the existence of tension stresses in the coating is still needed independently of the strain in order that cracking may take place. It is true that the contraction itself creates such tension stresses, but these are, by definition, insufficient to cause cracking by themselves (provided crazing is not taking place). It is very difficult to imagine how the appearance of a crack can be explained unless the additional system of stresses which has been induced in the coating by the application of the load to the specimen includes at least one principal tension stress.

M. de Leiris said that Durelli and de Wolf[7] appear to have been the first to recognize this fact and to attempt to interpret it. If the coating and the specimen have the same

Poisson's ratio then the stress systems which produce a given strain in the specimen and the coating will be in the ratio of the Young's moduli of the two materials. The Poisson's ratios of lacquer coatings are not well known but probably lie in the region between 0·4 and 0·5 as compared with approximately 0·3 for steel and up to 0·35 for other metallic materials. It follows, therefore, that the stress systems in the coating and in the specimen cannot be similar because each principal stress in the coating depends on the two principal stresses in the specimen.

If A_s and B_s are the two principal stresses in the specimen, and A_r and B_r are the two principal stresses in the coating, and E_s, E_r, σ_s, σ_r, are the elastic constants, then the equality of strain imposed by the adhesion of the coating to the specimen leads to the following relations:

$$A_r = \frac{E_r}{(1-\sigma_r^2)E_s}[A_s(1-\sigma_r\sigma_s) - B_s(\sigma_s - \sigma_r)]$$

$$B_r = \frac{E_r}{(1-\sigma_r^2)E_s}[B_s(1-\sigma_r\sigma_s) - A_s(\sigma_s - \sigma_r)]$$

Then assuming

$$\sigma_r = 0{\cdot}5 \text{ and } \sigma_s = 0{\cdot}3$$

put

$$A_r = \frac{E_r}{(1-\sigma_r^2)E_s}a \text{ and } B_r = \frac{E_r}{(1-\sigma_r^2)E_s}b$$

hence

$$a = 0{\cdot}85A_s + 0{\cdot}2B_s$$
$$b = 0{\cdot}85B_s + 0{\cdot}2A_s$$

Fig. 4 shows how a and b vary as functions of A_s and B_s. If A_s is the maximum principal stress, the section of the curves to be considered is for a that which is to the left of the

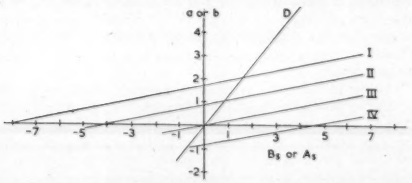

Fig. 4. Stresses in brittle lacquer coating as a function of those in the specimen: $\sigma_r = 0{\cdot}5$, $\sigma_s = 0{\cdot}3$

Line	A_s or B_s
I	2
II	1
III	0
IV	−1

straight line D, and for b that which is to the right. If B_s is a compression and A_s a tension, and if the ratio B_s/A_s is larger than 4·25, both the principal stresses in the coating are compressive. In this case it will not be possible to cause cracking by mechanical means even if the tension A_s has

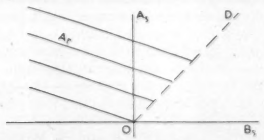

Fig. 5. Curves of equal stress in the lacquer coating: $\sigma_r = 0{\cdot}5$, $\sigma_s = 0{\cdot}3$, $A_s > B_s$

very large values (B_s increasing correspondingly). The question arises whether this should be interpreted as meaning that a criterion for cracking should be taken as the maximum value of the strain induced in the coating. This would lead to a linear relationship between the critical values for A_s and B_s shown in Fig. 5. From the scatter of the results it does not appear that such an equation can be justified. This is at least the opinion of Durelli and de Wolf, who propose the following empirical formula:

$$(\sigma_r - \sigma_s)\left(\frac{A_s}{T_s}\right)\left(\frac{B_s}{T_s}\right)^2 + \frac{A_s}{T_s} = 1$$

where T_s is a critical value of stress in a specimen subjected to simple tension.

Fig. 6 shows this empirical law and compares it with the other two criteria. It is interesting to note that the criterion

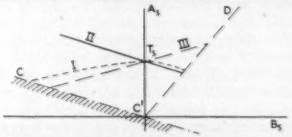

Fig. 6. Comparison of Durelli and de Wolf's results (Curve I) with that for the maximum stress (Curve II) and the maximum strains (Curve III): $\sigma_r = 0{\cdot}5$, $\sigma_s = 0{\cdot}3$, $A_s > B_s$; CC' coating in compression

of maximum stress fits in well enough with the empirical law as long as A_s and B_s are of the same sign. The position is entirely reversed with the criterion of maximum strain. It seems clear that the laws of cracking cannot be expressed simply in terms of the stresses in the specimen. Consequently, even if reproducibility is assumed with regard to the selected criterion, the quantitative interpretation of such tests will be neither simple nor clear unless the loading is of the most elementary type. In principle, it will be necessary to determine the two systems of isostatics and to determine according to a simple law the critical values found for these two families of curves. If only an approximation is desired, and a simple criterion like that of maximum strain is chosen, it may lead to errors of 30–50%.

M. de Leiris finished this section by saying that it appeared, therefore, that if a stress analysis of great accuracy is to be carried out it is only possible to obtain a pattern of isostatics from the brittle coating techniques. This is, in itself, of great value since it reduces by one-third the number of strain measurements to be made, and more reliable results can be obtained from strain measurements when the strain gauge is more or less shear-sensitive.

THE PNEUMATIC GAUGE

M. de Leiris devoted the second half of his paper to the description of a static strain gauge of very short gauge length (2 mm) and great sensitiveness (magnification factor 200 000) which allows precise strain measurements to be made under very difficult conditions.

Fig. 7 gives an outline of the pneumatic gauge constructed on the Solex principle. A hydraulic indicator fed with compressed air through an intake A delivers air at a constant pressure of 125 g/cm². This air flows through an orifice B, of a few tenths of a millimetre in diameter, into an intermediary container C where the pressure is measured by means of a hydraulic manometer D. The air is then led

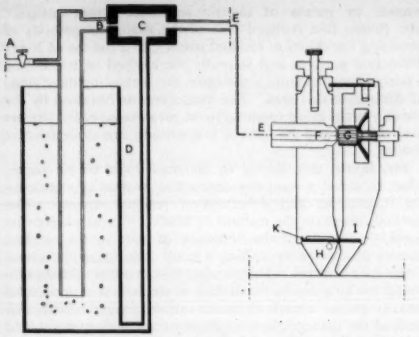

Fig. 7. Outline of pneumatic gauge constructed on Solex principle

through a rubber rube E to the escape jet F of the strain gauge proper. From this jet the air escapes into the space between its end and a plate E parallel to the plane of its opening. Under these conditions the pressure in the intermediary container provides a measure of this distance. The jet is built into the leg of the strain gauge which bears the fixed knife edge H, while the plate is attached to the moving knife edge I which is connected by a plate spring K to the fixed leg. The strain at the level of the jet is magnified mechanically in the ratio of 3 : 1 and from there it is transformed into a variation of pressure in the intermediary container.

Fig. 8 illustrates the strain gauge built on these principles. Its weight is 9 g and its total height is 32 mm. Its cross-section is 8 × 15½ mm, but the fact that it is cut away near the knife edges allows it to be used in very restricted spaces. The gauge is supplied with a locking device which is used when actual measurements are not being taken. The instrument is designed to be stable in itself, the length of the knife edges being 0·3 mm, which is not negligible in comparison with the gauge length of 2 mm. One leg of the gauge is pierced by a hole as low as possible; a small shaft 0·8 mm in diameter is passed through this hole and on its two projecting ends rest the Vees of a stirrup. A great number of arrangements to apply the holding force to the stirrup can be envisaged; one of these for use of the gauge in a restricted space is illustrated in Fig. 9. The spring above the connecting lever can be set so as to give the optimum holding force at the gauge which is between 1 and 1·5 kg, while the balancing reaction is taken up by the central suction pad.

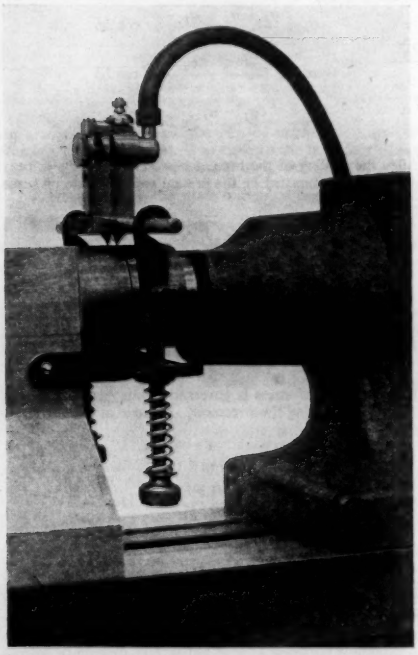

Fig. 8. Strain gauge built on pneumatic gauge principle illustrated in Fig. 7

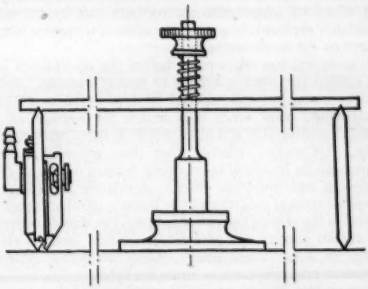

Fig. 9. Method of applying holding force to stirrup when using the gauge shown in Fig. 8, in a restricted space

As usual in Solex systems the calibration curve of the apparatus has a very long zone of inflexion, the central part of which is almost linear. This portion corresponds to a variation of pressure of 200 mm of water on the hydraulic indicator which has a range of 1 200 mm; it is possible to obtain a longer straight line characteristic by the use of a differential attachment.[11]

Tests are carried out on the linear portion of the calibration curve, the slope of which corresponds to a magnification of 200 000 when an orifice of 0·2 mm diameter is used. This means that in simple tension on steel a stress of 1 kg/mm² gives a variation of level on the indicator of 20 mm. The speaker summed up his opinion of this instrument by saying that if the precautions usual in precision measurements are taken[9] very well-defined stress curves are always obtained on which very small changes can be easily and clearly observed.

FATIGUE

Dr. D. G. Sopwith (Engineering Division, National Physical Laboratory) delivered a lecture on "Fatigue." Dr. Sopwith limited his remarks to those aspects of fatigue

of interest to the stress analyst and designer and did not refer the metallurgical aspects of this problem. He emphasized the importance of fatigue failures in practice, pointing out that in his experience of service failures 90% were due to fatigue, 9% due to impact and 1% due to other causes. The speaker, after dealing with some historical aspects of his subject, turned to a description of some of the machines used in investigating the endurance of specimens under repeated loading. He then discussed the correlation between the fatigue range of a material and its other mechanical properties. There is little or no correlation with the elastic limit or with yield or with the Izod impact value. The ultimate tensile strength (U.T.S.) shows the best correlation with the fatigue range. The ratio of the U.T.S. to the fatigue limit under reversed stress, known as the endurance ratio, has values lying within the range 0·35 to 0·65 for steels, decreasing somewhat as the U.T.S. increases, 0·3 to 0·45 for light alloys, 0·25 to 0·4 for copper alloys. Since hardness varies with the U.T.S. there is a good correlation between hardness and fatigue limit.

Dr. Sopwith then discussed the effects of various factors on the fatigue properties of a material. The effect of speed between a few hundred and ten thousand cycles per minute is negligible. This does not hold if other factors such as corrosion or high temperature are operative at the same time. The effects of temperature are complex and by no means completely explored; in general the effect is somewhat similar to that on the tensile strength.

If corrosion has taken place before the reversals of load are applied the effect is similar to that of notches. Simultaneous corrosion and reversal of load have a mutually accelerating action which may reduce the strength of the material considerably and often results in there being no safe range. Of surface effects, other than geometrical ones, plating can be beneficial in corrosion fatigue, as can be case-hardening and nitriding. When considering the effects of combined stresses the criteria to be borne in mind are generally similar to the criteria for elastic failure. For ductile materials the criteria adopted are generally maximum shear or strain energy or shear strain energy, while for brittle materials maximum principle stress or strain are taken.

Any sudden change of section produces local stress concentrations, which under static conditions with ductile materials would be relieved by yielding. In fatigue this does not occur to the same extent, particularly in materials which are "notch-sensitive." If the stress concentration factor is defined as the ratio of stress/nominal stress in the vicinity, the notch sensitivity can be defined as $(K-1)/(K_t-1)$ where K is the actual and K_t the theoretical stress concentration factor. Generally speaking, the harder the steel the more notch-sensitive it becomes. There is also a marked size effect on notch-sensitivity. Amongst the methods of relieving stress concentrations the following were mentioned: geometrical methods, improved finish, changes in design, work hardening, e.g. rolling wheel seats or oil holes, and favourable internal stresses.

Dr. Sopwith concluded his lecture by giving a number of examples of fatigue failures and discussing the way they had taken place and how they might have been avoided. He also threw out the suggestion that, as fatigue failures take place without preliminary deformation, this form of failure might sometimes be used to check stress analysis of complicated parts.

DETERMINATION OF RESIDUAL STRESSES

MR. R. G. BOITEN (Nijverheidsorganisatie T.N.O., Delft, Holland) read a paper on: "The determination of residual stresses by means of electric resistance strain gauges." Mr. Boiten first outlined two of the available methods of obtaining the values of residual stresses, first the use of X-ray diffraction patterns and secondly the method of trepanning a fairly large area from a specimen and measuring the change of stress over that area. The measurements obtained by the use of a strain gauge rosette give the mean value of the stresses over the area and the method is essentially one of destructive testing.

Mr. Boiten then turned to the main topic of his paper, what he called a semi-non-destructive method of obtaining the magnitudes and directions of residual stresses. The method, based on the method of Mathar[10] and adapted by Soete,[11] consists of the liberation of part of the residual stresses at a point by drilling a small hole (generally about 6 mm in diameter). The changes in the stress distribution round the hole due to the drilling of the hole is measured by radially placed electric resistance strain gauges. With this method the damage done to the structure is only slight and can be made good by plugging or welding. As the stresses are assumed to be uniform over a much smaller area in this method than in the trepanning method, high stress gradients, e.g. in the vicinity of welds, can be investigated by the former method.

Assuming a state of plane stress in the plate and referring to Fig. 10, where a is the radius of the hole, for a point (r, ϕ), where $(r < a)$:

$$\sigma_r = \frac{\sigma_1 + \sigma_2}{2} + \frac{\sigma_1 - \sigma_2}{2}\cos 2\phi$$

$$\sigma_t = \frac{\sigma_1 + \sigma_2}{2} - \frac{\sigma_1 - \sigma_2}{2}\cos 2\phi$$

$$\tau = -\frac{\sigma_1 - \sigma_2}{2}\sin 2\phi$$

After the drilling of the hole, a new state of stress appears which is superimposed on the present residual state of stress.

Fig. 10. Illustrating method of determining stresses by drilling a hole

This new state of stress is governed by an Airy stress function F', introducing the stresses σ'_r, σ'_t and τ' at each arbitrary point. Then:

$$\Delta'\Delta'F' = 0$$

$$\sigma'_r = \frac{1}{r}\frac{\partial F'}{\partial r} + \frac{1}{r^2}\frac{\partial^2 F}{\partial \phi^2}$$

$$\sigma'_t = \frac{\partial^2 F'}{\partial r^2} \text{ and } \tau' = \frac{1}{r^2}\frac{\partial F'}{\partial \phi} - \frac{1}{r}\frac{\partial^2 F'}{\partial r \partial \phi}$$

The solution of $\Delta'\Delta'F' = 0$ may be derived with the boundary conditions:

$$r = a \quad \sigma_r + \sigma'_r = 0$$
$$\tau + \tau' = 0$$

$$r \to \infty \quad \sigma'_r = \sigma'_t = \tau' = 0$$

Hence

$$F' = \frac{\sigma_1 + \sigma_2}{2} a^2 \log r + \frac{\sigma_1 - \sigma_2}{2} a^2 \left(1 - \frac{a^2}{2r^2}\right) \cos 2\phi$$

$$\sigma'_r = -\frac{\sigma_1 + \sigma_2}{2} \frac{a^2}{r^2} - \frac{\sigma_1 - \sigma_2}{2} \left(\frac{4a^2}{r^2} - \frac{3a^4}{r^4}\right) \cos 2\phi$$

$$\sigma'_t = \frac{\sigma_1 + \sigma_2}{2} \frac{a^2}{r^2} - \frac{\sigma_1 - \sigma_2}{2} \frac{3a^4}{r^4} \cos 2\phi$$

From this the liberated strains are found:

$$\epsilon'_r = \frac{1}{E}(\sigma'_r - \nu\sigma'_t)$$

$$\epsilon'_t = \frac{1}{E}(\sigma'_t - \nu\sigma'_r)$$

The three gauges are placed as shown in Fig. 11. It follows from the above equations that the magnitude of the strain decreases rapidly with increasing distance from the centre of the hole. To obtain as great an output as possible from

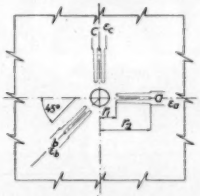

Fig. 11. Position of strain gauges around drilled hole (Fig. 10)

the gauges they must have the shortest practicable length of filament and must be placed as close to the boundary of the hole as possible. The indicated strain is given by $\epsilon'_m = \frac{\int \epsilon' dS}{S}$, where $\int \epsilon' dS$ is the strain integrated over the surface S of the filament of the strain gauge.

After some simplification it is found that:

$$\epsilon'_m = \frac{A}{E}\left(\frac{\sigma_1 + \sigma_2}{2}\right) + \frac{B}{E}\left(\frac{\sigma_1 - \sigma_2}{2}\right) \cos 2\phi$$

where A and B are constants depending on the location of the gauge, its dimensions, the radius of the hole and the value of Poisson's ratio. A first approximation may be obtained by assuming the width of the gauge to be negligible. If r_1 and r_2 denote the distances from the ends of the filament to the centre of the hole

$$\epsilon'_m = \frac{1}{r_2 - r_1} \int_{r_1}^{r_2} \epsilon'_r \, dr$$

According to Soete A and B are now given by

$$A = -(1 + \nu)\frac{a^2}{r_1 r_2}$$

$$B = \frac{a^2}{r_1 r_2}\left[(1 + \nu)\frac{a^2(r_1^2 + r_1 r_2 + r_2^2)}{r_1^2 - r_2^2} - 4\right]$$

In reality these expressions are more complicated. The constants A and B can be determined experimentally by drilling a hole in a plate which has been loaded mechanically so that the stress distribution is known beforehand. Mr. Boiten mentioned that at the time of speaking a number of tests were still in progress to determine the best values for gauge dimensions, distance of gauge from hole, etc. If A and B are made to have the same values for the three gauges, and the gauges are arranged as in Fig. 11, after some computation, the following expressions giving the residual strains in terms of the measured liberated strains are obtained:

$$\epsilon_a = C_1 \epsilon'_{ma} + C_2(\epsilon'_{ma} + \epsilon'_{mc})$$

$$\epsilon_b = C_1 \epsilon'_{mb} + C_2(\epsilon'_{ma} + \epsilon'_{mc})$$

$$\epsilon_c = C_1 \epsilon'_{mc} + C_2(\epsilon'_{ma} + \epsilon'_{mc})$$

where

$$C_1 = \frac{1 + \nu}{B}$$

$$C_2 = -\frac{\nu(A + B) - (A - B)}{2AB}$$

If the constants C_1 and C_2 are determined theoretically or experimentally for an accepted standard procedure the true residual strains can be calculated directly from the measured strains. From these the principal strains can be determined and hence the principal stresses may be calculated.

Mr. Boiten concluded by discussing the practical technique of the method. The main point, apart from usual strain gauge technique, was the great care taken to get the location of the gauges and the hole as nearly correct as possible. The gauges used were type A5 (by the Baldwin Instrument Co. Ltd.) or type GM4473 (by Philips Electrical Ltd.).

PHOTOELASTICITY

Dr. A. W. Hendry and Mr. J. K. Tattersall read a paper on "The application of the 'frozen stress' method of photoelasticity to the analysis of a buttress dam."

The work they described was carried out on behalf of the North of Scotland Hydro-Electric Board and arose in connexion with the design of a dam for one of their hydro-electric power schemes in Central Scotland. This dam is of unusual design as it is to be made up of a number of independent buttress units, placed side by side, each unit having three faces subjected to water pressure, as shown in Fig. 12.

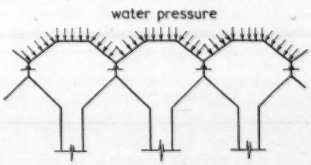

Fig. 12. Design of dam

The irregular outline of the unit and the complexity of the loading meant that the stress analysis of a buttress by classical theory, relaxation methods or the use of Airy stress functions, would have been extremely tedious if not impossible, unless many simplifying assumptions were made. In the drawing-office design of the dam, these simplifications were made and as the dam is some 1 300 ft long and a maximum of 130 ft high it was decided to carry out a closer study of the primary stresses developed. Accordingly a photoelastic investigation was put in hand at King's College, University of London. Three-dimensional scale models of one buttress unit were machined from solid blocks of Catalin 800 and the "frozen stress" technique was used. The object of these tests was two-fold: Firstly to see whether the stresses observed photoelastically in the web of a model buttress unit agree with

the calculated stresses, and secondly to observe the dispositions and magnitudes of the stresses in the buttress head.

To simplify the tests, two distinct load systems were recognized and examined separately: the hydrostatic load on the buttress face and the self-weight of the dam. The stresses obtained from the separate experiment were combined using Mohr's circle procedures.

The blocks of Catalin used for the models were roughly triangular in shape, 10 × 10 in and 2½ in thick, and were machined to within one-sixteenth of an inch of their final dimensions and greased until required. They were then machined down to final size, greased all over with Vaseline, and generally tested within 24 h. The Catalin used gave the unit fringe value/temperature curve shown in Fig. 13. This curve was derived by taking a disk of the material 1 in in diameter and ¼ in thick and compressing it across a diameter at a certain temperature, allowing it to cool under load and counting the fringe order which had been "frozen" in at the centre. Further disks were loaded at other temperatures yielding other points on the curve. The temperature selected from the curve was 85° C.

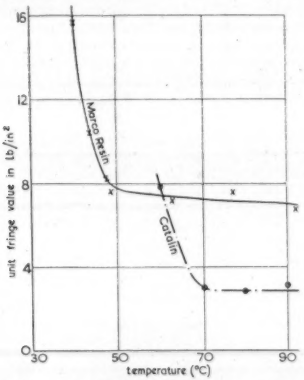

Fig. 13. Unit fringe value—temperature curves for Catalin and Marco Resin

For the hydrostatic loading tests a model was placed in a special jacking frame. Three banks, each of eight pistons, simulated the water pressure on each of the three water faces of the buttress head. The piston thrust was obtained from pressure oil behind each piston, all the pistons being connected to a common reservoir. The diameters of the pistons ranged from 0·161 in to 0·625 in, and were arranged to simulate the hydrostatic loading.

The model in its loading frame and a calibration disk cut from the same block of Catalin and loaded diametrically, were placed in an oven, slowly heated to 85° C, and allowed to soak at this temperature for 1½ h. The loads were then applied both to the model and the calibration disk; the model and disk were then allowed to cool, under load, down to room temperatures in about 3 h.

On completion of the loading cycle the model was sliced and examined in the polariscope. The location of the slices was considered carefully; they were to be examined two-dimensionally and therefore had to be cut in the plane of the third principal stress. It seemed reasonable to assume that this principal stress acted straight down the buttress head and in a preliminary model a slice down the centre of the head was examined as this was a plane of symmetry. This showed that one of the principal stresses was approximately parallel to the upstream faces and hence slices normal to the water face were examined. The unit fringe value was obtained from the calibration disk and the principal stresses in the buttress head slices and in the buttress web were evaluated. A typical fringe photograph of a buttress head slice is shown in Fig. 14.

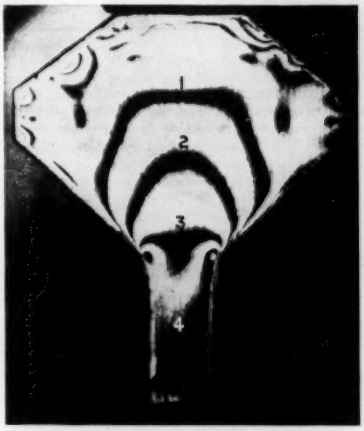

Fig. 14. Typical photoelastic pattern showing stresses in buttress head slice of dam (Fig. 12)

As a qualitative check on the work a series of tests was carried out on Catalin models of a two-dimensional normal section of the buttress head, the fringe pattern being directly observed in the polariscope as the load was applied. The magnitudes and directions of the principal stresses in the two-dimensional tests agreed reasonably with the values obtained from the three-dimensional "frozen stress" tests. The two-dimensional tests were, of course, very much more rapid and much cheaper than the three-dimensional tests; consequently the opportunity was taken of examining a series of slightly modified sections in order to arrive at the most satisfactory shape of the buttress head, the ideal to be aimed at being the absence of tension anywhere in the head.

The gravitational loading to obtain the stress pattern due to the self-weight of the dam presented quite a different set of problems. The sensitivity and density of Catalin are too small to obtain any fringes under the self-weight of the model. It was therefore decided to rotate a three-dimensional model in a centrifuge producing an effective gravitational field of 40*g*. The rotor arm was 10 ft 6 in long, being rotated about its centre and balancing counterweights were attached. A model, mounted on a special heat-insulating fixing, was heated in the oven. After soaking at 85° C for 1½ h, a kapok-filled cover was pulled over the model, still in the oven; the model was then removed from the oven and quickly secured to one end plate of the centrifuge rotor arm. A double-walled aluminium cover was slid over the model, the centrifuge run up to about 160 r.p.m. and kept at that speed

for some 2 hours by which time the model had reached room temperature and the fringe pattern was "frozen" in. The rotor arm of the centrifuge was made as long as practicable in order to produce a sensibly uniform gravitational field over the full height of the model.

After discussing the results obtained from some of these tests the authors turned to the problems encountered when investigating the stresses in the special buttress which is to accommodate a ground sluice and gate shaft. This gate shaft is, in effect, a vertical hole of rectangular cross-section down the buttress and, as it will be full of water, the shaft walls will be subject to hydrostatic pressure. Two-dimensional normal sections were examined and the frozen stress technique used. It was found necessary to use this method because the pressure on the model gate shaft would have been very large, involving considerable practical difficulties if the model had been loaded at room temperature. The model material used for these tests was Marco Resin of the following composition: 64 parts of resin, 28 parts of Monomer C, 1 part of catalyst, and 1 part of accelerator (all by weight). The mixture was cast in a mould formed of 2 glass sheets separated by vulcanized sheet rubber $\frac{1}{4}$ in thick. An aqueous solution of polyvinyl alcohol was used as a parting agent in the mould. After gelling, the sheet of Marco Resin, about $4 \times 3 \times \frac{1}{4}$ in thick, was removed from the mould and allowed to harden for 6 days before a model was cut from it. A unit fringe value against temperature curve was produced for the Marco Resin and is shown in Fig. 13. A temperature of 72° C was selected for the frozen stress tests using Marco Resin. A typical fringe pattern obtained in this part of the investigation is shown in Fig. 15.

MR. G. ROBERTSON (Technical College, Dundee) read a paper on "Stress analysis of pipe flanges by the photoelastic method."

The model material used by this speaker was the comparatively new material "Fosterite" which, although expensive, was found to be almost ideal for this work; it was found extremely easy to machine and, with ordinary care, free from machining stresses, while rind and time edge effects were negligible. It was also found that models which were annealed after having undergone a stress freeing cycle returned to a stress-free condition and regained their original dimensions.

The investigation was carried out in three parts: (*a*) the stress analysis of plane rings under dead weight loading; (*b*) the analysis of flanges with bolt holes and fillets but without the pipe under dead weight loading; and (*c*) the analysis of flanges integral with a short length of pipe, subjected to bolt loading and internal pressure.

The speaker dealt in some detail with some of the difficulties encountered in loading the models. In the first part of the investigation, concerned with the behaviour of plane rings, the load was applied through an annulus, the mean diameter of which represented the pitch circle of the bolt holes, while the support was provided by another annulus at the internal diameter of the ring. It was found that the most satisfactory method of transmitting the load was through dummy rings also made of Fosterite, which had the appropriate annular areas in contact with the model. The thicknesses of the rings tested varied between $\frac{3}{8}$ and 1 in which, on a scale of one to five, corresponded to 8 in pipe flanges of thicknesses between $1\frac{7}{8}$ and 5 in.

In the second series of tests, dealing with flanges under bolt loading only, two identical flanges were placed together as in the normal pipe joint, thus eliminating friction between the raised contact surfaces.

It was also necessary to ensure that the load was distributed equally between the bolt holes, which were varied in number between 4 and 16. The dead load was applied to each bolt hole by means of steel balls and buttons. The buttons projected into the bolt holes for a short distance only and were provided with heads to correspond in size to those of the bolts. A shallow indentation was made in the centre of each head to receive the ball. These indentations were made by a similar ball pressed into each head, the depth of indentation being made the same in each case and checked by a comparator. This arrangement, while not eliminating friction entirely, reduced it to within reasonable limits. Fig. 16 illustrates the flange loading device with the hood removed. When under test the steel hood shown was placed over the models and base, bearing on the balls and being located by the cylindrical base. The load was applied by

Fig. 15. Frozen stress pattern obtained with Marco Resin at 72° C

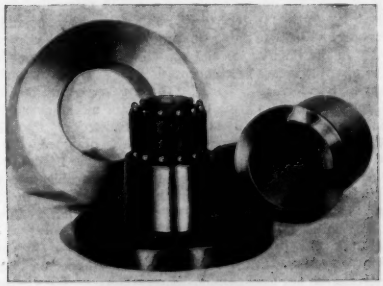

Fig. 16. Flange loading device with hood removed

means of steel rings, one of which is shown, which was placed over the hood and rested on the bottom collar.

The same apparatus was used for the bolt loading of the models in the third series of tests. The internal pressure was applied by means of a mercury column, placed outside the oven and connected with the model inside the oven through thick pressure tubing, the pressure being transmitted by water. Wide limbs were provided on the mercury U-tube so as to avoid the necessity for readjustments due to changes in the internal volume of the models. The "freezing" temperature for all the models was 185° F. The residual material fringe value obtained from calibration experiments was almost exactly 3 lb/in/fringe.

The models were first sliced radially, so as to obtain a number of radial slices and a number of radial sectors, each containing a plane of symmetry as its central plane. The radial sectors were then sliced into a series of tangential and transverse slices. To facilitate the large amount of slicing which had to be done special jigs were prepared which enabled the slicing to be done on a milling machine using a

Fig. 17. "Frozen stress" fringes with single slice

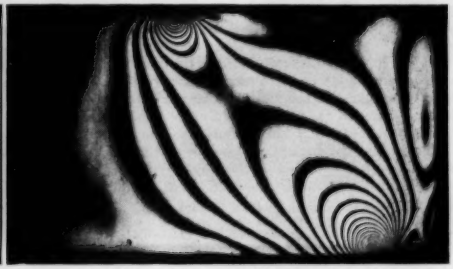

Fig. 18. "Frozen stress" fringes with six slices

$6 \times \frac{3}{64}$ in slitting saw. The surface finish obtained on the slices was satisfactory except at points where there was considerable stress concentration causing the fringes to lie very close together; such slices were lightly polished by hand, using fine-grade metallographic paper. For observation the slices were immersed in Halowax oil which has the same refractive index as Fosterite. It was, however, found that if the model was left in contact with the Halowax oil for a large number of hours the edges of the models were affected causing the fringes at the boundaries to become obscured.

It is generally necessary for accuracy to make the slices cut for use in the "frozen stress" method as thin as possible. This of course leads to only a small number of fringes becoming visible in the polariscope and consequently to the necessity of using some means of compensation for accurate measurement of fractions of a fringe. The speaker overcame this difficulty without resorting to compensator measurement by using a pile of identical slices in the polariscope. Figs. 17 and 18 show the improvement in the pattern obtained when a pile of six slices is viewed as compared with the fringes in a single slice. This technique requires considerable care in obtaining good alinement; but it should prove useful in the analysis of problems involving solids of revolution as these yield a number of identical slices fairly easily.

MR. R. G. HOARE and MR. K. G. HANCOCK (Messrs. Electro-Hydraulics Ltd., Warrington) read a paper on "The application of test loading by hydraulic power." The authors surveyed the field of hydraulic appliances, and dealt with jacks and their design, construction and calibration. After dealing with other components of hydraulic loading rigs they dealt in some detail with some of the circuits employed to apply static and dynamic loading. They also described the circuit aspects of constant stress and constant strain machines and the efficiency of hydraulic systems of this kind.

MR. H. G. EDMUNDS (University College, Cardiff) read a paper on "Edge stresses on free boundaries of photoelastic models." He described some work he had done on this topic while investigating stresses in rotating disks at the Cambridge University Engineering Laboratory. Speaking of time-edge stresses he pointed out that in the past it has been tacitly assumed that the connexion between time-edge fringes and time-edge stresses is the stress-optic law for the material. There is, in fact, no direct evidence for this and the speaker gave some speculative reasons for believing that this may not be so. From experiments he had carried out he thought it probable that the time-edge effect in Catalin 800 did not depend entirely on the water content as had been suggested. Turning to rind effect his experiments showed that, for the same material, the initial time-edge effect has little or no influence on the final rind effect produced by heating at the softening temperature. He was also satisfied that the fringes due to the rind effect and the fringes due to load were superimposed and that, therefore, the pattern due to the load only could be obtained by subtraction of the results from two models, one subjected to load and rind effect and the other to rind effect only. The speaker concluded by referring to certain difficulties he had encountered in regions where the stress gradient was large.

E. K. FRANKL

REFERENCES

(1) DIETRICH, O., and LEHR, E. *Z. Ver. dtsch. Ing.* (*VDI*), **76**, (8 October, 1932).
(2) PORTEVIN, A., and CYMBOLISTE, M. *C.R. Acad. Sci., Paris*, (1934).
(3) DE FOREST, A. V., ELLIS, G., and STERN, F. B., JR. *J. Appl. Mech.*, **9**, A, p. 184 (December 1942).
(4) SMITH, C. W. *Paint Manufacture*, **17** (10 October, 1947).
(5) KOHN, S., KARNOJITSKY, V., and TAGUET, G. *La Recherche Aeronautique*, No. 13 (January–February 1950).
(6) SALMON, B. *Analyse des Contraintes*, **1**, No. 2 (April 1950).
(7) DURELLI, A. J., and DE WOLF, T. N. *Proc. Soc. Exp. Stress Anal.*, **6**, No 2 (1949).
(8) DE LEIRIS, H. *Sur une nouvelle methode d'amplification pneumatique et ses applications en extensometrie.* Proc. VIIth Internat. Cong. Appl. Mech., London, 1948.
(9) DE LEIRIS, H. *The Machinist* (July 1950 and August 1950).
(10) MATHAR, J. *Arch. Eisenhüttenwesen*, **6**, p. 277 (1932–34).
(11) SOETE, W., and VANCROMBRUGGE, R. *Proc. Soc. Exp. Stress Anal.*, **8**, p. 17 (1951).

Liquid films formed by means of rotating disks

By B. E. Dixon, M.Sc., Ph.D., F.R.I.C., A. A. W. Russell, B.A., B.Sc., and J. E. L. Swallow, B.Sc.,
Department of the Government Chemist, London

[*Paper received* 30 *August*, 1951]

A study is made of liquid films ejected from the rims of rotating disks with liquid supplied at the centre. The variation in film area with alteration in experimental conditions is best explained by the assumption of a limiting film thickness, the "breaking thickness," for each liquid, below which the film can no longer exist unsupported in the air in the face of disruptive forces. This assumption is supported by experimental evidence including a study of the paths of liquid particles and liquid films before and after leaving the rotating disk, and a rough measurement of film thickness. A distinction is made between films tending to ellipsoidal shape whose peripheral thicknesses vary within fairly wide limits, and substantially horizontal films whose dimensions are governed by the "breaking thickness" of the liquid concerned. The mechanism of the formation and destruction of these liquid films is discussed and differences in the behaviour of water and glycol examined.

Liquid supplied to the centre of a rotating disk at an increasing rate of flow is ejected from the rim by the centrifugal effect, first in the form of drops, then as stems from which drops are formed, and finally as film which subsequently breaks up into drops. This property is applied industrially in spraying from various types of rotors, and also in gas absorption. In the present paper the stage of film formation only has been studied.

The only detailed study of liquid films rapidly moving in air appears to be that of Bond,[1] on which was based a method of surface tension measurement. Two liquid jets of water were caused to collide at an angle of 180°, forming a roughly horizontal sheet which ultimately curved downwards or broke down into drops. Over a limited range of conditions and subject to minor corrections the diameter of the film was found to be:

$$2R = Q\rho v/2\pi S \qquad (1)$$

where R = radius of liquid film (cm);
Q = volume of liquid supplied in unit time (ml/sec);
ρ = density of liquid;
v = initial linear velocity of liquid at point of supply (cm/sec);
S = surface tension (dynes/cm).

Puls[2] carried out similar experiments with mercury.

The conditions of the present study differ from those in Bond's work mainly in that (*a*) the unsupported film originates not from a point source but from a circle in a horizontal plane, and (*b*) the direction of flow within the film is not normal to the film boundary but varies with the experimental conditions.

MEASUREMENT OF FILM AREA

Experimental. A measured stream of liquid was fed vertically on to the centre of a horizontal brass disk mounted on the axis of a motor and rotated at a known speed with the minimum of vibration. The surfaces of the disks (of 10, 14 and 20 cm diameter) were carefully polished and the rim cut away at an angle of 45° to the upper surface. A camera was placed directly above the disk and focused to cover a horizontal field of film extending outwards from the rim and slightly below it. When steady conditions had been reached the camera shutter was opened and the field was illuminated with a flash of about 2 μsec from an Arditron apparatus. The area of the liquid film on the photograph was measured by means of a planimeter and the average width of film calculated.

The results obtained with ethylene glycol are shown in Fig. 1 where the average film widths are plotted against liquid flow rates for various rim linear velocities. The average film width is directly proportional to the flow rate over almost the whole range of conditions studied. It is only when flow rate,

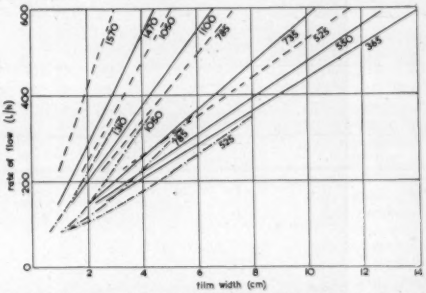

Fig. 1. Variation of width (R–R_1) of film with rate of flow of glycol
The numbers against the curves refer to linear velocities of the rim (cm/sec).
— — — disk of 20 cm diameter.
———— disk of 14 cm diameter.
— · — · — disk of 10 cm diameter.

linear speed, and disk size are all small that the curves show a tendency to curl upwards. Broadly speaking, the film width decreases with increasing rim velocity but it is evident that the disk size exerts some influence on the magnitude of the film width apart from its share in determining the rim velocity.

Appearance of film. A typical glycol film is shown in Fig. 2. The film forms a roughly circular plane terminating in a torus. In places the torus thickens and one or more drops are flung off either directly or at the end of short stems. Under favourable lighting conditions faint undulations in the film can be seen. The boundary is very irregular in shape but, nevertheless, the area of film produced by a given set of conditions is remarkably constant.

FILM THICKNESS

From Fig. 1 it was evident that the film radii did not increase with the liquid linear velocity, as required in equation (1), but on the contrary decreased with the linear velocity. Further, Bond's treatment of the phenomenon by balancing two opposing forces did not appear promising in our case in view of the greater complications. In particular the retaining

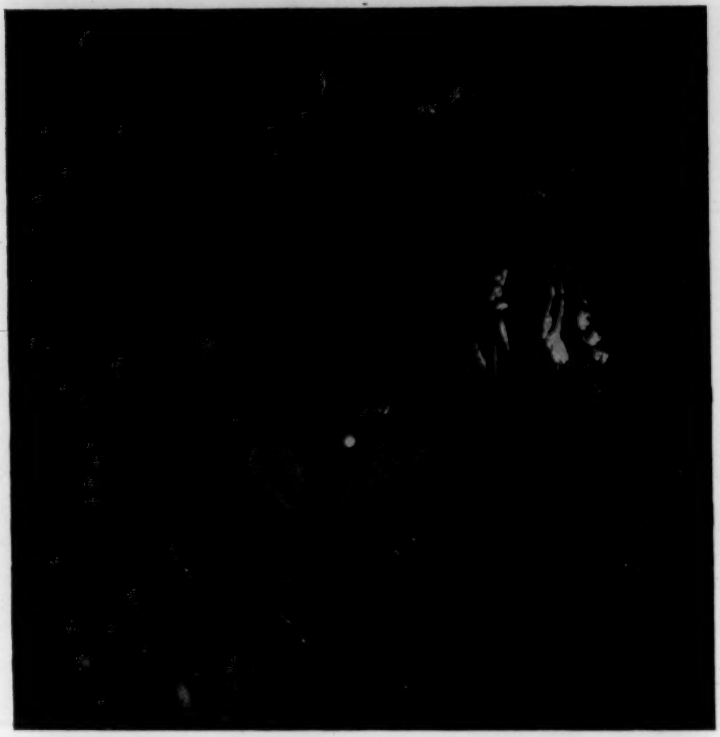

Fig. 2. Typical glycol film from a disk rotating in a clockwise direction

force could hardly be expressed in terms of boundary length, which is irregular and variable in the film from disks, whereas the ellipsoidal film from vertical jets yielded a circular periphery. It was accordingly decided to approach the problem by consideration of film thickness.

From a knowledge of the liquid flow rate, angular velocity, radius of the disk, and the film radius, the theoretical "breaking thickness," or thickness of the liquid film just prior to disintegration, can be calculated. Provided $(R - R_1)$ is not too small, the volume of liquid contained in an annular space of minimal width x at the film periphery is approximately Qx secant $\theta/R_1\omega$, which is equal to the product of the thickness δ and the annular area.

$$Qx \text{ secant } \theta/R_1\omega = \delta 2\pi Rx$$
$$\delta = Q \text{ secant } \theta/2\pi RR_1\omega \qquad (2)$$

where θ = angle made at the film boundary by the intersection of the film diameter and the tangent to the disk;
R_1 = radius of disk (cm);
ω = angular velocity of disk (radians/sec).

The validity of equation (2) rests on the following assumptions, which are discussed in a later section: (i) that the particles of which the film is composed move tangentially on leaving the rim; (ii) that the particles at the moment of ejection have essentially the velocity of the rim itself. It is also assumed that the loss in linear velocity of the liquid due to the air resistance is negligible.

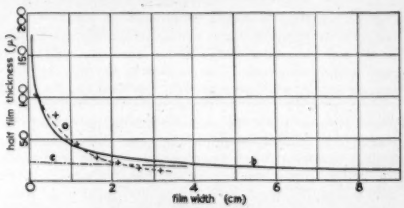

Fig. 3. Variation of thickness of glycol film with film width

(*a*) measured average thickness.
(*b*) thickness calculated according to equation (2).
(*c*) thickness calculated on the assumption of an outward flow of the film normal to the disk rim.

Rough measurement of film thickness. Some experimental confirmation of the validity of equation (2) was obtained by measuring the colour intensity of a film of dyed glycol. Photographs were taken of film extending from the rim outwards, and of thin glass wedges containing the same dyed glycol and covering approximately the same range of thicknesses. The intensities of the negatives were measured by means of a slit photometer over a width of 2 in and a front of 1 in. In Fig. 3 are shown (*a*) the measured average film thicknesses, (*b*) the thicknesses calculated according to equation (2), and, for contrast, (*c*) the thicknesses calculated on the assumption of an outward flow of the film normal to the disk rim. Curves (*a*) and (*b*) are seen to agree fairly closely. The appreciable local variations in thickness corresponding to visible undulations in the film did not warrant a more accurate determination of film thickness.

PATH OF LIQUID PARTICLES

Preliminary tests with various liquids, in particular glycol and water, showed a considerable difference in behaviour with respect to formation of film. It seemed likely that this was due to a difference in the path followed by the liquids from the moment of leaving the supply tube, this in turn depending on the physical properties of the liquids. Tests were carried out to elucidate this point.

Path on disk. Single drops of selected liquids were pipetted on to the centre of a disk rotating at a known speed and the track made by the drop on its way to the rim was observed. The track was usually made visible by the use of a dyed liquid and a disk covered with paper, but some liquids left clear tracks on the brass disk itself.

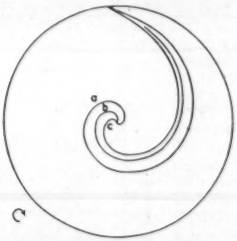

Fig. 4. Tracks made by drops of Aerosol solution on disk of 14 cm diameter at 1 000 r.p.m.
(*a*) 0·001% Aerosol solution of surface tension 73 dynes/cm.
(*b*) 0·005% Aerosol solution of surface tension 58 dynes/cm.
(*c*) 0·01% Aerosol solution of surface tension 51 dynes/cm.

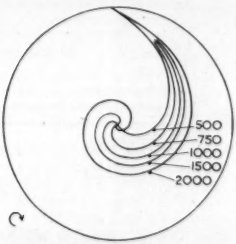

Fig. 5. Tracks made by drops of 0·01% Aerosol solution on disk of 14 cm diameter
The numbers against the curves refer to r.p.m.

The following solutions were used:

(1) Aerosol solutions of varying surface tensions (51 to 73 dynes/cm), but of substantially constant viscosity and density (Figs. 4 and 5).
(2) Sodium alginate solutions of varying viscosities (1·4 to 15·8 cP), but of substantially constant surface tension and density. Results similar in form to Figs. 4 and 5 were obtained.
(3) Glycol/water mixtures of varying strengths.

The results showed that an increase in the length of the path taken by a drop is caused by:

(i) An increase in the angular velocity of the disk.
(ii) An increase in the surface tension of the drop.
(iii) A decrease in the viscosity of the drop.

The tracks were spirals of the logarithmic type, of formula

$$p = r \sin \alpha$$

where r = radius vector of spiral (cm);
α = angle made by intersection of radius vector and tangent to the spiral;
p = length of perpendicular from the origin to the tangent to the spiral (cm).

The drops at any point on the disk are presumably subject to two main forces, one force centrifugal acting radially outwards, the other acting at right angles to the radius at that point and in a direction opposite to that of rotation. The resultant of these two forces at any point will be represented by the tangent to the spiral at that point, which makes a constant angle with the radius. Glycol, with a relatively low surface tension and a high viscosity, gives a track that is almost radial even at high angular velocities (i.e. α approaches zero). In this case presumably the maximum amount of centrifugal force is transmitted from the disk with the minimum degree of slip. A drop of glycol can therefore reasonably be assumed to be ejected from the disk at a velocity approximating to that of the rim. It is probable that this assumption with respect to the drop may be extended to a thin film of liquid.

Water drops, on the other hand, with their relatively high surface tension and low viscosity, yield spiral tracks of considerable length. Their linear velocity on ejection is therefore presumably appreciably less than that of the disk rim, especially at high angular velocities.

Path after leaving disk. The experiments with single drops described above were extended in order to observe the path of the drops after leaving the disk. The rotating disk was surrounded with a stationary annular strip of paper placed slightly below the plane of the disk. In the case of every liquid tested, the drop on leaving the disk was found to give a track apparently tangential to the rim.

In another experiment a stream of dyed glycol from a stationary jet was injected into the film of undyed glycol at a point on a rotating disk near the centre (Fig. 6). The boundary streak lines are not exactly tangential to the disk rim, but are inclined at an angle slightly more than 90° to the disk radii. This divergence from tangential flow is no doubt due to the influence of the radial component of the particle velocity, but no serious error in the computation of δ in equation (2) is thereby caused. The clear-cut boundary between dyed and undyed liquid indicates a negligible degree of diffusion. The use of a similar technique with water was not so successful, a considerable degree of diffusion resulting in blurred outlines. Better results were obtained by strewing the water film on

Fig. 6. Dyed glycol supplied from a stationary point to the layer of undyed glycol on a disk rotating in a clockwise direction

the disk with light, finely divided solid particles, e.g. sawdust, tinsel, and allowing an exposure time long enough to show a particle track of a few cm on the photographic plate (Fig. 7). In this and similar photographs the water is seen to leave the disk rim in directions inclined at from 10° to 20° to the tangent. There also appears to be a further slight change in direction of flow when the film breaks down into drops.

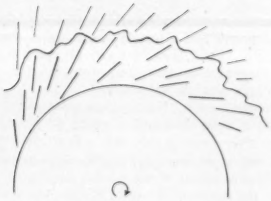

Fig. 7. Particle tracks formed by scattering sawdust on the layer of water on a rotating disk. Exposure $\frac{1}{10}$ sec

MECHANISM OF FILM FORMATION AND DESTRUCTION

It is now possible to form a clearer picture of some of the factors affecting the making and breaking of film in the comparatively simple case of a viscous liquid of fairly low surface tension such as glycol. Shortly after being fed on to the centre of the disk, the liquid becomes sufficiently attenuated to assume the rotational speed of the disk. It is impelled by centrifugal force radially outwards towards the rim and is then ejected in an approximately tangential and horizontal direction, and, given a sufficient supply of liquid, in the form of film.

The chief force maintaining the film in being is the surface tension acting in a direction difficult to define owing to the irregular and constantly fluctuating boundary. As the liquid travels away from the disk the film thins and ultimately disintegrates into drops. It seems reasonable to postulate a limiting film thickness ("breaking thickness") for each liquid below which the film can no longer exist unsupported in face of disruptive forces. It is possible that these forces may include oscillatory disturbances set up by contact with the air. It is to be expected that the breaking thickness will vary within relatively narrow limits with the experimental conditions.

In the following discussion the term "breaking thickness" will be confined to the thickness at the edge of substantially horizontal films, and not of films of mushroom shape. "Breaking thickness" refers to the thickness of the film just prior to the formation of the torus, which is of course actually thicker than the neighbouring parts of film.

The effect of an increasing angular velocity in reducing film width, and the inapplicability of equation (1) outside the limits laid down by its author, can be explained on the assumption of a roughly constant breaking thickness. If, for instance, the angular velocity of a disk is increased without altering the liquor flow rate, the thickness at the film boundary would hypothetically be reduced to a figure below the breaking thickness. In order therefore to maintain equilibrium the film must shrink until the proper breaking thickness is attained.

The assumption of a breaking thickness merely serves as a working hypothesis to interpret the variation in the film area and, of course, leaves unexplained the processes by which the film is destroyed.

Limits of breaking thickness. Although the calculated breaking thickness for a given liquid is approximately constant, it does in fact vary within narrow limits. The values for glycol, for instance, vary from 0·001 to 0·003 cm over a wide range of film widths ($R - R_1$) (0–13 cm) and of nominal film thicknesses at the rim (0·005–0·08 cm). As there are at least three variables governing film formation with a rotating disk it is difficult to ascertain the effect of each on the magnitude of the breaking thickness. The most important factor appears to be θ, the angle at which the liquid strikes the film boundary; the breaking thickness varies almost inversely with θ (Fig. 8). The effect of rate of liquor flow on breaking thickness is almost negligible in the case of water films from a stationary disk (Fig. 10) and is probably very small in other cases. Increase in rim linear velocity decreases the breaking thickness up to a point and thereafter has little effect.

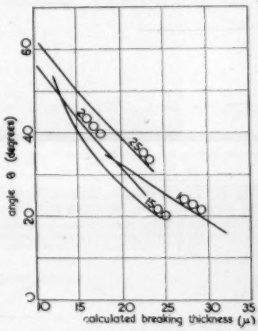

Fig. 8. Variation of calculated breaking thickness δ with the angle θ at which liquid particles strike the film boundary

Effect of initial velocity. Since in all the experiments described the liquid was supplied to the centre of the disk by means of a tube, the liquid always possessed an initial linear velocity which could be calculated from the rate of flow and

the tube dimensions. In the case of glycol with the small flows used the initial linear velocity was usually small compared with the imposed angular velocity. It was found that an increase in the initial linear velocity caused by reducing the diameter of the supply tube whilst maintaining the same flow resulted in a small decrease in film width.

WATER FILMS

When water, with its much higher surface tension and much lower viscosity, is substituted for glycol the case is more complicated. The water film never assumes the full linear speed of the disk even at low angular velocities and no assumptions can be made as to the thickness of the film. Experiments were therefore made in the first instance with a stationary brass disk.

Film with a stationary disk. A number of supply jets of various sizes were used. The velocity of the liquid film can be regarded as entirely derived from the initial velocity of the water in the vertical supply jet. A disk of diameter 2·5 cm was found to be large enough to impart a horizontal direction of flow and not so large as to cause undue loss of linear speed by friction. The diameter of the film was measured directly in several directions and where the curvature was appreciable a correction was made in order to ascertain the true path of the moving film.

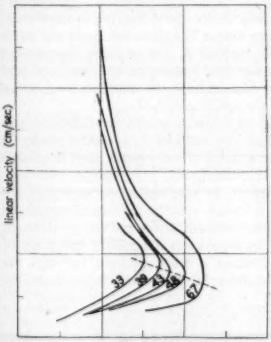

Fig. 9. Variation of film diameter ($2R$) with linear velocity of water

The numbers against the curves refer to water flow rates (ml/sec).

In Fig. 9 the film diameters are plotted against linear velocity at various rates of flow, and in Fig. 10 the calculated approximate film thicknesses at the periphery are plotted against linear speed. The dotted line in Fig. 9 indicates the observed transition between the horizontal type and the ellipsoidal or mushroom type of film. In every case this line cuts the flow rate curves at the point of maximum film diameter.

The process of film formation can perhaps be more clearly followed in Fig. 10. As the linear velocity of the liquid is increased, whatever the rate of flow, the calculated thickness at the film periphery is seen to decrease rapidly and the film diameter to grow, until a speed of 250 to 300 cm/sec is reached. Up to this point the film has been ellipsoidal or mushroom shaped, and, provided the loss in speed due to friction on the disk is taken into consideration, the film radius has corresponded roughly with R of equation (1). When this critical speed of 250 to 300 cm/sec has been passed, however, the film becomes substantially horizontal and the film thickness at the periphery is reduced to "breaking thickness" which remains relatively constant at 0·001–0·0025 cm as the linear speed continues to increase. The film, whose diameter is governed by breaking thickness and linear velocity, is therefore forced to shrink.

As in the case of glycol the breaking thickness of water film

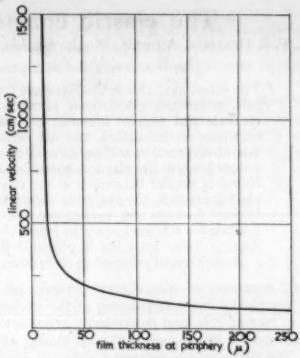

Fig. 10. Variation of calculated film thickness at the periphery of the film with linear velocity of water

varies within narrow limits, decreasing with increasing speed. The fact that points representing flow rates ranging from 33–67 ml/sec all fall very nearly on the curve in Fig. 10 shows that liquid flow rate has a negligible influence on the magnitude of the breaking thickness. Since in this experiment the angle θ is always nil there is no variation of the breaking thickness with θ.

Film with rotating disk. The comparatively simple case of formation of a water film from a stationary disk is greatly complicated when the disk is made to rotate. The following additional factors then come into operation:

(i) the water film never fully assumes the angular velocity of the disk and the greater the angular velocity the greater the degree of slip;

(ii) since the assumed angular velocity of the water film is always comparatively low, any initial velocity the water may have before reaching the disk has a correspondingly greater importance;

(iii) if a significant proportion of the disk's angular velocity is to be taken up by the film, the disk must be fairly large. Hence disk size is more important than in the case of glycol;

(iv) no attempt at calculating the film thickness can be made.

As a result of these complications the formation of films of water from a rotating disk does not show the regularity found in the case of glycol, although the linear relationship between film width and rate of liquor flow is maintained. Attempts were made to reduce the degree of slip and thus increase the linear velocity of the water at the rim by grooving the disk radially and also by roughening the surface. It was found that this treatment resulted in the expected reduction of film width.

ACKNOWLEDGEMENTS

The authors wish to thank the Government Chemist for permission to publish this paper. The discussions we have had with Mr. H. B. Squire and Dr. R. C. Pankhurst of the National Physical Laboratory, on the subject of film break-up, have been most helpful.

REFERENCES

(1) Bond, W. N. *Proc. Phys. Soc., Lond.*, **47**, p. 549 (1935).
(2) Puls, H. O. *Phil. Mag.*, **22**, p. 970 (1936).

The elastic constants of piezoelectric crystals

By R. F. S. Hearmon, A.Inst.P., Physics Section, Forest Products Research Laboratory, Princes Risborough, Bucks.

[*Paper first received* 14 *September*, 1951, *and in final form* 19 *November*, 1951]

The values available in the literature for the elastic constants of the piezoelectric crystals Rochelle salt, potassium dihydrogen phosphate, ammonium dihydrogen phosphate, quartz, sodium chlorate and sodium bromate are assembled. The averages and standard deviations of the estimates are calculated, and the variability of the results discussed. The direct extension and lateral contraction stiffnesses of Rochelle salt show great variability which, however, is much reduced when the elastic constants are expressed as compliances. Little, if any, evidence is found of similar behaviour in the other materials. For comparison with the results on piezoelectric crystals, the available determinations on the non-piezoelectric crystals sodium chloride, lithium fluoride and pyrites are also summarized. It is concluded that elastic constants of crystals are seldom known to better than 1%, and in many cases the uncertainty is considerably larger. This variability is probably due to inherent variability in the materials rather than to experimental error or to differences caused by the use of different experimental methods.

The elastic constants of piezoelectric crystals are of importance, practically in the calculation of the frequencies of vibration of rotated cuts, and theoretically in connexion with the atomic theory of piezoelectric and elastic effects in crystals. The constants are measured either as compliances S_{ik} or stiffnesses C_{ik}[1]; the former are appropriate when the strains are expressed in terms of elastic constants and stresses, and the latter when the stresses are expressed in terms of elastic constants and strains. A number of determinations of the elastic constants of the piezoelectric crystals Rochelle salt, ammonium dihydrogen phosphate (ADP), potassium dihydrogen phosphate (KDP), quartz, sodium chlorate ($NaClO_3$) and sodium bromate ($NaBrO_3$) are now available; the object of this paper is to collect these results, and to discuss their accuracy. The methods which have been used in the determinations are summarized in Table 1; for brevity the methods will be referred to later by the letter given in the second column of Table 1.

Brief descriptions of methods *R*, *T*, and *D* are given in Hearmon's review,[2] together with a more detailed discussion of method *S*. Methods *T*, *P* and *D* are dealt with at some length by Bergmann,[10] but for completeness, short accounts of the methods are given here.

Table 1. *Methods of measuring elastic constants*

Method	*Abbreviation*	*References*
Static	*S*	2, 3, 4, 5
Resonant frequencies	*R*	6, 7, 8, 9
Ultrasonic transmission	*T*	10, 11, 12, 13, 14, 15
Pulse transmission	*P*	10, 16, 17
Light diffraction	*D*	10, 18, 19, 20

In method *S*, the strain under static loading is measured, and the appropriate compliance is calculated from the ratio of stress to strain.[5] In method *R*, the resonant frequencies of appropriately cut and excited specimens are measured and the elastic constants are derived from the resonant frequencies and the dimensions of the specimens.[7, 9]

Methods *T*, *P* and *D* are of more recent development and are therefore less familiar. In method *T*, a quartz wedge is attached to one face of a plate of the crystal, and the other face is immersed in a suitable liquid. The wedge is set into vibration by application of an alternating voltage and the frequency of excitation is varied. At the resonant frequencies of the specimen, the transmission of ultrasonic energy through the specimen and into the liquid is a maximum; this state of affairs is detected by passing a beam of light through the liquid and observing the light diffraction effects produced by

Table 2. *Rochelle salt (orthorhombic)*

Author	*Method*	*Reference*	S_{11}	S_{22}	S_{33}	S_{44}	S_{55}	S_{66}	S_{12}	S_{13}	S_{23}
Mandell	*S*	4	46·9	32·0	28·2	60·9	306	80·2	− 8·0	−21·8	+16·8
Hinz	*S*	3	52·3	34·3	32·4	96·3	337	118	−21·8	−16·9	−13·4
Mason	*R*	9	51·8	34·9	33·4	79·8	328	101	−15·3	−21·1	−10·3
Sundara Rao	*T*	15	50·2	30·4	31·7	82·0	333	106	−11·6	−21·4	−8·9
Huntington	*P*	16	52·4	35·0	33·7	74·6	311	102	−15·4	−9·8	−9·1
All results	$\bar{S}$		50·7	33·3	31·9	78·7	323	101	−14·4	−18·2	−5·0
	σ_S		2·37	1·98	2·37	15·2	13·3	16·3	5·9	5·2	13·0
	V_S		4·7	5·9	7·4	19·3	4·1	16·1	41	29	260
Omitting static results	$\bar{S}$		51·5	33·4	32·9	78·8	324	103	−14·1	−17·4	−9·4
	σ_S		1·3	2·7	1·18	4·4	13·0	2·95	2·2	6·8	0·83
	V_S		2·5	8·1	3·6	5·6	4·0	2·9	16	39	8·8

Author	*Method*	*Reference*	C_{11}	C_{22}	C_{33}	C_{44}	C_{55}	C_{66}	C_{12}	C_{13}	C_{23}
Mandell	*S*	4	3·46	4·73	8·01	1·64	0·327	1·25	−0·78	3·14	−3·42
Hinz	*S*	3	6·82	10·31	9·66	1·04	0·297	0·848	6·83	6·38	7·83
Mason	*R*	9	4·25	5·15	6·29	1·25	0·304	0·996	2·96	3·57	3·42
Sundara Rao	*T*	15	4·06	5·20	6·40	1·22	0·300	0·95	2·56	3·46	3·20
Huntington	*P*	16	2·55	3·81	3·71	1·34	0·321	0·979	1·41	1·16	1·46
Jona	*D*	18	2·58	3·80	3·75	—	0·314	0·997	1·40	1·12	—
Omitting Jona's results	$\bar{C}$		4·23	5·84	6·81	1·30	0·310	1·005	2·60	3·54	2·50
	σ_C		1·84	2·80	2·56	0·26	0·013	0·173	3·28	2·25	4·8
	V_C		43	48	38	20	4·2	17	126	63	192
Omitting Jona's and static results	$\bar{C}$		3·62	4·72	5·47	1·27	0·308	0·975	2·31	2·73	2·69
	σ_C		1·0	0·82	1·59	0·071	0·012	0·027	0·91	1·42	1·15
	V_C		28	17	29	5·6	3·9	2·8	39	52	43

the ultrasonic "grating" in the liquid. The elastic constants are then found from the frequencies of maximum transmission and the thickness of the specimen. This method was devised and developed by Bhagavantam[11] and his co-workers in India, and its use has apparently been confined to that country.

Method *D* was devised and developed by continental workers and it has been used by them and by one Japanese.[19] A quartz transducer is attached to the specimen, which is set into vibration on excitation of the quartz by an alternating voltage. A beam of light is passed through the specimen itself, and the light is diffracted by the supersonic "grating" in the vibrating crystal. The diffraction pattern is photographed, and the elastic constants are derived from certain dimensions of the diffraction pattern, in conjunction with an apparatus constant.[10]

Table 3. *KDP (tetragonal)*

Author	Method	Reference	S_{11}	S_{33}	S_{44}	S_{66}	S_{12}	S_{13}
Mason	*R*	9	18	20	79	164	−4	−7
Zwicker	*D*	20	15·3	19·6	77·5	168	2·0	−3·8
Bantle and others	*R*	20	15·2	19·5	77·9	158	1·8	−4·5
Price and Huntington	*P*	17	14·7	19·5	79	159	1·7	−3·8
All results	$\bar{S}$		15·8	19·7	78·3	162	0·4	−4·8
	σ_s		1·62	0·25	0·73	4·9	2·9	1·57
	V_s		10	1·3	0·93	3·0	725	33
Omitting Mason's results	$\bar{S}$		15·1	19·5	78·1	162	1·8	−4·0
	σ_s		0·35	0·059	0·89	5·9	0·18	0·41
	V_s		2·3	0·30	1·1	3·6	10	10

Author	Method	Reference	C_{11}	C_{33}	C_{44}	C_{66}	C_{12}	C_{13}
Mason	*R*	9	7·8	7·7	1·27	0·61	3·23	3·84
Zwicker	*D*	20	6·91	5·56	1·29	0·600	−0·600	1·22
Bantle and others	*R*	20	7·08	5·84	1·28	0·633	−0·383	1·55
Price and Huntington	*P*	17	7·14	5·61	1·27	0·628	−0·49	1·29
All results	$\bar{C}$		7·23	6·18	1·28	0·618	0·439	1·98
	σ_c		0·44	1·05	0·0098	0·016	1·87	1·28
	V_c		6·1	17	0·77	2·6	426	65
Omitting Mason's results	$\bar{C}$		7·04	5·67	1·28	0·620	−0·491	1·35
	σ_c		0·14	0·17	0·012	0·019	0·128	0·195
	V_c		2·0	3·0	0·94	3·1	26	14

In method *P*, the elastic constants are obtained from the velocity of propagation of ultrasonic pulses in the crystal. A quartz transducer is attached to one face of the specimen, and pulses are applied to the quartz. These are transmitted through the material, reflected at the opposite face of the specimen, travel back and are picked up by the quartz. The pulses are produced, and the interval between launching and reception timed, by apparatus and techniques similar to those used in radar; this method has been devised, developed and applied mainly in the United States.[16, 17] From the transmission times, and the path lengths, the velocities of propagation are found, from which in turn the elastic constants are calculated.

Method *S* yields the compliances S_{ik} directly, method *R* yields the compliances or the stiffnesses C_{ik} according to the type of vibration, and the other three methods yield the stiffnesses directly. The original authors do not always give both the compliances and the stiffnesses, and in these cases the figures have been converted by the writer, using the appropriate conversion equations.[2, 5, 20, 21] In piezoelectric materials, the values of some of the elastic constants depend on the electrical conditions obtaining during the measurements, and are different, for example, at constant field *E* and at constant displacement *D*.[1, 9, 21] The results quoted in the present paper refer as a rule to constant field conditions, at ordinary temperature (*ca.* 20–30° C); Mason's results for Rochelle salt[9] are an exception since they refer to constant displacement conditions.* However, in practice the only elastic constants which are affected appreciably at ordinary temperatures by the electrical conditions are S_{44} and C_{44} of Rochelle salt and S_{66} and C_{66} of ADP.

Table 4. *ADP (tetragonal)*

Author	Method	Reference	S_{11}	S_{33}	S_{44}	S_{66}	S_{12}	S_{13}
Mason	*R*	9	17·5	43·5	114	163	7·5	−11
Zwicker	*D*	20	20·0	45·7	117	169	1·7	−12·9
Price and Huntington	*P*	17	17·4	42·2	117	168	2·0	−10·9
Bechmann	*R*	7	18·1	43·5	115	165	1·9	−11·8
All results	$\bar{S}$		18·3	43·7	116	166	3·3	−11·7
	σ_s		1·27	1·72	1·47	2·94	2·84	0·98
	V_s		6·9	3·9	1·3	1·8	86	8·4
Omitting Mason's results	$\bar{S}$		18·5	43·8	116	167	1·9	−11·9
	σ_s		1·53	2·07	1·18	2·36	0·18	1·18
	V_s		8·3	4·7	1·0	1·4	9·5	10

Author	Method	Reference	C_{11}	C_{33}	C_{44}	C_{66}	C_{12}	C_{13}
Mason	*R*	9	7·58	2·96	0·87	0·614	−2·43	1·30
Zwicker	*D*	20	6·17	3·28	0·85	0·592	0·72	1·94
Price and Huntington	*P*	17	6·89	3·35	0·856	0·595	0·40	1·89
Bechmann	*R*	7	6·77	3·38	0·868	0·608	0·59	1·99
All results	$\bar{C}$		6·85	3·24	0·861	0·602	−0·18	1·78
	σ_c		0·69	0·21	0·0098	0·0108	1·54	0·34
	V_c		10	6·5	1·1	1·8	855	19
Omitting Mason's results	$\bar{C}$		6·61	3·34	0·858	0·598	0·57	1·94
	σ_c		0·42	0·059	0·0106	0·0094	0·19	0·059
	V_c		6·4	1·8	1·2	1·6	33	3·0

Table 5. *Quartz (trigonal)*

Author	Method	Reference	S_{11}	S_{33}	S_{44}	S_{12}	S_{13}	S_{14}
Voigt	*S*	5	12·99	9·90	20·05	−1·66	−1·52	4·31
Atanasoff and Hart*	*R*	6	12·75	9·61	20·09	−1·79	−1·16	4·52
Mason	*R*	9	12·79	9·56	19·78	−1·53	−1·10	4·46
Bhagavantam	*T*	11	12·80	9·84	20·00	−1·59	−1·64	4·35
Bechmann	*R*	7	12·77	9·60	20·00	−1·79	−1·22	4·48
Nomoto	*D*	19	12·87	9·93	20·42	−1·85	−1·43	4·49
All results	$\bar{S}$		12·83	9·74	20·06	−1·70	−1·35	4·43
	σ_s		0·096	0·148	0·256	0·128	0·216	0·084
	V_s		0·75	1·52	1·28	7·5	16·0	1·9

Author	Method	Reference	C_{11}	C_{33}	C_{44}	C_{12}	C_{13}	C_{14}
Voigt	*S*	5	8·51	10·55	5·70	0·70	1·41	−1·69
Atanasoff and Hart*	*R*	6	8·67	10·68	5·79	0·69	1·13	−1·80
Mason	*R*	9	8·61	10·71	5·87	0·51	1·05	−1·83
Bhagavantam	*T*	11	8·69	10·68	5·76	0·69	1·56	−1·74
Bechmann	*R*	7	8·67	10·72	5·80	0·71	1·19	−1·78
Nomoto	*D*	19	8·64	10·46	5·66	0·79	1·36	−1·73
All results	$\bar{C}$		8·63	10·63	5·76	0·68	1·28	−1·76
	σ_c		0·072	0·104	0·084	0·112	0·204	0·056
	V_c		0·83	0·98	1·46	16·5	16·0	3·2

* Results corrected by Lawson.[18]

The compliances and stiffnesses are given in Tables 2–8; the units throughout are 10^{-13} cm²/dyn for S_{ik} and 10^{11} dyn/cm² for C_{ik}. It should be noted that hitherto in the literature the sign of S_{14} for quartz has been negative and that of C_{14} has been positive, whereas in Table 5 S_{14} is

* Mason's stiffnesses are quoted incorrectly by Huntington[16] and Jona.[18]

positive and C_{14} is negative. This change in sign is made in accordance with the recent I.R.E. standard.[1] Voigt's values for $NaClO_3$[5] have not been included in Table 6 because all the recent determinations show these values to be in error. The values given by Ramachandran and Wooster[22] for $NaClO_3$ have also been omitted. These workers used a new and ingenious method depending on the diffuse reflexion of X-rays from the crystal, and although the method is extremely promising it has not yet been developed to give accurate results.

Table 6. *$NaClO_3$ (cubic)*

Author	Method	Reference	S_{11}	S_{44}	S_{12}	C_{11}	C_{44}	C_{12}
Mason	*R*	9	23·3	85·4	−5·15	4·90	1·17	1·39
Sundara Rao	*T*	14	23·5	84·1	−5·30	4·92	1·19	1·45
Bhagavantam	*T*	12	22·9	84·7	−5·35	5·09	1·18	1·55
Jona	*D*	18	23·4	85	−5·2	4·89	1·17	1·39
Bechmann	*R*	7	22·9	85·4	−5·05	4·99	1·17	1·41
All results	Mean		23·2	84·9	−5·21	4·96	1·18	1·44
	σ		0·26	0·56	0·13	0·086	0·0086	0·069
	V		1·1	0·66	2·5	1·7	0·73	4·8

Table 7. *$NaBrO_3$ (cubic)*

Author	Method	Reference	S_{11}	S_{44}	S_{12}	C_{11}	C_{44}	C_{12}
Mason	*R*	9	20·6	65·0	−5·7	6·16	1·54	2·36
Sundara Rao	*T*	14	22·4	66·7	−5·8	5·45	1·50	1·91
Bechmann	*R*	7	20·4	65·7	−4·8	5·73	1·52	1·77
All results	Mean		21·1	65·8	−5·4	5·78	1·52	2·01
	σ		1·18	1·00	0·59	0·42	0·024	0·35
	V		5·6	1·5	11	7·2	1·6	17

Table 8. *NaCl and LiF (cubic)*

		S_{11}	S_{44}	S_{12}	C_{11}	C_{44}	C_{12}
NaCl (9 observations)	Mean	23·3	79·2	−4·9	4·83	1·26	1·25
	σ	0·61	2·1	0·27	0·11	0·031	0·041
	V	2·6	2·7	5·5	2·3	2·5	3·3
LiF (4 observations)	Mean	11·6	17·8	−3·4	11·3	5·64	4·5
	σ	1·46	1·36	0·55	0·99	0·46	0·66
	V	13	8	16	9	8	15

In addition to the individual values, Tables 2–8 also contain the average value of each elastic constant, and the standard deviation of the results. For a variable x, the former, $(\bar{x})$, is $(\Sigma x)/n$, where n is the number of observations, and the latter, (σ_x), is calculated from

$$\sigma_x = K(x_{max} - x_{min}) \tag{1}$$

where K depends on n as follows[23]:

n	3	4	5	6
K	0·59	0·49	0·43	0·40

The standard deviation σ_x is usually estimated from the formula

$$\sigma_x^2 = \frac{\Sigma(x - \bar{x})^2}{n - 1} \tag{2}$$

but for low values of n, it has been shown[23] that the estimate given by equation (1) is almost as efficient as that given by equation (2), and is, of course, simpler to calculate. However, as a check, calculations were made on all the constants of Rochelle salt and ADP using equation (2). Comparison with the results obtained from equation (1) showed that the differences between the two estimates, though sometimes appreciable, were not large enough to affect the conclusions drawn from the results, and the simpler method involving the range (equation 1) was therefore used in the remaining calculations. For the sake of uniformity, the standard deviations given in Tables 2 and 4 for Rochelle salt and ADP are also those obtained using equation (1).

Finally, the coefficient of variation (V) defined by

$$V = 100\sigma_x/\bar{x}$$

is included in the tables; this quantity gives a measure of the dispersion of the results which is independent of the units employed.

For comparison with the piezoelectric crystals, the results available in the literature for the non-piezoelectric crystals sodium chloride (NaCl) and lithium fluoride (LiF) have been summarized and the values are given in Table 8. The results for NaCl are based on nine sets of observations and those for LiF on four sets.

DISCUSSION

(1) *Rochelle salt.* The most significant result emerging from the observations on Rochelle salt is the large variation in the direct extension and lateral contraction stiffnesses C_{11}, C_{22}, C_{33}, C_{12}, C_{13} and C_{23}; this effect has been previously commented on by Sundara Rao.[15] The stiffnesses measured by Jona[18] are included for comparison, although Jona was unable to measure C_{44} and C_{23}, and for this reason his results have been omitted from the calculation of $\bar{C}$, σ_c and V_c. His results actually agree very closely with Huntington's[16] and Sundara Rao's agree with Mason's,[9] but the discrepancy between the two groups is very considerable. If the static results of Mandell[4] and Hinz[3] are included, V_c for the extensional constants C_{11}, C_{22} and C_{33} is approximately 50%, and for the lateral extension constants C_{12}, C_{13} and C_{23} is approximately 100%. By omitting the static results, V_c can be approximately halved, but is still very large. The picture, however, is quite different when the observations are expressed as compliances, S_{ik}. The value of V_s for the constants S_{11}, S_{22}, S_{33} is about 5%, and for S_{12} and S_{13} is about 30%. It is evident that Mandell's value[4] of S_{23} is open to suspicion and affects the V_s for this constant; the value of V_s when the static observations are omitted is 8·8%. In the orthorhombic system, to which Rochelle salt belongs, the shear stiffnesses C_{44}, C_{55}, C_{66} are simply the reciprocals of the corresponding shear compliances S_{44}, S_{55}, S_{66}, and there is accordingly no significant difference in the variability of these two sets of results. It is not possible, on the information available, to explain the large variation in the stiffnesses, but inherent variability of the material, reflected to a greater extent by the stiffnesses than by the compliances, cannot be ruled out, and further work would evidently be necessary to settle the question.

Recent work on the anomalous elastic, piezoelectric and dielectric behaviour of Rochelle salt has indicated that between the Curie points (− 18° C and 24° C), Rochelle salt normally consists of an aggregate of single domains, possessing monoclinic, rather than orthorhombic, symmetry.[21] The gross elastic properties of an assemblage of monoclinic domains may depend on the size and disposition of the individual domains, and it is probable that the domain structure of the specimens of Rochelle salt used by the workers quoted in Table 2 varied considerably. It therefore seems that domain structure may have to be taken into account in interpreting the variability of the elastic and other constants of Rochelle salt, but information on this point is not at present available. It is, however, a matter which should be borne in mind in any future work.

(2) *KDP and ADP.* There is no evidence for these two substances of the effects noted for Rochelle salt. The values of V_s and V_c are all quite small, except on the constants with suffixes 12 and 23 when Mason's results[9] are included. The figures attributed to Mason in Tables 3 and 4 have

actually been read as S_{ik} at 20° C from rather small-scale graphs, and converted to C_{ik}. Some of the discrepancies may be due to errors in reading the graphs, but the discrepancies in S_{12} on both materials, and to a lesser extent in S_{13} on KDP, make it probable either that Mason's material was genuinely different from that of the other workers, or that his results for the above constants are erroneous. For these reasons, the results have been summarized in two groups, the first including all the values and the second omitting Mason's values.

(3) *Quartz, $NaClO_3$, $NaBrO_3$, NaCl and LiF.* Quartz, $NaClO_3$, $NaBrO_3$, although piezoelectric, are not ferroelectric. There are no significant differences between the variability of the stiffnesses and the compliances, and on quartz and $NaClO_3$, the direct extension and shear constants (those having suffixes 11, 33, 44) are concordant to about 1%. The dispersion associated with the other constants ranges up to about 16%, which is the value for C_{12}, C_{13} and S_{13} of quartz. The values of V for NaCl are in the region of 2–5%, and for LiF and $NaBrO_3$ they are somewhat higher.

(4) *General.* Table 9 gives the highest and lowest values of V found when the constants are divided into three groups: (*a*) direct extension constants, i.e. those having suffixes 11, 22, 33; (*b*) direct shear constants, i.e. those having suffixes 44, 55, 66; (*c*) transverse constants, i.e. those having suffixes 12, 13, 23, 14.

Table 9 summarizes conveniently the points already made, namely that the direct extension and transverse stiffnesses C_{ik} of Rochelle salt show much greater variability than do the compliances S_{ik}, and that the evidence for such an effect with other materials is slight or non-existent. It also brings out the fact that for all substances the variability of the transverse constants is greater than that of the direct extension and shear constants. This is presumably a reflection of the difficulty of determining the transverse constants, which normally are measured by indirect procedures.

Table 9. *Maximum and minumum values of V*

Suffixes		11, 22, 33		44, 55, 66		12, 13, 23, 14	
Material	*Constants*	*Max.*	*Min.*	*Max.*	*Min.*	*Max.*	*Min.*
Rochelle salt, omitting Jona's results	*S*	7·4	4·7	19·3	4·1	260	29
	C	48	38	20	4·2	192	63
Rochelle salt, omitting Jona's and static results	*S*	8·1	2·5	5·6	2·9	39	8·8
	C	29	17	5·6	2·8	52	39
KDP, all results	*S*	10	1·3	3·0	0·93	725	33
	C	17	6·1	2·6	0·77	426	65
KDP, omitting Mason's results	*S*	2·3	0·30	3·6	1·1	10	10
	C	3·0	2·0	3·1	0·94	26	14
ADP, all results	*S*	6·9	3·9	1·8	1·3	86	8·4
	C	10	6·5	1·8	1·1	855	19
ADP, omitting Mason's results	*S*	8·3	4·7	1·4	1·0	10	9·5
	C	6·4	1·8	1·6	1·2	33	3·0
Quartz, all results	*S*	1·52	0·75	1·28	1·28	16	1·9
	C	0·98	0·83	1·46	1·46	16·5	3·2
$NaClO_3$, all results	*S*	1·1	1·1	0·66	0·66	2·5	2·5
	C	1·7	1·7	0·73	0·73	4·8	4·8
$NaBrO_3$, all results	*S*	5·6	5·6	1·5	1·5	11	11
	C	7·2	7·2	1·6	1·6	17	17
NaCl, all results	*S*	2·6	2·6	2·7	2·7	5·5	5·5
	C	2·3	2·3	2·5	2·5	3·3	3·3
LiF, all results	*S*	13	13	8	8	16	16
	C	9	9	8	8	15	15

The material showing the least variability in the direct constants is quartz, but even here V is about 1%. It may be recalled that if the observations are normally distributed, approximately 32% of them will have deviations from the mean numerically greater than the standard deviation. The value of V for the direct constants of NaCl is about 2·5% and for some other crystals reaches even higher values.

The present survey includes nearly all the materials for which more than three independent sets of measurements are available. It leads to the conclusion that the elastic constants of crystals are not, in general, known with high precision. As with the discrepancies for Rochelle salt discussed earlier, the cause of this lack of precision is not known, but it is probably due mainly to inherent variability in the materials themselves. Some support is given to this suggestion by the results of Doraiswami[13] who measured the elastic constants of four samples of pyrites by method *T* (Table 1). Doraiswami's results are analysed in Table 10, which also contains the average elastic constants obtained by including the earlier results of Voigt[5] (method *S*) and Bhagavantam[11] (method *T*).

Table 10. *Pyrites (cubic)*

		S_{11}	S_{44}	S_{12}	C_{11}	C_{44}	C_{12}
Mean (all results)		2·87	9·49	0·43	36·27	10·54	−4·73
Doraiswami	Mean	2·86	9·49	0·43	36·33	10·55	−4·74
	σ	0·083	0·31	0·054	0·85	0·35	0·44
	V	2·9	3·3	12·5	2·3	3·3	9·3

The results are very concordant in the sense that differences between the two means are never greater than about 0·35%. Nevertheless, the values of V derived from Doraiswami's results for the direct constants are very similar to those for NaCl (Table 8). For the transverse constants, V on pyrites is 2–3 times the value for NaCl. Thus, even when the results of a single worker, using a single method, are examined, the elastic constants show appreciable variability, indicating that there is almost certainly inherent variability in the material. This behaviour in pyrites is not, of course, proof that other materials behave similarly; pyrites is, in fact, abnormal in that S_{12} is positive (i.e. Poisson's ratio is negative), but the probability is that other materials will also show inherent variability. A final assessment of the magnitude of inherent variability, and of the accuracy of the experimental methods, could only be reached by a co-operative investigation in which the constants of different samples of a series of materials were determined by different workers, using different methods.

ACKNOWLEDGEMENT

This paper is published by permission of the Department of Scientific and Industrial Research.

REFERENCES

(1) *Institution of Radio Engineers, Standards on Piezoelectric Crystals, Proc. Inst. Radio Engrs*, **37**, p. 1378 (1949).
(2) HEARMON, R. F. S. *Rev. Mod. Phys.*, **18**, p. 409 (1946).
(3) HINZ, H. *Z. Phys.*, **111**, p. 617 (1939).
(4) MANDELL, W. *Proc. Roy. Soc.*, **A116**, p. 623 (1927).
(5) VOIGT, W. *Lehrbuch der Kristallphysik*, reprinted edn., 1928. (Leipzig: B. G. Teubner.)
(6) ATANASOFF, J. V., and HART, P. J. *Phys. Rev.*, **59**, p. 85 (1941).
(7) BECHMANN, R. *Proc. Phys. Soc., Lond.*, **B64**, p. 323 (1951).
(8) LAWSON, A. W. *Phys. Rev.*, **59**, p. 838 (1941).
(9) MASON, W. P. *Piezoelectric Crystals and their Application to Ultrasonics*. (New York: D. van Nostrand Co., Inc., 1950.)
(10) BERGMANN, L. *Der Ultraschall und Seine Anwendung in Wissenschaft und Technik*, 5th edn., pp. 402–482. (Zurich: S. Hirzel Verlag, 1949.)
(11) BHAGAVANTAM, S. 33rd Indian Science Congress, Bangalore, 1946. Presidential Address to Section of Physics.
(12) BHAGAVANTAM, S., and SURYANARAYANA, D. *Phys. Rev.*, **71**, p. 553 (1947).
(13) DORAISWAMI, M. S. *Proc. Indian Acad. Sci.*, **A25**, p. 413 (1947).
(14) SUNDARA RAO, R. V. G. *Curr. Sci.*, **18**, p. 204 (1949).
(15) SUNDARA RAO, R. V. G. *Proc. Indian Acad. Sci.*, **A30**, p. 173 (1949).

(16) HUNTINGTON, H. B. *Phys. Rev.*, **72**, p. 321 (1947).
(17) PRICE, W. J., and HUNTINGTON, H. B. *J. Acoust. Soc. Amer.*, **22**, p. 32 (1950).
(18) JONA, F. *Helv. Phys. Acta*, **23**, p. 795 (1950).
(19) NOMOTO, O. *Proc. Phys.-Math. Soc. Japan*, **25**, p. 240 (1943). (Quoted by Bergman.[10])
(20) ZWICKER, B. *Helv. Phys. Acta*, **19**, p. 523 (1946).
(21) CADY, W. G. *Piezoelectricity*. (New York: McGraw Hill Book Co. Inc., 1946.)
(22) RAMACHANDRAN, G. N., and WOOSTER, W. A. *Acta Cryst.*, **4**, pp. 335, 431 (1951).
(23) DEAN, R. B., and DIXON, W. J. *Analytical Chemistry*, **23**, p. 636 (1951).

A radio-frequency power supply system for high voltage accelerators

By P. A. DAVENPORT, M.A., Clarendon Laboratory, Oxford

[*Paper received* 29 *August*, 1951]

A radio-frequency power supply system for operating an ion source on a high-voltage accelerator is described. A multi-channel link for radio-frequency power is provided between the ground and the high-voltage terminal, each separate power requirement of the ion source assembly having its own channel. Oscillators at ground potential provide the power, and adjustment of their outputs gives positive control of the beam intensity and focus.

A problem in the production of a beam of high-energy particles in a high-voltage accelerator is the provision of electrical power to operate and control the ion source. The normal practice is to use a motor-generator driven by insulating belts and to operate the necessary controls by means of insulating strings. The disadvantages of having heavy machinery mounted at the high-voltage terminal of an accelerator are obvious.

In the power supply system described, a multi-channel link for radio-frequency power is provided between the ground and the high-voltage terminal. Each separate power requirement of the ion source assembly has its own channel; where d.c. power is necessary it is provided by rectification at the high-voltage terminal. Thus the operation of the ion source can be controlled completely from the ground without the use of mechanical remote controls.

METHOD

The radio-frequency ion source[1] used on the 1·2 MV accelerator in this laboratory is shown in Fig. 1. The power requirements for the complete assembly are:

(*a*) 300 W at 20 Mc/s for excitation;

(*b*) 20 W for heating the palladium leak controlling the flow of gas (hydrogen or deuterium) into the ion source;

(*c*) 5 kV at 20 mA for extracting the ions;

(*d*) 25 kV at 0·5 mA for the first focusing electrode of the accelerator.

These are the maximum powers required; (*a*) may be preset, but (*b*), (*c*), and (*d*) must be controllable independently during operation.

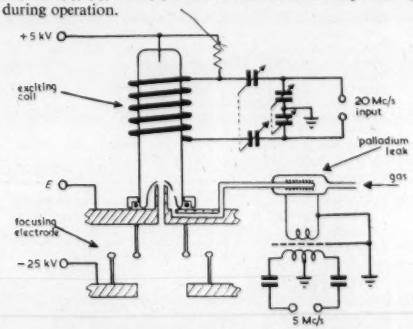

Fig. 1. Schematic diagram of ion source assembly

The four power requirements are provided by four oscillators at ground potential, operating at different frequencies. The oscillator outputs are mixed in a filter unit, and the power is taken up to the high-voltage terminal by a high-pass artificial transmission line designed to withstand the overall accelerator voltage between the input and output ends. The four frequencies are there separated by an identical filter unit. (*a*) is taken to the ion source via an impedance-matching unit; (*b*) to the palladium leak via a transformer. (*c*) and (*d*) are obtained by rectifying the power in the remaining two channels.

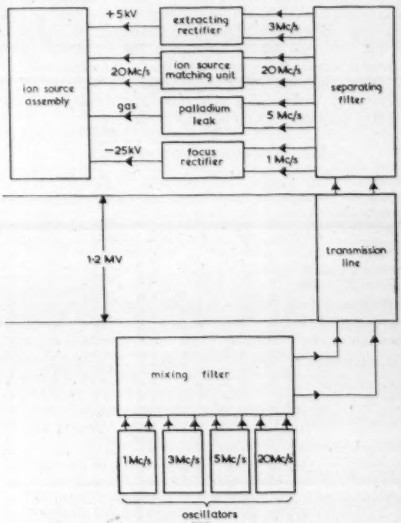

Fig. 2. Block diagram of power supply system

The degree of ion source excitation, the rate of gas flow, and the extracting and focusing voltages are all controlled by adjusting the power outputs of the appropriate oscillators. The complete system is shown schematically in Fig. 2.

THE ARTIFICIAL TRANSMISSION LINE

The characteristics of the line govern the design of the remaining units and the choice of the oscillator frequencies. Electrically the line is a simple balanced high-pass network. Inductors of 30 μH, wound on ceramic formers (Bullers type LEA14702), and capacitors of 0·0011 μF (Admiralty pattern 1059, 0·0011 μF $\pm$ 5%) are used, giving a cut-off frequency of 630 kc/s and a characteristic impedance of 234 Ω. Hence the lowest practicable oscillator frequency is about 1 Mc/s and the filter units must be designed to work into this impedance.

The line is constructed in units of eight sections. Each section is surrounded by a corona ring which is connected via a 1 MΩ resistor to the centre-point of the inductor. Spark gaps are provided between each ring to prevent the voltage across any section exceeding 25 kV. The capacitors are rated at 28 kV test, with a working voltage of two-thirds of this figure, so each unit of the line will withstand 150 kV under operating conditions. The units are stacked on top of one another and bolted together, eight being used on the 1·2 MV set. Details of the construction are shown in Fig. 3.

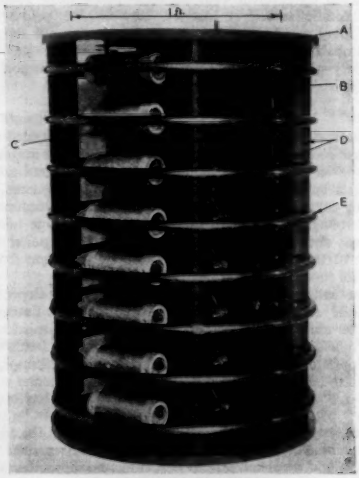

Fig. 3. Transmission line unit

A, bakelite end-plates; *B*, capacitors mounted on bakelite panel; *C*, coils mounted on capacitor terminals; *D*, bakelite pillars; *E*, brass corona rings. The spark gaps are mounted on the corona rings behind the capacitor panel.

THE OSCILLATORS

The power requirements (*a*) and (*c*) above are obtained from type ET4336 transmitters (by Radio Corporation of America), and (*b*) and (*d*) from laboratory-built oscillators. The latter are of the push-pull Hartley type, using two 807 tubes and two ACT6 tubes respectively. In order to obtain a balanced output from the R.C.A. transmitters a simple matching unit[2] was used. The circuit is shown in Fig. 4.

The choice of working frequencies was governed by the cut-off frequency of the line (630 kc/s), the range of the R.C.A. transmitters (2–20 Mc/s), the need for adequate separation of the frequencies to simplify the design of the filter units, and the fact that the difficulty of obtaining high voltages by the rectification of radio-frequency power increases with frequency. The frequencies chosen were (*a*) 20 Mc/s, (*b*) 5 Mc/s, (*c*) 3 Mc/s, and (*d*) 1 Mc/s, (*a*) being decided by the optimum working frequency of the ion source.

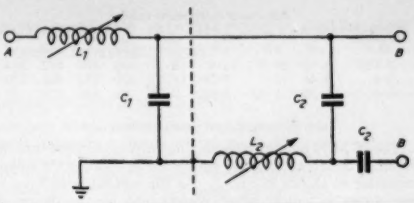

Fig. 4. Transmitter balancing unit

A, unbalanced input from power amplifier of R.C.A. transmitter; *BB*, balanced output. The condition for balance is $2\omega^2 L_2 C_2 = 1$. L_1 and C_1 form the impedance matching unit of the transmitter.

The oscillators are not crystal-controlled so that the circuits at the high-voltage terminal can be preset and final adjustments made by slight variation of the oscillator frequencies.

THE FILTER UNITS

Experiment showed that relatively simple filter units were adequate to mix and separate the four power channels with negligible interaction. This is due to the wide separation of the frequencies and also to the fact that the loads presented to the outputs of the separating filter unit are tuned circuits.

The two identical units each consist of three pairs of two-section complementary *m*-derived filters,[3] making three cross-over networks which are connected in series. The cross-over frequencies are chosen to lie nearly mid-way between the oscillator frequencies and to enable as many standard values of capacitors as possible to be used in the filters. The sections of the filters are screened from one another, and ceramic capacitors and coil formers are used throughout. The capacitor tolerance is $\pm$ 10% and the inductances are accurate to within 5%. The filter circuit is shown in Fig. 5 and the component values in the table.

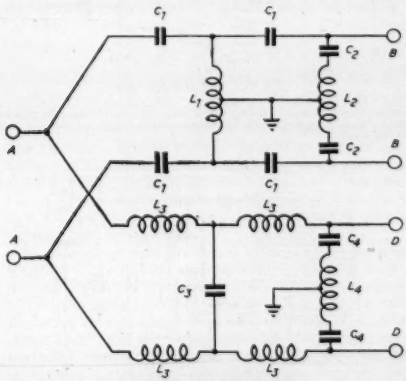

Fig. 5. Filter circuit

AA, mixed input; *BB*, high-pass output; *DD*, low-pass output.

Filter unit component values

Cross-over frequency Mc/s	L_1 μH	L_2 μH	L_3 μH	L_4 μH	C_1 μμF	C_2 μμF	C_3 μμF	C_4 μμF
2·125	8·72	29·2	13·9	18·7	400	600	642	384
3·4	5·46	18·2	8·75	11·7	250	375	400	240
10·6	1·75	5·83	2·80	3·73	80	120	128	77

THE ION SOURCE MATCHING UNIT

The 20 Mc/s output from the filter unit is matched into the resonant circuit exciting the ion source by splitting the tuning capacitor as shown in Fig. 1. As the parallel impedance of the circuit is almost wholly determined by the degree of excitation of the ion source, no simple equivalent circuit can be drawn. The capacitors are variable and the optimum values for a given power input are best found by trial and error. This matching circuit also allows the exciting coil to be connected to the extracting voltage electrode without additional blocking capacitors.

THE RECTIFIER UNITS

The rectifier units providing the extracting and focusing voltages are of conventional design. Figs. 6 and 7 show the circuits and physical layout. In the 5 kV unit the output from the filter unit is loosely coupled into a tuned circuit with a high ratio of inductance to capacity. A normal half-wave circuit is used. The rectifier is a 3B24 tube, whose filament is heated by means of a small coil coupled to the tuned circuit. The regulation is improved by connecting a resistor across the output. The 25 kV unit uses a voltage doubler circuit with 1B3–GT rectifiers, whose filaments are heated in a similar manner. In order to obtain as high a voltage as possible, the tuned circuit consists of a coil designed to resonate with the stray capacities at its supply frequency.

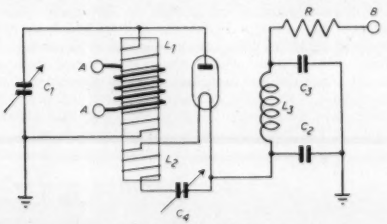

Fig. 6. 5 kV rectifier unit

AA, 3 Mc/s input; *B*, +5 kV output; C_1, tuning capacitor, 20 μμF max.; C_2, 0·0044 μF, 16 kV wkg.; C_3, 0·01 μF, 5 kV wkg.; C_4, filament adjusting capacitor, 150 μμF max.; L_1, resonant coil; L_2, filament heating coil; L_3, r.f. choke; *R*, surge-limiting resistor.

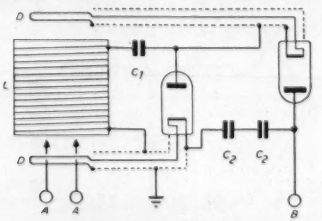

Fig. 7. 25 kV rectifier unit

AA, 1 Mc/s input to coupling coil inside resonant coil L_1; *B*, −25 kV output; C_1, 0·0011 μF, 18 kV wkg.; C_2, 0·002 μF, 16 kV wkg.; *DD*, filament heating loops.

The high voltages involved render it essential to make the coil physically large and of heavy gauge wire; otherwise excessive heating will occur. The coil used has an inductance of approximately 1·2 mH and is wound with 22 s.w.g. wire on a 4 in diameter low-loss former.

The lower limit to the output voltage of these units is governed by the falling off of the rectifier cathode emission as the input power is reduced. With the filament loop couplings adjusted to give normal filament voltages at the maximum outputs of 5 and 25 kV respectively, it is found that reduction of input power to give outputs of 2 and 10 kV is possible; further reduction leads to the output voltages dying away. This range of output is quite adequate for satisfactory operation; should lower output voltages be required the inclusion of some non-linear element such as a thermistor in the rectifier filament circuits should be practicable.

HEATING THE PALLADIUM LEAK

The element heating the palladium thimble has a resistance of 15 Ω and requires a maximum power of 20 W. This load is matched into the output of the filter unit by a simple air-cored transformer with the appropriate turns ratio. An electrostatic screen is inserted between the primary and secondary windings to enable the low-impedance output to be unbalanced, and series capacitors are included in the primary circuit to tune out the leakage inductance. The circuit is shown in Fig. 1.

CONSTRUCTION AND ALINEMENT

The oscillators and mixing filters are rack-mounted in the control room beneath the h.t. room containing the accelerator. The power is taken to the input end of the transmission line along a balanced feeder constructed of ¾ in diameter Dural tubing mounted on porcelain insulators. The units at the high-voltage terminal are rack-mounted in a large bun, and current and voltage meters are grouped on a panel in the floor of the bun so as to be visible by telescope from the control room.

The satisfactory performance of the system depends on accurate radio-frequency alinement. The oscillators and rectifier units must be well matched into the transmission line; any reflexions tend to cause instability. Lamp loads of the appropriate impedances, made from Robertson lamps, were found to be of great assistance during the alinement.

CONCLUSION

The system has been operating satisfactorily on the 1·2 MV accelerator since the summer of 1949 and has proved to be reliable and trouble-free. In particular, no difficulties due to short- or long-term frequency drift have been experienced. A second system is now being installed on the 600 kV accelerator in this laboratory.

ACKNOWLEDGEMENTS

The author wishes to express his gratitude to Professor Lord Cherwell for extending the facilities of the Clarendon Laboratory, to Dr. D. Roaf for his valuable advice and assistance, and to Dr. F. V. Price and the accelerator group for their help in the installation of the power supply system.

REFERENCES

(1) THONEMANN, P. C., MOFFATT, J., ROAF, D., and SANDERS, J. H. *Proc. Phys. Soc.*, **61**, p. 483 (1948).
(2) WHITEHEAD, J. W. *J. Sci. Instrum.*, **26**, p. 71 (1949).
(3) TERMAN, F. E. *Radio Engineers' Handbook*, Sec. 3, Para. 28 (New York and London: McGraw-Hill Publishing Co. Inc., 1943).

Pool surface and cathode spot temperature of mercury cathodes as a problem in heat conduction

By H. v. Bertele, Dr.techn., Dipl. Ing., A.M.I.E.E., Purley, Surrey

[*Paper first received* 5 *July*, 1951, *and in final form* 20 *August*, 1951]

The normal equilibrium of metal molecules and electron temperature is disturbed in the cathode spot. The heat transfer through the cathode pool is merely a matter of the molecular temperature and thus the metal temperature a consequence of the share, the heat conductivity through the pool takes in the total heat dissipation occurring in the discharge device in question. A particular transfer rate is only a convenient technical characteristic for individual arrangements, but no definite physical datum. Temperature of the metal surface at the actual spot position and at the neutral parts has to be discriminated. Average of the latter is mainly dependent on the actual cathode current, while the temperature in the spot is a variable feature following the fluctuations accompanying the spot phenomenon, like current subdivision in several spots, change of spot current, and momentary spot migration speed. Calculation of the thermal fields of moving spots yields about 240° C temperature rise for an average spot size of 6·7 A and a range of at least 80–400° C when considering the possible variations of spot current.

The thermal potential around each spot shows a strong gradient at the spot boundary. Most of the temperature rise occurs within three times the spot radius (0·03–0·1 cm).

The Mercury Pool Cathode Spot

Though the cathode spot has been known and extensively utilized for over fifty years, the mechanism of the emission process still remains largely unknown because of the difficulty of establishing any primary characteristic data. A wide variety of phenomena occur simultaneously with the spot emission, but careful investigations reveal their interrelation rather than their relation, if any, with the emission itself.

Among these accompanying features, the spot temperature attracts particular interest. Constancy of the spot temperature would obviously signify a close relation of the temperature to the emission. In view of both the general pressure level and the generation of vapour jets, surface temperature and temperature distribution in and around the spot on the surface are also of great importance in the design of mercury arc rectifiers and other discharge devices.

When dealing with cathode spot temperatures one must first take note of K. T. Compton's[1] statement that spot temperature cannot greatly exceed 200° C. In this way, a substantial support was gained for interpreting the cathode spot phenomenon as field emission. Compton obtained this numerical value by a carefully constructed energy balance taking into account all processes ever observed in connexion with spot emission by utilizing for this purpose the best numerical values obtainable at that time. Among these the rate of heat transfer through the cathode pool represented a prominent term. It will be shown that this, although throughout the literature assumed as a constant quantity, may, in fact, diverge by more than $\pm$ 50% from its accepted value. While such a fact does not affect the fundamental statement of Compton about the impossibility of a Richardson emission the indicated temperature limit becomes invalid.

But field emission theory itself did not succeed in explaining satisfactorily the various spot phenomena, in particular spot extension, under steady state conditions. Thus C. G. Smith[2] and J. Rothstein[3,4] recently promoted new ideas for the electron release. Smith, in particular, deduced in a gas-kinetic way the presence of a very thin layer of highly energized electrons close under the spot surface extending within the metal of the cathode pool. Energy transfer to the electrons of this layer is explained by direct impacts of recurrent electrons even more highly energized in the region of the cathode drop above. Heat exchange of such an electron layer towards the surrounding metallic body will be prevented largely by a strong Thomson heat; the discharge current observed must correspond to the difference between the total number of electrons escaping into the cathode drop space and those returning back into the layer with even higher energies. Rothstein, differing in the details, suggests also an electron transfer from the pool metal into the space above the cathode spot due to thermal energy. But he refers to a lack of image force, which within the spot area might disappear if the vapour density close above the metallic matrix increases up to values of about 10^{22} molecules/cm^3.

In the light of these recent theories, energy equilibrium between metal molecules and electrons is disturbed in the spot. Thus the spots form minute local surface anomalies plotted on an undisturbed metallic structure (matrix). For technical considerations this metal temperature is of prime interest and it is this temperature which is here particularly dealt with. The microvolume of the cathode space concentrates on the bright spots area; it shows, under steady-state conditions, a current density of about 4 000 A/cm^2 and possesses a perpendicular distance of about 0·004 cm[5] above and following C. G. Smith[2] 0·00002 cm below the pool surface. Release of the cathode losses will occur only in this very limited space. The energy thereof, Q, will correspond to the total emission current, I, times the difference between the actual cathode drop, V_{ca}, and the work function, ψ, for the electron release out of the metal: $\psi = 4{\cdot}5$ V for mercury and

$$Q = (V_{ca} - 4{\cdot}5)I \qquad (1)$$

One part Q_d of this energy is dissipated without entering the liquid mercury; the other, Q_m, is carried away in accordance with the thermal facilities offered by the macrostructure of the mercury pool. It splits up into evaporation heat Q_v and conduction heat Q_c through the pool towards the cooling bottom. Only the latter is susceptible to direct measurement and the ratio Q_c/I is generally referred to as pool heat transfer rate q. However, the thermal field resulting from this heat flow will determine the temperature distribution within the mercury pool boundaries.

In accordance with the recent concept of an undisturbed structure of the cathode pool metal up to the spot itself, one thus can, by means of potential theory, derive the temperature in the pool metal, the spot included. It is only the random motion of the spot across the usually very wide pool surface—about 2 000 times the steady-state spot area—which requires particular consideration. But before going into the details of average surface and spot temperature a survey on the numerical values of cathode drop and heat transfer rates through the pool, observed under practical operating

conditions, seems to be necessary in view of their bearing on the spot losses.

CATHODE DROP PERFORMANCE

Only little work has been published permitting the determination of the cathode drop performance under varying conditions. The following Table 1 presents the data available on this subject.

Table 1. *Measurements of cathode drop V_{ca}*

Year	*Author*	*Cathode drop V*	*Current range A*	*Pressure range*
1925	A. Güntherschulze[6]	8·0	up to 100	(about 100μ)*
1931	E. S. Lamar and K. T. Compton[7]	9·9	4·2–11	not indicated†
1932	J. Kömnick and E. Lübcke[8]	11·3	10	0·6μ‡
		9·0	10	16μ

* According to indications given about the experimental arrangement.

† A special cathode arrangement locating the spot within the boundaries of a quartz envelope and water cooling close under the surface was used.

‡ Anchoring of the spot on a tungsten sheet was used as well as cooling of the mercury and the adjacent discharge space with a water coil.

Although the experimental conditions do not agree completely, comparison of the cathode drop values yields a definite decrease in value with increasing pressure. Thus no accurate constancy of a cathode drop value should be expected with freely moving spots. Fluctuations of the local vapour density will result in permanent cathode drop fluctuations. Apart from that, motion of the spot relative to any measuring device will introduce a further element of uncertainty and render observations of the cathode drop values of moving spots even more statistic.

For the large number of spots at high currents of hundreds or thousands of amps such as occur in power rectifiers, general loss balances of steel tank rectifiers indicate an average cathode drop of 8·0–8·5 V in agreement with the first observation in Table 1.

THE HEAT TRANSFER THROUGH THE POOL AS A CONSEQUENCE OF THE THERMAL SYSTEM AS A WHOLE

A constant value $q = 2{\cdot}68$ W/A is usually given on the basis of Güntherschulze's[6] investigation of 1922 for the heat transfer rate through the mercury pool. But a substantially different heat transfer value was obtained when analysing the internal loss distribution over the various parts of the cooling surfaces of water-cooled steel tank rectifiers in the test-bed of the Siemens Rectifier Works in Berlin. The measurements were made by means of two thermometers inserted in the water inlet and outlet pipes of the cathode bottom,§ while the rate of water flow was observed with one of the usual integrating water flow meters. The value found was much lower than that quoted above; it was only 1·5 W/A cathode current. Only negligible deviations were found for various cathode loads and for different sizes of steel tanks of the same type. The large discrepancy between this low rate and the widely accepted value given by Güntherschulze necessitates a critical review of the significance of the "rate of heat transfer" as such, which will lead to very narrow ranges in which any rate of heat transfer can be assumed as constant.

Güntherschulze's method of investigating the rate of heat transfer consisted in calorimetering the heat transmitted from

§ The thermal system corresponding to this arrangement is shown in Fig. 1.

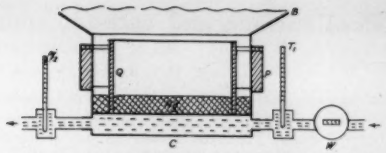

Fig. 1. Cathode heat transfer rate measuring arrangement with steel tank rectifiers

B = bottom of rectifier tank.
Hg = cathode mercury.
Q = protective quartz cylinder.
P = china insulator.
C = cathode bottom with water cooling.
W = water flow meter.
T_1 = inlet thermometer.
T_2 = outlet thermometer.

the bottom of a glass rectifier to the water in a surrounding container; screens were used to prevent radiation being absorbed by the water. The corresponding arrangement is illustrated in Fig. 2. The value of 2·68 W/A represented the average of a series of measurements taken with three glass bulbs of different sizes and largely varying cathode currents. As the individual values were in the narrow range 2·4–2·8 W/A it was tempting to consider the average thereof a characteristic of the heat transfer. The incorrectness of such an assumption follows easily by tracing the cathode loss dissipation as a whole, as indicated in Fig. 2.

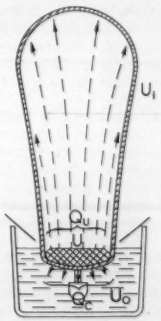

Fig. 2. Güntherschulze's measuring arrangement for the cathode heat transfer rate. The arrows indicate the directions of the two heat flows in the thermal system formed by the glass bulb rectifier used. The respective heat conductivities are:

(*a*) heat conductivity downwards: $S_1 = Q_c/(U - U_0)$.

(*b*) heat conductivity upwards: $S_2 = Q_u/(U - U_6)$

thus $S_1/S_2 \simeq Q_c/Q_u$

Owing to the random motion and the splitting up of the spots one may assume an even distribution of Q_m over the whole mercury surface which yields for the downwards flow Q_c heat resistance $1/S_1$. Although the upwards heat flow, $Q_u = Q_v + Q_d$ is dissipated in a complex manner from the surface by means of mercury evaporation momentum carried away by the high-speed mercury jets and spot radiation, it is finally transferred *in toto* to the ambient cooling medium through the container walls. This transfer occurs in proportion to the temperature difference of the system and gives a resulting upward heat resistance $1/S_2$. The cathode temperature thus will reach a steady value when the sum of the heat flows Q_c and Q_u equals the actual losses Q.

For the type of valves investigated by Güntherschulze with the particular cooling arrangement, and in his loading range, the ratio between the heat conductivities S_1 and S_2 did not vary very much and neither did the q values. Considering

the different level, but very similar performance, of the heat transfer rate with steel tanks, the conclusion is obvious that the ratio S_1/S_2 is an inherent characteristic for each valve type, thus a particular heat transfer rate only applies to certain designs of pool cathode devices. The much lower heat transfer rate found with water-cooled steel tanks can easily be understood by referring to the actual cooling conditions as expressed by the specific cooling areas given as figures of merit in an earlier paper of the author.[9] Much larger vessel surfaces with greater efficiency in heat dissipation due to the water cooling on the one hand, and the higher mercury filling in the cathode on the other, obviously increase S_2 and decrease S_1 respectively, thus yielding a lower heat transfer rate than found by Güntherschulze. But even for glass rectifiers in practical operation where the bulbs are simply air-cooled, Güntherschulze's rate seems inadequate. With air cooling the heat dissipation from the glass bottom to the air is much lower than with the experiment in question because of the smaller heat transfer rate from glass to air. The ratio (heat transfer glass to air)/(heat transfer glass to water) amounts to $\frac{1}{2}$ or $\frac{1}{3}$. This must lead to a noticeably different mercury temperature, under practical operating conditions.

While the upward heat conductivity S_2 does not lend itself easily to calculation, S_1 is susceptible to mathematical treatment as it results only from the heat conduction through the pool. Three typical cases will be dealt with below in order to demonstrate the particular performance of the heat flow and temperature distribution in a mercury pool cathode.

AVERAGE CATHODE SURFACE TEMPERATURE

Steady current conditions. The current subdivision into a multitude of spots beginning already at cathode currents of about 10 A and the random motion of them makes it obvious that the average surface temperature will follow the average current density i.

$$i = I/F \text{ A/cm}^2 \tag{2}$$

where I is the total cathode current (A) and F is the total pool surface (cm^2). In order to calculate the average surface temperature, an even heat flow from the surface to the means of cooling at the bottom of the pool through the mercury is assumed. As the radial dimensions of the cathode area F are usually much more extended than the depth H, replacement of the bowl-shaped cathode body by two infinitely extended layers is justified. Fig. 3 represents the corresponding thermal diagram. Then the temperature drop ΔU between surface and container bottom is easily expressed as follows:

$$\Delta U = iq\left(\frac{H_{mercury}}{\lambda_{mercury}} + \frac{H_{wall}}{\lambda_{wall}}\right) \tag{3}$$

where q is the pool heat transfer rate of the valve type in consideration (W/A);

$H_{mercury}$ is the height of mercury filling, 10 mm in glass and 20 mm in steel;

$\lambda_{mercury}$ is the average heat conductivity of the mercury pool 0·146 W/cm per °C at 100° C;

H_{wall} is the wall thickness, (*a*) iron approximately 0·5 cm, (*b*) glass approximately 0·4 cm;

λ_{wall} is the heat conductivity of wall, (*a*) iron 0·69 W/cm per °C, (*b*) glass 0·01 W/cm per °C.

Taking the case of a steel tank cathode, the influence of the cathode bottom does not amount to more than about 5%, so it seems justifiable to consider the mercury only. In a steel tank cathode the average surface temperature rise will amount

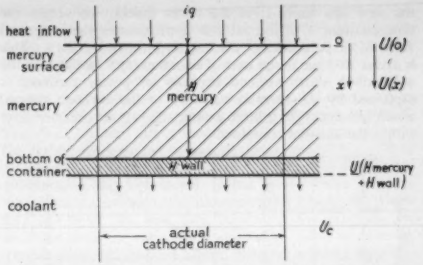

Fig. 3. Mercury cathode represented by a portion of infinitely extended mercury and bottom wall. Heat inflow of qi W/cm^2 on the surface assumed equal to outflow from bottom to coolant (air or water). Wall temperature on the coolant side assumed equal to coolant temperature U_c. Temperature at the cathode surface equals the sum of U_c plus the temperature rise $\Delta U(H_{mercury} + H_{wall})$ in mercury and wall

to about 45° C at $i = 2$ A/cm^2 current density, whereas with an air-cooled glass bulb actual measurements[10] show a corresponding value of about 70° C at nominal load. When substituting this temperature together with the usual glass bulb cathode surface density i of about 1·35 A/cm^2 in equation (3) one gets a heat transfer rate of only 1·2 W/A in striking contradiction to Güntherschulze's value, which confirms again the dependence of the "cathode heat transfer rate" on the particular arrangement.

Transient current conditions. In case of an abrupt current change, the average surface temperature follows with a time delay determined by the building up of the thermal field within the mercury pool. For an extended mercury layer corresponding to Fig. 3 with the temperature dropping only in one direction, the temperature performance in time can be derived from the differential equation of linear temperature distribution

$$U_t = a^2 \cdot U_{xx} \tag{4}$$

assuming an abrupt heat inflow iq per unit surface beginning at $t = 0$. The transient temperature performance of the layer then will follow the expression

$$U(x,t) = \frac{iq}{\lambda} \cdot H\left[\left(1 - \frac{x}{H}\right) - \frac{8}{\pi^2} \sum_{\nu=1,3,5\ldots\infty} \frac{1}{\nu^2} \cdot e^{-(\nu\pi/2H)^2 t\sigma} \cdot \cos\frac{\nu\pi x}{2H}\right] \tag{5}$$

$$\sigma = \lambda/c\gamma$$

where c is the specific heat of pool material for mercury, 0·033 cal/g per °C;

H is the pool height;

x is the distance of surface;

γ is the specific weight of pool material (13·6 g/cm^3);

t is the time elapsed after the current started.

Taking the cathode of a steel tank, $H = 2$ cm, as a practical example, equation (5) yields the surface temperature

$$\Delta U(0,t) = 20 \cdot 5i(1 - 0 \cdot 81e^{-0 \cdot 096t} - 0 \cdot 09e^{-0 \cdot 36t} - 0 \cdot 032e^{-2 \cdot 4t} \ldots) \tag{6}$$

referred to $U(H_{mercury}) = 0$. In the graph shown in Fig. 4 an approximation of equation (6) is plotted, restricted to

the first two terms. As the series quickly converges the time constant T of the cathode approximates the reciprocal value of the parameter of the first term dependent on t. This is about 10·3 sec in the case of equation (6). In this way the well-known short-overload capacity of power rectifiers is explained by the thermal structure of the cathode system, which influences, to a large extent, the vapour pressure level within the vacuum container.

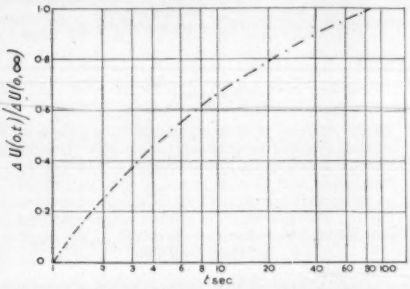

Fig. 4. Surface temperature performance in time at mercury pool cathodes after a sudden application of current

SPOT TEMPERATURE

The temperature of one particular fixed point of the pool will vary in accordance with the momentary distance from the nearest moving cathode spot. Considering a single cathode spot it can be expressed by the thermal potential of the cathode spot produced at each instant at the point in question. The potential field results from the heat inflow Q^* into a restricted area on the surface belonging to a semi-space with a heat conductivity λ. The area is assumed of a circular shape with a radius r_0 and moves around at random.

Random spot motion and staying time. According to E. Schmidt[11] the spot motion is similar to the Brownian motion. The average spot speed decreases when considering longer stretches of spot dislocation as deduced by Einstein[12] and Smoluchowsky.[13] The numerical relation found by Schmidt

$$\frac{\Delta x}{\Delta t} = \sqrt{\frac{15 \cdot 2}{\Delta t}}\ \text{cm/sec} \tag{7}$$

where Δx is the straight distance between two subsequent positions of the same spot;

and Δt is the time taken for the motion between the two positions considered;

is represented in Fig. 5. Conforming to the irregular motion of the spot, its thermal field moves at random within the pool material. As shown later, most of the temperature drop is concentrated in the immediate surroundings of the spot. Thus a substantial heat flow through the point considered will occur only when the spot approaches the position perpendicularly above it on the mercury surface. Bearing this in mind, it will be readily realized that the effect of spot motion is largely equivalent to a sudden heat application for such a time $\bar{t}$ (referred to as the "staying time") as the spot needs to travel a distance equal to its own width under normal motion, i.e.

$$\bar{t} = \text{spot width/migration speed of spot} \tag{8}$$

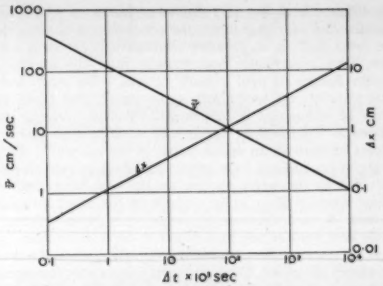

Fig. 5. Velocity performance of cathode spots on a mercury surface. Straight path Δx and velocity $\bar{v}$ have been derived from high-speed cinematographic records by E. Schmidt[11] for successive positions of individual cathode spots. Spot velocity calculated from equation (7)

When taking $\bar{t}$ from graph Fig. 5 by referring to a spot path $\Delta x = 2r_0$ the circuitous motion occurring in the small area of the cathode spot itself is taken into consideration by the definition of the migration speed.

Thermal potential of a moving spot. The thermal steady-state potential of a defined small source lying flat on the upper boundary of a conductive ground closely corresponds to earth electric potential. Ollendorff[14] dealt with both flat circular earthing electrodes having elliptical fields and hemispherical ones with spherical fields, the former only differing from the spherical ones in the closest neighbourhood to the conductor. Thus a hemispherical source boundary with a radius r_0, Fig. 6, was chosen, which, in this way, takes into account the vapour reaction on the surface, at the same time as it simplifies the Laplace transform required for dealing with the transient response. The general differential equation for a three-dimensional heat flow

$$U_t = \sigma^2 \,.\, \text{div grad}\, U \tag{9}$$

reads in spherical co-ordinates chosen in view of the hemispherical boundary

$$U_t = \sigma^2 (U_{rr} + \frac{2}{r} U_r) \tag{10}$$

Solution of equation (10) for an infinite semi-space yields

$$U(r,t) = \theta \frac{r_0}{r}\left\{1 - \phi\left(\frac{r - r_0}{2\sigma\sqrt{t}}\right) - e^{-[1-(r/r_0)-(\sigma^2/r_0^2)t]}\left[1 - \phi\left(\frac{r - r_0}{2\sigma\sqrt{t}} + \frac{\sigma\sqrt{t}}{r_0}\right)\right]\right\} \tag{11}$$

$$\sigma = \lambda / c\gamma$$

where U is the temperature at a part cular point of space;

t is the time;

λ is the heat conductivity
c is the specific heat
γ is the specific weight
} of substance where field occurs;

θ is the steady state potential;

ϕ is the Gaussian integral $(\alpha) = \phi \dfrac{2}{\sqrt{\pi}} \displaystyle\int_0^z e^{-x^2} dx$.

$U(r, t)$ defines the potential around the spot as a function of the time t elapsed after a heat flow leading to a steady-state

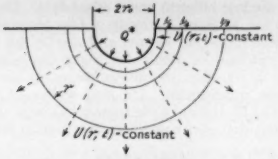

Fig. 6. Heat flow from a hemispherical source into an infinite mercury body after applying a uniform heat influx Q^* on the surface of the hemisphere. Distances of the isotherms are given by equation (11) for the transient period

temperature θ had been applied; according to Ollendorf[14] it is

$$\theta = Q^*/2\pi r_0^2\lambda \qquad (12)$$

For $t \to \infty$ the term in the curved brackets of equation (11) approaches unity, leading to the well-known hyperbolic potential drop along any radius. But during the transition period the bracketed term, depending both on r and on t, causes a greater temperature drop in the neighbourhood of the heat source.

On the mercury surface equation (11) is simplified to

$$U(r_0,t) = \theta\frac{r}{r_0}\left\{1 - e^{-(\sigma^2/r_0)t}\left[1 - \phi\left(\frac{\sigma\sqrt{t}}{r_0}\right)\right]\right\} \qquad (13)$$

The graph shown in Fig. 7 illustrates this surface temperature distribution around a spot of 0·035 cm radius (the dotted line corresponding to the simple r/r_0 potential drop is shown for comparison).

The space occupied by the main portion of the temperature field of the spot is minute. It does not extend to much more than about three times the spot radius, that is $\frac{1}{10}$ of a cm at the most. This very small distance now justifies the treatment of the pool as an infinite mercury body without any bottom boundary; it further justifies the sudden heat application adopted for the transient calculation in place of the gradual change occurring with the real spots moving irregularly and carrying with them the thermal field. In fact, calculation of a transient heat at a particular point on the pool surface practically corresponds to a spot crossing this point because temperature will not rise noticeably before the spot has approached a distance of about three times its diameter. Then it will increase rapidly till the spot is just about to leave the point. It will have dropped down again to the average surface temperature by the time the spot is three diameters away.

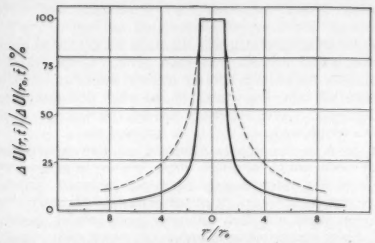

Fig. 7. Temperature distribution in the neighbourhood of the cathode spot calculated for the end of the staying time $\bar{t}$ for a 15 A spot. The hyperbolic potential distribution occurs only in an (imaginary) steady state

r, distance from spot centre; r_0, spot radius.

The exact amount of heat inflow Q^* into the spot is unknown, but limits for its value can easily be drawn. The lowest value will be the product of cathode spot current I_s times heat transfer rate q measured at the cathode bottom. The highest value cannot surpass the total losses $I_s(V_{co} - 4{\cdot}5)$ occurring in the spot. As radiation from the spot and energy contained in the high-speed vapour jets[15] have not yet been directly measured, the corresponding energy Q_a^* which does not enter the heat flow producing the thermals pot field can only be determined indirectly. This is done by consideration of the well-known rate of mercury evaporation. The surface evaporation corresponds namely to that part of heat inflow in the cathode spot which gradually deviates from the distribution shown in Fig. 6 by bending back towards the surface. But since the largest part of the temperature drop occurs close to the spot where the heat flow still corresponds to Fig. 6, this heat flow acts like the heat flow towards the bottom. Average mercury evaporation η from pool surfaces with freely moving spots is quoted by various authors with reference to cathode current unity.

Table 2. *Evaporation data*

Author	η	*Remarks*
I. v. Issendorff (from unpublished notes)	1–16 × 10⁻³ g/A, varying with emission current	includes sputtered droplets
I. v. Issendorff[16]	7·2 × 10⁻³ g/A	pure evaporation after deduction of sputtering
Wellauer[17]	4–6 × 10⁻³ g/A	measured under conditions similar to the operation of big steel tanks

An average mercury evaporation of 5 × 10⁻³ g/A per sec corresponds to an energy of 1·45 W/A cathode current based on an evaporation heat value of 68 cal/g for mercury and yields a total inflow $q_m = q + q_v$.

For steel tank mercury arc rectifiers q_m becomes 2·95 W/A and the more closely defined spot temperature of the last line of Table 3 holds in particular for this type of rectifier. With glass bulbs or other discharge devices with a lower heat transfer and a higher evaporation rate, even higher values than the top limits of Table 3 may be expected, particularly when the cathode drops exceed 8·5 V.

Cathode spot size is not uniform. For steady cathode currents above 15 A it is scattered between 3·5–15 A per spot, the majority being about 6·7 A according to E. Schmidt.[11] Table 3 is calculated from equation (13) and shows numerical values for the temperatures U at the end of the corresponding staying intervals $\bar{t}$ for the average, the smallest, and the

Table 3. *Range of cathode spot metal surface temperatures* $U(r_0,t)$

(*Final values at end of staying time*)

spot current I_s	3·5	6·7	15·0	Amps
spot radius r_0	0·017	0·023	0·035	cm
staying time Δt	0·07	0·14	0·32	×10⁻³ sec
lowest temperatures due to a 5 W/A heat transfer	79° C	102° C	150° C	
highest temperatures due to a 4 W/A heat transfer	210° C	270° C	400° C	
temperatures due to a 2·95 heat transfer W/A	170° C	240° C	340° C	

largest single spots to be expected when 1·5 W/A and 4·0 W/A respectively were used as heat inflow q for the lowest and the highest temperatures.

The temperature values of Table 3 mean final temperatures for various spot sizes, which one particular point on the pool surface will acquire at the end of the passage of a spot. Referring to the moving spots themselves temperature will be maintained constant therein as long as spot size and intensity does not change.

On the cathode pool surface a very uneven temperature distribution occurs. There are pronounced warm areas around each spot sharply distinguished from the average temperature level of the neutral surface and these follow the spot motion. This explains the rapid variation in the local evaporation and the random distribution of vapour jets, which follows the spots in position and actual size. The reaction of these vapour jets on the liquid mercury in turn will, at least to a certain extent, be responsible for the irregular spot motion itself.

Even the highest temperature found for cathode spots on liquid mercury in the spot area is much too low for thermionic emission; it is also insufficient to yield the high vapour density required by Rothstein. Still, the continuous fluctuations of local temperatures occurring with motion and change in size of the spots do not show any noticeable influence on the emission. Thus it is evident that no relation between electron release, however it may operate, and temperature of the pool metal, even in the emission zone, can exist.

ACKNOWLEDGEMENTS

The author has to express his gratitude to management of the Siemens-Schuckert Werke A.G., Erlangen, for permission to disclose hitherto unpublished data. He is further indebted to Mr. F. Geyer, formerly of Elin Aktiengesellschaft für Elektrische Industrie, Vienna; and also Dr. M. Steenbeck and Dr. Grünwald of Berlin for many discussions which helped him to develop the above theory of some of the cathode spot peculiarities. He also wishes to thank, in particular, Dr. D. Gabor of the Imperial College and Mr. G. Carcasson for their advice and help in preparing the paper.

REFERENCES

(1) COMPTON, K. T. *Phys. Rev.*, **37**, p. 1077 (1931).
(2) SMITH, C. G. *Phys. Rev.*, **62**, p. 48 (1942).
(3) ROTHSTEIN, J. *Phys. Rev.*, **73**, p. 214 (1948).
(4) ROTHSTEIN, J. *Phys. Rev.*, **75**, p. 1323 (1949).
(5) SMITH, C. G. *Phys. Rev.*, **69**, p. 96 (1946).
(6) GÜNTHERSCHULZE, A. *Z. Phys.*, **11**, p. 96 (1922).
(7) LAMAR, E. S., and COMPTON, K. T. *Phys. Rev.*, **37**, p. 1076 (1931).
(8) KÖMNICK, J., and LÜBCKE, E. *Physikalische Zeitschrift*, **33**, p. 215 (1932).
(9) BERTELE, H. v. *J. Instn Elect. Engrs*, **97**, p. 663 (1950).
(10) GÜNTHERSCHULZE, A. *Z. Phys.*, **11**, p. 260 (1922).
(11) SCHMIDT, E. *Ann. Phys., Lpz.*, **6/4/5**, p. 246 (1949).
(12) EINSTEIN, A. *Ann. Phys., Lpz.*, **17**, p. 549 (1905).
(13) SMOLUCHOWSKY, v. *Ann. Phys., Lpz.*, **21**, p. 756 (1906).
(14) OLLENDORFF, F. *Potentialfelder der Elektrotechnik* (Berlin: Springer, 1932).
(15) KOBEL, E. *Phys. Rev.*, **36**, p. 1636 (1930).
(16) ISSENDORFF, I. v. *Physikalische Zeitschrift*, **29**, p. 858 (1928).
(17) WELLAUER. *Bulletin des Schweizer Elektrotechnischen Vereines*, **23**, p. 94 (1932).

NOTES AND NEWS

New books

Ferromagnetism. By RICHARD M. BOZORTH, Ph.D. (New York: D. Van Nostrand Co. Inc.; London: Macmillan and Co. Ltd.) Pp. 968. Price §17.50; 130*s*. net.

There are many features of this book which attract attention immediately—its size, the large number of diagrams (825 in the 861 pages of actual text), the extensive bibliography (about 1,780 items) but most striking of all to British readers is undoubtedly the price! Excellent as the book is in many ways it is certainly expensive and this is all the more to be regretted, since there is a real need, amongst users of magnetic materials, for a unified account such as this.

Dr. Bozorth's contributions to ferromagnetism and to the development of magnetic materials are well known and his book presenting "the background knowledge that has been useful to various members of the Bell Telephone Laboratories who have been actively interested in ferromagnetism" is a worthy addition to the Bell Laboratories' series. It is a remarkable achievement, combining descriptions of the properties of almost all known ferromagnetic metals, alloys and compounds in the first part of the book, with later chapters on theoretical and experimental work on ferromagnetism. In the second part the emphasis is on the phenomenological aspects of the subject as distinct from the atomic aspects and the book will appeal particularly to the industrial physicist and to those interested in the use and development of magnetic materials. There are sections on the production of magnetic materials, the effects of composition, impurities, etc., and detailed information on each particular group of alloys with reference to the various commercial alloys. Then follow chapters on magnetic phenomena and theories, the observed results being considered with reference to the domain theory, and there is a chapter on the measurement of magnetic properties.

The book is more properly described as a handbook or encyclopaedia. One feels that every possible aspect of ferromagnetism has been mentioned and it is certainly convenient to have all this information in one book, but this method of treatment makes the book very impersonal and rather colourless. The order of presentation adopted means that properties of specific magnetic materials are discussed before any theoretical account has been given. Thus magnetic annealing or the relation between internal strains and coercive force are left completely unexplained when first mentioned, and there are no cross-references between the two parts of the book to enable such subjects to be followed up.

The book is remarkably complete, no serious omissions having been noted, although there are no details of one or two of the more recently developed magnetic materials (e.g. permanent magnet alloys with columnar crystals). Nor are there many mistakes, although more careful checking could have eliminated a number of minor but irritating errors such as Mo for MO and could have ensured that proper names were rendered correctly, the names of five authors known personally to the reviewer being incorrectly spelled. A number of statements, whilst not actually wrong, are given in a form which might be misleading. Thus it is

not strictly correct that the important attributes of a ferromagnetic, as distinct from a paramagnetic, material are saturation effects and dependence of permeability on field strength, although in a practical sense the statement is true. A more serious error is the statement that hysteresis loops can be displayed on a cathode-ray oscillograph at power frequencies. In the sense in which hysteresis is usually understood and in which Dr. Bozorth himself uses it, this is incorrect. Such a loop is a B–H loop whose area is proportional to the total energy loss in the material, including the effects of eddy currents, etc., as well as hysteresis. In many materials, e.g. Supermalloy, the distinction is very important.

Both the theory and practice of ferromagnetism have made great advances since Becker and Döring's *Ferromagnetismus* appeared in 1939. Dr. Bozorth's book, although written from a different point of view, should be an equally important landmark in the history of the subject and should make a great contribution to the better and wider understanding of magnetic phenomena.

A. E. De Barr

Applied atomic energy. By K. Fearnside, E. W. Jones and E. N. Shaw. (London: Temple Press Ltd.) Pp. 156. Price 8*s*. 6*d*. net.

Much has been written in recent years on the subject of the war-like potentialities of atomic energy. Despite the widespread use of radio-active "tracers" in biological research and in medicine, the peaceful applications of nuclear physics have all too often been neglected. For this reason an authoritative and well-written book in this field is to be welcomed.

The book presents a balanced and up-to-date picture of the production and uses of isotopes, both radioactive and stable. For the scientific worker specializing in fields other than nuclear physics, it should prove stimulating as the authors have been at pains to indicate possible new fields in which isotopic techniques might be helpful. As usual, that abstraction "the intelligent layman" may find it rather heavy going.

The first half of the book is concerned with miscellaneous but necessary introductory matter; a review of the basic physics of radioactivity and nuclear reactions, the preparation and distribution of radio-isotopes and techniques of measurement. A chapter on stable isotopes has been included for completeness and some notes on the legal aspects of atomic energy has also been added. An unnecessary blemish here is the introduction of an element of controversy by the inclusion of some views of the authors on the quite irrelevant topic of the international control of atomic energy.

The last five chapters contain a selection of examples of the use of radio-isotopes in pure research, biology, medicine, agriculture and industry. It concludes by listing the isotopes available on a routine basis from the Atomic Energy Research Establishment, Harwell, together with their chief physical properties. Altogether, this is a very worthwhile publication.

W. A. Langmead

La cybernetique—theorie du signal et de l'information. By Louis de Broglie. (Paris: *Editions de la Revue d'Optique Theorique et Instrumentale 1951*.) Pp. 318. Price 1 600 *f*.

In the spring of each year since 1944 the Seminar of Theoretical Physics of the Henri Poincaré Institute of Paris has organized a conference on an aspect of theoretical physics and the papers presented have been published in small volumes similar to the one under review. The subjects chosen in the successive years have been the meson, electron optics, mesomerism, centimetre waves, interaction between the nucleus and its attendant electrons, particle accelerators, and, in 1950, cybernetics, with particular reference to the theories of signalling and of information. Since the sub-title gives the accurate description of the contents of the volume, the use of the word cybernetics as title is perhaps unfortunate, in so far as the manner in which the two are associated may extend the impression which has apparently been formed by some engineers in this country that information theory and cybernetics are one and the same; or at any rate that the former is merely a constituent part of the latter. However, the relationship between the two is brought out clearly enough in Professor de Broglie's preface and in the introductory paper by M. Julien Loeb. The book contains twelve other papers dealing with stationary and Markoff processes, and entropy, by R. Fortet; the filtering and prediction of messages according to Norbert Wiener, by M. D. Indjoudjian; noise in telecommunications, by A. Blanc-Lapierre; the transmission of information, by P. Aigrain; analytic signals and their transformations, by J. Oswald; the theory of communications and of physics, by D. Gabor; measure of the quantity of information, by J. Ville; analysis of the quality of telephonic transmissions, by P. Chavasse; loss of information by dispersion, by S. Colombo; television and the transformation of information, by Y. Delbord; multiplex methods of communication, by J. Icole; frequency compression, by P. Marcou, and, coding and information, by E. Picault.

The papers are of high standard and constitute a very useful contribution to the literature of a subject which promises to become of rapidly increasing importance. They have a particular interest for telecommunication engineers but their significance extends into several other spheres of scientific activity.

Willis Jackson

The surface chemistry of solids. By S. J. Gregg, Ph.D., F.R.I.C. (London: Chapman and Hall Ltd.) Pp. ix + 297. Price 30*s*. net.

The study of surfaces is a subject of great and growing importance and has technical ramifications in an extremely wide field of physical and chemical processes. Surface science has indeed already inspired a number of monographs and treatises. However, Adam's classical work, written with exceptional elegance, is now ten years old and is devoted largely to the physics and chemistry of *liquid* surfaces and interfaces. Similarly Brunauer's stimulating account of the adsorption of gases and vapours deals with a rather specialized field and his theories have evoked many criticisms and modifications in the last seven years. In the present book Dr. Gregg has very courageously attempted to provide an up-to-date survey, in less than three hundred pages, of our current knowledge of the surface chemistry of solids. The subject covers an enormous field and the author has deliberately omitted such items as electrode processes, electrokinetic phenomena and colloidal solids. The book covers four main themes. Firstly it deals with the structure and contour of solid surfaces, the porosity and permeability of solid materials, surface energies and true surface areas. Secondly it discusses the adsorption of gases and vapours by solids, the spreading of liquids over solids and the adsorption of liquids by solid materials. Thirdly it describes the adhesion between solids and the effect of adsorption on it and the corresponding mechanism of friction and lubrication. Finally it deals with the part played by solid surfaces in chemical reaction, catalysis and chemisorption. In addition many of the more important practical applications such as the swelling of clays and proteins, the sintering in powder metallurgy, the preparation of active solids, smokes and dust; and their removal, soldering, flotation and water proofings chromatography and ion-exchange are discussed at each stage.

In a survey of this kind it is inevitable that some of the themes are dealt with more fully than others. To the present reviewer, for example, the section on the part played by surfaces in chemical reaction could with advantage have been expanded. But this is a fault which errs if anything on the right side. On the other hand the treatment of adsorption, the discussion of the various types of isotherms and adsorption theories, the account of the work of Harkin and Bangham on the true energy of spreading, provide a very sound and critical evaluation of our present-day knowledge of adsorption processes. It is in this field that Dr. Gregg has himself carried out original research.

In his preface to this book Dr. Gregg has pointed out that the underlying concept which unifies the whole subject of surface chemistry is the presence of an unsaturated field of force at the free surface of a solid (or liquid). This concept has been applied by him with considerable success to a discussion of adsorption, adhesion, spreading and catalysis in later chapters. It seems, therefore, a pity that he has not included a somewhat more detailed account of the nature of the surface fields of force but has used it throughout in a rather vague descriptive way. In a later edition Dr. Gregg may be able to rectify this omission.

On the whole, however, this is an extremely readable book which will be of value to workers in the field as well as to those who wish to acquire a general knowledge of the subject. It should be particularly valuable to physicists who often overlook the important physico-chemical properties of the surfaces with which they have to deal. D. TABOR

Servomechanisms and regulating system design. Vol. 1. By H. CHESTNUT and R. W. MAYER. (London: Chapman and Hall Ltd., New York: John Wiley and Sons Inc.) Pp. xiii + 505. Price 62*s*.

This book is a welcome addition to a respected series; it is considerable both in size and performance. On the flyleaf the series is dedicated to the advancement of engineering practice. With these terms of reference the authors have admirably pursued their ideal by sifting and compiling from many sources a coherent statement of design methods together with charts, graphs and devices by means of which system design is reduced to a simple and unambiguous procedure.

The volume aims to be a comprehensive and self-contained statement of current practice and to this end it starts at an elementary level. For so specialized a topic this is perhaps a fault; but at worst a fault only leading to additional length (and cost!) It does not deal with details of apparatus but lays a firm foundation of design method based primarily on the sinusoidal response method of analysis and design, with emphasis on the simplification arising from the use of the logarithm of the transfer function plotted to a base of log. frequency. Adequate examples are given in the text applying the recommended methods and covering a satisfactory range of practical applications. The authors' viewpoint throughout is one of furthering design practice rather than extending understanding of fundamentals. They are content to tell the reader how, if not why. They clearly believe in the philosophy behind their method of presentation. In the most advanced chapter in which they seek to extend Nyquist's criterion of stability they readily admit defeat at a difficulty by appealing to Routh's criterion of stability (which is arrived at on an entirely different basis). In a book of this type these are small defects. Later in this chapter amends are made by a correct enunciation of the Nyquist criterion for the so-called inverse plot, which is commonly given incorrectly.

The bibliography is excellent, containing over 100 references, and the problems on each chapter will be most helpful to the novice. The authors have been at pains to approach their subject gently. The book is intended for those who need to design control systems and is essential for those who must design, repeatedly and in haste. J. H. WESTCOTT

Les systèmes asservis. By PIERRE NASLIN. (Paris: Revue d'Optique.) Pp. 333. Price 1 500 *f*.

Since the war, French engineers have made notable contributions to the science of automatic control. At the recent Conference on Automatic Control organized by the Department of Scientific and Industrial Research a prominent part was played by the strong French contingent, amongst whom was Major Pierre Naslin. It was therefore a disappointment to find an almost complete lack of original treatment in Major Naslin's book; it consists mainly of translations of excerpts from the classic American volumes and some British papers. The reason for this appeared on reading the foreword; such a collected translation was made deliberately to satisfy the greatest present needs of the French engineer.

The greater part of the book is based on the volumes by James, Nichols and Phillips, Brown and Campbell, Bode, and MacColl. Well-chosen excerpts from these and other works are collected into a general theme which is developed in the first eight chapters. Chapter IV, on the stability of linear systems, includes a more original treatment in the discussion of the generalized Nyquist criterion, or as the author very aptly names it, the Nyquist–Cauchy criterion; this is excellent. Chapters IX to XI on pulsed systems, statistical analysis, and R.M.S.-error criterion, are condensed translations of the corresponding chapters of James, Nichols and Phillips. The remaining chapters form very short introductions to multi-loop systems, servos in analogue computers, simulators and the human operator.

The author's claim that the sacrifice of rigour in the treatment has resulted in clarity of explanation is well justified. His further claim that he has supplied all the information necessary for practical application of the methods described is misleading; for instance, there is his statement on p. 307 that the presence of the capacity in the feedback circuit of an electronic integrator is sufficient to ensure its stability.

The advance copy sent for review contained a number of misprints which no doubt will not appear in the published version. Otherwise the volume is generally accurate. Very full references to original texts, and acknowledgements to most of them, are given, and there is a useful bibliography. There is, unfortunately, no index. R. H. TIZARD

Basic electrotechnics. By B. L. GOODLET. (London: Edward Arnold and Co.) Pp. vii + 247. Price 21*s*. net.

This book was written, Professor Goodlet says, "to teach engineering students . . . the basic minimum of electromagnetic theory." He discusses not only electromagnetic waves but also d.c. and a.c. circuits, ferromagnetism, and machines. Although not intended for beginners, the book starts at the beginning; it goes on to survey the physical bases of electrical engineering.

The survey is skilful. By discussing technical details only where they illustrate fundamental principles, Professor Goodlet both teaches the principles, and shows how engineering depends always upon them. He gathers together topics which are often scattered, and presents a view of electrical engineering as a whole. Rationalized M.K.S. units are used throughout, and there are plenty of worked examples and exercises.

Some flaws in the book reflect the difficulties of writing a compact yet comprehensive review *ab initio*. As a logical

summary of the elementary work, the early chapters just fail: current is defined as rate of flow of charge, but charge is not defined. Also, the standard of difficulty is uneven: the formula for resistances in series is derived, but the conservative property of the electrostatic field is taken for granted.

Rigour and elegance have been sacrificed, to make the book "more comprehensible to engineers." The sacrifice has marred the chapters on electrostatics and electrodynamics, and seems hardly necessary: engineers nowadays will accept serious physics, if its relevance to engineering is made clear.

And Professor Goodlet does make its relevance clear. He has passages, such as that on dielectrics in practice, which will delight any engineer-physicist. For both teachers and students his book will make a happy companion.

P. PARKER

The hardness of metals. By Dr. D. TABOR. (London: Oxford University Press.) Pp. ix + 175. Price 15*s*. net.

In this book, the property of "hardness" of metals, as determined by static indentation tests (Brinell, diamond pyramid and Rockwell) is approached in a new way. From considerations of past and present theoretical work on plasticity, the author demonstrates the reality of the correlation between the stress-strain diagram which can be drawn from a tensile or compression test, and behaviour in the hardness test.

Well-known empirical relationships, such as Meyer's law and the ratio between the Brinell hardness and the ultimate tensile strength of steels, are derived from equations representing the stress-strain curve. Explanations are provided for phenomena such as the piling-up or sinking-in of material which occurs around hardness indentations and leads to the observed differences between the shapes of diamond pyramid impressions in annealed and heavily worked metals.

The conclusions reached are supplemented by a considerable amount of experimental data, much of which is drawn from researches of Dr. Tabor and his co-workers. In most cases, the agreement with the theories advanced is remarkably close. Dynamic hardness testing is not forgotten, and the final chapter, in which the results obtained for the static hardness tests are employed to examine the problem of determining the real area of contact between two flat (and nominally smooth) metal surfaces pressed together, is very illuminating.

It is a pity that the author has employed the term "Vickers hardness," and abbreviations "V.D.H." and "B.H.N." for diamond pyramid and Brinell hardness number respectively. The descriptions and symbols employed by the British Standards Institution might with advantage be universally adopted for new writing.

Notwithstanding its theoretical bias, this is a book which the mechanical testing engineer will wish to have ready to hand.

A. J. FENNER

Theory and design of valve oscillators. 2nd edition. By H. A. THOMAS. (London: Chapman and Hall Ltd.) Pp. xv + 317. Price 36*s*. net.

The first edition of this book dealt with the fundamental theory of oscillators: it described the various forms they could take and the effect of circuit and component design on frequency stability. In the second edition, now under review, this material has been rearranged and recent developments have been included. Five new chapters have been added. One of them is on resistance capacity oscillators. In this, the ladder type of phase shift oscillator is dealt with in detail, but the various bridge type feedback oscillators are not mentioned. There is a short chapter on crystal oscillators, and one describing the various types of special triodes for use at ultra-high frequencies. The last two chapters are devoted to velocity modulated oscillators and magnetrons and give a concise picture of their operation. The scope of the book has been considerably increased, it is well produced and has very few misprints. It can be thoroughly recommended.

A. BODLEY SCOTT

Mathematical engineering analysis. By RUFUS OLDENBURGER, Ph.D. (London: Macmillan and Co. Ltd.) Pp. xiv + 426. Price 45*s*. net.

This book is written with the excellent intention of helping the reader to express "physical situations in the form of equivalent mathematical relations," which the author rightly regards as "one of the most difficult tasks in industrial research." Research workers and teachers alike know full well the difficulties experienced in trying to translate a physical problem into mathematics; it demands physical insight as well as mathematical powers. This volume does not deal with special mathematical techniques but with the setting up of engineering problems in mathematical form. It derives from the author's industrial experience and is based on his lectures at the Illinois Institute of Technology and also at De Paul University.

The first part of the book deals with mechanics. Chapter I is a short survey of the dynamics of particles and rigid bodies; it has some unorthodox features which might attract the experienced reader but it is too general and concentrated for one with little previous knowledge. The second chapter turns to some practical problems concerned with cars, rockets, marine propellors and such machines as can be considered as combinations of springs, dash-pots and rigid bodies. All this would be much more valuable if the author had paid more attention to the formulation of the basic equations and he would thereby have more nearly achieved his avowed aim.

The same sequence of theory and problems is followed in the other four parts of the book, which deal with electricity and magnetism, heat, elasticity and fluid mechanics. The classical theory of electricity and magnetism is condensed into fifty pages; it is strange in a book such as this to find the potential of an electrostatic field defined mathematically and *later* given a physical interpretation. And Gauss's Theorem is "proved" by assuming Laplace's equation! Most of the practical examples discussed are associated with electric circuits. Maxwell's equations are derived and a few consequences discussed.

The heat section deals mainly with thermodynamics and heat transfer. Part IV opens with a general discussion of stress and strain, and passes on to the usual two- and three-dimensional problems in elasticity. After discussing, rather unsatisfactorily, the helical spring the author writes, "The above analysis would have little value unless verified by experiment, inasmuch as we have by-passed the fundamental equations of elasticity because of the more or less complicated shape of the wire in the spring"!

Units are treated carefully throughout (the slug is taken as the unit of mass!) and several examples of dimensional analysis are given. Also, the problems set for the reader are interesting and unusual in design and in keeping with the author's main aim. But one cannot help feeling that too much has been attempted in one volume; it is perhaps too ambitious to try and provide "a reference work for research directors" and at the same time to make clear the nature of mathematical engineering analysis.

J. TOPPING

Notes and comments

Elections to The Institute of Physics

The following elections have been made by the Board of The Institute of Physics:

Fellows: E. R. Andrews, R. W. Dunn, D. M. Heller, H. J. L. Herne, E. G. Richardson, D. Rogers, W. J. Thomas.

Associates: W. D H. Blackman, W. Bullerwell, J. L. W. Churchill, J. Dutton, K. D. Exley, P. G. Hambling, R. C. Hart, S. C. Haydon, J. Hurst, M. Kerridge, J. K. Lancaster, Miss E. Laverick, E. L. Lovering, R. G. Martin, C. G. Morgan, S. M. Mukherjee, B. W. Osborne, P. J. Palmer, F. Parry, L. W. Phipps, B. O. Smith, J. B. Smith, S. K. Stephenson, P. Vousden, H. M. Wilson, L. C. Wiltshire, R. Wolsey, D. Wroe.

Ninety-one Graduates, thirty-eight Students and seven Subscribers were also elected.

Fourth Conference on Industrial Physics

The Fourth Conference on Industrial Physics is being arranged by The Institute of Physics to take place in the Royal Technical College, Glasgow, from 24–28 June next. The subject of the conference is "Physics in the transport, shipbuilding and engineering industries." About 70 firms and Government and other research organizations have accepted invitations to take part in an exhibition of instruments, apparatus and books cognate to this subject. The programme includes lectures and discussions on the physics of metals, meteorology and industry, The education and training of industrial physicists in Scotland, Physics and sound reproduction, Applications of physics in naval architecture, Application of physics in transport, Automatic control of industrial processes and Noise and its suppression. In addition, a number of visits to research laboratories and local works have been arranged and some trips to local beauty spots. The social events include a civic reception and a conference lunch. All interested, whether members of the Institute or not, may attend the conference and there will be no conference fee; ladies will be welcome.

The conference is to be opened by Lord Bilsland, President of the Scottish Council, and has the support of distinguished scientists and industrialists. The Chairman of the organizing committee is Sir Andrew McCance, Joint Managing Director and Deputy Chairman of Colvilles Ltd.

Full particulars and forms of application for conference membership may be obtained from The Secretary, The Institute of Physics, 47 Belgrave Square, London, S.W.1, to whom they should be returned before 15 May next.

Physics as a career

The Institute has now published a small book entitled "Physics as a career" which has been written by the Deputy Secretary, Mr. N. Clarke, F.Inst.P. It is intended to provide school masters, university students, school boys and girls and their parents with authoritative information about courses of training in physics and the opportunities in different branches of the profession. The book, which is illustrated, is available at 6*s.* net from booksellers or direct from The Institute of Physics, 47, Belgrave Square, London, S.W.1.

Third International Spectroscopy Colloquium, 1952

The Industrial Spectroscopy Group of The Institute of Physics is arranging the Third International Spectroscopy Colloquium to be held in England from 1–3 September, 1952. The conference will be residential and will be held at High Leigh, Hoddesdon, Hertfordshire, about one-and-a-quarter hours journey from central London. As the total attendance is limited to about 120, early application for enrolment forms is necessary; there will be accommodation for a few married couples.

The programme will provide for papers and discussions in eight short sessions. Two sessions will probably be devoted to reviews of progress in some special aspects of spectroscopy and it is hoped also to have papers on various branches of absorption spectroscopy as well as on emission and direct-reading methods. All communications concerning the conference, including suggestions for speakers, should be addressed to The Honorary Colloquium Secretary, Mr. E. Van Someren, The Institute of Physics, 47 Belgrave Square, London, S.W.1.

Journal of Scientific Instruments

Contents of the April Issue

ORIGINAL CONTRIBUTIONS

Integrating and other galvanometers. By A. H. Bebb.

A fast amplitude discriminator and scale-of-ten counting unit for nuclear work. By F. H. Wells.

Manual temperature compensation of a substandard multi-range d.c. meter. By B. V. Hamon and R. L. Gregory.

A modified "thermal conductivity" gas analyser for measuring methane in air or carbon dioxide. By F. W. Pritchard.

A Fourier electron-density balance. By V. Vand.

Some considerations on the design of the re-entrant tube vapour trap. By D. W. Stops.

A brightness temperature pyrometer using a photoconductive cell. By E. C. Pyatt.

A simplified scanner for X-ray diffraction. By F. A. Underwood.

A method of measuring the depth of haemacytometer counting chamber cells. By L. O. C. Johnson.

LABORATORY AND WORKSHOP NOTES

Demountable vacuum seals. By J. R. W. Smith.

A miniature hot plate and radiant heat dryer. By F. Hudswell and K. L. Wilkinson.

A modified specimen mounting for a high temperature X-ray camera. By R. L. Berry and W. G. Henry.

Dead time correction for monitored counters. By W. H. Hall and G. K. Williamson.

Prevention of electric charge formation on plastic surfaces. By B. H. Parks.

Mounting of Nernst filaments. By J. L. Hales.

Preserving sodium iodide crystals. By A. J. Salmon and E. K. Inall.

CORRESPONDENCE

Substitution of a fast thermocouple for a bolometer in an infra-red spectrometer. From A. R. Roberts.

Double monochromator optical system based upon ideas of Czerny and Turner. From V. Roberts.

NOTES AND COMMENTS

THIS JOURNAL is produced monthly by The Institute of Physics, in London. It deals with all branches of applied physics (including theory and technique). All rights reserved. Responsibility for the statements contained herein attaches only to the writers.

EDITORIAL MATTER. Communications concerning editorial matter should be addressed to the Editor, The Institute of Physics, 47 Belgrave Square, London, S.W.1. (*Telephone:* Sloane 9806.) Prospective authors are invited to prepare their scripts in accordance with the *Notes on the Preparation of Contributions.* (Price 2*s.* 6*d.* including postage.)

ADVERTISEMENTS. Communications concerning advertisements should be addressed to the agents, Messrs. Walter Judd Ltd., 47 Gresham Street, London, E.C.2. (*Telephone:* Monarch 7644.)

SUBSCRIPTION RATES. A new volume commences each January, and annual subscriptions will only be accepted for complete volumes of the monthly parts (January–December). The charge is £4 per volume ($11.50 U.S.A.), including index (post paid), payable in advance. Single parts, so far as available, may be purchased at 8*s.* each ($1.15 U.S.A.), post paid, cash with order. Orders should be sent to The Institute of Physics, 47 Belgrave Square, London, S.W.1, or to any Bookseller.

SPECIAL REPORT

Report of conferences on electron microscopy—Washington and Philadelphia 1951

As part of its fiftieth anniversary celebrations, the National Bureau of Standards organized during 1951 a number of symposia on special topics in the physical sciences. That on electron physics, to which a number of visitors were invited from other countries, was held in Washington from 5 to 7 November. The annual meeting of the Electron Microscope Society of America (E.M.S.A.) was arranged to follow it, from 8 to 10 November, in Philadelphia. The two meetings together formed the most representative gathering of electron microscopists for some time, the leading workers from Germany, France, Britain and Japan being present as well as those from Canada and the United States. The contributions summed up the present state, and in some sense also the future prospects, of the subject. The papers dealing with the fundamental electron-optical and technical problems were given at Washington, whilst the Philadelphia meeting was concerned with specimen techniques and applications of the electron microscope. They are summarized in this report. Several sessions at Washington were also devoted to electron scattering in general, but these are not summarized in the report except where they concern electron microscopy.

The proceedings of the Washington symposium will be published in full, and the abstracts of the E.M.S.A. meeting in Philadelphia are already available,[1] so that only the outstanding contributions and certain general trends will be reported. The most striking feature of the symposium was that practically all the papers on theoretical electron optics came from Europe. The two exceptions were concerned with special topics not directly related to electron microscopy. Brillouin discussed the theory of the magnetron, to which Gabor also had ideas to contribute. Lachenbruch dealt with the theoretical aspects of the electron optical schlieren method for the micro-exploration of electron-magnetic field distributions. Apart from these, the American contributions dealt with instrumental matters such as electron scattering and phase contrast effects. It is characteristic of the present state of the subject on the two sides of the Atlantic that in Europe much attention is still being devoted to the properties of electron lenses as such, whilst in the United States efforts are directed to making the best use of the lenses, and the complete microscopes, which now exist. The new ways of treating aberrations theoretically, and of correcting or avoiding them in practice, are being developed in Europe. The most consistent high resolution is obtained in America, and electron microscopes are being produced at the fastest rate there.

The rigorous treatment of electron lenses was considerably clarified by Glaser with a wave-mechanical approach, avoiding the unsatisfactory combination of geometrical optics and wave optics usually employed in discussing aberrations. It takes account of the chief particular in which an electron beam differs from light in its interaction with an object: electron scattering is mainly forward, the object being much larger than the wavelength, so that the aperture is not filled as it is by the spherical scattering of a light wave. Starting from Schroedinger's equation, Glaser derives the complete paraxial behaviour of a lens, and then treats the aberrations by perturbation methods. The satisfying rigour of the treatment leads, however, to only slight modification in the numerical constants in the expressions for resolving power and optimum aperture. It gives a clear relation between the size of an opaque particle and the width of its disk of confusion, which is helpful in interpreting practically achieved resolution. A less fully developed wave-mechanical treatment was put forward by Bremmer.

The development of special types of electron microscopes, and of systems for avoiding or correcting spherical aberration, is again confined almost exclusively to Europe. The method of diffraction microscopy proposed by Gabor[2] was further developed by him in a theoretical paper, whilst Haine described the progress made experimentally in a modified electron microscope. Scherzer's scheme[3] for introducing cylindrical lenses as correction elements was clarified theoretically by the work of Regenstreif on electrostatic lenses with a central elliptical electrode, on which some British work also bore. Special microscopes for surface study by electron reflexion are being built at two places in Britain and one in France, and at least one scanning microscope for a similar purpose. Cosslett and Nixon described an X-ray shadow microscope, which allows living specimens to be observed with an ultimate resolution limited in the first place only by the exposure which can be tolerated. Marton proposed a similar scheme which would use the high intensity of emission from a cold tungsten cathode, and thus reduce exposure times. His laboratory is also developing the schlieren method of investigating electromagnetic fields with an electron beam.[4] The only other American work of a special nature is that of Becker, and of Dyke and Trolan, on the field emission point projector microscope. The perfector of this technique, E. W. Müller,[5] demonstrated it with a projection tube. There was some difference of opinion as to whether the effect of single atoms could be observed as he claimed. A new development is to reverse the polarity of the tungsten point, so as to form the image by means of previously adsorbed positive ions. If such a tube could be operated with protons, the resolution should be 3 Å instead of the 20 Å when electrons are used.

Development of the existing types of electron microscope is more balanced in location. The recently announced RCA table model[6] is the first to use permanent magnet lenses. A full discussion was given by E. Ruska of the design of magnetic circuits of variable reluctance for this purpose, which would permit continuously variable magnification and focusing. Liebmann and van Dorsten both dealt with the design of a magnetic lens of minimum focal length and chromatic aberration. The way is now open for the production of a relatively cheap magnetic microscope of sufficient flexibility and high enough performance for all routine purposes. Two electrostatic instruments of this type are in an advanced state of development in the U.S.A.

Technical details of the standard type of electron microscope were discussed in papers by Haine on electron gun performance, by Bertein on the breakdown between metal electrodes in a vacuum, and in a general session on experimental techniques. The latter revolved mainly around the

maintenance of high vacuum, and the source of contamination of specimens in the electron beam. The work of Ellis of the Radio Corporation of America and of Haine of Associated Electrical Industries Ltd. shows the practical impossibility of avoiding such trouble, except in an all-glass apparatus. It is especially disturbing in work at very high resolving power. Apart from linear resolving power, the question of contrast arises when particles approaching atomic dimensions are to be viewed. Many attempts have been made, based on theoretical laws of electron scattering, to estimate whether single atoms could be observed. The first experimental investigations of scattering in the circumstances prevailing in electron microscopy are now being made by Hall[7] and Ellis, the latter from the contrast of electron diffraction rings and the former from that of shadow edges and of images in the transition from bright to dark field. The cross-section thus obtained agrees fairly well with theory,[8] but gives a rather less optimistic estimate of minimum observable size. Individual atoms of uranium should be detectable, but only a 25 Å cluster of carbon atoms.

Now that very high resolutions are available, the use of very thin or very small objects for imaging leads to interference effects becoming visible in electron micrographs. Hillier described two such phenomena in thin plate-like crystals, such as graphite. Boersch gave a more general theoretical discussion of phase contrast effects which occur by elastic scattering from objects comparable in size with the resolution limit. Both Hall and Hillier drew attention to the false appearance which may arise in such cases if the image is slightly out of focus; a periodic structure will show wide variations in appearance in a through-focal series.

At Philadelphia, the E.M.S.A. programme was rather overcrowded, 56 papers being presented in two and a half days, with one afternoon given up to a symposium on "Elementary electron optics and factors affecting the electron microscopical image." The latter was mainly interesting as reflecting the standard of knowledge of the physical principles of the subject prevalent among American users of the instrument.

At an altogether different level was the discussion by Hillier of the factors standing in the way of attaining the high resolution which is theoretically possible even with existing electron lenses. These are mainly of a mechanical and thermal nature in the specimen, and electrical instabilities in the beam. He also drew attention to the need to use finer-grained, less sensitive photographic emulsions to obtain adequate contrast when working at the resolving limit of the microscope. Two more technical papers were contributed on the investigation of the sensitivity of emulsions to electrons. A bright spot of the meeting was the display of electron micrographs in colour, obtained by a special processing method; the colours do not of course necessarily correspond to those of the original object.

The reliability of Dow Latex 580G particles as a magnification standard was further discussed. A new investigation by Watson and Grube showed sizes up to 3 000 Å, compared with the previously accepted average of 2 700 Å.[9] Ellis had meantime proved, by deposition of samples at different concentrations, that extraneous material was present which settled as a blanketing layer over the particles and added considerably to their observed diameter, especially from concentrated suspension. He found a true size of approximately 2 450 Å, in good agreement with earlier measurements from a dilute suspension.[10]

A number of improvements in preparation techniques were reported, particularly for adequately dispersing particle suspensions. The droplet spraying method of Backus[11] has been extended by him to deal with pathogenic organisms safely, and by Williams to obtain larger bodies such as blood cells in drops of liquid so small that they can be rapidly freeze-dried. They then retain their three-dimensional form more perfectly than after ordinary drying, very much as in Anderson's triple-point method of desiccation,[12] further results of which were described by him.

The most notable advance has been made in methods of cutting thin sections. Several existing types of microtome have been adapted and a number of special models made, to cut sections of 0·1 μ and even thinner. The tendency is to avoid mechanical means of advancing the specimen block, relying on thermal expansion of the support to move it towards the knife at an adequate rate. A plate glass sliver is much favoured as cutting edge.[13] A great deal of critical investigation is being conducted into the best method of fixation of biological tissue for electron microscopy. Preference is given to formalin (Wyckoff) or osmic acid buffered at *p*H 7·3 (Pallade and Porter). Several papers presented results in which the electron micrographs were free of obvious artefacts and agreed well in their larger features with optical evidence. A critical paper by Bang and co-workers, on details of cell structure seen in tissue cultures, also showed good agreement between phase contrast and electron pictures. The beginnings of a reliable body of experience in electron microhistology is evident. In the same vein, Richards reported an extensive series of tests of heavy metal stains for insect cuticle.

In bacteriology the identification of the main components of cell morphology continues. Following the demonstration of the nuclear regions as those of low physical density in the normal cell,[14] Mudd presented evidence that the dense areas have the characteristics of mitochondria. Otherwise attention was concentrated on the formation and activity of bacterial viruses. Convincing evidence of the stages in their multiplication was shown by Levinthal and Fisher, the bacteria having been broken open at different times by a decompression technique.[15]

It remains to remark that no applications of a metallurgical nature were reported, and few to inorganic materials, aside from some work on the structure of clays and a number of particle-size studies. It may well be that the electron microscope is being as much used in America as in Europe for the study of metals, but if so the evidence is not published. The report of the committee of the American Society for Testing Materials on the reliability of replica techniques[16] has gone a long way to make electron microscopy respectable in metallurgy. Nevertheless, it is true that much more work appears to be done on biological applications, and now with a critical spirit which was absent from much of the early work.

V. E. COSSLETT

REFERENCES

(1) Proceedings of the Electron Microscope Society of America. *J. Appl. Phys.*, **23**, p. 156 (1952).

(2) GABOR, D. *Proc. Roy. Soc. A*, **197**, p. 454 (1949); *Proc. Phys. Soc. B*, **64**, pp. 244, 449 (1951).

(3) SCHERZER, O. *Optik*, **2**, p. 114 (1947); *J. Appl. Phys.*, **20**, p. 20 (1949).

(4) MARTON, L., and LACHENBRUCH, S. H. *J. Appl. Phys.*, **20**, p. 1171 (1949).

(5) MÜLLER, E. W. *Z. Phys.*, **106**, p. 541 (1937); **126**, p. 642 (1949).

(6) REISNER, J. H., and DORNFELD, E. G. *J. Appl. Phys.*, **21**, p. 1131 (1950).

(7) HALL, C. E. *J. Appl. Phys.*, **22**, p. 655 (1951).

(8) HILLIER, J., and RAMBERG, E. G. *Z. angew. Physik*, **2**, p. 19 (1950).
(9) GEROULD, C. H. *J. Appl. Phys.*, **21**, p. 183 (1950).
(10) COSSLETT, V. E. *Proc. Conf. Elect. Mic. Delft*, p. 64 (The Hague: N. Nijhoff, 1949).
(11) BACKUS, R. C., and WILLIAMS, R. C. *J. Appl. Phys.*, **21**, p. 11 (1950).
(12) ANDERSON, T. F. *J. Appl. Phys.*, **21**, p. 724 (1950); *Biol. Bull.*, **99**, p. 315 (1950).
(13) LATTA, H., and HARTMANN, J. F. *Proc. Soc. Exp. Biol. Med.*, **74**, p. 436 (1950).
(14) ROBINOW, C. F., and COSSLETT, V. E. *J. Appl. Phys.*, **19**, p. 124 (1948).
HILLIER, J., MUDD, S., SMITH, A. G., and BEUTNER, J. *J. Bact.*, **60**, p. 641 (1950).
(15) FRASER, D. *Nature, Lond.*, **167**, p. 33 (1951).
(16) Report of Sub-Committee on Microstructure of Steel. *Proc. Amer. Soc. Test. Mater.*, **50**, p. 444 (1950).

ORIGINAL CONTRIBUTIONS

Time-resolved spectroscopy of spark discharges

By F. TSUI, B.Sc., Department of Electrical Engineering (Electronics), University of Liverpool

[*Paper received* 25 *September*, 1951]

Using a rotating-mirror and a spectrometer, the spectra of the light emission from spark discharges in several gases have been photographed at different instants after the current-initiation. By triggering the discharge recurrently in synchronism with the mirror, the time-resolved spectral images of a number of sparks were superposed to obtain sufficient blackening on the photographic plate. The triggering circuit was activated by the rotating-mirror, and, when provided with a counter, the system could be left in automatic operation.

INTRODUCTION

In the spectroscopic studies of transient emission phenomena, either the method of rotating-mirror photography or the photomultiplier technique may be used in conjunction with a spectrometer. Of these, the latter is often the more convenient to use, by virtue of its relative simplicity in mechanical and optical arrangements, its better time-resolution and its more straightforward calibration. But when the emission under study happens to be rather complex in spectral content, it is often useful to obtain the complete spectrum first in a rotating-mirror photograph, which can then be used as a qualitative guide in the photomultiplier investigation and as an aid to the subsequent analysis of the results. If the emission is not strong enough in intensity, the phenomenon may be arranged to recur, and an accumulated time-resolved spectrum may be obtained.

Rotating-mirror photographs of the latter form have been obtained for spark discharges in several gases, including argon, helium, neon, and air.

DESCRIPTION OF THE APPARATUS

The discharge was between two pointed tungsten-electrodes separated at 1·0–1·5 cm in gases at atmospheric pressure, in a cylindrical glass chamber fitted with a flat window. A length of coaxial cable, charged to about 20 kV, was discharged through the gap, and gave sparks carrying 200 A square current-pulses of 4 μsec duration.

The luminous channel (C in Fig. 1, horizontal) of the spark discharge was first focused, by means of lens L_1, on and across a (vertical) slit S_1. The light from a narrow central section of the image thus selected and admitted by S_1 was then focused, by lens L_2 and after reflexion by mirror M (when it was in the correct position), on to the plane of S_2. When M was set into rotation about a vertical axis, the image formed at S_2 became smeared out along a horizontal time-axis.

When recurrent sparks were triggered in synchronism with the mirror-rotation, the time-resolved streak-shaped image obtained at S_2 would appear every time in the same position in space. By placing the front slit of a spectrometer here across the "streak," the emission from the discharge at a certain instant after the current-initiation was selected and dispersed into its spectral components. With a sufficient number of sparks superposed together, a time-resolved spectrum could thus be photographed.

A small auxiliary mirror M', fastened on the lower part of the main-mirror shaft, reflected the light from a fixed source into a photomultiplier-tube and generated pulses of the mirror-rotation frequency. The train of pulses was fed

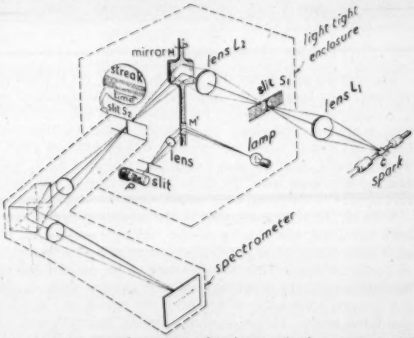

Fig. 1. Diagram of apparatus for time-resolved spectroscopy of spark discharges

C, 1–1·5 cm; L_1, $f = 2$ in at $f/1·5$; S_1, about 0·5 mm; L_2, $f = 5$ in at $f/2·9$; M, $2\frac{1}{4} \times 2\frac{1}{8} \times \frac{1}{16}$ in; S_2, about 20 μ; P, photomultiplier tube, Type 931A.

into a monostable-multivibrator circuit with large time-constants, reducing the frequency to the order of 1 pulse/sec. This time-selection operation was to allow ample time between successive sparks for the recharging of the square-pulse-forming cable to a full constant voltage.

To provide a fine adjustment by which the "streak" could be shifted continuously across the spectrometer slit, the low-repetition-frequency pulses were passed through a variable-delay circuit before they went to activate the blocking-oscillator unit which triggered the trigatron in the main discharge circuit.

The triggering circuit, shown in Fig. 2, was thus automatic in operation during the mirror-rotation. It was also provided

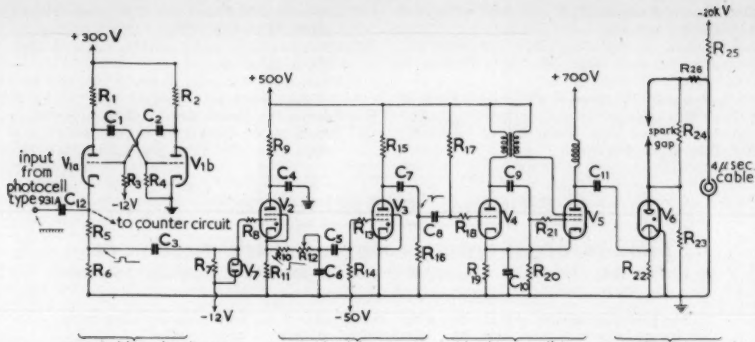

Fig. 2. Triggering circuit for photomultiplier

R_1 = 50 kΩ; R_2 = 47 kΩ; R_3 = 3·6 MΩ; R_4 = 25 kΩ; R_5 = 1·5 kΩ; R_6 = 4 kΩ; R_7, R_{14} = 1 MΩ; R_8 = 2 kΩ; R_9, R_{15} = 2·2 MΩ; R_{10}, R_{19} = 5 kΩ; R_{11} = 2 kΩ; R_{12} = 20 kΩ potentiometer; R_{13} = 220 Ω; R_{16} = 2·2 kΩ; R_{17} = 270 kΩ; R_{18} = 100 Ω; R_{20} = 470 kΩ; R_{21} = 360 Ω; R_{22} = 3 MΩ; R_{23} = 50 MΩ; R_{24} = 80 MΩ; R_{25} = 4 MΩ; R_{26} = 51Ω, 10 W; C_1, C_6, C_7, C_8 = 0·01 μF; C_2 = 0·25 μF; C_3 = 200 μμF; C_4, C_{12} = 0·1 μF; C_5 = 0·002 μF; C_9 = 220 μμF; C_{10} = 25 μF; C_{11} = 0·015 μF (10 kV); V_1 = 6SN7; V_2, V_3 = 2D21; V_4 = SP61; V_5 = CV73; V_6 = CV100; V_7 = VR92

with an electromagnetic counter to register the number of sparks photographed in superposition.

The spectrometer used was a small Hilger constant-deviation model, capable of giving spectra from 3 600 to about 6 700 Å in some 5·5 cm on the photographic plate. The slit-width used was about 20 μ.

OPERATION

The mirror was driven by a ¼ h.p. motor on controlled voltage. The speed of the mirror-rotation was measured to 1% accuracy by comparing the pulses from the multiplier with a standard oscillator on a double-beam oscilloscope. In the equipment used, the mirror-to-image distance (MS_2) was 7½ in (19·5 cm) so that the linear resolution at S_2 was about 1 mm/μsec when the mirror was turning at 400 r.p.s., and about 0·5 mm/μsec when at 200 r.p.s.

With all the voltage-supplies to the triggering circuit carefully stabilized, the jittering of the "streak" was found, by observation with a low-power microscope at S_2, to be within ± ½ μsec or less. This was believed to be mainly due to fluctuations in the blocking-oscillator circuit, since it did not become appreciably worse when the mirror was turning at a lower speed. Hence, in order to avoid excessive wear of the mirror bearings, the lower rotation-speed of 200 r.p.s. was decided upon and, with the slit S_1 at about 0·5 mm, the overall time-resolution at S_2 was about 1 μsec.

The selection of the finite instant after current-initiation for spectrographing was done by shifting the "streak" across the spectrometer slit, by changing either the position of the light-source for the auxiliary mirror or the variable delay in the triggering circuit, the latter being the finer adjustment. The time-lapse between the current-initiation and the instant chosen was, of course, given by the distance between the slit and the head of the "streak" divided by the linear resolution (in this case, 0·5 mm/μsec). This distance was conveniently determined by fixing a scale on the "earlier" side of the slit and observing the "streak" thereon through a small hand-mirror. On a scale graduated in millimetres, ½ mm (1 μsec) could be read with fair accuracy.

It was found that the lateral (up-and-down) movement of the channel could be considerably minimized, if sufficient pre-breakdown voltage was applied across the gap so that corona-discharge or in some cases intermittent streamers were allowed to take place and provide a pre-ionized path. That this streamer-discharge or other possible sources of unwanted stray-light did not make any detectable contribution to the spectrum or the actual background photographed, was later carefully checked by having the mirror stationary in the reflecting position and taking an exposure of an interval equivalent to or in excess of that in the case when the mirror was running.

The technique has been independently developed and used on high-current sparks and exploded wires in America,* where a greater section of the channel (or wire) was taken and the slit S_2 was placed parallel to the time-axis of the "streak." Of these different arrangements, the former served to reduce the loss of unused radiation, though at the expense of losing time-resolution and at the risk of introducing metal-vapour effects in the early stages of the spark. The latter, while making no difference in the time-resolution and the exposure required for a given equipment, had the ingenious advantage of showing the continuous variation of the spectra in the interval covered by the length of the slit. Unfortunately, such an arrangement becomes unsuitable when the discharge has a long afterglow or when, especially in the case of low-current sparks, the channel's lateral movement is comparable with its width.

The technique, if incorporated with emulsion-response calibrations, could be used also for quantitative measurements. But this was not pursued, since the photomultiplier seems a more time-saving alternative with a much simpler calibration procedure.

ACKNOWLEDGEMENTS

The writer wishes to express his gratitude to Messrs. Alfred Holt and Co. for their kind support of his work at the University of Liverpool, and to Dr. J. D. Craggs for his invaluable guidance and encouragement in the course of this work.

* GORDON, G., and CADY, W. M. *J. Opt. Soc. Amer.*, **12**, p. 852 (1950).

A graphical treatment of the tone reproduction problem in television systems*

By R. B. MACKENZIE, B.Sc.(Eng.), A.M.I.E.E., Research Laboratories, The General Electric Co. Ltd., Wembley, Middlesex

[*Paper first received* 27 *August*, 1951, *and in final form* 22 *October*, 1951]

The impracticability of analysing the tone reproduction properties of a television system in terms of simple mathematical laws is discussed. A construction for a tone reproduction chart is presented which enables a realistic assessment of the overall performance of a system to be made, subjective effects being taken into account. The use of the chart is demonstrated by examining the effects of altering certain parameters of the system.

The simple theory of tone reproduction, originating in photography and commonly applied to television, involves the assignment to each component of the system of a value of gamma (definable broadly as the average slope of the log output/log input curve). The product of the individual values gives the overall gamma, which is taken as a measure of the apparent increase or decrease in tone differences.

There appears to be a growing realization, however, that such a treatment is inadequate to account for observed effects. This paper surveys the factors in a television system which tend to limit the usefulness of mathematical analysis; one such factor often neglected is the response characteristic of the human eye.

NOMENCLATURE AND SYMBOLS

The nomenclature used in the present communication is in accordance with recent British practice. The physical quantity, variously denoted in the literature by "physical brightness," "objective brightness," "photometric brightness," and "brilliance," is termed luminance; the unit is the foot-lambert (ftl). The ratio between maximum and minimum luminance in a picture or scene is denoted by "luminance range." The response of the visual system to luminance is termed "luminosity." This supersedes such terms as "apparent brightness" and "subjective brightness."

List of Symbols

E_p = print exposure
k = constant
L = screen luminance (raster)
L_0 = luminance in original scene
L_r = luminance in reproduction
O = opacity of negative (= 1/transmission factor)
T = transmission factor of negative (= transmitted illumination/incident illumination)
v_c = camera output voltage (amplified to arbitrary level)
v_m = cathode-ray tube modulator/cathode voltage
v_n = cathode-ray tube drive voltage
v_r = virtual drive volts, i.e. modulator volts measured from virtual black-out point (see text)
α = constant
β = constant
$\gamma_1 = \Delta \log O / \Delta \log L_0$ at straight-line portion of curve
$\gamma_2 = \Delta \log L_r / \Delta \log (1/E_p)$ at straight-line portion of curve
$\gamma_3 = \Delta \log L_r / \Delta \log L_0$ at straight-line portion of curve
λ = slope of $\log L / \log v_r$ curve

VISUAL RESPONSE CHARACTERISTICS

General. As a general rule, the eye is the ultimate judge of quality in tone reproduction; i.e. it is the relation between reproduced and original luminosities, rather than luminances, that is of interest.

Luminosity, by definition, is a sensation. Whether or not sensations can be measured is still a matter for debate. For practical purposes, however, useful results can be obtained by estimating magnitudes in terms of just perceptible differences. A just perceptible difference at a given level of luminosity cannot with any exact meaning be said to be the same as a just perceptible difference at another level, and the units are, therefore, not necessarily strictly additive. It has been found, however, that by treating them as such results are obtained which are in accordance qualitatively with actual experience.

It is frequently stated that the eye has a logarithmic response to increments of luminance, i.e. luminosity is proportional to log. luminance. Obviously this can only be partially true, since it is a matter of common experience that for a given adaptation level there is a certain value of luminance below which the eye can no longer distinguish differences; the darkest part of a television picture usually approaches, if it does not reach, this limit, as judged by the eye. Television viewing must therefore utilize in part a non-logarithmic region of the visual response characteristic.

Luminosity/luminance curves directly applicable to the complex conditions of television viewing are not available. The ensuing investigation is based on a set of curves published by Hopkinson, Stevens, and Waldram,[1] which in turn are based on data derived from a number of sources. They are thought, therefore, to be possibly of more general application than those obtained by Jones,[2] which are qualitatively similar although somewhat different quantitatively. The application of these curves to television practice will now be discussed with reference to Fig. 1.

APPLICATION OF LUMINOSITY/LUMINANCE CURVES TO TELEVISION

(*a*) *Viewing conditions.* Under domestic television viewing conditions, the screen fills a sufficiently large portion of the field of view to play a considerable part in determining the effective adaptation level. This can be readily demonstrated by comparing the luminosity of the background with and without a picture on the screen.

The average background luminance can only be roughly estimated, but 0·5 ftl is thought to be a representative figure. If a maximum screen luminance of 15 ftl and a minimum of 0·15 ftl are assumed, as being representative of present-day practice, a reasonable estimate of the adaptation level, which need not be determined with any exactitude, would appear to be 1 ftl. The characteristic of the eye when adapted to 1 ftl is indicated by Curve I of Fig. 1.

(*b*) *Studio conditions.* The incident illumination in B.B.C. television studios has been quoted as 150 to 250 lm/ft^2, and luminance limits in one typical scene as 200 ftl and 3 ftl.[3] For the purpose of the present investigation a somewhat arbitrary lower limit of 1 ftl has been selected, and the adaptation level is estimated at 30 ftl. Curve II, then,

* Communication No. 482.

represents the visual response characteristic for typical studio conditions.

(*c*) *Outdoor conditions.* An extensive investigation, reported by Jones,[2] into the luminance ranges encountered in outdoor scenes under a wide variety of conditions, shows that luminance values may be as high as 11 500 ftl and that the range in one scene may be 750 ftl. The average luminance range for a large number of scenes was found to be 160 ftl.

Although there are cameras sensitive enough to transmit a scene having a peak luminance of 1 ftl, such conditions can be regarded as exceptional. The general conclusion can be drawn that in the vast majority of transmissions the average level of luminance on the screen is less than that in the scene viewed by the camera, the reduction factor being anything up to 800.

The condition selected for investigation is the extreme one where maximum and minimum luminances are 10 000 ftl and 13 ftl respectively, and adaptation luminance 1 000 ftl (Curve III of Fig. 1). The upper part of the curve, extending into the glare region, is somewhat conjectural.

The curves were obtained for white light; the assumption in the following treatment is that they are correct for all colours, and that the spectral response of the camera is also uniform. A more exact treatment, however, would call for the use of separate curves for each primary colour.

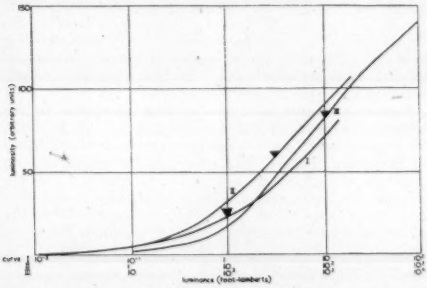

Fig. 1. Curves showing relationship between luminosity and luminance. The adaptation luminance for each curve is indicated by an arrow-head

APPARENT DISTORTION DUE TO THE EYE

Any substantial overall reduction in the luminance of a scene has a marked effect on the appearance of the scene to the eye. The effect is illustrated graphically in Fig. 2 for a reproduction at 1/700 of its original luminance of a scene in which the maximum and minimum luminance values are 10 000 and 13 ftl respectively. In this curve luminosity values in the reproduction as derived from Curve I of Fig. 1, are plotted against the corresponding luminosity values in the original, derived from Curve III of Fig. 1. The effect observed is that one just distinguishable step in the reproduction represents about one in the original towards the higher end of the scale, and about 4 towards the lower end; in other words, from grey to black there is an increasing loss of gradation.

Under the viewing conditions postulated the distinguishable steps in the reproduction cannot exceed about 80; some loss of gradation is therefore inevitable unless the steps visible in the original are also limited to 80, which corresponds to luminance limits of, say, 250–4 000 ftl or a luminance range of 16. It is only in exceptional scenes that the range does not exceed this figure. If it is accepted as a criterion of faithful

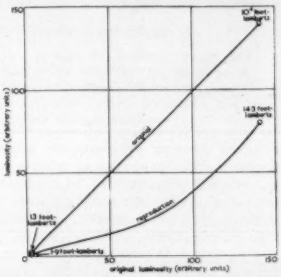

Fig. 2. Curves showing nature of relationship between luminosity in original scene and in reproduction when all luminances are scaled down in ratio 1 : 700 (deduced from curves of Fig. 1)

reproduction that luminosities of corresponding areas in reproduction and original should be equal, it follows that under these viewing conditions faithful reproduction of many scenes is impossible.

The achievement of proportionality might be suggested as a secondary standard. It is debatable whether this condition represents the nearest approach to faithful reproduction for given limitations, or whether it yields the most acceptable picture, but being clearly definable it forms a convenient standard of reference.

PHOTOGRAPHIC ANALOGY

Tone reproduction in photography. The essential features of the tone reproduction problem in photography may be illustrated by reference to Fig. 3.

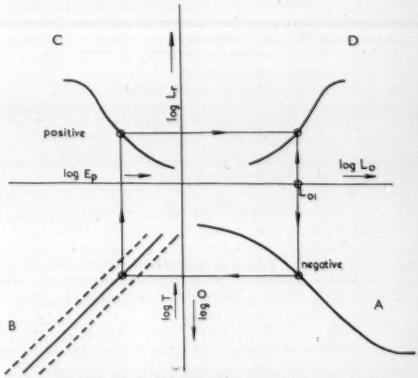

Fig. 3. Photographic tone reproduction chart

L_o = original scene luminance.
L_r = reproduced luminance.
O = opacity = incident illumination/transmitted illumination.
T = transmission factor = 1/opacity.
E_p = exposure (proportional to transmitted illumination × time).

The curves in quadrants *A* and *C* represent qualitatively the characteristic of a negative material and of a positive material (print or transparency), respectively. In so far as these curves follow power laws, they can be represented by straight lines, the gradients of which may be denoted by γ_1, γ_2 respectively. Then from simple mathematical considerations the $\log L_r/\log L_0$ curve will have a gradient of $\gamma_3 = \gamma_1 \times \gamma_2$. This is so because print exposure E_p is directly proportional to negative transmission factor T (or $1/E_p \propto O$). This relationship is represented in quadrant *B* by a straight line of unity gradient. The effect of varying the product (time of exposure × printing illumination) is merely to shift the line horizontally, as indicated by the dotted lines.

It is now widely recognized that many photographic materials have characteristics departing so widely from power laws as to render the simple theory, in terms of gamma, almost valueless. In practice, it is usually necessary to trace out the L_r/L_0 curve point by point, by successive projections through the quadrants; the procedure for one value (L_{01}) of L_0 is indicated by arrows.

For a detailed analysis it is necessary to invoke concepts such as gradient at a point, minimum useful gradient, and average gradient (defined, e.g. as the slope of the straight line joining the points where the gradient falls to some fraction of the average). Recent practice is exemplified in the paper by Jones previously cited.[2]

APPLICATION OF PHOTOGRAPHIC ANALOGY TO TELEVISION

It has been pointed out by previous writers[4,5] that a television system does not lend itself to analysis in terms of gamma characteristics. This is partly due to the fact that, as in photography, transfer characteristics frequently do not follow power laws. Another reason, peculiar to television, will now be discussed. The two elements of primary importance in conventional television systems, the camera and the reproducing cathode-ray tube, may be regarded as corresponding in a general way to the negative and positive in a photographic system. It is in the connecting link between the two that the analogy is weakest. In a television system the conversion of light input into an electrical signal confers degrees of freedom in determining the relation between camera output and tube input for which there is no parallel in a practical photographic system.

In Fig. 4 are shown hypothetical camera and cathode-ray tube characteristics; the graphical construction is similar to that of Fig. 3, but the co-ordinates are linear instead of logarithmic.

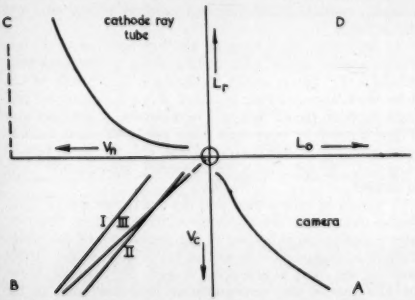

Fig. 4. Basic tone reproduction chart for television system

The curves in quadrant *B* represent the summation of all the stages of amplification, etc., between the camera and the tube. It is assumed that any non-linearity present in these stages is transferred to the camera characteristic. The v_m/v_c curves are therefore of the form $y = \alpha x + \beta$. The cathode-ray tube parameter v_m represents drive voltage, i.e. modulator voltage measured from some point having a fixed negative potential with respect to the cathode. Three of the possible forms of the v_m/v_c characteristic are shown by Curves I, II, and III (Fig. 4). The first two represent operation at the same gain but a different bias level. An increase in gain and a further change in bias level gives Curve III.

If the operative parts of the camera and cathode-ray tube characteristic curves were exactly definable by power laws, then the extrapolated curves would pass through the origin. By choosing a v_m/v_c curve which also passed through the origin (e.g. Curve III), or in other words by putting $\beta = 0$, the product of the camera and tube gammas would give the overall gamma. A special significance, in a mathematical sense at least, would therefore attach to curves such as III which passed through the origin.

In general, however, power laws do not obtain in practice. Also, because of the complexity of the visual response characteristic, discussed earlier, the overall gamma would not be a direct measure of the apparent expansion or compression of tone differences. In practice, then, the problem usually amounts to selection of a suitable v_m/v_c characteristic, by manipulation of bias and gain controls, to give an optimum result as judged subjectively. This optimum characteristic may be one such as Curve III, but may equally well be of the form of I or II. Mathematical analysis, if possible, is likely to be extremely complex and to yield little useful result. Graphical methods appear to hold much greater promise.

Before developing further the subject of graphical analysis, it is necessary to discuss briefly the nature of practical cathode-ray tube and camera characteristics.

CATHODE-RAY TUBE CHARACTERISTICS

Reliance on graphical methods for the complete system analysis, it is suggested, increases the possibility of a limited application of mathematical concepts to individual component characteristics; these may be defined in terms of parameters chosen without regard to the necessity for relating them mathematically to parameters of other components. Such concepts are of value in comparing characteristics of different cathode-ray tubes or cameras. A method of defining the cathode-ray tube modulation characteristic in mathematical terms has been discussed elsewhere,[10] and will only be briefly summarized here.

Practical characteristics. Figs. 5 and 6 show static modulation characteristics for, respectively, a standard commercial electromagnetic tube and a special electrostatic monitor tube. These curves are plotted in accordance with the method referred to above. Briefly, a value (in this case 15 ftl) is assumed for maximum luminance (measured on a plain raster); from measurement of the modulator/cathode voltage v_m at 15, 1·5, and 0·15 ftl a value of v_m, described as the virtual black-out point, is derived. Modulator voltage measured positively from this point is termed virtual drive voltage v_r. If then luminance L is plotted against v_r on logarithmic co-ordinates the three points corresponding to 15, 1·5, and 0·15 ftl lie on a straight line. The slope of this straight line might be described as the gamma of the tube;

it is, however, preferred to use the symbol λ, to denote the particular method of derivation. To derive the dynamic characteristics it is necessary to take into account the effect of stray light.

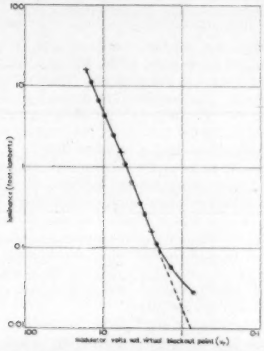

Fig. 5. Modulation characteristic of electro-magnetic cathode-ray tube ($\lambda = 2{\cdot}4$). Dotted line represents power law; full line curve is derived from experimental readings

O experimental points. + key points.

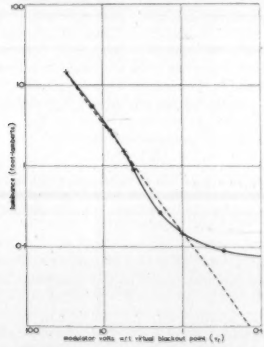

Fig. 6. Modulation characteristic of electrostatic cathode-ray tube ($\lambda = 1{\cdot}4$). Dotted line represents power law; full line curve is derived from experimental readings

O experimental points. + key points.

Luminance range. In an aluminized tube, minimum luminance is determined only by stray light originating from the lighter parts of the picture and reflected from the protective glass panel, the tube surround, etc. It may be about 1% of maximum picture luminance.

An area close to one of high luminance, however, receives additional light due to halation in the end wall of the tube. In a discussion on the subject of luminance range, Law[6] quotes a minimum figure of 6 and a maximum of 34 for closely adjacent areas. The latter was obtained with a dusted screen with 15% optical contact on glass having an absorption of 20%.

A figure of 10 for detail luminance range and 100 for overall range would appear to afford a good working basis.

CAMERA CHARACTERISTICS

These vary considerably with type of camera and operating conditions. Generally speaking, the output current/luminance relationship of the Iconoscope or Emitron type is represented on log-log co-ordinates by a curve, the slope of which is about 0·7 in the middle of its range and decreases towards higher luminance. Orthicon and C.P.S. cameras, on the other hand, have a substantially linear characteristic, i.e. the slope on log-log co-ordinates is unity. Characteristics of other types appear to be intermediate.[4, 5, 7] To compensate for the average characteristic of commercial receiving tubes, however, the C.P.S. camera output is normally passed through a correcting circuit[8] so that the effective characteristic can be regarded as not widely different from that of the Iconoscope.

The dynamic characteristic of a camera tube differs from the static characteristic on account of stray light (lens flare) and, in certain types of cameras, electron redistribution. (Tilt and bend correction mitigates but does not annul the effects of re-distribution.) Because of the random nature of these effects, camera output, for a given picture, is not a unique function of scene luminance; the camera characteristic, like that of the cathode-ray tube, can only be fully represented by an infinite number of curves.

From the literature it appears that under the most favourable conditions the luminance range which can be accepted by a present day television camera does not exceed 100. Any luminance values lying outside this range will fall beyond the toe or the knee of the curve.

OVERALL SUBJECTIVE CHARACTERISTIC

Graphical construction. The necessary data is now available for the construction of a tone reproduction chart from which can be derived a curve relating luminosities in a reproduction to those in the original scene.

Such a chart is shown in Fig. 7. This is a development of a form of chart originally published in the *Photographic Journal*.[9] Quadrants *A*, *B*, *C*, and *D* correspond to those of Fig. 4, but the co-ordinates are logarithmic instead of linear. For the sake of convenience in plotting, the parameter v_c is defined as the camera output voltage amplified to an arbitrary maximum level of 1 V. By the construction shown in Fig. 3, a curve of reproduced against original luminance is derived in quadrant *D*. To convert luminance to luminosity, quadrants *E*, *F*, and *G* are added. *E* and *F* contain, respectively, appropriate portions of Curves I and III of Fig. 1.

In order that the luminance and luminosity reproduction curves should appear with corresponding co-ordinates horizontal, a 45° line is drawn in quadrant *G*. Points on the luminance curve are then projected through quadrant *E* and reflected from the 45° line in *G* horizontally, to intersect with a line formed by projection from the same point through quadrant *F* and reflexion from the 45° line in a vertical direction. By this means the luminosity reproduction curve is derived.

It should be emphasized that no exact quantitative significance can be attached to this curve; its shape does, however, give a qualitative indication of the appearance of the reproduction as compared with that of the original scene. If the slope of the curve at any point is unity, for example, it can be said that a just distinguishable brightness step in the original, at the average level represented by that point, will

be just distinguishable in the reproduction. The slope at a point may conveniently be referred to as the visual gradient.

The 45° line, although primarily inserted for constructional purposes, also serves as a reference standard for faithful reproduction. The graphical construction described will now be employed to examine the effect of varying certain

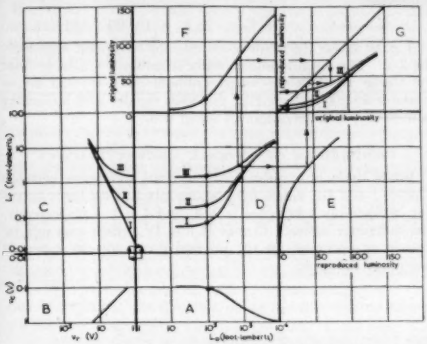

Fig. 7. Television tone reproduction chart
$\lambda = 2{\cdot}4$; $v_r = 16{\cdot}5v_c$.

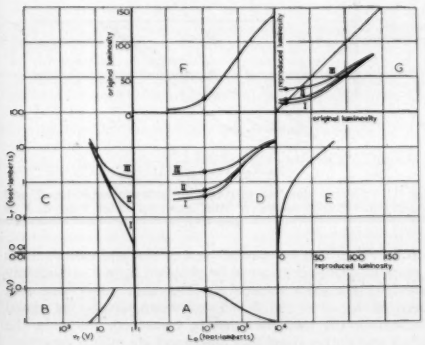

Fig. 8. Television tone reproduction chart
$\lambda = 2{\cdot}4$; $v_r = 14{\cdot}5v_c + 2$.

parameters. The camera characteristic assumed throughout is a somewhat generalized one, broadly representative of the Iconoscope or Emitron type. To avoid undue complications, the characteristic is represented by a single curve.

The cathode-ray tube characteristic is represented in Figs. 7 and 8 by three curves. The static characteristic (I) is a straight line having a gradient λ; maximum luminance is assumed to be 15 ftl. The dynamic characteristics for luminance ranges of 100 (II) and 10 (III) are derived by adding, respectively, 0·15 ftl and 1·5 ftl to all luminance values of Curve I.

As the average picture probably contains large areas of uniform luminance as well as fine detail, the effective characteristic can only be described as being bounded by Curves II and III.

EFFECT OF VARYING SELECTED PARAMETERS

$\lambda = 2{\cdot}4; v_r = 16{\cdot}5v_c$; $L_0 = 10\,000$–13 ftl.

Fig. 7 is drawn for the above conditions.

The luminance limits are such as might exist in a sunlit scene with deep shadow. This rather extreme case has been chosen to illustrate the maximum degree of distortion likely to occur. The cathode-ray tube characteristic is the same as that discussed with reference to Fig. 5. In quadrant *B*, the v_r/v_c relationship is defined by a straight line of unity gradient; one point on the line is located by the requirement that 10 000 ftl in the original should correspond to 15 ftl in the reproduction.

Several points of interest arise from a study of the chart. Firstly, while there is a considerable divergence between Curves II and III in quadrant *G*, that between Curves I and II is so small as to be almost insignificant. The conclusion can be drawn that any increase in brightness range beyond 100 at the luminance levels assumed for the cathode-ray tube, would have a negligible effect on the appearance of the picture. An increase from 10 to 100 in detail range would, however, produce an appreciable improvement.

Secondly, it may be observed that comparatively little is lost by reason of the dynamic brightness range of the camera being limited to 100. The dots on the curves indicate points corresponding to 1/100 of maximum scene luminance; from the curves of quadrant *G* it can be seen that only about 16 units of luminosity in a total of 140 are lost by virtue of the camera limitation.

Thirdly, by comparison of the curves in quadrants *D* and *G*, it may be seen that while the fall in slope towards peak white is partially compensated by the visual characteristic, the fall in slope towards black, due to the camera and the cathode-ray tube, is accentuated by the visual characteristic.

Fourthly, whereas according to the simple theory a combination of a camera of gamma 0·7 and a cathode-ray tube of gamma 2·4 would result in an increase in luminosity differences by a factor of about 1·7 the visual gradient does not in fact exceed unity.

The greatest departure from faithful reproduction is in the excessive loss of gradations in about the lower third of the original luminosity scale. An improvement in this respect may be effected by adjustment of bias and gain to bring the minimum camera voltage to a higher-slope portion of the cathode-ray tube characteristic, while maintaining the same peak luminance.

$\lambda = 2{\cdot}4$; $v_r = 14{\cdot}5v_c + 2$; $L_0 = 10\,000$–13 ftl

The result obtained when the bias point is moved 2 V positive, and the gain reduced to keep the maximum value of v_r the same as before, is shown in Fig. 8.

For ease of comparison, Curve II of quadrant *G* in Fig. 7 is re-plotted as Curve I in Fig. 11 and similarly Curve II of quadrant *G* in Fig. 8 is re-plotted as Curve II of Fig. 11. Curve II is chosen for purposes of comparison rather than III because it probably represents the effective characteristic for a much greater proportion of the picture area; also, it is probably the nearest practicable approach to Curve I, which represents a fundamental limit for the assumed luminance values and camera characteristic. In Fig. 11 the segment of each curve corresponding to original luminance below 100 ftl (the assumed camera limit) is omitted.

The general effect of the change in operating conditions is to decrease the visual gradient over most of the range of gradations (the maximum value being about 0·8), but to increase it towards black. At the same time the darkest tones are shifted further from subjective black (zero luminosity).

The characteristic obtainable from the electrostatic tube ($\lambda = 1{\cdot}4$) under different operating conditions will now be examined.

$$\lambda = 1{\cdot}4;\ v_r = 29{\cdot}7v_c;\ L_0 = 10\,000\text{–}13\ \text{ftl}$$

The cathode-ray tube characteristic for a luminance range of 100 only is used in Fig. 9. The effects associated with the assumed detail luminance range of 10 have, it is thought, been sufficiently demonstrated in Figs. 7 and 8.

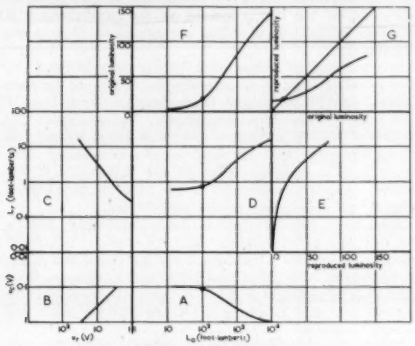

Fig. 9. Television tone reproduction chart
$\lambda = 1{\cdot}4;\ v_r = 29{\cdot}7v_c$.

The final curve in quadrant *G* is re-plotted in Fig. 11 (Curve III). The maximum visual gradient is 0·7 or rather less than in Curve II. The principal difference between the curves is that the gradient in Curve III is lower towards white and higher towards black. There is therefore less variation in gradient than in Curve II. The minimum value is about 0·25 compared with 0·17; that is to say, a luminosity difference of 4 just perceptible steps in the original will be perceptible in the reproduction, the corresponding figure for Curve II being 6.

To utilize more fully the lower end of the cathode-ray tube characteristic, it is necessary to move the bias point negatively.

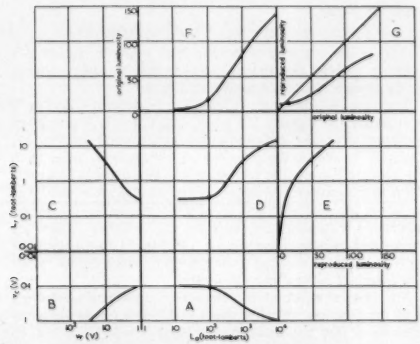

Fig. 10. Television tone reproduction chart
$\lambda = 1{\cdot}4;\ v_r = 31{\cdot}7v_c - 2$.

The curvature thus introduced into the log v_r/log v_c characteristic, in contradistinction to that in Fig. 8, is such as to minimize the falling off in slope towards black to which the camera, the cathode-ray tube and the eye all contribute. The possibility of decreasing minimum reproduced luminosity without reducing the minimum visual gradient is thereby indicated.

$$\lambda = 1{\cdot}4;\ v_r = 31{\cdot}7v_c - 2;\ L_0 = 10\,000\text{–}13\ \text{ftl}$$

Fig. 10 shows the result of shifting the bias point negatively by 2 V. The minimum luminosity is reduced nearly to that of Curve I, while the visual gradient does not fall below about 0·25 (as in Curve III), and rises rapidly with increasing luminosity, to a maximum of about 0·8.

COMPARISON OF OVERALL CHARACTERISTICS

While there is a quite clearly defined difference between Curves I and III, which may be described as the basic curves for cathode-ray tubes of $\lambda = 2{\cdot}4$, and $\lambda = 1{\cdot}4$ respectively, the difference between Curves II and IV, which may well be chosen as optimum for the respective cathode-ray tubes, is less easily definable.

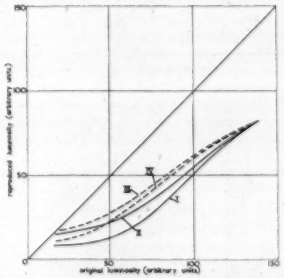

Fig. 11. Curves showing relationship between reproduced and original luminosity, re-drawn from quadrant *G* of Figs. 7, 8, 9 and 10

It is evident that by manipulation of bias and gain controls a range of characteristics can be obtained from a cathode-ray tube having a given value of λ. The ranges associated with tubes of $\lambda = 2{\cdot}4$ and $\lambda = 1{\cdot}4$ overlap, so far as visual gradient in the medium tones is concerned. It is in the lighter and darker tones that differences are mainly observed. The value of 1·4 gives a more nearly uniform visual gradient.

Of the four curves in Fig. 11, Curve IV approaches most closely to a straight line through the origin, i.e. to the secondary standard suggested earlier.

GENERAL REMARKS

Reproduction of a studio scene has not been considered in detail. The effects of distortion due to the eye are more clearly brought out by consideration of a sunlit scene; also, studio illumination being, at the present day, determined by requirements of camera sensitivity and not by the natural requirements of the scene, there is a wide variation in the relationship between the scene as it appears in the studio and the picture as it is intended to appear on the screen.

How far the curves of Fig. 11 do actually represent the relation between an observer's impression of a reproduction and of an original scene is a question which could only be

satisfactorily answered by extensive experimental work, using the techniques of subjective appraisal which have been increasingly developed in recent years. Direct comparison of a reproduction and an original, with all the parameters of the system accurately known, calls, of course, for a considerable experimental effort. Such limited observations as have been made, however, suggest that the shape of the curves at least gives a good impression of the relative effects of viewing cathode-ray tubes with different values of λ, and operating under, different conditions.

It is not intended to draw any conclusions or express any opinions as to what form of reproduction characteristic is most desirable. There can, however, be little doubt that there are instances where faithful reproduction is not desirable —where, in fact, the television system can improve on the eye and convey the maximum of information or enhance the aesthetic value of a scene by emphasizing certain luminosity differences at the expense of others. To a large extent the value of such distortions must be a matter of personal preference.

What constitutes the most desirable form of characteristic is, again, a question which calls for large-scale experiment on a subjective basis; factors such as signal-to-noise ratio and the effect of the characteristic on apparent definition have to be taken into account.

Reference may be made in passing to the results of Jones's investigation into the preferences of a large number of observers in the matter of photographic prints.(2) This investigation tends to show that preferred prints are those in which the gradient of the $\log L_r/\log L_0$ curve is approximately unity for the medium tones, and that a greater fall in the gradient is acceptable towards black. It would be unwise to assume, however, that the results obtained are necessarily applicable to television practice, where the form of the transfer characteristics and the viewing conditions are different. One general principle which does not seem to be in dispute is that, whereas a considerable tolerance exists when the reproduction is in monochrome, colour calls for a much closer approach to fidelity in luminosity reproduction.

Large-area luminance range in modern aluminized cathode-ray tubes, in the absence of external light, appears to offer little scope for worth-while improvement. It is worth noting, however, that the importanee of good detail luminance range in determining the subjective quality of television pictures has been stressed by Law(6) and other writers.

Assuming that an optimum characteristic, or range of characteristics, can be defined, practical realization of the optimum raises a number of issues, e.g. the relative contributions of the transmitting and receiving apparatus to the overall result, and whether the desired objective can best be arrived at by selection of the camera or cathode-ray tube characteristic or by suitable circuit design.

It is hoped that the present communication may help to clear the ground for further investigation of these and other related problems.

REFERENCES

(1) Hopkinson, R. G., Stevens, W. R., and Waldram, J. M. *Trans Illum. Engng Soc., Lond.*, **6**, p. 37 (1941).
(2) Jones, L. A. *Photographic Journal*, **89B**, p. 126 (1949).
(3) Birkinshaw, D. C. *B.B.C. Quarterly*, **4**, p. 105 (1949).
(4) Fink, D. G. *Proc. Inst. Radio Engrs*, **29**, p. 310 (1941).
(5) Schade, O. H. *RCA Rev.*, **9**, pp. 490 and 653 (1948).
(6) Law, R. R. *Proc. Inst. Radio Engrs*, **27**, p. 511 (1939).
(7) McGee, J. D. *Proc. Instn Elect. Engrs*, **97**, Part III, p. 377 (1950).
(8) White, E. L. C. and Harker, M. G. *Proc. Instn Elect. Engrs*, **97**, Part III, p. 393 (1950).
(9) Hopkinson, R. G., Mackenzie, R. B., and Nixon, R. D. *Photographic Journal*, **91B**, p. 2 (1951).
(10) Mackenzie, R. B. *Brit. J. Appl. Phys.*, **3**, p. 54 (1952).

Mechanical strength of piezoelectric crystals

By R. Bechmann, Ph.D., and P. L. Parsons, B.Sc., A.R.C.S., Post Office Research Station, Dollis Hill, London

[*Paper first received* 5 *November*, 1951, *and in final form* 22 *November*, 1951]

A direct mechanical method and an electrical method have been used to determine the mechanical strength of the piezoelectric materials sodium chlorate, sodium bromate, ammonium dihydrogen phosphate, ethylene diamine tartrate, and lithium sulphate monohydrate. New measurements have also been made on quartz as a check on the methods. A formula for the current due to the piezoelectric polarization is given which covers the longitudinal flexural, contour, and thickness modes of vibration considered. The maximum safe current for piezoelectric resonators has been calculated for specific cuts of the various materials.

INTRODUCTION

The mechanical strength of a piezoelectric crystal is of interest since it determines the maximum safe current that can be passed by a piezoelectric resonator made of this material. In the proportioning of bars and plates for practical use, the question of maximum allowable loading is of importance. If the elastic stress exceeds the breaking strength of the material, the resonator will fracture. The maximum current depends on the vibrational mode, the dimensions and the material. A simple relationship exists between the current flowing through the crystal and the elastic stress or strain which is present during vibration. The resonance current can be easily measured, so that it is convenient to define the maximum allowable loading by the maximum safe current. In the case of longitudinal vibrations the limit of the loading is set by the strength under longitudinal stress (tensile strength) which can be determined either electrically or by direct mechanical measurements. No figures have yet been published for the strength of a number of synthetic materials which have recently been investigated, but the mechanical strength of quartz is known quite accurately.(1)

A simple mechanical method was used to determine the breaking strength in extension of bars of various materials and orientations, and a check was provided by measurements of the current required to break longitudinally vibrating bars at their resonance frequency. From these results the maximum safe current for various types of resonator of different materials was calculated. A few electrical measurements on ethylene diamine tartrate (EDT) $X_{77°}$ plates,(2) both square and circular, have also been made.

ELECTRICAL DETERMINATION OF BREAKING STRENGTH

General considerations. The current $|I_p|$ due to the piezoelectric polarization in a resonator excited by one pair of

electrodes can be expressed for any mode[3] by the following formula:

$$|I_p| = vaF\,|T| \qquad (1)$$

where $|T|$ is the stress related to its point of maximum value, v the frequency, a the area of the fully plated crystal, and F a factor dependent on the mode, orientation, and the material of the specimen. The modes of bars and plates considered here comprise: longitudinally vibrating bars, longitudinal mode 1 of square plates, contour shear mode of square plates, and thickness modes of plates. The co-ordinate system used is shown in Fig. 1. For longitudinal mode 1 of square plates

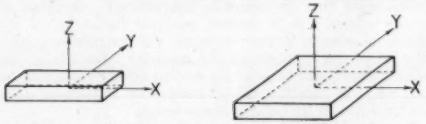

Fig. 1. Co-ordinate system used for bars and plates

the conditions $s_{11} = s_{22}$ and $d_{31} = -d_{32}$, were assumed, and for the shear mode, $s_{16} = s_{26} = 0$, as discussed in an earlier paper.[3] Table 1 gives the strain-stress relation, the maximum amplitude A_0 of displacement, the elastic constant γ,[3] and the factor F of equation (1) for the particular mode and zero electrode gap.* A_0 is given in terms of the stress $|T|$ at the point of maximum value, which occurs in the above cases at $x = 0$, $y = 0$. The factor F is proportional to the effective piezoelectric constant. In the case of the thickness mode the expression for F is derived on the assumption of uniform distribution of motion. For any arbitrary orientation of bars and plates the transformed values for the piezoelectric constants d_{ik} or e_{ik} must be used.

For modes where the frequency is determined by the length of the specimens (longitudinal mode of bars, contour modes of plates) the formula (1) reduces to:

$$|I_p| = NbF\,|T| \qquad (2)$$

where N is the frequency constant and b the width of the specimen.

In practice, the total current I_t through the crystal is the vectorial sum of the polarization current I_p and the current I_C due to the parallel capacitance C of the crystal, unless this capacitance is neutralized by an external circuit. The relation between the magnitudes of the current $|I_p|$ and the total current $|I_t|$ is given by

$$|I_p| = |I_t|\frac{1}{\sqrt{(1+\Delta^2)}}, \text{ where } \Delta = \frac{\Gamma}{Q} \qquad (3)$$

and Γ is the capacitance ratio C/C_k, Q the quality factor, and C_k is the dynamic capacitance of the equivalent electric circuit. In practice the Q for crystals is normally very high and thus the correction is small.

The current $|I_p|$ can also be expressed in terms of strain or maximum displacement as shown in an earlier paper.[3] The equation in terms of strain agrees with the formula (371) given by Cady[4] for the case of longitudinally vibrating bars.

Experimental method. The circuit arrangement adopted is shown in Fig. 2. The output of a carrier frequency oscillator with fine tuning control is amplified and applied to the crystal specimen under test in series with a carbon resistor R, usually of about 3 000 Ω. A valve voltmeter M records the voltage drop across R. The oscillator is tuned to the series resonance of the crystal, shown by a maximum reading of M, and the oscillator output increased until fracture occurs, the reading of M at fracture being noted. The specimens were silvered on the major faces and held at the nodal point by spring clamps, care being taken to obtain a low contact resistance.

With specimens of weak excitation, the correction for the parallel capacitance of the crystal becomes significant. This

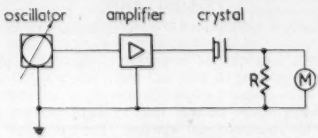

Fig. 2. Circuit arrangement for measurement of breaking strength

was made by noting the reading of M at resonance, V_r, and at a frequency sufficiently far from resonance V_p, using an output insufficient to cause breaking. Then if V' is the reading of M obtained for fracture at resonance, the corrected value is $V = V'\sqrt{[1-(V_p/V_r)^2]}$, from which can be calculated the breaking current I_p and the maximum tensile strength using equation (1).

Table 1. *Properties for various modes of bars and plates considered*

Mode	*Strain-stress relation*	*Amplitude A_0 of displacement in terms of maximum stress $\|T\|$*	γ	F
longitudinally vibrating bar	$T_1 = \gamma S_1$	$\frac{1}{\gamma k}\|T_1\|$	$\frac{1}{s_{11}}$	$4d_{31}$
longitudinally vibrating square plate, mode 1	$T_1 = \gamma S_1$ $T_2 = \gamma S_2$	$\frac{1}{\gamma k}\|T_1\|$	$\gamma_{11} - \gamma_{12}$ $= 1/(s_{11} - s_{12})$	$\frac{16}{\pi}d_{31}$
shear vibrating square plate	$T_6 = \gamma S_6$	$\frac{1}{2\gamma k'}\|T_6\|$	$\gamma_{66} = \frac{1}{s_{66}}$	$2\pi\frac{\sin\kappa}{\kappa}d_{36}$
thickness mode of plates	$T_t = \gamma S_t$	$\frac{1}{\gamma k''}\|T_t\|$	c	$4e/c$

where s, c, γ are elastic constants, d, e piezoelectric constants;
and S_i, T_i, are components of strain and stress, $k = \pi/l$, $k' = 2\kappa/l$, $k'' = \pi/t$;
$\kappa = 2{\cdot}088$, and l, t, length and thickness of specimen.

* Equation (1) can also be applied to the case of flexurally vibrating narrow bars with two pairs of electrodes. For the fundamental mode of a bar with identical orientation to that of the longitudinal bar considered ($d_{ik} = d_{31}$),

$F = \pi\sqrt{(2)}d_{31}\frac{\sqrt{(\cosh^2\varepsilon + \cos^2\varepsilon)}}{\cosh\varepsilon - \cos\varepsilon}\frac{\tan\varepsilon}{\varepsilon}$, where $\tan\varepsilon + \tanh\varepsilon = 0$ ($\varepsilon = 2{\cdot}3650$).

MECHANICAL METHOD FOR DETERMINATION OF BENDING STRENGTH

Attempts to use a conventional extensional loading of the crystal bars to obtain the tensile strength were abandoned owing to difficulties in holding the specimens and in ensuring axial loading. However the modulus of rupture (bending strength) was determined using a three knife edge method. This quantity is defined as the maximum longitudinal stress to cause fracture under application of a bending moment,[1, 5] where the effects of shear forces are small. The bar is supported horizontally by two knife edges N_1, N_2 (Fig. 3).

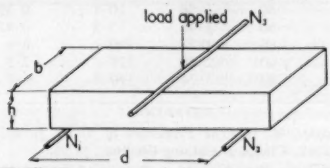

Fig. 3. Arrangement for the determination of bending strength of a bar

A gradually increasing vertical load is applied to the upper face midway between the two supports by a third knife edge N_3. The load was obtained by slowly pouring lead shot into a container. The bars tested had the same dimensions as those for electrical test.

The longitudinal stress is a maximum at the midpoint of the bar, and in fact the break usually occurs close to this point.

If W is the total load applied to N_3 to cause fracture, then the bending strength B_0 can be determined from the equation[1]

$$B_0 = \frac{3}{2}\frac{Wd}{bh^2} \qquad (4)$$

where d is the separation between the supports N_1 and N_2, b the width and h the thickness of the bar. In this method, a shear stress W/bh is incidentally applied to the bar. The ratio of maximum extensional stress to shear stress is the ratio d/h. With the bars used this quantity was of the order 10–15, and the effect of the shear stress has been assumed negligible.

EXPERIMENTAL RESULTS

New measurements of tensile and bending strength. The breaking strengths of bars of sodium chlorate, sodium bromate, ammonium dihydrogen phosphate (ADP), ethylene diamine tartrate (EDT), lithium sulphate monohydrate, and quartz have been investigated by both electrical and mechanical methods. In the case of ADP (tetragonal), EDT and lithium sulphate (monoclinic), specimens of various orientations distributed over the three crystallographic axial planes were used, except where the crystal symmetry made some specimens unnecessary. Usually two specimens of each orientation were used for electrical and two for mechanical testing. In the case of quartz and of the cubic crystals, sodium chlorate and sodium bromate, specimens of one orientation only were used. The dimensions of the bars tested were about $2 \times 3 \times 25$ mm.

It appears that in all cases the variation of breaking strength with orientation was not significant compared with the experimental uncertainties caused by the use of relatively few specimens of each orientation. Accordingly, the experimental results in Table 2 do not include the detailed orientation of each specimen.

General agreement is obtained between mechanical and electrical results, but the longitudinal strength determined by bending (modulus of rupture) is 20–50% higher than the tensile strength determined from electrical breaking, with the exception of sodium chlorate for which only six specimens in all were tested. A similar discrepancy between bending and tensile strength has been previously found by purely mechanical methods[1] for other materials.

The breaking current was also determined for several EDT $X_{77°}$ square plates, vibrating in contour shear mode. Using equation (1) and Table 1 the mechanical strength was found to range from 115–160 kg/cm² with a mean of 135 kg/cm². This agrees with the value obtained from bars quoted in Table 2. For circular plates vibrating in contour mode the expression for F in formula (1) is not known, but the experimental value for $F|T|$ obtained from circular EDT $X_{77°}$ plates appears to agree with the value obtained from the square plates of the same orientation.

Earlier results. A summary of the mechanical measurements of the strength of quartz has been given by Sosman.[1] According to Berndt's[3] determination for quartz, the tensile strength parallel to the optic axis is 1 160–1 210 kg/cm² and perpendicular to the axis 850–930 kg/cm², the bending strength parallel to the axis is 1 400–1 790 kg/cm² and perpendicular to the axis 920–1 180 kg/cm². The first figure refers to the average strength and the second to the maximum.

From longitudinally vibrating X-bars of different width/length ratios, b/l, and with frequencies in the range 50–300 kc/s, v. Beckerath[6] obtained values for the tensile strength of 600–1 400 kg/cm², with a mean value of 1 000 kg/cm². For smaller b/l ratios the values are nearer the upper limit, but for wider bars ($b/l \sim 0{\cdot}5$) the values are closer to the lower limit.

The breaking strength for thickness-shear quartz plates has also been measured. For AT cuts, using circular bevelled plates at 350 kc/s, v. Beckerath[6] showed that the value was greater than 900 kg/cm². One of the authors has previously obtained values in the range 1 100–1 300 kg/cm², using circular bevelled plates in the frequency range 600–5 000 kc/s. In both determinations uniform distribution of the motion was assumed.

MAXIMUM SAFE CURRENT

The maximum safe loading is assumed to be half the mean tensile strength and is given for the materials considered in Table 2. The maximum effective safe current $(I_p)_{rms}$ in mA, due to piezoelectric polarization, has been calculated for

Table 2. *Maximum tensile and bending strength of various materials in kg/cm²*

Material	*Tensile strength (electrical)*			*Bending strength (mechanical)*			*Maximum safe loading*
	Number of specimens	*Range*	*Mean*	*Number of specimens*	*Range*	*Mean*	
Sodium chlorate	3	180–560	350	3	260–420	330	170
Sodium bromate	3	260–350	290	3	340–370	350	150
ADP	8	200–290	250	25	210–480	335	130
EDT	25	65–240	125	41	70–250	160	60
Lithium sulphate	22	150–350	240	29	180–490	290	120
Quartz perpendicular to axis	5	700–870	800	5	1 190–1 380	1 270	500

Table 3. *Maximum safe current for various cuts and materials in mA calculated from the values for maximum safe loading given in Table 2*

Material	Cut	Mode	Frequency kc/s	Area of electrode cm²	F 10^{-8}	$(I_p)_{rms}$ mA
Quartz	$X_{0°}$ bar	flexural	6	1·40	11·4	0·11
	$X_{0°}$ bar	flexural	30	0·69	11·4	0·27
	$X_{0°}$ bar	longitudinal	60	3·47	27·8	6·7
	CT square plate	contour shear	150	4·20	14·9	10·8
	DT square plate	contour shear	150	1·91	21·0	6·9
	AT plate	thickness shear	1 000	4·15	38·7	186
	BT plate	thickness shear	6 000	0·79	17·0	93
Sodium chlorate	$X_{45°}$ bar	longitudinal	60	1·56	10·5	0·39
Sodium bromate	$X_{45°}$ bar	longitudinal	60	1·46	15·5	0·47
ADP	$Z_{45°}$ bar	longitudinal	60	1·27	290	6·6
EDT	$Y_{0°}$ bar	longitudinal	60	2·29	121	2·3
	$X_{77°}$ square plate	contour shear	60	3·74	150	6·7

specific cuts from these figures using equation (1). The values for the piezoelectric coefficients d_{ik} have been taken from recent determinations.(3) The value for the maximum safe stress for quartz has been taken as 500 kg/cm² and is also used in the calculation on quartz plates vibrating in contour-shear and thickness shear modes. For all bars the same breadth/length ratio 0·17 has been used. A summary of these results is given in Table 3.

ACKNOWLEDGEMENT

Acknowledgement is made to the Engineer-in-Chief of the General Post Office for permission to make use of the information contained in this paper.

REFERENCES

(1) SOSMAN, R. B. *The Properties of Silica*, p. 482 (New York: Chemical Catalog Co. Inc., 1927).
(2) BECHMANN, R. *Proc. Phys. Soc., B*, **63**, p. 577 (1950).
(3) BECHMANN, R. *Proc. Phys. Soc., B*, **64**, p. 323 (1951).
(4) CADY, W. G. *Piezoelectricity*, p. 324 (New York: McGraw-Hill Publishing Co. Inc., 1946).
(5) BERNDT, G. *Verhandl. Deutsch. Phys. Ges.*, **21**, p. 110 (1919).
(6) v. BECKERATH, H. *Elektrische Nachrichten Technik*, **19**, p. 45 (1942).

The bending and twisting of anisotropic plates

By R. F. S. HEARMON, A.Inst.P., and E. H. ADAMS, Physics Section, Forest Products Research Laboratory, Princes Risborough, Bucks

[*Paper received* 14 *September*, 1951]

The theory of the deflexion of anisotropic plates under bending and twisting loads is summarized; experimental methods for investigating the theory are described and tested on metal plates. The results of experiments on plywood cut at various angles to the grain are given and found to conform with the theory.

1. INTRODUCTION AND THEORY

There has been considerable development recently in the theory of elasticity applied to anisotropic systems, and the two-dimensional theory has been used to calculate stress distribution, buckling loads, frequency of vibration and deflexion under load of anisotropic plates, particularly those made from wood and plywood.(1) Much work on problems of anisotropic elasticity has also been carried out in Russia, and is described, for example, by S. G. Lekhnitskii (*Anizotropnye plastinki*, Moscow and Leningrad, Ogiz Gostekhizdat, 1947). The present paper sets out the general theory of the deflexion of anisotropic plates under bending and torsional loading and compares the observed with the calculated behaviour, using plywood as the experimental material.

In the notation of Voigt(2) the strains in a two-dimensional anisotropic system are given in terms of the stresses by the equations:

$$\left.\begin{aligned} x_x &= s_{11}X_x + s_{12}Y_y + s_{16}X_y, \\ y_y &= s_{21}X_x + s_{22}Y_y + s_{26}X_y, \\ x_y &= s_{61}X_x + s_{62}Y_y + s_{66}X_y, \end{aligned}\right\} \quad (1)$$

where x_x = extensional strain in the x direction;

y_y = extensional strain in the y direction;

x_y = shear strain in the xy plane;

X_x = extensional stress in the x direction;

Y_y = extensional stress in the y direction;

X_y = shear stress in the xy plane;

s_{ik} are the elastic compliance constants which obey the relations:

$$s_{ik} = s_{ki}, \quad (2)$$

so that equations (1) become:

$$\left.\begin{aligned} x_x &= s_{11}X_x + s_{12}Y_y + s_{16}X_y, \\ y_y &= s_{12}X_x + s_{22}Y_y + s_{26}X_y, \\ x_y &= s_{16}X_x + s_{26}Y_y + s_{66}X_y. \end{aligned}\right\} \quad (3)$$

The compliances s_{11}, s_{12} and s_{66} can be expressed in terms of Young's moduli, E_x, E_y, Poisson's ratios, σ_{xy}, σ_{yx},* and rigidity modulus, G_{xy}, as follows: $s_{11} = 1/E_x$; $s_{22} = 1/E_y$; $s_{12} = -\sigma_{xy}/E_x = -\sigma_{yx}/E_y$; $s_{66} = 1/G_{xy}$. The compliances s_{16} and s_{26} are constants of proportionality between a shear stress and the resulting extensional strain or between an extensional stress and the resulting shear strain. They are not encountered in elastic theory as applied to isotropic

* The first suffix denotes the direction of the applied stress and the second the direction of the lateral strain.

systems, and, in the general case, cannot be expressed in terms of familiar elastic constants.

In some materials, and in particular in plywood, the anisotropy is restricted by the existence of axes of elastic symmetry, which, for plywood, coincide with the directions along and at right angles to the grain direction in the face plies. Materials with this type of symmetry are often termed "orthotropic," and the remainder of this paper will be concerned with such materials. The principal directions will be distinguished by capital letters; thus the direction parallel to the face grain of the plywood will be denoted by OX, and the direction perpendicular to the face grain by OY (Fig. 1). The compliances measured in the principal directions will be similarly distinguished by the use of capital letters; for an orthotropic material $S_{16} = S_{26} = 0$, and the stress-strain relations (3), referred to the principal axes, become:

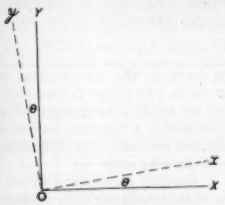

Fig. 1. Rotated axes. OX and OY are the principal directions.

$$\left.\begin{aligned} x_x &= S_{11}X_x + S_{12}Y_y = \frac{X_x}{E_X} - \frac{\sigma_{XY}Y_y}{E_X},\\ y_y &= S_{12}X_x + S_{22}Y_y = -\frac{\sigma_{YX}X_x}{E_Y} + \frac{Y_y}{E_Y},\\ x_y &= S_{66}X_y = \frac{X_y}{G_{XY}}. \end{aligned}\right\} \quad (4)$$

In an isotropic material,

$$\sigma_{XY} = \sigma_{YX} = \sigma,\ E_X = E_Y = E,$$

and, in addition,

$$G = E/2(1+\sigma),\ \text{i.e. } S_{66} = 2(S_{11} - S_{12}). \quad (5)$$

If the axes OX, OY in the orthotropic material are rotated through a counterclockwise angle θ to Ox, Oy (Fig. 1), the compliances are given by the equations:[1, 2, 3]

$$\left.\begin{aligned} s_{11} &= S_{11}m^4 + (2S_{12} + S_{66})m^2n^2 + S_{22}n^4,\\ s_{22} &= S_{11}n^4 + (2S_{12} + S_{66})m^2n^2 + S_{22}m^4,\\ s_{16} &= mn[2S_{22}n^2 - 2S_{11}m^2 + (2S_{12} + S_{66})(m^2 - n^2)],\\ s_{26} &= mn[2S_{22}m^2 - 2S_{11}n^2 - (2S_{12} + S_{66})(m^2 - n^2)],\\ s_{12} &= (S_{11} + S_{22} - S_{66})m^2n^2 + S_{12}(m^4 + n^4),\\ s_{66} &= 4(S_{11} + S_{22} - 2S_{12})m^2n^2 + S_{66}(m^2 - n^2)^2, \end{aligned}\right\} \quad (6)$$

where $m = \cos\theta$, $n = \sin\theta$.

Thus, in a general direction in an orthotropic material, s_{16} and s_{26} differ from zero and the stress-strain equations (3) must be used, with the compliances given by (6).

Now consider a plate $ABCD$ (Fig. 2), cut from an orthotropic material; if the angle θ is 0° or 90°, the plate is termed "specially orthotropic," and if θ has any other value, the plate is termed "generally orthotropic." Suppose the plate is subjected to uniform bending moments M_x per unit length of side along AD, BC, M_y per unit length along AB, CD, and a uniform twisting moment M_{xy} per unit length along all four sides. Thielemann[3] has shown that the general expression for the deflexion of a thin plate under these conditions is:

$$\left.\begin{aligned} h^3w = {} & 6M_x(s_{11}x^2 + s_{12}y^2 + s_{16}xy)\\ & + 6M_y(s_{12}x^2 + s_{22}y^2 + s_{26}xy)\\ & + 6M_{xy}(s_{16}x^2 + s_{26}y^2 + s_{66}xy), \end{aligned}\right\} \quad (7)$$

where w is the small deflexion, normal to the plane of the plate, of the point whose co-ordinates with respect to the centre of the plate are x, y, and h is the plate thickness.

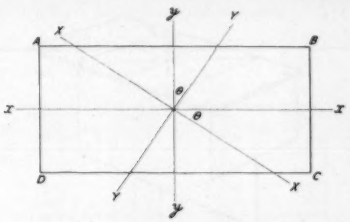

Fig. 2. Plate cut from orthotropic material

It is evident from equation (7) that for isotropic and specially orthotropic plates ($s_{16} = s_{26} = 0$) the deflexion is symmetrical about the lines $x = 0$, $y = 0$ when $M_{xy} = 0$ and antisymmetrical about these lines when $M_x = M_y = 0$. The first case corresponds with pure bending, and the second with pure torsion. The compliances s_{16} and s_{26} are not zero for the generally orthotropic plate, and, if $M_{xy} = 0$, some twisting will occur owing to the existence of the terms $s_{16}xy$ and $s_{26}xy$ in equation (7). Similarly, in the absence of bending moments ($M_x = M_y = 0$), some symmetrical bending will occur owing to the presence of the terms $s_{16}x^2$ and $s_{26}y^2$.

2. EXPERIMENTAL METHODS

2.1. *Bending.* As suggested by Thielemann,[3] the bending experiments were carried out using a method originally described by Bergsträsser.[4] The plates were rectangular, and measured $12\frac{1}{2} \times 6$ in. They were loaded at the points marked L (Fig. 3) by means of the arrangement illustrated diagrammatically in Fig. 4; ball bearings provided support at the points S and the load P was applied by dead weights added to a pan.

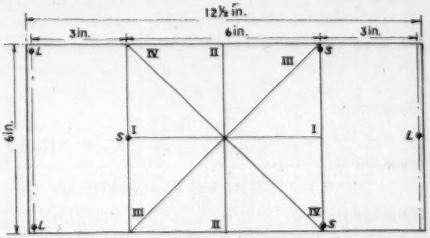

Fig. 3. Plate for bending test, showing dimensions, loading points L, support points S, and lines along which deflexions are measured. The origin of co-ordinates is at the centre of the plate.

The central lines I and II and the diagonals III and IV (Fig. 3) were marked on the central 6×6 in square of the plates, and the deflexions along these lines measured by a dial

gauge, reading directly to 10^{-4} in, mounted on a metal platform as shown in Fig. 5. The foot of the gauge B was placed on the central point of the plate, with the fixed feet A and C on the required line (say I). The third fixed foot D was used simply as a support so that the gauge and platform would stand on the test plate. With the gauge in position, readings were then taken at a suitable series of loads P. By repeating the procedure with the line ABC, coinciding

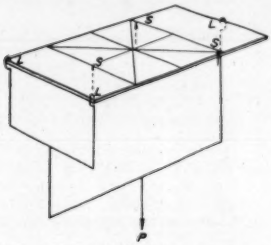

Fig. 4. Method of making bending tests

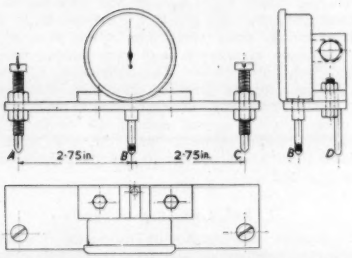

Fig. 5. Platform mounted dial gauge for measurement of deflexion. The gauge reads to 1/10 000 in

successively with lines II, III and IV, the deflexions under load along all four lines were obtained.

Now, if a bending moment M_x only is applied to the plate (i.e. $M_y = M_{xy} = 0$), equation (7) becomes:

$$h^3 w = 6M_x(s_{11}x^2 + s_{12}y^2 + s_{16}xy),$$

and, under the conditions of the experiment,*

$$M_x = \frac{P}{2} \cdot \frac{3}{6} = \frac{P}{4}.$$

Along line I:

$$x = 2{\cdot}75 \text{ in}, y = 0, \text{ and } \frac{w}{P} = \frac{11{\cdot}35 s_{11}}{h^3}, \text{ i.e. } s_{11} = \frac{wh^3}{11{\cdot}35P}.$$

Along line II:

$$x = 0, y = 2{\cdot}75 \text{ in}, \text{ and } s_{12} = wh^3/11{\cdot}35P.$$

Along line III:

$$x = y = 2{\cdot}75/\sqrt{2}, \text{ and } s_{11} + s_{12} + s_{16} = wh^3/5{\cdot}67P.$$

Along line IV:

$$x = -y = 2{\cdot}75/\sqrt{2}, \text{ and } s_{11} + s_{12} - s_{16} = wh^3/5{\cdot}67P.$$

* Inch-pound units are used throughout this paper. The conversion factors to metric units are: 1 in = 2·54 cm; 1 lb = 454 g = 0·454 kg; 1 in²/lb = $14{\cdot}5 \times 10^{-6}$ cm²/dyn = 14·2 cm²/kg.

Measurements on the specially orthotropic plates ($\theta = 0°$ or 90°) yield the principal constants as follows:

0° *plate.* Line I: $S_{11} = wh^3/11{\cdot}35P$;
Line II: $S_{12} = wh^3/11{\cdot}35P$;
Lines III and IV: $S_{11} + S_{12} = wh^3/5{\cdot}67P$.

90° *plate.* Line I: $S_{22} = wh^3/11{\cdot}35P$;
Line II: $S_{12} = wh^3/11{\cdot}35P$;
Lines III and IV: $S_{22} + S_{12} = wh^3/5{\cdot}67P$.

2.2 *Torsion.* The method used in the torsion tests is illustrated in Fig. 6. The test plates were square in shape and the ends of the plates used in the bending experiments were therefore cut off to leave the central 6 × 6 in square, on which the torsion experiments were carried out. The deflexions were measured exactly as in the bending tests.

As will be seen from Fig. 6, the plate is subjected to concentrated loading at one pair of diagonally opposite corners, and supported (in the present experiments on ball bearings) at the other two corners. The theory of this method of loading as applied to isotropic materials has been discussed

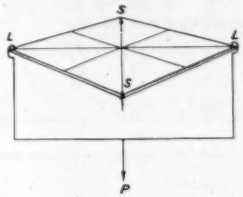

Fig. 6. Method of making torsion tests

by Nadai[5] and Timoshenko,[6] and tests on isotropic materials have been made by Nadai[5] and Bergsträsser.[4] March, Kuenzi and Kommers[7] have used the method to measure the rigidity modulus of specially orthotropic plywood plates, and Thielemann[3] has suggested its application to generally orthotropic plates.

The theory given by Nadai and Timoshenko shows that concentrated loads $P/2$ at each corner, acting as shown in Fig. 6, produce a torsional moment M_{xy} per unit length along each side equal to $P/4$. Hence from equation (7),

$$2h^3 w = 3P(s_{16}x^2 + s_{26}y^2 + s_{66}xy),$$

and, along line I, $s_{16} = wh^3/11{\cdot}35P$;

along line II, $s_{26} = wh^3/11{\cdot}35P$;
along line III, $s_{16} + s_{26} + s_{66} = wh^3/5{\cdot}67P$;
along line IV, $s_{16} + s_{26} - s_{66} = wh^3/5{\cdot}67P$.

For the specially orthotropic plate there should be no deflexion along lines I and II; along line III, $wh^3/5{\cdot}67P = S_{66}$ and along line IV, $wh^3/5{\cdot}67P = -S_{66}$.

In both the bending and torsion experiments, the deflexions were kept "small," i.e. not greater than about $h/10$. Even so, the incremental deflexion for a given load increment sometimes tended to fall off as the load increased, indicating the development of some direct stresses. In such cases the deflexion taken was that corresponding with the first load increments, giving, in effect, the slope of the deflexion-load curve at the origin.

3. EXPERIMENTAL RESULTS AND DISCUSSION

3.1. *Metal plates.* In order to test the validity of the methods, experiments were made on four metal plates. The deflexions per unit load increment are given in Table 1. After taking a set of readings along all four lines on any one plate, the plate was reversed, so that the deflexions occurred in the opposite direction, and the observations repeated. The two sets of observations obtained in this way are distinguished in Table 1 by the letters A and B.

The values of the compliances, calculated from the mean values of w/P in Table 1, are given in Table 3. Assuming that the materials are isotropic, the values of S_{11} and S_{12} derived from the observations along lines I and II in bending are sufficient in theory to specify completely the behaviour of the plates both in bending and in torsion, because the observations along lines III and IV in bending should yield $S_{11} + S_{12}$, and in torsion, should yield S_{66}, which, by equation (5), is equal to $2(S_{11} - S_{12})$ for isotropic materials.

Table 1. *Tests on metal plates*

Values of $10^4\ w/P$ (unit = in/lb) and $(10h)^3$ (unit = in^3)

Line	Bending				Torsion			
	Aluminium (a)	*Aluminium (b)*	*Brass*	*Mild steel*	*Aluminium (a)*	*Aluminium (b)*	*Brass*	*Mild steel*
IA	22·5	4·58	3·60	6·86	0·0	0·1	0·0	0·0
IB	21·0	4·50	3·46	6·80	−0·5	0·0	0·0	−0·1
Mean	21·7	4·54	3·53	6·83	−0·25	0·05	0·0	−0·05
IIA	−7·0	−1·27	−1·00	−2·40	0·0	0·0	0·0	−0·2
IIB	−6·0	−1·15	−1·00	−2·46	0·0	0·0	0·0	0·0
Mean	−6·5	−1·21	−1·00	−2·43	0·0	0·0	0·0	−0·1
IIIA	8·0	1·60	1·27	2·40	27·2	6·0	4·6	9·0
IIIB	7·3	1·65	1·20	2·26	28·5	5·8	4·6	8·6
Mean	7·7	1·63	1·23	2·33	27·9	5·9	4·6	8·8
IVA	7·5	1·82	1·20	2·30	−28·0	−6·0	−4·6	−8·8
IVB	8·0	1·58	1·27	2·33	−27·5	−5·8	−4·4	−9·4
Mean	7·7	1·70	1·23	2·31	−27·7	−5·9	−4·5	−9·1
$(10h)^3$	0·533	2·406	2·147	0·574	0·533	2·406	2·147	0·574

Examination of Table 1 shows that individual readings along a given line differ in one or two instances by as much as 10%, when the direction of deflexion is reversed, but normally the differences are less than this. Comparison of the mean values along line III with those along line IV suggests, however, that when the average of the deflexions in both directions is taken, the uncertainty in the results is reduced to a maximum of about 3%.

The compliances are calculated from the observed values of w/P by means of the equations in Table 2.

Table 2. *Compliance equations, isotropic plates*

Line	Bending	Torsion
I	$S_{11} = wh^3/11{\cdot}35P$	0
II	$S_{12} = wh^3/11{\cdot}35P$	0
III	$S_{11} + S_{12} = wh^3/5{\cdot}67P$	$S_{66} = wh^3/5{\cdot}67P$
IV	$S_{11} + S_{12} = wh^3/5{\cdot}67P$	$S_{66} = -wh^3/5{\cdot}67P$

Table 3. *Compliances for metals*

(unit = 10^{-6} in^2/lb)

	Aluminium (a)	*Aluminium (b)*	*Brass*	*Mild steel*
S_{11}	0·102	0·096	0·0667	0·0345
S_{12}	−0·031	−0·026	−0·0189	−0·0123
$S_{11} + S_{12}$ (obs.)	0·072	0·071	0·0466	0·0235
$S_{11} + S_{12}$ (calc.)	0·071	0·070	0·0478	0·0222
S_{66}	0·261	0·250	0·172	0·0906
$2(S_{11} - S_{12})$	0·266	0·244	0·171	0·0936

The observed and calculated values of $S_{11} + S_{12}$ and S_{66} are compared in Table 3. The agreement is very satisfactory, and justifies the methods of loading, and of deriving the compliances from the observations.

3.2. *Plywood plates: results.* Experiments were carried out on plates of the following plywoods: afara three-ply

Table 4. *Tests on maple 5-ply wood*

Values of $10^4\ w/P$ (unit = in/lb)

Plate No.	Deflexion direction	Angle (deg.)	h (in)	Bending				Torsion			
				Line				Line			
				I	*II*	*III*	*IV*	*I*	*II*	*III*	*IV*
1	A	0	0·224	5·24	−0·65	3·71	1·75	1·8	0·8	36·5	−31·0
	B			5·36	−0·73	3·27	1·42	1·8	0·3	33·5	−30·7
2	A	0	0·222	5·58	−0·80	2·08	2·84	0·0	1·2	31·5	−31·0
	B			5·67	−0·87	2·40	2·84	0·2	1·3	31·5	−31·2
3	A	22½	0·224	10·9	−3·93	9·38	−2·18	12·5	−6·7	25·5	−19·8
	B			10·9	−3·93	9·82	−2·40	12·2	−5·7	26·2	−20·2
4	A	45	0·226	21·8	−9·06	9·10	3·99	4·6	6·5	17·0	−6·5
	B			21·8	−8·72	9·06	4·20	4·8	6·0	17·7	−6·7
5	A	45	0·226	20·7	−8·72	8·72	3·60	4·5	6·5	18·5	−6·3
	B			20·7	−8·72	8·72	3·82	4·3	6·2	17·7	−6·5
6	A	67½	0·225	19·8	−4·80	4·80	11·3	−7·5	12·1	25·0	−20·0
	B			19·6	−4·80	4·36	10·7	−7·1	12·2	24·2	−19·5
7	A	90	0·223	16·8	−0·73	8·07	8·07	−0·7	−0·3	32·5	−33·5
	B			17·0	−0·55	7·52	8·40	−0·5	−0·3	32·0	−33·2
8	A	90	0·224	16·8	−0·44	8·73	8·07	0·1	−0·5	30·0	−32·0
	B			16·6	−0·51	8·73	8·07	1·1	−0·9	32·0	−32·5

($h \simeq 0{\cdot}185$ in); maple five-ply ($h \simeq 0{\cdot}225$ in); and gaboon three-ply ($h \simeq 0{\cdot}305$ in). The plates were cut with the face grain making angles of 0, $22\frac{1}{2}$, 45, $67\frac{1}{2}$ and 90° with the long sides of the plates; the experimental technique was exactly as described earlier for the metal plates. As an example of the readings obtained, the observed values of w/P for the maple plywood are given in Table 4.

If we write

$$s = wh^3/kP, \tag{8}$$

where $k = 11{\cdot}35$ for lines I and II, and $k = 5{\cdot}67$ for lines III and IV, then the discussion of sections 2.1 and 2.2 shows that s on the generally orthotropic plate is equivalent to the expressions given in Table 5. These expressions are, of course, simplified if the plate is specially orthotropic, because then $s_{16} = s_{26} = 0$.

Table 5. *s for generally orthotropic plates*

Line	*Bending*	*Torsion*
I	$s = s_{11}$	$s = s_{16}$
II	$s = s_{12}$	$s = s_{26}$
III	$s = s_{11} + s_{12} + s_{16}$	$s = s_{16} + s_{26} + s_{66}$
IV	$s = s_{11} + s_{12} - s_{16}$	$s = s_{16} + s_{26} - s_{66}$

The observed mean values of w/P were converted to s using equation (8), and the results are given in columns 1, 3 and 5 of Tables 6(*a*) and 6(*b*).

The calculated values in columns 2, 4 and 6 of Tables 6(*a*)

Table 6. *Observed and calculated values of s*

(Unit = 10^{-6} in²/lb)

6(*a*). *Bending*

Plywood			*Afara—3-ply*		*Maple—5-ply*		*Gaboon—3-ply*	
Column number			1	2	3	4	5	6
Angle deg.	*Line*	$s =$	*Obs.*	*Calc.*	*Obs.*	*Calc.*	*Obs.*	*Calc.*
0	I	S_{11}	0·511	0·511	0·535	0·535	0·78	0·78
0	II	S_{12}	−0·140	−0·135	−0·074	−0·065	−0·09	−0·107
0	III	$S_{11} + S_{12}$	0·486	0·376	0·560	0·47	0·76	0·67
0	IV	$S_{11} + S_{12}$	0·466	0·376	0·430	0·47	0·90	0·67
$22\frac{1}{2}$	I	s_{11}	1·93	1·60	1·08	1·20	1·84	2·21
$22\frac{1}{2}$	II	s_{12}	−0·473	−0·42	−0·39	−0·56	−0·17	−0·27
$22\frac{1}{2}$	III	$s_{11} + s_{12} + s_{16}$	3·74	3·70	1·90	2·02	4·52	5·32
$22\frac{1}{2}$	IV	$s_{11} + s_{12} - s_{16}$	−0·762	−1·34	−0·45	−0·76	−1·16	−1·44
45	I	s_{11}	3·56	3·84	2·16	2·09	4·94	5·42
45	II	s_{12}	−0·73	−0·70	−0·89	−1·06	−0·33	−0·43
45	III	$s_{11} + s_{12} + s_{16}$	5·00	5·91	1·81	1·59	9·3	9·3
45	IV	$s_{11} + s_{12} - s_{16}$	0·796	0·37	0·79	0·47	0·13	0·68
$67\frac{1}{2}$	I	s_{11}	5·62	5·51	1·98	1·99	7·7	8·3
$67\frac{1}{2}$	II	s_{12}	−0·423	−0·42	−0·48	−0·56	−0·64	−0·27
$67\frac{1}{2}$	III	$s_{11} + s_{12} + s_{16}$	6·12	6·48	0·92	0·83	9·6	10·8
$67\frac{1}{2}$	IV	$s_{11} + s_{12} - s_{16}$	4·06	3·70	2·22	2·03	4·5	5·31
90	I	S_{22}	6·05	6·05	1·66	1·66	9·4	9·4
90	II	S_{12}	−0·13	−0·135	−0·055	−0·065	−0·123	−0·107
90	III	$S_{22} + S_{12}$	5·52	5·92	1·63	1·60	9·3	9·3
90	IV	$S_{22} + S_{12}$	6·08	5·92	1·61	1·60	9·1	9·3

6(*b*). *Torsion*

Plywood			*Afara—3-ply*		*Maple—5-ply*		*Gaboon—3-ply*	
Column number			1	2	3	4	5	6
Angle deg.	*Line*	$s =$	*Obs.*	*Calc.*	*Obs.*	*Calc.*	*Obs.*	*Calc.*
0	I	0	0·07	0·00	0·09	0·00	0·0	0·0
0	II	0	−0·07	0·00	0·09	0·00	0·1	0·0
0	III	S_{66}	8·90	9·1	6·50	6·32	11·9	11·7
0	IV	$-S_{66}$	−9·12	−9·1	−6·06	−6·32	−11·5	−11·7
$22\frac{1}{2}$	I	s_{16}	2·72	2·52	1·21	1·39	3·2	3·37
$22\frac{1}{2}$	II	s_{26}	1·31	1·39	−0·61	−0·60	2·4	2·72
$22\frac{1}{2}$	III	$s_{16} + s_{26} + s_{66}$	11·0	11·9	5·10	5·09	17·3	17·1
$22\frac{1}{2}$	IV	$s_{16} + s_{26} - s_{66}$	−3·22	−4·06	−3·95	−3·51	−6·3	−4·93
45	I	s_{16}	2·13	2·77	0·46	0·56	4·6	4·31
45	II	s_{26}	2·80	2·77	0·64	0·56	4·5	4·31
45	III	$s_{16} + s_{26} + s_{66}$	11·0	12·4	3·59	3·46	20·3	19·0
45	IV	$s_{16} + s_{26} - s_{66}$	−1·28	−1·29	−1·32	−1·22	−1·8	−1·77
$67\frac{1}{2}$	I	s_{16}	1·14	1·39	−0·73	−0·60	2·7	2·72
$67\frac{1}{2}$	II	s_{26}	2·39	2·52	1·21	1·39	3·5	3·37
$67\frac{1}{2}$	III	$s_{16} + s_{26} + s_{66}$	11·8	11·9	4·94	5·09	16·4	17·1
$67\frac{1}{2}$	IV	$s_{16} + s_{26} - s_{66}$	−4·92	−4·06	−3·96	−3·51	−3·9	−4·93
90	I	0	0·11	0·00	0·00	0·00	0·1	0·0
90	II	0	−0·30	0·00	−0·05	0·00	−0·1	0·0
90	III	S_{66}	9·0	9·1	6·24	6·32	12·1	11·7
90	IV	$-S_{66}$	−9·4	−9·1	−6·48	−6·32	−11·1	−11·7

and 6(*b*) were derived by substituting in equations (6) the estimates of the principal constants obtained as folllows:

S_{11} from line I, 0° plate in bending;
S_{22} from line I, 90° plate in bending;
S_{12} from line II, 0° and 90° plates in bending;
S_{66} from lines III and IV, 0° and 90° plates in torsion.

By adding and subtracting the experimental results for lines III and IV, further comparisons can be made both between independent experimental measurements, and between experimental and calculated values. Thus, in bending, from Table 5,

$$s_{III} + s_{IV} = 2(s_{11} + s_{12}),$$
$$s_{III} - s_{IV} = 2s_{16},$$

where the Roman suffixes indicate the lines along which the measurements are made. Similarly, in torsion,

$$s_{III} + s_{IV} = 2(s_{16} + s_{26}),$$
$$s_{III} - s_{IV} = 2s_{66}.$$

than the agreement between either and the theoretical estimates, implying that the errors of measurement are less than the errors introduced by assuming the material to have the same properties at all points in the sheet.

The two sets of experimental values for s_{16} are generally in close agreement. One of these sets is derived from bending, the other from torsion, experiments. The correspondence is therefore a good test of the reciprocal relations (2). If these relations were invalid, the bending experiments would measure s_{16} and the torsion experiments s_{61} [cf. equations (1) and (7)]. The results show that the two constants are, in fact, indistinguishable within the limits of experimental error, and the relations (2) therefore hold.

A valuable feature of the methods under investigation is that they enable the compliances s_{16} and s_{26} to be measured directly, and as far as is known this has not hitherto been done. The compliance s_{12} is related to the Poisson's ratios of the plywood by the equations:

$$\sigma_{yx} = -s_{12}/s_{22};\ \sigma_{xy} = -s_{12}/s_{11},$$

and the methods should therefore be of use for studying the

Table 7. *Compliances for plywood*

(Unit = 10^{-6} in²/lb)

Plywood			*Afara—3-ply*			*Maple—5-ply*			*Gaboon—3-ply*		
Angle			22½	45	67½	22½	45	67½	22½	45	67½
Compliance	*Lines*	*Type of experiment*									
$s_{11} + s_{12}$ (obs.)	I + II	Bending	1·46	2·83	5·20	0·69	1·27	1·50	1·67	4·61	7·06
$s_{11} + s_{12}$ (obs.)	½(III + IV)	Bending	1·49	2·90	5·09	0·73	1·30	1·57	1·68	4·71	7·05
$s_{11} + s_{12}$ (calc.)	—	—	1·18	3·14	5·09	0·64	1·03	1·43	1·94	4·99	8·04
s_{16} (obs.)	½(III − IV)	Bending	2·25	2·10	1·03	1·17	0·51	−0·65	2·84	4·59	2·55
s_{16} (obs.)	I	Torsion	2·72	2·13	1·14	1·21	0·46	−0·73	3·2	4·6	2·7
s_{16} (calc.)	—	—	2·52	2·77	1·39	1·39	0·56	−0·60	3·37	4·31	2·73
$s_{16} + s_{26}$ (obs.)	½(III + IV)	Torsion	3·89	4·86	3·44	0·57	1·13	0·49	5·5	9·3	6·3
$s_{16} + s_{26}$ (obs.)	I + II	Torsion	4·03	4·93	3·53	0·60	1·10	0·48	5·6	9·1	6·2
$s_{16} + s_{26}$ (calc.)	—	—	3·91	5·54	3·91	0·79	1·12	0·79	6·09	8·62	6·09
s_{66} (obs.)	½(III − IV)	Torsion	7·11	6·14	8·36	4·53	2·45	4·45	11·8	11·1	10·2
s_{66} (calc.)	—	—	7·97	6·83	7·97	4·31	2·33	4·31	11·0	10·4	11·0

The experimental quantities calculated from these equations are given in Table 7, which also contains the experimental values for $(s_{11} + s_{12})$ from lines I and II in bending and s_{16} from line I in torsion, together with the corresponding theoretical values.

3.3. *Plywood plates: discussion.* It is evident from Tables 6 and 7 that the general agreement between the experimental and theoretical values is close, although in some instances fairly large discrepancies occur. It has to be remembered, however, that the properties of the plywoods will vary to some extent from point to point in the sheets from which the test plates are cut. Thus the basic constants from which the theoretical values are calculated are derived from measurements on the 0° and 90° plates, and the properties of this material may not be exactly the same as those of the plates cut at the other angles. Some support is given to this suggested explanation by the fact that the discrepancies are smaller on the maple than on the afara and gaboon plywoods. Examination of the plywoods shows that the grain in the maple is straighter and more regular than in the afara and gaboon, and for this reason, the variation of properties with position should be smaller on the maple plywood.

Further support to the suggestion is given by the results of Table 7, which shows that in most cases the agreement between two independent experimental estimates is better

Poisson's ratios of plywoods. The principal elastic constants of the plywood (i.e. those measured with respect to axes parallel and perpendicular to the face grain) are:

$$E_X = 1/S_{11};\ E_Y = 1/S_{22};$$
$$\sigma_{XY} = -S_{12}/S_{11};\ \sigma_{YX} = -S_{12}/S_{22};$$
$$G_{XY} = 1/S_{66}.$$

The values of these constants are collected in Table 8 and compared, in the case of E and G, with independent measurements made by a dynamic bending method for E and a dynamic torsion method for G [reference (1), pp. 13 and 14].

Table 8. *Principal elastic constants*

(Unit for E and G = 10^6 lb/in²)

Constant	*Afara—3-ply*	*Maple—5-ply*	*Gaboon—3-ply*
$E_X = 1/S_{11}$	1·96	1·87	1·28
E_X (dynamic)	1·82	1·89	1·24
$E_Y = 1/S_{22}$	0·165	0·60	0·11
E_Y (dynamic)	0·160	0·59	0·11
$G_{XY} = 1/S_{66}$	0·110	0·159	0·085
G_{XY} (dynamic)	0·111	0·167	0·073
σ_{XY}	0·26	0·12	0·14
σ_{XY}	0·022	0·039	0·011

The elastic constants found by the two methods do not

differ by more than a few per cent; the differences could easily be due to the fact that the strips for the dynamic measurements and the plates for the bending and torsion experiments were cut from different parts of the original plywood sheets.

Finally, it can be concluded from the results of Tables 6, 7 and 8 that the theory given in section 1 represents very closely the behaviour of plywood plates under the influence of uniform bending and torsional moments.

4. ACKNOWLEDGEMENT

The work described above was carried out as part of the programme of the Forest Products Research Board and is published by permission of the Department of Scientific and Industrial Research.

REFERENCES

(1) HEARMON, R. F. S. *The Elasticity of Wood and Plywood.* (London: H.M. Stationery Office, 1948.)
(2) VOIGT, W. *Lehrbuch der Kristallphysik.* (Leipzig and Berlin: B. G. Teubner, 1910, reprinted 1928.)
(3) THIELEMANN, W. *FGH Report No.* 150/19 (1945), Ministry of Supply, Translation TIB T 3418 (1949).
(4) BERGSTRÄSSER, M. *Z. techn. Phys.*, **8**, p. 355 (1927).
(5) NADAI, A. *Elastische Platten*, p. 26. (Berlin: Springer Verlag, 1925.)
(6) TIMOSHENKO, S. *The Theory of Plates and Shells*, p. 47. (New York and London: McGraw-Hill Book Company, Inc., 1940.)
(7) MARCH, H. W., KUENZI, E. W., and KOMMERS, W. J. *U.S. Dept. Agric., Forest Products Laboratory, Madison, Mimeograph* 1301 (1942).

The two-dimensional magnetic or electric field inside a semi-infinite slot terminated by a semi-circular cylinder

By N. DAVY, D.Sc., and N. H. LANGTON, M.Sc., A.Inst.P., The University, Nottingham

[*Paper received* 25 *September*, 1951]

The field is investigated inside (*a*) a semi-infinite slot with a semi-circular closed end in a magnetized ferromagnetic body, such as a slotted armature or a polepiece, or (*b*) a hollow electrical conductor of the same shape. Tables of calculated values of the field at important points, and the corresponding graph, are given.

The effects upon the electrical stresses surrounding charged conductors caused by rounding off their corners has many practical applications and such problems have aroused interest for many years, but few complete exact solutions of this type of problem have been obtained. Cockcroft[1] approximated to the case where the curved portion of the conductor was part of a cylinder and it is also possible to obtain approximate results by the use of relaxation methods. In this paper an exact result is obtained where the rounded portion of the conductor is part of a cylinder.

Fig. 1 represents a cross-section of a two-dimensional system, viz. either a semi-infinite slot in a magnetized but not saturated ferromagnetic body or a semi-infinite cavity in a charged electrical conductor. The field inside such a slot or cavity is investigated, the mathematics being the same in the two cases. The face of the slot or cavity is an equipotential. First a geometrical transformation is obtained by which the edge *BAODB′*, in the *z*-plane, is transformed into the real axis of a *c*-plane, not shown, and the interior of *BAODB′* into the upper half of the *c*-plane. This transformation gives *z* as a function of two solutions of the hypergeometric equation, the independent variable being $c = k^2$, where k is the modulus of the elliptic integrals K, K', E and E'. z is expressed as a function of these quantities in the geometrical transformation.

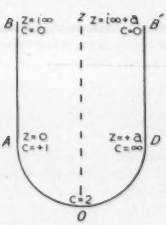

Fig. 1. Semi-infinite slot terminated by a semi-circular cylinder in the *z*-plane

Next, a magnetic or electric transformation is required, to link the geometrical with the physical properties of the system. If U is the stream function of the field, magnetic or electric, in Fig. 1, and V the corresponding potential, and if $W = U + iV$, then a second diagram (Fig. 2), the W-plane, is constructed to represent the magnetic or electric state at each point in Fig. 1. In Fig. 2 the infinitely long horizontal line *BAODB′* corresponds to the edge *BAODB′* in Fig. 1. A transformation $W = f_2(c)$ is obtained, which changes this line in Fig. 2 into the real axis of the *c*-plane (not shown) and the region below the line into the upper half of the *c*-plane. Combining the two transformations we can express $W = U + iV$ as a function of z and then get equations of lines of force and equipotentials. The modulus of dW/dz gives F, the field strength, and the numerical value of F is found at all points on the edge *BAODB′* of Fig. 1 and also along the axis *OZ* of that figure. Expressions for dF/dz and $d(F^2)/dz$, likely to be of use in atomic beam work, are also found.

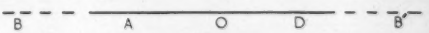

Fig. 2. W-plane. The infinitely long horizontal straight line *BAODB′* has the equation $W = U + iV_0$. It represents the electric or magnetic state of the slot in Fig. 1 which is at constant potential V_0. Points below *BAODB′* correspond to internal points of the slot in Fig. 1

THE TRANSFORMATIONS

(*a*) *The geometrical transformation.* To transform the edge *BAODB′* of Fig. 1 into the real axis of the *c*-plane (not shown) and the interior of *BAODB′* into the upper half of the *c*-plane, we first note that *BA*, *AOD* and *DB′* are three sides of a curvilinear triangle. The sides are arcs of circles, *AOD* having a finite radius, while *BA* and *DB′* have infinite radii and are straight. The internal angles of the triangle are zero at *O*, and π radians at *A* and *D*, respectively. By a theorem due to Schwarz the geometrical transformation is obtained by solving the hypergeometrical equation

$$d^2z/dc^2 + [\gamma - (\alpha + \beta + 1)c]/[c(1 - c)] \cdot dz/dc - \alpha\beta z/c(1 - c) = 0$$

In this case z is the dependent variable and c the independent variable. α, β and γ are linked with the angles of

the corresponding curvilinear triangle $\lambda\pi$, $\mu\pi$ and $\nu\pi$ by the equations $\lambda^2 = (1-\gamma)^2, \mu^2 = (\alpha-\beta)^2, \nu^2 = (\gamma-\alpha-\beta)^2$.

In our particular case $\lambda = 0$, $\mu = 1$, $\nu = 1$. Of the various values of α, β and γ possible as solutions, we have selected the convenient set $\alpha = -\frac{1}{2}$, $\beta = +\frac{1}{2}$, $\gamma = +1$. On substituting these values the hypergeometric equation reduces to

$$d^2z/dc^2 + 1/c \,.\, dz/dc + z/c(1-c) = 0 \tag{1}$$

According to Forsyth[2] (p. 292), one solution of (1) is

$$z = A\int_0^1 v^{\beta-1}(1-v)^{\gamma-\beta-1}(1-cv)^{-\alpha}dv \tag{2}$$

$$= A\int_0^1 v^{-1/2}(1-v)^{-1/2}(1-cv)^{+1/2}dv \tag{3}$$

Substituting $v = \mathrm{sn}^2 u$ to modulus $k = c^{\frac{1}{2}}$, we get after clearing

$$z = 2A\int_0^K dn^2u \,.\, du = 2AE \tag{4}$$

where E is the second complete elliptic integral.

By equation VII, Forsyth[2] (p. 215), another solution to equation (1) is obtained by replacing α by $\gamma-\alpha$, β by $\gamma-\beta$, γ by $\gamma-\alpha-\beta+1$ and c by $1-c=c'$. Using this we get new values $\alpha = +3/2$, $\beta = +\frac{1}{2}$ and $\gamma = +2$ respectively. Also according to Forsyth (p. 214) we can and do exchange the new values of α and β so that finally we get $\alpha = +\frac{1}{2}$, $\beta = +3/2$ and $\gamma = +2$.

By equation VII, Forsyth[2] (p. 215) makes the new solution

$$z = Ac'\int_0^1 v^{1/2}(1-v)^{-1/2}(1-c'v)^{-1/2}dv \tag{5}$$

Put $v = \mathrm{sn}^2 u$ to modulus $k' = \sqrt{c'}$. We then get

$$z = 2Ac'\int_0^{K'} \mathrm{sn}^2 u \,.\, du$$

so that

$$z = 2A(K'-E') \tag{6}$$

By Schwarz's theory the two values of z given by equations (4) and (6) are combined to give the required transformation in the form

$$z = [B_1E + B_2(K'-E')]/[C_1E + C_2(K'-E')] \tag{7}$$

where B_1, B_2, C_1 and C_2 are constants to be determined. To determine their values we apply the conditions at the three corners B, A and D. At the point B (Fig. 1), $z = i\infty$ and at B' $z = a + i\infty$, $c = 0$, $E = \pi/2$, $E' = +1$, $K' = \infty$, whence $C_2 = 0$. At the point A, $z = 0$, $c = +1$, $E = +1$, $E' = \pi/2$, $K' = \pi/2$, so that $B_1 = 0$. At D, $z = +a$, $c = \infty$ from which we can deduce nothing useful.

We therefore go back to the points B and B' where $z = +i\infty$ and $a + i\infty$. In crossing the gap BB' of Fig. 1 from right to left the value of z decreases by a cm. The corresponding value of c changes from a very small real and positive to a very small and real negative value. When c has a very small positive value $c = k^2 = +\epsilon$, then according to Cayley[3] (p. 54) $K' = \ln 4/k$ approx., $= \frac{1}{2}\ln 16/\epsilon$ approx., $E' = 1$ approx., $E = \pi/2$ approx., and when $c = -\epsilon$, $K' = \frac{1}{2}\ln 16/(-\epsilon)$ approx., $= \frac{1}{2}\ln 16 - \frac{1}{2}\ln(-\epsilon) = \frac{1}{2}\ln 16 - \frac{1}{2}\ln\epsilon - \frac{1}{2}\ln(-1) = \frac{1}{2}\ln 16 - \frac{1}{2}\ln\epsilon - i\pi/2$. Also $E' = 1$ approx., $E = \pi/2$ approx. By equation (7) the corresponding change of z is

$$B_2/C_1 \,.\, 2/\pi \,.\, [(\tfrac{1}{2}\ln 16 - \tfrac{1}{2}\ln\epsilon - 1) - (\tfrac{1}{2}\ln 16 - \tfrac{1}{2}\ln\epsilon - 1 - i\pi/2)] = iB_2/C_1$$

From Fig. 1 we see that the same change of z consists in going from $(i\infty + a)$ to $i\infty$, i.e. is $(-a)$. Hence $iB_2/C_1 = -a$ and $B_2/C_1 = +ia$. Equation (7) now reduces to

$$z = ia(K'-E')/E \tag{8}$$

THE MAGNETIC OR ELECTRIC TRANSFORMATION

Let $W = U + iV$, where U is the stream function and V the potential at any point in Fig. 1. In Fig. 2, the W-plane, the W's of every point along the edge $BAODB'$ in the z-plane are represented by the various points along the infinitely long horizontal straight line $BAODB'$. The line $BAODB'$ in the W-plane has the equation $W = U + iV_0$ and is to be made to correspond to the edge of the conductor, thus raising it to the required potential $+V_0$. The real axis of the W-plane (not shown) has the equation $W = U$ and corresponds to a zero equipotential in the z-plane. In the z-plane, the lines of force from the conductor will terminate at the point at infinity, which will therefore have a potential of $-\infty$. Thus the whole of the W-plane from the line $BAODB'$ down to $W = -i\infty$ must be transformed into the upper half of the c-plane. This can be performed by a change of variable and an inversion about the point O.

Let $W_1 = W - iV_0$, then the line $BAODB'$ in Fig. 2 becomes the real axis of the W_1-plane. The complex inversion $W_1 = A/c$ then transforms the lower half of the W_1-plane into the upper half of the c-plane as required. Thus the transformation from the W-plane to the c-plane is

$$W = (A/c) + B \tag{9}$$

where A and B are constants.

Hence

$$dW = -A \,.\, dc/c^2 \tag{10}$$

Now $W = iV_0$ when $c = \infty$, hence $B = iV_0$ and when c is real, $W = U + iV_0$ so that the line $BAODB'$ in the W-plane does transform to the perimeter of the conductor. In general, any point in the z-plane corresponds to complex c, but c is wholly real along the edge.

THE FIELD STRENGTH

The magnetic or electric intensity (field strength) at any point in Fig. 1 is

$$F = |dW/dz| = |dW/dc \,.\, dc/dz| = |dW/dc \,.\, dc/dk \,.\, dk/dz|$$

Now by equation (9)

$$dW/dc = -A/c^2 \tag{11}$$

and since $c = k^2$

$$dc/dk = 2k \tag{12}$$

By differentiating z in equation (8) with respect to c we get

$$dz/dk = -i\pi a/2kE^2 \quad \text{or} \quad dz/dc = -i\pi a/4cE^2 \tag{13}$$

Combining these results we get $F = |-4AE^2/\pi ac|$. Hence at B, when $c = 0$, F is infinite. At A when $c = 1$, $F = |-4A/\pi a|$. At D, when $c = \infty$, $F = |-4A/\pi a|$ the same as at the point A. To get this last result we have to use the relation that when $k \to 1/k$, $E \to [E - k'^2K - i(E' - k^2K')]/k$.

Numerical values of z are calculated for points along the boundary $BAODB'$, and along the internal axis of symmetry OZ. From B to A, along the side, c is real and less than unity and ordinary tables of E can be employed. From A to O, however, $1 < c < 2$, i.e. c is greater than unity, and we have again to use the relation that when

$$k \to 1/k, \quad E \to [E - k'^2K - i(E' - k^2K')]/k$$

the values in the bracket relating to values of k between 0 and unity (see Table 2 and Fig. 3). Along the internal axis of symmetry OZ, c is complex.

Writing $$c = 2/(1 + c_2) \quad (14)$$

or $$c_2 = 2/c - 1 \quad (15)$$

we see that at 0, i.e. when $c = 2$, $c_2 = 0$. Symmetry, with respect to c_2 is thus introduced. Along OZ, c_2 is of the form $c_2 = -i\alpha$, where α is real and positive. The inside of $BAODB'$ of Fig. 1 and of the region below the line in Fig. 2 now corresponds to the lower half of the c_2-plane (not shown). Also writing $\alpha = \sin x/(1 + \cos x)$ so that $c_2 = -i\alpha = -i \tan(x/2)$ we get $c = 2/(1 + c_2) = 1 + e^{ix} = k^2$.

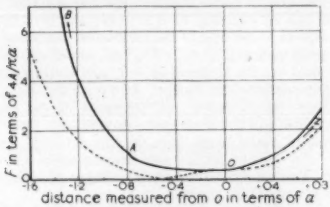

Fig. 3. Variation of F along boundary OAB and along centre line OZ. *Full curve:* slot investigated. *Dotted curve:* slot with straight end

Values of E for various values of x and α can be found by the aid of special tables by Cambi.[4] These give values of K and $(K - E)/\pi$ for $k^2 = 1 + e^{ix}$, whence, after some labour, values of E can be obtained. Table 1 shows values of the field strength F along OZ as well as along the edge BAO, and Fig. 3 includes a part representing the value of F along OZ. As expected the graph of F shows a cusp at the point A (or D), for A is a definite corner. The result found that F is steadily increasing along OZ in the direction of Z, is supported by a similar result for the internal field of a semi-infinite rectangular body.

In view of their importance in experimental work with atomic or molecular beams, the expressions for dF/dz and $d(F^2)/dz$ have been worked out. They are

$$dF/dz = |+ 16iAE^3K/\pi^2a^2c| \quad (16)$$

$$d(F^2)/dz = |- 128iA^2E^5K/\pi^3a^3c^2| \quad (17)$$

RESULTS

(1) *Field strength F on the axis OZ.*

The field strength F (e.s.u. or e.m.u. according to whether the problem is an electrostatic or magnetic one) is expressed as a multiple of $4A/a\pi$, the constant in the equation for F, i.e. the table gives $a\pi F/4A$. The distance z of the point concerned from O is expressed as a multiple of $ia/2$, i.e. the table gives $2z/ia$. The modulus c of the elliptic integrals is complex, except at O itself, where $c = +2$.

Table 1. (See also Fig. 3)

c	2·0000	1·9511 +i0·3090	1·8090 +i0·5878	1·5878 +i0·8090	1·3090 +i0·9510	1·0000 +i1·000
$2z/ia$	0·0000	0·302	0·504	0·722	0·902	1·084
$Fa\pi/4A$	0·355	0·498	0·645	0·830	1·06	1·35

(2) *Field strength F on the circular edge OD.*

s is the distance of the point concerned, measured along the edge from O. The radius of the edge is $a/2$ and the table gives $2s/a$, i.e. the distance along the edge as a multiple of $a/2$. The modulus c is real and greater than unity except at the point D, where it is equal to unity and $F = 4A/a\pi$, $s = \pi/2 \cdot a/2 = 1{\cdot}571a/2$.

Table 2. (See also Fig. 3)

c	2·0000	1·704	1·333	1·137	1·000
$2s/a$	0·0000	0·5672	1·0386	1·3492	1·571
$a\pi F/4A$	0·355	0·3735	0·477	0·690	1·000

(3) *Field strength F on the straight side DB.*

s is the distance of the point concerned from D. The table gives $2s/a$, i.e. distances as a multiple of $a/2$. The modulus c is real and less than unity except at D, where it is equal to unity.

Table 3. (See also Fig. 3)

c	1·0000	0·9699	0·8830	0·7500	0·5868	0·5000
$2s/a$	0·000	0·0496	0·1704	0·3524	0·6208	0·7490
$a\pi F/4A$	1·000	1·118	1·422	1·955	2·90	3·66

c	0·4132	0·3290	0·2500	0·1786	0·1170	0·03014	0·007604
$2s/a$	0·9110	1·0786	1·3352	1·5310	1·8160	2·724	3·606
$a\pi F/4A$	4·70	6·23	8·62	12·58	19·87	80·4	323·5

COMPARISON WITH A RECTANGULAR SLOT

It is interesting to compare the field of the slot investigated above with that of a semi-infinite rectangular slot of the same width a. The two slots differ only in that the two parallel sides BA and $B'D$ in the second case are joined by a straight line instead of the semi-circular arc AOD. The field of a semi-infinite slot has been investigated by one of the authors.[5] He showed that the electric intensity F inside the slot is given by

$$F = |(-i\pi C_3 \sinh u)/a| \quad (18)$$

where C_3 is a constant and u a variable given by $t = \cosh u$. If $u = p + iq$, it can be shown that the intensity along the straight end of the slot is given by

$$F = |(\pi C_3 \sin q)/a| \quad (19)$$

where q is in radians, and distances are measured from the centre point O of the straight end. Similarly it can be shown that the intensity along a vertical side is given by

$$F = |(i\pi C_3 \sinh p)/a| \quad (20)$$

where p is in radians.

The intensity along the centre line of the slot is given by

$$F = |(\pi C_3 \cosh p)/a| \quad (21)$$

Thus a graph of the variation of F along the perimeter and centre line of the conductor can be plotted. This curve is shown dotted in Fig. 3 for comparison. In order to render comparison easier, the constant C_3 of equations (18–21) has been adjusted so that both conductors have the same value of F at the origin O. This is done by putting $C_3 = (1{\cdot}42A)/\pi^2$.

Fig. 3 shows that the intensity at any point along the perimeter or centre line of the straight-ended slot is less than the intensity at the corresponding point of the circular-ended slot the same distance away from the origin O. Also, whilst the intensity increases as we move from the origin in the case of the circular-ended slot, in the other case F decreases to zero as we approach a corner.

REFERENCES

(1) Cockroft, J. D. *J. Instn Elect. Engrs*, **66**, p. 385 (1928).
(2) Forsyth, A. R. *Differential Equations*. (London: 6th Ed. 1933).
(3) Cayley, A. *Elliptic Functions*, 2nd Ed. (London, 1895).
(4) Cambi, E. *J. Maths. and Phys.*, **26**, p. 234 (1948).
(5) Davy, N. *Phil. Mag.*, **36**, p. 694 (1945).

Measurement of die pressures in wire drawing by photoelastic methods

By P. M. Cook, B.Sc., A.Inst.P., A.I.M., and J. G. Wistreich, M.Sc.(Eng.), D.I.C., A.M.I.Mech.E.,
Metal Working Laboratory, British Iron and Steel Research Association, Sheffield

[*Paper received* 9 *October*, 1951]

Wire drawing has been simulated by drawing lead-tin alloy strips through a wedge-shaped die made of stress-optically sensitive plastic, and the pressure normal to the die-metal interface has been measured by the photoelastic method. This is a comparatively uncommon application of photoelastic stress analysis, in that the externally applied pressure is deduced from the stress pattern in the interior of the model. For this reason the experimental techniques and the computational procedure are described in detail. Filon's method of stress analysis was chosen in preference to other methods on account of restrictions imposed by the conditions of the experiment. The accuracy of the graphical computation was enhanced by the use of alternative methods and paths of integration which lent themselves to cross-checking. The pattern of isoclinics was found to have features which are not discussed in standard textbooks on photoelasticity, and which call for some modification of the usual computational procedure.

The results are in good agreement with a theory of drawing due to Hill,[1] and extended by Green.[12]

INTRODUCTION

Whilst several attempts have been made in recent years to deduce from theory the stresses present in wire drawing, experimental evidence, apart from measurements of the drawing force, is lacking. The theory cannot be compared satisfactorily with measurements of the drawing force because of ignorance about friction in the die. The pressure between wire and die, however, is much less sensitive to friction than the drawing force[1]; for this reason it seemed most desirable to measure the die pressure in order to compare experiment with theory. It was also hoped that the knowledge of the variation of pressure along the die-wire interface might help to explain the non-uniform wear of wire drawing dies.

The photoelastic method has already been applied to this problem by Thompson and Barton,[2] who used a celluloid model to represent the section of wire passing through a die. The model was placed between two wedge-shaped steel dies and subjected to a longitudinal pull. In these circumstances, however, the "wire" remained at rest and was not plastically deformed. In the present investigation a metal strip was actually drawn through a die made of a stress-optically-sensitive plastic, and the stress pattern was recorded whilst the strip was in motion.

Whereas one fundamental requirement of physical similarity with wire drawing was thus satisfied, in another respect the experiments were not strictly comparable with wire drawing, which is a three-dimensional process; the experiments were two-dimensional. The photoelastic "stress-freezing" technique, which is designed for the study of three-dimensional stress problems, was not attempted for two reasons. First, at the relatively high loading temperature that is needed in this method the plastic die would be too soft to support, without gross distortion, the heavy stresses accompanying the drawing of even the softest metal; second, the drawing operation, even if possible, would have to continue for several hours whilst the die cooled to room temperature, so that even with a very low drawing speed a great quantity of wire would have to be drawn through the die. There is, however, good reason for exploring the two-dimensional problem, since the most recent theory[1] is concerned with the drawing of sheet, or of strip under conditions of plane strain.

This paper is concerned with the investigation principally as an example of a fairly uncommon problem in photoelasticity. The implications of the findings for wire drawing theory are only briefly touched upon, and will be examined in greater detail in another paper.

DETAILS OF APPARATUS AND MATERIALS

Drawing equipment. The device for drawing the metal strip is shown in the centre of Fig. 1. The jig holding the die appears in greater detail in Fig. 2. It consists of two L-shaped backing plates *A*, which support and locate the halves of the plastic die *B*. Stress-free glass plates *C*, 1·25 mm thick, and held in place by the outer frame *D*, prevent lateral spread of the metal strip *E* during drawing.

Photoelastic equipment and materials. A polariscope with a 3½ in (89mm) diameter working field was designed on conventional lines, and is shown in Fig. 1 fully assembled, with the drawing equipment in place. Details of the components are listed below:

(1) Two alternative swivel-mounted light sources; a 150 c.p. Pointolite lamp and a 250 W Siemens Sieray mercury vapour lamp, the latter fitted with a $\frac{1}{8}$ in (3mm) diameter aperture;

(2) 2 in (51 mm) diameter × 2 mm thick heat filter (Chance ON19 glass);

(3) Wratten No. 77 light filter, which passes monochromatic light of wavelength 5461 A from the Sieray lamp;

(4) 5 in (127 mm) diameter plano-convex lens of 8 in (203 mm) focal length;

(5) Polaroid sheets, 4 in (102 mm) square, in graduated, rotatable mounts;

(6) Mica quarter-wave plates, 4 in (102 mm) square,

secured between thin sheets of stress-free glass in graduated, rotatable mounts;

(7) 8 in (203 mm) diameter plano-convex lens of 30 in (762 mm) focal length. (The large diameter and long focal length serve to minimize spherical aberration);

(8) 14 in (356 mm) focal length, f 5·6 camera lens.

(9) Half-plate stand camera with lens removed.

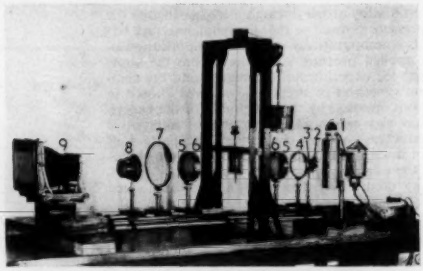

Fig. 1. Equipment used in experiments

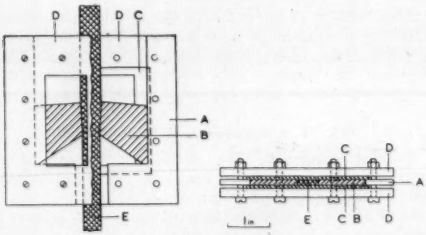

Fig. 2. The die jig

Two types of stress-sensitive plastic were used for the die: CR.39, an allyl styrene resin, with a stress-optical coefficient of approximately 35 brewsters, and Perspex type B (polymethyl methacrylate) with a coefficient of approximately 4 brewsters. The former material was used for recording the isochromatics; the latter served for recording the isoclinics, because owing to its lower sensitivity it displays fewer isochromatics and therefore offers a clearer background to the isoclinics. Both materials were shaped and polished by standard methods[3, 4] to a thickness of 0·140 in, and no trouble was experienced with machining stresses. The model fringe value of the CR.39 plastic, determined in a compression test, was 680 lb/in^2 per fringe.

DETAILS OF EXPERIMENTS

In preliminary tests pure lead was drawn through a die similar in shape to the cross-section of a conventional wire-drawing die. In order to photograph the stress pattern whilst the metal was being drawn, a steady speed of the order of 1 in per minute was desirable. The pure lead, however, would not draw smoothly at this slow speed owing to recrystallization. At first it yielded at a fairly low load. Then, the deformation caused the lead to work-harden sufficiently for the drawing to cease temporarily. The interruption of deformation, however, enabled the lead to recrystallize and with the consequent lowering of the yield stress drawing recommenced. Drawing thus proceeded in jerks. For this reason lead-tin alloys, which do not recrystallize at room temperature, were adopted for the main experiments.

Metal strips were made of commercially pure lead, alloyed with small amounts (3% and 5%) of tin, and cast into a heated, split mould of steel. The cast strips, measuring $\frac{1}{4} \times \frac{1}{2} \times 18$ in, were rolled in a hand-operated assay mill to 0·138 × 0·500 in. The 5% alloy was annealed when 0·173 in thick, the 3% alloy after the final rolling operation. The anneal consisted of soaking at 210/220° C, followed by cooling in air. The finished strips were painted with a concentrated solution of wire-drawing soap in water and left to dry. The thin and well-adhering soap film served as a lubricant in the drawing operation.

The preliminary tests demonstrated that the conventional die shape, shown in Fig. 3, was unsuitable for photoelastic stress analysis, because outside the shaded

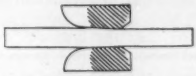

Fig. 3. Conventional die-shape

areas the die was so lightly stressed and the isoclinics so ill-defined that the principal stress trajectories could not be traced with any certainty. Since, as is explained below, it is essential that these trajectories should be accurately known starting from a free boundary, the shape of the die had to be altered by stages until the desired result was obtained. The shape finally adopted is shown at *B*, Fig. 2. It may be argued that since this shape departs from the conventional one the stresses in the die will be different. It should, however, be noted that the principal aim of the investigation was to study the stresses at the die/wire interface and these are determined solely by the plastic properties of the metal and the shape of the deformation zone. The latter could be expected to remain unchanged to the first order of magnitude, since the die is distorted only elastically. Consequently the chosen shape of the die was deemed acceptable for the purpose in view. The inclination of the die face to the wire axis was 4·5°, and the strip was reduced 21% in width.

One experiment with each alloy was performed; the same die was used in both experiments. The difference between the two experiments lay in the different mechanical properties of the two alloys. True-stress/logarithmic-strain curves (Fig. 4) were obtained by compressing small cylinders cut out from the strip with their axes normal to the direction of drawing. The compression test data

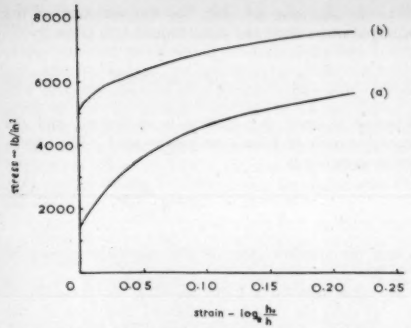

Fig. 4. Stress-strain curves for the two alloys
(*a*) Annealed 3% alloy. (*b*) Work-hardened 5% alloy.

were corrected so as to refer to plane strain conditions. Since both experiments presented similar problems in photoelastic stress analysis, only the one using the 3% alloy will be discussed in detail.

In order to avoid dismantling the die jig half-way through the experiment (which might disturb the conditions at the interface), one half of the die was made of the CR.39 plastic and the other from the Perspex. The isochromatic fringe patterns in the CR.39 half were photographed in monochromatic light and with both bright and dark backgrounds, thereby showing the position of every half fringe. The isoclinic lines in the Perspex half of the die were photographed in white light and with a dark background. Isoclinics of parameters 60° to 80° by 5° intervals, and 82½° to 95° by 2½° intervals, were needed for the subsequent stress analysis, making a total of thirteen photographic exposures for each experiment.

The isochromatic pattern obtained by drawing the 3% alloy is shown in Fig. 5. The isoclinics near the metal/die interface were rather diffuse and difficult to trace accurately, owing to the fact that in this region the principal stresses did not change direction very rapidly. Examples of clear and diffuse isoclinics may be seen in Figs. 6 and 7.

The isoclinics and isochromatics were traced on to a master diagram of the die from 6 × 9 in enlargements of the thirteen photographs in the following manner. The

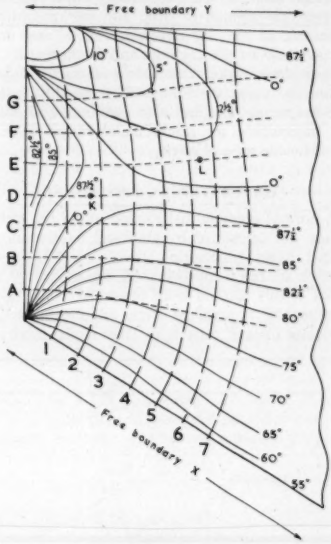

Fig. 8. Master diagram
——— Isoclinic lines. — — *p* stress trajectories.
– – – – *q* stress trajectories.

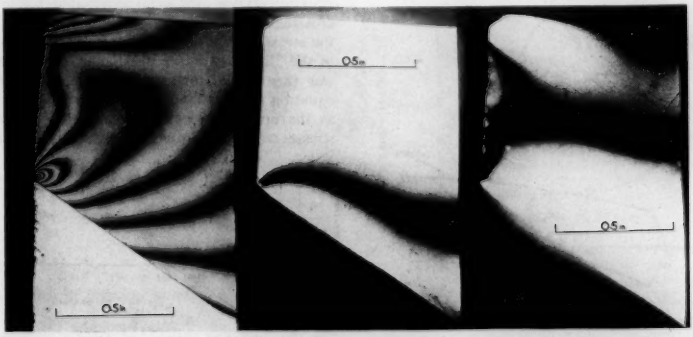

Fig. 5. Isochromatic pattern

Fig. 6. 75° Isoclinic

Fig. 7. 87½° Isoclinic

photographic prints were made on sensitized aluminium foil to ensure that no change in dimensions occurred during processing. By reversing the appropriate negatives in the enlarger the isoclinics and isochromatics were made to refer to the same half of the die. The centre line of each isoclinic and isochromatic was then located by visual examination and, together with the outline of the die, was marked by a series of pin-holes through the aluminium foil. A sheet of tracing paper was placed over each photograph in turn, and the underside was illuminated, so that the pin-holes enabled one to trace the centre lines of the isoclinics and isochromatics. The principal stress trajectories were constructed from the isoclinics by using the "tangent" method.[5, 6] Fig. 8 shows the master diagram with isoclinics and principal stress trajectories; the isochromatic fringes have been omitted for the sake of clarity.

COMPUTATIONAL PROCEDURE

The normal pressure distribution along the metal/die interface was calculated by graphical integration along principal stress trajectories, based on Filon's transformation of the Lamé–Maxwell equations.[7, 8] Two variants of this method were employed. The first was used whenever a principal stress trajectory intersected the isoclinic lines at reasonably large angles (above, say, 50°). In this case (cf. Fig. 9*a*) the variation of the principal stress along the stress trajectory is given by

$$p_n = p_1 + \int_1^n (p - q)\cot\psi d\theta \qquad (1)$$

When ψ is small this method is inaccurate, and the second variant of Filon's method is used. The appropriate equation is

$$p_n = p_1 + \int_1^n (p - q)\frac{ds_1}{ds_2}d\theta \qquad (2)$$

where the symbols refer to the quantities shown in Fig. 9*b*.

In either method a curve showing the variation of $(p - q)$ along the trajectory is plotted, and from this the values of $(p - q)$ at the points 1 to n in Fig. 9 are read off. These values are then multiplied by cot ψ (or divided by ds_2 when the second method is used) and the products are likewise plotted. The mean values between points 1–2, 2–3, etc., are then multiplied by $d\theta$ (or $d\theta \cdot ds_1$) to give the increments by which p increases or decreases from point to point. It should be noted that cot ψ, $d\theta$, ds_1, and ds_2 may be either positive or negative, and care must be taken to give each increment of the integral its correct sign.[9] A curve showing the variation of p along the trajectory can then be plotted. The value of the other principal stress q at any point is found by referring to the appropriate value of $(p - q)$ derived from the curve already plotted.

It will be apparent from this description of the computational procedure that there are many possible sources of error and that the individual errors are additive. For this reason the paths of integration in this problem were so chosen as to afford as many check points as possible. In fact (as is shown below) the errors were, on the whole, surprisingly small.

Referring to Fig. 8, the graphical integration was first performed along the p stress trajectories, starting at points 1 to 7 along the boundary X. In each case equation (1) was used as far as possible (e.g. to the second crossing of the 87½° isoclinic for line 1). In the case of the stress trajectories 3 to 7, which are cut by isoclinics of the "loop" type (see discussion below), another start was then made from the other free boundary Y, and equation (1) was used along the five trajectories as far as the opposite sides of the looped isoclinics. The p stresses were then plotted and it was found that the values

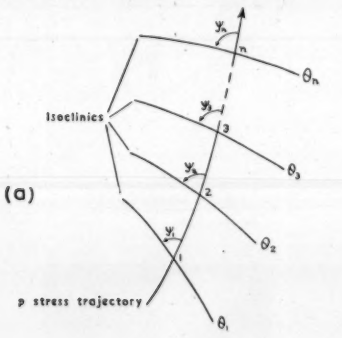

Fig. 9. Filon's method for calculating separate principal stresses

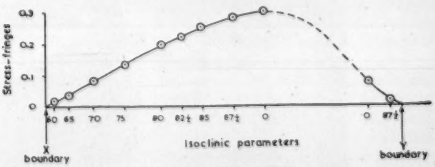

Fig. 10. Variation of principal stress, p, along trajectory 7
Model fringe value = 680 lb./sq. in/fringe.

inside the isoclinic loops could be safely interpolated. The longest gap between the two series of integrated values was that inside the 0° isoclinic along line 7; but even here the shape of the two branches of the curve was such that they could be joined without the risk of serious error, as may be judged from Fig. 10. Lines 1 and 2 were not continued to the Y boundary because the isoclinics were too congested for reliable integration. The integration along line 1 from the second crossing of the $87\frac{1}{2}°$ isoclinic to the 0° isoclinic was completed with the aid of equation (2).

Next, the values of the q stresses were deduced from the values of p at all the points of intersection of the two orthogonal families of trajectories, and were plotted along the lines terminating at points A to G. It was originally hoped that the curves so produced might be extrapolated to give the values of the q principal stresses at the contact boundary, but check calculation revealed the unsoundness of this idea. The check consisted of integrating along the q stress trajectories, starting with values of q deduced from the p stress trajectories. The integrations along trajectories A, B and C were started at the points of intersection with line 7; equation (2) was used up to the 80°, 85°, and $87\frac{1}{2}°$ isoclinics respectively, and from thereon equation (1) was used. The good agreement between the q stress curves so produced and those deduced from the p stress trajectories, is indicated in Fig. 11(*a*); the largest difference between the two curves is only 2%. At the same time it is clear that the q stress at the boundary could not have been determined by extrapolation because of the change in shape of the stress curve close to the boundary. The largest differences between the curves for trajectories A and C were 6% and 3% respectively.

The integration along line D was also started from the intersection with line 7, but because of the unusual isoclinic pattern no progress could be made beyond the point K. The integrated curve up to this point, however, showed such close agreement with the curve deduced from the p stress trajectories, cf. Fig. 11(*b*), that confidence could be placed in an extrapolated value of q at the intersection with the $87\frac{1}{2}°$ isoclinic, from which point equation (1) could be applied without further difficulty right to the boundary.

Because of the "loop" type of isoclinic lines, the integrations along lines E, F and G were started progressively nearer to the boundary, and the starting values of q at these points were again read off the curves deduced from the p stress trajectories. The greatest difference between the integrated curves and those deduced from the p stress trajectories was 6% for line E (see Fig. 11c); for lines F and G the differences were 5% and 3% respectively.

The principal stresses q along the contact boundary of the die did not act in directions normal to the surface, but were inclined at angles to the normal which varied from approximately $\frac{1}{2}°$ in the vicinity of point A, to approximately 5° in the vicinity of points E and F. Such inclination was, of course, expected owing to the presence of friction. The normal pressure σ was computed with the aid of the equation

$$\sigma = \tfrac{1}{2}(p + q) - \tfrac{1}{2}(p - q)\cos 2\theta$$

where θ is the angle between q and σ.

The curves depicting the variation of normal pressure along the metal/die interface are shown for both alloys in Fig. 12. The stresses at the points of entry to, and

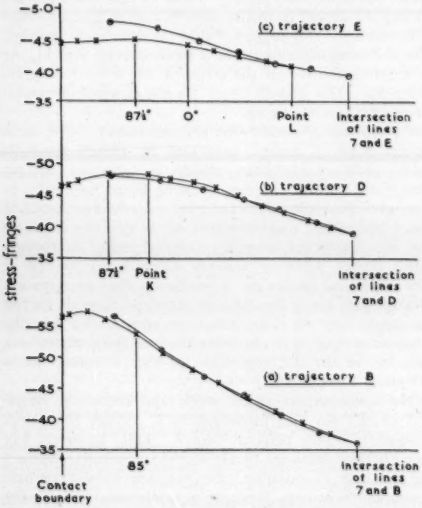

Fig. 11. Variation of principal stress, q, along trajectories B, D, and E

Model fringe value = 680 lb/sq. in/fringe.
—○—○—○— Curves deduced from p stress trajectories.
—×—×—×— Curves obtained by integration.

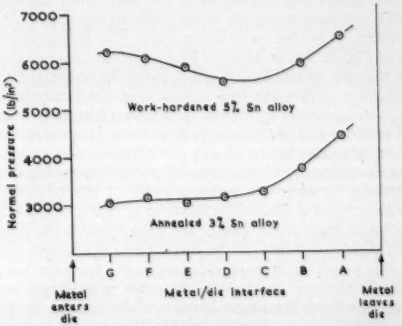

Fig. 12. Variation of normal pressure along metal/die interface

exit from the die could not be evaluated, because it was impossible to resolve the isoclinic patterns at these points.

DISCUSSION

The choice of the method of stress analysis was restricted by the conditions of the experiment. It was not possible, for example, to base the analysis on isopachic patterns, because the model had to be constrained laterally in order to satisfy the condition of plane strain. Again, owing to the peculiar shape of the model, which is constrained on two opposite sides, the method employing the numerical solution of the Laplace equation was also unsuitable, and in the circumstances Filon's method had to be used. The efficacy of this method depends to a large extent on the geometry of the isoclinic and isochromatic patterns and on the accuracy with which the individual isoclinics (and isochromatics) are located. Difficulties were experienced on both counts and deserve to be discussed in detail.

Peculiarities of the isoclinic pattern. An unusual problem arises when computing the principal stress function along a trajectory which crosses a system of looped isoclinics, similar to that exhibited in the upper half of Fig. 8. Equation (1) cannot be used to integrate the stress function between opposite sides of a loop since, with $d\theta$ equal to zero, the increment is zero, implying—usually quite incorrectly—that the stress is the same on either side of the loop. Equation (2), on the other hand, fails because neighbouring isoclinics rapidly deviate from the trajectory lying between them, so that the transverse ds_2 measurements cease to be reliable. The gap between opposite sides of a loop can, of course, be reduced by determining one or more intermediate isoclinics; one might, in fact, completely map out the area inside the loop. It follows from geometrical considerations that one isoclinic inside the loop is tangent to the trajectory, but since at the point of tangency (which, as a matter of interest, is a point of inflexion in the stress trajectory) $\cot \psi = \infty$, equation (1) is still inapplicable. In these circumstances, the method adopted in the present investigation—of approaching the loop from opposite sides and completing the stress curve by interpolation—appears to be the only alternative. The interpolation, as in Fig. 10, can be justified by a qualitative examination of the change of $(p - q)$ and ψ along the portion of the trajectory within the loop. Referring, for example, to the p stress trajectory 7 (Fig. 8), it is seen that an isoclinic of parameter approximately 2° will be tangent to the stress trajectory in the vicinity of its intersection with the q stress trajectory F. The value of $(p - q)$ is approximately constant between the opposite sides of the looped 0° isoclinic, and ψ clearly increases in a steady manner as we move from either side of the loop towards the point of tangency. Since, at the same time, $d\theta$ changes sign at this point, the stress decreases steadily from the lower branch of the 0° isoclinic to the point of tangency, and increases from the upper branch of the isoclinic to the point of tangency. It is reasonable, therefore, to suppose that inside these looped isoclinics the stress changes monotonically.

Another feature of the stress system worth mentioning here is found in the vicinity of point K (in Fig. 8). The 0° isoclinic which starts from the die exit is, clearly, a "degenerate loop," and therefore the isoclinic pattern in this region contains one isoclinic, with parameter between 87½° and 0°(90°), which consists of four branches radiating from a point. The directions of principal stresses change, however, so very little in this region that this isoclinic would be extremely difficult to locate. At the same time, since the fringe order in this region is also fairly constant, the principal stresses do not change much and can therefore be safely extrapolated (cf. Fig. 11*b*).

Accuracy of stress analysis. Photometric and other methods which enable the fringes and isoclinics to be located with remarkable accuracy,[10, 11] are time-consuming. They were unsuitable in the present investigation because the photoelastic pattern had to be recorded whilst drawing was in progress; consequently visual examination of the photographs had to be relied upon. Difficulties with locating the isoclinics by visual examination, which were encountered in exploratory experiments, were overcome by substituting the insensitive Perspex for the CR.39 plastic and by suitable choice of photographic techniques.

The errors in the actual computation, which depend upon the measurements of the fringe order $(p - q)$, distances ds_1 and ds_2 and the angles ψ, are estimated to be not more than $\pm 2\%$. None of the values plotted in Fig. 12 depart from the smooth curves by more than this amount. It is suggested that the differences between the two computations of the q stress curves, Fig. 11, are a rough indication of the errors in the master diagram (Fig. 8). The overall error in the normal pressures probably does not exceed $\pm 5\%$.

Comparison of results with drawing theory. The most recent drawing theory, proposed by Hill,[1] accounts more satisfactorily than earlier theories for certain observed relations between drawing force, reduction in size, and die angle. However, for reasons mentioned in the introduction, measurements of the drawing force do not afford sufficient scope for a crucial test of the theory. Hill's theory, however, sharply differs from the rest in one important particular; it predicates that the pressure at any point along the die-wire interface depends on the die angle and the *total* reduction effected by the die, whereas according to the other theories the pressure is a function of the die angle and of the reduction *up to* the point considered.

The combination of die angle and reduction which was chosen for this investigation is outside the range covered by Hill's original theory. This, however, has recently been extended by Green,[12] according to whom* (in the case in question) the pressure should at first decrease, then pass through a minimum, and finally increase towards the die exit. (According to older theories the pressure decreases continuously from entry to exit.) Fig. 12 shows that this prediction is in

* Private communication.

qualitative agreement with the behaviour of the already work-hardened alloy, but not with that of the annealed one. This difference is to be expected because the theory is based on the assumption that the metal does not work-harden; it can be applied in a qualitative manner to a work-hardened metal, but not to the initial working of a fully annealed metal.

The effect of friction. Friction at the die-wire interface is responsible for the inclination of the principal stresses to the interface normal. Unfortunately, owing to the difficulty of locating the isoclinics in closest proximity to the interface, the degree of inclination could not be measured with the desired precision. Nevertheless, the measurements are sufficiently reliable for stating that the coefficient of friction varied between about 0·05 and 0·01, being largest near the die entry and smallest near the die exit. The upper value is of the order attributed to wire drawing by many investigators, the lower value, though surprisingly low, is in accord with certain results reported by Thompson and his co-workers.[13]

Whilst drawing was in progress fine "ripples" appeared from time to time in the isochromatic pattern in closest proximity to the interface. These "ripples" invariably propagated from die entry towards die exit. Similar disturbances occurred in isoclinics located close to the interface. These disturbances, which are clear evidence of varying friction, did not influence the main stress pattern.

Elastic v. *plastic "loading."* The stress pattern, and particularly the isoclinic pattern, were notably different before drawing commenced, during drawing, and when drawing was interrupted and the strip partly unloaded. It was originally found, for example, that the 0° isoclinic starting from the die exit during drawing, would start from the die entry when drawing was interrupted and the strip was loaded only elastically. This observation substantiates the argument which led to the adoption of the present experimental technique in preference to Thompson and Barton's, namely that the interfacial stresses in the elastic loading of strip are not equivalent to those prevalent during drawing.

ACKNOWLEDGEMENTS

The authors gratefully acknowledge Col. H. T. Jessop's invaluable advice on the design and use of the polariscope, and helpful suggestions in the course of the investigation. They also greatly profited by frequent discussions with Dr. R. Hill and their colleague, Mr. A. P. Green, on the theory of strip drawing.

This paper is published by permission of the Director of the British Iron and Steel Research Association.

REFERENCES

(1) Hill, R. *Mathematical Theory of Plasticity*, p. 163 (London: Oxford University Press, 1950).
(2) Thompson, F. C., and Barton, J. *Carnegie Scholarship Memoirs, J. Iron Steel Inst.*, **19**, p. 39 (1930).
(3) Frocht, M. M. *Photoelasticity*, Vol. I, 2nd ed., p. 349 (New York: John Wiley and Sons Inc., 1948).
(4) Jessop, H. T., and Harris, F. C. *Photoelasticity*, p. 123 (London: Cleaver-Hulme Press Ltd., 1949).
(5) Frocht, M. M. Reference (3) above, p. 198.
(6) Jessop, H. T., and Harris, F. C. Reference (4) above, p. 131.
(7) Frocht, M. M. Reference (3) above, p. 287.
(8) Jessop, H. T., and Harris, F. C. Reference (4) above, p. 79.
(9) Frocht, M. M. Reference (3) above, pp. 294–308.
(10) Brown, A. F. C., and Hickson, Y. M. *Brit. J. App. Phys.*, **1**, p. 39 (1950).
(11) Fisher, W. A. P. *Research*, **3**, p. 298 (1950).
(12) Green, A. P. *Phil. Mag.*, **42**, p. 365 (1951).
(13) Baron, H. G., and Thompson, E. C. *J. Inst. Metals*, **78**, p. 415 (1950).

NOTES AND NEWS

New books

Some recent developments in rheology. Edited by V. G. W. Harrison, B.Sc., Ph.D., F.Inst.P. (London: United Trade Press Ltd.) Pp. vii + 140. Price 20*s*.

This book consists of a series of papers read at a conference held by the British Rheologists Club at Bedford College in October 1946. The first part deals with soft materials—greases—in papers by E. G. Ellis, who gives a review of conventional methods of measurement and some all-too-rare results of temperature variations. J. W. Amner and J. F. T. Blott review viscometers including the pendulum one. Chapter III consists of a paper by K. Weissenberg on the geometry of rheological phenomena which was illustrated by demonstrations and models at the meeting; these are not described here at all but just mentioned—an omission which seriously reduces the value of the contribution. The next chapter by S. M. Freeman described as "the practical application of Dr. Weissenberg's proposal of a 'rheogoniometer' " is quite incomprehensible in the absence of illustration and diagram. It reads in fact rather like a description of one of the inventions of Dr. Strabismus.

Chapter V, by the late H. Green, is important insofar as the author most definitely insists upon the existence of a hysteresis loop—that is, a time lag in re-equilibriation of a system under shear—as the criterion of thixotropy. This view is unacceptable in this country but seems to be accepted widely in the United States.

Chapter VI is a survey of methods used for the examination of the rheology of pastes and doughs. Chapter VII by J. M. Buist is on hardness testing of the rubber-like state; Chapter VIII by C. M. Blow and J. A. Schofield describes: "the measurement of stress relaxation of unvulcanized rubber by means of the Mooney shearing—disk viscometer." Chapter IX is a very complete analysis of the problems arising in wood by W. W. Barkas. The last contribution, by L. R. G. Treloar, is a survey entitled "the meaning and use of certain rheological terms." The book illustrates all too well the rapid change which has come over this subject. Once upon a time many workers used non-Newtonian viscosity to obtain information of the nature of the particles which caused the non-Newtonian behaviour by a dissipation of energy over

and above that required for the normal Newtonian flow of the dispersion medium. To-day the rheologist seems to regard the problem as one of fluid mechanics only and is satisfied by being able to say that his material is of type X7, or whatever it may be, in some chart of all the possible systems. This seems to your reviewer to be a singularly sterile approach, but not because he regards a more physical view as less revealing than a more chemical one. The history of the change of outlook is really that those who call themselves "rheologists" are mostly applied scientists working on the very difficult problems of consistency in commercial materials where this usually high consistency is its commercially valuable property. They never therefore dilute their systems or heat them enough to approach fluidity in its normal sense. The academic scientist always tries to dilute his system to such an extent that mutual interaction of particles of the disperse phase is eliminated: effects then observed are those due to and resulting from interaction of each individual particle with its fluid environment and subject to such changes of that fluid environment as the experimenter may choose to make. He then has a zero state from which he may proceed to find the effects of particle interaction by increasing the concentration of the system. It would be most unfortunate if this approach were excluded from rheology.

A. S. C. LAWRENCE

Magnetic and electrical methods of non-destructive testing. By D. M. LEWIS, B.Sc., A.I.M. (London: George Allen and Unwin Ltd.) Pp. 242. Price 35*s*.

This book, which covers a deliberately restricted field, is an excellent review of the subject. The wise exclusion of methods, such as radiography, which only incidentally employ electrical techniques and equipment, enables full reference to be made to original papers on a subject in which, as Professor Bates says in his foreword, the diversity of the work already carried out is surprising even to the expert. The first half of the book covers crack detection, starting with magnetic ink and powder methods, followed by a shorter section on the use of other devices, such as search coils. The information set out in this half is a result of extensive practical experience of crack detection and will enable the industrial user coming new to the field to get a complete picture not only of the problem, but also of many of its solutions. The presentation of a full list of references enables some technical details to be omitted, and an overall picture to be presented in an understandable manner. The second half of the book sets out many methods for characterizing metals, for example, according to composition, heat treatment and the presence of fatigue. As this section contains details of more recent work, much of which has been carried out only in America, it is of greater value for indicating possibilities of technique than as a guide to available types of equipment.

Since the book has been vetted by a committee of experts it is probably the most authoritative British work on this subject. It is the more surprising, therefore, that the author should not have been more positive in some of his statements: for example, on page 21 the reference to the roving field technique implies that this is going out of fashion, without any statement as to whether this is because of scientific or technical shortcomings. Again, on page 42 the very real danger of using a.c. methods for magnetizing (especially for routine inspection) is not sufficiently stressed and the methods to be used to overcome the dangers are not made sufficiently clear. It is surprising that more work has not been carried out on control of field strength in crack detecting, the statement on page 55 that instruments are being applied would indicate that very little has been done so far to overcome the effects of ineffective magnetization which have been appreciated for the past ten years.

The division of the subject of crack detection into its various fields would have been helped by cross-references; the combined a.c. and d.c. methods, for example, are included under testing procedures and only casually mentioned under methods of magnetizing, where one would obviously first look for them. As a radiologist, the reviewer feels that the implication on page 72 that only very serious shrinkage cavities can be located by radiography, gives a wrong impression of the strength of this alternative technique.

The book is probably the most useful starting point for anyone entering this field; the possible methods are given and details can easily be obtained from the appropriate paper among the 274 references given. The appendices also will assist the inexperienced person in deciding upon the type of test for any particular inspection requirement.

R. JACKSON

Colour cinematography. 3rd edition. By ADRIAN CORNWELL-CLYNE, M.B.E., F.R.P.S. (London: Chapman and Hall Ltd.) Pp. xvi + 780. Price 84*s*.

This is a third and a very much enlarged edition of the earlier book, the second edition of which was published in 1939. Many sections have been expanded in particular the section on three-colour subtractive processes which has grown from 34 to 158 pages. New sections have also been added for example those entitled trichromatic analysis, background or process projection, colour film sound tracks, and stereoscopic motion picture in colour. In addition to the expansion, which is to be expected in a treatise on this growing subject, a change of atmosphere has crept in since the previous edition. The whole book has taken on a scientific air. The machinery of the C.I.E. colour measuring system is introduced at a very early stage—long before its foundations are discussed in the subsequent theoretical section—and continues to be used throughout the book. While it cannot be assumed that the application of colour measurement is the single and indisputable criterion in the valuation of colour reproduction, yet it cannot but be indispensable in clarifying the functions of art and precise technique in this field. R. DONALDSON

Modern magnetism. 3rd edition. 1951. By L. F. BATES, Ph.D., D.Sc., F.R.S. (London: Cambridge University Press.) Pp. xii + 506. Price 30*s*.

The second edition of this well-known book was published in 1948 and consisted essentially of the text of the first, published in 1939, with a number of additional chapters and notes giving an account of the more recent researches in magnetism. The whole book has now been rearranged so that the various topics lumped together at the end of the second edition appear in their appropriate contexts. There are also two largely new chapters: one on the properties of paramagnetics and ferromagnetics in alternating fields, including paramagnetic dispersion and nuclear resonance; the other on domain effects and hysteresis in ferromagnetics, including an account of recent work on these subjects by the author and his collaborators.

The book now covers a very wide range of subjects, both experimental and theoretical, and this has involved some drastic compression in the discussion of certain of them; but those whose interest in any particular topic is aroused, as it may well be by the author's account, will be greatly helped in studying it further by the many references which are given to original papers.

P. RHODES

The illumination of photographic darkrooms. By G. WEBER. (Copenhagen: Fr. Bagges Kgl. Hofbogtrykkeri.) Pp. 278. Price Danish Kr. 15.00.

This book is a thesis for a technical doctorate, and deals with problems of designing the lighting arrangements for photographic darkrooms. The author sets out the broad problems and after briefly reviewing the literature on the research work on this subject, discusses the available commercial lighting equipment. By considering the extent to which the photographic material and the eye receive and evaluate light it is shown how it is possible to determine the optimum colour of illumination, and also the quantity which is permissible.

The author's experimental measurement of the colour sensitivity of photographic materials has been dealt with comprehensively. Photometric units and measuring methods are considered in detail, and to a lesser extent, the spectral transmission of the light filters. A survey of the commercial safelight filters of the dyed gelatine type, even if not current, shows that the manufacturers of photographic materials appear to solve the problems in similar ways.

The general use of any lighting equipment means that specific designs of filters and lamps cannot always be used to best effect. The author does not draw up a code of lighting which would enable illuminating engineers to schedule a darkroom lay-out. The reason for this may lie in the brevity of the outline to the physiological aspects of vision at low illuminations. Although no experimental work had been carried out a more extensive review of this aspect together with the psychological aspects of darkroom lighting might well have lead the author to have formulated a few psychological and physiological rules which are needed to guide a lighting engineer.

As the first book on this subject it is to be welcomed particularly for the care with which it is written; and although the emphasis is not on those points which any engineer would appreciate most, its technical data is nevertheless of great value. R. B. MORRIS

The interpretation of X-ray diffraction photographs. By N. F. M. HENRY, H. LIPSON and W. A. WOOSTER. (London: Macmillan and Co. Ltd.) Pp. 249. Price 42*s*.

This book is an important contribution to the literature of crystallography. It is designed to meet the needs of the physicist or chemist who wants to train himself to use the methods of X-ray crystallography, and of the crystallographer who wants the information on techniques which is scattered through the literature brought compactly and authoritatively into one volume. It does both admirably.

It opens with an account of crystal geometry and notation, followed by an explanation of the stereographic and other projections, and an introduction to the concept of the reciprocal lattice. A short chapter on X-rays serves to emphasize those aspects which are relevant to crystallographic work. The different types of X-ray photograph are considered in detail, the methods of interpretation being illustrated by actual examples. There are chapters on related topics such as preferred orientation, line broadening, and measurement of intensities. One particularly valuable chapter deals with the symmetry of the lattice, with special attention to the relationship of hexagonal and rhombohedral lattices, which is notoriously confusing. The authors' treatment is clear and authoritative, and the chapter may well become the standard reference work on the subject.

No previous knowledge of crystallography is required of the reader, nor any advanced mathematics, but much of the book will be lost on anyone who is not prepared to follow the examples in detail and familiarize himself with the geometry and notation. For those who take that trouble, it is clear, straightforward and helpful. The experienced crystallographer is likely to find it essential as a work of reference. Details of technique may go out of date, but the principles of the methods are well established and not likely to change; the main emphasis of the book is on the underlying geometry, and this remains unaltered.

One might question the relative importance accorded to different sections of the book, or to different methods within a section, but such criticism is likely to depend on one's own particular interests. The general effect is well balanced. It is a pity that the paragraph on X-ray wavelengths (Chapter 2) does not emphasize the danger of confusion between kX and Ångström units in consulting the older literature, and explain how to avoid it. In Chapter 15, the structure intensity should be denoted by $|F|^2$, not F^2; the incorrect expression not only provides an unnecessary stumbling-block for beginners, but may in the future lead to real confusion, since recent methods of analysis do in fact make use of F^2, which is a complex quantity. But these are small points, which can be corrected.

In general, it is obvious that a high standard of accuracy has been aimed at, and largely achieved. Definitions are given with care and words are used in their exact sense. Misprints are very few. There are useful tables, and solutions to the illustrative exercises are given in an appendix. The print and diagrams are clear, and the book is pleasant to handle. The price is not high by present standards.

H. D. MEGAW

Wavelength tables of sensitive lines. By L. H. AHRENS. (U.S.A.: Addison-Wesley Press Inc.) Pp. 86. Price $3.00.

Tables of sensitive lines, forming an appendix to the author's book *Spectrochemical Analysis* (1950), have now been revised and published separately in convenient form for frequent reference. After a brief discussion of line sensitivity and detection-limit concentrations, the most sensitive lines in arc spectra together with possible interfering lines within $\pm$ 0·4 to 0·5 A of each sensitive line are tabulated. Wavelengths and approximate arc intensities are taken from the M.I.T. Wavelength Tables (1939). Recent data on sensitive rare earth element lines are also included. D. M. SMITH

Fifty years of British Standards 1901–1951. (London: British Standards Institute.) Pp. 103. Price 7*s*. 6*d*.

This survey begins by describing the nature and formulation of British Standards and emphasizes that the term "standardization" is interpreted as the maintenance of high standards of quality and performance.

The historical development of the British Standards movement is summarized. The formation of the original Standards Committee followed suggestions made by Mr. H. J. Skelton in a letter to *The Times* in 1895, and in a paper read by him before the British Iron Trade Association in 1900.

Examples are quoted of the results of some of the early work, providing striking proof of the effectiveness of the members in reducing the number of sizes of iron and steel products, and illustrating the nature of the benefits derived by both users and manufacturers.

Several chapters are devoted to summaries of the extensive growth of the movement and the penultimate chapter emphasizes the co-ordination between standardization and research, several examples of which are given.

Notes and comments

The scientific education of physicists

The Institute of Physics has just published a new report, *The scientific education of physicists*. Copies are available, price 2*s*., on application to the Secretary, The Institute of Physics, 47 Belgrave Square, London, S.W.1. The report includes, as appendices, factual data relating to the physics departments of all the universities and university colleges of Great Britain and Northern Ireland and of those technical colleges recognized by the Institute. The information should be of value to those studying for a degree in physics or contemplating such a course of study, as well as to others who have a close interest in the facilities for advanced training in physics.

Notes on the preparation of papers

A revised and enlarged edition of the booklet *Notes on the preparation of contributions to the Institute's journals and other publications* is now available. These notes, first issued in 1931, are intended to assist less experienced authors and to serve as a reference book for all who contribute to the Institute's publications. Apart from the special information concerning these publications the notes deal with the preparation, length and cost of publishing papers, the form of script and diagrams required, the setting out of tables and mathematics, and the correction of proofs. A short bibliography of dictionaries and books on writing is included. The appendix contains notes and examples of spellings, symbols and abbreviations, the Greek alphabet (so often unrecognizably written in scripts) and printers' marks for correcting proofs.

Copies of the booklet may be obtained from The Institute of Physics, 47 Belgrave Square, London, S.W.1, price 2*s*. 6*d*. Orders should be accompanied by remittance.

Safe transit of scientific instruments

From time to time, research laboratories making delicate scientific measurements need to exchange instruments, for purposes of comparison, with similar laboratories in other countries. If these instruments are to reach their destination undamaged, they must be handled with extreme care during customs inspection in both exporting and importing countries. An arrangement proposed by UNESCO provides for the inspection of these instruments to be made in the laboratories themselves, under competent supervision, rather than in customs depots at national frontiers.

It has been suggested by the United Kingdom that a customs officer should supervise the packing of an instrument at an exporting laboratory and affix an internationally recognized label which would allow the package to be forwarded unopened to its destination, where it would be opened in the presence of a customs official. UNESCO would keep a register of laboratories designated by governments and would periodically send to interested countries a list of these laboratories, as well as details of operation. Information reaching UNESCO by 1 June, 1952, will be included in the first circular. The scheme seeks to extend an arrangement already operating between eight institutions which maintain regular contact with the International Bureau of Weights and Measures (IBWM) for the purpose of exchanging apparatus and scientific data. Both the IBWM and the International Council of Scientific Unions have endorsed the proposal as a practical means of reducing obstacles to the international exchange of scientific information.

Instrumentation and atomic energy

We have received a copy of a report on the tripartite conference held at the Atomic Energy Research Establishment, Harwell, in May 1951, on instrumentation and atomic energy. The purpose of the conference was to review the latest advances made in the electronic equipment and techniques used in the atomic energy projects of the United States, Canada and the United Kingdom. The report gives details of the more important items discussed and copies may be obtained from the Chairman of the conference, Dr. D. Taylor, Atomic Energy Research Establishment, Harwell, Didcot, Berks.

Journal of Scientific Instruments

Contents of the May issue

ORIGINAL CONTRIBUTIONS

A method of correcting the cosine error of selenium rectifier photocells. By G. Pleijel and J. Longmore.

Potentiometer circuit for measurement of high potential. By T. B. Rymer and K. H. R. Wright.

Display of transistor characteristics on the cathode-ray oscillograph. By G. B. B. Chaplin.

A visual and a photoelectric portable colour temperature meter. By H. G. W. Harding.

A direct method for measuring the high voltage stability of the electron microscope. By T. Mulvey.

Stray light in monochromators. By R. Donaldson.

Furnace construction and thermocouple arrangements for a high temperature X-ray camera. By Z. S. Basinski, W. B. Pearson and J. W. Christian.

Apparatus for the determination of moisture in samples of air. By R. S. Vincent.

A single-channel pulse-height discriminator of high speed and stability. By G. T. Wright.

LABORATORY AND WORKSHOP NOTES

A multi-electrode all-glass cap for electrolytic cells. By E. C. Potter.

A calibrating device for impact testing machines. By G. L. Brown.

A self-starting low pressure mercury arc. By J. D. S. Goulden.

A wide-range electronic ratio timer. By C. D. Kinloch.

The measurement of temperature within tubes at high pressures and low temperatures. By A. G. Monroe and D. J. Penny.

Monitoring device for use with an X-ray diffraction cylindrical camera. By M. S. Ahmed.

A universal mounting for X-ray goniometer arcs. By A. L. Mackay.

A deuterium electrolysis plant. By J. T. Lloyd.

A friction drive for a carriage on an optical bench. By Y. R. Meyorowitz.

A greaseless mercury-sealed vacuum-tap. By H. M. Stanier and J. H. Beynon.

CORRESPONDENCE

A simple resistance thermometer. From H. S. Eisner.

Synchrotron magnet construction. From O. Wernholm.

The extension of the magnification range of a two-stage electron microscope. From C. E. Challice.

NOTES AND COMMENTS

Erratum

In the article *Liquid films formed by means of rotating disks*, by B. E. Dixon, A. A. W. Russell and J. E. L. Swallow, published in the April issue, the scales on Fig. 9, p. 119, *should read*: (horizontal axis) 0 to 30 cm, (vertical axis) 0 to 1 600 cm/sec.

THIS JOURNAL is produced monthly by The Institute of Physics, in London. It deals with all branches of applied physics (including theory and technique). All rights reserved. Responsibility for the statements contained herein attaches only to the writers.

EDITORIAL MATTER. Communications concerning editorial matter should be addressed to the Editor, The Institute of Physics, 47 Belgrave Square, London, S.W.1. (*Telephone*, Sloane 9806.) Prospective authors are invited to prepare their scripts in accordance with the *Notes on the Preparation of Contributions*. (Price 2*s*. 6*d*. including postage.)

REPRODUCTION. The Institute of Physics is a signatory to The Royal Society's Fair Copying Declaration. Details may be obtained upon application from The Royal Society, London, W.1.

ADVERTISEMENTS. Communications concerning advertisements should be addressed to the agents, Messrs. Walter Judd Ltd., 47 Gresham Street, London, E.C.2. (*Telephone*: Monarch 7644.)

SUBSCRIPTION RATES. A new volume commences each January, and annual subscriptions will only be accepted for complete volumes of the monthly parts (January–December). The charge is £4 per volume ($11.50 U.S.A.), including index (post paid), payable in advance. Single parts, so far as available, may be purchased at 8*s*. each ($1.15 U.S.A.), post paid, cash with order. Orders should be sent to The Institute of Physics, 47 Belgrave Square, London, S.W.1, or to any Bookseller.

Recent research on radio-luminescence*

By G. F. J. Garlick, B.Sc., Ph.D., F.Inst.P., Physics Department, University of Birmingham

During the last few years the development of sensitive photoelectron multipliers and of single crystals has made possible a quantitative study of luminescence in solids excited by electrons or by heavy particles. Previous empirical relations found between luminescence, electron potential and beam current are shown to be due to the complex structure of the powder-form screens used. Much simpler behaviour is indicated when the luminescence emission due to excitation of single crystals by single particles is investigated. In many inorganic crystals the luminescence is found to be proportional to the energy absorbed. Deviations from this linearity, particularly in organic crystals, provide indications of the nature of energy transport mechanisms in crystals. Studies of phosphors deposited as optically clear films on glass provide similar evidence and enable range energy relations to be studied for the exciting electrons. Recent theoretical researches have provided ideas on the nature of non-radiative processes in particle excited phosphors. These processes are of practical interest since they account for at least 80% of the energy absorbed by phosphor screens.

The last review of research in cathodoluminescence (i.e. luminescence due to electron excitation) published in 1950[1] showed that the information available was almost entirely obtained from experiments on screens of microcrystalline phosphors as used in conventional cathode-ray tubes. The chief interest was in the practical requirements of the cathode-ray tube screen such as the achievement of high brightness for given tube potentials and electron beam current densities. From studies of the characteristics of zinc sulphide, zinc silicate and other phosphor screens certain empirical relations were found between the luminescence emission intensity, the electron beam current and its energy or potential. These relations are best illustrated by examples taken from very careful measurements due to Strange and Henderson.[2] Fig. 1 gives the variation of luminescence intensity with

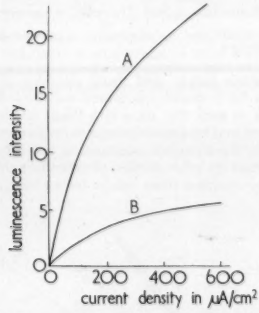

Fig. 1. Variation of cathodoluminescence with electron current density for a Zn_2SiO_4–Mn phosphor
A, 10 kV; *B*, 4 kV

electron beam current for two different accelerating potentials for a manganese activated zinc silicate phosphor screen. These curves show two things, first that the relation between luminescence and current density is not linear, except at very small beam currents, and secondly that the form of the relation, i.e. the tendency to a saturation effect at high current densities is independent of the accelerating potential, i.e. of the electron energy. Fig. 2 shows the relation between

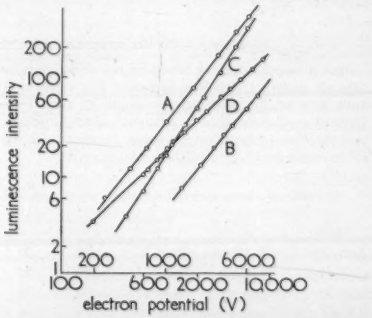

Fig. 2. Variation of cathodoluminescence with electron potential at fixed current densities for different phosphors
A, ZnS–Ag: 10 μA/cm²; *B*, ZnS–Ag: 550 μA/cm²; *C*, Zn_2SiO_4–Mn: 5 μA/cm²; *D*, ZnS–Mn: 10 μA/cm².

luminescence and accelerating potential for different phosphor screens and for different beam currents.[2] These results may be expressed by the simple relation:

$$L = f(i)(V - V_0)^q \qquad (1)$$

where L is the luminescence intensity, i the beam current density, V the accelerating potential, V_0 a so-called dead voltage which is zero when the screen is uncontaminated on its surface, and q is a constant for a given screen but varies between 1 and 3 for different screens.

The fundamental interpretation of the above characteristics is exceedingly difficult, but reference may be made to previous discussions of their significance.[1, 2, 3] Equation (1) shows that if q is greater than unity then the luminescence efficiency (L/iV) increases with electron beam energy. The complex

* Based on a lecture given to the Electronics Group of The Institute of Physics at the Institute's House, London, on 11 December, 1951.

nature of the phosphor surface presented to the electron beam prevents any useful analysis of the effect in terms of penetration of the electrons.

A fact of practical interest is the intrinsic conversion efficiency of a phosphor screen which according to recent studies of zinc sulphide-cadmium sulphide phosphors by Longini[4] may be of the order of 20%. This means that 80% of the available energy is lost in non-radiative processes in the phosphor crystal grains. The nature of the latter processes was still obscure until some recent studies of single crystal phosphors referred to below. Claims of 80% conversion efficiencies made by Riehl[5] for the luminescence in zinc sulphide excited by α-particles have been shown to be erroneous by the results of other investigators reviewed by Klasens.[6]

In the present review the very recent advances in knowledge of radio-luminescence, that is luminescence due to excitation by various particles, including electrons, are considered. It is now possible to obtain much more precise and significant information because of two important advances:

(*a*) The production of good single crystals or uniform transparent films of luminescent materials.

(*b*) The development of very sensitive photoelectron multipliers which respond to the relatively few quanta emitted during the bombardment of a crystal by a single energetic particle.

SINGLE CRYSTAL PHOSPHORS

Before considering the luminescence characteristics of single crystals under particle bombardment it is useful to give a brief summary of the materials available in such form and an indication of their absolute efficiency of response to α-particles and electrons, where this is known, together with the approximate mean decay time of the luminescence.[7]

Table of characteristics of single crystal phosphors

Phosphor	*Size of crystals*	*Emission colour*	*Efficiency (%) α-particles*	*electrons*	*Decay time (μsec)*
ZnS–Ag	5–10 mm	blue	~20	~20	>10
CdS–Ag	1–2 cm	red	~20	~20	>10
NaI–Tl	many cm	blue	~20	~20	0·25
KI–Tl	many cm	blue	5	5	> 1
NaCl–Ag	many cm	u.v.	15	10	0·2
CsI–Tl	many cm	white	15	15	> 1
LiI–Tl	many cm	blue-green	10	10	> 1
LiF	many cm	—	10	2	< 1
CaF_2	many cm	green	—	—	0·15
$CaSO_4$	many cm	blue	2	5	3
Zn_2SiO_4–Mn	1–2 cm	green	—	~10	10^4

This table does not include the organic crystals such as naphthalene, anthracene, stilbene, etc. In general these substances have a 10% efficiency for electrons but only 1 or 2% efficiency for heavier particles.

In most of the researches described below the significant feature of the measurements is that the luminescence output is measured for a single particle entering the crystal. In previous cathodoluminescence studies the output for a steady or pulsed electron current was measured. Investigation of the luminescence due to individual particles provides a clearer indication of the fundamental mechanism of energy conversion in phosphors. There are some practical difficulties in the measurement of light emitted by crystals when a single particle is absorbed. For example, it is difficult to collect the light emitted in crystals of high refractive index so that most of it shall fall on the photocathode of a photomultiplier. Even for α-particles of 5 MeV energy incident on a crystal the maximum number of photo-electrons released from the photocathode is about 400. In this case statistical fluctuations in output pulse size are ± 5% and some care is needed in the analysis of the results.

Luminescence due to heavy particles.

One of the first attempts to determine the relation between particle energy and the emitted luminescence was that of Kallmann[8] using cadmium sulphide crystals and 5 MeV polomium α-particles. His results involved a measurement of mean current output from the photomultiplier and not the measurement of individual pulses due to single particles. However, they show a linear relation between particle energy and luminescence emitted. Since then more precise measurements have been made by many different workers on other phosphor crystals using α-particles, protons, deuterons and other heavy particles and observing the effects due to each particle. Fig. 3 taken from recent results,[9] shows the relation

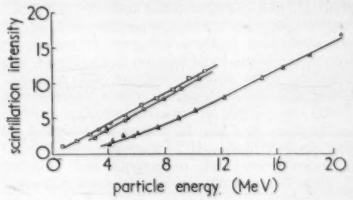

Fig. 3. Responses of NaI–Tl crystal to various particles
○—molecular H_2^+ ions; □—deuterons; △—α-particles; ●—protons; ▲—Po_{84} α-particles.

between particle energy and mean intensity of individual scintillations for a thallium activated sodium iodide crystal. In general it is seen that there is a linear relation between particle energy and luminescence intensity with some departure from linearity for α-particle excitation at low energies, a fact since confirmed by other studies of different workers. It is interesting to compare these results for an inorganic crystal

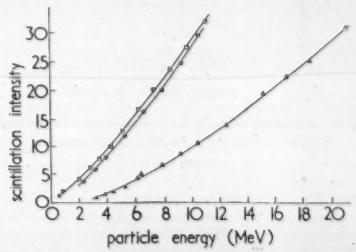

Fig. 4. Response of anthracene crystal to various particles
○—molecular H_2^+ ions; □—deuterons; △—α-particles; ×—Birks' data for α-particles.

with those typical of an organic crystal such as anthracene given in Fig. 4.[9] Non-linearity between particle energy and luminescence is a common feature of organic crystals and liquids and a theoretical comparison of luminescence mechanisms, organic and inorganic crystals, is made below.

Luminescence due to electrons.

There are two different methods of exciting a phosphor crystal with electrons. For energies in the range 0–10 keV a cathode-ray tube system can be used and the light output measured for constant beam current density conditions as for the results of Fig. 2. For higher electron energies in the range up to 600 keV the crystal may be bombarded by mono-energetic γ-rays to produce conversion electrons of similar energy inside the crystal. Results obtained in this way by Taylor and others are given in Fig. 5 for different crystals.[10]

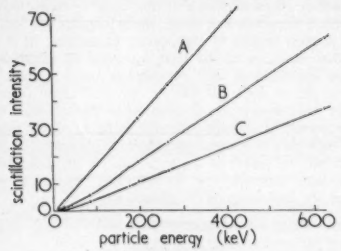

Fig. 5. Response of different crystals to electrons

A, NaI–Tl; *B*, anthracene; *C*, stilbene.

Again the inorganic crystals show a sensibly linear behaviour in comparison with the organic crystals.

In the above work electron beams have also been used to determine the response of crystals to lower energy electrons in the range of interest for the cathode-ray tube.[10] Results are given in Fig. 6 which includes a curve for higher energy

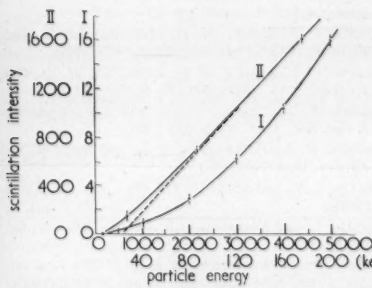

Fig. 6. Response of anthracene crystal to electrons

I—0–5 keV electrons; II—0–200 keV electrons.

electrons for purposes of comparison. From all the above results certain characteristics of crystals are evident:

(i) Over a wide range of energy the inorganic crystals show a sensibly linear relation between luminescence emission and energy deviations being greatest for heavy particles and low energies.

(ii) For all types of particle the organic crystals depart from the linear relation characteristic of inorganic crystals.

(iii) The efficiency of inorganic crystals is about the same for electrons and heavy particles, that of organic crystals is similar for electrons but much lower for heavy particles.

EXPERIMENTS WITH THIN PHOSPHOR FILMS

Recently Studer, Cusano and Young[11] have made thin films of zinc sulphide phosphors by chemical deposition on glass. Such films, made by evaporating zinc on to glass plates at 500–600° C in an atmosphere of hydrogen sulphide at a pressure of a few mm of mercury are from 0·1 to 0·5 μ thick and are optically transparent. The most efficient of these films, a layer of manganese activated zinc sulphide, was about one-half of the brightness of the corresponding micro-crystalline powder screen for 0–10 kV electrons. The lack of comparable response in films of silver or copper activated zinc sulphides may be due to the failure to include a halogen in the constitution of the atmosphere or of the material to be evaporated. Such an inclusion is essential to the formation of the luminescence centres in such phosphors.[12]

Measurements on these films using a cathode-ray beam have been made by Koller and Alden.[13] A linear relation is found between electron energy and luminescence emission except when the range of the electrons exceeds the film thickness. From these results the constants of the Thomson–Widdington penetration law may be obtained. When electron scattering is accounted for it appears that 90% of the primary electron energy is lost in the first half of the electron range. The use of such thin films offers considerable possibilities for study of the fundamental mechanism of cathodoluminescence under relatively simple conditions.

Deterioration of phosphors under particle bombardment.

There has always been a practical interest in the deterioration or "burn" of cathode-ray tube screens under prolonged use, but the nature of the process was not known, particularly at low electron energies. Recent studies by Broser and Warminskey[14] have provided more definite indications of the changes in single crystals of zinc sulphide due to prolonged exposure to α-particles. The fall in luminescence efficiency with particle dosage is quite different if ultra-violet light is used for excitation than if particles are employed. These workers give a satisfactory interpretation of their results in terms of a recent theoretical model due to Schön.[15] Experiments are beginning in the author's laboratory in which the effects of other particles on single crystal phosphors are to be examined. Such experiments will help to determine the nature of non-radiative processes in such crystals.

THEORETICAL DISCUSSION

To obtain the more fundamental significance of the results contained in the above figures it is useful to derive the specific luminescence dL/dx, i.e. the luminescence emission per unit path of the particle in the crystal and to compare it with the specific energy loss dE/dx. Now dE/dx can be computed from

range energy relationships for the particles in question, dL/dE from the experimental curves and so by combination the quantity dL/dx is obtained. In Fig. 7 the relation between specific luminescence and specific energy loss is given for different particles exciting an anthracene crystal. This curve

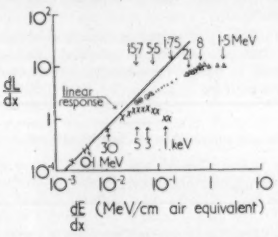

Fig. 7. Relation between specific luminescence dL/dx and specific energy loss dE/dx for an anthracene crystal and for different particles

●—protons; △—α-particles; ×—electrons; ○—protons (Princeton results).[6,10]

shows immediately that high ionization densities are detrimental to a linear response of the crystal. Birks[16] has derived a theoretical relationship which agrees very well with the above results. In an organic crystal the absorbed energy is transferred from the molecule by a resonance process until it is radiated as luminescence. Any ionization will tend to upset this transfer by "destroying" molecules and perturbing the crystal lattice. The theoretical relation obtained by a quantitative consideration of the system is:

$$\frac{dL}{dx} = A.\frac{dE}{dx}\Big/\left(1 + B.\frac{dE}{dx}\right) \qquad (2)$$

where A and B are constants.

Considerable departures from this relation are indicated in Fig. 7 for low energy electrons, but this may be due to conditions in the crystal surface since the penetration of a 1 keV electron is only $2{\cdot}5 \times 10^{-6}$ cm in anthracene.

Recent experiments by G. T. Wright in the author's laboratory have yielded relations between dL/dx and dE/dx for inorganic crystals, notably fluorite, diamond, calcium, tungstate and thallium activated potassium iodide. The behaviour of single crystals of zinc and cadmium sulphides are also now being studied. Although it is a little premature to discuss these results it is noteworthy that inorganic crystals in which transport of energy is due to electron migration show similar effects to organic crystals at very high ionization densities.

Non-radiative processes.

It has already been stated that at least 80% of the energy absorbed by phosphor crystals when excited by particles is dissipated non-radiatively. In recent theoretical studies Schön[15] has suggested a model for non-radiative losses. In inorganic phosphors excitation removes electrons from luminescence centres and some of the electrons are trapped. At ordinary temperatures electrons from lattice atoms may neutralize these centres leaving "positive holes" in the crystal which migrate to the trapping sites and are neutralized by the electrons there which undergo non-radiative transitions on combining with the "positive holes." Perturbation and destruction of the phosphor crystal creates more trapping states and so increases the probability of such electron-"positive hole" combination. Thus the luminescence emission due to the recombination of electrons with luminescence centres decreases. As stated above the experimental studies of Broser and Warminsky[14] tend to support this theory.

CONCLUSION

It is seen that the interest in luminescent crystals as detectors of nuclear particles has considerably advanced the knowledge of phosphor characteristics and that these investigations are of practical importance to those whose interests are confined to the applied aspects of cathode-ray excitation. It is now clear that relations of the type expressed in equation (1) between luminescence and cathode-ray beam current and potential are of empirical interest only and result from the complex conditions in conventional phosphor screens. What is now needed is a more extensive study of single crystals and of thin films of conventional sulphide phosphors in order to elucidate the nature of the non-radiative processes which so seriously diminish the luminescence efficiency when particles are used to excite the phosphors.

REFERENCES

(1) Garlick, G. F. J. *Advances in Electronics*, Vol. II, p. 152 (New York: Academic Press, 1950).
(2) Strange, J. W., and Henderson, S. T. *Proc. Phys. Soc.*, **58**, p. 369 (1946).
(3) Fano, U. *Phys. Rev.*, **58**, p. 544 (1940).
(4) Longini, R. L. *Phys. Rev.*, **75**, p. 335 (1949).
(5) Riehl, N. *Ann. Phys. Lpz.*, **11**, p. 103 (1931).
(6) Klasens, H. A. *Trans Faraday Soc.*, **42**, p. 666 (1946).
(7) *Nucleonics*, p. 72 (May 1950).
(8) Kallmann, H. *Research*, **2**, p. 62 (1949).
(9) Taylor, C. J., Remley, M. E., Jentschke, W. K., and Kruger, P. G. *Phys. Rev.*, **83**, p. 169 (1951).
(10) Taylor, C. J., Remley, M. E., Jentschke, W. K., and Kruger, P. G. *Phys. Rev.*, **83**, p. 170 (1951).
(11) Studer, F. J., Cusano, D. A., and Young, A. H. *J. Opt. Soc. Amer.*, **41**, p. 559 (1951).
(12) Kroger, F. A., Hellingman, J. E., and Smit, N. W. *Physica*, **15**, p. 990 (1949).
(13) Koller, L. R., and Alden, E. D. *Phys. Rev.*, **83**, p. 684 (1951).
(14) Broser, I., and Warminsky, R. *Z. Naturforsch.*, **6a**, p. 85 (1951).
(15) Schön, M. *F. Naturforsch.*, **6a**, p. 251 (1951).
(16) Birks, J. B. *Proc. Phys. Soc. A*, **63**, p. 1294 (1950); **64**, p. 874 (1951).

A method for the electron and optical microscopic examination of identical areas

By E. D. HYAM, B.A., and J. NUTTING, M.A., B.Sc., Ph.D., Department of Metallurgy, University of Cambridge

[*Paper received* 12 *December*, 1951]

The difficulties involved in attempting to obtain optical and electron micrographs from the same area of a metal surface using the standard dry-stripping technique are outlined. An attachment is described which fits over the objective lens of a bench metallurgical microscope, and enables replica supporting grids to be precisely positioned over a feature of interest in the microstructure. By this method, optical and electron micrographs of the same area of the surface may be readily obtained. The mode of operation is described in detail and the applications of the method are indicated.

Many attempts have been made to obtain optical and electron micrographs of the same area of an etched metal surface, since a comparative study of such pairs will yield information about the fidelity of the replica technique and its possible limitations. The difficulty in identifying a micro-area of a plastic replica, as seen in the electron microscope, with the area of the etched specimen surface from which it was originally stripped, lies in the high magnifications (e.g. × 2 500) normally used in electron microscopic examination, and in the fine scale upon which detail is generally present in metallurgical structures. A reference mark of some kind is essential if an area on both the replica and the original surface is to be identified successfully.

The usual dry-stripping technique has been used to obtain optical and electron micrographs of the same area of a pearlitic structure, by stripping the replica from the region of two small intersecting scratches on the surface of the specimen. Ellis[1] has similarly obtained optical and electron micrographs from an area of a spheroidal structure in the region of a fine needle scratch; however, it is difficult to position the supporting grid over the reference scratch sufficiently accurately by hand. This is particularly true when the replica must be examined in an electron microscope of a type which allows only a limited central area of the grid to be scanned.

Moreover, there are further difficulties which arise:—

(i) The replica may strain or rupture at the scratch if the latter is not made fine enough.

(ii) Since the grid bars obscure more than 50% of the plastic film supported by them, the scratches are not always observed favourably in the electron microscope for the subsequent successful identification of any particular area. When a suitable portion of a scratch is observed, it is unlikely that the same area will be favourably observed in subsequent replicas similarly stripped from the specimen.

The difficulty of making reference scratches on the surface fine enough to allow stripping without strain or rupture, has been overcome by the use of a fine diamond point, lightly loaded, to produce a grid of scratch lines, each less than 0·2 μ in width.[2] Agar and Revell[3] have succeeded in obtaining comparison optical and electron micrographs of the same area of a surface by the use of scratches made with a normal laboratory micro-hardness tester by Vickers Ltd.

The method to be described is a refinement of the usual stripping technique. It enables the replica supporting grid to be positioned more precisely over the specimen surface and does not always involve the use of surface scratches. One essential requirement is to be able to recognize a given grid square in both the optical and electron microscopes. By using the electro-formed copper grids now available, having a centrally placed diamond-shaped stop, this requirement is easily fulfilled.

DESCRIPTION OF METHOD

An attachment has been designed for the ×40 objective lens of a normal bench metallurgical microscope, fitted with a ×10 eyepiece and eyepiece graticule (Figs. 1, 2). This

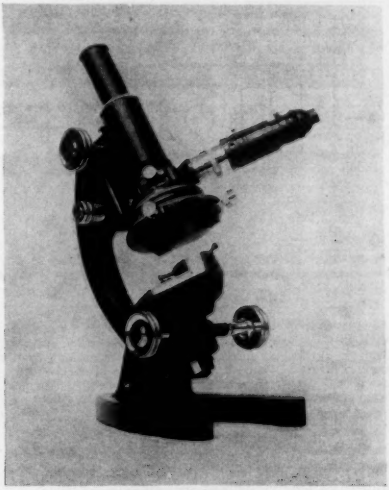

Fig. 1. Microscope with attachment fitted

attachment consists essentially of a number of concentric sleeves fitting smoothly around the objective lens, and an upper and lower collar. Rotation of the upper threaded collar raises or lowers the sleeve bearing the lower collar. The latter can be rotated freely and smoothly and carries on its underside two smooth traversing slides working at right angles and operated by two fine screw adjustments. A small square brass frame carries the replica supporting grid and tape, and this fits firmly by means of four pins into one of the slides just below the objective lens. The grid is mounted

over a $\frac{1}{4}$ in diameter hole punched centrally in a $1\frac{1}{2}$ in length of cellulose tape. This leaves the grid supported at its periphery with the central portion free from contact with the tape. The ends of the tape are bent back upon themselves and stuck to the frame, so that when the latter is pinned in position to the attachment, the grid and the adhesive side of the tape are towards the stage.

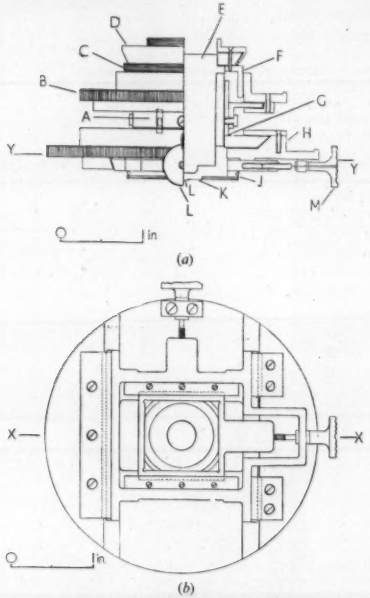

Fig. 2. Attachment assembly

(*a*) sectional elevation through *X*–*X*

A, Key-way allowing vertical movement only; *B*, focusing control; *C*, threaded steel collar; *D*, objective holder, *E*, objective; *F*, push-fit sleeve (steel); *G*, brass sleeve keyed to inner steel sleeve; *H*, smooth rotational movement for grid orientation; *J*, notched supporting frame; *K*, Scotch tape; *L*, grid; *M*, traversing controls.

(*b*) underside plan on *Y*–*Y*

The specimen grid, when mounted thus in position, may be raised or lowered beneath the objective until in focus, traversed in two directions at right angles until centrally in position in the field of view, and rotated to any desired orientation without reference to the positions of either the microscope tube or stage. It is essential, however, that the play between the moving parts of the attachment be as small as possible. In addition, the guides of the microscope tube and stage adjustments must be parallel to the optical axis of the instrument. The normal stage has been replaced by a brass ring carrying three fixing screws, in which the specimen can be mounted firmly in position, with the prepared surface perpendicular to the optical axis and approximately central beneath the objective lens.

When the feature of interest in the microstructure is large and of distinctive shape, the sequence of operations for stripping a replica from the chosen area with the aid of this device is as follows:—

(i) The specimen is held firmly in the holder by the three screws, with the feature of interest focused under the central line of the graticule.

(ii) The microscope is tilted and the 2% Formvar solution is applied to the specimen surface in the usual way. The frame carrying the grid and tape is mounted in position, the grid is focused, orientated, and centred with a chosen grid square under the central line of the graticule. The position of the chosen grid square relative to the diamond-shaped stop is noted.

(iii) After breathing on the Formvar film, the microscope is tilted to the upright position. The stage is raised until the specimen nearly touches the grid; the latter is checked to ensure that it has not moved, and the microscope tube is then lowered carefully until the grid and tape are pressed firmly to the specimen surface.

(iv) The tape is cut at the V-notches on the sides of the frame, and the microscope tube is raised to leave the grid and tape adhering to the Formvar coated surface. After a quick check to ensure that the grid has been correctly placed on the surface with the feature of interest outlined in the chosen grid square, the replica is stripped.

(v) A second grid is transferred to the surface in exactly the same position as the first. This serves for identification of the chosen area when the specimen is examined with a metallurgical microscope suitable for photography.

It was found that movement of the Formvar film with respect to the grid occurred during stripping, and that grids correctly placed on the specimen surface did not always show the feature of interest in the chosen grid square on subsequent examination in the electron microscope; frequently this feature was obscured by an adjacent grid-bar.

This difficulty was overcome by punching a small hole in the centre of the grid with a needle, but this made recognition more difficult because the field to be searched was greater.

Where large features of distinctive shape are absent, however, as in eutectoid pearlitic or spheroidal carbide structures in steels, it becomes difficult to identify areas by this method alone, and it was found necessary to rule scratch lines on the specimens to reduce the labour involved in searching. By means of a micro-hardness tester, with a load of $\frac{1}{2}$–1 g, it was found possible to rule fine even scratches, less than 1 μ in width, to form around any chosen feature on the surface a small distinctive pattern of a size which would be covered by 15–25 squares of a grid.

There was no difficulty in stripping replicas from the pattern of scratch lines, nor in correlating the electron micrographs taken at $\times$ 2 500 with the optical microstructure, provided that the orientation of the electron micrographs with respect to the pattern of scratches was known. Electron micrographs at higher magnifications (e.g. $\times$ 5 000 or $\times$ 10 000) are not readily identifiable with the corresponding optical field unless a portion of a scratch line is present on the plate.

If the slipping of the Formvar film with respect to the grid during stripping were to be overcome, the pattern of thick and thin grid bars adjacent to the diamond-shaped stop would themselves form a sufficient reference system. There would then be no necessity to punch a hole in the grid or to

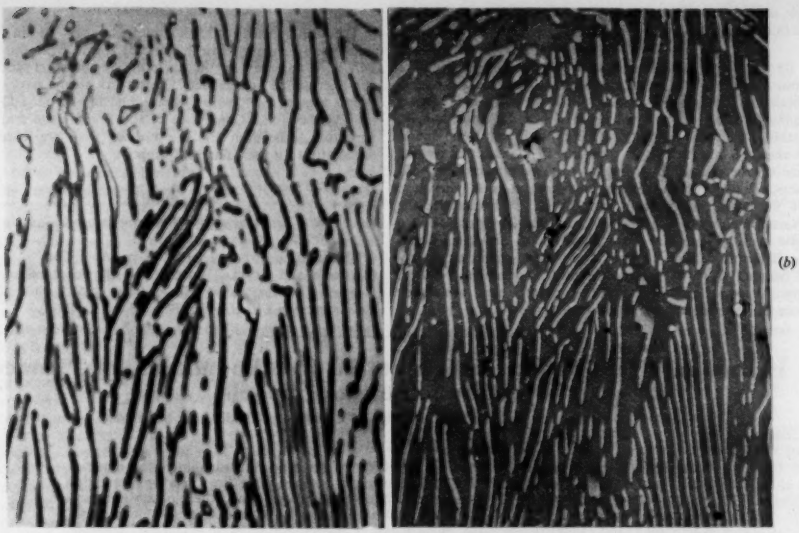

Fig. 3. 0·8% carbon steel, normalized, showing coarse pearlite, magnification × 4 000. (*a*) Optical micrograph; (*b*) electron micrograph

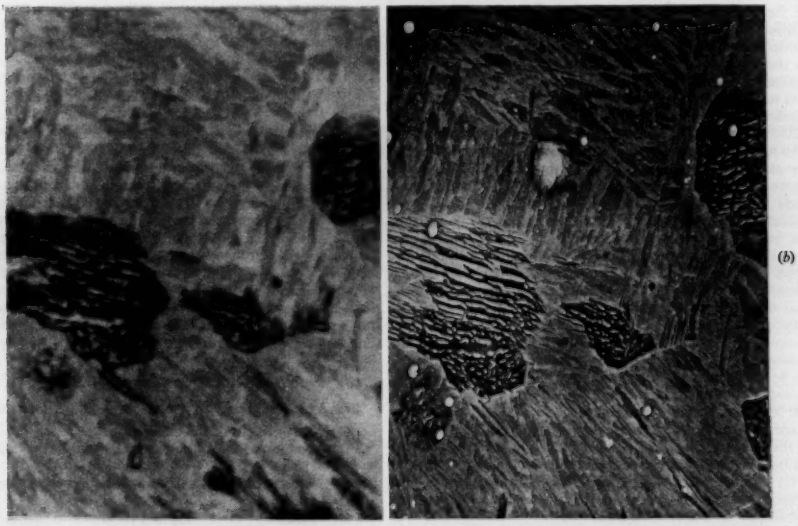

Fig. 4. 1·2% carbon steel, quenched from 900° C at critical cooling rate showing intermediate transformation products, magnification × 3 500. (*a*) Optical micrograph. (*b*) electron micrograph

rule scratches on the specimen for many of the structures to be examined.

USES OF THE METHOD

By the method described, optical and electron micrographs from the same area of a specimen surface can be readily obtained (Figs. 3, 4). It also allows a series of Formvar replicas to be dry-stripped from the same chosen area, enabling the reproducibility of the dry-stripping technique to be checked, and facilitating the study of the effect of etching time on the electron microstructure of metallographic specimens. In cases where the electron micrographs of a structure are unfamiliar, the method may serve to characterize the phases by direct comparison with optical micrographs of the same area. There may be applications in biological fields, e.g. if the need arises to strip a previously identified colony of bacteria from its growth medium, and generally in the examination of particular features on any type of surface from which a replica can be obtained.

ACKNOWLEDGEMENTS

The authors wish to thank Professor G. W. Austin for his interest and encouragement, and Mr. F. T. Bridgeman and Mr. T. K. Saunders for their help in designing and producing the microscope attachment. This work forms part of the programme of the Electron Microscope and Electron Diffraction Methods Sub-Committee of the British Iron and Steel Research Association and the authors wish to thank the Association for their financial support.

REFERENCES

(1) ELLIS. *Yearbook of the American Iron and Steel Institute* (1950).
(2) HAAS, DE. *Nature, Lond.*, **166**, p. 482 (1950).
(3) AGAR and REVELL. Institute of Physics conference on electron microscopy, St. Andrews, 1951. (Summarized report in *Brit. J. Appl. Phys.*, **3**, p. 26 (1952).)

Errors in stress determination at the free boundaries of "frozen stress" photoelastic models

By V. M. HICKSON, B.Sc., The National Physical Laboratory, Teddington, Middlesex*

[*Paper first received* 3 *July*, 1951, *and in final form* 6 *November*, 1951.]

An attempt has been made to list the errors, apart from those due to the use of imperfect material, which may occur in the determination of free boundary stresses from direct relative retardation observations on slices cut from "frozen stress" photoelastic models and, where possible, to estimate their magnitudes. Particular regard is paid to the important case of a stress concentration, where small radii will introduce errors which would be negligible at other points on the boundary.

1. INTRODUCTION

The "frozen stress" technique as generally practised consists of the fabrication of a model in transparent plastic of the engineering component under study, the subjection of the model to thermal treatment whilst loaded in the same manner as the component is loaded in service, and the subsequent slicing of the model. The slices are viewed in a polariscope and relative retardation measurements taken of the permanent birefringence induced by the process; these measurements allow a quantitative estimate of the stress in the component. The regions of a model of greatest interest to the engineer are the stress concentrations, which nearly always occur on the outer surface at points where one or both of the principal radii of curvature are small. These small radii, with their accompanying high rates of change of stress, put a limit on the permissible thickness of slice, with consequent low relative retardations and necessity to use compensation methods for observations. In general the curvature at the boundary causes apparent thickening of the projected edge of the slice, which will not permit a direct observation at the edge, and necessitates extrapolation of observations taken within the boundary. A procedure for taking observations has been described by the author,(1) and the errors and corrections to be investigated are based on this procedure of which the essential points are noted below. It should be remarked that the routine is basically the same whether the observations are made on a conventional slice containing two principal stresses at the boundary, or whether it is intended to use the "oblique incidence" method as described in reference (1).

(1) Cut the slice so that the normal to the boundary at the point under study—the reference point—lies as nearly as possible in the plane of the slice.

(2) Take relative retardation observations, by the Tardy compensation method supplemented by photocell detection of minimum intensity, for light passing in planes parallel to the tangent plane at the reference point. Matched immersion liquid is used to avoid refraction effects.

(3) Observations for each incidence angle are made at not less than three positions very close to the boundary along the normal to the boundary at the reference point.

2. ERRORS IN STRESS DETERMINATION AT THE BOUNDARY

It is the primary purpose of this paper to investigate errors which are due to measurement techniques and to the use of slices of finite thickness. There may be considerable errors due to the use of imperfect material or to non-correspondence of the stress in the model and the engineering component it represents, e.g. through having a different value of Poisson's ratio, or excessive strains. Perfect material is, of course, not yet available, but the introduction of materials such as Fosterite encourages the hope that the ideal may eventually be approached. With the assumption of perfect material, one may classify the errors into the two types.

(*A*) Measurement errors.
(*B*) Errors due to the finite thickness of slice.

Errors of class *A* may be in the following observations:

(*A*1) Measurement of the thickness of the slice.
(*A*2) Location of the aperture with respect to the reference point.
(*A*3) Angle settings of the slice with respect to the incident ray.
(*A*4) Polariscope errors, leading to errors in Tardy compensation.
(*A*5) Finite size of photometer aperture.

* Now at Royal Aircraft Establishment, Farnborough, Hants.

Errors of class *B* may be attributed to:

(*B*1) Variation of magnitude of stress through the thickness of the slice.

(*B*2) Change in directions of principal stresses through the thickness causing variation in secondary principal stress difference.

(*B*3) Tardy compensation error due to variation in direction of polarization planes through the thickness ("rotation").

The errors are treated separately in Section 3 and, where possible, correction formulae are derived. The basic assumption is made that the thickness of the slice is small in comparison with the minimum surface radius of curvature; the boundary in the region of the reference point may therefore be treated as if it were an infinitesimally small element of a general surface. Certain of the errors are not independent; with the above proviso on the relative thickness of the slice, they are all small quantities. There is no reason to believe that independent consideration results in appreciably lower estimates for the errors.

The important criterion of error in the measurements is not the percentage error in the particular observation which is being made. For example, if the true relative retardation at a particular location on a slice were zero, any finite error would represent an infinite percentage error, which would be meaningless. The absolute error is of practical significance; to assess its importance it may be expressed as a percentage of the maximum relative retardation per inch path in the model. In Section 3, this maximum retardation is assumed, for convenience, to occur in the region being investigated.

3. INVESTIGATION OF ERRORS

*Error A*1. *Thickness measurement.* The thickness of the slice in the region of the reference point is measured to 2 μ by means of a travelling microscope. As the practical lower limit of slice thickness at present is 0·5 mm, it should be possible to take this measurement to 0·4%, which would lead to an uncertainty of this amount in the determination of relative retardation per inch path.

*Error A*2. *Aperture location.* In the previous paper[1] it is stated that the photometer aperture can be located on the reference point image to 0·0005 inch in terms of distance on the slice. The rate of change of stress along the boundary normal may be very high, in fact, in the experimental example quoted the relative retardation dropped 20% in 0·01 in at certain incidence angles, leading to 1% error due to imperfect location of the aperture. This figure may be taken as a rough guide for the location error when the minimum surface principal radius of curvature is $\frac{1}{4}$ in; the percentage errors for other radii would be in inverse proportion. An accurate estimate may, of course, be made from the actual observations on a slice.

*Error A*3. *Angle setting.* The relative retardation per inch path for a ray travelling parallel to the tangent plane at the reference point is

$$n = [(p - r)\sin^2\phi + (q - r)\cos^2\phi]/F$$

where F = the fringe value of the material

p, q = principal stresses in the plane

r = principal stress normal to the surface of the model

ϕ = the angle made by the ray with the p stress direction (see Fig. 1).

The maximum variation of retardation with ϕ occurs where

$$d^2n/d\phi^2 = (2/F)(p - q)\cos 2\phi = 0, \text{ i.e. } \phi = 45°$$

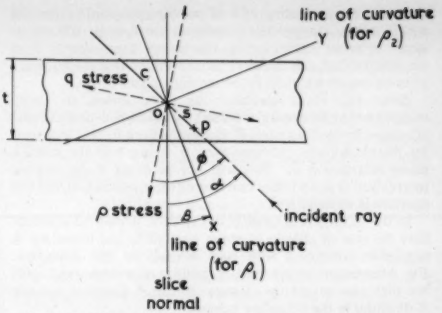

Fig. 1. Diagram showing edge of slice with angle relations between surface principal stresses, slice normal, lines of curvature and incident ray

At this angle, the change in n for a change in ϕ of $\Delta\phi°$ is

$$\Delta n = (\pi/180F)(p - q)\Delta\phi$$

This will have the greatest absolute value when $(p - q)/F$ is the maximum relative retardation in the model. The percentage of this maximum is $1{\cdot}75\Delta\phi$, thus in the most unfavourable case an error in angle setting of 1° will result in an error of nearly 2%. For safety, angle settings should therefore be made to better than $\frac{1}{2}$°.

*Error A*4. *Polariscope errors.* The possible causes of error in Tardy compensation due to polariscope defects are:

(1) Variation in direction of polarization over the areas of polarizer and analyser.

(2) Variation in transmission over the areas of the components.

(3) Incorrect quarter-wave plates.

It is presumed that scales, mounting, etc., are to a high standard.

The first two possibilities of error may be avoided by using selected Polaroid sheet for the components. It may not be possible to get quarter-wave plates of exactly $\pi/2$ relative phase retardation, but in this event a correction may be applied. R. D. Mindlin[2] gives an expression for the intensity transmitted in a general polariscope. Substituting the Tardy conditions when imperfect quarter-wave plates are used, it is found that

$$\tan 2\theta' = \sin\delta/(\tan\epsilon_1 \sin\epsilon_2 + \cos\epsilon_2 \cos\delta) \text{ for extinction}$$

instead of $\tan 2\theta' = \tan\delta$ which applies to the perfect polariscope. The symbols have the following meaning:

δ = relative phase retardation.

θ' = rotation of analyser for extinction.

ϵ_1 = 1st quarter-wave plate phase error.

ϵ_2 = 2nd quarter-wave plate phase error.

With known values ϵ_1 and ϵ_2, a table may be constructed giving values of δ corresponding to readings θ'.

The effective fringe value of Fosterite has been stated by Levens[3] to be 3·85 lb/in² tension per inch thickness per fringe, and the optical proportional limit 190 lb/in²; this represents a maximum relative retardation of 49 wavelengths per inch, or one wavelength in a 0·02 in thick slice. With optimum loading of the model, this is the maximum retardation to be expected in a slice of this thickness, and it therefore appears

that an error in reading of 0·01 wavelength would represent a 1% error. In practice, optimum loading is difficult to attain without knowing the maximum stress which it is required to find; it is therefore recommended that the accuracy of compensation should be better than 0·005 fringe.

Error A5. Finite aperture. As noted above, in Tardy compensation (assuming a perfect polariscope), the analyser is rotated through an angle θ' when minimum light is indicated by the photometer galvanometer, θ' being half the relative phase retardation δ. This will not be exact if the relative retardation is not a linear function of the co-ordinates and the aperture is of finite size.

In the vicinity of a stress concentration it may be assumed that the rate of change of stress parallel to the boundary is negligible compared with that normal to the boundary. Fig. 4 represents an aperture of radius a on a stress field, with the high rate of change of stress in the Z direction, i.e. the Z direction is the boundary normal.

The light intensity at an element of area in the aperture circle is given by:

$$I = C \sin^2 [(\delta/2) - \theta] = [1 - \cos(\delta - 2\theta)]C/2$$

The total light entering the aperture

$$L = C\int_{-a}^{a} (a^2 - Z^2)^{\frac{1}{2}}[1 - \cos(\delta - 2\theta)]dZ$$

This will be a minimum when $\partial L/\partial\theta = 0$.

i.e.
$$\int_{-a}^{a} (a^2 - Z^2)^{\frac{1}{2}} \sin(\delta - 2\theta')dZ = 0$$

Let $v = Z/a$ and $\delta = \delta_0 + k_1 v + k_2 v^2$

Then
$$\int_{-1}^{1} (1 - v^2)^{\frac{1}{2}} \sin(\delta_0 + k_1 v + k_2 v^2 - 2\theta')dv = 0$$

or

$$\tan(2\theta' - \delta_0) = \int_{-1}^{1} (1 - v^2)^{\frac{1}{2}} \cos k_1 v \sin k_2 v^2 dv \Big/ \int_{-1}^{1} (1 - v^2)^{\frac{1}{2}} \cos k_1 v \cos k_2 v^2 dv$$

Practical limits may be assigned to the values of the constants from general experience.

(*a*) δ_0 may have any value between 0 and 2π. (In Tardy compensation the relative retardation is measured from the nearest whole fringe.)

(*b*) k_1 is half the difference between the relative phase retardations at the extremities of the aperture. It is necessary to restrict the size of aperture to cover only a fraction of the distance between two fringes otherwise the variation in intensity on rotation of the analyser may be considerably reduced. k_1 is therefore restricted to the value $\pi/4$ or less.

(*c*) The maximum value of k_2 may be fixed on the assumption that the spacing between the first pair of three adjacent fringes is twice that between the second pair. The numerical magnitude of k_2 is assumed not to exceed $\pi/12$. It is believed that these limits of rate of change of slope will cover any practical case in which the slope is not $> \pi/4a$.

The error in fractions of a wavelength is $e = (2\theta' - \delta_0)/2\pi$. The formula for e may be evaluated approximately if the above limits are fixed. It is found that

$$e = [1 - (k_1^2/8)]k_2/8\pi \text{ to } 0{\cdot}001 \text{ wavelength}$$

A successive approximation method is given below if it is required to apply the formula to a set of observations.

Application of the formula. Having taken at least three Tardy readings at different positions along the Z axis, the results are plotted in wavelengths and a smooth curve drawn through them. If there is no curvature k_2 disappears and the correction is nil. Fig. 4 shows a portion of a curve where the correction may be applied. Ordinates are measured at $Z = \pm a$ from the point where the correction is required; we thus have three values δ_1, δ_2, and δ_3. Then

$$k_1 = (\delta_3 - \delta_1)/2,\ k_2 = (\delta_1 - 2\delta_2 + \delta_3)/2$$

The error e is given by substitution of these numerical values in the formula and the corrected value of δ_2 is given by $\delta_2 - e$. The process may be repeated with a new curve drawn through the corrected points.

Error B1. Variation of principal stress magnitudes. This error cannot be predicted without prior knowledge of the stress distribution in the vicinity of the reference point. However, if an estimate can be formed of the change of relative retardation in the direction of the transmitted ray, e.g. by taking successive slices, this will assist materially in correction. Neglecting rotation effects, which are treated separately, the total relative retardation for a ray parallel to the tangent plane at the reference point is the sum of the retardations due to elements of the path.

Referring to Fig. 1, let

n = relative retardation per inch at a point P in the path.
n_0 = relative retardation per inch on the normal to the reference point.
s = distance of the point from the normal.
c = distance to the surface of the slice from the normal.

The distribution may be represented by the parabola

$$n = n_0 + a_1 s + a_2 s^2$$

The total relative retardation along the path is

$$\int_{-c}^{c} n ds = \int_{-c}^{c} (n_0 + a_1 s + a_2 s^2) ds = 2[n_0 c + (a_2 c^3/3)]$$

If all elements of the path had relative retardation per inch n_0 the total retardation would be $2n_0c$. The error is therefore $\frac{2}{3}a_2c^3$, which is equivalent to $\frac{1}{3}c^3\, d^2n/ds^2$; it will only be significant when d^2n/ds^2 is high, as at a stress concentration. An estimate of d^2n/ds^2 has been made for the grooved cylinder described in reference (1) and it was found that the percentage error could be as high as $60(t/\rho)^2$ for certain orientations of the ray and slice. Lacking further data on other types of notch, this figure may be taken provisionally as the maximum to be expected.

When we have no knowledge of the distribution, such as is usually the case, it is still possible to make part correction by using the device of an "effective" boundary which may be used for extrapolation instead of the reference point. The assumption is made that the distribution of stress relative to the boundary along parallels to the normal to the surface at the reference point is constant through the thickness of the

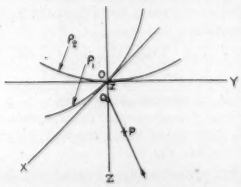

Fig. 2. Error *B*1. Correction for boundary curvature

slice; the effective distance of the ray from the boundary will then be its mean distance.

Referring to Figs. 1 and 2, the vertical distance of an element P from the surface is

$$e = Z + [(x^2/2\rho_1) + (y^2/2\rho_2)]$$

The mean distance of the ray QP is given by

$$\bar{e} = \frac{1}{2c}\int_{-c}^{c} eds \quad \text{where} \quad c = t/2\cos\alpha$$

$$x = s\cos(\alpha - \beta), \quad y = s\sin(\alpha - \beta)$$

On integration it is found that

$$\bar{e} = Z + \Delta Z$$

Where

$$\Delta Z = -(t^2/24\cos^2\alpha)\left\{[\cos^2(\alpha-\beta)/\rho_1] + [\sin^2(\alpha-\beta)/\rho_2]\right\}$$

Application of correction. The principal normal planes and radii of curvature are known from the geometry of the model. β is measured in a counter clockwise sense to the principal normal plane appertaining to ρ_1. Radii of curvature are accounted positive if their centres of curvature are outside the boundary. Compensator measurements having been made at known distances from the reference point, relative retardations per inch thickness or secondary principal stress differences are calculated and plotted against distance. The curve is extrapolated to an ordinate at distance ΔZ from the reference point.

Error B2. Variation of secondary principal stress difference through "rotation." This error is due to variation in the angle of the transmitted ray with respect to the principal axes of the birefringent elements as the ray progresses through the slice; the secondary principal stresses, hence the relative retardations, will vary through the thickness, even if the actual principal stresses were constant.

The chief factor causing this error is the change of direction of the r stress, i.e. of the boundary normal. Fig. 3 shows an

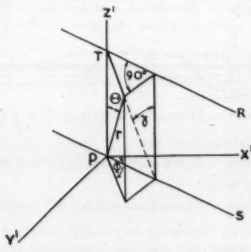

Fig. 3. Inclined boundary normal at point P

inclined boundary normal r corresponding to the point P; its direction is defined by polar angles Θ and Φ. It can be shown that

$$\tan\Phi \simeq (\rho_1/\rho_2)\tan(\alpha - \beta)$$

$$\tan\Theta \simeq \Theta \simeq s\left\{[\cos^2(\alpha-\beta)/\rho_1^2] + [\sin^2(\alpha-\beta)/\rho_2^2]\right\}^{\frac{1}{2}}$$

The most unfavourable case for the error is where Θ has maximum variation and rotation has occurred about the q stress (taken as the lower numerical value), the transmitted ray travelling in the index ellipsoid principal plane containing the p direction. This occurs where $\alpha = 45°$, $\beta = 0°$ or $90°$, and the p and q stresses are at 45° to the plane of the slice. Again assuming p and q constant, an approximation to the total relative retardation along the path of the ray may be made.

$$\tan\Theta \simeq \sin\Theta \simeq (s/\sqrt{2})[(1/\rho_1^2) + (1/\rho_2^2)]^{\frac{1}{2}}$$

therefore $p\cos^2\Theta \simeq p\left\{1 - s^2/2[(1/\rho_1^2) + (1/\rho_2^2)]\right\}$

The secondary principal stress difference at an element will be $p\cos^2\Theta - q$. The mean relative retardation per inch along the path is

$$n = \frac{\sqrt{2}}{Ft}\int_0^{t/\sqrt{2}}\left\{p[1 - (s^2/2)(1/\rho_1^2 + 1/\rho_2^2)] - q\right\}ds$$

$$= 1/F\left\{p[1 - (t^2/12)(1/\rho_1^2 + 1/\rho_2^2)] - q\right\}$$

The error will have its maximum value when $p - q$ is a maximum and $q = 0$. The percentage error is then

$$8\cdot3t^2[(1/\rho_1^2) + (1/\rho_2^2)]$$

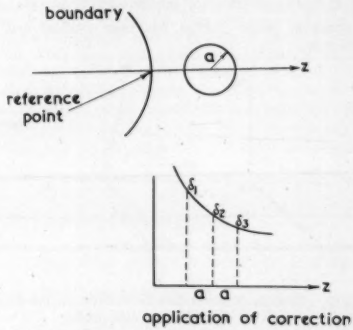

Fig. 4. Error *A5*. Finite photometer aperture

Error B3. Tardy compensation error due to "rotation." The simple relation $\tan 2\theta' = \tan\delta$ for Tardy compensation no longer applies exactly when the secondary principal stresses change in orientation along the path of the ray. In this sub-section an approximation to the maximum rotation that may be expected at the edge of a slice is given, and also a calculation of the compensation error for a given rotation, together with a proposal for applying corrections.

Referring again to Fig. 3, *PTRS* represents a plane through the Z' axis and the ray SP. The total rotation of the surface normal through the slice will be twice the projection angle γ of r on a plane parallel to the Z' axis and at right angles to the plane *PTRS*, P being at the entrance point of the ray.

We have $\tan\gamma = \tan\Theta\sin[\Phi - (\alpha - \beta)]$

The total projected rotation γ_0 of r in the direction of the transmitted ray is given by substituting $s = t/\cos\alpha$. γ_0 will have its maximum value when ρ_1 and ρ_2 are small and of opposite sign, $\alpha - \beta = 45°$ and $\alpha = 45°$, i.e. $\beta = 0°$.

Let $\rho_1 = -\rho_2$. Then $\tan\gamma_0 = t\sqrt{2}/\rho$. γ_0 will be the actual rotation of the secondary principal stresses if the birefringent elements are uniaxial, i.e. if any two of p, q and r are equal in magnitude and sign. If the elements are biaxial, the angle may be slightly increased or decreased dependent on the disposition of the optic axes with respect to the incident ray.

*Effect on Tardy compensation.** Drucker and Mindlin[4] have calculated the amplitude and phase relationships of the two rays propagated through a stressed photoelastic material for the case of uniform principal stress difference and a linear relation between angle of principal stress rotation and distance in the direction of propagation. These conditions apply fairly closely at the boundary for a thin slice.

Let x = distance from entrance face.
$\delta = 2kx$ = relative retardation in radians.
$\sigma = xA/2$ = rotation, $\sigma/\delta = R/2$, $S = [1 + R^2]^{\frac{1}{2}}$.

v and w are vibration components parallel and perpendicular to one principal stress direction. On the entrance point at $x = 0$ the components on the YOX and ZOX planes are $v_0 = M\cos\omega t$, $w_0 = N\cos\omega t$ (Fig. 5). The expressions given in reference (4) for v and w on the exit planes are

$$v = [-(R/S)N\sin\eta + M\cos\eta]\cos\omega t - (M/S)\sin\eta\sin\omega t \quad (1)$$

$$w = [(R/S)M\sin\eta + N\cos\eta]\cos\omega t + (N/S)\sin\eta\sin\omega t \quad (2)$$

The common phase change has been omitted and k/Sx written as η.

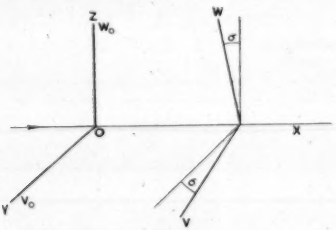

Fig. 5. Change of stress directions through the slice, showing entrance and exit planes

Isoclinic. For determining the isoclinic parameter the polarizer and analyser are usually linked together with their planes of polarization at right angles, and the assembly is rotated with respect to the slice until minimum light is observed. Let the incident plane polarized light $B\cos\omega t$ be polarized at angle ν to v_0, i.e. to the y direction.

In this case $M = B\cos\nu$, $N = B\sin\nu$. The exit components are

$$v = B\{[-(R/S)\sin\nu\sin\eta + \cos\nu\cos\eta]\cos\omega t - (1/S)\cos\nu\sin\eta\sin\omega t\} \quad (3)$$

$$w = B\{[-(R/S)\cos\nu\sin\eta + \sin\nu\cos\eta]\cos\omega t + (1/S)\sin\nu\sin\eta\sin\omega t\} \quad (4)$$

Resolving these components on the analyser plane which is at $(90° + \nu)$ to v_0 it is found that the resultant vibration is

$$U = B\{[(R/S)\cos\sigma\sin\eta + \sin\sigma\cos\eta]\cos\omega t + (1/S)\sin\eta\sin(2\nu - \sigma)\sin\omega t\}$$

The amplitude has its minimum value when $2\nu = \sigma$. Thus the isoclinic parameter is at $\sigma/2$ to the y axis, i.e. it corresponds to the average principal stress direction.

Compensation. For the measurement of relative retardation circularly polarized light is incident on the slice, and the second quarter-wave plate has its principal planes at 45° to the isoclinic parameter as determined above. Take the two separate conditions each representing plane polarized light

(*a*) $v_0 = M\cos\omega t$, $w_0 = 0$, i.e. $N = 0$.
(*b*) $v_0 = 0$, $w_0 = N\cos[\omega t + (\pi/2)]$, $N = M$.

Substitute the two conditions in equations (1) and (2) and add.

The sums of the two pairs of components v and w represent the resultant vibrations when circularly polarized light is incident, i.e.

$$v = M[\cos\eta\cos\omega t - (1/S)(1 - R)\sin\eta\sin\omega t]$$
$$w = M[-\cos\eta\sin\omega t + (1/S)(1 + R)\sin\eta\cos\omega t]$$

On exit from the slice v is at an angle σ to the y axis. The second quarter-wave plate has its fast plane at $-45°$ to the average direction of v through the slice. Fig. 6 shows the

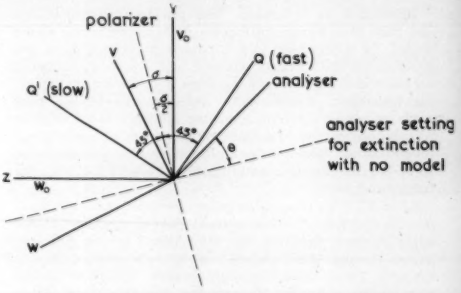

Fig. 6. Tardy compensation when rotation is present

relative angles of the slice entrance and exit planes, isoclinic parameter, quarter-wave plate planes, and the analyser at an arbitrary angle θ. Resolving v and w on to the planes Q and Q' and applying a phase change $-\pi/2$ to Q'

$$Q = (M/\sqrt{2})\{[\cos\eta\cos\omega t - (1/S)(1 - R)\sin\eta\sin\omega t][\cos(\sigma/2) - \sin(\sigma/2)] + [\cos\eta\sin\omega t - (1/S)(1 + R)\sin\eta\cos\omega t][\cos(\sigma/2) + \sin(\sigma/2)]\} \quad (5)$$

$$Q' = (M/\sqrt{2})\{[\cos\eta\sin\omega t + (1/S)(1 - R)\sin\eta\cos\omega t][\cos(\sigma/2) + \sin(\sigma/2)] + [\cos\eta\cos\omega t + (1/S)(1 + R)\sin\eta\sin\omega t](\cos\sigma/2 - \sin\sigma/2)\} \quad (6)$$

This, in general, represents elliptically polarized light. The analyser is turned until the light transmitted is of minimum intensity, i.e. the components Q and Q' resolved on to the analyser plane give minimum amplitude.

Let $Q = A_1\cos\omega t + B_1\sin\omega t$
$Q' = A_2\cos\omega t + B_2\sin\omega t$

The required amplitude C is given by

$$C^2 = (A_1^2 + A_2^2 + B_1^2 + B_2^2) - 2\cos 2\theta(A_1A_2 + B_1B_2) + \sin 2\theta(A_1^2 - A_2^2 + B_1^2 - B_2^2)$$

There is a maximum or minimum when

$$d(C^2)/d\theta = 0$$

i.e. $\tan 2\theta' = \frac{1}{2}(A_2^2 - A_1^2 + B_2^2 - B_1^2)/(A_1A_2 + B_1B_2)$ (7)

* It should be noted that the correction formulae derived apply equally well to Sénarmont compensation.

Note that θ' is measured from the analyser position for minimum light when no slice is present.

Substituting from equations (5) and (6) into (7),

$$\tan 2\theta' = 2(S\cos\sigma\cot\eta - R\sin\sigma)/[S^2\cot^2\eta - (1-R^2)] \quad (8)$$

The error in the Tardy reading in fringes is $(2\theta' - \delta)/360$. When high accuracy of measurement is required and the fringe order is low this error may be a significant factor, but may be corrected if the angle σ is known. A slight modification to the Tardy compensation procedure will permit the measurement of σ and the evaluation of the error.

(1) Turn linked polarizer and analyser until minimum light is observed.
(2) Rotate polarizer and analyser independently in opposite sense by equal amounts until a lower minimum is observed. This extra rotation of either component is $\sigma/2$.
(3) Set quarter-wave plate principal planes at 45° respectively to polarizer and analyser.
(4) Turn analyser until minimum light is again observed. θ as before is measured from the bisector of the right angle between the second quarter-wave plate planes.

Under these conditions the value of θ for compensation is given by

$$\tan 2\theta'' = 2S\cot\eta/[S^2\cot^2\eta - (1-R^2)] \quad (9)$$

Curves derived from the two formulae (8) and (9) are drawn in Fig. 7 and show the error in fractions of a fringe to be expected for various values of σ and δ.

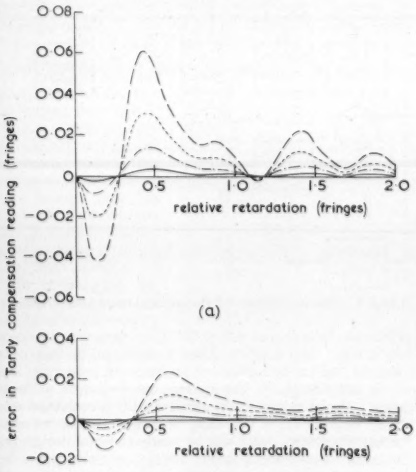

Fig. 7. Error in Tardy compensation due to rotation

(*a*) Conventional Tardy compensation (θ').
(*b*) Modified Tardy compensation (θ'').

——— $\sigma = 6°$. —·—·— $\sigma = 12°$.
– – – – $\sigma = 18°$. ———— $\sigma = 24°$.

4. MAXIMUM THICKNESS OF SLICE

From the foregoing consideration of errors it is possible to draw some conclusions on the permissible thickness of slice and the minimum surface radius of curvature such that measurement and geometrical factors should not introduce excessive error. An estimate of the total error under specified conditions may be made by addition of the separate errors calculated as in section 3. It is not possible here to tabulate the total errors for a representative series of conditions since the number of variables is so large. However, an estimate formed by simple addition of the separate maximum errors (which will not necessarily be co-existent) will give a conservative guide to the minimum radius of curvature which may be dealt with satisfactorily, and the permissible thickness of slice.

It is necessary to state the maximum allowable error. This, of course, depends on the nature of the problem; for convenience, an arbitrary figure of 2% of the maximum relative retardation per unit thickness in the model has been chosen. It is assumed that one slice only is available and that the effective boundary device is applied for correction of error *B*1. We have two general cases, one in which no corrections are applied, and the other in which all possible corrections are applied. Limits of t, ρ, and t/ρ noted below define the ranges within which the 2% error will not be exceeded.

(*a*) No corrections applied.

If $t > 0{\cdot}05$ in, then ρ must be $> 0{\cdot}5$ in, and $t/\rho < 0{\cdot}1$.

(*b*) All possible corrections applied.

If $t > 0{\cdot}05$ in, then ρ must be $> 0{\cdot}25$ in, and $t/\rho < 0{\cdot}2$.

For the thinnest practicable slice.

$t = 0{\cdot}02$ in, then ρ must be $> 0{\cdot}2$ in, and $t/\rho < 0{\cdot}1$.

CONCLUSIONS

Approximations to the errors in relative retardation observations on "frozen stress" slices at angles of incidence up to 45° have been calculated. It is observed that the error due to "rotation" is not negligible in thin slices and correction curves for this effect have been calculated. It has been found possible to specify minimum surface radii of curvature and maximum slice thicknesses such that a certain error should not be exceeded.

ACKNOWLEDGEMENTS

The work described above has been carried out as part of the research programme of the National Physical Laboratory and this paper is published by permission of the Director of the Laboratory.

The author wishes to acknowledge the assistance of Mathematics Division, National Physical Laboratory, in the evaluation of the definite integrals in error *A*5.

REFERENCES

(1) Hickson, V. M. *Brit. J. Appl. Phys.*, **2**, p. 261 (1951).
(2) Mindlin, R. D. *J. Opt. Soc. Amer.*, **27**, p. 289 (1937).
(3) Leven, M. M. Scientific Paper. Westinghouse Research Laboratories (1948).
(4) Drucker, D. C., and Mindlin, R. D. *J. Appl. Phys.*, **11**, p. 724 (1940).

The application of molecular resonance to microwave frequency stabilization*

By H. R. L. Lamont, M.A., Ph.D., A.M.I.E.E., A.Inst.P.,† and E. M. Hickin, A.M.I.E.E., Research Laboratories, The General Electric Company Ltd., Wembley, Middlesex

[*Paper received* 24 *September*, 1951]

A method is described of stabilizing the frequency of an oscillator by means of the molecular absorptions which occur in the microwave spectrum of some gases. Circuit details are given of an apparatus used with ammonia at wavelengths near 1·25 cm, and factors affecting performance are discussed theoretically. An N.P.L. test gave a measured stability figure of $\pm$ 6 parts in 10^7. Possibilities for other wavelengths are considered.

1. Introduction

It has long been known that certain gases absorb electromagnetic radiation of particular wavelengths. The case of ammonia, predicted theoretically and confirmed experimentally in 1934 by Cleeton and Williams,[1] is the best known, having a strong absorption band which at atmospheric pressure occupies a wavelength band extending from about 1·0 cm to 2·0 cm. The discovery by Bleaney and Penrose[2] in 1946 that decrease of pressure causes this band to split up into individual resonance lines which eventually become very narrow, was the next major step in a study which has since been extended to many gases over wide frequency ranges, and is now called microwave spectroscopy.

The frequencies of the resonance lines are functions of the possible quantum states of the gas molecules, and, at pressures sufficiently low that the lines appear as distinct individuals, are independent of pressure. These lines can therefore be used as standard reference frequencies. As a further step, they can be used to control the frequency of a centimetre wave oscillator. Ammonia is the best gas yet found for this purpose, since it has a number of suitably intense lines. Its molecule, which is in the form of a tetrahedron, has quantum states defined by two quantum numbers, J, K, which represent respectively the total number of units of angular momentum, and the number of units of angular momentum about the axis of symmetry. The intense lines have frequencies in the region of 24 000 Mc/s, corresponding to wavelengths around 1·25 cm.

2. Frequency Stabilization

2.1. *Introduction.* Two general methods of using absorption lines for stabilization of an oscillator have been suggested. One method is to produce a microwave discriminator as developed by Pound,[3] using, instead of a tuned cavity to produce the required characteristic, a length of waveguide filled with the gas. The complex dielectric constant of the gas can be shown to vary around the resonance frequency in such a way as to provide the required discriminator characteristic. This method has been developed by Smith, de Quevedo, Carter and Bennett.[4] The other method, suggested by Hershberger and Norton[5] but described only in outline, uses an auxiliary scanning oscillator to sweep through the resonance line and transfers the discriminator problem from the high frequency part. It is this method which has been used in these laboratories, and the circuits evolved for it and the results obtained are described here.

2.2. *General description of method.* The block diagram of Fig. 1 shows the arrangement of the system, and Fig. 2 is a photograph of the essential parts of the complete stabilizer, some details of which have already been published.[6] The scanning oscillator (Osc. *A*, Fig. 1) is a 1·25 cm reflex Klystron (type VX 302) which is swept over a small frequency range (not exceeding 5 Mc/s) in the neighbourhood of a chosen ammonia resonance frequency at a recurrence rate of 2 kc/s. Neither the repetition rate of the sweep nor its frequency range is critical. The output of the valve is taken through a cavity wavemeter and a variable attenuator to the ammonia cell. This consists of a 6-metre length of standard waveguide

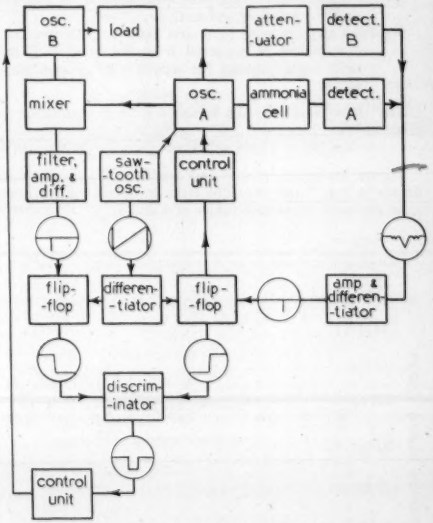

Fig. 1. Block diagram of stabilizer showing waveforms

of internal dimensions 0·420 × 0·170 in, bent for convenience into a coil. This guide is closed at each end by thin mica windows and has connexions to an ammonia gas supply and an oil diffusion pump, the pressure being read on a Pirani gauge. The other end of the ammonia coil is connected to a crystal detector (type VX 4026) A, (Fig. 1). The rectified current from this crystal will be nearly constant during the frequency sweep except at the absorption point when the momentary drop of output gives rise to a short recurrent pulse. This pulse can be seen in the top trace of Fig. 12(*a*), where it consists of the main absorption line with satellite lines on either side of it. To avoid trouble due to variations in oscillator output over the sweeping range some of the output of the scanning oscillator is taken through a directional coupler and a second attenuator to a second crystal detector *B*

* Communication No. 485.

† Now at Royal Technical College, Glasgow.

connected in parallel with the first but with reversed polarity. By adjustment of one of the attenuators the two crystal outputs can be arranged to cancel except at the absorption point, whatever may be the variation of oscillator output.

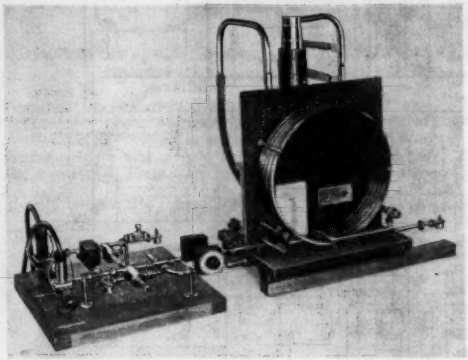

Fig. 2. R.F. components of stabilizer and vacuum pump

The oscillator to be stabilized, the "controlled oscillator" (also type VX 302, *B* in Fig. 1), assumed for the moment to be set at a frequency differing by a few megacycles per second from the absorption frequency, feeds power to a crystal mixer which is also connected through a directional coupler to the scanning oscillator. On the output side of the mixer is connected a narrow-band filter, followed by a detector and amplifier, which accepts the variable beat-frequency between the two oscillators over only a narrow range, thereby producing a second recurrent pulse. The variation of time difference between the pulses from these two sources is a measure of the frequency variation of the controlled oscillator.

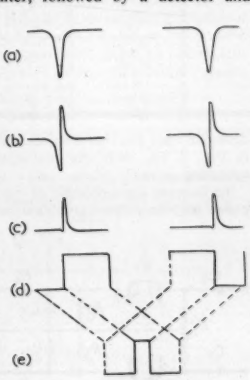

Fig. 3. Pulse waveforms, showing control voltage generation

To stabilize the frequency of the controlled oscillator it is necessary to derive a voltage dependent in magnitude and sign on the time difference between the two pulses. As a first step each pulse, which displayed along a time axis appears as in Fig. 3(*a*), is amplified, differentiated [Fig. 3(*b*)], and limited [Fig. 3(*c*)] to give a pulse with a steep rise at the position of the peak of the original pulse. The leading edge of this pulse is used to trigger on a multivibrator which is switched off at the end of the sweep by means of a pulse derived from the fly-back of the sweep voltage generator. The two rectangular waves thus produced [Fig. 3(*d*)] are subtracted to give a rectangular wave of duration equal to the time difference between the peaks of the two original pulses [Fig. 3(*e*)], and sign dependent upon their order of arrival. The d.c. component of this pulse has the characteristic of a discriminator circuit and may be fed back to control the oscillator frequency, the complete circuit forming a servo system.

2.3. *Circuit details.* For a stabilized frequency exactly equal to the absorption frequency the filter (in Fig. 1) must give its maximum output at zero frequency. Although this requirement can be met by an amplifier with a low frequency response extending down to zero the time constants of the following detector, required to give the envelope of the response, proved difficult. It was found better to offset the stabilized frequency from the absorption frequency by a small amount, and to use as a filter for the beat frequency a sharply tuned amplifier stage. For this purpose a single stage 16 Mc/s amplifier (type Z77 tuned grid and anode) is quite adequate. The detector is a germanium diode whose output is the envelope of the response curve of the amplifier.

This envelope is further amplified as a pulse by a three-stage amplifier with about 60 db gain, the circuit of which is shown in Fig. 4 (V_{12}–V_{14}). The response of this amplifier is deliberately reduced at frequencies below 1 kc/s, in order to avoid trouble from hum. A differentiating circuit couples the output to a fourth valve V_{15} which runs with zero bias and a grid current limiting resistance. The anode waveform of this stage which is that shown in Fig. 3(*c*) is in the form of a positive pulse and is used to trigger a cathode-coupled multivibrator V_{16}. A negative "cancelling" pulse, derived from the fly-back of the sweep voltage generator V_{8a}, is supplied via a decoupling valve V_9.

The three-stage amplifier with limiter and multivibrator is duplicated (V_1–V_3) to provide amplification for the combined outputs of the two crystal detectors (*A* and *B* of Fig. 1).

The outputs of the two multivibrators are passed to two twin-diode limiting circuits V_6, V_{17} which maintain equality of output in a common load R_{49}. This is obviously essential otherwise a permanent error will arise. At first the two multivibrator outputs were taken from dissimilar anodes (as shown in Fig. 4) to obtain the necessary inversion, but some trouble was experienced with incomplete cancellation at the end of each cycle and this was greatly eased by using similar anodes and passing one square-wave through an inverting valve. Any residual voltage can be removed by adjustment of R_{25}, R_{86}, C_{28} and C_{29} (associated with V_5, V_9 and V_{16}), or by a diode clamp operated by the fly-back pulse.

The voltage appearing across the common diode load R_{49} may be smoothed to leave the d.c. component and then applied directly to the reflector electrode of the "controlled oscillator." However, this electrode in the VX302 valve runs at approximately − 1 800 V with respect to the resonator, which is an integral part of the metal work of the valve and so is most conveniently run at earth potential. Some method of transferring this control potential to the − 1 800 V level is therefore desirable. One system which has been commonly used is shown in Fig. 5. The d.c. control voltage V_c is fed to a control valve whose anode load forms part of a potentiometer chain from + 350 V to some potential more negative from the reflector, say − 2 kV. The reflector voltage is taken off by a variable tapping. The objections to this system are that a greater negative potential is required for its operation than is needed by the valve, and that the proportion

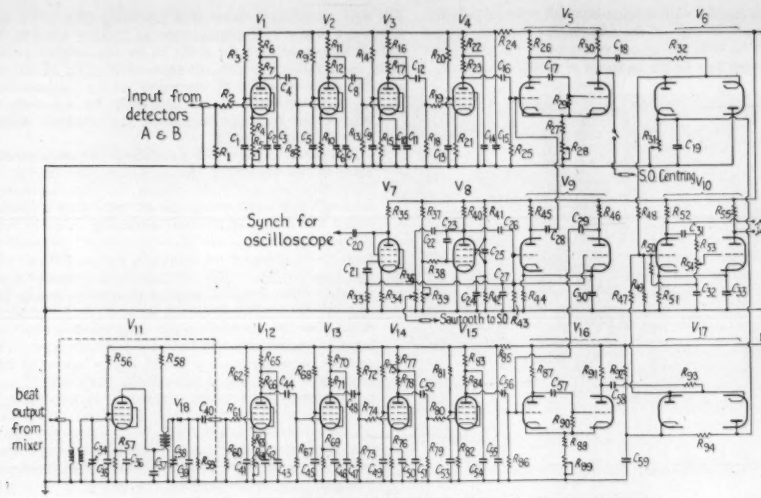

Fig. 4. Circuit diagram of amplifiers and control voltage generators

$C_1 = 0{\cdot}1\ \mu F$
$C_2 = 20\ \mu F$
$C_3, C_4, C_5 = 0{\cdot}1\ \mu F$
$C_6 = 20\ \mu F$
$C_7 = 0{\cdot}1\ \mu F$
$C_8 = 0{\cdot}01\ \mu F$
$C_9, C_{10}, C_{11} = 0{\cdot}1\ \mu F$
$C_{12} = 330\ pF$
$C_{13}, C_{14} = 0{\cdot}1\ \mu F$
$C_{15} = 8\ \mu F$
$C_{16} = 0{\cdot}001\ \mu F$
$C_{17} = 0{\cdot}01\ \mu F$
$C_{18} = 0{\cdot}1\ \mu F$
$C_{19} = 25\ \mu F$
$C_{20} = 0{\cdot}1\ \mu F$
$C_{21} = 0{\cdot}002\ \mu F$
$C_{22} = 0{\cdot}1\ \mu F$
$C_{23} = 0{\cdot}002\ \mu F$
$C_{24} = 330\ pF$
$C_{25} = 68\ pF$

$C_{26} = 0{\cdot}002\ \mu F$
$C_{27} = 0{\cdot}01\ \mu F$
$C_{28}, C_{29} = 0{\cdot}002\ \mu F$
$C_{30} = 25\ \mu F$
$C_{31} = 0{\cdot}1\ \mu F$
$C_{32} = 20\ \mu F$
$C_{33} = 25\ \mu F$
$C_{34} = 3{-}30\ pF$
$C_{35} = 0{\cdot}1\ \mu F$
$C_{36} = 0{\cdot}002\ \mu F$
$C_{37} = 0{\cdot}1\ \mu F$
$C_{38} = 3{-}30\ pF$
$C_{39} = 10\ \mu F$
$C_{40} = 0{\cdot}002\ \mu F$
$C_{41} = 0{\cdot}1\ \mu F$
$C_{42} = 20\ \mu F$
$C_{43} = 0{\cdot}1\ \mu F$
$C_{44} = 0{\cdot}002\ \mu F$
$C_{45} = 0{\cdot}1\ \mu F$
$C_{46} = 20\ \mu F$

$C_{47} = 0{\cdot}1\ \mu F$
$C_{48} = 0{\cdot}002\ \mu F$
$C_{49} = 0{\cdot}1\ \mu F$
$C_{50} = 20\ \mu F$
$C_{51} = 0{\cdot}1\ \mu F$
$C_{52} = 330\ pF$
$C_{53}, C_{54} = 0{\cdot}1\ \mu F$
$C_{55} = 8\ \mu F$
$C_{56} = 0{\cdot}001\ \mu F$
$C_{57} = 0{\cdot}02\ \mu F$
$C_{58} = 0{\cdot}1\ \mu F$
$C_{59} = 25\ \mu F$

V_1–V_4 = Z77
V_5 = B65
V_6 = D77
V_7, V_9 = Z77
V_8, V_{10} = B65
V_{11}–V_{15} = Z77
V_{16} = B65
V_{17} = D77
V_{18} = GEX44

$R_1, R_2 = 47\ k\Omega$
$R_3 = 22\ k\Omega$
$R_4 = 270\ \Omega$
$R_5, R_6, R_7 = 10\ k\Omega$
$R_8 = 100\ k\Omega$
$R_9 = 22\ k\Omega$
$R_{10} = 470\ \Omega$
$R_{11}, R_{12} = 10\ k\Omega$
$R_{13} = 57\ k\Omega$
$R_{14} = 22\ k\Omega$
$R_{15} = 470\ \Omega$
$R_{16}, R_{17}, R_{18} = 10\ k\Omega$
$R_{19}, R_{20} = 47\ k\Omega$
$R_{21} = 100\ \Omega$
$R_{22} = 47\ k\Omega$
$R_{23} = 10\ k\Omega$

$R_{24} = 1\ k\Omega$
$R_{25} = 470\ k\Omega$
$R_{26} = 0{\cdot}68\ k\Omega$
$R_{27}, R_{28} = 2{\cdot}2\ k\Omega$
$R_{29} = 470\ k\Omega$
$R_{30} = 22\ k\Omega$
$R_{31} = 4{\cdot}7\ k\Omega$
$R_{32} = 100\ k\Omega$
$R_{33} = 220\ k\Omega$
$R_{34} = 1\ k\Omega$
$R_{35} = 47\ k\Omega$
$R_{36} = 1\ M\Omega$
$R_{37} = 100\ k\Omega$
$R_{38} = 1\ M\Omega$
$R_{39} = 47\ k\Omega$
$R_{40} = 100\ k\Omega$
$R_{41} = 150\ k\Omega$
$R_{42} = 47\ k\Omega$
$R_{43} = 2\ k\Omega$
$R_{44} = 330\ \Omega$

$R_{45}, R_{46} = 47\ k\Omega$
$R_{47}, R_{48}, R_{49} = 100\ k\Omega$
$R_{50} = 470\ k\Omega$
$R_{51} = 150\ \Omega$
$R_{52} = 50\ k\Omega$
$R_{53} = 470\ k\Omega$
$R_{54} = 100\ k\Omega$
$R_{55} = 50\ k\Omega$
$R_{56} = 47\ k\Omega$
$R_{57} = 150\ \Omega$
$R_{58} = 22\ k\Omega$
$R_{59} = 4{\cdot}70\ k\Omega$
$R_{60} = 4{\cdot}7\ k\Omega$
$R_{61} = 47\ \Omega$
$R_{62} = 22\ k\Omega$
$R_{63} = 270\ \Omega$
$R_{64}, R_{65}, R_{66} = 10\ k\Omega$
$R_{67} = 100\ k\Omega$
$R_{68} = 22\ k\Omega$
$R_{69} = 470\ \Omega$

$R_{70}, R_{73} = 10\ k\Omega$
$R_{72} = 3{\cdot}9\ M\Omega$
$R_{73} = 100\ k\Omega$
$R_{74} = 47\ k\Omega$
$R_{75} = 22\ k\Omega$
$R_{76} = 470\ \Omega$
$R_{77}, R_{78}, R_{79} = 10\ k\Omega$
$R_{80}, R_{81} = 47\ k\Omega$
$R_{82} = 100\ k\Omega$
$R_{83} = 47\ k\Omega$
$R_{84} = 10\ k\Omega$
$R_{85} = 1\ k\Omega$
$R_{86} = 470\ k\Omega$
$R_{87} = 68\ k\Omega$
$R_{88}, R_{89} = 2{\cdot}2\ k\Omega$
$R_{90} = 470\ k\Omega$
$R_{91} = 22\ k\Omega$
$R_{92} = 68\ k\Omega$
$R_{93} = 100\ k\Omega$
$R_{94} = 2{\cdot}2\ k\Omega$

of the control valve anode voltage change which reaches the reflector depends upon the reflector setting (which is frequency dependent) and is never very high.

The method developed for the present equipment uses the a.c. component of the out-of-balance voltage developed across the diode load R_{49}. This is amplified (V_{10}) and split into two parts, the one an inverted image of the other, and these two alternating voltages are condenser-coupled to a twin rectifier circuit of the type shown in Fig. 6. Each rectifier will respond only to positive pulses and therefore a positive or negative change will occur at the reflector depending upon which rectifier is operating. The operation of the normal reflector voltage control is not affected by this circuit. The input-output characteristic of this system will depend upon whether the rectifiers have loads high enough for them to operate as peak voltmeters. In this desirable case the characteristic will assume the form shown in Fig. 7, i.e. with the maximum possible slope at the operating point.(7)

To increase the sensitivity of the discriminating system the pulses may be further amplified before being applied to the

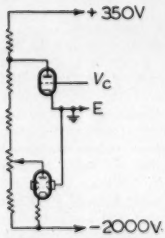

Fig. 5. Circuit diagram of d.c. control voltage coupling to Klystron reflector

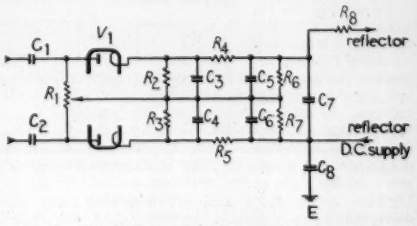

Fig. 6. Circuit diagram of a.c. control voltage coupling to Klystron reflector

$R_1 = 220\ k\Omega$
$R_2, R_3 = 5{\cdot}6\ M\Omega$
$R_4, R_5 = 1\ M\Omega$
$R_6, R_7 = 10\ M\Omega$
$R_8 = 100\ k\Omega$

$C_1, C_2 = 0{\cdot}02\ \mu F$
$C_3, C_4 = 500\ pF$
$C_5, C_6 = 2\,000\ pF$
$C_7 = 0{\cdot}07\ \mu F$
$C_8 = 2\ \mu F$

V_1 = D77

rectifiers. By limiting pulses in the negative direction the voltage swing of the positive pulses may be increased.

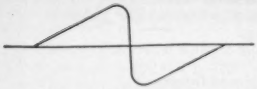

Fig. 7. Form of discriminator characteristic

A further use of this control voltage transference technique has been made in connexion with the scanning oscillator. It will be understood from the earlier discussion that unless the absorption line occurs within the sweep of this oscillator the stabilizer will not operate. Therefore some form of stabilization is desirable in order roughly to "centre" the oscillator on the absorption. This has been achieved by the circuit of Fig. 8, in which the output of the absorption pulse

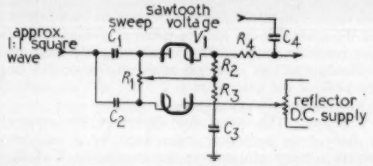

Fig. 8. Circuit diagram of centring circuit for sweeping oscillator

$R_1 = 220\ \text{k}\Omega$ $C_1, C_2 = 0{\cdot}02\ \mu\text{F}$ $V_1 = \text{D77}$
$R_2, R_3 = 470\ \text{k}\Omega$ $C_3 = 2\ \mu\text{F}$
$R_4 = 100\ \text{k}\Omega$ $C_4 = 0{\cdot}5\ \mu\text{F}$

multivibrator (V_5 of Fig. 4) is fed to another rectifier circuit in the reflector lead of the sweeping oscillator. When the absorption occurs in the middle of the sweep this output will be a square wave of 1 : 1 on-off ratio, and the rectifier outputs will balance. Any deviation from this will cause a positive or negative voltage to be injected in series with the reflector in such a manner as to reduce the magnitude of the error.

Another form of discriminator which has been successfully constructed uses the grid base of a high slope pentode as the

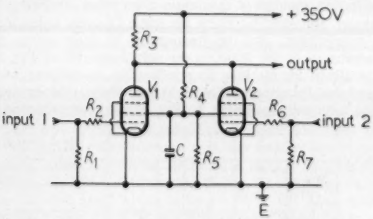

Fig. 9. Circuit diagram of high gain discriminator

$R_1 = 68\ \text{k}\Omega$ $R_5 = 10\ \text{k}\Omega$ $C = 16\ \mu\text{F}$
$R_2, R_3 = 15\ \text{k}\Omega$ $R_6 = 15\ \text{k}\Omega$
$R_4 = 47\ \text{k}\Omega$ $R_7 = 68\ \text{k}\Omega$ $V_1, V_2 = \text{Z77}$

limiting device. The two square waves are fed to a pair of valves of type Z77 having a common anode load. A substantial gain results from this system, the circuit of which is shown in Fig. 9.

2.4. *Theory.* If the centre of the chosen absorption line is at a frequency f_a, and f_i is the resonance frequency of the filter, then the control circuits will set the oscillator frequency f_s to a value such that $f_s = f_a \pm f_i$. There are thus two stable positions equally displaced from the absorption frequency. If f_i is made zero the frequency of stabilization becomes equal to the absorption frequency, but, as has been stated, it is much simpler to use a finite value of f_i, which should be high enough for the two frequencies to be readily separated.

A change of magnitude Δf_s in the oscillator frequency due to an external cause such as a change of voltage will be reduced by the negative feedback to a value $\Delta f_s/S$, where S is the stabilization factor. This factor is given by the relation

$$S = 1 + kg \qquad (1)$$

in which k is the sensitivity of the discriminator and its associated amplifiers in volts per unit frequency change, and g is the oscillator frequency sensitivity per control volt.

Any variation in the position of the ammonia line or of the position of the initiating pulse generated from it will, however, be transferred directly to the stabilized oscillator as a change in frequency. The position of the centre of the ammonia line is considered to be independent of temperature and pressure.* In order therefore that the position of the initiating pulse should be as precise as possible the absorption line should be as narrow as possible. The limitations on the width of the line are well known, being determined mainly and in varying degrees by intermolecular collision broadening, broadening due to collisions with the cell walls, Doppler broadening and saturation effects.[9]

Intermolecular collision is the most important factor influencing line shape when the pressure is not extremely low. It has been shown[9] that for the strongest line in ammonia the line half-width Δf, that is, half the width of the line between points where the absorption has fallen to half the maximum, is proportional to pressure over the pressure range from approximately 0·1 to 100 m of mercury, and is given by

$$\Delta f = 27 \times 10^6 p \text{ c/s} \qquad (2)$$

where p is the pressure in millimetres of mercury. The Doppler effect accounts for a half-width of about 36 kc/s for ammonia at room temperature. For a waveguide of internal dimensions 0·42 × 0·17 in as used here collision with the guide walls produces at room temperature a half-width of about 10 kc/s. The total half-width will be the sum of these separate factors, and thus it would appear that by sufficient reduction of pressure the half-width could be readily reduced to a value of less than 100 kc/s. Unfortunately, however, as the pressure is decreased a saturation effect becomes evident, when the incident power is sufficient to raise molecules to the excited state at a rate comparable with their return to their former state. Since collisions between molecules is their principal means of returning to the unexcited state this effect becomes increasingly important as the pressure is decreased. The result of this is to reduce the absorption at the peak of the curve, giving an apparent increase in line width. Carter and Smith[10] give the following expression which relates the actual half-width $\Delta f'$ for an input power density W (watts/cm²) to the asymptotic value of half-width Δf attained for vanishingly small input power:

$$\Delta f' = \Delta f\left[1 + \frac{1{\cdot}7 \times 10^{14} W}{(\Delta f)^2}\right]^{\frac{1}{2}} \qquad (3)$$

If Δf is replaced by its value in terms of pressure given by equation (2), then equation (3) becomes

$$\Delta f' = [(27 \times 10^6 p)^2 + 1{\cdot}7 \times 10^{14} W]^{\frac{1}{2}} \text{ c/s} \qquad (4)$$

and it is evident that, as the pressure is reduced,

$$\Delta f' \to 1{\cdot}3 \times 10^7 W^{\frac{1}{2}} \text{ c/s} \qquad (5)$$

* Margenau[8] has shown theoretically that it should be dependent on the pressure p in the form $f_a(1 + Ap^2)$, but the constant A is so small that the effect has not so far been observed.

The two terms in equation (4) become equal when

$$p \simeq 0{\cdot}5W^{\frac{1}{2}} \text{ mm} \tag{6}$$

and when, for a given power, p is appreciably below this value it ceases to have any further effect on the line width. This is illustrated in Fig. 10 which shows the variation in $\Delta f'$ with p as given by equation (4) for an assumed value of $W = 10^{-4}$ W/cm². This theory neglects the effect of the containing cell and assumes a uniform distribution of field. The exact analysis gives much more complicated expressions whose actual values, however, differ very little from those given here.

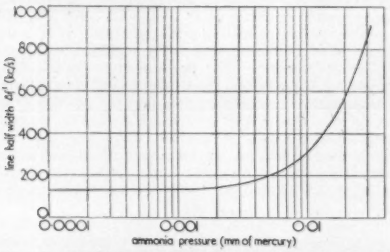

Fig. 10. Variation of line half-width with pressure for an input power of 100 μW

Thus the minimum power required for detection without appreciable interference from crystal noise will determine the minimum line width. A good crystal detector is thus of primary importance in the operation of the stabilizer.

One of the sets of triggering pulse is derived by differentiation of the absorption pulse obtained from the two detector crystals, and thus this triggering pulse will be steepest and hence its operation most precise when the curvature at the peak of the absorption curve is a maximum. It is possible to find a value for the length of the guide which makes this curvature a maximum. The absorption coefficient α (cm^{-1}) of the gas in the cell at any frequency f is related to the peak absorption α_a at the frequency f_a by the equation

$$\alpha = \frac{\alpha_a(\Delta f)^2}{(f - f_a)^2 + (\Delta f)^2} \tag{7}$$

If P_0 is the power input to a waveguide of length l having an attenuation constant α_g (cm^{-1}) due to conductor loss, then the power P_{rA} received in crystal A will be

$$P_{rA} = P_0 e^{-(\alpha + \alpha_g)l}$$

The balancing power P_{rB} in crystal B is

$$P_{rB} = P_0 e^{-\alpha_g l}$$

For square law crystal responses the voltage V of the triggering pulse will have the form

$$V = KP_0 e^{-\alpha_g l}(1 - e^{-\alpha l})$$

If α_g is assumed constant over the small frequency range of the sweep then α is the only frequency dependent term, and the curvature at the peak of the absorption curve is given by

$$\left(\frac{d^2V}{df^2}\right)_{f=f_a} = \frac{2KP_0\alpha_a l}{(\Delta f)^2} e^{-(\alpha_a + \alpha_g)l} \tag{8}$$

Before making this a maximum with respect to l one has to decide how the power has to be allowed to vary, bearing in mind that it must be kept to the minimum usable value. Since Δf is dependent on the power in the guide, and the power varies along the length of the guide, it is probably best to stipulate that the average power along the guide should remain constant as the length is varied.

If, then, P_0 in equation (8) is replaced by P_{ave}, where

$$P_{ave} = \frac{P_0}{(\alpha_a + \alpha_g)l}\left[1 - e^{-(\alpha_a + \alpha_g)l}\right]$$

maximizing (8) with respect to l gives

$$(\alpha_a + \alpha_g)l \simeq 1{\cdot}6 \tag{9}$$

For the copper waveguide used the attenuation constant is about 0·005 db/cm, and thus

$$\alpha_g = 1{\cdot}2 \times 10^{-3} \text{ cm}^{-1}$$

The value in space of α_a for the (3, 3) ammonia line[10] is $7{\cdot}9 \times 10^{-4}$ cm^{-1}, but in the waveguide this must be multiplied by $\lambda g/\lambda$, giving $\alpha_a = 9{\cdot}7 \times 10^{-4}$ cm^{-1}. The optimum value for the guide length determined through equation (9) is thus about 7 m, although on account of the variation of Δf along the guide this can only be taken as a rough indication of the optimum length. The length of guide used in the experiments was 6 m. The gas attenuation over this length at the peak of the absorption is 2·5 db, with an additional 3-db loss due to waveguide losses.

2.5. *Results.* The actual frequencies of the absorption lines have been accurately determined by a number of observers in terms of quartz crystal standards. Kisliuk and Townes[11] give a comprehensive list of molecular resonance frequencies published up to the beginning of 1950. Most of these have been determined to one or two parts in 10^6.

During experiments with the equipment a search was made for the detectable ammonia absorption lines. All the known lines, twenty-three in number, within the range of the wavemeter were identified and these are shown in Fig. 11 plotted on the wavemeter calibration curve. It will be noticed that five of these lines (numbered below the curve) are for the $N^{15}H_3$ isotope, present to its natural extent of 0·38%. However, many of these absorptions are very weak, and while they are of great importance for calibration work they are not suitable for operating the stabilizer. From the experimental work a rough criterion has been established that satisfactory stabilization requires a maximum asborption coefficient in excess of 10^{-4} cm^{-1}. There are some 15 lines which meet this requirement, and the frequencies of those within the wavemeter range are listed on the right-hand side of Fig. 11, the length of the marking lines indicating the relative intensities of the absorptions. The (3, 3) line, which is the strongest in the ammonia spectrum, having a maximum absorption

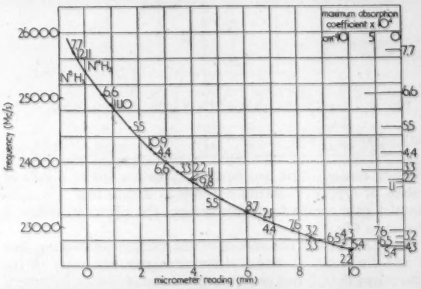

Fig. 11. Wavemeter calibration showing identified lines and relative intensities of those suitable for stabilization

coefficient of $7{\cdot}9 \times 10^{-4}$ cm^{-1}, is shown in the photograph of Fig. 12(*a*) together with the triggering pulse derived from it (cf. Fig. 3). The (5, 4) line with its derived initiating pulse is shown in Fig. 12(*b*). This line, with a maximum absorption coefficient of $1{\cdot}9 \times 10^{-4}$ cm^{-1}, has also given satisfactory stabilization. The small satellite lines shown on either side of the main (3, 3) line in Fig. 12(*a*) and also in Fig. 13 are a useful guide to the scale of frequency: the two inner ones are separated by 3·37 Mc/s, the outer two by 4·65 Mc/s.

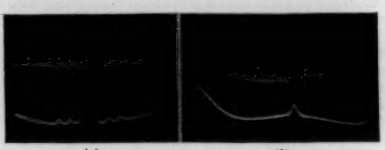

(*a*) (*b*)

Fig. 12. Photographs of $N^{14}H_3$ lines (with differentiated pulses above). (*a*) 3, 3 line; (*b*) 5, 4 line

As has been discussed in Section 2.4 the line width of the absorptions depends upon pressure, temperature, cell size and power absorbed, but these have no effect on the absorption frequency. The effect of pumping out the system can be seen in the photographs of Fig. 13. The swept frequency range is some 7 Mc/s, and the highest pressure in the series is about 1 mm of mercury. The amplifier gain has been increased between Fig. 13(*d*) and 13(*e*), but it is clear that the line width has reached an almost stationary value.

It has been found that the minimum input power for satisfactory operation is about 50 μW, although of course this depends on the particular crystal detector used. This corresponds to a value of input power density of about 100 μW/cm^2, and hence, by equation (5), to a limiting line-width ($2\Delta f'$) of 260 kc/s. In accordance with equation (6) and Fig. 10, the line width will approach this value when the pressure has been reduced to about 5×10^{-3} mm of mercury, and further reduction of pressure will have little effect. These figures were confirmed by the experiments, which gave a limiting line width of about 300 kc/s, changing little for pressures below 10^{-2} mm of mercury. This value of 300 kc/s corresponds to a Q value of 80 000.

Discriminator sensitivities have been steadily improved as the apparatus developed. The simplest type, shown in Fig. 6, had a sensitivity of some 150 V per Mc/s. The addition of limiters and amplifiers increased this to some 600 V per Mc/s, and it was in this condition that the tests at the National Physical Laboratory to be described in Section 2.6 were made.

The improved discriminator of Fig. 9, which was a later development, gave a sensitivity of 10^4 V per Mc/s without amplifiers, and 10^5 V per Mc/s when these were added.

How closely the frequency can be held on the centre of the discriminator curve depends on the design of the pulse circuits. With a line width of 300 kc/s it will probably be difficult to reduce the uncertainty below $\pm$ 5 kc/s. The stabilizing factor S, therefore, need only be sufficient to limit possible oscillator drift to within about $\pm$ 1 kc/s. If one assumes that the unstabilized frequency deviations can amount to 10 Mc/s, then this can be achieved by a value of S equal to 10^4. Thus, since the frequency sensitivity g for the type VX302 Klystron is about 1 Mc/s per volt, then equation (1) gives a value of the required discriminator sensitivity k as 10^4 V per Mc/s. Thus the values quoted above for the later discriminator circuits are sufficient to realize the full accuracy of the system.

2.6. *Check on stabilized frequency.* Through the courtesy of the Superintendent, Electricity Division of the National Physical Laboratory, both the bandwidth and mid-band frequency of the oscillator have been measured by Dr. Essen in terms of the N.P.L. quartz crystal frequency standard. The results are published by permission of the Director of the N.P.L.

The method employed a 5 Mc/s crystal-controlled oscillator whose output was multiplied and amplified up to 250 Mc/s. This power was then fed to a type CV113 silicon crystal rectifier mounted in a 3×1 in waveguide cavity tuned to 3 000 Mc/s. This was in turn coupled to a second crystal rectifier mounted in a length of $0{\cdot}42 \times 0{\cdot}17$ in waveguide in which harmonic power at 24 000 Mc/s was generated. This was mixed with the output of the ammonia-stabilized oscillator, of nominal stabilized frequency 23 870 $\pm$ 16 Mc/s, to give a beat at 114 or 146 Mc/s. Owing to the presence of a strong 50 Mc/s component, stronger and more convenient beats were in fact found at 64 and 96 Mc/s, and these were used for the measurements. While the measurements were being made a check was kept on the frequency of the 5 Mc/s oscillator in terms of the 100 kc/s N.P.L. frequency standard. Two sweep frequencies were used, 2 000 c/s and about 800 c/s, but no particular difference in behaviour between them was found. The results which were taken with the discriminator of Fig. 6 were:

(*a*) Sweep frequency 2 000 c/s	
Measured frequency with I.F. filter frequency added	23 886·40 Mc/s
Measured frequency with I.F. filter frequency subtracted	23 854·02 Mc/s
Mean frequency	23 870·21 Mc/s
Oscillator bandwidth	0·1 Mc/s
(*b*) Sweep frequency 800 c/s	
Measured frequency with I.F. filter frequency added	23 886·36 Mc/s
Measured frequency with I.F. filter frequency subtracted	23 854·01 Mc/s
Mean frequency	23 870·18 Mc/s
Oscillator bandwidth	0·15 Mc/s

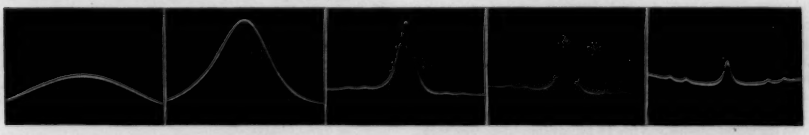

(*a*) (*b*) (*c*) (*d*) (*e*)

Fig. 13. Effect of reducing pressure on the absorption pulse. Swept frequency range is some 7 Mc/s and the highest pressure (*a*) about 1 mm of mercury. Amplifier gain increased between (*d*) and (*e*)

These mean frequencies when compared with the present accepted figure of 23 870·11 Mc/s for the 3, 3 line of ammonia show a discrepancy of about 4 parts in 10^6. An examination of the method of stabilizing shows that the most likely source of error lies in the generation of the square waves from the differentiated envelopes of the absorption and the beat pulses. There may be a tendency for the wavefront to lag behind the true mid-point of the pulse and while this effect would cancel if the two pulses were of identical shape the beat pulse is in fact steeper due to the narrow bandwidth of the I.F. filter. This would cause the stabilizer to lock to a higher frequency if the sweep were from low to high frequency which is the case in this apparatus.

The bandwidths noted, which represent the amount of oscillator jitter, were greater than anticipated and the reasons for this are not clear. The power supplies used were ordinary laboratory units and were not highly stabilized, but the impression was formed during the test that the ammonia stabilizing mechanism itself was introducing a jitter. This may be due to the manner in which a "sample" is taken of the relative frequencies of oscillator and absorption each cycle of sweep, since the error voltage generated from this information can in fact have been applied to the oscillator, and a substantial frequency change have resulted, before the next sample is taken. Limitation of the rate at which this error voltage is applied to the oscillator, however, did not appear to improve matters substantially. It is hoped to investigate both these matters more fully.

However, the centre point of the oscillator bandwidth could be defined to about 10 kc/s, and over a period of several hours the variations were within $\pm$ 15 kc/s, despite intentional wide changes in control settings. This represents an accuracy of $\pm$ 6 parts in 10^7.

2.7. *Harmonic working.* It has been shown in Section 2.3 that the oscillator to be stabilized need not be at the frequency of an absorption line, as a beat frequency filter of up to several hundred megacycles per second can be employed. Stabilization at frequencies even further removed from a convenient absorption line is perfectly feasible. The only requirement is that there should be sufficient energy present at the mixer from both oscillators for a reliable beat to be detected and amplified. This energy may be present as harmonics of either the stabilized valve or of the sweeping valve. For example, the 3, 3 line of ammonia at 23 870 Mc/s can be used to stabilize a valve at 47 750 Mc/s by using the second harmonic of the sweeping valve and a 10 Mc/s filter. Similarly the harmonics of a lower frequency oscillator can be mixed with energy at 24 000 Mc/s to provide a controlling voltage. Also, since a power of only a few microwatts is required at the input to the ammonia cell, it is possible to use a scanning oscillator whose frequency is a sub-harmonic of the absorption frequency. A similar method to this has been used by the National Bureau of Standards in Washington.[12] In their equipment the harmonics of a 100 kc/s quartz-crystal-controlled oscillator are employed, suitable frequency multiplication, modulation and amplification being provided.

The harmonic working technique has been successfully applied in these laboratories to a small glass-envelope magnetron of the resonant segment (type E1210). The seventh harmonic of this valve, oscillating at 3 412 Mc/s (8·8 cm), was developed by feeding the power into a crystal distorter, and in this case additional amplification at 16 Mc/s was used between the mixer crystal and the 16 Mc/s filter. The feedback voltage was made to control the oscillator valve frequency by variation of the current in a coil surrounding the permanent magnet of the oscillator.

2.8. *Future developments.* As a result of experience with this equipment a number of improvements can be suggested.

The bulk of the equipment could be greatly reduced if a sealed-off system were used, thereby dispensing with the pumping system seen adjacent to the waveguide coil in Fig. 2. This is not possible with copper waveguide, since copper adsorbs ammonia to an appreciable extent. There is not much information available on adsorption of ammonia, but investigation might show some more suitable metal.

The length of guide used is more than is necessary with the more intense lines; a length of about 1 m would be adequate for the (3, 3) line. Again, this is very dependent on the sensitivity of the crystal, and any improvement here would allow further reduction in the guide length. As indicated in Section 2.4 the line-width could be reduced a little by increasing the cross-section of the waveguide.

If 10^{-4} cm^{-1} is taken as a rough criterion of the smallest value of the maximum absorption coefficient of a line to give satisfactory stabilization a search of the substances whose attenuation has so far been investigated[11] gives the cyanogen compounds, ClCN, BrCN, ICN and HCN, which have resonances in the region of 9 mm and 3·5 mm wavelength, and carbonyl sulphide, COS, with resonances near 5 and 6 mm wavelength.

Comparison of the line-widths of these molecules shows that they are all similar to those of ammonia with the exception of carbonyl sulphide, which has a line width about one-fifth of that of ammonia. In view of this sharpness it is unfortunate that the strong lines of COS occur at wavelengths where the difficulties of generation are as yet considerable. There is, however, a COS line at 12 mm (24 326 Mc/s) which may yet prove useful, although its absorption coefficient is approximately half the minimum which can at present be tolerated.

3. CONCLUSIONS

It has been demonstrated that stabilization of an oscillator to an accuracy of 1 part in 10^6 is readily possible, but it appears that with existing techniques the width of the ammonia line will prevent anything better than about 1 part in 10^7 being obtained. The use of a waveguide of larger size and a lower temperature would improve matters by decreasing the line width, but the best solution lies in finding substances with still sharper lines.

REFERENCES

(1) CLEETON, C. E., and WILLIAMS, N. H. *Phys. Rev.*, **45**, p. 234 (1934).

(2) BLEANEY, B., and PENROSE, R. P. *Proc. Roy. Soc., A*, **189**, p. 358 (1947).

(3) POUND, R. V. *Proc. Instn Radio Engrs*, **35**, p. 1405 (1947).

(4) SMITH, W. V., DE QUEVEDO, J. L. G., CARTER, R. L., and BENNETT, W. S. *J. Appl. Phys.*, **18**, p. 1112 (1947); **19**, p. 83 (1948).

(5) HERSHBERGER, W. D., and NORTON, L. E. *R.C.A. Rev.*, **9**, p. 38 (1948).

(6) LAMONT, H. R. L. *Physica*, **17**, p. 446 (1951).

(7) British Patent Appl. No. 20047/50 (General Electric Co. Ltd. and E. M. Hickin).

(8) MARGENAU, H. *Phys. Rev.*, **76**, p. 1423 (1949).

(9) BLEANEY, B., and PENROSE, R. P. *Proc. Phys. Soc.*, **60**, p. 83 (1948).

(10) CARTER, R. L., and SMITH, W. V. *Phys. Rev.*, **73**, p. 1053 (1948).

(11) KISLIUK, P., and TOWNES, C. H. *J. Res. Nat. Bur. Stand.*, **44**, p. 611 (1950).

(12) *Tech. News Bull. Nat. Bur. Stand.*, **33**, p. 17 (1949).

The atomization of liquid in a flat spray

By R. G. Dorman, B.Sc., A.R.C.S., D.I.C., Grad.Inst.P., Chemical Defence Experimental Establishment, Porton, Wilts.

[*Paper first received* 13 *November*, 1951, *and in final form* 11 *December*, 1951.]

The drop-size distribution in flat sprays produced by agricultural nozzles is discussed and an equation has been derived by dimensional analysis relating a mean drop diameter to operating conditions at the nozzle. The equation has been applied to experimental data for agricultural nozzles with satisfactory results. The development of the spray sheet with pressure increase is shown by high-speed photographs.

INTRODUCTION

This paper has its origin in an investigation of the performance of some commercial flat spray nozzles used for agricultural spraying. There is an extensive literature on the break-up of jets, but little has been written on the dispersion of a liquid when it issues from a nozzle in the form of a flat sheet. It was therefore decided to study, by flash photography, the mechanism of the atomization, and to determine the size-distribution of the droplets produced, in an endeavour to relate the parameters characterizing the distribution to the physical properties of the liquid and the conditions of dispersion. Although the spray nozzles were from normal production and not made with special precision, they gave consistent and reproducible results.

DESCRIPTION OF SPRAY NOZZLES AND MECHANISM OF BREAK-UP

The nozzles were standard production types from different makers, seven being of brass whilst two were of ceramic construction. The delivery rates varied from about 7 c.c./sec for the smallest to more than 70 c.c./sec for the largest over the range of pressure 45–105 lb/in^2. Although the nozzles differed in construction and appearance, the method of forming the liquid sheet was similar in all cases; Fig. 1, a

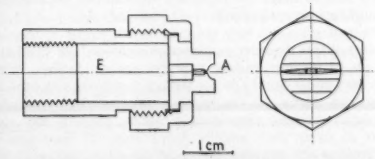

Fig. 1. Section and end view of a flat-spray nozzle

diagrammatic section and end view of one of the nozzles, shows that from the entrance chamber *E* there is a channel to the orifice *A*, just behind which the inner walls begin to converge. It is in this convergence that the orifice is cut by a V-shaped milling tool, producing an elliptically shaped mouth. The essence of the formation of a flat spray is this narrowing of the channel, whereby the liquid on the periphery is accelerated towards the centre, giving rise to an axial pressure and a velocity at right angles to the convergence, in a plane containing the major axis of the ellipse. At very low pressures the sheet of liquid emerging from the orifice is oval in shape and very large drops are produced (Fig. 2). With slight increase of pressure the sheet grows larger but retains much the same shape until further increase produces the form shown in Fig. 3. With larger liquid velocities a fan-like sheet is formed, the leading edge breaking into droplets whilst the sides thicken and break into fewer but somewhat larger drops. It is this stage with which we are concerned, a stage where the fan angle or spray-angle (Fig. 4) grows slightly with pressure whilst the length of the liquid sheet decreases. The high-speed photograph, Fig. 5, shows clearly the wavy nature of the liquid sheet breaking into ligaments

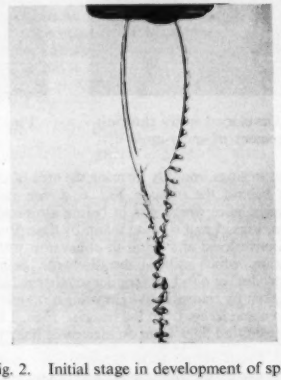

Fig. 2. Initial stage in development of spray

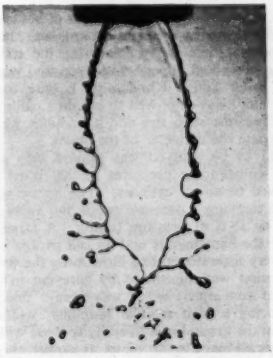

Fig. 3. Second stage in development of a flat spray

which subsequently break into droplets. These ligaments are not all of the same thickness, and indeed in a particular ligament the thickness may vary at different points. As a general rule the distance between ligaments increases with distance from the orifice and the droplets appear to be

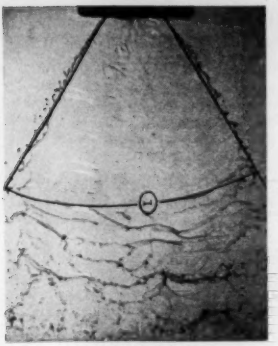

Fig. 4. Developed spray showing measurement of spray-angle θ

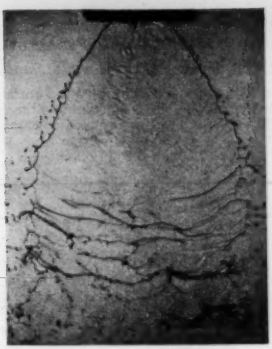

Fig. 5. Fully developed spray at pressure of 60 lb/in^2

Fig. 6. Side view of spray

concentrated in rings, roughly forming the arcs of circles with centres just behind the orifice. Fig. 6, a side view, clearly shows the turbulence which sets in before atomization. The photographs, Figs. 5 and 6, were taken by flash from a spark apparatus, constructed at Porton in connexion with research on atomization, which utilized the discharge, between magnesium electrodes, of a 0·1 μF condenser charged to 6 000 V. They were taken by transmitted light using a double extension plate camera some 30 cm from the nozzle. Figs. 2 and 3 were taken by transmitted light from an electronic flash tube.

EXPERIMENTAL METHOD FOR DETERMINING SIZE DISTRIBUTION OF DROPLETS

The tests were carried out at pressures of between 45 lb/in^2 and 105 lb/in^2 spraying dyed water, and later, kerosene, the drop size being estimated by measuring the stain diameter produced on absorbent paper. The dyes used were Croceine Scarlet for water and a Rhodamine B base for kerosene. A microburette[1] was employed to obtain a calibration curve of drop size against stain size and a Luminex magnifier was used to estimate the diameter of the stains.

The liquid to be sprayed was poured into a 4 gal can capable of withstanding pressures of 200 lb/in^2 and which was connected to an air cylinder. The nozzle was screwed into a lance carrying a pressure gauge and valve and joined to the can by 15 ft of pressure tubing. A large room was required for the experiments and an old garage was chosen. There was very little draught to blow away the finer droplets and evaporation was minimized by spraying in the vapour of the liquid concerned; water was always present on the floor, producing a high relative humidity, whilst before a kerosene trial the ground was liberally sprayed with kerosene. The tests were all made in the winter at temperatures of about 12° C and evaporation losses were considered unimportant.

The layout to be sprayed consisted of a line of about 25 filter papers each approximately 29 cm square. Pressure having been applied to the liquid the operator positioned himself about 6 ft from one end of the line and 12 ft to the side of it. He adjusted the pressure at the nozzle to the agreed value by means of the valve whilst spraying into a can, and then carried the nozzle smartly across the layout, spraying horizontally and pointing down the line. The filter papers were removed after allowing a few seconds for the smaller drops to settle. This method gives a representative sample on a line parallel to the nozzle and it is only necessary to count and size stains from equal areas on each paper to obtain the distribution. The largest drops were sprayed further than the fine ones, although winnowing into size groups was not complete. The number of the small drops near the operator often amounted to more than 200/in^2, whilst the number of large drops distant from him was less than ten to a filter paper so that it was usual to count larger areas of the more distant papers and to make the necessary adjustments when adding the numbers on each paper.

The method is not very accurate for the sizing of drops of less than 100 μ diameter as the stains produced are small and difficult to measure with a magnifying glass; further, stains from very small drops are not always round, the dye running along the fibres of the paper. Nevertheless, practised observers obtained reproducible results, and in any case errors in sizing these smaller drops were not important in determining the relevant statistical diameters, although the use of filter papers is not to be recommended for sizing distributions smaller than those reported in this work. Some difficulty has also been experienced when spraying oils since dyes must be found which will not spread with the oils, otherwise the stains are liable to run one into the other.

METHOD OF EXPRESSING SIZE DISTRIBUTION OF DROPLETS IN A SPRAY

The equations which are most commonly used to express the distribution of sizes in sprays are the Rosin–Rammler, the logarithmic normal and the Nukiyama–Tanasawa equations. All these equations are empirical, the use of the first two arising mainly from their ability to fit particle sizes resulting from grinding operations whilst the formula of the Japanese, Nukiyama and Tanasawa, was devised as a result of size measurements on sprays from gas atomizing nozzles. It has been found that the frequency of occurrence of drops at the high and low ends of the range is small and gradually increases to a maximum at some intermediate value. The three equations mentioned fit results tolerably well but

predict an infinite size maximum drop, although in the practical case there must be a finite maximum. They show, however, that the frequency of occurrence of the larger drops rapidly falls to an insignificant value and they may be used to calculate most statistical diameters with reasonable accuracy.

Two statistical diameters in use to define the sizes of droplets in sprays are the mean-volume-surface diameter D_o, and the mass median diameter D_m. The mass median diameter is that diameter of droplet, above or below which is found half the mass of the spray. It is simple, though tedious, to calculate from experimental data without pre-supposing any size distribution equation. The method, which has long been in use at The Chemical Defence Establishment, consists of plotting on logarithmic probability paper the cumulative percentage of drops below a diameter x against the diameter x and drawing a smooth curve through the points (Fig. 7).

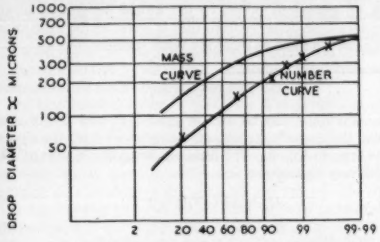

Fig. 7. Drop-size distribution plotted on logarithmic probability paper

Convenient size intervals are taken and the percentage number in each is read off from the smoothed curve and multiplied by the cube of the mean diameter, giving the relative mass in each interval. These relative masses are converted into percentage masses and the cumulative percentages plotted against the higher interval values on the same graph paper. The value at 50% mass is then read directly from the graph.

The mean-volume-surface diameter (or Sauter mean diameter) is defined as the diameter of a single drop having the same ratio of surface to volume as the whole spray, and may be written

$$D_o = \int_0^\infty x^3 dn \Big/ \int_0^\infty x^2 dn \qquad (1)$$

where x is the drop diameter in microns and n the number with diameters less than x. In value it is a little less than D_m.

A series of experiments carried out by the writer on the distribution from nozzles showed that the drop spectrum fitted the Nukiyama–Tanasawa equation closely, except for the smaller droplets of less than 100 μ diameter, and that there was extremely good agreement between the values of D_m calculated by the Porton method and by the method of the Japanese. It was therefore decided to adopt this method of computing D_o and D_m, without in any way prejudicing the use of the Rosin–Rammler or logarithmic normal methods. A new diameter, designated D_g, the value at 99·99% number, was also introduced, being considered a superior parameter to the "largest drop seen" used by some writers.

THE DROP-SIZE DISTRIBUTION EQUATIONS

The equation of Nukiyama and Tanasawa[2, 3] may be written as follows:

$$dn/dx = ax^2 \exp(-bx^q) \qquad (2)$$

where x is the diameter of an individual drop in microns, dn the number of drops with diameters between x and $x + dx$ in the sample and a, b and q are constants. q was found to be equal to unity for all the commercial nozzles described in this paper. Equation (2) may be rewritten as,

$$\log(x^{-2}dn/dx) = \log a - xb/2{\cdot}3 \qquad (3)$$

A plot of $\log(x^{-2}dn/dx)$ against x should therefore yield a straight line of slope $-b/2{\cdot}3$. Substituting equation (2) in (1) and integrating it is found that $D_o = 5/b$. The value of D_o can thus be calculated from the slope of the line given by equation (3). Assuming the applicability of the Nukiyama–Tanasawa equation it is comparatively easy to find relationships between D_o and other statistical diameters.

When $q = 1$

and

$$D_m/D_o = 1{\cdot}14 \qquad (4)$$

$$D_g/D_o = 2{\cdot}78 \qquad (5)$$

The cumulative percentage number curve was drawn from the experimental data and from this smooth curve the 99·99% number, D_g, was read, and dn/dx was found for various values of x (n being expressed as a percentage). On plotting $\log(x^{-2}dn/dx)$ against x a good straight line was obtained from which D_o was calculated. The fact that the experimental results for the smaller drops did not show particularly good agreement with the Nukiyama–Tanasawa equation has little effect on the diameters calculated, the Japanese stating in their paper that the larger drops have most bearing on the results. Any slight discrepancies on the graph for drops of less than 100 μ diameter were therefore neglected and the best line drawn for drops of 100 μ and above.

DIMENSIONAL TREATMENT OF FLAT SPRAY BREAK-UP

The spraying of insecticides had shown that although the tendency was for drop size to increase with viscosity the effect was not large. The assumption was therefore made, that as a first approximation, the viscosity could be neglected over the range of normal free flowing liquids. It was also assumed that disintegration of the sheet took place evenly over the front edge, although Figs. 3 and 5 show some break away from the thickened sides.

D, some statistical diameter of the droplets formed (measured in cm), may then be expressed as

$$D = C(Q/\theta)^x \gamma^y \rho^z v^a \qquad (6)$$

where C is constant, Q is the liquid throughput in c.c./sec, θ is the spray angle in radians, γ is the surface tension in dynes/cm, ρ the liquid density in g/c.c., and v the velocity in cm/sec.

In order to solve the equation the power of one of these quantities must be assumed. Rayleigh[4] in his work on jets found that the diameter of drop depended on the one-third power of the surface tension and since the Rayleigh jet bears considerable likeness to the flat spray break-up the value $\frac{1}{3}$ was tentatively assigned to y. On substituting $y = \frac{1}{3}$ in equation (6) it was found that

$$x = \tfrac{1}{3},\ a = -1,\ \text{and}\ z = -\tfrac{1}{3}$$

Since $v \propto p^{\frac{1}{2}}\rho^{-\frac{1}{2}}$ the equation takes the form

$$D = C(Q/\theta)^{\frac{1}{2}}\gamma^{\frac{1}{2}}\rho^{\frac{1}{2}}p^{-\frac{1}{2}} \quad (7)$$

The throughput Q is proportional to $p^{\frac{1}{2}}$ so that for any particular nozzle $D \propto p^{-\frac{1}{2}}$ neglecting small changes in θ. Equation (7) is similar to that of Hodgkinson[5] who undertook a detailed mathematical treatment of the control by surface tension upon a fluid emerging from an orifice in the form of a conical sheet. Assuming the fluid to have axial and radial velocities only and neglecting the reaction of the air he arrived at a formula

$$D = (2{\cdot}12/\pi \sin \beta)^{\frac{1}{2}}(Q\gamma)^{\frac{1}{2}}\rho^{\frac{1}{2}}p^{-\frac{1}{2}} \quad (8)$$

where β = half spray cone angle.

No very accurate experiments have been carried out to investigate the change in drop size with viscosity, but it would appear that drop size depends on less than the one-tenth power of the viscosity. The introduction of such a small term will modify but slightly the powers of the quantities in equation (7).

RESULTS AND DISCUSSION

The experiments were first carried out with water as the sprayed fluid and showed that $D \propto (Q/\theta)^{\frac{1}{2}}p^{-\frac{1}{2}}$ within the limits of experimental error. The ratio D_g/D_o was found to be 2·7, a little smaller than the 2·78 predicted by the Nukiyama–Tanasawa equations, but even so, in satisfactory agreement. Kerosene, surface tension 28 dynes/cm measured by the weighed drop method, and density 0·8 g/c.c., was used to test the validity of the surface tension term in equation (7). The predicted variation of drop size with density has been included in the calculations although the experiments were not accurate enough to show the existence of such a small variation. To save time only six tests were carried out with kerosene, using three different nozzles, and full calculations for D_o were made in only the first two tests; in the remainder D_g only was read and D_o calculated by dividing D_g by 2·7. A considerable amount of tedious work was thereby saved, it being only necessary to measure the sizes of the larger stains whilst the rest were merely counted in order to provide a total from which to find D_g. The plots of D_g and D_o against $(Q/\theta)^{\frac{1}{2}}\gamma^{\frac{1}{2}}\rho^{\frac{1}{2}}p^{-\frac{1}{2}}$ (Fig. 8) are straight lines and seem to point to $D \propto \gamma^{\frac{1}{2}}$ although tests with a greater number of liquids would have been desirable. γ, the surface tension value, is that at the point of break-up, and whilst this is easily measurable in the case of pure liquids, it is not so simple with liquids containing surface active agents, since in such cases there is a time lag before the surface tension drops to the static value. Work on emulsions points to the surface tension at break being very little different from that of water as the drop sizes are almost the same as those for water sprays.

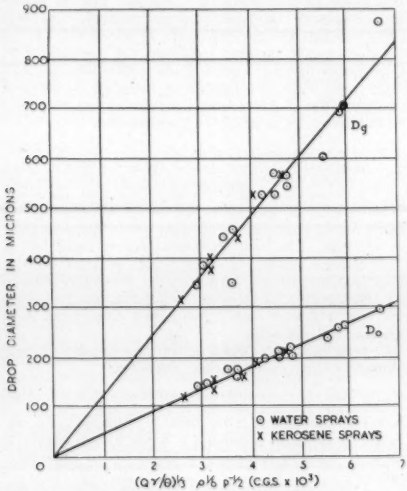

Fig. 8. Experimental points for all nozzles used connecting D_g and D_o with $(Q\gamma/\theta)^{\frac{1}{2}}\rho^{\frac{1}{2}}p^{-\frac{1}{2}}$

CONCLUSIONS

The equations may be used to predict D_g and D_o for new nozzles, the numerical constants being taken from the slopes of the lines in Fig. 8. The final equations for liquids which are not very viscous are

$$D_g = 12(Q/\theta)^{\frac{1}{2}}\gamma^{\frac{1}{2}}\rho^{\frac{1}{2}}p^{-\frac{1}{2}} \quad (9)$$

and

$$D_o = 4{\cdot}4(Q/\theta)^{\frac{1}{2}}\gamma^{\frac{1}{2}}\rho^{\frac{1}{2}}p^{-\frac{1}{2}} \quad (10)$$

The standard errors of the coefficients are 0·7 and 0·15. In these equations the units of the various quantities are the same as those in equation (6). Throughput and pressure measurements are both quickly made and θ, the spray angle, may be measured sufficiently accurately for most purposes by placing a protractor under the nozzle whilst spraying; in this work θ was measured from negatives of spark shadowgraphs.

ACKNOWLEDGEMENTS

The author wishes to record his appreciation of the work of Mr. T. D. Narracott of the National Institute of Agricultural Engineering who collaborated in the first part of these experiments, and to thank Mr. J. M. Creasey and Mr. B. W. Philipson for assistance with the experiments.

Much of this work was carried out whilst the writer was employed by the National Institute of Agricultural Engineering and seconded to the Chemical Defence Experimental Establishment to members of the staff of which he is grateful for advice and encouragement. The paper is published by permission of the Chief Scientist, Ministry of Supply.

REFERENCES

(1) LANE, W. R. *J. Sci. Instrum.*, **24**, p. 98 (1947).
(2) NUKIYAMA, S., and TANASAWA, Y. *Trans. Soc. Mech. Engrs (Japan)*, **4**, pp. 86, 138 (1938); **5**, pp. 63, 68 (1939); also **6**, II, pp. 7, 18 (1940).
(3) LEWIS, H. C., EDWARDS, D. G., GOGLIA, M. J., RICE, R. I., and SMITH, L. W. *Industr. Engng Chem.*, **40**, p. 67 (1948).
(4) RAYLEIGH, LORD. *Proc. Roy. Soc.*, **29**, p. 71 (1879).
(5) HODGKINSON, T. G. Unpublished paper (1950).

The rheology of plastic dispersions

By P. A. Briscoe, B.Sc., W. J. Dunning, B.Sc., Ph.D., and R. C. Seymour, B.Sc., A.Inst.P., Department of Physical and Inorganic Chemistry, The University, Bristol

[*Paper first received* 21 *May*, 1951, *and in final form* 21 *January*, 1952]

An account is given of the behaviour of a system containing 80% by volume of a powdered solid, which shows plastic deformation but does not conform to the Bingham or Freundlich concepts of plasticity. The term "dilatant plasticity" is suggested for such systems which have a small sedimentation volume, are dilatant, non-thixotropic and can be moulded, but shear harden showing a series of yield values dependent on their previous history. Under a force exceeding one yield value, deformation does not proceed continuously but approaches a limiting value.

The deformation properties of this system are characterized by two parameters. k measures the shear hardening due to changes in the geometry and structure of the powdered solid, and c expresses the relation between the limiting compression and the weight required to produce it. On roll milling, the parameters change in a reciprocal way, the product kc remaining approximately constant.

A solid dispersed in a liquid modifies the flow properties of the liquid in a manner which depends upon the following factors: volume concentration; size distribution and shapes of the solid particles; flow properties of the liquid and the surface properties and structure of the solid–liquid interphase which determine the forces between the particles.

At low concentrations of solid, the flow properties of the liquid are but slightly modified. As the concentration increases, interaction between the particles[1] modifies the form of the simple Einstein formula. Freundlich and Röder[2] showed that an aqueous suspension containing over 43% by volume of a quartz powder with an average particle size of 1 to 5 μ, behaves as a Newtonian fluid for small rates of shear, the mobility of the suspending fluid allowing the structure to relax. On increasing the stress, a disproportionately high resistance appears at a certain rate of shear, and any further increase in the shearing stress only serves to maintain this maximum rate of shear. At this high rate of shear, the structure cannot relax quickly enough. This phenomenon has been called "inverted plasticity."[3]

When forces between the particles are present, it is to be expected that the structure will be more permanent, and the effects of structure formation will be apparent at smaller values of the solid concentration. Very strong forces will introduce deviations from Newtonian behaviour at quite small concentrations, and the structure may be present in the undisturbed system so that shearing breaks it down rather than builds it up. It has been suggested by Freundlich and Röder that the time taken by the structure to reform after such disturbances is the feature which distinguishes thixotropy from false-body.[4] Such thixotropic systems conform to the Bingham plasticity equation[5] and, in particular, exhibit Bingham yield values.[2, 6]

The systems investigated in the present research consist of about 80–85% by volume of solid in a grease-like medium. They exhibit a very mild secular thixotropy in that they become slightly harder after about six months' storage and can be softened by a moderate amount of manipulation. The experiments were always carried out on fresh samples so that the thixotropic effect—already of secondary importance—was negligible. The most characteristic feature of these putty-like materials is their mouldability and, in the common usage of the word, they are very plastic. On deformation, the surface becomes dry, due to Osborne–Reynolds dilatancy.[7] Here we have a system displaying interesting features in that it is plastic, dilatant and virtually non-thixotropic. Freundlich and Jones[8] contrast the properties of plasticity and dilatancy inferring that, in general, a system which is plastic is also thixotropic, whilst a non-plastic system is not, in general, dilatant. We shall show that the conception of plasticity used by Freundlich and his co-workers (essentially that of Bingham) is too limited and must be broadened, unless we are to refuse the term "plastic" to these materials, which would be contrary to the common usage of the word.

EXPERIMENTAL

When a liquid is added drop by drop to an insoluble powdered solid of suitable particle size distribution, the mass, after working, remains dry and crumbly until a certain proportion of liquid has been added; it then becomes coherent and plastic. In this state it can be continuously moulded, and retains its shape so long as the sample is not so large that excessive gravitational forces, due to its weight, are present to deform it further. The addition of further quantities of liquid makes the mixture more and more easily deformable until the gravitational force on even a small sample causes it to flow, and the plasticity is then destroyed. The range of liquid content over which the mixture is plastic, and the flow properties of the mixture, depend upon the factors mentioned above. An example which will serve to illustrate the type of plastic material under discussion is given by putty. Experiments were made on a putty-like material containing 78% by volume of a certain powdered solid, which was mixed with 22% by volume of soft mineral jelly, the jelly being heated to facilitate mixing. This mixture, on cooling, formed a "short," crumbly, sugary mass with very little coherence. It was then passed through a laboratory Torrance roll mill a number of times. After milling a certain number of times, it became smoother and more coherent, and could then be readily moulded. It lost its crumbly brittleness and could be drawn out between the fingers into thin strings, which smoothly extended, necked and broke.

A cylinder of material was rolled out between two glass plates separated by glass rollers, 15 mm in diameter, so that this became the cylinder's diameter. The ends were squared up by cutting carefully with a razor-blade, thus making a cylinder 1 in long. This cylinder was placed between the platform and piston of a compression plastometer, the whole being thermostated at 25° C. A weight was put on the piston and, after the latter had been released, the height of the cylinder was measured at 10-second intervals for 10 minutes.

There was a rapid compression during the first seconds and fractions of a minute, and then the rate of compression slowed down until, at the end of 10 min, there was only a "creep" remaining. (On lifting the compressing weight and piston from the cylinder at this stage, no (less than 0·1%) elastic recovery was measurable.) Analysis of the compression-time curves for each compressing weight shows (Fig. 1) that they could be described by the equation

$$-dt/dh = kt + a \qquad (1)$$

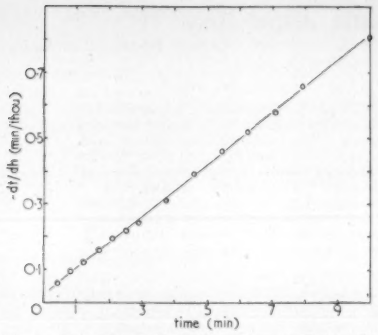

Fig. 1. Dependence of velocity of compression on time

In Table 1, the values of k, derived for different values of the compression weights, are given.

Table 1. *First sample.* *Temp.* 25 ± 0·5° C

W grams	k	Δh_{10} (thou)	$\log_e h_{10}/h_0$
0	—	27·2	0·0270
30	—	58·2	0·0598
50	0·082	96·5	0·1015
80	0·078	132·8	0·1428
100	0·092	163·0	0·178
130	0·089	199·0	0·222
150	0·111	216·0	0·244
200	0·092	260·0	0·305

The value of c from Fig. 3, curve b, is 0·00135 g, giving an average value of $kc = 0{\cdot}122$

The value of k from 50 to 200 g is approximately constant, and it is very probable that the value of k is independent of the compressing weight.

In order to find the form of a, equation (1) is integrated, giving

$$t = a(e^{k\Delta h} - 1)/k \tag{2}$$

Inserting this value of t in equation (1),

$$-\left(\frac{\partial h}{\partial t}\right)_W = \frac{1}{a}e^{-k\Delta h} \qquad (W \text{ constant}) \tag{3}$$

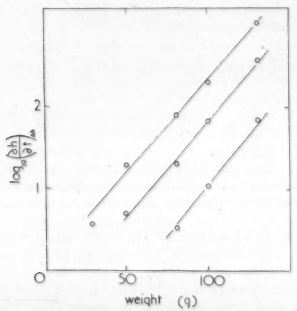

Fig. 2. $\text{Log}_{10}(\partial h/\partial t)_{\Delta h}$; plotted as a function of the compressing weight for separate compression of each cylinder

The velocity of compression, $-dh/dt$, was read off from each of the curves obtained for different weights and the velocity found when the amount of compression had reached a fixed value ($\Delta h = 40$, 80, 120 × 10^{-3} in). It was found (Fig. 2) that $\log_{10}(\partial h)/(\partial t)_{\Delta h}$; was a linear function of the weight. Hence a is an exponential function of W, and equation (3) can be rewritten as

$$-(\partial h)/(\partial t) = je^{\beta W - k\Delta h} \tag{4}$$

where β is a constant independent of Δh and W.

If, in a family of $\Delta h/t$ curves for different compressing weights, points which have the same velocity of compression are selected on the curves, these points satisfy equation (4) in the form

$$je^{\beta W - k\Delta h} = -(\partial h)/(\partial t)_W = \text{constant} \tag{5}$$

or

$$\beta W - k\Delta h = \text{constant}$$

i.e.

$$\Delta h = \beta(W - \text{constant})/k \tag{6}$$

The velocity of compression after 10 min is almost the same for all curves, and in this case, equation (5) predicts a linear relation between Δh_{10} (amount of compression after 10 min) and W.

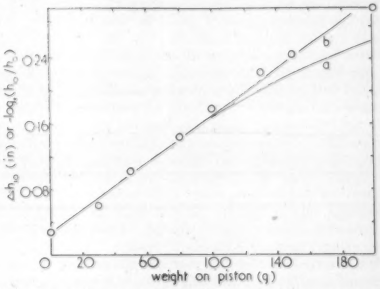

Fig. 3. Amount of compression as a function of load

A plot of Δh_{10} against W (Fig. 3) is linear for small values of Δh_{10}*, i.e.

$$\Delta h_{10} = c(W - W_0) \tag{7}$$

in agreement with equation (6) with

$$kc = \beta \tag{8}$$

and putting W_0 for the constant in equation (6). From equations (5) and (7) we have

$$j = -(\partial h)/(\partial t)_{W_0} \cdot e^{kcW_0} \tag{9}$$

and substituting for j in equation (4),

$$\partial h/\partial t = (\partial h)/(\partial t)_{W_0} \cdot e^{k(c\overline{W - W_0} - \Delta h)} \tag{10}$$

This gives the relation between the velocity of compression $\partial h/\partial t$, the compressing weight and the amount of compression Δh. The value of W_0 depends upon the value of $(\partial h/\partial t)_{W_0}$, chosen for equation (7).

According to equation (10), the value of $\partial h/\partial t$ depends only on W and Δh and vice versa. This means, for example, that equation (7) is independent of the history of the sample. To test this, another series of experiments was carried out on another example of the same composition (second sample). The same cylinder was compressed by a succession of increasing weights, each weight being allowed to compress the

* It is interesting to find that, by plotting not Δh_{10} but $\log_e h_{10}/h_0$ against the compressing weights (Fig. 3), the line is straight, up to about 25% compression.

plastic for 10 min. Thus, in the first experiment, the cylinder was compressed for 10 min by a 50 g weight, and then the weight increased to 100 g, and so on. The compressing weights were 50, 100, 150, 200, 300 and 400 g. In the second

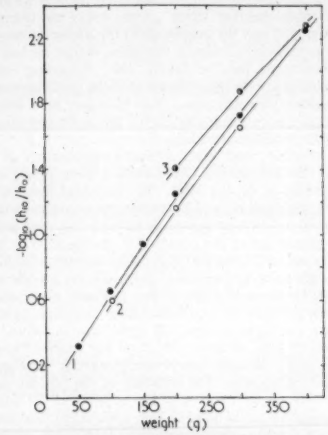

Fig. 4. $\text{Log}_{10}(h_{10}/h_0)$ as a function of W for successive compression of the same cylinder

experiment, they were 100, 200, 300 g and in the third experiment 200 and 400 g. The results are plotted in Fig. 4 and with the same proviso concerning $\log h_{10}/h_0$ as previously,

$$\Delta h_{10} = c(W - W_0)$$

The points lie close to a single straight line. The amount of compression appears then to depend only upon the compressing weight, subject to the condition that the rate of compression is small (i.e. that the compression-time curve has reached the "plateau"). This conclusion is of importance when we come to interpreting equation (10).

The effect of progressive roll milling. The powder was mixed with 21·8% by volume of the jelly and passed through a roll mill. After each passage a sample was put aside. Each of eight samples was subjected to compression tests; the values of k and c are given in Table 2 and plotted in Fig. 5 against the number of millings. It is seen that k shows a minimum and c a maximum near the fifth and sixth millings. Subjective evaluation by various persons, who moulded and

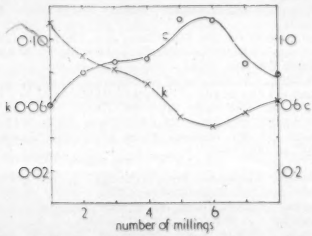

Fig. 5. Reciprocal behaviour of k and c on milling

worked the samples in their hands, indicated that the "most plastic" sample was either the fifth or sixth. This suggests that k and c are significant in relation to what is subjectively considered "good plasticity."

Table 2. *The effect of milling on the parameters k and c*

No. of millings	k	$c \times 10^{-3}$ *per sec*	$k \times c \times 10^3$
1	0·110	0·60	6·6
2	0·090	0·80	7·2
3	0·082	0·86	7·05
4	0·073	0·88	6·45
5	0·053	1·13	6·0
6	0·047	1·10	5·2
7	0·053	0·83	4·56
8	0·062	0·78	4·85

In the fourth column of Table 2, it is interesting to note that again the product $k \times c$ is (approximately) constant.

The changes in particle size distribution, as a result of the progressive milling, are shown in Fig. 6. After removal of the jelly by means of a solvent, microscopic examination showed the particles to be roughly spherical.

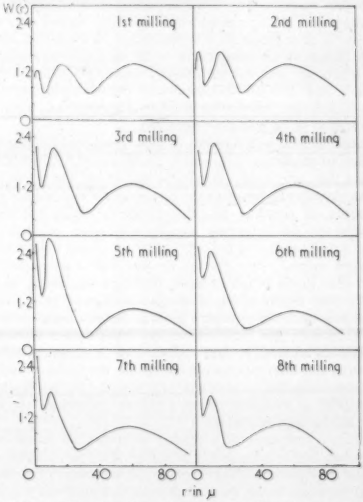

Fig. 6. Change of particle size distribution on milling

PLASTICITY, THIXOTROPY AND DILATANCY

The value of the shear hardening constant k depends upon the particle size distribution of the powder. This suggests that the shear hardening is due to changes in the geometry and structure of the powdered solid. This view is supported by qualitative observations. A cylinder of plastic, held between the fingers, becomes stiff when extended or compressed; its surface loses its wet, glistening appearance and becomes dry.* This effect is most noticeable in plastics with

* A similar phenomenon has been observed in clay by Macey.(9) He noticed that the effect became more marked as the frequency of cycles of compression and extension was increased. A series of slip planes were sometimes produced in the surface.

a high degree of shear hardening (e.g. $k = 0{\cdot}90$). For such plastics, one can feel the particles making contact with each other.

A mass of hard particles in contact possesses a property called dilatancy by Reynolds; it is "the property of undergoing a definite change in bulk consequent upon any definite change of shape or distortional strain." This dilation is a geometrical necessity for spheres in close packing, since the forces between the spheres are directed towards their centres. It can be shown, for example, that if a pile of identical spheres of unit density, arranged in tetrahedral packing, is sheared until the spheres are uniformly cubically packed, an overall increase of 40% in the bulk volume must result. In our system, we are dealing with a random arrangement of non-uniform rough spheres and the geometry is therefore much more difficult to discuss. Nevertheless, similar considerations should apply with modifications.

McMillen[10] has expressed the view that the thixotropy and plasticity of two-phase systems are inseparable twin phenomena, both of which have a common origin. The connexion between thixotropy and plasticity has also been stressed by Freundlich and Jones, who studied the plastic properties of paste-like suspensions. Their experiments led them to the opinion that plastic pastes were generally thixotropic and showed large sedimentation volumes and no dilatancy, whilst those pastes which exhibited a small sedimentation volume and dilatancy, but no thixotropy, were not plastic. Our systems have a small sedimentation volume, dilatancy, very little thixotropy, and yet are plastic. This contrasts with the conclusions of the authors mentioned.

The difference in the points of view rests mainly upon the concept of plasticity. Our materials are undoubtedly plastic, in that they are readily mouldable and retain their moulded shape; they do not, however, conform entirely with Wilson's[11] definition of plasticity as "that property which enables a material to be deformed continuously and permanently without rupture during the application of a force that exceeds the yield value." Our plastics do not have a characteristic yield value in the Bingham sense; the shear hardening, which results from deformation, gives a succession of yield values depending upon the previous history, and so, under a force which exceeds one yield value, the deformation does not proceed continuously, but approaches a limiting value. Houwink has discussed such systems and the systems studied by Roller[12] appear to be of a similar nature. In fact, Roller's "coefficient of renitence" bears a strong resemblance to our shear hardening constant k.

Wilson's definition is a verbal summary of Bingham's researches, and is adequate in defining "Bingham plasticity." We feel it would be wrong to refuse the description "plastic" to our materials merely because they are not Bingham plastics, but prefer to retain the word "plastic," and to distinguish their nature by the term "dilatant plasticity."

The essential difference between Bingham plastics and dilatant plastics lies in the two ranges of volume concentration of the solid in the liquid for the two types of systems. Bingham plasticity is found in the range of volume concentration less than about 50%. Vand has shown that suspensions of glass spheres in a glycerol–water–zinc iodide solution behave as Newtonian fluids up to a volume concentration of solid of 47%. Presumably in this system there are no interparticulate forces present, and the concentration is low enough for the particles to behave more or less independently. At such concentrations, in the presence of attractive forces between the particles, the latter would form a structure and the system would be thixotropic. The minimum shear stress necessary to rupture the structure would constitute a definite yield value of the Bingham type. When the attractive forces are sufficiently powerful, such structure and Bingham plasticity would appear at very low concentrations of the solid. If we consider a system of about 45% solid concentration without forces, the rate of strain-shearing stress graph would be linear and Newtonian. If now the magnitude of the forces are imagined to be progressively increased, the graph would deviate more and more from the Newtonian line, becoming concave towards the axis of the rate of strain, until the graph approached the Bingham limiting type. We thus see that Bingham plasticity can be considered as derived by continuous modification from a Newtonian liquid.

On the other hand, with a solid concentration of 75% upwards, dilatant plastics would seem to be related more to the properties of the dry solid. We may here imagine their properties as being derived by a continuous process whereby the interstitial fluid is progressively added to the solid powder, and the properties of the powder are modified. The arches and columns of Terzaghi[13] and the loosely and tightly packed regions of Reynolds and Brown[14] are modified with increasing amounts of fluid. When sufficient fluid has been added, the particles become independent and these structures no longer exist; the system will then have a volume concentration of solid of about 50% and will display "inverted plasticity" and "dilatant non-plastic properties" as discussed in the last paragraph. The structure of the powder will be possible even in the absence of forces between the particles if the concentration of solid is high enough, so that dilatant plasticity is possible when there are no such forces present.

The range of solid concentration, over which dilatant systems are plastic, will depend also upon the viscosity of the interstitial fluid. It should be sufficiently viscous to oppose the rapid relaxation of the shear hardening contacts, so that the number of such contacts will depend upon the amount of shear. If the liquid is mobile, however, the contacts relax too quickly and the behaviour becomes similar to those dilatant systems studied by Freundlich and Röder where the number of contacts depends upon the rate of shear and not upon the amount of shear.

ACKNOWLEDGEMENTS

We wish to thank Mr. D. McKenzie and Dr. J. W. Rowe of the Ministry of Supply for the considerable interest they have taken in the work, and for the advice they have given us on the solution of many problems.

This paper is published by permission of the Chief Scientist, Ministry of Supply.

REFERENCES

(1) Vand. *J. Phys. Coll. Chem.*, **52**, p. 309 (1948).
(2) Freundlich and Röder. *Trans Faraday Soc.*, **34**, p. 308 (1938).
(3) Williamson and Heckert. *Industr. Engng Chem.*, **23**, p. 667 (1931).
(4) Pryce-Jones. *J. Oil. Col. Chem. Ass.*, **19**, p. 295 (1936).
(5) Bingham. *Fluidity and Plasticity* (New York: McGraw Hill Book Co. Inc., 1922).
(6) Houwink. *Second Report on Viscosity and Plasticity*, pp. 189 and 191 (Amsterdam: Noord-Hollandsche U.M., 1938).
(7) Reynolds. *Phil. Mag.*, **20**, p. 469 (1885).
(8) Freundlich and Jones. *J. Phys. Chem.*, **40**, p. 1217 (1936).
(9) Macey. *J. Sci. Instrum.*, **19**, p. 159 (1941); *Nature, Lond.*, **147**, p. 146 (1941).
(10) McMillen. *J. Rheology*, **3**, p. 179 (1932).
(11) Wilson. *Ceramics–Clay Technology*, p. 55 (New York: McGraw Hill Book Co. Inc., 1927).
(12) Roller. *J. Phys. Chem.*, **43**, p. 457 (1939).
(13) Terzaghi. *J. Rheology*, **2**, p. 253 (1931).
(14) Brown. *British Coal Utilisation Research Association Bulletin*, **9**, p. 113 (1945).

The solution of temperature distribution problems by computation and electrical analogy

By J. C. WILLIAMS, B.Sc., A.Inst.P., James A. Jobling and Co. Ltd., Wear Glass Works, Sunderland

[*Paper first received* 19 *November*, 1951, *and in final form* 5 *March*, 1952]

The computational method of Dusinberre[1] and the use of an electrical analogy for the solution of problems involving temperature distribution in solid bodies with various boundary problems are discussed briefly. The two methods are used to solve a simple problem, and the results compared with an analytical solution. The computation solution can be made as accurate as required by lengthening the calculation, an accuracy of 1% being easily obtained. The electrical solution, using simple and inexpensive apparatus, agrees with the analytical solution within 2%; this accuracy is obtained when the temperatures at the boundaries of the solid are either uniform or sinusoidal, an error of 4% being found for other boundary conditions. Change of thermal properties with temperature is neglected. The application of both methods to the solution of industrial problems involving conduction in one, two or three dimensions, with heat losses from surfaces, is discussed.

For the determination of temperature distribution in solid bodies with time-varying boundary conditions the methods available include the computational method of Dusinberre[1] and the use of an electrical analogy. The author has found both techniques useful in the investigation of thermal problems arising from glass pressing operations.

LIST OF SYMBOLS USED

Thermal

a = thermal diffusivity.
θ = temperature.
T = absolute temperature.
k = thermal conductivity.
c = specific heat.
ρ = density.
V = volume.
x = distance.
A = area.
t = time.

Electrical

R = resistance.
C = capacity.
τ = time.

Scaling factors

$\beta = C/V$.
$\gamma = R/\frac{x}{A}$
$\epsilon = \tau/t$.

COMPUTATIONAL METHOD

In the computation method the solid is divided into "lumps" of a convenient size. It is then assumed (i) that in a short interval of time the heat flow into any lump is determined only by the conditions in adjacent lumps, and (ii) that the temperature conditions at the beginning of the time interval can be taken as constant throughout the interval. The method is best explained by a simple example, which will be referred to as problem (1). Linear heat flow takes place through a plate 5 cm thick, the thermal diffusivity of the material of the plate being 0·09 cm/sec. One face of the plate is kept at a constant temperature of 100° C, and the temperature of the other face is given by

$$100[1 + \sin(2\pi/132)t] \qquad (1)$$

Consider in the plate an element of width 1·25 cm, as shown in Fig. 1, the thickness of the element normal to the plane of the paper being 1 cm. The element is divided into lumps by the horizontal lines, with five reference points numbered 1 to 5. Points 2, 3 and 4 lie at the centre of lumps of heat capacity $1 \cdot 56c\rho$. For flow between any pair of adjacent points the conductance is equal to the thermal conductivity.

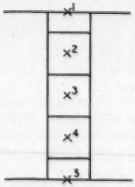

Fig. 1. Division into "lumps" in problem (1)

It is now assumed that a small time interval can be chosen so that assumptions (i) and (ii) can be made. If the time interval chosen is Δt, then equating the heat flow into lump 2 with the increase in heat content leads to:

$$\theta_2' = [a\Delta t/1 \cdot 56][\theta_1 + \theta_3] + \theta_2[1 - (2a\Delta t/1 \cdot 56)] \qquad (2)$$

θ_1, θ_2, and θ_3 are the temperatures at points 1, 2 and 3 at the beginning of a time interval, and θ_2' is the temperature at point 2 at the end of the interval. In order that θ_2 may have a positive effect on the value of θ_2' it is necessary that $1 - (2a\Delta t/1 \cdot 56) > 0$, i.e. $\Delta t < 8 \cdot 65$ sec. An interval of 5·77 sec is chosen as it is seen that this gives coefficients in the governing equation which permit the calculation to be made mentally. Equation (2) can now be written:

$$\theta_2' = \tfrac{1}{4}(\theta_1 + \theta_2 + \theta_3) \qquad (3)$$

Similar equations apply for θ_3' and θ_4'.

We can now proceed to the calculation of temperatures. A table is drawn up as in Table 1. The temperatures at points 1 and 5 are known, and if the body is initially at temperature 100° C this value is entered in the table for all points at time zero.

Table 1. *The computational table*

Time intervals	*Reference points* 1	2	3	4	5
0	100	100	100	100	100
1	127	100	100	100	100
2	152	109	100	100	100
3	173	120	103	100	100
etc.					

The temperatures at points 2, 3 and 4 after each time interval are found by successive applications of equation (3). The first five or six steps will not give very reliable values, but for later time intervals the temperature at each point will be traced out. If only the steady state is of interest the length of the computation can be reduced by guessing the initial temperature at points 2, 3 and 4. As in relaxation calculations the correct answer will be obtained whatever the initial guess, but the better the guess the less is the amount of computation to be done.

It is evident that greater accuracy can be obtained by using a smaller value of Δt. A technique similar to that of "advance to a finer mesh" in relaxation calculations[2] can be adopted. Problem (1) was recalculated using $\Delta t = 2 \cdot 88$ sec, the result of the previous calculation being used as a starting point; the results, which are given in Table 2, show that a considerable improvement in accuracy was obtained.

OTHER BOUNDARY CONDITIONS

More complicated forms of the boundary temperatures can be handled just as easily; it is merely necessary to write the

known temperatures in the table, and they are incorporated in the calculations. Thus a set of experimental temperatures of non-mathematical form can be used. If the rate of heat loss from the surface at point 5 to an atmosphere at temperature θ_0 is h cal/cm² sec °C, then for point 5 we have

$$\theta'_5 = (2a\Delta t/1{\cdot}56)\theta_4 + (2h\Delta t/1{\cdot}56c\rho)\theta_0 + \theta_5\{1 - (2\Delta t/1{\cdot}56)[(h/c\rho) + a]\}$$

If the value of h is known, then the coefficients can be evaluated to give the governing equation for θ'_5. In a similar manner radiation heat losses can be dealt with; if, in the above example, the heat loss from point 5 is equal to $r(T_5^4 - T_0^4)$, where r is a constant, the governing equation for point 5 is:

$$T'_5 = (2a\Delta t/1{\cdot}56)T_4 + (2r\Delta t/1{\cdot}56c\rho)T_0^4 + T_5[1 - (2a\Delta t/1{\cdot}56) - (2r\Delta t T_5^3/1{\cdot}56c\rho)]$$

If the value of r is estimated the coefficients in this equation can be evaluated, but the presence of T_5^3 in the final term lengthens the calculation.

In problem (1) only linear flow was considered. The method is not limited to such problems, for any body can be divided into suitable lumps, and the calculation proceeds as before.

THE CAPACITANCE-RESISTANCE NETWORK

The use of the capacitance-resistance network to solve transient heat flow problems is well known; the method has been developed and used particularly by Paschkis[3] in America. It seemed that a simple and inexpensive model might give solutions of temperature distribution problems sufficiently accurate for industrial purposes, when temperature variation of thermal properties can be neglected. To investigate the usefulness of a simple model, a network has been constructed using twenty-five capacitors (0·0263 μF $\pm$ 1%), each enclosed in a brass screen, the whole being contained in a wax-filled wooden box. Adjustable resistors may be connected between the capacitors to complete the network.

Solution of problem (1) *by capacitance-resistance network.* Coyle[4] has worked out the condition for an analogy between heat flow and air flow. The reasoning for an electrical analogy is exactly the same, and the condition for the analogy to hold is

$$\gamma = \epsilon/\beta a \qquad (4)$$

where a is the thermal diffusivity of the material and β, γ and ϵ are scaling factors defined earlier in the list of symbols. Differences of potential in the electrical model are then proportional to differences of temperature in the heat transfer case. Using this scaling condition problem (1) was solved by the electrical analogy. The analogous circuit is shown in Fig. 2, the resistances being $10^5\,\Omega$. The scaling condition is satisfied by a suitable choice of frequency and in this case the boundary condition is simulated by applying to point 1 in the network an a.c. of frequency 50 c/s.

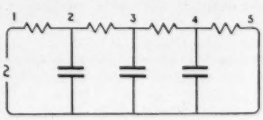

Fig. 2. Analogous circuit for problem (1)

Generally, the method used to investigate the change in amplitude, phase and waveform was to connect the plates of a cathode-ray oscilloscope directly across each condenser in turn, and photograph the wave forms. When the applied wave form is sinusoidal a more accurate measurement of amplitudes is obtained by varying the input voltage by means of an autotransformer and adjusting the input voltage to give the same amplitude at each of the condensers; the input voltages then give an inverse measure of the amplitudes. The results given in Table 2 were obtained by this method.

Results of problem (1). Carslaw and Jaeger[5] give an analytical solution for problem (1). The results obtained by analysis, computation and capacitance-resistance network are summarized in Table 2.

Table 2. *Results of problem* (1), *giving amplitudes at the various reference points*

Depth cm	Analysis	Computation $\Delta t = 5{\cdot}77$ sec	Computation $\Delta t = 2{\cdot}88$ sec	CR network
0	100	100	100	100
1·25	53·5	55	53·2	53·5
2·5	29·5	31·6	29·6	30·2
3·75	14·0	15·5	14·1	14·1
5·0	0	0	0	0

From these results it will be seen that in the computation solution with $\Delta t = 5{\cdot}77$ sec the error at depth 3·75 cm is 11%; with $\Delta t = 2{\cdot}88$ sec all the calculated results are within 1% of the analytical solution. The results from the capacitance-resistance network agree with the theoretical solution within 2%. In the treatment of this problem five reference points were used because Paschkis[6] has shown experimentally that this gives accurate results. A solution was obtained from the capacitance-resistance network using seven reference points, the resistances being adjusted accordingly. The solution obtained was the same as that given with five reference points, thus verifying Paschkis' conclusion.

A further problem [*problem* (2)]. Problem (1) was modified so that the applied boundary condition at point 1 was a square wave, the frequency being unaltered. A solution of this new problem (problem 2) was obtained by computation using $\Delta t = 5{\cdot}77$ sec, and the result used as a starting point for a calculation with $\Delta t = 2{\cdot}88$ sec. The solution is shown graphically in Fig. 3(*a*). The same problem was solved by the capacitance-resistance network and tracings of the photographs of the cathode-ray oscilloscope screen are shown in Fig. 3(*b*). Values of the peak to peak amplitudes given by the two methods are compared in Table 3.

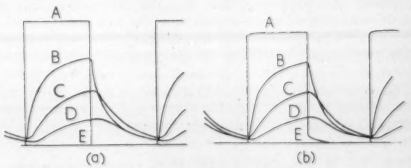

Fig. 3. Solutions to problem (2)

(*a*) By computation, using $\Delta t = 2{\cdot}88$ sec; (*b*) by capacitance-resistance network. Depth below surface: $A = 0$, $B = 1{\cdot}25$ cm, $C = 2{\cdot}5$ cm, $D = 3{\cdot}75$ cm, $E = 5{\cdot}0$ cm.

Table 3. *Amplitudes in problem* (2)

Depth cm	Computation $\Delta t = 2{\cdot}88$ sec	CR network	% difference
0	100	100	—
1·25	66·5	68	2
2·5	38·8	40·5	4
3·75	18·5	19·1	3
5·0	0	0	—

FURTHER APPLICATIONS

Some means by which the computational method can be used for more difficult problems have already been noted. In the same way the scope of the electrical method can be extended. The assembly of twenty-five condensers allows the solution of two-dimensional problems, the condensers being connected in five banks of five; three-dimensional problems in which there is axial symmetry can be solved by regarding them as two-dimensional. Convective heat loss from a surface is simulated by allowing a current to leak to earth through a suitable resistance. Radiation heat losses can be dealt with by estimating the surface temperature at the surface and using a suitable leakage resistance; a method of successive approximation may be necessary. The computational method gives more accurate results, but for complicated problems the length of the calculation may be considerable; in such a case the capacitance-resistance network may be used; the same accuracy is not attained, but the amount of work is reduced. The electrical network may be regarded as a type of calculating machine for performing the computation, and is particularly suitable for carrying out a series of investigations, involving only slight changes in the network.

ACKNOWLEDGEMENTS

This paper is published by permission of the directors of James A. Jobling and Co. Ltd., in whose laboratories the work described has been performed. The writer also wishes to thank Mr. P. L. Kirby for his advice, and Mr. A. B. Rogers for assistance in the experimental work and in computation.

REFERENCES

(1) DUSINBERRE, G. M. *Numerical Analysis of Heat Flow* (McGraw-Hill Book Company, 1949).
(2) SOUTHWELL, R. V. *Relaxation Methods in Theoretical Physics* (Oxford: University Press, 1946).
(3) PASCHKIS, V., and BAKER, H. D. *Trans. Amer. Soc. Mech. Engrs*, **64**, p. 105 (1942).
(4) COYLE, M. B. *Brit. J. Appl. Phys.*, **2**, p. 12 (1951).
(5) CARSLAW, R. S., and JAEGER, J. C. *Conduction of Heat in Solids* (Oxford: University Press, 1947).
(6) PASCHKIS, V., and HEISLER, M. P. *Elect. Engng, N.Y.*, **63**, p. 165 (1944).

Permanent magnets for spectrographs and nuclear physical research

By D. HADFIELD,* M.Sc.(Eng.), A.M.I.E.E., A.I.M., and D. L. MAWSON, Grad.Inst.P., Magnetic Research Laboratory, W. Jessop and Sons Ltd., Sheffield

[*Paper first received* 11 *July, and in final form* 22 *November*, 1951]

Composite permanent magnets, embodying the latest anisotropic alloys, are being used increasingly in equipment for research in many branches of applied physics. Among the advantages are freedom from power supplies, and also constancy of field, when compared with the electromagnet. Flexibility is achieved in the electro-permanent magnet by either reinforcing the permanent magnet field or artificially aging to a reduced value of field strength. Particular applications are for cosmic-ray traps, nuclear magnetic resonance apparatus, mass spectrometers, and β-ray spectrographs; the design of a magnet for the latter purpose being discussed in detail.

1. INTRODUCTION

In the past, when high and constant magnetic fields in large air gaps were required, bulky d.c. electro-magnets, with elaborate voltage stabilizing devices and water-cooled coils, were necessary. To-day, however, owing to the progress made in permanent magnet materials,(1) field strengths of the same order of magnitude and considerably greater constancy may be obtained more efficiently with compact permanent magnets.

The development of the anisotropic nickel-aluminium-copper-cobalt-iron alloys with higher stored magnetic energies has permitted the use of permanent magnets made from these materials for β-ray and mass spectrographs and other apparatus for research in nuclear physics. For these instruments, the magnetic field must be of a specified strength and possess a uniformity constant to within a few parts in ten thousand. Generally, the uniform magnetic field has to deflect a high-velocity stream of electrons into a certain orbit, which is defined by the value of $H\rho$, the product of the field strength and the radius of curvature of the electron path.

An electro-permanent magnet has the advantage that its field can be adjusted to a desired value by means of the auxiliary electro-magnetic field, which can either reinforce or oppose the existing permanent magnetic field. Variations in supply voltage introduce little effect, since the strength of the auxiliary field is only a fraction of that of the permanent magnet field. If, however, absolute constancy is desired, these fluctuations cannot be neglected, and accordingly, auxiliary fields are not used.

* Now Chief of Research and Development, Swift Levick and Sons Ltd., Sheffield.

2. EARLY DESIGNS

A permanent magnet system was designed and constructed by Cockroft, Ellis and Kershaw(2) in 1932 for a Cavendish Laboratory β-ray spectrograph. The pole-piece magnet material used was 35% cobalt steel with soft-iron yoke and

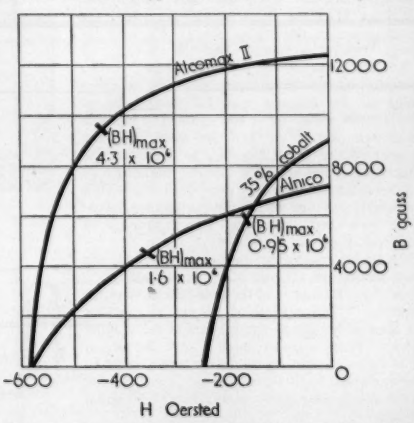

Fig. 1. Demagnetization curves of Alcomax II, Alnico and 35% cobalt steel

pole tips, designed to give a field strength of 2 000 oersted in a gap length of 5·5 cm and of area 17 × 29 cm, although a uniform field was necessary only over a gap area of 12 × 24 cm. The total weight of the finished assembly was in the region of 2 400 lb and the $H\rho$ factor desired was approximately 20 000 oersted-cm.

At a later date, a further β-ray spectrograph magnet was designed and constructed at the Randal Morgan Laboratory of Physics, University of Pennsylvania, by Plesset, Harnwell and Seidl,[3] giving a field strength of 2 800 oersted in a gap of 40·6 × 20·3 × 4 cm long. They considered that for fields below 10 000 oersted, a permanent magnet would be cheaper than an electro-magnet. Isotropic Alnico alloy (the demagnetization curve of which is shown in Fig. 1, together with those of 35% cobalt steel and Alcomax II) was used for the permanent magnet poles, comprising 64 blocks each 2 × 2 × 6 in, the total weight being 450 lb. A double-yoke design was adopted, the yoke and pole tips of high permeability iron weighing 2 000 lb. Thus, the total weight was approximately 2 450 lb. The non-uniformity of the field was less than 0·2% to within 2 cm from the edge of the pole-pieces.

3. RECENT DESIGNS

Several designs of diverse character have been developed and constructed by the authors to suit particular applications and requirements. Some will be discussed in detail and others referred to briefly.

Experimental prototype. A β-ray spectrograph magnet was required having an adjustable field of the same order of field strength in the same gap size as the one used by Cockroft, Ellis and Kershaw, i.e. to give a value of Hp equal to 20 000 oersted-cm. A reduction in size and weight was to be achieved by the use of the higher energies available in anisotropic Alcomax alloy. The magnetic circuit adopted by Cockroft, Ellis and Kershaw was used, except that Alcomax alloy replaced the 35% cobalt steel in the pole-pieces. Coils were placed on both pole-pieces and were used in initial magnetization and for the variation of the gap field strength.

Permanent magnet blocks. The permanent magnet material employed was anisotropic Alcomax II alloy (this work preceded the development of the higher energy Alcomax III alloy), having a mean value of $(BH)_{max}$ of $4{\cdot}0 \times 10^6$ gauss-oersted for large masses. From optimum design considerations[4] the working point of the magnet material should be at $B = 10\,000$ gauss, $H = 400$ oersted. Using a reluctance factor of 1·1 (to allow for the magnetomotive force necessary to overcome the reluctance of the magnetic circuit), the length of magnet material necessary was 30·2 cm, with a cross-sectional area of 200 cm² (a leakage factor of 2 was used, following the experience of Cockroft, Ellis and Kershaw).

To ensure maximum uniformity of field, the cross-section of magnet alloy was made 11 × 19 cm, i.e. in the ratio of the pole-face dimensions required. The total area of 209 cm² allowed for the area of the cored fixing holes in the magnet blocks. Since a single magnet of cross-section 11 × 19 cm cannot be efficiently heat treated to give optimum magnetic properties, it was decided to sub-divide the magnet material into four equal blocks.

Pole tips. The specified dimensions of the gap and of the permanent magnet poles determined the shape of the soft-iron pole tips. The pole tips were thus tapered down from 17 × 29 cm to 11 × 19 cm with a taper of 37°. The tips were drilled and tapped to take the non-magnetic stainless-steel bolts which clamped the blocks to the yoke.

Soft-iron yoke. As other components governed the width and distance between the inside of the limbs of the soft-iron yoke, it remained to fix the cross-sectional area of soft-iron necessary to carry the flux emanating from the permanent magnet blocks. In order to under-saturate the iron slightly, the section had to be at least five-eighths of that of the Alcomax II pole-pieces;[4] as the magnet poles and yoke were approximately equal in width, the thickness of the latter had to be 7 cm.

Coils. Two coils, one on each pole-piece, were used for initial magnetization, for altering the strength of the permanent magnet field and for reinforcing this field when required. The necessary A-turns (NI) per coil were calculated in terms of magnetizing force, H (oersted), and coil length l cm from $H = 4\pi NI/10l$. To ensure saturation of the blocks during initial magnetization, a minimum magnetizing force of 3 000 oersted was used (five times the coercive force of Alcomax II), equivalent to 36 000 A-turns per coil. As this value was required only for momentarily magnetizing and demagnetizing, it was adjudged that the wire could be overloaded at least five times and hence 1 440 turns of cotton-covered 16 s.w.g. wire were used for each coil.

Assembly. The method adopted for clamping the permanent magnet blocks to the yoke by non-magnetic stainless-steel bolts screwed into the pole tips is indicated in Fig. 2. Brass supports were made for the pole tips to relieve bending strain on the fixing bolts.

Performance of magnet. The approximate weights of the finished components were:

Alcomax II blocks	100 lb
Armco iron yoke	270 lb
Armco iron pole tips	60 lb
Coils	100 lb
	530 lb

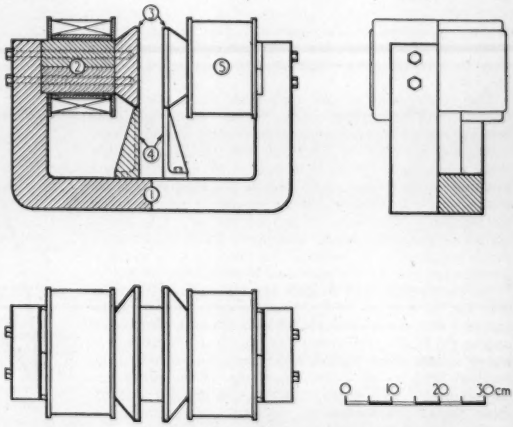

Fig. 2. Assembly drawing of magnet for β-ray spectrograph
1, soft-iron yoke; 2, Alcomax blocks; 3, soft-iron pole tips; 4, brass supports; 5, coils.

After initial magnetization, the mean permanent magnet field strength was 1 600 oersted. (This, the average of the values in six different positions over the pole face area of the field strength, was measured by means of a rotary flux meter manufactured by the General Electric Co. Ltd.) It was found that the maximum non-uniformity within an area of 24 × 12 cm was 2·5%, and that the mean non-uniformity within this area was 2·2%. A reinforcing electro-magnetic field was applied by passing suitable currents through the magnetizing coils. The gap field strengths in terms of the various applied fields are shown in Fig. 3. By reversing the current, it was possible to reduce the field strength to zero.

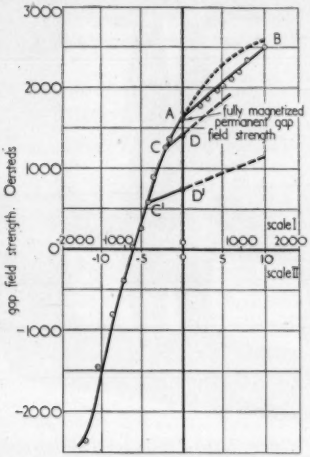

Fig. 3. Effect on gap field strength of applying and removing superimposed reinforcing and demagnetizing fields

Scale I, applied magnetic field: H (oersted).
Scale II, current (per coil): A.

It will be seen from the results shown plotted in Fig. 3 that the curve through the plotted points resembles the part of a hysteresis loop in the second and third quadrants, i.e. the decrease in gap field strength from the fully magnetized value down to negative values represents a portion of the hysteresis loop of a magnet having a series air-gap. The part of the curve *AB* representing the increase in resultant field strength due to the reinforcing magnetic field is a recoil line, as are also the straight lines (e.g. *CD* or *C'D'*) representing the rise in gap field strength (from *C* to *D* or *C'* to *D'* respectively) when a small demagnetizing field is removed. It is possible, therefore, to determine the value of the demagnetizing field, and thus the current to be applied, in order to demagnetize the Alcomax II blocks to give a certain permanent magnet field strength less than the fully magnetized gap field strength. For a field strength above that given by the permanent magnet blocks alone the graph shows the extent of the reinforcing field which must be applied to give the required value. As the maximum continuous safe current which may be used is approximately 7 A, the maximum resultant field obtainable is of the order of 2 200 oersted, producing a value of $H\rho$ of 26 400 oersted-cm.

Thus, it can be seen that by the use of anisotropic Alcomax II the total weight of the magnet assembly was reduced from 2 400 lb (the weight of the magnet by Cockroft, Ellis and Kershaw) to 530 lb, without materially affecting the performance. The satisfactory design and construction of this magnet made it possible to undertake similar ones, brief descriptions of which will be given.

Mass spectrometer magnet. A mass spectrometer magnet constructed for the Royal Institution,[5] shown in Fig. 4, is identical with the one described in detail above, except that special semi-circular truncated pole tips were fitted in place of the flat rectangular type. These pole-pieces were hollowed

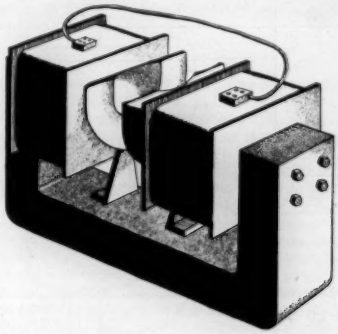

Fig. 4. Mass spectrometer electro-permanent magnet

out in the centre in the form of a saucer and a concave semi-circular portion left on the rim of mean radius 12 cm (which was the desired radius of curvature for the electron particles). The semi-circular portion of the pole tips was made slightly concave to achieve a uniform field strength. The gap length at this outer rim was 5·5 cm as before, but the modifications in pole-tip shape gave an increase in field strength from 1 600 oersted to approximately 1 780 oersted, uniform to within ± 2%.

β-ray spectrograph magnet. Another magnet for a β-ray spectrograph, closely resembling that already described, required a gap volume of 6·5 × 26 × 39 cm, and a field strength of 1 200 oersted. In view of this increase in gap volume it was necessary to increase the cross-sectional area of permanent magnet material by roughly one-third. The performance of the finished magnet closely agreed with the field strength aimed at, the observed permanent magnet field at the centre of the gap being 1 220 oersted, with variations not exceeding 2% over the whole gap area. The maximum field strength available with electro-magnetic reinforcement was 2 600 oersted, and the gap field strength and $H\rho$ factor could thus be varied over a wide range.

Cosmic-ray trap magnet. The application depends on the deflexion of charged particles, such as mesons, by a magnetic field.[6] The tracks of the particles are recorded on photographic plates, which are inserted in the air gap of a magnet and subjected at high altitudes to bombardment by cosmic rays. The permanent magnet assembly shown in Fig. 5 was designed and constructed for this purpose for Professor C. F. Powell at the University of Bristol, and gives a very high

field strength of about 15 000 oersted in a gap 0·6 cm long having an area of 7·5 × 7·5 cm². In this case (due to the difficulties of successfully heat treating the very large masses of Alcomax required) it was necessary to depart from the normal composite soft-iron yoke "C" type of circuit. A double "C" design was therefore adopted (the two yokes being magnetically "in parallel"), using Alcomax II permanent magnet alloy throughout, with pole tips of high saturation intensity cobalt-iron alloy, tapered to give the required gap area. The total height of the assembly was 60 cm and the total weight 3¼ cwt. The field strength obtained was over 15 000 oersted.

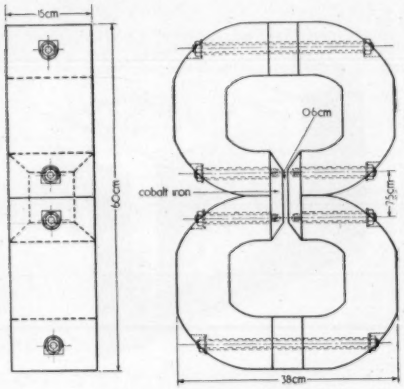

Fig. 5. Cosmic-ray trap magnet

Nuclear magnetic resonance magnet. The largest electro-permanent magnet in Great Britain, weighing about 1¼ t, and shown in Fig. 6, has been developed and constructed recently by William Jessop and Sons Ltd. for nuclear magnetic resonance research work at St. Andrews University. The design followed that of Plesset, Harnwell and Seidl, and in order to achieve the extremely high uniformity of field necessary (variations of less than 0·02%), pole tips designed according to a paper by Rose[7] have been incorporated.

Alcomax III permanent magnet poles (composed of 90° circular segments to facilitate heat treatment) were encompassed by the magnetizing and adjusting coils, and special Armco iron recessed pole-pieces abutted on to the ends of the Alcomax III blocks and clamped them to the iron yoke. The weight of the permanent magnet alloy was about 800 lb, producing a fully magnetized gap field strength of 5 500 oersted in a gap of 5·5 cm long × 20 cm diameter. Field uniformity obtained over a central volume of 1 cm cube was better than 1 part in 5 500. The overall efficiency factor on which this design was based was just under 50%, but this was probably a little too high, a more realistic value being of the order of 40%.

4. CONCLUSIONS

Some advantages of the permanent and electro-permanent magnet over the electro-magnet have been discussed and successfully demonstrated by practical applications in the fields of mass and β-ray spectrography and other branches of particle research.

The widespread application of permanent magnets in these fields of research has been made possible by the development of new alloys of high magnetic energy. Formerly, an electro-magnet was less bulky than a permanent magnet producing the same gap energy, whereas now the permanent magnet may be smaller and cheaper, and in addition independent of fluctuations in power supplies. In view of this it is to be

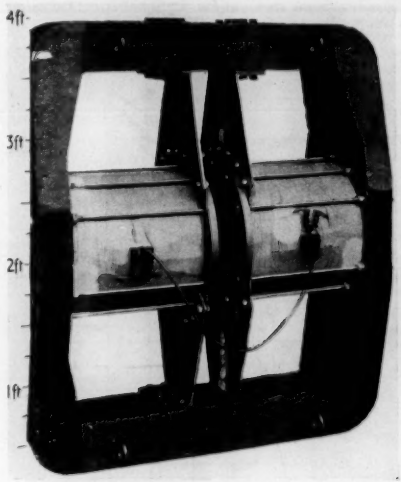

Fig. 6. Nuclear magnetic resonance electro-permanent magnet

expected that research workers will, in the future, look increasingly towards the use of permanent magnets as an obvious solution for providing constant strong magnetic fields in large air-gaps.

ACKNOWLEDGEMENTS

The authors wish to thank Mr. D. A. Oliver, Director of Research, the B.S.A. Group of Companies, for his help and encouragement; and Mr. B. Sugarman for valuable criticism in the preparation of this paper.

REFERENCES

(1) Oliver, D. A., and Hadfield, D. *J. Instn Elect. Engrs*, **95**, Pt I, p. 531 (1948).
(2) Cockroft, J. D., Ellis, D. C., and Kershaw, H. *Proc. Roy. Soc. A.*, **135**, p. 628 (1932).
(3) Plesset, E. H., Harnwell, G. P., and Seidl, F. G. P. *Rev. Sci. Instrum.*, **13**, p. 351 (1942).
(4) Hadfield, D. *Elect. Times*, **3**, p. 323 (1947).
(5) Robertson, A. J. B. *Proc. Roy. Soc.*, **199**, p. 394 (1949).
(6) Powell, C. F., and Rosenblum, S. *Nature, Lond.*, **161**, p. 473 (1948).
(7) Rose, M. E. *Phys. Rev.*, **53**, p. 715 (1938).

Correspondence

Aerial prospecting and the absorption of γ-radiation

There is evidence that the value of the absorption coefficient of radium γ-radiation in air quoted in Peirson and Franklin's paper, Aerial prospecting for radioactive minerals, published in the October issue, is erroneous. Their value, $\mu_a = 10^{-4}\,cm^{-1}$, quoted from Heitler's book,(1) refers properly only to "narrow-beam" conditions where scattered radiation is prevented from reaching the detector. For the conditions which hold in aerial prospecting, the coefficient would be expected to be much smaller due to the inclusion of the scattered radiation and this has been verified by direct experiment. Using sodium iodide scintillation crystals and radium sources, observations in the open air have shown that μ_a varies somewhat with distance from the source, and gave an average value over the interval from ground level to 500 ft altitude of $\mu_a = 3{\cdot}5 \times 10^{-5}\,cm^{-1}$ measured at 15° C. This much lower value markedly affects the feasibility of aerial prospecting. For instance, in Fig. 10 of the paper, the γ-radiation intensity from a uniform concentration of radioactive matter in the ground is shown to be "less than 1/10th of the ground level value" at 500 ft; the correct fraction is about 1/3rd. Further, at 500 ft the fraction of radiation from a localized deposit on the ground absorbed by the air is only 40%, rather than 80%, as would be given by the larger value of μ_a.

Another criticism may be offered concerning the method adopted by Peirson and Franklin of evaluating results on the basis of a "signal/noise" ratio. This would be satisfactory if the "noise" were of instrumental or cosmic-ray origin and therefore substantially constant. With a good detector, however, such noise has been found to be insignificant compared with the "noise" fluctuations arising from the varying activity of the terrain over which the flight takes place. Our experience is that when flying over open water the background signal is small and practically constant, but when flying over land the background signal is large and fluctuating. The size of the irregularities varies with the type of terrain. Evidently the fluctuations of the background over land are due chiefly to real changes in the radioactivity of the terrain. An equal signal appearing superimposed on these backgrounds, if evaluated by the "signal/noise" method, would fail in some cases to indicate a useful deposit over relatively active terrain. Consistent results for a figure of merit for the detector are unlikely to be obtained from the "signal/noise" ratio observed by flying over a source placed on land since it depends on the local radioactivity of the land. In our experience the source should be located, floating or on ice, at the middle of a large lake, in as nearly standard condition as it is possible to obtain and, instead of a "signal/noise" ratio, the ratio between the signal and this background should be used as the figure of merit since it takes into account factors such as the freedom of the aircraft from radioactivity.

Aerial prospecting has been carried out successfully on an experimental basis in the North-West Territories of Canada with Geiger counters during Summer 1949 and with scintillation counters since Summer 1950. Even with a sensitive detector the chief difficulty has proved to be the problem of distinguishing, at the operational height of 500 ft, between the signals from localized deposits which are probably valuable and those from extensive areas of very low grade rock.

This work was initiated by the Eldorado Mining and Refining (1944) Limited and carried out by the National Research Council (N.R.C.) Atomic Energy Project, Chalk River, and the N.R.C. Flight Research Section, Arnprior, with co-ordination by the Geological Survey of Canada, Dept. of Mines and Technical Surveys, Ottawa.

National Research Council of Canada, Atomic Energy Project, Chalk River, Ontario. J. F. STELJES

REFERENCE

(1) HEITLER, W. *The Quantum Theory of Radiation* (London: Oxford University Press, 1944).

The value adopted in our paper for the absorption coefficient in air of the γ-radiation from the uranium series ($\mu_a = 10^{-4}\,cm^{-1}$) is supported by observation of the variation with altitude of the background counting rate due to the gamma activity of the earth's surface. The variation was observed in flight by aircraft and also by stationary measurements in several localities from a balloon or radio mast. All measurements were conducted with Geiger–Müller counting tubes similar to those described in our paper. The variation of this background from ground level to 500 ft is consistent with a mean value of $\mu_a = 10^{-4}\,cm^{-1}$; from ground level to 100 ft the effective absorption coefficient appears to be somewhat greater than this value. As this evidence was not considered to be conclusive, the uncertainty in the estimated figure was emphasized in our paper. The feasibility of aerial prospecting is unaffected by this uncertainty since over the normal range of operational altitudes our reported performance figures rely upon experimental measurement.

In the calculation of γ-ray flux in our paper it was necessary, to avoid great complication, to assume a simple exponential absorption in air equivalent to the total effect of complex processes. Thus the factor μ_a represents the effective absorption coefficient for γ-radiation having the diverse energies characteristic of a uranium or radium source. It is reasonable to assume that μ_a will decrease with increasing distance from the source for several mean free paths (1 m.f.p. $\simeq$ 300 ft) owing to the rapid absorption of the softer components. The distribution of energy in the beam is also affected by the incidence of scattered quanta, degraded in energy, upon the detector under "wide-beam" conditions, and will vary with distance from the source.

The value of $\mu_a = 3{\cdot}5 \times 10^{-5}\,cm^{-1}$ reported by Steljes relates to a direct measurement of the coefficient using a scintillation counter. It is difficult to reconcile this figure with our observations of the variation of background with altitude reported above. It is possible that the discrepancy between the two values for μ_a may be partly accounted for by the different efficiency *versus* γ-energy characteristics of the two detectors.

No direct evidence is available from other work. Conversion of results of absorption measurements in water,(1) using γ-radiation of mean energy about 1·2 MeV from cobalt 60, to the case of air gives a coefficient for this energy of $5{\cdot}8 \times 10^{-5}\,cm^{-1}$, which applies for distances greater than 3 m.f.p. In the aerial prospecting case we are concerned with distances < 2 m.f.p. over which range this and similar experiments using comparatively massive media are in-

applicable, since the dimensions of the detector become comparable with the source-detector distance thereby modifying the scattering geometry. A theoretical assessment of the effect of multiple scattering has been made by Hirschfelder and Adams[2] from whose calculations may be derived an effective value for the coefficient, for an energy of 1 MeV and over the first few m.f.p., of $4 \cdot 9 \times 10^{-5}$ cm^{-1}. These results must be interpreted in terms of the energy spectrum (mean energy $\simeq 0 \cdot 7$ MeV) of the γ-radiation from the uranium series.

The method of evaluating experimental flight results based on our performance factor, i.e. on a "signal/noise" ratio, is justified by the necessity to measure not only the sensitivity but also the detecting power of the apparatus. Therefore the performance factors are measured by the ratio of peak signal to the standard deviation of the background observed over the same testing ground. The standard deviation is obtained from the square root of the mean background counting rate read from the calibrated recorder scale, rather than from an estimate of statistical fluctuations about the mean value.

This letter is published by permission of the Director of this Establishment.

Atomic Energy Research Establishment, Harwell, Berks.

D. H. PEIRSON
E. FRANKLIN

REFERENCES

(1) COCKING, S. J. A.E.R.E. (private communication).
(2) HIRSCHFELDER, J. O., and ADAMS, E. N. *Phys. Rev.*, **73**, p. 863 (1948).

New books

Encyclopedia on cathode-ray oscilloscopes and their uses. By RIDER and USLAN. (London: Chapman and Hall Ltd.) Pp. viii + 982. Price 75*s*.

To cover in a single volume, even the size of the present one (pages 11 × 8 in) the operation and main applications of the cathode-ray oscilloscope is a considerable achievement. Messrs. Rider and Uslan have succeeded in doing it, and have supplied additional material which is not usually regarded as pertaining to oscillography. The text is often brief and sometimes comes near to being misleading, but the book contains, in twenty-two chapters and three appendices, information on basic principles of cathode-ray tubes, deflexion systems and time-bases of several types, the testing of audio-frequency circuits, transmitters and television receivers, visual alinement of a.m., f.m., and television receivers, general industrial and engineering applications and cathode-ray tube photography.

There is a chapter on special-purpose cathode-ray tubes which includes all the normally used camera tubes and a description of the graphecon. Circuit diagrams and data on some seventy-five commercial oscilloscopes occupy nearly one hundred and fifty pages. One British oscilloscope is described. A feature of the book is that nearly sixteen hundred complex waveforms are reproduced, all of which were photographed from an oscilloscope screen. The purchaser of the book will be the best judge of their usefulness.

It is not surprising to find mistakes in a book of this size. There are a few misprints and one or two of the figures are wrongly numbered, or entitled. More notably, attention is drawn to the circuit diagrams in Figs. 9–49 and 9–97. The first shows a thyratron time-base in which both anode and cathode of the thyratron are connected to the h.t. line, and the second a constant-current charging pentode running under anything but constant-current conditions. Omar Khayyám, among others, would be surprised at Figs. 11–29 and 11–30, where a grid voltage waveform is shown going backwards in time because of the incorrect graphical addition of a sine wave and an exponential curve.

There is a useful bibliography containing a pleasingly high proportion of references to British authors. The book should find considerable use as a comprehensive reference volume and some sections of it will provide good introductory matter for students.

R. D. NIXON

Electromagnetic waves. By SIR JOHN TOWNSEND, F.R.S. (London: Hutchinson's scientific and technical publications.) Pp. 60. Price 6*s*.

Townsend rejects Maxwell's theory and the concept of displacement current but retains Faraday's law of electromagnetic induction. He sets himself the task of deriving the same results for the case of waves from oscillatory circuits by constructing the well-known field of, for example, an Hertzian oscillator from the retarded contributions of both its current and the electrostatic charges on its ends. The electric field due to the former is postulated to be everywhere parallel to the current (i.e. to the axis of the oscillator) and the latter, the electrostatic contribution, is to consist not only of the Coulomb field but also of a retarded longitudinal field, decreasing only inversely with the first power of distance and depending on the change of charge with time.

In the last ten pages of the book Townsend endeavours to give a mechanistic illustration by means of an aether model which now has to transmit also these longitudinal waves and thus differs from the incompressible solid aether of Maxwell's theory. He claims that it rather resembles a gas.

Townsend's main objection against Maxwell's theory is that the auxiliary concept of a charge which oscillates in magnitude and which is used by Townsend in his derivations (quite legitimately, the reviewer thinks, as a virtual concept) cannot be treated by Maxwell's theory. But the reason for this is surely that such an oscillatory charge, taken as a single reality, violates the conservation of charge. Townsend overlooks that in his own treatment these oscillatory charges will never occur as single entities but always in pairs attached to the ends of a current whenever he treats a real problem; thus his objection to Maxwell's theory would be valid only in cases which are not realizable in nature.

Nevertheless, Townsend's methods could also be considered as an original re-interpretation of the well-known retarded potentials solutions of electromagnetic theory, in which the terms are collected and arranged in a way different from the usual one; but in this book his treatment of waves from oscillatory circuits is an inductive one, based on three basic laws and employs only elementary mathematics. A further problem treated is the field due to an alternating current in a small closed loop.

H. PELZER

The preparation of programs for an electronic digital computer. By M. V. WILKES, D. J. WHEELER and S. GILL. (U.S.A.: Addison-Wesley Press Inc.) Pp. 167. Price $5.00.

This book is a welcome addition to the small amount of published material on the detailed process of organizing calculations for automatic calculating machines, a process usually called "programming." To the potential or prospective user, this subject is as important as the provision of a machine itself, and one which has to be learnt before he can avail himself of the facilities which the machine offers.

In the early machines, the Harvard Mark I and ENIAC for example, numbers and operating instructions were represented in the machine in quite different forms. One of the most important subsequent developments has been the use of the same form, in the machine, for operating instructions as for numbers. This has the consequence that the facilities of the arithmetical unit can be used for building up and for modifying the operating instructions themselves in the course of the calculation, this being done quite automatically as the result of other operating instructions, and perhaps being conditional on the results of the calculation itself. The possibility of doing this has a profound influence on the process of programming.

One way of lightening the programmer's task, and thereby enlarging the range of kinds of calculations to which it is practicable to apply the machine, is to associate with the machine a library of sets of instructions, usually called "sub-routines," for various standard processes such as interpolation, quadrature, and evaluation of polynomials, exponential and circular functions. To be of practical value these library sub-routines must be drawn up in such a form as to provide the variants which different users may want in their particular calculations, and facilities must be provided for incorporating the appropriate variants of library sub-routines into the program for any calculation.

This book provides the first detailed account of a system of programming in which full advantage is taken of the possibility of instructing the machine to modify its own operating instructions, and for which a considerable library of sub-routines has been built up; further, this system has been tested by two years of practical operating experience. It has been developed by the group working with the EDSAC at the Mathematical Laboratory of the University of Cambridge, but most of the general ideas and much of the detailed programming could be taken over to other machines using a one-address order code and serial storage for instructions; it is notable how little reference the authors have had to make to the physical form of the store or of the arithmetical unit.

The book is divided into three sections. The first is explanatory and gives a survey of the method of programming, how parameters are used to give the required flexibility to sub-routines, how sub-routines are entered and left, a summary of contents of the library of sub-routines which has been developed for use with the EDSAC, and some examples of the construction of complete programs. The second section gives the specifications of all the sub-routines in this library at the time of writing; these specifications give enough information for the programmer to use the sub-routines, without having to inquire *how* they do what they do. The third section gives detailed and annotated programs of selected sub-routines.

The book has been printed by a photographic process from copy prepared on a typewriter; the result is clear and easily readable, except that suffixes and indices are much lighter than the rest of a page. The reviewer is glad to see the use of the English spelling "program"; this, although perhaps a result of the book being published in America, is not an Americanism (see Fowler's *Modern English Usage* and the *O.E.D.*); we do not use the French form in "diagram" and similar words, why retain it in "programme"?

D. R. HARTREE

Quantum mechanics of particles and wave fields. By ARTHUR MARCH. (London: Chapman and Hall Ltd.) Pp. x + 292. Price 44*s*.

It is a sign of the times that several recent introductory accounts of quantum mechanics have included a treatment of the quantization of wave fields. Professor March's book is in line with this development, about half of the text (Chapters 6–9) being devoted to a description of relativistic wave equations (for particles of spin 0, $\frac{1}{2}$ and 1) and their quantization. Perturbation theory treatments are also given for several problems in quantum electrodynamics and meson theory.

The earlier chapters of the book form a very readable account of the wave and matrix mechanics of systems with a finite number of particles. The conceptions are clearly explained, and generally the emphasis is on principles rather than examples. Fuller analytical treatment is, however, given to a few problems, such as the linear oscillator and the hydrogen and helium atoms. Generally, these first nine chapters can be recommended for the uniform clarity of the exposition.

In its last chapter the book enters upon less certain ground. Some of the divergence difficulties of field theories have been earlier discussed. One of the proposed methods for their removal—the introduction of a fundamental length—is now presented in some detail. The method has scarcely, however, the finality which would justify its appearance in a book. It is particularly unfortunate that part of the experimental material chosen by Professor March as a justification for his procedure should be based on a misapprehension. The conflict between the small nuclear scattering cross-section observed for cosmic-ray mesons and the strong meson-nuclear coupling required for other reasons (such as nuclear forces) was resolved when it was shown that two different types of meson, π and μ, were involved. J. C. GUNN

Textbook of electrochemistry. Vol. II. By G. KORTÜM and J. O'M. BOCKRIS. (London: Elsevier Publishing Co. Ltd.) Pp. xiii + 530. Price 70*s*.

In my review of the first volume* the need for more attention to practical technique with applications was emphasized. In this second volume this part of the criticism is completely met. A large part of the text (nearly one-quarter of the whole book) is given over to examples graded in order of difficulty. They cover the subject matter of each chapter. The examples are admirable and many of them have been taken from original papers. In addition, the more difficult problems are solved with explanatory notes. Clear diagrams of both apparatus and circuits are given throughout the book.

The main text, comprising approximately half the total contents, consists of four chapters. These are on: electrical phenomena at interfaces; irreversible electrode processes; electrochemistry of gases; and experimental methods of electrochemistry. They are extremely well presented and are up to date. The use of the modern electronic equipment (e.g. the cathode-ray oscillograph and the thyratron) in

* *Brit. J. Appl. Phys.*, **2**, p. 367 (1951).

electrochemical measurements is well described. While the footnotes are extensive and often helpful, they tend to break up the continuity of the text.

Sections 3 and 4 of the tables of physico-chemical constants (properties of electrolytes and electrolytic solutions and data on electrode processes and electrode potentials) place a great deal of information, which might otherwise be difficult to obtain, at the disposal of readers. Most of the physical data in Sections 1 and 2 (universal constants, ratios and physical data) may be obtained in ordinary standard compilations of tables (e.g. Kaye and Laby). From the point of view of economy they could be omitted or made more selective. The two volumes are obviously intended to be used as a unit since only one index is given, yet the pages given over to "Important Symbols" are repeated in Volume II, but with some variations which may be confusing. The symbol P in Vol. I is pressure and in Vol. II it is used in addition for molar polarization, proton affinity and force.

JOSEPH REILLY

Fundamentals of electronics. By PROFESSOR F. H. MITCHELL. (U.S.A.: Addison-Wesley Press Inc.) Pp. xi + 243. Price $4.50.

One of the aims claimed for this book is to give the non-specialists in electronics—be they engineers or physicists—an insight into the fundamental devices and circuits of this subject. The level achieved is no higher than that of an intermediate degree or national certificate and any sixth-form schoolboy with a taste for electronics will find no difficulty in following the text throughout.

Direct and alternating current circuits, valves of several types, amplifiers, oscillators, gas-filled valves, wave-shaping and controlling circuits are all treated adequately for the purpose. Chapter Eleven, however, on special purpose tubes and devices, treats all of these too scantily. It might have been more profitable to have omitted many of the very special devices such as magnetrons, velocity-modulation tubes, etc., and to have devoted separate small chapters to the photocell (discussed in two pages) and the cathode-ray oscilloscope as being of far greater use to the majority of readers of the book.

A. J. MADDOCK

Sound insulation and room acoustics. By PER V. BRUEL. (London: Chapman and Hall, Ltd.). Pp. xi + 275. Price 35*s*.

Dr. Bruel has given us a nicely balanced combination of the theory and practice of the branches of acoustical engineering connected with sound in buildings. The translation of technical terms is always difficult and, while to the expert the meaning is seldom in doubt, the technical idiom has sometimes been missed, e.g. "optimum" instead of "maximal." Readers in Britain and the U.S.A. must beware of his use of sabins in sq. m instead of sq. ft and of his indiscriminate use of "phons" when only "db" is justified. He does not draw attention to the difference between them. The concept of "true impedance" in ρc units is very useful in simplifying the calculations associated with sound reflexion. He also shows the simplicity of the tube method compared with the reverberation method for determining the absorption coefficient, especially when only small quantities of material are available.

The particular arrangement which he shows for calibrating a microphone by a Rayleigh disk in a resonant tube is unsuitable for high frequencies and he does not point out that the tube works for odd harmonics. He deals comprehensively with absorbents, both theoretically and practically, bringing out the importance of thickness in porous materials at low frequencies. He deals similarly with the reduction of noise by solid and porous walls, multiple walls and absorbents. However, he advocates corners or bends in lined ducts to increase attenuation at high frequencies and does not mention the much more effective way of subdividing the air path into narrow passages by absorbent "splitters." He illustrates some useful ways of reducing structure-borne impact sounds, but his suggested velocity scale for vibration measurements calls for more explanation and justification. A velocity scale is appropriate from the point of view of sound radiation, but it follows from Fig. 39 that acceleration is more pertinent to feeling. Resilient mountings are referred to in a few lines and some references. In his treatment of room acoustics he is naturally at home and gives much useful information for the design of theatres and studios.

There are 126 references, or groups of references, and a bibliography of about 100 items.

A. J. KING

Radiation monitoring in atomic defence. By DWIGHT E. GRAY and JOHN H. MARTENS. (London: Macmillan and Co. Ltd.) Pp. iv + 120. Price 15*s*.

This book is directed to those civil defence workers whose duties in the event of an emergency involving atomic energy hazards would include some responsibility for the radiation safety of others. The first half of the book gives basic information about health physics, radiation hazards and the protective measures which can be taken against an atomic explosion; the second half of the book describes the instruments developed by the American Atomic Energy Commission for the detection and quantitative determination of these radiation hazards.

In many ways the book is disappointing. Thus, on page 26 the authors give the effect of acute doses 25 to 600 röntgens of γ-radiation assuming whole body radiation. On page 27 they state that the effect is different if the exposure is spread over a series of days instead of being given in a short time, but they fail to discuss this important case. Similarly, they point out in Chapter V the danger of radioactive contamination resulting from deposited fission products in the event of a low-altitude, or an underwater explosion, but they give no quantitative information about this hazard. In some places the information presented is misleading. Thus, on page 30 the authors give the impression (rightly) that the hazard due to α-active materials is negligible, but they devote the whole of a later chapter to the description of an instrument for measuring α-radiation.

It is thought that civil defence workers with scientific knowledge will find much of interest in this book, but it is fairly certain that they will agree with the present reviewer—that it is a disappointing book.

DENIS TAYLOR

Advanced five-figure mathematical tables. By C. ATTWOOD, B.Sc., A.M.I.Mech.E., A.M.I.E.E. (London: Macmillan and Co. Ltd.) Pp. vi + 70. Price 4*s*. 6*d*.

This small book includes tables of sines and cosines of angles in decimals of a degree (interval $0{\cdot}1^\circ$) and in radians (interval $0{\cdot}001r$) and similar tables of tangents and secants, with a reduced interval in the appropriate range of argument. Hyperbolic sines (0·000–0·001–1·000–0·01–6·00), cosines and tangents, the exponential function, factorial function and complete elliptic integrals of the first and second kind are also given. There are also twelve pages of useful notes on the tables and on interpolation. The type face used for the tables is good and altogether this is an excellent little book which should be useful to students. It is a pity the binding is not in stiff boards, even though this would have increased the present modest price.

N. CLARKE

Rubber technology. Edited by R. C. W. MOAKES and W. C. WAKE. (London: Butterworths Scientific Publications.) Pp. xiv + 199. Price 25*s*.

A modern treatise covering the wider aspects of rubber technology is long overdue. This book, which constitutes an account of the lectures given at the 1951 Summer School of the Research Association of British Rubber Manufacturers is necessarily limited in scope and therefore can hardly be said to live up to its rather ambitious title. It does, however, bring together in a convenient form the results of much recent work.

Except for the sections on latex and textiles the work is produced by members of the staff of the R.A.B.R.M., with a short introduction by the Director, Dr. J. R. Scott, who discourses provocatively on present and possible future aspects of rubber processing and compounding.

Dr. W. J. S. Naunton discusses "Latex: from the tree to the finished article," in a clear and interesting manner, but the growing importance of the subject merits a fuller account, particularly of processing and manufacture, than is given here. In contrast, the section on "Recent developments in compounding," by Mr. R. C. W. Moakes, attempts to crowd too much data into a limited space. It is useful to the experienced compounder in summarizing a varied assortment of recent information, but would have been more helpful to non-specialists if more attention had been given to principles and less to the results of actual experiments.

Mr. J. Mann's account of the various kinds of deterioration of rubber, including exposure cracking, oxidative ageing and light stiffening, is well done and up to date. In the limited space at his disposal Mr. A. L. Soden has given a good survey of the many physical test methods employed in rubber laboratories. The section on statistics by Mr. W. C. Wake suffers from an attempt to combine in too short a compass the application of a particular statistical technique to rubber production problems with a discussion on operational research. Professor W. E. Morton discusses the "Resources of the woven fabric designer" in a most interesting manner, but the article, which gives no indication of applications to the rubber industry, seems out of place in a book devoted to rubber technology.

D. PARKINSON

An introduction to applied mathematics. By J. C. JAEGER. (London: Oxford University Press.) Pp. xiii + 445. Price 35*s*. net.

This stimulating book will be welcomed by those who are interested in mathematics as a tool. It does not, however, attain the author's aim of being "useful to physicists and engineers," and "to give good training for mathematicians." The statement (p. 77) that the term

$$\sin(\omega t + \beta - \phi) \cdot F_0/m \cdot [(n^2 - \omega^2) + 4k^2\omega^2]^{\frac{1}{2}}$$

"builds up" is one example of an imprecision of statement that could have been easily avoided, and the treatment of vectors to include small rotations is to be regretted. The alternative treatment mentioned in the footnote on p. 162 would have been far better.

Engineers and others will probably find that the book assumes too great an understanding of mathematics, and too few of these readers will know enough partial differentiation, especially at "intermediate standard," to follow Section 54, or Section 113 on conformal representation. Much of the algebra is too severely shortened, for example $f(t + 0) = \underset{\tau \to t + 0}{Lt} f(\tau)$ is an explanation only for those who know what is meant by "tending towards a discontinuity from the right."

The dual aim of this book is perhaps responsible for the lack of balance which the author to some extent anticipates in his preface. There is much that is beyond the scope of the student at "intermediate" level, and the author would no doubt have written a better book for non-mathematicians at a more advanced stage. The book is, however, a valuable handbook for those using mathematics, and contains adequate reference when more exhaustive investigation is required.

C. SNELL

Ultrasonics. By P. VIGOUREUX. (London: Chapman and Hall Ltd.) Pp. vi + 144. Price 25*s*.

The extent of the recent developments in ultrasonics is seen by comparing the 1938 English edition of Bergmann's book, having 264 pages and 483 references, with the 1949 Swiss edition having 748 pages and 2 322 references. Dr. Vigoureux' is the first English book to give an up-to-date account of some of the main topics. Attention is concentrated mainly upon work with gases and liquids.

The treatment is divided into five main sections dealing in turn with generation, propagation, observation, gases, and liquids, together with a bibliography of publications starting in 1939. To attempt to give, in 160 pages, an account of all aspects of ultrasonics including its technological applications, would have led to little more than a superficial catalogue. Instead Dr. Vigoureux has written a concise account of those parts of the subject in which the physical principles can be clearly stated and in which precision measurements can be made. For instance, in the chapter on observation three techniques, the interferometer, optical diffraction and echo pulse methods are selected for detailed treatment, but first of all a clear discussion of physical principles is given. This type of treatment extends throughout the book. Mathematical treatments are kept as simple as possible. There are 74 figures in the text and 25 tables of results relating chiefly to velocity and absorption measurements on gases and liquids. All these features, together with the exceptionally clear type and the arrangement of the book, make it the best English introduction to ultrasonics for physicists. For the benefit of other readers wishing to know also of applications of ultrasonics outside the physics laboratory, in such topics as metallurgy, chemistry, biology and medicine, a more exact title might have been chosen.

W. H. GEORGE

General astronomy. (3rd edition.) By SIR HAROLD SPENCER JONES. (London: Edward Arnold Co. Ltd.) Pp. x + 456. Price 30*s*.

A new edition of the Astronomer Royal's well-known textbook on general astronomy will be a welcome addition to the bookshelves of astronomers and of a much wider group of interested readers. This edition has been completely revised and many additions and alterations have been made to bring the book up to date. Such names as Edlén and Bethe appear in the index for the first time. Although the book has been considerably enlarged something has had to go, but one is sorry to see dropped the reference to the discovery of the spiral nature of nebulae by the Earl of Rosse. A comparison of the indexes of this and earlier editions gives a good idea of the rate and direction of the modern developments of astronomy. The one growing point which has not been adequately treated is that of radio-astronomy, perhaps because it is growing so fast. Speculative cosmogony has been largely ruled out but the author has selected Weizsäcker's theory of the origin of the solar system as the most promising among recent studies.

F. J. M. STRATTON

The conduction of electricity through gases. 3rd edition. By K. G. EMELEUS, M.A., Ph.D. (London: Methuen and Co. Ltd.) Pp. x + 99. Price 5*s*. 6*d*.

The first two editions of this little book were published in 1929 and 1936, and this third one differs from them only in minor respects. It cannot, of course, compare with the larger treatises, but most of the important parts of the subject are dealt with in a concise and elementary manner. The explanations are clear, and brevity is largely achieved without resulting in inaccuracy.

It is perhaps a pity, in view of the widespread use of electric discharge lamps for lighting, that space could not be found for some discussion of the spectral properties of the positive column. The book will continue to prove useful to non-specialists interested in the subject. V. J. FRANCIS

Steels in modern industry. Edited by W. E. BENBOW. (London: Iliffe and Sons Ltd.) Pp. viii + 562. Price 42*s*.

This book is a small encyclopaedia covering a subject which is of great importance to everyone who uses steel. It has the advantages and disadvantages of an encyclopaedia as compared with a book by a single author. Some of the advantages are that every part of the subject is covered by someone who knows it more intimately than a single author could possibly hope to do, that one can look in the index for such headings as creep, corrosion fatigue, temper brittleness or plastic deformation and find their relation to many different uses of steel and that the points of view of the users, the steelmakers and the fabricators can all be presented. The disadvantages are the obvious ones that there is a certain inevitable overlap between certain sections and that some authors assume more prior knowledge on the part of the reader than others. Some of the authors are perhaps not sufficiently critical on, for example, the disputed existence of a mechanical equation of state for metals, and some recent work of practical importance such as Tabor's work on hardness could usefully have been included.

Nevertheless the book can be recommended to the physicist for two reasons. Firstly, when the physicist uses steel in his apparatus the knowledge he requires coincides with that of the industrial engineer whether it be in regard to the mechanical strength under various types of load and at various temperatures, to the resistance to chemical attack or to electrical and magnetic properties. Secondly, while the metal physics treatment of the properties of steel, which has made such progress in the hands of Mott, Cottrell, Orowan, Nabarro and many others, is hardly mentioned in the book because it has not yet borne sufficient practical fruit, yet it is valuable to the metal physicist to have a handy reference to the various technical properties of steel which he is concerned to explain, such as blue brittleness or weld decay. M. W. THRING

Report on interlingual scientific and technical dictionaries. Pp. 33. Price 1*s*. 6*d*.

Bibliography of interlingual scientific and technical dictionaries. Pp. 227. Price. 4*s*.

By J. E. HOLMSTROM, Ph.D. (Paris: U.N.E.S.C.O., 1951).

This report and accompanying bibliography have resulted from an attempt to make as complete a survey as possible of the supply of special dictionaries. The bibliography, which is now published separately, details 1 044 works grouped under 224 subject heads in accordance with the Universal Decimal Classification, and is indexed under 45 languages. It includes, however, a large proportion of works which are out of print. This is the second edition of the report and it has been revised to include developments of some of the ideas which have originated by discussion of the original edition and further comment is invited.

F.B.I. register of British manufacturers—1951–2. 24th edition. (London: Kelly's Directories Ltd., and Iliffe and Sons Ltd.) Pp. 882. Price 42*s*.

The 1951–2 register comprises seven sections. These include a products and services section which lists over 6 000 member firms under more than 5 000 alphabetical trade headings. The addresses section is an alphabetical directory giving full information of every member firm. Other sections list useful details of trade associations, brands, trade names and marks. The whole production once more attains its usual high standard.

Journal of Scientific Instruments

Contents of the June issue

SPECIAL ARTICLE

The Physical Society's Exhibition—London 1952. By E. J. Harris.

ORIGINAL CONTRIBUTIONS

A device for the automatic control of electrical power up to 2 kW. By W. T. Bane and J. S. Appleby.

A printing recorder for use in conjunction with scaling units. By A. R. Lang.

An objective method for measuring the daylight factor. By W. Koch and D. Kaplan.

A crystal-photomultiplier gamma counter for hospital use. By A. H. Ward and P. G. Jensen.

Power supply for a thermionic ion source. By C. Reutersward.

Apparatus for the measurement of the dynamic shear modulus and hysteresis of rubber at low frequencies. By W. P. Fletcher and A. N. Gent.

The RADIAC slide rule for the computation of external radiation dose from nuclear fission products. By B. W. Soole.

Demountable X-ray tube for crystallography. By T. B. Rymer and P. G. Hambling.

The simultaneous measurement of the magnitude and dispersion with wavelength of a small birefringence. By J. E. H. Braybon and H. G. Jerrard.

Apparatus for conversion of infra-red spectrometer records to percentage transmission. By R. A. G. Carrington and J. G. Reynolds.

LABORATORY AND WORKSHOP NOTES

A multiple exposure camera for use with a single crystal X-ray goniometer. By H. J. Grenville-Wells.

An interferometer for calibrating extensometers. By W. K. G. Floor.

A combustion chamber for the semi-micro determination of carbon monoxide and hydrogen. By G. T. Rogers.

A torsion balance for weighing evaporated films. By P. L. Clegg and A. W. Crook.

A pilot tone alarm circuit. By E. J. Miller.

The use of aluminium contacts in electro-polishing. By H. J. Hartley.

An easily made flexible vacuum-tight joint. By J. Norbury.

A shock operated switch with small time lag. By A. Watson.

NEW INSTRUMENTS, MATERIALS AND TOOLS

Rayleigh interference refractometer
X-ray photograph illuminator
High-speed laboratory grinding mill
Corona voltage stabilizer tube
Two-speed precision drives
Absorption wavemeter
Manometer

NEW BOOKS

Prism and lens making
Materials technology for electron tubes
H.M. King George III collection, descriptive catalogue.
Correction tables for radioactive decay
Lenses in photography

MANUFACTURERS' PUBLICATIONS

THIS JOURNAL is produced monthly by The Institute of Physics, in London. It deals with all branches of applied physics (including theory and technique). All rights reserved. Responsibility for the statements contained herein attaches only to the writers.

EDITORIAL MATTER. Communications concerning editorial matter should be addressed to the Editor, The Institute of Physics, 47 Belgrave Square, London, S.W.1. (*Telephone:* Sloane 9806.) Prospective authors are invited to prepare their scripts in accordance with the *Notes on the Preparation of Contributions*. (Price 2*s*. 6*d*. including postage.)

REPRODUCTION. The Institute of Physics is a signatory to The Royal Society's Fair Copying Declaration. Details may be obtained upon application from The Royal Society, London, W.1.

ADVERTISEMENTS. Communications concerning advertisements should be addressed to the agents, Messrs. Walter Judd Ltd., 47 Gresham Street, London, E.C.2. (*Telephone:* Monarch 7644.)

SUBSCRIPTION RATES. A new volume commences each January, and annual subscriptions will only be accepted for complete volumes of the monthly parts (January–December). The charge is £4 per volume ($11.50 U.S.A.), including index (post paid), payable in advance. Single parts, so far as available, may be purchased at 8*s*. each ($1.15 U.S.A.), post paid, cash with order. Orders should be sent to The Institute of Physics, 47 Belgrave Square, London, S.W.1, or to any Bookseller.

SPECIAL ARTICLE

The method of dimensions*

By E. W. H. Selwyn, B.Sc., A.R.C.S., D.I.C., F.Inst.P., Research Laboratories, Kodak Ltd., Harrow, Middlesex

The fundamental theory of the method of dimensions, here given in a way which shows why variables appear as products in physical formulae, indicates that any physical quantity which has a character peculiar to itself, and which may be measured by addition of units of the same character (if necessary by distortion of scale), may be attributed a dimension and used in dimensional arguments. Examples are given.

INTRODUCTION

The method of dimensions has been in use for a very long time yet its fundamental basis seems still not to be well understood. Except for the discussion by Bridgman,† most treatments depend upon the intuitive assumption that it is not possible to equate physical quantities of different sorts, and also assume that any physical quantity is expressible either as a product of other physical quantities each raised to some power or as a series of such terms. It can be proved, however, that these are necessary consequences of the system of measurement adopted in physics. The object of this article is to offer an account, free from the objections which may be raised against others so far available, of the reasons why the method is what it is. We shall then understand better what sort of quantities may legitimately be used in dimensional arguments and the meaning of the results which are obtained. This may be regarded as worth doing, because, although dimensional arguments may tell us very little about the physics of any phenomenon other than what has been introduced into the arguments, they can give an answer when a more detailed analysis is impossible.

Units of measurement may on occasion be a mere convenience. But units of measurement are a necessity in physics, because physics deals with the variation of quantities. To represent a variable it is necessary to have some standard of reference against which the variation can be measured. The size of the standard is immaterial, but it is convenient if some commonly agreed standard is adopted. Such standards are normally spoken of as units.

The relations between variables are expressed by mathematical equations or an equivalent graphical representation. The size of a variable is expressed by the number of units in it, and mathematical operations are carried out on this number. It is not necessary that the variation should be expressed in this fashion. For instance, the variation might be described by the convention that doubling the size of the variable increased the number in the equation by unity. But the normal convention is the simplest because it is directly connected with the arithmetic scale of numbers and enables the quantity to be measured by simple addition of units. If the size of the unit be changed so that x new units are equal to the original unit then the number of new units in a given measure is increased in the ratio x. This, as pointed out by Bridgman, is the fundamental proposition on which the theory of the method of dimensions rests.

It is possible to take an empirical view of any equation of physics, regarding it as directly derived in every case from an adequate number of observations on the phenomenon which it represents. This process of derivation is hardly ever followed. Most equations of physics start from some theoretical foundation, some foundation, that is, derived from previous experience. But formally the empirical view is sound, because unless observations fit the theoretically derived equation it is the equation which is thrown overboard. On this basis let us consider an experiment in which a tin can with a hole perforated in the side near the bottom is maintained just full of water by running water into it continuously. Water issuing from the lower hole then describes a curve. If this experiment were performed by an Englishman in London and a Frenchman in Paris, and they used the same can, practically identical curves would be produced. But if, in attempting to determine a mathematical function to represent the curve, each observer takes off horizontal (x) and vertical (y) co-ordinates, the Englishman using inches and the Frenchman centimetres, they might obtain co-ordinates representable, in a hypothetical example, by the equations

$$y = 1{\cdot}0\,x^2 \text{ (inches)}, \quad y = 0{\cdot}394\,x^2 \text{ (centimetres)}.$$

The difference between the units makes a difference in the "constant" in the equation, but does not alter the essential character of the equation, namely the parabolic variation of y with x. It is easy to see why the "constant" varies with the units of measurement. For if we calculate, from two particular co-ordinates, y_1 and x_1, the value of the constant, namely y_1/x_1^2 and then change the unit of length, so that A new units make an original one, the new value of the constant is $Ay_1/A^2x_1^2$, which bears the ratio $1/A$ to the original value.

This example illustrates a feature invariably found in the equations of physics. An equation is made to give the correct answer, whatever the units in which the variables in it are measured, by making constants in the equation vary with the units when necessary.

THEORETICAL

The quantities to be found in a physical equation, then, are variables and constants the numerical values of which are dependent upon the sizes of the units in terms of which the variables are measured, and variables and constants the numerical values of which are not dependent upon units. Let us consider a quantity (whether variable or constant) which varies with one or more units and which has the numerical value a for certain units. If one of the units be changed in size, by a ratio the logarithm of which is x, the value of a becoming changed in consequence to a^*, then a^* depends upon a and x. That is

$$a^* = \Phi(a, x).$$

For another ratio, with logarithm x^*, and the quantity consequently taking another value a^{**},

$$a^{**} = \Phi(a, x^*).$$

But a^{**} may also be calculated from a^* and $x^* - x$, since the size of the units can have no influence on the functional relation. Thus

$$a^{**} = \Phi(a^*, x^* - x).$$

If the numerical values specified in the three preceding

* Communication No. 1484 H.

† Bridgman. *Dimensional Analysis* (New Haven, Conn., and London, 1922 and 1931).

equations be plotted graphically as in the figure (using any curve to represent the functional relation) it is easily seen that the curve through (0, a^*) is necessarily equidistant in the x-direction from that through (0, a). Consequently the relation must take the form

$$f(a^*) = f(a) + x$$

where the function is arbitrary. If more than one type of unit be involved, and the logarithms of the ratios in which their sizes are changed be $x, y, z \ldots$ then

$$f(a^*) = f(a) + \alpha x + \alpha' y + \alpha'' z \ldots$$

where $\alpha, \alpha', \alpha'', \ldots$ are constants.

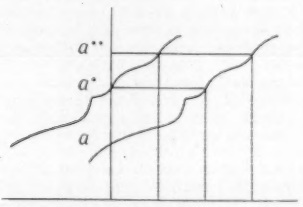

To show that $f(a^*) = f(a) + x$

Now $f(a)$ is a valid measure of a, whatever the form of the function, all that is implied being a distortion of the scale of measurement if we use $f(a)$ instead of a. But if measurement be the only requirement then some particular form or forms of function will be preferred. In fact the automatic choice is to make $f(a)$ equal to $\log a$. Then

$$\log a^* = \log a + \alpha x + \alpha' y + \alpha'' z + \ldots$$

and

$$a^*/a = x^{\alpha} \cdot y^{\alpha'} \cdot z^{\alpha''} \ldots \qquad (1)$$

Although the measurement of a involves several units the principle of simple additivity is preserved, whatever the size of the units. For adding two quantities a_1 and a_2 together implies that the corresponding quantities a_1^* and a_2^* are also added together. Or we may observe that the ratio of a_1 to a_2 is the same as the ratio of a_1^* to a_2^*. This latter was adopted by Bridgman as a fundamental requirement of physical variables. As we have seen it is not an essential requirement but largely a convenience. On either view (they are really the same) the quantity a may be regarded as measured in terms of a single unit which is a combination of the individual units.

An example may make the point concerning the choice of the form of f clear. Suppose an apparatus be set up with a small translucent diffusing disk in a black surround, behind it a shutter giving very short exposure times t, and behind that a lamp movable to different distances d from the translucent disk. A patient enough observer could then make estimates (especially if he were given two patches of different fixed brightnesses for reference) to suggest a relation

$$B = \phi(t/d^2),$$

where B is a psycho-physical estimate of brightness. The function $\phi(t/d^2)$ would be peculiar to the observer and the conditions of the experiment. But if a physicist did this, he would almost automatically write the equation as

$$B' = \text{constant } (t/d^2),$$

turning the brightness into a physical light-flux by defining it in terms of t and d, and attribute any non-linearity in the first equation to peculiarities of the eye, which he would regard as unsatisfactory, to some extent at least, as a physical instrument.

It is now a simple matter to establish a theorem due to Buckingham which is of fundamental importance in discussing the form of any physical equation known or suspected to involve a set of given physical quantities, namely, quantities, whether constants or variables, the numerical values of which depend upon the sizes of units. Such equations are usually given in a form which expresses a variable as a function of the other variables. By dividing both sides by the dependent variable we can write it as

$$F^*(a, b, c, \ldots) = 1.$$

If one of the units is changed in the ratio x, the quantities $a, b, c, \ldots$ become, say,

$$x^{\alpha}a,\ x^{\beta}b,\ x^{\gamma}c, \ldots$$

in accordance with equation (1).

The equation may also be written in the new units:

$$F^{**}(xa^{1/\alpha},\ xb^{1/\beta},\ xc^{1/\gamma}, \ldots) = 1,$$

or

$$F^{***}(xa^{1/\alpha},\ xb^{1/\beta}/xa^{1/\alpha},\ xc^{1/\gamma}/xa^{1/\alpha}, \ldots) = 1,$$

the modification of the variables being made only on those affected by the change in the unit.

Since x cancels in all terms other than the first, thus making these terms independent of the size of the particular unit under consideration and because F^{***}, being equal to unity, must also be independent of the size of this unit, the first term cannot appear in the equation. Thus the equation is now

$$F^{***}(b^{1/\beta}/a^{1/\alpha},\ c^{1/\gamma}/a^{1/\alpha}, \ldots) = 1,$$

The number of terms is now reduced by one, with the elimination of the dependence on x. Each of the new terms will be of the usual form, involving units raised to powers and the same argument as before may be followed. The final result is that we shall arrive at an expression

$$F(\pi_1, \pi_2, \pi_3 \ldots) = 1,$$

where the π's are independent variables such that each π is a product of the variables $a, b, c, \ldots$ each raised to powers making each π independent of the units. If there are m variables involving n units altogether the number of π's will be $m - n$, as is easily seen by considering the process of deduction of the equations. The exponent to which any given variable is raised in any π can be made unity or any other arbitrary value, provided the other exponents are suitably adjusted. The argument establishes that any physical equation may always be expressed in the above form. The most useful form, or that which best expresses its physical content can, of course, always be derived by transformation. The simplest transformation is to solve for one of the arguments, say $a^{-1}b^{\lambda}c^{\mu} \ldots$, so that the equation becomes

$$a = b^{\lambda}c^{\mu} \ldots \psi(\pi_2, \pi_3, \ldots). \qquad (2)$$

The quantity a may then be said to have the dimensions λ in the unit in which b is measured and μ in the unit in which c is measured. Dimensional analysis is concerned with the discovery, somehow, of the variables involved in the phenomenon under discussion and then sorting them out into groups independent of variations in the units. The methods

of doing this are so well known that it is not necessary to discuss them. The first part is the more difficult.

NATURE OF PERMITTED VARIABLES AND EQUATIONS

So far the only restriction which has been placed on the variables in a physical equation is that the numerical value of any of them shall be inversely as the size of the unit in which it is measured. Since the size of the unit may extend from indefinitely small to indefinitely large, the numerical values of any variable must also extend from zero to infinity for the purposes of the equation. These are indeed the only restrictions required, apart from the common-sense one that all the variables (including physical constants) involved in the phenomenon under discussion, and none which are irrelevant, should be included in any equation. It is deciding which variables are important that requires thought. But this is not peculiar to the method of dimensions: even if one is mathematician enough to solve problems without using it, there is no escape, except by luck, from the necessity of thinking about the physics of a physical problem. There are physical variables, however, which are limited in magnitude, such as angle which is limited to $0 - 2\pi$ (or $0 - 360°$), or optical transmission which may be zero, but cannot be greater than unity (or 100%), or velocity which, since the theory of relativity, may not be greater than that of light. In such cases a graphic representation of any function involving them must stop short along the axis representing a variable with a limited value. In respect of the numerical values which occur in the function, therefore, the limiting value must appear as a physical constant. By Buckingham's theorem the corresponding variable then appears in the function as a ratio to its limiting value, and this quantity is independent of the units of measurement. The example from the theory of relativity must not be taken too seriously. Most velocities are so far below that of light that the possible range of velocities may be taken as infinitely great for most purposes. This point will be referred to again.

The argument has been cast into a form based upon experiment in order to avoid any implication that results which might be deduced from a knowledge of the units involved in a phenomenon have any special significance. The question whether an equation or formula is "true" is irrelevant; the only question is whether any equation represents the phenomenon it purports to represent with an accuracy or adequacy sufficient for the purpose in view. Any equation can and should be made to fit the dimensional requirements. Many physical equations fit the possible observations over a limited range only, though the equation itself will operate, on paper, to infinite values of the variables, both positive and negative. Provided, however, that one does not take the result beyond the bounds of fit with the variables, any operations, including dimensional arguments, may be performed on such an equation. According to the theory of relativity, coupled with dimensional arguments, velocities should always appear in ratio to the velocity of light in free space. The equations are such, however, that for small velocities the ordinary laws of addition of velocities hold with ample accuracy and to this accuracy the velocity of light may be dropped from the equations. In dimensional arguments involving small velocities, therefore, the velocity of light need not, and usually, if useful results are to be obtained, should not, be introduced.

EXAMPLES

The following examples have been chosen to illustrate the flexibility possible in choice of units, and the advantages which come from this. It is also intended that they should show that physical insight into a problem is helpful.

(1) *Flow through a pipe.* A standard example of the use of the method of dimensions is that of flow of a liquid through a straight horizontal pipe. First let us use the "blindfolded" method, in which one picks out the variables involved uncritically, to examine the situation when the flow is slow and is not affected by the density—even here we have to have a little peep through the blind-folding to the extent that we realize that if there are no accelerations the density of the liquid will not affect the motion. The relevant quantities are then (1) the pressure difference P between the two ends of the pipe; (2) the length, l; and (3) the diameter, d, of the pipe; (4) the mean velocity, v_0, measured by the volume flow, for example; and (5) the viscosity, η. The units are length, mass and time, and the equation comes out, by any of the usual methods, to

$$v_0 = (Pd/\eta)\Phi(d/l).$$

We cannot be sure, therefore, of the influence of d or l on the rate of flow, since we have no guidance on the form of the unknown function Φ.

The difficulty may be circumvented in several ways. No element of liquid will tend to move under uniform pressure. If motion occurs then it must be under the influence of a pressure gradient. Alternatively one may argue, more formally, that the flow through two pieces of pipe each of length $l/2$, with pressure at the ends of P and $P/2$ for one, and $P/2$ and 0 for the other, will be identical, since the viscosity of fluids is not appreciably affected by pressure. Consequently these two pipes may be connected in series, giving a single pipe of length l and with the pressures P and 0 at the ends, with exactly the same flow. The flow therefore depends on P/l and not on either separately. P/l may, therefore, be used as a single variable.

Conclusions of this type are often reached in all sorts of problems by intuition alone, but although they are usually correct it is often worth while to check them by an argument similar to the above. A little consideration will show that the above problem is an idealized one and forces the conclusion that P/l is the relevant variable. The lines of flow at the ends of the pipe are determined to some extent by the way in which the liquid is fed into the pipe and allowed to flow out. To avoid the necessity of specifying these conditions it must be supposed that the pipe is indefinitely long, the length thereby becoming undefinable and leaving P/l, the pressure gradient, as the only possible variable.

Using P/l as a single variable the result is

$$v_0 = \text{constant } Pd^2/l\eta.$$

An alternative and more direct method is as follows. Viscosity is defined by the force (caused by the viscous drag) per unit area on a plane lying along the lines of flow when the velocity along the lines of flow has a gradient across the lines of flow. The linear dimension in the force, in the velocity and one in the unit area are directed along the pipe in the problem under consideration, while the other two remaining linear dimensions are directed transversely to the pipe. This differentiation suggests that we might use different units for measuring lengths in three directions at right angles. We therefore take X as the length dimension along the pipe, Y along a radius and Z at right angles to the other two. The dimensions of viscosity, from the definition of it, are then

$$(MXT^{-2}/XZ)/(XT^{-1}/Y) \text{ or } MX^{-1}YZ^{-1}T^{-1}.$$

The other dimensions relevant to the problem are

l	X
d	Y
P	$MXY^{-1}Z^{-1}T^{-2}$
v_0	XT^{-1}

with the result $v_0 = \text{constant } Pd^2/l\eta$.

This is, of course, Poiseuille's law. The more usual form giving the rate of volume flow is to be obtained by multiplying v_0 by a factor containing the area of cross-section of the tube or d^2. Poiseuille's law is well established, and is, therefore, adopted as a starting point for extension of the argument to other conditions under which it does not apply.

When the velocity of flow is increased Poiseuille's law does not hold: the motion of the liquid ceases to be regular and it requires greater pressure than would be calculated by Poiseuille's law to maintain the flow. This is due, as was shown by Reynolds in 1883, to the occurrence of wavy or turbulent motion in the liquid. We are then no longer permitted to make use of three different scales of length, for if we try to describe the action of viscosity we must follow the lines of flow, at angles to the axis of the tube. These angles will be measured by ratios of lengths, and this automatically requires all lengths to be measured, in effect, on the same scale.

Wavy motion implies acceleration of elements of the liquid (since they move in curved paths) and the forces required to maintain such accelerations will be determined by the accelerations and the density of the liquid. The list of variables, with their dimensions, is then

v_0	LT^{-1}
d	L
ρ	ML^{-3}
η	$ML^{-1}T^{-1}$
P/l	$ML^{-2}T^{-2}$

The number of possible non-dimensional arguments is therefore 2 by Buckingham's theorem. We have already discovered one, namely $(P/l)d^2/v_0\eta$, and it will be convenient not to use P/l in the second. Dropping this from the list, it turns out that $v_0d\rho/\eta$ is independent of units. The required relation is therefore

$$F[(P/l)d^2/v_0\eta,\ v_0d\rho/\eta] = 0,$$

so that if $(P/l)d^2/v_0\eta$ be plotted against $v_0d\rho/\eta$ a single graph is obtained, true for all values of the variables. That this is so is well established experimentally.

The considerations, other than the facts of his experiment, by which Reynolds was led to the recognition of the importance of the dimensionless quantity $v_0d\rho/\eta$, since known as Reynolds number, were not those just given, but were based on the equations of motion of a viscous liquid. Somewhat similar but more detailed arguments had previously been used by Stokes (1850) and Helmholtz (1873). The following is probably the most easily intelligible form.

The equations of motion, of which only one need be discussed, take the form

$$\frac{\partial u}{\partial t} + \frac{u\partial u}{\partial x} + \frac{v\partial u}{\partial y} + \frac{w\partial u}{\partial z} + \frac{1}{\rho}\cdot\frac{\partial p}{\partial x} = \frac{\eta}{\rho}\left(\frac{\partial^2 u}{\partial x^2} + \frac{\partial^2 u}{\partial y^2} + \frac{\partial^2 u}{\partial z^2}\right),$$

where u, v, w, are velocities in the directions of the rectangular axes of x, y, z, at the point with the co-ordinates x, y, z, and p is the pressure. If the unit of length be taken as the diameter of the pipe, d, and the unit of velocity as the mean velocity of flow v_0, then the unit of time is necessarily d/v_0. In place of choosing a unit of pressure it is convenient to use a unit of pressure gradient, namely P/l. In terms of these units the equation becomes

$$\frac{\partial u'}{\partial t'} + \frac{u'\partial u'}{\partial x'} + \frac{v'\partial u'}{\partial y'} + \frac{w'\partial u'}{\partial z'} + \frac{(P/l)d}{\rho v_0^2}\left(\frac{\partial p}{\partial x}\right)' = \frac{\eta}{\rho d v_0}\left(\frac{\partial^2 u'}{\partial x'^2} + \frac{\partial^2 u'}{\partial y'^2} + \frac{\partial^2 u'}{\partial z'^2}\right)$$

where the primed quantities are in the new measures. The boundary conditions, expressed in terms of the new units, are the same for all tubes and conditions. Consequently the nature of the solution to this equation is controlled by the values of $(P/l)d/\rho v_0^2$ and $\eta/\rho d v_0$. But if these are fixed there will be only one solution, whatever the diameter of the tube or the mean velocity of flow. That is to say, the motions of the liquid will be exactly similar, the only differences being that the geometry of the motions will be on a scale proportional to the mean velocity of flow. Conversely the conditions for similarity of motion are that $(P/l)d/\rho v_0^2$ shall not vary, nor $\eta/\rho d v_0$. This is essentially the same result as that already discovered by the standard method of dimensions.

The argument based on the equations of motion is in some ways the more satisfying—which is only what might be expected since we have had to delve deeply (or more probably somebody else has) into the physics of the flow of liquids in order to establish the equations. But the satisfaction is somewhat illusory, because when it is realized that any specifiable characteristic velocity could replace v_0, any characteristic length replace d, or any characteristic pressure gradient replace (P/l), in the ordinary dimensional argument, the fact of similarity of the motions when $(P/l)d/\rho v_0^2$ and $\eta/\rho d v_0$ are fixed can easily be established. Moreover the equations of motion are not exact.

(2) *Child's law.* In a diode consisting of a cathode emitting electrons and an anode maintained at a positive potential, V, with respect to the cathode, the electrons, while they are between cathode and anode, form a "space charge" which opposes the action of the anode potential and slows down the electrons nearer the cathode. We propose to examine the nature of the dependence of the current, C, between cathode and anode on V. If electric charge be regarded as a physical quantity in its own right and given the dimension Q, then electric current has the dimensions Q/T, and V has the dimensions of the ratio of energy to charge or ML^2/T^2Q. The electrons will move to the anode only under the influence of a force, namely that provided by the charges which supply the potential V, acting on the charges of the electrons. The force between two charges varies inversely as the square of the distance between them, providing the dimensional relation

$$ML/T^2 = KQ^2/L^2,$$

where K is a constant with the dimensions ML^3/Q^2T^2. Any characteristic length l in the geometry of the diode will have dimension L.

With the quantities mentioned above no answer is possible, but on consideration we see that, treated purely as an electrical and not an electromagnetic problem, the charges will move with infinitely great velocity if they have no mass associated with them and in any diode produce an infinitely large current. The force on any charge is proportional to the charge but the acceleration produced is inversely as the mass. We therefore introduce a quantity m/e, the mass associated with unit charge, with dimensions, M/Q. For these quantities only one

product exists which is independent of units, giving the current as proportional to

$$(e/m)^{\frac{1}{2}}V^{3/2}/K.$$

If we use m and e independently an undetermined function is left in the solution. If the diode be assumed to have the form of an infinitely long cathode surrounded by an infinitely long cylindrical anode of radius r it is not possible to discuss the current since that also will be infinitely large, but the current per unit length of cathode, which is a finite quantity which can be discussed, turns out to be proportional to

$$(e/m)^{1/2}V^{3/2}/Kr,$$

whereas if the cathode and anode be infinite flat plates spaced d apart and parallel, the current per unit area of cathode is proportional to

$$(e/m)^{1/2}V^{3/2}/Kd^2.$$

The preceding formulae show that the cathode emits an infinite current when the anode potential is infinite, and we have, in fact, assumed this to be possible. If C_0 is the maximum current which the cathode can emit, the first of the above formulae becomes, by straightforward application of Buckingham's theorem,

$$C/C_0 = \Phi[(e/m)^{1/2}V^{3/2}/KC_0].$$

The same results are obtained if one uses the old electromagnetic or electrostatic system with dielectric constant with dimensions $L^{-2}T^2\mu^{-2}$ or K respectively, but the gain in clarity by not adopting these systems is substantial. The numerical work is also less liable to mistakes. The M.K.S. system is based on the choice of charge as a physical entity in its own right.

(3) *An uncommon unit.* A peculiar situation arises with optical transmission. Since this quantity appears in all equations as a ratio to the maximum transmission, that is as $X/1$ or $X\%/100\%$, it has to be regarded as independent of the units of measurement. But if we take the logarithm of the reciprocal of the transmission as a variable then it becomes a regular physical quantity, variable with the unit. The quantity may extend from zero to infinity, and the unit may be changed by changing the base of the logarithm. Physically the situation is then not essentially different from that of lengths or weights. Two pieces of grey glass of equal transmission T, placed face to face, have a total transmission T^2. But

$$\log 1/T^2 = \log 1/T + \log 1/T$$

and the quantities defined by the logarithms of the reciprocals of the transmission are additive. These quantities are commonly spoken of as "densities." A scale of density may be set up by adopting a piece of grey glass as a standard, making others equal to it, and stacking them together, in a manner exactly similar to that in which a scale of length or weight is established. There are, of course, difficulties with reflexions from the faces of concrete units of density, but these may be overcome. Opportunities for making use of this property of density are limited but it has proved useful.

Owing to the irregular distribution of the grains of silver in developed photographic materials the density fluctuates somewhat from point to point. Suppose we imagine a network to be drawn on the sample so as to divide it up into small equal squares. Then we assume that the mean fluctuation, Δ, of the densities of these squares of the material will be dependent upon some property, G, of the sample and upon the area, a, of any one of the squares. Since there are only three quantities Buckingham's theorem shows that

$$G = \Delta a^{\frac{1}{2}}.$$

Starting from this point application of the theory of probability to the calculation of the fluctuation of density of pairs of squares taken together leads, under certain assumptions, to the result that

$$\Delta = G/a^{1/2}.$$

G, therefore has the dimensions of density multiplied by length.

The irregularity of density tends to obscure detail recorded in a photograph and reasons have been found for believing that at the threshold of resolution the density difference between detail and background is proportional to GR, where R is the reciprocal of some characteristic length in the detail. This relation can easily be deduced by the method of dimensions on the assumption that these are the only quantities involved in the phenomenon, but in fact more must be taken into account. This is one of the failings of the method: it can only decide the form of the equation between assumed variables. The resolving power of a system combining photography and optical image formation is therefore to be found by equating the density difference between detail and background (which is a function, of the size of detail, characteristic of the system) and GR. When such an equation has been solved for R the dimension of density has disappeared, for if the base of the logarithm be changed both sides of the equation are changed in the same ratio. Although, therefore, the symbol G remains in the expression for the resolving power the only dimension it can retain is that of length. Now in an investigation of a group of lenses an empirical formula was found for the average resolving power R over a field of semi-angle, θ, in negatives made with lenses of focal length f and focal ratio (f-number) A, namely,

$$R = \text{constant } (A/\tan^2\theta)^{0\cdot 3}/f^{1/2}.$$

The constant depended upon what film was used for taking the photographs. On examining the formula it is obvious that the left-hand side has the dimensions of a reciprocal of a length, since the resolving power is measured in lines per mm. To make the formula applicable whether one uses millimetres or inches the constant must have the dimensions of the reciprocal of the square root of a length. Since it varies with the film one must look for a property of film involving length. On using G, as suggested by the preceding considerations, the formula becomes

$$R = \text{constant } (A/\tan^2\theta)^{0\cdot 3}/f^{1/2}G^{1/2},$$

the constant now being purely numerical and independent of any units. On trying measured values of G in the formula agreement was found to a degree better than could reasonably be expected.

Qualms can easily be felt about the disappearance of the dimension of density from G. The equation

$$\Delta = GR$$

can, however, be written

$$T_\Delta = T_G^R,$$

where T_Δ is the transparency fluctuation corresponding with Δ and T_G a constant involving transparency fluctuation, corresponding with the constant G. The form of this equation suggests that it would have been much more difficult to deal with the problem if transmission had been used instead of density as a variable. The frequent occurrence of exponential formulae in physics may provide excuses for the same trick of taking the logarithm in order to use dimensional arguments, but it is not known whether it would be worth while.

Radiation intensity from high energy accelerators

By J. D. Lawson, B.A., Atomic Energy Research Establishment, Harwell

[*Paper received* 21 *January*, 1952]

It is shown that the forward radiation intensity from high energy electron accelerators may be calculated quite simply for targets of thickness up to 0·1 radiation length, and that an estimate to within about 15% is often possible for considerably thicker targets. A measurement of the forward radiation from a linear accelerator with a thick copper target operating at 7·3 MeV was made by means of a thick-walled ionization chamber, and found to be in satisfactory agreement with theory.

At energies below about 5 MeV it is not easy to calculate the relationship between electron current and forward X-ray intensity from either thick or thin targets, nevertheless a satisfactory empirical formula has been found which is valid up to an energy of 2 MeV at least.[1] In the present paper it is shown that above about 5 MeV a reasonably accurate calculation can be made quite simply for targets up to about 0·1 radiation lengths in thickness, and that a fair estimate can often be made without difficulty for considerably thicker targets. As an example a calculation is made of the radiation from a thick water-cooled copper target in a linear accelerator operating at 7·3 MeV. The calculated value of the radiation intensity agrees reasonably well with the measured value.

Calculation of the forward radiation intensity

We shall first consider the radiation from a target sufficiently thin that the straggling and energy loss by ionization of the electrons is negligible, but sufficiently thick that multiple scattering is important. The fraction of the electron energy appearing as radiation per unit solid angle in the forward direction from such a target is given approximately by the formula[2]

$$R_0 = (\sigma/\pi c) \ln (E^2 ct/1 \cdot 78\ \mu^2) \qquad (1)$$

where t = thickness of target in "radiation lengths" (for the definition and a table of radiation lengths for some common materials see the appendix).

σ = fractional loss of energy by radiation per radiation length. (A table of values of σ, which is of order unity, is given in the appendix for various materials as a function of energy.)

c = mean squared angle of scattering of the electrons per unit thickness of target.

E = kinetic energy of electrons in MeV.

μ = rest energy of the electron in MeV = 0·51.

The value of c may be expressed in terms of the product of the momentum of the electron, p, and its velocity relative to that of light, β.[3] At energies above about 5 MeV, where $\beta \simeq 1$, we have

$$c = 440/p^2\beta^2 \simeq 440/E(E + 2\ \mu) \qquad (2)$$

Substituting in equation (1), and neglecting 2 μ compared with E under the logarithm, we get

$$R_0 = \frac{\sigma E(E + 2\ \mu)}{440\ \pi} \ln \frac{440\ t}{1 \cdot 78 \mu^2}$$

$$\simeq \frac{\sigma E(E + 1)}{1\ 380} \ln 950\ t \qquad (3)$$

At energies above about 5 MeV this formula should be correct to within about 5% for a target thickness of between 0·01 and 0·1 radiation lengths. If the target thickness is increased above this figure the forward intensity does not increase very much. Even if the electrons lost all their energy in accordance with the above formula the contribution from the rest of the target would not be a large fraction of the total (about $\ln 10/\ln 950 \simeq 30\%$). In fact the contribution will be less than this, both because energy is lost by ionization, and because the r.m.s. angle of scattering per unit thickness increases as the electron energy decreases. Even for a target one radiation length thick we have therefore upper and lower limits to the radiation intensity which are in the ratio of about 3 : 2. Even a rough estimate of the radiation from that part of the target at a depth of more than 0·1 radiation lengths should enable an estimate of the forward radiation within about 15% to be made. Such an estimate must be made with reference to the material and thickness of the target, and must take account of the absorption of radiation in the target. The absorption term is appreciable only for targets greater than about 0·1 radiation length thick, and since most of the radiation comes from the front face of the target it is sufficient to multiply the forward radiation by an attenuation constant α given by

$$\alpha = \int \phi(W) \exp [-\tau(W)t] dW / \int \phi(W) dW \qquad (4)$$

where $\phi(W)$ is the "thin target" spectrum and $\tau(W)$ the absorption coefficient due to Compton effect and pair production as a function of W.

Experimental confirmation of the theory

In order to verify the theory a measurement was made of the X-ray flux from the linear accelerator constructed by Metropolitan-Vickers Electrical Co. Ltd. for the Medical Research Council.[4] The machine was operated at an energy of 7·3 MeV and a current of 5 μA, and the radiation from a water-cooled copper target was measured with a thick-walled aluminium ionization chamber placed 100 cm from the target. The result of this measurement is shown in the figure, where the ratio of the current per c.c. of the cavity in the ionization chamber to the current in the accelerator is plotted against the thickness of the front wall of the chamber.

In order to calculate the radiation intensity we must know the sensitivity of the ionization chamber. Calibration curves for such a chamber in terms of $S_0(W)$, the fraction of incident energy converted to ionization per cm of aluminium as a function of X-ray energy have been given by Flowers, Lawson and Fossey.[5] The overall sensitivity s, defined as the fraction of the incident energy converted to ionization per cm of air space, can be found if the air equivalent of aluminium and the X-ray spectrum are known. The air equivalent of aluminium is shown by Flowers, Lawson and Fossey[5] to be $1 \cdot 1 \times$ (density of air)/(density of aluminium) = $5 \cdot 25 \times 10^{-4}$, and

the radiation spectrum was taken to be of the form given by Rossi and Greisen for 7·3 MeV electrons, multiplied by the absorption coefficient of the whole target. This is not seriously in error since most of the forward radiation comes

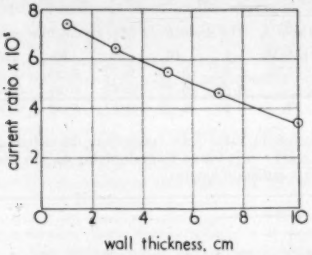

Ratio of the current per c.c. of cavity in the aluminium ionization chamber to the current in the linear accelerator. Ionization chamber 100 cm from target, accelerator energy = 7·3 MeV

from the front face of the target, furthermore the chamber sensitivity is not strongly dependent on the shape of the spectrum at these energies. The overall sensitivity of the chamber is therefore given by

$$s = 5{\cdot}25 \times 10^{-4} \frac{\int(\phi W)\exp[-\tau(W)t]S_0(W)dW}{\int\phi(W)\exp[-\tau(W)t]dW} \qquad (5)$$

This expression may easily be evaluated by numerical integration.

The following quantities are needed to deduce R, the fraction of electron energy converted to radiation per unit solid angle in the forward direction:

I_a = accelerator current = 5×10^{-6} A.
E = accelerator voltage = $7{\cdot}3 \times 10^6$ V.

Details of the method of measuring I_a and E are given by Miller.[4]

t = target thickness = 8·5 g/cm² of copper + 0·48 g/cm² of water (for details see below).
s = overall chamber sensitivity given by equation (5) = 21×10^{-6}.
v = number of electron volts to produce 1 ion pair = 32 eV.
V = volume of air space in ionization chamber = 0·48 c.c.
I_c = ionization chamber current with 5 cm wall thickness = $1{\cdot}31 \times 10^{-10}$ A.
d = distance between target and chamber = 100 cm.

In terms of these quantities

$$R = I_c d^2 v / I_a E s V$$
$$= 0{\cdot}11.$$

The accelerator has a water-cooled target consisting of alternate layers of copper and water. The thickness of the layers starting with the copper are $\frac{1}{16}$, $\frac{1}{16}$, $\frac{1}{8}$, $\frac{1}{16}$, $\frac{1}{8}$, $\frac{1}{16}$, $\frac{1}{16}$ in. The total thicknesses of copper and water being $\frac{3}{8}$ and $\frac{3}{16}$ in respectively. Some relevant properties of the target materials are shown in Table 1.

Unfortunately the condition that the ionization loss should be rather smaller than the radiation loss does not hold for such a light element as copper at this energy, so that equation (3) must be applied with caution. It should be valid,

Table 1. *Properties of the target materials*

	Copper	*Water*
Thickness in g/cm²	8·5	0·475
Thickness in radiation lengths	0·68	0·011
Ionization loss in MeV/g/cm² at 7·3 MeV	1·5	1·9
σ	0·72	0·66

however, without much error for a thickness of target such that the energy loss by ionization and radiation together is less than 10%. A simple calculation based on the table shows that a 10% energy loss corresponds to a target thickness of approximately 0·035 radiation lengths. The radiation intensity from this thickness of target may be found from equation (3), substitution of σ, E and t give $R = 0{\cdot}11$, this represents a lower limit to the total forward radiation from the target. An upper limit may be found by substituting in equation (3) a value of t given by the range of the electrons. The average range is given by the expression

$$r = \int_0^E dE/[-(dE/dt)_c - (dE/dt)_R] \qquad (6)$$

where $-(dE/dt)_c$ and $-(dE/dt)_R$ are the expressions for collision and radiation loss respectively. Convenient expressions for these quantities are given by Heitler,[6] and an evaluation of equation (6) gives a range of 0·4 radiation lengths. Substitution of this figure in equation (3) gives $R = 0{\cdot}19$. The true value of R is certainly therefore between 0·11 and 0·19, and may be quoted as $0{\cdot}15 \pm 0{\cdot}04$ for certain with a probable error of very much less than this. Before comparing this value of R with the measured R we must allow for absorption of energy in the target. This can be done by multiplying the calculated R by α defined in equation (4). The value of α was computed and found to be 0·64. A reasonable estimate of R would then be $0{\cdot}64 \times 0{\cdot}15 \pm 15\% = 0{\cdot}096 \pm 15\%$. This is in satisfactory agreement with the measured value of $R = 0{\cdot}11$.

CONCLUSION

It has been shown that at energies above about 5 MeV the forward radiation intensity from a fairly thin electron accelerator target is given by a simple formula, and that for thicker targets each case must be considered individually, although a reasonable estimate can often be arrived at quite simply. An example of a more accurate calculation for a specific case may be found in a recent paper by Lanzl and Hanson,[7] where excellent agreement between the shape of the theoretical and measured curves is reported, although an absolute measurement of the forward intensity was not made. In general, however, it will probably be more profitable to investigate the radiation from thick targets experimentally, and to use thin targets in experiments where an accurate knowledge of the spectrum and intensity is required.

ACKNOWLEDGEMENTS

The author is indebted both to the Medical Research Council and Metropolitan-Vickers Electrical Co. Ltd., Manchester, for permission to use the linear accelerator, and would like to acknowledge the help and co-operation of Mr. C. W. Miller and the research team at Manchester during the experiment. This paper is published by permission of the Director, the Atomic Energy Research Establishment, Harwell.

REFERENCES

(1) Kaye, G. W. C., and Binks, W. *Brit. J. Radiol.*, **16**, p. 193 (1940).

(2) LAWSON, J. D. *Phil. Mag.*, **43**, p. 306 (1952).
(3) ROSSI, B., and GREISEN, K. *Rev. Mod. Phys.*, **13**, p. 240 (1941).
(4) MILLER, C. W. Metropolitan-Vickers Research Report No. 4882. To be published.
(5) FLOWERS, B. H., LAWSON, J. D., and FOSSEY, E. B. *Proc. Phys. Soc., Lond.*, **65B**, p. 286 (1952).
(6) HEITLER, W. *The Quantum Theory of Radiation*, 2nd Ed. (London: Oxford University Press, 1944).
(7) LANZL, L. H., and HANSON, A. O. *Phys. Rev.*, **83**, p. 959 (1951).

APPENDIX

The *radiation length* is defined as $720A/Z^2 \ln 183Z^{-\frac{1}{3}}$, where A = atomic weight and Z = atomic number.[3]

Table 2. *The thickness in g/cm² of one radiation length of some common substances*

Substance	H	C	O	H_2O	Al	Cu	Pb
g/cm² per radiation length	138	52	39·7	43	26·3	13·3	5·9

Table 3. *The dependence of σ on electron energy*

Energy (MeV)		5	10	20	50	100	500
σ	H_2O	0·61	0·70	0·77	0·85	0·89	0·95
	Cu	0·66	0·77	0·82	0·88	0·92	0·97
	Pb	0·69	0·78	0·83	0·89	0·93	0·98

The values in Table 3 are taken from the curves on p. 173, reference (6). σ is found by multiplying ϕ_{rad} by the number of cm in a radiation length.

An improved apparatus for the differential thermal analysis of minerals

By J. J. THERON, B.Sc., National Chemical Research Laboratory, Pretoria, South Africa

[*Paper received* 29 *May*, 1951]

An automatic apparatus for carrying out the differential thermal analysis of minerals is described. The apparatus used by some other authors is discussed briefly. The electronics of the proportioning temperature control is described and circuit diagrams and an indication of the performance of the control and differential amplifiers are given.

INTRODUCTION

Differential thermal analysis has become one of the major techniques in the identification and characterization of clays, but is also applicable to other minerals. Although the basic technique itself was applied by le Chatelier[1] as long ago as 1887, it is only comparatively recently that the method has found general application. Various types of apparatus have been used by workers in this field and it is the purpose of this paper to describe an apparatus which is believed to combine the advantages of previous apparatus while avoiding the disadvantages.

Briefly, the procedure and principle of differential thermal analysis may be outlined as follows: The mineral under consideration is heated to about 1 000° C in a furnace at a given rate. During the run the sample undergoes reactions such as loss of adsorbed water, loss of crystalline water, crystalline inversion, crystallization, partial fusion, etc., all accompanied by evolution or absorption of heat. Therefore during reaction the sample is at a higher or lower temperature than the furnace. This temperature difference is measured by means of a differential thermocouple, the other junction of which is placed in some thermally inert material such as calcined alumina, which is assumed to be at furnace temperature during the run. The plot of differential temperature (or voltage) with furnace temperature constitutes the differential thermal curve which is used to characterize and identify the sample.

DISCUSSION OF PREVIOUS APPARATUS

The apparatus for carrying out a differential thermal analysis may be described conveniently under four headings: (i) furnace, (ii) sample and thermocouple holder, (iii) heating programme controller, and (iv) differential recorder.

(i) *Furnace.* Furnaces have invariably been electrically heated, tube furnaces being mounted either horizontally or vertically. Judging from the literature there seems to be no reason to prefer one or the other mode of mounting.

(ii) *Sample and thermocouple holder.* Different authors have proposed various types of sample and thermocouple holders. Some prefer a nickel or stainless steel block with holes drilled to contain thermocouples and sample,[3,4,8] while others[5,9,10] prefer a ceramic block with noble metal or refractory cups, made for insertion into either a horizontal or vertical furnace as the case may be. Herold and Planje[10] use a composite sample holder made of platinum and platinum/rhodium alloy as the differential thermocouple itself, mounted in a refractory block. There are certain objections against these methods of holding the sample. In the case of the nickel or stainless steel holder the metal acts as a large reservoir of heat with high thermal conductivity which tends to decrease the magnitude of the differential voltage since heat is rapidly removed from or supplied to the reacting mineral. On the other hand, if the sample is held in a refractory block the magnitude of the differential voltage is appreciably increased, but there is a large thermal gradient between sample and furnace, and the accurate control of the furnace by means of the temperature measuring thermocouple imbedded in the ceramic block becomes difficult due to large thermal lag.

Gruver[8] overcomes these particular difficulties by containing the sample and alundum in small removable platinum crucibles suspended from a refractory tube. The temperature measuring thermocouple is permanently fixed between the two crucibles, in free air. Since the containers themselves have low heat capacity but high conductivity, the differential voltage is a maximum, while there is no appreciable lag between the furnace and sample. Experiment has shown that in the case of quartz the sensitivity of this type of holder is about four times that of the metal block type at 15° C/min heating rate.

(iii) *Heating programme.* The heating programme may be obtained in several ways. Since the rate of heating affects

the position of most peaks it is necessary to maintain a reproducible rise in temperature with time whatever the heating gradient in order to obtain comparable results. Manual control, maintenance of fixed wattage,[9] motor-driven variable transformers[3,4,7] and liquid rheostats[2] have been used, but the modern and more precise way is to use an electronic or electrical programme controller.[5,6,8,10] These instruments have the further advantage that the controlled rate of heating can be set usually by merely rotating a dial knob. Thus, for instance, a programme controller of Leeds and Northrup Co. maintains a substantially linear rate of heating between 0° C and 50° C/min.

(iv) *Differential recorder.* In principle it is easy to obtain the differential record since an ordinary galvanometer may be used and the deflexions at different furnace temperatures noted manually. A number of difficulties must be overcome if this voltage is to be recorded automatically. The photographic recording described in earlier papers[2,3,4] is a tedious process necessitating dark room facilities and light-tight equipment. Quite apart from this the fact that the differential record cannot be observed while the run is progressing is a definite disadvantage.

In all except a few cases the voltages obtained from the differential thermocouple are small, of the order of 50–500 μV, and even using the most sensitive electronic recorders commercially available, some form of amplification is necessary to obtain records with good definition. Since great difficulty is experienced in obtaining satisfactory operation of ordinary direct coupled amplifiers, other means of obtaining an amplified differential record have to be resorted to. The procedure often followed is to interrupt the d.c. thermocouple voltage by means of a synchronous vibrator. This interrupted d.c. may then be amplified by conventional a.c. methods and rectified by some form of phase sensitive rectifier and then recorded on an ordinary d.c. recorder. However, leakage currents in the electrically heated furnace cause the amplifier to give a spurious response at high temperatures when current is flowing in the furnace windings, especially if the vibrator is driven at mains frequency.[13] This effect may be reduced by driving the vibrator at some other frequency by means of a vacuum tube oscillator, but even then these leakage currents may be troublesome at high sensitivities. This type of amplifier is inevitably fairly complicated and expensive. The method used by the National Building Research Institute of the South African Council for Scientific and Industrial Research with satisfactory results employs a commercial feed-back galvanometer photocell d.c. amplifier.[11] The fact that this device, like all galvanometer instruments, is sensitive to vibration necessitates rigid mounting, but this has not affected the results.

DESIGN OF PRESENT APPARATUS

(*a*) *General considerations.*

The apparatus described in this paper and at present in use in this laboratory has been designed with due consideration given to the factors pointed out in the above discussion, and embodies the following features:

(i) Four Kanthal *A*-wound tube furnaces after the design of Gruver,[8] any one of which may be selected by means of a switch.

(ii) Thermocouple and sample holder after the design of Gruver.[8] Platinum/platinum, 13% rhodium thermocouples are used for the differential and temperature recording thermocouples since their very much longer life compared to that of chromel-alumel thermocouples makes them preferable in spite of the much lower e.m.f. developed by them. The cold junctions are maintained at 0° C in a vacuum flask containing ice.

(iii) Electronically controlled linear heating programme with heating rate variable between 0° C and 50° C/min up to 1 100° C.

(iv) Full-scale deflexion on differential recorder of voltages between 75 μV and 1 500 μV in eleven steps, using a feed-back galvanometer type d.c. amplifier.

(v) Simultaneous recording of temperature and differential voltage on one chart only by a 6-point centre-zero Speedomax recording millivoltmeter (f.s.d. = 3 mV), manufactured by the Leeds and Northrup Co.

(vi) Completely automatic operation after certain initial adjustments have been made.

(*b*) *Heating programme and associated mechanism.*

Heating rates are controlled by varying the voltage applied to the furnace winding, using a Variac driven by a reversible split-field d.c. motor. The heating programme is obtained by driving a potentiometer with a synchronous clock motor. This potentiometer supplies a direct current e.m.f. which is balanced against the e.m.f. from the controlling (and recording) platinum/platinum, 13% rhodium thermocouple in the furnace, to supply a difference voltage. This difference voltage is used to activate the motor driving the Variac after amplification. [See Section (*c*).]

Provision is made by a system of relays to apply voltage to the amplifiers used for measurement and control without applying power to the furnace or the synchronous motor driving the programme potentiometer. The furnace and programme motor are brought into operation by a press-button switch through relays, when it is desired to commence a run. The recording meter may be brought into operation for calibration purposes only or is placed under control of the button switch by a two-position toggle switch. A contact on the programme potentiometer which is reached at the end of a run switches off the power to the whole instrument.

A 2 V accumulator is used to supply the voltage to the programme potentiometer and this voltage is calibrated against a standard cell using an electron ray tube as detector through the control amplifier. A battery charger is built in to charge this battery as well as the 6 V accumulator used to heat the filaments of the first two stages of the control amplifier.

Unlike the chromel-alumel temperature-e.m.f. relationship, that of platinum/platinum, rhodium is non-linear to a considerable extent and this factor complicates the design of the programme potentiometer. This can only be overcome by using a non-linear potentiometer wound in such a way that the linear angular movement of the moving contact with time will give the required temperature-time relationship. The discrete voltage increments from one winding of the potentiometer to the next should also be so small that no heating surges will take place in the furnace due to the movement of the variable contact. This was satisfactorily accomplished by winding 1 000 turns of 18# manganin wire on a Perspex former, machined to dimensions calculated from standard temperature-e.m.f. tables. It was necessary to machine all dimensions to a tolerance of $\pm$ 0·001 in. At no point was the voltage error more than $\pm$ 5 μV, and in fact overall performance indicates that the programme over the whole range varies by no more than $\pm$ 1° C from the nominal setting.

To obtain the variable heating rate of the programme two synchronous motors are used, one running all the time and driving a small wheel with point contacts on it which operate two micro-switches. One micro-switch is fixed while the other can be rotated through about 330°. The angle

between the micro-switches determines, with the aid of a double-pole, double-throw relay, the percentage time which the other synchronous motor which drives the programme potentiometer, is running. An angle of 0° corresponds to 0% running time and an angle of 330° to 100% running time, i.e. to a temperature rise of 50° C/min. A dial may then be calibrated directly in degrees/min temperature rise. This cycle is repeated every 20 sec, causing voltage increments in steps of about 150 μV at 50° C/min temperature rise. Due to thermal inertia these small steps are not apparent in the recorded temperature-time curve.

(c) Temperature control and measurement and associated mechanism.

Temperature control is obtained by feeding the out-of-balance voltage between the furnace thermocouple and programme potentiometer to a breaker type d.c. amplifier which actuates one of two thyratrons according to the polarity of the difference voltage. The circuit diagram of the control amplifier is given in Fig. 1. Each thyratron controls one of

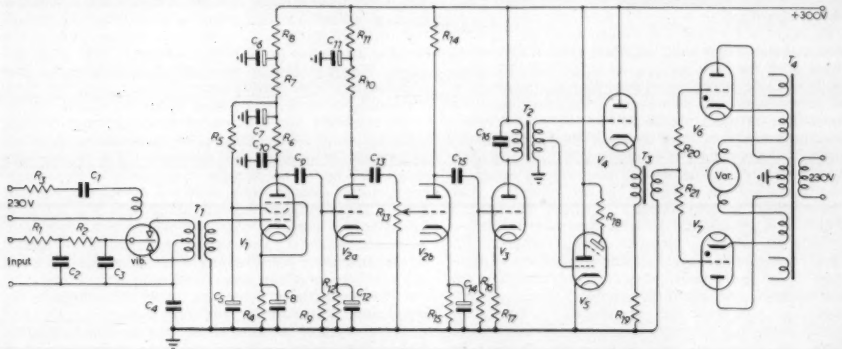

Fig. 1. Circuit diagram of programme control amplifier

R_1, R_2 = 5 kΩ
R_3 = 10 kΩ, 10 W (w.w.)
R_4 = 1 kΩ
R_5 = 250 kΩ
R_6 = 95 kΩ (precision w.w.)
R_7, R_8 = 10 kΩ
R_9 = 1 MΩ
R_{10} = 0·5 MΩ
R_{11} = 0·25 MΩ
R_{12} = 3 kΩ
R_{13} = 1 MΩ
R_{14} = 0·5 MΩ
R_{15} = 3 kΩ
R_{16} = 1 MΩ
R_{17} = 5 kΩ
R_{18} = 1 MΩ
R_{19} = d.c. resistance of T_3
R_{20}, R_{21} = 10 kΩ

C_1 = 0·25 μF, 600 V
C_2, C_3 = 8 μF
C_4 = 5 μF
C_5, C_6, C_7 = 8μF, 450 V
C_8 = 25 μF, 25 V
C_9, C_{10} = 0·02 μF, 600 V
C_{11} = 8 μF, 450 V
C_{12} = 25 μF, 25 V
C_{13} = 0·02 μF, 600 V
C_{14} = 25 μF, 25 V
C_{15} = 0·1 μF, 600 V
C_{16} = 0·5 μF, 600 V

V_1 = 6SJ7
V_2 a + b = 6SL7-G
V_3 = 6SF5
V_4 = 6V6
V_5 = 6U5-G
V_6, V_7 = FG27-A

T_1 = input transformer in electronic recording millivoltmeter
T_2 = 1 : 4 interstage transformer
T_3 = 1 : 1 interstage transformer
T_4 = transformer for thyratron plate filament and bias supply

Vib = synchronous vibrator in recording millivoltmeter

the field coils of the d.c. motor driving the Variac. Thus the Variac is caused to turn in a direction which will oppose and tend to cancel the difference voltage. The furnace temperature thus follows the programme.

The furnace temperature is directly recorded from the control thermocouple on one point of the 6-point Speedomax recording millivoltmeter. A voltage divider divides the thermocouple voltage in the ratio 3 : 11·81 since 11·81 mV is the e.m.f. of a platinum/platinum, 13% rhodium thermocouple at 1 100° C. (Cold junction at 0° C.) Due to the fact that the recorder is a centre-zero instrument, variable bias from a dry cell is supplied to spread the temperature record over the whole chart. Another of the six points is used to indicate the bias voltage only. The temperature is then read from this line by means of a calibrated scale.

The input circuit, which is similar to that used by Leeds and Northrup Co. in their recording electronic millivoltmeters, is fed on to a pentode type 6SJ7 through a synchronous vibrator and isolating transformer, and earthed through a capacity only, thus minimizing hum pick-up. The fact that the input impedance of the balancing and thermocouple network is low (about 10 Ω) is, however, chiefly responsible for the elimination of interference, as also the fact that lead wires are twisted wherever possible. The filaments of the first two stages are run off a 6 V accumulator, since a.c. heated filaments caused interference. Biasing the filaments with respect to the cathode showed no improvement. A considerable amount of trouble was experienced due to d.c. thermocouple voltages in soldered connexions, but it was found that selection of the input carbon filter resistances gives a minimum of about 15 μV d.c. potential on the input side. This voltage did not vary once operating temperature had been reached. Wire-wound resistors proved completely unsatisfactory. Further sources of trouble were high frequency vibrator "mush" and valve noise. It was possible to obtain a noise level of about 0·5 μV by carefully selecting components in this circuit and peaking the input valve's response to a frequency much lower than mains frequency (50 c/s) to reject high frequency noise and subsequently tuning at a later stage to reject low frequency noise.

The two thyratrons are powered by a centre-tapped transformer and are transformer-biased to cut-off in the cathode circuit. One of the split-field windings of the motor is in each cathode circuit and the return to earth is completed through the armature of the motor driving the power Variac. Since positive and negative potentials are transformed into sine waves 180° out of phase with each other, positive d.c. potentials will fire one thyratron only and negative d.c. potentials the other, provided that these sine waves are in correct phase relationship with the cathode biasing voltage. The phase shift in the amplifier is about 90° and this is corrected for by feeding the vibrator through a condenser which further advances the

phase angle by 90°. At full gain (about 2×10^6) a signal of 3 μV either way is sufficient to actuate one or the other thyratron, while normally the threshold voltage is set at about 10 μV. This voltage serves as a stimulating signal to

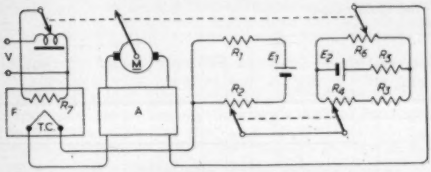

Fig. 2. Schematic diagram of temperature control feed-back loop. (All resistors except R_1 and R_5 are made of manganin wire)

R_1 = 300 Ω
R_2 = programme potentiometer shunted by 2·5 Ω
R_3 = 0·06 Ω
R_4 = 0·14 Ω
R_5 = 150 Ω
R_6 = 20 Ω
R_7 = 2 kW Kanthal-*A* furnace winding

E_1 = 2 V accumulator
E_2 = 1½ V telephone cell

A = amplifier
M = split-field d.c. motor
V = 2 kVA Variac
F = furnace

drive the Variac in the correct direction to bring the system to equilibrium again.

A diagram to illustrate the function of the control system is shown in Fig. 2. Suppose that a positive out of balance signal is fed into the control amplifier *A* (i.e. corresponding to a temperature greater than that required by the programme), then the Variac *V* would be turned down by the motor *M* in an attempt to balance out the signal and would continue downwards until balance is reached. As soon as this occurs the Variac would stop. However, due to thermal lag effects between the thermocouple *TC* and heater winding R_7, too much heat will have been lost and this loss will have to be made up by increasing the voltage on the winding until the temperature indicated by the thermocouple exceeds that required by the programme. The measured temperature will therefore oscillate about the required temperature by a certain amount. Whatever the speed of the Variac (experimentally varied between 10 r.p.m. and $\frac{1}{200}$ r.p.m.), these oscillations were of the order of $\pm$ 50° C. It therefore became necessary to inject a correcting signal as well as the out of balance voltage into the amplifier and this was done in the following way: A potentiometer R_6 is mounted on the Variac shaft which on rotation of the Variac injects a signal of such polarity that it allows only a limited movement of the Variac brush, the system then coming to balance. As soon as unbalance occurs (the speed of the Variac is about 5 r.p.m.), the Variac moves to a new position in phase with the unbalance voltage, thus restoring balance. This is in contrast to the state of affairs without the injection of the correcting signal, where there is a phase lag between unbalance and restoration of balance. Since the Variac must perform two functions, i.e. (*a*) supply the average amount of power to the furnace to cause it to rise linearly in temperature according to the programme, (*b*) correct any chance deviation from the programme, it is necessary to make the balance position of the Variac rise synchronously with the programme. Experimentally it was found that a voltage of about 100 V across the furnace winding was necessary to start the run with, while the potential difference at the end rises to about 180 V. It was

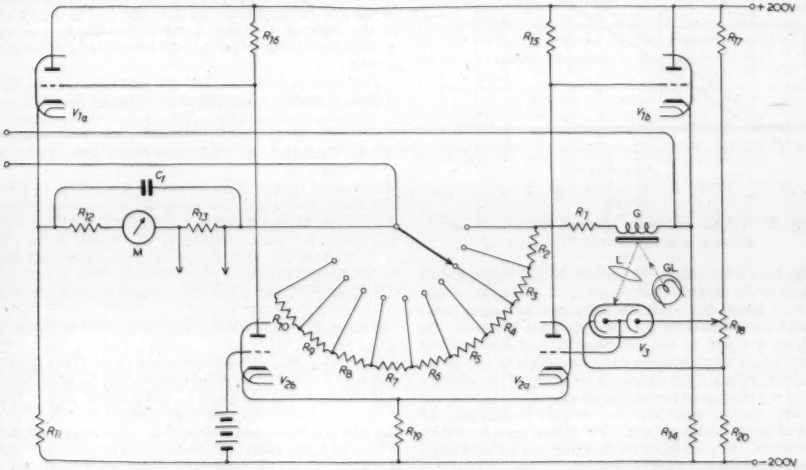

Fig. 3. Circuit diagram of feed-back photoelectric galvanometer d.c. amplifier

R_1 = 0·05 Ω
R_2, R_3, R_4, R_5 = 0·025 Ω
R_6 = 0·05 Ω
R_7, R_8, R_9 = 0·1 Ω
R_{10} = 0·5 Ω
R_{11} = 50 kΩ
R_{12} = 25 kΩ
R_{13} = 1 Ω
R_{14} = 50 kΩ
R_{15}, R_{16} = 0·5 MΩ
R_{17} = 2 MΩ
R_{18} = 1 MΩ (volume control)
R_{19} = 65 kΩ
R_{20} = 0·18 MΩ

C_1 = 4 μF, 100 V
S_1 = 10 position single pole stud switch
G = galvanometer (40 Ω coil resistance, 2 sec period, sensitivity: 15 mm/μA at 1 meter)

L = focusing lens
G.L. = galvanometer lamp (3·5 W, 6 V)
V_{1a+b} = 6SL7 − *G*
V_{2a+b} = 6SL7 − *G*
V_3 = 920

assumed that the rise in potential with time was linear, as a first approximation. This proved satisfactory, but better control would be obtained where there is a large thermal lag between winding and control element, if the Variac voltage followed the correct curve with time. A second potentiometer R_4 was therefore fitted to the shaft of the programme potentiometer R_2 and brings about a linear rise of voltage from a certain threshold as the programme is carried out.

(d) Recording and amplification of differential voltage.

In view of the complexity and cost of the differential amplifier described by Theron, Heydenrych and Anderson,[13] as well as its inherent disadvantages, it was decided to use a feed-back galvanometer photocell amplifier to amplify the differential voltage.[11, 12] It is similar in principle to the amplifier described by Gall[11] as well as a photo-electric recording potentiometer obtainable commercially. The circuit diagram is given in Fig. 3.

The optical system is simple, consisting only of a light source focused by one lens on to the galvanometer mirror from where it is reflected directly on to the photocell which is placed about 15 cm away. The light source, photocell and galvanometer are rigidly mounted on a chassis supported by anti-vibration mounting in a wooden box which in turn is mounted on rubber supports. The whole instrument must also be rigidly mounted.

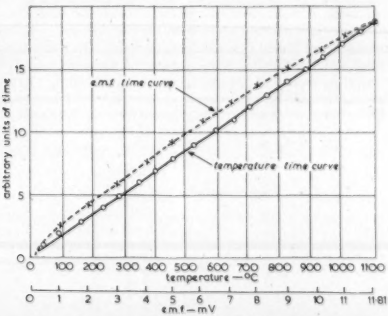

Fig. 4. Typical record of derived temperature-time curve at a heating rate of 15° C/min

The light beam should be equally divided between each cathode of the photocell and the single stage balanced amplifier is so biased that when this is the case no current flows between the cathodes of the output cathode followers. On applying a signal to the galvanometer, unbalance of the system occurs which causes a restoring current to flow in the feed-back resistor until balance is attained. This restoring current is a measure of the original signal and may be recorded as such. Various sensitivities are obtained by changing the value of the feed-back resistor. The system must be slightly overdamped and conditions for damping and self-oscillation are similar to those treated by Gall.[11]

This amplifier has so far given satisfactory service for about seventy runs. The noise level is low and after a preliminary warm-up of about 5 min, no further drift is evident even at high sensitivities. The input impedance is of the order of 50 000 Ω, but in spite of this long leads may be used since "pick-up" does not affect the amplifier.

RESULTS

A plot of the e.m.f.-time curve with the corrected temperature-time curve is given in Fig. 4 at a heating rate of 15° C/min. Except for a slight undershoot at low temperatures, the programme is adhered to, to within ± 1° C over the whole range.

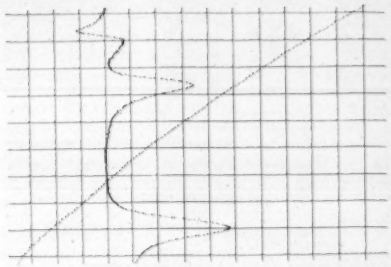

Fig. 5. Curve of Wyoming bentonite illustrating the actual type of record obtained. Sensitivity 350 μV full-scale deflexion

Some differential curves are given in Fig. 5 to illustrate the records obtained by the apparatus.

ACKNOWLEDGEMENTS

I am indebted to Mr. J. Wanklyn of the National Chemical Research Laboratory and to Mr. N. T. van der Walt of the National Physical Laboratory, South Africa, for their frequent advice and help. Thanks are also due to Mr. H. Heystek of the National Chemical Research Laboratory who constructed the differential furnace and sample and thermocouple holders.

This paper is published with the permission of the South African Council for Scientific and Industrial Research.

REFERENCES

(1) LE CHATELIER, H. *Bull. Soc. Franc. Min.*, **10**, p. 204 (1887).
(2) NORTON, F. H. *J. Amer. Ceram. Soc.*, **22**, p. 54 (1939).
(3) GRIM, R. E., and ROWLAND, R. A. *J. Amer. Ceram. Soc.*, **27**, p. 5 (1944).
(4) SPEIL, S., BERKELHAMER, L. H., PASK, J. A., and DAVIES, B. *U.S. Bureau of Mines*, Technical Paper No. 664 (1945).
(5) KERR, P. F., and KULP, J. L. *Amer. Mineral.*, **33**, p. 387 (1948).
(6) KERR, P. F., and KULP, J. L. *Amer. Mineral.*, **34**, p. 839 (1948).
(7) BECK, C. W. *Harvard University Ph.D. Thesis* (1946).
(8) GRUVER, R. M. *J. Amer. Ceram. Soc.*, **31**, p. 323 (1948).
(9) GRIMSHAW, W., HEATON, E., and ROBERTS, A. L. *Trans. Brit. Ceram. Soc.*, **44**, p. 69 (1945).
(10) HEROLD, P. G., and PLANJE, T. J. *J. Amer. Ceram. Soc.*, **31**, p. 21 (1948).
(11) GALL, D. C. *J. Instn Elect. Engrs*, **89**, Part II, No. 11 (1942).
(12) *Vacuum Tube Amplifiers*, Vol. 18, Radiation Laboratory Series, pp. 487–91 (New York: McGraw-Hill Book Co., 1948).
(13) THERON, J. J., HEYDENRYCH, J. C. R., and ANDERSON, F. *J. Sci. Instrum.*, **26**, p. 7 (1949).

Conduction of heat in tissue supplied with blood

By Professor J. C. Jaeger, M.A., D.Sc., F.Inst.P., The Australian National University, Canberra

[*Paper received* 2 *April*, 1952]

A linear partial differential equation is suggested as a crude approximation to the equation of conduction of heat in tissue supplied with blood. Solutions of some simple cases are given and compared with experimental results.

Cook[1] has recently measured the rise in temperature of human tissue when irradiated with microwaves. He concludes that when the blood supply is cut off the observed skin temperature agrees very well with that calculated from the mathematical theory of conduction of heat provided the thermal conductivity of the tissue is taken to be 0·005 (units are c.g.s. and °C throughout). But in the presence of blood supply the observed temperature behaves in a very different way (tending to a horizontal asymptote instead of increasing steadily) and can only be fitted on the assumption that the conductivity of the tissue increases by a factor of three over a time of the order of a minute. Similar effects were observed by Mendelssohn and Rossiter,[2] who measured subcutaneous temperatures when the skin was placed in contact with a burning iron and found them to tend to temperatures substantially less than that of the iron. In both cases the effects are ascribed to a change in conductivity with temperature caused by the blood flow, so that the problem becomes non-linear and no exact theoretical solutions are available.

The object of this note is to draw attention to a crude approximation to the effect of the blood flow which still leads to a linear differential equation, which can be solved in a wide variety of cases. Suppose the tissue has conductivity K, density ρ, specific heat c, and diffusivity $\kappa = K/\rho c$, all of which are constants. Suppose also that v is its temperature at the point (x, y, z) and that heat is supplied at the rate H_0 per unit time per unit volume throughout the solid (e.g. by microwave radiation). The approximation to the effect of blood flow referred to above consists of assuming that mass m of blood of specific heat c' is removed per unit time per unit volume at each point at the temperature v at that point and is replaced by the same mass at a fixed temperature V.

Then the differential equation satisfied by the temperature v becomes

$$\nabla^2 v - \frac{1}{\kappa}\frac{\partial v}{\partial t} - \frac{mc'}{K}(v - V) = -\frac{H_0}{K} \qquad (1)$$

This equation is linear and, for one-dimensional systems at least, is readily solved by the Laplace transformation method. The three simplest cases are given below; there is no difficulty in extending them, e.g. by taking $V \neq 0$ and including an initial temperature variation in (i) and (ii), but the formulae become rather clumsy. Composite solids with different values of m in different regions can also be studied.

(i) *The region* $x > 0$ *with* $V = 0$, $H_0 = 0$, *and zero initial temperature. The surface* $x = 0$ *maintained at constant temperature* V_0 *for* $t > 0$.

In this case equation (1) becomes

$$\frac{\partial^2 v}{\partial x^2} - \frac{1}{\kappa}\frac{\partial v}{\partial t} - \frac{mc'}{K}v = 0 \qquad (2)$$

and its solution with $v = V_0$ when $x = 0$ is

$$v = \tfrac{1}{2}V_0\left\{\exp(-\beta x)\operatorname{erfc}\left[\frac{x}{2\sqrt{(\kappa t)}} - \beta\sqrt{(\kappa t)}\right] + \exp(\beta x)\operatorname{erfc}\left[\frac{x}{2\sqrt{(\kappa t)}} + \beta\sqrt{(\kappa t)}\right]\right\} \qquad (3)$$

where

$$\beta = (mc'/K)^{\frac{1}{2}} \qquad (4)$$

and

$$\operatorname{erfc} z = \frac{2}{\sqrt{\pi}}\int_z^\infty e^{-u^2}\,du, \quad \operatorname{erf} z = 1 - \operatorname{erfc} z.$$

For large values of the time the temperature tends to

$$V_0 \exp(-\beta x) \qquad (5)$$

and so β is determined if this value is known. This is an approximation to the conditions of Mendelssohn and Rossiter.[2]

(ii) *The region* $x > 0$ *with* $V = 0$, $H_0 = 0$, *and zero initial temperature. At* $x = 0$ *for* $t > 0$ *there is heat transfer from a medium at* V_0 *at the rate* $Kh(V_0 - v_s)$, *where* h *is a constant and* v_s *is the surface temperature of the region.*

Here the solution is

$$v_s = \frac{hV_0}{h^2 - \beta^2}\left[(h - \beta\operatorname{erf}\beta\sqrt{(\kappa t)}\right] - \frac{h^2 V_0}{h^2 - \beta^2}\exp\left[-\kappa t(\beta^2 - h^2)\right]\operatorname{erfc} h\sqrt{(\kappa t)} \qquad (6)$$

where β is defined in equation (4). As $t \to \infty$ the surface temperature tends to $hV_0/(h + \beta)$, and if this is known it gives the ratio h/β. This result, and its extensions to non-zero V and initial temperature may also be used to discuss the experiments of Mendelssohn and Rossiter.

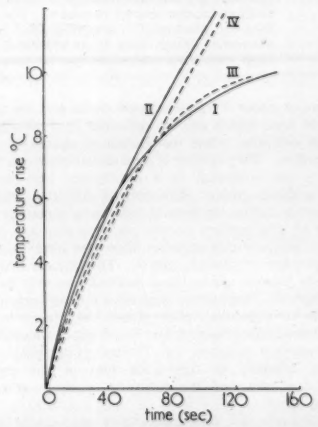

Skin temperature of tissue heated by microwaves.

Curves I and III are calculated and observed, respectively, for unimpeded blood supply. Curves II and IV are for occlusion of blood supply

(iii) *The region $x > 0$ with no loss of heat from the surface $x = 0$. The initial temperature $V(1 - e^{-ax})$, and the rate of heat production $H_0 = A_0 e^{-ax}$.*

The exponential form of initial temperature is chosen because the results are easy to calculate, $a = 0{\cdot}56$ leads to the surface gradient of 2° C per cm used by Cook.[1]

The surface temperature is found to be

$$\frac{A_0}{K(\beta^2 - \alpha^2)\beta}\{\beta - \alpha \operatorname{erf} \beta\sqrt{(\kappa t)} - \beta \exp\left[-\kappa(\beta^2 - \alpha^2)t\right] \operatorname{erfc} \alpha\sqrt{(\kappa t)}\} + V - V \exp\left[-\kappa(\beta^2 - a^2)t\right] \operatorname{erfc} a\sqrt{(\kappa t)} \quad (7)$$

where β is defined in equation (4). As $t \to \infty$ the surface temperature tends to

$$V + \frac{A_0}{K\beta(\beta + \alpha)} \quad (8)$$

This corresponds to the problem of Cook[1] in which all the quantities are known numerically so that quantitative comparison is possible. Taking the values of his Fig. 4, namely, $K = \kappa = 0{\cdot}005$, $\alpha = 1{\cdot}5$, $A_0 = 0{\cdot}184$, assuming $V = 3{\cdot}6°$ C (the excess of blood heat above initial skin temperature), and that the final skin temperature is 11° C above its initial value, gives $\beta = 1{\cdot}6$, which, with $c' = 1$, $K = 0{\cdot}005$ in equation (4), corresponds to a blood supply of 0·013 g per c.c. per sec. Curve I of the figure gives the calculated surface temperature for this case with $a = 0{\cdot}56$, and Curve II the corresponding case with occlusion, $m = 0$. The dotted Curves III and IV are the corresponding observed results from Cook's Fig. 4. The fit is by no means perfect but it gives a reasonable representation of the results and it could have been improved by changing the assumed values of A_0, α, and K.

I am indebted to Dr. Cook for pointing out that the rate of supply of blood found above, namely 0·013 g per c.c. per sec, is about six times the normal rate, and that this ratio seems reasonable in view of the vaso-dilatation on heating. It may also be remarked that, in the absence of other sources of heat, supply of blood at the normal rate of about 0·0022 g per c.c. per sec leads to surface temperature gradients of the right order of magnitude: for example, if the surface is maintained at 3·6° C below blood heat, the steady temperature gradient at the surface will be 2·4° C per cm.

Finally it may be mentioned that the same considerations have been found useful in a study (unpublished) of the heating of the retina of the eye by infra-red radiation.

REFERENCES

(1) Cook, H. F. *Brit. J. Appl. Phys.*, **3**, p. 1 (1952).
(2) Mendelssohn, K., and Rossiter, R. J. *Quart. J. of Exp. Physiol.*, **32**, p. 301 (1944).

The saturation curve at high ionization intensity

By J. W. Boag, B.Sc., F.Inst.P., and T. Wilson, B.Sc.(Eng.),* Radiotherapeutic Research Unit, Hammersmith Hospital, London

[*Paper received* 30 *January*, 1952]

In this paper the form of the saturation curve is investigated theoretically and experimentally. It is shown that saturation curves taken under different conditions on a parallel plate ionization chamber are transformed into a single general curve when plotted in terms of a dimensionless product of the several variables. The experimental work utilized an ionization chamber with thin foil electrodes. A coin-shaped region between the foils was ionized by a beam of fast electrons. Dose rates up to 100 000 e.s.u./cm³ × sec could be attained. It is shown that very high ionization intensities can be measured in a parallel plate chamber, provided the spacing of the plates is small.

In a previous paper[1] formulae were developed for the proportion of ions which can be collected in a parallel-plate ionization chamber when the ionization occurs in instantaneous pulses. The problem of the ionization current flowing through a gas subjected to a continuous high radiation intensity presents greater mathematical difficulty. Although J. J. Thomson set up the general differential equation for the transport of ions between parallel plates as long ago as 1900, explicit solutions of this equation have been obtained in only a small number of special cases.[2] The equation has been attacked by various approximate methods, notably by Mie[3] and Seeliger.[4] Seemann[5] determined experimentally the saturation curve between plane parallel electrodes in air at normal atmospheric pressure, and found good agreement with Mie's numerical solution of Thomson's equation. The ionization intensity in this work was of the order of 1 e.s.u./c.c. × min and the electrode spacing varied from 1 to 5 cm.

Mie had shown that saturation curves taken under different experimental conditions should be capable of transformation to a standard form by taking as ordinate the collection efficiency (which we shall denote by f), that is, the ratio of measured ionization current to theoretical saturation current, i/i_m, and as abscissa another dimensionless parameter, V/Ri_m,

where V = collecting voltage;
i_m = saturation current;
R = apparent resistance of the ionized gas at very low collecting voltage.

Seemann confirmed experimentally that a transformation of this kind was possible, but he did not determine R directly, as his apparatus was not suitable for this purpose. He merely brought the different saturation curves into coincidence at an arbitrary point near the knee of the curve (the point $f = 0{\cdot}6$) and showed that, when this was done, the portions above and below the arbitrary matching point agreed extremely well. It is not easy to measure R accurately from the gradient at the origin, since curvature persists down to very low collecting voltages. Moreover, the quantity R is not usually of direct interest, nor is it of use in designing an ionization chamber for a given ionization intensity. Mie's parameter is not, therefore, the most suitable one for the abscissa of a general saturation curve.

* Now at the British Electricity Authority Research Laboratory, Leatherhead.

Table 1. *Dimensional analysis*

Fundamental units: Length (L), Time (T), Charge (Q)

Name of quantity	*Symbol*	*Dimensional formula*
Collecting voltage	V	QL^{-1}
Electrode spacing	d	L
Ionization intensity	q	$QL^{-3}T^{-1}$
Recombination coefficient	α/e	$Q^{-1}L^{3}T^{-1}$
Ionic mobilities	k_1, k_2	$Q^{-1}L^{2}T^{-1}$
Ionization current density	i	$QL^{-2}T^{-1}$

The experimental variables which influence the saturation curve between plane parallel electrodes in a uniformly ionized gas, are listed in Table 1. These are all the independent quantities which enter into the differential equation governing the phenomena. Other variables, such as the field strength X at distance x from the positive plate, may also appear in the differential equation, but a subsidiary equation such as $V = \int_0^d X dx$ permits each dependent variable to be eliminated from the final solution, at least in principle. The saturation curve is, of course, influenced by the type of gas used and by its temperature and pressure. These variables do not appear explicitly in Table 1 because we assume that they influence only the recombination coefficient α and the mobilities of the positive and negative ions, k_1 and k_2. We assume:

(1) That recombination occurs at the rate $\alpha n_1 n_2$ ion pairs per cm^3 per sec where n_1, n_2 are the numbers of ions of either sign present per cm^3, and α is a constant characteristic of the gas. This expression may equally well be written in the form $-(\alpha/e)\rho_1\rho_2$ e.s.u. of charge destroyed per cm^3 per sec where the ρ's represent units of charge per cm^3 and e is the electronic charge.

(2) That the drift velocity of the positive ion, when in an electric field of strength X, is $k_1 X$ cm/sec in the direction of the field while that of the negative ion is $k_2 X$ in the opposite direction, k_1 and k_2 being constants.

The dimensional formulae of the several variables, in terms of the units chosen as fundamental, namely, length, time, and charge, are given in Table 1. The most general form of the product of powers of the variables is

$$(V)^{\beta}(d)^{\gamma}(q)^{\delta}(\alpha/e)^{\kappa}(k_1)^{\lambda}(k_2)^{\mu}(i)^{\nu}$$

Substituting the dimensional formula for each of the variables into this expression and equating the indices of the three fundamental units to zero, we have the following three equations between the seven variables:[6]

$$\left.\begin{aligned} \beta + \delta - (\kappa + \lambda + \mu) + \nu &= 0 \\ -\beta + \gamma - 3\delta + 3(\kappa + \lambda + \mu) - 2\nu &= 0 \\ -\delta - (\kappa + \lambda + \mu) - \nu &= 0 \end{aligned}\right\} \quad (1)$$

After solving the equations (1) for γ, δ, λ, in terms of the other indices, we obtain for the general dimensionless product

$$\left(\frac{V\sqrt{k_1}}{d^2\sqrt{q}}\right)^{\beta}\left(\frac{\alpha}{ek_1}\right)^{\kappa}\left(\frac{k_2}{k_1}\right)^{\mu}\left(\frac{i}{qd}\right)^{\nu} \quad (2)$$

Since the combination of variables within each bracket is raised to an arbitrary power, each such combination must form a subsidiary dimensionless product. The general solution of the problem may then be written

$$\frac{i}{qd} = \phi\left[\frac{k_1}{k_2}, \frac{\alpha}{ek_1}, \frac{d^2\sqrt{q}}{V\sqrt{k_1}}\right] \quad (3)$$

where ϕ is an unknown function of the three dimensionless arguments. The l.h.s. of this equation is the ratio of actual current density to saturation current density, i.e. it is the collection efficiency, f. Moreover, two of the arguments of the function ϕ involve only the mobilities, the recombination coefficient and the electronic charge. For a given gas under standard conditions all these are constant. We may, therefore, conclude that under these circumstances

$$f = \phi\left(\frac{d^2\sqrt{q}}{V}\right) \quad (4)$$

where ϕ is to be read simply as an unknown function, whose form, however, can be determined experimentally for a particular gas under standard conditions of temperature and pressure.

EXPERIMENTAL MEASUREMENTS

The ionization chambers used in this work have already been described.[7] The saturation curves illustrated below were taken in a 1·2 MeV electron beam emerging from a thin aluminium window at the end of the accelerating tube of a Van de Graaff generator. The beam entering the ionization chamber was defined by a circular hole in a 3/16 in thick aluminium "stop" placed immediately above the upper aluminium foil of 0·001 in thickness which formed the chamber wall. The beam diameter was in some cases 1 cm and in others 0·7 cm. Even with the larger beam, the radial variation in ionization intensity in the chamber did not exceed 5%, so the experimental arrangement permitted a well-defined coin-shaped region between the parallel foils to be irradiated to a high and fairly uniform ionization intensity. One of the ionization chambers used (Chamber *B*, Fig. 1, in the paper by Boag, Pilling and Wilson[7]) had provision for varying the spacing of the foils, from a fraction of a millimetre up to several millimetres. In the experiments described below the two outer foils were adjusted to be at equal distances from the central foil, so that the characteristics of the two gaps from which the total current was collected were always identical.

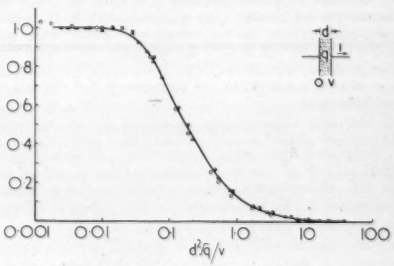

Fig. 1. General saturation curve in air at 764 mm and 17·1° C for plane parallel geometry. Ionization intensity was constant while the plate spacing was varied

$q = 1\,000$ e.s.u./c.c. × sec.
○ $d = 0{\cdot}0625$ cm.
△ $d = 0{\cdot}126$ cm.
□ $d = 0{\cdot}253$ cm.

In the first series of measurements the ionization intensity was set to give 1 000 e.s.u./c.c. × sec in air at normal pressure and room temperature and saturation curves were taken for electrode spacings of 0·0625 cm, 0·125 cm and 0·25 cm. The collection efficiency in these measurements is plotted in Fig. 1 to a base of $d^2\sqrt{q}/V$, and it can be seen that (within the experimental error) the points for all three electrode spacings

lie on a single curve. The full line is based on an approximate theory which we shall discuss below.

In the second series of measurements the electrode spacing was held constant at 0·126 cm and the ionization intensity was set at 1 890 e.s.u./c.c. × sec, 18 800 e.s.u./c.c. × sec and 118 000 e.s.u./c.c. × sec, successively. For each intensity a complete saturation curve was taken, and the collection efficiency for each measured point is plotted against $d^2\sqrt{q}/V$ in Fig. 2. As before, the points for all three intensities lie on a single curve, and as the full line is identical with that in Fig. 1, it can be seen that within the limits quoted—namely 0·0625 cm to 0·25 cm and 1 000 e.s.u./c.c. × sec up to 118000 e.s.u./c.c. × sec—the collection efficiency f is indeed a function of $d^2\sqrt{q}/V$ only.

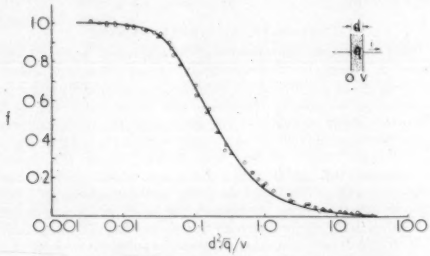

Fig. 2. General saturation curve in air at 764 mm and 17·1° C for plane parallel geometry. Spacing of plates was held constant while the ionization intensity was varied

$d = 0{\cdot}126$ cm.
○ $q = 118\,000$ e.s.u./c.c. × sec.
△ $q = 18\,800$ e.s.u./c.c. × sec.
□ $q = 1\,890$ e.s.u./c.c. × sec.

The curves in Figs. 1 and 2 were all taken on the same day, so that atmospheric conditions were constant. Curves taken on different days over a period of months did not always agree with one another quite so closely, but the divergences were principally at the low voltage end of the curve. As a guide to the voltage required for saturation the general curve has proved entirely satisfactory. It is proposed to investigate the effect of air pressure and temperature, but this has not yet been done.

APPROXIMATE THEORIES

By ignoring space charge, it is possible to obtain an approximate solution of Thomson's equation which should be valid in the near-saturation region. Mie's numerical solution (reference (3), Fig. 3) shows that for 90% collection efficiency in air at atmospheric pressure and room temperature the field strength varies only about ± 20% from its mean value. At higher collection efficiency the variation will be less. The assumption of constant field strength between the plates may be introduced into the equations in several ways, and these lead to slightly different solutions. Thus, Townsend[3] assumes that the ions of either sign move with constant velocities, $k_1(V/d)$ and $k_2(V/d)$, in the field between the electrodes. The steady state is then determined by the equations (in our notation)

$$q = \frac{\alpha}{e}\rho_1\rho_2 + \frac{d}{dx}(\rho_1 u_1) \tag{5}$$

$$i = \rho_1 u_1 + \rho_2 u_2 \tag{6}$$

where ρ_1, ρ_2 = charge densities of positive and negative ions respectively;
u_1, u_2 = velocities of positive and negative ions respectively;
i = ionization current density.

The solution of these equations for u_1, u_2 constant, can be shown to be[8]

$$\sqrt{\left(\frac{4qu_1u_2}{(\alpha/e)i^2} - 1\right)} \tan\left[\frac{\alpha}{e}\frac{di}{4u_1u_2}\sqrt{\left(\frac{4qu_1u_2}{(\alpha/e)i^2} - 1\right)}\right] = 1 \tag{7}$$

Now putting $u_1 = k_1 V/d \qquad i = fqd$
$u_2 = k_2(V/d)$

$$\xi = \sqrt{\left(\frac{\alpha}{ek_1k_2}\right)}\frac{d^2\sqrt{q}}{V} = m\frac{d^2\sqrt{q}}{V}$$

say, where m is a constant, we obtain

$$\sqrt{\left(\frac{4}{f^2\xi^2} - 1\right)} \tan\left[\frac{f\xi^2}{4}\sqrt{\left(\frac{4}{f^2\xi^2} - 1\right)}\right] \tag{8}$$

We cannot express f in terms of ξ explicitly, but the solution can be put into the parametric form

$$\left.\begin{aligned} f &= \frac{\omega}{(1+\omega^2)\tan^{-1}\omega} \\ \xi &= 2\sqrt{(1+\omega^2)}\tan^{-1}\omega \end{aligned}\right\} \tag{9}$$

where ω is a variable parameter, $0 < \omega < \infty$.

An alternative approximation is obtained by assuming that the positive ion density between the electrodes rises linearly from zero at the positive plate to a maximum at the negative plate, while the negative ion density varies linearly in the opposite direction. If the field were truly uniform and no recombination occurred, this model, which is illustrated in Fig. 3, would be correct. Close to the negative plate the current i is carried entirely by the positive ions whose density there is $\rho_{1\,max}$, and whose velocity we take as $k_1(V/d)$. Then

$$\left.\begin{aligned} \rho_{1\,max} &= \frac{i}{k_1(V/d)} = \frac{fqd^2}{k_1V} \\ \text{Similarly} \quad \rho_{2\,max} &= \frac{i}{k_2(V/d)} = \frac{fqd^2}{k_2V} \end{aligned}\right\} \tag{10}$$

The densities of positive and negative ions at any distance x from the positive plate are then

$$\left.\begin{aligned} \rho_1(x) &= \left(1 - \frac{x}{d}\right)\frac{fqd^2}{k_1V} \\ \rho_2(x) &= \frac{x}{d}\frac{fqd^2}{k_2V} \end{aligned}\right\} \tag{11}$$

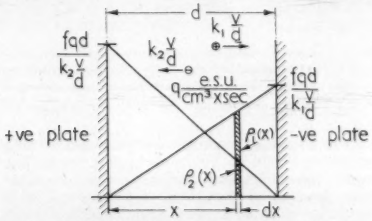

Fig. 3. Distribution of charge density in the air gap under near-saturation conditions

and hence the average rate of recombination throughout the space is

$$\mathscr{R} = \frac{1}{d}\int_0^d \alpha e \rho_1(x)\rho_2(x)dx = \frac{\alpha}{e}\frac{f^2q^2d^4}{6k_1k_2V^2} \qquad (12)$$

Now the fraction of the total charge liberated per unit volume which is destroyed by recombination is $(1 - f)$. Therefore $\mathscr{R} = (1 - f)q$. Hence

$$f = 1 - \frac{\mathscr{R}}{q} = 1 - \frac{f^2}{6}\frac{\alpha}{ek_1k_2}\frac{d^4q}{V^2} = 1 - \tfrac{1}{6}f^2\xi^2 \qquad (13)$$

where $\xi = m(d^2\sqrt{q}/V)$ as before.

This is a quadratic equation for f whose only positive root is

$$f = 2/[1 + \sqrt{(1 + \tfrac{2}{3}\xi^2)}] \qquad (14)$$

If we calculate pairs of values of f and ξ from equation (9), and for comparison determine from equation (14) the value of f for each of these values of ξ, we find that the two equations (9) and (14) are almost entirely equivalent. This comparison is given in Table 2.

Table 2. *Comparison of the values of f determined from equations* (9) *and* (14)

		$\omega = 0{\cdot}1$	$0{\cdot}2$	$0{\cdot}4$	$0{\cdot}8$	$1{\cdot}0$	$2{\cdot}0$	$4{\cdot}0$
Eqn. (9)	$\xi =$	$0{\cdot}1994$	$0{\cdot}4026$	$0{\cdot}8196$	$1{\cdot}728$	$2{\cdot}221$	$4{\cdot}951$	$10{\cdot}933$
	$f =$	$0{\cdot}9930$	$0{\cdot}9742$	$0{\cdot}9062$	$0{\cdot}7230$	$0{\cdot}6366$	$0{\cdot}3613$	$0{\cdot}1775$
Eqn. (14)	$f =$	$0{\cdot}9934$	$0{\cdot}9743$	$0{\cdot}9079$	$0{\cdot}7328$	$0{\cdot}6512$	$0{\cdot}3873$	$0{\cdot}2004$

We can then confine our attention to the simpler expression for f which is provided by equation (14), and can test this formula against the experimental results by regarding m as an empirical constant. The full line in Figs. 1 and 2 represents equation (14) with m put equal to 19·4. It is surprising that this formula fits the observations not only in the near-saturation region, for which the approximation was set up, but also over most of the curve.

The values of the recombination coefficient and of the ionic mobilities reported in the literature are by no means all concordant. Thomson surveyed the data up to 1927 in his book.[2] For air at atmospheric pressure and 0° C the smallest of the several values of α/e reported is 3 200 (reference (2), p. 40). According to Erikson[9, 10] α/e varies inversely as the 7/3 power of the absolute temperature. At 20° C one should, therefore, have $\alpha/e = 2\,730$. Widely different values have been reported by different observers for k_1, k_2 in air. Thomson's survey recommends

$$\begin{cases} k_1 = 1{\cdot}36 \text{ cm/sec per volt/cm} \\ k_2 = 2{\cdot}1 \text{ cm/sec per volt/cm} \end{cases}$$

as the most probable values. However, Erikson[11] found that the positive ion, when freshly formed, had the same mobility as the normal negative ion. Substituting $\alpha/e = 2\,730$, $k_1 = k_2 = 2{\cdot}1$ in the expression for m we find

$$m = \sqrt{(\alpha/ek_1k_2)} = \sqrt{(2\,730/2{\cdot}1 \times 2{\cdot}1)} = 24{\cdot}9 \qquad (15)$$

Although we have selected from the reported values of the constants those which would tend to make m as small as possible, the figure which results is considerably higher than the empirical value of 19·4. We conclude that, in our experiments, α/e was smaller than normal or k_1k_2 larger. The most likely source of the discrepancy is the mobility of the negative ion. The latter is usually formed by the attachment of a free electron to a molecule, although bombardment by fast electrons does lead, in some cases, to the direct splitting of a diatomic molecule into positive and negative ions.[12] With the short inter-electrode spacings and high field strengths used in our experiments, some of the electrons may cross the gap without attachment, thus increasing the apparent value of k_2. The extent to which this may happen is examined in the next section.

ATTACHMENT OF ELECTRONS TO MOLECULES

Only a small fraction, say $1/n$, of all collisions between free electrons and molecules result in the formation of a negative ion by electron capture. Thomson has shown (reference (2), p. 137) that the probability of an electron drifting a distance d in a uniform field of strength X without becoming attached to a molecule is then

$$P(d) = e^{-vd/n\lambda kX} = e^{-\psi}, \text{ say,}$$

where v is the velocity of agitation, λ is the mean free path, and k is the mobility of the electron in the gas under the given physical conditions. If electrons are liberated uniformly in the space between two plane electrodes at a distance d apart, then the proportion crossing unattached will be

$$P'(d) = \frac{1}{d}\int_0^d P(x)dx = (1 - e^{-\psi})/\psi \qquad (16)$$

Data on the quantities n, v, λ, and on the drift velocity kX have been collected and published by Healey and Reed.[13] For air their values are based on the experiments of Townsend and Tizard[14] and of Bailey.[15]. The quantities are all functions of the ratio of field strength to gas pressure. For air at 1 atmosphere and a field strength of 2 kV/cm, the values obtained by interpolation in Healey and Reed's tables are:

$n = 2{\cdot}9 \times 10^6$, $v = 6 \times 10^7$ cm/sec, $\lambda = 4{\cdot}2 \times 10^{-5}$ cm and $kX = 2{\cdot}1 \times 10^6$ cm/sec.

Hence

$$\psi = \frac{vd}{n\lambda kX} = \frac{6 \times 10^7 \times d}{2{\cdot}9 \times 10^6 \times 4{\cdot}2 \times 10^{-5} \times 2{\cdot}1 \times 10^6} = 0{\cdot}234\,d = 0{\cdot}0234 \text{ for } d = 0{\cdot}1 \text{ cm}$$

In this case $P'(d) = (1 - e^{-\psi})/\psi = 0{\cdot}985$ and so only 1·5% of the electrons would form ions in crossing a 1 mm gap with 200 V across it. It must be noted, however, that the value of n which should be used is very uncertain. Thus Loeb[16, 17] found $n = 0{\cdot}7$–$6{\cdot}4 \times 10^4$ in air at atmospheric pressure for small field strengths. Moreover, Healey and Reed's value refers to dry air, and a small amount of moisture may increase the probability of attachment (reference (2), p. 155). If the true value of n for our experimental conditions were 1/10 of the value used above we should have $P' = 0{\cdot}893$; if it were 1/100, $P' = 0{\cdot}386$. It seems that for a 1 mm gap and a field of 2 kV/cm, which is typical of the field strength required to produce saturation in many of our experiments, a considerable proportion of the electrons liberated in the gap will reach the positive plate without having formed ions.

The approximate formulae derived in an earlier section to represent the saturation curve were based on the assumption that the mobilities of the positive and negative ions were independent of the field strength. Free electrons do not show a constant mobility (reference (2), p. 146). Moreover, we had assumed that the field in the near-saturation region would be almost uniform across the gap. If a considerable proportion of the negative charge carriers are electrons, there will be a residual positive space charge and the field at the negative plate will always be higher, and often much higher, than at the positive plate. It appears that, under these conditions, a different approach must be made. In some gases,

such as argon and hydrogen, electron attachment does not occur, and, in the absence of impurities, the current should be carried by positive ions and electrons only. It is of interest to consider this case, if only because conduction in air must lie somewhere between this extreme and the other, for which we have already obtained an approximate solution.

CONDUCTION BY POSITIVE IONS AND ELECTRONS

The drift velocity of electrons in an electric field is about one thousand times that of positive ions, and in the near-saturation region the electronic space charge is therefore negligible compared with that due to the positive ions. Instead of assuming constant field strength across the gap, we can determine the spatial variation of the field for the case in which no recombination occurs and assume that this field distribution still holds in the near-saturation region.

Let X be the field at distance x from the positive plate, and ρ_1, ρ_2 the charge densities of the positive ions and electrons, respectively, at that plane.

Then

$$\frac{dX}{dx} = 4\pi(\rho_1 - \rho_2) \tag{17}$$

$$\frac{d}{dx}(k_1 X\rho_1) = q \tag{18}$$

$$\frac{d}{dx}(k_2 X\rho_2) = -q \tag{19}$$

Combining these equations and eliminating ρ_1, ρ_2 we obtain

$$\frac{d^2X^2}{dx^2} = 8\pi q\left(\frac{k_1 + k_2}{k_1 k_2}\right) = \theta \text{ (say)} \tag{20}$$

where θ is independent of x. Now the positive ion density in the vicinity of the positive plate is zero, and if we assume that the electron space charge, even at the positive plate, is negligible, then $dX/dx = 0$ for $x = 0$ and the solution of equation (20) is

$$X^2 = X_0^2 + (\theta/2)x^2 \tag{21}$$

where X_0 is the field at the positive plate. We may write this as

$$\left(\frac{X}{X_0}\right)^2 = 1 + \zeta^2\left(\frac{x}{d}\right)^2 \tag{22}$$

with $$\zeta = \sqrt{\left[\frac{4\pi(k_1 + k_2)}{k_1 k_2}\right]}\frac{d\sqrt{q}}{X_0}$$

Now

$$V = \int_0^d X dx = X_0 d\int_0^1 \left(\frac{X}{X_0}\right) d\left(\frac{x}{d}\right) = X_0 d\int_0^1 \sqrt{(1 + \zeta^2 u^2)}\, du$$

$$= \frac{X_0 d}{2}\left\{\sqrt{(1 + \zeta^2)} + \frac{1}{\zeta}\log\left[\zeta + \sqrt{(1 + \zeta^2)}\right]\right\}$$

Hence

$$\sqrt{\left[\frac{k_1 k_2}{4\pi(k_1 + k_2)}\right]}\frac{V}{d^2\sqrt{q}} = \frac{1}{2}\sqrt{\left[\frac{k_1 k_2}{4\pi(k_1 + k_2)}\right]}\frac{X_0}{d\sqrt{q}}$$

$$\left\{\sqrt{(1 + \zeta^2)} + \frac{1}{\zeta}\log\left[\zeta + \sqrt{(1 + \zeta^2)}\right]\right\}$$

or $$\frac{1}{\xi'} = \frac{1}{2\zeta}\left\{\sqrt{(1 + \zeta^2)} + \frac{1}{\zeta}\log\left[\zeta + \sqrt{(1 + \zeta^2)}\right]\right\} \tag{23}$$

where ξ' is a dimensionless variable containing $d^2\sqrt{q}/V$ as a factor. Equation (23) gives the value of X_0 corresponding to given values of d, q, and V, the mobilities k_1 and k_2 being supposed known. Knowing X_0, the field distribution between the plates is then fully determined by equation (22). The curves in Fig. 4 illustrate the shape of this distribution, for several values of ξ'.

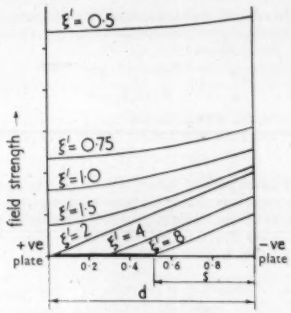

Fig. 4. Variation of field strength across the air gap when the electrons cross the gap without attachment, for several different values of ξ'

From the field distribution given by equation (22) one can calculate the positive and negative charge densities present at any plane x. The rate of recombination at x is then given by $(\alpha/e)\rho_1\rho_2$. By integrating this expression over the whole width of the gap one obtains the total recombination occurring per unit time, and hence the collection efficiency. The algebra involved in this integration is tedious and on substituting the appropriate numerical values into the final result, one finds that, as long as X_0 differs even very slightly from zero, the proportion of ions and electrons which recombine, is negligible. Until recently the recombination coefficient for electrons and positive ions in argon was thought to be about 2×10^{-10} cm^3/sec, but measurements by Biondi and Brown[18] using microwave techniques have given the much higher value of 3×10^{-7} cm^3/sec. This is the value which was used in the numerical test just described. What then is the field distribution for collection efficiencies lower than unity when electrons are the negative charge carriers?

As the applied voltage V is decreased, the field X_0 at the positive plate falls until, at a certain voltage V', we have $X_0 \simeq 0$. The field strength between the plates then follows the simple law [cf. equation (21)]

$$X = \sqrt{\left(\frac{\theta}{2}\right)}x = \sqrt{\left[\frac{4\pi q(k_1 + k_2)}{k_1 k_2}\right]}x \tag{24}$$

If the applied voltage be reduced below V', the point of (almost) zero field must shift towards the negative plate, for we see from equation (24) that dX/dx depends only on q, k_1 and k_2, and so the slope of the line cannot change as V is reduced. When the applied voltage is less than V' there is, therefore, a region of width $(d - s)$ (Fig. 4), in which the field is extremely low. This is only possible, of course, if the net space charge is negligible, that is to say, if electrons and positive ions are present in nearly equal concentrations in this region. These concentrations will be in equilibrium when the rate of recombination equals the rate of production, i.e. when

$$(\alpha/e)\rho_1\rho_2 = q \quad \text{or} \quad \rho_1 = \rho_2 = \sqrt{(qe/\alpha)}$$

The width of the region s is obtained from the relation

$$V = \int_0^s X dx = \frac{s^2}{2}\sqrt{\left(\frac{\theta}{2}\right)}$$

Hence
$$s = \sqrt{\left(\frac{2V\sqrt{2}}{\sqrt{\theta}}\right)} = \sqrt[4]{\left[\frac{k_1 k_2 V^2}{\pi q(k_1 + k_2)}\right]} \qquad (25)$$

Now in this case the collection efficiency f is simply the ratio s/d.

Hence
$$f = \frac{s}{d} = \sqrt[4]{\left[\frac{V^2}{d^4 q}\,\frac{k_1 k_2}{\pi(k_1 + k_2)}\right]} = \sqrt{\frac{2}{\xi}} \qquad (26)$$

For $V > V'$ we have $X_0 > 0$ and $f = 1$.

The foregoing approximate theory may be compared with measurements made in argon, in an ionization chamber having 0·5 mm electrode spacing [Ref. (7), Fig. 1A]. The argon was taken, without purification, from a commercial cylinder and was allowed to flow continuously through the ionization chamber. The only impurity was said to be 2% of nitrogen. Saturation curves were taken for three different ionization intensities—10^3, 10^4 and 10^5 e.s.u./cm^3 × sec, respectively. The separate points obtained are plotted in Fig. 5 and they evidently lie on a common curve. The dashed curve (A) is that derived from equation (26). with the constants* appropriate to argon inserted in the formula, the chain-dotted curve (B) is the experimental curve for air, as given in Figs. 1 and 2, while the full line (C) is that given by equation (14) of our earlier approximate theory for ionic conduction in air, putting $m = 24{\cdot}9$ in accordance with equation (15).

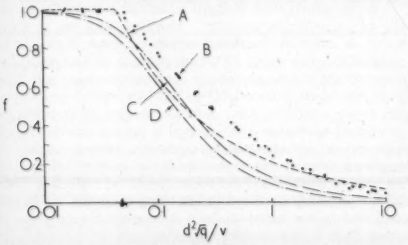

Fig. 5. General saturation curve in argon at 770 mm and 16·5° C for plane parallel geometry, at three different ionization intensities. The points were determined experimentally

A = theoretical curve for electron conduction in argon.
B = experimental points for argon at 10^3, 10^4 and 10^5 e.s.u./c.c. × sec.
C = experimental curve for air ($m = 19{\cdot}4$).
D = curve for air from ionic mobilities ($m = 24{\cdot}9$).

The agreement between theory and experiment is as good as could be expected, in view of the simplicity of our theoretical model, and the difficulty of measuring accurately the internal ½ mm airgaps in the ionization chamber. The latter was not specially designed for these measurements, but for general use. It would doubtless be possible to improve both theory and experiment, but the results presented in Fig. 5 do at least show: (i) that when the negative charge carriers are electrons, saturation curves taken at different ionization intensities coincide if plotted in terms of the parameter $d^2\sqrt{q}/V$; (ii) that even in the complete absence of negative ion formation saturation difficulties arise only a little later than when negative ions are present. In Fig. 6 saturation curves in

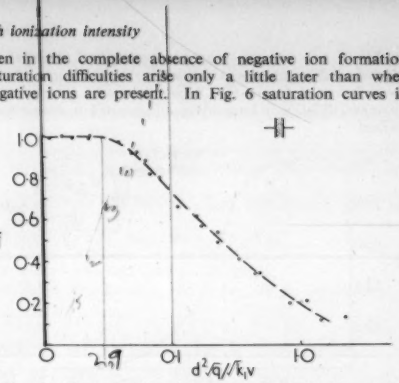

Fig. 6. General saturation curves for hydrogen and argon with plane parallel geometry, plotted in terms of the same dimensionless parameter

○ hydrogen $k_1 \simeq 1{\cdot}7$ cm²/V × sec
● argon $k_1 \simeq 7{\cdot}6$ cm²/V × sec
} for freshly formed ions.

hydrogen and in argon, taken under identical geometrical conditions (i.e. in the same ionization chamber) have been brought into coincidence by introducing the factor $\sqrt{k_1}$ into the denominator in order to obtain a dimensionless product in accordance with equation (3).

CYLINDRICAL AND SPHERICAL GEOMETRY

If space charge can be neglected it is not difficult to develop formulae which bring cylindrical and spherical geometry within the scope of this survey. This was done in a previous paper on pulsed radiation,[1] and, in the case of ionic conduction, the formulae for "equivalent gap length" are the same for continuous as for pulsed radiation. Extensive experimental investigations with variable geometry would be required to check the validity of the underlying assumptions, and these have not been made. If one considers only a particular cylindrical or spherical ionization chamber, however, saturation curves taken at different ionization intensities can be brought into coincidence by plotting f against $\sqrt{q}/V$.

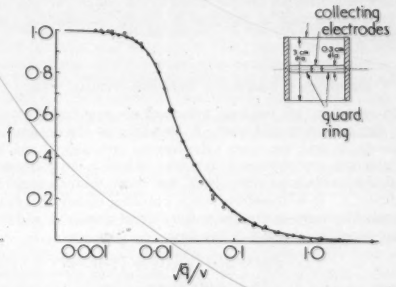

Fig. 7. Saturation curve in air at 770 mm and 16·5° C for a cylindrical ionization chamber at two different intensities

○ $q = 0{\cdot}21$ e.s.u./c.c. × sec. ● $q = 0{\cdot}037$ e.s.u./c.c. × sec.

* Only k_1 is of importance in the formula since the ratio k_2/k_1 is about 1 000 and k_2 therefore cancels with $(k_1 + k_2)$. For argon $k_1 \simeq 1{\cdot}7$ cm²/V × sec for freshly formed ions.

In Fig. 7 two separate runs on a cylindrical chamber are plotted in this way, the intensities for the two runs differing by a factor of 6. In Fig. 8 two runs on a hemispherical chamber, differing in intensity by a factor of 4·6, are similarly plotted.

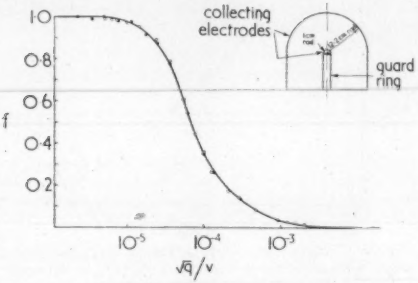

Fig. 8. Saturation curve in air at 753 mm and 16·6° C for a hemispherical ionization chamber at two different intensities

○ $q = 3{\cdot}4 \times 10^{-6}$ e.s.u./c.c. × sec.
● $q = 0{\cdot}73 \times 10^{-6}$ e.s.u./c.c. × sec.

For high intensity measurements pronounced cylindrical or spherical geometry is, of course, quite unsuitable. In the first place, the radial air gap will usually have to be larger than can easily be achieved with plane electrodes, and it has to be multiplied by a factor greater than unity before it is comparable with the plane case. In the second place, the field strength at the inner electrode, due to a given applied voltage, may be several times as high as that which the same voltage would produce across a plane gap of equal length. Multiplication of ions by collision will therefore occur at considerably lower applied voltage, and this will set an upper limit to the intensity for which the ionization chamber can be used.

A spherical or cylindrical design of chamber in which the ratio of inner electrode radius to outer electrode radius approximates to unity is, on the other hand, merely a plane gap folded into a convenient form, and, provided no pockets of low field strength are permitted in the design and the gap is kept short, such a chamber is entirely suitable for high intensity work.

EMPIRICAL FORMULA FOR PRACTICAL USE

In equation (14) we have presented an empirical formula for the collection efficiency, f, in terms of the ionization intensity, q, and the other experimental variables, d and V. In practical measurements, however, q has to be estimated from the ionization current itself, and to do this one requires to know f. It is therefore worth recasting equation (14) to express f in terms of the ionization current density, i, and the other variables, d and V. We have

$$f = i/qd = 2/[1 + \sqrt{(1 + \tfrac{2}{3}\xi^2)}] \qquad (14)$$

where $\xi = m(d^2\sqrt{q}/V)$

Hence

$$\frac{i}{qd}\frac{m^2qd^4}{6V^2} = \xi^2/3[1 + \sqrt{(1 + \tfrac{2}{3}\xi^2)}] = \eta \text{ (say)} \qquad (27)$$

where $\eta = (m^2/6)(id^3/V^2)$ is a dimensionless variable embodying the current density i. If we eliminate ξ between the two equations (14) and (27) we are left with

$$f = 1/(1 + \eta) \qquad (28)$$

Putting $m = 19{\cdot}4$ in accordance with the experimental measurements in air, Figs. 1 and 2, we have

$$\eta = 62{\cdot}7(id^3/V^2) \qquad (29)$$

with i expressed in e.s.u./cm² × sec, d in cm, and V in volts,

or $$\eta = 1{\cdot}88 \times 10^5(i'd^3/V^2) \qquad (30)$$

with i' in μA/cm².

For different atmospheric conditions, or for gases other than air, equation (28) should still provide a good fit to the saturation curve, if a suitable value is chosen for m. The appropriate value is best found by taking a complete saturacurve, plotting $(1 - f)/f$ against id^3/V^2, and determining the slope of the best-fitting straight line. This slope is equal to m^2.

UPPER LIMIT FOR IONIZATION INTENSITY

The highest ionization intensity which can be measured in a parallel plate ionization chamber depends upon (i) the minimum permissible spacing of the plates and (ii) the maximum field strength that can be used.

The minimum plate spacing is determined by the quality of workmanship available, the feasibility of measuring accurately the spacing, and the risk of floating dust bridging the gap. In our experiments we have used a chamber with a ½ mm gap over long periods without trouble.

The maximum field strength is limited principally by the risk of ionization by collision. Provided there are no sharp points or edges in the design of the chamber, it should be possible to work up to 10 kV/cm without the occurrence of ionization by collision. On one occasion the saturation curve in air was taken up to a field of 13 kV/cm without any indication of ion multiplication. A further danger which has to be considered when thin foils are used is the deformation of the foils due to the electrostatic attraction between them. A simple calculation shows that, with the type of foil used in the present work,[7] the deflexion should be negligible if the foil is adequately stretched before being cemented. This was confirmed by measuring under a microscope the deflexion of typical foils at various field strengths.

Let us consider ½ mm spacing and 10 kV/cm as practical limits, and suppose that we are content with 90% collection. This does not mean that the 10% correction depends entirely on theory. The complete general saturation curve of the ionization chamber can be plotted at lower ionization intensity and we then depend on this curve with $d^2\sqrt{q}/V$ as abscissa, to determine the degree of saturation obtaining at the higher intensity. For $f = 0{\cdot}9$ we require $d^2\sqrt{q}/V$ to be less than 0·04.

Therefore $$\sqrt{q} = \frac{0{\cdot}04 \times 10^4}{0{\cdot}05} = 8\,000$$

that is, $$q = 64 \times 10^6 \text{ e.s.u./c.c. × sec}$$

If the foregoing limits for d and V/d are replaced by the less exacting values $d = 1$ mm, $V/d = 3\,000$ V/cm and if we put $f = 0{\cdot}9$ as before, we find

$$q = 1{\cdot}44 \times 10^6 \text{ e.s.u./c.c. × sec}$$

Thus 10^6 e.s.u./c.c. × sec is readily measurable in a plane parallel ionization chamber, and 10^8 e.s.u./c.c. × sec can probably be measured with some difficulty.

REFERENCES

(1) BOAG. *Brit. J. Radiol.*, **23**, p. 601 (1950).
(2) THOMSON. *Conduction of electricity through gases*, Vol. 1 (London: Cambridge University Press, 1928).
(3) MIE. *Ann. Phys., Lpz.*, **13**, p. 857 (1904).
(4) SEELIGER. *Ann. Phys., Lpz.*, **33**, p. 319 (1910).
(5) SEEMANN. *Ann. Phys., Lpz.*, **38**, p. 781 (1912).
(6) BRIDGMAN. *Dimensional Analysis* (Yale University Press, 1931).
(7) BOAG, PILLING and WILSON. *Brit. J. Radiol.*, **24**, p. 341 (1951).
(8) TOWNSEND. *Electricity in gases*, p. 72 (London: Oxford University Press, 1915).
(9) ERIKSON. *Phil. Mag.*, **18**, p. 328 (1909).
(10) ERIKSON. *Phil. Mag.*, **23**, p. 747 (1912).
(11) ERIKSON. *Phys. Rev.*, **20**, p. 117 (1922).
(12) MASSEY. *Negative ions* (London: Cambridge University Press, 1938).
(13) HEALEY and REED. *Behaviour of slow electrons in gases* (Sydney: Amalgamated Wireless (Australasia) Ltd., 1941).
(14) TOWNSEND and TIZARD. *Proc. Roy. Soc. A.*, **88**, p. 336 (1913).
(15) BAILEY. *Phil. Mag.*, **50**, p. 825 (1925).
(16) LOEB. *Phys. Rev.*, **17**, p. 89 (1921).
(17) LOEB. *Phil. Mag.*, **43**, p. 229 (1922).
(18) BIONDI and BROWN. *Phys. Rev.*, **76**, p. 1697 (1949).

A method of studying the formation of cracks in a material subjected to stress

By R. JONES, B.Sc., Ph.D., Road Research Laboratory, Harmondsworth, Middlesex

[*Paper received* 5 *November*, 1951]

A method is described to determine the onset of cracking in specimens of concrete subjected to tension or compression in mechanical testing machines. While the loads were being applied, measurements were made at intervals of the velocities of ultrasonic pulses passing through the test-piece in the axial and/or transverse directions. In compression, the velocity of the ultrasonic pulses in the direction of loading remained constant while the load was increased to failure, but in the transverse direction a fall in the velocity started at only a fraction of the ultimate load, and the velocity then decreased with increase of load. This indicated that cracking occurred internally parallel to the direction of loading. The load at which it started depended on the strength of the concrete and the uniformity of the stress distribution. In tension, fracture was preceded by only a very small, and often insignificant, amount of cracking which occurred at right angles to the direction of loading.

INTRODUCTION

In recent years, considerable theoretical and experimental effort has been directed to determining the behaviour of a specimen of material loaded to failure in a mechanical testing machine. Usually, the distribution of stress across the principal cross-section is not uniform, and it is difficult to determine precisely which mechanical property of the material is being determined by the test. In some cases studies have been possible by photoelastic methods. With metallic specimens, the behaviour of the internal structure of the material when subjected to stress has been studied by X-ray crystallographic analysis. The present paper describes a method of determining the onset of cracking in specimens subjected to tension or compression, and of obtaining information concerning the orientation of such cracks. The experimental investigation has dealt solely with concrete, but this technique has been applied to examine the distribution of voids in other materials showing brittle fracture.

In the experiments to be described, cubes, cylinders, bobbins and beams of concrete were tested to destruction in mechanical testing machines of conventional design. While the loads were being applied, measurements were made at intervals of the velocities of ultrasonic pulses passing through the test-piece in the axial and/or transverse directions. The onset of cracking was indicated by a marked drop in the velocity of the pulse. In compression tests, the effects of varying the shape of the specimen, the rate of loading, and the end restraint, on the stress just causing cracking were investigated.

EXPERIMENTAL PROCEDURE

The arrangements of the test specimen and of the transducers for transmitting and receiving the ultrasonic pulses are shown diagrammatically in Fig. 1.

The velocity of the ultrasonic longitudinal waves in a given direction through the specimen was determined by accurately timing the passage of the pulse between two transducers placed in contact with opposite faces of the specimen. Both transducers contained piezoelectric quartz crystals, and each transducer had a thin film of lubricating oil between it and the concrete to improve the acoustical matching. The ultrasonic pulse was produced by electrically shock-exciting one of the transducers and, after passing through the concrete, the mechanical pulse was received by the second transducer and converted into an electrical signal. The received signal was then amplified and applied to the Y-plates of one beam of a double-beam cathode-ray tube, giving a visual trace.

Timing marks were produced on the trace of the second beam of the tube at intervals of 1·017 μsec while, to facilitate measurement, larger marks were produced at intervals of 10·17 μsec. These timing marks gave the scale for determining the time taken for the leading edge of the pulse of longitudinal waves to pass through the concrete. The time of transmission was the difference between the times of arrival of the leading edge of the pulse when the transducers were placed on opposite sides of the concrete and in direct contact. A typical display on the cathode-ray tube is reproduced in Fig. 2.

The time of transmission of the pulse through the specimen in a given direction was determined before applying a load. The leading edge of the pulse on the cathode-ray tube was aligned on a cursor and also on a timing mark. When application of the load caused a change in velocity of the pulse, the change in time of arrival of the leading edge of the pulse was measured to within 0·2 μsec. Full details of the apparatus have been given by Jones.(1)

When measurements were made across the cylindrical cross-

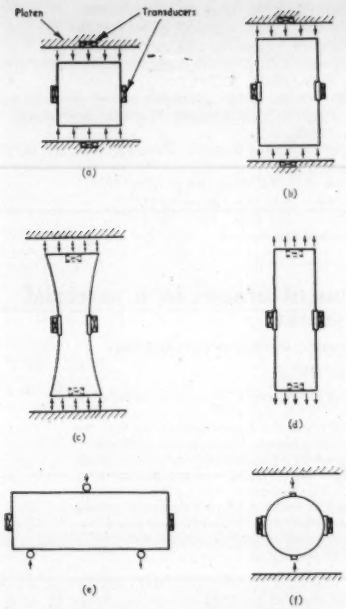

Fig. 1. Arrangement of test specimens and transducers for measuring the velocity of ultrasonic pulses

(*a*) Cube in compression, (*b*) cylinder in compression, (*c*) bobbin in tension or compression, (*d*) cylinder in tension, (*e*) beam in bending, (*f*) cylinder in compression across a diameter.

section of a specimen, the ultrasonic transducers had faces curved to fit the test-piece, and were held in contact by light springs. With some compression specimens, measurements were made in the axial direction by transducers embedded in the faces of steel blocks placed between the test-piece and the platens of the testing machine. When tensile specimens were stressed axially, the tension was applied through a ring of reinforcing bars embedded in the ends of the specimens, and transducers were placed in contact with the concrete in the centre of the ring.

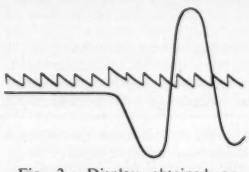

Fig. 2. Display obtained on double-beam cathode-ray tube

Fig. 1(*f*) shows a method used by Carneiro[2] of applying tensile forces across a vertical cross-section of a cylinder by compressing it on its side. Thin wooden strips were used between the cylinder and the platens of the testing machine. When a cylinder of diameter d is subjected to a concentrated, vertical, diametral load P per length t, the horizontal tension is constant ($= 2P/\pi td$) across the vertical central section, i.e. along the line of the loads, while the vertical compressive stress varies from infinity at the loading points to a minimum of $6P/\pi td$ at the centre of the cross-section.

Across the horizontal section through the axis of the cylinder, the horizontal tensile stress at a distance x from the axis is given by:

$$\sigma_x = \frac{2P}{\pi td}\left[\frac{d^2 - 4x^2}{d^2 + 4x^2}\right]^2$$

while the vertical compressive stress is:

$$\sigma_y = \frac{-2P}{\pi td}\left[\frac{4d^4}{(d^2 + 4x^2)^2} - 1\right]$$

Both stresses vanish on the circumference, i.e. at the ends of the horizontal diameter, and the maximum stresses developed at the centre are as given for the vertical central section.

SPECIMENS TESTED IN COMPRESSION

General. The compression tests were made on cubes, cylinders and bobbins [see Figs. 1(*a*) to 1(*c*)]. In all cases the velocity of longitudinal waves in the direction of loading remained constant while the load was increased to failure. In the transverse direction, perpendicular to the direction of loading, the velocity remained constant only up to a fraction of the ultimate load (25–30% for cubes) and then decreased with increasing load as shown in Fig. 3. This sharp fall of velocity in the transverse direction, taken in conjunction with the constant velocity in the axial direction, indicates that, under these stress conditions, internal fracture occurs by cracking parallel to the direction of loading.

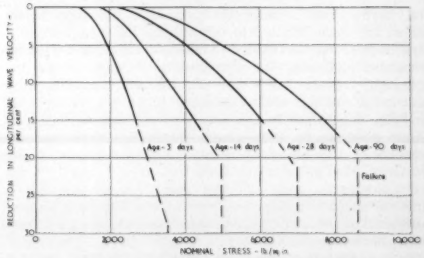

Fig. 3. Specimens tested in compression—effect of stress on longitudinal wave velocity in transverse direction

An indirect proof of this assumption was obtained from experiments on cubes of 4 in side which contained single cracks near their centre, 0·002 in thick and 0·5, 1·0 or 1·5 in wide by 4 in long. The cracks were produced by casting strips of foil into the concrete and withdrawing them prior to testing at an age of twenty-eight days. A significant increase of 2½–3% in the time of transmission occurred when the transducers were on opposite sides of the 1 in and 1·5 in cracks due to the diffraction of the pulse around the crack. Measurements made with the crack parallel to the path between the transducers gave no increase in the transmission time. This was to be expected owing to there being a direct path through the concrete for most of the surface area of the transducers.

Effect of loading conditions. The curves relating the velocity of ultrasonic pulses to the applied load were not altered by varying the rate of loading from 600–5 000 lb/in²/min.

When the applied load was sufficiently great to cause a fall of the longitudinal wave velocity in the transverse direction, maintenance of the load for 12 h produced no further change of velocity.

Fig. 4 shows the effect of the longitudinal wave velocity of reversing the load applied to the test specimens. In the transverse direction, a decrease of velocity occurred during both loading and unloading. This depended, however, upon the maximum load, and, when the initial change of velocity was less than 5%, the subsequent decreases of velocity were small and occurred principally during unloading.

In the axial direction, a decrease of longitudinal wave velocity occurred when the average stress was less than 1 000 lb/in².

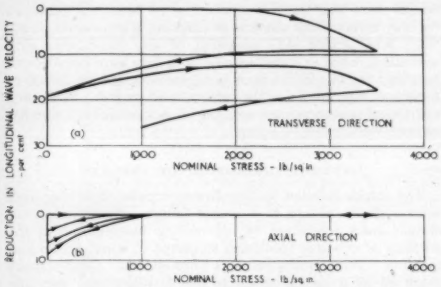

Fig. 4. Specimens tested in compression—effect of loading cycles

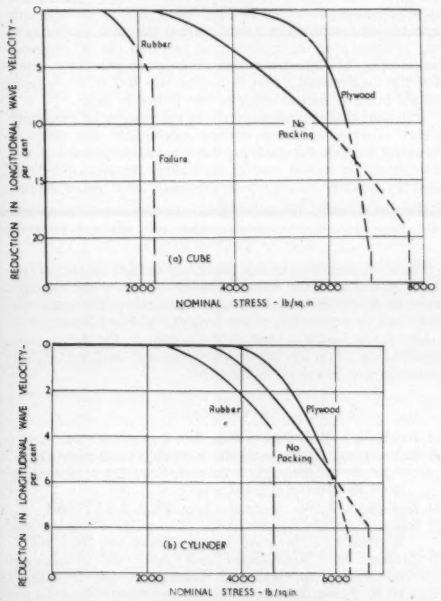

Fig. 5. Specimens tested in compression—effect of varying end packing

Effect of varying end restraint. Fig. 5 shows the effect of interposing hard rubber and plywood packings, each 0·125 in thick, between the ends of the specimens and the platens of the testing machine. The tests were made with cubes and cylinders.

Compared with specimens tested between the steel platens, the load at which the initial decrease of longitudinal wave velocity occurred in the transverse direction was reduced by using rubber packing and increased by employing plywood. The effect was smaller with cylindrical specimens than cubes.

When cubes were tested with rubber packing, ultimate failure occurred by two cracks through the centre of the cube parallel to the vertical sides. After test, the rubber showed permanent deformations consistent with maximum stresses being developed in these two mutually perpendicular directions. The fracture of the cube may have been due, therefore, to aggravated lateral expansion of the ends imposing tensile stresses which the concrete could not withstand. A similar type of failure occurred with cylinders tested with rubber packing; in this case radial and circumferential cracks appeared.

When plywood packing was employed, the change of longitudinal wave velocity in the transverse direction occurred at a higher load than when no packing was used. This may have been due to the gradual compression of the plywood, giving a more uniform distribution of stress in the concrete.

Effect of shape of specimens. The table summarizes the results which have been collected from the other sections of the work and shows the effect of employing various shapes of test-piece.

Effect of varying shape of specimen

Shape of specimen	*Packing*	*Applied pressure at which: Change of transverse velocity occurred* (P_c) lb/in²	*Ultimate failure occurred* (P_f) lb/in²	P_c/P_f %
Cube of 4 in side	none	2 500	7 700	33
	plywood	3 600	6 900	55
Cylinder 12 in long by 6 inches in diameter	none	3 500	6 700	52
	plywood	3 900	6 300	62
Bobbin of 17 in overall length, ends of diameter 5 in and with central parallel portion 8 in long by 3 inches in diameter	none	3 200	4 800	65

Thus internal cracking occurred at a greater proportion of the ultimate strength when the specimens were made more symmetrical and the length/cross-sectional area was increased.

Specimens tested in compression—discussion of results. The results show that, in general, the ultimate failure of specimens of concrete subjected to uniaxial compression is preceded by internal cracking parallel to the direction of loading. The load at which this occurs depends on the strength of the concrete and on the uniformity of the stress distribution, which can, of course, be affected by change of end packing and of shape of test-piece.

The opening of interstices within cylindrical specimens

subjected to uniaxial load has been observed by Bridgman.[3] In this work a dilatometer was used to measure the volume changes occurring as the load was increased to near failure. The materials tested included several types of rock which showed an irreversible increase of volume.

Since the cracks form parallel to the direction of loading, lateral pressure should prevent their formation. Smith and Brown[4] tested cement-mortar cylinders in a triaxial machine using lateral pressures of 0, 800, 1 600 and 2 400 lb/in^2. An analysis of their results by the method of Mohr's circle is given in Fig. 6. With lateral pressures, the circles had a

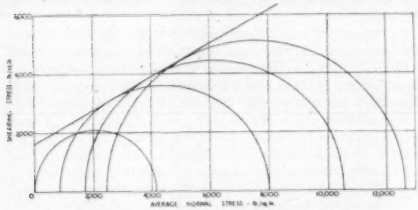

Fig. 6. Effect of lateral pressure on the failure of cement-mortar cylinders (Smith and Brown[4])

common tangent from which the shear strength of the material may be deduced. Without lateral pressure, however, the appropriate Mohr's circle was below the common tangent, indicating that the mortar failed before the shear strength was reached.

It is difficult to account for the lateral stresses which cause internal cracking parallel to the applied loading. The theory of elasticity gives no satisfactory explanation, and a rheological explanation involving relative lateral acceleration suggested by Reiner[5] has not yet been solved mathematically.

SPECIMENS TESTED IN TENSION

In this work, tests were made on bobbins, cylinders, beams tested in flexure, and cylinders tested on their sides [see Figs. 1(*c*) to 1(*f*)].

Specimens subjected to direct tension. When cylinders and bobbins were tested in direct tension, no change in the longitudinal wave velocity occurred in the transverse direction, but significant decreases of velocity occurred in the direction of stressing. Fig. 7 shows the results obtained with a cylinder 18 in long by 4 inches in diameter, the type of specimen giving the greatest change of velocity in the axial direction.

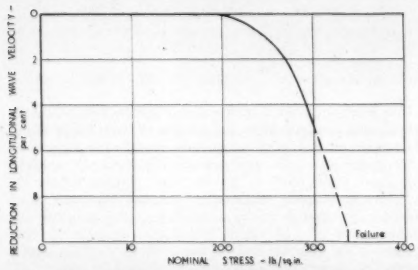

Fig. 7. Specimens tested in direct tension—effect of stress on longitudinal wave velocity in axial directions

Specimens tested in tension by an indirect technique. With concrete beams tested in flexure, and cylinders compressed on their sides to generate tensile stresses across a vertical plane, the longitudinal wave velocity in the direction of the tensile stresses did not vary significantly until failure occurred.

Specimens tested in tension—discussion of results. The results show that fracture of concrete by tension is preceded by only a very small amount of cracking if any occurs at all. Such pre-cracking only appeared of any significance with specimens tested in direct tension, and may have been due to localized faults such as poor bond between the underside of a piece of aggregate and the cement-sand mortar. With long cylindrical specimens cast vertically, it is possible for a number of such weaknesses to occur.

GENERAL DISCUSSION OF RESULTS

The cracks detected by the ultrasonic pulse technique were always of the nature of a tensile failure. Berg[6] observed similar crack formation by microscopic examination of the surfaces of concrete specimens subjected to compression and bending. Here, measurements showed that micro cracks occurred at a lateral strain of 10^{-4}, which was also the deformation limit for concrete in tension. It was concluded that the theory of maximum strain applies up to the ultimate strength of concrete. Calculations were made of the strains at which cracks occurred in the present tests on cylinders in tension and compression, assuming that the stress distribution was uniform over the cross-section and that the deformation was elastic. The lateral strain in compression was $1{\cdot}5 \times 10^{-4}$ and the longitudinal strain in tension was $0{\cdot}7 \times 10^{-4}$, both results being of similar order to that found by Berg.

It is clear that the measurement of the velocity of ultrasonic pulses through specimens during mechanical test offers a powerful weapon for studying the internal behaviour of the test-pieces. It should lead to reasonable theories of failure, possibly initially in regard to materials of a more homogeneous character than concrete.

ACKNOWLEDGEMENTS

The work described in this paper was carried out as part of the programme of the Road Research Board of the Department of Scientific and Industrial Research. The paper is published by permission of the Director of Road Research.

Mr. E. N. Gatfield assisted the author in the design and construction of the ultrasonic apparatus and took part in the measurements described in the paper.

REFERENCES

(1) Jones, R. *Mag. Concr. Res.*, No. 2, p. 67 (1949).
(2) Carneiro, F. *Une nouvelle méthode d'essai pour déterminer la résistance à la traction du béton* (Paris: Réunion des Laboratoires d'Essai, 1947).
(3) Bridgman, P. W. *J. Appl. Phys.*, **20**, p. 1241 (1949).
(4) Smith, F. C., and Brown, R. Q. *University of Washington Engineering Experiment Station Bulletin* No. 106 (1941).
(5) Reiner, M. *Deformation and flow: an elementary introduction to theoretical rheology*, p. 307 (London: H. K. Lewis, 1949).
(6) Berg, O. Ya. *Dokl. Akad. Nauk, SSSR*, **70**, p. 617 (1950).

A castable polyester resin for photoelastic work

By B. SUGARMAN, M.Sc., A.Inst.P., G. O. MOXLEY, B.Sc., A.R.I.C., and I. A. MARSHALL, B.Sc.,
The B.S.A. Group Research Centre, Sheffield

[*Paper first received* 17 *September*, 1951, *and in final form* 15 *October*, 1951]

Photoelasticity has, until the last few years, been, in the main, restricted to two-dimensional examination because of the limitations of model-making materials. Requirements for three-dimensional model-making plastics are discussed in detail, and the faults of the few materials used to date listed. The introduction of a cross-linked polyester resin, readily available, into this field permits further investigations to be conducted. The chemical and physical properties of this new resin are considered, and a theory explaining the "frozen" effect propounded. The resin is castable in the user's laboratory, and provided adequate care is taken, castings can be obtained to the near finished size. Mottle, which, it is thought, is developed during the setting period of the resin, and edge effects which appear during the freezing cycle, are the main limitations of this new plastic. Methods of overcoming both these defects have been devised and the techniques adopted are described in detail. The results indicate that the figure of merit (a criterion which may be adopted as an indication of the sensitivity of the material) of this particular resin is only slightly lower than that of the latest American material, Fosterite.

Until recently the science of photoelasticity has been limited to two-dimensional investigations. This has, in the main, been due to the non-existence of suitable materials for three-dimensional investigations. Of later years it has been possible, by the introduction of new resins into the plastic field, to extend the application of this science. Bakelite BT-61893 and Catalin 800 have, in the past, been used by workers adopting the frozen stress technique. This technique, amply described in the literature (notably by Frocht[1]), embodies the requirement that at a certain "critical temperature" the plastic deforms by an amount proportional to the stress. After cooling and removal of the load this type of plastic displays, when examined in a polariscope, a frozen pattern proportional to the stress which enables the stress distribution within the model to be determined. A perfectly frozen model may be cut or machined without disturbing the pattern.

The American manufactured plastic BT-61893 has been almost universally adopted in the past, as the most suitable one for this work, even though it is only obtainable in 12 × 6 in sheets of 1¼ in maximum thickness. Some workers in this country have used Catalin 800, which bears a great similarity to Trolon, adopted in Germany before the last war. In spite of the limitations of Columbia Resin 39 (C.R.39), a glass-clear plastic, this material has been used to a slight extent for two-dimensional frozen stress investigations, but owing to its inherent manufacturing stress, it cannot be used as a truly three-dimensional material. It is, however, remarkably free from some of the defects which detract from the usefulness of BT-61893 and Catalin 800. Although alkyd resins have been manufactured for some years, the use of a styrene alkyd resin as a three-dimensional photoelastic plastic is only a recent development. Fosterite,[2] a material of this class now manufactured in the U.S.A., is much superior to materials used in the past and has consequently been adopted by many workers there; its cost and availability, however, preclude its general industrial use in this country.

The results published in this paper have been obtained from tests on a cross-linked polyester resin which is obtainable in this country at a reasonable price, and they suggest that this plastic or a modification of it will prove to be better in all respects than BT-61893 and Catalin for general use. It appears also that its properties are similar to those reported by various workers on Fosterite, and, in fact, it is considered that it might easily prove to be a suitable alternative for workers unable to afford or to purchase Fosterite.

GENERAL REQUIREMENTS FOR A MATERIAL FOR THREE-DIMENSIONAL PHOTOELASTICITY

Frocht[1] and Fisher[3] have both tabulated the main requirements for a material to be used for three-dimensional photoelasticity, and the salient requirements are briefly repeated here. (*a*) The material should be homogeneous and free from residual stress. Materials displaying initial birefringence are obviously unsuitable and lack of homogeneity, which in general appears as a mottle, cannot be tolerated. In some cases residual stress can be removed by annealing, but in others annealing has no appreciable effect on the fringe pattern. (*b*) The plastic should be capable of easy machining without producing machining stresses or chipping. If excessive heat is generated during machining it is likely that frozen stresses may be produced. (*c*) There should be an easily determined critical temperature at which the material behaves elastically. Stresses, once frozen in, should not be disturbed by subsequent machining. In addition, at this critical temperature the material should be free from optical or strain creep. (*d*) Edge effects, either "time edge" or "rind" effects, should not occur. At room temperature, the majority of three-dimensional plastics slowly absorb or evolve moisture and possibly alternative constituents at the surface. This transference causes edge stress of a compressive or tensile nature which cannot be removed by subsequent treatment, apart from machining. Some plastics display this effect only when subjected to heat, and this reaction is again non-reversible unless special techniques are adopted. (*e*) The product of the "frozen" modulus of elasticity and the "frozen" sensitivity should be as high as possible. This

is tantamount to saying that the figure of merit, which is defined as the effective modulus divided by the effective fringe value, should also be as high as possible. The photoelastician requires the minimum deformation of his model with the maximum number of fringes. Associated also with this particular requirement is the ultimate tensile strength. When the plastic is at the critical temperature, it is obvious that a high figure of merit is not the sole consideration, for the plastic itself, when hot, must withstand a reasonable stress without fear of fracture. (*f*) In addition to the previous requirements, the material should be easily available at a moderate cost and, if possible, should be capable of being cast within the confines of the user's laboratory. The first of these requirements means that although a material might satisfactorily meet all the technical requirements, a lack of availability may preclude its use in this country. The second would assist a user in eliminating waste. If the model can be cast to its near finished shape or size, machining time, cost, and material wastage are reduced.

The above conditions are, in the main, fulfilled by Fosterite. However, this material is neither easily available nor inexpensive, and it does possess a certain inherent mottle. Bakelite BT-61893 and Catalin fail on several counts, since both are available only in limited thicknesses and sizes, they cannot be cast, and possess severe edge effects which are aggravated by heating. Further, Bakelite BT-61893 has a low figure of merit owing to the low value of Young's modulus at the freezing temperature, and Catalin possesses severe creep recovery. This defect is probably the greatest disadvantage occurring with Catalin. The possibility of using Marco type resins which are readily available in Great Britain was therefore explored.

MARCO RESINS

Marco resins (by Scott Bader and Co. Ltd., of London) are polymers of the type known as modified polyesters, originally developed and introduced industrially in the U.S.A. as low-pressure laminating resins. Their potentialities as casting resins soon became obvious, and several types developed purely for this purpose are now commercially available. Of these resins we have found Marco Resin S.B.26.C to be the most satisfactory for photoelastic purposes. On copolymerizing with styrene (Monomer C), under the correct conditions it sets to a very pale amber glass-like solid, which may be machined to almost any desired shape provided the correct techniques are employed. Chemically S.B.26.C is a linear polyester, based on a dihydric alcohol and a mixture of saturated and unsaturated dicarboxylic acids. The proportions of the materials employed, and the conditions of the reaction are closely controlled in the process of manufacture, with the result that photoelastically only very small differences are observed between two different batches of resin. The product, which is a thick golden syrupy liquid, is subsequently copolymerized with a monomer, of which styrene is the most commonly used. The copolymerization is initiated by a peroxide catalyst, and accelerated by a solution of a metal naphthenate in styrene. Owing to the presence of more than one double bond per molecule of base resin the reaction results in a cross-linked macro-molecular structure (i.e. a thermoset resin). Obviously the amount of monomer employed in the reaction will influence the degree of cross-linking, and it is actually found in practice that both the Young's modulus and the sensitivity alter with styrene content. The readiness with which Marco resins may be cast to give relatively stress-free products may be explained by the fact that the transition from liquid to solid state is achieved by a polymerization reaction in which no volatile products are evolved, and only a small volume change occurs.

THEORY

In order to possess satisfactory properties for three-dimensional analysis the plastic must be cross-linked to some extent. A hypothesis which is advanced to explain the three-dimensional phenomenon is similar to the "diphase" theory proposed by Frocht,[1] but does not require the existence of two separate and distinct phases. It is suggested that the photoelastic effect is due to the polarization of the chemical bonds present in the plastic, caused by their being strained when an external stress is applied. In this type of plastic we have true covalent chemical bonds (primary bonds) which link up the individual atoms in the three-dimensional mesh structure, and we also have secondary bonds (caused by Van der Waals' forces), which are weak linkages between neighbouring atoms in different chains of the structure. These latter bonds are analogous to the crystal forces existing in normal organic compounds and are easily disrupted when thermal energy is absorbed. At the "critical temperature" or above it these secondary bonds cannot exist, and the properties of the material will be entirely due to the primary covalent bonds. At still higher temperatures, these latter will be fractured and the material will decompose.

The formation of the fringe pattern, therefore, during a freezing cycle is caused by the following effects. On loading the specimen at room temperature, a fringe pattern develops, which is due to the combined polarizations of the primary and secondary bonds. As the temperature is raised, the secondary bonds are progressively eliminated, until at the "critical temperature" the fringe pattern is due to the polarization of the primary linkages only. After cooling and on removing the load there is some relaxation which is once again due to the combined effect of the primary and secondary bond polarizations (which will, in general, be different and possibly even of opposite signs). The primary bond sensitivity appears to be almost independent of temperature as the overall sensitivity varies little above the critical temperature. By postulating positive and negative sensitivities for the two effects where necessary, the photoelastic phenomena as observed in Catalin and Fosterite may be satisfactorily explained.

CASTING

The technique developed at the B.S.A. Group Research Centre for the production of standard castings up to about 4 lb in weight and of maximum sensitivity, is as follows (the catalyst and accelerator quantities mentioned may have to be adjusted for different batches of resin). Half a part by weight of catalyst H.C.H. is dissolved in 40 parts of "Monomer C" (styrene), with slight warming if necessary. This mixture is then added to one hundred parts by weight of resin S.B.26.C and stirred until a completely homogeneous product is obtained. Finally, one and a half parts of "Accelerator E" are thoroughly stirred in. If perfectly clean castings are desired it is advisable to filter at this stage. After standing to allow air-bubbles to rise to the surface, the mix is poured into the mould contained in a water bath maintained at room temperature. If very large castings are required, the temperature of the cooling bath may have to be reduced even further. Certain substances, such as rubber and brass, inhibit, or are attacked by the resin and therefore care should be taken in the selection of the mould materials. Glass, aluminium and ferrous metals are perfectly satisfactory for this purpose, while as an additional safeguard, a thin film of polyvinyl alcohol, which also acts as a parting agent, may be deposited on the surface of the mould from a dilute aqueous solution of the polymer.

After an interval (usually about two days), depending both on the temperature of the mixture and the proportions of accelerator and catalyst used, a rapid increase in viscosity occurs, the mixture assuming solid properties giving a soft rubbery product known as a gel. Subsequently the gel hardens, with the evolution of considerable quantities of heat. This is the critical stage in the casting of large blocks of resin, as if the temperature of the mass is allowed to rise the rate of the reaction increases accordingly, and a severely stressed casting may result. This type of defect cannot be removed by annealing, and is probably due to the introduction of stresses of thermal origin while primary bonds are still being formed in the body of the gel. In extreme cases extensive cracking may occur. The only way of controlling this strongly exothermic reaction is by adjusting the accelerator and catalyst concentrations, and ensuring that the initial temperature of gelation is sufficiently low. Unfortunately, the mottle effect appears to be accentuated when the rate of gelation is retarded in this manner, but this problem is considered in detail below.

RESULTS

In order to compare the properties of Marco resin containing different amounts of cross-linking, the following programme was carried out: five sheets compounded with different percentages of styrene were cast and subjected to the same annealing and machining treatment. Four specimens were obtained from each sheet and were tested simultaneously. It was considered that only the effective Young's modulus, and the effective material fringe value of the plastic need be determined, the experimental technique adopted being as follows: pairs of fiduciary marks were engraved on opposite faces of each specimen, and the lengths measured between each pair, when cold. By evaluating Young's modulus from results obtained from opposite faces of the specimen, allowance could be made for any slight bending which may have occurred owing to unsymmetrical loading.

The "effective" extension was determined from the specimen lengths after they had been subjected to the following cycle: the four tensile specimens (cut from one sheet) were mounted in the oven and loaded at room temperature. The oven temperature was raised to 96° C in 35 min and maintained to within $\pm \frac{1}{4}$° C of this temperature for a further 25 min. Earlier experiments had proved that at 96° C the plastic behaved elastically, was free from optical and strain creep, and generally fulfilled requirement (*c*) listed above. The oven was then automatically switched off and the specimens cooled to room temperature in about 3 h. The frozen fringe order was recorded for each specimen and yielded the effective material fringe value for each sample.

From the moduli and fringe value results the means were recorded. After a period of a week the four specimens were carefully annealed, and after a further week the schedule was repeated to determine whether the previous history had any appreciable effect upon the properties of the material. The results of these experiments are illustrated in Table 1.

Table 1. *Properties of Marco resin containing different amounts of cross linking*

% styrene added	Mean effective material fringe value lb/in² tension/(fringe/in (λ_v = 5 893 Å)		Mean effective modulus lb/in²		Mean figure of merit	
	Test	Retest	Test	Retest	Test	Retest
20	12·6	13·0	4 620	4 550	367	350
30	9·6	9·6	5 090	5 300	532	553
40	8·3	8·1	5 400	4 710	652	578
40	8·1	8·2	4 640	4 620	571	562
45	7·7	7·9	4 720	4 340	611	552

From the results it can be seen that the effective fringe value decreases with increasing monomer concentration, while the effective modulus increases to a maximum and then decreases. The value of the quotient, modulus divided by fringe value (the figure of merit), reaches a maximum at approximately 40% styrene, and consequently this was chosen by us as the best mix. The previous history of the specimen appears to have no appreciable effect on its properties.

Of the requirements to be met by a perfect photoelastic material Marco resin S.B.26.C possesses all but two to a satisfactory degree. Firstly it displays an "edge effect" when heated in air as shown in Fig. 1(*a*). It differs from that observed in Catalin in that a freshly machined edge shows no stress over long periods until it is heated. At the "critical temperature" the effect develops extremely rapidly and reaches a stable value in a matter of a few minutes. At the most it is of the order of one fringe of tensile stress in a $\frac{1}{4}$ in thickness. If the

specimen temperature rises too far above 96° C, crazing of the surface may be observed. Secondly, a typically cast block of the plastic normally possesses serious mottle when observed in a polariscope. The form which the mottle takes—a series of irregular light and dark streaks orientated chiefly in a vertical direction, suggests that the phenomenon is in some way bound up with convection currents which are present in the gelling resin. This results in differential thermal effects in the mass, causing premature gelation of isolated tracts of resin, which is later followed by diffusion effects, causing inhomogeneity of the finished product. To a lesser extent it may be criticized in three respects: (*a*) the ultimate tensile strength at the critical temperature could, with advantage, be higher; (*b*) the average figure of merit is slightly less than that of Fosterite; (*c*) it does possess a certain degree of brittleness.

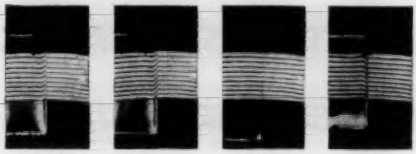

(*a*) (*b*) (*c*) (*d*)

Fig. 1. Effect of the annealing medium on the edge effect of specimens of Marco resin, $\frac{1}{2}$ in thick. Annealed in (*a*) air, (*b*) glycerine, (*c*) 13½% water in glycerine, (*d*) water

When machining Marco resin, it should be treated in a similar manner to thermoplastics, such as polystyrene and Perspex. For example, for turning: (*a*) tools should be sharp and have ample top rake and clearance; (*b*) it is an advantage to apply copious quantities of soluble cutting oil coolant or preferably impinge a strong air blast at the seat of cutting; (*c*) cutting speeds should be as high as practicable. (Speeds of the order of 100 ft/min have been found suitable.) We have found engraving to be a satisfactory method of producing intricate recessed sections.

REDUCTION OF EDGE EFFECTS

Preliminary experiments aimed at inhibiting the edge effect by immersing the plastic in various liquids, as other materials have been treated in the past. Immersion in silicone and hydro-carbon oils was tried without success. It was then shown that water, as a surrounding medium, reversed the sign of the edge effect (see Fig. 1(*d*)). Further, it was found that *in vacuo* the edge effect was "normal" (tensile), in pure water vapour "abnormal" (compressive), which led to the idea of balancing the humidity of the annealing atmosphere. The practical difficulties involved in controlling the atmosphere in the oven without special apparatus, however, proved too great, and recourse was made to annealing in a liquid medium, containing the correct proportion of water in a hygroscopic constituent miscible with it in all proportions. Glycerine was selected as this second component, as it has these properties, and because when used alone as the surrounding medium it gave a "normal" edge effect.

A number of standard size test-pieces were made and annealed in solutions containing 50%, 40%, 30%, 20% and 10% by volume of water in glycerine. The abnormal edge effect in each succeeding mix was found to be reduced, until with the 10% solution a small "normal" effect was observed. New solutions were tested containing 8%, 12% and 15% water, and of these only a trace of edge effect was found in the solution containing 12% water, 88% glycerine. We may therefore assume that at some optimum concentration of water, the edge effect may be reduced to negligible proportions. Fig. 1 shows specimens ($\frac{1}{2}$ in thick) which have been carefully annealed in air, glycerine, 13½% v/v water in glycerine, and water respectively. As a result of these experiments, it is postulated that on heating, water (possibly with other components) is lost from the surface of the plastic, and it was actually determined that a specimen lost 0·0005 g/cm² after heating for 1 hour at 100° C. The following experiment was conducted in an attempt to identify the evolved component. A litre flask with a gas-delivery tube was charged with 215 g of finely divided Marco shavings, which had been carefully dried at room temperature. A stream of dry nitrogen was then passed through the apparatus which was heated in an oven at about 96° C, and the issuing vapours condensed in a trap cooled in ice. During the first 6 h of heating, two colourless immiscible liquids collected in the trap, and although heating was continued for a further 15 h, very little further change occurred. Table 2 gives the physical constants of the two liquids collected, and their relative proportions in the mixture.

Table 2. *Analysis of Marco resin*

	n_D^{22}	D_4^{22}	quantity present	water content
Component A	1·4669	0·898 g/cc	0·8 g.	—
Component B	1·3968	1·058 g/cc	0·6 g	30% w/w

The total amount of mixed liquids obtained after 20 hours' heating was 1·4 g. Component A had the characteristics of a typical hydrocarbon and was probably an impurity incompletely eliminated during manufacture. Its proportion was found to vary considerably between different batches of resin, as would be expected if this were the explanation of its presence. The proportion of component B was found to vary only slightly between different batches and it is almost certainly produced by some reaction at the surface of the plastic. Its water content was estimated (employing the Karl Fischer reagent) as 30% by weight. The identity of the remaining 70% is uncertain as insufficient of component B was obtained for a full analysis to be carried out. It is possible, however, from a consideration of the structure of the resin, that this material is ethylene glycol.

REDUCTION OF MOTTLE

This effect consists mainly of a series of alternate dark and light irregular streaks in the material when observed

between crossed Polaroids. It is incapable of being removed by annealing. It had been suggested that this undesirable effect could be eliminated by suitable rotation of the mould during casting. To test this hypothesis a cylinder was cast while rotating about a horizontal axis

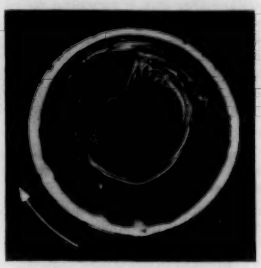

Fig. 2. Showing orientation of mottle by rotation

through the length of the cylinder at speeds of rotation of the order of 200 r.p.m. It was found that the mottle was orientated chiefly in the direction of rotation (see Fig. 2), and was most pronounced at the point through which the axis of rotation passed. Cylindrical castings approximately 1·1 in diameter by 3·25 in long were also prepared in a centrifuge rotating at 2 000 r.p.m., and a disk cut from a similar casting prepared in the normal manner. Fig. 3(*b*) shows the same arrangement with a stress pattern introduced to show any distortion of the fringes caused by the mottle. The gravitational fields at the top of the rotating cylinders were estimated as 42*g* and 168*g*. The success of the centrifugal method may be explained on the "convection" theory, as if the gravitational field is increased sufficiently, the convection currents become so rapid that temperature differences cannot exist for any significant length of time.

CONCLUSION

Marco Resin S.B.26.C as normally cast is not completely satisfactory for three-dimensional photoelasticity, owing to the mottle developed during setting and the edge effect appearing during the freezing cycle. Centrifugal casting, however, reduces the mottle to negligible amounts, although care must be taken to avoid the formation of gravitational casting stresses. By conducting all heating cycles in a balanced mixture of glycerine and water, edge effects can be eliminated. A 40% styrene mix yields a plastic which possesses a figure of merit of the same order as that of Fosterite, at the critical temperature of 96° C.

ACKNOWLEDGEMENTS

The assistance given by Mr. B. Parkyn of Messrs. Scott Bader and Co. Ltd. is gratefully acknowledged, as are the helpful discussions with members of the Stress Analysis Group of The Institute of Physics. Guidance and continued support from Mr. D. A. Oliver, Director of Research, the B.S.A. Group Research Centre, Sheffield, facilitated the execution of this investigation.

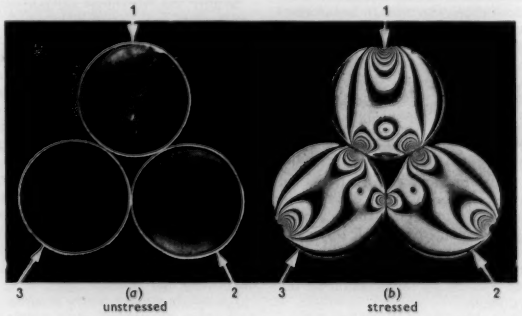

Fig. 3. Showing reduction of mottle by centrifugal casting at gravitational fields of (1) *g*, (2) 42 *g*, and (3) 168 *g*

some encouraging results were obtained. It was found that the mottle was almost eliminated, but care had to be taken not to continue centrifuging too long after initial gelation had occurred, otherwise gravitational stresses were "frozen" in. (These stresses were found to be similar to the "fixed" type, and were not affected by annealing.)

Further tests were conducted employing controlled speeds of rotation of 500, 750 and 1 000 r.p.m. Fig. 3(*a*) shows disks cut from the region of the top of the cylinders rotating at 500 and 1 000 r.p.m. in comparison with such

REFERENCES

(1) FROCHT, M. M. *Photoelasticity*, Vols. I and II (New York: John Wiley and Sons Inc., 1941 and 1948).
(2) LEVEN, M. M. *Proc. Soc. Exp. Stress Analysis*, Vol. VI, Nos. I and II (1948).
(3) FISHER, W. A. P. *Proc. Instn Mech. Engrs*, **158** (1948).

New books

Physics as a career. By N. CLARKE. (London: The Institute of Physics.) Pp. 70. Price 6*s*.

This book gives guidance on the available avenues of training which lead to professional recognition as a physicist, together with factual information and comments on the main openings for employment. These include industrial, university, Government, research association, technical college, school and hospital posts, to each of which a chapter is devoted. The other chapters are: On finding a job, Other posts, and Institutions and Societies. A short introductory chapter, followed by a brief outline of physics and its applications, is intended for the convenience of those not familiar with the subject.

The President of The Institute of Physics writes in his foreword: "In writing this book Mr. Clarke (deputy secretary) has had two objects in mind. One is to provide the essential information required by those who contemplate entering upon a career in physics. The other is to give them advice which they may find helpful both during their period of training and in the exercise of their profession. The former mainly comprises facts which are already available to those who know where to find them, but it is, nevertheless, extremely valuable to have them collected together and systematically arranged. The latter is even more valuable, since it derives from extensive personal experience which has endowed Mr. Clarke with quite exceptional qualifications for this task. As he points out, he takes full responsibility for the opinions expressed, but few experienced physicists will be found to differ from him, and many less experienced might profitably bear them in mind. . . . I believe that this book will be of real assistance to all those who wish to be informed on the nature and prospects of a career in physics, as well as to many who have already embarked upon their period of training."

Tensor analysis. By I. S. SOKOLNIKOFF. (London: Chapman and Hall Ltd.) Pp. 335. Price 48*s*.

This attractive volume in the Wiley Applied Mathematics series is based on graduate lectures given by Professor Sokolnikoff at the University of California and elsewhere. The first chapter deals with linear transformations and matrices, and is a useful preliminary to the discussion of the algebra and calculus of tensors to which the second chapter is devoted. The approach here is entirely pure-mathematical, the applications being reserved for separate treatment later. However, the exposition is lucid and compact and will be appreciated by those who have had an elementary introduction to the subject; others may find it difficult.

The remaining four chapters of the book deal with the uses of tensors in geometry and in mechanics. There is an interesting account of Newtonian mechanics and generalized dynamics, followed by a short chapter on relativity which discusses the main results of the special theory as well as some applications of the general theory. The final chapter on the mechanics of continuous media will be of interest to physicists working on non-linear problems in elasticity.

The printing is excellent throughout. J. TOPPING

Elements of thermodynamics and statistical mechanics. By E. O. HERCUS. (London: Cambridge University Press. Melbourne: Melbourne University Press. Pp. ix + 153. Price 21*s*.

This little book gives a useful development of the formulae and applications of thermodynamics, and as such will be of value for reference as well as for study. It does not enter into such questions as the evidence for the first and second laws of thermodynamics. After this, it presents a parallel course of statistical mechanics which is clear, accurate and within the capacity of a student reading for a degree in physics to understand and assimilate.

The average student, however, will probably feel that a guinea for this is more than he can spare, and that for such a sum he ought to get the whole of his course in heat.

J. H. AWBERY

Progress in biophysics and biophysical chemistry, Vol. 2. Edited by J. A. V. Butler and J. T. Randall. (London: Pergamon Press Ltd.) Pp. viii + 323. Price 50*s*.

This second volume of eight further articles reviewing recent developments in the application of physical and physico-chemical methods to biological and medical problems is of the same high standard as the first. The articles, in order, are Birefringence of cytoplasm and cell membranes by M. M. Swann and J. M. Mitchison; Biophysical aspects of polysaccharide structure in plants by R. D. Preston; Physico-chemical properties of the nucleic acids by D. O. Jordan; Physical principles underlying the clinical use of radioactive isotopes by W. K. Sinclair and L. F. Lamerton; Biophysical aspects of nervous function by W. D. Wyke; Quantum physics of vision: theoretical discussion by M. H. Pirenne; Electron microscopy of developing bacteriophage and other viruses by R. W. G. Wyckoff; and Biological actions of ionizing radiations by L. H. Gray.

Swann and Mitchison do not discuss techniques. They concentrate upon conclusions which have been drawn from the results, strongly criticizing inaccuracies of the Swedish school of workers and offering their own conclusions, including a new concept of the structure of a new cell membrane. Preston's article is largely written around the polysaccharide cellulose while Jordan has chosen to emphasize the chemical aspects of the nucleic acids. The article dealing with radioactive isotopes seemed the least inspiring of the volume, but this may be due to the reviewer's more intimate contact with this subject. The documentation of the most interesting articles by Wyke and by Gray must be of the greatest value to workers in these fields. Pirenne provides a lucid discussion of a fascinating field of work and Wyckoff's article, with its beautiful set of electron micrographs makes very clear the new field of interpretation which the electron microscope has opened up.

The whole volume seems to show that as a result of the application of physical and physico-chemical methods to biological problems, data are being collected with considerable speed and in considerable quantity. Complete and fully satisfying explanations of the data are much more difficult to find. In this respect all workers in these fields would do well always to bear in mind the following remarks from Wyke's article in this volume:—

"It would appear at present that the principal function of the biophysicist is to expedite the application of recent advances in the physical sciences to biological problems. This implies a close relationship between the biophysicist and his more biologically-minded colleague: but in some instances biophysics seems to be acquiring a false independence from biology, and the biophysicist is in danger of being divorced from biological reality by undue concentration

upon physical models which attempt to represent certain aspects of animal function."

The book is well produced and only a very few minor printer's errors seem to have escaped the proof readers. The most disturbing of these for the reader may be the references on page 269 which apparently refer to pages in the manuscript and not in the text. C. W. WILSON

Proceedings of the International Conference on Low Temperature Physics—Oxford 1951. Edited by R. BOWERS. (Oxford: The Clarendon Laboratory.) Pp. xiv + 165. Price 15*s*.

The International Union of Pure and Applied Physics, in conjunction with UNESCO, sponsored a conference on low temperature physics which was held in Oxford from 22–28 August, 1951.

The proceedings now published correspond more with the series of "summarized proceedings" of conferences which are published from time to time in this *Journal*. The volume is of foolscap size and is a reproduction of the original typescript. The text was prepared by fifty reporters who, between them, covered the 100 lectures and discussions and usually had the assistance of the lecturers' notes. It is assumed that the work described at the conference will be published in scientific journals by the lecturers in due course.

The two introductory lectures were on "Paramagnetism" and on "Limitations of the two-fluid theory." The other lectures were grouped under the headings: Thermal properties, Electrical resistivity, Liquid helium, Superconductivity and Magnetism.

The Editor and his colleagues are to be congratulated on their work, although the title "Proceedings" is perhaps a little misleading for a collection of abstracts. It is interesting to speculate on how far this method of prior partial publication of new work is desirable when it is intended to submit most of it later in full to well-established scientific journals; there is much to be said on both sides. H. R. LANG

Absorptions—Spektralanalyse. By F. X. MAYER and A. LUSZCZAK. (Berlin: Walter De Gruyter and Co.) Pp. xiv + 238. Price 14 marks.

This book is an account of the practical methods of absorption spectrophotometry in the visible and ultra-violet regions as developed on the European continent. The methods are almost without exception based on photographic techniques as little photoelectric equipment has as yet become available to the continental research worker. The basic principles of spectrophotometry are thoroughly expounded and its application in qualitative and quantitative analysis is illustrated by many examples covering a wide range of analytical problems. It is doubtful whether the book will appeal to workers in this country because here photoelectric instruments with their greater quantitative accuracy and ease of operation have largely superseded photographic ones.

W. C. PRICE

Principles of lighting. By W. R. STEVENS, B.Sc. (London: Constable and Co. Ltd.). Pp. x + 482. Price 35*s*.

This book will in time come to be regarded as a standard text-book on the design of lighting equipment and the fundamentals of installation design, for in its 420 pages of reading matter and 60 pages of appendices the author has condensed much of the basic knowledge of the expert illuminating engineer. It is of the same calibre as that great book, *The Theory and Design of Illuminating Engineering Equipment*, written twenty years ago by Jolley, Waldram, and Wilson, and now out of print, and it will be welcomed as a comprehensive description of methods of applying current theories and rules of good practice.

The opening chapters deal with fundamentals, the units of measurement, the properties of the eye, the applied physics of light production and the measurement of light and of colour. There are two very practical chapters on the optical, thermal, and mechanical considerations in the design of lighting fittings, and then ten chapters dealing with the special requirements of different types of lighting installations. In all these chapters the author gives direct and practical guidance on the matter under consideration and gives methods of applying the principles which have been set forth in general terms in documents such as the *Code for the Lighting of Buildings* issued by the Illuminating Engineering Society.

Instrumentation is an important part of illuminating engineering and, although lighting is an art and its results are not easily assessed by physical measurement, the recent developments in light sources and in principles of design have only been achieved by the invention and use of elaborate and accurate instruments. In this book, the reader is brought up to date by an excellent twenty page summary of photometric methods in Chapter IV, supplemented by a short list of references for general reading.

The production of the book makes it a pleasure to read, and the half-tone and line illustrations, 200 in all, are of uniformly good quality. The references have obviously been selected impartially from many sources, and the index is unusually good. Although intended to be used by students preparing for the City and Guilds Final Examination in Illuminating Engineering, its main service should be to engineers, architects, and others, in this country and overseas, concerned with good lighting. J. G. HOLMES

Electrical phenomena at interfaces. Edited by Dr. J. A. V. BUTLER. (London: Methuen and Co. Ltd.) Pp. vii + 309. Price 32*s*. 6*d*.

In many branches of experimental science the investigation of electrical phenomena at interfaces is of importance. The subject is a wide one and involves the study of electrically charged surfaces, electrophoresis, overpotential, stability of colloidal solutions, membrane potentials, polarization, the deposition of metals, etc. In the monograph of some 300 pages by Dr. J. A. V. Butler, practically all the basic research on this subject has been collected and correlated with the aid of six recognized experts. An excellent compilation has been produced with good diagrams and an index. The book is produced in the usual high standard of Methuen and the price is reasonable. It can be highly recommended.

J. REILLY

Dictionary of mathematical sciences. Vol. 1: German–English. By LEO HERLAND. (London: Hafner Publishing Co. Ltd.) Pp. 235. Price 24*s*.

If we define a good dictionary as one which tempts the reader to browse in it, this dictionary is certainly a good one largely owing to the very liberal cross-references which are specially copious and useful in the mathematical entries. Another useful feature is the illustration of mathematical terms in their context, model usages being given in great detail. The dictionary also covers certain fields of application such as mathematical logic, statistics and commercial terms. One feels that at least the latter are somewhat out of place and have been treated as a "cinderella"; the English reader will find many of the commercial entries useless since American terminology is used almost exclusively. The book is thoroughly recommended to those who wish to consult or translate German mathematical works. W. F. BERG

Notes and comments

Elections to The Institute of Physics

The following elections have been made by the Board of The Institute of Physics:

Fellows: J. W. Boag, H. R. Heath, R. F. Thyer, E. J. Whitmore.

Associates: G. R. Bainbridge, J. G. Campbell, M. W. Clutterbuck, R. Deighton, L. T. Draycott, A. S. Gladwin, G. R. Goldman, W. L. Harries, H. Hughes, R. C. Kell, W. F. Kilby, P. H. Knight, D. N. Layton, E. B. Nicholls, J. A. Place, D. E. Thomas, G. Thomas, C. H. Vincent, B. N. Watts.

Twenty-three Graduates, thirteen Students and ten Subscribers were also elected.

Autumn Conference of the Manchester Branch

A one-day conference has been arranged by the Manchester Branch of The Institute of Physics to take place on 29 October, 1952, under the chairmanship of Dr. F. C. Toy, a past president of the Institute. The programme is divided into two sessions:—

First session 2 *p.m.*	*Title*
Professor W. T. Astbury, F.R.S., Leeds University	Review
Dr. Nils Gralen, Swedish Institute of Textile Research	Electron microscopical studies of keratinous objects
Dr. Muhlethaler, Pflanzenphysiologisches Institut, Zurich	Electron microscopical studies of fibres and plant cell walls
Mr. J. Ames, I.C.I. Nobel Division	Sectioning technique for electron microscopy and its application to protein fibres
Second session 5.30 *p.m.*	*Title*
Mr. J. M. Preston, College of Technology, Manchester	Review
Dr. A. Elliott, Courtaulds Ltd., Maidenhead	Infra-red dichroism of polypeptides
Mr. R. Meredith, British Cotton Industry Research Association	Measurement of orientation in cotton by optical methods
Mr. R. Faust, British Rayon Research Association	An interferometric method of studying radial variations in refractive indices

The conference will be held in the Schuster Building, University of Manchester. Tea will be available in the University Refectory between the afternoon and evening sessions. Persons who wish to attend the conference should apply to the Conference Secretary, Mr. A. G. Thompson, Research Department, Tootal Broadhurst Lee Co. Ltd., Oxford Street, Manchester.

Electronics symposium and exhibition

The Electrical and Electronics Section of the Scientific Instrument Manufacturers' Association will be holding its Fourth Symposium and Exhibition at the Examination Hall, Queen Square, London, W.C.1, from Tuesday, 2 September, to Friday, 5 September, 1952.

As in previous years, a series of technical papers will be read. There will also be a comprehensive display of the latest types of British scientific and electronic instruments, most of which will be shown in operation during the period of the exhibition.

The following programme of technical papers has been arranged:

Tuesday afternoon—2 *September.*

Electronic control systems for large astronomical telescopes.
(G. H. Hickling, B.Sc., A.M.I.E.E., of Sir Howard Grubb, Parsons and Co.)

Wednesday morning—3 *September.*

(*a*) The development of resistive elements and wave-guide attenuators from a semi-conducting ceramic.
(J. M. Herbert, B.Sc., A.R.I.C., of The Plessey Co. Ltd.)

(*b*) Electronics in strain measurement.
(D. L. Johnston, B.Sc., and D. W. Hobbs, of Elliott Brothers (London) Ltd.)

Wednesday afternoon—3 *September.*

Electronic instruments developed by the E.R.A. for research in the electrical industry.
(G. Mole, Ph.D., F.Inst.P., of the Electrical Research Association.)

Thursday morning—4 *September.*

(*a*) Electronic measurement and control for industry.
(J. R. Boundy, B.Sc., A.M.I.E.E., of Evershed and Vignoles Ltd.)

(*b*) Electronics in temperature control.
(D. K. Das Gupta, M.Sc., and R. J. Russell-Bates, of Elliott Brothers (London) Ltd.)

Thursday afternoon—4 *September.*

The application of high power ultrasonics.
(B. E. Noltingk, Ph.D., A.Inst.P., of Mullard Research Laboratories.)

Friday morning—5 *September.*

User forum—an open discussion of instrument users' problems.

Time will be allowed for brief discussion following each paper. Entrance to the Symposium itself will be by ticket of admission (covering also the Exhibition), obtainable on application to the Secretary of the Scientific Instrument Manufacturers' Association, 20 Queen Anne Street, London, W.1.

Journal of Scientific Instruments

Contents of the July issue

ORIGINAL CONTRIBUTIONS

A sedimentation balance for particle size analysis in the sub-sieve range. By W. Bostock.
An electronic device for measuring small transient displacements. By J. J. Trott.
A simple hot stage for the study of polarizing microscope interference figures at elevated temperatures. By E. G. Steward.
The use of diffraction gratings with an infra-red spectrometer. By J. D. S. Goulden.
An apparatus for the measurement of multiple scattering of tracks in nuclear emulsions. By N. C. Barford and R. M. Tennent.
The Pitot cylinder as a static pressure probe in turbulent flow. By A. H. Glaser.
Two viscometers for rapid measurements at definite shearing stresses. By R. S. Higginbotham and J. J. Benbow.
The elimination of errors due to stray capacitances in certain Schering bridge measurements. By H. C. Hall.
A differential-voltmeter using a temperature-limited diode. By V. H. Attree.
A recording raingauge. By E. Nothmann.
A Weissenberg X-ray diffraction camera. By C. A. Beevers.

LABORATORY AND WORKSHOP NOTES

Wavelength calibration of infra-red spectrometers in the wavelength region 15–25 μ and the selection of solvents. By L. W. Marrison.
Improvements in the construction of molecular models. By J. C. McGowan and K. Moss.
A dispersion unit for clays. By A. R. Carthew and W. F. Cole.
A photoelectric balancing device for use with "chainomatic"-type balances. By P. W. Allen and R. D. Wright.
An adjustable Debye–Scherrer X-ray camera for specimens of large diameter. By A. Taylor.
A quick-release seal for vacuum desiccators. By J. H. Fremlin.

NEW INSTRUMENTS, MATERIALS AND TOOLS
NEW BOOKS
NOTES AND COMMENTS

THIS JOURNAL is produced monthly by The Institute of Physics, in London. It deals with all branches of applied physics (including theory and technique).

All rights reserved. Responsibility for the statements contained herein attaches only to the writers.

EDITORIAL MATTER. Communications concerning editorial matter should be addressed to the Editor, The Institute of Physics, 47 Belgrave Square, London, S.W.1. (*Telephone:* Sloane 9806.) Prospective authors are invited to prepare their scripts in accordance with the *Notes on the Preparation of Contributions.* (Price 2*s.* 6*d.* including postage.)

REPRODUCTION. The Institute of Physics is a signatory to The Royal Society's Fair Copying Declaration. Details may be obtained upon application from The Royal Society, London, W.1.

ADVERTISEMENTS. Communications concerning advertisements should be addressed to the agents, Messrs. Walter Judd Ltd., 47 Gresham Street, London, E.C.2. (*Telephone:* Monarch 7644.)

SUBSCRIPTION RATES. A new volume commences each January and annual subscriptions will only be accepted for complete volumes of the monthly parts (January–December). The charge is £4 per volume ($11.50 U.S.A.), including index (post paid), payable in advance. Single parts, so far as available, may be purchased at 8*s.* each ($1.15 U.S.A.), post paid, cash with order. Orders should be sent to The Institute of Physics, 47 Belgrave Square, London, S.W.1, or to any Bookseller.

The physics of transistors*

By E. Billig, D.Sc.Tech., M.I.E.E., Research Laboratory, Associated Electrical Industries Ltd., Aldermaston, Berks.

Some of the fundamental concepts of the solid state which are required for an understanding of transistor action are discussed. The results of wave mechanics when applied to the solid state are outlined in simple non-mathematical language. The discrete levels of electron energy in single atoms and molecules become widened into energy bands in the solid. The large difference in the physical properties characteristic of such solids as metals, insulators, intrinsic and extrinsic semiconductors, can be accounted for by the width and relative position of their energy bands. When two different solids are brought into contact electrical potential barriers arise which pass electrons more freely in one direction than in the other. If electrons and holes are present simultaneously in a semiconductor, interaction occurs between them and this can be used to produce transistor action, i.e. to effect control over the flow of relatively large currents in a solid by means of weak optical or electrical signals.

1. THE THEORY OF SOLIDS

One of the main problems of the solid state concerns the energy of the electrons. This problem can be solved by the equation which governs the motion of electrons in general, i.e. by Schrödinger's wave equation,

$$\nabla^2\psi + \frac{2m}{\hbar^2}(E - V)\psi = 0 \qquad (1)$$

The essential feature of a differential equation of this type is that in order to give a proper solution, the coefficient of ψ may assume only certain discrete values. This is well known, for example, from the case of any vibrating mechanical system whose frequency can assume only certain definite values. Similarly, an electron moving in the potential V of a proton in a hydrogen atom, or in the field of several nuclei in a molecule, can exist only in certain states with definite energy E_1, E_2 ... [Fig. 1(*a*)].

Metals. In the solid also, electrons can take on only certain discrete energy levels. A satisfactory theory of metals was given by Sommerfeld, who translated Drude's old idea of "free electrons" into wave mechanical language. Each metal atom is assumed to release its one outer electron into the crystal where it is then quite free to move throughout the whole volume. Apart from the constraint at the surface which prevents the electron from leaving—at least at normal temperatures—there are no forces acting on it, the "inner potential" V_0 in the metal is uniform. Once the main parameter V was fixed in this way, the wave equation could be solved. The result may be described as follows [Fig. 1(*c*)]. Each electron has to be fitted into the "box" as a standing wave, and must have an antinode at each wall. The longest possible wave has a wavelength $2l$. Using de Broglie's relation,

$$\lambda = h/mv \qquad (2)$$

this corresponds to a minimum speed v and kinetic energy $\frac{1}{2}mv^2$ of the electron. Now, according to Pauli's exclusion principle, there cannot be more than two electrons (of opposite spin) in this lowest state; the next pair of electrons must go into a state of higher quantum number, corresponding to one half the wavelength or twice the energy; the next one into a state with wavelength $\frac{1}{3}$ and so on. Now realizing that there are about 10^{22} electrons to be accommodated per cm^3, we see that, in spite of the very close spacing between adjacent levels ($\simeq 10^{-15}$ eV), the highest electrons will have rather large energy. All the states of low energy available in the

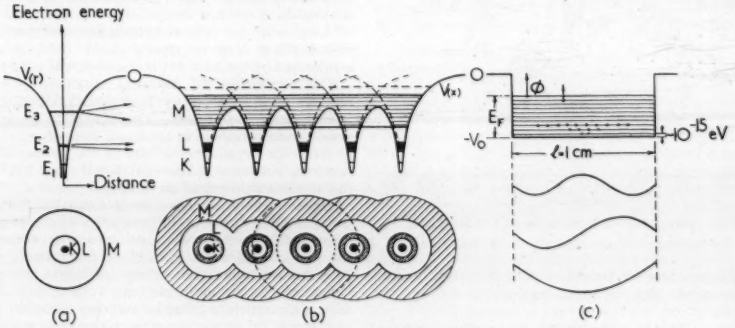

Fig. 1. Electronic energy levels

(*a*) Free atom. (*b*) Periodic solid (Bloch). (*c*) Metal (Sommerfeld).

* Based on a lecture given before the Electronics Group of The Institute of Physics on 18 March, 1952.

metal are filled with electrons up to this "Fermi level" E_F. For sodium, for example, which is an almost ideal metal, the width of the band filled with electrons is 3·16 eV.

With this very simple model we can understand some of the most fundamental properties of a metal, such as the work function ϕ required to lift an electron over the potential barrier at the surface, the specific heat and the electrical and thermal conductivity. The first essential requirement for a solid to be metallic is that some of its electrons must be free; they must extend sufficiently far from their parent atom. In the isolated atom, the electron should have a large orbit, or low ionization potential. This is demonstrated by Fig. 2 where the first ionization potential of the elements is plotted against their atomic number. Almost without exception, all

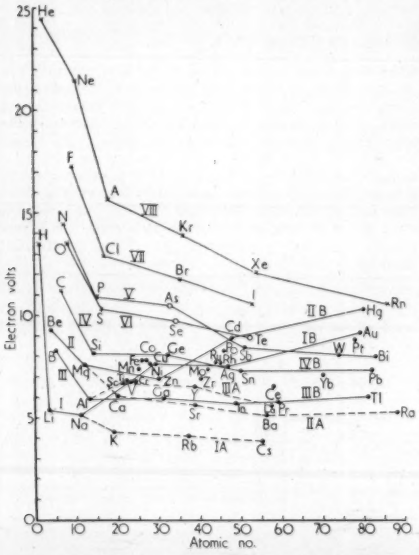

Fig. 2. First ionization potential of the elements
× non-metals. ○ semi-metals. ● metals.

metallic elements have an ionization potential below, and all non-metals above 10 V, with the semi-metals forming the borderline.

Insulators. However successful in certain respects, Sommerfeld's model still left unanswered a number of other problems, the chief one being, why should certain solids be good conductors and others good insulators? The answer was given by Bloch, who refined that model by observing that the potential within a solid is not really constant, but has the periodicity of the lattice, in the order of a few Å. Now substituting into Schrödinger's equation (1) a periodic potential function V, Bloch obtained a mathematical solution showing that the electrons in the crystal do not, in fact, pile up indefinitely with higher energy, but that there are certain ranges of energy which are "forbidden" [Fig. 1(*b*)]. This result might seem rather surprising, but it can be given a simple physical interpretation. In a monovalent metal one free electron is contributed from each atom, and these electrons fill the conduction band just to the halfway mark; twice as many electrons, two per atom, could go into the band. In sodium, for example, the electrons of highest energy have a wavelength of 6·9 Å (equation 2). Let us now put some more electrons into this band, as we might do by replacing some sodium by magnesium atoms, each of which contributes two free electrons. The Fermi level is now raised beyond the halfway mark and as we continue, the wavelength of the highest electron approaches twice the lattice spacing. Now when a wave falls on to a grating whose line spacing is of the order of half the wavelength, interference will cause diffraction and reflexion. In the standard electron diffraction experiment, electrons impinging on to a crystal set at the Bragg angle are totally reflected from the corresponding set of lattice planes. Similarly for electron waves *within* the crystal: as their wavelength approaches twice the lattice parameter, they are *internally* reflected and can, in fact, not be propagated within the crystal. This is the meaning of the "forbidden energy zone" which separates an allowed full band from a higher one that might be partially or completely empty.

No electron in a full band can absorb small parcels of energy. The lower electrons cannot do so as all the levels above are full, and those at the top cannot, as levels with higher energy are forbidden. The solid is therefore transparent to infra-red radiation. Similarly electrons in such a solid cannot be accelerated by the application of an electric field, as such acceleration would be equivalent to absorbing energy. No current can flow, the solid is an insulator.

We can now state the second essential requirement for a solid to be metallic: it must have an energy band which is only partly filled with electrons. The highest electrons in this "conduction band" will then be able to accept small amounts of energy; they will contribute to the specific heat by absorbing thermal energy; they will cause the absorption of long-wave, i.e. infra-red, radiation and finally they will absorb energy from an applied electric field, i.e. they can be accelerated by the field and cause electrical conductivity.

The mechanism of electrical conductivity in no way requires perfect periodicity, it can be explained on Sommerfeld's simple "box" model. The mere fact that metals remain good conductors even in the liquid state shows that it is not so much the regular periodicity of the lattice field which is required, but rather a large number of close neighbours, and this remains unimpaired on melting.

There is an interesting case of transition from insulators to conductors in the covalent solids silicon and germanium. These solids have the very open structure of diamond, with the low co-ordination number of four closest neighbours. They have a rather high entropy of fusion, $\simeq 6$ cal/mol °K, indicating that strong bonds have to be broken. When they melt, their structure collapses and they shrink by about 20% in volume; the atoms move more closely together and some of the four outer electrons previously used for the formation of strong electron-pair bonds, are released to move freely about the whole lattice: the liquid shows considerably higher electrical conductivity, it is much more metallic than the solid, and this in spite of a much less regular atomic arrangement. The case of tin is quite analogous; at low temperature grey tin has the same (diamond) structure and is a semiconductor; on heating above 13° C it changes to the tetragonal structure of white tin which is again about 20% more dense, has a higher co-ordination number and shows metallic conductivity.

Intrinsic semiconductors. An electron in a full band *can*

accept a rather large amount of energy, sufficient to carry it over the forbidden range into the next allowed band. This it could do, for instance, by absorbing a photon of ultra-violet radiation, the gap width E_g of most insulators being in the order of a few electron volts.

Take, for example, a crystal of potassium chloride. It cannot absorb visible radiation and is, in fact, completely transparent: the gap must be larger than 3 eV. The probability

$$\gamma = \exp(-eE_g/2kT) \tag{3}$$

that an electron gets this much energy from the thermal vibrations of the crystal is negligible. Even with 10^{22} electrons per cm³ there will not be a single one obtaining sufficient energy to make the crossing; electronic conductivity in alkali halides is practically nil. On the other hand, in a solid with an intermediate gap, as in a crystal of germanium with 0·72 eV, an electron at room temperature has a chance of one in a million of getting across. On the average about 2×10^{13} electrons per cm³ are lifted into the conduction band from the full band where they leave the same number of holes behind. Now holes are practically just as free to move about in the valency band as are electrons in the conduction band, and both make a contribution to the current when a potential difference is applied.* The number of mobile electrons and holes, $n_i = p_i$, existing in such an "intrinsic semiconductor" depends only on the gap width and the temperature.

Extrinsic semiconductors. A perfect lattice as discussed so far is, of course, an abstraction. Even faultless single crystals retain their perfect periodicity and sharp energy bands only at zero temperature; at any higher temperature the periodicity of the lattice is disturbed by its thermal vibrations and the band edges become diffuse. A photon of slightly less energy, i.e. of longer wavelength, will then be sufficient to lift an electron across the narrowed gap. A crystal of cadmium sulphide, for example, having an energy gap of 2·4 eV absorbs all visible radiation of wavelength shorter than 0·512 μ and will, therefore, appear yellow. When the crystal is heated, the energy gap is reduced and the "absorption edge" is shifted by about 1 Å/°C, causing a deepening of the colour.†

Actual crystals, even if they do not show any separate grains, still have many faults such as dislocations, vacant sites, interstitial atoms, etc., which constitute a considerable deviation from the true periodicity on an atomic scale. As regards purity, even with the best chemical processes to keep impurities down to a level of one part per million, is quite exceptional and this still implies about 10^{16} impurity atoms per cm³! In order to fix ideas, consider a perfect germanium crystal and replace one of its atoms by one of arsenic. Apart from having one additional charge on its nucleus and an extra electron in its outer shell, there is not much difference between this and the surrounding germanium atoms; the arsenic atom will fit quite snugly into the lattice. Very little energy is required to detach the extra electron from the arsenic atom because of the high dielectric constant of germanium, about 18. The thermal vibrations of the lattice, even below room temperature, are quite sufficient to achieve that. However, with the "valency" band completely full, the extra electron can only go into the next higher band where it is then quite free to move and thereby makes "extrinsic" conduction possible. By adding a certain amount of the "donor" impurity arsenic to intrinsically pure germanium, we have, in fact, produced n-type germanium (n for negative carriers), i.e. we have increased the number of electrons n beyond their intrinsic number n_i.

The situation is quite analogous when trivalent gallium is added instead of the pentavalent arsenic. Such an "acceptor" impurity causes an increase in the number p of holes and makes the material p-type (p for positive carrier). There is a general rule which follows from statistical thermo-dynamics, that the product of electron and hole concentration remains constant,

$$np = n_i p_i = n_i^2 \tag{4}$$

i.e. independent of any change in the number of either electrons or holes; if we increase the number of electrons the number of holes decreases, and *vice versa*. This rule is important in so far as it limits the type of material that can be used for such devices as transistors which rely for their operation on the simultaneous presence of holes and electrons.

2. CONTACT OF TWO SOLIDS

Contact of two metals. We shall now discuss the contact of two different metals such as copper and sodium. We then have to consider one type of carrier only, electrons. The inner potential V_0 will, in general, be different in the two metals, as will also their Fermi levels [solid lines in Fig. 3(*a*)].

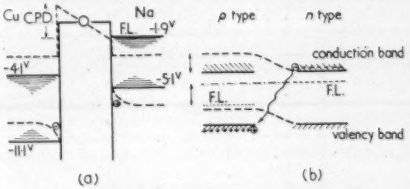

Fig. 3. Potential diagram for two solids in contact

(*a*) Two metals.
(*b*) p–n junction.
——— before, – – – after contact.

As we bring them closely together, it becomes possible for the electrons from sodium to jump across to copper, where empty levels are available for them in the conduction band. Electrons from the copper, however, do not find any empty levels at the same height in sodium, as these are all occupied. A net stream of electrons will thus flow into the copper and will leave a charge deficit, a positive ionic charge, on the sodium. This charge distribution will lower the general level of the potential in the bulk of the sodium, and raise it in the copper. The process will continue until the Fermi levels in both metals become equal when the overall energy is at a minimum [broken lines in Fig. 3(*a*)]. The excess charges cannot go deeply into either metal as the bulk of each will tend to remain neutral for minimum energy as it was to start with. In fact, the charges transferred correspond to only about 1/500 of a single atomic layer and they will become separated by the smallest possible distance, i.e. they will remain directly at the interface. Whilst the conduction band in both metals will be filled to the same (Fermi) level, the bottom of the band corresponding to the inner potential will vary with distance as indicated. The small separation of the charges corresponds to a rather large capacitance, of the order of a μF/cm².

* A simple two-tier model with steel balls representing electrons in a full band was demonstrated during the lecture to illustrate the mechanism of intrinsic semiconduction.

† The experiment was performed during the lecture.

Contact of two non-metals. Contact phenomena in non-metals can be discussed in a similar way. Charge separation will always take place until the overall energy has been reduced to a minimum. The most convenient way of dealing with these problems is to widen the concept of the Fermi level so as to include non-metals.

Rather loosely, the Fermi level (F.L.) of any solid may be described as the average of the energy levels of all its free charges (electrons, holes, ionized donors and acceptors). In an intrinsic semiconductor there are as many electrons as holes, and the F.L. lies halfway in the forbidden energy zone. In an extrinsic semiconductor the position of the F.L. depends on the ratio of extrinsic to intrinsic carriers; it is, therefore, determined by the concentration of ionized donors and acceptors, and by the width of the forbidden band as well as by the temperature. In an *n*-type semiconductor there are more electrons free (in the conduction band) than there are holes (in the valency band) and the F.L. lies in the upper half of the forbidden band and, similarly, in the lower half for *p*-type material. Fig. 4 shows the variation of the F.L. of 10^{15}/cm³, for instance, is practically intrinsic at any temperature above 150° C.

n-type germanium

Intrinsic carrier concentration $n_i = p_i = 2{\cdot}3 \times 10^{13}$ cm^{-3} at 300° K.
Intrinsic conductivity $\sigma_i = 0{\cdot}0195\ (\Omega\ \text{cm})^{-1}$ at 300° K.

Resistivity (at 300° K)	51·5	10	1	0·1	Ω cm
Extrinsic electrons (n_D)	0	$1{\cdot}4 \times 10^{14}$	$1{\cdot}7 \times 10^{15}$	$1{\cdot}74 \times 10^{16}$	cm^{-3}
Intrinsic temperature*(T_i)	—	73	162	306	°C

* Intrinsic temperature, T_i, here is defined as the temperature at which the number of intrinsic carriers equals that of the extrinsic ones.

Once the F.L. has been determined, the relative shift in potential on establishing contact is easily obtained for any two solids—even if neither is a metal—simply by taking their F.L.s at the same height.

Potential barriers. The change in potential between the two contacting solids, i.e. the shape of the potential barrier,

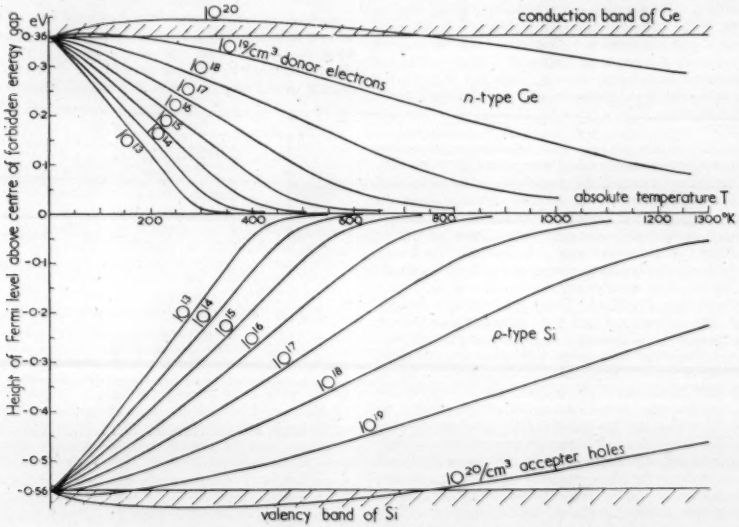

Fig. 4. Variation of Fermi level with temperature in *n*-type germanium and *p*-type silicon

with varying temperature; the upper half of the figure applies to germanium containing various amounts of *n*-type, and the lower half to silicon containing various amounts of *p*-type impurities, all ionized. At low temperatures no (intrinsic) carriers are excited across the gap, the F.L. coincides with the level of the extrinsic carriers.* At intermediate temperatures the Fermi level approaches the centre of the forbidden band and reaches this level at a lower temperature the purer the semiconductor. Germanium with an impurity content depends on individual circumstances. The width of the barrier is much greater in non-metals: to transfer a given amount of charge, a much greater depth of the semiconductor has to be drained of its relatively few mobile charges. The capacitance of semiconducting barrier cells is thus reduced to an extent which makes their operation possible up to reasonably high frequencies. Similarly, the potential gradient in the barrier is much lower, enabling it to operate at reasonably high voltages without breaking down.

Fig. 5 shows some typical asymmetric barriers which have been postulated for various rectifiers.

(i) There is the simple Mott type of barrier consisting in effect of a thin layer of insulating material with all its positive

* If the concentration of donors is sufficiently high, e.g. $> 2{\cdot}4 \times 10^{19}$/cm³ at room temperature, the F.L. may lie even within the conduction band, just as in the case of a metal.

charges transferred to one side—at the semiconducting end—and the negative ones to the other, in contact with the metal electrode. In this insulating layer the electric field is uniform, the electron potential dropping linearly from the metal electrode to the interior of the semiconductor. The capacitance of such a barrier depends mainly on the separation of the charges and will be independent of applied voltage, temperature and frequency. The barrier is assumed to have a potential step of fixed height V_0 at the metal/semiconductor contact, corresponding to the difference in the two work functions, and to merge into the potential of the semiconductor at the other end. Constant capacitance is found experimentally in copper oxide rectifiers and Mott's model is, therefore, applied to them.

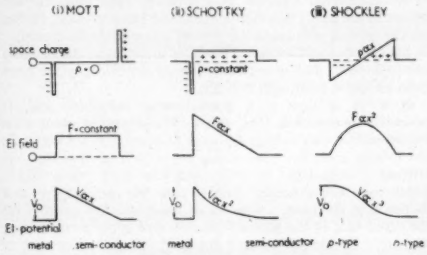

Fig. 5. Three types of potential barrier

(ii) Schottky's barrier is more appropriate to semiconductors containing a definite concentration of impurity centres. The electrons originating from these centres are transferred to the metal electrode leaving a uniform density of fixed positive charge (ions) within the barrier region and a thin layer of corresponding negative charge sitting on the metal interface. The strength of the field in the barrier drops linearly, and the potential with the square of the distance. The potential step at the interface is assumed as above, independent of the applied voltage. The width of the barrier, however, and hence also its capacitance, should now vary with the square root of the applied voltage. Such variation is actually observed in selenium rectifiers.

Whilst there is no fundamental difficulty in analysing these potential barriers, troubles do arise in practice due to complications at the surface. Quite apart from the "surface states," which always arise in any solid owing to its finite size, there are the asperities in the surface which may lead to "weak spots," its contamination by adsorbed gases, and possible chemical reactions at the interface. All these factors affect the potential distribution to a considerable extent, with the result that the barrier height V_0 which largely controls the operating characteristics of the barrier cannot readily be correlated to the properties of the two contacting solids.

(iii) All these uncertainties are eliminated when one is not dealing with free surfaces, but with barriers within a single crystal. Take as an example the extreme case of a single crystal of germanium or silicon, in one region of which most impurities are of the acceptor type and in an adjacent one mostly donors. As stated, the F.L. in the *p*-region will be lower than in the *n* (Fig. 4). As the two parts are brought into contact [Fig. 3(*b*)], electrons from the *n*-part drop into holes of the *p*, annihilating each other in the process and leaving the central region denuded of mobile carriers. The fixed acceptor and donor charges set up a dipole layer which shifts the potentials until in equilibrium the F.L.s of the two regions line up.* The height of the barrier in the resulting *p–n* junction becomes equal to the difference in the F.L.s and is therefore unaffected by such complications at the surface as mentioned above. However, the barrier height now becomes very sensitive to changes in the temperature. As the temperature is raised and large numbers of electron-hole pairs are excited across the forbidden gap, their number soon swamps whatever carriers there might have been present originally from the impurity centres. The whole difference between *n*- and *p*-regions disappears, the crystal becomes uniform throughout and there is no barrier left. In Fig. 5(*c*) a simple *p–n* barrier is illustrated in which the density of fixed charges, donors minus acceptors, is assumed to vary linearly with distance. The field and potential distribution, determined mainly by the fixed ionic charges, vary respectively with the square and cube of the distance.

3. RECTIFICATION

When it comes to accounting in detail for the observed rectifier characteristics, there are several distinct possibilities. In the *diode* theory the net current is regarded as the difference of two currents, one being emitted over the barrier from the semiconductor into the metal and the other one in the opposite direction. When a voltage is applied, the two currents are of different magnitudes owing to the different height the barrier presents to an electron arriving from either side [Fig. 6(*a*)]. If, on the other hand, electrons suffer many collisions on their way over the barrier, the mechanism of current flow is more in the nature of a *diffusion* process and the carriers tend to accumulate at regions of lowest potential energy. In that case the two opposing factors controlling current flow are, on the one hand, the electric field which causes electrons to run down the potential hill from the metal into the semiconductor and, on the other, the higher concentration of carriers which drives them in the opposite direction.

It is rather significant that both these theories predict the same type of *i*/*u* characteristic. However, neither of them can account for the large increase in current which is observed when a high inverse voltage is applied to a rectifier, with the carriers passing from the metal into the semiconductor. Several processes may be responsible for this part of the characteristic: As the barrier gets very thin on the application of high inverse voltage [thickness *t* in Fig. 6(*a*)], some electrons can get across the barrier by tunnelling through rather than by climbing over it with the aid of their thermal energy. In a *p–n* junction tunnelling may take place from the valency into the conduction band, when the applied voltage causes the field to exceed a certain critical "breakdown value" in the order of 10^5 to 10^6 V/cm. Alternatively, the image force may lower the barrier to such an extent that electrons from the metal can get over it much more readily. Finally, once the leakage current has started rising the increasing power loss may cause a rise in temperature which in turn raises the current.

Turn-over. Germanium diodes, in particular, exhibit a characteristic "turn-over" of the voltage and the magnitude of

* It should be noted that as long as no external potential is applied the electrostatic potential of the free electrons is equal in the bulks of either solid. If, however, both electrons and holes are present, this is no longer so; the potential of an electron in the conduction band will be lower in the *n*- than in the *p*-region and electrons will therefore accumulate there (and conversely for holes in the valency band of the *p*-region). In this case, it is the F.L.s that will line up throughout the junction.

the voltage at which this happens is a useful indication of the purity of the germanium used. However, the current/voltage characteristic is a genuine property of the rectifier only *before* the voltage turns over; only then is the current determined entirely by the rectifier. Beyond that voltage, the rectifier loses control and the current is limited mainly by external resistances. If such resistances are absent, the rectifier may be destroyed by drawing excessive current. This would happen, for example, if two diodes were connected back to back straight across an a.c. supply and excessive voltage applied to them.*

The turn-over voltage at low temperatures is quite high, but drops steadily as the ambient is raised. The turn-over current remains almost independent of temperature but rises quite sharply above 150° C or so. The sudden rise in current is demonstrated in a striking way when single pulses are applied. With the voltage set near its critical value, a very slight increase will cause a sharp increase in current.*

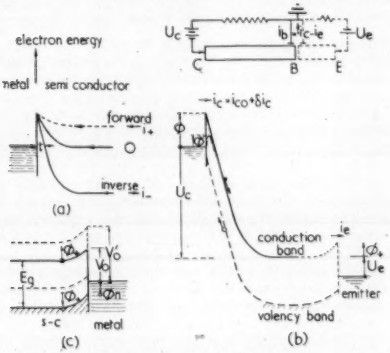

Fig. 6. Potential diagram of point contact transistor

(*a*) Rectifying barrier.
(*b*) Point contact transistor.
(*c*) Emitter contact.
——— for $V_0 < E_g$,
– – – – for $V_0' > E_g$ (hole emission).

When the power dissipated at turn-over is plotted against ambient, a straight line is obtained which intersects the zero line at about the same critical temperature at which the current started rising. Whatever the ambient, the voltage will turn over when the contact point reaches this temperature. The value of this temperature is identical with the intrinsic temperature, around 150° C for the grade of germanium ($\simeq 2\ \Omega$ cm) used in the particular experiment.

The precise mechanism of turn-over has been something of a puzzle so far. For *n*-type material, for example, the electron current flows from the metal into the germanium on the application of an inverse voltage; yet the number of electrons available in the metal is not affected, even when the germanium reaches intrinsic temperature. The explanation seems to be that, on reaching intrinsic temperature, a large number of holes are created at the same time in the valency band and there is no potential barrier to stop them: they readily float up the potential hill into the metal and can carry an almost unlimited current.

* This was demonstrated during the lecture.

4. TRANSISTOR ACTION

The possibility of gaining control over the current flow in a solid by means of a relatively weak signal has, of course, been in the minds of physicists for almost as long as metal rectifiers have been made. One of the earliest attempts consisted of inserting a third electrode in the form of a grid into the barrier layer of a selenium rectifier, in analogy with the grid of a vacuum triode. There was, however, little success.

There is a case, however, where amplification of current in the solid has been achieved, and used, for many years: it is in secondary photo-conductors where a weak optical signal is used to initiate the flow of comparatively large current. Cadmium sulphide, for example, is an excellent insulator in the dark, with a resistivity of about $10^{15}\ \Omega$ cm. When connected straight to a battery, very little current passes in the dark; however, a moderate beam of light, falling on the crystal, will cause the flow of a considerable current,† in the order of milliamps. This is far in excess of the primary photo-current, and quantum yields up to 10^5 or more have been obtained with such crystals.

Now let us look at a point contact transistor and its potential distribution [Fig. 6(*b*)]. The collector point *C* is biased with a high voltage U_c so as to operate as a rectifier in the inverse direction. Assuming *n*-type germanium, electron current i_c—say 1 mA at 50 V—will flow from the collector point over the potential barrier into the germanium and thence into the base. Now let us place another point *E* on the other face of the germanium disk and apply a small bias, say, $U_e = 1$ V, in the forward direction. Electron current i_e of about the same order of magnitude will flow from the interior of the germanium into this emitter point over the low residual barrier. The two currents are, of course, quite independent of each other and if the two bases were joined together, the current there would simply correspond to the difference, $i_b = i_c - i_e$. Now, if the thickness of the disk *w*, i.e. the distance between the two contact points, is made small enough, say 0·001 in, the two currents become interdependent: as the emitter current is increased, so the collector current rises and the effect may be used for voltage amplification: a small current signal δi_e flowing in the emitter circuit of low input resistance will produce a current change of the same order of magnitude in the much higher load resistance in the collector circuit, giving a greatly amplified voltage output.

On this diagram it is hard to see how a change in the emitter current can effect a change in the collector circuit. An entirely new phenomenon is involved. Fig. 7 shows an experiment on a thin filament of *n*-type germanium in which current is supposed to be carried by electrons. A current pulse is applied to ϵ, but the electrons which make up the pulse current are kept out of the right half of the filament by the negative bias there. Yet some μsec after the pulse is applied, a signal is picked up by electrode *c*, and its polarity indicates that positive carriers are involved. In other words, in this filament of *n*-type germanium where the vast majority of available carriers are electrons, the pulse current is carried by holes.

This possibility of carrying current simultaneously in the conduction band (by electrons), and in the valency band (by holes) is at the root of transistor action. It must be realized, of course, that electrons and holes if present in any large number within the same region will soon recombine, their lifetimes are in the order of 1 to 100 μsec. But within that interval of time a hole in *n*-type germanium has a good chance

† The experiment was demonstrated during the lecture.

of diffusing over a distance l up to 0·1 to 1 mm. In the presence of an electric field, it can, of course, drift much farther in that time. A hole injected from the emitter would certainly not survive the journey to the base, but it stands a good chance of reaching the collector; the ratio of survivors

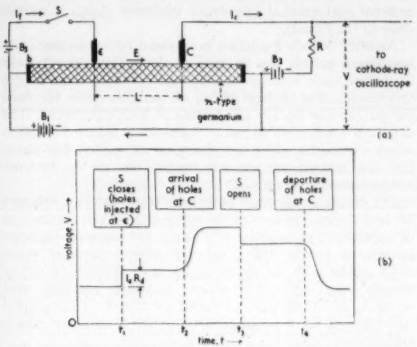

Fig. 7. Hole injection into *n*-type germanium

increases as the distance between the two electrodes is reduced. In a transistor, the large negative bias on the collector will, of course, favour the arrival of holes from the germanium; electrons coming from the interior meet an insuperable barrier at the collector whilst holes can float up the potential hill very easily indeed, just as easily as the electrons slide down in the other direction once they have got into the germanium from the collector point [Fig. 6(*b*)].

Now as the hole current δi_e arrives at the collector, electrons from the conduction band drop into them and an additional electron current $\delta i_c = \alpha \delta i_e$ is drawn through the external collector circuit. For any given collector voltage the current flowing is thus made up as the sum of the original leakage current i_{co} determined by the rectifying characteristics of the collector point, plus a contribution which is proportional to the emitter current, $i_c = i_{co} + \delta i_c$. For the point contact transistor the leakage current i_{co} rises appreciably with higher potential, mainly due to the rise in temperature of the point, and we obtain the family of current/voltage characteristics of Fig. 8(*a*), whilst in the junction type of transistor the leakage current is much lower and nearly saturated—as it should be according to theory in the absence of any large rise in temperature—hence the collector current remains almost independent of the collector voltage [Fig. 8(*b*)].

Current multiplication. Now, what is the magnitude of the collector current? In the first place we have already mentioned the decay of the holes as they recombine with electrons on their way to the collector. The loss of hole current can be quite large for the standard point contact transistor, but is quite small in good junction types if the base layer is made sufficiently thin.

The other factor concerns current multiplication. We know that electrons tend to accumulate at places of lowest potential, and holes at the highest. As the holes arrive at the collector their concentration grows and forms a positive space charge in the germanium which lowers the barrier there, and electrons can now pass more freely from the collector. However, these in turn will now partly neutralize the space charge of the holes, and this sets a limit to the possible increase in electron current. The concentration of electrons in front of the collector must always remain somewhat less than that of the holes so that the barrier can still be reduced. In other words, the additional electron current can never exceed about twice the hole current as the mobilities are in that ratio. The total collector current cannot, therefore, exceed about three times the emittor current—and current multiplication in point contact transistors is usually less than 3 times. No such mechanism of barrier depression and current amplification is conceivable in the standard junction type of

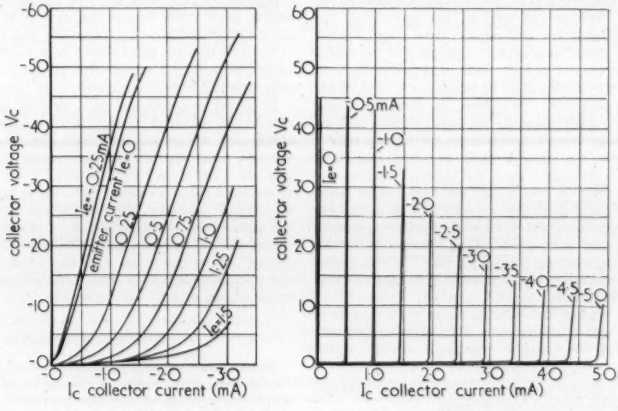

Fig. 8. Current/voltage characteristics of point contact (*a*) and junction type (*b*) transistors

transistor and the collector current changes almost by the same amount as the emitter current* [see Fig. 8(*b*)].

Hole injection. Although this has been demonstrated beyond doubt it is still somewhat uncertain why the current at the emitter should consist of holes rather than electrons, or, put differently, why electrons near the emitter should travel in the valency band rather than in the conduction band.

There is one obvious possibility. Consider the barrier at the emitter. With bias applied in the forward direction, Fig. 6(*c*), both electrons and holes have still to overcome a potential barrier of the same, rather low, height (ϕ_+), but this they can do quite easily with the aid of their thermal energy. However, the electrons in the valency band would require an additional amount of energy (ϕ_h) to pass into the metal, whilst no such energy is needed for the electrons in the conduction band. On the other hand, it is known that the height of the barrier (V_0) is in the order of 0·6 eV and this would bring the top of the valency band quite close to the Fermi level in the metal; should the barrier height exceed the width of the forbidden band (0·72 eV in germanium), then electrons will pass quite readily from the metal into the valency band of the germanium and this would satisfactorily explain hole emission. In fact, we have recently obtained some evidence in this laboratory that the barrier is indeed higher than 0·72 eV over certain patches of the contact. Hole injection would then be preferred from these spots of large barrier height, whilst "weak spots" of much lower height would be mainly responsible for the comparatively low contact resistance and barrier height observed at low temperatures, as well as for the onset of thermal instability.

Limitations of transistors. One of the most serious limitations concerns the *highest frequency* at which a transistor can operate. As shown in Fig. 6(*b*), by far the largest part of the applied potential difference is dropped in the narrow barrier at the collector. Within the bulk of the germanium the potential is nearly uniform and current flow there is more in the nature of a diffusion process. A signal starting with a sharp front at the emitter would arrive at the collector with its front broadened by diffusion (to an extent $l = \sqrt{(Dt)}$, where the diffusion constant $D \simeq 50\ \text{cm}^2/\text{sec}$ in germanium and the transit time t is determined by the hole velocity) and the arrival of the signal would, accordingly, be spread over a certain time. If now the signal is varied at a high frequency, comparable to this spreading time, the collector current will drop. Rough calculation of the effective field can be made from the geometry and gives the correct order of magnitude for the cut-off frequency, about 10 Mc. Further spreading of the signal is due to some holes taking a longer path than others. By applying a strong magnetic field it has been found possible to force all holes into the same path and to raise the cut-off frequency thereby.

In the junction type of transistor the maximum frequency is limited much more severely by the large capacitance ($\simeq 0{\cdot}1\ \mu\text{F/cm}^2$) of the collector barrier. As the signal frequency is increased beyond the audio range, a large fraction of the signal current is used to build up the space charge layer instead of passing into the collector circuit, the effective time constant of the output circuit becomes rather large. It is possible to reduce the effect to some extent by a drastic reduction of the load resistance, but such a mismatch of external and internal impedance obviously causes a serious drop in the output.

Another serious limitation is imposed by *temperature*. It was stated before, that as soon as the intrinsic temperature is reached there is no more difference between *n*- and *p*-type germanium, and devices relying on such junctions for their barrier become equally conducting in both directions. The situation is not quite so bad in metal/semiconductor rectifiers where the barrier does not disappear altogether, but there, too, the leakage current will rapidly rise as the intrinsic temperature is approached.

The precise temperature at which a semiconductor becomes intrinsic depends mainly on the energy gap and on the number of impurities; germanium of 1 Ω cm, for example, becomes intrinsic at around 160° C (see the table). However, transistor action is by no means exclusive to germanium, it has already been reported in silicon, cadmium sulphide, lead sulphide, and there will, no doubt, be others. The essential requirements for a semiconductor to show transistor effects are:

(i) It must be able to carry simultaneously electrons and holes in reasonable concentration, i.e. the energy gap which directly fixes the product $n \cdot p$ should not be too large.

(ii) The barrier should remain of reasonable height up to fairly high temperatures, without the material becoming intrinsic; the energy gap should therefore not be too small, especially if *p–n* junction devices are to be used.

(iii) The carriers must easily be excited from their impurity centres even at the lowest temperature of operation, hence the material should have a reasonably high dielectric constant.

(iv) The carriers should have high mobility and long life before recombining, the material should therefore be reasonably pure and perfect, preferably in the form of single crystals.

If silicon is considered as a possible alternative to germanium, it is rather surprising that, in spite of its larger energy gap, silicon has never been made to withstand inverse voltages even approaching the values obtained with germanium. The author suspects that if it could only be purified to the same extent as germanium, say to an impurity content of $10^{14}/\text{cm}^3$ or better, the resistivity of silicon should be of the same order of magnitude as of germanium, the carriers should have about the same mobility and life, and should be excited just as easily; on the other hand, the larger energy gap will allow silicon to remain intrinsic up to much higher temperatures, around 500° C (see Fig. 4).

* By the use of a further junction—in the "*p–n* hook" arrangement—current amplification has been achieved.

ACKNOWLEDGEMENTS

Thanks are due to Dr. T. E. Allibone for permission to publish this paper, and to Dr. W. Shockley and *The Physical Review* for permission to reproduce Figs. 7 and 8(*a*).

A comparison of the dielectric behaviour of pure water and human blood at microwave frequencies

By H. F. Cook, B.Sc., Ph.D., A.I.M.E.E., F.Inst.P., Department of Physics Applied to Medicine, The Middlesex Hospital, London, W.1

[*Paper received* 21 *February*, 1952]

Methods used to measure the complex dielectric constant of water and blood at frequencies from $1 \cdot 7 \times 10^9$ to $2 \cdot 4 \times 10^{10}$ c/s are described. The results obtained for water at temperatures between 0 and 60° C are given and analysed with relation to the Debye and the Cole–Cole dispersion equations. The possibility that the dispersion in water is characterized by a narrow spectrum of relaxation times is briefly discussed. The complex dielectric constant of whole human blood has been measured at temperatures between 15 and 35° C. The dispersion observed is attributed entirely to water relaxation. It is shown to fit the Debye dispersion equations if the effects of a frequency-independent ionic conductivity are allowed for. Comparison of the results for blood with those for water leads to approximate estimates of the erythrocyte intracellular ionic conductivity and haemoglobin hydration.

As part of the initial stage in investigations of the propagation of hyper-high-frequency radio energy in human tissues, a study has been made of the dielectric properties of pure water and blood in the frequency range $1 \cdot 7 \times 10^9$ to $2 \cdot 4 \times 10^{10}$ c/s. It was anticipated that the electrical behaviour of these liquids would be similar at such high frequencies, and that a comparison would yield information regarding the electrical properties of the intracellular contents of human erythrocytes in their normal environment.

The anomalous dielectric dispersion of water at microwave frequencies has been widely investigated in the past. The serious lack of agreement between the results of various early workers has been attributed to several causes, notable among these being the use of sources producing damped waves. The advent of stable continuous wave sources of microwaves and improved techniques of measurement has enabled more reliable measurements to be made in recent years. However, at the time of the commencement of the present work serious discrepancies between the results of the most recent workers were apparent. The work of Connor and Smyth,[1] Abadie,[2] and Saxton and Lane[3] showed lack of agreement regarding the relaxation time when the results were analysed in terms of Debye's dispersion equations:

$$\epsilon' = \frac{\epsilon^* - \epsilon_\infty}{1 + (\omega\tau)^2} + \epsilon_\infty$$

$$\epsilon'' = \frac{\epsilon^* - \epsilon_\infty}{1 + (\omega\tau)^2}\omega\tau$$

where $\epsilon = \epsilon' - j\epsilon''$ is the dielectric constant at frequency $\omega/2\pi$,

ϵ^* and ϵ_∞ are the low and high frequency values of ϵ' on either side of a dispersion frequency region (ϵ^* is not necessarily the static constant)

and τ is a generalized relaxation time.

While the present work was in progress Collie, Hasted and Ritson[4] published the results of a comprehensive investigation of the dielectric properties of water at microwave frequencies. They pointed out the discrepancies between previous workers' results and claimed that their own satisfied the Debye equations (with a single relaxation time) within their experimental error (approximately $\pm 2\%$ in both ϵ' and ϵ''). At the same time, the results of workers in America came to general notice (Montgomery[5]) and large differences between these results and those of Collie and others were apparent. Whereas the latter indicated a single relaxation time for water, the American results showed a wide relaxation time spectrum to be present. Thus the present work was continued with an object additional to the primary one in that a full investigation of the dielectric behaviour of water in its dispersion region might confirm one or other of the above conclusions.

In the case of whole human blood little reliable work in any range of frequency in the radio frequency spectrum was known to the author. Work on the blood of various animals has been reported[6, 7, 8, 9] and the observed dispersion discussed in terms of an extension of Wagner's theory for inhomogeneous dielectrics.[10, 11] The only work at frequencies higher than about 10^9 c/s is that on whole human blood by England and Sharples[12] and England.[13] Their method of measurement of the dielectric constant of blood in the frequency range 3×10^9 to $2 \cdot 4 \times 10^{10}$ c/s was not well suited to the measurement of a material of such high dielectric constant and loss. The present investigation was intended to obtain results of higher accuracy than was achieved by these workers, and to use similar specimens at all frequencies.

DESCRIPTION AND PRINCIPLE OF THE EXPERIMENTAL METHODS

The essential feature of the methods used was that the measured quantities were largely, or completely, independent of an air-liquid reflexion coefficient. With high dielectric constant materials the measurement of such a coefficient to an accuracy sufficient to obtain $\pm 1\%$ accuracy in ϵ' is very difficult. Thus methods were employed where the liquid propagation constant, $\alpha + j\beta$, was measured directly, as far as possible, to an accuracy commensurate with limits of error of approximately $\pm 1\%$ in ϵ' and $\pm 2\%$ in ϵ''.

The derivation of the relationships between $\epsilon' - j\epsilon''$ and the propagation constants for materials contained in coaxial lines or wave-guides and carrying travelling or standing waves is well known[14] and it suffices only to state them:

$$\epsilon' = \left[\beta^2 - \alpha^2 + \left(\frac{2\pi}{\lambda_c}\right)^2\right]\left(\frac{\lambda}{2\pi}\right)^2$$

$$\epsilon'' = 2\alpha\beta\left(\frac{\lambda}{2\pi}\right)^2$$

where λ = free space wavelength and λ_c = cut-off wavelength.

For coaxial lines $\lambda_c = \infty$ for the principal wave, and in

the wave-guide it is dependent on the guide geometry and order of mode. Where λ and λ_c are known to high accuracy it follows that, when $\beta^2 \gg \alpha^2$, to obtain the required accuracy in $\epsilon' - j\epsilon''$ it is necessary to measure β to within $\pm 0{\cdot}5\%$ and α to within $\pm 1{\cdot}5\%$.

(*a*) *Methods used at frequencies lower than* 5×10^9 *c/s.* To enable a wide frequency range to be covered in one apparatus a coaxial line method was employed. This was the coaxial version of the twin-wire method used by Knerr[15] and Cooper[16], and is similar to a method described by Abadie. A diagrammatic section of the apparatus is shown in Fig. 1. The theory of the method has been given by Knerr

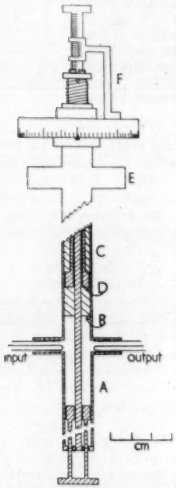

A, resonant air section; *B*, thin mica window; *C*, liquid filled section; *D*, plunger, movement of which is measured by micrometer or scale and vernier, *F*; *E*, liquid reservoir. (Not shown are the joint in the line at *B*, and the water jacket which extends from above *E* to below *B*.)

Fig. 1. Diagrammatic section of coaxial line apparatus used at frequencies lower than 5×10^9 c/s

and Cooper. Briefly, the method consists of varying the signal output of the air-filled section (previously tuned to resonance) by movement of the reflecting plunger in the liquid-filled section. Maxima and minima of the signal output occur and are related to the position of the plunger. The maxima and minima recur for successive movements of the plunger through $\pi/2\beta$, and their relative amplitudes are related to α. The accuracy of the method depends upon:

(i) the stability of the signal generator output power and of the signal detection apparatus;
(ii) the accuracy of measurement of frequency, plunger movement and temperature.

The klystron oscillators used were operated from well-stabilized power supplies derived from automatically regulated alternators. Their outputs were very stable. Similarly, the signal measuring apparatus, consisting of a microwave mixer and intermediate frequency amplifier, was operated on independent supplies and gave very stable amplification. The relationship between the second detector current (read on a 6 in, 1 mA full-scale meter) and the relative signal input to the mixer was established by use of inputs from an accurate cut-off attenuator. Frequencies near 3×10^9 c/s were measured to an accuracy of $\pm 0{\cdot}05\%$ by means of a cavity wavemeter, while other frequencies were measured to $\pm 0{\cdot}1\%$ by the use of a line wavemeter. The plunger movement was normally between 1 and 4 cm, corresponding to a number of half wavelengths in the liquid equal to, or greater than, three. It was measured by a micrometer providing length readings accurate to $\pm 0{\cdot}01$ mm. Temperature was controlled by a large water jacket surrounding the apparatus. During a set of observations at any one temperature this remained constant to within $\pm 0{\cdot}1^\circ$ C except at the highest temperatures employed. The final accuracy of measurement of β was estimated to be $\pm 0{\cdot}4\%$, and of α to be $\pm 2\%$, for water at temperatures near room temperature. Thus the best accuracy achieved for water was approximately $\pm 1\%$ in ϵ' ($\beta^2 \gg \alpha^2$) and $\pm 2{\cdot}5\%$ in ϵ'', with somewhat greater limits of error at temperatures lower than 10° C and higher than 30° C.

At a frequency of 3×10^9 c/s a second method was also used for measurements on water. A cylindrical water-filled wave-guide (H_{11} mode) was provided with a movable pick-up loop. The signal output was fed to an air-filled wave-guide section, into which was also fed a constant phase output from a cut-off attenuator (see Fig. 2). The attenuation in the water-filled guide was measured directly, and β was obtained from

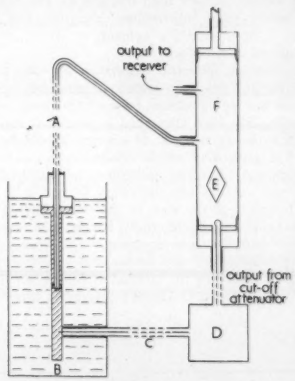

Fig. 2. Diagram of wave-guide apparatus used at 3×10^9 c/s

A, rack and pinion with scale and vernier; *B*, water jacket; *C*, lossy cable; *D*, signal generator; *E*, attenuator; *F*, rectangular guide, 3 × 1 in.

the movements of the pick-up loop providing successive nulls in the combined output of the air-filled guide. The accuracy of measurement of both α and β was considered to be $\pm 1\%$, giving limits for ϵ' and ϵ'' of $\pm 2\%$.

(*b*) *Method used at approximately* 10^{10} *c/s and* $2{\cdot}4 \times 10^{10}$ *c/s.* Buchanan[17] has described a null method of measurement at these frequencies, and the measurements on water and blood were made using his apparatus at 10^{10} c/s, and, at the highest frequency, on similar apparatus set up by Haggis[18] for work on protein solutions.

Briefly, the principle of the method is that on which the cylindrical wave-guide method used at 3×10^9 c/s was based

and which followed a suggestion by Buchanan. At the higher frequencies, rectangular wave-guide cells were used, the outputs from this and from a cut-off attenuator being fed to the arms of a hybrid tee and thence to a mixer and intermediate frequency amplifier. Movements required in the signal pick-up mechanisms of the liquid cell and attenuator to obtain successive nulls in the output of the hybrid tee are directly related to β and α for the H_{01} mode. An important feature of the method is that the measurements are largely independent of oscillator output instability, an annoying property of valves working at these frequencies. The best accuracy attainable for water near room temperature was $\pm$ 1% for both ϵ' and ϵ''.

EXPERIMENTAL RESULTS

(*a*) *Water.* Results at four frequencies were obtained and are listed in Table 1. They have all been interpolated from

Table 1. *Experimental values of* $\epsilon' - j\epsilon''$ *for pure water*

Temp. (°C)	*Frequency* (c/s) $3{\cdot}00 \times 10^9$	$4{\cdot}63 \times 10^9$	$9{\cdot}39 \times 10^9$	$2{\cdot}377 \times 10^{10}$
0	$(80{\cdot}2 - j\,24{\cdot}0)$	$(71{\cdot}4 - j\,33{\cdot}4)$	$(43{\cdot}4 - j\,41{\cdot}1)$	$(14{\cdot}5 - j\,26{\cdot}5)$
5	80·0	20·3) 73·1	28·7 49·6	39·2 18·0 29·7
10	79·4	17·5 74·3	25·2 54·4	37·1 22·0 32·5
20	77·7	13·0 74·0	18·8 61·5	31·6 31·0 35·7
30	75·3	$9{\cdot}9_0$ 73·1	14·6 64·8	25·6 38·5 35·6
40	72·6	$7{\cdot}5_5$ 70·7	12·0 65·5	20·9 43·0 34·0
50	69·7	$5{\cdot}9_5$ 68·5	$9{\cdot}4_0$ 64·6	17·0 (46·3 30·8)
60	66·4	$4{\cdot}6_0$ 66·3	$7{\cdot}4_0$ —	—

graphs of a large number of observations made at different temperatures and at each frequency. Those for 3×10^9 c/s are the means from the two methods used at this frequency, the agreement obtained between these being well within the calculated limits of error.

(*b*) *Whole human blood.* The specimens were selected from normal males so that the red cell concentrations were within the limits 4·8 to $5{\cdot}0 \times 10^6$ per mm³. The corresponding total cell volume was 43%. 1·9 mg heparin was added to each 10 ml of whole blood to prevent coagulation. This substance does not ionize, and, in such low concentration, it was considered unlikely to affect the electrical properties of the specimens. The measurements were carried out in the apparatus used for water. A fortunate result of the use of a plunger or signal pick-ups moving in the liquid cells was that the blood was kept well stirred by this means alone. Measurements were made at a frequency lower than 3×10^9 c/s (the lowest used for water) to give more accurate information on the ionic contribution to dielectric loss. The full results, interpolated from experimental curves through a large number of individual observations at each frequency, are listed in Table 2.

Table 2. *Experimental values of* $\epsilon' - j\epsilon''$ *for whole human blood (cell concentration* $4{\cdot}9 \times 10^6$ *per mm³)*

Temp. (°C)	*Frequency* (c/s) $1{\cdot}77 \times 10^9$	$2{\cdot}99 \times 10^9$	$9{\cdot}39 \times 10^9$	$2{\cdot}377 \times 10^{10}$
15	$(59{\cdot}2 - j\,17{\cdot}8)$	$(59{\cdot}9 - j\,19{\cdot}9)$	$(42{\cdot}4 - j\,26{\cdot}7)$	
25	56·8	17·8 57·5	17·1 45·5	23·0 (25·0 − *j* 24·8)
35	56·2	18·1 56·0	15·9 47·8	19·7 30·2 26·0

The results are considered to be within $\pm$ 2% for ϵ' and $\pm$ 5% for ϵ'' of the true values for male blood containing average cells in concentration $4{\cdot}9 \times 10^6$ per mm³ (43% of total volume).

ANALYSIS OF THE RESULTS AND COMPARISON WITH PREVIOUS WORK

(*a*) *Water.*

Analysis. The results for water were analysed in relation to both the Debye dispersion equations and the empirical form of these due to Cole and Cole.[19] These authors show that many materials behave in their dispersion regions according to the equation:

$$\epsilon - \epsilon_\infty = \frac{\epsilon^* - \epsilon_\infty}{1 + (j\omega\tau)^{1-\alpha}}$$

where α is a parameter depending on the width of a spectrum of relaxation times characterizing the dispersion. For a single relaxation time α is zero and the equation then becomes identical with the corresponding Debye equation.

The outcome of the analysis can be summarized as follows:

(i) The best average fit of the experimental results to values calculated from the Debye equations was obtained if ϵ^* was taken as the static dielectric constant as given by Lattey and others,[20] ϵ_∞ was 5·0, and the single values of τ shown in Fig. 3 were used. Only half the experimental values agreed with calculated ones within the experimental error.

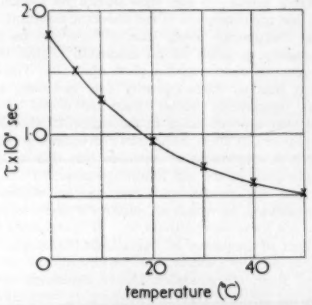

Fig. 3. Variation of relaxation time with temperature for pure water

(ii) Slightly better overall agreement was obtained between the experimental results and values calculated from the Cole and Cole equation if $\epsilon_\infty = 4{\cdot}0$ (the far infra-red value[21, 22]), $\alpha = 0{\cdot}02$ at all temperatures, and τ had values approximately 2% lower than those of Fig. 3. In this case two-thirds of the experimental results agreed with calculated ones within experimental limits of error.

(iii) In both the above cases ϵ_∞ was assumed independent of temperature. Improved agreement was obtained when ϵ_∞ was allowed to vary with temperature, but the results are not sufficiently accurate to warrant any conclusions regarding any systematic dependence of ϵ_∞ on temperature. Similarly, in (ii), agreement was improved when α was allowed to vary with temperature.

It must be concluded that the accuracy of the present results is not sufficiently high to be able to state that the anomalous dispersion of water is definitely characterized by a single relaxation time and a temperature independent ϵ_∞. The possible existence of a narrow relaxation time spectrum

cannot be ruled out. The latter possibility is attractive in that the far infra-red results can be linked with those in the microwave region without introducing an additional dispersion process at frequencies between the two regions.

Comparison with previous work. Good agreement exists between the present results and those of Collie and others. The relaxation times shown in Fig. 3 are within 2% of these workers' values. Whereas Collie and others found $\epsilon_\infty = 5{\cdot}5$ gave the best average fit to the Debye equations, the present work provides a lower estimate of 5·0. It should be noted that their experimental results can also be fitted reasonably well to the Cole and Cole equation with $\alpha > 0$. The results referred to by Montgomery are approximately consistent with the Cole and Cole equation with $\epsilon_\infty = 15$ and $\alpha = 0{\cdot}19$ and differ markedly from the present results and those of Collie and others. The large discrepancies may be due to the use by the American workers of techniques unsuited to dielectric measurements on water. Saxton analysed the results of Saxton and Lane and found water to obey the Debye equations with $\epsilon_\infty = 5{\cdot}5$. Later work (private communication) by Saxton and Lane suggests 4·9 as the value of ϵ_∞ to use in the Debye equations to obtain best agreement between theory and experiment.

(*b*) *Whole blood.* It has been shown by Danzer and by Schwan that the dispersion of the dielectric constant of animal blood at frequencies lower than 10^8 c/s can be explained approximately in terms of an extension of the theory for inhomogeneous dielectrics due to Wagner.[23] The effects of dispersion due to inhomogeneity are, however, negligibly small at frequencies higher than 10^9 c/s.[8] ϵ' remains constant over a small range in the region of this frequency. The present results show dispersion at frequencies higher than this and it is reasonable to conclude that this is due to the large water content and not inhomogeneity.

Therefore, the results were analysed in relation to the Debye equations, in which an additional term was included to allow for ionic conductivity, σ. It is assumed that σ is independent of frequency at hyper-high frequencies. It was found that all the experimental results agreed with values calculated from the modified Debye equations, within the experimental limits of error, if, in these, ϵ_∞ was taken as 4·5 and the values of the other constants used were as in Table 3.

Table 3. *Whole blood—constants derived from analysis of experimental results*

Temp. (° C)	ϵ^*	τ (sec)	σ (Ω^{-1} cm^{-1})
15	62·0	$1{\cdot}19 \times 10^{-11}$	0·010
25	58·0	$0{\cdot}90 \times 10^{-11}$	0·012
35	56·0	$0{\cdot}70 \times 10^{-11}$	0·014

Comparison of the values of $\epsilon' - j\epsilon''$ at 35° C in Table 2 can be made with the results of England and Sharples, and England, for a temperature of 37° C. Allowing for the wider range of cell concentrations and higher temperature of their specimens, reasonable agreement exists between the two sets of results.

DISCUSSION OF THE DIELECTRIC PROPERTIES OF BLOOD

For the purposes of this discussion the effect of cells other than erythrocytes present in blood will be neglected, since the erythrocytes far outnumber the other cells.

(*a*) *Dispersion at radio frequencies.* The phenomena observed can be discussed in terms of Wagner's extension of Maxwell's theory for inhomogeneous dielectrics possessing ionic conductivity. Maxwell considered the case of a heterogeneous medium consisting of strata of materials with different dielectric constants and ionic conductivities and showed that dispersion would result. Wagner extended the theory to cover the case of spheres, and bodies of other shapes, suspended in a medium of different dielectric properties. This Maxwell–Wagner theory is well established and has been discussed by many authors (see, for instance, Jackson[24] and Hartshorn[25]). Briefly, the theory proposes that dielectric dispersion occurs in such a heterogeneous medium as a result of restricted movement of ions at the boundaries of the constituents. For example, if a constant potential difference is set up in such a medium, ionic accumulations occur at the boundaries of the constituents. These lead to polarization electromotive forces being set up in opposition to the applied potential difference, and then to a simple, or complex, exponential decay of current depending on the number of different types of boundary present. This is a relaxation process and can be described by dispersion equations similar in form to those of Debye for dipole relaxation.

Danzer applied the theory to the type of inhomogeneity represented by blood and derived equations which can be written

$$\epsilon' = \frac{\epsilon_s - \epsilon^*}{1 + \omega^2 T^2} + \epsilon^*$$

$$\sigma = \sigma_s + \frac{(\epsilon_s - \epsilon^*)}{(1 + \omega^2 T^2)} \frac{\omega^2 T}{4\pi}$$

where ϵ_s is the dielectric constant at zero frequency,
ϵ^* is the value of ϵ' between the dispersion regions due to inhomogeneity and water relaxation,
σ_s is the conductivity at zero frequency,
σ is the conductivity at a frequency, $\omega/2\pi$,
T is a time constant (relaxation time), related to the radius and thickness of the cell membrane and its dielectric constant, and to the conductivity of its contents.

Schwan has used Danzer's equations to discuss the dispersion of blood observed at frequencies well below those of microwaves. He shows that the published results on animal blood are approximately consistent with the theory if ϵ_s is about 5 000 and T between 10^{-7} and 10^{-8} sec. Confirmation that blood has such a high dielectric constant at low frequency is provided by the results of Iwase who obtained $\epsilon' = 3\,150$ at 30 kc/s for rabbits' blood at 14·5° C. Rajewsky and Schwan have more recently obtained results on sheep's blood at wavelengths between 36·5 and 185 cm, showing agreement between the experimental results and those calculated from Danzer's equations.

The present results have provided the values of ϵ^* and σ. No measurements were made of ϵ_s for the specimens used in the investigation, but σ_s was measured at 1 000 c/s in a cell designed to minimize the effects of polarization. Using the values thus obtained for σ_s, and those for σ from Table 3, the time constants, T, for human blood have been calculated on the assumption that $\epsilon_s - \epsilon^* = 5\,000$. Table 4 lists the results.

Table 4. *Whole blood—the time constant, T*

Temp. (° C)	σ_s (Ω^{-1} cm^{-1})	σ (Ω^{-1} cm^{-1})	T (sec)
15	0·0050	0·010	$8{\cdot}9 \times 10^{-8}$
25	0·0060	0·012	7·4
35	0·0072	0·014	6·5

Following Schwan, these values of T are approximately consistent with the following properties of spherical cells: internal conductivity 0·01 Ω^{-1} cm^{-1}, membrane dielectric

constant = 6, membrane thickness = 30 Å, and cell radius = 3×10^{-4} cm. The foregoing shows that the ionic contribution to dielectric loss observed at hyper-high frequencies is reasonably consistent with existing dispersion theories and approximate cell data. It will now be of value to compare the observed microwave ionic conductivity of whole blood with that of blood plasma, since this leads to information regarding the internal conductivity of the cells.

(*b*) *Intracellular conductivity.* The relationship between the specific conductivity of whole blood, blood plasma and cell contents given by Danzer can be written

$$\sigma = \sigma_1\left(1 + 3\rho\frac{\sigma_2 - \sigma_1}{\sigma_2 + 2\sigma_1}\right)$$

where σ, σ_1, and σ_2 are the conductivities of whole blood, blood plasma, and cell fluid respectively, and ρ is the volume concentration of cells.

This appears to be the approximation for spheres at low concentration to the relation derived by Fricke[26] for any suspension:

$$\frac{\sigma - \sigma_1}{\sigma + x\sigma_1} = \rho\frac{\sigma_2 - \sigma_1}{\sigma_2 + x\sigma_1}$$

where x is a numerical factor dependent on the shape of the suspended particles and on σ_2/σ_1. For spheres, $x = 2$, and, when σ nearly equals σ_1, the equation can be simplified to the form given by Danzer.

Applying Fricke's relation to blood at microwave frequencies it is necessary to assume that the cell membrane reactance is negligible at such frequencies, and that the relation holds for high concentrations. Fricke[27] has shown the theory to apply in the cases of the low-frequency conductivity of blood and of cream up to a concentration of 62% of cream in skimmed milk. He has also given the values of x for spheroids of various axial ratios and for the full range of variation of σ_2/σ_1.[26] It is established[28] that human erythrocytes behave electrically at low frequencies (according to Fricke's relation) as oblate spheroids of axial ratio 1 : 4. Table 5 shows the results of calculations made using Fricke's equation. Here, the ionic conductivities of

Table 5. *Whole blood—ionic conductivities of blood, plasma, and cell contents*

Temp. (° C)	σ (Ω^{-1} cm^{-1}) Blood	Plasma	Cells	x
15	0·010	0·0108	0·0090	1·90
25	0·012	0·0128	0·0100	1·92
35	0·014	0·0155	0·0122	1·88

whole blood are taken from Table 3, and those for the plasma are the ionic conductivities measured at low frequency (1 000 c/s) and assumed to be unchanged at hyper-high frequencies.

The ionic conductivity of the intracellular fluid is lower than that of the plasma, the ratio of the two being approximately that calculated from published data[29] for the ion balance of normal human erythrocytes and plasma. There appears to be no previous dielectric work on human erythrocytes leading to an estimate of intracellular conductivity. Cole and Curtis[30] list the results of several workers on the cells of other animals. The present work indicates that the intracellular ionic conductivity of human erythrocytes is higher than that for erythrocytes of other animals.

(*c*) *The dispersion of the dielectric constant in the microwave region.*

(i) *Relaxation time.* It has been noted that the dispersion in this frequency region is characterized approximately by a single relaxation time. Comparison of the relaxation times of blood with those of water at the same temperature show the former to be nearly 10% longer. Thus the dispersion in blood can be attributed to water relaxation with times increased probably by hydrogen bond formation to active groups of other types of molecule. (A large increase in relaxation time has recently been reported when water associates with dioxan.)[31, 32]

(ii) *Interpretation of* ϵ^* *in terms of hydration.* Comparison can also be made between the values of ϵ^* for blood and water. In the case of blood it can safely be assumed that contributions to the polarization corresponding to ϵ^* from protein relaxation are negligibly small, since the relaxation times of proteins in aqueous solution lie in the region of 10^{-7} sec.[33] The polarization can then be attributed to the orientation polarization of water molecules and to the atomic and electronic polarizations of all the constituents of blood.

When the value of ϵ^* for blood is calculated using any existing dielectric theory for solutions, mixtures or suspensions, it is found that the experimental value is lower than the calculated one. Following previous workers, the explanation for this is that some water is bound in such a way to ions and proteins as not to contribute to orientation polarization. Estimates of hydration can thus be made from a comparison of dielectric constants, the estimate depending upon which dielectric theory is assumed to apply.

Dielectric measurements at frequencies lower than in the microwave region have already been used to obtain hydration estimates. Errara[34] and Girard and Abadie[35] have worked with colloidal suspensions, gluten and other systems. Much of the work done on protein solutions has been summarized by Oncley. More recently, Hasted and others[36] showed that dielectric measurements at microwave frequencies could lead to hydration estimates in aqueous ionic solutions, and Haggis and others have extended the work to protein solutions.

In the present case of blood a hydration estimate for haemoglobin can be made. It is necessary to use a dielectric theory accounting for inhomogeneity since the dielectric constant of the cell contents differs from that of the plasma. The dielectric theories of Maxwell,[37] Wiener[38] and Fricke[39] all lead to the relation

$$\frac{\epsilon - \epsilon_1}{\epsilon + x\epsilon_1} = \rho\left(\frac{\epsilon_2 - \epsilon_1}{\epsilon_2 + x\epsilon_1}\right)$$

identical in form to the conductivity equation. Hence ϵ, ϵ_1 and ϵ_2 refer to the suspension, suspending and suspended media respectively. x is Fricke's numerical factor, dependent on shape and ϵ_2/ϵ_1.

Table 6 gives the dielectric constants, ϵ^*, of blood plasma, whole blood and red cell contents.

Table 6. *Whole blood—the dielectric constant,* ϵ^*, *of blood, plasma and cell contents*

Temp. (° C)	ϵ^* Blood	Plasma	Cells
15	62·0	78·3	43·9
25	58·0	74·3	40·1
35	56·0	70·6	39·8

Those for plasma have been calculated from pure water values allowing for ionic and protein depression of the dielectric constant. The erythrocyte values have been obtained using the above equation with $\rho = 0{\cdot}43$ and $x = 1{\cdot}70$ (from Fricke, for oblate spheroid of axial ratio 1 : 4).

From the values of ϵ^* for red cell contents one can proceed

to derive the partial volume of the intracellular hydrated haemoglobin. It will be assumed that the erythrocyte contents represent an inhomogeneous dielectric and that the above relation applies. Using average cell data[40] and assuming a hydrated haemoglobin molecule is equivalent to an oblate spheroid of axial ratio = 1 : 2 and $x = 1{\cdot}72$, the partial volumes and hydration estimates shown in Table 7 have been obtained.

Table 7. *Human erythrocytes—partial volume and hydration of haemoglobin*

Temp. (° C)	Partial volume Hb. + water	Hb.	Hydration (g water per g)
15	0·340	0·266	0·21
25	0·361	0·266	0·27
35	0·340	0·266	0·21

The further assumptions that have been made are: (*a*) the partial molar volume of haemoglobin = 0·75, (*b*) the hydrated haemoglobin molecules have a dielectric constant of 2·0 and are dispersed in a medium of dielectric constant equal to that of a saline solution of ionic conductivity as shown in Table 5, and (*c*) constituents other than water, haemoglobin and ions occupy 1·5% of the total volume and have a dielectric constant of 2·0.

Full consideration of all the limits of error involved shows that, as in all hydration estimates, the accuracy of the final estimate is very low. The best that can be claimed here is that the haemoglobin hydration for human erythrocytes is $0{\cdot}23 \pm 0{\cdot}16$ g water per g, assuming the inhomogeneous dielectric theory to apply. Agreement with the results of Haggis and others, who used aqueous solutions of haemoglobin, is reasonably good, though the hydration in a living cell may differ from that in a more dilute aqueous solution. It should be noted that if the hydration is calculated from simple volume proportions[41, 9] the estimate obtained is approximately double the above figure.

CONCLUSIONS AND SUMMARY

(*a*) *Water.* The present results show that the dispersion in water is such that ϵ' falls through the dispersion region from the static value to a value of 5·0 if a single relaxation time is assumed; but also that a fall to the infra-red value of 4·0 is equally possible if relaxation is characterized by a narrow spectrum of relaxation times. A decision between the two would only be possible if results of greater accuracy over a wider frequency range were obtainable. This would also enable any variations of ϵ_∞ with temperature to be detected.

(*b*) *Blood.*

(i) The dispersion at hyper-high frequencies is closely related to the "free" water content and to the ionic conductivity.

(ii) The dispersion effects of inhomogeneity, so great at lower frequencies, are negligibly small at hyper-high frequencies.

(iii) The values obtained for the dielectric constant and ionic conductivity at frequencies just lower than those where water dispersion becomes significant are consistent with Danzer's theory and with published results in the radio frequency region.

(iv) These values give reasonable estimates for the erythrocyte intracellular conductivity and haemoglobin hydration if Fricke's theory and data for inhomogeneous dielectrics is assumed to apply for high concentrations.

ACKNOWLEDGEMENTS

The author wishes to acknowledge the assistance he has received from his colleagues. In particular, thanks are due to Mr. T. J. Buchanan and Dr. G. H. Haggis for the use of apparatus set up by them, and for helpful discussions, and to Dr. J. W. Stewart for providing blood specimens.

The work formed part of a research programme leading to the Ph.D. degree of the University of London. It gives pleasure to thank Professor J. E. Roberts for his guidance and interest during the investigations.

REFERENCES

(1) Connor, C. P., and Smyth, W. P. *J. Amer. Chem. Soc.*, **65**, p. 382 (1943).
(2) Abadie, P. *Trans. Faraday Soc.*, **42A**, p. 143 (1946).
(3) Saxton, J. A., and Lane, J. A. *Meteorological Factors in Radio-wave Propagation*, p. 278. (London: The Physical Society, 1946.)
(4) Collie, C. H., Ritson, D. M., and Hasted, J. B. *Proc. Phys. Soc., Lond.*, **60**, p. 145 (1948).
(5) Montgomery, C. G. *The Principles of Microwave Circuits*, p. 380. (New York: McGraw-Hill Book Co. Inc., 1948.)
(6) Gsell, G. *Z. Phys.*, **43**, p. 101 (1942).
(7) Osswald, K. *H.F. Tecknik u. Elektroak.*, **49**, p. 40 (1937).
(8) Rajewsky, B., and Schwan, H. *Naturwissenschaften*, **10**, p. 315 (1948).
(9) Iwase, Y. *Theory and Application of High Frequency Phenomena*, p. 21 (Japan: Hokkaido University, 1950).
(10) Danzer, H. *Ann. Phys., Lpz.*, **20**, p. 463 (1934).
(11) Schwan, H. *Ann. Phys., Lpz.*, **40**, p. 509 (1941).
(12) England, T. S., and Sharples, N. A. *Nature, Lond.*, **163**, p. 487 (1949).
(13) England, T. S. *Nature, Lond.*, **166**, p. 480 (1950).
(14) Jackson, W. *Trans Faraday Soc.*, **42A**, p. 91 (1946).
(15) Knerr, H. W. *Phys. Rev.*, **52**, p. 1054 (1937).
(16) Cooper, R. *J. Instn Elect. Engrs*, **93** (*Pt. III*), p. 69 (1946).
(17) Buchanan, T. J. *Proc. Instn Elect. Engrs*, **99** (*Pt III*), p. 61 (1952).
(18) Haggis, G., Buchanan, T. J., and Hasted, J. B. *Nature, Lond.*, **167**, p. 607 (1951).
(19) Cole, K. S., and Cole, R. H. *J. Chem. Phys.*, **9**, p. 341 (1941).
(20) Lattey, R. T., Gatty, O., and Davies, W. G. *Phil. Mag.*, **12**, p. 1019 (1931).
(21) Cartwright, C. H. *Nature, Lond.*, **135**, p. 872 (1905); **136**, p. 181 (1935); *Phys. Rev.*, **49**, p. 470 (1936).
(22) Rubens, H. *Verh. Deutsch. Phys.*, **17**, p. 315 (1915).
(23) Wagner, K. W. *Die Isolierstoffe der Elektrotechnik*, Chap. 1 (Berlin: J. Springer 1924).
(24) Jackson, W. *J. Instn Elect. Engrs*, **75**, p. 93 (1934).
(25) Hartshorn, L. *J. Instn Elect. Engrs*, **64**, p. 1152 (1926).
(26) Fricke, H. *Phys. Rev.*, **24**, p. 575 (1924).
(27) Fricke, H. *Cold Spring Harbor Symposia*, **1**, p. 117 (1933).
(28) Ponder, E. *Medical Physics*, p. 1203 (Chicago: The Year Book Publishers Inc., 1944).
(29) Muntwyler, E. *Medical Physics*, **2**, p. 317 (Chicago: The Year Book Publishers Inc., 1950).
(30) Cole, K. S., and Curtis, H. J. *Medical Physics*, **2**, p. 82 (Chicago: The Year Book Publishers Inc., 1950).
(31) Hasted, J. B., Haggis, G., and Hutton, P. *Trans Faraday Soc.*, **47**, p. 577 (1951).
(32) Cook, H. F. *Trans Faraday Soc.*, **47**, p. 751 (1951).

(33) ONCLEY, J. L. *Proteins, Amino Acids and Peptides*, p. 543 (New York: Reinhold Publishing Corp., 1943).
(34) ERRARA, J. *J. Chim. Phys.*, **29**, p. 577 (1932).
(35) GIRARD, P., and ABADIE, P. *Trans Faraday Soc.*, **42A**, p. 40 (1946).
(36) HASTED, J. B., RITSON, D. M., and COLLIE, C. H. *J. Chem. Phys.*, **16**, p. 1 (1948).
(37) MAXWELL, J. C. *Treatise on Electricity and Magnetism*, p. 314 (Oxford: University Press, 1892).
(38) WIENER, O. *Leipzig, Ber.*, **62**, p. 256 (1910).
(39) FRICKE, H. *Physics*, **1**, p. 109 (1931).
(40) DIGGS, L. W. *Medical Physics*, **2**, p. xxiv (Chicago: The Year Book Publishers Inc., 1950).
(41) OSTER, G. *J. Amer. Chem. Soc.*, **68**, p. 2036 (1946).

The spectrophotometry of light sources

By S. T. HENDERSON, Ph.D., F.Inst.P., and M. B. HALSTEAD, B.Sc., Grad.Inst.P., Thorn Electrical Industries Ltd., London

[*Paper first received* 21 *February, and in final form* 24 *March*, 1952]

The calibration and use of simple, non-automatic equipment for spectrophotometry of light sources is described, with particular attention to precautions required for accuracy. The computation of chromaticity from the spectral energy distribution curves is illustrated, with results for a variety of lamps. These results show better agreement with visual colorimetry than in other recently published work. The change of chromaticity of fluorescent lamps with varied loading is analysed by the same methods, and the application to the study of phosphors briefly mentioned.

Spectrophotometry has been widely practised in the determination of transmittance and reflectance factors, and perhaps to a lesser degree in the study of light sources. Automatic instruments have been developed for this latter application.[1–3] The methods used, whether in automatic operation or otherwise, are well known in principle, and are surveyed in a National Bureau of Standards handbook,[4] but there is often a lack of experimental detail available to guide those interested in the technique. This paper shows how, with some precautions, simple apparatus may be used to give results which are not inferior in accuracy to those obtained by more elaborate methods, and which are valuable in problems concerning fluorescent lamps.

The curve of spectral energy distribution (s.e.d.) in the visible region, expressed as energy per unit wavelength interval against wavelength, is fundamental to considerations of colour and colour rendering. Examples of its use are: (i) the chromaticity or colour appearance of the light source can be calculated from this curve, while the agreement with a visual match on a reliable colorimeter is a crucial test of the accuracy of the experimental work; (ii) the curve is of considerable value in the investigation of solid inorganic phosphors, especially those in which preparative conditions are critical for the development of any desirable type of emission; (iii) the s.e.d. curve can be reduced to luminance ordinates instead of energy. From this, any division can be made into bands of specified wavelength intervals with a view to measuring the total luminance in each band. This method, probably not yet in its final form, provides a concise though approximate description of the colour rendering properties of the light source.

APPARATUS

A wavelength spectrometer by Adam Hilger Ltd., with glass prism ($n = 1{\cdot}74$) and wavelength drum was used as a monochromator with the entrance slit narrower than the exit slit, the latter normally at constant width (see below). The entrance slit received light directly from a fluorescent lamp held vertically and run at constant wattage or current as desired. The whole of the emergent beam from the spectrometer was received on the cathode of a 1P22 photomultiplier cell by Radio Corporation of America mounted in a metal box provided with a tube fitting into the exit tube of the spectrometer. The sensitivity of this multiplier extends well into the red end of the spectrum: its very much higher sensitivity at the blue end is compensated by increasing absorption in the yellowish glass of the spectrometer prism. A stabilized a.c. supply and half-wave rectifier circuit provided the multiplier with about 1 kV during operation, while a potential divider ($\simeq 2$ MΩ total resistance) supplied about 100 V to each of the nine stages of amplification and about 50 V between the anode and the ninth dynode. The output was fed through a universal shunt (10 kΩ) to a d'Arsonval galvanometer (450 Ω) by the Cambridge Instrument Co. Ltd. with a sensitivity of about 1 300 mm/μA at 1 m, which was the scale distance used. For calibration of the apparatus by light of known s.e.d. a 1 kW tungsten projector lamp standardized for colour temperature was found convenient, with a magnesium oxide screen illuminated thereby fixed in front of the spectrometer slit.

PROCEDURE

After an initial period of running to stabilize the multiplier circuit and the fluorescent lamp, and to fatigue the photosurface, readings were taken of the galvanometer deflexion for each 50 or 100 Å interval on the wavelength drum, proceeding from red to blue. The total voltage on the multiplier was held constant at a value in the range 1 000–1 050 V by a variable 1 MΩ resistor in series, and the lamp loading controlled over the narrow range necessary by a variable resistor in series with the choke. Galvanometer deflexions were restricted to about 35 cm, above which a higher range on the universal shunt was introduced. This was chiefly required for the mercury line measurements which in the final form of the experiment were made after the readings through the spectrum of the phosphor bands. For each mercury line the maximum was found by trial adjustment of the drum, and two separate peaks recorded for the yellow doublet.

For calibration, numerous separate runs were made with the tungsten lamp at a colour temperature of 2 848° K (old temperature scale), firstly with an unstabilized a.c. supply with Variac control, which produced some unsteadiness in the resulting deflexions; secondly by a d.c. battery supply, with much improved stability. The observations agreed closely with the averaged a.c. ones. The smooth curve resulting from the mean of ten sets of d.c. observations was taken for the derivation of a table of factors F (F_λ = relative energy at λ of Planck radiator at 2 848° K/deflexion at λ), determined at each wavelength normally used, including those of the mercury lines, for application to all the readings taken for other light sources. The effects of variable exit waveband (in Å), uneven photocell sensitivity and certain instrument errors, were thus eliminated, while the error due to divergence of the standard

lamp from Planckian distribution was taken as negligible according to the usual custom.[4] The validity of this last assumption has been criticized recently by Stair,[5] but his more elaborate calibration methods do not seem to lead to greater ultimate accuracy. In particular some uncertainty must result from his use of an average factor taken from widely differing values for different mercury lines.

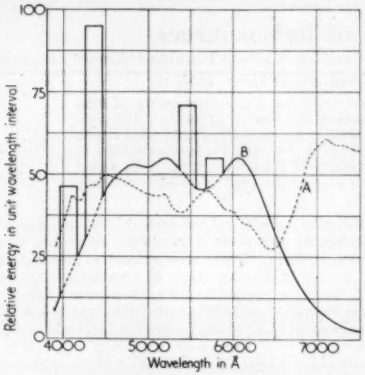

Fig. 1. Spectral energy distribution curves
A, incandescent + OB 9 glass. *B*, Northlight lamp.

The energy values for the phosphor and the mercury lines were computed as described below and recorded in the form of diagrams like Fig. 1(*b*). On these the mercury lines, having no appreciable width, are represented by blocks above the phosphor curve. The area of a block gives the total energy of the line on the same scale as that for areas below the phosphor curve.

SOURCES OF ERROR

The initial trials with the method gave only fair agreement between the known chromaticity of fluorescent lamps and the values calculated from s.e.d. curves (x or y differences in the C.I.E. system up to 0·015). The sources of error detailed below were then examined and corrected where possible, with very marked improvement in the chromaticity computations.

(*a*) *Scattered light.* Double monochromators are usually regarded as essential in this type of work to ensure purity of the narrow spectral band being measured at any time. For single dispersion instruments it is possible to use colour filters to eliminate unwanted radiation in regions where this is likely to form an appreciable proportion of the radiation being measured, for example at the extreme ends of the visible spectrum. Attempts were made with Ilford 202 (red) and 621 (blue) filters in front of the entrance slit when measuring radiation above 6 000 Å and below 4 800 Å respectively. It was found that errors due to uncertainty in the transmission factors at any wavelength were of the same order as the resulting corrections for scattered light, and the method was abandoned. The calibration by tungsten lamp will, of course, compensate for scattered light to an extent depending on the similarity of the s.e.d. curves for the standard and unknown sources. It is possible, however, that the insensitivity of chromaticity to extreme red or blue light conceals the errors due to this cause.

Visual inspection revealed stray images in the beam emerging from the prism. A considerable improvement was made by a circular aperture (14 mm diameter) in the telescope tube about half way between lens and exit slit. This reduced the light transmission by about 7%. There was little or no chromatic aberration in the telescope lens so that it was unnecessary to consider progressive refocusing of the beam on to the exit slit; in any case this procedure is impracticable unless alternate observations are made on standard and unknown source at each wavelength setting.[2] Care was taken to fill the collimator lens with light by a suitable slit to source distance (15 cm). No condenser was used between source and slit as any lack of mechanical rigidity in the arrangement might lead to difficulties.

(*b*) *Slits.* An examination of mercury line profiles was made at various slit widths, and these agreed reasonably well with the deductions of Hogness, Zscheile and Sidwell[6] assuming an image of uniform intensity. This treatment has been extended to the case of close pairs of lines. Let d be the line separation, s_1 the entrance slit width, and s_2 the exit slit width (all measured in the same units). The overall magnification is 1 in the present case, hence the image of the entrance slit is of width s_1. It appears that (*a*) the two peaks can be resolved (with a minimum between them) if $s_1 < d > s_2$; (*b*) the peaks can be separately measured, though with a maximum between them, if $s_2 - s_1 < d < s_2$; (*c*) a peak equivalent to the sum of the two lines is obtained if $d < s_2 - s_1$. Further, with $s_2 = s_1$, (*d*) resolution requires $d > s_2$; (*e*) if $d \leqslant s_2$ one peak is recorded which increases as d decreases but a complete summation is never achieved. These deductions are shown graphically and lettered as above in Fig. 2 for two lines of equal intensity. Thus for the mercury yellow lines $d = 21$ Å, and with $s_1 = s_2 = 50$ Å, as often used,[5,13] neither resolution nor accurate summation can occur: the same is true of the violet lines at 4 047 and 4 078 Å.

In the present work s_2 was about 0·2 mm, or 22 Å at 5 791 Å and 7 Å at 4 047 Å. By the strict theory this should make the yellow lines just overlap as in (*b*), Fig. 2, but in practice they are just resolvable, probably because of diffraction effects which have been ignored in the above treatment. The entrance slit width varied according to source intensity but was generally 0·06 mm; the exit slit length was 3·5 mm.

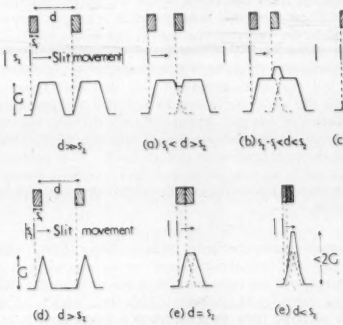

Fig. 2. Relation of galvanometer deflexions (ordinates) to line separation and slit widths, for ideal images

It will appear below that the exit slit width (in Å) is a necessary constant in computing the mercury line energies.

The width was measured directly on the wavelength drum, using cadmium and mercury lines, and averaged values obtained from a smoothed curve. This is a difficult measurement to make and is considered to be the least satisfactory part of the present work. In future development it is desirable to use some more accurate method, preferably a slit adjustable to a known width by a graduated ring instead of the symmetrically opening but uncalibrated "shutter eyepiece" which was the only type available when this work was done.

(*c*) *Wavelength errors.* Since the entrance slit was not symmetrically opening, accurate agreement between the known wavelength of a mercury line and the drum reading for maximum photomultiplier output on this line could not be expected for all settings of the slits. The maximum differences were about 5 Å. However, with a difference assumed to be 20 Å throughout the spectra of the tungsten standard and a fluorescent lamp (apart from the mercury lines), the calculation of chromaticity showed only small changes. For a daylight lamp both x and y increased by about 0·001, or the colour was apparently more yellow for too high drum readings. The direction of the changes will depend on the shape of the phosphor s.e.d. and the proportion of mercury emission, but the correction is negligible for the present purpose.

(*d*) *Magnesium oxide screen.* The fluorescent lamp sources were viewed directly, the calibrating tungsten lamp via a magnesium oxide screen. The reflectance of the latter is therefore involved in the calculations. Using the data given by Benford, Lloyd and Schwarz,[7] the changes in chromaticity for a daylight fluorescent lamp were less than 0·0005 in x and y and therefore negligible. The corrections for magnesium oxide were not used henceforward, especially as Middleton and Sanders[8] claim that the effect of magnesium oxide is the reverse of that described by Benford. The use of multiple reflexions from magnesium oxide, as in the use of an integrating sphere, is to be avoided unless the reflectivity is deliberately lowered by addition of a black pigment. Otherwise any slight spectral absorption is magnified by repeated reflexions, and the issuing light may be perceptibly altered in chromaticity. In order that the position of the white screen should be the same with respect to the entrance slit as that of the fluorescent lamp, the oxide was smoked in a thick layer on to the glass wall of a similar lamp held in the same clamps.

(*e*) *Tungsten standard lamp.* The voltage on the lamp was held within 1 V of the operating level of 184 V on a.c., and more closely on d.c. There is little information on the relation between voltage and colour temperature, but the indications are that a variation of 1 V would cause only minor changes in the lamp chromaticity, of the order of 0·001 in x.

(*f*) *Photomultiplier and galvanometer.* The dark current tended to vary, and to increase during the course of a run, hence frequent zero determinations were necessary. The cell was fatigued before use[9] by about ten minutes' exposure to yellow light from the fluorescent lamp, with the wavelength or entrance slit adjusted to give about the maximum deflexion used on range 1 (0·25 μA). In view of the larger fatigue effects to be expected from the powerful mercury lines, it was found advisable to measure these after the phosphor band. The cell should have a linear response since the range of operation was well within the makers' limits. Several checks were made to confirm the linearity of the galvanometer and cell combination. A tungsten lamp run on d.c. was used as in calibration, with the addition of a variable sector rotating at high speed to vary the light intensity incident on the spectrometer slit. The response was shown to be very nearly linear, and within 1% over the range used.

The nominal values of the ranges on the universal shunt (3 and 10) were replaced by values determined by repeated trials (3·04 and 10·02).

APPLICATIONS

(*a*) *Fluorescent lamp s.e.d. and chromaticity by selected ordinate method.* The energy value E_λ for the phosphor emission at any wavelength λ is the product of the galvanometer deflexion G, the shunt range R, and the factor F derived from the calibration procedure. The phosphor emission so derived is almost always smooth as curve B in Fig. 1. In general, these curves can be drawn through the individual points, though a few points may lie as much as 2% in ordinate from the smooth curve in its central part, with occasional divergences up to 5% below 4 500 Å and above 6 500 Å.

The chromaticity of the phosphor emission was determined by a variant on Hardy's "selected ordinate" method,[10] though the thirty ordinates (or wavelengths) were a set calculated from Wright's table of distribution coefficients for the equal energy spectrum.[11] The positions of these ordinates differed no more than 5 Å from the published ones[12] based on Hardy's tables, except for the sixth $\bar{x}$ ordinate which was at 5 230 Å in the present work and 5 316 Å in the other. In some cases ten ordinates selected from the usual thirty were used to test the precision of the method; also 100 ordinates were specially calculated for the same purpose. The following descriptions of the details of computation are confined to the X tristimulus coefficient of chromaticity, except in the numerical example; the Y and Z values are determined in exactly similar fashion.

The X contribution of the phosphor is given by $\Sigma E_\lambda \,.\, \bar{x}_\lambda \,.\, \Delta\lambda_x$ over the whole visible spectrum. The selected ordinates are at spacings $\Delta\lambda_x$ such that $\bar{x} \,.\, \Delta\lambda_x$ is constant for each, and the required sum is this constant times the sum of the energy ordinates at the thirty wavelengths. Now since $\Sigma\bar{x}$ (or $\Sigma\bar{y}$ or $\Sigma\bar{z}$) at regular 50 Å spacings between 3 800 Å and 7 800 Å is 21·37 in Wright's table,[11] then for the thirty selected ordinates the constant $\bar{x} \,.\, \Delta\lambda_x$ equals the area of the $\bar{x}$ *vs.* λ curve divided by 30, or $50 \times 21{\cdot}37/30 = 35{\cdot}61$ Å.

To find the mercury line contributions to the chromaticity the energy for a line is first calculated as $E = (GRF - B)$, where B is the phosphor energy ordinate (or background level per Å) at the particular wavelength, read off from the curve already drawn. Next the energy value must be multiplied by the exit slit width s_2 (in Å) because of the difference between photomultpilier response to a continuous phosphor band and to a line. In both cases the response is proportional to the entrance slit width s_1, but with $s_2 \geqslant s_1$ the value of s_2 is immaterial for an isolated line whereas the energy transmitted from a band is proportional to s_2 over the usual range. The lines may now be represented on the s.e.d. curve by blocks of arbitrary width and area s_2E, and so appear on the same energy scale as the phosphor curve. The values for wavelengths 4 047 and 4 078 Å are added, also those for 5 770 and 5 791 Å, since it is an unnecessary refinement to treat these close lines separately either in the diagrams or in the chromaticity determinations. The blocks are conveniently made 200 Å wide (Fig. 1).

Conversion of the s_2E values into coefficients of X involves multiplication by the $\bar{x}$ values at the line wavelengths, except that weighted values are used for the close pairs of violet and yellow lines. In practice it is convenient to omit the factor $\bar{x} \,.\, \Delta\lambda_x$ in the phosphor computation and instead use its reciprocal K in the line computation. The following is an

example for the Northlight lamp whose s.e.d. curve is shown in Fig. 1.

Phosphor:

ΣE_λ = 1 877·7 by summation of the 30 $\bar{x}$ ordinates.
1 987·8 by summation of the 30 $\bar{y}$ ordinates.
1 758·8 by summation of the 30 $\bar{z}$ ordinates.

Mercury lines:

$K = 1/35{\cdot}61$ in units of Å^{-1}. s_2 is measured in Å at each wavelength.

λ Å	$\bar{x}$	$\bar{y}$	$\bar{z}$	s_2E	$s_2EK\bar{x}$	$s_2EK\bar{y}$	$s_2EK\bar{z}$
4 047, 4 078 A	0·023	0·00065	0·111	6 794	4·4	0·1	21·2
4 358	0·332	0·0178	1·643	17 340	161·2	8·7	800·0
5 461	0·376	0·984	0·0124	6 460	68·1	178·5	2·2
5 770, 5 791	0·887	0·888	0·0017	2 080	51·7	51·9	0·1
					285·4	239·2	823·5

Lamp chromaticity:

Coefficient of $X = 1\,877{\cdot}7 + 285{\cdot}4 = 2\,163$
$Y = 1\,987{\cdot}8 + 239{\cdot}2 = 2\,227$
$Z = 1\,758{\cdot}8 + 823{\cdot}5 = 2\,582$
$C = 0{\cdot}311X + 0{\cdot}319Y + 0{\cdot}370Z.$

Fig. 1(*A*) also shows (not on the same scale of ordinates) the curve for the combination of the standard tungsten lamp with a Chance OB 9 glass filter, Table 1(*A*). The calculation here is simpler, involving no mercury lines. The time taken for two operators to set up and measure a lamp, and to make the computation of chromaticity, is about 1½ h. A simple adding device (the "Exactus Mini-Add," metric version) is of great assistance.

The results are collected in Table 1. The agreement between the visual colorimetry and the computed values is satisfactory for the tungsten + OB 9 sources (*A*) and (*B*). For the fluorescent sources the mercury 4 358 Å line often has a considerable effect on chromaticity and the apparent systematic error in the results (mean differences $-0{\cdot}004X$, $-0{\cdot}002Y$) could be due to this if s_2 were not accurately determined. The general agreement is, however, adequate for both near-white and strongly coloured lamps, and is better than that claimed by Jerome[13] and Stair.[5] For future work it will probably be better to use a wider exit slit, which need not affect resolution adversely for most phosphors.

The values in Table 1 were obtained at the National Physical Laboratory on a Donaldson 6-stimulus colorimeter and are understood to be accurate, by comparison with spectrophotometry, to within 0·003 in X, Y or Z (usually within 0·002). Computations given elsewhere in this paper were made at somewhat different lamp loadings than the standard conditions applicable to Table 1, and therefore do not give values strictly comparable with these.

In Table 2 are shown some comparisons from different degrees of approximation. In terms of colour appearance the differences are significant only for the Peach lamp.

Table 2. *Computed chromaticity at different stages of approximation*

No. of ordinates	Northlight lamp x	Northlight lamp y	Peach lamp x	Peach lamp y
10 selected	0·314	0·324	0·468	0·394
30 selected	0·315	0·324	0·474	0·389
100 selected	0·315	0·321	0·476	0·386
38 unselected	0·314	0·323	0·474	0·387

(*b*) *Chromaticity by unselected ordinate method.* Table 2 includes the results of a somewhat different computation by thirty-eight evenly spaced ordinates at 100 Å intervals. The X coefficient for the phosphor curve is given by $\Sigma E_\lambda \,.\, \bar{x}_\lambda \,.\, \Delta\lambda$, where $\Delta\lambda$ is 100 Å, and requires the more lengthy summation of the separate products $E_\lambda \,.\, \bar{x}_\lambda$. As in the selected ordinate method, the constant factor is transferred to the mercury line contributions which become $s_2E\bar{x}_\lambda/100$.

(*c*) *Fluorescent lamp loading.* An aspect of lamp performance which can be examined by this method is the change of chromaticity with varied loading. Increase of loading increases the wall temperature, arises the mercury vapour pressure and alters the phosphor response. From the work done it is now clear that the usual loss of colour saturation as loading is increased is due to (i) a small change in the phosphor chromaticity, and (ii) a much greater change in the mercury emission which becomes greener and relatively brighter with increased temperature. Table 3 refers to the calcium silicate and Northlight lamps appearing in Table 1 and to a lamp without a phosphor coating. It is difficult to show the changes on small diagrams and only the lamp showing the most marked changes is represented in Fig. 3, where the mercury chromaticity determinations lie close to the straight line A between $x = 0{\cdot}205$, $y = 0{\cdot}155$ (low current) and $x = 0{\cdot}230$, $y = 0{\cdot}260$ (high current). Lamps of different sizes cover different parts of this range and there may also be

Table 1. *Chromaticity of light sources*

(Bracketed values are independent determinations on other lamps of same batch.)

Lamp colour	Visual colorimetry x	Visual colorimetry y	Computed x	Computed y	Differences 10^3x	Differences 10^3y
(*A*) Incandescent + OB 9	0·313	0·320	0·313	0·319	0	− 1
(*B*) Incandescent + OB 9	0·363	0·367	0·369	0·369	+ 6	+ 2
Northlight	0·314	0·326	0·311	0·319	− 3	− 7
			(0·308)	(0·326)	(− 6)	(0)
Daylight 1*	0·369	0·369	0·366	0·367	− 3	− 2
Daylight 2	0·362	0·364	0·359	0·366	− 3	+ 2
			(0·358)	(0·365)	(− 4)	(+ 1)
Natural daylight	0·372	0·342	0·370	0·341	− 2	− 1
White	0·408	0·384	0·403	0·378	− 5	− 6
Warm white	0·424	0·383	0·419	0·380	− 5	− 3
			(0·418)	(0·379)	(− 6)	(− 4)
Peach	0·478	0·393	0·470	0·388	− 8	− 5
Calcium silicate (Mn, Pb) phosophor*	0·482	0·380	0·478	0·380	− 4	0
Green	0·252	0·604	0·246	0·603	− 6	− 1
Blue	0·183	0·156	0·182	0·162	− 1	+ 6

* 2 ft 40 W lamps, all others 4 ft 40 W.

Table 3. *Change of computed chromaticity and luminance of phosphor, mercury and lamp with change of lamp current*

Lamp	Current A	Phosphor x	Phosphor y	Phosphor Y_1	Mercury x	Mercury y	Mercury Y_2	Lamp x	Lamp y	Y_1/Y_2
Calcium silicate	0·25	0·581	0·413	1 179	0·213	0·189	150	0·501	0·365	7·9
2 ft 40 W lamp	0·30	0·577	0·418	1 294	0·215	0·201	169	0·500	0·372	7·7
	0·40	0·576	0·419	1 490	0·220	0·215	209	0·499	0·376	7·1
	0·55	0·577	0·419	1 814	0·225	0·238	299	0·498	0·378	6·1
	0·70	0·579	0·419	2 059	0·228	0·245	387	0·493	0·377	5·3
	0·80	0·576	0·421	2 101	0·235	0·253	421	0·490	0·379	5·0
	0·90	0·575	0·423	2 155	0·235	0·263	480	0·485	0·381	4·5
Northlight	0·25	0·334	0·348	1 344	0·208	0·154	144	0·309	0·310	9·3
5 ft 80 W lamp	0·30	0·329	0·346	1 568	0·209	0·169	173	0·307	0·314	9·1
	0·40	0·328	0·346	1 900	0·211	0·176	226	0·306	0·314	8·4
	0·55	0·327	0·348	2 349	0·216	0·193	306	0·306	0·318	7·7
	0·70	0·327	0·343	2 648	0·223	0·215	381	0·308	0·319	7·0
	0·80	0·328	0·345	2 850	0·225	0·220	441	0·308	0·321	6·5
	0·90	0·328	0·343	2 945	0·226	0·227	492	0·307	0·319	6·0
Uncoated	0·25				0·215	0·224	159			
2 ft 40 W lamp	0·30				0·217	0·226	184			
	0·40				0·219	0·236	243			
	0·55				0·222	0·238	315			
	0·70				0·225	0·255	411			
	0·80				0·227	0·260	477			
	0·90				0·229	0·266	541			

some dependence on the particular phosphor used. The ratio of Y contributions by phosphor and mercury spectra (Table 3) shows how the relative luminance increases in favour of the mercury spectrum with increased current. From the absolute values the mercury luminance Y_2 is seen to increase by a factor of about 3·3, and it is of interest that this increase is very closely linear with current increase, in spite of changing chromaticity. On the other hand, the phosphor spectrum luminance Y_1 increases about twofold, and not in a linear manner; there may again be some dependence on the phosphor type. The wattage consumption increases by about 2·5 times over the range considered.

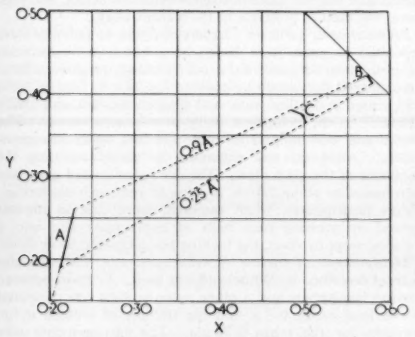

Fig. 3. Changes of chromaticity with loading
A, mercury; *B*, phosphor (calcium silicate); *C*, lamp.

(*d*) *Emission of phosphor powders.* The work is being extended to the examination of phosphor powders, which are enclosed in a metal box with a quartz window, through which excitation is produced by mercury radiation at 2 537 Å. The phosphor capsule is mounted close to the entrance slit and irradiated by light from a "germicidal" lamp. It is thus possible to test phosphors without the necessity of making lamps, or phosphors which will not withstand the usual lamp processing conditions. Measurement of the mercury lines is not required in this section of the work.

ACKNOWLEDGEMENTS

The authors are indebted to Mr. J. W. Perry, of Hilger and Watts Ltd., and to their colleagues, for helpful discussions. This paper is published by permission of the Directors of Thorn Electrical Industries Ltd. The visual colorimetry determinations in Table 1 were made at the National Physical Laboratory, and thanks are due to the Director for permission to publish the data.

REFERENCES

(1) Zworykin, V. K. *J. Opt. Soc. Amer.*, **29**, p. 84 (1939).
(2) Studer, F. J. *J. Opt. Soc. Amer.*, **37**, p. 288 (1947).
(3) Parsons, S. L., Martin, A. E., and Roberto, S. N. *J. Electrochem. Soc.*, **97**, p. 41 (1950).
(4) Gibson, K. S. *Spectrophotometry.* Nat. Bur. Stand., Circular 484 (1949).
(5) Stair, R. *J. Res. Nat. Bur. Stand., Wash.*, **46**, p. 437 (1951).
(6) Hogness, T. R., Zscheile, F. P., and Sidwell, A. E. *J. Phys. Coll. Chem.*, **41**, p. 379 (1937).
(7) Benford, F., Lloyd, G. P., and Schwarz, S. *J. Opt. Soc. Amer.*, **38**, p. 445 (1948).
(8) Middleton, W. E. K., and Sanders, C. L. *J. Opt. Soc. Amer.*, **41**, p. 419 (1951).
(9) Hillert, M. *Brit. J. Appl. Phys.*, **2**, p. 164 (1951).
(10) Hardy, A. C. *Handbook of colorimetry* (Massachusetts: Technology Press, 1936).
(11) Wright, W. D. *The measurement of colour*, p. 209 (London: Adam Hilger Ltd., 1944).
(12) Bowditch, F. T., and Null, M. R. *J. Opt. Soc. Amer.*, **28**, p. 500 (1938).
(13) Jerome, C. W. *Illum. Engng, N.Y.*, **45**, p. 225 (1950).

Frictional and elastic properties of high polymeric materials

By B. LINCOLN, B.Sc., Wool Industries Research Association, Leeds

[*Paper received* 11 *March*, 1952]

The relationship of the elastic properties of solids to their frictional properties is discussed. By applying Hertz's equation for deformation of solids in contact, it is shown that while the asperities on metallic surfaces are deformed plastically even at the smallest loads, this is not necessarily true of materials having lower elastic modulus. This is confirmed by measurement of the area of contact between a nylon hemisphere and a glass surface, and by frictional measurements on various nylon specimens. It is shown further that the observed decrease in friction of some high polymers on rough surfaces may be explained in terms of elastic deformation of the asperities.

The relationship between the coefficient of friction and the elastic constants of solids has been discussed by Bowden and Tabor[1] in the case of metals, and these workers have shown that the frictional force between metallic surfaces is directly proportional to the load, as a result of plastic deformation of the surface asperities. The frictional properties of high polymers have been studied by Shooter and Thomas,[2] who have shown that Amontons' law is followed for the range of loads 1–4 kg, thus demonstrating that plastic deformation occurs under these conditions. The frictional force is assumed to arise from the necessity of shearing the junctions formed between the two surfaces, and the magnitude of the frictional force is determined by the area of real contact multiplied by the shear strength of the junctions. Under smaller loads, however, it is not certain that plastic deformation occurs in high polymer friction, and the results of King,[3] Olofsson,[4] and Howell[5] suggest that a more complicated relationship exists between frictional force and load than has been established for metallic friction. In any event, the frictional force F may be related to the load W by an expression of the form

$$F = S \cdot f(W, E, R) + F_0 \qquad (1)$$

where E is an elastic property of the material;

S is the shear strength of the real areas of contact;

R is a geometrical term;

and F_0 is a term representing any component of the frictional force not due to variation of area of contact with load. Olofsson and Howell obtain such an intercept F_0 on the F-axis of the curve relating F to W.

If it is assumed that the critical mean pressure, over the real area of contact, for onset of plasticity is given by $P_m = 1{\cdot}1\,Y$, where Y is the elastic limit of the material, the corresponding critical load W_p in the case of an asperity of modulus E_1 and of spherical form, pressed on a plane surface of modulus E_2, is[1]

$$W_p = (\pi \times 1{\cdot}1\,YC)^3 R^2 \left(\frac{1}{E_1} + \frac{1}{E_2}\right)^2 \qquad (2)$$

where R is the radius of the asperity;

and C is $[\frac{4}{3}(1 - \sigma^2)]^{2/3}$, σ being Poisson's ratio.

The application of this criterion to metallic contact leads to the result that plastic flow occurs in the asperities at loads of the order of 10^{-5} to 10^{-3} g for $R = 10^{-4}$ cm. However, if we consider the elastic properties of high polymers, the elastic modulus is lower by a factor of about 10^2 while the elastic limit is roughly of the same order as in metals. Nylon at 65% R.H. has[10] an elastic limit of about 5×10^9 dyn/cm^2 and an elastic modulus of 2×10^{10} dyn/cm^2. The corresponding values for mild steel are[1] $6{\cdot}5 \times 10^9$ and 2×10^{12} dyn/cm^2 so that the critical load for onset of plastic flow for equal values of R in the case of nylon in contact with a steel surface is greater than that for steel in contact with steel, by a factor of around 10^4; for a nylon-nylon contact, the factor is of a slightly higher order. The corresponding critical load is of the order of 10 to 100 mg for $R = 10^{-4}$ cm and increases as R^2, so that the frictional properties of high polymers might be expected to conform to a relationship based on elastic deformation (and hence on the relationship $F = KW^{2/3}$) with consequent deviation from the classical laws of friction. The work to be described here was undertaken with the object of examining the validity of this conclusion.

EXPERIMENTAL

The methods hitherto employed for determination of the frictional properties of textile fibres have been of the type where interfibre friction is measured,[4,5] or where a fibre is made to slide around a cylindrical surface.[3] The area of contact between the surfaces is not easy to determine in certain of these methods,[3,5] however, and the normal load varies, in the work of King and Olofsson, along the whole length of the contact. The method employed by Whitehead[6] and Parker and Hatch[7] does not suffer from this defect, and was, therefore, used in principle in the present work.

Preparation of surfaces. Layers of nylon 66 polymer were deposited on glass, from 20% w/v* solution in formic acid. To ensure firm adhesion of the nylon coating, the glass surfaces were cleaned previously by soaking for 24 h in fuming nitric acid, rinsed in distilled water and absolute alcohol, and finally "flamed" in the colourless flame of a bunsen burner. The formic acid was allowed to evaporate in a water-free atmosphere. Adhesion was enhanced by gently warming the underside of the glass plate. The dry nylon-coated glass was then heated to about 240° C *in vacuo* to remove irregularities. Nylon hemispheres, when required, were cast in moulds formed by pressing steel balls of appropriate size into a polished sheet of silver, the melting being conducted *in vacuo*.

Measurement of friction of nylon surfaces. The stick-slip method described by Whitehead was used. Friction between a nylon hemisphere and a plane nylon surface was measured in the load range 0–1 g and the friction of crossed nylon cylinders for the range 0–70 mg. The measurements were made at 70° F and 65% R.H. Preliminary cleaning of the nylon hemisphere and plane was not necessary as freshly prepared surfaces were employed. The nylon cylinders (commercially extruded filaments about 0·060 cm diameter) were selected for uniformity of cross-section and extracted in petroleum ether, using Soxhlet apparatus for 4 h prior to use, and then allowed to reach moisture equilibrium in a dust-free enclosure.

In addition to the above measurements in atmospheric conditions, the friction of a ring sliding on a rod was measured *in vacuo* so that a higher degree of cleanliness could be

* I.e. 20 g nylon per 100 ml of solution.

attained. The method consisted of measuring the angle of limiting friction of the system. A nylon-coated ring R (Fig. 1), resting on a glass rod S similarly coated, could be made to slide by tilting the tube C which was pivoted about the axis XX'. The pivot was formed by a conical joint leading to a temperature-controlled water reservoir T. To clean the surfaces an electric discharge was passed between the filament F and the anode A. The rod S could be rotated so that, by means of an auxiliary support, the nylon surfaces were completely exposed during the cleaning process. The complete apparatus was enclosed in an air thermostat and was evacuated by means of a diffusion pump with an intermediate vapour trap. The tube C was rotated by means of a rod (not shown) co-axial with XX' and attached outside the thermostat to a pointer moving over a scale graduated in degrees. The water content of the nylon was controlled by varying the temperature of the water reservoir T and hence the vapour pressure in the system, and was measured by means of the sorption balance B which consisted of a spiral quartz spring

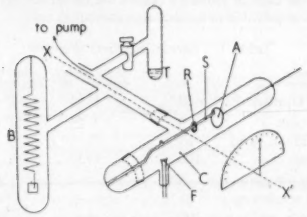

Fig. 1. Apparatus for measuring angle of friction between ring and rod

on which was suspended a sample of nylon film prepared in an identical manner to the friction surfaces. The angle of friction λ was measured for clockwise and anti-clockwise rotation and one half the total movement was taken as the value of λ, to eliminate zero error.

Measurement of variation of geometrical area of contact with load. The radius r of the circular area of contact between two spherical surfaces has been shown by Hertz[8, 9] to be

$$r = \left[\frac{3}{4}\pi W \frac{(k_1 + k_2)}{R_1 + R_2} R_1 R_2\right]^{1/3} \qquad (3)$$

where W is the load;

R_1 and R_2 are the radii of curvature of the two surfaces,

$$k_1 = (1 - \sigma_1^2)/\pi E_1$$

$$k_2 = (1 - \sigma_2^2)/\pi E_2$$

where E_1 and E_2, σ_1 and σ_2 are the elastic moduli and Poisson's ratios of the two materials.

If the second surface is plane, and $E_2 \gg E_1$ the relationship becomes

$$r = \left[\frac{3}{4} W \frac{(1 - \sigma_1^2)}{E_1} R_1\right]^{1/3} \qquad (4)$$

If r can be measured, then E_1 can be found. This principle was employed to compare the value of E_1 so obtained, with the value resulting from tensile measurements.

A nylon hemisphere N (Fig. 2) was mounted on a rigid arm L (pivoted on a knife-edge F), and was pressed on the underside of a sheet of optical glass E by suspending weights on the opposite end of the arm. The area of contact was observed in the microscope M fitted with a graticule eyepiece, and the surfaces were illuminated by a sodium lamp S to produce interference fringes. The edge of the area of contact was not perfectly circular at small loads but was sufficiently well defined to enable the diameter to be estimated. This was taken as being that of the central dark fringe.

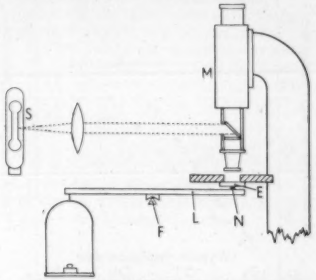

Fig. 2. Measurement of area of contact between hemisphere and plane under various loads

Measurement of shear strength. Cylindrical specimens were prepared by moulding in a glass tube, and were subjected to double shear by means of a triple clamp, the middle element being pulled out to produce the shearing action. The clamp was mounted in a recording tensile tester, and five specimens were tested at 70° F and 65% R.H.

RESULTS

The results of the measurement of area of contact between the nylon hemisphere and a glass plate are shown in Fig. 3. They indicate that the gross or geometrical area of contact is proportional to $W^{2/3}$ over the range of applied load (0–125 g wt) for a hemisphere of radius 0·158 cm. This area will not necessarily be the true area of contact owing to the presence of asperities, the mode of deformation of which is irrelevant. It is, however, possible to obtain from these results the elastic modulus by using Hertz's formula, and therefore to obtain a closer estimate of the range over which elastic deformation occurs in an asperity of given radius. The results in Fig. 3 indicate that hemispherical asperities with a radius of curvature greater than $1{\cdot}4 \times 10^{-2}$ cm will deform elastically in the load range 0–1 g wt.

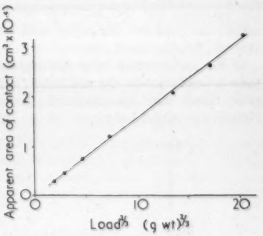

Fig. 3. Variation of apparent area of contact with load. (Nylon hemisphere 0·158 cm radius)

The friction measurements are shown in Fig. 4. In the case of the nylon hemisphere the linear relation between frictional force and $W^{2/3}$ is obtained. The relation for crossed cylinders shows a similar variation. The two sets of

experimental points represent two separate determinations on different samples of the same radius. They are in reasonable agreement and indicate that a uniform standard of cleanliness was attained. It may be concluded, then, that the frictional force varies as $W^{2/3}$.

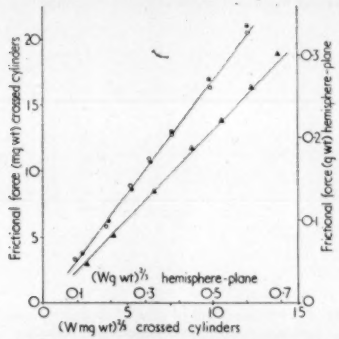
Frictional force (mg wt) crossed cylinders
Frictional force (g wt) hemisphere-plane
(Wg wt)^⅔ hemisphere-plane
(W mg wt)^⅔ crossed cylinders

Fig. 4. Variation of frictional force with load
● ○ crossed cylinders; ▲ hemisphere-plane.

The experimental value of the elastic modulus is in reasonably good agreement with published values for fibres.[10] It should be emphasized that nylon in textile fibres possesses a high degree of molecular orientation so that strict comparison of the moduli is not possible.

Friction and elastic properties. The observed variation of area of contact and of frictional force with load indicate that elastic deformation occurs in the corresponding range of loads. The results of friction measurements on nylon fibres[5] also conform satisfactorily (Fig. 5) to the relationship $F = KW^{2/3}$. It is evident, therefore, that this interpretation of the relationship between frictional force and load avoids the necessity for the inclusion of a term F_0 representing additional cohesion forces, as was considered necessary by Howell, Olofsson and others.

If the deformation over the region of contact is elastic, then an estimate of the apparent or geometrical area for a given load may be obtained by using the appropriate Hertzian equation [reference (9), p. 339]. Having obtained a value for the apparent area, the effective shear strength S' over this area may be calculated by substitution in the relationship $F = S'A$, where F is the frictional force corresponding to the load for which the apparent area has been calculated. The values of S' calculated in this manner are $3{\cdot}6 \times 10^6$ dyn/cm² for the hemisphere-plane system and 7×10^7 dyn/cm² for the crossed cylinders. If a similar calculation is made from Howell's results, assuming $R = 10^{-3}$ cm and $E = 3 \times 10^{10}$ dyn/cm² we obtain $S' = 1{\cdot}8 \times 10^8$ dyn/cm². Comparing these values with the shear strengths of the bulk material ($7{\cdot}2 \times 10^8$ dyn/cm²), it is evident that true contact does not exist between the surfaces over the apparent or geometrical area of contact as a result either of the presence of asperities or of contamination. The increase of the value of S' with decreasing radius of curvature of the surfaces (assuming constant contamination) is in agreement with the conclusion of Bowden and Tabor that in a system of crossed cylinders of small radius of curvature the real and apparent areas of contact are approximately equal, and it is probable that in the case of Howell's results the difference between S' and S is largely due to surface contamination only.

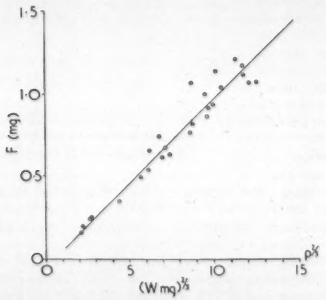

Fig. 5. Friction of crossed nylon fibres. (Howell[5])

Table 1. *Elastic constants of nylon*

Method of measurement	*R.H.*	*Elastic modulus* dyn/cm² × 10¹⁰	*Shear strength* dyn/cm² × 10⁸
Area of contact	65%	1·65	—
Tensile tests	0%	3·25	—
(Speakman and	65%	2·15	—
Saville)	100%	1·30	—
Shearing of cylin-	0%	—	9·0
drical specimens	65%	—	7·2
	100%	—	6·4

Variation of friction of nylon with moisture content. The elastic constants of polar polymers vary with relative humidity, as a result of moisture sorption. The frictional properties should exhibit a corresponding variation, and this effect has been studied by King for nylon and wool fibres. The variation of frictional force with moisture content (Fig. 6) as measured with the ring-rod system, is similar to that reported by King. It should be pointed out that as a consequence of the elastic nature of the deformation the frictional coefficient cannot be assumed to be tan λ, where λ is the angle at which slip commences.

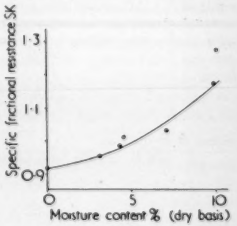

Fig. 6. Variation of friction of nylon with moisture content
● experimental points;
○ theoretical points.

The relationship now becomes $mg \sin \lambda = S'K(mg \cos \lambda)^{2/3}$ where λ is the mass of the sliding ring, S' is the apparent shear strength of the surface of contact and K is a geometrical constant, or $S'K = \left(\frac{mg \sin^3 \lambda}{\cos^2 \lambda}\right)^{1/3}$. An attempt has been made to correlate this variation with the shear strength and the elastic modulus. Values of the shear strength were obtained by direct measurement (Table 1) at total dryness, 65% R.H. and saturation, and the relative values of E were calculated from the data of Speakman and Saville. The

three values of $S \cdot E^{-2/3}$ so obtained were fitted at zero R.H. and are seen to conform to the experimental curve. This supports the view that the frictional force is a function of the shear strength and the elastic modulus under clean conditions.

The effect of surface contamination is illustrated in Fig. 7, which shows the decrease of the frictional coefficient with time of exposure to the atmosphere. It is clear from these results that surface contamination is likely to cause serious error in evaluation of high polymer friction if the shear strength of the bulk material is used as a basis for calculations.

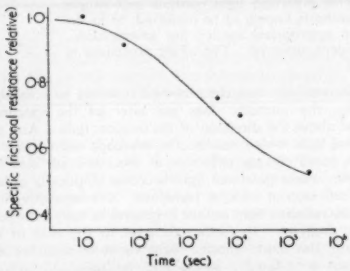

Fig. 7. Decrease of friction of nylon when exposed to atmospheric contamination

Effect of surface roughness. King has noted that under certain circumstances the coefficient of friction may decrease with increasing surface roughness. He found that the friction between a wool fibre and cylinders of various materials decreased on scratching the surface of the cylinder. The author has measured the friction of nylon fibres against stainless steel cylinders, using King's method, and the results, together with those of King, are shown in Table 2. It has been suggested that the decrease in friction might be due to the difficulty of cleaning a rough surface, but in both sets of observations it was found that prolonged cleaning did not produce any significant increase in the value of μ. A further argument against the suggestion is that the fibre will be supported on the tops of the asperities, which are likely to be of the same degree of cleanliness in a wide range of surface roughness.

Table 2. *Effect of surface roughness on friction* (*R.H.* 60%)

Fibre	*Cylinder*	*Surface condition of cylinder*	μ
Wool[4]	ebonite	smooth	0·60*
		rough	0·50*
Wool	horn	smooth	0·49*
	keratin	rough	0·42*
Nylon	stainless steel	polished	0·95
		machined	0·47
		sandblasted	0·38

* μ root-tip.

It is now proposed to develop an argument to show that the decrease in friction may be caused by the variation in the number of points of contact when deformation is elastic. It will be assumed that the same considerations apply when a hard asperity presses against a soft plane surface as when a soft asperity presses against a hard plane surface [reference (1), pp. 10–17].

If we consider a simple case where N_0 asperities of equal height and equal radius R_0 are in contact with a perfectly smooth surface, we obtain a value for the real area of contact

$$A = yN_0^{1/3}\left(\frac{WR_0}{E}\right)^{2/3} \qquad (5)$$

where y is a constant, and W is the total load.

Tnis suggests that the shape of the asperities is relatively more important than their total number, and to satisfy the condition that the friction decreases with increasing surface roughness, R_0 and N_0 should increase as the surface becomes smoother. If it is possible to assume that R_0 is a function $f(N_0)$, the necessary condition for decrease of friction with increasing surface roughness is then

$$\frac{d}{dN}[N_0^{1/3}(fN_0)^{2/3}] > 0$$

It is thus possible to define surface roughness in a way which is compatible with an explanation of the decrease of frictional force with increasing roughness.

CONCLUSIONS

(i) In contrast to the behaviour of metals, it is found that high polymers deform in an elastic manner under small loads, and the area of contact consequently varies as $W^{2/3}$, where W is the load. In consequence there is no unique value of the coefficient of friction and it is preferable to express F in terms of $W^{2/3}$.

(ii) Although contact between high polymer surfaces at small loads may occur only on the surface asperities, in many cases these are deformed elastically at loads in excess of those calculated for onset of plastic flow in the contact of metallic surfaces.

(iii) The frictional force, in perfectly clean conditions, is the product of the shear strength of the material and the real area of contact but, in practice, is often less than 1/10 of its theoretical value as a result of incomplete contact.

(iv) There is no evidence of any cohesional forces other than those implied in the relationship $F = SA$.

(v) As a result of the elastic deformation of high polymers, they may exhibit anomalous behaviour in respect of surface roughness, i.e. for the same value of the load, a greater frictional force may be associated with a smooth surface than with a relatively rougher surface.

ACKNOWLEDGEMENTS

I am indebted to Dr. A. B. D. Cassie, Director of Research, and the Council of the Wool Industries Research Association for permission to publish this account, and to Mr. G. King for helpful discussions and encouragement. Thanks are also due to Miss N. B. Wilson for assistance with the experimental work.

REFERENCES

(1) Bowden, F. P., and Tabor, D. *The friction and lubrication of solids* (Oxford: The Clarendon Press, 1950).
(2) Shooter, K. V., and Thomas, D. *Research, Lond.*, **2**, p. 533 (1949).
(3) King, G. *J. Text. Inst., Manchr*, **41**, p. T153 (1950).
(4) Olofsson, B. *Text. Res. J.*, **20**, p. 476 (1950).
(5) Howell, H. G. *J. Text. Inst., Manchr*, **42**, p. T521 (1951).
(6) Whitehead, J. R. *Proc. Roy. Soc. A*, **201**, p. 109 (1950).
(7) Parker, R. C., and Hatch, D. *Proc. Phys. Soc., Lond. B*, **63**, p. 185 (1950).
(8) Hertz, H. *J. Reine angew. Math.*, **92**, p. 156 (1881).
(9) Timoshenko, S. *Theory of elasticity* (New York: McGraw Hill Book Co. Inc., 1934).
(10) Speakman, J. B., and Saville, A. K. *J. Text. Inst., Manchr*, **37**, p. 241 (1946).

The use of polarized light for the examination of etched metal crystals and their orientation

By P. DUNSMUIR, M.Sc., A.Inst.P., Research Laboratory, The British Thomson-Houston Co. Ltd., Rugby

[*Paper received* 10 *March*, 1952]

This paper draws attention to the use of polarized light as an additional tool in studies of the orientation of etched metal crystals by goniometric methods. Observation of the state of polarization of the reflected light enables single and multiple reflexions to be distinguished in cases where this ambiguity exists. Furthermore, in specific cases the orientation of crystallographically etched crystals may be determined by inferring from the reflected polarized light whether single or multiple reflexion has occurred. This polarized light method uses simple apparatus and is of greatest use where a certain orientation is known to be preferred, as in the case of cold-rolled silicon iron alloys. Choosing an appropriate section for examination, inspection shows whether the expected orientation is indeed achieved. The whole procedure is extremely rapid.

The simplicity of etch pit methods for the determination of the orientation of metal crystals is a great attraction, particularly when appreciable numbers of separate crystals have to be examined. One requires only to know which crystal planes are exposed when the given metal is etched with some suitable chemical reagent. The directions of the traces of the etch pit sides in the surface of the specimen are then observed, or else reflexions are obtained from the faces of the etch pit, usually by using a goniometer. The goniometer method is the best, but it is complicated by the possibility of multiple reflexions of the light at the faces of the pits.

In the case when the collimator and telescope of the goniometer are parallel, Barrett and Levenson[1] have shown the danger of observing double or triple reflexions from etch pits of cubic shape and wrongly inferring that an etched facet lies normal to the light beam. To avoid this danger they separated the telescope and collimator by an angle, so that multi-reflected light returned to the collimator instead of reaching the telescope. In fact, this procedure is not always a solution to the problem. When the plane of incidence of the light is inclined to each of the faces of the cubic pit, then the incident and doubly-reflected rays are skew, and it is possible to receive light in the telescope even when an angle separates it from the collimator. Despite the lower intensity of the doubly-reflected light, there is still the danger of making false deductions. With non-cubic etch pits it can be even more difficult. Each case requires separate consideration of how to exclude multiple reflexions. It is shown below that if polarized light is used for goniometric observations on etch pits in cubic metals then single reflexions can be distinguished from multiple ones.

With non-cubic metals the use of polarized light affords contrast between the appearance of one grain and the next except when the metal consists of a single crystal, or when there is a very high degree of preferred orientation. This effect occurs without the metal being etched and is very well known. It will not be considered further here.

GONIOMETRIC OBSERVATION OF ETCHED METAL CRYSTALS WITH POLARIZED LIGHT

The necessary apparatus consists of a goniometer in which telescope and collimator are parallel. The specimen may be rotated about an axis coinciding with the direction of the light. The incident light is plane polarized and an analyser crossed with respect to the polarizer is interposed between the telescope and the eye. With this arrangement singly reflected light can only be observed after striking the reflecting facets at normal incidence. For metals of the cubic system, with which one is generally concerned, incident plane polarized light is then reflected still as plane polarized light and the analyser cuts the observed intensity to a minimum. Further, the intensity does not alter as the specimen is rotated about the direction of the incident light. Any multi-reflected light which reaches the telescope must result from two or more oblique reflexions at successive surfaces of the etch pit. Plane polarized light becomes elliptically polarized upon reflexion at oblique incidence. Consequently, in this case, the reflected light cannot in general be fully extinguished by the analyser. In further contrast to the case of single reflexion, the multi-reflected light varies in intensity as the specimen is rotated. Single and multiple reflexions can therefore be clearly distinguished when polarized light is employed.

Unfortunately, it is not practicable to extend the method to make quantitative measurements of ellipticity and predict therefrom the orientation of the metallic reflecting facets. In a review of the theoretical work Stratton[2] remarks: "the complexity of what appeared at first to be the simplest of problems—the reflexion of a plane wave from a plane, absorbing surface—is truly amazing. The formulas are far too involved to be understood from a casual inspection, and the nature of the reflection phenomenon becomes apparent only when one treats certain limiting cases." Despite this discouraging complexity it is shown in the following section how information concerning the orientation of etched metal crystals may in certain cases be extracted, using polarized light. The practical case of examining cold-rolled silicon-iron alloys for preferred orientation is discussed in detail.

PREFERRED ORIENTATION IN COLD-ROLLED SHEETS OF SILICON IRON ALLOY

Preferred orientation of the crystals in transformer sheet gives it valuable properties for certain electrical engineering applications. Speedy routine tests of the uniformity of crystal orientation are required. Alloys have been studied consisting of up to 4% silicon and the remainder almost entirely iron. The crystal structure of such an alloy is the same as for α-iron, that is, it belongs to the cubic system and the unit cell is body-centred. By suitable cold-rolling and heat treatment it is possible to produce polycrystalline sheet in which the various crystals are almost perfectly similarly aligned. A cube edge, the [100] axis, lies along the rolling direction and a (110) plane lies in the plane of the sheet. This orientation is briefly designated [100], (110) (see Fig. 1), and is of particular interest.

Preparation of specimens. The surfaces of polycrystalline specimens of silicon-iron sheet are polished and etched. The etching reagent used is chosen to expose facets parallel to (100) planes of the lattice. Ferric sulphate has been found to be suitable.

Apparatus and method. The simple apparatus used consists essentially of a microscope with a vertical illuminator and a rotating stage *G* (see Fig. 2). The specimen *S* is placed

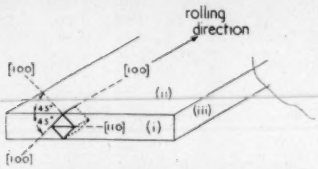

Fig. 1. The aspect presented by the crystals to the thin surface (iii), which is parallel to the rolling direction, is similar to that presented by the crystals to the large flat surface (ii)

on the horizontal stage, which is marked in degrees. A polarizer *P* is placed in the illumination system and an analyser *A* is conveniently placed beyond the eyepiece *E*. Pieces of Polaroid sheet are used here. An objective of 3 in focal length gives a satisfactory compromise between the two following requirements: (*a*) illumination of the specimen at approximately normal incidence; and (*b*) ability to distinguish separate grains of the specimen. (For this latter reason a goniometer is not used for polycrystalline specimens.) The following preliminary adjustments are made:

(i) Centre the turntable.
(ii) With analyser removed, rotate the polarizer until maximum brightness of the field is observed.
(iii) Replace analyser, and rotate until it is crossed with respect to the polarizer.

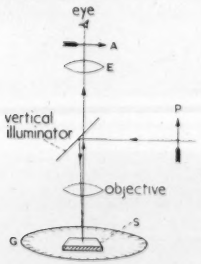

Fig. 2. Diagram of apparatus

First consider the appearance of an etched polycrystalline specimen with no preferred orientation when it is placed in position and the turntable is rotated. The grains are seen to fall into the following three groups.

(*a*) Grains of group (*a*) appear always of minimum intensity and do not change their appearance during rotation. These grains return the light after a single reflexion at normal incidence, so that the reflected light is still plane polarized and is extinguished by the analyser. Since the reflecting facets are known to be (100) planes, these crystals have a (100) plane in the plane of polish. That is, the plane of polish includes two [100] axes.

(*b*) Grains of group (*b*) exhibit four cycles of variation through maximum and minimum intensity as the specimen is rotated through 2π. These grains return the light after a double reflexion at oblique incidence and have a (110) plane and one [100] axis near the plane of polish. A theoretical treatment of this case was given by Jones,[3] who calculated the intensity of the light transmitted by the analyser as a function of the angle of rotation ϕ of the specimen about the axis of the microscope. Despite the fact that Jones wrongly added the amplitudes of two components of the reflected light without any regard to their time phase, nevertheless the correct result was given. This was due to the fact that the phases did not depend on the azimuth ϕ.

(*c*) Grains of group (*c*) exhibit variations in intensity as the specimen is rotated, other than the specific fourfold variation shown by crystals of group (*b*). Such grains have no [100] axes near to the plane of polish and return the light after a threefold oblique reflexion. The theory for three-fold reflexions is not nearly so simple as for double reflexions and the author does not know of a result obtained for this case. Grains of group (*c*) may simply be described as having a [111] axis nearly normal to the plane of polish.

Now consider a sample of polycrystalline sheet having a high degree of the preferred orientation indicated in Fig. 1. It is clear that if one polishes three different sections parallel to the surfaces designated (i), (ii) and (iii) in that diagram, and then etches the sample so as to expose (100) facets, the surface topography of the various surfaces becomes different. The thin section (i) perpendicular to the rolling direction consists of crystals having a (100) plane near the plane of polish [that is, grains of group (*a*)]. When the specimen is examined in polarized light the grains remain dark as the stage is rotated [see Fig. 3(*a*)]. The degree of preferred

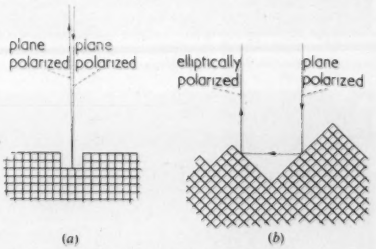

Fig. 3. (*a*) Section (i) polished and etched. (100) facets are parallel to the plane of polish. The light, both incident and reflected, is plane polarized
(*b*) Section (ii) or (iii) polished and etched. (110) is parallel to the plane of polish and (100) facets are at 45°. Plane polarized light is reflected as elliptically polarized

orientation may be estimated at once from the proportion of grains exposed which belong to group (*a*). Such grains necessarily have a [100] axis within a few degrees of the rolling direction of the sheet. For each of the sections (ii) and (iii) shown in Fig. 1, which are parallel to the rolling direction, the (100) facets which are exposed make angles of 45° to the plane of polish. The surfaces are covered with

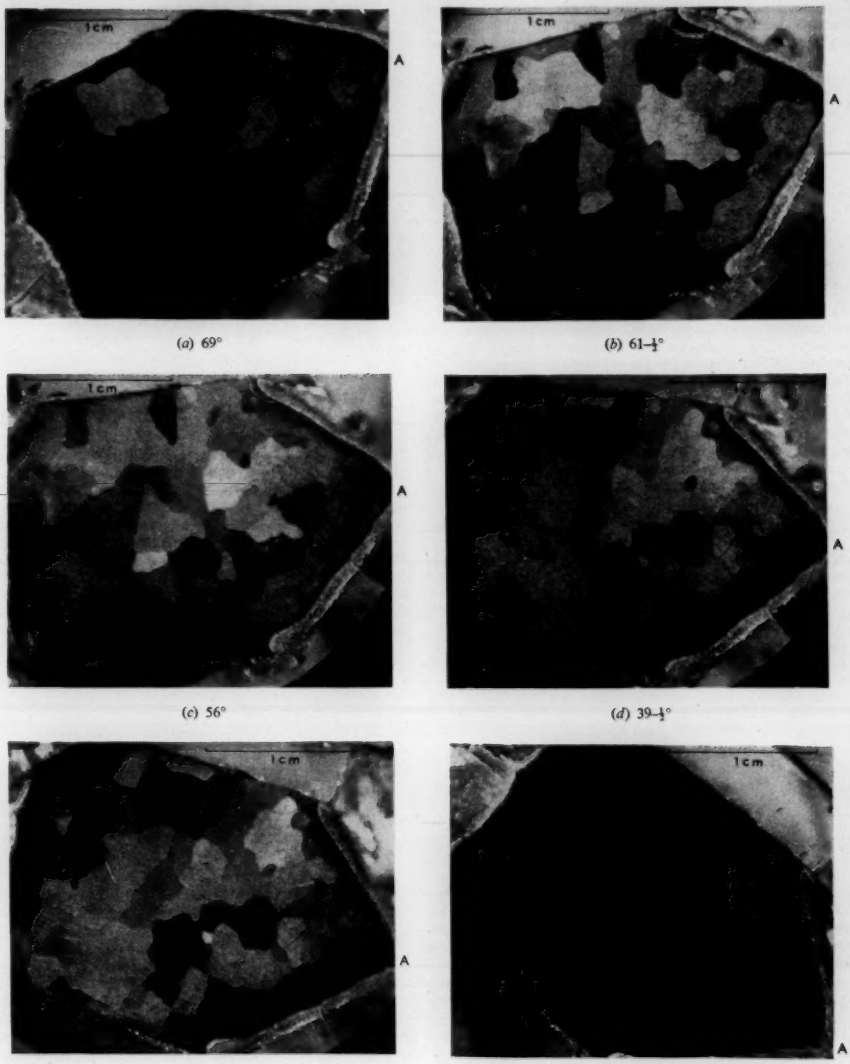

(*a*) 69° (*b*) 61–½°

(*c*) 56° (*d*) 39–½°

(*e*) 23° (*f*) 2°

Fig. 4. The photographs show the appearance of a typical etched specimen of cold-rolled silicon-iron when viewed in polarized light. The photographs were taken with the rolling direction at various angles with the plane of polarization of the analyser

etched furrows and light incident normally on the specimen returns after a two-fold oblique reflexion [that is, the grains belong to group (*b*)] as shown in Fig. 3(*b*).

Light reflected from group (*b*) grains is of minimum intensity whenever the [100] axis defining the ridge of each furrow is parallel to the plane of polarization either of the analyser or of the polarizer. Maximum intensity occurs when the [100] axis is at 45° to the polarization planes. Thus, when either of the sections of the specimen parallel to the rolling direction are observed in polarized light, the grains go through four maxima and four minima in one complete rotation of the specimen. The positions of the minima give the spread in angle between the [100] axes of the various grains and the rolling direction of the sheet, thus affording a useful and quick method for observing the degree of preferred orientation. In some cases the preferred orientation is so pronounced that (owing to the breadth of the maxima and minima) perhaps 90% of the area viewed appears bright (or dark) at the same angular position of the specimen.

An average sample of cold-rolled silicon iron sheet is shown in Fig. 4 (*a* – *f*). The etched surface, whose appearance is shown in polarized light, is the one marked (ii) in Fig. 1. The rolling direction is parallel to the longer edge of the specimen. The individual crystals vary in brightness as the specimen is rotated to successive positions as shown by the six photographs in Fig. 4. For each photograph the angular position of the rolling direction with respect to the plane of polarization of the analyser is given. A fair degree of preferred orientation is apparent, since a majority of the crystals become bright and dark in synchronism and belong to group (*b*), having orientation [100], (110). A few small crystals may be seen which are always dark (one is near the point *A* of the specimen) and these have a (100) plane nearly in the plane of the sheet. The background on which the specimen is mounted may be seen to remain constant in brightness for all the pictures. Any change in brightness of individual crystals is due solely to the position of the specimen with respect to the polarizer and analyser.

After the completion of the work herein described the attention of the author was drawn to a paper by Weerts,[4] who makes use of the elliptical polarization produced by oblique reflexion of plane polarized light in order to set a crystal face accurately normal to the incident light in a goniometer. No mention is made of multiple reflexions, but his work depends upon the same principles.

ACKNOWLEDGEMENTS

It is a pleasure to record my indebtedness to Mr. J. E. Stanworth and to my colleagues who have helped with discussions and advice. I also wish to thank Mr. L. J. Davies, Director of Research, British Thomson-Houston Co. Ltd., for permission to publish this paper.

REFERENCES

(1) BARRETT and LEVENSON. *Trans Amer. Inst. Min. Metall. Engrs*, **137**, p. 76 (1940).
(2) STRATTON. *Electromagnetic Theory*, Section 9.9 (New York: McGraw Hill Book Co. Inc., 1941).
(3) JONES. *Phil. Mag.*, **48**, p. 207 (1924).
(4) WEERTS. *Z. techn. Phys.*, **9**, p. 126 (1928).

The viscosity of suspensions of rigid spheres

By R. ROSCOE, Ph.D., A.Inst.P., Physics Department, King's College, Newcastle-upon-Tyne

[*Paper received* 7 *January*, 1952]

An explanation is given of the dependence of the relative viscosity on the size distribution of the suspended spheres, an effect recently observed by Ward and Whitmore.(1) It is shown theoretically that if the spheres are of very diverse sizes, the relative viscosity is $(1 - c)^{-2.5}$ for all values of the volume concentration c. For spheres of equal size, the validity of the Einstein expression for the relative viscosity $(1 + 2{\cdot}5c)$ is restricted to concentrations well below $c = 0{\cdot}05$; while for medium and high concentrations the relative viscosity is given by the theoretical expression $(1 - 1{\cdot}35c)^{-2{\cdot}5}$. The use of the latter formula in interpreting measurements on the viscosity of solutions is briefly indicated.

An important series of observations on the relative viscosity of suspensions of smooth rigid spheres has recently been published by Ward and Whitmore.(1) These writers found that while the relative viscosity is independent of the viscosity of the suspending liquid and the absolute size of the spheres at a given concentration, it is a function of their size distribution, decreasing with increasing size range to a constant value. They also concluded that, at very high dilution, the slope of the relative viscosity/volume concentration curve approaches a value which varies from 4·0 for spheres with a 1 : 1 size ratio to 1·9 for size ratios of over 3 : 1. It was further noted that inconsistent results are obtainable with suspensions in non-polar liquids, since these suspensions are thixotropic; thus only results obtained with polar suspending liquids should be compared with the results of ordinary hydrodynamic theory.

The two main conclusions are surprising, for it has been shown by Einstein(2) that for extreme dilution, the relative viscosity (η_r) should be connected with the volume concentration of the spheres (c) by the relation

$$\eta_r = 1 + 2{\cdot}5c \qquad (1)$$

This formula follows directly from the well-established principles of hydrodynamics and is valid at extreme dilution irrespective of the size distribution of the spheres, so that the slope of the $\eta_r - c$ curve at extreme dilution should be 2·5 in all cases; while Ward and Whitmore give values for this quantity ranging from 4·0 to 1·9 according to the size distribution. It must be pointed out, however, that the latter figures were obtained by a rather questionable extrapolation to the limiting cases of complete equality and great diversity of sizes respectively, the extreme size ratios actually used being 1·17 : 1 and 2·74 : 1. Assuming that the $\eta_r - c$ curve is sensibly linear up to the lowest concentration used ($c = 0{\cdot}05$), Ward and Whitmore's results give the slope at extreme dilution as 3·6 and 2·1 for these two size ratios respectively. The authors estimate the accuracy of the viscosity measurements as within 2%, so that the greatest errors to be expected in the measured slopes amount to about ± 0·45. Thus, while the measured slope for the most diverse spheres used does not differ significantly from 2·5, the slope for the most uniform spheres is appreciably higher.

The primary object of the present work is to give an

explanation of the dependence of η_r upon the size distribution; and to show theoretically that, in the case of spheres of nearly uniform size, the validity of the Einstein relation is restricted to concentrations well below $c = 0{\cdot}05$, so that there is actually no conflict between theory and observation.

SPHERES OF VERY DIVERSE SIZES

Consider a suspension containing a small volume concentration c_1 of spheres of very small size into which is placed a small concentration c_2 of spheres of much larger size, and into this again a small concentration c_3 of spheres of yet larger size, and so on up to n sets of spheres, and let the total concentration be c. Then on adding another set of spheres of concentration c_{n+1}, the new total concentration is $c(1 - c_{n+1}) + c_{n+1}$, so the increase in concentration is $dc = c_{n+1}(1 - c)$. Now as all the other spheres are much smaller than the new set, the original suspension can be regarded as a homogeneous liquid in its flow round the new spheres, and as the volume concentration of the latter is small, the ratio of the viscosity of the new suspension to that of the original is approximately $1 + 2{\cdot}5c_{n+1}$ by equation (1). Thus

$$\eta + d\eta = \eta(1 + 2{\cdot}5c_{n+1})$$

whence

$$d\eta/dc = 2{\cdot}5\eta/(1 - c)$$

For a given finite concentration c, the diversity of sizes can be increased by increasing the number of sets of spheres and reducing the concentration of spheres in each set, with a consequent increase in accuracy for the above equation which thus becomes strictly valid in the limiting case of extreme diversity. Integration of this equation gives $\eta = \eta_0(1 - c)^{-2{\cdot}5}$, the constant η_0 being the viscosity of the suspending liquid, so that

$$\eta_r = (1 - c)^{-2{\cdot}5} \qquad (2)$$

This relation is valid for all concentrations, and reduces to equation (1) at great dilution. It is shown as curve *B* in Fig. 1 for comparison with the observations made by Eilers[3] on a suspension of spheres having a wide range of sizes, 25% by volume of his spheres having diameters below $3{\cdot}4\,\mu$ and 25% above $6{\cdot}0\,\mu$. The observations lie somewhat above the curve at the higher concentrations. The most diverse size distribution used by Ward and Whitmore (the 2·74 : 1 size ratio) had 25% by volume of the spheres with diameters lying below $150\,\mu$ and 25% above $190\,\mu$, and being less diverse than that used by Eilers gives higher values of η_r. The remainder of Ward and Whitmore's results show a progressive increase in η_r with increasing uniformity of size up to the most uniform set of spheres used (the 1·17 : 1 size ratio) for which the results are also plotted in Fig. 1.

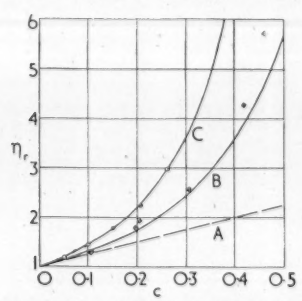

Fig. 1. Relative viscosity of suspensions of spheres

A, Einstein relation, equation (1); *B*, curve for spheres of very diverse sizes from equation (2); *C*, curve for spheres of equal size from equation (3). ◇ = spheres of diverse sizes (Eilers). ○ = spheres of 1·17 : 1 size ratio (Ward and Whitmore).

SPHERES OF EQUAL SIZE: HIGH CONCENTRATIONS

In order to extend the range of validity of equation (1), several attempts have been made to estimate the effect of the interaction of spheres at close range which is neglected in Einstein's treatment. These give additional terms on the right-hand side of equation (1) proportional to the square and higher powers of c, but there is little agreement between the magnitude of the terms so obtained by different writers. An important advance along this line of approach was made by Vand[4] who pointed out the importance of collisions between the spheres, and found that an appreciable number of temporary "collision doublets" or pairs of spheres in actual contact should be present even in quite dilute suspensions when undergoing shear. A certain amount of liquid is effectively frozen between the two spheres composing each doublet and this increases the effective concentration of the suspension, the resulting increase in the calculated value of η_r being comparable with the increase obtained by taking into account the close range interaction of spheres not in actual contact. Although Vand did not extend his calculations to the region of high concentrations, he noted that as the concentration is increased, appreciable numbers of temporary "triplets" and aggregates of higher order should be formed, until, at high concentrations, nearly all the spheres are combined in large closely packed aggregates of varying size and roughly spherical form. So at high concentrations, the liquid "frozen" in these aggregates increases the effective concentration by a factor of $3\sqrt{2}/\pi$ or 1·350.

Thus it follows from Vand's argument that a suspension containing a high concentration c of uniform spheres can be treated as a suspension of spheres of very diverse sizes and concentration $1{\cdot}35c$, so that η_r is given at once by equation (2) as

$$\eta_r = (1 - 1{\cdot}35c)^{-2{\cdot}5} \qquad (3)$$

The fact that the aggregates are not strictly spherical should not appreciably affect the validity of this formula, for it is clear from the calculations of Burgers[5] that small amounts of ellipticity in the suspended particles do not sensibly alter the factor 2·5 occurring in equation (1) which is used in the derivation of equation (2), so that the latter is valid for slightly elliptic particles of very diverse sizes. Values for η_r calculated from equation (3) are shown as curve *C* in Fig. 1 for comparison with Ward and Whitmore's results for spheres having a 1·17 : 1 size ratio.

It is to be noted that for a suspension of spheres of equal size equation (3) gives η_r rising to infinity at $c = 0{\cdot}740$, the concentration at which the suspension becomes closely packed and rigid. On the other hand, for spheres of very diverse sizes equation (2) gives η_r rising to infinity only at $c = 1$, since in this limiting case the whole of the space occupied by a suspension may be filled with spheres and rigidity is only attained at 100% concentration. For intermediate cases, the suspension becomes rigid at values of c between 0·740 and 1. This provides a simple qualitative explanation of the decrease

of η_r with increasing diversity of size observed at high concentrations.

SPHERES OF EQUAL SIZE: LOW CONCENTRATIONS

It remains to explain theoretically why the Einstein relation is not valid for suspensions of spheres of nearly equal size at the lowest concentrations for which observations have been made: a fact well illustrated by the results for the 1·17 : 1 size ratio spheres plotted in Fig. 1, which lie close to the theoretical high concentration curve over the whole range and do not fall near to the Einstein line at low concentrations.

In discussing the process of shear for very dilute suspensions of spheres of equal size, Vand concluded that each sphere spends a fraction $4c$ of its time in contact with other spheres, that is to say combined in temporary "collision doublets," and he considered that each doublet behaves as a solid bounded by two hemispherical caps joined by a cylindrical surface of length $2a$, all of the same radius a as the constituent spheres. He then treated this solid as if it were a prolate spheroid of the same volume $\pi a^3 10/3$ and axial ratio 2 : 1. The details of his work may be criticized in that he estimates the average time spent in a collision on the tacit assumption that angular momentum is conserved on impact, whereas in fact momentum considerations are irrelevant in cases of slow motion in a viscous fluid. A more correct treatment takes the two spheres together with the "frozen" liquid as forming a rigid body which rotates with approximately the same angular velocity as a single sphere, that is to say with an angular velocity equal to half the rate of shear. A calculation on these lines, however, leads to the same value $4c$ for the fraction of its time spent by each sphere as a member of a doublet. On the other hand, it appears that Vand considerably underestimates the volume of "frozen liquid" carried by each doublet. In the case of those doublets which contribute most in their effect upon the viscosity, the maximum stress concentration occurs at points near to the most distant points on the two spheres; so the mechanical influence of a doublet can best be simulated by that of a prolate spheroid which fits the spheres closely at their extreme points. Such a spheroid has a major semi-axis of length $2a$ and a minimum radius of curvature a, and hence has a volume of $\pi a^3 16/3$ (or twice the volume of the spheres together) and an axial ratio of $\sqrt{2} : 1$. Now according to Burgers' calculations, a spheroid of this axial ratio behaves very nearly as a sphere of the same volume, so that the "frozen liquid" effectively doubles the volume of those spheres which are in temporary contact, thus increasing the effective concentration from c to $c + 4c^2$. At $c = 0{\cdot}05$, for instance, the effective concentration is 0·06, while at $c = 0{\cdot}075$ it is 0·0975.

Although the above estimation is based on rather crude approximations and neglects the formation of triplets and higher aggregates, it serves to show that even when c is as low as 0·05 the effective concentration is appreciably greater than the actual, and is rapidly rising towards the value $1{\cdot}35c$ obtained for high concentrations. Thus the lowest concentration used so far in experimental work is well above the region of validity of the Einstein formula and the slope of the $\eta_r - c$ curve at this concentration does not correspond to the slope at extreme dilution. It is also apparent that with rising concentration the number of doublets, triplets and higher aggregates rapidly increases, so that the suspension very soon behaves as one of spheres of very diverse sizes and concentration $1{\cdot}35c$; and this explains why the observations agree with equation (3) for medium as well as high concentrations.

APPLICATION OF THE RESULTS

The theory developed in the preceding sections may prove useful for the interpretation of observations on the viscosity of solutions and suspensions. The measurements of η_r for aqueous solutions of dextrose made by Powell[6] may be briefly considered as an example. In Fig. 2 the values of η_r

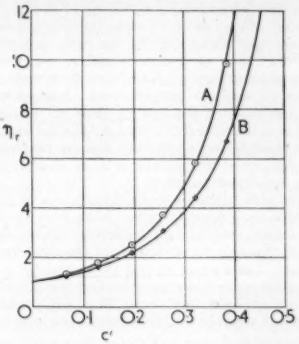

Fig. 2. Relative viscosity of aqueous solutions of dextrose

A, curve calculated from equation (3) with $c = 1{\cdot}16c'$; *B*, curve calculated from equation (3) with $c = 1{\cdot}03c'$. Powell's observations: ○ = 25° C; ◇ = 50° C.

obtained at the extreme temperatures used are plotted against c', the volume of solid dextrose dissolved in unit volume of the solution. These results are fitted closely by equation (3) if it is arbitrarily assumed that $c = 1{\cdot}16c'$ at 25° C and $1{\cdot}03c'$ at 50° C. Thus the dextrose molecules behave in solution as if they were spheres whose volumes are 1·16 and 1·03 times the volume they occupy in the solid state at 25° C and 50° C respectively. The measurements made on aqueous solutions of sucrose by Bingham and Jackson[7] can be treated in the same way, but it is found here that the ratio of the effective volume in solution to the volume in the solid state varies slightly with the concentration. Thus at 0° C it rises from 1·53 at $c' = 0{\cdot}126$ to 1·68 at $c' = 0{\cdot}378$, and at 85° C it rises from 1·06 at $c' = 0{\cdot}126$ to 1·28 at $c' = 0{\cdot}378$; but it is interesting to note that these ratios, like those for dextrose, are much nearer unity than the corresponding figures deduced from the semi-empirical formula used by Bredée and de Booys.[8]

REFERENCES

(1) Ward, S. G., and Whitmore, R. L. *Brit. J. Appl. Phys.*, **1**, p. 286 (1950).
(2) Einstein, A. *Ann. Phys., Lpz.*, **19**, p. 289 (1906); **34**, p. 591 (1911).
(3) Eilers, H. *Kolloid Z.*, **97**, p. 313 (1941).
(4) Vand, V. *J. Phys. Coll. Chem.*, **52**, p. 277 (1948).
(5) Burgers, J. M. *Second Report on Viscosity and Plasticity*, p. 145 (Amsterdam: N. V. Noord-Hollandsche Uitgeversmaatschappij, 1938).
(6) Powell, C. W. R. *J. Chem. Soc.*, **105**, p. 1 (1914).
(7) Bingham, E. C., and Jackson, R. F. *Bull. Bur. Stand., Wash.*, **14**, p. 59 (1918–19).
(8) Bredée, H. L., and de Booys, J. *Kolloid Z.*, **91**, p. 39 (1940).

New books

Heat and thermodynamics. 3rd Edn. By MARK W. ZEMANSKY. (London: McGraw-Hill Publishing Co.) Pp. xiv + 465. Price 42*s*. 6*d*.

The 20% increase in number of pages as compared with the first edition represents not only several major additions, but also a very painstaking programme of detailed improvements mainly concerned with a more rigorous presentation of certain important topics such as the basic concept of temperature, the laws of thermodynamics, etc. The most prominent new feature is a full and well-illustrated chapter on the physics of very low temperatures. A good account is given of the work of the last 15 years on helium. Heat transfer is now the subject of a separate chapter incorporating some new material on convection and on heat-exchangers. A useful feature of this edition is a set of answers to the numerous well-chosen problems.

In certain parts of the book one is conscious of the absence of references to original papers. Also, it is surprising to find the author retaining the somewhat confusing title of "centigrade thermodynamic scale" for the ideal gas scale of temperature. There seems no end to the changes in thermodynamic symbols: in this edition we find that the Helmholtz function has changed from F to A at the moment when British learned societies are recommending a reversion from A to F!

Such minor matters, however, do not alter the fact that the new edition is a substantial improvement on the original strikingly lucid and well-written book. Starting at a level suitable for the student in the first year of his honours course it takes him by easy stages to the degree standard and is a book to which he will constantly turn in later life.

K. A. MACFADYEN

Careers in physics. By A. W. SMITH. (Columbus: Long's College Book Company.) Pp. 271. Price $4.00.

In this book the Emeritus Professor of Physics of the Ohio State University attempts "to outline briefly the meaning and scope of modern physics, to indicate some of the professional activities in which physicists engage, and to give high school and college students and teachers of physics a better understanding of physics as a profession." He writes, of course, for American readers; but some sections are, or should be, equally applicable in other countries. Perusal of the book will give a good idea of the scope of physics, although some chapters read more like a college syllabus and will require a knowledge of physics to understand them. The sections on professional and ethical standards are rather dogmatic and seem to me to be politically biased. Most parents and prospective physicists would expect to find some figures indicating approximate commencing salaries and the normal order of ceiling salary that might reasonably be expected in different branches of the profession. This information would, I suggest, be more helpful than such statements as (p. 51): "Indeed some apprehension about future financial needs for one's self or his family may be a stimulus to increased effort and better work" or (p. 25): "Physical comforts, satisfactions and conveniences must be pushed aside by those who would learn about the ways of nature."

Readers may well get the impression from this book that, in general, physicists are only engaged in research and teaching. I am not in a position to say how far this is true in America, indeed, there are hints in the book that industrial physicists are otherwise occupied; they "try to apply existing physical data and principles to current industrial problems" (p. 73), and therefore the remarks about rewards quoted above may not apply to them. In this country only about one-third, or less, of the qualified physicists are really engaged in "extending the boundaries of knowledge." Far more are engaged in applying existing knowledge to production and development problems and to improving, testing and calibrating instruments in industry or in Government service and quite a few are full-time teachers. While the majority of them no doubt find satisfaction in their work, as they would in any other profession, it must be admitted that, with some exceptions, they do so primarily in order to support themselves and their families. In fact, they have often chosen their posts because of the pleasant conditions, the security of tenure and reasonable prospects they offer.

There is an amusing misprint on p. 205 where it is stated that "The first type of x-ray tube was gall filled"!

The book will form a useful addition to a college library, but cannot be recommended to individuals seeking information about prospects for physicists in *this* country.

H. R. LANG

Engineering metrology. By K. J. HUME, B.Sc., A.M.I.Mech.E., M.I.Prod.E. (London: Macdonald and Co. (Publishers) Ltd.) Pp. xvii + 293. Price 18*s*.

Precise measurement as a branch of engineering is of recent growth, though for generations most nations have had a standard of length and mass. Not until the beginning of the twentieth century did Whitworth and Johannson first attempt to bring precise measurement and, in its train, interchangeability into the engineering workshop. Mr. Hume spent a number of years at the National Physical Laboratory where, during the First World War under the stimulus of Sears, Rolt and Eden, the science of measurement rapidly advanced. Rolt's book *Gauges and fine measurements*, published in 1929, remains the standard work on this subject.

In the inter-war years Engineering Metrology was introduced as a subject for the Higher National Certificates in Mechanical and Production Engineering, and recently a School of Engineering Metrology has been set up at the Manchester College of Technology. Towards the end of the recent war many Technical Colleges were equipped with certain basic measuring devices, not only for instructional purposes but with a view to extending the testing facilities of the country, and these were "approved" by the National Physical Laboratory as suitable for the examination of certain types of gauge. This scheme gave rise at once to a requirement for the teaching of metrology on a wider scale than heretofore, and it is this need which Mr. Hume's book so admirably fills.

The book commences by teaching the essential mathematics of the subject but no more, and where it becomes necessary to refer, for example, to the wavelength of light as a unit of length a section is introduced explaining the phenomenon of interference. The whole book is well balanced as between theory and practice. It is essentially a practical book, giving to the student that measure of theory which he requires, saving him from recourse to text-books on either mathematics or physics though, should he desire to explore any avenue more fully, an excellent bibliography has been provided. There are some discrepancies in the book but none are serious. Some of the diagrams are cramped and for this reason sometimes confusing.

In the past 25 years many instruments have been evolved to measure and compare length, angles, forms of screw threads,

etc. The author has avoided the pitfall of an attempt to describe all of these, but has only directed the attention of the reader to the original models, the most essential and the more commonly used. Precision production of engineering components is to-day of great importance in the national economy. It is not merely that the component parts of weapons, wherever they may be produced, must be readily assembled, but that a tractor or mine excavator rendered useless through the breakage of a component may be put back into service with the minimum delay through dispatch of a spare by air freight. The replacement component must be truly interchangeable since skilled fitters do not exist in remote parts of the world, and if these markets are to be captured and held, so must components be machined and held to fine tolerances. To this end the teaching and practice of engineering metrology is essential. G. A. WHIPPLE

Textbook of physics, Vol. 2. Heat. By Dr. R. C. BROWN. (London: Longmans, Green and Co. Ltd.) Pp. ix + 270 + viii. Price 13*s*. 6*d*.

This book forms the second volume of Dr. Brown's Textbook of physics for Intermediate students. The author covers the usual syllabus work, with some differences in emphasis which reflect the outlook of a university teacher who very properly insists on a thorough understanding of elementary principles. Fundamental ideas are explained very carefully and in detail, with numerous examples; and the experiments described are chiefly those which a student would be expected to meet himself during his course.

The book is intended for both Intermediate students and Advanced Level General Certificate candidates, and can be thoroughly recommended for work up to these standards. Scholarship candidates would need a little more than it contains, but could use it very profitably for their main source of fundamental groundwork. G. R. NOAKES

Radio astronomy. By B. LOVELL and J. A. CLEGG. (London: Chapman and Hall Ltd.) Pp. 238. Price 16*s*.

Astronomy is one of the oldest sciences, and throughout the centuries spectacular advances have been made from time to time as a result of new observing techniques. The telescope increased the number of observable stars from the few thousand seen with the naked eye to many millions. Astrophysics owes its remarkable discoveries mainly to the spectrograph. In recent years, the application of radio and radar techniques is producing advances of similar magnitude. Radio astronomy was born in 1931, when Jansky detected radio waves from space, but the new science has progressed rapidly only since 1945 when it became possible to apply the more refined radio methods developed during the war. Since then the achievements of radio astronomy have been impressive. For example, the number of known meteor showers has almost been doubled by radio observations, and new radio "stars," which cannot be perceived by conventional astronomical methods, have been discovered. British scientists have played a prominent part in this work and it is appropriate that two of them should write an up-to-date and authoritative book on the subject.

The book opens with two chapters on classical astronomy, followed by two chapters on electromagnetic waves and radio techniques. These introductory chapters provide a useful background for the reader who has no specialized knowledge of radio or astronomy. The remainder of the book discusses comets and meteors; the measurement of meteor velocities; radio waves from the sun and from the galaxy; and radio investigations of the aurora, the moon and the planets. A useful feature is that, in addition to references to important original papers, a bibliography of a more general type is appended to each chapter to indicate where the reader can find more detailed accounts of the subject-matter. The book is well illustrated; the diagrams are clear and helpful but some of the half-tone plates of aerial systems could have been better reproduced as line sketches.

On the whole, the subject is carefully expounded and any reader with some general scientific knowledge should have no difficulty in following the text, and should derive considerable enjoyment from this fascinating story.

J. S. FORREST

A bibliographical survey of flow through orifices and parallel-throated nozzles. By T. H. REDDING, A.M.I.Mech.E., A.F.R.Ae.S. (London: Chapman and Hall Ltd.) Pp. 196. Price 32*s*. 6*d*.

This collection into a single book of over 600 references to orifices and nozzles will prove invaluable to all who are engaged on research into these devices. All those whose interest is mainly fundamental, industrial or historical will readily find appropriate material. Extensive cross-references are given. The book does not set out to be a code of practice and no formulae are included which could be used for design purposes.

The demand for a book of this type dealing with such a narrow field of knowledge will presumably be very limited and in view of the author's great ability in the collection and classification of data, one hopes that he will be encouraged to extend his activities to wider fields. The term -1 has been omitted from the exponent in equation (2), p. 5.

M. P. NEWBY

An introduction to electronic circuits. By R. FEINBERG, Dr.-Ing., M.Sc. (London: Longmans, Green and Co. Ltd.) Pp. xiv + 163. Price 18*s*.

Intended primarily as an introductory course in electronics for undergraduates, this book will also interest those who have a practical knowledge of electronics and wish to put that knowledge on a sounder theoretical basis.

In the earlier chapters the basic principles of the operation of thermionic valves, cathode-ray tubes and magnetrons are discussed fully. This is followed by a description of valve amplification at audio and radio frequencies, and the effects of feedback and non-linearity. Further chapters are devoted to valve oscillators, gas-filled valves and other specialized types of valve. Each chapter contains several suggested experiments, and concludes with a selection of numerical examples and references. Most of the references are to more advanced work on subjects mentioned in the text, the student is not referred to any other introductory books or articles on electronics.

The treatment is largely mathematical, but the standard required is unlikely to worry the average student. An exception is the use of the "a.c.-vector" method, which is as confusing as ever, especially to those having any experience of vector methods in other subjects.

The book is a welcome addition to the range of introductory literature on electronics, and can be recommended for its accuracy, clarity and style. R. C. HART

The gyroscope through the ages. (Brentford: The Sperry Gyroscope Co. Ltd.). Pp. 44. Gratis.

This illustrated booklet has been issued to mark the centenary of Foucault's demonstration of the gyroscope as we know it to-day. The development of its general applications to stability and navigations of ships and aircraft are briefly traced and its uses in peace and war are outlined.

Notes and comments

The Institute of Physics

At the Annual General Meeting of The Institute of Physics held on 5 June, 1952, Dr. C. Sykes (Managing Director, Thos. Firth and John Brown Ltd., Sheffield) was elected President. Mr. O. W. Humphreys and Dr. T. L. Ibbs were elected Vice-Presidents and Dr. S. Whitehead was elected Honorary Treasurer. Dr. B. P. Dudding was re-elected Honorary Secretary. The four new ordinary members of the Board elected were Mr. H. Barrell, Dr. N. A. de Bruyne, Dr. W. H. Taylor and Mr. R. G. Wood. Sir Owen W. Richardson was elected to Honorary Fellowship, the highest honour which the Institute can bestow. Sir Owen was Professor of Physics at King's College, London, for many years and is known for his distinguished fundamental work on thermionics. In 1928 he was awarded the Nobel Prize for physics.

The Board's Report for 1951, which was adopted at the meeting, shows that 524 applications for membership or transfer to higher grades were considered during the year compared with 627 the previous year. The Board modified the interpretation of the regulations governing election to Associateship so as to permit the admission of candidates whose training in physics is adequate but who may have graduated in subjects other than physics. Nine technical colleges which had applied for recognition or for an extension of recognition by the Institute were inspected during the year. The system of inspection and recognition which has been established in recent years has already resulted in substantial improvements in the facilities offered by the colleges for teaching physics.

An important development recorded was the issue of regulation and syllabuses for the Institute's new Graduateship examination which is to be held for the first time in 1952. The number of candidates for National Certificates in Applied Physics showed a substantial increase compared with the previous year; twelve colleges entered candidates at the ordinary level and five at the higher stage. The Report mentions the several other educational activities of the Institute.

In 1949 the Board of the Institute decided upon a rapid development in the amount of its publications and while the Report shows that this has been largely implemented it states that these developments have been hampered by the substantial rise in the cost of printing and of paper. The Institute now publishes two Journals, monthly, the *Journal of Scientific Instruments*, and this *Journal*, besides a monthly *Bulletin* which also contains a list of vacancies and the circulation of which is restricted to members. In addition, two further monographs were added in 1951 to its "Physics in Industry" series. The Report announces that the Institute is to sponsor a series of small books suitable for university students and those studying for Higher National Certificates in Applied Physics, each of which will cover some branch of applied physics and be written by an authority in that field. Some further books were published for the Institute by Messrs. Edward Arnold and Co.

The "Report on the second Survey of Salaries and Emoluments paid to Fellows and Associates resident in Great Britain and Northern Ireland" was published in the *Bulletin* during the year under review and again proved of great value to members and others. Among other professional matters dealt with by the Board were contracts of service, the Ministry of Labour's report on the supply and demand for physicists, and scientists' rights of travel.

The Institute's fifteen local Branches and specialist subject Groups held over one hundred meetings in addition to some short conferences on branches of applied physics. An innovation was the exhibition of scientific instruments and apparatus arranged by the Australian Branch in Melbourne which was visited by some 4 000 persons during the four days it was open.

Elections to The Institute of Physics

The following elections have been made by the Board of The Institute of Physics:

Fellows: A. D. Booth, T. W. F. Brown, K. Deutsch, R. Meredith, H. S. Peiser, J. Savage.

Associates: F. Bovey, W. S. Brown, P. L. Degen, A. Fonda, N. F. Godwin, S. Guest, J. P. Morrison, R. G. Rhodes, N. Sheppard, E. D. Thomas, C. E. Williams.

Twenty-four Graduates, six Students and three Subscribers were also elected.

Journal of Scientific Instruments

Contents of the August issue

ORIGINAL CONTRIBUTIONS

A high speed transient recorder. By D. R. Hardy.
A radiation monitor for demonstration purposes. By K. E. G. Perry and F. S. Goulding.
A simple automatic gas flow-limiting valve. By F. Call.
A high temperature sintering furnace. By J. H. Rendall.
A device for marking event positions on the surface of nuclear emulsions. By E. W. Titterton and W. Barneveld.
An automatic thermal analyses recorder. By R. L. Cunningham, H. M. Weld and W. P. Campbell.
A four channel dynamic strain-recorder. By C. H. G. Mills and J. R. Bristow.
A simple method of determining orientation in recrystallized wires of the cubic system. By T. S. Hutchison.
The high temperature Pirani gauge. By J. H. Leck.
A simple furnace temperature controller. By M. Shepherdson.

LABORATORY AND WORKSHOP NOTES

An automatic solenoid operated switch for extending the range of electronic recorders. By T. L. Webb.
A laboratory timer for intermittent operations. By R. S. Young, R. Snaddon and V. A. Tullett.
A flexible vacuum joint. By J. H. Fremlin.
A charging device for pocket electrometers. By W. H. Sutherland and R. G. Wood.
A simple method of determining the azimuthal orientation of single crystals with the Weissenberg goniometer. By D. S. Beard.

CORRESPONDENCE

Ho coefficient—correction and comment. From J. Pollard; D. Latham.
A simple conversion of an X-ray dose-rate meter into an integrating dose-meter. From C. L. Smith.
Modified Hilsch apparatus for producing hot and cold air streams. From J. Bertin.
A single-relay scale of two counting unit. From B. D. Corbett.

NEW BOOKS

MANUFACTURERS' PUBLICATIONS

NOTES AND COMMENTS

THIS JOURNAL is produced monthly by The Institute of Physics, in London. It deals with all branches of applied physics (including theory and technique).

All rights reserved. Responsibility for the statements contained herein attaches only to the writers.

EDITORIAL MATTER. Communications concerning editorial matter should be addressed to the Editor, The Institute of Physics, 47 Belgrave Square, London, S.W.1. (*Telephone:* Sloane 9806.) Prospective authors are invited to prepare their scripts in accordance with the *Notes on the Preparation of Contributions*. (Price 2*s.* 6*d.* including postage.)

REPRODUCTION. The Institute of Physics is a signatory to The Royal Society's Fair Copying Declaration. Details may be obtained upon application from The Royal Society, London, W.1.

ADVERTISEMENTS. Communications concerning advertisements should be addressed to the agents, Messrs. Walter Judd Ltd., 47 Gresham Street, London, E.C.2. (*Telephone:* Monarch 7644.)

SUBSCRIPTION RATES. A new volume commences each January, and annual subscriptions will only be accepted for complete volumes of the monthly parts (January–December). The charge is £4 per volume ($11.50 U.S.A.), including index (post paid), payable in advance. Single parts, so far as available, may be purchased at 8*s.* each ($1.15 U.S.A.), post paid, cash with order. Orders should be sent to The Institute of Physics, 47 Belgrave Square, London, S.W.1, or to any Bookseller.

Summarized proceedings of the fourth industrial physics conference —Glasgow, June 1952

The fourth industrial physics conference on "Physics in the transport, shipbuilding and engineering industries" was held in the Royal Technical College, Glasgow, from 24 to 28 June, 1952. The programme consisted of seven papers, a discussion and a public discourse which are summarized in this report. An exhibition of instruments, apparatus and books cognate to the subjects of the conference was also held in the college.

The conference, which was attended by close on 400 people, was formally opened by LORD BILSLAND (President, the Scottish Council) who referred to the key position held by the physicist in engineering and called for closer co-operation between science and industry.

METALLURGY

The first paper, presented by SIR ANDREW MCCANCE (Colvilles Ltd.), was a survey of "Physics in the service of metallurgy." The transformation of metallurgy from a craft to an observational science was briefly traced, with particular reference to the introduction of the microscope by Sorby, the hypothesis of the allotropy of iron advanced by Osmond and the platinum-rhodium thermocouple. SIR ANDREW then discussed the more recent contributions of the physicist to the development of the science and practice of metallurgy dealing, in particular, with the fields of pyrometry, spectrographic analysis, the application of X-rays and γ-radiography and the detection of flaws.

Pyrometers utilizing the intensity of radiation are being applied in the automatic control of furnace temperature and operation and, with the advent of pyrometric control of the reversing schedule in gas-fired furnaces, the day of the fully automatic steel-melting furnace is within sight. The introduction of radio-active tracer techniques promises still further advances in automatic metallurgical control.

Within a period of some 10 years, the wet chemical methods of routine metallurgical analysis have been largely replaced by physical methods, mainly spectroscopic, which enable rapid estimations of the elements in a sample to be made; their application to the analysis of non-conducting slags and refractories represents a development of real importance. Promising results are being obtained by applying the principles of the mass spectrometer to the estimation of gases and elements of low atomic weight.

The foremost and longest established use of X-rays has been for the examination of imperfections in castings and welds and particularly now that welded fabrication of cylindrical high-pressure boilers and reaction vessels has replaced hollow forging from solid ingots. In circumstances where such high-voltage X-ray equipment is cumbersome, as with steam valves and turbine casings of complicated section, γ-radiography is being increasingly employed using Tantalum^{182} and Cobalt^{60}. Other applications of X-rays are in the measurement and control of the thickness of sheets during the high-speed cold-rolling process which forms part of the continuous hot-strip mills of America.

Several methods have been developed for the detection of flaws and cracks. One of the first was the magnetic crack detector depending on the concentration of flux that takes place in a magnetized material at the edges of a small air-gap. This method is not very convenient for irregular shapes and to deal with them the use of fluorescent liquids is increasing rapidly, cracks into which such liquids have penetrated showing up as bright lines when viewed under ultra-violet light. The ultrasonic pulse technique has made considerable progress.

The lecturer finally turned to modern trends. Tremendous advances in the study of the mechanical properties of metals in the polycrystalline state have resulted from the technique of growing single crystals and from the physicist's skill in measuring the elastic constants along their crystallographic axis. Attempts to explain the discrepancies between theory and experiment have involved postulating that in all materials there are hidden flaws which are now regarded more as crystal imperfections or dislocations, but uncertainty exists as to the extent to which they influence actual physical properties. Much new information on the mechanical behaviour of metals has come from recent studies on damping, the viscous element of Maxwell's theory being replaced by a whole spectrum of damping effects which were enumerated. Damping effects arising from atomic diffusion were dealt with in some detail in order to illustrate the behaviour of carbon and nitrogen in solution in iron. A development of some significance arising from this work on damping is the possibility that the effects or orientation in a solid solution may influence the physical properties of the solvent just as profoundly as the distribution effects. Of equal significance may be the recent idea that rivalry may exist between two sites within a lattice for accommodating a single atom.

METEOROLOGY

SIR ROBERT WATSON-WATT (Sir Robert Watson-Watt and Partners Ltd.) speaking on "Meteorology in industry," indicated that his address had been designed not so much for the purpose of presenting facts but in the hope of stimulating discussion on industry's meteorological needs.

Hitherto, industry had been concerned mainly with the weather and its effects, but industrial meteorology covered a much wider field. The Meteorological Office obtains information synoptically on the physical conditions existing on and above the whole surface of the earth, collates the data and issues compact statements, for public use, on a national as well as regional scale. There is still a definite need, however, for industry itself to maintain specialists who can interpret such data for the benefit of individual industries.

It had been shown, in war, that a thorough appreciation of the fighting man's requirements was just as important as the scientist's ability to apply his knowledge. In the same way the meteorologist in industry, who must be as highly qualified as those in the state service, must first learn the needs of industry and then mould his knowledge to suit the needs if he is to make the important contributions to industrial efficiency that lie within his power. SIR ROBERT concluded with some industrial examples where the meteorologist could be employed with advantage.

The discussion was opened by SIR NELSON JOHNSON (Director, Meteorological Office). Meteorology during the

last 10 years had been mainly directed towards understanding the physical processes involved, this being clearly the initial step to an assessment of the meteorological problems facing industry. Forecasting advances had not been as great as had been hoped and it was emphasized that long-range forecasting was not round the corner. The application of electronic computing to forecasting resolved itself into a question of deciding what mathematical equations the electronic brain should be called upon to solve and the punched-card system for storage of data had been in use for years. As to the function of the state meteorological service which was itself highly specialized, as instanced by the studies on atmospheric turbulence, information and facilities available were at the disposal of industry which did not, however, make full use of them. There was undoubtedly a definite scope for meteorological research in industry, but it might well be that lack of prospects would restrict recruitment of suitably qualified personnel.

MR. R. A. WATSON (Meteorological Office, Edinburgh) was of the opinion that the Meteorological Office could satisfy the needs of industry more effectively than a private individual on account of the tremendous wealth of information available and the specialized staff it could call upon. Better service would be rendered if only industry provided the fullest information as to its requirements. Mr. M. G. BENNETT (Railway Executive), on the other hand, felt that there was a field for individual meteorological research outside the Meteorological Office which knew the facts but not the circumstances of the problems.

EDUCATION AND TRAINING

The discussion on "The education and training of industrial physicists in Scotland" was opened by DR. J. TAYLOR (Imperial Chemical Industries Ltd., Glasgow). He emphasized that this country had contributed more than its share to new scientific discoveries but had been very remiss in applying them to industry. One reason for this failure to apply basic knowledge was that the sound training in the fundamental principles now given by universities was not followed by an adequate technological education. The speaker advocated post-graduate or advanced courses in applied physics, but that due allowance should be made for different aptitudes.

PROFESSOR P. I. DEE (University of Glasgow), who followed, was of the opinion that university courses which were mainly devoted to the basic classical physics in the years leading up to and including the first post-graduate degree and were followed by concentration on the nuclear field and associated techniques for the Ph.D. degree, gave the right training for industrial research even though only certain aspects were as yet of direct use to industry. From such training would emerge a man with a sound basic knowledge of the fundamentals coupled with originality and adaptability. If university courses became too specialized only a few industries would be interested; on the other hand, if courses were designed to suit many industries, they would become too diffuse.

PROFESSOR J. S. RANKIN (The Royal Technical College, Glasgow) considered that if students were to be fitted to the wider demands of modern industry, the training provided by the universities in the fields of pure science should be complementary to a technological training at university level. The engineers and the chemical technologists were well established in industry, yet the status of physicists, as comparable with them, had still to be fully recognized even though the physicist was proving himself essential to industry. The applied physicist, he considered, supplied the missing link in scientific education for industry, bridging the gap between the laboratory and the works. He stated that the course in applied physics instituted four years ago at the Royal Technical College combined fundamental science with practical applications, these being supplemented by works experience during the summer vacation. PROFESSOR RANKIN ended with a plea that every student of adequate academic standard should be given every opportunity, if he so desired, to obtain a degree in applied physics.

All the speakers were of one mind in that a thorough training in the fundamentals was a pre-requisite, but opinions differed not only as to the need for additional training of a technological character but as to the form and time it should take. In the discussion that followed from the floor each point of view had its own supporters. One speaker, however, pointed out that only one side of the picture had been presented and the industrialist's view had not been considered. A new attitude of mind should be adopted by both sides. Another contributor referred to the training scheme established by his organization which opened up the field of management to successful candidates. There was no reason why such a process could not be applied to scientifically trained entrants. Finally, a suggestion was made that information as to the demand existing in industry for applied physicists would be of great assistance.

SOUND REPRODUCTION

"Physics and sound reproduction" was the subject of the public discourse given by Mr. D. T. N. WILLIAMSON (Ferranti Ltd.), and the outline presented clearly conveyed the dependence of the principles of sound reproduction and its development on physics. After a brief reference to systems whose objects are the clear transmission of information (e.g. the telephone) and the simultaneous reinforced reproduction of the original sound (e.g. the public address system) the lecturer turned his attention to a third and most important group whose object is to create the illusion that the original sound is being heard (e.g. the cinema, broadcasting, etc.). The means employed to achieve this object and the difficulties encountered were described and illustrated by recordings.

The various links in the chain connecting the artist to the listener serve the purpose of transforming the original acoustical wave-form into an identical electrical wave-form which, in turn, is converted to its acoustical counterpart. The purely electrical links in the chain can be made as perfect as desired, but the electro-mechanical links are in a far less advanced stage of development and it is this aspect of sound reproduction that gives rise to many of the imperfections.

MR. WILLIAMSON then discussed the various types of distortion encountered, all of which tend to destroy the illusion of hearing the original sound. In the first category were the distortions due to defects in the equipment which could be minimized by careful design and engineering. Some distortions arise from fundamental limitations to the single-channel system which is the one almost invariably used. A stereophonic or multi-channel system, which is not practicable at present on a large scale, overcomes these faults and also masks other forms of distortion. The final form of distortion lies outside the control of the engineer and listener and concerns the relation between the acoustics of the studio, on the one hand, and of the auditorium, on the other. In order to achieve an acceptable degree of realism over the wide range of conflicting conditions to be catered for, it is clear that the design of a loudspeaker for use with

a single-channel system involves considerable compromise supported by subjective listening tests. A loud speaker, designed with these factors in mind, was demonstrated.

The lecturer then turned to the storage of sounds by means of disk and tape recordings. In disk recording the links in the chain are the tracing of a replica of a sound wave-form by cutting a V-shaped groove in a smooth disk and converting, electro-mechanically, the lateral movements of a stylus tracing the groove to give the electrical counterpart of the original sound wave-form. Distortion occurs, principally, in the replay when the radii of curvature of the groove wave-form and tracing stylus become comparable and when the mass of the tracing mechanism is such as to set up, at the high accelerations experienced, high forces between stylus and groove wall which may result in record wear or damage. To overcome these effects, use is made of an elliptically shaped sapphire stylus attached to a very light metal ribbon vibrating in a magnetic field and acting as the electro-mechanical converter.

Full development of magnetic-tape recording did not occur until the advent of the thermionic valve for amplification and the application of a thin layer of magnetic material to a non-magnetic base tape. In principle, tape recording consists of passing a tape at constant speed over gaps in each of three heads which respectively perform the functions of erasing, recording and replaying. Each head carries a winding whose purpose it is to convert electrical wave-forms into corresponding variations in the magnetizing force. After outlining the limitations and advantages of tape recording, MR. WILLIAMSON concluded by stating that the present-day level of efficiency in sound reproduction owes much to advances in physics and a plea was made for multi-channel stereophonic reproduction which will remove the last barrier to the achievement of absolute realism.

NAVAL ARCHITECTURE

PROFESSOR A. M. ROBB (University of Glasgow) had designed his paper on "Some applications of physics in naval architecture" to draw attention to some of the major problems facing naval architects and in the solution of which the fundamental approach of the physicist could be of the greatest assistance.

Stability was first properly understood when Bougeur's conception of the metacentre was allied with the expression developed by Atwood which not only holds for vessels of rectangular and parabolic cross-sections, but is very nearly true for vessels of rectangular cross-section and up to the angle at which the deck enters the water. When extended, however, to deal with a ship rolling in still water and on a sinusoidal wave the equations of motion derived are generally intractable and, where solutions have been possible, they have been unreliable due mainly to inadequate knowledge of the resistance involved. Whatever the variation of resistance with velocity, however, both mathematical investigation and experience show that the nature and magnitude of the resistances to rolling motion are not of major importance. In any case a solution is needed of the seemingly simpler problem of resistance to steady motion.

While experience has enabled the power required to propel ships at normal speed to be predicted with some degree of reliability there is as yet no clear conception as to the genesis of the resistance which is overcome. Application of classical hydrodynamics does not seem to be helpful. Some progress has been made through aerodynamics where the problem of resistance is simpler since an aircraft moves only in one fluid whereas a ship moves in two fluids with a well defined motion at their surface of separation. Some light has also been thrown on the subject by Kelvin's investigation of the disturbance of fluid caused by a travelling pressure point. Evidence suggests that one minor feature of resistance can be linked with the occurrence of a double wave Kelvin pattern and a marked increase in resistance associated with the disappearance of the stern wave pattern which is also associated with separation of flow.

Alongside every body moving ahead through a fluid three types of motion are encountered. Laminar motion with low resistance occurs over the leading portion of the body and turbulent motion with increased resistance abaft, both types being confined within a thin boundary layer beyond which the motion seems to be that of an ideal fluid. This boundary layer creates a resistance due to pressure differences. If the boundary layer breaks away from the body, pressure difference and resistance increase. There is no clear conception, however, of the circumstances which bring about this separation of flow. On this subject the physicist could help by determining the conditions under which laminar flow with low resistance breaks down into turbulent flow with greatly increased resistance and by determining the circumstances for which separation of flow occurs.

TRANSPORT

Mr. M. G. BENNETT (Research Department, Railway Executive) in giving the first of the two papers on "Some applications of physics in transport" discussed some novel fields of activity outside the conventional role of physics in which the physicist, by virtue of his training, might be of still further service to transport.

There is the important problem of finding a means of adequately assessing the efficiency of industrial undertakings, and it seems that no single unit of measurement can completely define efficiency, itself a term which has a different connotation for different people. Time is an essential ingredient in assessing the adequacy of a transport system and is closely related to the nature of the services required. Some of the simpler factors might be dealt with by a unit having dimensions MLT^{-1} and having subsidiary correction factors to cater for other features, some of which, however, may well be imponderable. In the marketing of home grown food there is need for a measure which balances the advantages of the large central market against the transport effort involved. Assessment of the effects of fatigue, ease of operation, climate and noise on human efficiency requires the collaborative efforts of scientists and engineers in order to determine the easiest way of performing a job in the interest of maximum efficiency and maintenance of reserves of energy. The problem of traffic control might be tackled by analogy with fluid flow in pipes, the main difficulty being that traffic rarely reaches a steady state amenable to mathematical treatment. Despite all improvements, fog remains a most serious hazard and nuisance to transport.

Mr. T. A. EAMES, of the same organization, who followed, dealt mainly with the work done in the Physics Division of the Railway Executive Research Department which covers the more fundamental aspects, a wide range of physical measurements, instrumentation and an assortment of problems not readily classified, among which the application of mathematics and computing services to help on the theoretical side is becoming increasingly important.

Varied problems, frequently of an urgent character, call for a high degree of ingenuity, improvisation and skill in

designing and making instruments not normally obtainable and of which many must be portable and suitable for field work. Such instruments had been developed for measurement of low intensity illumination, humidities in wall cavities, electrical resistance of wooden railway sleepers where track circuiting is employed and gas flow in locomotive boilers under conditions of unsteady, pulsating flow.

Another important field of study is that of physical measurement related to subjective phenomena such as noise, colour, comfort and fatigue. There are problems which began as purely field or practical investigations of a specific nature and developed into fundamental studies. Two examples in this category are the refrigerated transport of perishable goods and the breakage of glass water level tubes in boilers.

Finally, reference was made to the mathematical attack on certain problems, usually to assist parallel experimental investigations, an example of which was the use of relaxation methods for solving problems involving variable heat flow and the stresses in engine frames and rails under load.

Dr. D. PARKINSON (Dunlop Rubber Co. Ltd.) in opening the discussion referred to the common interest of road and rail transport in such problems as friction, inertia, stability and comfort, although the lines of attack might be very different. Road transport, however, had its own particular problems many of which were related to the increased speed of road travel. The physicist was intimately concerned with the quality, tread pattern and wear of tyres, the ability to corner at speed and the absorption of high energy vibrations. Other speakers referred to the use of operational research and automatic control in rail transport problems and to the adjustment of tyre pressures to meet the conflicting demands of comfort and life of tyres. The final point discussed was the possibility of using rubber tyres or rubber covered wheels in passenger rail transport to eliminate the noise made by wheels when passing over rail joints and points.

AUTOMATIC CONTROL

The opening paper on the last day of the Conference was delivered by MR. A. J. YOUNG (Imperial Chemical Industries Ltd., London) on "Automatic control of industrial processes." Automatic methods not only achieved more consistent control than the human operator, thereby producing a saving in plant and materials, but of greater importance perhaps is that they enable skilled men to be released for other work. Automatic control makes it possible for one skilled man to supervise a large number of machines or, alternatively, to devote more time to the study of the machine or plant and its operation than to its maintenance. The important point is to decide what type of control—manual or automatic, separate or in combination—is likely to give the most economic performance.

Any control system forms a closed loop of which the machine or plant to be controlled is an integral part, the other components comprising a measuring unit, a manual or automatic controller and a regulating unit. Since the over-all performance of a system is governed by the performance of the components each should be designed to this end. In general, it is the machine or plant itself that falls short of this requirement. The characteristics required in the measuring, controlling and regulating units are reliability, sensitivity, speed of response and a suitable indication or record of measurements. The requisite reliability and sensitivity are almost invariably achieved without difficulty. Speed of response is adequate in all but the detecting element where, in many instances, it is not merely inadequate but unknown and a time lag not recognized can produce serious results.

In industrial automatic control installations, the instrumental readings and record trends of the conditions must be kept continually under review. There is an increasing tendency to concentrate such instruments in a single control room and to group them so as to facilitate supervision and, when necessary, manual control. A great deal of work on this problem is being carried out in many fields and its scope extends beyond the obvious factors and involves physiological and psychological studies.

When a controller is installed on a plant it is necessary to adjust its range of action so as to maintain steady control at the desired value irrespective of disturbances normal to the plant. By introducing into a smoothly running plant, not fitted with control, an alien disturbance of known characteristics and comparing the magnitude of the injected disturbance with that of the disturbance induced on passing through the plant, information is obtained as to the characteristics of the plant. Such an analysis, now known as the "frequency response" method, is of great value, when setting up new control installations, in predicting both the type of controller required for a given purpose and the adjustments to be made. Considerable attention is being devoted to this technique with the object of supplying data to the plant designer that will enable him to make his plant as easily controllable as possible.

NOISE AND ITS SUPPRESSION

The Conference lectures closed with a paper by MR. N. FLEMING (National Physical Laboratory) on "Noise and its suppression." As mechanization increases, noise tends to increase. Since the power wasted by a machine in producing noise is usually an insignificant fraction of that employed in useful work any incentive to reduce noise arises not from the need to conserve power, but lies in the alleviation of the psychological and physiological effects upon a person. Though noise may be physically harmful and may reduce efficiency, the most common reason for desiring its reduction is simply because it is a nuisance at work or in leisure hours. Data on the physical characteristics of noise, associated subjective effects and methods of measurement are essential preliminaries to the design of schemes for reducing noise. These factors were briefly described as well as various scales of measurement expressed in terms of sound pressure, relative loudness, subjective assessments of fractional changes in loudness or a frequency spectrum.

Reduction of sound may be sought either by suppressing it at the source or by preventing its transmission. In such tasks as riveting noise is inextricably associated with the process and reduction at its source is impracticable. Where re-design is out of the question, a local sound insulating or absorbing treatment is employed which may involve measures not only to reduce the sound directly produced but also against vibrations communicated to the structure which may appear as noise elsewhere. To reduce transmission of such vibrations, the machine must be mounted on resilient supports correctly designed in relation to the mass of the machine and the frequency of its vibration.

Insulation against air-borne sound requires enclosing the source of noise or, alternatively, the space from which noise needs to be excluded. While the principles are the same, the type of insulation may range from a complete double walled room to a simple box or even a partial enclosure. Full benefit of a sound insulation treatment is not obtained unless there is a certain degree of sound absorption in the system. The normal furnishings may sometimes suffice, but a machine shop or a quiet room in a works would each require

special absorptive measures. A high degree of insulation involves complete enclosures, doors and windows receiving special attention and, where direct ventilation is necessary, air should be led in and out through specially designed ducts split into parallel channels by sheets of sound absorbing material. A test house for an aero-jet engine provides an extreme case of the ventilation aperture problem. Partial remedial measures are often worthwhile such as confining a noisy machine to a bench surrounded by absorbent screens at sides, back and top; an absorbent hood for a telephone in noisy surroundings or general absorption treatment to the ceiling and upper walls of a machine shop. The pyschological effects of such partial measures are often greater than might be expected from the degree of reduction achieved.

If reduction of escaping noise is the primary consideration, improvements to the insulating of the external shell of the building may be necessary which, in existing buildings, may lead to major constructional alterations. Doors, windows and glass roofs are the main outlets and best results are obtained with permanently closed double windows, insulated artificial ventilation and general absorptive treatment to the roof or the provision of a heavier false ceiling at eaves height. Effective design of all such remedial measures demands a knowledge of the frequency spectrum of the noise. The degree of reduction at which to aim is one of the most difficult design problems, each case needing individual attention, and even the time of day has to be considered for the requirements are more stringent at night.

During the course of the lecture, a description was given of the special rooms available in the National Physical Laboratory and the methods used for accurate measurement of sound insulation of various types of construction and insulating materials. A mobile laboratory was also described which enables experiments to be carried out at the site of the noise.

Contributions from the floor were mainly confined to requests for information on specific problems covering the methods of measuring impact noises (e.g. hammer blows), decorative materials that are also sound absorbing, the relative merits of solid and sandwich insulation materials, the difficulties of subjective measurements and the psychological effect of induced sub-sonic vibrations of indeterminate quality.

THE EXHIBITION

An exhibition of instruments, apparatus and books cognate to the subject of the conference was held in the Royal Technical College, in which 75 firms, Government departments and Research Associations participated. Arrangements were made for non-members of the conference and senior scholars from local schools to visit the exhibition. An account of the principal exhibits is published in the current issue of the *Journal of Scientific Instruments*. A few copies of the 128-page descriptive catalogue are available from The Institute of Physics, price 1s. 3d. post paid.

VISITS AND SOCIAL FUNCTIONS

Some of the laboratories of the University and the Royal Technical College were open for inspection by parties of members from the conference and visits were also made to the Loch Sloy hydro-electric scheme, Messrs. John Brown & Co., Ltd., the Thorntonhall Laboratories of the Mechanical Engineering Research Organization, Messrs. Colvilles Ltd., Messrs. Albion Motors Ltd., and Messrs. North British Locomotive Co., Ltd.

The official Conference Luncheon, presided over by Sir Andrew McCance (Chairman of the Conference Committee), was attended by some 200 members and guests; the toast of "The Institute of Physics" was proposed by Dr. D. S. Anderson (Director of the Royal Technical College) and Dr. S. Whitehead (Vice-President of the Institute) replied. The Corporation of Glasgow gave the conference members and their guests a civic reception and dance in the beautiful City Chambers. On the last day of the conference (Saturday, 28 June) a large party enjoyed a day's steamer excursion on the River Clyde and Firth of Clyde, and a smaller party had an all-day motor coach tour to local beauty spots; others spent their time looking more closely at the exhibition.

W. RHEINALLT THOMAS

Summarized proceedings of a conference on structures of silicate minerals—London, November 1951

A Conference of the X-ray Analysis Group of The Institute of Physics was held in London on 2–3 November, 1951. The first day's discussion related to the structures of calcium silicates and the second day's to layer lattice silicates. An evening lecture was delivered on the felspars.

The first paper was given by DR. A. M. B. DOUGLAS (Department of Mineralogy and Petrology, Cambridge) on "Dicalcium silicate structures." She noted the similarity of the α and γ forms to *glaserite*[1] ($K_3Na(SO_4)_2$) and *olivine*,[2] respectively. Crystals of the α' form, *bredigite*, which is similar to βK_2SO_4, have been extracted from *spiegeleisen* slags and examined in order to investigate the structure more fully. The two structures are not identical since the a and b dimensions of bredigite are approximately twice those of βK_2SO_4, and the space group is *Pmcn* for the latter and either *Pmnn* or *P2nn* for the former; the application of Wilson's statistical methods to the analysis of the distribution of X-ray intensities indicates that *Pmnn* is more probable. Additional reflexions from some slag specimens suggest the presence of a trigonal phase, which is probably α dicalcium silicate. The structures of the α, α' and β forms can be derived from one another by rotations of some of the SiO_4 tetrahedra accompanied by slight relative shifts of the cations.

MRS. C. M. MIDGLEY (Building Research Station, Watford) gave details of the "Crystal structure of β dicalcium silicate." The space group, $P2_1/n$, and unit cell dimensions, $a_0 = 5{\cdot}48 \pm 0{\cdot}02$ Å, $b_0 = 6{\cdot}76 \pm 0{\cdot}02$ Å, $c_0 = 9{\cdot}28 \pm 0{\cdot}02$ Å, $\beta = 94° 33'$, were determined from synthetic crystals, twinned on (100) or (001). Two-dimensional electron density syntheses show that the structure is built up of isolated SiO_4 tetrahedra and calcium ions. Half of the calcium ions have six close oxygen neighbours arranged so as to leave a large gap, which is partially filled by the more distant oxygens.

The presence of holes in the structure may be important for an understanding of the special hydration properties of the mineral. The close structural similarity of the β form to the α and α' forms, which have higher symmetry, offers an explanation of the fact that the crystals are always twinned. The speaker also mentioned that *nagelschmidtite* ($7CaO \cdot P_2O_5 \cdot 2SiO_2$) has a hexagonal unit cell which is a multiple of that proposed for αCa_2SiO_4 with $a_0 = 21{\cdot}8$ kX ($4 \times 5{\cdot}45$ kX) and $c_0 = 21{\cdot}5$ kX ($3 \times 7{\cdot}18$ kX). In reply to questions by Dr. W. A. Wooster (University of Cambridge) she said that there is no information on the effect of pressure on twinning and that the crystal size was 0·5 cm.

In his paper Dr. J. W. Jeffery (Birkbeck College, London) described some "Unusual X-ray diffraction effects shown by mono- and tri-calcium silicates." *Wollastonite*, $CaSiO_3$, exists in two structurally related forms,[3,4] one monoclinic and the other triclinic. Crystals of a specimen from Devon when oscillated about the *b* axis show systematic absences on even layer lines corresponding to a *C* face centring, but no systematic absences on odd layers. Odd layer Weissenberg photographs also show streaks in the a^* direction and two sets of diffuse reflexions on row lines parallel to a^*. One set is more diffuse than the other and may be indexed in terms of the monoclinic cell, whilst the sharper reflexions can be accounted for by assuming the presence of both right- and left-handed triclinic forms. Dr. Jeffery interpreted these diffraction effects in terms of a structure of alternating plates, lying parallel to *bc*, of monoclinic and right- and left-handed triclinic forms, each plate being only a few cells thick.

The structure of the *alite* form of tricalcium silicate is monoclinic,[5,6] but strongly pseudo-rhombohedral. This gives rise to weak satellites grouped around the main rhombohedral reflexions. All the satellites may be indexed in terms of the true monoclinic cell.

Dr. H. F. W. Taylor (Birkbeck College, London) read a paper on "Crystallography of the hydrated calcium silicates." Two calcium silicate hydrates (I and II), readily formed synthetically at room temperature, give rather poor X-ray powder photographs. The least diffuse reflexions from calcium silicate hydrate I are mainly (*hk*) reflexions from a two-dimensional lattice with $a_0 = 5{\cdot}62$ Å, $b_0 = 3{\cdot}66$ Å, $\gamma = 90°$. The long spacing varies between 13 Å and 11 Å, and is probably a function of the degree of hydration. Both I, which may have a lime/silica ratio between 1·0 and 1·5, and II, with a composition always close to that of a dicalcium silicate hydrate, appear to have layer structures similar in some respects to those of clay minerals. Samples of I produced hydrothermally appear to be more crystalline.

A number of naturally occurring hydrated calcium silicates are poorly crystalline and fibrous, the fibre axis repeat distance being very close to an integral multiple of 3·6 Å (see Table 1). The most interesting of these minerals is *riversideite*, which is an alteration product of *wilkeite* (an isomorph of *apatite*). Rotation photographs of about a dozen specimens of riversideite all show spots, which fit the wilkeite lattice with its *c*-axis along the fibre axis, together with preferred orientation streaks, which may be interpreted in terms of calcium silicate hydrate I crystallites with their 3·66 Å spacing parallel to the fibre axis. It appears that the material consists of an intergrowth of the original mineral and its alteration product.

"The crystal structure of afwillite" was described by Dr. H. D. Megaw (Cavendish Laboratory, Cambridge). The unit cell is monoclinic with $a_0 = 16{\cdot}27$ Å, $b_0 = 5{\cdot}632$ Å, $c_0 = 13{\cdot}23$ Å, $\beta = 134° 48'$, and the space group is *Cc*. The structure was refined by means of three-dimensional Fourier syntheses, and it is estimated that the bond lengths are correct to within 0·05 Å. The positions of the hydrogen atoms were deduced from a consideration of the electrostatic valencies of the different types of oxygen, the cation–oxygen bond-lengths and the oxygen–oxygen distances. The evidence from these three lines of argument leads to the same arrangement of long and short hydrogen bonds, which form a continuous chain running through the structure in the [101] direction.

Table 1. *Natural fibrous calcium silicate hydrates*
(Fibre axes in bold type)

Mineral	*CaO*	SiO_2	H_2O	*Crystallographic data* (Å)
Okenite	1	2	2	Monoclinic: 12·2, **7·2**, 20·3; 119°
Crestmoreite	2	3	2	
Riversideite	2	2	1	Orthorhombic: 5·62, **3·66**, 11 to 14
Xonotlite	5	5	1	Orthorhombic: 7·05, **3·65**, 8·50
Foshagite	5	3	3	Monoclinic: 10·0, 7·6, 12·3; 104° (**7·2**, fibre axis spacing)
Hillebrandite	2	1	1	**3·6**

The structure has other interesting features. It is the first substance in which the structure determination gives definite proof of a direct linkage of hydroxyl groups to silicon atoms.[7] The co-ordination of the calcium ions is irregular with six oxygen neighbours arranged either as a distorted octahedron or as a distorted trigonal prism, and a seventh neighbour further away. Finally, it is interesting to compare the environment and arrangement of bonds in the two different types of water molecules.

In her paper "The thermal decomposition of afwillite," Mrs. K. M. Moody (Woolwich Polytechnic, London) described the changes which take place when afwillite is heated.[8] Three experiments were made in which afwillite was heated to temperatures of 500° C, 1000° C and 1300° C respectively, and the products identified from powder photographs. The product at 500° C gave a photograph with only a few diffuse lines which correspond to reflexions from γCa_2SiO_4 and calcite together with one line which was identified as the strongest reflexion from quartz. The calcite appears to be formed when calcium oxide, probably the initial product, reacts with atmospheric carbon dioxide. There was no reversion to afwillite when the material was rehydrated. Powder photographs of the products at 1000° C and 1300° C showed that in each case *rankinite*, $Ca_3Si_2O_7$, was formed. Again, on addition of water there was no reversion to afwillite.

A differential thermal analysis showed an endothermic reaction proceeding in several stages at low temperatures with its maximum effect at about 370° C, and an exothermic reaction at about 820° C. No complete explanation has so far been given of these changes at lower temperatures, but possibly the conversion of a third of the calcium in afwillite into calcium oxide according to the equation

$$Ca_3(SiO_3OH)_2 \cdot 2H_2O \rightarrow 3H_2O + Ca_2SiO_4 + SiO_2 + CaO$$

can be correlated with the fact that one type of calcium has a different environment from the other two. A similar 2 : 1 division of calcium has been noted by Parry and Wright.[9]

Answering a query by Professor J. D. Bernal (Birkbeck College, London) the speaker said that no single crystal work could be done because of disintegration at about 300° C.

DR. R. W. NURSE (Building Research Station, Watford) asked for details of the endothermic reaction and was informed that there was a large peak at 370° C together with subsidiaries in the range 250-450° C. Dr. H. F. W. Taylor mentioned that he had synthesized afwillite under pressure from lime, silica and water at temperatures between 120° C and 160° C.

MRS. L. HELLER (Birkbeck College, London) read a paper on "The crystal structure of dicalcium silicate α hydrate." Short period hydrothermal treatment of β dicalcium silicate yielded orthorhombic plates of the α hydrate, having unit cell dimensions $a_0 = 9{\cdot}34$ Å, $b_0 = 9{\cdot}22$ Å and $c_0 = 10{\cdot}61$ Å. There are eight formula units of $2CaO \cdot SiO_2 \cdot H_2O$ per unit cell and the space group is $P2_12_12_1$, although there is pseudo-symmetry which would correspond to a space group *Pbca*. Consideration of the Patterson synthesis of the *ac* projection together with the general properties of the compound led to a structure based on discrete $[SiO_3(OH)]^{3-}$ tetrahedra which are linked together through Ca^{2+} and $(OH)^-$ ions. The hydroxyls have been identified from chemical and not crystallographic evidence. Observed and calculated structure factors of low order $(h0l)$, $(hk0)$ and $(0kl)$ reflexions show satisfactory agreement. The structure of *hillebrandite* $(2CaO \cdot SiO_2 \cdot H_2O)$, which is formed by more prolonged hydrothermal treatment of β dicalcium silicate, may be related to that of the α hydrate by rotations of the silicate tetrahedra.

Professor Bernal, in discussing "The crystal chemistry of hydration of silicate systems," drew attention to possible relationships between the group of hydrated calcium silicates and other hydrated silicates. A common feature seems to be the existence of silicate tetrahedra, with one or more corners occupied by hydroxyl groups, leading to the series $(SiO_4)^{4-}$, $[SiO_3(OH)]^{3-}$, $[SiO_2(OH)_2]^{2-}$, $[SiO(OH)_3]^-$, and terminating in the silicic acid molecule $Si(OH)_4$ which may occur in fresh silica gel and is the active form in water vapour above 100° C. In many silicate structures $(SiO_4)^{4-}$ tetrahedra are linked together, but it is not known whether this is possible if one or more of the oxygens is replaced by a hydroxyl group. Evidence from sulphates and phosphates tends to suggest that this type of replacement can occur in linked tetrahedra.

The hydrated calcium silicates, whether in mineral form or synthetically prepared, do not crystallize well, and little information about the part played by water in the structures can be obtained from powder photographs. However, in afwillite, which is the only hydrated calcium silicate whose structure has been completely determined, there is definite proof of the existence of $[SiO_3(OH)]^{3-}$ groups, and it is very probable that these groups also occur in dicalcium silicate α hydrate. Evidence for the existence of the $[SiO_2(OH)_2]^{2-}$ tetrahedral groups may be obtained from the 3·6 Å periodicity found in many hydrated calcium silicates (see Table 1), for there is only one way of arranging silicate tetrahedra to give such a short spacing and the close approach of highly charged Si^{4+} cations can only be explained by the presence of hydrogen bonds between the tetrahedra. The chemical evidence based on the study of calcium sodium hydrated silicates by Thilo[10] also supports the existence of easily polymerized $SiO_2(OH)_2$ chains.

In his paper "X-ray examination of Portland cement by powder methods" DR. H. G. MIDGLEY (Building Research Station, Watford) mentioned the difficulty of identifying different calcium silicate minerals when they occur in cements, because of the masking effect of the strong alite pattern, which is almost always present. For example, weak reflexions must be used to identify β dicalcium silicate, which can therefore only be detected in proportions exceeding about 20%. Concentration by mineralogical techniques has proved impracticable, but differential hydration has been found useful although the process takes three months. So far only the β form of the dicalcium silicate has been identified in cements. Frequently found in cements is a calcium alumino ferrite phase, which has a wide range of composition and which may be concentrated magnetically. The second strongest line from this phase ($d \simeq 1{\cdot}9$ Å) shifts with composition so it is possible to estimate the composition of the phase in different cements; in Portland cements this is always close to $4CaO \cdot Al_2O_3 \cdot Fe_2O_3$.

In general discussion Dr. Nurse drew attention to the existence of cements other than Portland cement, e.g. the very strong hydrated mono-calcium aluminate, which is much less fibrous than the calcium silicates and more crystalline. A cement need not necessarily have a regular crystal structure, nor need it contain hydrous minerals.

Professor Bernal related the rate of growth of fibres to their thickness and mentioned that a rapid rate would give dendritic growth followed by thickening of the dendrites. Practically all substances can be made to grow in this way and therefore all substances are potentially cements under the right conditions.

In the evening lecture, DR. W. H. TAYLOR (Cavendish Laboratory, Cambridge) described the tetrahedron framework of the felspar structure and showed how its properties explain many features characteristic of felspar minerals. The existence of the different varieties of potash felspar, $KAlSi_3O_8$ —*microcline* (triclinic), *adularia* (triclinic or monoclinic), *orthoclase* and *sanidine* (both monoclinic)—is thought to be due to differences in the distribution of the Al atoms among the tetrahedra, but a direct test of this suggestion, from high-accuracy structure analyses, has still to be completed. It is certain that the form of the potash felspar depends upon the thermal history of the material. The existence of a high-temperature form of *albite*, $NaAlSi_3O_8$, is now clearly established by both X-ray and optical methods, and high-accuracy analyses of both high- and low-albite structures are in progress.

Perthitic potash-soda-felspars contain a potash-felspar component and *several* triclinic soda-felspar components, the *latter* in pairs related by either the Albite or the Pericline twin law. A monoclinic soda-felspar may also be present. Some success has been achieved in attempts to correlate the type of soda-felspar observed with the nature of the twin-orientation.

The *plagioclases* are much more complex than would be imagined from the gradual variation in axial ratios and interaxial angles on passing from albite ($NaAlSi_3O_8$) to *anorthite* ($CaAl_2Si_2O_8$). The albite-type structure persists from pure $NaAlSi_3O_8$ to about 30% $CaAl_2Si_2O_8$, with a *C*-face-centred cell having a *c*-axis $\simeq 7$ Å, but the anorthite-type structure is based on a true cell with a *c*-axis $\simeq 14$ Å, the 7 Å axis being now only a pseudo-periodicity. There is a variation of symmetry (from body-centred to primitive) within the range 70% to 100% $CaAl_2Si_2O_8$ in which this type of structure exists. Intermediate plagioclases (30% to 70% $CaAl_2Si_2O_8$) show diffraction effects explicable in terms of alternating slabs of albite-like and anorthite-like structures, but it is not yet possible to fill in all the details of this model.

DR. G. W. BRINDLEY (University of Leeds) opened the second session with a paper on "X-ray analysis of clay mineral structures," and remarked that the numerous books[11–14] which have appeared within the last year indicate the great current interest in this subject. X-ray examination

of clay minerals has three main objectives—structure analysis, mineral identification and estimation, and a study of mineral transformations. Powder analysis is often the only method available and in recent years several powder cameras have been designed for the examination of clay minerals. Details were given of cameras used by MacEwan[15] and in the author's laboratory. A new camera based on the principle of the multiple camera of de Wolff[16] is now being used extensively by Brindley and Crooke.

Few detailed structure analyses of clay minerals have appeared since that of *kaolinite*,[17] increasing attention now being given to the peculiar features of the diffraction patterns from two-dimensional lattices and to effects arising from the interstratification of different types of layer. *Amesite*[18] has a two-layer kaolin-type structure and should not therefore be classified as a *chlorite*. A green ferrous iron silicate occurring in many iron ores and known as *chamosite*[19] has monoclinic and orthorhombic kaolin-type structures, but differs structurally from the type mineral from Chamoson, France, which is a *chlorite*.[20] The relative merits of the two alternative structures for *montmorillonite* proposed by Hofmann and others[21] and by Edelman and Favejee[22] have not yet been finally established, for although the former is more generally accepted, the latter has recently gained some ground from the results obtained by organic chemists on the bonding of organic derivatives. The method usually adopted for the estimation of Al^{IV}/Si^{IV} has been confirmed experimentally by Brindley and Youell[23] in the case of a chlorite.

Identification of the components in a mixture of clay minerals requires the use of subsidiary thermal and/or chemical treatments, e.g. heating at 500–600° C will "remove" kaolin minerals and modify chlorites, whilst dilute HCl removes carbonates and chlorites.

Single crystal examinations of the dehydration and recrystallization of minerals on heating have now been carried out on chlorites (→ olivine),[24] *chrysotile* (→ *forsterite*)[25] and *pyrophyllite* (→ *mullite*).[26]

In the discussion Dr. F. A. Bannister (British Museum, Natural History) asked if it might not be better to classify chamosite with the trioctahedral minerals chrysotile and *antigorite* rather than with the kaolins, and if preference should not be given to *cronstedtite* as the iron analogue of antigorite. Dr. Brindley replied that although chamosite was more closely related to chrysotile and antigorite, he preferred to include both di- and trioctahedral minerals in the kaolin group; cronstedtite had been omitted from his remarks because of its comparative rarity. With regard to the two possible structures for montmorillonite, Dr. G. Nagelschmidt (Safety in Mines Research Establishment, Sheffield) mentioned that the cation exchange had recently been explained in terms of the Hoffmann structure, whilst Mr. R. Greene-Kelly (Rothamsted Experimental Station, Harpenden) thought that the evidence in favour of the Edelman structure from organic chemistry had been over-estimated.

In his paper "Interlamellar reactions of montmorillonite and related minerals" Dr. D. M. C. MacEwan (Rothamsted Experimental Station, Harpenden) outlined the information which may be deduced solely from the basal (00*l*) X-ray reflexions. To balance the net charge on the talc-type layers there are, between successive layers, mobile cations, which may be inorganic or organic and which are readily replaceable. A second type of interlamellar adsorption involves the uptake of *neutral* molecules. Adsorption of either type pushes the layers apart and increases $d(001)$. For the neutral straight chain alcohols[27] with more than two carbon atoms $d(001)$ increases by 4·1 Å, indicating that the adsorbed molecules form a monolayer lying as flat as possible; with chains containing one or two carbon atoms the expansion is just sufficient for two flat monolayers. Similar experiments by Jordan[28] with adsorbed ionic amine chains show that as the number of carbon atoms in the chain increases $d(001)$ increases in discrete steps. Similar effects are obtained on plotting $d(001)$ as a function of vapour pressure of sorbate[29] or as a function of the polarity of the molecules.[16] In general, the number of adsorbed monolayers between successive mineral layers may vary. The theory of diffraction from such a turbostratic structure[30,31] has been applied, and details of one such case follow in the paper by Mr. G. Brown.

In favourable cases it is possible to obtain one-dimensional electron density syntheses from the (00*l*) intensities, either by assuming the basic structure of the more strongly scattering mineral layers or by determining the signs of the structure factors directly from the variation of $I(00l)$ with l. Because of the turbostratic structure, however, it is not possible to obtain information concerning the arrangements of molecules *within* the adsorbed layers. This is a feature of the problem in which electron diffraction may help considerably.

Dr. K. Robinson (Cavendish Laboratory, Cambridge) in a paper with Dr. B. M. Oughton (University of Uppsala) on the "Crystal structures of chlorites" described the polymorphic forms which have been found amongst single crystals of these minerals. The structures may be divided into three groups, ordered, partially ordered and disordered. In terms of unit cells, having orthogonal axes parallel to the basal cleavage plane ($a_0 \simeq 5{\cdot}3$ kX, $b_0 \simeq 9{\cdot}2$ kX), the reflexions are of two types. Those for which $k = 3n$ (n integral) are similar in almost all chlorites and confirm the *ac* projection of the structure determined by McMurchy[32] from powder data. The much weaker reflexions for which $k \neq 3n$, which were not recorded by McMurchy, show wide variations even in crystals from the same sample. Only the tetrahedral Si–O networks contribute to these reflexions, and in each chlorite layer there are three alternative positions of one such network relative to the other which still leave unaltered those reflexions for which $k = 3n$. Relative to any fixed direction these three possibilities represent three different chlorite layers which are simply related by rotations of $2\pi n/3$ about c^*.

Moreover, there are also three different ways in which one chlorite layer may stack upon its neighbour without altering reflexions for which $k = 3n$. These three possibilities correspond to a shift of $-a/3$ along each of the three "hexagonal" a-axes. Thus, relative to any fixed set of orthogonal axes, each chlorite layer may have any one of nine sets of (a, b) coordinates. Regular sequences give rise to normal (hkl) reflexions when $k \neq 3n$ and correspond to ordered structures, four of which have been determined in detail.[33] Random sequences give rise to two-dimensional (hk) streaks when $k \neq 3n$ and correspond to the disordered structures.

Mr. E. J. W. Whittaker (Ferodo Ltd., Chapel-en-le Frith) in a paper dealing with "Asbestos minerals" confined his attention to chrysotile. Stationary and rotating fibres of this mineral give identical photographs. The pattern from a Quebec chrysotile may be indexed in terms of a monoclinic cell with a significant variation of b_0 with Bragg angle; this variation has been explained by Warren[34] and Aruja[35] on the assumption that $(0kl)$ reflexions are due to diffraction from independently scattering two-dimensional lattices. Padurow's attempt[36] to explain the effect by using a triclinic cell has been discounted.[37] A better explanation is afforded by the theory of diffraction by cylindrical layers of radius about 65 Å (Fock and Kolpinsky).[38]

Other specimens show additional reflexions from an orthorhombic form. The whole pattern is due to an intimate mixture of clino- and ortho- forms, the relative proportions of which vary from almost pure clino- from Quebec to almost pure ortho- from Silesia.

The intensity distribution in the unsymmetrical reflexions has been studied with photographs taken on a Weissenberg goniometer without screens and with a camera traverse of a few millimetres. A Weissenberg goniometer in the equi-inclination setting without screens or camera movement has been useful for determining the presence of a small amount of ortho-chrysotile in the Quebec sample. This technique has also been used to study weak subsidiary layer-lines corresponding to a repeat of 9·2 Å.

In reply to a question by Dr. Bannister, Mr. Whittaker said that on heating chrysotile the ortho- and clino- patterns disappear simultaneously.

Dr. G. NAGELSCHMIDT (Safety in Mines Research Establishment, Sheffield) commented on the different forms in which mica may occur. In clays micaceous minerals are usually called illites and give rise to broadened general (*hkl*) reflexions. The ratio of sodium to potassium content varies considerably with location, but there seems to be an excess of potash in sedimentary rocks compared with the amount known to be present in sea-water. There is, in general, an excess of micaceous minerals in sedimentary rocks, and it is suggested that after weathering of the parent rocks (e.g. felspars) the potash is recovered in the form of micaceous minerals, whereas the soda is not so readily deposited in mineral form. The proportion of potash decreases considerably through the series of minerals:—muscovite, illite, vermiculite, montmorillonite.

MR. G. BROWN (Rothamsted Experimental Station, Harpenden) presented a contribution in conjunction with Mr. R. GREENE-KELLY on "Diffraction by randomly superposed layers in a clay mineral." The Hendricks and Teller theory[30] has been applied to the lithium montmorillonite-glycerol system. After heating to 190° C lithium montmorillonite loses its power of interlamellar sorption of glycerol at room temperature, but it will still take up amounts which increase as the temperature is raised from 30° C to 100° C. This effect has been used to prepare samples of lithium montmorillonite with different fractions (f) of interstratified glycerol layers. There is good agreement between the observed intensity distribution and interplanar spacings and those calculated on the Hendricks and Teller theory (see Fig. 1 and Table 2).

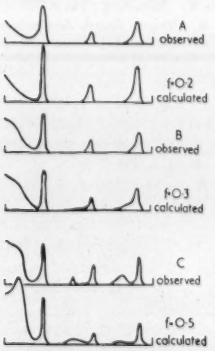

Fig. 1. Comparison of observed and calculated intensity distributions for different lithium montmorillonites

Table 2. *Observed and calculated spacings (kX) for lithium montmorillonite complexes*

Complex	A		B		C	
f	obs. 0·2	calc. 0·2	obs. 0·26	calc. 0·3	obs. 0·48	calc. 0·5
					?	18·52
	9·25	9·24	9·20	9·13	9·08	9·07
					5·65	5·72
	4·63	4·63	4·61	4·59	4·52	4·51
					$3{\cdot}41_5$	3·45
	$3{\cdot}08_5$	$3{\cdot}08_5$	3·07	$3{\cdot}05_5$	$3{\cdot}01_5$	3·01

MISS A. MILNE, DR. A. MCL. MATHIESON AND DR. G. F. WALKER (Macaulay Institute for Soil Research, Aberdeen) discussed "Some considerations arising from Fourier syntheses of vermiculite." They showed one-dimensional (00*l*) electron density syntheses of vermiculite calculated from thirty-one observable orders of reflexion (see Fig. 2). Particular attention was drawn to the resolution of the (Si, Al)

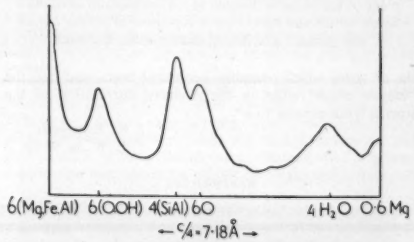

Fig. 2. One-dimensional (00*l*) electron density synthesis of vermiculite

and oxygen sheets and to the position of the exchangeable magnesium cations lying between two sheets of water "molecules." Confirmation of the magnesium positions is obtained from the results after substituting Sr^{2+} for Mg^{2+}; the peak marked 0·6 Mg then increases in height. Substitution of Li^+ or Ba^{2+}, however, produces only a single sheet of interlamellar water "molecules."

In the general discussion PROFESSOR L. ONSAGER (Yale University) proposed an explanation for the unusual diffraction effects observed for antigorite by Aruja.[39] He suggested that the layer structure inverts every 43·4 Å in the *a*-direction; the bending of the layers then produces an undulating plate and not the cylindrical habit in which chrysotile develops. The manner in which the proposed inversion takes place is shown in the *ab* projection in Fig. 3. Instead of the normal hexagonal array of silicons, these atoms form rectangles and octagons in projection at the inversion line. The distance between successive inversions is $8\frac{1}{2}$ times the *a*-dimension of the Si–O network (5·2 Å), but in this distance there are only sixteen octahedral groups of the brucite layer, and not

seventeen as would normally be the case. In addition to explaining the crystal habit and the long *a*-axis of antigorite the proposed structure explains the variation of intensity in

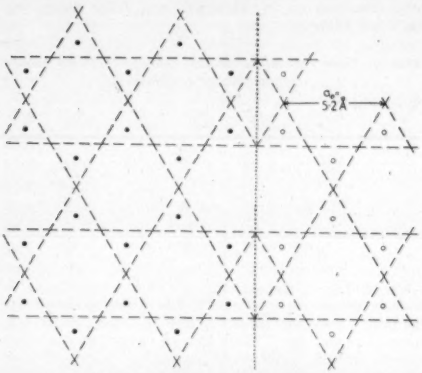

Fig. 3. The *ab* projection of the proposed chrysotile structure. The black circles represent Si atoms above the plane of the oxygens (located at the intersection of dashed lines), whilst the open circles represent Si atoms below this plane. The line of discontinuity is dotted

the a^* rows, which resembles acoustical beats, and also the "bicycle chain" effect in the intensity distribution of the streaks lying parallel to c^*.

K. Robinson
E. R. S. Shaw

REFERENCES

(1) Gossner, B. *Neues Jahrb. f. Min.*, **57A**, p. 89 (1928).
(2) Bragg, W. L., and Brown, G. B. *Zeit. f. Krist.*, **63**, p. 538 (1926).
(3) Barnick, M. *Dissertation, Berlin* (1936); see *Strukturbericht* IV, pp. 71 and 207 (1936).
(4) Warren, B. E., and Biscoe, J. *Zeit. f. Krist.*, **80**, p. 391 (1931).
(5) Jeffery, J. W. *Proc. Phys. Soc. Lond.*, **64A**, p. 1003 (1951).
(6) Jeffery, J. W. *Acta Cryst.*, **5**, p. 26 (1952).
(7) Megaw, H. D. *Acta Cryst.*, **2**, p. 419 (1949).
(8) Moody, K. M. *Min. Mag.*, **29**, p. 838 (1952).
(9) Parry, J., and Wright, F. E. *Min. Mag.*, **20**, p. 277 (1925).
(10) Thilo, E., and Funk, H. *Zeit. anorg. Chem.*, **262**, p. 185 (1950).
(11) Brindley, G. W. (Editor). *X-ray Identification and Crystal Structures of Clay Minerals* (London: Mineralogical Society, 1951).
(12) *Trans. Fourth International Congress of Soil Science*, (4 vols), Amsterdam (1950).
(13) *Analytical Data on Reference Clay Materials* (Amer. Petr. Inst. Columbia Univ., 1950).
(14) Jasmund, K. *Die Silikatischen Tonminerale* (Weinheim: Verlag Chemie, 1951).
(15) MacEwan, D. M. C. *J. Soc. Chem. Ind.*, **65**, p. 298 (1946).
(16) de Wolff, P. M. *Acta Cryst.*, **1**, p. 206 (1948).
(17) Brindley, G. W., and Robinson, K. *Min. Mag.*, **27**, p. 242 (1946).
(18) Brindley, G. W., Oughton, B. M., and Youell, R. F. *Acta Cryst.*, **4**, p. 552 (1951).
(19) Brindley, G. W. *Min. Mag.*, **29**, p. 502 (1951).
(20) Orcel, J., Hénin, S., and Caillère, S. *C.R. Acad. Sci., Paris*, **229**, p. 134 (1949).
(21) Hofmann, U., Endell, K., and Wilm, K. *Zeit. f. Krist.*, **86**, p. 340 (1933).
(22) Edelman, C. H., and Favejee, J. Ch. L. *Zeit. f. Krist.*, **102**, p. 417 (1940).
(23) Brindley, G. W., and Youell, R. F. *Acta Cryst.*, **4**, p. 495 (1951).
(24) Brindley, G. W., and Ali, S. Z. *Acta Cryst.*, **3**, p. 25 (1950).
(25) Hey, M. H., and Bannister, F. A. *Min. Mag.*, **28**, p. 333 (1948).
(26) Bradley, W. F., and Grim, R. E. *Amer. Min.*, **36**, p. 182 (1951).
(27) MacEwan, D. M. C. *Trans. Faraday Soc.*, **44**, p. 349 (1948).
(28) Jordan, J. W. *Min. Mag.*, **28**, p. 598 (1949).
(29) Glaeser, R. *Trans. Fourth International Congress of Soil Science*, **III**, p. 65 (1950).
(30) Hendricks, S. B., and Teller, E. *J. Chem. Phys.*, **10**, p. 147 (1942).
(31) Méring, J. *Acta Cryst.*, **2**, p. 371 (1949).
(32) McMurchy, R. C. *Zeit. f. Krist.*, **88**, p. 420 (1934).
(33) Brindley, G. W., Oughton, B. M., and Robinson, K. *Acta Cryst.*, **3**, p. 408 (1950).
(34) Warren, B. E., and Hering, K. W. *Phys. Rev.*, **59**, p. 925 (1941).
(35) Aruja, E. *Nature, Lond.*, **154**, p. 53 (1944).
(36) Padurow, N. N. *Acta Cryst.*, **3**, p. 204 (1950).
(37) Whittaker, E. J. W. *Acta Cryst.*, **5**, p. 143 (1952).
(38) Fock, V. A., and Kolpinsky, V. A. *J. Physics (U.S.S.R.)*, **3**, p. 125 (1940).
(39) Aruja, E. *Min. Mag.*, **27**, p. 65 (1944).

The measurement of velocities for solid-fluid flow in a pipe

By C. JONES, B.Sc., A.Inst.P., and G. HERMGES, B.A., Central Research Establishment, National Coal Board, Cheltenham

[*Paper received* 3 *April*, 1952]

When a stream of particles is conveyed by air or water in a glass pipe two photographs of a portion of the stream are superimposed on the same photographic negative. The pictures are taken by the light from a pair of discharge lamps, the time interval between the flashes being variable and measured by a rotating disk. A more satisfactory light source is a high speed stroboscope, the interval between flashes being predetermined by a setting of a multivibrator. The velocity of a particle is obtained from its displacement measured on the photograph. The method is illustrated by its application to the movement of gravel by air and coal by water.

In the study of the physics of transportation of material in a pipe by pneumatic or hydraulic means, it is essential to know the velocities of the solid and fluid as accurately as possible at various places along the pipe. Various methods have been reported in the past but they do not give the velocity at a point on the pipe nor are they reliable or sufficiently accurate.[1, 2, 3] This article gives a brief account of the successful application of modern equipment to a problem of wide interest. Although the technique can be applied to many solids and transparent fluids two examples are sufficient to illustrate the procedure.

Particles of gravel about $\frac{1}{8}$ inch in size were to be observed in a 1 in diameter glass pipe when carried at speeds up to 40 ft/sec by a stream of air. Their velocities were obtained by taking two photographs of a part of the stream on the same photographic negative, with a very short time interval between the exposures. Two Microflash units, Type 1702B, by Dawe Instruments Ltd., were used, each of which had an effective photographic duration of only a few microseconds. They were flashed off at about a millisecond time interval between them by means of two pairs of contacts on an a.c. mains operated relay, variation in the time interval being obtained by altering the relay voltage.

Another method of flashing the tubes made use of two enclosed microswitches. These were mounted horizontally and side by side and were operated by two set screws on a falling lever. Alteration of the time interval was obtained by adjustment to the screws or by changing the angle of fall of the lever.

The magnitude of the time interval was obtained from the angular rotation of a disk which was photographed in a position behind the pipe. The disk speed was adjustable up to 3,500 r.p.m. and the actual speed was measured by a calibrated tachometer at the time when each photograph was taken. Fig. 1 is an example of the photograph obtained. It shows the two positions of each particle together with the angular rotation of the disk. The scale factor for each photograph was known by measurement of the pipe's external diameter at the position where the particles were observed.

The second example concerned the measurement of the velocity of pieces of coal when conveyed at speeds up to 20 ft/sec by a flow of water in pipes. Again, two photographs of the particle stream were taken, but the light source and the time interval between flashes were obtained with a power stroboscope that was more reliable, accurate and convenient

Fig. 1. Movement of gravel by air

although more costly than the previous method. The stroboscope is manufactured by Turner Electrical Instruments Ltd., and has been fully described in the technical press.[4] A few flashes of the stroboscope were triggered off simultaneously with the operation of the Compur shutter of a good plate camera. The shutter speed was selected so that only two pictures of each particle were taken at a predetermined time interval. The interval was selected by setting the flashing rate at the required value within the range of 100 to 4,000 flashes per sec. The accuracy was within 2%. Fig. 2 is a typical photograph for coal in water.

to increase the flashing rate of the stroboscope so that more than two images were obtained very close together.

Once the particle velocity was determined at the required point along the pipe together with the mass throughput of solid and fluid, a simple calculation gave the fluid velocity at that point. However, with low concentrations of material the correction to be made to the mean fluid velocity, as determined by division of the fluid flow by the cross-sectional area of the pipe, was small enough to be neglected once the particles had acquired a small velocity. The technique has certain limitations and these will be mentioned in conclusion.

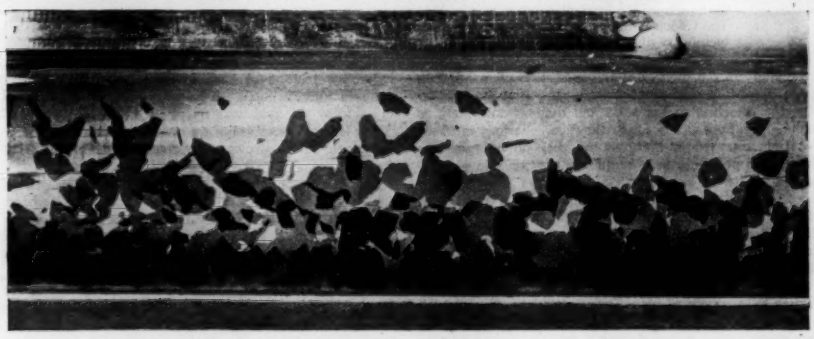

Fig. 2. Movement of coal by water

The light output of the Dawe Microflash unit was high enough to operate with a lens aperture of *f*/18 and in the case of the Turner stroboscope *f*/22 gave ample exposure. In both cases quarter-plate Ilford HP3 cut film was used and developed in Kodak D.76 developer.

Measurement of the distance between the two positions of each particle was facilitated by choosing a prominent angular point on the particle as the measuring point. The average of these measurements together with the measurement of the time interval gave the particle velocity. With light or moderate concentrations of material it was always possible to include in each photograph pairs of images for at least ten particles. With the same conditions of flow observed at a later stage the particle velocities were all within 5% of the mean.

With particles of irregular shapes recognition of the pairs of images of each particle was easily achieved by means of such prominent characteristics as the sharp points of the particle, recognizable angles in the outline, the obvious ratio of length to width, the size of the particle, special contours shown up by the flashes or the position of the particle in relation to the others and to the pipe. Of course, in practice more than one of these special features were normally used. It was also an advantage to use the light from an angle of about 45° to the pipe, as this side light revealed the contours of the particle more readily than direct frontal lighting. Once some knowledge of the distances between images had been obtained from measurement of the particles moving in isolated paths it was quite easy to select images from among closely packed groups of particles. For spherical particles resort was made to the grouping of the particles, their size and surface markings (if any). It also helped in identification

As the method is a photographic one it can only be used with transparent sections of the pipeline and with particles greater than about 0·5 mm for good definition. If there is much spinning of the particles it becomes difficult to identify the two positions of the same particle when the time interval between the flashes is too long. This difficulty also arises with spherical particles, and, in addition, the time interval may also need adjustment for ease of identification so that the distance traversed between flashes does not coincide with the actual distance between particles in the stream. The inaccuracy of measuring small distances between pairs of images can be reduced by taking the measurements from an enlargement or projection of the negative. The heaviest concentrations of material do make it more difficult to select many pairs of images, but it is usual to find a sufficiently representative number. It is only when choking conditions are being approached that the method is of small use, but under these conditions particle velocity varies within a very much wider range of values and, as a result, it takes on a different meaning.

This paper is published by permission of the Director General, Scientific Department, National Coal Board.

REFERENCES

(1) Cramp, W. *J. Roy. Soc. Arts*, **69**, p. 283 (1921).
(2) Cramp, W., and Priestley, A. *Engineer, Lond.*, **137**, p. 34 (1924).
(3) Gasterstadt, V. D. I. Forschungsarbeiten, No. 265 (1924).
(4) Chesterman, W. D., Glegg, D. R., Peck, G. T., and Meadowcroft, A. J. *Proc. Instn Elect. Engrs*, Pt II, **98**, p. 619 (1951).

The effect of frequency on the behaviour of rubber under cyclical deformation

By D. M. Davies, B.Sc.(Eng), A.M.I.Mech.E., University of Nottingham

[*Paper received* 16 *April*, 1952]

A new testing machine is described which records autographic hysteresis loops, and which has an unlimited low frequency range. Graphs are presented showing the variation of stiffness with frequency over the range 0·05–1 000 c/min for a rubber with 60 parts of lamp-black. The overall variation can amount to anything up to 50%, depending on the amplitude. A range of amplitudes is covered in compression from 3–11% of the undeformed specimen height. The behaviour of the rubber is compared with that of the combined models of Maxwell and Voigt. A possible law emerges for the variation of stiffness in the frequency range 0–300 c/min where almost the entire variation occurs. Upwards of 400 c/min stiffness varies little. Further graphs show the variation of resilience; over the same range resilience falls anything up to 10% depending on the amplitude. Above 200–300 c/min again there is little variation. Similar tests on a gum-stock rubber with no carbon black showed negligible hysteresis, and the overall variation of stiffness with frequency was less than 7%.

The deformation of a rubber-like material under the action of an applied force is known to be a function of time, and the stiffness of the material is consequently a function of the rate of deformation. In cyclical deformations one would expect stiffness to be a function of frequency, and so it is surprising to find that most investigators report stiffness to be virtually constant in the range 300–8 000 c/min.[1–6] All agree, however, that this constant dynamic stiffness is higher than the "static" value, though no precise meaning seems to have been assigned to the term "static" in this context.

The primary object of the work reported in this paper was to investigate the behaviour of rubber over a range of low frequencies, and so possibly to establish a law governing the variation of stiffness with frequency. Furthermore, it has long been considered desirable to confirm, by a more direct method, the findings reported above—namely, that upwards of 300 c/min the graph of stiffness *versus* frequency appears to be flat—since these conclusions were arrived at indirectly from observations of the resonant amplitude and frequency of a forced vibration applied to a rubber specimen. During the course of the present investigation such confirmation was provided by Wilkinson and Gehman[7] in America. These investigators used a machine of a type that had been developed earlier,[8] in which the transient force *versus* deformation relationship for rubber subjected to a cyclical force was recorded optically. As the force was applied by means of a rotating eccentric mass, however, it was not possible for them to explore the low frequency range where the considerable variation of stiffness occurs. The resonance method is even more limited in its low frequency range. There appears to be only one investigation in which very low frequencies were possible,[9] but in this work the parameter given pride of place was temperature rather than frequency, and only three frequencies are quoted below 1 000 c/min. Furthermore, the apparatus did not record the transient force *versus* deformation relationship during a cycle, so that the equally important hysteresis of the rubber could not be measured directly.

At the outset of the present work, therefore, the need was felt for a new testing machine capable of giving cyclical force *versus* deformation records over a frequency range which might be extended indefinitely at the low end. The machine developed for the purpose is shown in principle in Fig. 1. An eccentric imparts a reciprocating motion to the lower platten *C* on which the specimen *B* rests. The top of the specimen bears against the underside of cantilever *A*. When the lower platten rises, the specimen is deformed by a force which is proportional to the consequent displacement of the end of the cantilever. This displacement is converted into a proportionate and approximately horizontal movement of the scribing point *H*, at the lower end of the light pointer *F*, which is rigidly attached to the end of the cantilever. A piece of smoked glass *G*, on which the scriber ultimately records, is housed at one end of a strip of spring steel *E* rigidly attached at its other end to the bracket *D* carried by the reciprocating member driving the lower platten. The relative vertical displacement between the scribing point and the screen is thus equal to the axial deformation of the specimen, whilst

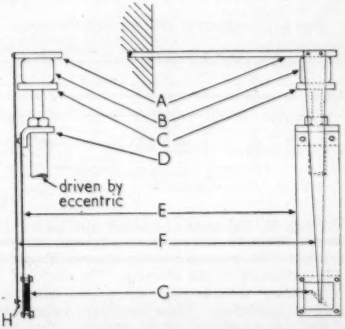

Fig. 1. Diagrammatic arrangement of machine

the relative horizontal displacement is proportional to the force on the specimen. Thus a miniature autographic record of force *versus* deformation is obtained which can subsequently be enlarged by projection. The purpose of the spring strip *E* is to enable records to be taken only when desired. Normally the smoked glass is clear of the scribing point, and a record is only obtained when they are brought into contact. This is achieved by manual deflexion of the spring strip. The machine was ultimately fitted with an encastré beam in place of the cantilever, and the load recording pointer was then attached at the point of contraflexure.

Compression testing was chosen for the initial investigation mainly to simplify the preparation of the specimens, and a rubber of specification CS. 2507 (60 parts of lamp-black to 100 parts of rubber by weight) was used on the advice of the Ministry of Supply Advisory Service on Rubber. Moulded cylindrical specimens of nominal diameter ½ in and height

$\frac{1}{2}$ in were used throughout, and preliminary investigation showed that with unbonded specimens bearing on ground steel plattens the end restraint was complete. A disadvantage of compression testing lies in the complexity of the stresses and strains involved in the barrel shape assumed by the deformed specimen. Mathematical analysis in such conditions is made difficult and empirical shape factors are usually resorted to. The large variation in shape of the specimen is a serious drawback of testing methods in which changes of stiffness are measured by changes in deformation under a constant cyclical load. In the present method it is the applied cyclical deformation which is kept constant, and changes of stiffness are measured by changes in the recorded force, so that shape variations are minimized. Thus, over each of the varying frequency curves mentioned below, the shape of the specimen is virtually constant.

Figs. 2 and 3 show the results of varying frequency tests down to the lowest frequency possible with the existing speed reducing gear. The spacing of the points was dictated by the gear ratios available on the machine. The curves of Fig. 3 show a tendency towards finite asymptotic values as zero frequency is approached. These asymptotic values might be termed the "static stiffness" of the material. Thus the stiffness of this rubber at a frequency of 1 000 c/min can exceed its static stiffness by anything up to about 50%, depending on the amplitude of the cyclical deformation. When Fig. 2 is viewed in the light of the previous investigations mentioned it would seem that in these graphs asymptotic values are approached as the frequency is increased. The apparatus, at present, is not provided with a temperature control so that at the higher end of the frequency range a rise in the temperature of the specimen occurs. It is known, however, that around room temperature the variation of stiffness with temperature is small.

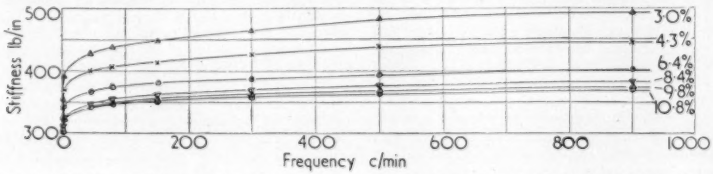

Fig. 2. Variation of stiffness with frequency. Parameter is the amplitude; constant mean deformation 20%

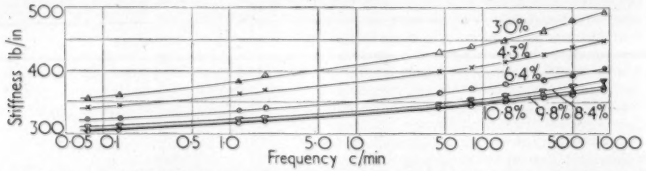

Fig. 3. Variation of stiffness with log N. Parameter is the amplitude; constant mean deformation 20%

Mechanical models made up of springs and dash-pots have been used extensively to illustrate the behaviour of rubber-like materials.[10] Such a model is shown in Fig. 4, and it is of interest to see how closely the behaviour of this model agrees with the behaviour of the rubber in question. If this model be compressed by an amount l and then, after settling down, subjected to a further sinusoidal deformation of the form

$$y = A(1 - \cos \omega t) \tag{1}$$

where A is the amplitude and $\omega/2\pi$ the frequency, it can be shown that the steady state force P exerted on the model is given by

$$P = (l + A)(\lambda_1\lambda_2)/(\lambda_1 + \lambda_2) + B \sin \omega t + C \cos \omega t \tag{2}$$

where
$$B = \lambda_1^2 A\omega/\eta(\omega^2 + k^2)$$
$$C = [\lambda_1^2 Ak/\eta(\omega^2 + k^2)] - \lambda_1 A$$
$$k = (\lambda_1 + \lambda_2)/\eta$$

The force *versus* deformation graph given by equations (1) and (2) forms an elliptical hysteresis loop as shown in Fig. 5. The hysteresis loops for rubber obtained in the present investigation are so pointed at their ends that no appreciable error is involved if the ends of the major axis of the loop in Fig. 5 are taken at $\omega t = 0$ and $\omega t = \pi$. Substituting these values in equation (2) will give for the mean dynamic stiffness S of the model

$$S = (P_2 - P_1)/2A = \lambda_1 - [\lambda_1^2 k/\eta(\omega^2 + k^2)] \tag{3}$$

where P_1 and P_2 are the values of P in equation (2) when $\omega t = 0$ and $\omega t = \pi$ respectively.

This expression for S has a finite value at $\omega = 0$ and $\omega = \infty$, and when plotted against ω gives a graph of the same form as those in Fig. 2. Thus, there is a semblance of agreement between the behaviour of the model and that of rubber. To see how far the analogy might be taken a linear relationship is desirable. Such a relationship can be obtained as follows.

Substituting for k in equation (3) and replacing ω by

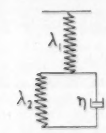

Fig. 4. Mechanical model. λ_1 and λ_2, spring stiffnesses; η, the damping constant of the dash-pot

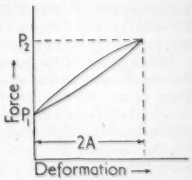

Fig. 5. Force *v.* deformation relationship for mechanical model

$2\pi N/60$, where N is the frequency in c/min, the dynamic stiffness S becomes

$$S = \lambda_1 - D/(\eta^2 N^2 + E) \quad (4)$$

where $D = (30/\pi)^2 \lambda_1^2 (\lambda_1 + \lambda_2)$

$$E = (30/\pi)^2 (\lambda_1 + \lambda_2)^2$$

Putting $N = \infty$ gives $S_\infty = \lambda_1$

and $N = 0$ gives $S_0 = \lambda_1 - D/E$ or $D/E = S_\infty - S_0$

Combining these relationships with equation (4)

gives $$(S_\infty - S)\eta^2 N^2 = E(S - S_0) \quad (5)$$

so that $$\log (S - S_0)/(S_\infty - S) = 2 \log N + \log (\eta^2/E) \quad (6)$$

Here is a linear relationship between $\log (S - S_0)/(S_\infty - S)$ and $\log N$, whose slope is 2. Fig. 6 shows graphs of these quantities for rubber. In the frequency range 0·07 to about 300 c/min these graphs are consistently linear, but their slopes are far from 2, so that the model, as it stands, is ruled out. Examination of equations (5) and (6) shows that if η were a function of N, such that $\eta^2 N^2$ were proportional to N^n, then the result would be a linear relationship similar to equation (6), but having a slope n. In terms of the model, this would entail having a dash-pot with a damping constant controlled by the frequency of the applied deformation.

Putting $$\eta^2 N^2 = K^2 N^n$$

i.e. $$\eta = K N^{n/2-1} \quad (7)$$

where K is a constant of proportionality, reduces equation (6) to

$$\log (S - S_0)/(S_\infty - S) = n \log N + \log (K^2/E) \quad (8)$$

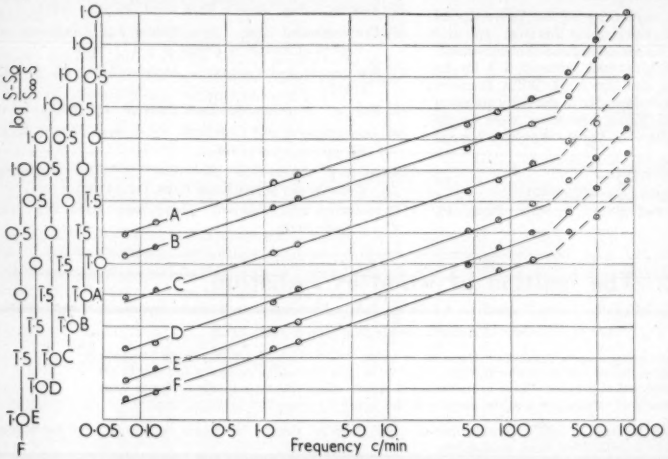

Fig. 6. Variation of $\log (S–S_0)/(S_\infty–S)$ with $\log N$. S is the stiffness of the rubber and the suffixes indicate frequency

	Amplitude %	Slope n
A	3·0	0·32
B	4·3	0·32
C	6·4	0·33
D	8·4	0·34
E	9·8	0·35
F	10·8	0·34

The linear graphs of Fig. 6 with appropriate values of n, as tabulated, conform to this equation, so that, whether a model analogy is applicable or not, it can be said that up to a frequency of 300 c/min the variation of stiffness follows closely a law of the form

$$S = U - V/(N^n + W) \quad (9)$$

where U, V, W and n are constants. For the rubber in question, n has a value of about 0·34, and is virtually independent of amplitude. This makes η proportional to $N^{-0.83}$. In a previous investigation[6] it was suggested that η was proportional to N^m, where m varied between −0·70 and −0·95 depending on the composition of the rubber. These investigators, however, used a resonance method based on the classical equation for forced vibrations, so that the mechanical model involved in their case would consist merely of a spring and dash-pot in parallel.

It seems that with further increase of frequency the stiffness of rubber, unlike that of the model, does not remain independent of frequency. A linear increase of stiffness with frequency has been observed in the range 200–600 c/s.[11] The results of Aleksandrov and Lazurkin, although limited to an upper frequency of 1 000 c/min, also suggest the possibility of this second rise of stiffness at high frequency. Furthermore, their results indicate that the lower the temperature of the specimen, the lower the frequency at which this rise of stiffness occurs. The machine described in the present paper is now being modified to incorporate temperature variation and control down to as low as −40° C, and at the same time it is hoped to extend the frequency range so that a more ambitious test programme may be undertaken.

The variation of hysteresis energy with frequency recorded in the present tests followed curves similar to those of Figs. 2 and 3, with a maximum variation of over threefold. Unlike stiffness, however, the area of the hysteresis loop varies appreciably with the temperature of the specimen, so that a full analysis cannot be attempted until a temperature controlling device has been developed. Nevertheless the temperature variation will not be great, as the specimen is in intimate contact at both ends with a considerable mass of metal. Fig. 7 shows the variation of resilience with frequency. Here resilience is defined as the percentage ratio of energy output to energy input in a cycle of deformation, and was measured by a planimeter from the force *versus* deformation

records. Only one other type of rubber of controlled specification was readily available at the time of these tests. This was a gum-stock with no carbon-black, which proved to have negligible hysteresis. The variation of stiffness for this rubber over the same frequency range was less than 7%, so that it was not possible to confirm the law suggested in equation (9).

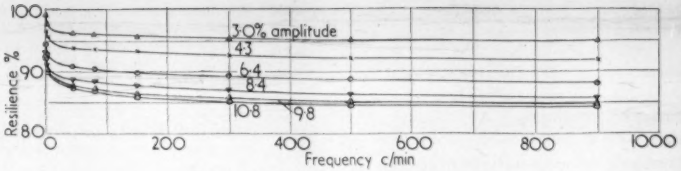

Fig. 7. Variation of resilience with frequency

ACKNOWLEDGEMENTS

Thanks are due to the authorities of the University of Nottingham for facilities for carrying out this work, and also to Professor J. A. Pope for his advice and constant encouragement. The author also wishes to thank Professor S. J. Davies of King's College, London, and Mr. A. H. Willis, formerly of the same college, for their assistance in the early stages of the work. The controlled rubber specimens were kindly supplied through the Ministry of Supply Advisory Service on Rubber.

REFERENCES

(1) GEHMAN. *J. Appl. Phys.*, **13**, p. 402 (1942).
(2) DILLON, PRETTYMAN and HALL. *J. Appl. Phys.*, **15**, p. 309 (1944).
(3) GEHMAN, WOODFORD and STAMBAUGH. *Industr. Engng Chem.*, **33**, p. 1032 (1941).
(4) STAMBAUGH. *Industr. Engng Chem.*, **34**, p. 1358 (1942).
(5) KOSTEN. *Proc. Rubber Tech. Conf.*, p. 987 (1938).
(6) FLETCHER and GENT. *Instn Rubber Ind. Conference on Aspects of Rubber in Engng*, p. 1–17 (1950).
(7) WILKINSON and GEHMAN. *Analyt. Chem.*, **22**, p. 283 (1950).
(8) ROELIG. *Proc. Rubber Tech. Conf.*, p. 821 (1938).
(9) ALEKSANDROV and LAZURKIN. *Acta phys.-chim. URSS*, **12**, pp. 647–668 (1940).
(10) ALFREY. *Mechanical Behaviour of High Polymers* (New York: Interscience Pubs. Inc., 1948).
(11) NAUNTON and WARING. *Trans. Instn Rubb. Ind.*, **14**, p. 340 (1939).

The ignition of wood by radiation

By D. I. LAWSON, M.Sc., M.I.E.E., F.Inst.P., and D. L. SIMMS, B.Sc., Fire Research Station, Boreham Wood, Herts

[*Paper first received* 15 *January, and in final form* 6 *June*, 1952]

The minimum intensities of irradiation required to ignite wood, with and without the presence of a pilot flame, have been determined, and found to be approximately constant for nearly all species. Empirical expressions have been obtained which relate the time taken to ignite with the intensity of irradiation and the density of the wood for these two types of ignition.

Although wood is probably the most common combustible material in general use, little attention has been paid to the factors which contribute to its ignition. Most of the literature deals with tests which are applicable only to special conditions, the only published work of a general nature being that of Bamford, Crank and Malan[1] relating to the thermal conditions in burning wood. The work described in this paper sets out to relate the time taken to ignite wood, when subjected to various intensities of irradiation, with the thermal properties of the wood. Two types of ignition have been studied; first, with a pilot flame half an inch from the plane of the surface acting as igniting source, and second, ignition without a pilot flame. This has been termed spontaneous ignition. The problem is not one which yields readily to a theoretical treatment, for combustible materials by their very nature change during the course of irradiation. Nevertheless, by making a theoretical analysis in which the material to be ignited is considered to be an inert substance, the parameters in which the experimental results may be interpreted have been found.

EXPERIMENTAL PROCEDURE AND RESULTS

The materials examined had densities ranging from 0·24 to 0·72 g/cm³. These are listed below:

(i) 0·5 in thick fibre insulation board;
(ii) 0·75 in thick western red cedar (*thuja plicata*);
(iii) 0·75 in thick American whitewood (*liriodendron tulipifera*);
(iv) 0·75 in thick African mahogany (*khaya ivorensis*);
(v) 0·75 in thick freijo (*cordia goeldiana*);
(vi) 0·75 in thick oak (*quercus robur*);
(vii) 0·75 in thick iroko (*chlorophora excelsa*).

Specimens 2 in square were cut so that the faces were parallel with the grain and these were dried for 24 h in an oven at 90° C. After drying they were allowed to cool for two days or more over phosphorus pentoxide in a desiccator. The density was obtained from the volume and the weight, when oven-dry. The results are shown in Table 1, together

Table 1. *The thermal properties of the materials tested*

Material	*Density* g/cm³	*Thermal conductivity* ⊥ *to grain*, cal/cm²/sec/° C ×10⁵	*Specific heat*, cal/g/° C	$K\rho s \times 10^5$ C.G.S. units
Fibre insulation board	0·24	8·5	0·34	7
Western red cedar	0·36	21·2	0·34	26
American whitewood	0·47	28·5	0·34	45
African mahogany	0·56	32·5	0·34	62
Freijo	0·58	33·0	0·34	65
Oak	0·61	35·4	0·34	73
Iroko	0·72	41·2	0·34	101

with the values of thermal conductivity perpendicular to the grain, taken from a paper by Maclean.[2] The value of 0·34 cal/g for the specific heat of the various species of wood is taken from a publication by Dunlap.[3]

The specimen was placed in a holder on which was mounted a pilot gas jet, length 0·5 in, giving a flame 0·5 in above and in front of the surface to be irradiated. The specimen holder was rapidly moved into place in front of a radiation panel and the time taken for the pilot flame to ignite the combustible gases evolved was noted. The radiation panel, which was a surface combustion heater 1 ft square, burned a coal gas/air mixture; its temperature was found by means of a total radiation pyrometer. This enabled the intensity of irradiation, I, to be calculated at the surface of the specimen, for, if the temperature of the radiant panel is T_1, and that of the surroundings is T_3, the intensity I incident upon the specimen is given by

$$I = \epsilon\phi\sigma(T_1^4 - T_3^4)$$

where ϵ is the emissivity of the radiator from a point on the surface of the specimen: for the radiation surface used, this approximates to unity.
σ is the Stefan–Boltzmann constant
$= 1{\cdot}37 \times 10^{-12}$ cal/cm²/sec/° C⁴, and
ϕ is the configuration factor.

For a square radiator

$$\phi = \frac{4}{\pi}\,\frac{l}{(l^2 + d^2)^{\frac{1}{2}}}\tan^{-1}\frac{l}{(l^2 + d^2)^{\frac{1}{2}}}$$

where l is half the length of the square radiator (6 in)
and d is the distance of the specimen from it.

The experiment was repeated for intensities of irradiation ranging from 0·15 to 1·50 cal/cm²/sec obtained by altering the distance of the specimen from the radiator. These results are shown in Fig. 1. Experiments were next carried out without the use of a pilot flame. The specimen was irradiated until it burst into flame. The times taken for ignition to occur for various intensities of incident radiation are shown in Fig. 2. Most points on the curves are the mean of three experiments. The extreme variation was about ± 25%, but most results were within the range ± 10% of the mean value. Fibre insulation board gave the most consistent results.

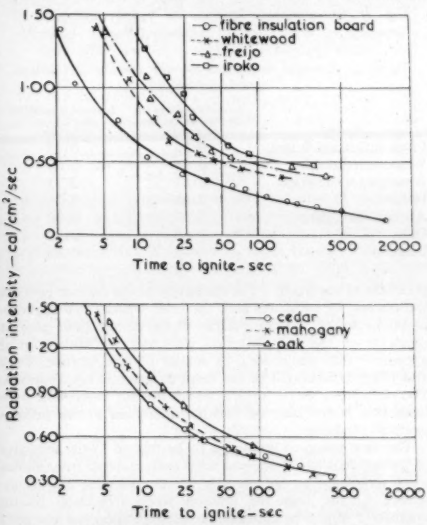

Fig. 1. Pilot ignition of wood; time to ignite as a function of intensity of radiation

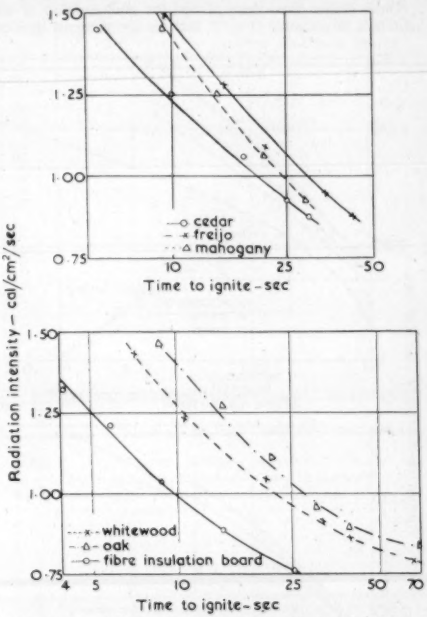

Fig. 2. Spontaneous ignition of wood; time taken to ignite as a function of intensity of radiation

DISCUSSION OF RESULTS

If radiation of intensity I falls on a slab of inert material it may be shown,[4] assuming that the surface cooling is Newtonian and that there is no appreciable rise in temperature of the back surface during the experiment, that the surface temperature rise θ after a sufficiently long time ($t > 2K\rho s/\Psi^2$) is given by

$$\theta = \frac{I}{\Psi}\left[1 - \frac{1}{\Psi}\left(\frac{K\rho s}{\pi t}\right)^{\frac{1}{2}}\right] \qquad (1)$$

where K is the thermal conductivity,
ρ is the density,
s is the specific heat of the material,
and Ψ is the rate of loss of heat per unit area for each degree rise in temperature.

If wood were an inert material which ignited at a time t when the surface had been brought to some critical temperature, the graph of I plotted against $I/\sqrt{t}$ would be a straight line for values of time which were sufficiently long

and the intercept on the intensity axis when $I/\sqrt{t} = 0$ would be the critical intensity I_0, that is, the minimum intensity of irradiation at which ignition can occur.

This may be seen by writing equation (1) in the form

$$I_0 = I(1 - a\sqrt{t})$$

where $I_0 = \theta\Psi$

and $a = (1/\Psi)\sqrt{(K\rho s/\pi)}$

These graphs have been plotted for pilot ignition of the materials investigated (Fig. 3) and for spontaneous ignition

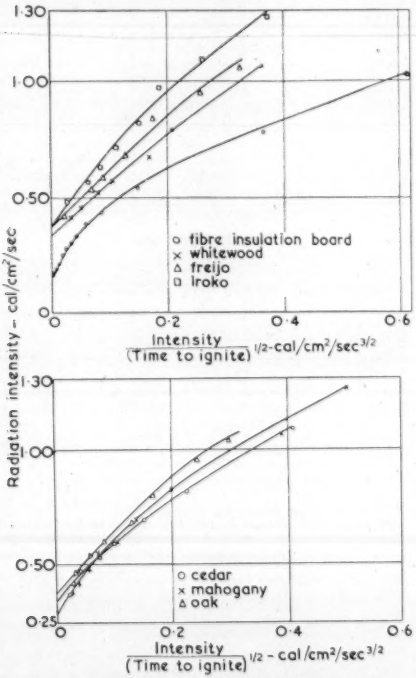

Fig. 3. Pilot ignition of wood; intensity of radiation as a function of intensity/(time to ignite)$^{1/2}$

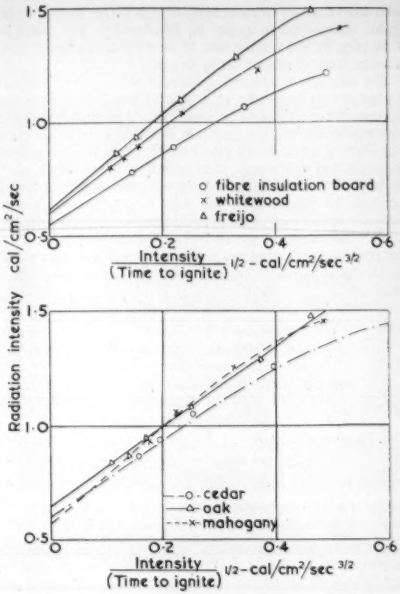

Fig. 4. Spontaneous ignition of wood; intensity of radiation as a function of intensity/(time to ignite)$^{1/2}$

Table 2. *Critical intensities for the ignition of various species of wood*

Material	*Intensity required for spontaneous ignition, cal/cm²/sec*	*Intensity required for pilot ignition, cal/cm²/sec*
Fibre insulation board	0·57	0·15
Western red cedar	0·64	0·35
American whitewood	0·61	0·35
Freijo	0·63	0·36
African mahogany	0·57	0·30
Oak	0·66	0·36
Iroko	—	0·36

(Fig. 4). The critical intensities for spontaneous and pilot ignition are both almost independent of the species of wood for those tested; the values are shown in Table 2. The only large variations occur in the values for fibre insulation board and iroko; for the latter, the critical intensity for spontaneous ignition is much higher than those of other species.

The critical intensity might be expected to be independent of the species, since it is the intensity of irradiation required to ignite the wood after a long time, by which time the transfer of heat into the wood has ceased. Under this condition the thermal constants of the wood have no effect. The only operative factors are the emissivity of the wood surface and the nature and proportion of the gaseous decomposition products of the wood. The emissivity of the surface governs the cooling by radiation and, for most woods, this approximates to unity. Precise analysis of the combustible gaseous products of the woods tested were not available, but it appears[5] that about 30% by weight of pine, spruce, birch and beech is liberated in the form of gaseous combustibles. The differences in the critical intensities for iroko and fibre insulation board may be due to differences in the decomposition products.

The time taken to ignite has to be related to the intensity of the incident radiation, and since each material only ignites when irradiated by an intensity greater than the critical intensity I_0, the time for ignition when irradiated by an intensity I might be expected to depend upon the quantity $(I - I_0)$. In order to explore this relation, graphs of the results for each material were plotted relating the quantities

$\log (I - I_0)$ and $\log t$. For the results for each material, and for both types of ignition, a straight line having the same slope could be drawn through the experimental points. Thus the required law for pilot ignition is $(I - I_p)t^{2/3} = A$, where A is a constant which varies with the different species investigated, as may be seen from the curves, shown in Fig. 5. For spontaneous ignition, the law is $(I - I_s)t^{4/5} = B$, where B is a constant, which again varies with the different

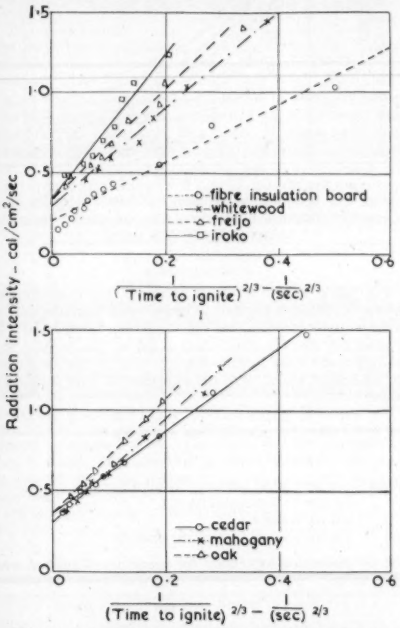

Fig. 5. Pilot ignition of wood; intensity of radiation as a function of 1/(time to ignite)$^{2/3}$

species considered. These are shown in Fig. 6. Equation (1) is founded on two hypotheses, (i) that wood is an inert material, and (ii) that the surface cooling is Newtonian, which suggests that the thermal properties should appear in the expression relating the intensity of irradiation with the time to ignite in the form of the product $K\rho s$.

Graphs were therefore plotted of $(I - I_p)t^{2/3}$ against $K\rho s$ for the different materials investigated and a straight line relationship was obtained. This is shown in Fig. 7 and indicates that the required expression for pilot ignition is

$$(I - I_p)t^{2/3} = 0{\cdot}025 \times 10^6(K\rho s + 68 \times 10^{-6}) \qquad (2)$$

where I_p is the critical intensity for pilot ignition.

For spontaneous ignition, $(I - I_s)t^{4/5}$ is plotted against $K\rho s$ (Fig. 8) and this indicates that the required expression is

$$(I - I_s)t^{4/5} = 0{\cdot}05 \times 10^6(K\rho s + 35 \times 10^{-6}) \qquad (3)$$

where I_s is the critical intensity for spontaneous ignition.

A family of curves for given values of $K\rho s$ are also plotted

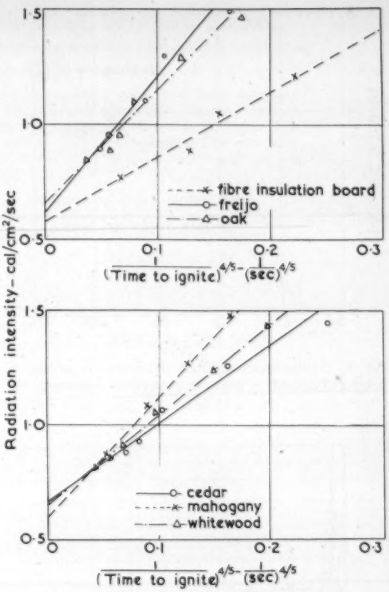

Fig. 6. Spontaneous ignition of wood; intensity of radiation as a function of 1/(time to ignite)$^{4/5}$

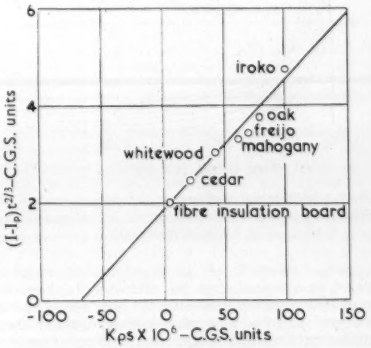

Fig. 7. Pilot ignition of wood; (intensity in excess of critical) × (time to ignite)$^{2/3}$ as a function of $K\rho s$

for both pilot and spontaneous ignition (Figs. 9 and 10). Since the value of $K\rho s$ over the species investigated varied between (10 and 100 $\times 10^{-6}$), the quantity 68×10^{-6} appearing in the bracket in expression (2) considerably reduces the variations in the time for pilot ignition due to differences in $K\rho s$. The corresponding numerical factor for

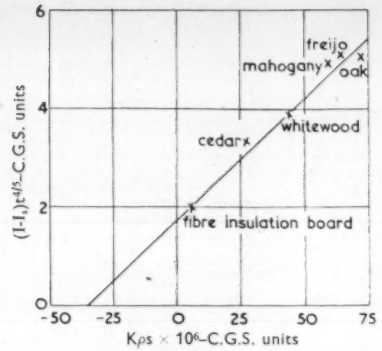

Fig. 8. Spontaneous ignition of wood; (intensity in excess of critical) × (time to ignite)$^{4/5}$ as a function of $K\rho s$

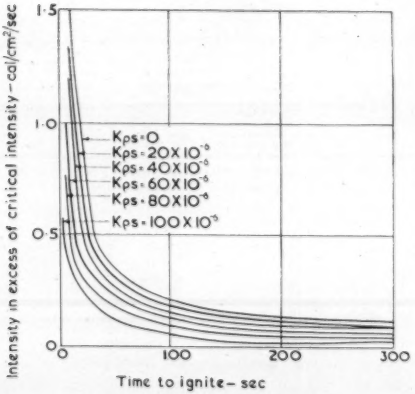

Fig. 9. Pilot ignition of wood; intensity in excess of critical as a function of time to ignite for various values of $K\rho s$ (C.G.S. units)

spontaneous ignition is not so large; thus the instant of ignition is more dependent on the value of $K\rho s$ and therefore varies more with the species investigated. For a given intensity of incident radiation with pilot ignition, ignition always occurs sooner than with spontaneous ignition. One cause may be that since the radiation energy density in the vicinity of the irradiated surface is much less than that of a pilot flame, before spontaneous ignition can occur, a richer mixture requiring a lower energy density for ignition must be formed, and this concentration of combustible gas takes longer to generate. If the radiation energy were too low then the mixture may never attain the required concentration for spontaneous ignition although pilot ignition would be possible.

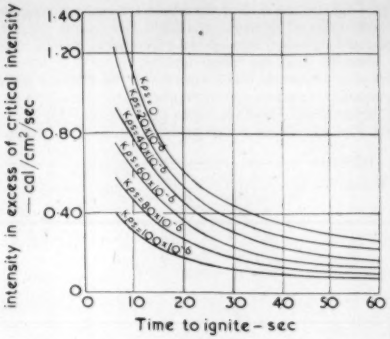

Fig. 10. Spontaneous ignition of wood; intensity in excess of critical as a function of time to ignite for various values of $K\rho s$ (C.G.S. units)

CONCLUSIONS

For nearly all the materials examined, the minimum intensity of radiation required to ignite wood spontaneously is approximately constant, the only exception being iroko. If a small pilot flame is placed near to the surface, ignition will take place at a lower incident intensity which is again constant for all species tested, with the exception of fibre insulation board.

For intensities greater than the critical intensity it was found the time t taken for pilot ignition was given by

$$(I - I_p)t^{2/3} = 0{\cdot}025 \times 10^6(K\rho s + 68 \times 10^{-6})$$

where I_p is the critical intensity for pilot ignition,
K is the thermal conductivity,
ρ is the density
and s is the specific heat of the material.

The corresponding expression for spontaneous ignition was found to be

$$(I - I_s)t^{4/5} = 0{\cdot}05 \times 10^6(K\rho s + 35 \times 10^{-6})$$

where I_s is the critical intensity for spontaneous ignition.

ACKNOWLEDGEMENT

The work described in this paper forms part of the programme of the Joint Fire Research Organization of the Department of Scientific and Industrial Research and Fire Offices' Committee; the paper is published by permission of the Director of Fire Research.

REFERENCES

(1) BAMFORD, C. H., CRANK, J., and MALAN, D. H. *Proc. Camb. Phil. Soc.*, **42**, pp. 168–82 (1946).
(2) MACLEAN, J. D. *Trans Amer. Soc. Heat. Vent. Engrs*, **47**, p. 1184 (1941).
(3) DUNLAP, F. *U.S. Department of Agriculture, Forest Service Bulletin, No.* 110 (1912).
(4) LAWSON, D. I., FOX, L. L., and WEBSTER, C. T. *Dep. Sci. Industr. Res. and Fire Offices' Committee, Fire Res. Spec. Rep., No.* 1 (H.M. Stationery Office (1952).
(5) BUNBURY, H. M. *The Destructive Distillation of Wood.* Table XLVI, p. 79 (London: Benn Brothers, 1923).

The properties of semi-conducting ceramic glaze

By D. H. Lucas, B.A., A.Inst.P., British Electricity Authority, Research Laboratories, Leatherhead

[*Paper received* 21 *April*, 1952]

The surface resistivity and contact resistance of semi-conducting glaze have been measured over the range of temperature, − 177 to 110° C. The rectifying effect with a metal point and the thermo-electric power indicate that the conduction process is electronic (*n*-type). The conductivity is thought to be mainly due to mixed crystals of $ZnCr_2O_4$–Fe_3O_4. The deterioration of glaze in service is due to electrolytic corrosion occurring at the interface with surface films of water.

The use of semi-conducting glaze to control the surface resistivity, and hence the voltage distribution of outdoor insulators, has been described.[1, 2] These descriptions covered the constitution and properties of semi-conducting glaze and also stated that in one way its performance was disappointing. Although, as a glaze, it might have been expected to have excellent durability and weather resistance, it was found to deteriorate in service, and in a bad case might become unserviceable in a few weeks. It is the purpose of the present paper to explain the nature of this process of failure and to add to the information on the properties of the glaze.

PHYSICAL PROPERTIES

Dependence of glaze resistance on temperature and voltage. At a number of temperatures the glaze was subjected to a range of currents from the smallest measurable to the highest that could be used without appreciable heating of the glaze. The contacts were of Aquadag, each 2 mm wide. In each case two specimens of different lengths were used. For a number of currents, by simultaneous equations for the two specimens, the measured resistance was resolved into its two components—the surface resistivity of the glaze and the contact resistance per cm. The results are shown plotted in Figs. 1 and 2. It is apparent that the resistance of the glaze is reduced when the voltage is increased and this is quite independent of any heating effect. However, the resistance tends to a fairly obvious limit as the voltage tends to zero and this limit is taken as the resistance at any given temperature.

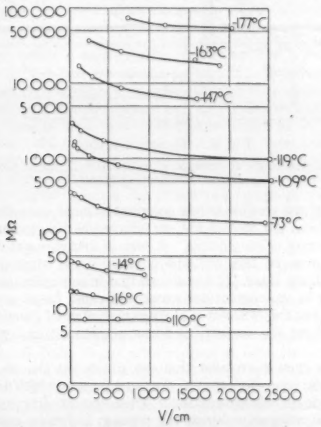

Fig. 1. Surface resistivity of glaze

This resistance is shown plotted against $1/T$ in Fig. 3. It shows a continuous deviation from the straight line that would be expected for a simple semi-conductor.

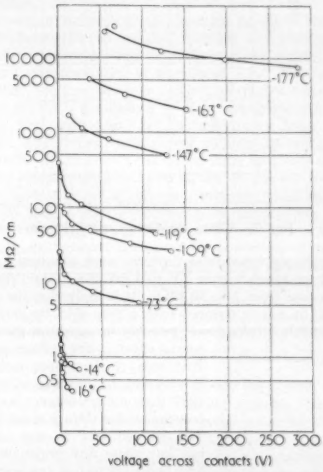

Fig. 2. Contact resistance of graphite-glaze contact

Glaze constituents. The semi-conducting glaze in question consists of ordinary ceramic glaze containing a suitable mixture of Cr_2O_3, ZnO and Fe_3O_4. The nature of the reaction between these oxides and the constituents of the ordinary glaze is not fully known. However, it is likely that mixed crystals of $ZnCr_2O_4$ and Fe_3O_4 are formed and it has been shown[3] that the resistivity curve of such mixed crystals is of the form shown in Fig. 4. It seems probable that the mixed crystal, $ZnCr_2O_4$–Fe_3O_4, is responsible for the main conductivity of the glaze, but that the curve of Fig. 4 is modified to the curve of Fig. 3 by the many other chemical compounds which may be present.

Voltage sensitivity of glaze resistivity and contact resistance. The decrease of resistivity with increase of voltage gradient is only pronounced when the voltage gradient is high and is in any case a normal property of semi-conductors. The decrease of contact resistance with increase of voltage roughly corresponds to the resistivity change at high voltage gradients, but at low voltages the effect is very marked and it appears that the contact resistance increases without limit as the voltage tends to zero. A specimen was prepared of relatively great length of contact (300 cm) so that even with

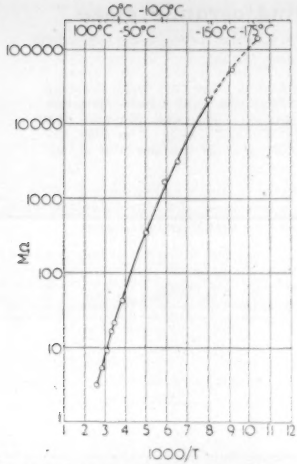

Fig. 3. Glaze resistivity—temperature

small voltages measurable currents were obtained. As the applied voltage fell from 2 V to 1 mV the contact resistance per cm rose from 2 to 50 MΩ. It is likely that the glaze is covered, or nearly covered with a very thin insulating film and that this breaks down, possibly by quantum mechanical tunnel effect, as the voltage increases from zero. If the surface of the glaze is removed by rubbing with emery cloth the contact resistance is virtually constant as the voltage tends to zero. The surface film is not complete but has many tiny punctures. If a fine point contact is traversed over the glaze it normally makes no electrical contact, provided the test voltage is low, but occasionally contact is made. The size of these minute holes is of the order of 0·02 mm. Their area is a few per cent of the total glaze area.

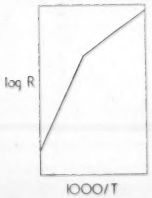

Fig. 4. Type of resistivity curve for mixed crystals of $ZnCr_2O_4$ and Fe_3O_4

If a number of these point contacts is tested for rectifying properties, by putting each in series with a supply of 50 c/s a.c. and a long period galvanometer, the galvanometer occasionally deflects. The deflexions are invariably in the same direction and indicate that the direction of easy current flow is from metal to glaze. According to the theory of rectification of Schottky and Hartman[4] this implies that the conduction process is *n*-type.

Thermo-electric power. The thermo-electric power of the glaze was measured to give further evidence on the nature of the conduction process. A sample of porcelain, glazed with semi-conducting glaze, was cut from a cap-and-pin insulator using a metal bonded diamond wheel. The sample had the shape shown in Fig. 5 and the two ends were immersed in mercury cups. The mercury made good electrical and thermal contact with the glaze, so that voltage and temperature measurements could be conveniently made. It was found necessary to have the mercury thoroughly dry to avoid electrolytic voltages which, with undried mercury, were of the same order as the measured quantity. It was also necessary to provide a very sensitive galvanometer for the potentiometer used, because the source impedance was many megohms. The thermo-electric voltages finally measured were closely linear with temperature and reproducible, and indicated a thermo-electric power of 290 μV/° C. The direction of current flow at the cold junction is from mercury to glaze, which again implies that the conduction is *n*-type.

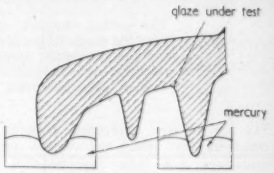

Fig. 5. Glaze with mercury contacts

GLAZE DETERIORATION

Experience in service. A diagram of a typical insulator is shown in Fig. 6. When the insulator is in service, a.c. flows from cap to pin by way of the glaze. A layer of cement is interposed in the current path at both cap and pin. The glaze deteriorates at both these places, but more severely near the pin. Failure also occurs at other places on the glaze surface but not with the same frequency or intensity. When the glaze-cement contact at the pin is silvered over, the attack is less severe, and when an area of higher conductivity glaze is provided at the contact there is a further improvement.

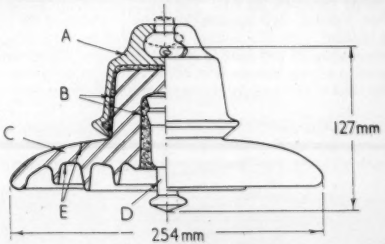

Fig. 6. Typical insulator

A, metal cap; *B*, cement; *C*, porcelain; *D*, metal pin; *E*, semi-conducting glaze.

However, the trouble is not completely cured, and the areas remote from the contact are not affected by this treatment.

The nature of the process. It was at first thought that the contact was in fact a "bad contact," and that sparking destroyed the glaze. It was shown that in some circumstances sparking at the contact did occur and could be an accessory process, but this was not a likely explanation of deterioration remote from the contact, and was abandoned as a primary cause.

It was then postulated that the attack on the glaze was electrolytic corrosion, that is, the same process which dissolves the anode in electro-plating. This was at first sight an unnatural suggestion since the process is firmly associated with metals whereas the material deteriorating on the insulator

is a glaze. It is, however, a conducting glaze and this is the significant point. It can act as an anode and in so doing will be attacked by the cations it discharges. The suggestion might also appear unlikely because the current used is a.c. and in the case of the electro-plating cell, for instance, the metal removed during one half cycle of a.c. is restored during the next and the net electrolytic effect is nil. However, if the process in the case of the glaze is not *exactly* reversible, in time a net result will be apparent. If the process is irreversible, a.c. attack will be as severe as d.c.

The proof that semi-conducting glaze was susceptible to electrolytic attack was made difficult by the high resistance of the glaze. In principle, all that was required was a piece of glaze dipping into an electrolyte at one end and making contact with a conductor at the other. In practice, if the conductor was near the surface of the electrolyte, the latter rapidly bridged the gap and defeated the aims of the arrangement; if the gap was large enough to meet this hazard, its total resistance was so large that only a minute current flowed. After many partly successful attempts the arrangement shown in Fig. 7 was devised.

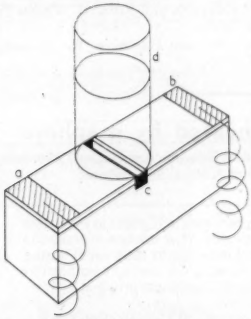

Fig. 7. Electrolytic cell with glaze electrodes

Graphite contacts *a* and *b* were painted on the glaze. A complete break *c* was made in the continuity of the glaze but it was bridged by an electrolyte. The electrolyte was contained by the glass cylinder, *d*, which was sealed to the specimen with Araldite (made by Aero Research Ltd.). The current density used was of the same order as is used on insulators—100 μA/cm. After current had been passed for a few hours, deterioration was visible to the practised eye. After a week, severe attack was obvious. The duration of a test was limited because the attack took place in the region of the seal and this was successively undercut until the electrolyte could escape.

The test was carried out with a.c. and with d.c., using as electrolytes a solution of salt and rain water (from an industrial area). When d.c. was used, the anodic glaze became covered with rust-like encrustations, turned lighter in colour and ultimately became pitted. The cathodic glaze was relatively lightly attacked and received a deposit of white crystals. Bubbles of gas were evolved at both electrodes and were assumed to be hydrogen and oxygen produced electrolytically. When a.c. was used the attack was, of course, symmetrical and appeared to be at least as severe as with d.c. The test was finally carried out without cutting the glaze at *c*, but the results were quite unaffected. The conductivity of the electrolyte was so much higher than that of the glaze that the bulk of the current left the glaze just as before.

The actual mass of glaze attacked in the cell, before the seal was broken, was so small that analysis of the products of attack was very difficult. It was possible to prove conclusively, however, that iron had gone into solution during the attack. It is probable that the other metals present in the glaze were also dissolved while the glaze was anodic. It also seems likely that the glaze was subjected to a different sort of attack while it was cathodic. It was seen that there was a slight attack on the cathode in the d.c. case and it is possible that the silica or even the alumina of the glaze was dissolved. If this alternating form of attack does in fact occur with a.c., it explains the effectiveness of a.c. in destroying the glaze.

Deterioration in service. It remains to show that the artificial electrolytic cell just described has its counterpart on the insulator in service and to show that the experience as previously described can be accounted for. The films of water which form on insulators when the relative humidity is above about 75% are known to have strong electrolytes in solution, and may have surface resistivities from 10 kΩ upwards. The surface resistivity of semi-conducting glaze is of the order of 20 MΩ. The water films normally tend to cover the whole insulator, but it can be shown that this situation cannot be stable because the current which would be carried by such a film would raise the temperature of the insulator sufficiently to dry the film. In practice, as soon as the drying process has interrupted the continuity of the film, the current is reduced and the majority of the film is not dissipated. A dry belt is created round the insulator and remains in equilibrium with the current through the film. If the resistance of the belt tends to fall, the current increases and its heating effect reverses the tendency, and conversely. Other things being equal, the dry belt will tend to form where the current density is highest.

In the case of the cap-and-pin insulator the current density is highest at the contact with the pin cement. Since the cement will normally have a much lower resistance than the glaze, it will remain cool and wet. The situation is shown in Fig. 8. At *a* and *b* there is a passage of current between glaze and film. *a* is always at the point where the glaze joins the cement and will be severely attacked, particularly because the cement is charged with electrolytic salts and furthermore acts as a sponge. The point *b* will tend to wander and the total attack will be more diffuse.

A dry belt may also be formed where a portion of the insulator is sheltered from the deposition of pollution and

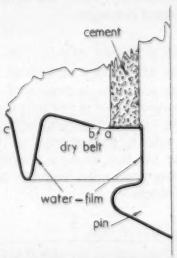

Fig. 8. The break in the water-film

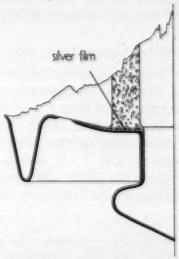

Fig. 9. The effect of silvering

water. Again attack will occur at the edges of the dry belt. Regions of deterioration are found at places such as *c*, Fig. 8. In general, wherever the thickness of the glaze or the thickness of the film changes, there will be a transfer of current and deterioration will follow.

If the cement is silvered over as shown in Fig. 9 the attack is known to be less severe. The dry belt now forms at the edge of the silver. The silver will remain wet since it has a low resistance and the current will have little heating effect. The attack will be less severe because the line of contact is much longer and the current density is less. Further, the tendency of the cement to aggravate the attack has been countered.

If high conductivity glaze is used at the contact it merges gradually into the main glaze. Where the conductivity is high the glaze remains wet and the dry belt is more remote from the pin. As in the silvered case, the line of contact is longer and cement hazard is removed. Again, since the transition is gradual the location of the dry belt probably varies from day to day and the attack is distributed.

CONCLUSIONS

The resistivity of the glaze is nearly constant with variation of voltage gradient when the latter is small, but the resistivity decreases considerably when the voltage gradient is large. The resistivity of the glaze increases with decrease of temperature. Over a large range, the curve deviates from the simple semi-conductor law, but it shows some resemblance to the curve for mixed crystals of $ZnCr_2O_4$–Fe_3O_4. The contact resistance between graphite and the glaze varies considerably with voltage and appears to tend to infinity as the voltage tends to zero. There is a thin insulating film over the surface of the glaze which is not, however, quite complete. The rectifying effect with a fine metal point and the thermo-electric power, both indicate that the conduction process is *n*-type. The cause of deterioration of semi-conducting glaze in service is electrolytic corrosion.

ACKNOWLEDGEMENT

This work was carried out in the Research Laboratories of the British Electricity Authority under the direction of Dr. J. S. Forrest, who has taken an active interest in the progress of the investigations.

REFERENCES

(1) Forrest, J. S. *J. Sci. Instrum.*, **24**, p. 211 (1947).
(2) Forrest, J. S. *Bull. Soc. Belge Elect.*, **66**, No. 3 (1950).
(3) Verwey, Haayman and Romeyn. *Philips Tech. Rev.*, **9**, p. 243 (1947).
(4) Schottky, W., and Hartman, W. *Z. techn. Phys.*, **16**, p. 512 (1935).

Heat flow in an infinite medium heated by a sphere

By H. Goldenberg, M.Sc., A.R.C.S., The British Electrical and Allied Industries Research Association, Greenford, Middlesex, and Professor C. J. Tranter, M.A., Military College of Science, Shrivenham

[*Paper received* 8 *April*, 1952]

A solution is given of the heat conduction problem in which a sphere generating heat at a constant rate is embedded in an infinite medium of different thermal properties. The solution is of use in a consideration of the disinfestation and sterilization of biological materials by differential heating due to the application of h.f. fields. Typical curves are given showing the transient temperature at the centre of the sphere for various ratios of the physical constants involved.

The disinfestation and sterilization of biological materials by differential heating due to the application of h.f. fields has led to a demand for the solution of the heat conduction problem in which a homogeneous sphere generating heat at a constant rate per unit volume is embedded in a homogeneous infinite medium.(1) A previous paper by one of the authors(2) has given the solution of this problem in a form suitable for practical application when the physical constants of the sphere and medium are equal. The present paper gives the solution to the more general problem in which the sphere and medium possess different physical constants.

THE EQUATIONS AND THEIR FORMAL SOLUTION

Consider a homogeneous sphere of radius a embedded in an infinite homogeneous medium and heat is produced in the sphere for time $t > 0$ at the constant rate A per unit time per unit volume. Both the sphere and medium are initially at zero temperature. If suffixes 1 refer to the sphere, 2 to the medium, and V, K, and k denote the temperature, thermal conductivity and diffusivity respectively, we require the solution of the boundary value problem—

$$\left.\begin{aligned} \frac{1}{k_1}\frac{\partial V_1}{\partial t} &= \frac{1}{r^2}\frac{\partial}{\partial r}\left(r^2\frac{\partial V_1}{\partial r}\right) + \frac{A}{K_1}, 0 \leqslant r < a, \\ \frac{1}{k_2}\frac{\partial V_2}{\partial t} &= \frac{1}{r^2}\frac{\partial}{\partial r}\left(r^2\frac{\partial V_2}{\partial r}\right), r > a, \end{aligned}\right\} t > 0 \quad (1)$$

$$V_1 = V_2 = 0, \text{ when } t = 0 \quad (2)$$

$$\left.\begin{aligned} V_1 &= V_2 \\ K_1\frac{\partial V_1}{\partial r} &= K_2\frac{\partial V_2}{\partial r} \end{aligned}\right\} \text{ when } r = a \quad (3)$$

$$V_1 \text{ finite as } r \to 0 \text{ and } V_2 \text{ finite as } r \to \infty \quad (4)$$

Introducing the Laplace transform of V, defined by

$$\bar{V} = \int_0^\infty e^{-pt}V(t)dt = L[V(t)]$$

the subsidiary equations are

$$\left.\begin{aligned} \frac{d^2}{dr^2}(r\bar{V}_1) - rq_1^2\bar{V}_1 &= -\frac{rA}{K_1 p}, 0 \leqslant r < a \\ \frac{d^2}{dr^2}(r\bar{V}_2) - rq_2^2\bar{V}_2 &= 0, r > a \end{aligned}\right\} \quad (5)$$

$$\left.\begin{aligned} \bar{V}_1 &= \bar{V}_2 \\ K_1\frac{d\bar{V}_1}{dr} &= K_2\frac{d\bar{V}_2}{dr} \end{aligned}\right\} \text{ when } r = a \quad (6)$$

$$\bar{V}_1 \text{ finite as } r \to 0 \text{ and } \bar{V}_2 \text{ finite as } r \to \infty \quad (7)$$

where $q_1^2 = p/k_1$, $q_2^2 = p/k_2$.

The solution of equations (5), (6) and (7) is

$$\bar{V}_1 = \frac{Ak_1}{K_1 p^2}\left[1 + \frac{K_2}{K_1}\frac{a \sinh q_1 r}{r D(p)}\right] \tag{8}$$

$$\bar{V}_2 = \frac{Ak_1}{K_1 p^2}\frac{a}{r}\frac{[\sinh q_1 a - q_1 a \cosh q_1 a]\exp[-q_2(r-a)]}{(1+q_2 a)D(p)} \tag{9}$$

where

$$D(p) = \frac{\sinh q_1 a - q_1 a \cosh q_1 a}{1 + q_2 a} - \frac{K_2}{K_1}\sinh q_1 a \tag{10}$$

The inversions to be performed are simplified by using the theorem[3] that if

$$L[\phi(t)] = \Phi(p), \text{ then } L[\lambda\phi(\lambda t)] = \Phi(p/\lambda) \tag{11}$$

where λ is any real positive number. Writing

$$\gamma_1 = \frac{a^2}{k_1}, c = 1 - \frac{K_2}{K_1}, b = \frac{K_2}{K_1}\sqrt{\left(\frac{k_1}{k_2}\right)}, \sigma = \left(\frac{r}{a} - 1\right)\sqrt{\left(\frac{k_1}{k_2}\right)} \tag{12}$$

and

$$F(p) \equiv (c - b\sqrt{p})\sinh\sqrt{p} - \sqrt{p}\cosh\sqrt{p} \tag{13}$$

this leads to

$$V_1 = \frac{Ak_1}{K_1} f_1(t)$$

where

$$\frac{1}{\gamma_1} f_1(\gamma_1 t) = L^{-1}\left\{\frac{1}{p^2} + \frac{aK_2}{rK_1}\frac{[1+\sqrt{(k_1 p/k_2)}]\sinh[(r\sqrt{p})/a]}{p^2 F(p)}\right\} \tag{14}$$

and

$$V_2 = \frac{Ak_1}{K_1}\frac{a}{r} f_2(t)$$

where

$$\frac{1}{\gamma_1} f_2(\gamma_1 t) = L^{-1}\left[\frac{(\sinh\sqrt{p} - \sqrt{p}\cosh\sqrt{p})\exp(-\sigma\sqrt{p})}{p^2 F(p)}\right] \tag{15}$$

To evaluate $f_1(\gamma_1 t)$, $f_2(\gamma_1 t)$ in equations (14) and (15) we apply the Mellin inversion theorem for the Laplace transformation. This gives

$$\frac{1}{\gamma_1} f_1(\gamma_1 t) = \frac{1}{2\pi i}\int_{s-i\infty}^{s+i\infty} e^{pt}\left\{\frac{1}{p^2} + \frac{aK_2}{rK_1}\frac{[1+\sqrt{(k_1 p/k_2)}]\sinh[(r\sqrt{p})/a]}{p^2 F(p)}\right\} dp \tag{16}$$

where s is to be so large that all the singularities of the integrand lie to the left of the line $(s - i\infty, s + i\infty)$. Since the integrand in equation (16) has a branch point at the origin we use the contour of Fig. 1 with a cut along the negative real axis. In deriving $\bar{V}_2$ in equation (9) so that $\bar{V}_2 \to 0$ as $r \to \infty$, we have assumed that $-\pi < \arg p < \pi$ and it can be shown that, for physically possible values of b and c, no zeros of $F(p)$ occur within or on the contour of Fig. 1. It may also be shown that the integrals over the arcs BF, CA tend to zero as the radius of these arcs tends to infinity. The proof of this is somewhat tedious, but quite straightforward, and follows from a lemma given by Carslaw and Jaeger.[4] Hence the line integral in equation (16) can be replaced by a real infinite integral, derived from the integrals along CD and EF, together with the contribution from the small circle about the origin. On CD and EF we write $p = y^2\exp(-i\pi)$ and $y^2\exp(i\pi)$ respectively and find that the integral derived from those along CD and EF is

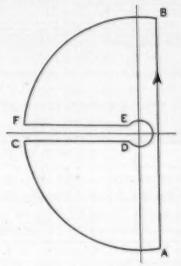

Fig. 1. Contour of integration

$$-\frac{2ab}{r\pi}\int_0^\infty \frac{\exp(-y^2 t)}{y^2}\frac{(\sin y - y\cos y)\sin(ry/a)}{[(c\sin y - y\cos y)^2 + b^2 y^2 \sin^2 y]}dy.$$

To evaluate the contribution from the small circle about the origin, the expansion of the integrand of equation (16) in ascending powers of p gives

$$\left[\frac{1}{3}\frac{K_1}{K_2} + \frac{1}{6}\left(1 - \frac{r^2}{a^2}\right)\right]\frac{1}{p} + \text{terms of higher orders},$$

so that the integral round the small circle gives, in the limit as its radius tends to zero,

$$\frac{1}{3}\frac{K_1}{K_2} + \frac{1}{6}\left(1 - \frac{r^2}{a^2}\right)$$

The final expression for the temperature inside the sphere, derived from equations (12) and (14) is therefore

$$V_1 = \frac{a^2 A}{K_1}\left\{\frac{1}{3}\frac{K_1}{K_2} + \frac{1}{6}\left(1 - \frac{r^2}{a^2}\right) - \frac{2ab}{r\pi}\int_0^\infty \frac{\exp(-y^2 t/\gamma_1)}{y^2}\frac{(\sin y - y\cos y)\sin(ry/a)}{[(c\sin y - y\cos y)^2 + b^2 y^2\sin^2 y]}dy\right\} \tag{17}$$

where

$$b = \frac{K_2}{K_1}\sqrt{\left(\frac{k_1}{k_2}\right)}, c = 1 - \frac{K_2}{K_1} \text{ and } \gamma_1 = \frac{a^2}{k_1} \tag{18}$$

The temperature at the centre of the sphere is

$$(V_1)_{r=0} = \frac{a^2 A}{K_1}\left\{\frac{1}{3}\frac{K_1}{K_2} + \frac{1}{6} - \frac{2b}{\pi}\int_0^\infty \frac{\exp(-y^2 t/\gamma_1)}{y}\frac{(\sin y - y\cos y)dy}{[(c\sin y - y\cos y)^2 + b^2 y^2\sin^2 y]}\right\} \tag{19}$$

Expressions corresponding to equations (17) and (19) for the particular case when the sphere and medium possess the same physical constants have previously been obtained by

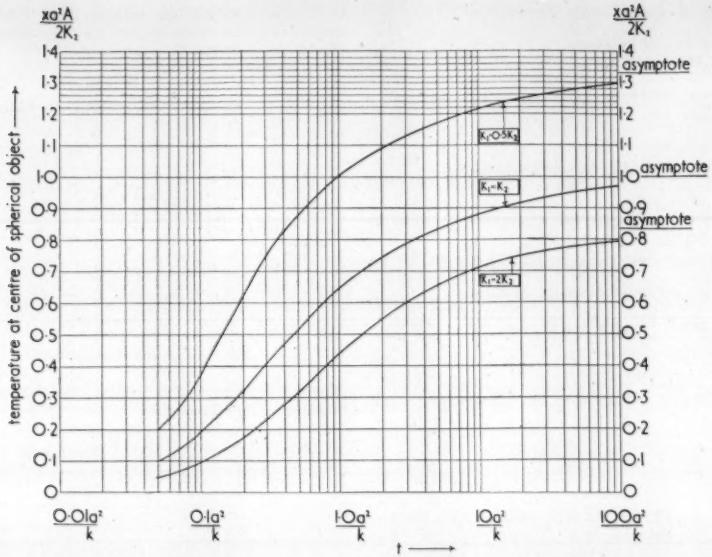

Fig. 2. Transient temperature at sphere centre for various ratios of thermal conductivities of the sphere and medium

K_1 = thermal conductivity of sphere.
K_2 = thermal conductivity of medium.
k = common thermal diffusivity of sphere and medium.
A = heat/unit volume/unit time generated in the spherical object only.
a = radius of sphere.
t = time from start of heating.

one of the authors[2] and a comparison of the results leads to some interesting equalities. For example, the equality corresponding to equation (19) is

$$\int_0^\infty \frac{\exp(-ay^2)}{y^3}(\sin y - y\cos y)dy = \frac{\sqrt{(\pi a)}}{2}\exp\left(-\frac{1}{4a}\right) - \frac{\pi}{2}\left(a-\frac{1}{2}\right)\operatorname{erf}\left(\frac{1}{2\sqrt{a}}\right)$$

for $a > 0$, and this may be verified by expansion and term by term integration.

A similar procedure applied to equations (15) gives, for the temperature outside the sphere,

$$V_2 = \frac{a^3A}{rK_1}\left\{\frac{1}{3}\frac{K_1}{K_2} - \frac{2}{\pi}\int_0^\infty \frac{\exp(-y^2t/\gamma_1)}{y^3} \frac{(\sin y - y\cos y)[by\sin y\cos\sigma y - (c\sin y - y\cos y)\sin\sigma y]dy}{[(c\sin y - y\cos y)^2 + b^2y^2\sin^2 y]}\right\} \quad (20)$$

with b, c, γ_1 as in equations (18) and

$$\sigma = \left(\frac{r}{a} - 1\right)\sqrt{\left(\frac{k_1}{k_2}\right)}$$

NUMERICAL RESULTS

The transient temperature at the centre of the sphere for the particular cases $K_1 = 2K_2$ and $K_1 = 0{\cdot}5K_2$, with the diffusivities of the sphere and medium equal in each case, has been computed from equation (19) by numerical integration. This integration is straightforward and, because of the rapid decrease of the term $\exp(-y^2t/\gamma_1)$ for increasing y and fixed t, is not too laborious. The resulting transient temperature curves are given in dimensionless form in Fig. 2. On the same diagram is reproduced, from a previous paper by one of the authors,[2] the corresponding curve when the sphere and medium possess equal physical constants. Similar computations applied to equations (17) and (20) would yield temperature curves for any point of the sphere or medium for any physical constants.

ACKNOWLEDGEMENTS

The authors wish to thank the Director of the Electrical Research Association and the Commandant of the Military College of Science for permission to publish this paper.

REFERENCES

(1) THOMAS, A. M. *Report Ref. W/T23* (London: Electrical Research Association, to be published).
(2) GOLDENBERG, H. *Brit. J. Appl. Phys.*, **2**, p. 233 (1951).
(3) CARSLAW, H. S., and JAEGER, J. C. *Operational methods in applied mathematics*, 2nd ed., p. 250 (Oxford: University Press, 1948).
(4) CARSLAW, H. S., and JAEGER, J. C. *Operational methods in applied mathematics*, 2nd ed., p. 76 (Oxford: University Press, 1948).

Some mechanical and adhesive properties of indium

By A. C. Moore, M.A., Ph.D., A.Inst.P.,* and D. Tabor, Ph.D., Research Laboratory on the Physics and Chemistry of Surfaces, Department of Physical Chemistry, Cambridge

[*Paper received* 29 *April*, 1952]

Experiments are described showing that (in the absence of surface contamination) the adhesion between indium and metal surfaces depends only on the area of contact and on the time of breaking. The detailed behaviour may be correlated with the creep properties of indium. With non-metals such as diamond, glass, thick metal oxides and certain plastics very strong adhesions to indium are observed whilst with polytetrafluoroethylene, which has a very low coefficient of friction, the adhesion is negligibly small. These results suggest that in the sliding of non-metals, adhesion at the interface plays a part in the frictional mechanism analogous to the cold-welding process in the friction of metals.

CREEP PROPERTIES OF INDIUM

Indium has been used by various workers to investigate the fundamental adhesive properties of ductile metals.[1-5] In an earlier paper[1] it was found that for clean surfaces the adhesion of indium to other metals depends on the time of loading. The following experiments show that this may be simply explained in terms of the creep properties of indium under tension and compression.

The yield stress of indium under tension was measured in a Hounsfield tensometer using indium tensile specimens cast in dry plaster-of-paris moulds. The specimens were cast with an initial diameter of 0·500 in but after stretching their diameter decreased and the experiment could then be repeated with the thinner specimen. As indium is self-annealing at room temperature the state of the specimen is essentially unchanged. The results for three mean diameters (0·500, 0·455 and 0·405 in) are plotted in Fig. 1. It is seen that the

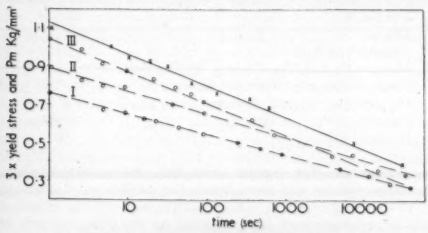

Fig. 1. Creep properties of indium

– – – –, 3 × yield stress Y of cylindrical indium specimens under tension as function of time of loading. Mean diameters of specimens: I, 0·500; II, 0·455; III, 0·405 in

———, mean pressure P_m over a spherical indenter (Meyer hardness) as function of time of loading. P_m is very nearly equal to $3Y$ for the most heavily deformed tensile specimen.

yield stress falls off logarithmically with time. Assuming the simple creep relation suggested by Dushman, namely:

$$\text{rate of creep} = Ae^{\alpha Y}$$

where Y is the stress and A and α are temperature dependent constants, it is easy to show that under the conditions of the test this reduces to a relation of the type

$$Y = \text{constant} - \frac{1}{\alpha}\log_e t$$

where t is the time. This relationship is followed by the curves in Fig. 1. It is seen that as the diameter of the tensile specimen decreases the yield stress increases. This is not work hardening in the ordinary sense of the word, but is probably due to the closing up of flaws in the indium as deformation proceeds.

Measurements were also made of the indentation hardness (Meyer hardness) or mean yield pressure P_m of a flat bar of cast indium using a lightly greased steel ball (diameter $\frac{1}{4}$ in) as the indentor and a load of 2 kg. The results are plotted in Fig. 1. It is seen that P_m falls off logarithmically with time and is nearly equal to $3Y$ when compared with the most heavily deformed tensile specimen. This is in good agreement with the theory of hardness of materials which do not work harden.[6]

Comparison with adhesion experiments. If a clean steel ball is pressed on to a clean indium surface with a constant load the force required to break the junctions (for a fixed time of breaking) steadily increases with the time of loading, though the adhesive force per unit area of contact remains constant. A typical result[2] is plotted in Fig. 2. These

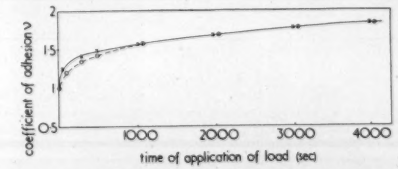

Fig. 2. Cofficient of adhesion of steel ball on clean indium surface as function of time of application of joining load for a fixed time of breaking

—×—, experimental values from paper by McFarlane and Tabor[2]
—o—o, values calculated from P_m in Fig. 1 assuming a constant breaking time of 10 sec.

results may be correlated with the creep experiments by assuming that if the surfaces are loaded for a time t and then pulled apart for the same time t the adhesive force will always be equal to the loading force whatever the value of t. If the time of loading is increased but the time of breaking is kept constant the adhesion will then increase proportionately to the creep growth of the area of contact. Assuming a constant breaking time of 10 sec for the results in Fig. 2 the Meyer hardness values from Fig. 1 have been used to calculate this increase. The calculated values are shown dotted and agree well with the experimental curve.

Rotation experiments. Some experiments were carried out on the adhesion of a clean copper hemisphere to a freshly scraped indium bar under constant load, with rotation about the axis of the hemisphere superposed. Rotation leads to a large increase of adhesion by as much as a factor of five,

* Now at Telecommunications Research Establishment, Malvern.

but the adhesive force per unit area of contact remains substantially constant if the time of breaking is kept constant. Practically the whole of the increase in adhesion is due to the growth in area of contact which occurs during rotation. This growth is due to the combined effect of thermal stress and shear stress on the plastic flow of the indium.[7]

Discussion. In all these experiments the specific adhesion, i.e. the adhesion per unit area of contact, is constant and depends only on the time of breaking of the junctions. To a first approximation, the specific adhesion for a given time of breaking is three times the uniaxial yield stress of indium as determined for the same time of stressing. These results are simple consequences of the fact that for the experiments described here, the interfacial adhesion is greater than the strength of the indium so that yielding always occurs in the indium itself. In the presence of contaminant films or for very short times of loading[5] this is no longer true and the adhesion behaviour is more complex.

ADHESION WITH NON-METALS

Adhesion experiments with indium have been extended to a number of non-metals. A modified apparatus was used in which one surface was held fixed while the other was mounted at the centre of a flat spring steel strip held under tension. The surfaces were pressed together by moving the spring strip towards the fixed surface by a massive screw thread. The force between the surfaces was measured by the deflexion of the spring strip which in turn was measured by strain gauges. The adhesion was simply determined by moving the spring strip away from the fixed surface and again determining its deflexion at the instant of separation. With this arrangement the applying load and breaking force were applied normally to the surfaces with a minimum of twist or lateral motion.

The indium test surface was either a flat, the other surface being a hemisphere of diameter $\frac{1}{4}$ in, or the indium was in the form of a cone of semivertical angle 30°, the other surface being flat. The indium was cleaned immediately before use by scraping or turning with a clean degreased tool. The other surfaces were cleaned by abrasion, cutting with a degreased tool or by vigorous rubbing with degreased cloth. The adhesion experiments were carried out with approximately equal loading and breaking times. The coefficient of adhesion ν, defined as adhesion force/loading force was found to be independent of the load over a load range of 0·3 to 3 kg. In general the indium cone gave somewhat greater adhesions on a flat surface of the other material than the converse arrangement. This is probably because there is greater flow of indium around the tip of the indium cone and this facilitates the break-up of oxide or other contaminant films on the indium. This is supported by an examination of the transfer of indium to the other surface in those cases where good adhesion occurred. A small crater of indium was detached from the end of the cone, but at the very centre where the tip of the indium cone first made contact with the surface no detectable transfer of indium was observed (Fig. 3). Some flow of the indium apparently facilitates adhesion. The flow of the indium also tends to displace contamination from the flat surface.

A simplified summary of the chief results is given in the table.

Adhesion of indium to various materials

Material	*Coefficient of adhesion* ν
Diamond	0·9–1
Glass	1
Tungsten carbide	1
Metals; Fe, Cd, Zn, Co, Ag, Pt, Cu, Au	1
Thick oxides of copper and silver	1
Plastics: polystyrene, Perspex	0·5–0·7
Plastics: P.V.C., polythene	0·02
Plastics: P.T.F.E.	0

Discussion. The results show that for diamond, glass, tungsten carbide and most metals the coefficient of adhesion is of the order of unity. These results mean that the adhesion at the interface is at least as great as the bulk strength of indium. This is supported by the observed transfer of indium to the surface. The results on the metals and on the thick metal oxides are of interest. When indium adheres strongly to a freshly cleaned copper surface ($\nu = 1$) it is probable that the indium is in fact adhering to the oxide layer on the copper surface. To investigate this further, a copper surface was heated at one end to give oxide layers of different thicknesses (and colours) over the surface. Adhesion measurements with an indium cone showed that over all parts of the surface the adhesion was limited by the strength of the indium itself, the coefficient of adhesion at all points being $\nu = 1$. However, the transfer of indium was much heavier on the thick oxide layer than on the "unoxidized" portions. A similar effect was observed with silver but not with a platinum surface that had been heated at one end. It is evident that strong adhesions can occur between a metal and an oxide; true metal-metal contact is not necessary. This is consistent with the view that the friction between oxide-covered surfaces involves adhesion as for metallic sliding[8] though in general the oxide-oxide adhesion is smaller than when true metallic contact occurs.

Fig. 3. Micrograph showing crater of indium left adhering to oxidized copper surface after an indium cone has been pressed on to the surface with a load of 2 kg and then pulled away. At the centre of the crater, where the tip first makes contact with the surfaces, there is no detectable transfer. Magnification × 50

With plastics the adhesion behaviour falls into three main groups. For polystyrene and Perspex the adhesion is high. For P.V.C. (polyvinyl chloride) it is low but this is due to the much greater elastic recovery of the plastic when the load is removed.(9) With P.T.F.E. (polytetrafluoroethylene) the elastic recovery is negligible but the intrinsic adhesion is small. This is consistent with the very low friction observed with this plastic. However, even here some transfer of the plastic occurs.(9) The results obtained with indium on diamond, glass, tungsten carbide, metal oxides and certain plastics show that strong adhesion can occur between very dissimilar materials and that junctions may be formed of the same order of strength as indium-metal junctions. It is probable that in the sliding of non-metals strong adhesion at the interface of the type described in this paper plays a part in the frictional mechanism analogous to the cold-welding process in the friction of metals.(10)

ACKNOWLEDGEMENTS

We wish to express our thanks to Dr. F. P. Bowden for his interest in this work, to the Ministry of Supply (Air) for a research grant and to the Ministry of Supply for a maintenance grant to one of us (A. C. M.).

REFERENCES

(1) McFarlane, J. S., and Tabor, D. *Seventh Int. Congr. Appl. Mech. London*, **4**, p. 31 (1948).
(2) McFarlane, J. S., and Tabor, D. *Proc. Roy. Soc. A*, **202**, p. 224 (1950).
(3) McFarlane, J. S., and Tabor, D. *Proc. Roy. Soc. A*, **202**, p. 244 (1950).
(4) Parker, R. C., and Hatch, D. *Proc. Phys. Soc., Lond.*, **63**, p. 185 (1950).
(5) Crook, A. W., and Hirst, W. *Research, Lond.*, **3**, p. 432 (1950).
(6) Tabor, D. *The Hardness of Metals* (Oxford: Clarendon Press, 1951).
(7) Hill, R. *Mathematical Theory of Plasticity* (Oxford: Clarendon Press, 1950).
(8) Whitehead, J. R. *Proc. Roy. Soc. A*, **201**, p. 109 (1950).
(9) Shooter, K. V. Ph.D. Dissertation, Cambridge (1951).
(10) Bowden, F. P., and Tabor, D. *Friction and Lubrication of Solids* (Oxford: Clarendon Press, 1950).

NOTES AND NEWS

New books

Practical electron microscopy. By V. E. Cosslett. (London: Butterworths Scientific Publications.) Pp. xiii + 299. Price 35*s*.

It has long been the opinion of successful light microscopists that the light microscope is often misused, owing largely to inadequate instruction of the research workers in its various fields of application in the selection and best use of appropriate microscopical methods. How common is the cry "this high dry objective is no good," when the fault usually lies in the preparation and is, in fact, usually due to faulty cover-glasses, particularly those available to us in these last few years! This failure to use light microscopes to best advantage is not directly the fault of the research workers themselves, since little formal instruction in light microscopy has been available, and even less has been included in their normal academic curricula, save in a few noteworthy cases.

It is greatly to be hoped that a similar situation will not arise with the newer forms of microscopy now becoming available, and a welcome will therefore be extended to all publications and lectures designed to provide authoritative information on these new techniques. We are particularly fortunate in having so lucid a writer as Dr. Cosslett to record his own experience and that of other advanced workers in the field of *electron* microscopy so that those who wish to enter it may find the fullest information ready for them both on points of detail and of general background. The author points out that his book is complementary to Dr. Drummond's *Practice of electron microscopy* [*J. Roy. Micr. Soc.*, **LXX**, p. 1 (1950)] and certainly the two together give an invaluable introduction to the practical side of the subject. They will find places on the bookshelf of every worker and potential worker in this field. The author has also been responsible for initiating and organizing summer schools in electron microscopy at Cambridge University and the lessons learned there are incorporated in his book.

Comment could be made on many points of detail in the book, but they are all minor matters which will, no doubt, be eliminated in subsequent editions. Misprints are rare and there is surprisingly little to show that the book was not printed in Great Britain. But surely this must be the first book on electron microscopy in which the name *de Broglie* does not find a place in the name index?

F. W. Cuckow

The oxide-coated cathode. Vol. II. By Dr. S. Wagener. (London: Chapman and Hall Ltd.) Pp. xiv + 311. Price 42*s*.

The first volume of Wagener's book on the oxide-coated cathode, which was reviewed in the February number of this *Journal*, dealt with the manufacture of the cathodes. The subject matter of the second volume covers a much wider field than its main title suggests, and indeed, the first three chapters, occupying more than half of the book, are devoted to the physics of thermionic emission from metals and phenomena in ionic solids. Both the theoretical arguments and the experimental evidence are clearly presented, and this part of the book will be of considerable value to students and to those who are beginning work in this branch of solid physics.

In the treatment of fundamental phenomena associated with thermionic emission from metals, the statistical method is chosen in preference to the thermodynamical approach since, as the author points out, the former method "allows the behaviour of electrons to be more clearly observed in any particular emission problem." Pure metals and the influence of adsorbed layers of foreign materials on emission and work function are considered, and the first chapter concludes with a discussion on the effects of surface field on work function. The various methods of measuring the work functions of metals are critically discussed in Chapter 2, and the most reliable experimental data for a large number of metals are given. One minor criticism may be mentioned here: in view of the importance of technique in such measurements and the difficulty of weighting experimental results, it is questionable whether the average values quoted in Table 5 are significant. Later in the book, on pages 158–60, there appears an even

less justifiable averaging of the experimental results of different workers.

The semi-conductor model of the oxide cathode is introduced by a chapter on ionic solids, and diffusion and electrical conduction phenomena in such solids are discussed. Chapters 4 and 5 deal with the mechanism of emission from fully activated cathodes, first treating single oxides and then considering the properties of mixed oxides, in particular the barium-strontium mixture which has such wide commercial use. The evidence in favour of the excess semi-conductor model is clearly presented. Much of the present knowledge about the oxide-coated cathode has resulted from recent studies of the activation and decay of emission. These phenomena and their interpretation are treated in the final chapter.

There is a useful and up-to-date bibliography and the diagrams are well produced. The book can be thoroughly recommended both to the specialist and to those who wish to be brought up to date in a field of inquiry which, to quote from the preface to O. W. Richardson's book written thirty-six years ago, "still suggests for investigation many interesting questions which are either of theoretical or of practical interest."

G. W. WARREN

Electronic and ionic impact phenomena. By H. G. W. MASSEY and E. H. S. BURHOP. (London: Oxford University Press.) Pp. xviii + 669. Price 70*s*.

Electronic devices, in the operation of which the interaction of particles plays an essential part, become increasingly important both practically and as instruments of scientific investigation. It is unfortunately not true that the only or even the major obstacle to complete understanding of the operation of such devices is lack of knowledge of the characteristics of particle impact phenomena and the quantitative data associated therewith. It is, however, true that few complete theoretical investigations can be made until much more information of this kind is available. While, therefore, a comprehensive review would in any event have been welcome, an authoritative volume by these authors, discussing in detail the present state of knowledge, is doubly so. As far as the reviewer is aware, this new volume of the International Series of Monographs in Physics is the most exhaustive treatment of the subject in any language.

The authors have written the book primarily from an experimental standpoint, but they give in addition an excellent theoretical treatment. Even in a volume as large as this, some limitations are necessary. Electron diffraction at solid surfaces is omitted, for example; but with a few such exceptions, practically all aspects of the subject are treated. Of the ten chapters, five deal with impact of electrons; two of them, excellent chapters, discuss the experimental and theoretical analysis of cross sections; and one is concerned with processes involving radiation. There is a chapter on secondary electron emission, and one dealing with the collision of positive ions and neutral atoms with surfaces.

This is not a book for the beginner, but the lucid presentation of the theory and critical discussion of experimental results make for easy reading. The production is excellent, the diagrams and references adequate, and if there are any errors they are not at all obvious.

V. J. FRANCIS

Fundamentals of technical electricity. By H. G. MITCHELL. (London: Methuen and Co. Ltd.) Pp. xii + 543. Price 18*s*.

This egregious volume in no way justifies its near-sumptuous production. Though not based on any syllabus, it covers all the National Certificate work; it purports to be logical and modern. Its modernity embraces Ticonal, atomic energy, and an attempt to develop electromagnetism without unit poles—which collapses after ten pages. The author tells us that the e.m.f. of a source is the work done in taking unit charge completely round a circuit containing the source; and that a diamagnetic sets across the field, because of "the dispersion of the lines of force" through it (the diagram shows it along the field, and does not make its polarization clear). The author uses terms like string-electrometer, dead-beat, V.A., without explanation. He defines effective resistance correctly, and then confuses it with reactance. He has a few good ideas, but is incapable of carrying them out.

P. PARKER

Mathematics, queen and servant of science. By E. T. BELL. (London: G. Bell and Sons, Ltd.) Pp. xx + 437. Price 21*s*.

Professor Bell, of the California Institute of Technology, has re-written two earlier popular accounts of mathematics and combined them as one volume. It is neither a formal mathematical text nor a history of mathematics, but an attractive review of the fundamental ideas and techniques in pure mathematics as well as of some of the applications in science, mainly in physics. It ranges from early Greek mathematics to modern mathematical physics and recent developments in mathematical logic. If the Queen is given regal honours, the Servant is not unacclaimed.

Although the author has an exceptional gift of clear exposition, the book in places is not easy reading, but there is so much that is excellent that the mathematical amateur, to whom it is intended to appeal, should follow D'Alembert's advice recommended by the author: "Go on, and faith will come to you."

Through common and uncommon algebras and geometries, group theory and the tensor calculus, he is led to the favourite domain of the Queen, the theory of numbers. After a glimpse at the work of Maxwell and Newton, he is introduced to the "chief instrument of applied mathematics" and the theory of probability. Throughout he will be stimulated by Professor Bell's pungent comments on men and affairs.

J. TOPPING

Thermal properties of buildings. By N. S. BILLINGTON, M.Sc., M.I.H.V.E. (London: Cleaver-Hume Press Ltd.) Pp. xii + 208. Price 25*s*.

The chief merit of this book is the confidence it inspires. There have been many books written about the thermal properties of materials but seldom has such a coherent whole been made of the subject as related to buildings. The author is obviously a physicist, but a physicist with exceptional practical insight and the ability to relate the two aspects. He has read widely and critically in his subject and interprets his reading in a succinct and interesting manner.

The book is divided into seven main sections, and those dealing with the unsteady flow of heat and the problems of condensation are of particular value. The diagrams and graphs throughout are up-to-date and informative and many useful tables are given. There is an excellent bibliography, and the text abounds with short but vivid descriptions of the author's experimental work and also that of many others. Some mathematical theory is given but many physical concepts are conveyed quickly and clearly without recourse to symbolism.

This book should be of great interest both to the scientifically-minded heating engineer and to others for general reading on a subject which touches most people very nearly.

M. V. GRIFFITH

Automatic and manual control. Edited by PROFESSOR A. TUSTIN, M.I.E.E. (being the papers read at the conference organized by the Department of Scientific and Industrial Research in July 1951, and material presented during the discussions on those papers). (London: Butterworths Scientific Publications Ltd.) Pp. xiii + 584. Price 50*s*.

This tome, which measures 10 × 7½ in and weighs 3½ lb, has been produced under the guidance of a strong editorial committee whose aim has been to produce a volume that will be useful not only as a book of reference for those engaged in the design of control equipment, but also as a book for students and others who have some knowledge of the principles of the subject and who wish to bring their knowledge up to date or to extend it in various more specialized directions. Indeed, the wide range of subjects covered by the 37 papers and symposia makes it highly probable that all those interested in this subject will, in fact, find sections of it of importance to them. The sections deal with (i) educational problems, arising from the growing importance of feed-back systems and the demand for skill in this field; (ii) the development and co-ordination of improved methods of mathematical analysis for such systems; (iii) the extension of the methods to a widening range of technical and other problems; and (iv) the attempt to deal more adequately with such problems as non-linearities and intermittent data. The similarity of the problems that confront economists in the analysis of the behaviour of economic systems with the problems that confront engineers in the analysis of the behaviour of physical systems has often been noted, and the conference devoted an informal evening session to an exchange of views on this topic. A brief report of this discussion is included. A number of interesting demonstrations and exhibits formed part of the conference and accounts of these are also printed. Most of the leading authorities from this country and many from overseas participated in this conference, and as Sir Ben Lockspeiser writes in his Foreword, "this volume will mark an important stage of consolidation and development of this subject."

Professor Tustin and his colleagues and all those associated with the production of this volume are to be congratulated. The printers were the Pitman Press, and they have made a nice job of the difficult mathematics required and of the printing generally. H. R. LANG

Corrosion testing procedures. By F. A. CHAMPION. (London: Chapman and Hall Ltd.) Pp. xi + 369. Price 36*s*.

The advice on corrosion resistant materials that is generally available from their suppliers is best taken into account at the stage when new structures, machines and instruments are being designed. Even so, many physicists are likely to be faced during their career with a corrosion problem which existing information is inadequate to solve. Then it is best to put the problem to an experienced corrosion chemist whose philosophy will bring forth appropriate testing procedures for the selection of more suitable materials. Just how deep this specialist philosophy must be, and how complex the considerations involved, will be clear to non-specialist readers of Dr. Champion's book.

It is addressed principally to the investigator of practical problems in the corrosion of metals. For the investigator who is already experienced in the field, the book undoubtedly provides a valuable compilation of testing methods and of studies in the assessment of corrosion damage and the interpretation of results.

Unfortunately there is a shortage of corrosion chemists, and designers may well have to settle some of their own corrosion problems. When they turn to Dr. Champion's book for advice they must be embarrassed by the choice of tests and of methods of assessment of the results. It is too much, no doubt, to expect that over the whole field of corrosion testing a small number of tests could be standardized, along with one method of expressing the results. At least the author, who is himself responsible for one generalized scheme for assessing corrosion damage, seems to hold out little hope in this direction. G. L. J. BAILEY

Tungsten. (3rd edition). By COLIN J. SMITHELLS. (London: Chapman and Hall Ltd.) Pp. xii + 326. Price 75*s*.

The metallurgy of tungsten is not only of importance intrinsically, but also historically in view of the widespread use of powder metallurgical techniques, many of which had their origin in the development of processes for the production of ductile tungsten.

When Dr. Smithells's book on Tungsten first appeared in 1926 it filled a gap in the literature of the subject. The second edition of 1936 was recognized to be the standard work on the subject in the English language. With the 1952 edition in which Dr. Smithells has assumed the role of editor the whole of the material has been brought up to date and the scope of the volume has been substantially increased. In the re-writing of many of the chapters Dr. Smithells has had the assistance of specialist workers in the various fields and they have been able to bring their expert knowledge to bear on the subject. As a result the original work of some 160 pages has been expanded to about twice the size and the new edition is noteworthy for the completeness of the treatment in the various sections. The illustrations have also been brought up to date and they indicate the latest type of plant and equipment used for the production and processing of tungsten bars, rod and wire.

Possession of the latest edition of Dr. Smithells's book will enable both the student and the expert to gain a good general acquaintance with the state of the art not only of the preparation of ductile tungsten from the ore but also of its metallurgy and properties.

The chapter on the thermionic properties of tungsten is of considerable value in view of the widespread use of thin tungsten wires as thermal electron emittors. The remaining sections dealing with tungsten iron alloys, tungsten steels and other tungsten alloys and carbides give a good general picture of the position.

It is a well-written and excellently produced volume with good, clear illustrations, adequate references and a useful index, and should be on the shelves of not only those who have found the earlier editions valuable, but also in the reference libraries of schools, technical colleges, universities and research institutions of all kinds. J. N. ALDINGTON

Currents and fields in electrical engineering. By H. E. M. BARLOW. (London: H. K. Lewis and Co. Ltd.) Pp. 19. Price 5*s*.

Professor Barlow's inaugural lecture, printed here, is a call for a change of emphasis in studies of electrical engineering. He wants attention focused upon basic considerations, illustrated by selected examples from technology; the electromagnetic field, he says, should be presented as the fundamental concept, with lumped-circuit theory as a simplification of limited validity. At present many students, even of telecommunications, have little or no acquaintance with Poynting's theorem when they graduate. Let us hope that this charming and persuasive lecture will help to change all that. P. PARKER

Notes and comments

Fortieth anniversary of the discovery of X-ray diffraction

To celebrate the fortieth anniversary of the discovery of X-ray diffraction the X-ray Analysis Group of The Institute of Physics is holding a Conference at the Royal Institution, London, on 24–25 October, 1952. There will be a dinner on the evening of the 24th at which the guest of honour will be Professor Max von Laue. Professor von Laue is the Honorary President of the International Union of Crystallography, and it is hoped that the Executive President, Professor J. M. Bijvoet, will also be present. The scientific meeting will be opened by Professor Sir Lawrence Bragg, with a historical survey of the subject; and survey papers will be given by him and by Professor J. D. Bernal, Dr. D. Hodgkin and Professor G. V. Raynor. Further details may be obtained from the Honorary Conference Secretary, Dr. J. Thewlis, Atomic Energy Research Establishment, Harwell, Berks.

The international commission on glass

The international commission on glass held its annual meetings from Monday, 30 June, to Saturday, 5 July, 1952. The technical work of the commission occupied three full days, one of them devoted to an open session, the two other days to committee work on a variety of subjects classified under the group headings of Glass literature—Chemical properties of glasses; Physical properties of glasses; Glass furnace problems. Reports were presented on tasks or projects previously undertaken by affiliated organizations; agreements were reached on a number of fundamental issues, and plans were prepared for further collaboration. The International Standards Organization sent, by invitation, two observers to the meetings.

Professor W. E. S. Turner, to whom illuminated addresses were presented from Germany and Japan, will, after being continuously in office for twenty years, retire from the Presidency in 1953. He will be succeeded by Dr. B. P. Dudding, Honorary Secretary of The Institute of Physics, and at present Secretary of the Commission. M. Henri Vandecapelle, Director of the Institut National du Verre, Charleroi, was appointed Secretary-elect.

Japanese Applied Mechanics Institute Reports

We have received the first two issues of *Reports of Research Institute for Applied Mechanics*, published by Kyushu University, Fukuoka, Japan. This new Institute has been formed by the amalgamation of the Fluid Engineering and Elasticity Engineering Institutes of that University, each of which previously published its own reports. The papers in these parts are: Note on the hydrodynamical roughness length of a grass-field, by M. Kurihara; A contribution to mechanics of hardened mortar, by K. Shinohara; On the forms of hen's eggs, by J. Okabe; Calculation of the stresses of the orthotropic strip with a hole, by M. Higuchi; Elastic stability of the square plate with a central circular hole under edge thrust, by T. Kumai; On the calculation of free oscillations with intermediate non-linearity, by H. Yamada; An approximate calculation of the laminar nonisothermal flow in a circular pipe, by M. Ohji.

Copies of all papers in these issues may be obtained free of charge from the Librarian of the above Institute.

Comparison between British and American standards for short-circuit testing

A sixteen-page booklet compares the British and American Standards for the short-circuit rating, performance, selection and testing of oil circuit-breakers. Its main sections are headed: Assessment of rating and performance; Calculation of fault currents and selection of circuit-breakers; Other factors affecting performance; Short-circuit test code; Practical comparisons; Comparison of rating and performance between BS and ASA circuit-breakers selected for the same duty; Comparison between British and American Standards for the short-circuit rating, performance, selection and testing of oil circuit-breakers. The booklet is available from The Association of Short-Circuit Testing Authorities (Inc.), 36 and 38 Kingsway, London, W.C.2, price 10*s*.

Journal of Scientific Instruments

Contents of the September issue

SPECIAL ARTICLE

The Institute of Physics' exhibition of physical instruments and apparatus of value to the transport, shipbuilding and engineering industries—Glasgow, June 1952. By M. W. Thring.

ORIGINAL CONTRIBUTIONS

On the preservation of groove-form in replicas of diffraction gratings. By G. D. Dew.

The transient behaviour of thermionic filaments with temperature-limited emission. By F. H. Hibberd.

A flame photometer for routine biochemical use. By R. L. Warren.

An oscillating specimen holder for an X-ray microbeam camera. By P. Gay and A. Kelly.

Unbonded wire resistance strain gauge accelerometers. By J. R. Bristow and F. G. Ellames.

A furnace constant temperature controller and its modification as a programme controller. By J. R. Beattie and A. J. Milne.

A photocell amplifier for infra-red spectroscopy. By D. A. H. Brown.

LABORATORY AND WORKSHOP NOTES

A simple method of purifying hydrogen, nitrogen and the inert gases. By E. R. Harrison.

Some disturbing effects in glass Geiger–Müller counters. By L. Carlbom and C. Taylor.

The design of high vacuum valves. By L. Riddiford and H. Lilley.

Shunted thermocouple vacuum gauge. By N. A. Florescu.

A device for calculating complex X-ray structure factors. By D. C. Phillips.

A laboratory galvanometer stand. By S. C. Baker.

Exposure time measurement in electron microscopy using a visual photometer. By A. E. Ennos.

A gas control valve for flow proportional counters with facilities for flushing. By P. Holton.

Adaptation of a lathe for crystal grinding. By L. Cartz and E. Nave.

CORRESPONDENCE

NEW INSTRUMENTS, MATERIALS AND TOOLS

MANUFACTURERS' PUBLICATIONS

NOTES AND COMMENTS

British Journal of Applied Physics

Original contributions accepted for publication in future issues of this Journal

Secondary electron emission from barium oxide. By J. Woods and D. A. Wright.

On two problems in potential theory and their application to the design of magnetic recording heads for digital computers. By A. D. Booth.

A study of the oil-film formation in gears by electrical resistance measurements. By T. B. Lane and J. R. Hughes.

Electrical measurement of the cathode temperature of diodes. By D. A. Bell, J. C. Cluley and H. O. Berktay.

A quick method of distortion measurement in nuclear emulsions. By J. V. Major.

THIS JOURNAL is produced monthly by The Institute of Physics, in London. It deals with all branches of applied physics (including theory and technique).

All rights reserved. Responsibility for the statements contained herein attaches only to the writers.

EDITORIAL MATTER. Communications concerning editorial matter should be addressed to the Editor, The Institute of Physics, 47 Belgrave Square, London, S.W.1. (*Telephone:* Sloane 9806.) Prospective authors are invited to prepare their scripts in accordance with the *Notes on the Preparation of Contributions*. (Price 2*s*. 6*d*. including postage.)

REPRODUCTION. The Institute of Physics is a signatory to The Royal Society's Fair Copying Declaration. Details may be obtained upon application from The Royal Society, London, W.1.

ADVERTISEMENTS. Communications concerning advertisements should be addressed to the agents, Messrs. Walter Judd Ltd., 47 Gresham Street, London, E.C.2. (*Telephone:* Monarch 7644.)

SUBSCRIPTION RATES. A new volume commences each January, and annual subscriptions will only be accepted for complete volumes of the monthly parts (January–December). The charge is £4 per volume ($11.50 U.S.A.), including index (post paid), payable in advance. Single parts, so far as available, may be purchased at 8*s*. each ($1.15 U.S.A.), post paid, cash with order. Orders should be sent to The Institute of Physics, 47 Belgrave Square, London, S.W.1, or to any Bookseller.

SPECIAL REPORT

Summarized proceedings of a conference on X-ray analysis —Edinburgh, April 1952

The Spring Conference of the X-ray Analysis Group of The Institute of Physics, which was a joint meeting with the Scottish Branch, was held in the Chemistry Department of the University of Edinburgh on 3–5 April, 1952. In contrast to the usual type of group conference in which one or two chosen topics are discussed, this one covered almost the whole field of X-ray crystallography, forty-five papers being presented in the three days of the conference.

The outstanding impression left by the conference is of the great vitality of X-ray crystallography and of the versatility and power of X-ray methods applied in subjects as diverse as, say, biophysics and atomic energy. Examples were given of their success not only in crystal physics or the structural problems of organic chemistry but also in applications in connexion with chemical and metallurgical industry. Much of this success is due to improvements in the performance and reliability of X-ray diffraction equipment, and a small exhibition of the latest types of commercial apparatus served to emphasize the wide range of problems to which X-ray techniques can be applied as well as to enable members to inspect the newest designs.

BIOPHYSICS

Perhaps the most fascinating subject was that discussed by PROFESSOR J. T. RANDALL (King's College, London) in his evening discourse on "Some aspects of structural biophysics," in which he spoke of some of the results of X-ray, infra-red, electron and optical microscopy investigations on the structure of living matter. The two topics considered in this lecture were the nucleic acid content of cells and the origin and structure of fibrous tissue. On the first of these, optical methods, notably the use of the polarizing microscope, have shown that although the amounts involved are of the order of 10^{-12} g the nucleic acids are mostly concentrated in the nucleus of the cell. X-ray methods help, however, and some excellent fibre photographs in varying conditions of humidity showed the strongly crystalline nature of these materials. Professor Randall went on to discuss the structure of fibres of the collagen groups and showed a film of fibrogenesis in a fibre tissue culture. Emphasizing the persistence of the essential structural features of the fibres he observed that their characteristic striations persisted even when the fibres were dissolved in acid and reprecipitated and he showed slides of intact collagen fibres taken from a 10 000-year-old mammoth tusk and showing the same features. The crystal structure of collagen fibres still presents some difficulties and recent infra-red data is not in accord with previously proposed models, but supports the suggestion that the fibres form a sheet structure tilted at 41° to the fibre axis.

X-RAY METHODS IN INDUSTRY

One session of the conference was devoted to three specially invited papers on "X-ray methods in industry" which were intended to show the uses to which X-ray methods can be put and their value in an industrial laboratory. DR. B. RAISTRICK (Scottish Agricultural Industries Ltd.), who spoke on "Chemical industry and X-ray methods," pointed out that X-ray methods are only to be preferred if they are more effective and more economic. Emphasizing the advantages of the X-ray method over the chemical method in that it gives not only the nature of the ions present but also their state of combination, Dr. Raistrick gave examples of the use of the X-ray method of qualitative analysis in checking the operation of a large chemical plant. Quantitative analysis is an extension of the procedure used for qualitative analysis, and it is particularly valuable when chemical analysis is tedious, inaccurate or impossible, when phase differentiation is necessary or when a knowledge of the state of combination of the ions is important. This, too, he illustrated with reference to an industrial process and showed how a simple, home-made microdensitometer could yield valuable results with an accuracy of $\pm 1\%$. But of all the benefits offered by X-ray methods to chemistry probably the most important of all is the advantage of knowing the structure of the materials with which one is working. This was illustrated with reference to the reactions occurring during the hydration of phosphorus pentoxide and to the use of chain polyphosphates to inhibit scale formation with hard water or electrochemical corrosion. A knowledge of crystalline size, easily obtained by X-ray methods, often enables chemical processes to be carried out more efficiently whilst the ability to recognize preferred orientation can assist in the solution of many chemical problems.

The second paper in this series, by MR. H. S. PEISER and DR. J. R. RAIT (Hadfields Ltd.), was on "The metals industry and X-ray methods." Mentioning what he called the easier problems to which X-ray methods could contribute—identification and composition of slags, refractories and carbides, etc., or radiography—Mr. Peiser went on to stress the importance to industry of a knowledge of the latest structural information on alloys. Thus the high-temperature creep of ferritic gas turbine blades is intimately related to their composition and X-ray structural studies have enabled such steels to replace expensive austenitic steels in many cases. Tool steels provide another example. Here a knowledge of carbide structures enables the use of lower alloy steels. Mr. Peiser also drew attention to the economies in design which are permitted by the use of newer materials and stressed that, as the efficient use of valuable raw materials is so vital, the industry could not afford to be without the information which can be provided by X-ray methods. On actual procedure he showed how the great power of X-ray methods means that relatively simple equipment can provide results of more than adequate accuracy for most purposes.

DR. J. THEWLIS (Atomic Energy Research Establishment, Harwell), in the third paper on "X-ray analysis and atomic energy," paid tribute to the immense amount of structural work on the transuranic elements done by Zachariasen. He reviewed some of the material problems encountered in the construction and operation of nuclear reactors, such problems

as the structure and purity of graphite or the deformation structures of metals, in all of which X-ray methods have contributed. On the other side of the picture Dr. Thewlis mentioned some of the applications of nuclear diffraction techniques being developed at Harwell and elsewhere, and studies of the effects of nuclear bombardment on elements and alloys.

The contributed papers seemed to fall into four groups—metallurgical, chemical, X-ray physics and techniques.

METALLURGICAL SUBJECTS

Of the metallurgical subjects discussed, perhaps the most interesting at the present time are the investigations of the texture of cold-worked and annealed metal. Dr. P. Gay and Dr. P. B. Hirsch (Cavendish Laboratory, Cambridge) described measurements of the breadths of X-ray reflexions leading to estimates of the density of dislocations as 10^9 per cm^2 in cold-worked metal and 10^7–10^8 per cm^2 in annealed material. From the same laboratory Mr. A. Kelly showed how, using microbeam techniques, the Debye–Scherrer ring obtained from a deformed polycrystalline aggregate has a wavy nature, waviness being due to spots displaced from the ring. This has been shown to be due to particles of varying lattice parameter and the strain involved has been estimated to be equal to the yield point for the material. Dr. G. K. Williamson (University of Birmingham) presented Geiger-counter studies of the effects of cold-working on integrated intensities and line breadths. Measurements on aluminium suggest that the total reflected intensity is unaltered, the sharp line intensity decreasing by about 7% and there being a corresponding increase in the general background scatter. The observed line broadening is again attributed to lattice strains.

From the Atomic Energy Research Establishment, Harwell, Dr. J. Adam reported on the effects of neutron bombardment on ordered Cu_3–Au alloy. The observed changes of electrical resistivity suggest that ordering and disordering mechanisms operate simultaneously. Changes in the lattice constant do, on the whole, confirm this idea but not all of the observed effects are yet completely explained. Dr. J. Thewlis (A.E.R.E., Harwell) gave the results of some interesting X-ray measurements on Li^6F and Li^7F which confirm the theoretically predicted variation of atomic volume with mass number, the observed lattice parameters being 4·0271 kX and 4·0262 kX respectively at 25° C.

Dr. C. J. Milner (British Thomson-Houston Co. Ltd., Rugby) suggested alternatives to pole figures for representing the texture of rolled sheet and described a moving film camera capable of forming directly on the film a recognizable projection of the reference sphere.

CHEMICAL SUBJECTS

Mr. C. W. Bunn (I.C.I., Ltd., Welwyn) gave a report on the notable determination of the structure of "terylene" determined from its fibre photograph. Experience with tilted crystal methods played a valuable part in this work. Other reports covered investigations on thiourea dioxide, l-glutamine, quinaldil, some nucleosides and nucleotides, benzanthrone, some new compounds containing a five-membered ring with two sulphur atoms, and some acid salts of monocarboxilic acids. The structural investigations of some of these compounds gave valuable chemical evidence. Work on the orientation of the crystallites of bone was described by Dr. J. Iball (University of St. Andrews), and some conclusions were reached by Dr. P. B. Hirsch concerning the structure of coal as determined by diffraction methods. Dr. Iball also showed some remarkable photographs produced by built-up films of barium stearate and palmitate, and a suggestion was made by Professor A. R. Ubbelohde (Queen's University, Belfast) that such films may prove useful as monochromators.

X-RAY PHYSICS

The problem of extinction is one which has presented difficulties for many years and it is interesting to see that several new attacks on this and related subjects are now being made. Dr. G. E. Pringle (University of Leeds) described the application of extinction theory to the interpretation of the observed distributions of energy in divergent beam photography. He spoke of attempts to correlate the photographic density of the lines obtained with the mosaic structure deduced from their angular width. Then Dr. P. Gay discussed the intensities of asymmetric X-ray reflexions from quartz crystals and their interpretation in terms of the dynamical theory of X-rays, and Dr. P. B. Hirsch considered the anomalous absorption of X-rays incident at the Bragg angle (the Borrman effect). He showed that the intensities of X-rays reflected and transmitted through perfect absorbing crystals can be expressed in terms of a single parameter depending upon absorption in the crystal. The reduction in intensity of the transmitted beam (extinction) for thin perfect crystals changes to an increase in intensity for thick absorbing crystals due to the reduction of absorption when the X-rays are incident at the Bragg angle.

TECHNIQUES

Mr. A. R. Lang (Cavendish Laboratory, Cambridge) described some interesting variants of the Bragg–Brentano system applied to Geiger-counter spectrometers. As the requirement is only that those rays diffracted at the Bragg angle under observation shall be focused, new geometrical arrangements are possible and these can be exploited to give diffraction patterns in which resolution, intensity and purity exceed that obtainable with the usual film methods. Four techniques using diffracted beam monochromatization were described and illustrations of their success included suppression of fluorescent background, observation of very high angle reflexions and separation of $\alpha_1\alpha_2$ doublets.

In another paper Mr. Lang described the considerable advantages of the proportional counter in accurate intensity work. From the Manchester College of Technology (Dr. H. Lipson and Dr. C. A. Taylor) came the report of optical methods by which the approximate structure of purpurogallol was found. These methods are of especial interest in that they demonstrate so well the physical principles of diffraction. Computational aids in X-ray analysis were covered in a note by Dr. V. Vand (University of Glasgow) on an improvement in the Fourier balance, and in a report by Dr. W. Cochran (Cavendish Laboratory, Cambridge) on his experience with XRAC at Penn State College.

C. A. Beevers
A. E. De Barr

On two problems in potential theory and their application to the design of magnetic recording heads for digital computers

By A. D. Booth, D.Sc., Ph.D., F.Inst.P., Electronic Computer Project, Birkbeck College, London

[*Paper first received* 6 *February, and in final form* 6 *May*, 1952]

An examination of two sets of examples shows that the external field arising from the gap in a magnetic digit recording head is very insensitive to the pole-piece shape. It follows that head design should be decided by facility of manufacture rather than by theoretical perfection.

During the past five or six years, a period of intense development in the design of electronic calculating machines, there has been considerable discussion—and some practical experiment using the electrolytic tank[1]—as to the optimum pole piece shape for a magnetic recording head to be used in conjunction with magnetic drum storage units.[2] It is the purpose of this note to give two results of two-dimensional potential theory and to indicate their implications in the theory of recording head design.

The first problem is essentially that of the edge effect in a parallel plate condenser: it appears to have been first treated by Helmholtz,[3] and the solution is given by Jeans.[4] *AB*, *CD* (Fig. 1) are the parallel plates of a condenser; *B* and *C*

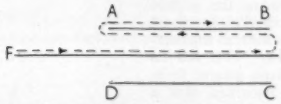

Fig. 1. Parallel plate condenser boundary

are assumed infinitely distant. The solution obtained by means of a Schwarz transformation, is

$$x = U + e^U \cos V \qquad (1)$$

$$y = V + e^U \sin V \qquad (2)$$

where V is the potential and U its orthogonal.

The parallel plates are seen to correspond to the lines $y = \pm\pi$ from $x = -1$ to $x = -\infty$ and to be at potentials $V = \pm\pi$. The x axis is the equipotential $V = 0$.

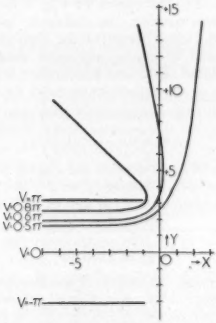

Fig. 2. Equipotentials for parallel plate case

Fig. 2 is a scale drawing of the equipotentials. From the point of view of the later discussion, important functions are the field intensity distributions along and perpendicular to the x axis. These are obtainable from the expression:

$$E = \left|\frac{dw}{dz}\right| = 1/|1 + e^w| = 1/(1 + 2e^u \cos V + e^{2u})^{\frac{1}{2}} \qquad (3)$$

and it can be seen at once that, on $y = 0$, for large x, $E \simeq 1/x$, whilst, on any line perpendicular to $y = 0$, for large y, $E \simeq 1/y$. In Fig. 3, the full curve gives the value of E along $y = 0$ and in Fig. 4 is represented the variation of E along $x = 1{\cdot}731$.

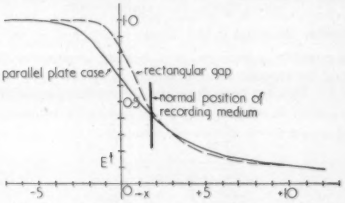

Fig. 3. Variation of intensity along axis of symmetry

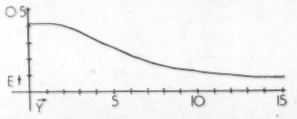

Fig. 4. Variation of intensity along $x = 1{\cdot}731$ for the parallel plate case

The second problem is the somewhat more complicated one shown in Fig. 5. Here the field is required in the space surrounding the conductors *ABC*, *DEF*. The system can be replaced by the polygon consisting of the lines *AB*, *BC* and the reflexion plane *GH*. The appropriate Schwarz transformation is readily seen to be given by:

$$\frac{dz}{d\zeta} = c\frac{(\zeta - 1)^{\frac{1}{2}}}{\zeta}$$

together with the auxiliary transformation

$$W = \log \zeta$$

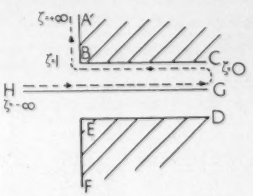

Fig. 5. Ideal recording gap boundary

from which, after integration and substitution:

$$z = \sqrt{(e^w - 1)} - \cos^{-1} e^{-w/2} \qquad (4)$$

To obtain this result the constant of integration has been put equal to zero and the value of C taken as unity.

The dimensions of the system represented by equation (4) can be obtained by the following process.

(*a*) Put $V = 0$ in equation (4), then:

$$x + iy = \sqrt{(e^u - 1)} - \cos^{-1}e^{-u/2}$$

Two cases arise:

$u > 0$ the right-hand side is real and consequently

$$x = \sqrt{(e^u - 1)} - \cos^{-1}e^{-u/2}$$
$$y = 0 \qquad (5)$$

$u < 0$ the right-hand side is imaginary and

$$x = 0$$
$$y = \sqrt{(1 - e^u)} - \cosh^{-1}e^{-u/2} \qquad (6)$$

The boundary therefore consists of $y = 0$ from $x = 0$ to $x = +\infty$ and of $x = 0$ from $y = 0$ to $y = -\infty$.

(*b*) Put $V = \pi$ in equation (4)

$$x + iy = i\sqrt{(e^u - 1)} - i\sinh^{-1}e^{-u/2} - \pi/2$$

whence this equipotential is the line $x = -\pi/2$ and

$$y = \sqrt{(e^u - 1)} - \sinh^{-1}e^{-u/2} \qquad (7)$$

which takes all values in the range $-\infty < y < +\infty$

It is possible to separate the variables in equation (4) and obtain a parametric representation of x and y in terms of U and V. This has been done and the resultant equipotentials

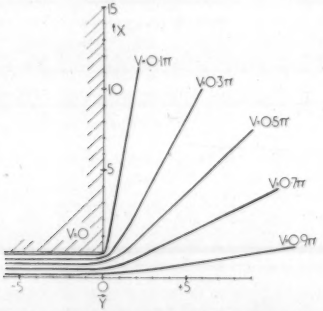

Fig. 6. Equipotentials for ideal gap case

are given in Fig. 6. The detailed formulae are easily verified to be:

$$x = \left[\frac{e^u \cos V - 1 + \sqrt{(e^{2u} - 2e^u \cos V + 1)}}{2}\right]^{\frac{1}{2}} - \cos^{-1}\left[\frac{e^{-u} + 1 - \sqrt{(e^{-2u} - 2e^{-u}\cos V + 1)}}{2}\right]^{\frac{1}{2}}$$

$$y = \left[\frac{1 - e^u \cos V + \sqrt{(e^{2u} - 2e^u \cos V + 1)}}{2}\right]^{\frac{1}{2}} - \cosh^{-1}\left[\frac{e^{-u} + 1 + \sqrt{(e^{-2u} - 2e^{-u}\cos V + 1)}}{2}\right]^{\frac{1}{2}}$$

The field intensity is given by:

$$E = \left|\frac{dw}{dz}\right| = 2/|\sqrt{(e^w - 1)}| \qquad (8)$$

and on $V = \pi$

$$E = 2/|\sqrt{(1 + e^u)}| \qquad (9)$$

The intensity variation along the axis of symmetry has been calculated from equation (9) and is shown in the dashed curve of Fig. 3. The scale has been so arranged as to correspond in gap size and gap field strength with that of the previous example.

Now, although the two solutions given above were derived for an electrostatic system, the results apply equally to any magnetic system in which the conductors are replaced by a magnetic circuit whose permeability (μ) can be assumed to be infinite compared with that of air ($\mu \simeq 1$). This is true of the materials used for the construction of magnetic recording heads (e.g. Mumetal $\mu = 20\,000$, Radiometal $\mu = 10\,000$) if, as is usual, they are not worked near to magnetic saturation. It is also assumed that the recording medium does not disturb the magnetic fields, and this is also approximately true, at least for dispersed particle media of the iron oxide type.

Thus in Fig. 2 the field will not be disturbed if the magnetic conductor has the shape of *any* equipotential. The curves of Fig. 2 can therefore be considered to represent a set of head profiles such that each produces an identical external field. In case it should be argued that the profiles are of unlikely shapes, Fig. 7 gives a smaller scale version which shows clearly that from the macroscopic viewpoint the profiles are quite similar to those generated in normal engineering operations. This will be seen with even greater force when it is remarked that a customary value for the gap width in a recording system is 0·001 in.

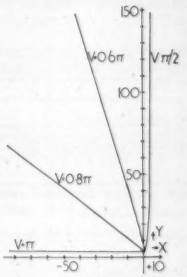

Fig. 7. Small scale version of Fig. 2

It is also normal practice, in the design of high-speed magnetic storage devices, to operate with the medium separated from the front of the gap by about one half of the gap width. The curve of Fig. 4 was constructed to give the variation in field strength at about this distance from the profiles of Fig. 2. The curves of Fig. 3 show that at and beyond the above spacing, the difference between the field produced by an "ideal" head of the type shown in Fig. 5 and that produced by almost any other shape is negligible. It is to be remarked that these conclusions are in full accord with the results of the experimental work carried out in this laboratory.

ACKNOWLEDGEMENTS

The author wishes to express his thanks to Dr. Kathleen Booth and Miss Beryl Marchington for assistance with the drawing and computation of the figures given in this paper.

REFERENCES

(1) See, for example, the reports of the Harvard Computation Laboratory. U.S. Air Force. Harvard University Press.
(2) BOOTH, A. D. *Electronic Engng*, **21**, p. 234 (1949).
(3) HELMHOLTZ, H. VON. *Ges. Abh.*, **1**, 154.
(4) JEANS, J. H. *Electricity and Magnetism*, p. 274 (Cambridge: University Press, 1923).

A quick method of distortion measurement in nuclear emulsions

By J. V. Major, B.Sc., The Physical Laboratories, The University, Manchester

[*Paper received 5 May*, 1952]

A rapid method for measuring the curvature distortion in the tracks of cosmic-ray particles in photographic emulsions is described. The method is applied to the determination of curvature distortion contours on a 400 μ thick G5 nuclear research plate.

Definitions and Theory of the Method

Following Cosyns, the horizontal displacement Δ, of a point at a height z in an emulsion of thickness d, may be represented by the series:

$$\Delta = K_1(z/d) + K_2(z/d)^2 + \ldots$$

The first term $K_1(z/d)$ represents a linear displacement and the type of distortion which it produces is termed "K_1-distortion." A straight track undergoing K_1-distortion remains a straight track, but its orientation in the emulsion is altered. The second term $K_2(z/d)^2$ gives rise to curvature distortion and is called "K_2-distortion." The higher order terms contribute little to curvature distortion in emulsions of the thicknesses now in common use. Thus the displacement Δ_2, at a height z in an emulsion of thickness d, due to K_2-distortion is:

$$\Delta_2 = K_2(z/d)^2$$

In Fig. 1 is shown part of a processed emulsion. Let us assume that in the absence of distortion, the track of a particle

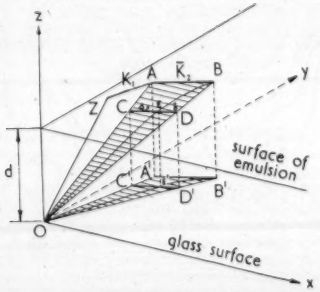

Fig. 1. Linear and curvature distortions in a nuclear emulsion

lies along OZ. As a result of K_1-distortion the track is caused to lie along OA and with K_2-distortion the track assumes the curve OB. The line AB is the distortion vector K_2 in magnitude and direction. The projection of the distorted track in the plane of the glass is the curved line OB'; OA appears as OA'. Since the surface of the emulsion is parallel to the surface of the glass,

$$K_2 = AB = A'B'$$

Because of K_2-distortion, the point C, at a height z in the emulsion is displaced by $\Delta_2 = K_2(z/d)^2$ to the point E on the distorted track. CE produced meets the chord joining the ends of the distorted track at D. Let ED be written as δ. Since CD is also parallel to the surface of the glass,

$$\Delta_2 = CE = C'E' \quad \text{and} \quad \delta = ED = E'D'$$

where $C'E'$ and $E'D'$ are the projections of CE and ED on the glass. By similar triangles,

$$K_2/(\Delta_2 + \delta) = d/z$$

This gives $K_2(z/d) = \Delta_2 + \delta$ and since $\Delta_2 = K_2(z/d)^2$

$$K_2(z/d)^2 - K_2(z/d) + \delta = 0$$

Thus K_2 can be determined by a measurement of δ at a given height z in the emulsion, where δ is the separation, at z, of the track and the chord joining the ends of the track.

The optimum height z', at which to measure the separation δ of the track and chord, is that which gives a maximum value to δ. Differentiating the above equation for δ with respect to z, the optimum value of z is $z' = d/2$, that is, half-way through the emulsion. Substituting this value of z' in the equation for δ, at half-way through the emulsion,

$$\delta = K_2/4 = \Delta_2$$

Hence a measurement of the separation of the track and chord at a height $z = d/2$ enables K_2 to be easily computed. Further, since δ is parallel to K_2 its direction gives the direction of K_2.

The method of measuring δ is explained by reference to Fig. 2. The track is arranged so that its projected chord lies

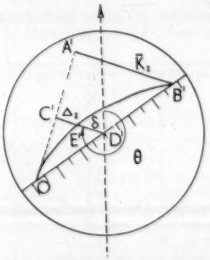

Fig. 2. The measurement of curvature distortion in the emulsion

equally about the centre of the scale, which centre is coincident with the field of view. Thus D' is the midpoint of the chord joining the ends of the track. The track is seen in the microscope as the locus of a black spot which moves along the curved track OB' as different layers of the emulsion are brought into view. The black spot is followed through the emulsion to the point E' corresponding to the half depth. The scale is rotated about D', $E'D'$ is measured and its direction is measured on a goniometer scale. The point corresponding to the half depth should always be approached in such a direction as to avoid backlash.

Comparison with the Method of Cosyns and Vanderhaeghe

The method has been checked with that of Cosyns and Vanderhaeghe.* Ten tracks, at each of six points in the emulsion, were selected and the distortion measured in them

* Cosyns, M., and Vanderhaeghe, G. *Bull. du Cen. de Phys. Nuc. de l'Université Libre de Bruxelles*, No. 15 (1950).

by both methods. The results for the six points are shown in Fig. 3. The ordinates K_N represent measurements made by the method described above, and the abscissae K_C are measurements made by the method of Cosyns and Vanderhaeghe. The agreement between the measured directions is shown in Fig. 4. In both Figs. 3 and 4 the results lie about an expected straight line at 45° to the axes. The uncertainties indicated on the measurements are probable errors.

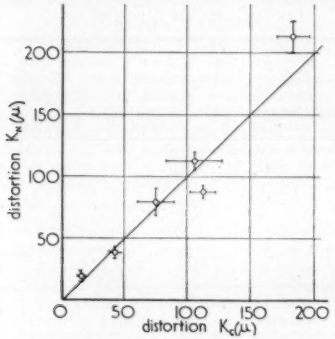

Fig. 3. Comparison of Cosyn's method and the author's method of measuring the magnitude of distortion.

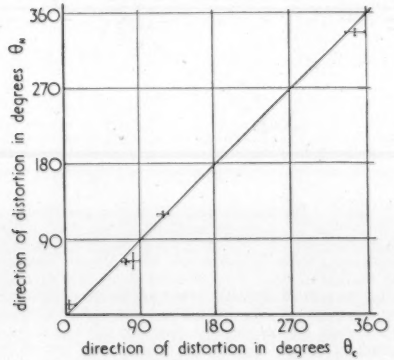

Fig. 4. Comparison of Cosyn's method and the author's method of measuring the direction of distortion

Since, at the midpoint of the emulsion, the separation δ of the track from the chord joining its ends, is equal to the separation Δ_2 of the track from the tangent drawn at its lower end, a test on the equality of Δ and δ constitutes a further check on the method. Lack of equality would be due to higher order distortions. This test has been carried out on nine tracks at a point in an emulsion. The co-ordinates of the end points and midpoint of each track were measured together with the direction of the tangent to the lower end of the track; these points and tangents were set out on squared paper and δ and Δ_2 measured. The test is a sensitive one since Δ_2 depends greatly on the measured position of the track at the half depth of the emulsion and the direction of the tangent. On the other hand, δ is quite constant over the central position of the track. Because of backlash in the microscope which affected the measurement of Δ_2, it was found desirable to measure the midpoint from the bottom of the emulsion. Since the tracks were all at one point in the emulsion δ should have been constant. δ had a mean value of $13{\cdot}1 \pm 0{\cdot}5\,\mu$. The mean value for Δ_2 was $14 \pm 1\,\mu$. Hence the measurements on one track give quick and direct readings of the magnitude and direction of the second order distortion vector K_2.

APPLICATION

The method has been used to plot the distortion contours on a 2×2 in plate which was originally coated with 400 μ thick Ilford G5 emulsion. As a result of processing the thickness was reduced to 200 μ. The distortion was measured in two tracks at each of the points at 5 mm intervals along traverses 5 mm apart. From the distribution of distortion along the X and Y axes plotted from these results, points of equal distortion were found. The contours have been drawn in Fig. 5. The direction of distortion is approximately

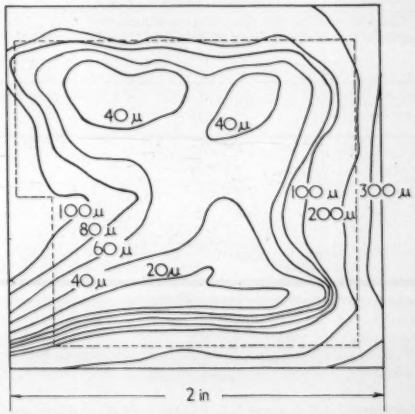

Fig. 5. Distortion contours in a badly distorted emulsion

perpendicular to the contours. The dotted line encloses the area in which measurements were made. Although it is not the purpose here to analyse the contours in detail, the almost closed contours indicate a centrally directed distortion, which would lead to a zero minimum at the centre of the plate. The displacement of this minimum indicates a shearing distortion across the plate. In this way, distortion contours should indicate the sources of distortion in nuclear emulsions.

ACKNOWLEDGEMENTS

I should like to thank Dr. G. D. Rochester for his encouragement and interest. I am indebted to M. M. Séys of the Centre de Physique Nucléaire, l'Université Libre de Bruxelles, for drawing the figures, and to the D.S.I.R. for the award of a maintenance allowance.

Production and separation of small glass spheres

By W. Paul, M.A., Ph.D., and Professor R. V. Jones, C.B., C.B.E., D.Phil., F.Inst.P., Natural Philosophy Department, University of Aberdeen

[*Paper received* 22 *May*, 1952]

Glass spheres free from gaseous inclusions have been made in the size range 1–40 μ. They have been separated with relatively high accuracy into narrow ranges of size by a new sedimentation method using a liquid column containing a gradient of density.

1. Introduction

Small uniform spheres of diameters between 1 and 40 μ have many possible applications as standard particles. For example, experimental investigations of the scattering of radiation by particles require small spheres of uniform size and of known refractive index and absorption coefficient. These investigations enter into such diverse fields as the transmission of light through mist and fog, the measurement of droplet size in a Wilson chamber, the covering power of pigment particles, and the optical characteristics of colloids. Spheres of uniform size and of known optical and mechanical properties provide the best means of testing and calibrating apparatus intended for the size analysis and surface area determination of powders, particularly when the apparatus depends on the phenomena of light scattering and absorption. The spheres can also be used in experiments on flocculation and adhesion, and on fluid and heat flow through packings.

The main purpose of this paper is to describe how spherical glass particles can be made and separated into fractions having a small spread in size, in the hope that the technique may be generally useful. A subsidiary purpose will be to describe the method of separation, which may have general application as a method of size analysis with a relatively high resolving power.

2. Preparation of the Spheres

(*a*) Methods for the production of glass spheres have been described by Sklarew,[1] Sollner,[2] and Bloomquist and Clark.[3] After the glass has been ground and powdered to the desired size, each individual particle is raised to fusion temperature while free to take up spherical shape, and kept in that shape until it has cooled to a rigid solid. We have extended the methods of the above workers towards producing an apparatus which is compact and easy to operate, which is efficient in the avoidance or elimination of particles that are non-spherical or have impurity inclusions, and which collects a high proportion of the original powdered glass in spherical form.

(*b*) *Experimental method*

Prior to fusion, the glass is ground to the desired size and dried for 12–24 h in an oven at 300° C to remove most of the moisture so that the particles do not lump together or stick to the walls of the container. The apparatus shown in Fig. 1 is used. A blowpipe T is fed by ordinary coal gas and an oxygen-air mixture which becomes loaded with glass particles on passing through the container A. The flame is first enclosed in a cylinder C_1 and at its tip is placed a baffle B having a circular hole concentric with the flame and of about the same diameter. Behind B is placed the cylinder C_2; a cold air stream S at right angles to this cylinder at its far end ejects the fused glass particles into a water trough R.

The oxygen-air ratio in the feed to the blowpipe is adjusted to give a "roaring" flame; this imparts sufficient velocity to the glass to carry it into the receiver and gives sufficient heat to fuse most of the particles. The bottle A and the connecting tubes to the blowpipe are thoroughly dried before operation to prevent the glass powder clogging. The inlet to A from the oxygen-air source is by way of a glass tube bent into a semi-circle to create a swirl loading the stream with glass powder. The formation of pockets of powder that may shoot through the flame without dispersion into individual particles must be prevented. The blowpipe should deliver a broad, long flame. The glass particles are injected centrally into the flame from the air-oxygen tube. The cylinder C_1 confines the flame and creates a path to the receiver that is more uniformly heated than if the flame were in the open.

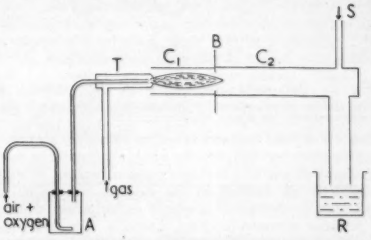

Fig. 1. Sketch of apparatus for production of glass spheres

A glass particle might be ejected sideways from the flame so quickly that it does not fuse. To prevent this, the particles might be guided through the whole length of the flame; this would be very difficult experimentally. Alternatively, they might be made to stay longer in the flame by reducing the flame velocity or they might be heated more quickly by increasing the flame temperature. Some of these requirements are mutually exclusive, and, in practice, fusion time and fusion temperature are adjusted to give the maximum number of spherical particles and any non-spherical ones are prevented from entering the collecting apparatus by the baffle B. The efficiency of collection is thereby reduced, but the non-spherical component is completely eliminated.

After ejection from the flame the spheres are confined to the cylinder C_2 and allowed to cool before final extraction. The air stream S cools them still further and pumps them along C_2 into the receiver R.

(*c*) *Results*

When soda and Pyrex glasses are fused, inclusions are often noticed under microscope examination (see Fig. 2). These inclusions have a lower refractive index than glass, as observed by the Becké line test, and a lower density, as is easily verified in separation of the spheres by centrifugation in a liquid of density near to the glass density. The inclusions are probably gaseous and may be caused by the "freezing in" of expanded bubbles of gas in the glass or by the trapping of air when several small particles fuse into one large one.

The production of gas bubbles could be reduced by lowering the flame temperature to the lowest usable value; however, there would be some variation in temperature in a cross-section perpendicular to the length of the flame so that

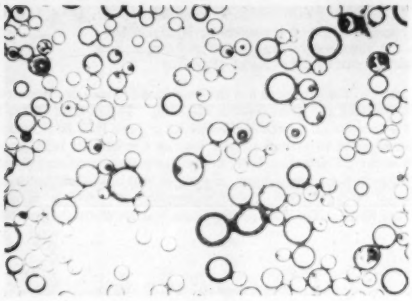

Fig. 2. Photomicrograph of soda glass spheres, immersed in water, showing inclusions. Diameter 1–40 μ

differently situated particles would be differently treated. The trapping of air between particles would be lowered by reducing the density of particles in the air-oxygen stream. When these precautions are applied in the case of soda glass, some improvement ensues, but a wholly inclusionless sample has not yet been obtained (cf. Figs. 2 and 3). The final product, when Hysil glass is used, contains uniformly spherical particles of diameters ranging from less than 1 μ to greater than 40 μ (see Fig. 3). There are few particles that are seriously a-spherical. Measurements of the worst-shaped member of a random sample of twenty particles gave a maximum to minimum diameter ratio of 1·02. No extra difficulty is anticipated in fusing other materials by a similar technique.

Experiments were carried out on the production of spheres

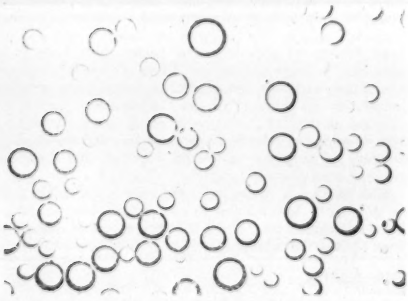

Fig. 3. Photomicrograph of Hysil glass spheres, diameter 1–40 μ, immersed in water

by dropping glass through a silica furnace 30 cm long run at 1 000° C. A long wide furnace that can be maintained at a steady high temperature would fuse most types of glass. Further, the better control and estimation of temperature would allow the exact determination of the best conditions of fusion to avoid inclusions and strains. A more effective cooling device could be established and a higher percentage of the ultimate product collected. The preliminary experiments carried out were only moderately successful, the main difficulty lying in the initial dispersion of the powder sample. In the present method of separation Hysil glass spheres fused in a flame as described above are used.

3. SEPARATION OF THE SPHERES INTO CLOSELY-SIZED FRACTIONS

Different definitions of the term "size" are appropriate in different methods of particle separation and analysis. In this discussion the size is measured by the actual sphere diameter.

(a) Accepted methods

There exist several established methods of separating particles of the size required; however, none of these gives very uniform fractions even with considerable expenditure of effort. The sieves available are unsuitable for producing sharply defined graded fractions, the proportional variation in sieve opening increasing as the opening becomes smaller. A possible modification of the sieve, a slit mechanism of narrow aperture, was constructed with a slit length of approximately 1 cm and adjustable down to slit widths of approximately 2 μ. The variation of slit width over the whole length was of the order of 5% at 5 μ. Glass spheres

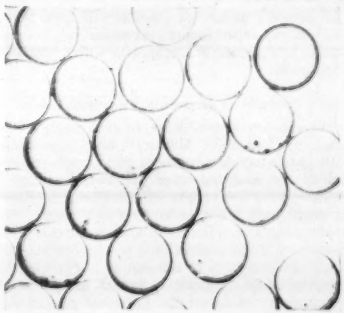

Fig. 4. Photomicrograph of Chance glass spheres immersed in water. Diameter 216–224 μ

were vibrated vertically in a suitably shaped closed cavity above the horizontal slit. The relative velocity of spheres and slit was probably less than 100 cm/sec and there was no observable deterioration in the condition of the slit jaws due to abrasion by the glass. It was found that the yield for spheres smaller than 40 μ was very low owing to clogging of the slit by spheres suffering electrostatic attraction. Spheres larger than these were separated quite efficiently. Successive separations at slightly different slit widths succeeded in giving a sample inside a narrow size range. Fig. 4 shows spheres of Chance glass, size 216–224 μ, separated by this means. The size corresponds exactly with the slit settings. In the size range greater than 40 μ there seems to be little difficulty in thus producing monodisperse samples.

Small homogeneous spheres settle in a fluid with limiting

velocities dependent on some power of their diameter. The usual applications of this in separation work are in the well-known techniques of sedimentation with decantation, in elutriation, and in centrifugation. Sedimentation followed by decantation is a laborious process involving large quantities of liquid, which never gives complete separation. It is a useful way of producing a wholly "under-size" fraction. The elutriator tube, which uses an upward fluid flow to balance the fall with limiting velocity under Stokes' Law, has several inherent disadvantages—variations in fluid velocity in different parts of the tube, wall effects, temperature effects—that spoil its performance. The ordinary centrifuge method faces difficulties similar to those of the decantation procedure, and in any case is usually employed in the size range below 1 μ.

Electrostatic methods of separation are theoretically possible, but the experimental difficulties are considerable.

(*b*) *Method used*

(i) The density gradient. The equation of motion of a particle falling under streamline flow in a fluid medium is

$$m\ddot{x} = (m - m')g - kd\eta\dot{x}$$

where mg = weight of particle, $m'g$ = upthrust of liquid, d = diameter of particle, η = viscosity of liquid, k = constant. The particle, starting from rest, accelerates until the resistance due to the fluid viscosity balances the resultant gravitational pull, whence it moves with a terminal velocity v given by

$$v = \frac{k'(\rho - \rho_0)d^2}{\eta}$$

where ρ, ρ_0 = densities of particle and liquid, k' = constant. In our experiments the conditions necessary for the application of Stokes' Law to the fall of the particles may be assumed to be satisfied.

It is necessary in the ordinary sedimentation procedure to settle and decant a large number of times to produce reasonably good size separation. If the particles could be released simultaneously at the top of the sedimentation vessel and allowed to fall with their terminal velocities, they would reach the bottom in order of size. In practice, the particles swirl downwards like a blob of ink, large and small mixed, and no application of grids and baffles reduces the convection. The instability of the column is caused by the larger mean density of the layer containing the particles over the layer below.

Dr. F. C. Frank suggested that if the particles were made to settle against a density gradient there would be no tendency for a swirl to develop, and the particles would settle with their limiting velocity under Stokes' Law.* That this is borne out in practice has already been summarily reported.(4) In choosing liquids to form a density gradient several considerations have to be borne in mind:

(*a*) the liquids should mix over a considerable range of proportionate volumes;

(*b*) the liquids should have a density difference sufficiently high to make that between successive layers greater than a certain minimum. This minimum is dependent on the liquids used, and is just large enough to prevent the layers mixing immediately on contact;

(*c*) none of the liquids used should coagulate the particles to be separated;

(*d*) the liquids should not react with the container, producing precipitated particles or giving any product likely to coagulate the particles to be separated or interfere with their free fall.

Mixtures of alcohol and water are found to be satisfactory in the separation of glass particles. Mercuric chloride was usually added to the alcohol-water mixture to prevent organic growths, which were a troublesome feature of initial experiments with the density gradient column. Diffusion at the interfaces between layers provides a gradual change-over in density. The layers can be made thin and numerous so that a sensibly continuous gradation of density is obtained, especially at the top of the sedimentation column. The gradient persists for a long time and is not upset by small oscillational movements or temperature fluctuations. Convection currents are damped out and the column obtains an equilibrium state with a gradient of density from 0·86 to 1·0 g/c.c. from top to bottom.

The densities of the mixtures used in setting up the gradient are in steps of 0·01 g/c.c. from 1·0 to 0·86 g/c.c. The containing vessel is filled with water, and a tube with a flanged end lowered on to the water surface. Liquid of density 0·99 g/c.c. is slowly pipetted down the side of the tube. At the flange the downward velocity is reduced and a flow outwards across the water surface produced. With a density difference of 0·01 g/c.c. it is relatively easy to create a step in density at the water surface. The procedure is repeated with further layers. The thickness of the different layers is adjusted to provide a steep gradient at the top of the sedimentation vessel. A typical gradient is shown in Fig. 5.

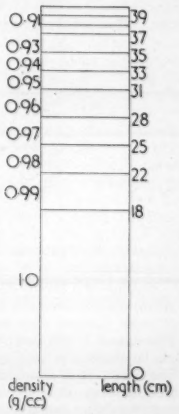

Fig. 5. Typical construction of alcohol-water column having a gradient of density

(ii) The instrument. The gradient is incorporated in the instrument of Fig. 6. The sedimentation vessel *A* is locked to the detachable top *C* of a large cylindrical container *B* at a point near the circumference. A number of small glass dishes are mounted round the circumference of a plate *D* which is rotatable about a central stem *E* in such a way as to bring the dishes successively beneath *A*, which may be of any length and may have a wide variation in diameter. The length is determined by the size of particles being separated (the larger the particles, the greater the length required) by the resolution required in the separation, by the time considered necessary for the completion of a separatory run and by the time taken to change the dishes in position without introducing any tendency for the liquid in *B* to swirl. The vessels used varied in length from 20 cm to 100 cm and in diameter from 6 cm upwards. The bottom part of *A* is wax-sealed into a cylindrical brass container *H* which in turn is locked securely through a hole in the Perspex plate *C* by the ring *J*, screwed tightly to the threaded bottom portion *K* of *H*. Rubber washers are used to perfect the liquid-tight

* Mr. W. H. Walton has independently developed the same method—private communication.

seal between Perspex and brass. A stopcock *F* empties *A* as required. The top Perspex plate *C* is fixed to *B* by a brass ring *L* and twelve bolts and nuts *M* spaced round *B*. *B* is constructed of brass and has a stopcock *G*.

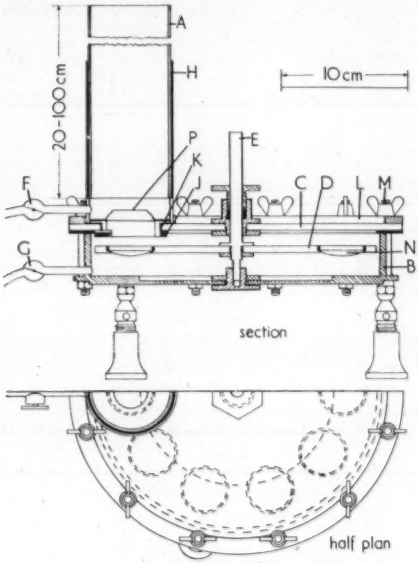

Fig. 6. Apparatus for separation of glass spheres

Through the centre of *C* is sealed the stem *E* which has attached to its lower end a Perspex plate *D* carrying a number of small, concave glass dishes *N* fixed in position by circlips. The size of *D* and position of the dishes are such that they can be revolved in turn, by *E*, into position under the vessel *A*. The height of *D* is adjusted until the dishes are under, and as close as possible to, the brass end *H*, to ensure that any particles falling out of *A* will settle in a glass receiving dish. The instrument is levelled by mounting the three feet of *B* on adjustable jacks.

When the vessel *B* is being filled it is advisable to prevent the trapping of air bubbles on any part of *B* or the apparatus inside *B*. An air bubble released during a run which rises through the sedimentation column spoils the separation by causing swirls along its path. This difficulty can be avoided in several ways, e.g. by coning part of the underside of the top *C* and trapping the air in the cone apex, or by providing an escape port by suitably slotting the locking ring *J* and the bottom threaded part of *H*.

(iii) Use of instrument. When the instrument has been assembled and the liquid column with its gradient of density established, a dilute suspension of spheres in pure alcohol is run down on to the top of the column using the flanged tube as before. The dishes are then rotated under the sedimentation vessel at times determined by the size of particles required and their velocity of fall as calculated from Stokes' Law and empirical calibration of the gradient for density and viscosity. Several precautions improve the quality of the separation.

(*a*) The instrument and the liquids used must be as free as possible from extraneous particles.

(*b*) The glass introduced in suspension must be completely deflocculated and must stay dispersed during the time of the separation. A combination of mechanical dispersion and suitably chosen liquids provides good deflocculation. Water-alcohol mixtures are especially suitable for glass.

(*c*) Particles which stick to the walls and are dislodged may eventually fall into the "wrong" receiving dish. They are eliminated by inserting, at the bottom of the vessel *A*, a baffle ring *P* designed to present a sharp edge to the falling spheres at such an angle that they are unlikely to attach themselves to the edge itself.

(iv) Results and conclusions. Spheres with diameters up to 40 μ have been separated in one operation giving over 90% of all those in one dish within $\pm$ 5% of the mean size. Fig. 7 shows a typical separation. The separated particles can be used in any application requiring a small amount of uniformly spherical particles of the same size. The amount of material separated in each operation is small, being of the order of 0·3 g, but it is possible to make at least 3 runs in the same column without destroying the density gradient.

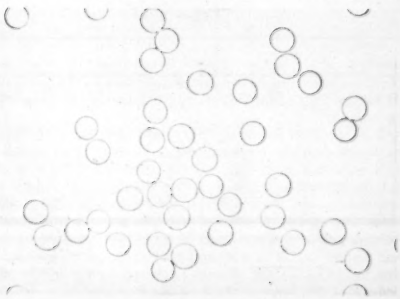

Fig. 7. Photomicrograph of Hysil glass spheres immersed in water. Mean diamater 14 μ

The method may be used for any material if two liquids can be found that maintain dispersion of the particles and are of suitable density and viscosity. The method of separation may be applied directly to the size distribution analysis of powders and has been used in a method depending on the scattering of light by the particles as they cross a horizontal section of the sedimentation vessel.

REFERENCES

(1) Sklarew, S. *Industr. Engng Chem. Anal. ed.*, **6**, p. 152 (1934).
(2) Sollner, K. *Industr. Engng Chem. Anal. ed.*, **11**, p. 48 (1939).
(3) Bloomquist, C. R., and Clark, A. *Industr. Engng Chem. Anal. ed.*, **12**, p. 61 (1940).
(4) Paul, W., and Jones, R. V. *Research*, **3**, p. 98 (1950).

A study of the oil-film formation in gears by electrical resistance measurements

By T. B. LANE, M.Sc., A.Inst.P., and J. R. HUGHES, B.Eng., G.I.Mech.E., The Shell Petroleum Co. Ltd., Thornton Research Centre, Chester

[*Paper received 5 May*, 1952]

In pursuit of information concerning the nature of lubrication in gears, measurements of the electrical resistance between the meshing teeth of rotating gears have been made using a cathode-ray oscillograph. Photographs of the trace on the screen of the cathode-ray oscillograph are shown indicating values of resistance ranging from infinity to zero. The variation of resistance depends on the load, though the resistance is always lowest where the sliding speed is highest and has its maximum value in the neighbourhood of the pitch-line where there is no sliding motion. Absolute values of film-thickness could not be determined.

The mechanism of oil-film formation between meshing spur-gear teeth is not completely understood, and although various conflicting theories have been put forward based on indirect experimental evidence, no direct investigation of this problem, to our knowledge, has yet been undertaken. Lubrication of gear teeth may be by full-fluid film or by an adsorbed boundary film or, as has recently been suggested,[1] by a solidified oil film. Frictional values are useful indications of the type of lubrication and values of 0·1[2] and 0·05[3] have been quoted for the coefficient of friction in gears. A value of 0·1 suggests that lubrication is predominantly by boundary films whereas 0·05 suggests that hydrodynamic action is also playing a part. Bowden[4] has stated that light mineral oils have no boundary-lubricating properties at temperatures above 90° C, whereas experiments on the Institution of Automobile Engineers' (I.A.E.) 3½ in centres gear rig[5] using a spindle oil supplied at this temperature show that an appreciable load can be carried, indicating that boundary films cannot be solely responsible for the lubrication. As a direct approach to the problem, measurements of the electrical resistance between the meshing teeth of rotating gears have been made, since differences in oil-film thickness might be expected to be reflected by changes in the measured resistance. It was thought unlikely that quantitative results would be obtained but at least it was expected that some general idea of the magnitude of the film thickness might be deduced.

EXPERIMENTAL

The I.A.E. 3½ in centres gear rig was used for this work. The test gears were those normally employed, but, for the purpose in view, each gear was separately insulated from its shaft and provided with a short extension shaft carrying a metal disk which was partially immersed in mercury. Electrical connexion to the gear could thus be made through the mercury bath. The electrical circuit is shown in Fig. 1.

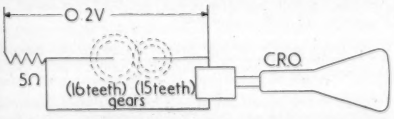

Fig. 1. Electrical circuit for resistance measurements

The potential difference across the gears was measured by a cathode-ray oscillograph, the time-base of which was controlled to correspond with the period of revolution of the sixteen-toothed gear. The trace on the screen of the oscillograph was recorded photographically, provision being made to record a single trace only to avoid confusion. With the circuit used, a half-scale deflexion was obtained when the gear-contact resistance was 5 Ω. The measurements were therefore very sensitive in the region of low resistance, a fact which permitted early detection of any tendency for the teeth to be separated by an oil film.

Fig. 2 shows a selection of photographs taken during an experiment using a mineral oil of viscosity 1·3 poise at the operating temperature of 60° C. In these photographs, the left-hand side of the trace represents the start of the horizontal sweep and corresponds in every case to the same tooth on the sixteen-toothed wheel. Two photographs were taken at each load increment, one as near the start as possible and the other just before the end of the running period, which was of 5 min duration for each load. All photographs taken at the beginning of the runs are included, and in addition, two, (*c*) and (*g*), which were taken at the ends of their respective runs, and one, (*h*), taken after scuffing had occurred, but at a lower load than the scuffing load. The condition of tooth engagement corresponding to the start of the time-base of the cathode-ray oscillograph was identified by observing the gears by stroboscopic flashes synchronized with the time-base. Fig. 3 shows a selection of photographs taken during a run using an oil (of viscosity 0·13 poise at the operating temperature of 60° C) containing 1·5% w of an extreme pressure additive. They all relate to the start of the loading interval except (*f*), which was taken at the end of the period in which scuffing was found to have occurred.

DISCUSSION

The traces recorded in Figs. 2 and 3 show that variations of resistance occur throughout the meshing period, except with the heavier oil at the lowest load [(*a*), Fig. 2]. When the resistance is very high the teeth must be completely separated by an oil film. The interpretation of resistances between the very high values and zero is not so easy. Assuming that the value of the electrical conductivity of the oil in bulk may be applied to the thin films existing in the gear contact, an estimate of the order of resistance expected may be obtained. The conductivity of mineral oil varies quite rapidly with temperature and is affected by moisture and oxidation products. In the present experiments, which were carried out at 60° C, some oxidation will have taken place and some moisture may still have been present. Measurements have shown that the conductivities of the oils in bulk, even for the used oil containing the additive, were all less than $10^{-12}\ \Omega^{-1}\ cm^{-1}$. The area of contact between the teeth for a load of 25 lb on the lever is approximately $10^{-2}\ cm^2$. The resistance of a film 10^{-5} cm thick (of the order of the height of the asperities on the gear teeth) will therefore be

greater than $10^{12} \times 10^{-5}/10^{-2} = 10^9\,\Omega$. Accordingly resistances of a few ohms, as observed, must indicate metallic contact or at any rate extremely thin films of molecular dimensions.

Concerning measurements of this nature Bowden and Tabor[6] have stated ". . . the least separation of the surface beyond the region of boundary lubrication introduces resistance values ranging from several ohms to millions of ohms. Consequently a contact resistance exceeding, say, 100 Ω, means that the surfaces are completely separated by a lubricant film, . . . on the other hand a contact resistance considerably less than 1 Ω means that there is either intimate metallic contact between the surfaces, or at best a regime of boundary lubrication." The resistance of very thin films must, however, be regarded with caution. Needs,[7] using an applied potential of 0·025 V, found that films began to conduct at a thickness of 10^{-4} in and at "60×10^{-6} in conducted as well as copper wire." Cameron[3] found that the resistance of an oil film between rotating disks fell as the applied voltage increased, but that constant values of the resistance were obtained when the applied voltage was less than a few tenths of a volt. Similarly Courtney-Pratt and Tudor[8] in their measurements of contact resistance between a piston ring and cylinder wall found that as long as the applied voltage was less than 0·4 V the oil film behaved in an ohmic manner. Therefore an applied voltage of 0·2 V seemed reasonable in the present experiments. With this value the potential gradient for a film 10^{-5} cm thick is 2×10^4 V/cm which is less than the values of dielectric strength (10^5 V/cm) usually associated with mineral oils in bulk.

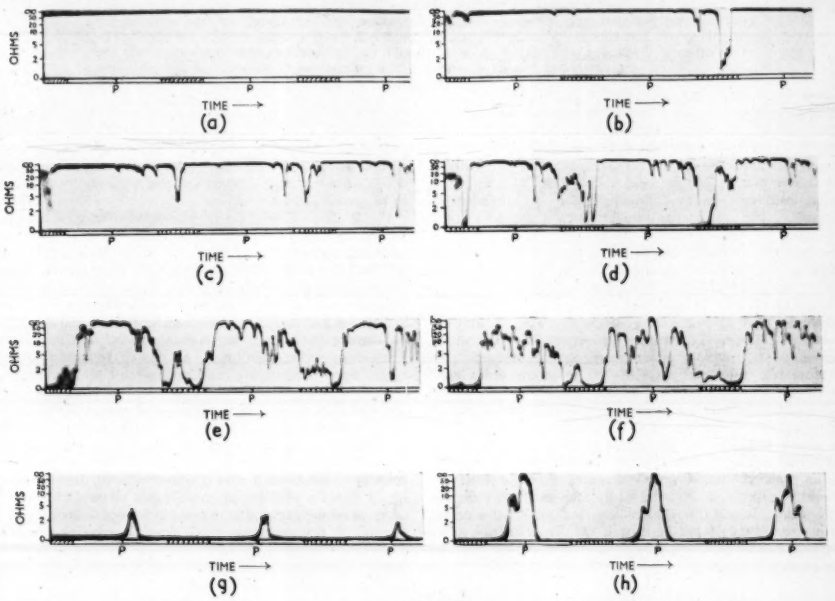

Fig. 2. Oscillograph traces showing the variation of oil-film resistance with meshing position when using a mineral oil of viscosity 1·3 poise at the operating temperature of 60° C. Pinion speed: 2 500 r.p.m.

(*a*) 10 lb beginning of run, (*b*) 20 lb beginning of run, (*c*) 20 lb end of run, (*d*) 30 lb beginning of run, (*e*) 40 lb beginning of run, (*f*) 50 lb before scuffing, (*g*) 50 lb after scuffing, (*h*) 40 lb scuffed gear.

In spite of the limitations of this kind of measurement the present results are valuable because they do give some indication of the changes in the oil-film thickness over the meshing cycle. Whether a low resistance means that metallic contact has occurred or merely that the oil film has been punctured by the applied voltage, it does in either event show that the film is thinner than when the resistance is high. Fig. 2 shows the effect of load. At the lowest load the teeth are separated at all times by a thick film and here it may be

inferred that hydrodynamic action is responsible. The value of $\eta(u_1 + u_2)/W$, a measure of the hydrodynamic-film-forming tendency, where η = dynamic viscosity, u_1, u_2 = surface speeds of gear teeth relative to the line of contact, W = the unit line-loading of the teeth (all in consistent units), is 10^{-5} at the pitch point under these conditions, which is somewhat lower than the value of 10^{-3} deduced by Blok[2], from friction measurements, for the onset of hydrodynamic lubrication. As the load is increased the film becomes thinner until finally, at the scuffing load (*f*) (see Fig. 2), values of resistance greater than 50 Ω are rarely obtained. When scuffing occurs the trace changes immediately to the type shown in (*g*), the value of the resistance being zero for most of the time. (*h*) was obtained after scuffing had occurred but at a lower load, and comparison with (*e*) (obtained under the two pairs of teeth, which would be expected to reduce the tooth loading and hence encourage the formation of a thicker film, but dynamic loads, due to the change from one- to two-pair contact, may disturb this tendency. The best conditions (highest resistances) occur in the neighbourhood of the pitch point, where one pair of teeth carries the total load. It will be interesting to examine the hydrodynamic-film-forming tendencies at points corresponding to these two conditions.

The film thickness depends on $\eta(u_1 + u_2)R/W$ where R is the relative radius of curvature of the two contacting teeth at the point considered. In the I.A.E. 3¼ in centres gear rig $(u_1 + u_2)R$ increases by approximately 40% between the points where the tooth engagement begins (and when two pairs of teeth are in contact) and the pitch point where one pair of teeth only carries the load. Thus the film would be

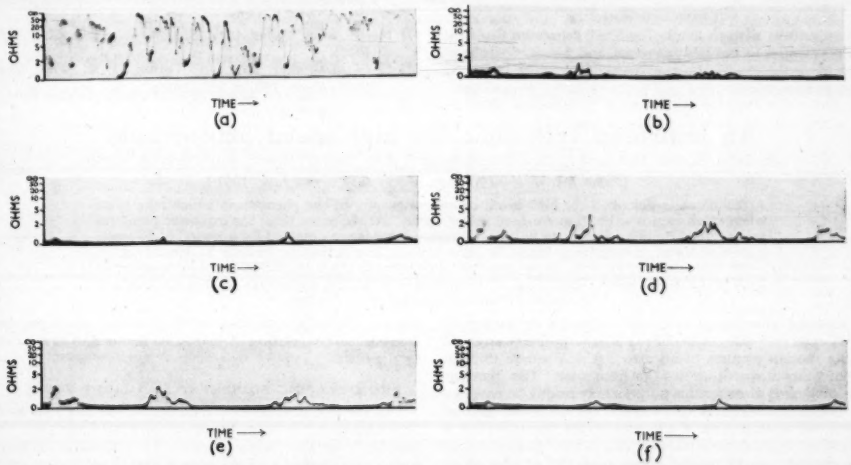

Fig. 3. Oscillograph traces showing the variation of oil-film resistance with meshing position when using a mineral oil of viscosity 0·13 poise at the operating temperature of 60° C containing an E.P. additive. Pinion speed: 2 500 r.p.m.
(*a*) 10 lb, (*b*) 30 lb, (*c*) 50 lb, (*d*) 60 lb, (*e*) 70 lb before scuffing, (*f*) 70 lb after scuffing.

same load but before scuffing had occurred), shows the change in contact conditions brought about by a scuffed profile. During most of the five-minute runs the trace on the screen of the oscillograph indicated a progressive deterioration in the state of lubrication. This effect is illustrated in (*b*) and (*c*) (Fig. 2,) which were obtained at the beginning and end respectively of the five-minute running period. These two photographs show that continued running—at any rate with the finely-finished gears used—does not improve the lubrication. The change noted in the present instance is probably due to the effect on the oil film of gradual heating of the gear.

Relating the resistance traces to the position of the contact on the gear teeth shows that the worst conditions (lowest resistances) occur during the period when two pairs of teeth are in contact at the same time. Although part of this reduced resistance must be due to the fact that during this period there are two electrical contacts in parallel, it is notable that the resistance still falls to zero at many points, in spite of the fact that during this period the load is shared between expected to be thinnest during the period of one-pair contact—since the favourable increase of up to 40% in the value of the function $(u_1 + u_2)R$ is more than offset by the nominal increase of 100% in the value of W. The observed condition is opposite to this and may be due to the influence of dynamic loads, already referred to, or, more likely, to the effect of sliding speed. At first and last contact the sliding speed is high and the consequent rise in temperature might be enough to affect the oil film; at the pitch point the sliding speed is zero, there is little generation of heat and so the viscosity of the oil will not fall very much.

Fig. 3 shows photographs of traces taken during an experiment in which a light oil containing an E.P. additive was used. By comparison with Fig. 3 the effect of viscosity is immediately apparent—the oil films are very much thinner than with the heavier oil. At loads greater than 10 lb the traces rarely depart from a value of zero, and even when scuffing has occurred [(*f*), Fig. 3] the trace is little different from the earlier ones. These low values of resistance probably mean

that boundary films were responsible for the lubrication throughout most of this experiment.

CONCLUSIONS

These experiments show that the thickness of the oil film is not uniform over the tooth surface but appears to depend on sliding speed, being thinnest where the sliding speed is highest. An increase in load reduces the thickness of the oil film; at low loads using a heavy oil the film is comparatively thick whereas at high loads and particularly with a light oil fortified with a load-carrying-capacity improver of the chemically-active type, the lubricant film may be very thin. The interpretation of electrical resistance in terms of film thickness was not possible but the low values obtained suggest that metallic contact may occur particularly in those areas where the sliding speed is highest.

ACKNOWLEDGEMENTS

The authors wish to thank The Shell Petroleum Co. Ltd., for permission to publish this paper, and Mr. R. C. Robson, who made the electrical arrangements and assisted with the experimental work.

REFERENCES

(1) CLARK, O. H., WOODS, W. W., and WHITE, J. R. *J. Appl. Phys.*, **22**, p. 474 (1951).
(2) BLOK, H. *Papers and Discussion presented at the Symposium on Gear Research, Brunswick* 1950, p. 153 (Brunswick: Friedr. Vieweg and Sohn).
(3) CAMERON, A. *Papers and Discussion presented at the Symposium on Gear Research, Brunswick* 1950, p. 139 (Brunswick: Friedr. Vieweg and Sohn).
(4) BOWDEN, F. P. *Proc. 3rd World Petroleum Congress, The Hague* 1951, Sec. VII, p. 328 (Leiden: E. J. Brill, 1951).
(5) MANSION, H. D. *J. Inst. Petrol. Paper presented at the Gear Lubrication Symposium* 1952 (In the press).
(6) BOWDEN, F. P., and TABOR, D. *The Friction and Lubrication of Solids*, p. 248 (Oxford: University Press, 1950).
(7) NEEDS, S. J. *Trans Amer. Soc. Mech. Engrs*, **62**, p. 331 (1940).
(8) COURTNEY-PRATT, J. S., and TUDOR, G. K. *Proc. Instn Mech. Engrs*, **155**, p. 293 (1946).

An improved technique for high-speed photography

By D. A. SENIOR, M.A. and C. O. J. GROVE-PALMER, B.Sc., Royal Naval Scientific Service, Rosyth

[*Paper first received* 20 *May, and in final form* 4 *June*, 1952.]

A technique is described for high-speed cine-photography of the phenomena which take place when small explosive charges are fired under water. At the same time, the explosive pressures are recorded by piezo-electric technique. Pressure records are obtained for a period of 60 msec, and high-speed photographs taken by means of a 16 mm Fastax camera at speeds up to 4 000 frames/sec. At the maximum speed, a cine record in black and white or colour is obtained for a period of 80 msec. The layout of equipment is described, and details of time marking and sequence timing arrangements are given.

In studying phenomena associated with the detonation of small explosive charges under water, the problem arose of taking motion pictures of an area 3 ft 6 in square through 9 ft of water at speeds up to 4 000 frames/sec. The illumination of limited areas for this purpose may readily be provided by means of continuous light sources, but the power requirements are considerable if the area to be photographed is extensive. (Calculations showed that, in this instance, colour photography would require about 1 000 kW of photoflood lighting, which was clearly impracticable.) High intensities of illumination may, however, be provided for limited periods by means of photoflash bulbs,[1, 2, 3] and the technique which is described is based upon this principle. Photographs are taken simultaneously of phenomena above and below the water surface. The equipment has been designed so as to synchronize the photography with other methods of recording. The photographs cover a period of 80 msec at maximum speed, and therefore give the general history of the explosion phenomena; most information is obtained by projecting the records as a film at normal speed. From a study of the film it is possible to decide at which points more detail and time resolution are required. The detailed study is then carried out by taking microsecond flash photographs at suitable times from the instant of detonation.

Water treatment. Experiments have been carried out in a cylindrical tank of diameter 12 ft and depth 8 ft, around which has been built a laboratory to provide cover over the tank itself and accommodation for control and recording equipment. Water clarity is maintained by careful exclusion of dust and continuous filtration (the filter handles one tank volume per day). An alkalinity of pH8 is maintained by the addition of sodium carbonate (about 6 g of the anhydrous salt per day). The addition of 0·6 g potash alum per day then ensures coagulation of suspended matter and its removal by the filter.

PHOTOGRAPHIC EQUIPMENT AND LIGHT SOURCE

The Western Electric 16 mm Fastax camera has been used. This camera has a maximum speed of 4 000 frames/sec, the exposure time then being 80 μsec. Two modifications have been found desirable. The lens provided by the makers, with focal length 2 in, did not give a sufficiently large field of view. It has therefore been replaced by a Dallmeyer "Reverse Telephoto" lens which has an effective focal length of 1 in. The comparatively large distance of 2 in from the rear component to the focal plane makes it possible to use this lens in spite of the space occupied by the rotating glass block, which is a feature of the camera. No time marker is available with the camera as manufactured. A crater tube (Sylvania type R.1130.B) has therefore been installed to operate at a tuning-fork controlled frequency of 5 kc/s. The light is focused by means of a small mirror and lens on to the film on the sprocket wheel in the space between the perforations and the edge of the film. (The arrangement is shown in Fig. 2.)

Light is provided by firing a sequence of flash bulbs, the wire-filled type being used in preference to those with foil filling. The advantages are that, with the wire-filled variety, the time interval between the application of voltage and maximum light output is constant within close limits; the percentage of bulbs which fail to fire is very small; the bulbs do not fire sympathetically and may thus be mounted compactly in groups without the use of partitions. They are, moreover, robust, and able to resist explosive shock.

Reflector units have been built to take twelve or twenty-four bulbs which are fired at intervals of 16 msec. Their light outputs overlap to give an even illumination throughout the sequence.

Provision is made for firing a maximum number of 192 bulbs in groups over periods varying from 80 to 320 msec. The following formula, derived experimentally, gives the number of flash bulbs required (bulbs used being Philips P.F.56 with an output of 56 000 lm sec):

$$N = (f^2d^2S4D/10)/(30Z)$$

where f is the lens aperture,

d is the distance from the light source to the subject in feet,

D is the water path in feet traversed by the light between light source and camera,

S is the speed of the camera in thousands of frames/sec (with the Fastax camera the exposure time is approximately one-third the time per frame),

Z is a factor which varies inversely with the speed of the film used and has a value of unity for Kodachrome,

N is the number of bulbs in each group, the number of groups being determined by the length of record required.

The layout of the photographic equipment is shown in Fig. 1. The camera is mounted with its axis running vertically through the centre of $\frac{1}{4}$ in plate glass window in the bottom

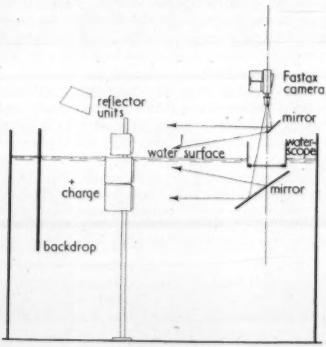

Fig. 1. Photographic layout

of a brass box (the waterscope). The function of the waterscope is to eliminate optical distortion by the water surface. A mirror is arranged beneath the waterscope at an angle of about 45° to the vertical, the depth and angle of the mirror both being adjustable. A surface silvered mirror is introduced between the camera and waterscope when photographs above the water surface are required. Photography is carried out by reflected light against a black background. The reflector units are clipped on to vertical poles which may be withdrawn from the water in order to change the bulbs. No waterproofing is provided as the bulbs operate quite satisfactorily under water. The explosive charge, a fifteen-grain electric detonator, is supported upon stiff wires which serve also as firing lead. Orange and green-coloured cable is used so that the colour rendering may be checked in colour films.

Pressure recording. Shock wave pressures are recorded for a period of 60 msec by piezo-electric technique. Two $\frac{1}{4}$ in diameter tourmaline crystal gauges are connected to amplifiers and the pressures recorded by an oscilloscope and drum camera. Time marking is provided by means of a crater tube operating in parallel with the tube in the Fastax camera. The two records are synchronized by interrupting the timing traces for 0·2 msec about 16 msec after firing the charge. In order to facilitate comparison of pressure records, the drum camera speed is adjusted to 750 r.p.m. before the Fastax camera is started, the speed being checked as follows: a radial line painted upon the driving pulley of the drum is illuminated by means of a neon stroboscope operating at a tuning fork controlled frequency of 50 flashes per sec. When the drum is running at 750 r.p.m. the line is seen as a cross. The charge is fired when the cross appears stationery.

SEQUENCE TIMING AND CONTROL CIRCUIT

The technique of timing the photographic and pressure records is influenced by features of the design of the oscillograph recording camera which will first be described with the aid of Fig. 2. The film is wrapped around a drum 7 ft in circumference, the ends of the film being threaded through a slot in the periphery of the drum and held in place by means of a wedge. Exposure of the film during one revolution of

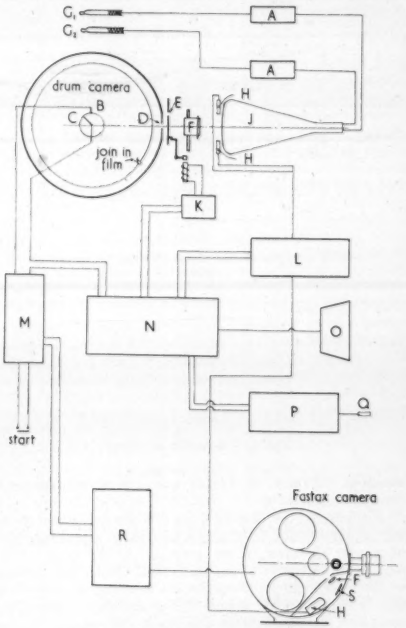

Fig. 2. Schematic circuit diagram

A, amplifier; *B*, brush; *C*, contactor; *D*, gate; *E*, shutter opening; *F*, lens; G_1, G_2, piezo-electric gauges; *H*, time marker; *J*, cathode-ray oscilloscope; *K*, shutter control circuit; *L*, time marker amplifier; *M*, delay circuit; *N*, flash control circuit; *O*, reflector unit; *P*, firing circuit; *Q*, charge; *R*, camera control circuit; *S*, mirror.

the drum is regulated by the shutter (Fig. 2). The shutter consists of a brass plate, constrained to fall vertically, a slot in the plate permitting exposure of the film as the shutter passes the gate in the body of the camera. The shutter is released by an electromagnetic trigger at such a time that exposure of the film begins a few inches after the join in the film has passed the gate. Timing is effected by means of the contactor C mounted on the spindle of the camera drum, the angular position of the contactor segment being adjustable with respect to the position of the join in the film.

The whole sequence will now be clarified by Figs. 2 and 3. The drum camera is first run up to speed. When the speed is

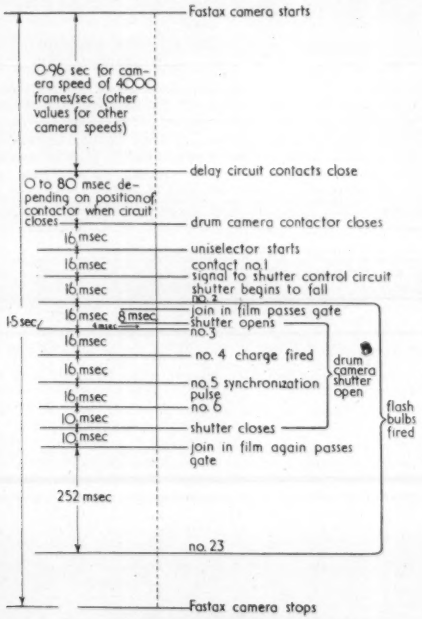

Fig. 3. Sequence of events

steady at 750 r.p.m. the Fastax camera is started; thereafter timing is regulated by two circuits. The first, a simple delay circuit, governs the time of firing the charge relative to the start of the camera. Contacts are closed at a predetermined time after the start of the camera. (This circuit is not required in cameras such as the Eastman high-speed camera, which incorporates a mechanical switching device.) This closure completes the circuit to the contactor. When the contactor segment reaches the brush, the second control circuit is set in operation. Details of this circuit, which is built around a Post Office uniselector, are given below. On receipt of the signal from the contactor, relays are operated which allow the uniselector to perform one cycle. The cycle is performed in twenty-five steps at intervals of 16 msec. The flash bulbs are fired on step number 2 and on subsequent steps. (The number of steps used depends upon the length of record required.) A signal is supplied to the circuit which operates the drum camera shutter on step number 1. The charge is fired on step number 4. On step number 5 a synchronization pulse is injected into the time marker supply.

The sequence control circuit is designed (i) to time the opening of the shutter in the drum camera used in pressure recording, (ii) to provide a synchronization pulse to the time markers on the Fastax and drum cameras, (iii) to fire a sequence of photoflash bulbs, and (iv) to fire the charge. These operations are performed by a Post Office uniselector (type 42A). The remainder of the circuit starts the uniselector at the appropriate time, ensures that it performs one cycle only and permits the testing of the uniselector without firing the flash bulbs. The circuit is shown in Fig. 4; it is operated by connecting the terminal marked "start" to the negative side of the 110 V supply. The duration of this contact may be either prolonged or as short as a few milliseconds. In either case, the uniselector performs one cycle and then stops. If the switch S is in the open position, the circuit re-sets itself automatically when the starting contact is removed. When the switch S is closed, the circuit must be re-set by hand before another cycle is performed. This feature (hand re-set) is necessitated by the nature of the contact which operates the circuit in practice. As has been mentioned, this circuit is started by the rotary contactor on the drum camera. Consequently, once the circuit to this contactor has been made, impulses of about 2 msec duration are repeated at intervals of 80 msec—once for each revolution of the drum. With automatic re-setting between impulses the uniselector would operate repeatedly with consequent damage.

The control circuit must thus fulfil two conditions: (i) it must operate on a short duration starting pulse, and (ii) it must then provide power to the uniselector for a long enough period to make one step. After this the uniselector takes control. The power supply must, however, be removed before the completion of the whole cycle in order to avoid the initiation of a further cycle. The first condition is achieved by the rapid closure of the double wound relay X (Fig. 4). This relay is energized initially on a voltage of 110 V through the contacts X_3 which are normally closed. This permits a surge of current to flow until operation of the relay opens the contacts X_3. Relay X is then maintained by the reduced current which flows through the series resistor R_2. Under these conditions the operation of relay X is sufficiently rapid to respond to the starting pulse (which is of duration 2 msec). The relay is also maintained by the operation of contacts X_2 which connect the second exciting coil of the relay to the negative end of the supply through the switch S (which is shown closed in the position for "hand re-set"). The operation of the contacts X completes the circuit to the driving magnet M of the uniselector through the first wiper W_1 and the single contact on which the wiper normally rests. After the first step the wiper gains contacts with the "homing" arc H. The driving current through the magnet M and the self drive contacts is then maintained until the uniselector has completed a cycle of twenty-five steps. The wiper W_1 then comes to rest again on the single contact mentioned above.

By this time the circuit to the positive end of the supply must be broken if a second cycle is to be avoided. This is brought about by the contacts Y_1. Relay Y is operated by the closure of the contacts X_2. It is loaded with a capacitor C_1 and supplied through the resistor R_4, and therefore closes relatively slowly. Consequently,

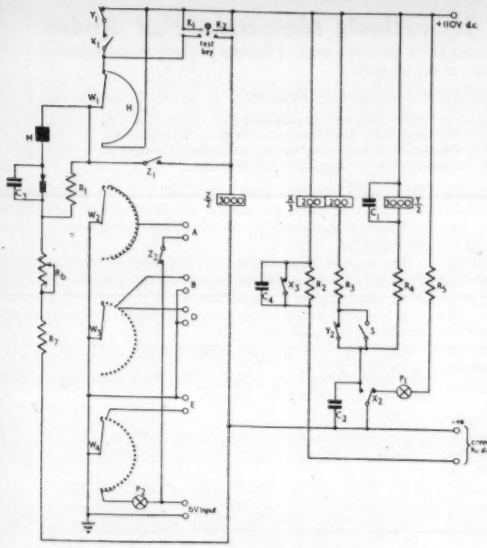

Fig. 4. Control circuit

A, to output sockets; *B*, to charge firing circuit; *D*, time marker synchronization pulse; *E*, to drum camera shutter control.

$R_1 = 100\ \Omega$ $R_2 = 1\,000\ \Omega$ $R_3 = 1\,000\ \Omega$ $R_4 = 15\,000\ \Omega$ $R_5 = 1\,000\ \Omega$ $R_6 = 100\ \Omega$ $R_7 = 20\ \Omega$ $C_1 = 0{\cdot}6\mu F$ $C_2 = 0{\cdot}1\mu F$ $C_3 = 0{\cdot}1\mu F$ $C_4 = 0{\cdot}1\mu F$

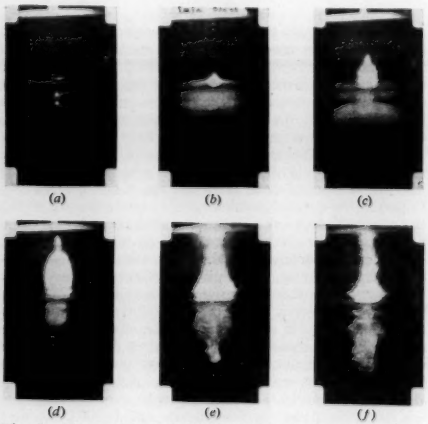

Fig. 5. Frame enlargements from a typical motion picture record. Explosion of a detonator showing above and below surface phenomena

(*a*) 0·15 msec; (*b*) 0·4 msec; (*c*) 1·15 msec; (*d*) 2·5 msec; (*e*) 18 msec; (*f*) 30 msec.

current is supplied to the driving magnet of the uniselector during the interval between the operation of relays *X* and *Y*. This interval is adjusted, by choice of the values of R_4 and C_2, and is just sufficiently long for the wiper W_1 to gain contact with the "homing" arc *H*. Operation of relay *Y* also causes the contacts Y_2 to open. The circuit may therefore be re-set by opening and closing the switch *S*. This de-energizes relay *X* which in turn breaks the supply to relay *Y*. Relay *Y* is then maintained for a short time by C_1, so that the contacts X_1 open before Y_1 re-closes and re-setting does not initiate another cycle. The contacts X_2 also operate a pilot lamp which is alight when relay *X* is not energized, i.e. when the circuit is ready for operation. Automatic re-setting is arranged by leaving the switch *S* open. Operation of relay *Y* causes the contacts Y_2 to open. Relay *X* is de-energized at this stage or when the starting contacts are opened, if this should occur later. This in turn de-energizes relay *Y* and leaves the circuit ready for operation. Contacts 2 to 23 inclusive on the second bank of the uniselector are brought out to the socket to which the reflector units are plugged. Arrangements are made to fire the bulbs on contacts 2 to 6, 2 to 12, or 2 to 23.

Provision is made for testing the control unit and checking the speed of the uniselector without firing the flash bulbs. K_1 and K_2 are contacts on a non-locking test key. Closure of K_1 maintains the uniselector for as many cycles as are desired. Relay *Z* operates when K_2 is closed and is maintained *via* contacts Z_1 and the homing arc until the end of the cycle during which K_2 is opened. The contacts Z_2 break the circuit to the flash bulbs which consequently do not fire during testing. The pilot lamp P_2 is wired so as to light once per cycle as wiper W_4 passes over the last four contacts of the bank. The speed of the uniselector is controlled by means of the variable resistor R_6.

RESULTS

Typical photographs from a high-speed motion picture record are given in Fig. 5. These show the water phenomena associated with the detonation of a fifteen-grain charge. The lower portion of the picture shows the bubble formed in the water by the products of the explosion. The upper portion shows the formation of the "dome" and "column" typical of an underwater explosion.

ACKNOWLEDGEMENTS

The writers wish to thank Mr. D. R. Leah for his assistance with the design of the control circuit, and Messrs. W. L. Millar and F. Winfield for their work during the development of the technique.

This paper is published with the approval of the Lords Commissioners of the Admiralty but the responsibility for any statement of fact or opinion rests solely with the authors.

REFERENCES

(1) LESTER, H. M. *Gen. Elect. Rev.*, **47**, pp. 19–20 (1944).
(2) PALME, A. *Amer. Photog.*, **39**, pp. 34–36 (1945).
(3) LESTER, H. M. *J. Soc. Mot. Pict. Engrs*, **45**, pp. 358–69 (1945).

Electrical measurement of the cathode temperature of diodes

By D. A. Bell, M.A., B.Sc., J. C. Cluley, M.Sc., and H. O. Berktay, B.Sc., Electrical Engineering Department, University of Birmingham

[*Paper first received* 9 *April and in final form* 13 *May*, 1952]

Comparison of "electrical" and pyrometric temperatures for several different types of diode show that the electrical method can be reliably used with oxide-coated cathodes. The method may be of use in determining the surface temperature of indirectly-heated cathodes in practical valve structures which are not accessible for pyrometric measurements.

It is known in a general way that the retarding-field anode current in a diode is governed by a factor $\exp(-eV/kT)$ where e is the electronic charge, V the magnitude of the retarding potential on the anode, and kT the equipartition energy for the cathode temperature. There was at one time some doubt whether the oxide-coated cathode would give the same type of characteristic as a pure metal cathode,[1] but experiments which might have revealed the occurrence of selective electron-reflexion at a surface barrier[2] (either at cathode or anode surface) failed to reveal any modification of the characteristic due to this cause. (Phenomena such as the "ten-volt effect" which are found with accelerating fields are not relevant to the retarding-field characteristic.)

Two practical difficulties are (i) the effect of space-charge at any substantial magnitude of current-density, and (ii) the modification of the retarding-field characteristic when the diode is cylindrical rather than planar. When space-charge is present the transit of electrons is no longer governed solely by their initial velocities. Since the effect of space-charge can only be to reduce the actual anode current, the latter increases with rising anode potential less rapidly than in the absence of space-charge, or conversely it is cut off less rapidly with falling anode potential and therefore suggests a higher electron temperature than the true value. In a plane diode, one merely plots the characteristic back until the slope remains constant, indicating that space-charge is no longer significant. In a cylindrical diode the retarding-field characteristic in the absence of space-charge would not be a simple exponential throughout, but for small retarding potentials would show a deviation which can be computed from Schottky's analysis[3] and is in the same direction as the effect of space-charge. An observed modification of the characteristic could be definitely related to the calculated effect of cylindrical geometry only in the absence of space-charge. Space-charge can be detected through the departure from unity of the "smoothing-factor" F^2 in the shot-noise expression $2F^2ied f$; and in this work measurements of F^2 gave a value of unity (within $\pm 2\%$) over the greater part of the characteristic, so that reduction of F^2 was a reliable criterion of the commencement of space-charge. It was then found that in the particular diodes here used, space-charge commenced at about the same potential as that at which the effect of cylindrical geometry is likely to be significant. This is not surprising, because the cylinder-effect depends on the average tangential component of emission velocities, which is less than the average normal component of emission velocity. The cylinder-effect is therefore associated with low velocities, which also favour the development of space charge.

At large currents (accelerating-field) or at abnormally low temperatures the characteristic of a diode may be modified by the resistance of the cathode coating, or of a coating/core interface, but at normal working temperature this resistance will not be significant in the retarding-field region. There is also the question of "patch effect," but this is only significant near the transition from retarding to accelerating fields, and the latest work[4] attributes a lesser magnitude to patch effect than has sometimes been suggested. It can therefore be assumed that when the current has been reduced sufficiently to eliminate space-charge, all other secondary effects will also be negligible.

The slope of the retarding-field characteristic was measured in terms of resistance, following MacDonald and Fürth,[5] using the fact that if the current is $i = i_0 \exp(-eV/kT)$ and r_a is the differential resistance of the diode (measured at an amplitude of about 5 mV), then

$$ir_a = -idV/di = kT/e = 8{\cdot}598 \times 10^{-5}T.$$

The figure shows a plot of ir_a *versus* i for a diode, type EA50, at three different heater voltages.

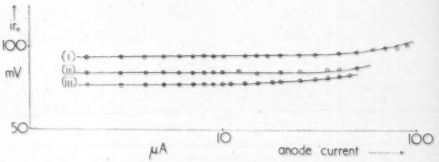

Plots of ir_a versus i for EA50 diode

(i) Heater supply = 6·21 V
(ii) Heater supply = 5·0 V
(iii) Heater supply = 4·0 V

In order to prove this method of temperature determination, comparative measurements were made with an optical (disappearing-filament) pyrometer where possible. In these optical-pyrometer measurements, the figure used for the emissivity of the cathode surface at the pyrometric wavelength was that given by the American Institute of Physics[6] and a correction for absorption in the glass bulb was estimated at 5° C (compare Parker's[7] figure of 5·4° C at 800° C), as a result of observing the effect on the pyrometer reading of inserting a piece of clean glass between it and a test body. In general the optical pyrometer could only be focused on the *end* of a cathode, so that its reading might be expected to be a little below the average temperature of the cathode. A set of temperatures determined electrically, with optical temperatures where available, is given in the following table.

In every case where a comparison is available, the pyrometric temperature is below the "electrical" temperature by an amount which is consistent with the effect of the cooler end section of the cathode. It is therefore thought the error in the electrical value is likely to be less than the difference between electrical and optical values, namely 2 to 3% in absolute temperature. The optical pyrometer available for this work could not be used below 720° C (993° K), and optical pyrometry is necessarily difficult for temperatures below about 1 000° K. The electrical method may therefore be valuable for cathodes operated at the minimum temperatures which are practicable for oxide coatings, e.g. in order to obtain long life.

Valve type	Sample no.	Heater voltage	Cathode temperature Pyrometric	Cathode temperature iR_a method
EA50	2	6·21	1 075	1 085
EA50	3	6·21	—	1 090
EA50	3	5·00	—	— (986)*
EA50	3	4·00	—	920
EA50	6	5·21	1 060	1 080
EA50	6	5·00	—	977
EA50	6	4·00	—	890
6H6	1	6·21	—	970
6H6	2	6·21	—	930
6H6	3	6·21	1 056	—
6H6	4	6·21	1 081	1 110
6X5	1	6·21	1 081	1 110

(*Deduced from slope of retarding-field characteristic.)

REFERENCES

(1) NOTTINGHAM, W. B. *Phys. Rev.*, **41**, p. 795 (1932).
(2) For example, BROWN, A. A., NEELANDS, L. J., and FARNSWORTH, H. E. *J. Appl. Phys.*, **21**, p. 1 (1950). HUNG, C. S. *J. Appl. Phys.*, **21**, p. 37 (1950).
(3) SCHOTTKY, W. *Ann. Phys., Lpz.*, **44**, p. 1011 (1914).
(4) WRIGHT, D. A., and WOODS, J. *Proc. Phys. Soc., Lond., B*, **65**, p. 134 (1952).
(5) MACDONALD, D. K. C., and FÜRTH, R. *Proc. Phys. Soc., Lond.*, **59**, p. 375 (1947).
(6) AMERICAN INSTITUTE OF PHYSICS. *Temperature, its measurement and control in Science and Industry.* (New York: Reinhold Publishing Corp., 1941). See also MARTIN, S. L., and WESTON, G. F. *Brit. J. Appl. Phys.*, **1**, p. 318 (1950).
(7) PARKER, P. *Electronics.* (London: E. Arnold and Co., 1950).

Secondary electron emission from barium oxide*

By J. WOODS, Ph.D., and D. A. WRIGHT, M.Sc., F.Inst.P. The M.-O. Valve Co., at the G.E.C. Research Laboratories, Wembley, Middlesex

[*Paper received* 10 *April*, 1952]

The effect of temperature on the secondary emission of barium oxide is found to be small between room temperature and 600° C. With evaporated layers, the d.c. value of the secondary emission coefficient at a bombarding energy of 240 V falls from near 3 at 10^{-6} cm to about 2 at 10^{-4} cm. The pulsed value is about twice as large as the d.c. for the thinner films. For sprayed coatings the coefficient is near 2, and is the same for d.c. as for pulsed. During operation there are rather complex short time effects, but over a long period the coefficient falls, and decomposition of the oxide occurs.

This paper deals with the secondary emission of barium oxide as a function of its thickness, its temperature, the method of preparation and the time of operation under electron bombardment. As with other non-metals, all these features are relevant, in addition to the energy of the primary electrons and their angle of incidence, which are the only important parameters affecting the secondary emission of metals. The secondary emission coefficient of barium oxide is large under suitable conditions, as with the other alkaline earth oxides. With all of them, however, the coefficient is low when the physical properties of the oxide are unfavourable and, whatever the initial value, a fall occurs in long periods of operation drawing secondary emission.

The main object of the present work was to study the changes in secondary emission with time for barium oxide, and to associate them with the physical properties of the oxide and with the behaviour of the thermionic emission. A secondary object was to observe the effect of temperature, since in the case of mixed barium–strontium oxide coatings there have been conflicting results in earlier work. Pomerantz[1] found an increase in secondary emission coefficient with temperature, in agreement with Morgulis and Nagorsky.[2] Johnson[3] found a small decrease between room temperature and 600° C, while Jones[4] found very little change with temperature up to 850° C. Johnson observed above 600° C an increase in the apparent secondary emission with time, which he attributed to an enhancement of thermionic emission under electron bombardment. D.c. and pulsed measurements have been made, and both secondary and thermionic emission have been measured as functions of time of operation and of temperature, with layers of barium oxide formed in various ways. This paper gives an account of the effect of temperature, the comparison of pulsed and d.c. operation, and preliminary results on time of operation and on structure of the oxide. These last two aspects will form the subject of a further paper.

* Communication No. 513.

PROCEDURE

The tube used for measuring the secondary emission coefficient, δ, is of the electro-static deflexion type. The bombarding beam, drawn from the primary oxide cathode through a rectangular slot in an accelerator electrode, is deflected through an angle of 20° as it passes between two deflector plates. The beam is incident normally on the target under test, which is maintained at a positive potential, V_p. The emitted secondaries are drawn off to two inclined collector plates held at a potential, V_c, which is greater than V_p. These plates are disposed in such a way that the primary electron beam can be made to pass between them before striking the target. The deflector voltage is adjusted to achieve this and to focus the bombarding beam on to the target. The target can be rotated through 90° from its normal operating position so that barium or barium oxide can be evaporated on to it. This design of tube ensures that material evaporated from the primary cathode during operation does not contaminate the target under test. The current density of the incident beam of electrons can be varied up to 2 mA/cm², while target potentials up to 900 V and collecting potentials ($V_c - V_p$) up to 250 V can be used before interception of the primary beam by the collector becomes troublesome.

Several kinds of coating have been studied. These include thin films formed by evaporation of barium on to a nickel target and subsequent oxidation in oxygen at a pressure of 10^{-2} mm of mercury. The oxidation was performed either by heating to 500° C or by passing a radio-frequency discharge. Other thin films were formed by evaporating barium oxide from platinum spirals. Thicknesses from 10^{-6} to

10^{-4} cm have been examined. Coatings of barium oxide have also been formed by spraying barium carbonate on to the targets and converting to oxide by heating in vacuum. The thickness was generally 0·1 mm, although coatings as thin as 0·02 mm have been used. The target base metal was usually pure nickel or cathode nickel ("*o*-nickel"), although some tests with evaporated films on molybdenum have been made.

The tubes were pumped on a mercury in glass diffusion pump with liquid air trap. After degassing the getter and metal electrodes by eddy current heating to 850° C, the target was outgassed. This routine was followed whether the target was sprayed or not. After heating all metal parts again, the primary cathode carbonates were decomposed, the various electrodes were again heated to 850° C and the target was flashed at 1 000° C for 1 min. When working with sprayed targets, the tubes were sealed off and gettered at this point, but with evaporated films the evaporation was carried out at this stage. Some sprayed and evaporated coatings were examined during continuous exhaust on the pump.

The d.c. measurements of δ were made by placing known voltages V_p and V_c on the target and collector with V_c sufficiently greater than V_p to saturate the secondary current. This condition was usually met if $V_c = V_p + 30$ V, but in our experiments V_c was 100 V greater than V_p in most cases. By adjusting the accelerator voltage the current density of the bombarding beam could be varied, and the deflector potential was set so that the collector and target currents were both at a maximum. This ensured that there was minimum interception of the primary beam by the collector. The fact that most layers examined fluoresced under bombardment provided a visual check. As the deflector voltage was altered the luminescent patch, whose sides were sharply defined, moved across the target. δ is determined once the target and collector currents I_T and I_c are known, since $\delta = I_c/(I_c + I_T)$. I_T is of opposite sign to I_c when $\delta > 1$.

Pulse measurements were made by pulsing the accelerator positive with respect to the primary cathode, and displaying the target and collector currents on the screen of a high speed cathode-ray oscillograph. This was done by allowing the pulsed currents to return to earth *via* a low impedance formed by a 0·005 μF condenser and a 2 200 Ω resistor in series. The voltage developed across the 2 200 Ω resistor was the actual quantity measured. High resistances in the h.t. leads ensured that the current through the supply was negligible. Pulses were square, several lengths from 1 to 20 μsec were used, and the repetition rate was 50 c/s.

EXPERIMENTAL RESULTS

δ as a function of V_p and V_c. Fig. 1, curve *A*, shows a plot of the d.c. value of δ against V_p, the target potential, when V_c, the collector potential, is kept 100 V higher than V_p. Similar curves taken under d.c. conditions have been obtained for all tubes investigated. On average $\delta = 1$, when $V_p = 40$ V, and assumes its maximum value, δ_m, when $V_p = 600$ V. Fig. 2, curve *A*, illustrates the dependence of δ on the collecting potential, $V_c - V_p$, when the target potential is held at 240 V. Both these curves were taken for evaporated films at 18° C, and are typical of all three methods of forming such films. Sprayed coatings give lower values of δ, as in curves *C*, Figs. 1 and 2.

Difference between pulsed and d.c. values of δ. Curve *B*, Fig. 1, shows the δ–V_p relationship for an evaporated film when 2 μsec pulses are used. It will be observed that pulsed values of δ are considerably larger than d.c. ones for this film. In Fig. 2, curve *B* shows a secondary emission saturation curve under pulsed conditions. It was found that the pulse/d.c. difference was present in all tubes with evaporated films of barium oxide formed in any of the three different ways. With the sprayed coatings, however, giving lower values of δ under d.c. conditions, there was no difference between pulsed and d.c. values.

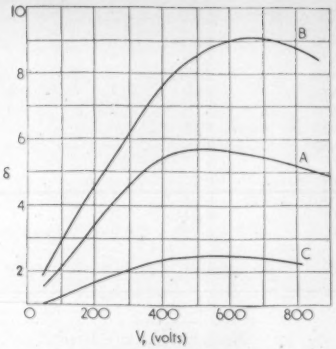

Fig. 1. Secondary emission coefficient δ as a function of target voltage V_p

A, evaporated film by d.c. method; *B*, evaporated film by pulsed method; *C*, sprayed coating by d.c. and pulsed methods.

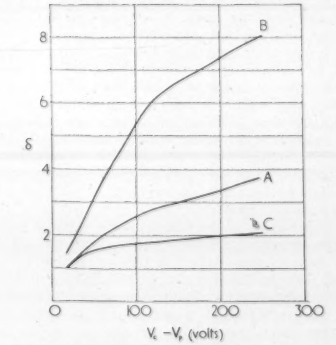

Fig. 2. Secondary emission coefficient δ as a function of collecting potential V_c–V_p

A, evaporated film by d.c. method; *B*, evaporated film by pulsed method; *C*, sprayed coating by d.c. and pulsed methods.

At room temperature, δ_m measured under d.c. conditions is between 4 and 7 for evaporated coatings, and between 7 and 15 under pulsed conditions. With sprayed coatings δ_m is from 3 to 4. The secondary emission performance of any type of coating used here did not appear to be influenced by the nature of any of the three base metals used. The pulse shapes were square, and failed to reveal any changes with time within 20 μsec. In order to gain some idea of the time necessary to produce the transition from pulsed to d.c. values of δ in evaporated films, a sinusoidal r.f. signal of variable

frequency was applied to the accelerator. The display on the cathode-ray oscillograph was a rectified sine wave. In Fig. 3, results for two thin films, taken over a considerable frequency range, are compared with d.c. and pulsed measurements on the same tubes. It will be seen that the change from pulsed to d.c. values occurs at 10^{-5} to 10^{-4} sec from the beginning of the bombardment.

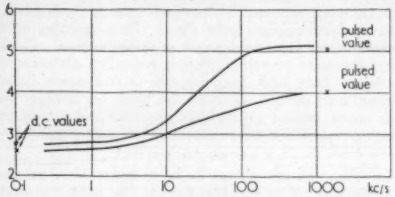

Fig. 3. δ as a function of frequency for two evaporated films

Effect of the electric field at the surface of the coating. In another experiment the target was used as a thermionic cathode with the collector as an anode. The anode was pulsed positive with respect to the cathode, and the slopes of the anode current/anode voltage curves in the accelerating field region were measured at various cathode temperatures. The slope was plotted as a function of saturated current and the resulting curve used to determine the slope at any given saturated current. The slopes of the pulsed secondary emission saturation curves (such as curve *B*, Fig. 2) beyond the "knee" were compared with the thermionic slopes in the accelerating field region when the saturated secondary current was equal to the saturated thermionic emission. It was found that these slopes were identical for both sprayed and evaporated coatings. It appears, therefore, that the high slope beyond saturation in curves *A* and *B*, Fig. 2, is associated with the external electric field at the surface of the oxide. An alternative possibility that high fields in the coating are responsible for this effect is unlikely, since the effect is present at higher temperatures where the resistance of the oxide is very much lower.

δ as a function of temperature. In Fig. 3 and in all the later work, values of δ refer to target and collector potentials of 240 and 340 V respectively. This value is more convenient to measure than that of δ_m, and 240 V is more typical of the target voltage used in practical devices than is 600 V, at which δ is a maximum. The temperature range over which the experiments were performed was limited to 600° C at the higher end. This was due to space charge difficulties caused by the onset of considerable thermionic emission. It was found preferable to use the pulse technique in this investigation, since the thermionic and secondary emission currents were then automatically separated. Typical curves for evaporated and sprayed coatings are shown in Fig. 4. δ rises slowly in both cases to a flat maximum in the vicinity of 500° C and subsequently appears to collapse at higher temperatures. This collapse is not real but due to space charge effects. In one or two cases there have been indications that after passing the maximum there is a genuine small decrease in δ before the rapid collapse obscures the situation. Some d.c. results have also been obtained and they show a similar trend. It is interesting to note that the pulse–d.c. difference for evaporated coatings is maintained at temperatures of 600° C.

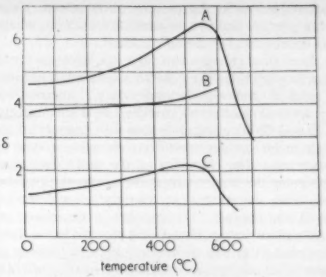

Fig. 4. Secondary emission coefficient δ as a function of temperature. (Note: values above 550° C are unreliable due to space charge)

A, evaporated film by pulsed method; *B*, evaporated film by d.c. method; *C*, sprayed coating by d.c. and pulsed methods.

δ as a function of thickness of evaporated films. In tubes where barium oxide was evaporated from the platinum spirals, δ was studied as a function of thickness in the range 10^{-6} to 10^{-4} cm. The thicknesses were estimated from the interference patterns formed by reflexion. In order to exercise good control during the formation of the films the evaporation was carried out at 1 200° C, so that films 10^{-4} cm thick were formed in 20 min approximately. It was found that the initial value of δ, measured under d.c. conditions, was dependent on the thickness of the coating. For layers 10^{-6} cm thick, δ was about 2·8; at increasing thicknesses up to 10^{-5} cm, δ remained constant, but at greater thicknesses it decreased until at 10^{-4} cm it reached a value of 2·2. This value was not altered by further evaporation. It is significant that 2·2 is the value usually observed with sprayed coatings of barium oxide. It seems possible that the decrease in δ with thickness is due to a roughening of the surface occurring as a result of crystallization. To test this view, a sprayed coating was compressed under a pressure of 2 t/in² so that its surface took on a glazed appearance. As a result of this treatment δ had increased to 2·8, the value typical of thin evaporated films.

Time changes. During prolonged running drawing secondary emission under d.c. conditions, δ changes with time. The time changes may be divided into two categories: those occurring within 15 min of beginning a run, and those taking place over 100 h or more. All types of coating show a decay in yield over periods of hours, and this decay is more rapid at higher target temperatures. In one tube, with an evaporated film on pure nickel, δ fell from 4·2 to 2·5 after 250 h operation with the target at room temperature. In a similar tube, operated with the target at 700° C, δ fell from 6·6 to 1·6 in 150 h. After this run the film was invisible to the naked eye. A sprayed coating showed a decay in δ from 2·0 to 1·0 in 200 h. Another sprayed coating operated at 700° C showed an even more rapid decay, while the coating had turned almost black and possessed a metallic lustre. Earlier experiments[5] using an electro-magnetic deflexion tube established that the rate of decay increased with current density. With this type of tube, the bombarded area was small, and with evaporated films a change of colour of this area was observed during 300 h operation at 500° C. Heating at 1 000° C for a few seconds gave the appearance of clean nickel in this region, the rest of the oxide being unaffected.

This, combined with the present observations, shows that these changes are due to a process of reduction, whereby the oxide is decomposed to metallic barium.

The short time changes can take one of three forms, (i) a rise to a steady value; (ii) a rise to a maximum followed by a decay; and (iii) a straightforward decay. At room temperature the sprayed coatings all give short time effects of type (iii). Types (i) and (ii) are commonly seen with evaporated coatings, although under certain conditions changes of type (iii) are also observed. The character of the short time changes is dependent on the target temperature, the thickness of evaporated films, the method of evaporation and the previous history of the coating. The changes in secondary emission which take place are associated with changes in the thermionic emission, and there is a definite correlation between the two processes. This aspect and the whole subject of short time effects has been subjected to an extensive investigation, the results of which will be reported in a later paper.

CONCLUSIONS

The effect of temperature on the secondary emission of barium oxide is not very large. There is a small increase between room temperature and 500° C, and a small decrease above 600° C. This result is in agreement with those of Johnson and Jones, rather than those of Pomerantz and Morgulis and Nagorsky. No effect has been observed corresponding with the enhancement of thermionic emission described by Johnson.

The pulsed values of secondary emission are greater than the d.c. for thin films, but not for sprayed coatings. The reason for this is not known. The effect does not appear to be associated with the resistivity of the oxide, since the difference is maintained up to 600° C. The d.c. value of the secondary emission coefficient of evaporated films has an initial value near 3, at a bombarding energy of 240 V, for thicknesses of 10^{-6}–10^{-5} cm. At larger thicknesses, the coefficient is less, decreasing to a value near 2 at 10^{-4} cm. This value is similar to that of sprayed coatings. This decrease with thickness appears to be due to the roughening of the surface of the layer as a result of crystallization. During long periods of operation drawing secondary emission, the coefficient falls, and decomposition of the oxide occurs. During short periods, 15 to 30 min, there are changes with time which depend on the type of coating, thickness and temperature. These will be described in a later paper.

ACKNOWLEDGEMENTS

In conclusion the authors desire to tender their acknowledgements to the M.-O. Valve Co. Ltd., on whose behalf the work described in this publication was carried out.

REFERENCES

(1) Pomerantz, M. A. *Phys. Rev.*, **70**, p. 33 (1946).
(2) Morgulis, N., and Nagorsky, A. *J. Tech. Phys., USSR*, **5**, p. 848 (1938).
(3) Johnson, J. B. *Phys. Rev.*, **73**, p. 1058 (1948).
Johnson, J. B. *Phys. Rev.*, **83**, p. 49 (1951).
(4) Jones, T. J. *Nature, Lond.*, **161**, p. 846 (1948).
(5) Harrisson, L. E. Private communication.

An ultrasonic phase lag method for measuring the thickness of rubber

By P. Hatfield, M.Sc., A.Inst.P., Dunlop Rubber Co. Ltd., Research Centre, Birmingham

[*Paper first received* 21 *February, and in final form* 11 *June*, 1952]

An ultrasonic phase lag method for measuring the thickness of rubber when only one surface is available is described. This method, working at 50 kc/s frequency, was chosen because at this frequency ultrasonic absorption losses in rubber are low. The method was developed to measure thickness of rubber in the range 5–20 mm with an accuracy of ±1 mm.

In the rubber industry, it is essential to know fairly accurately the wall thickness of enclosed rubber products when it is not possible to see or handle the inside surface. The present method of measuring wall thickness is by hand pressure, which can give erroneous results, and it was decided to develop an ultrasonic method. A low-frequency method was selected because, for most rubbers, there is a rapidly increasing absorption of ultrasonic waves with increasing frequency. This physical factor rules out the commercial ultrasonic pulse apparatus, operating at frequencies above $\frac{1}{2}$ Mc/s. Attempts to use such equipment to measure the thickness of natural rubber slabs in the range 3–20 mm at $\frac{1}{8}$ mc/s frequency were unsuccessful. As considerable experience in propagating low-frequency ultrasonic waves in rubber had been gained by this laboratory in detecting internal air voids in rubber products, it was thought that a phase lag method working at 50 kc/s frequency might be successful.

DESCRIPTION OF METHOD

The phase method is a simple one, and the main details are shown in Fig. 1. An electrical oscillation was fed by a coaxial cable to a transmitting X-cut quartz crystal, at or near its resonant frequency, and to the X-plates of a cathode-ray oscilloscope. The transmitting crystal was pressed lightly on the rubber surface, the thickness of which was to be measured and the rubber surface wetted with water to obtain maximum ultrasonic transmission between the crystal and rubber. A longitudinal ultrasonic wave was propagated into the rubber and totally reflected from the far rubber surface because it was backed by air. The received ultrasonic wave was detected by a receiving X-cut quartz crystal, identical to the transmitter, the receiver being placed as close as possible to the transmitter. The received ultrasonic wave was converted by the receiving crystal into electrical oscillations, which were amplified and then fed on to the Y-plates of the cathode-ray oscilloscope. The two alternating voltages on the X and Y plates combined to form a simple Lissajous figure.

The elliptical figure shown on the cathode-ray tube is a convenient way of measuring the phase lag between the transmitted and received ultrasonic waves in the rubber. A change in phase of 360° corresponds to a rubber thickness of approximately 15 mm at 50 kc/s frequency. The ellipse gives a number of ambiguities in measuring a phase change of 360°, but fortunately, in this application, a change in amplitude as well as phase resolves most of these ambiguities, and also the thickness limits are known. Fig. 2 shows typical Lissajous figures, which were traced from the cathode-ray tube, for varying known thicknesses of rubber. Fig. 3 shows how the amplitude of the received signal varies with

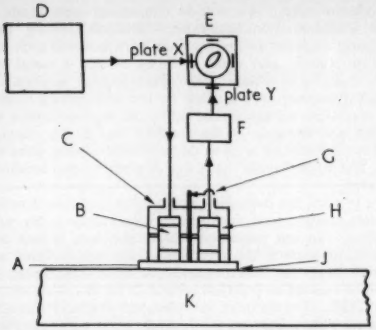

Fig. 1. Block diagram of ultrasonic apparatus for measuring thickness which is determined by the shape of the figure on the cathode-ray tube

A, rubber pad (known thickness); *B*, transmitter crystal (50 kc/s); *C*, brass crystal holder; *D*, oscillator (50 kc/s frequency); *E*, cathode-ray tube; *F*, amplifier; *G*, metal diaphragm; *H*, receiver crystal (50 kc/s); *J*, water coupling; *K*, rubber (unknown thickness).

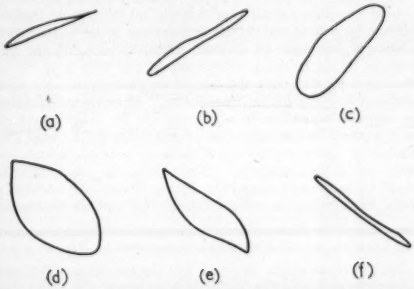

Fig. 2. Typical Lissajous figures for different thicknesses of rubber

(*a*), 13 mm; (*b*) 15 mm; (*c*) 16 mm; (*d*) 17½ mm; (*e*) 20 mm; (*f*) 21 mm.

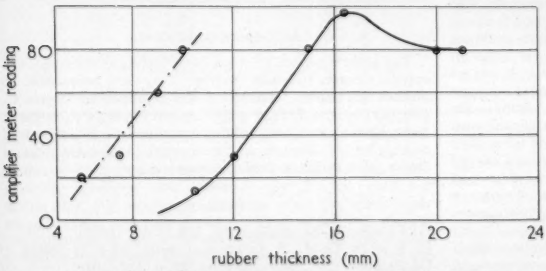

Fig. 3. Graph of meter readings with varying thickness of rubber

—·—·—· = maximum amplifier gain ———— = ampifier gain reduced

thickness. Above 10 mm the shape of the ellipse gives an accurate measure of thickness, but below 10 mm an almost linear relation exists between thickness of rubber and the amplifier meter reading.

The apparatus was calibrated against samples of rubber of known thickness. It was essential that these samples have a thick air layer on the surface opposite that on which the crystals are placed, as it was found that if they were placed directly on to a wooden or metal bench some energy was transmitted into the bench, reflected back into the rubber and detected by the receiving crystal. This caused errors in thickness reading. Although there was a thin air layer between the rubber and the bench, the slight pressure on the top rubber surface by the crystal head was sufficient to allow a small percentage of energy to pass from the rubber into the bench, because parts of the rubber surface were in intimate contact with the bench. This difficulty was overcome by placing the samples of rubber on a pad of foam rubber 0·5 cm thick. This provided an air backing on the under surface of the samples and 100% reflexion of the ultrasonic energy occurred at this surface. The type of foam rubber is not critical, but in these experiments Dunlopillo, density 0·2 g/c.c. pore size 0·01 to 0·03 cm, was used. The enclosed rubber vessels, of unknown thickness, automatically have this thick air layer.

Normally, the rubber samples of known thickness are made from the same compound as the rubber to be tested for thickness. This is not essential since the variation of the velocity of sound waves in common rubbers is small. One reason for the large variation of amplitude with thickness was that at 50 kc/s frequency a wide beam of ultrasonic energy was emitted from the crystal. The area of the crystal was 2·5 × 1·2 cm² and the semi-angle of the radiated beam was about 60°. The receiving crystal was identical with the transmitter and had the same polar diagram. For very thin sections of rubber the polar diagrams of receiver and transmitter did not overlap and no received signal was picked up. For thicker sections of the rubber the polar diagrams did overlap and energy was received by the receiver.

EXPERIMENTAL DETAILS

The two crystals were identical X-cut steel quartz assemblies. The area of the crystal faces in the first crystal assembly was 1·2 × 2·5 cm², but for some applications smaller area crystals 1 × 1·25 cm² were used. These latter crystals had the advantage that they could be used more easily on curved surfaces. The two larger crystals were mounted in a brass crystal holder approximately 2·7 cm × 3·0 cm × 6 cm. The crystals were clamped at their mid-point, placed side by side, and electrically screened from each other and from outside electrical radiation. Although the crystals were placed as close together as possible, it was essential that the sides of the crystals did not touch the brass crystal housing; otherwise vibrations would have been picked up by the receiving crystal direct from the transmitting crystal. This danger was overcome by inserting a thin layer of foam rubber 2 mm thick between the crystals, as shown in Fig. 4. This prevented any cross pick-up between the crystals. By careful machining, it has now been found that the foam rubber is not needed and a constant small air gap can be kept between the crystals. A coaxial cable was connected to

each crystal through a small brass tube and a rubber sleeve prevented any movement of the cable within the crystal housing (see Fig. 4). The top of the brass crystal housing was removable to facilitate the mounting of the crystals. The face of each crystal electrode projected slightly from the crystal housing, and could be pressed directly on to the rubber surface.

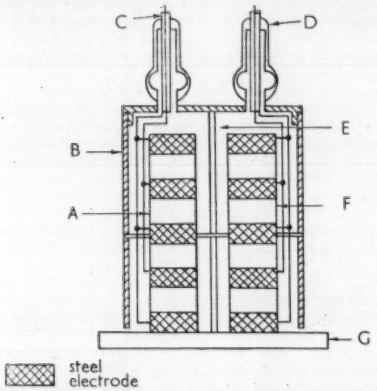

Fig. 4. Crystal holder, showing the clamp at the mid-point

A, transmitter crystal; *B*, brass housing; *C*, coaxial cable; *D*, rubber sleeve; *E*, brass plate; *F*, receiver crystal; *G*, rubber pad, 3 mm thick, stuck on to steel electrodes.

Fig. 3 shows that for thin rubber sections the amplitude of the received wave was small. By inserting a known thickness of rubber, which was thoroughly wet on both surfaces, between the crystals and the rubber product of unknown thickness, a large amplitude received signal was obtained and a suitably shaped ellipse displayed on the cathode-ray oscilloscope. The shape of this ellipse gave the thickness of rubber from which the rubber slab of known thickness could be subtracted to give the unknown thickness. This technique is also useful when the surface of the rubber is badly pitted and it is difficult to make good contact between the rubber and crystals. A soft wet rubber pad pressed into the rough surface gives good contact. Fortunately, the acoustic resistivity of rubber and water are very nearly equal, which means that when one pad of rubber of known thickness is added to the rubber of unknown thickness, no reflexion occurs at the rubber/rubber interface provided it is wetted with water. A pad of rubber 3 mm thick was now stuck on the crystal face, and left permanently on the crystal. No received signal was picked up by the receiving crystal with this pad of rubber stuck on to the electrodes, and no surface wave was transmitted through the rubber from one crystal to the other. A further advantage of having this rubber pad on the crystal face was that it prevented ingress of moisture into the crystal housing and prevented short circuits across the electrodes.

The electrical equipment was standard but care was taken to screen adequately each section, amplifier, oscillator and cathode-ray tube. All outside connexions were made by 80 Ω impedance coaxial cable. The cathode-ray tube, oscillator, amplifier and power pack were mounted each on a separate chassis, and made a sliding fit into a metal box, 2 ft × 1 ft × 1 ft. About 100 V peak-to-peak amplitude at 50 kc/s frequency was applied to the transmitting crystal. The maximum voltage picked up by the receiver crystal was 750 mV and the gain of the amplifier was 60 db. Because of space restrictions a 2½ in diameter cathode-ray tube was used, and consequently the X and Y plate voltage sensitivity was low.

The method has been designed to suit a particular practical problem where rubber thickness must be known in the range 5–20 mm. In one particular factory problem, it was only required to know if the thickness of the rubber vessel was below 8 mm. For this purpose, the meter reading on the amplifier was set at 0·5 (full scale 1·0) for a rubber sample 8 mm thick. The operator only observed whether the reading obtained, when measuring the thickness of the enclosed rubber vessel, was below or above 0·5, and ignored the cathode-ray tube indication. It is essential, using this technique, that the available rubber surface is thoroughly wetted, otherwise readings of thickness are too low because of reflexion of energy at the surface. The wetting can be improved by adding non-foaming detergents to the water, e.g. Carbowax or Ucon.

Obviously, this method, using the same frequency, could be used for thicker sections of rubber, but to measure thinner sections of rubber the crystal would have to be loaded with a known thickness of rubber. Alternatively, higher frequencies could be used. The method has been used up to 200 kc/s frequency but the phase lag changes rapidly with thickness at these higher frequencies. To operate the phase lag method satisfactorily would require the replacement of the Lissajous figure indication of phase lag by a phase discriminator meter, which would indicate rubber thickness in terms of phase angle.[2,3] The thickness measurements would be more accurate at the higher frequencies because a given phase change would correspond to a smaller thickness.

OTHER APPLICATIONS

This method could be used for plastics whose acoustic resistivities do not differ radically from water. It could also be used to detect large areas of internal looseness in a rubber-walled vessel, provided they were parallel to the crystal faces. An internal fissure at right angles to the crystal faces could be detected if the fissure occurred on a line at right angles to the mid-point between the two crystals.

ACKNOWLEDGEMENTS

The author wishes to thank the Technical Director, Research Centre, Dunlop Rubber Co., for permission to publish this paper. Thanks are also expressed to Messrs. C. Cropper and L. I. Farren of the General Electric Co. Research Laboratories, for their helpful contributions to this work, and to Mr. V. Warner, of the General Electric Co. Service Depot, who built the prototype apparatus.

REFERENCES

(1) ERWIN, W. S. *Engineering*, **158**, p. 487 (1944).
(2) SCHUCK, O. H. *J. Acoust. Soc. Amer.*, **20**, p. 26 (1948).
(3) FARREN, L. I. *Wireless Engr*, **23**, p. 330 (1946).

The development of a multi-flash camera and its application to the study of liquid jets

By M. A. Mahrous, M.Sc., Ph.D.,* King's College, Newcastle upon Tyne

[*Paper received* 11 *June*, 1952]

An apparatus to operate a micro-flash tube a number of times in rapid succession is described and applied to obtain cinematograph pictures of a water-jet at a number of stations along its length. As the speed of efflux is increased three stages in the form of the jet may be discerned in which (i) the jet becomes varicose, (ii) it becomes sinuous and (iii) pieces are sheared off the sides by friction with the air. It appears that, below speeds of the order 20 m/sec, the liquid always breaks into pieces of a size comparable with the width of the jet. Subsequent break-up of individual drops into smaller units occurs owing to their high speed through the air.

A number of high-speed cinematograph cameras have been developed. These are all intended for a comparatively large field of view and, in a number of them, the definition is not sufficiently good for the examination of the fine details of a rapidly moving small object. For a number of purposes a series of sharp photographs in rapid succession of a fixed "field" a few square centimetres in area are required. Such a subject is a fine liquid jet in the region in which it breaks into droplets, and the present device, though of general application, was developed to make a detailed study of such a break-up.

ARRANGEMENTS FOR MULTI-FLASH ILLUMINATION

For this purpose a micro-flash tube was adapted to give about eight successive flashes. The circuit for the repeated flashing of the tube is shown in Fig. 1. A condenser C_2 of 8 μF charged to 6·5 kV acts as a reservoir of potential. A high-speed commutator successively charges a condenser C_1 of 0·25 μF and discharges it through the tube, so reducing the charge on C_2 step-wise.

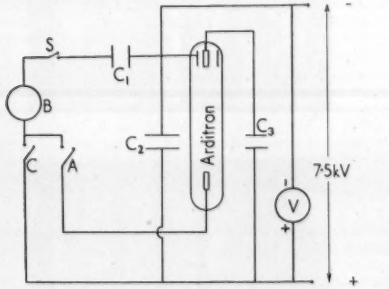

Fig. 1. Circuit for multi-flash operation of arditron lamp

The high-speed commutator [Fig. 2(*a*)] consists of a rotating Tufnol disk 5 in diameter, carrying a stud with spring contacts, which in rotation at 50 r.p.s. makes contacts with studs on two fixed disks each side of the rotating one (compare the developed view shown in Fig. 2(*b*) in which the spring stud is pictured as stationary while the other studs move past it). The eight contacts on one of the fixed disks *B* are connected to each other and, through the control switch, to one end of the operating condenser. The other end of the operating condenser is connected to the plate of the tube and to one end of the reservoir condenser. The eight contacts on the other disk are divided into two groups, *A* and *C*, each with four contacts connected alternately. Group *C* is permanently connected to the other end of the reservoir condenser and the positive end of the power supply. Group *A* is permanently connected to the lower end of the tube (see Fig. 1).

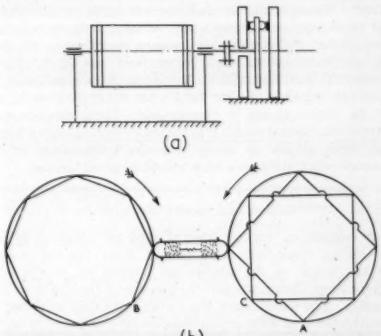

Fig. 2. (*a*) Form of commutator. (*b*) Developed sketch of commutator

When the moving stud comes into line with one contact of group *C* it brings C_1 into parallel connexion with C_2, whereby the former is charged up to the voltage across the large condenser C_2. Later, when the moving stud comes into line with one of the contacts of group *A*, a spark bridges the gap and supplies the positive voltage to the anode of the arditron. The small condenser C_3 (about 0·01 μF) applies the pulse also to the grid of the tube so that the arditron breaks down and flashes. The moving stud now moves on until it lines up again with another contact of group *C*, whereby C_1 is again charged and then discharged through the tube when the moving stud lines up again with another contact of group *A*. In each case the condenser C_1 charges up to the full—or nearly full—original voltage of C_2. The flashing goes on until the voltage across C_2 has dropped to a value below which the arditron will not trigger (about 4 kV).

Thus the size of C_2 can be estimated to give the required total number of flashes. The value of C_1 depends on how much light is required; the higher the capacity, the greater the light output of the flash. This is limited by (i) the power that can be dissipated through the arditron without damaging the tube, and (ii) the number of successive flashes that can

* Now at the Ibrahim Pasha University, Cairo, Egypt.

be obtained with a certain capacity C_2 as starting reservoir. Though the light output is increased by increasing C_1, yet the number of successive flashes that can be obtained is considerably diminished, necessitating some compromise in these two factors. With the motor rotating at 3 000 r.p.m., and four pairs of contacts, flashing every 1/200th sec was assured. Later another commutator was built giving flashes every 1/400th sec.

In the first model the two contacts were mounted on one spiral spring. This was found to be inefficient, especially at high speeds, and was replaced by separate mountings of steel spheres. (Actually ball catches were used.) These provided good contact, but it was noticed that ordinary steel spheres still wore out and they tended to engage the spiral spring in a manner which prevented them from rotating around themselves. In the latest model two small hardened steel spheres were used to overcome this difficulty.

Although the discharge in the lamp is about 2 cm long the illumination over the arc is not uniform. An enlarged image of the more intense portion of the arc was cast by a system of lenses and slits on to the jet, backed by a ground-glass screen. The light afterwards fell on to a mirror which reflected the beam into the stationary camera, ready with open shutter. The mirror was rotated by a constant speed motor, the shaft of which carried another commutator having a pair of contacts to start the arditron flashing at the moment when the image of the field of view fell on the extreme left-hand side of the plate exposed in the camera. These contacts were part of the control switch S in the multi-flash circuit of Fig. 1, but were subject to heavy sparking. Operation of the control switch through a relay would be an advantage.

PHOTOGRAPHY OF JETS

A number of workers have studied the break-up of jets, by taking single-flash photographs, from the two aspects (i) the length of the continuous portion up to the point where drops break off, and (ii) the size of the drops so produced. The latest data are to be found in a paper by Merrington and Richardson,[1] in which references to earlier papers are to be found. Lane[2] has recently published some excellent single-flash photographs of large drops in the process of disruption by a stream of air. In the present work the object was to present a series of photographs of a water jet issuing from a nozzle (made of precision glass tubing) to enable the process of break-up to be followed in more detail than is possible if isolated photographs are taken. The stages in the break-up have already been described by a number of workers—for example Merrington and Richardson. As the velocity of the issuing liquid is raised, three stages may be distinguished; (i) the "varicosities" of Rayleigh, (ii) "waggling" of the jet from side to side, and (iii) shearing of the skin of the jet into fragments.

Fig. 3(*a*) shows the break-up of a jet from a wide nozzle (4 mm) in the first stage. When the swellings and contractions starting from the nozzle have reached such an amplitude that the drops are detached, the bulk forms drops of the order of the jet diameter, the "necks" which formerly joined them to their fellows forming little satellite drops between the main ones. At a higher speed the varicosities are less regular, giving the jet, just before it breaks up, the appearance of a string of beans of irregular length having nodules separated by filaments. In this stage any slight disturbance, probably originating at the nozzle, grows and makes the whole jet waggle from side to side [Fig. 3(*b*, *c*)]. A point which does not appear to have been noted before is that this waggling is superimposed on the varicosities—the nodules previously mentioned—so that when the jet does break up finally [Fig. 3(*d*)] the bulk of the drops originating in the nodules still have a diameter comparable in size with the nozzle. The

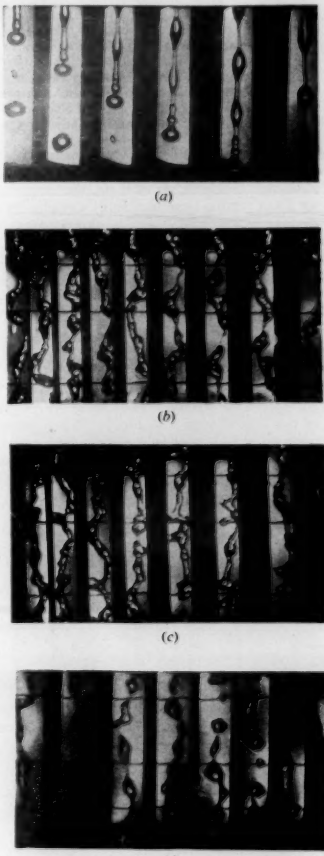

(*a*)

(*b*)

(*c*)

(*d*)

Fig. 3. Stages in break-up of jet emerging from 4 mm nozzle

(*a*) at 3 m/sec, 10 cm below orifice (*b*, *c*, *d*) at 13·2 m/sec.
(*b*) 20 cm, (*c*) 30 cm, and (*d*) 42 cm, below orifice.

first break is usually into a group containing several nodules. In the third stage it was not profitable to take multi-flash photographs, but in Fig. 4 three single-flash photographs at different points along the same jet issuing at 23·5 m/sec are shown. The fine particles formed by the shearing action of

the air on the boundary layer of the jet can be clearly seen. This layer thickens as more fine drops are sheared off, but at the last [Fig. 4(*c*)] there is still a considerable quantity of liquid in the core going into large pieces. That there is still some periodicity in the initial disturbance can be seen in the view nearest the nozzle [Fig. 4(*a*)], though it is lost in later photographs. It is, of course, possible to produce the same shearing effect by letting the liquid issue at a moderate speed into a coaxial high-speed jet of air. Green[3] has published such a photograph which does not differ in essence from those of Fig. 4.

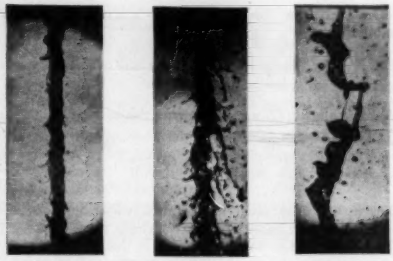

(*a*) (*b*) (*c*)

Fig. 4. Jet from 4 mm nozzle at 23·5 m/sec
(*a*) 10 cm, (*b*) 18 cm, and (*c*) 56 cm, below orifice.

There are other observations which one can make from a study of a series of multi-flash photographs at the lower velocities. The wavelength of axial-symmetrical disturbance which grows most rapidly and ultimately breaks the jet is about nine times the radius, in agreement with Rayleigh's (1879) calculation. At the first stage [Fig. 3(*a*)] the detached drops continue with nearly the same (constant) velocity with which the liquid left the nozzle, but in the second stage [Figs. 3(*b*, *c*)] the bent-up sections of jet seem to be constantly changing in appearance from photograph to photograph and are strongly decelerated. Eventually the nodules at the bend are thrown off with a horizontal component of acceleration in a sort of whipping action at a velocity considerably less than that with which, as part of the general flow, they left the nozzle.

Whereas the "continuous length" of the jet is proportional to the efflux velocity in both the varicose and sinuous stages, this is no longer true when the break-up is due to shear. Indeed, in this third stage, no definite value can be assigned to the length of the jet.

DROP-SIZE DISTRIBUTION IN JETS

Fig. 5 shows typical analyses (at one pressure) of the size distribution from nozzles of different diameter, showing that the mean drop diameter is about twice the nozzle diameter. When the pressure is increased up to the "atomization" stage, this is still true, though there is some change in the size range covered. Evidently, then, the relationship between mean drop size *at a distance* and efflux velocity reported by Merrington and Richardson is due to the subsequent break-up of larger drops into smaller ones, as they are exposed to air blasts on release at different speeds. This is the phenomenon already investigated by Lane. Only at the third stage where the jet has small drops sheared off it as it falls is it possible to find in the photographs a mean drop size which diminishes as the velocity of the jet increases.

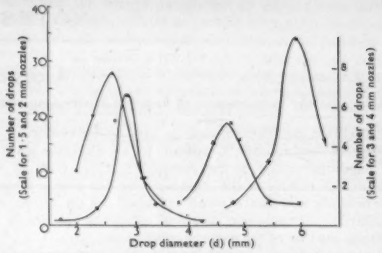

Fig. 5. Drop-size distribution from different nozzles
Nozzle diameters: ● = 1·5 mm; ○ = 2·0 mm; × = 3·0 mm; + = 4·0 mm.

PRACTICAL IMPLICATIONS

It is a problem in a number of industrial processes to produce a liquid in the form of a fine dispersion. When small quantities only are required, ultrasonic agitation or the "spinning top" of Walton and Prewett[4] may be used. The work described in this and other papers indicates that the high-speed jet and the swirl atomizer are still the most economical ways of producing a dispersion in larger quantities. So far all methods tried fail to give a spray with a mass median below 10 μ. Whether this limit is significant of a fundamental property of liquids the author is unable to state.

ACKNOWLEDGEMENTS

The author is indebted to Mr. R. S. Allen of the Royal Naval Scientific Service for suggesting the method of producing multiple flashes of the arditron and to Dr. J. F. W. Bell of this university for first developing the circuit used. He also thanks Dr. E. G. Richardson for advice during the course of the work.

REFERENCES

(1) MERRINGTON, A. C., and RICHARDSON, E. G. *Proc. Phys. Soc., Lond., B*, **59**, p. 1 (1947).
(2) LANE, W. R. *Industr. Engng Chem.*, **43**, p. 1312 (1951).
(3) GREEN, H. K. *Aspects of Fluid Flow*, p. 75 (London: E. Arnold and Co., 1950).
(4) WALTON, W. H., and PREWETT, W. C. *Proc. Phys. Soc., Lond., B*, **62**, p. 341 (1949).

Correspondence

A note on the measurement of damping in vibrating rods

My attention has been drawn by Mr. K. H. Griffin of the College of Aeronautics, Cranfield, to an algebraic error in my paper published in the November, 1951, issue of this *Journal*. It occurs in the expansion of the cosine term of equation (4) and has a small influence on the subsequent calculation. It does not, however, affect the validity of the methods used or of the general conclusions.

It can be largely corrected by replacing ω_0 in equation (5c) and thereafter by W, where:

$$W = \omega_0/(1 - 3/8\ Q_\omega^2)$$

If this is done, the only remaining corrections necessary are small modifications of the intermediate equations (7) and (10) (in the ϵ only), and of the definition of γ, which now becomes:

$$\gamma = \tfrac{1}{4}\delta^2[(8 + 7k - k^2) + \lambda\delta^2(20{\cdot}5 + k + k^2) + \lambda^2\delta^4(26{\cdot}3 + 41k + 9k^2)]$$

Also the last sentence but one before equation (8), regarding the variation of E, should be deleted. In the final results of the paper, these changes can lead in a very unfavourable case to a difference of 0·4% in the resonance frequency derived from equation (8), and about 1% in Q derived from equation (16).

I am indebted to Mr. Griffin for the helpful advice and criticism he has given on this problem.

Physics Department, Imperial College, London, S.W.7. — G. G. Parfitt

Calculation of the propagation constants of an inhomogeneously-filled waveguide

In his paper published in the January 1952 issue of this *Journal*, Mr. Chambers, extending a Lagrangian formalism, applies the Rayleigh–Ritz method to find the propagation constants of an inhomogeneously-filled waveguide. The following variational procedure leads, I feel, more directly to a determinantal equation for such constants. Although one may readily apply it to a waveguide, I will illustrate its application to a microwave cavity, considered as a closed conservative system.

Let a microwave cavity of arbitrary shape be filled with a lossless medium whose dielectric and magnetic properties, ϵ, μ, are constant in time but may be arbitrary functions of position in the cavity. The actual electric vector field in the cavity may be expanded, following Slater,* in a series:

$$E = \Sigma e_a E_a$$

Here the e_a are amplitude coefficients and the E_a are a complete orthonormal set of vectors representing modes of the empty cavity. The vectors E_a are independent of time and satisfy the following equations and conditions:

$\nabla \times E_a = k_a H_a$, $\nabla \cdot E_a = 0$, $\hat{n} \times E_a = 0$ on the cavity walls,
$\nabla \times H_a = k_a E_a$, $\nabla \cdot H_a = 0$, $\int E_a \cdot E_b d\tau = \delta_{ab}$

(integrations (v) are over cavity volume).

* Slater. *Microwave electronics*, Chap. IV (New York: Van Nostrand, 1950).

The H_a form a second orthonormal set of vectors, associated with the E_a.

The actual fields in the cavity satisfy the Maxwell field equations and boundary conditions,

$$\nabla \times H = j\omega\epsilon E\ (1),\ \nabla \times E = -j\omega\mu H\ (2),\ \hat{n} \times E\Big|_w = 0\ (3)$$

Consequently they also satisfy the relation derived by Mr. Chambers,

$$\int_v (\mu|H|^2 - \epsilon|E|^2)d\tau = 0$$

Using equation (2) we may rewrite this as:

$$\int_v \left(\frac{|\nabla \times E|^2}{\omega^2\mu} - \epsilon|E|^2\right)d\tau = 0 \qquad (4)$$

Let us consider small independent variations, δE, of E about the correct value. These variations must preserve the boundary condition on E, and will, in due course, turn out to be variations of the e_a. The variation of equation (4) yields:

$$\int_v \left[\epsilon(\delta E \cdot E^* + E \cdot \delta E^*) - \frac{j}{\omega}(H \cdot \nabla \times \delta E^* - H^* \cdot \nabla \times \delta E)\right]d\tau$$

Now:

$$\int_v \nabla \cdot (H \times \delta E^*)d\tau = \int_v (\delta E^* \cdot \nabla \times H - H \cdot \nabla \times \delta E^*)d\tau = \oint_w H \cdot \delta E^* \times \hat{n}d\sigma = 0$$

So

$$\int_v \left[\delta E \cdot \left(\epsilon E^* + \frac{j}{\omega}\nabla \times H^*\right) + \delta E^* \cdot \left(\epsilon E - \frac{j}{\omega}\nabla \times H\right)\right]d\tau = 0 \qquad (5)$$

In words, the coefficients of the variations δE and δE^* vanish in a variation of equation (4), if the actual fields satisfy equation (1).

We may now substitute in equation (4) the expansion given above for E. It is convenient to write here $\epsilon = \epsilon_0(1 - \eta)$, $\mu = \mu_0(1 + r)^{-1}$, and $k_a^2 = \omega_a^2\mu_0\epsilon_0$. Let us also define symmetric matrix elements:

$$M_{ab} = \int_v \eta(E_a \cdot E_b)d\tau,\ N_{ab} = \int_v r(H_a \cdot H_b)d\tau$$

Then we may rewrite equation (4) as:

$$\sum_a e_a^2\left(1 - \frac{\omega_a^2}{\omega^2}\right) - \sum_a \sum_b e_a e_b\left(M_{ab} + \frac{\omega_a\omega_b}{\omega^2}N_{ab}\right) = 0$$

According to equation (5) the coefficient of δe_c, a small variation in some amplitude e_c, is to be zero; so we find:

$$e_c(1 - \omega_c^2/\omega^2) = \sum_b e_b(M_{cb} + \omega_c\omega_b N_{cb}/\omega^2)$$

From the set over c of such variations we derive finally the secular determinant:

$$|(1 - \omega_a^2/\omega^2)\delta_{ab} - M_{ab} - \omega_a\omega_b N_{ab}/\omega^2| = 0$$

This is essentially the determinant which Mr. Chambers obtains.

J. A. BRADSHAW

Division of Applied Science,
Harvard University,
Cambridge, Massachusetts.

I am grateful for the opportunity of commenting on Mr. Bradshaw's remarks. My paper was intended to indicate the possibilities of using the Rayleigh–Ritz method in waveguide theory. I did not wish to bother the reader with the rigorous theory, as I felt that the method would be more intelligible if presented in a rather heuristic manner. The rigorous theory has, however, been submitted for publication elsewhere and will, I hope, be available shortly.

I think, however, that I ought to make it clear that my method applies only when there are pure T.E. or T.M. waves, and that this is only possible when there is no variation in field along the surfaces of discontinuity.*

I hope shortly to investigate the possibilities of applying an approximate method to the case where the waves are neither pure T.M. nor pure T.E.

LL. G. CHAMBERS

Military College of Science,
Shrivenham,
Wilts.

* PIRCHELE, L. *Phys. Rev.*, **66**, p. 118 (1944).

Pool surface and cathode spot temperature of mercury cathodes as a problem in heat conduction

In his paper published in the April 1952 issue of this *Journal* Dr. von Bertele's approach to the problem of spot emission and thermal fields might well lead to more general methods of analysing the design parameters of mercury-arc devices with pool cathodes. However, whilst his results on the heat transfer rate of water-cooled cathodes seem justified by experiment, the figures given for air cooling indicate neglect of the rate of heat transfer between glass and air, although the author earlier draws attention to the difference between this rate and that between glass and water.

Although the problem of heat transfer from a plane surface parallel to the airstream is one on which few data are generally available, experience shows that, in fact, the greater part of the overall temperature drop will occur across the airstream. Thus, equation (3) should include a term which takes into account the heat transfer rate of the bottom, and therefore read

$$\Delta U = iq\left(\frac{H_{mercury}}{\lambda_{mercury}} + \frac{H_{wall}}{\lambda_{wall}} + \frac{1}{\alpha}\right)$$

For water-cooled steel tank cathodes, $1/\alpha$ is small enough to be neglected.

Young* has given experimental coefficients for air-cooled radiators which might be of use. For an air speed of 1 000 ft/min—which is typical for a medium rectifier—he gives $\alpha = 25 \times 10^{-4}$. Substituting this in the revised equation (3) gives $q = 0{\cdot}116$—one-tenth of the author's figure and even more strikingly contrasted to that of Günterschulze. It does, however, support the contention that the heat transfer rate is more dependent on the cathode arrangement than the spot emission.

R. TUCKER

18 Malvern Road,
Enfield, Middlesex.

* YOUNG, A. J. *Marconi Rev.*, **94**, p. 85 (1949).

I am grateful for Mr. Tucker's comments which I also consider as a further proof of the heat transfer rate of a pool cathode being only a consequence of the thermal resistance of the particular system and not a basic feature of the spot emission.

When using the extended formula for calculating the surface temperature of air-cooled valves, one gets values about 30° C higher than those found in water-cooled systems, which explains the more elaborate screening of the empirically-developed anode systems of the air-cooled valves.

H. VON BERTELE

6 Warren Road,
Purley, Surrey.

New books

The theory of relativity. By C. MØLLER. (London: Oxford University Press.) Pp. xii + 383. Price 35*s*.

Professor Møller intends his book primarily as a students' textbook and, careful to approach the subject as a physicist, develops all relations at first in three-dimensional concepts. Chapter I is an excellent historical introduction, Chapter II deals with relativistic kinematics, and relativistic mechanics is introduced in Chapter III in a self-contained way without any borrowings from electrodynamics. The three-dimensional formulation is a most useful and attractive feature of the book.

When in Chapter IV the four-dimensional approach is introduced, this is done at once with imaginary time components which is certainly the most elegant and symmetrical formulation. (A real time variable does not reappear until general relativity is treated in Chapters VIII–XII.) One may perhaps regret that the pseudo-Euclidean approach is not given here, which means that Minkowski's graphical representation introducing the unit hyperbolae is missing. An exposition of special relativity in four-dimensional notation but without imaginaries would have also been of advantage to those who wish to apply it later to quantum theory, as it avoids the necessity to distinguish between the imaginary unit arising from quantum theory and that from relativity.

Chapter V deals with vacuum electrodynamics. In Section 55 of this chapter a derivation of the retarded potentials is given by a much used method which has its origin in a derivation by Herglotz who already in 1904, i.e. before relativity, employed an elegant integration in the complex time plane. But it has been pointed out that the development of this method, used notably by Sommerfeld, is very unsatisfactory: When reading (p. 147) "We therefore deform the original path of integration along the real axis into a loop round this (i.e. the lower) part of the imaginary axis . . ." most readers will receive the impression

that the value of the integral remained unchanged by this deformation. This, however, is not so, as can be seen from the statement on page 148, that whilst the path so deformed yields the retarded potentials, a corresponding upwards deformation into a corresponding upwards loop would have yielded the advanced potentials. The textbooks by Abraham and Becker on the theory of electricity (Vol. 2) and the earlier editions of M. v. Laue's *Relativitätsprinzip* expressly object to this method for mathematical reasons and prefer older, if perhaps less elegant, methods.

Chapter VII deals with non-closed systems, electrodynamics in dielectric and paramagnetic substances, and with thermodynamics. Here the modern view is adopted, that Minkowski's and not Abraham's electrodynamics of material media is correct; on this point there was much argument until quite recently.

Professor Møller has wisely deferred the general tensor calculus to the last chapters of his book so as not to burden those readers who are mainly interested in the physical aspects of the subject. They will still be able to read Chapter VIII on the foundations of general relativity, the last section of which treats the much discussed clock paradox neatly and in great detail. Thus Chapter VIII and Chapter XI on the fundamental laws of gravitation stress perhaps too much what (by other authors) is often called "Mach's principle," i.e. the explanation of inertia effects by the "distant masses of the universe." If one does not give way to wishful thinking one has to admit that this principle has not been established by relativity. The arguments quoted in support in Chapter XI have been criticized by Lanczos (*Z. Phys.*, **14**, 204, 1923), but though this criticism has never been refuted the arguments are still quoted in most expositions, including Einstein's own.

Chapter X on the influence of gravitational fields on physical phenomena begins with two sections in which the freely falling particle is also treated from the three-dimensional aspect, an innovation which will promote physical understanding.

The three points critically discussed above at such length as to take nearly all space of this review should not give a wrong impression about this book which is excellent and fills a gap among textbooks in the English language. It is warmly recommended. H. PELZER

Department of Scientific and Industrial Research—Report for the year 1950/51. (London: H.M. Stationery Office). Pp. 271. Price 7*s*. 6*d*.

The Report opens with a strong plea for removal of the delays preventing the Department from giving full effect to its post-war plans which it is estimated will now cost £7·5 M. But these delays are not only on account of finance; they include building delays and difficulties in recruitment of staff which now numbers just over 4 000. Recruitment should, the Report states, be at least 150 net a year and it has dropped to 110.

The gross expenditure of the Department in the year ending 31 March, 1951, was about £5 M of which the Research Associations had about £1½ M, while grants to students cost about £¼ M.

The Report summarizes the vast range of work carried out by the Department and the Research Associations and makes interesting and, in places, fascinating reading. It covers work connected with almost all the country's major industries; there are now forty-one Research Associations. Physics and its applications, as might be expected, are playing an ever-increasing part in the work of the Department and the Associations, and often this involves the development of special and sometimes large and expensive instruments and machines. The Report states that it was expected that its grants to universities for the machines for accelerating particles to high energies would cease at the end of the current university grants quinquennium, on 31 July, 1952, but that it will be necessary to continue them over the next quinquennium.

Applied research in the United States. EUGENE W. SCOTT (Editor), (Washington D.C.: Publication 21a, National Research Council, National Academy of Sciences). Pp. 90. Price $1.00.

Visitors to the United States see evidence on every hand of intense activity in scientific research. In the universities and great research institutions, in government and industrial laboratories, scientific knowledge is being applied to practical ends on an unprecedented scale. Yet any attempt to get the picture in true perspective or to assess the magnitude of the effort in numbers of men employed and dollars expended is not easy. Here is a report which gives us the answers to many of the questions at a most opportune time. Within its ninety pages the reader will find a mine of authoritative and up-to-date information on this subject.

As the title indicates, the report is restricted to research carried out for practical ends as distinct from research resulting from personal curiosity or purely scientific interest. It reviews very thoroughly and in a most readable form the developments in the various types of organization concerned and the many factors which operate in this remarkable field.

Any short summary of the contents of such a condensed statement might be misleading, but from the many data quoted the following are of exceptional interest. Out of a total population of over two million reaching the age of 18 annually some 70 000 ultimately take degrees in science and engineering and, of 600 000 of working age with such degrees, roughly 140 000 are employed in research and development, 45 000 of them in Government laboratories. The overall annual expenditure on research and development by all sources is nearly 3 000 million dollars, 50% of which comes from the Government. Government-sponsored university research is an outstanding feature of the American scene and in 1950 this activity was represented by a total obligation of 90 million dollars distributed among 194 colleges.

The report provides a valuable insight to the American philosophy of applied research and the willingness to change which is so prevalent everywhere. It will be read with profit by many of those in this country who see in applied research a great opportunity for maintaining and raising our standards of living and of securing our national prosperity.

P. DUNSHEATH

Dimensional analysis. By Dr. H. E. HUNTLEY. (London: Macdonald and Co. Ltd.) Pp. 150. 20*s*.

The aim of this book is practical application of the method of dimensions and it is addressed to students of physics. To that end it includes little more than a bare statement, in its most primitive form, of the operation of the method and a considerable collection of examples. The only novel feature is a discussion of the use of different units for measuring the components of a length along three co-ordinate axes and the division of the customary unit of mass into one of mass and one of inertia. Both devices are useful, but by neglecting any consideration of the fundamental basis of the method the author has misled himself into believing that the size of the unit for measuring a radius is the square root of the product of the units used for measuring lengths along two axes at right angles. Correctness of the answers the author gets by

believing this is not evidence of the correctness of the belief! I am surprised that the author should consider as many as at least four books on this subject a "dearth," and also that it should require 150 pages to deal with the parts he has selected.

E. W. H. SELWYN

Allgemeine metallkunde. By E. BRANDENBERGER. (Basel: Ernst Reinhardt.) Pp. 333. Price Fr. 16.50.

This book gives a condensed survey of a wide range of subjects connected with the structure and properties of metals and alloys. It is divided into five sections dealing with pure metals, substitutional solid solutions, interstitial phases, intermediate phases or intermetallic compounds and the chemical reaction of metals. With the increasing tendency towards specialization, the book will be of interest to those who wish to obtain a general survey, but in places it suffers from over condensation, and, except for a list of books at the end of the volume, there is an almost complete failure to provide the reader with the references or suggestions for further reading which are necessary if a book of this kind is to fulfil its purpose.

W. HUME-ROTHERY

Low temperature physics—Four lectures. By F. E. SIMON, N. KURTI, J. F. ALLEN and K. MENDELSSOHN. (London: Pergamon Press Ltd.) Pp. vi + 132. Price 21*s*.

This book is based on a series of lectures delivered at the Royal Institution early in 1950, since revised to cover developments up to the end of 1951. It includes a general introduction to low-temperature problems by Professor Simon, followed by more detailed discussions of the temperature range below 1° K, and the problems of liquid helium and superconductivity, by Dr. Kurti, Professor Allen and Dr. Mendelssohn respectively. The book as a whole forms an admirably lucid introductory survey of the whole field of low-temperature physics, and can be recommended both to general physicists who wish to keep abreast of modern developments and to students who intend later to specialize in this field. Criticisms are few: Figs. 3(*a*) and 4 of the first lecture, and Fig. 3 of the third, are slightly obscure; more important and surprising is the lack of any discussion of the recent radio-frequency measurements on superconductors by Pippard. Perhaps it was felt that an adequate discussion of these new and exciting results would require a fifth lecture.

R. G. CHAMBERS

The sensations, their functions, processes and mechanisms. By HENRI PIERON. (London: Frederick Muller Ltd.) Pp. xxiii + 468. Price 42*s*.

This is a valuable book, ably conceived and well translated. It falls naturally into four distinct but inter-related parts. These are, briefly, (i) Stimulus and sensation, (ii) Excitation mechanisms, (iii) Qualitative appreciations, and (iv) Quantitative appreciations.

If there is a tendency to write around the references, this can scarcely be avoided in a work of this character; it will probably be consulted more upon specific issues than read from cover to cover. For example, no better treatment of the physics of vision is likely to come the student's way, but he will have to go elsewhere if he wishes to learn what this entails for fluoroscopy at very low brightness levels. And correspondingly for the other "senses." We are, in fact, on the frontier between classical and quantum concepts, and a little more geometry (in appropriate cases) might have been better than some of the empirical formulae provided. An advantage, however, is that a bridge is thrown across between the natural sciences and psychology, especially gestalt theory. In this way, a balance is kept between too mechanistic a view of sensation and unbridled philosophical speculation. Towards the end, a study of retroactive stimulation is presented. This view of the build-up of the threshold in sensation is impressive, and perhaps capable of expression in more rigorous terms later on.

F. I. G. RAWLINS

Methods of algebraic geometry. Vol. 2. By W. V. D. HODGE and D. PEDOE. Pp. x + 394. (London: Cambridge University Press.) Price 42*s*.

This is the second of three volumes, of which the first appeared in 1947. It is concerned with the properties of a set of numbers $(x_0, x_1, \ldots x_n)$ which satisfy a group of simultaneous equations $f_i(x_0, \ldots x_n) = 0$ $(i = 1, 2, \ldots k)$. These numbers may be thought of as the co-ordinates of a set of points usually infinite in number, belonging to a space of n dimensions, and lying on the intersections of the k generalized surfaces $f_i = 0$. They are referred to as an algebraic variety. Their behaviour under various transformations, and their relationship to change of axes and other geometrical operations, form the substance of this book. Transformations of this type occur quite frequently in theoretical physics, and no doubt this book, which is excellently written and produced, contains a good deal that might be useful, particularly when these varieties occur as linear spaces on a quadric, and when they are made to throw light on the elementary divisors (or factors) of a matrix. But the approach is, naturally, entirely formal, and any physicist who wants to use this book, will have to be prepared to dig pretty deeply before he finds his treasure.

C. A. COULSON

Fouriersynthese von Kristallen. By W. NOWACKI. (Basle: Verlag Birkhäuser.) Pp. 237. Price Fr. 34.30 (60*s*.).

This book describes, in a most thorough and compact manner, the more advanced methods of crystal-structure determination. The author has confined himself rigidly to the title of the book, starting, for example, with the assumption that the basic theory is already known, and that there is no need to derive the basic structure-factor and electron-density equations. The book should therefore be extremely useful to the German-speaking world. To the average German-reading Englishman, however, the book is not likely to appeal greatly, except as an excellent source of references; roughly two-thirds of the papers referred to are written in English, and people in this country are likely to derive more benefit from consulting these papers than from reading this German digest of them.

H. LIPSON

The mechanical properties of cheese and butter. By MARGARET BARON. (London: Dairy Industries Ltd.) Pp. 106. Price 15*s*.

This compact book contains an unusually large amount of information on the subject of the measurement and interpretation of the physical properties of dairy products. Dr. Baron gives an admirable survey of this whole field of research in a very readable form, and with adequate references. It is evident that definite progress is being made in the devising of objective tests to replace subjective judgments, though there is still a long way to go.

Diverse industries frequently present strikingly similar rheological problems, and one would like to underline the following remark which appears in the foreword contributed by Dr. G. W. Scott Blair. "Her book is addressed mainly to those in the dairy industry, but I feel sure that many others, rheologists, psychologists and technicians working in other industries, will read her story with interest."

L. R. G. TRELOAR

Notes and comments

Second international congress on rheology

The British Society of Rheology, supported by the Joint Commission on Rheology of the International Council of Scientific Unions, is arranging the Second international congress on rheology, to be held at St. Hilda's College, Oxford, from 26–31 July, 1953. The congress will cover the whole field of the study of the deformation and flow of matter, except such specialized subjects as have come to be regarded as branches of applied mechanics, e.g. the classical theory of elasticity or aerodynamics. The programme will include a presidential address, a number of invited lectures, and a discussion on the international organization of rheology. Arrangements will be made for excursions, visits to colleges, etc., during the congress. Accommodation will be provided in colleges, or rooms in Oxford. Further information may be obtained from the organizing secretary, Dr. G. W. Scott Blair, The University, Reading, Berkshire.

Ramsay's centenary exhibition

An exhibition has been organized in collaboration with University College, London, to mark the centenary of the birth of Sir William Ramsay, and to commemorate, among other work, the discovery of the inert gases. The exhibition will be held at the Science Museum, South Kensington, London, and will remain open for three months, 2 October, 1952, to 3 January, 1953. It will be divided into three main sections. The first section will include general biographical material; in the second section will be included some of the original apparatus used by Ramsay, and the third section will illustrate some modern applications of inert gases.

Notes on the preparation of papers

A revised and enlarged edition of the booklet *Notes on the preparation of contributions to the Institute's journals and other publications* is available. These notes, first issued in 1931, are intended to assist less experienced authors and to serve as a reference book for all who contribute to the Institute's publications. Apart from the special information concerning these publications the notes deal with the preparation, length and cost of publishing papers, the form of script and diagrams required, the setting out of tables and mathematics, and the correction of proofs. A short bibliography of dictionaries and books on writing is included. The appendix contains notes and examples of spellings, symbols and abbreviations, the Greek alphabet (so often unrecognizably written in scripts) and printers' marks for correcting proofs.

Copies of the booklet may be obtained from The Institute of Physics, 47 Belgrave Square, London, S.W.1, price 2*s*. 6*d*. Orders should be accompanied by remittance.

The scientific education of physicists

The Institute of Physics has published a report, *The scientific education of physicists*. Copies are available, price 2*s*., on application to the Secretary, The Institute of Physics, 47 Belgrave Square, London, S.W.1. The report includes, as appendices, factual data relating to the physics departments of all the universities and university colleges of Great Britain and Northern Ireland and of those technical colleges recognized by the Institute. The information should be of value to those studying for a degree in physics or contemplating such a course of study, as well as to others who have a close interest in the facilities for advanced training in physics.

Overhead-line charts

We have received a 30-page booklet entitled *Overhead-line charts* (second series), by V. T. Morgan of British Electricity Laboratories, Kingston Road, Leatherhead, Surrey. This summary is supplementary to Memoir No. 1 which was issued in 1949 and has been prepared to meet demands for voltage-drop charts for lines not included in the first memoir. This memoir is divided into two parts. Part I for distribution lines up to 66 kV, and Part II for transmission lines working at 275 and 380 kV.

Conference on ash and clinker in industry

The Institute of Fuel is holding a conference on ash and clinker in industry to be held in London on the 28 and 29 October, 1952. The subjects to be covered will include consideration of the occurrence and fundamental properties of ash, methods of sampling and analysis, and the partial removal of ash from coal by cleaning processes. The conference is the opening function of a special study of the subject to be carried out by the Institute during this session. Fuller details and forms of application may be obtained from the Secretary, The Institute of Fuel, 18 Devonshire Street, Portland Place, London, W.1.

Journal of Scientific Instruments

Contents of the October issue

ORIGINAL CONTRIBUTIONS

An electronic computer. By M. Beard and T. Pearcey.
The design of thermocouple transformers for infra-red chopped beam systems. By T. S. Robinson.
The estimation of photographic resolving power from visual observations alone. By P. G. Powell.
Radiac instrumentation. By D. Taylor.
A source of computing voltage with continuously-variable output. By R. W. Williams and G. M. Parker.
A fast scanning mechanism for use with a Geiger counter X-ray spectrometer. By J. Adam.
A photoelectric correlation meter. By M. J. Tucker.
The effective radius of curvature of knife edges. By G. F. Hodsman and F. A. Chappell.

LABORATORY AND WORKSHOP NOTES

A piston type volume recorder. By C. P. Luck.
A structure-factor calculator. By E. Stanley.
A liquid nitrogen level indicator. By M. G. Davies and H. Kronberger.
A means of stabilizing the field of an electromagnet. By G. Suryan.
O-ring sealed vacuum valves. By P. A. Shatford.
A device for charging electroscopes. By A. O. Mathai.
A balancing and calibrating device for resistance strain gauge circuits. By P. Savic.
A galvanometer lamp and a clamp with four degrees of freedom. By R. V. Jones.

CORRESPONDENCE

Relay scaling circuits. From B. E. Swire.
The initial performance of a proton accelerator tube; deterioration and its causes. From D. R. Chick and F. J. Miranda.

NEW INSTRUMENTS, MATERIALS AND TOOLS

NOTES AND COMMENTS

THIS JOURNAL is produced monthly by The Institute of Physics, in London. It deals with all branches of applied physics (including theory and technique).

All rights reserved. Responsibility for the statements contained herein attaches only to the writers.

EDITORIAL MATTER. Communications concerning editorial matter should be addressed to the Editor, The Institute of Physics, 47 Belgrave Square, London, S.W.1. (*Telephone*: Sloane 9806.) Prospective authors are invited to prepare their scripts in accordance with the *Notes on the Preparation of Contributions*. (Price 2*s*. 6*d*. including postage.)

REPRODUCTION. The Institute of Physics is a signatory to The Royal Society's Fair Copying Declaration. Details may be obtained upon application from The Royal Society, London, W. 1.

ADVERTISEMENTS. Communications concerning advertisements should be addressed to the agents, Messrs. Walter Judd Ltd., 47 Gresham Street, London, E.C.2. (*Telephone*: Monarch 7644.)

SUBSCRIPTION RATES. A new volume commences each January. The charge is £4 per volume ($11.50 U.S.A.), including index (post paid), payable in advance. Single parts, so far as available, may be purchased at 8*s*. each ($1.15 U.S.A.), post paid, cash with order. Orders should be sent to The Institute of Physics, 47 Belgrave Square, London, S.W.1, or to any Bookseller.

Summarized proceedings of a conference on microwave physics—Oxford, July 1952

The 1952 summer meeting of the Electronics Group of The Institute of Physics was held on 11–13 July in the Clarendon Laboratory, Oxford. Four papers on microwave physics were read and discussed and one morning was spent viewing the work being carried out in the Clarendon Laboratory. The titles of the papers were: Paramagnetic resonance in crystalline solids; Microwave phenomena in gases; Precision measurements with microwaves; and Techniques and ultimate sensitivity in microwave spectroscopy. The papers and the discussions on them are summarized in this article.

PARAMAGNETIC RESONANCE IN CRYSTALLINE SOLIDS

The opening paper was by Dr. B. Bleaney (Clarendon Laboratory, Oxford) on "Paramagnetic resonance in crystalline solids." After some introductory account of the behaviour of gases and liquids in the presence of microwave radiation, Dr. Bleaney explained that with solids the interaction time between the atoms was too long for resonance effects to be observed due to the electric dipole moments of the atoms. If, however, there were atoms with magnetic dipole moments in the solid, then the lower strength of these compared with the electric gave the possibility of observing resonance phenomena with adequate resolution. The system was one in which the alternating magnetic field due to the microwaves was superimposed on a steady magnetic field, this being achieved by placing the solid in a cavity resonator which was between the poles of an electromagnet. The Q of the resonator was measured while the magnetic field was modulated over a small range including the resonance value. The specimen could be oriented in different ways in the cavity and preferably consisted of a single crystal, since in many solids the effects were anisotropic, and then with polycrystalline material the resolution was lost. Resonance was to be expected for any chosen frequency ν when the external field passed through the value H_R where

$$h\nu = g\frac{eh}{4\pi mc}H_R \text{ or } \omega = g\left(\frac{e}{2mc}\right)H_R \qquad (1)$$

At resonance the orientation of the dipoles was changed relative to the external field with a corresponding change in energy.

With copper Tutton salts, scanning the applied field through resonance gives two resonance peaks, each of width several hundred gauss. There are two because two types of copper ion are present, and the lines are broad because the fields of the neighbouring ions are appreciable, and varying. To raise the resolution the ions must be more widely separated, as in a complex salt; further separation can be achieved in a complex salt by replacing some of the copper by zinc, which is not paramagnetic. It is now found that each broad line is resolved into a set of eight strong lines and four faint ones; the eight strong lines are two sets of four produced by the two isotopes; there are four in each set because of interaction with the field of the nucleus. The moment of the nucleus is small, but its field is nevertheless strong at the distance of the electrons. The spin of the copper nucleus is 3/2, with four possible orientations, so that four fields are encountered, giving the four lines. The outer pairs of lines due to the two isotopes are readily distinguished, but the inner pairs are not fully resolved. The four faint lines are produced because the nucleus has an electric quadrupole moment, and therefore produces an electric field which affects the electron motion. The isotopes are not separated in these faint lines. The strong lines have a width of 12 gauss, which is due to the field of the protons of the water molecules of the complex salt. This width is reduced to 4 gauss if the salt is made using heavy water. Even better resolution is obtained if a salt can be prepared which contains no water of crystallization; the cyanide is one possibility, giving good results since carbon has no nuclear magnetic moment, and that of nitrogen is small. Thus using $K_3Cr(CN)_6$, the structure due to the chromium ion is observed. The isotope 53 gives a structure with four lines, indicating a nuclear spin of 3/2 as for copper. This value was not known until these four lines were observed. In the case of manganese there is an electron spin term of 5/2, giving six energy levels and five transitions; each transition has six components, since the nuclear spin is also 5/2, thus there are five sets each of six resonance peaks.

With neodymium, 80% of the isotopes have no magnetic moment, but masses 143 and 145 each have a moment, and each gives a set of eight resonance lines. This indicates eight nuclear orientations, and therefore a spin term of 7/2 for each isotope. This also was unknown before the use of microwave spectroscopy. The method is, of course, confined to atoms with a magnetic moment, i.e. paramagnetic ions, and those of the transition and rare earth metals.

Fuller accounts of the work described by Dr. Bleaney will be found in the literature.[13–15]

Dr. E. E. Schneider (Kings College, Newcastle-on-Tyne, University of Durham) next described some experimental results on paramagnetic resonance obtained at Newcastle. The first example was manganese at low concentration in zinc sulphide phosphor powder. With 1% manganese there was a broad band, but at 0·1% hyperfine structure was obtained, with six peaks due to the 5/2 spin term. With 0·001% manganese the six peaks showed further splitting, due to the axial components of the crystalline field; this was with zinc sulphide of wurtzite structure, in zincblende the sixfold nuclear splitting only was present. In the next experiments, manganese was present as a trace impurity in sodium chloride single crystals. At 0·001% there was at first a smooth broad peak, but after heating, a fine structure appeared, which was particularly complex after heating and quenching. This could be attributed to movement of vacant lattice sites; it appears that aggregation of the manganese suppresses the structure. The method might therefore be developed for the study of vacancy behaviour.

In the third part of the work, resonance had been observed due to the colour centres in alkali halides. The spin of the electron bound at the negative ion vacancy (Schottky defect) was responsible for this. Fourthly, resonance had been obtained with aqueous solutions, for example with manganese. In the fifth series, hyperfine splitting of paramagnetic

resonance, due to interaction with nitrogen nuclei, had been observed with an organic radical, both in dilute solution in benzene, and in solid solution in Perspex. The sixth reference was to the effect of irradiating Perspex with X-rays. This produces a resonance pattern with nine peaks, although there was no effect before irradiation. There is presumably a bond breakage, and interaction with the spins of the freed electrons.

In the discussion following these two papers, MR. KEELEY (University of Oxford) asked about the permanence of the effect of X-ray irradiation on Perspex. Dr. Schneider said that the effect remained present for several months, and was more stable in dyed Perspex. MR. PROUD (National Physical Laboratory) recalled that at the N.P.L. flashes had been detected by scintillation counters when Perspex was irradiated with X-rays. MRS. DUNSMUIR (British Thomson-Houston Co. Ltd.) asked how it was that Dr. Schneider could obtain hyperfine structure using polycrystalline material, in view of Dr. Bleaney's emphasis of the need to use single crystals. The answer was that with manganese the interaction is nearly isotropic. Dr. Bleaney remarked that structure had been obtained from plasticine due to traces of manganese. DR. ESSEN (National Physical Laboratory) asked whether resonance could be observed due to the nuclear field alone, and Dr. Bleaney replied in the affirmative, quoting as an example the case of neodymium. Dr. Schneider said that the zero-field effect was especially striking when a strong nuclear quadrupole interaction was present. DR. DUNSMUIR (British Thomson-Houston Co. Ltd.) asked for further details of the energy transfer process at resonance. Dr. Bleaney replied that the energy absorption produced a state of higher potential energy, which was dissipated as heat by transfer to the lattice vibrations. The energy was stored in a metastable state, sometimes for less than 10^{-11} sec. This time became very much longer when the temperature was lowered. DR. HOULDIN (College of Technology, Birmingham) inquired as to other effects of temperature, and in reply Dr. Bleaney stated that in addition to an increase in intensity and the decrease in line width (due to a longer relaxation time) with falling temperature, there was a change in spacing of the lines of the fine structure, following the changes in the dimensions of the surrounding lattice, with which the electronic dipole interacts. There were also more complicated effects, as in the case of the copper ion in a crystal with threefold symmetry; here at low temperature the cube axes formed axes of symmetry, with corresponding anisotropic effects in the hyperfine structure, whereas at high temperatures the spectrum was isotropic.

MR. WRIGHT (General Electric Co. Ltd.) asked whether one would expect resonance to be obtained with the electron at a Frenkel defect in an ionic crystal, as had been observed with an electron at a Schottky defect, i.e. a colour centre. If not, this might offer a criterion for distinguishing between the two types of defect. There was no information on this point, but Dr. Schneider said that attempts had been made to detect the presence of Cu^{++} ions in cuprous oxide, and it was intended to study the silver halides from this point of view. Dr. Bleaney remarked that no true resonance had been observed with semi-conductors, though this might be obscured by damping due to the Hall effect. Dr. Schneider said that with semi-conductors it would be necessary to work at low temperatures, where not too many of the electrons were free.

MICROWAVE PHENOMENA IN GASES

In the next paper, MR. P. O. HAWKINS (Services Electronics Research Laboratory) dealt with "Microwave phenomena in gases." He said that in considering the interaction between microwaves and the plasma of a discharge, the basic effects are of two kinds, firstly a loss of energy, corresponding with a resistive load, and secondly a lowering of the dielectric constant of the medium, corresponding with a capacitative load. The change in dielectric constant is a function of the electron density, while the loss of energy depends on the electron mean free path, and microwave frequency. The experimental method of Adler[1] was described, in which the discharge tube is introduced into a cavity resonator. This produces changes both in the frequency and in the Q of the circuit. From these effects it is possible to calculate the complex conductivity of the plasma. The results have been found to agree with the Margenau theory,[2] taking parameters of the discharge as indicated by probe techniques. Thus microwaves can be used in conjunction with the Margenau theory to obtain information under conditions where probes cannot be employed.

The second experimental procedure described was that of Biondi, using pulse techniques. Here a magnetron source is used to excite a discharge tube, and the source is switched off. The ionization decays, and with it the resonance frequency alters. This is in fact proportional to the free electron density, so that its variation after removing the source of power gives information about recombination and diffusion processes. Two interesting results were described, firstly that with helium the recombination coefficient was much larger than the theoretical,[3] and secondly that in some cases the electron density rose at first before decaying, indicating ionization by collision with metastable atoms.[4]

The third experiment involved observation of the microwave radiation emitted from a discharge plasma. This can be regarded as thermal radiation, and should depend directly on the electron temperature of the plasma, if this has any real significance. It has in fact been confirmed that the plasma radiates as a black body, the radiation indicating a temperature similar to that deduced from the gas kinetic properties of the plasma. The behaviour depends on pressure and on the ionization potential of the gas in the manner expected from theory.[5] The effects of changing the tube dimensions and microwave frequency are also self-consistent. One important result is that if the experiment is arranged to give the ratio between the imaginary and the real components of the plasma conductivity, the calculated value of the electron mean free path is different from that obtained by other methods.

In the discussion, DR. GARBOR (Imperial College, London) asked what were the electron concentration and the frequency used in these last experiments, and what was the magnitude of the discrepancy in mean free path. Mr. Hawkins gave the electron density as of the order of 10^{11} per cm^3, and the frequency as 36 000 Mc/s. The mean free path was less than that indicated by other methods, by a factor of 3 in the case of argon, and 10 in the case of neon. No mercury was present in these gases. In reply to Dr. Garbor, Mr. Hawkins said that allowance had been made for the Ramsauer change in section. Dr. Garbor pointed out the difficulty involved in accepting that the plasma in a discharge tube positive column radiated as a black body, since if this were generalized, one would expect no passage of radiation through the Heaviside layer: possibly the effect in the discharge tube was localized at surfaces. In connexion with the low mean free path, DR. THONEMAN (Atomic Energy Research Establishment) suggested that the scattering by excited atoms might be responsible, since as much as 30% of the gas might be excited at low pressures, and have an increased collision cross-section.

Dr. Garbor thought that, at an electron density of 10^{11} per cm^3, this might give a factor of two in mean free path, and would not explain the results with neon. Other unpublished experiments on air at 0·05 mm of mercury pressure, at 1 200 and 3 000 Mc/s, had given collision frequencies a hundred times as great as the theoretical, emphasizing the discrepancy. MR. BRADLEY (Elliott Bros. (London) Ltd.) showed a slide illustrating this point in another way. A plot of attenuation against pressure showed experimentally a maximum at twice the pressure deduced either from the simple or the Margenau theory, also indicating a low mean free path. Mr. Hawkins inquired as to the upper limit of pressure at which the simple theory of the positive column broke down, and Dr. Garbor said that the limit was near 1 mm of mercury.

Mr. Hawkins then gave a brief account of experiments at higher charge density, at which the normal plasma analysis is invalid. He introduced the conception of zones in the plasma at which the charge density was such that the dielectric constant effectively vanished, so leading to a resonance effect. Zones of intense activity had been found using probes,[6] and also localized luminosity had been observed in electrodeless discharges excited by microwaves. These zones were normally sheaths near the boundaries of the discharge. Dr. Garbor thought that this type of work should be carried out at higher frequencies than those used so far. Oscillations in sheaths in mercury vapour had been observed, unaccompanied by external radiation, because the plasma reflects the sheath radiation. MR. STRATTON (Royal Aircraft Establishment) asked how the regions were distinguished, where the plasma analysis was or was not valid. In reply Dr. Garbor said that the analysis was valid when the radiation frequency was high compared with the plasma frequency.

PRECISION MEASUREMENTS WITH MICROWAVES

DR. L. ESSEN (National Physical Laboratory) gave the next paper, on "Precision measurements with microwaves." He said that his contribution would be concerned mainly with the details and refinements of microwave measurements rather than with their physical principles. It was nevertheless interesting to notice that the particular feature of microwave work was that it was possible to combine radio frequency techniques with the optical technique of interferometry. The magic T, for example, was the analogue of the Michelson interferometer and the cavity resonator of the Faby–Perot interferometer. These interferometers enabled the wavelength of the wave in a guide or in air to be measured with great precision. The values of wavelength obtained were converted into free-wave values from a knowledge of the boundary conditions and these combined with the frequency of the waves gave the velocity. The work obviously required very stable sources of oscillation of accurately known frequencies, and it was found in recent work at the N.P.L. that a Pound stabilized microwave oscillator could be made stable to 1 part in 10^8 per hour and that its frequency could be measured in terms of the quartz clock with a precision of a few parts in 10^{10}.

In the first cavity resonator experiments at the N.P.L. a copper resonator of fixed dimensions was used, in an evacuated enclosure. The frequency of the oscillator was varied smoothly in the region of 3 000 Mc/s until resonance was obtained and it was then measured in terms of the standard. The free space velocity was calculated from the formula

$$C = \frac{f(1 + 1/2Q)}{[(r/\pi D)^2 + (n/2L)^2]^{\frac{1}{2}}} \qquad (2)$$

where Q is the quality factor of the resonator, D its diameter, L its length, n the number of half-wavelengths and r is a Bessel function. The repetition accuracy under fixed conditions was a few parts in 10^6 and the accuracy of the final result was therefore limited by the small systematic errors inherent in the experiment. The later experiment using a resonator which could be varied in length was designed to reduce these errors. It can be seen from equation (2) that by performing the experiment with different values of f or r it is possible to measure the effective value of the diameter D in terms of frequency and length. Moreover since the values of length are obtained by differences they are independent of end effects and surface imperfections. The final result obtained was

$$C = 299\,792{\cdot}5 \pm 1 \text{ km/s}$$

In the third experiment (carried out by Dr. Froome, N.P.L.) a path in air about 15 m long constituted one arm of a Michelson interferometer. In the detector successive minima were observed as the length of the path was changed by one-half-wavelength, and the total change for 359 half-wavelengths was measured. The value of the wavelength determined in this way was corrected for diffraction effects and the velocity then found from the wavelength and the frequency. The validity of the diffraction correction was checked by measurements at a number of distances with a number of reflectors; and systematic errors were eliminated as far as possible by the experimental procedure. The result obtained was

$$C = 299\,792{\cdot}6 \pm 0{\cdot}7 \text{ km/s}$$

In this experiment it was necessary to correct for the refractive index of the air. The value had not been determined previously with sufficient accuracy and a new method was therefore devised by Essen and Froome. The principle of the method was simply to determine the resonant frequency of a cavity when filled with air and when evacuated, but in order to obtain the required accuracy this resonant frequency needed to be determined with a precision exceeding 1 part in 10^7. This was achieved by connecting the resonator in a waveguide bridge circuit and measuring the frequency of a stabilized oscillator directly in terms of a quartz standard. The values for the various constituents of air and for samples of dry air and moist air were determined; and an equation giving the value for moist air under a wide range of conditions was developed.

In the discussion of Dr. Essen's paper, DR. LAVERICK (General Electric Co. Ltd.) asked about the form and accuracy of the reflecting mirror used in the interferometer experiments, and MR. STRATTON asked whether multiple scattering had been allowed for. Dr. Essen said that as the wavelength was 1·25 cm, the accuracy of the mirror need not be high, while the scattering was corrected by the procedure of taking a number of readings at short intervals over a range of half a wavelength. In reply to Mr. Stratton, Dr. Essen said that the Q of the cavity in the sliding piston resonator was 30 000–100 000. Dr. Schneider asked whether there was any evidence to support the view that the velocity of light was altering with epoch. Dr. Essen replied that there was no evidence in support of this if realistic values were taken for the accuracies of the various results. Dr. Dunsmuir pointed out that it should be possible to calculate the Q of the resonator taking account of the wall losses, and asked whether calculated and observed values agreed. Dr. Essen replied that the observed values were about three-quarters of the theoretical, if the calculations employed the bulk values of conductivity for copper or silver. This is reasonable, since

there were irregularities in the surface and in the plating, and the silver may be tarnished with silver sulphide. Other workers have obtained the theoretical Q by electroforming or polishing. Dr. Houldin inquired as to the uniformity of the inside diameter of the cavity and the method of measurement. In reply, Dr. Essen said that the hardened steel was uniform to 10^{-5} in, but after plating, the figure was slightly worse. The measurement involved an optical system for comparison of the inside diameter with a gauge block. MR. HICKIN (General Electric Co. Ltd.) asked about the effect of moisture, and Dr. Essen said that this was very important in the interferometer work. The procedure was to measure the refractive index of air as a function of moisture content, and then to measure the moisture content of the air in the room at the time of an interferometer experiment. The moisture measurement was not highly accurate, and it would be necessary if higher accuracies were required to measure the refractive index of the actual sample. MR. RODDA (Edison Swan Electric Co. Ltd.) asked what changes there were in the acceptable values of other physical constants, in view of Dr. Essen's accurate value of the velocity of light. Dr. Essen agreed that it had been necessary to recalculate other constants, though the change was near the limit of significance.

Fuller accounts of the work described by Dr. Essen will be found in the literature. [7-10]

TECHNIQUES AND ULTIMATE SENSITIVITY IN MICROWAVE SPECTROSCOPY

The final paper was by DR. E. E. SCHNEIDER (Kings College, Newcastle-on-Tyne, University of Durham) on "Techniques and ultimate sensitivity in microwave spectroscopy." He included both gases and solids showing paramagnetic resonance. He first made the general point that an absorption coefficient of the radiation α could be introduced, such that the intensity at depth l in the medium was $I = I_0 e^{-\alpha l}$. The absorption could be attributed to classical oscillators, but whereas in optical work α was of the order $1\ m^{-1}$, it was much smaller with microwaves. The number of oscillators was much less than the total number of atoms or molecules, whereas in optics it was of the same order; this implies that with microwaves only a few atoms or molecules in the medium are in the state corresponding with the equivalent oscillator. Many are in the wrong phase for there to be absorption of energy, and in fact some will be able to give up energy to the radiation. The rate of absorption depends on the type of resonator, but there is in fact little difference between electric and magnetic dipoles, although the interaction energy is less in the latter case. This is because the number of magnetic dipoles in the state for absorption is larger, and the line width is less in the magnetic case.

In one type of experiment a wave-guide absorption cell is used, the gas is introduced into it and the absorption is determined as a function of frequency by varying the frequency of the oscillator. Dr. Schneider described how by means of the Stark effect shift it was possible to label the absorption frequency, and to eliminate spurious signals produced by the apparatus. A second method involved a cavity resonator fed at a fixed frequency, and placed in a variable external magnetic field. The development of this to give a bridge method was described, using the hybrid ring.[11]

It was possible to obtain an expression for the signal amplitude at absorption as compared with that with no absorption, in terms of α and of the circuit constants. Then knowing the minimum detectable signal in terms of the receiver noise, the theoretical minimum detectable value of α could be determined. This was as low as $10^{-10}\ m^{-1}$. This is not in fact attainable, because of other sources of noise, in particular that due to frequency fluctuations, and also general interference by pick-up and microphony. Usually the minimum detectable value of α was about 100 times the theoretical value for the particular method, and the best figure obtained so far was $2 \cdot 10^{-9}\ m^{-1}$.[12]

The apparatus at Newcastle had been considerably improved in the last two years, by introducing a frequency stabilization scheme, and by using battery supplies to the klystron. The noise was thereby reduced, and the minimum detectable value of α lowered.

Opening the discussion of Dr. Schneider's paper, Dr. Essen said that the frequency stability of a stabilized klystron depended markedly on mains fluctations, and was better if the heater was supplied by d.c.; this gave about as much improvement as the use of batteries, and 20 c/s in 10 000 Mc/s were easily obtainable. The avoidance of mechanical vibration was important, and the cavity for the velocity of light experiments had walls $\frac{1}{2}$ in thick. There was then a brief discussion between Mr. Stratton and Dr. Schneider in which the former suggested that a magic T might be preferable to a hybrid ring, since amplitude modulation following shifts in frequency could thereby be avoided in a system using wide band width. Dr. Schneider remained unconvinced, thinking that the hybrid ring was easier to match and to adjust. With his procedure, he was concerned solely with frequency, not amplitude variation. His instability difficulties were equivalent to an r.m.s. frequency fluctuation of 5 c/s in 10 000 Mc/s, with negligible amplitude noise.

MR. WILLSHAW (General Electric Co. Ltd.) asked about receiver sensitivity, he had heard 6 db claimed at 5 mm. Dr. Schneider was doubtful whether this was possible using a crystal, though it had been achieved with a bolometer detector. Mr. Hickin asked what was the effect when measuring any particular gas if another gas was present as an impurity. Dr. Schneider replied that there was no effect depending only on magnetic resonance, but the line width would be affected, if the impurity introduced a quadrupole moment, e.g. in the case of nitrogen added to oxygen.

In reply to Dr. Essen, Dr. Schneider said he had avoided mention of molecular beam methods for observing magnetic resonance, as this was a large field and a subject in itself.

D. A. WRIGHT

REFERENCES

(1) ADLER, F. P. *J. Appl. Phys.*, **20**, p. 1125 (1949).

(2) MARGENAU, H. *Phys. Rev.*, **69**, p. 508 (1946); 73, p. 297 (1948).

(3) BIONDI, M. A., and BROWN, S. C. *Phys. Rev.*, **76**, p. 1697 (1949).

(4) BIONDI, M. A. *Phys. Rev.*, **82**, p. 566 (1951).

(5) COBINE, J. D. *Gaseous Conductors*, p. 236 (New York and London: McGraw Hill Book Co. Inc., 1941).

(6) WEHNER, G. *J. Appl. Phys.*, **22**, p. 761 (1951).

(7) ESSEN, L., and GORDON-SMITH, A. C. *Proc. Roy. Soc.*, *A*, **194**, p. 348 (1948).

(8) ESSEN, L. *Proc. Roy. Soc.*, *A*, **204**, p. 260 (1950); *Nature, Lond.*, **165**, p. 582 (1950); **167**, p. 258 (1951); *Science Progress*, **157**, p. 54 (1952).

(9) ESSEN, L., and FROOME, K. D. *Nature, Lond.*, **167**, p. 512 (1951); *Proc. Phys. Soc.*, *B*, **64**, p. 826 (1951).

(10) FROOME, K. D. *Nature, Lond.*, **169**, p. 107 (1952); *Proc. Roy. Soc., A*, **213**, p. 213 (1952).

(11) SCHNEIDER, E. E., and ENGLAND, T. S. *Physica*, **17**, p. 221 (1951).

(12) BERINGER, R., and CASTLE, J. G. *Phys. Rev.*, **75**, p. 1963 (1949).

(13) BAGGULEY, D. M. S., BLEANEY, B., GRIFFITHS, J. H. E., PENROSE, R. P., and PLUMPTON, B. F. *Proc. Phys. Soc. Lond.*, **61**, pp. 542 and 551 (1948).

(14) BLEANEY, B. *Physica*, **17**, p. 175 (1951).

(15) BLEANEY, B., and STEVENS, K. W. H. "Paramagnetic resonance," *Rep. Phys. Soc. Progr. Phys.* To be published.

SPECIAL ARTICLE

Secondary processes active in the electrical breakdown of gases

By PROFESSOR LEONARD B. LOEB, S.B., Ph.D., Department of Physics, University of California, Berkeley, California*

Recent advances in techniques and consequent results indicate the complexity of gaseous breakdown mechanisms. The three cathode mechanisms and two anode mechanisms are carefully analysed indicating their relative importance and conditions of appearance. They are shown to lead to the same type of generalized breakdown threshold condition with statistical fluctuations and subject to alteration by space charges. This condition masks the processes active rendering analysis difficult. The threshold mechanisms alone do not determine the breakdown for this involves the ultimate resulting discharge. The factors modifying the discharge are gas type and state, electrodes, geometrical factors and external circuit constants. The discharge types to which these lead and governing circumstances are presented. In conclusion proper modern methods of discharge analysis are indicated.

INTRODUCTION

There used to be a maxim that nature intrinsically acts in a simple fashion. The current developments in nuclear physics and in atomic physics, especially as exemplified through gaseous breakdown, render this classical maxim slightly fallacious. The development of the theories of electrical breakdown in gases under the aegis of the concept of simplicity have rendered chaotic a proper interpretation of the complex phenomena as revealed by the more recent static and dynamic analyses of the processes active in the various breakdown sequences. It is thus imperative that a summary be made of the processes known to be active and the conditions and circumstances of their appearance.

Primary processes. It will be taken for granted that the primary process in all gaseous breakdown is the multiplication of electrons in a gas by cumulative ionization by electron impact in advancing in the direction of the electrical field. This is characterized by a coefficient α representing the number of new electrons and ions created by one electron moving 1 cm in the field direction. The ratio of α to pressure p, α/p, is some function of the ratio of field strength X to pressure p, X/p, over most of the active range which can be evaluated by direct measurement. The number of new electrons created by one electron in progressing a distance a in any field is expressed as $\exp\left(\int_0^a \alpha dr\right)$ in the most general case. This group of electrons is termed an *electron avalanche*. The positive ions created in an avalanche remain essentially at rest during the creation of the avalanche, since the electrons move some 10^2 to 10^3 times faster than do the ions. The ions do, however, move, but on a time scale 100 or more times greater. Accompanying the avalanche of electrons there are created in the gas some ω photons of various energies per cm of electron path in the field direction. These photons can be segregated into special groups by appropriate subscripts. The quantity $f = \omega/\alpha$ then gives the ratio of the number of photons created per ion of the avalanche. The quantity f varies with the average electron energy and the energies of the photons created. As X/p increases for any given photon group, f at first increases and later declines.

Secondary processes. For the consummation of any discharge, or electrical breakdown, there is required a secondary process acting in conjunction with the primary process. There are in essence two categories of secondary processes that are relatively frequently encountered. These are:

1. secondary processes at the cathode;
2. secondary processes in the gas.

1. SECONDARY PROCESSES AT THE CATHODE

Experiment has revealed that the cathode processes, generally designated by a symbol γ, consist of the liberation of (*a*) secondary electrons by positive ion bombardment, γ_i, (*b*) secondary electrons by photoelectric processes, γ_p, and (*c*) secondary electrons by metastable atoms, γ_m. The coefficients γ represent the net number of secondary electrons moving from the cathode in the gas per ion incident for γ_i, per active photon liberated in the avalanche γ_p, or per metastable atom created γ_m. In static studies of these processes, it is often hard to distinguish which γ process is active, although in general 1(*b*) photoelectric processes, γ_p, occur more prominently at lower X/p, while 1(*a*), or γ_i processes, occur more prominently and with increasing values at high X/p. Dynamically studied, if triggered by avalanches initiated within short-time and narrow-distance intervals, the various γ processes are clearly distinguished by their temporal characteristics. For the γ_p process involves electron transit times which are 10^{-2} of the ion transit times needed for the γ_i process and 10^{-3} or more, of those involved in the γ_m

* Much of the later work here was done in the author's laboratory under grants from the Office of Naval Research and the Research Corporation of America.

process. The metastable process being a diffusive one would show a broad response in time intervals, whereas Y_i and Y_p would not be much broadened beyond the duration of the triggering pulse. H. L. von Gugelberg[1] has shown another dynamic form of analysis by which the processes can be separated in the case of spark discharge. These differ somewhat from the pulse techniques of R. W. Engstrom and W. S. Huxford,[2] J. A. Hornbeck,[3] J. P. Molnar,[4] L. Colli, E. Gatti and U. Facchini,[5] and E. J. Lauer.[6]

(*a*) Again these processes must be regarded relative to the fields existing at the cathode. If the ionizing potential E_i of the ion is above the work function of the cathode, ϕ_e, the Y_i process will yield secondaries at impact near thermal energy.[7, 8, 13] All ions irrespective of their ionization potential relative to ϕ_e, if they have energies which are sufficient (say, in excess of 60 eV), will liberate electrons from a cathode surface on impact. The vacuum yield of these electrons per incident positive ion, Y_i, increases as the energy of impact increases.[8]

It can be expected unless X/p is very high, leading to very energetic positive ions, that Y_i will depend very critically on positive ion species. It is not always possible to know what ions are active. Even in the inert gases, helium, neon and argon, the ions can be He^+, Ne^+ and A^+, or He_2^+, Ne_2^+ and A_2^+. The relative proportions of these change from all atomic to all molecular ions with pressure and time after creation.[9] At one X/p H. D. Hagstrum[10] found in helium with clean tungsten that Y_i for He_2^+ was 0·6 of that for He^+. Thus Y_i values in any gas-metal system can change unpredictably with changing conditions. The values of Y_i as studied for clean outgassed metal surfaces in vacuum are not those met with in gases under discharge conditions. The nature of the gas, the past history of the cathode surface, and the discharge conditions, including the current density, alter the cathode surface and determine ϕ_e and Y.[11, 12] Ideally, it is assumed that all positive ions drawn to the surface penetrate it and have a chance of liberating a secondary electron. In some cases the ion neutralizes to an excited or metastable state before it enters the lattice. Such atoms are known to suffer some reflexion at the surface.[13] Thus 0·75 of the argon metastables of 500 V are reflected from clean tungsten, while only 0·21 of the hydrogen molecules of 1 100 V are reflected.[13] Of those ions that enter the lattice a certain fraction liberates electrons that escape from the metal surface in vacuum. Call Y_c the fraction of positive ions directed toward the cathode that cause electrons to be emitted on impact, including in Y the fraction of ions that do not enter the metal. Y_c should depend on work function, ion species and energy of impact. Of the electrons emitted only a fraction ν will get into the gap if gas is present. The others willn to retur the cathode by *back diffusion*.[14]* The quantity ν increases with X/p near the cathode. It decreases as the average energy of the emitted electrons increases. Such energy of emission is large (of the order of 10 eV), when the ionization potential E_i is large compared to ϕ_e and relatively small (of the order of 0·1 eV), where electrons are emitted by impact of fast ions. Attachment of electrons to form ions in the gas somewhat decreases ν. Over the *range of discharge conditions* encountered the value of Y_c will vary from perhaps less than 0·01 to at most 0·5,[8, 15] while ν will range from perhaps 0·005 at very low X/p with electron energy 10 eV to around 0·5 at high X/p and low energy of emission.[14] Thus observed values of Y_i range from 0·40[3] down to 5×10^{-5}.[6]

(*b*) The value of Y_p will be composed of many factors. It is reduced by a geometrical factor g, which is anywhere from 0·8 to a small value on a small cathode since photons radiate in all directions. In a plane parallel gap with reflexion from the anode it will be perhaps 0·7. Y_p is reduced by a factor $\exp(-\mu x)$ where μ is the absorption coefficient in the gas and x is the distance to the cathode. Of the incident photons on the cathode only a fraction θ_p will liberate electrons. This fraction is small and may range from 0·1 to 10^{-4}. Again, of the electrons liberated from the cathode only a fraction ν will escape back diffusion. With photoelectric action the energy of emission is usually low so that ν is larger than with Y_i. Thus, Y_p is expressed by $Y_p = \nu g\theta \exp(-\mu x)$. Compared to Y_i the value of Y_p of itself will tend to be the smaller. However, only $\exp \int \alpha dr$ ions are created and $f \exp \int \alpha dr$ photons are created. At low X/p, f can be large so that fY_p can be as large or larger than Y_i. Values of fY_p of 0·1 have been observed by D. H. Hale[15] in hydrogen on a sodium surface at an X/p of 8 to 13 and values of 5×10^{-5} have been observed by E. J. Lauer[6] in hydrogen on outgassed nickel at $X/p = 0{\cdot}3$ and $p = 400$ mm. Note that f decreases as X/p increases while ν increases as X/p increases. The many variables make the action of Y_p difficult to predict. It does occur at *effective values* at lower X/p than Y_i and produces important actions.

(*c*) The quantity Y_m depends for its effectiveness on the value of fY_m relative to Y_i. It contains a geometrical loss factor which can be important if electrodes are of unequal area since diffusion as with photons is random in direction. It also suffers a loss owing to destruction in the gas which can be set as $\exp(-\mu_m x)$. Its chance of electron liberation from the cathode θ_m is perhaps of the order of 0·1 to 0·3.[13] Back diffusion loss ν is high and diminishes the electrons escaping. Thus Y_m is expressed by $f_m Y_m = \nu f_m g_m \theta_m \exp - \mu m x$ and should be less than Y_i but greater than Y_p in gases where it can occur. It also acts at lower X/p as does Y_p.

Unless pressures are very low so that diffusion in avalanches is large, actions produced by Y_i are localized in a cylindrical region symmetrical about the track of the first avalanche whose diameter corresponds to ion diffusion over the time of successive avalanches. Unless photon absorption is very great or $1/\mu$ is very small compared to gap lengths the diffusive nature of photon emission will spread the secondary Y_p processes well over the cathode area. Entrapment of resonance radiation will enhance this even when $1/\mu$ is smaller.[16, 17] Similar diffusive action characterizes Y_m. Thus Y_i conditioned breakdown will generally be more localized while Y_m and Y_p discharges are diffuse.

Currently too little is known about the work function of surfaces, their variation in the presence of gases and variation with past history. Very clean, outgassed surfaces of pure elements have clearly defined values of the work function. Studies of Y_i and Y_p have on occasion been made on such surfaces, notably with inert gas ions.[8] In general, such surfaces have lower values of Y than do gassy surfaces. C. W. Oatley and G. L. Weissler and his associates have noted the variation of the work function of platinum, tungsten, molybdenum and silver as a function of treatment with gases, such as hydrogen, oxygen, nitrogen and argon.[18] Prolonged heating at high temperatures cleans up surfaces of tungsten according to F. M. Penning.[19] Weissler[18] finds both electron bombardment and heating less effective than heavy bombardment with ions of relatively inert gases such as nitrogen and argon. J. K. Theobald[14] also reports that

* An intensive study of back diffusion is currently being concluded in the author's laboratory by J. K. Theobald. Covering as large a range as possible in X/p for standard gases and for emission energies the data indicate the influence of ν to be of considerable importance. This is borne out by E. J. Lauer's[6] values in *A*.

bombardment yields more stable photoelectric emitting surfaces. In general, hydrogen lowers the work function, while oxygen increases it. Changes observed amount in range to about 2 V. Theobald[14] finds that work function, a gross average surface value, may not directly correlate with secondary emission which may come from a selected few, but varied, numbers of points of low work function. Total surface emission may increase manyfold on activation treatment which increases the number without affecting the average work function nor the distribution in energy of emitted photoelectrons. Certain metals, such as those acting as surface catalysts with certain gases may behave differently with the gases that they catalyse than with others.[20] In some instances certain gases deactivate surfaces of otherwise high γ. Thus nickel, iron, copper and platinum are deactivated, or "poisoned," by oxygen, carbon dioxide, sulphur dioxide, and probably by mercury. Drastic action, including bombardment, may alter the behaviour markedly.[11, 21] Initially, no metal surfaces are clean or in the condition which they reach when a gaseous discharge operates. All cathodes, then, can be expected to undergo changes in time under ion bombardment in the process of building up, or operating, a discharge. These can raise or lower the work function and thus alter the γ values by factors of powers of ten. The time rate of change will depend on previous condition, gas present, nature of the ions used, and ion current density, as well as X/p. Where a reactive gas like O_2 is present, ion bombardment may clean up the cathode while a competing chemical reaction to reform a surface layer by incident O atoms could act to restore it.[12] The value of γ and changes therein might thus depend very much on gas pressure and ion current density as well as other variables mentioned. Starting from a low order discharge the positive ions can cause, at a certain current density, a rather abrupt change in the surface condition of the cathode. It is important to stress the existence of this phenomenon as it may abruptly alter the order of magnitude of γ. Such a change in γ will precipitate an abrupt change in current sometimes of uncontrolled and catastrophic dimensions.[12] Thus, under many conditions discharges dependent on cathode processes may not be reproducible, controllable, or stable, and being unstable they may lead to current-potential relations *showing a marked overshoot in potential*, or what are termed hysteresis effects. Where such effects are observed, then discharges dependent on cathode action, i.e. on γ, must be expected. The higher X/p, the more likely such cathode instability and behaviour may become. In some cases continued bombardment may deactivate a surface reducing γ.[21]

2. SECONDARY PROCESSES IN THE GAS

Returning now to the gas-conditioned phenomena, these may, for most discharges so far observed, at once be limited to only two mechanisms since ionization of the gas by *positive ion impact* is unlikely.[22] These are: (i) ionization of the gas by *avalanche-produced metastable atoms*, and (ii) the *photoelectric* ionization of the gas, by *avalanche-produced photons*, which are created directly by electron impact, or indirectly in consequence of such action.

Metastable action in the gas. If the metastable atoms of one gas have an energy such that they can ionize the atoms or molecules of a second gas present in a mixture, the effect on secondary processes can be described in one of two ways. If the most of the metastable atoms ionize the gas near the anode where most of them are formed in a uniform field (large interaction cross-section and enough molecules), then the net effect is the same as if the new electrons had been created by electron impact along with the others of the avalanche. This leads to an effective increase in the first coefficient and can be detected as such. This action was first noted by F. M. Penning[23] in neon, admixed with small quantities of argon. It will be termed hereafter the *Penning effect*. Where the metastables diffuse a long way before creating the ions, so that they are effective near the cathode, there is created a time lag in ion formation. The end result is essentially an effective increase in γ, with some smearing of time resolution in pulsed discharge analysis for ion-producing flashes of short duration.[2, 4]

The Penning effect with some diffusion of metastables before ionizing is strikingly shown with coaxial cylinders.[24] With fine inner anode wire diffusion largely takes ion-forming metastables from the anode where they are formed so that secondary electrons are created outside the ionizing zone. All of these produce avalanches as if from the cathode (simulated γ), and sparking potential is much lower. With fine inner cathode wire metastables are created away from the cathode and largely diffuse to the anode region liberating electrons which add to the current (increased α), while only a few diffuse to the cathode and give a γ_m and avalanches that count. Sparking potential here is little changed.

Photoelectric ionization in the gas. The photoelectric ionization of gases by photons created in an electron avalanche in a gas was first noted simultaneously and independently by A. M. Cravath,[25] using a corona discharge in air and by G. Dechêne,[25] using a spark discharge in air and other gases. At various times such photoelectric ionization in gases has been reported in Geiger-counter studies by E. Greiner[25] and others[26] and in cloud track photographs of H. Raether[26] and his students. It cannot be disputed that wherever there is a mixture of two gaseous species, such that one species has an ionization potential higher than the other, photons of the gas of higher ionization potential can and will ionize the other species. When gases like air, inert gasorganic vapour-filled Geiger-counter mixtures, or the hydrogen-water-alcohol mixtures of cloud chambers, are used, photoelectric ionization in the gas can be expected and is surprisingly large. When what appear to be essentially pure gases composed of homogeneous molecules, or atoms, such as the molecular gases, hydrogen, nitrogen and oxygen, or any molecular species, *remain unaltered* during ionization and excitation in the avalanche formation, then there could hardly be much photoelectric ionization. The same applies to atoms like the inert gases and mercury or similar vapours. However, as avalanches build up and as *low-level* forerunners of breakdown, namely the pre-discharge currents, corona currents, etc., build up, actions producing *essentially new species of atoms or molecules occur*. First, all of the molecules or atoms mentioned are excited by electron impacts. Most of these radiate within 10^{-9} to 10^{-7} sec. of excitation The chance of these being photoionized by a second photon of appropriate energy is relatively small. However, under appropriate conditions the early studies of Webb and Messenger, and Zemansky[16] have shown that the escape of the photon—and thus the loss of the excited states from the gas—is delayed by *entrapment of resonance radiation*. Recent accurate studies of T. Holstein and of A. O. McCoubrey have shown that the entrapped radiation may endure for 10^{-5} to 10^{-4} sec.[17] Such conditions lead to accumulations of quite a concentration of photoionizable species in the appropriate gases *if there is any appreciable current density* set up by pre-threshold discharge. Again, where metastable

atoms or molecules are formed and are not destroyed by collisions, these form very readily photoionizable reservoirs as they build up in concentration. Very recently, in the argon-mercury mixtures used in fluorescent tubes, Kenty[27] and his associates have proven the existence of unexpectedly high concentration of the $^3P_0$ and $^3P_2$ states of mercury. The molecular gases, hydrogen, nitrogen and oxygen, obviously can undergo dissociation and in the case of O and H there can be formed O_3 and H_3.

Finally, when direct photoelectric ionization studies were made of vapours of mercury, sodium, potassium, caesium, etc., by F. L. Mohler,[28] E. O. Lawrence, and N. E. Edefsen,[28] and G. Houtermans,[28] *positive ions were observed in all cases well below the long wavelength limit for photoelectric ionization.* In some vapours, such as K, there were appreciable numbers of K_2 molecules present, say as much as 20% at the ambient temperatures. K_2 can be ionized by photons from K. In Cs various ions came from interaction of excited Cs atoms which in impact yield Cs_2^+ ions and electrons. The yields observed are sufficiently great to indicate that lifetime of the excited atoms was being prolonged by absorption of resonance radiation. Cross-sections for such action are large as evidenced by the large cross-sections for the inverse process of dissociative recombination.[29] In mercury the ionization was due to interaction of excited $^3P_1$ and metastable $^3P_0$ states. Recent studies by J. A. Hornbeck[30] indicate the production at appropriate X/p of He_2^+ and A_2^+ ions by collision of atoms with excited states within 1·5 V of the ionization potential. The cross-sections for these interactions have been measured and are remarkably large, yields of molecular ions being comparable with those of atomic ions created by direct impact.[31]

It may thus be concluded that as regards *photoelectric ionization in gases by photons produced in the gases by avalanche electrons, there is no gas which has not under proper conditions been observed to show this phenomenon.* When it comes to a question of yields, or efficiency, the following comments may be made. Depending on the gaseous species in any mixed or soiled gases, the effect should readily be observed and strong. Certain admixtures obviously are more effective than others. The effects should in such gases appear in greater or less measure at all current densities and below thresholds for self-sustaining discharges. In what are initially simple, or essentially uncontaminated homogeneous gases, *such ionization will be relatively rare in avalanches below thresholds of self-sustaining discharges. Above such thresholds*, depending on pressure, geometry, current density, and the nature of the gases, what are essentially two-gas systems capable of photoelectric ionization appear in increasing measure as current densities increase. Thus, in the limit of currents below sparkover, in positive corona discharges, enough photoelectric ionization is present to lead to streamer breakdown. How high the current densities must be to achieve this depends on the individual circumstances. Apparently it can occur in hydrogen at an anode wire when current densities of the order of A/cm² occur. Regarded from the viewpoint of regenerative avalanche production at cathodes in uniform fields, photoelectric ionization in the gas is largely ineffective as a secondary mechanism.[32] If the free paths for photoelectric ionization and electron ionization $1/\mu$ and $1/\alpha$ are commensurate the net result is an effective increase in the first coefficient α to $\alpha' = \alpha(1 + f\xi_p)$, where f_p is the fraction of photons per avalanche and ξ_p is the chance of photoelectric ionization within $1/\alpha$ of the photon origin. If $1/\mu$ is commensurate with the gap length then the photons will usually yield a cathode Y_p. Quantitative analysis of the effect of intermediate values of $1/\mu$ indicates that except for unexpectedly large values of f and cross-sections for interaction at mid-gap the influence is trivial. *Secondary action of photons in the gas must thus be looked for in conjunction with other factors that only occur at highly stressed anodes.*

3. THE ANODE BREAKDOWN

Burst pulses. From what has preceded it is clear that photoelectric ionization in a dense gas is relatively ineffective as a secondary mechanism in a uniform field gap. This action must be associated with high field gradients near the anode of the discharge gap. In consequence the character of the breakdown will depend on the field geometry, its distortion by space charges and the values of $1/\mu$ and $1/\alpha$. Consider an anode in an asymmetrical gap with at least one of its radii of curvature, a, small and placed at a potential such that there is a high field gradient near its surface. If this radius a be such that r_0 the distance from the surface at which ionization becomes negligible is comparable with a, while a and r_0 are materially greater than $1/\alpha$, but $1/\mu$ is commensurate with but greater than r_0, the following type of action will occur. Avalanches $\exp\int_0^{r_0}\alpha dr$ feed into the anode triggered by electrons produced by external sources in the gap. These yield $f\exp\int_0^{r_0}\alpha dr$ photons capable of ionizing the gas out to about $1/\mu$. An appreciable fraction $(1-g)$ of these photons is lost through random emission. Roughly a fraction $g\exp(-B\mu)$ creates electrons beyond r_0 from the surface of the anode. These electrons are drawn to the anode and create new avalanches. At the point where

$$g\exp(-B\mu).\exp\int_0^{r_0}\alpha dr = 1 \qquad (1)$$

the system goes into a self-sustaining discharge independent of externally produced electrons. Roughly $g = 0{\cdot}5$ and $B = 1{\cdot}86$ for a hemispherically capped cylindrical anode.[32] This discharge being created by photon action will be diffusive. It will *spread laterally over the surface of the anode* where fields are adequate. The discharge will be one with maximum luminosity at the anode surface.

As the various terms of equation (1) are averages each subject to statistical fluctuation, *equation* (1) *sets a threshold for a discharge*, but every avalanche sequence started will not materialize. Also at threshold all such sequences will eventually break off. The electrons enter the anode and the positive ions gradually drift away. Their space charge reduces the anode surface field. It thus aids in choking off the statistically intermittent discharge at the threshold of equation (1). Thus fields can materially be increased above threshold while intermittence of discharge persists. When the fields become so high that space charges are compensated and avalanches reach such size that fluctuations no longer terminate them the discharge is self-sustaining and continuous. The fluctuating discharges were discovered by G. W. Trichel[33] in positive point corona in air at 760 mm of mercury and called burst pulses. They were independently discovered in coaxial geometry at lower pressures to be the operating mechanism of the self-quenching Geiger counters. The potential range of intermittent discharge is the Geiger-counter regime. The theory setting the threshold for Geiger-counter pulses is in principle the same as that of equation (1).[34]

Streamers. If the photoionizing free path $1/\mu$ becomes very short, less than r_0 but still somewhat larger than $1/\alpha$, the lateral spread of the discharge over the surface becomes slow. The positive ion space charges concentrate in local areas and build up over several successive avalanches. If the geometry of the anode field is such that avalanches converge on a limited area the action is enhanced. Thus with concentration of ionization at some localized area of the anode, and with slow lateral diffusion there will be created a very high local positive ion space density and space charge field, once the avalanche electrons enter the anode. This field adds vectorially to the gap field. Along that axis at which the total field is maximum α is materially increased. For in these discharges initial fields are such that α is in a region where it increases most rapidly with increase in field. Thus $1/\alpha$ decreases and more ionizing acts per unit distance occur along the increased field axis. The increased density of photoelectric ionization $f\exp\int\alpha dr$ then showers the localized region with photons and more avalanches feed into the positive space charge. In consequence the *positive space charge channel progresses out into the gap.* It advances its intense tip field and produces new photoelectrons to start further avalanches ahead. As it advances an electron current flows up the channel. This discharge advancing into the gap away from the anode as indicated is called a *streamer.* If the current into the anode is sufficient to maintain the point potential so as to sustain the current up the channel and if the gap field ahead of the tip is adequate to supplement the space charge tip field this positive streamer advances across the gap. If it crosses the gap it shorts the gap with a channel of conducting plasma and the brilliant return stroke called an electric spark takes place. The streamers were noted by the author in corona in 1936.[35] They were observed in overvolted uniform field gaps with cloud chamber techniques by E. Flegler and H. Raether[35] in 1935 and since have been studied in some detail. They sometimes occur near threshold in the Geiger-counter, or burst pulse corona regime, as noted by A. F. Kip.[35] They are called pre-onset streamers and are usually relatively weak. The streamers invariably appear again before spark breakdown as noted by the author[35] and A. F. Kip.[35] When they occur under breakdown conditions they produce the well-known filamentary spark. In overvolted uniform field gaps they appear as mid-gap streamers as noted by Raether[35] and earlier by F. G. Dunnington.[36] In the overvolted uniform field gap the fields are such that before crossing the gap the electron cloud density ahead of the avalanche and the positive ion space charge cloud density at the cathode-directed section of the avalanche become unstable. Then by photoelectric ionization ahead the anode-directed electron streamer advances towards the anode and a cathode-directed positive streamer advances towards the cathode from somewhere in mid-gap, depending on the percentage overvoltage. As the sparking threshold for various gases is approached with decreasing overvoltage it appears that there is first created a self-sustaining Townsend discharge of low order.[37] Such discharge builds up a space charge field in the gap which eventually reaches a value producing a mid-gap streamer.[38]

A semi-empirical quantitative theory neglecting photoelectric ionization terms for streamer propagation was derived by J. M. Meek[39] for the positive streamer advance and a similar equally valid theory was independently later derived by H. Raether[39] for the negative streamer advancing toward the anode. Quantitatively Meek and Raether's theories nearly yield the observed sparking threshold for air where the Townsend pre-discharge threshold is 2% below the streamer threshold. The writer and Wijsman[40] much later derived a more complete theory including photoelectric ionization yielding the threshold for positive streamer formation. This theory would yield sparking potential values of the same order as those of Meek and Raether, but is not open to quantitative test as the variables needed are unknown. It also would set a threshold for most gases lying above the threshold of the Townsend pre-discharge. Direct study has yielded many data on streamers.[41] Roughly speaking pre-onset streamers occur when $1/\mu$ is of the order of 10^{-2} cm in air. The photoionizing range fixes the radius of the streamers, though electrostatic and magnetostrictive forces may aid to keep radii small. Observation indicates that the streamers advance into the gap at a speed of 5×10^7, or more, cm/sec.[42] They create between 5×10^9 and 10^{10} ions per cm advance.[41] The current is of the order of 0·05 A, the channel radii are about 0·01 cm, the ion density is of the order of several times 10^{13} ions/cm^3, and the current density up the streamer channel is about 200 A/cm^2. The rate of current rise is of the order of $2{\cdot}5 \times 10^6$ A/sec. This makes the streamers electrically noisy. Breakdown streamers have been studied by Meek and Saxe[43] for impulse point to plane breakdown across a 55·4 cm gap. These create 10^{12} ions per cm advance in channels roughly 0·17 cm in radius. Ion densities vary as the velocity of these streamers change. Initially they range around 10^{13} ions/cm^3. As the streamers advance across the gap the tip velocity increases from 3×10^6 cm/sec at 10 cm to 2×10^7 cm/sec at 40 cm. The ion current increases in proportion from 2 A at 10 cm to 14 A at 40 cm. Current densities vary with the speed but range in the order of 200 A/cm^2. In these streamer channels heating occurs as the currents rise, causing roughly a fourfold rise in temperature and a corresponding decrease in density. The streamer channel radius on a microsecond time scale thus expands by a factor of two as it nears the end of the 50 cm gap. These streamers as they bridge the gap are observationally followed by the brilliant return stroke, characterizing the spark, that ionizes the channel by a potential wave of velocity above 10^9 cm/sec.

4. THE ROLE OF THE Υ PROCESS IN BREAKDOWN, AND THE TOWNSEND BREAKDOWN CRITERION

It is now essential to indicate the role of the first and second coefficients in gaseous breakdown and to correlate these with processes in the gas. When the secondary Υ processes at the cathode are active, it is possible to show that in a rough general fashion the initial ionization current i_0 for simplicity assumed liberated, from the cathode, is multiplied to a value i, by the field in terms of a relation of the general form,

$$i = i_0 \exp\int\alpha dr/[1 - \Upsilon(\exp\int\alpha dr - 1)] \qquad (2)$$

which holds as long as $\Upsilon\exp\int\alpha dr < 1$. Here the general symbol Υ can stand for any one of the three cathode processes or a composite of them. The current i is called a *field intensified current.* It does not cause breakdown. It reduces to zero when i_0 the external ionization is removed. At the point where

$$\Upsilon\exp\int\alpha dr = 1 \qquad (3)$$

Equation (2) is indeterminate, but for every initial electron avalanche $\exp\int\alpha dr$ the value of Υ is such that on the average a new avalanche will start and continue a succession of avalanches, i.e. a *self-sustaining current* is established. This *current can be initiated by a single electron* and is independent

of i_0. Equation (3) thus *sets the threshold for a self-sustaining, or Townsend discharge.**

While the self-sustaining threshold is set by equation (3) and involves no i_0, there are conditions where a field intensified i depending on i_0 can create space charges modifying the field distribution in the gap, or alter Y at the cathode, so as to lower or raise the breakdown threshold. Stated another way, while thresholds occur independent of an external i_0, requiring but one electron to start an avalanche, it is possible for an i_0 properly field intensified, so to alter the gap conditions as to yield a different threshold than that with no i_0. For example, too high an i_0 from ultra-violet illumination of the cathode in point to plane geometry effectively raises the threshold for Trichel pulses.[45] In plane parallel gaps, if the α/p–X/p function is below the point of inflexion the space charges created by a field intensified i_0 current can lower the sparking threshold by space charge accumulations.[46]

It was noted that for Y processes at the cathode a general equation (3) of the form $Y \exp \int \alpha dr = 1$ set the threshold for a transition from a field-intensified current to some form of self-sustaining discharge. Such a threshold will generally be termed a *Townsend discharge*. The theory of the two anode processes involving photoelectric ionization *in the gas* leading to burst pulses over the anode, or streamers from the anode, or in mid-gap, again permits the threshold condition for the event to be written as

$$\Omega \exp \int \alpha dr = 1 \qquad (4)$$

In this case under Ω there may be gathered a number of complicated relations which lumped together yield the equivalent of a secondary action probability akin in function to Y.

It is therefore clear that the factors $\exp \int \alpha dr$ and Ω or Y, which are probabilities leading to fluctuations, quite generally fix all thresholds and that space charges will play an inhibiting or an accelerative role in all of them. Further, in all these criteria the numerically dominant term is the $\exp \int \alpha dr$, for it is an exponent. Thus small changes in $\int \alpha dr$ compensate for larger variations in Ω or Y, especially since α can vary very rapidly with α or better X/p. This renders the threshold potentials very sensitive to primary action and *not sensitive to secondary action*.

It can at once be seen that quite generally an equation of the same basic form but indicating widely different physical processes sets the threshold for practically all gaseous breakdown. What is worse the dominating term in setting the thresholds is that for the primary processes which fixes the value of the exponent and is largely dependent on gas type and field geometry and thus not basically characteristic of the mechanism. Accordingly small variations in potential, or field conditions at thresholds, often poorly defined by statistical fluctuations, can mask the values of the secondary terms Ω or Y which are characteristic of the mechanism. Thus with many varied breakdown mechanisms, masked by a generalized threshold criterion and complicated by the ultimate discharge conditions that depend on external and internal circuit constants, slight variations of which may completely alter the course of events, it is not surprising that interpretation is difficult.

5. FACTORS INFLUENCING THE END STATE AT A BREAKDOWN WHICH DETERMINE THE NATURE OF THE PHENOMENA ABOVE A THRESHOLD

In the preceding sections the basic mechanisms and the relations which fix only the threshold for gaseous breakdown are all that have been presented. The course of the breakdown and the manner in which these mechanisms are brought into play to give a specific discharge state depend on various factors not so far considered. Since the conspicuous part of a transition from a non-existent discharge, or an existent form, to some other form obviously depends on the end state these modifying agencies must be enumerated.

(i) Of prime importance is the gas, its excitation, metastable and ionizing energies and cross-sections. Further factors are the transparency of the gas to photons, its susceptibility to photoelectric ionization, its elasticity to electron impacts, its Ramsauer free paths, its attachment of electrons to form negative ions, its sensitivity to impurities, its chemical affinities to electrode materials and alteration by discharge, as well as temperature and pressure.

(ii) Also of importance are electrode materials, primarily those of the cathode, their work functions, or a secondary response, their melting- and boiling-points, their reactions with the gas, their reactions under ion bombardment, the ionizing potential of the vapour, their past history and obviously the field to gas pressure ratio, X/p at their surface.

(iii) Next in importance is the geometry of the gap and its influence on potential gradients across the gap. Uniform field gaps require high potentials for breakdown. Once breakdown begins the discharge tends to be as heavy and complete as external circuit constants permit. Once breakdown fields are reached the discharge is cataclysmic, irreversible and transitory operating on an exceedingly short time scale making sequence of events impossible of analysis. Symmetrical gaps with non-uniform fields and low field regions require high potentials for spark over and complete breakdown. However, partial breakdown will begin at a lower potential at one or both electrodes before the spark. Depending on conditions such as rate of rise of potential and duration of applied potential, breakdown will start at lower potentials under some conditions at the positive, under other conditions at the negative electrode. Frequently at lower pressures the negative electrode breaks down first. If the fields are both non-uniform and asymmetrical as with coaxial cylinders, or point to plane geometry, *a sequence of breakdown phenomena* with increasing potential may occur at the highly stressed electrode of small radius which terminate in a spark at highest potentials. These breakdowns will be termed coronas. They differ materially for positive and negative points. They permit quite a detailed study of mechanisms leading to the ultimate spark. They allow actions at the highly stressed electrode to be studied independently of secondary actions at the low field electrode.

(iv) Another important feature lies in factors governing the time variation of potential at the electrodes and its scale factor in relation to the time scales of primary and secondary processes. The rate of rise of potential depends on the current supply to the electrode, electrode capacity, and the drains of current caused by the breakdown process. It is obvious that a rapid increase in potential can lead to predominence of mechanisms with short characteristic times such that changes in this factor alter the whole course of the

* Properly speaking it is not correct to set the threshold in this fashion. In 1931 M. Steenbeck set up the condition for the temporal growth of a Townsend discharge with a Υ process.[44] This approach yields a *correct threshold condition including the characteristic time constant of the process.* Except for time constant it is not essentially different from the criterion here set. Later Bartelomeyczyk[44] derived a more complete expression, including Υ_i and Υ_p. These were partially tested by Schade[44] and nicely confirmed by H. L. von Gugelberg(1) in his dynamic studies.

discharge.[1] If at breakdown the charge available is limited the discharge will be transitory, while large charges or heavy current supply may lead to several forms of sustained discharge.

(v) The time element also involves the presence of triggering electrons in the right locations at the opportune instants which govern initiation of the processes and time lags.

(vi) Once a non-transitory breakdown is achieved there will always be some limiting form of current which depends on the gas type, electrodes, field disposition, external resistance and capacity of the external power supply. If low field regions exist in the gap these will lead to space charge accumulations. If the geometry leads to the movement of ions of one sign into the low field regions these build up a space charge. To keep the current flowing added potential is required to maintain the flow. Such conditions represent an *internal resistance* in the gap. This limits the current flow and gives the discharge a positive resistance characteristic with dV/di positive. If the low field regions are too short, or pressures are low and the carriers accumulating are mobile electrons, while positive ions are confined to high field regions of active ionization near cathodes, the discharge can well become unstable with dV/di negative. Then the discharge will be controlled only by an external resistance. Such unstable conditions are inherent in many high field cathode conditioned discharges through the disposition of positive ions, high energy ion impacts, and clean up of the cathode which in the absence of any internal resistance all act autocatalytically to augment the current flow. Where by one of many mechanisms including the streamer spark unstable cathode conditions occur without space charge resistance the currents will in time progressively increase in magnitude and density until a power arc is achieved.

6. THE END STATE BREAKDOWN TYPES

It is recognized that once threshold is reached a wide variety of breakdown forms may result. These can be classified as sparks having a short duration which can be long or short, low pressure or high pressure, impulsive or static. How intense the spark resulting, or whether the gap remains in its highly conducting state yielding an arc, depends on the external circuit. The less dramatic breakdowns can be classified as glows or coronas which can be further qualified as to sign and pressure conditions. Some of the coronas are typified as burst pulse or streamer from anodes and Trichel pulses, glow or Townsend discharges from cathodes. Closely related to the negative point coronas are the familiar Geissler or glow discharges in long tubes at low pressures, between symmetrical electrodes but with non-uniform fields. The latter discharges have high cathode potentials and positive resistance. They and negative point coronas[47] have a characteristic structure next the cathode, with Crookes dark space, negative glow, Faraday dark space and positive column resulting from space charge accumulations and potential distributions characteristic of non-uniform fields and Y mechanisms. Finally, beyond these come the highly conducting low potential fall arcs. One type of discharge previously not recognized, because of its inconspicuous character and low current, is coming into prominence. It is a self-sustaining current of the Townsend type, probably with a photoelectric Y_p at the cathode and currents ranging from 10^{-11} to 10^{-8} A. It is called a *pre-discharge current*. It serves either to build up a space charge distortion in the gap leading to a streamer spark, or to condition the cathode by clean up through positive ion bombardment until a high value of Y is reached. It precedes many corona and glow discharge breakdowns and sets the threshold for the uniform field spark breakdown.[37, 38]

8. CONSTRICTION, FLARING AND DIFFUSION OF DISCHARGES

Near the highly stressed cathodes the positive ions accumulate in excess and build up a high field, the electrons moving into the gap. Near the highly stressed anodes the electrons are withdrawn and a positive ion space charge of high density is created next the anode that drifts outward in the gap. This extends the anode potential into the gap, reduces the anode field and creates a stronger field in the gap beyond. If the discharge from electrodes of small radii be regarded, the potential at the electrodes in the adjoining gap regions where there is no discharge will have a potential fall *lying below the potential along the discharge axis at the anode*. Thus the field will urge electrons from the region of no discharge into the discharge axis. Stated otherwise the equipotential surfaces will be so distorted near the discharge as to exert a constrictive force confining ionization to the axis channel. Likewise, and in a greater measure, the undistorted potential fall at the cathode will be negative to the potential fall along the discharge axis. Again, there will be a constrictive field component acting to compress the discharge toward the axis. These constrictive forces were first pointed out by the writer for negative point[47] corona and later independently confirmed in direct potential measurements by W. Finkelnburg[47] at cathodes and anodes of arc discharges. If current densities are high and diffusive secondary actions at the electrodes are absent the forces are high and constrict the discharges. Thus, in negative point corona with the Y_i mechanism and in streamers from anodes with small $1/\mu$ there are observed constricted discharges of high current density. Where photon diffusion acts as in burst pulses there is no constriction. At low pressures in glow discharges the diffusive action in the *normal cathode fall regions* is just overcome by constrictive forces. In this case, however, care must be used in drawing conclusions because of wall charges. Where the axial discharge potential falls below the undistorted field, discharges will spread and flare normal to the axis. This accounts for the brushes in negative[47] and some positive coronas.

The constriction of the cathode spots in many discharges increases current density and limits the total current which a single cathode spot can carry. If the spot becomes overloaded other spots form as seen in negative point corona and in many low boiling-point metal vapour arcs.[49] The electrostatic field surrounding such spots cause the spots to repel each other.[47]

Further factors affecting lateral spread arise from basic processes, for as already noted the cathode Y_i mechanism confines the sequence of avalanches to a relatively narrow channel. On the other hand, the Y_p and Y_m are highly diffusive, and except for very special geometry they will even at higher pressures yield diffuse breakdown. Likewise photoelectric ionization in the gas leading to anode burst pulses is diffusive while in contrast the photoelectric ionization of short $1/\mu$ leads to the highly constricted streamer. All discharges below pressures of some 10 mm become diffuse because of electron movement.

9. CONCLUSION

From the foregoing it is clear that the mechanism of electrical breakdown of gases is intricate and complicated.

There are many secondary processes whose relative importance may well be radically changed by seemingly insignificant changes in gas, electrode, circuit or temporal arrangements. In drawing conclusions relative to mechanisms active in a given breakdown sequence it does not suffice to investigate the breakdown by a study of one or two controlled variables alone, e.g. through current potential characteristics or oscillographic study. Proper investigation must involve observations of the physical appearance of the discharge, its variation with pressure, its current-potential relations including the insignificant pre-threshold currents. It must involve a knowledge of electrode properties and gas nature and purity. Spectroscopic characteristics cannot be ignored. Finally, the nature of the transition as regards the end state of discharge must be considered in relation to external circuit constants and internal geometry and field characteristics.

No conclusion as to mechanism is really complete without a properly planned dynamic analysis of the time sequence of events in current and potential with a cathode-ray oscilloscope of high time resolution accompanied by a dynamic luminosity analysis using a photo-multiplier tube.[43, 48] The investigation of the sequence of currents must be made at different sweep rate scales and with a range of sensitivities. Using some of the newer pulsed or triggering devices such as 1/10 μsec flashes of ultra-violet light [3, 4] on the cathode, or carefully collimated single α-particle ionization,[5, 6] amazingly accurate knowledge can be gained. Care must, however, be used in interpretation of such oscillograms since with improper circuitry or circuit constants, induced currents by space charge movement may obscure other phenomena.[3, 4, 48]

REFERENCES

(1) VON GUGELBERG, H. L. *Helv. Phys. Acta*, **20**, p. 307 (1947).

(2) ENGSTROM, R. W., and HUXFORD, W. S. *Phys. Rev.*, **58**, p. 67 (1940).

(3) HORNBECK, J. A. *Phys. Rev.*, **80**, p. 297 (1950); **83**, p. 374 (1951).

(4) MOLNAR, J. P. *Phys. Rev.*, **83**, pp. 933, 940 (1951).

(5) COLLI, L., GATTI, E., and FACCHINI, U. *Phys. Rev.*, **80**, p. 92 (1950); **84**, p. 606 (1951).

(6) LAUER, E. J. *J. Appl. Phys.*, **23**, p. 300 (1952).

(7) LOEB, L. B. *Fundamental Processes of Electrical Discharge in Gases* (New York: John Wiley and Sons, 1939).

(8) Ref. (7), Chapter IX, Sec. 4, p. 377; Sec. 5, p. 382; Sec. 7, p. 392.

(9) HORNBECK, J. A. *Phys. Rev.*, **80**, p. 297, (1950); **82**, p. 458 (1951); **84**, p. 615 (1951).
BIONDI, M. A. *Phys. Rev.*, **79**, p. 733 (1950); **83**, p. 1078 (1951).
BIONDI, M. A., and HOLSTEIN, T. *Phys. Rev.*, **82**, p. 962 (1951).
JOHNSON, R. A., MCCLURE, B. T., and HOLT, R. B. *Phys. Rev.*, **80**, p. 376 (1950).
PHELPS, A. V., and BROWN, S. C. *Phys. Rev.*, **86**, p. 102 (1952).

(10) HAGSTRUM, H. D. Paper A2, *Bull. Amer. Phys. Soc.*, **26**, p. 8, Programme 310 Meeting Amer. Phys. Soc., Berkeley, California, 27 Dec., 1951.
See also HORNBECK, J. A. Paper A4, Gaseous Electronics Conference, Schenectady, New York, 4–6 Oct., 1951.

(11) LLEWELLYN-JONES, F., and DAVIES, D. E. *Proc. Phys. Soc., Lond. B*, **64**, pp. 397, 519 (1951).
KRUITHOFF, A. A. *Physica*, **7**, p. 519 (1940).

(12) MILLER, C. G., and LOEB, L. B. *J. Appl. Phys.*, **22**, p. 614 (1951).

(13) GREENE, D. *Proc. Phys. Soc., Lond.*, **63**, p. 876 (1950). Gives complete list of references on Y_1 and Y_m.

(14) Ref. 7, Chapter VII, Sec. 3, p. 310. See also footnote, p. 342.

(15) HALE, D. H. *Phys. Rev.*, **55**, p. 815 (1939); **56**, p. 1199 (1939).

(16) HAYNER, L. J. *Phys. Rev.*, **26**, p. 364 (1925).
ZEMANSKY, M. W. *Phys. Rev.*, **29**, p. 513 (1927).
KENTY, C. *Phys. Rev.*, **42**, p. 823 (1932).
WEBB, H. W., and MESSENGER, H. A. *Phys. Rev.*, **33**, p. 319 (1929).

(17) HOLSTEIN, T., ALPERT, D., and MCCOUBREY, A. O. *Phys. Rev.*, **76**, p. 1257 (1949); **85**, p. 985 (1952).
HOLSTEIN, T. *Phys. Rev.*, **72**, p. 1212 (1947); **83**, p. 1159 (1951).

(18) WEISSLER, G. L., and KOTTER, G. *Phys. Rev.*, **73**, p. 538 (1948).
OATLEY, C. W. *Proc. Phys. Soc., Lond.*, **51**, p. 318 (1939).
WEISSLER, G. L., and WILSON, T. N. *Phys. Rev.*, **76**, p. 591 (1949).
WEISSLER, G. L., and WILSON, T. N. *J. Appl. Phys.* To be published.

(19) PENNING, F. M. Paper B1. Gaseous Electronics Conference, Barbizon Plaza Hotel, New York, 19–21 Oct., 1950.

(20) CURTIS, L. F. *Phys. Rev.*, **31**, pp. 1066, 1127 (1928).

(21) BANDEL, H. W. *Phys. Rev.*, **84**, p. 96 (1951).

(22) Ref. (7), Chapter IX, Sec. 3, p. 374.
See also LOEB, L. B., VARNEY, R. N., HASELTINE, W. R. *Phil. Mag.*, **29**, p. 379 (1940).

(23) KRUITHOFF, A. A., and PENNING, F. M. *Physica*, **3**, p. 515 (1936); **4**, p. 430 (1937).

(24) Ref. (7), Chap. X, Sec. 7, p. 509.
See also PENNING, F. M. *Phil. Mag.*, **11**, p. 961 (1931).

(25) CRAVATH, A. M. *Phys. Rev.*, **47**, p. 254 (1935).
DECHÈNE, G. *J. Phys. Radium*, **7**, p. 533 (1936).
GREINER, E. *Z. Phys.*, **81**, p. 593 (1933).

(26) COSTA, H. *Z. Phys.*, **113**, p. 531 (1939); **116**, p. 508 (1940).
SCHWIECKER, W. *Z. Phys.*, **116**, p. 562 (1940).
RAETHER, H. *Z. Phys.*, **110**, p. 611 (1938).
STEVER, H. G. *Phys. Rev.*, **61**, p. 38 (1942).

(27) KENTY, C. *J. Appl. Phys.*, **21**, p. 1309 (1950).

(28) LOEB, L. B. *Atomic Structure*, Chap. XIII, Sec. 2, p. 266, contains a good summary (New York: John Wiley and Sons, 1938).
See also HUGHES, A. L., and DU BRIDGE, L. A. *Photoelectric Phenomena*, p. 249 (New York: McGraw-Hill, 1932).
HOUTERMAN, G. *Z. Phys.*, **41**, p. 619 (1927).

(29) BATES, D. R. *Phys. Rev.*, **77**, p. 718 (1950); **78**, p. 492 (1950).
JOHNSON, R. A., MCCLURE, B. T., and HOLT, R. B. *Phys. Rev.*, **80**, p. 376 (1950).
BIONDI, M. A. *Phys. Rev.*, **79**, p. 733 (1950); **83**, p. 1078 (1951).
BIONDI, M. A., and HOLSTEIN, T. *Phys. Rev.*, **82**, p. 962 (1951).
PHELPS, A. V., and BROWN, S. C. *Phys. Rev.*, **86**, p. 102 (1952).

(30) HORNBECK, J. A. *Phys. Rev.*, **80**, p. 297 (1950); **83**, p. 574 (1951); **84**, p. 615 (1951).
HORNBECK, J. A., and MOLNAR, J. P. *Phys. Rev.*, **84**, p. 621 (1951).

(31) HORNBECK, J. A. Paper A4, Gaseous Electronics Conference, Schenectady, New York, 4–6 Oct., 1951.
(32) LOEB, L. B. *Phys. Rev.*, **73**, p. 798 (1948).
(33) TRICHEL, G. W. *Phys. Rev.*, **55**, p. 382 (1939).
(34) ALDER, F., BALDINGER, E., HUBER, P., and METZGER, F. *Helv. Phys. Acta*, **20**, p. 73 (1947).
(35) LEIGH, W., and LOEB, L. B. *Phys. Rev.*, **51**, p. 149 (1937).
KIP, A. F. *Phys. Rev.*, **54**, p. 149 (1938).
LOEB, L. B., and KIP, A. F. *J. Appl. Phys.*, **10**, p. 142 (1939).
LOEB, L. B., and MEEK, J. M. *J. Appl. Phys.*, **11**, pp. 438, 447 (1940).
FLEGLER, E., and RAETHER, H. *Z. Techn. Phys.*, **16**, p. 435 (1935); *Naturwissenschaften*, **23**, p. 591 (1935); *Z. Phys.*, **99**, p. 635 (1936); **103**, p. 315 (1936); **104**, p. 219 (1936).
RAETHER, H. *Ergebnisse der Exakten Naturwissenschaften*, **XXII**, p. 73 (1949).
(36) DUNNINGTON, F. G. *Phys. Rev.*, **38**, p. 1935 (1931).
LAWRENCE, E. O., and DUNNINGTON, F. G. *Phys. Rev.*, **35**, p. 396 (1930).
(37) FISHER, L. H., and BEDERSON, B. *Phys. Rev.*, **81**, p. 109 (1951).
FISHER, L. H., and KACHIKAS, G. A. *Phys. Rev.*, **79**, p. 232 (1950).
(38) LOEB, L. B. *Phys. Rev.*, **81**, p. 287 (1951).
(39) MEEK, J. M. *Phys. Rev.*, **57**, p. 722 (1940).
RAETHER, H. *Arch. Elektrotech.*, **34**, p. 49 (1940); *Z. Phys.*, **117**, pp. 394, 524 (1941).
(40) LOEB, L. B., and WIJSMAN, R. J. *J. Appl. Phys.*, **19**, p. 797 (1948).
(41) KIP, A. F. *Phys. Rev.*, **55**, p. 549 (1939).
ENGLISH, W. N. *Phys. Rev.*, **71**, p. 638 (1947); **74**, p. 170 (1948); **77**, p. 850 (1950).
(42) RAETHER, H. *Ergebnisse der Exakten Naturwissenschaften*, **XXII**, p. 86 (1949).
(43) MEEK, J. M., and SAXE, R. F. *Nature, Lond.*, **162**, p. 263 (1948).
(44) STEENBECK, M. *Wiss. Veröff. Siemens-Werk*, **9**, p. 43 (1930).
VON ENGEL, A., and STEENBECK, M. *Elektrische Gasentladungen*, **2**, p. 178 (Berlin: J. Springer, 1934).
BARTELOMEYCZYK, W. *Z. Phys.*, **116**, p. 235 (1940).
SCHADE, R. *Z. Phys.*, **104**, p. 487 (1937).
(45) BANDEL, H. W. *Phys. Rev.*, **84**, p. 94 (1951).
(46) WHITE, H. J. *Phys. Rev.*, **48**, p. 113 (1935).
ROGOWSIKI, W., and WALRAFF, A. *Z. Phys.*, **97**, p. 758 (1935).
VARNEY, R. L., WHITE, H. J., LOEB, L. B., and POSIN, D. Q. *Phys. Rev.*, **48**, p. 818 (1935).
VON ENGEL, A., and STEENBECK, M. *Elektrische, Gasentladugen*, **2**, p. 54 (Berlin: J. Springer, 1934); *Proc. Phys. Soc., Lond.*, **52**, p. 547 (1940).
(47) LOEB, L. B. *J. Appl. Phys.*, **19**, p. 887 (1948).
FINKELNBURG, W., and SEGAL, S. M. *Phys. Rev.*, **80**, p. 258 (1950).
(48) ENGLISH, W. N. *Phys. Rev.*, **77**, p. 850 (1950).
(49) FROOME, K. D. *Proc. Phys. Soc., Lond. B*, **63**, p. 377 (1950).

ORIGINAL CONTRIBUTIONS

Effect of vertical divergence on the displacement and breadth of X-ray powder diffraction lines

By J. N. EASTABROOK, B.Sc., Grad.Inst.P., Viriamu Jones Laboratory, University College, Cardiff

[*Paper received 6 August*, 1952]

A treatment is given of the aberrations caused by the extension of the X-ray source, specimen and receiving slit normal to the plane of the camera or spectrometer. A detailed examination is made of the aberrations which occur: (*a*) when the height of the specimen is the sole cause, and (*b*) when the vertical divergence of the X-ray beam is limited by Soller slits, the displacement and profile of the line being determined in each case. It is shown that vertical mis-alinement of a spectrometer can cause an additional broadening of the lines, especially in the back-reflexion region.

Different expressions for the effect of specimen height in powder cameras have been given without proof by Bradley and Jay,[1] Lipson and Wilson,[2] and Keith.[3] Expressions for the effect of slit and specimen height in Geiger-counter spectrometers have been derived by Alexander[4, 5] and quoted uncritically by Wilson.[6] The argument used by Alexander to obtain the effect of specimen height is in error, for the diffraction haloes intercepted by the plane *GG'* [reference (4), Fig. 1] are not circles but other conic sections, usually ellipses.

The present paper treats the effect of focal, specimen and receiver height in both spectrometer and camera by an extension of the method used by Wilson.[7] The expression obtained for the effect of specimen height alone is consistent with those given by Wilson and Lipson and Wilson for the error in spacing introduced by specimen height, and agrees with that of Bradley and Jay for the limiting case of a distant source giving an almost parallel incident beam. The results of Alexander and Keith appear to be in error.

Experimental conditions are rarely, if ever, well enough defined to enable the instrumental broadening to be calculated accurately, and it is doubtful whether any valid deductions can be made about the physical state of the specimen from a comparison of observed line profiles with the calculated effects of instrumental aberrations. (Some method of comparing sharp and broadened lines is required.) In the author's opinion the main value of calculations such as those presented here is that they give an idea of the general behaviour and order of magnitude of the effects involved, and enable the best compromise to be obtained between high intensity and

high resolution and accuracy. It is, for instance, a waste of intensity to restrict an aperture beyond the point at which the contribution to line shift and breadth is less than that of each of the other causes.

CALCULATION OF THE ELEMENTARY DISPLACEMENT

In Fig. 1, AOB is the horizontal median plane of the instrument. (It is convenient and conventional to consider the goniometric plane as being horizontal, and to describe the deviation of X-rays from this plane as "vertical divergence," although many instruments are not so placed.) The source of X-rays is in the vertical line AC, and the powder

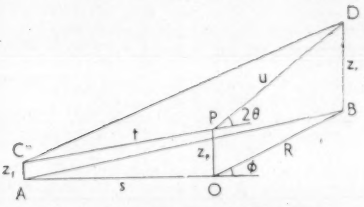

Fig. 1. Geometry of vertical divergence

specimen is in the vertical line OP, distance s from AC. The receiver, which may be a film or the scanning slit of a Geiger counter, lies on a cylinder of radius R and axis OP. X-rays from C, at a height z_f, are diffracted from P, at a height z_p, into a cone making an angle 2θ with CP. One of the rays in this cone cuts the cylinder in the point D, the perpendicular distance DB to the median plane being denoted by z_r. The angle ϕ between AO and OB is the angle at which the spectrometer must be set to receive the X-rays at D. The quantity required is the difference between $\phi/2$ and θ.

Denote the distances CP and PD by t and u. The theorem of Pythagoras and its extension give equations (1–5):

$$AB^2 = s^2 + R^2 + 2Rs\cos\phi \tag{1}$$

$$CD^2 = t^2 + u^2 + 2tu\cos 2\theta \tag{2}$$

$$t^2 = s^2 + (z_p - z_f)^2 \tag{3}$$

$$u^2 = R^2 + (z_r - z_p)^2 \tag{4}$$

$$CD^2 = AB^2 + (z_r - z_f)^2 \tag{5}$$

Subtracting equation (1) from equation (2), and using equations (3), (4) and (5) gives

$$(z_r - z_f)^2 = (z_p - z_f)^2 + (z_r - z_p)^2 + 2tu\cos 2\theta - 2Rs\cos\phi,$$

which becomes on reduction

$$tu\cos 2\theta - Rs\cos\phi = (z_r - z_p)(z_p - z_f)$$

On elimination of t and u by using equations (3) and (4) this becomes

$$Rs\cos\phi = [s^2 + (z_p - z_f)^2]^{\frac{1}{2}}[R^2 + (z_r - z_p)^2]^{\frac{1}{2}}\cos 2\theta - (z_r - z_p)(z_p - z_f) \tag{6}$$

For convenience put

$$\left.\begin{aligned}(z_p - z_f)/s &= \alpha\\ (z_r - z_p)/R &= \beta\end{aligned}\right\} \tag{7}$$

and

When the square roots of equation (6) are expanded by the binomial theorem there results as a very close approximation

$$\cos\phi = \cos 2\theta[1 + \tfrac{1}{2}(\alpha^2 + \beta^2)] - \alpha\beta \tag{8}$$

Put

$$\phi = 2(\theta - \epsilon) \tag{9}$$

where ϵ is the amount by which half the angle measured on spectrometer or film is less than the Bragg angle. Then

$$\sin\epsilon = \frac{(\alpha^2 + \beta^2)\cos 2\theta}{4\sin(2\theta - \epsilon)} - \frac{\alpha\beta}{2\sin(2\theta - \epsilon)} \tag{10}$$

If 2θ is near $0°$ or $180°$, equation (6) can give $\cos\phi$ greater than $+1$ or less than -1. Physically this means that the cone of X-rays diverging from the point P no longer intersects the cylinder at a height z_r. The Bragg angles θ_1 and θ_2 at which the measured angles become 0 and $\pi/2$ respectively are obtained by putting $\cos\phi$ equal to ± 1 in equation (8).

$$\left.\begin{aligned}\theta_1 &= \tfrac{1}{2}|\alpha - \beta|\\ \theta_2 &= \tfrac{1}{2}\pi - \tfrac{1}{2}|\alpha + \beta|\end{aligned}\right\} \tag{11}$$

At angles sufficiently remote from θ_1 and θ_2, ϵ is small and equation (10) reduces to

$$\epsilon = \tfrac{1}{4}(\alpha^2 + \beta^2)\cot 2\theta - \tfrac{1}{2}\alpha\beta\,\mathrm{cosec}\,2\theta \tag{12}$$

This is a very good approximation for practical values of α and β, and for all but the highest and lowest values of θ.

LIMITING VALUES OF ϵ

Where the focus, specimen and receiver are spread out over vertical lines, z_f, z_p and z_r take a range of values and the powder line is spread over an angular range which can be found by putting the appropriate limiting values of α and β in equation (12). It may sometimes be useful to find this range even if the distribution of intensity within it is not determined. As an example, compare the case where R and s are equal, a point specimen is at 0 and the focus and receiver extend from $-d$ to $+d$, with the case where the focus extends from 0 to $-2d$ and the receiver from 0 to $+2d$. The first case represents a well-adjusted instrument, and the second case represents the sort of mis-adjustment which can occur when the vertical alinement is done by using the direct beam. Equation (12) shows that in the first case ϵ extends from

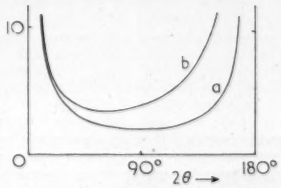

Fig. 2. Overall line breadth in minutes against 2θ. (*a*) Correct alinement, (*b*) incorrect alinement

$-d^2\tan\theta/2R^2$ to $d^2\cot\theta/2R^2$, whereas in the second case it extends from $-2d^2\tan\theta/R^2$ to $d^2\cot 2\theta/R^2$. Fig. 2 shows the corresponding variation of overall line breadth with angle when d is 0·25 cm and R is 15 cm.

LINE PROFILES

It is clear from equation (12) that the effects of focus, specimen and receiver height do not obey the "principle of linear superposition" and hence cannot be dealt with separately and then combined with each other by the convolution ("folding") method.[5,8] For this reason a general treatment of the effect of vertical divergence on line profile is difficult and will not be given; further discussion is confined to two cases which are thought to have practical significance.

EFFECT OF SPECIMEN HEIGHT ALONE

If, as in many arrangements of powder camera, the height of the focus is small compared with the illuminated length of the specimen, and if the film is examined along the median line, z_f and z_r are small and

$$\epsilon = z_p^2\left[\frac{\cot 2\theta}{4}\left(\frac{1}{R^2}+\frac{1}{s^2}\right)+\frac{\operatorname{cosec} 2\theta}{2Rs}\right]$$

If the specimen extends from $-p$ to $+p$ the line is spread over a range of ϵ from 0 to

$$\epsilon_{max} = p^2\left[\frac{\cot 2\theta}{4}\left(\frac{1}{R^2}+\frac{1}{s^2}\right)+\frac{\operatorname{cosec} 2\theta}{2Rs}\right] \tag{13}$$

The centroid of the line is displaced towards lower angles by the average value of ϵ:

$$\langle\epsilon\rangle = \frac{1}{p}\int_0^p \epsilon dz_p = \frac{\epsilon_{max}}{3} \tag{14}$$

The part of the specimen between z_p and $z_p + dz_p$ diffracts an amount of X-rays proportional to dz_p into the range between ϵ and $\epsilon + d\epsilon$. The line profile is therefore

$$I(\epsilon) = \frac{dz_p}{d\epsilon} = \epsilon^{-\frac{1}{2}}\left[\cot 2\theta\left(\frac{1}{R^2}+\frac{1}{s^2}\right)+2\frac{\operatorname{cosec} 2\theta}{Rs}\right]^{-\frac{1}{2}} \tag{15}$$

For a Geiger-counter spectrometer and for some powder cameras s and R are equal and equations (13) and (15) reduce to

$$\epsilon_{max} = p^2\cot\theta/2R^2 \tag{13a}$$

$$I(\epsilon) = (2\epsilon\cot\theta)^{-\frac{1}{2}} \tag{15a}$$

The shape of the line is shown in Fig. 3.

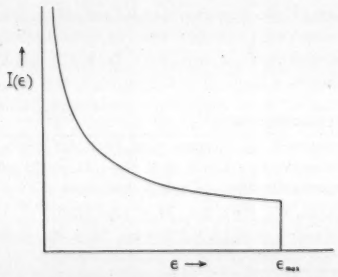

Fig. 3. Line profile for specimen-height broadening

Equation (13*a*) can also be derived directly by a consideration of the distance of the ends of the specimen from the parafocusing surface described by Brentano.[9]

SPECTROMETER WITH SOLLER SLITS

In one design of spectrometer[10] the focal line, specimen and scanning slit are all about a centimetre high and the vertical divergence is limited by louvres of the type described by Soller*[11] placed before and behind the specimen. This arrangement, which has considerable advantages, limits both α and β to the range $\pm\delta$, where δ is the distance between adjacent foils divided by their length. The extreme values of ϵ are thus

$$\left.\begin{aligned}\epsilon_{max} &= \tfrac{1}{4}\delta^2(\cot 2\theta + \operatorname{cosec} 2\theta) = +\tfrac{1}{4}\delta^2\cot\theta\\ \text{and}\quad \epsilon_{min} &= \tfrac{1}{4}\delta^2(\cot 2\theta - \operatorname{cosec} 2\theta) = -\tfrac{1}{4}\delta^2\tan\theta\end{aligned}\right\} \tag{16}$$

The range between these extremes is $\delta^2\operatorname{cosec} 2\theta$.

The following derivation of the line profile is not exact, because it does not consider end effects resulting from the finite height of focus, specimen and receiver slit, nor the detailed effect of the Soller slits themselves, but the error will normally be unimportant.

Of the X-rays leaving the focus at an angle between α and $\alpha + d\alpha$ an amount proportional to $(1 - |\alpha|/\delta)d\alpha$ passes through the first set of Soller slits. The fraction of this which, after diffraction at the specimen, passes through the second set of Soller slits at an angle between β and $\beta + d\beta$, is approximately proportional to $(1 - |\beta|/\delta)d\beta$. The intensity between ϵ and $\epsilon + d\epsilon$ is thus given by

$$I(\epsilon)d\epsilon = Kd\epsilon\int\left(\frac{\delta-|\alpha|}{\delta}\right)\left(\frac{\delta-|\beta|}{\delta}\right)\frac{d\beta}{d\epsilon}d\alpha \tag{17}$$

From equation (12),

$$\beta = [\alpha \pm \sin 2\theta(\alpha^2 + 4\epsilon\cot 2\theta)^{\frac{1}{2}}]/\cos 2\theta \tag{18}$$

$$(d\beta)/(d\epsilon) = \pm 2/[(\alpha^2 + 4\epsilon\cot 2\theta)^{\frac{1}{2}}] \tag{19}$$

The line profile is, from equations (17), (18), and (19),

$$I(\epsilon) = \frac{2K}{\delta^2}\int\frac{(\delta-|\alpha|)[\delta-|\alpha\sec 2\theta+\tan 2\theta(\alpha^2+4\epsilon\cot 2\theta)^{\frac{1}{2}}|]d\alpha}{(\alpha^2+4\epsilon\cot 2\theta)^{\frac{1}{2}}} + \frac{2K}{\delta^2}\int\frac{(\delta-|\alpha|)[\delta-|\alpha\sec 2\theta-\tan 2\theta(\alpha^2+4\epsilon\cot 2\theta)^{\frac{1}{2}}|]d\alpha}{(\alpha^2+4\epsilon\cot 2\theta)^{\frac{1}{2}}} \tag{20}$$

The integrals are to be taken over all values of α for which the factors of the numerator are positive and the denominator is real. The two integrals are equal, since one can be obtained from the other by altering the sign of α.

With $$a = \alpha/\delta,\ e = \epsilon/\delta^2 \tag{21}$$

equation (20) becomes

$$I(\epsilon) = 4K\int\frac{(1-|a|)[1-|a\sec 2\theta+\tan 2\theta(a^2+4e\cot 2\theta)^{\frac{1}{2}}|]d\alpha}{(a^2+4e\cot 2\theta)^{\frac{1}{2}}} \tag{22}$$

The lower limit is -1 and the upper limit, which is the value

* Soller's original slits were used to limit the *horizontal* divergence.

of a which makes the second factor of the integrand zero, depends on e and θ. Where $e \cot 2\theta$ is positive it is

$$\sec 2\theta - \tan 2\theta(1 + 4e \cot 2\theta)^{\frac{1}{2}}$$

and where $e \cot 2\theta$ is negative it is

$$-\sec 2\theta + \tan 2\theta(1 + 4e \cot 2\theta)^{\frac{1}{2}}$$

The solution has three ranges.

(i) For values of e from 0 to $\frac{1}{4}\cot 2\theta$:

$$\frac{I(e)}{4K} = (1 - 2|e|\operatorname{cosec} 2\theta)\ln\left|\frac{(\sec 2\theta - \tan 2\theta)[1 + (1 + 4e\cot 2\theta)^{\frac{1}{2}}]}{1 - (1 + 4e\cot 2\theta)^{\frac{1}{2}}}\right| - 4|e|\operatorname{cosec} 2\theta \ln|\sec 2\theta - \tan 2\theta| + |\tan 2\theta| - 6|e| + 8(e\cot 2\theta)^{\frac{1}{2}} - (2 + |\sec 2\theta|)(1 + 4e\cot 2\theta)^{\frac{1}{2}} \quad (23)$$

(ii) For e between $\frac{1}{4}\cot\theta$ and the end of range (i):

$$\frac{I(e)}{4K} = (1 + 2e\operatorname{cosec} 2\theta)\ln\left|\frac{(\sec 2\theta - \tan 2\theta)[1 + (1 + 4e\cot 2\theta)^{\frac{1}{2}}]}{1 - (1 + 4e\cot 2\theta)^{\frac{1}{2}}}\right| - \tan 2\theta + 2e - (2 - \sec 2\theta)(1 + 4e\cot 2\theta)^{\frac{1}{2}} \quad (24)$$

(iii) For e between $-\frac{1}{4}\tan\theta$ and the end of range (i):

$$\frac{I(e)}{4K} = (1 - 2e\operatorname{cosec} 2\theta)\ln\left|\frac{(\sec 2\theta - \tan 2\theta)[1 + (1 + 4e\cot 2\theta)^{\frac{1}{2}}]}{1 - (1 + 4e\cot 2\theta)^{\frac{1}{2}}}\right| + \tan 2\theta - 2e - (2 + \sec 2\theta)(1 + 4e\cot 2\theta)^{\frac{1}{2}} \quad (25)$$

Line profiles at three different angles are shown in Fig. 4. The profile of a line for which 2θ is $90° + A$ is the mirror image of that of a line at $90° - A$.

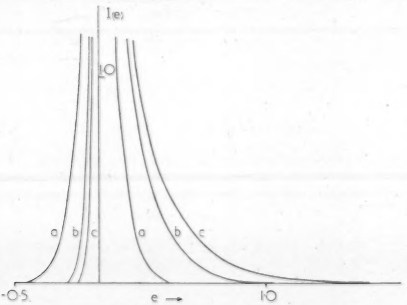

Fig. 4. Line profiles obtained with Soller slits: (*a*) $2\theta = 90°$, (*b*) $2\theta = 45°$, (*c*) $2\theta = 30°$

The displacement of the centroid of the line towards lower angles is

$$\langle e\rangle = \int eI(e)de / \int I(e)de = (\cot 2\theta)/12 \quad (26)$$

The integral breadth and half-height breadth are both zero. A suitable measure of the width of the line is the second moment $\langle e^2\rangle$. It is found that

$$\langle e^2\rangle = \left(1 + \frac{27}{10}\cot^2 2\theta\right)/144 \quad (27)$$

The reduced second moment, or variance, which is of value in combining the broadening from several sources,[8] is

$$\langle (e - \langle e\rangle)^2\rangle = \langle e^2\rangle - \langle e\rangle^2 = \left(1 + \frac{17}{10}\cot^2 2\theta\right)/144 \quad (28)$$

Fig. 5 shows line displacement and breadth as a function of angle.

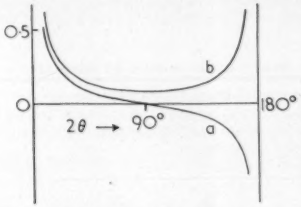

Fig. 5. (*a*) Displacement of mean position of line towards lower angles $\langle e\rangle$. (*b*) Root-mean-square line breadth $\langle (e - \langle e\rangle)^2\rangle^{\frac{1}{2}}$.

In an instrument constructed by the author, which is modelled on that described by Parrish,[10] the Soller slits have an aperture of 2°, so that δ is 1°. When 2θ is 20° the centroid of the line is shifted toward lower angles by 0·24′, and the root-mean-square line breadth $\langle (\epsilon - \langle\epsilon\rangle)^2\rangle^{\frac{1}{2}}$ is 0·33′. This is comparable with the broadening caused by slit width, focal width, or horizontal divergence.[12] When 2θ is 45° the line shift is only 0·09′ and the breadth is only 0·14′. It appears that in the range of 2θ between 40° and 140° Soller slits of wider aperture would provide an increase in intensity with very little increase in line width.

ACKNOWLEDGEMENTS

I am indebted to Dr. A. J. C. Wilson for his direction, and to the British Iron and Steel Research Association for financial assistance.

REFERENCES

(1) Bradley, A. J., and Jay, A. H. *Proc. Phys. Soc., Lond.*, **44**, p. 563 (1932).
(2) Lipson, H., and Wilson, A. J. C. *J. Sci. Instrum.*, **18**, p. 144 (1941).
(3) Keith, H. D. *Proc. Phys. Soc. B, Lond.*, **63**, p. 208 (1950).
(4) Alexander, L. *J. Appl. Phys.*, **19**, p. 1068 (1948).
(5) Alexander, L. *J. Appl. Phys.*, **21**, p. 126 (1950).
(6) Wilson, A. J. C. *Brit. J. Appl. Phys.*, **1**, p. 165 (1950).
(7) Wilson, A. J. C. *Ph.D. Dissertation, Cambridge University* (1941).
(8) Spencer, R. C. *J. Appl. Phys.*, **20**, p. 413 (1949).
(9) Brentano, J. C. M. *J. Appl. Phys.*, **17**, p. 420 (1946).
(10) Parrish, W. *Science*, **110**, p. 368 (1949).
(11) Soller, W. *Phys. Rev.*, **24**, p. 158 (1924).
(12) Wilson, A. J. C. *J. Sci. Instrum.*, **27**, p. 321 (1950).

Some problems in the analysis of steels by X-ray fluorescence

By E. Gillam, B.Sc., M.Sc., and H. T. Heal, B.Sc., A.Inst.P., British Iron and Steel Research Association, Battersea, London

[*Paper first received* 16 *May*, 1952, *and in final form* 16 *July*, 1952]

The measurement of the proportion of elements of atomic numbers higher than 20 in steels by X-ray fluorescence using a Geiger-counter spectrometer has been investigated, primarily with a view to determining the suitability of the method as a rapid means of analysis during the steel-making process, particularly for high alloy steels. A monitoring system to compensate for fluctuations in X-ray tube output is described and shown to increase the accuracy, though it gives higher variances than theoretical ones obtained by assuming a Poissonian distribution of counting events, and shows "drift" over long periods. From measurements on some iron/chromium/nickel steels it appears that unless a very powerful X-ray tube is used the method gives quick results of high accuracy only when more than about 10% of the alloying element is present. It is also shown that in some cases standard diagrams would have to be drawn up to allow for "mutual fluorescence." Certain possible improvements are noted. An Appendix gives the theory of this X-ray fluorescence analysis.

INTRODUCTION

The use of fluorescent X-rays for non-destructive quantitative analysis, which was first investigated by Von Hevesy in 1929, has recently been taken up with renewed interest because of the improvements made since that time in the efficiency of X-ray tubes and the means of measuring the intensities of weak radiations.

The method consists of placing the specimen in a strong X-ray beam chosen so that each element in the specimen is excited and emits its own characteristic radiation. The resultant radiation is analysed by means of an X-ray spectrometer. Photographic methods of intensity measurement have been described by Kochanovska[1] and von Hamos,[1] but they appear to be slower and more troublesome than the method adopted by Friedman and Birks[2] using a Geiger-counter spectrometer. This apparatus has also been discussed in papers by Abbott[3] and Cordovi.[4] Recent applications of the method for metals,[5] lead and bromine in aviation fuel,[6] and for detecting the presence of uranium in aqueous solution[7] have also been described.

Obvious advantages are that the method is non-destructive and that little preparation of the specimen is required, it being necessary only to grind a flat surface about an inch square. It is immaterial in what form the elements are combined, and as a comparatively large area of the specimen is used the effect of any inhomogeneity of the sample is reduced. Friedman and Birks have pointed out that the method is best suited for the analysis of elements with atomic numbers between 20 and 51 using the Kα characteristic rays and that elements of atomic numbers higher than 51 can be dealt with using the weaker L lines. For elements of atomic number less than 20, however, the fluorescent radiation is strongly absorbed by air, and analysis in this region would necessitate evacuation of the apparatus. Since these elements include sulphur, phosphorus, silicon, aluminium, carbon and magnesium, it is apparent that the application of the method to steelmaking practice is very limited.

APPARATUS

This is similar to that of Friedman and Birks with the addition of a monitoring system to correct for fluctuations in the output of the X-ray tube. In Fig. 1 the specimen is shown near to one window of an X-ray tube with its flat face at 45° to the emergent beam. The fluorescent rays are collimated by a bundle of brass tubes and pass to the Geiger counter spectrometer for analysis. Fluorite, calcite, rocksalt and quartz crystals were tried on the spectrometer and it was found that the 110 face of fluorite gave the most suitable dispersion and reflexion coefficient over the required range of wavelengths. The collimator consists of a bundle of brass tubes 4 in long, 1/16 in diameter and 0·002 in wall thickness mounted in a brass case of rectangular cross section 1 × ¼ in.

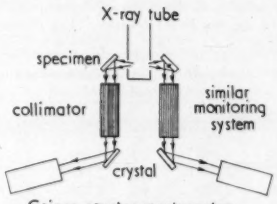

Fig. 1. Diagram of apparatus for analysis of steels by X-ray fluorescence

The Geiger counter is filled with argon and alcohol and has an aluminium window 0·001 in thick. This counter has an efficiency of 42% for FeKα and NiKα radiation, and 33% for CrKα rays. A similar system (Fig. 1) receives radiation from the opposite window of the X-ray tube. This serves as a monitoring device and automatically corrects for any fluctuations in tube output (though with limitations described

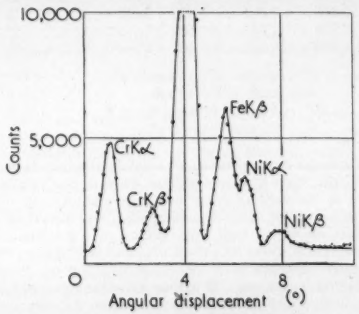

Fig. 2. Typical trace from recorder

later), the number of photons detected by the analysing counter being taken, not over a fixed time interval, but over the time taken for the monitoring counter to detect a fixed number of photons, 5 000 in the work here described. An automatic recorder[8] was used to plot the spectrum of the fluorescent radiation, counts being recorded to the last 100 at intervals of Bragg angle of 0·1°. With this apparatus, the half width of a line was found to be 0·8°, and the FeKα and CrKα lines were completely resolved by the fluorite crystal. The background count due to cosmic rays and stray scattered radiation was reduced to 300/min for a count of 6 000/min, which was the number obtained at the peak of the Cr line with an alloy steel containing 18% Cr, running the X-ray tube at 50 kV and 10 mA. Fig. 2 shows a typical trace from the recorder.

EXPERIMENTAL RESULTS

Single γ-ray source. To check the accuracy of the recording system the analysing counter was first irradiated by a γ-ray source, and the number of counts recorded in a fixed time interval of 78 sec was measured, a time switch replacing the monitoring system for this purpose. Seven sets of readings at different mean counting rates were taken, each set consisting of about twenty determinations, and the variances of the sets were calculated. The results are shown in Table 1(*a*).

Table 1. *Statistical data for unmonitored and monitored systems*

(*a*) *γ-rays*

K	$\bar{n}$	S^2
25	5 100	8 330
27	5 400	5 000
21	5 460	4 500
23	6 350	8 200
24	7 760	11 700
17	7 810	11 300
30	8 550	8 600

(*b*) *X-rays*

K	$\bar{n}$	S^2	t^2
63	3 709	4 721	6 340
62	3 697	7 448	6 300
62	3 726	9 077	6 380
63	3 760	7 900	6 450
64	3 740	8 100	6 420
67	6 397	18 180	14 600
70	6 460	17 760	14 800
69	6 472	16 472	14 800
70	6 496	11 884	14 950
79	6 431	12 930	14 720
72	6 480	18 530	14 900
76	6 337	17 990	14 400
60	9 017	36 859	25 300
60	9 042	23 833	25 400
60	9 000	22 203	25 200
60	9 010	39 729	25 200
60	9 015	27 398	25 200
60	8 958	32 519	25 200

(*c*) *γ-rays monitored*

K	$\bar{n}$	S^2
18	6 450	16 100
13	2 850	7 600
18	4 830	8 200
35	9 160	26 300

where K = number of readings in set
$\bar{n}$ = mean of K readings
S^2 = observed variance about $\bar{n}$
t^2 = theoretical variance

If the events detected have a Poisson distribution, as might be thought, then it is known that there is one chance in twenty of the variance lying outside $\bar{n} \pm 2(2/K)^{\frac{1}{2}} . \bar{n}$. This does in fact occur with the first reading, and indeed all the variances are rather high. Application of a X-squared test to these results shows that the probability of obtaining these or greater variances is of the order of 3% if the Poisson distribution is assumed. It is thus seen that calculations of the accuracy which can be obtained based on this assumption cannot be relied upon, and recourse must be made to experiment to determine the reproducibility of results. The reason for these departures from the expected distribution, which do not appear to be adequately accounted for by the dead time losses in the counter, is not known.

Two γ-ray sources. In these experiments the monitoring system was used, both counters being subjected to γ-radiation and the number of counts detected by the analysing counter taken over the time for the monitoring counter to count 5 000 events. It can be shown that the variances would increase from $\bar{n}$ for the unmonitored system to $(\bar{n}/5\,000)(\bar{n} + 5\,000)$ in this case, assuming that the events detected by both counters have a Poisson distribution. These results are given in Table 1(*b*).

Of these eighteen sets of readings, three lie outside the one in twenty probability limit, showing again that the assumption of a Poisson distribution is not justified.

Single X-ray source. Since the use of a monitoring system increases the variance of a group of counts, if the largest likely error due to X-ray tube fluctuations is less than this additional error, then the monitoring system is superfluous. Accordingly, the results of Table 1(*a*) were repeated with an X-ray source replacing the γ-ray source, the voltage and current being maintained as steady as possible by hand. The results are shown in Table 1(*c*). The variances are of the same order as those obtained with a monitor, the use of which appears to be justified provided that a monitoring count of not less than 5 000 is used.

X-ray source with monitor. Tests were then made with the apparatus complete with monitor to analyse the fluorescent radiation from a binary alloy. A specimen containing 16·98% Cr and 82% Fe was used and rigid stops were fitted to the spectrometer so that the peak of the CrKα line and a convenient part of the FeKα line could be alternately observed. The following results were obtained:

Table 2. *Results obtained from X-ray source with monitor*

number of readings in group	*mean FeKα count*	*variance*	*mean CrKα*	*variance*	*Fe/Cr count ratio*
10	7 720	34 040	5 650	13 750	1·366
10	7 400	11 850	5 520	8 850	1·341
10	7 480	22 550	5 570	13 570	1·343
10	7 650	27 950	5 480	6 650	1·396
10	7 590	28 450	5 570	11 550	1·363
10	7 440	5 150	5 560	16 450	1·338
10	7 400	18 550	5 570	18 350	1·328
Mean of above	7 530	27 230	5 560	14 210	1·353

The theoretical variance of the FeKα count is $(7\,530 + 5\,000) . 7\,530/5\,000 = 18\,900$, and for the CrKα count is $(5\,560 + 5\,000) . 5\,560/5\,000 = 11\,720$ so that the variances obtained are considerably higher than those given by the assumption that the distribution is Poissonian. Using the observed values it is seen that the standard error of the mean of a group of ten readings is $(27\,230/10)^{\frac{1}{2}} = 52$ for the Fe counts and $(14\,210/10)^{\frac{1}{2}} = 38$ for the Cr count. This means that by taking such a group of ten counts, which operation takes about 15 min, there is only one chance in twenty that the result will be more than $(2 \times 52)/7\,530 = 1·38\%$ in error in the case of the Fe count. The corresponding figure for the Cr count is $(2 \times 38)/5\,560 = 1·37\%$. If a single count lasting only 75 sec is used these figures become 4·38% and 4·28% respectively. An attempt to increase the accuracy by increasing the counting period leads to difficulties due to the measured intensity changing with time, as is

shown in the Table 3 which gives a set of readings collected over an interval of three hours.

Table 3. *Changes of measured intensity with time*

number of readings in group	*mean FeKα count*	*variance*	*mean CrKα count*	*variance*	*Fe/Cr count ratio*
10	8 110	5 150	6 020	11 550	1·347
10	7 820	27 450	5 850	24 850	1·337
10	7 650	14 050	5 760	4 850	1·328
10	7 860	7 150	5 610	26 050	1·400
10	7 530	27 450	5 520	16 050	1·363
10	7 260	11 850	5 720	18 250	1·270

It appears that the means decrease slowly with time. An attempt was made to locate the cause of the drift by irradiating both counters with γ-rays and taking a series of several hundred readings over a period of several hours. No drift could be observed, which eliminated the possibility that the counters and scaling units varied in sensitivity over this period. Since changes in the intensity of the output of the X-ray set were compensated for by the monitoring system the only possibilities that remained were that the angular distribution of the emergent radiation changed with time, due perhaps to the focal spot "wandering" over the target or that the quality of the radiation varied, which could occur if foreign matter such as tungsten from the filament was being deposited on the target. It was in an endeavour to eliminate the latter effect that the counting and monitoring beams were made to traverse similar paths in so far as the monitoring beam was derived by fluorescence from a steel specimen and subsequent reflection from a crystal.

As the application of the method to steelmaking, in which the time permitted for analysis is a few minutes only, was the main consideration, no further refinements of the monitoring system to improve the long-term stability were attempted. It was also apparent that the method was only applicable to alloys containing 10% or more of alloying element in order that a count sufficiently large to ensure a reasonable accuracy could be obtained in the time available.

ANALYSIS OF A NUMBER OF IRON/CHROMIUM/NICKEL ALLOYS

The method appeared to be well adapted to the analysis of alloys of Fe, Cr, and Ni, in which alloys the Cr and Ni are usually present in appreciable quantities. Accordingly, a series of such alloys with various Cr and Ni contents was examined in order to see to what extent the determination of the amount of one alloying element was influenced by the presence of others. Fig. 3 shows the CrKα count plotted against Cr content for various Ni contents. It is seen that the presence of Ni does not greatly affect the Cr count. Use of the theory outlined in the Appendix shows that even complete substitution of Ni for the remaining Fe will cause only about a 10% reduction of the Cr count. This is due to the fact that Cr having the lowest atomic number is caused to fluoresce by Fe and Ni radiation alike and the Cr radiation is absorbed to roughly the same extent by Fe and Ni. Similar considerations show that the Ni count will not be greatly affected by the presence of Cr, since Ni is absorbed to about the same extent by Fe and Cr and is caused to fluoresce by neither Fe nor Cr radiation since it has the highest atomic number of the three.

Fig. 4 shows the Fe count plotted against Fe content for different Cr contents, the balance being Ni. It is seen that Cr has a marked effect on the Fe count, 18% of Cr reducing

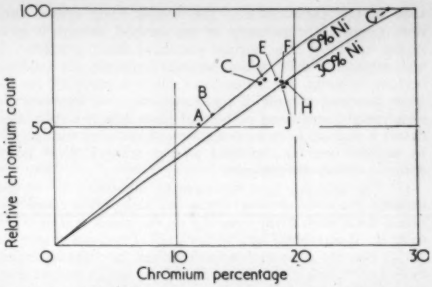

Fig. 3. Chromium count against chromium percentage for varying amounts of nickel in iron/chromium/nickel alloys

A, 12% Ni; *B*, 0·39% Ni; *C*, 0·24% Ni; *D*, 1·69% Ni; *E*, 8·92% Ni; *F*, 9·35% Ni, 1·56% Mo; *G*, 15·36% Ni; *H*, 30·82% Ni; *J*, 10·94% Ni, 3·55% Mo.

the Fe count by about 30%. The reason for this is that Fe is caused to fluoresce by Ni radiation but not by Cr, and Cr strongly absorbs Fe radiation whereas Ni does not. The substitution of Cr for Ni thus reduces the intensity of the Fe radiation produced within the specimen and enhances its absorption on the way out. The determination of Fe in such

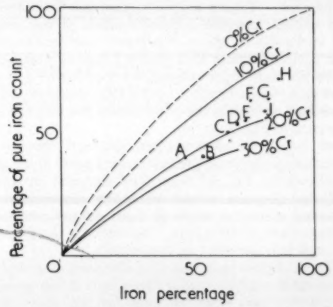

Fig. 4. Iron count against iron content for varying amounts of chromium in iron/chromium/nickel alloys

A, 19% Cr; *B*, 27½% Cr; *C*, 19% Cr; *D*, 18¾% Cr; *E*, 18½% Cr; *F*, 12% Cr; *G*, 17% Cr; *H*, 13% Cr; *J*, 17% Cr.

an alloy is not of much practical use, but it may be of importance to note that the analysis of Ni would be similarly affected by the presence of elements of higher atomic number, such as molybdenum, and the analysis of Cr would be affected in the same way by the presence of elements of lower atomic number, such as titanium.

PROBLEMS AND RECOMMENDATIONS

The work described is seen to raise a number of points which must be considered before this method can be used as a rapid steel works analysis.

(1) A monitoring system is desirable to counteract X-ray

tube output variations and the double beam system used does improve the accuracy of the method, though it gives higher variances than normal statistical theory predicts. It also exhibits a "drift" which becomes important for counting periods of hours, but the effect of which is negligible for the short counting periods of rapid analysis. An improvement which might repair one or both of these defects would be to devise a method of monitoring the counter used for analysis by another counter operating off the primary X-ray beam before it strikes the specimen.

(2) The accuracy of a measurement depends only on the number of counts obtained above the background count and hence, for a given X-ray intensity, on the length of time taken to do it. It was found for a binary alloy of iron and chromium (17%) that the counting period required for a measurement to $\pm$ 1·37% was 13 min using 50 kV and 10 mA and a cobalt target. The use of a much more powerful X-ray tube, such as a rotating anode tube operating at 100 mA, can certainly considerably decrease the time taken for a given accuracy, and it should be possible to make a measurement of the quantity of an element present to the extent of 1% with a result of 1% $\pm$ 0·02% in 5 min.

(3) Theory and experiment show that the measurement of the amount of a particular element present can be affected by the presence of other elements, so that care has to be taken in the interpretation of the results. Analysis where this effect is shown is simplest when the element contains either two or three principal elements, the amounts of any others being comparatively negligible. For such an analysis a set of carefully prepared "analysis diagrams," each like Fig. 4, could be used. Taking a specific example from the results already quoted, consider a determination of the amount of iron in an Fe–Cr–Ni alloy. The iron count for the specimen and for a piece of pure iron gives a range of possible values of the Fe, Cr and Ni percentages, marked out by a horizontal line on Fig. 4. A chromium count for the specimen, compared to a standard, then fixes the point on the line which is correct, by reference to Fig. 3.

Where only two elements are involved (binary alloy), the procedure is simpler as the first measurement alone gives the result also from Fig. 4. For four elements or more the use of the diagram would be more complicated unless the presence of one or more of them did not interfere with the measurement of the others. Reference to the theory of the method can indicate this (see Appendix).

Finally, it should be noted that standard diagrams drawn up for routine analysis would apply only if the wavelengths of the primary rays were the same for the measurement as for the data used in the standard diagrams, a point that the theory also makes clear.

CONCLUSIONS

Analysis by X-ray fluorescence has a limited application in the rapid works analysis of steels. It is most suitable for elements of atomic number higher than 20, and unless very powerful X-ray tubes are used, for amounts of these elements above 10%.

A second monitoring beam to correct for variations in X-ray tube intensity increases the accuracy, but this method of monitoring might be improved upon.

The effects of mutual absorption and fluorescence depend on the particular elements present, affecting the results in some cases but not in others. Analysis diagrams would be necessary where the mutual fluorescence effect is large, and these would be simplest to use for alloys containing two or three main elements.

Some indication of the present accuracy of this method is given by the following measurements for the chromium content in a binary alloy of iron and 17% of chromium, the X-ray tube being run at 50 kV and 10 mA.

Counting period	*Percentage error in measurement*
1 min 20 sec	$\pm$ 4·28% (i.e. Cr content 17% $\pm$ 0·75%)
13 min	$\pm$ 1·37%

The use of very powerful X-ray tubes can considerably increase the accuracy for a given counting period.

ACKNOWLEDGEMENTS

We should like to thank several of our colleagues at the British Iron and Steel Research Association for their help, and in particular Mr. D. G. Nickols of the Mathematics Section for his work on the statistics of monitored counting. We are also grateful to Mr. W. E. Bardgett of the United Steel Companies for supplying the alloy steels mentioned in the text.

REFERENCES

(1) *Transactions of the Instruments and Measurements Conference, Stockholm* (Stockholm: Royal Swedish Academy of Engineering Sciences, 1947).
(2) FRIEDMAN, H., and BIRKS, L. S. *Rev. Sci. Instrum.*, **19**, p. 323 (1948).
(3) ABBOTT, J. L. *Iron Age*, **162**, pp. 58 and 121 (1948).
(4) CORDOVI, M. A. *Steel*, **123**, p. 88 (1948).
(5) BIRKS, L. S., and BROOKS, E. J. *Analyt. Chem.*, **22**, p. 1017 (1950).
(6) BIRKS, L. S., BROOKS, E. J., FRIEDMAN, H., and ROE, R. M. *Analyt. Chem.*, **22**, p. 1258 (1950).
(7) BIRKS, L. S., and BROOKS, E. J. *Analyt. Chem.*, **23**, p. 707 (1951).
(8) HEAL, H. T. *Physics Communication No. 138* (London: British Iron and Steel Research Association, 1951).

APPENDIX

THEORY OF X-RAY FLUORESCENCE ANALYSIS

Fluorescence excited by the primary X-rays. Only the strongest (Kα) lines of those emitted are considered, and initially mutual fluorescence is neglected, the fluorescent rays being regarded as produced only by photoelectric absorption of the incident beam. For this to take place for any given element in the specimen, the wavelength of the incident beam must be lower than that of the K absorption limit of the element.

Notation: a suffix denotes *of* and a prefix denotes *with respect to*. Thus $_{\lambda}\mu_A$ is the total atomic absorption coefficient of element A with respect to radiation of wavelength λ.

Consider an element containing N_A atoms of element A

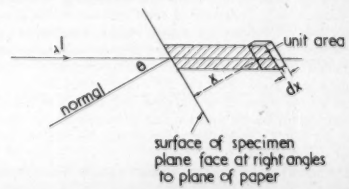

Fig. 5. Incident X-rays being absorbed by the specimen

per unit volume, N_B of element B and so on, so that the total number per unit volume is $\Sigma N_K = N$. Let monochromatic X-rays of wavelength λ and frequency ν be incident on a plane face of the specimen at an angle θ (Fig. 5) and consider an elementary volume dx within the specimen formed by unit areas parallel to the plane face at distances x, $x + dx$ normally from it. The energy absorbed in photons per second by this volume dx is

$$dI = ({}_\lambda I/h\nu) \cdot \exp(-{}_\lambda\mu Nx \sec\theta) \cdot {}_\lambda\mu N dx \qquad (1)$$

where ${}_\lambda\mu$, the total atomic absorption coefficient of the specimen for the wavelength λ is given by

$$N_\lambda\mu = \Sigma N_K \cdot {}_\lambda\mu_K \qquad (2)$$

Only photons absorbed photoelectrically give rise to fluorescent rays, and, in fact, only a proportion of these, given by the fluorescent yield factor Y which is different for each element.[1] Thus the fluorescent photons emitted per second uniformly in all directions by the volume dx is

$$dP = (Y \cdot {}_\lambda I/h\nu) \exp(-{}_\lambda\mu Nx \sec\theta) \cdot {}_\chi\tau N dx \qquad (3)$$

${}_\chi\tau$ being the photoelectric absorption coefficient.

In practice a small fraction K of these rays is collected by a collimator consisting of a bundle of small tubes pointing at the specimen at an angle ϕ, one of which is shown in Fig. 6. This fraction may be considered constant for all values of x,

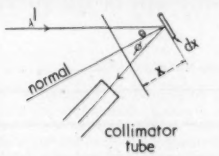

Fig. 6. Fluorescent X-rays emitted by an elementary volume and collected by a collimator tube

since, although dP is integrated from $x = 0$ to $x = \infty$, the effective values of x are very small compared to the length and breadth of the collimator. Allowing for absorption in the specimen on the way out the number of photons collected by the collimator from the volume dx is given by

$$dQ = (KY \cdot {}_\lambda I/h\nu) \exp - Nx({}_\lambda\mu \sec\theta + {}_F\mu \sec\theta) \cdot {}_\chi\tau N dx \qquad (4)$$

Where ${}_F\mu$ refers to the fluorescent wavelength. Thus, for a mixture of elements of which the fluorescent rays of element A are considered, the number of "A" photons collected in the collimator per second is

$$Q_A = \int_{x=0}^{x=\infty} dQ_A = (K \cdot Y_A \cdot {}_\lambda I \cdot N_A \cdot {}_\chi\tau_A/h\nu)(\Sigma N_K \cdot {}_\lambda\mu_K \sec\theta + \Sigma N_K \cdot {}_A\mu_K \sec\phi)^{-1} \qquad (5)$$

Comparison with experimental results for a binary alloy. Usually $\theta = \phi = 45°$, and if under these conditions two elements only, A and B, are present and no mutual fluorescence occurs

$$Q_A = (C \cdot Y_A \cdot {}_\lambda I \cdot N_A \cdot {}_\chi\tau_A/h\nu) N_A[({}_\lambda\mu_A + {}_A\mu_A) + N_B({}_\lambda\mu_B + {}_A\mu_B)]^{-1} \qquad (6)$$

C being a geometrical constant, with a corresponding expression for Q_B. Friedman and Birks[2] give experimental results for a binary alloy of iron and silver (for which mutual fluorescence is negligible) using a tungsten target at 35 kV

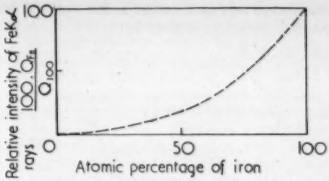

Fig. 7. Experimental curve for binary alloy of iron and silver
(after Friedman and Birks)

(Fig. 7). Available intensity distribution curves for such a target do not extend beyond a wavelength of 1 Å so that Q_A cannot be integrated over the part of the spectrum used (below 1·74 Å for the iron fluorescent rays). However, it can be shown that the theory developed above gives a qualitative account of the measurements of Friedman and Birks who plot the relative percentage intensity, i.e. 100 Q_{Fe}/Q_{100} (where Q_{Fe} is given by equation (6) and Q_{100} is the value of Q_{Fe} when there is no silver present), against the atomic percentage, 100 N_{Fe}/N, of iron.

From equation (6),

$$100Q_{Fe}/Q_{100} = [N_{Fe}({}_\lambda\mu_{Fe} + {}_{Fe}\mu_{Fe})100][N_{Fe}({}_\lambda\mu_{Fe} + {}_{Fe}\mu_{Fe}) + N_{Ag}({}_\lambda\mu_{Ag} + {}_{Fe}\mu_{Ag})]^{-1}$$
$$= 100N_{Fe}/[N_{Fe} + (N - N_{Fe})M/N]$$

where $$M = ({}_\lambda\mu_{Ag} + {}_{Fe}\mu_{Ag})$$

and $$N = ({}_\lambda\mu_{Fe} + {}_{Fe}\mu_{Fe}).$$

It can be shown that if the atomic percentage of Fe is n% then 100 Q_{Fe}/Q_{100} is also n% if $M/N = 1$; is greater than n% if $M/N < 1$ and is less than n% if $M/N > 1$, the curves being as in Fig. 8.

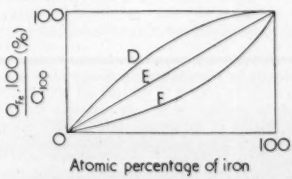

Fig. 8. Theoretical relative iron count against atomic percentage of iron for various values of M/N

$$D, \frac{M}{N} < 1;\ E, \frac{M}{N} = 1;\ F, \frac{M}{N} > 1$$

The atomic absorption coefficient of silver is greater than that of iron for any wavelength in the range 0·35 Å to 1·74 Å, so that in this case M is always greater than N. The theoretical curve for iron is therefore concave upwards as Friedman and Birks found experimentally.

Mutual fluorescence. The above theory is readily extended to calculate the additional fluorescent radiation of one element, A, resulting from the photoelectric absorption of the fluorescent rays of another element B, the latter being excited by the primary rays. The restriction still holds, of course that the wavelength of the B rays should be below the K absorption edge of the element A. The number of photons/sec

of the fluorescent rays of A excited in this way and collected as before by a collimator is given by

$$q_A = \left(\frac{K}{2}\cdot\frac{\lambda I}{h\nu}\cdot\frac{N_A N_B}{N^2}\cdot Y_A Y_B\cdot\frac{\chi\tau_{B\,.\,B}\tau_A}{\chi\mu\sec\theta + {}_A\mu\sec\phi}\right)\left[({}_A\mu\sec\phi)^{-1}\log\left(1+\frac{{}_A\mu\sec\phi}{{}_B\mu}\right) + ({}_\lambda\mu\sec\theta)^{-1}\log\left(1+\frac{\chi\mu\sec\theta}{{}_B\mu}\right)\right] \quad (7)$$

for a binary alloy of A and B. This is an additional term to be added to Q_A [equation (5)]. The fraction of fluorescence due to mutual fluorescence is

$$\frac{q_A}{Q_A} = \frac{1}{2}\frac{N_B}{N}\cdot\frac{\chi\tau_{B\,.\,B}\tau_A}{\chi\tau_A}\cdot Y_B\cdot F \quad (8)$$

Where F is the function in the second bracket of equation (7). This varies with λ; taking MoKα monochromatic rays for the incident beam, of wavelength 0·7097 Å, and an alloy of 80% of iron and 20% of nickel the value of q_A/Q_A is found to be 0·11, using figures for the coefficients from *Internationale Tabellen*[3] and the paper quoted by Backhurst. In this particular case, therefore, the effect of mutual fluorescence on the iron count is as much as 10%.

Conclusions. The theory developed above gives results of the same order as experimental ones for alloys of iron and silver, but the difficulty of integrating over all incident wavelengths prohibits a complete analysis, and makes necessary the use of empirical analysis diagrams such as those described above. Using monochromatic MoKα primary rays on an alloy of 80% of Fe and 20% of Ni, calculation shows that to neglect mutual fluorescence would involve an error of 10%. The theory can thus indicate to what extent the mutual fluorescence effect is important for a given case, and hence how to set up analysis diagrams for the analysis of a particular kind of alloy.

REFERENCES

(1) BACKHURST, I. *Phil. Mag.*, **22**, p. 737 (1936).
(2) FRIEDMAN, H., and BIRKS, L. S. *Rev. Sci. Instrum.*, **19**, p. 323 (1948).
(3) *International Critical Tables*, Vol. 6 (New York: McGraw Hill Publishing Co. Inc., 1933). *Internationale Tabellen zur Bestimmung von Kristallstrukturen*, Vol. 2, p. 579 (Ann Arbor, Michigan: J. W. Edwards, 1944).

Current densities of free-moving cathode spots on mercury

By H. v. BERTELE, Dr.techn., Dipl. Ing., A.M.I.E.E., Purley, Surrey

[*Paper first received* 18 *April*, 1952, *and in final form* 6 *August*, 1952]

Although a current density of about 4 000 A/cm² is generally considered as characteristic of cathode spots on mercury pools, much higher values have recently been measured, which may lie between 10^4 and 10^7 A/cm². When these densities are plotted against the time which has elapsed since spot initiation, a curve is obtained which shows a steady decrease of current with the life time of the spot. From this curve which holds for a single spot, and from the distribution of spot sizes which is found to exist when a number of spots are simultaneously present on the pool surface, it may be concluded that a continuous expansion of the area of each spot takes place. Hence the current density is not a significant constant of spot emission, but its value may show considerable variation. Only when the life time is large, e.g. in temperature investigations of the mercury pool of technical discharge devices, can the low classical value for the current density be used.

A knowledge of the current density of a cathode spot moving freely on a mercury pool is of interest not only for an understanding of the mechanism of spot emission, but is essential for the calculation of the temperature of both the spot and the pool surface[1] when designing technical discharge devices such as mercury arc rectifiers.

Recently, Cobine and Gallagher[2] have measured current densities in cathode spots on mercury pools of 50 000 A/cm², whilst Froome[3] has obtained values for the density as high as 5×10^6 A/cm². These values are in striking contrast to the generally accepted value of 4 000 A/cm² which was given some 30 years ago by Günther Schulze.[4] A careful examination shows that the large variation in the values for the current densities obtained by these investigations is not due to the measuring procedures which were used. It appears that the only difference in the procedures was the time, after spot initiation, at which the densities were measured. Plotting the logarithm of the above current densities against the logarithm of the corresponding time at which they were measured, the curve shown in Fig. 1 is obtained, which indicates a steady decrease of the density with the life time of the spot.

If the emission current is kept constant, the spot area will increase at the same rate as the current density decreases, and for this spot expansion a simple numerical relationship can be obtained from the curve of Fig. 1, namely

$$\log(i_2/i_1) = -0{\cdot}56\log(t_2/t_1) \quad (1)$$

or

$$(i_2/i_1) = (t_1/t_2)\,0{\cdot}56 \quad (2)$$

where i = current density in A/cm:

t = observation time in seconds counted from the instant of spot initiation. The suffixes 1 and 2 of t in equations (1) and (2) refer to the order of observation.

Assuming a circular spot area, then the emission current I is

$$I = i\,.\,r^2\pi \quad (3)$$

and the spot growth can conveniently be expressed by the rate at which the spot radius r increases. Eliminating i from equation (3) by means of equation (2) we obtain

$$(r/r_1) = (t/t_1)^{0.28} \quad (4)$$

and differentiating this with respect to t gives for the speed with which the spot radius grows

$$v = dr/dt = 0{\cdot}28\,r_1\,.\,(1/t_1)^{0.28}\,.\,(1/t)^{0.72}\ \text{cm/sec} \quad (5)$$

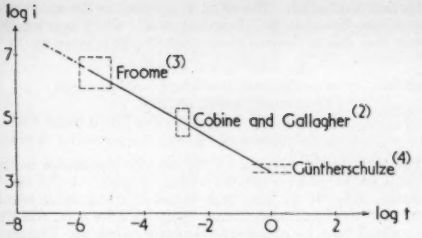

Fig. 1. Decay of current density i(A/cm²) of cathode spot with time t (sec) after spot initiation. The ranges investigated by various workers are indicated by the dotted lines.

Thus, even the latest values of Cobine and Froome cannot in general be regarded as characteristic of the cathode spot. They are approximately correct when the duration of the observation is much shorter than the spottage. In fact equation (4) can be used to explain the scatter, for example, in Froome's measurements as a result of spot expansion. Substituting his numerical data into this equation, a value for the dispersion range is obtained, which is in good agreement with the value of $\pm$ 50% quoted by Froome.

Continuous spot expansion according to equation (4) gives a current density in the spot of 4 000 A/cm² after a time of about 0·9 sec. However, in view of its empirical character, this equation cannot be expected to give any reliable information for such times, or for greater times. It is generally assumed that the spot persists in a steady state, but it is an open question how this steady state is reached, and what kind of coercive forces are active to confine the emission to a definite area of the mercury pool.

It is usual to visualize a spot in the steady state as completely free so that it can move about in a random manner, unhampered by any forces acting upon it. When forces are present, such as are caused for example by magnetic fields, vapour repercussions or spot anchoring, the behaviour of the spot and its motion will be completely different from the free spot with its random motion which is of the Brownian type.

In the course of some earlier investigations by the author and his collaborators, two peculiar features in the performance of free spots were observed which seem to throw light on the spot performance in the region where equation (4) ceases to be valid. These are the random spot extinction in a well-defined current region near the lower current limit required for the ignition of the cathode spot, and the existence of a probability distribution of the spot size for currents above the random extinction range.

RANDOM SPOT EXTINCTION AT CONSTANT LOW CATHODE CURRENTS

It is generally known that a critical lower current limit exists for mercury-pool cathodes, below which no spot can be maintained. The values quoted for this limit, for plain mercury surfaces vary between 3 and 6 A. When examining the excitation of glass or steel tank rectifiers, i.e. the circuit which ensures continuous operation of the rectifier in the event of an interruption of the main circuit, a relationship between the value of the exciter current and the corresponding life time of the spot was noticed. In order to study this more thoroughly, tests under controlled conditions were made over a period of 6 weeks on a small 10 A glass bulb of normal design. The bulb was run with its excitation only, having its current increased in small steps, and at each current level the number of reignitions of the automatic ignition device was counted. Reignition was achieved in the usual manner by dipping into the mercury an electrode which produced a spark on being withdrawn. With this arrangement it was noticed that, for currents below 3 A, only instantaneous flashes occurred each time the contact with the mercury surface was broken. For currents above 3 A cathode spots formed which, however, were of a temporary nature and eventually were extinguished.

Although the time intervals between successive reignitions appeared to be very irregular, prolonged observations with gradually increasing current gave a well-defined distribution function for the life time of the randomly extinguished spots, which is shown in Fig. 2. It can be seen from this figure

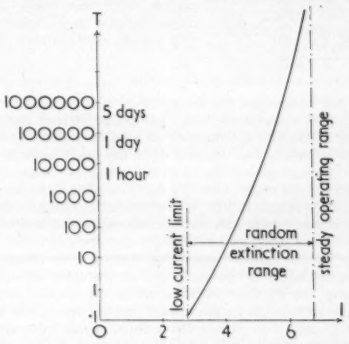

Fig. 2. Average life time T (sec) of cathode spots on a mercury pool as a function of cathode current I (A)

that for a current above 7 A, the curve rises very steeply and random spot extinction completely disappears. The room temperature during the test was kept between 15 and 18° C, and this small variation affected the vapour pressure of the mercury, which, in turn, slightly changed the current limits inversely with the pressure. It appeared, however, that this did not affect the random character of the spot extinction.

In general, in this unsteady range of operation a single cathode spot seems to provide the whole emission. However, a closer inspection showed that occasionally new spots appeared at the edge of the original one. As a rule these new spots disappeared again very quickly, but sometimes they were found to replace the original one and the random spot extinction seemed to coincide with this change of spots.

DISTRIBUTION OF SPOT SIZES IN MULTIPLE SPOT EMISSION

The experiments on cathode spots on mercury pools were continued later and the results published by E. Schmidt[5] in connexion with the newly observed similarity between the speed of spot migration and the Brownian movement. This work also revealed an unexpected distribution for the spot sizes in the current region far above the random extinction level. Above this level, emission takes place from several

or many spots simultaneously and hence the measurement of the current contribution from an individual spot is not possible. Using a high-speed cine-camera, however, the average spot current can be determined at any instant from the number of spots observed at this instant. Both the number of spots and their size vary continually and rapidly, but the variations lie between relatively narrow limits and give rise to distribution functions similar to the error function. Fig. 3

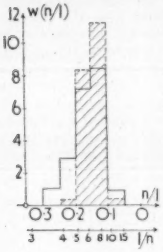

Fig. 3. Histograms of current subdivision on n separate spots for $I = 75$ A – – –, and $I = 16{,}3$ A——. Ordinates are the probabilities $w(n/I)$ of 180 subsequent observations plotted as a function of n/I, the spot number per unit current, and the lower abscissae indicate the corresponding average spot currents I/n

shows the histograms for the number of spots and the size of the spots respectively, the data being derived from 180 pictures taken with a frequency of 3 000 per second. From the histograms it can be seen that the spot currents may have any value between 3 and 15 A with a definite preference for values in the region of 6 to 7 A. From Fig. 3, in conjunction with the results of Fig. 2, two conclusions may be drawn. First, the size of the spot varies continually and second, the spots only expand, and ultimately disappear, in the same way as for the random extinction region. The scarcity of low current spots is obviously due to the instability of the spots near the low current limit, whilst the scarcity of spots with high currents seems to indicate that the ageing rate of the spot is greater than the current reinforcement from already extinguished spots.

To sum up, one may say that a freely moving individual spot never seems to attain a steady state, but instead performs a kind of "life cycle." After emerging with a very small cross-section, it grows as time proceeds until its existence comes to an end, either by its complete disappearance, or by its breaking up into new spots if the general conditions are conducive to spot propagation.

The tendency of spot expansion also throws some light on the emission mechanism itself. Whatever the nature of this mechanism, the expansion of the spot, as described above, must be due to some action of the emission zone on the adjacent neutral metal. Extrapolation of the current density values shown in Fig. 1 beyond Froome's value, towards the instant of spot ignition (i.e. $t = 0$), gives very high densities, in excess of 10^7 A/cm^2. These values are sufficiently high for field emission to become operative, so that spot initiation can be explained in this way. Later, however, the densities become too low for this type of emission and it is worth while to consider instead C. G. Smith's recent hypothesis[6] which postulates local disturbances of the electron temperatures equilibrium in the surface layer of the pool, where the spot is situated. In this region, the electron temperature is assumed to be much higher than elsewhere in the metal. The energy dissipation by heat conduction from the highly energized spot layer is counteracted by the Thomson heat. (Whenever heat and current flow coincide in a metal, they interact, according to Thomson, in such a way as to reduce the heat conduction. This effect is explained by the occurrence of a heat flow Δq, the "Thomson heat," which opposes the heat flow due to thermal conduction.[7] Δq is given by

$$\Delta q = 10^7 \times \sigma \times i \, d\theta/dz$$

where σ = Thomson coefficient (volt/grad/cm)
i = current density (A/cm^2)
θ = Electron temperature in liquid metal (°K)
$d\theta/dz$ = Gradient of electron temperature (°K/cm).

The coefficient σ depends on the electron conditions in the metal and its value for mercury is approximately $-1 \cdot 1 \times 10^{-5}$. Hence, only for the very high values of i and $d\theta/dz$ which occur in the immediate vicinity of the cathode spot, will the Thomson heat be effective.) However, since the Thomson heat at any point is dependant on the density of the current flow, it will be much smaller parallel to the pool surface than perpendicular to it, with the result that a much stronger energy dissipation will take place along this surface. This, in turn, will tend to widen the region of the disturbed metal electron equilibrium, the expansion occurring at the edge of the spot and just below the pool surface. In this expansion process the specific energy of the electrons in the spot decreases as the spot area increases and the emission will cease from those points where the local specific electron energy falls below a critical minimum value. Local differences in the energy exchange at the spot circumference are bound to occur at random, so that the direction of the spot expansion will continually change, causing a random motion of the spot.

The "life cycle" phenomenon of freely moving spots dispenses with the need for spot concentrating forces. It therefore gives experimental support to C. G. Smith's theory which was unable to satisfy the conventional picture of a steady spot, for it did not provide the coercive forces which, according to this picture, are necessary for such spots.

Technical devices, using mercury pool cathodes, operate in general with cathode currents above the random extinction range. Several cathode spots contribute to this current. Their number and size vary continually and hence, according to their age, so also does their current density. However, as the life time of a spot increases, it will remain longer in the low current density regions than in the higher ones. For example, it will be seen from Fig. 1 that a current density of 5 000 A/cm^2 corresponds to a life time of about 0·2 sec, whilst a density of 100 000 A is associated with a life time of about 0·001 sec. It is thus the low classical density values which must be used in considerations where the time matters, as, for example, in investigations concerning the spot or pool temperatures.

ACKNOWLEDGEMENT

The author wishes to acknowledge the help he received in the preparation of the manuscript from Dr. H. Tropper of the Queen Mary College, London.

REFERENCES

(1) H. v. Bertele. *Brit. J. Appl. Phys.*, **3**, p. 127 (1952).
(2) J. D. Cobine and C. J. Gallagher. *Phys. Rev.*, **74**, p. 1524 (1948).
(3) K. D. Froome. *Proc. Phys. Soc.*, **62**, p. 802 (1948); *Proc. Phys. Soc.*, **63**, p. 377 (1950).
(4) A. Günterschulze. *Z. Phys.*, **11**, 1922, p. 96.
(5) E. Schmidt. *Ann. Phys., Lpz.*, **6**, p. 246 (1949).
(6) C. G. Smith. *Phys. Rev.*, **62**, p. 48 (1942).
(7) A. Sommerfeld and N. H. Frank. *Rev. Mod. Phys.*, **3**, p. 1 (1931).

A similarity theorem in electrical contacts

By P. M. DAVIDSON, Ph.D., Department of Physics, University College of Swansea

[*Paper first received* 16 *May, and in final form* 16 *June*, 1952]

The opening of a contact, up to the melting stage, causes a progressive change in the radius l of the interface; and the opening of contacts in different circuits may conveniently be described as similar processes provided (i) at any given stage (meaning at any given value of the contact potential) the maximum temperature is the same in all the contacts, (ii) the spatial temperature distributions, when mapped on scales which make all their l's unity, give a single diagram, characteristic of the stage; (iii) the same is true of their potential distributions; and (iv) the ratio of their l's is the same at all stages. The conditions under which similarity will occur are investigated, the matter being of importance in contact theory and in the interpretation of experimental results.

INTRODUCTION

Consider two contact electrodes[1] (not necessarily of the same metal, but free from tarnish or adsorption film) pressed together, the rest of the circuit consisting of a battery of e.m.f. E, a resistance R and an inductance L, all in series. If, from time zero ($t = 0$) onwards, the electrodes are progressively separated, the radius l of the area of contact will progressively change from its initial value l_0 until, somewhere in the electrodes, melting begins; the process will not be considered beyond that stage. Suppose now a number of such systems are considered, obtained by varying, not E or the anode and cathode metals, but quantities which will be called the parameters, namely, R, L and the values of l at all positive times. These conditions will be described as similar if, and only if, at any given stage (that is at any given value of the contact potential V) the maximum temperature θ_m (not usually situated in the interface) is the same in all the contacts, and the spatial temperature distributions in the contacts, when mapped on scales which make all their l's unity, give a single diagram characteristic of the stage; and the same is true of their potential distributions; and the ratio of their l's (which will be called the scale ratio) is the same at all stages. It may be noted that in a set of systems having this similarity property the contact resistances r at a given stage will evidently be in the inverse ratio of their l's. (The ratio of the r's will thus be the same at all stages.)

A SIMILARITY THEOREM

Writing x, y, z for spatial co-ordinates in the contact, we will define new variables by

$$x = x/l_0, \text{ etc.}, \quad l = l/l_0, \quad t = t/l_0^2, \quad r = l_0 r, \quad R = l_0 R, \quad L = L/l_0 \tag{1}$$

Each system must satisfy the equation

$$E - \left(\frac{R + r}{r}\right)V = L\frac{d}{dt}\frac{V}{r} \tag{2}$$

and must also satisfy in the contact region the equation

$$s\rho(\partial\theta/\partial t) = \text{div}\,(\lambda\,\text{grad}\,\theta) + (\text{grad}\,\phi)^2/\sigma \tag{3}$$

and its boundary conditions (for which the usual assumptions that the temperature is atmospheric in remote parts of the electrodes and that the radiation losses in the contact region may be neglected are made). The differentials in the operators div and grad are with respect to x, y, z. The density, specific heat, thermal conductivity and specific resistance are ρ, s, λ, σ, all varying with temperature and differing in the two metals. ϕ is the potential (its values in parts of the electrodes well away from the contact differing by V on the two sides). ∂t means the rate of change with t in a given particle of metal. Moreover, the equation $\text{div}\,[(\text{grad}\,\phi)/\sigma] = 0$ must be satisfied in both metals, and also the equations expressing the continuity of current (both thermal and electric) at the interface between them. It may here be remarked that though for simplicity the thermoelectric, electrodynamic and electromagnetic effects in the contacts have been neglected, the similarity theorems which follow will remain valid when they are taken into account.

The mathematical solution of the differential equations (2), (3), etc., for given values of R and L and with l an arbitrary function $f(t)$ of t (having $f(0)$ unity) will evidently apply to all the physical systems obtained from it by giving different values to l_0 in the definitions (1); and it is thus evident that the systems so obtained will have similarity, as defined above. The physical relationships between the similar systems are immediately evident from definitions (1); for if it is noted that the relation $l = f(t)$ may be written $l = l_0 f(t/l_0^2)$ it can be seen that the systems are similar if, when l_0 is varied, L is varied as l_0 and R inversely as l_0, and if the relation between the l's in the various systems is of the form $l = l_0 f(t/l_0^2)$, where f may be any function having $f(0)$ unity.

[Certain conditions have been omitted which, though required for strict similarity, are of slight practical importance; such as that near the circle of contact the shapes of the electrodes shall be similar (in different systems) with scale proportional to l_0; and that, in fact, to take account of the skin effect in the external circuit, the wires and configuration of the external circuits should only differ by this geometrical factor. This last condition contains the two relationships, L varies as l_0 and R inversely as l_0, and is a more stringent form of them.]

The scale ratio of the systems may be thought of as either the ratio of the l_0's, or of the initial currents I_0, or as the inverse ratio of the R's; and the conditions required for similiarity may evidently be stated in different but equivalent ways. One of the most convenient is to say that, in the systems with different I_0's, L must be proportional to I_0 and l/I_0 must be some function of t/I_0^2; this last condition may also be expressed by saying that l_0 must be proportional to I_0, and dl^2/dt must be a function of t/I_0^2.

PRACTICAL APPLICATIONS

In practical measurements one does not specify the rate of separation of two electrodes by the variation of l with time, but by a separation velocity v, meaning the relative velocity (usually varying with time) of two points, of which one is in each electrode and neither is in the region of deformation around the contact area itself. Thus to give a direct practical significance to the conditions for similarity, stated at the end of the last section, the condition concerning l must be rewritten in terms of v. To do so it might be assumed that

the limits of elasticity are not exceeded in the contact, but the case of plastic yielding is of more interest. On the basis of the accepted formulae for plastic yielding[2] it will be assumed that in a set of similar systems

$$\left.\begin{aligned} P &= AI_0^2 \\ \text{and} \qquad dl^2/dt &= -BI_0 g(\theta_m)v \end{aligned}\right\} \qquad (4)$$

where P is the initial compressive force; A and B are constant throughout a set of similar systems and depend on the elastic and plastic properties of the metals, B being usually of the order 10^2; $g(\theta_m)$, unity at atmospheric temperature, is a function of θ_m (it could be regarded alternatively as a function of l or t) which has been inserted to allow for the thermal changes in volume and elasticity during the separation of the electrodes.

By definitions (1), $dl^2/dt = dl^2/dt$, which in a set of similar systems is a function of t only. Thus by assumption (4) I_0v must be a function of t/I_0^2. Alternatively, it may be said that I_0v must be a function of t/I_0^2. Thus by assumption (4) the conditions for similarity stated at the end of the last section may be rewritten thus: when P is varied, L and I_0 must be varied as $P^{1/2}$, and $P^{1/2}v$ must be a function of t/P. Alternatively, it may be said that when I_0 is varied, L must be varied proportionately, and P as I_0^2; and I_0v must be a function of t/I_0^2.

Important types of separation used in experimental work are those with constant acceleration and those with an "impulsive" separation intended to make v as nearly as possible constant during the separation. From the relations just given, it can be seen that in the first case similarity requires that the acceleration should be proportional to $P^{-3/2}$ and in the second case the constant velocity be proportional to $P^{-1/2}$.

APPROXIMATIONS TO SIMILARITY

The conditions required for similarity are seen to be decidedly restrictive; therefore consider to what extent they may be relaxed without serious loss of similarity. The following cases are of interest.

(*a*) Even if the current varies by a considerable percentage during the separation, the requirement imposed on L may evidently be omitted if L is small enough to be of negligible effect. This will be so if $Ldl/dt \ll \sigma_0(E/V)^2$, which by assumption (4) may be written $LBv \ll \sigma EV_0(E - V)/V^3$. In these expressions σ refers to the more resistive metal and the suffix $_0$ refers to the initial state; v, V and dl/dt have their values at the melting stage. These inequalities, and those in the following sections, may be obtained by straightforward and fairly short calculations.

(*b*) The requirement imposed on L may be omitted if the current is practically constant during the separation (that is, if it only varies by a few per cent). This will be so for all values of L if a rough estimate of V at melting shows that it is small compared with E. Even if this V is not small compared with E the current will be practically constant if L is large [say if $L \gg \sigma l_0/(dl^2/dt)$] in which σ refers to the more resistive metal and the quantities may be given mean values during the separation. By assumption (4) the relation may be written $L \gg \bar{\sigma}/B\bar{v}$). It is evident that in a set of contacts in which the various currents I are practically constant during the separation, not only the requirement imposed on L may be omitted, but also the requirement that the circuits shall be of the type considered in the Introduction, all having the same E. Provided the currents are practically constant during the separation the external e.m.f.s may be different in different members of the set; in fact the external circuits may be of quite different types in different members. Referring back to the similarity theorem, we see that similarity will occur if l_0 is proportional to I_0 and dl^2/dt a function of t/I_0^2.

(*c*) In cases where the separation velocity is sufficiently small to make the left-hand side of equation (3) a relatively small term in the hottest parts of the contact, there exists what is known as thermal equilibrium. Lander and Germer[3] have noted that in practical contacts thermal equilibrium will usually prevail when the liquid bridge has been formed, but will be conspicuously absent in the stages leading up to melting with which this paper deals. It would occur if, in those stages $(\sigma/\sigma_0)(dl^2/dt) \ll \lambda/s\rho$, in which σ and σ_0 refer to the more resistive metal and the right-hand side should be given the smallest value in the contact in those stages. From assumption (4) the relation may be written $B\sigma I_0 v \ll V_0\lambda/s\rho$. Generally speaking this condition will only be satisfied, in those stages, in purely experimental contacts which are either at rest or have a very slow mechanically controlled separation. The conditions for similarity would become very simple, but there would be little purpose in discussing them.

(*d*) Finally, consider a type of approximate similarity which will be of interest in the case of systems in which, as always, the anode and cathode metals are not varied and which satisfy the following conditions: (i) the current is practically constant during the separation, (ii) v is practically constant in time though varying from system to system, (iii) θ_m is initially only a small fraction of the melting temperature.

Make assumption (4) and, as a first simple case, take $g(\theta_m)$ as unity. Consider a set S with various I_0's and P's, and with v's proportional to $P^{-1/2}$; thus $vP^{1/2}$ has the same value, say $C^{1/2}$, in the whole set. By assumption (4) dl^2/dt has thus the same constant value $-B(C/A)^{1/2}$ in all the systems. They are not similar unless the I_0's happen to be proportional to the l_0's and thus to the $P^{1/2}$'s; but compare them with a hypothetical set S_1 with the same constant currents and with l_0's proportional to the currents (the constant of proportionality being chosen so that in two systems with the same currents the l_0 in the S_1 system is always larger than the l_0 in the S system), and with dl^2/dt equal to $-B(C/A)^{1/2}$ in the whole set. It need not be considered how the l's in the set S_1 could be given that particular time variation; but only noted that, from what was said at the end of (*b*) above, the set S_1 would have similarity. However, as regards the l's, the only difference between the two contacts in the sets S and S_1 with the same current is that the S_1 contact starts from a larger l_0 and diminishes (with constant dl^2/dt) to the l_0 of the S contact; both are then at low temperatures, and since the subsequent changes of l with time are the same in both, and since both carry the same current, it is evident that when the important high-temperature stages are reached the conditions in the two contacts will be practically the same. Thus S is, practically speaking, a similarity set, and the scale ratio is the ratio of the currents. The argument is readily extended to the case when $g(\theta_m)$ is not constant, and leads to the same result, namely, that a set with $vP^{1/2}$ constant is a similarity set and the scale ratio is the ratio of the currents. In particular, if the contacts all have the same initial compressive forces they are approximately similar if they all separate with the same constant velocity.

Similar states of transfer. In deriving the conditions for similarity it has been supposed that the anode and cathode each consist of a single metal. But now, instead, suppose that one electrode is coated with a layer of metal from the

other. If the sets of systems considered above are modified in this way, then (except for those considered in (*d*) of the last section), the corresponding modification in the conditions required for similarity is simple; it is merely to impose the extra condition that the thicknesses of the layers (in the contact regions) shall be in the scale ratio of the systems. Thus if the contacts were originally each of a single metal, and if, with prolonged use, a progressive transfer of this kind occurred, the conditions for similarity, which in their original form are applicable to the initial state, are also the conditions for similarity in what may be called corresponding states of layer formation (meaning states in which the layer thicknesses are in the scale ratio).

Influence of contact films. As previously remarked, the absence of adsorption films has been assumed. In general, they would impair the similarity properties deduced above. Suppose, for example, that the contacts are stationary or are opening very slowly so that there is practically thermal equilibrium. If there is no film, then, whatever the external circuit may be, all the contacts will, at a given V, have the same θ_m and their temperature distributions will only differ by a geometrical scale factor, proportional to the contact radius (that is, to the current through the contact). But an air film, if of the same thickness in all the contacts, will produce a modification which will be least in the largest contacts (in a sufficiently large contact the film is a negligible fraction of the total contact resistance, and its effects are thus negligible). If, as Kohler[4] has suggested by wave-mechanical arguments, the heat associated with the film resistance is actually generated in the surface of the anode electrode, so that even in the case of identical contact metals with negligible thermoelectric effects there will be temperature asymmetry (making the anode hotter than the cathode) the asymmetry will be least in the very large contacts. On the other hand, as remarked above, the temperature asymmetry due to thermoelectric effects in contacts free from film would not impair the similarity property.

ACKNOWLEDGEMENTS

This work forms part of a programme of research on the fundamental processes in electrical contacts being carried out in the Physics Department of the University College of Swansea.

REFERENCES

(1) A general discussion of the physics of separating contacts is given in *Fundamental Processes in Electrical Contact Phenomena*: Llewellyn-Jones, F., *Radio Research Special Report*, No. 24. H.M. Stationery Office. (To be published.)

(2) See, for example, HOLM, R. *Electrical Contacts.* (Uppsala) 1946; or LANDER, J. J., and GERMER, L. E. *J. Appl. Phys.*, **19**, p. 910 (1948).

(3) LANDER, J. J., and GERMER, L. E. *J. Appl. Phys.*, **19**, p. 910 (1948).

(4) See, for example, JUSTI, E. and SCHULTZ, H., *Abh. der Braun. Wiss. Gesell.*, **1**, No. 1, p. 89 (1949).

NOTES AND NEWS

Correspondence

Transit time oscillations in triodes

The recently published paper by Critchley and Gavin[1] appears to fill an important gap in the field of experimental results on oscillations maintained by the "transit time" negative conductance in triodes. It appears to the writer, however, that the mathematical discussion in the same paper is out of touch with some of the original (and most relevant) work on the subject, and the purpose of this note is to mention briefly the possible relationship between these new experimental results and those predicted by the small signal transit time theory of negative grid triodes.

With the type of circuit used in the experiments, the "double concentric line of the common-grid earthed-anode oscillator," the space-charge limited diode conductance[2,3] is not necessarily applicable, and the input conductance of the common-cathode triode circuit with the anode tied to the cathode[4] is certainly not applicable. The triode, having three accessible terminals, has three distinct pairs of terminals across each of which, under suitable conditions, a transit time negative conductance can appear. Three well defined calculable cases occur when the anode and cathode, or anode and grid, or grid and cathode are effectively short-circuited. These three cases may be realized by using lines as circuit elements in the manner shown in the figure at (*a*), (*b*) and (*c*) respectively, the short-circuits at the appropriate pairs of electrodes being obtained by half wavelength short-circuited lines.

An approximate theory of all three cases emerges on suitable application of Benham's original results.[5] These results were expressed in the form of equivalent networks (Fig. 3 of Ref. 5) with curves giving the values of the elements

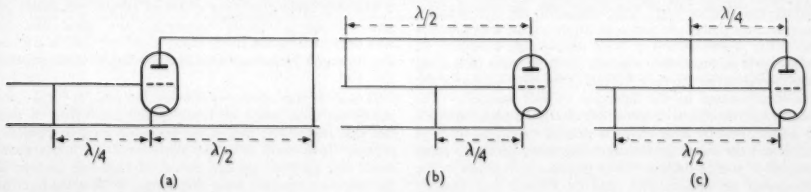

(Figs. 6 and 7 of Ref. 5), but they can readily be translated into conductance and susceptance components. Case (*a*) may also be treated on the lines of North's method.[4] The theoretical results show that, except in case (*b*), the assumption that the triode conductance functions are similar in form to the diode conductance function, is not justified. Taking the grid-anode transit to be one-third of the cathode-grid transit time, it is found that in case (*a*) the first maximum of negative conductance occurs at a cathode-grid transit angle of 7·9 radians, with a magnitude of about $0{\cdot}8\ g_m$, where g_m is the triode mutual conductance. In case (*b*) the first maximum of negative conductance occurs at a cathode-grid transit angle of 7·6 radians, and is of approximate magnitude $0{\cdot}25\ g_m$; while in case (*c*) the angle is 4·7 radians and the magnitude is $0{\cdot}8\ g_m/\mu$ where μ is the triode amplification factor. Other types, intermediate between these three "pure" cases, can doubtless be realized by various circuit adjustments.

It should perhaps be mentioned that, owing to the presence of a potential minimum at an appreciable negative potential relative to the cathode and at an appreciable distance from the cathode, the simple formula for the cathode-grid transit time [equation (7) of Ref. 1 which, incidentally, is misquoted by a factor of 3] gives too large a value of transit time, even when allowance has been made for the negative contact potential.

In view of the theoretical possibilities mentioned, it would be interesting to know the type of circuit adjustment made by the authors[1] in deriving their experimental results, what the d.c. conditions (voltage and current) were, and to which, if either, of the arrangements (*b*) or (*c*) they consider their circuit most closely approximated.

Meadow View,
Burnham Avenue,
Beaconsfield, Bucks.

I. A. HARRIS

REFERENCES

(1) CRITCHLEY, O. H., and GAVIN, M. R. *Brit. J. Appl. Phys.*, **3**, p. 92 (1952).
(2) BENHAM, W. E. *Phil. Mag.*, **5**, p. 641 (1928).
(3) LLEWELLYN, F. B. *Proc. Instn. Radio Engrs., N.Y.*, **23**, p. 112 (1935).
(4) NORTH, D. O. *Proc. Instn. Radio Engrs., N.Y.*, **24**, p. 108 (1936).
(5) BENHAM, W. E. *Phil. Mag.*, **11**, p. 457 (1931).

In his interesting letter Mr. Harris criticizes the "mathematical discussion" of the input impedance of a triode in a paper which is essentially empirical. The significant fact appears to be that the experimental evidence shows that the maximum negative conductance does occur at approximately that value of the transit angle, about 7·5 radians, which is predicted by theory for a number of widely differing arrangements. Small signal theory indicates that the critical value of transit angle applies to most cases of transit across a gap—for longitudinal or transverse fields, with or without space charge and with or without initial velocities. The value may be modified to some extent if consideration is given to the conditions outside the gap. Such modification (5% or less) is seen in Mr. Harris's cases (*a*) and (*b*). His arrangement (*c*) with a short-circuit between grid and cathode is of little significance with reference to the possibility of negative input conductance. With this circuit transit time oscillations would occur most favourably in the grid-anode space. Maximum negative conductance would then occur with a grid-anode transit angle of 7·5 radians.

The circuit arrangement which gave most favourable oscillations approximated to short-circuited quarter wavelengths for both transmission lines. The anode voltage ranged from 100 to 350 V, and the anode current from a few milliamps to about 50 mA. Grid current was usually less than 1 mA. The maximum current density was about 400 mA per cm^2.

The authors of the paper are indebted to Mr. Harris for pointing out the omission of the factor 3 in equation (7). The correct value was, of course, used in calculating the transit times.

Department of Physics and Mathematics,
College of Technology,
Birmingham 1.

M. R. GAVIN

New books

Mass spectrometry. Report of a conference organized by the Mass Spectrometry Panel of The Institute of Petroleum and held in Manchester, April, 1950. Pp. 205. Price 30*s*.

Conference reports are apt to be somewhat disjointed; but this has been avoided here to some extent by presenting the work discussed in four main groups. In the first group concerned with the ionization and dissociation of molecules, four papers by Evans, Waldron and Wood, McDowell and Warren, and Warren and Craggs deal with the measurement of appearance potentials and application of the experimental data to the determination of bond dissociation energies. In this group is included also a paper by Robertson discussing some theoretical problems involved in the application of the mass spectrometer to the detection of free radicals. The second group dealing with some instrumental aspects contains two papers, one by Reis giving a general survey of work in France and the other by Barnard discussing generally some problems of source design. Four papers are included in the third group on applications, one by Palmer and one by Bentley on isotopic work, one by Nicholson on hydrocarbon analyses and finally one by Winter and Houghton on isotopic exchange of ^{18}O. The final group deals with problems involved in the preparation of standard gases. Three papers by Johns, Kronberger and London, Thomas, and Herington are presented.

To each group is appended a brief report of the discussion at the conference of the papers and allied subjects. Finally, a valuable bibliography is added of papers published in the period January, 1938, to November, 1950. This bibliography was prepared by the Intelligence and Interchange Section of the Research Department of Metropolitan-Vickers Electrical Co. Ltd.

It is clear that many workers in the field of mass spectrometry will find much of value in this collection of papers; but it is regrettable that it has taken so long to publish this report. It is more than two years since the conference was held; and an even greater period of time has elapsed since the papers presented were prepared. With a subject that is

still very much in the making, it is evident that new data, changes of emphasis or modifications of opinion would appear in similar papers prepared to-day. This delay is largely the consequence of the spasmodic birth of a formal conference from a desire amongst certain workers for an opportunity for informal discussion of the manifold problems of mass spectrometry. It is to be hoped that if future conferences are held under the auspices of the Institute of Petroleum, the publication time will be very substantially reduced. It is felt also that the title of the volume, viz. *Mass Spectrometry*, is too general in that it may foster an impression of a more comprehensive survey of the subject than is, in fact, the case.

However, in spite of these criticisms, many workers will find this volume valuable. Only a few misprints have been noted and the standard of production is good.

G. P. BARNARD

An introduction to acoustics. By R. H. RANDALL. (Cambridge, Mass.: Addison-Wesley Press Inc.) Pp. xii + 340. Price $6.50.

This book is of a standard which we are led to infer has not previously been available in America "except for British imports," and is assigned a level intermediate between the texts due to Watson and to Morse. It provides a good survey of modern acoustics; and, although it is on the whole more concerned with the mathematical basis than experimental methods, care has been taken to link theory with practical applications. The roles played by diffraction and by absorption have received, very justifiably, more than their usual emphasis; and adequate use is made of "electrical analogs." Only one obvious slip has been noticed, but some confusion may possibly result from the "envelope" of the stationary wave pattern produced by partial reflexion, and also from the fact that the spectrum analysis of the "ee" sound of pp. 203–4 differs from that of p. 208. Each chapter concludes with a series of problems, some non-mathematical, and answers are provided to the odd-numbered questions. The reviewer of another book in which this procedure was followed has characterized it as "a subtle touch which shows that Mr. X is a wise and experienced teacher": it seems legitimate to substitute Randall for X.

E. J. IRONS

Phase microscopy. (Principles and applications.) By A. H. BENNETT, H. JUPNILL, H. OSTERBERG and O. W. RICHARDS. (London: Chapman and Hall Ltd.) Pp. 320. Price 60*s*.

Twenty years have elapsed since Zernike first put forward his theory of phase contrast and applied it to the study of transparent microscopic objects. Despite the attempts of Zernike and, in this country, of Burch, to convince potential users of the usefulness of this application, it is only in the post-war years that the method has become generally available. Whilst many papers have been written on the subject of the application of phase contrast to particular problems during this period, little has appeared in print, other than the original papers, to give a detailed account of the principles and applications of the technique. This book, the first to be devoted entirely to phase contrast, or as the American authors have entitled it, "Phase microscopy," is indeed welcome.

It is sometimes difficult in such a book to give a full enough account of the theory of a technique without using mathematical methods beyond the understanding or requirement of many of the readers; Alva Bennett and his colleagues have succeeded in this by roughly dividing the book into three sections which deal with the principle, the instrumentation and the applications of the technique, together with an appendix which deals with the diffraction theory of phase microscopy in a comprehensive manner. Nothing is lost, even by those who cannot tolerate so much as an integral sign in mathematics, as almost invariably throughout the first part of the book the authors quote in succeeding chapters the results obtained in the immediately preceding ones.

For the practical microscopist the instrumentation should provide ample interest—practical details of the design and manufacture of phase microscope components are given, although only brief mention is made of the simpler methods which would be more within the capabilities of the research worker. Features of instruments produced by various manufacturers are included together with details of recent advances in polarizing phase contrast and continuously variable phase systems. Hints on the preparation of biological specimens for examination by phase contrast should be of help to those who may have recourse to this method, whilst the chapter on industrial applications reveals the many problems that can be tackled by phase microscopy. From tissue culture to clays and paints may seem a long way but this gives some idea of how varied are the applications of the technique, and microscopists, no matter what their field of research, will find this a welcome addition to their library.

K. W. KEOHANE

The principles of the control and stability of aircraft. By W. J. DUNCAN. (London: Cambridge University Press.) Pp. xvi + 384. Price 40*s*.

It is not so very long ago that many aircraft designers subscribed to—and even possibly believed—the formula that, to produce a flyable aeroplane, all that was needed was a far-forward centre of gravity position, a fin perhaps a little larger than the one on their previous machine, and a brave pilot. But evolution has outgrown the art of recipe. The problem of the stability and control of modern aircraft requires exacting analysis and careful experiment; it is the study of the motion of a body possessing several degrees of freedom and subjected to a complicated and often incalculable system of air reactions.

This would hardly appear to be a subject which could be dealt with adequately in a book of 384 pages. Indeed, anyone but a first-class teacher would not make the attempt. Fortunately, in Professor Duncan we have the first-class teacher; he has with admirable skill been able so to manipulate the reader's path as to make palatable both the mathematical problem of formulating and solving the equations of motion and the physical problem of predicting the aerodynamic forces created during the motion. Detail has been most wisely avoided where it can be supplied readily by other treatises: on the other hand, he has not hesitated to repeat classical proofs where, presumably, he believes his own treatment has the advantage of clarity and emphasis on physical principles. This is illustrated by the chapters describing the derivation of the equations of motion of a rigid body and the conditions for its stability to small disturbances.

As a guide to its scope, a few of the topics dealt with in the book may be mentioned: the characteristics of flap controls, theory of manœuvrability, analysis of the spin, the effects of structural distortion and compressibility of the air, the measurement of aerodynamic forces in the wind tunnel, as well as the more conventional criteria for longitudinal and lateral stability involving such terms as stick-fixed and stick-free neutral points, manœuvre margin, dutch roll and spiral stability. Professor Duncan and Professor Young, who

contributed two chapters on the stall and landing flaps, must be congratulated on producing what will surely be the standard text-book for some time to come, on the control and stability of aircraft. P. R. OWEN

Radio. Vol. 1. By JOHN D. TUCKER and DONALD WILKINSON. (London: The English University Press Ltd.) Pp. ix + 177. Price 7*s.* 6*d.*

This book is intended as a course book for the C.G.L.I. Radio I syllabus. It assumes that the student will also be studying for the Telecommunications (Principles) II examination, but includes a chapter on basic electricity and magnetism for those studying for the "Radio Amateurs" Examination. The treatments in the book are, in the main, non-mathematical, although a number of elementary relations are derived, for example, that giving the gain of a resistance loaded triode.

In spite of the obvious necessity to keep the book short, the authors do seem to give undue emphasis to the older type of screened grid valve (p. 101) and to the behaviour of primary cells (pp. 106–112). Criticism could also be made of some points of detail, but on the whole the explanations are sound, and the information reliable. The printing and binding are good, and misprints few. The book should be useful to students beginning the study of radio, especially those lacking the background acquired by work in the radio industry. H. S. BARLOW

Physical properties of glass. By J. E. STANWORTH. (London: Oxford University Press.) Pp. vii + 224. Price 21*s.*

This book is the sixth volume in a series of monographs on the physics and chemistry of materials edited by Professors Willis Jackson, H. Fröhlich and N. F. Mott and intended to summarize the recent results of academic or long-range research in materials and allied subjects. A more appropriate title might well have been chosen, for no attempt has been made to summarize in detail the mass of published technical information on the physical properties of glass. In fact the reader is directed to Morey's *Properties of Glass* or to W. Eitel's *Glastechnische Tabellen* for such information. The purpose is, the author states, to present the noteworthy advances in the present theories of the nature and structure of inorganic glasses.

In pursuing this aim a short statement is given of the wide range of materials which form glasses and of the manifold purposes to which they can be applied. Comprehensive as this introductory chapter is, it would have been of greater value if some brief reference had been made to the general principles—of which Mr. Stanworth is an outstanding exponent—which now guide industrial chemists and physicists in the selection of glass compositions for various applications. Such a reference to the necessarily empirical methods frequently used would have served to focus attention on the advances in our knowledge which are described in the remaining chapters.

There is little doubt that in the second and longest chapter (56 pp.), entitled the structure of glasses, the author goes a long way towards achieving his object. Although, as he states, there is no attempt to describe the modern (and controversial) views of the types of bond existing between the atoms, this chapter is a clear, concise and yet fairly detailed account of the present position.

The remainder of the book contains a critical account of a wide, but by no means an exhaustive list of physical properties: mechanical strength and fracture (51 pp.), electrical properties in the "solid" state (17 pp.), surface properties (15 pp.), properties in the transformation range (28 pp.), viscosity and surface tension (11 pp.), annealing (8 pp.) and devitrification (11 pp.). The properties have been chosen to illustrate the fundamental relationships which have been found and the theories proposed. There is, for example, no detailed account of the thermal-expansion of glasses except in its bearing on the statement of the properties in the so-called "transformation range" of temperatures.

In each section the facts presented are explained by reference to the theories given in the second chapter or by the presentation of alternative explanations. By this means an attempt is made to build up a detailed picture of the glassy state. It is difficult to see, however, how the uninitiated reader will be able to follow all the complex evidence presented without confusing this picture. For example A. Q. Tool's conception of "fictive temperature," convenient as it may well be, hardly helps to produce a clear picture of the phenomena of rearrangement which affects so markedly the physical properties of glasses in the "transformation range" of temperatures.

Within the limits imposed by the purpose of the book, Mr. Stanworth is to be congratulated on producing a well-balanced, full and thoughtful account of the more recent progress on the nature and structure of glass. Despite the author's commendable desire to present with fairness every side of the picture, a desire which has been allowed to detract to some extent from the clearness of his theme, this book should be of great value to physicists and chemists who are interested in the structure of both liquids and solids.

JAMES BOOW

Mechanics and properties of matter. By R. J. STEPHENSON. (London: Chapman and Hall Ltd.) Pp. x + 371. Price 48*s.*

Theory of mechanics. By K. E. BULLEN. (London: Cambridge University Press.) Pp. xvi + 368. Price 21*s.*

These two books, though differing in standard and in treatment, have much in common. Both are by university professors of considerable experience in the teaching of mechanics, who appreciate the student's difficulties and are emphatic that the physical principles of the subject must be thoroughly understood. And both are written with an enthusiasm for the subject which should encourage the reader to put forth his best efforts to master it.

The standard of Dr. Stephenson's book approaches that of the pass degree in physics, and in some places is above this level. The material has been selected and presented with the needs of the physics and engineering student in mind. The elements of vector methods, potential theory, and Fourier analysis are included, and there are very full discussions of oscillations, rigid dynamics, and wave motion. The chapter on statics deals with the solutions to a number of important practical problems, and the same is true of the sections on the properties of matter which are on the whole of a more elementary nature than the rest of the book. Dr. Stephenson writes clearly and does what he sets out to do, taking great pains to see that the principles are not submerged in analysis and manipulation. The exercises at the end of each chapter are searching and well-chosen, but no answers are provided. It is unfortunate that the price is likely to put this excellent book beyond the reach of the average English student.

Dr. Bullen's book is less advanced, and is directed more clearly to the needs of the first-year student of applied mathematics. It would be fair to say that its aim is to train

the student to solve problems intelligently from first principles, instead of by recondite processes which may get the answer. The many examples in the text are worked out in great detail, and each ends with a discussion of the method used and the points the example was chosen to illustrate—the technique of the tutor rather than of the conventional textbook. Students will appreciate it, and should derive great help from it; and it seems to embody the most sensible way of introducing applied mathematics to the future physicist.

G. R. NOAKES

Exercises in experimental physics. By N. C. B. ALLEN and L. H. MARTIN. (London: Cambridge University Press.) Pp. xiii + 237. Price 30*s*.

The seventy-four experiments described in this book are planned to occupy the second year of the physics course at the University of Melbourne. The text is lucid, well printed and clearly illustrated. The thirty-five groups of experiments are each preceded by a useful discussion of the relevant theory. A desirably modern outlook with a somewhat applied bias is given by the inclusion of experiments not usually found in courses for students: examples are the use of slip gauges; the improvement of the resonance tube method by the use of loudspeaker and microphone; the measurement of small radii of curvature by a microscope method; the study of room illumination; the determination of the thermal conductivity of a gas; the use of a Geiger counter. Many useful practical hints are given to facilitate the making of observations whilst an introductory chapter on statistical theory is very helpful.

There is, however, a regrettable lack of detail of how to set up apparatus in discussing some of the experiments: the discussion of apparatus for determining the specific charge on the electron and the brief description of scaler circuits are but two instances of such inadequacies. The chief disadvantage of the book for general use is, however, that only one year's course is considered. Consequently many of the experiments considered vital to a graduate course are omitted. This limitation of the text—doubtless done to keep the price down—will possibly and unfortunately restrict the wide use of an attractive volume.

J. YARWOOD

Correspondence on—

Fundamentals of technical electricity. By H. G. Mitchell. (London: Methuen and Co. Ltd.) Pp. xii + 543. Price 18*s*.

The review of my book which appeared in your September issue contains few expressions of opinion but consists largely of grossly inaccurate statements.

(i) The reviewer states ". . . it purports to be logical and modern. Its modernity embraces Ticonal, . . ." If these words mean anything, they indicate that nothing more modern than the topics referred to can be found in the book. Such an implication is entirely false, as can be shown, for example, by reference to the text and diagrams of "C"-core transformers, information about which could only be released to the public while the book was in the proof stage.

(ii) The statement that "The author tells us that the e.m.f. of a source is the work done in taking unit charge completely round a circuit containing the source" is false. The sentence which has been misquoted appears on p. 24 and reads "electromotive force (e.m.f.) . . . is measured, in volts, by the work in joules done in taking 1 coulomb completely round a circuit containing the source."

(iii) The reviewer states that "The author uses terms like string-electrometer, dead-beat, V.A., without explanation."

(*a*) On p. 25 there is a diagram of a string-electrometer (Fig. 2.1.). The term string-electrometer first appears on p. 25 in the sentence "For example, if the plates of a string-electrometer are made of copper and zinc respectively and are connected at the base (Fig. 2.1.), the string will . . ."

(*b*) The term dead-beat first appears on p. 191 in the sentence "To overcome this difficulty and to make the instrument dead-beat so that the pointer moves to the appropriate position and stays there, . . ."

In both these cases the explanation of the term is given in the sentence in which the term is introduced. In case (*b*) there is additional explanation in the preceding sentence which describes what happens in an instrument which is not dead-beat.

(iv) "He defines effective resistance correctly, and then confuses it with reactance." Effective resistance is defined on p. 335 and the term reactance is introduced on p. 336 where it is stated that "The effective resistance due to the inductance L (is) known as the reactance in the circuit." The next sentence explains that the effective resistance of the circuit is normally due not only to the reactance, but also to the ohmic resistance in the circuit, and is known as the impedance in the circuit. There then follows an equation showing how the effective resistance (impedance) can be calculated from the reactance and ohmic resistance. This is the exact opposite of what is stated by the reviewer.

(v) The comment "an attempt to develop electromagnetism without unit poles—which collapses after ten pages . . ." is most unfair. Reference to the preface (p. v) shows that I claim to "introduce" and not "develop" electromagnetism in this manner. Further, on p. 154, the tenth page of the chapter on electromagnetic theory, the reviewer could have read "Although an isolated magnetic pole does not exist, it is often convenient in the development of electromagnetic theory to assume something to which we can only approximate in practice." The fact that this statement precedes any theory involving unit magnetic poles belies his criticism.

Whether or not my methods are desirable is a matter of opinion, but the continued success of my *Textbook of Electricity*,* in which similar techniques are used, suggests that they appeal to more than a few. I might even add that a Professor of Electrical Engineering at an English University, commenting on the suitability of the book under review, has written "I can recommend the book with every confidence and am of the opinion that it is a model second year syllabus. I am recommending the book to both staff and students here."

Finally, your reviewer's last statement "He has a few good ideas, but is incapable of carrying them out" would appear to be a criticism not of the book but of my professional status to which it is damaging. I should be glad if you would bring these comments to the attention of your reviewer and publish a refutation of his statements.

H. G. MITCHELL

[Unfortunately, the reviewer was killed in a recent mountaineering accident. I know that the last sentence of his review was intended to be no more than his judgment of the author's treatment of the subject of his book and not to reflect in any way on Mr. Mitchell's professional competence—an idea that must have arisen because of the rather unfortunate choice of words used to convey the meaning.—ED.]

* A successful textbook by the same author.

Notes and comments

Elections to The Institute of Physics

The following elections have been made by the Board of The Institute of Physics:

Fellows: K. W. Andrews, C. H. Carlisle, T. J. Heal, J. W. Jeffery, J. H. Martin, P. B. Moon, B. E. Noltingk, G. de Q. Robin.

Associates: W. Bardsley, S. T. Bayley, P. R. Briggs, D. Bulgin, K. H. Clarke, P. T. Davies, A. D. Dobson, W. H. Dowland, W. H. Evans, L. C. J. Fricker, A. J. Herz, W. C. A. Hutchinson, N. C. Jain, D. Jakeman, L. A. King, C. S. Lees, W. O. Lock, A. H. Morton, P. F. Morton, R. W. R. Muncey, M. R. Padhye, G. S. Parry, I. W. Ramsay, B. C. Raychaudhuri, H. Scouloudi, D. S. Stark, E. W. Tapper, H. Tipton, M. J. Tucker, A. R. Wilson, J. G. R. Young.

Twenty-seven Graduates, seven Students and three Subscribers were also elected.

Journal of the mechanics and physics of solids

We have received a copy of the first issue of the new quarterly *Journal of the mechanics and physics of solids*, which is produced under the joint editorship of Dr. R. Hill, of the University of Bristol, and Professor W. M. Baldwin, Jr., of the Case Institute of Technology, Ohio. The issue before us is of 76 pages, measuring $6\frac{1}{4} \times 10$ in, and contains the following papers:

Plastic instability under plane stress, by H. W. Swift.
On discontinuous plastic states, with special reference to localized necking in thin sheets, by R. Hill.
Calculations on the influence of friction and die geometry in sheet drawing, by A. P. Green and R. Hill.
Rheology of metals at elevated temperatures, by A. E. Johnson and N. E. Frost.
The time laws of creep, by A. H. Cottrell.
The yield phenomenon in polycrystalline mild steel, by W. M. Lomer.

The production generally is not quite as high as most of the established English scientific journals. The publishers are Pergamon Press Ltd., of London, S.W.1. The subscription price is £4 10*s*. 0*d*. per volume.

Recently developed techniques in high-speed photography

The September–October issue of *The Photographic Journal*, Vol. 92B, pp. 130–166 (1952), contains a series of papers on high-speed photography which deals with some of the most recently developed techniques. The contents include: Flash cinematography, by R. H. J. Brown; A synchronized flash-discharge system for high-speed 35 mm cinematography, by W. D. Chesterman and G. T. Peck; Image converter tubes and their application to high-speed photography, by J. S. Courtney-Pratt; Image converter techniques applied to high-speed photography, by R. A. Chippendale; An electronically operated Kerr cell shutter, by K. D. Froome; Electro-optical shutters as applied to the study of electrical discharges, by J. M. Meek and R. C. Turnock.

The journal is published by The Royal Photographic Society of Great Britain, 16 Princes Gate, London, S.W.7, from whom copies may be obtained, price 5*s*.

Errata

In the article "The method of dimensions," by E. W. H. Selwyn, published in the July issue of this *Journal*, x, y and z in equation (1) *should be* replaced by X, Y and Z, where $x = \log X$, $y = \log Y$ and $z = \log Z$. In what follows x *should be* replaced by X. Up to and including the equation previous to (1) x is the logarithm of the ratio of the sizes of the units and from the modified equation (1) onwards X is the ratio itself.

In the "Summarized proceedings of a conference on X-ray analysis—Edinburgh, April 1952," published in the October issue of this *Journal*, the word "nuclear" which appears on p. 306, column 1, lines 4 and 6, *should read* "neutron." The units kX which appear on lines 43 and 44 *should be* Å.

Journal of Scientific Instruments

Contents of the November issue

ORIGINAL CONTRIBUTIONS

An optical slit mechanism. By R. V. Jones.
A versatile equipment for thermocouple switching using a Post Office type uniselector. By H. Burton and S. F. Suffolk.
Infra-red solar spectroscopy in a high-altitude aircraft. By J. Yarnell and R. M. Goody.
A photomechanical wave analyser for Fourier analysis of transient waveforms. By T. B. Whiteley and L. R. Alldredge.
A simple gas-flow-control of high efficiency. By D. H. James and C. S. G. Phillips.
A low-temperature X-ray powder camera. By N. C. Tombs.
A dynamometer for the human calf muscles. By O. C. J. Lippold, P. F. D. Naylor and E. E. E. Treadwell.
Instantaneous measurement of a varying frequency. By L. U. Hibbard and D. E. Caro.
A method of measuring the magnetic permeability of rod specimens. By H. Aspden.
A rotating coil fluxmeter. By M. S. Wills.

LABORATORY AND WORKSHOP NOTES

Electron beam plotting in cathode-ray tubes. By L. S. Allaru and D. B. Clayson.
A simple a.c. mains operated thyratron relay. By G. K. M. Pfestorf.
A multi-channel switch for operation in a microwave circuit. By H. M. Barlow and H. G. Effemey.
The construction of a liquid dielectrics test cell. By S. Baxter and H. A. Vodden.
A powder camera modification for high temperature photographs. By H. T. Heal, E. Gillam and D. G. Cole.

NEW INSTRUMENTS, MATERIALS AND TOOLS NEW BOOKS NOTES AND COMMENTS

British Journal of Applied Physics

Original contributions accepted for publication in future issues of this Journal

The motional impedance of simple sources in an isotropic solid. By H. Pursey.
A note on the use of extrapolation techniques with electrical network analogue solutions. By R. Culver.
Stability and accuracy of numerical solutions of the heat flow equation. By P. H. Price and M. R. Slack.
Absorption and scattering of radiation by water sprays of large drops. By P. H. Thomas.
Second-order transition points in high polymers. By K. L. Floyd.
A simple goniometric method for examining preferred orientation in etched metal polycrystals. By P. Dunsmuir.
Propagation in waveguides filled longitudinally with two or more dielectrics. By I.I.G. Chambers.
Spectrophotometric measurements in the vacuum ultra-violet: the use of photomultipliers. By J. H. Bolton and S. E. Williams.
High power solenoids: stresses and stability. By J. M. Daniels.
The compression and bearing capacity of cohesive layers. By G. G. Meyerhof and T. K. Chaplin.
Laboratory drying of herbage by radio-frequency dielectric heating. By J. N. Merridew and W. F. Raymond.
The use of X-ray diffraction cameras as recording optical goniometers. By E. Stanley.
A vibrating reed microbalance for susceptibility measurements in weak fields. By Y. L. Yousef.
The electrical measurement of moisture in granular materials. By D. J. Millard.

THIS JOURNAL is produced monthly by The Institute of Physics, in London. It deals with all branches of applied physics (including theory and technique). All rights reserved. Responsibility for the statements contained herein attaches only to the writers.

EDITORIAL MATTER. Communications concerning editorial matter should be addressed to the Editor, The Institute of Physics, 47 Belgrave Square, London, S.W.1. (*Telephone:* Sloane 9806.) Prospective authors are invited to prepare their scripts in accordance with the *Notes on the Preparation of Contributions*. (Price 2*s*. 6*d*. including postage.)

REPRODUCTION. The Institute of Physics is a signatory to The Royal Society's Fair Copying Declaration. Details may be obtained upon application from The Royal Society, London, W.1.

ADVERTISEMENTS. Communications concerning advertisements should be addressed to the agents, Messrs. Walter Judd Ltd., 47 Gresham Street, London, E.C.2. (*Telephone:* Monarch 7644.)

SUBSCRIPTION RATES. A new volume commences each January. The charge is £4 per volume ($11.50 U.S.A.), including index (post paid), payable in advance. Single parts, so far as available, may be purchased at 8*s*. each ($1.15 U.S.A.), post paid, cash with order. Orders should be sent to The Institute of Physics, 47 Belgrave Square, London, S.W.1, or to any Bookseller.

Summarized proceedings of the third international spectroscopy colloquium—Hoddesdon, September 1952

The third international spectroscopy colloquium was held at High Leigh, Hoddesdon, Hertfordshire, from 1 to 4 September, 1952, and was arranged by the Industrial Spectroscopy Group of The Institute of Physics. The papers and the discussions on them are summarized in this report. The subjects covered were: Detectors of radiation, Spectroscopic light sources, Emission spectroscopy, Direct reading spectroscopy, Infra-red and Raman spectroscopy.

DETECTORS OF RADIATION

The colloquium was opened by DR. C. SYKES, President of The Institute of Physics. The first paper was "Detectors of radiation," by DR. W. L. HYDE (American Embassy, London). In reviewing the characteristics of radiation detectors, the examples of Geiger counters, photographic plates, the human eye and the television camera were quoted as approaching the ideal of producing a signal for every quantum in the incident radiation. In the infra-red region of the spectrum, however, the radiation must be degraded into heat, so that radiation measurement becomes a branch of thermometry. Gas thermometers, thermocouples and resistance thermometers are all used as detectors, but they were much inferior in sensitivity. Dr. Hyde then compared the fundamental limits of the various techniques of measurement.[1]

At the evening session DR. F. POHL (Technische Hochschule, Graz, Austria) presented a paper describing the value of emission spectroscopy as an aid to the microchemist (Dr. F. Rohner, Switzerland, in the Chair). As a preliminary to spectrographic analysis, specially sensitive organic reagents were employed for selective concentration of the traces of metals to be determined (chiefly those of biological importance).

Among the many points raised in discussion, PROF. J. GILLIS (Ghent) observed that this method of concentration was also of value in absorptiometric analysis. DR. G. GORBACH (Graz) explained the value of the method by the fact that these organic reagents could be purified by purely organic means, thus avoiding the possibilities of contamination inherent in other chemical methods.

Two demonstrations followed: "Interference filters," by DR. A. C. MENZIES (Hilger and Watts Ltd., London) and "The measurement of slit widths," by MR. R. A. MOSTYN (Chemical Inspectorate, Ministry of Supply, London).

Dr. Menzies and colleagues demonstrated a novel apparatus in which the wave-band required was selected by the use of sharp interference filters of an all dielectric type. MR. M. MILBOURN (Imperial Chemical Industries Ltd., Birmingham) instanced the possible use of such filters for detecting aluminium in copper alloys. DR. H. KAISER (Dortmund) compared the performance of interference and absorption filters on the basis of the concept of "light conductivity" and mentioned the Lyot polarizing type of interference filter. Dr. Menzies stressed the necessity for very careful temperature control in using the Lyot filter. PROF. M. V. MIGEOTTE (Institut d'Astrophysique, Liège), however, had used such a filter for the determination of magnesium in aluminium.

Mr. R. A. Mostyn described a simple diffraction pattern method, proposed by Preuss, for the measurement of slit widths, which showed good agreement with those of independent microscopic and metrological methods. Statistical analysis indicated a precision of $\pm 0{\cdot}5\ \mu$ on zero estimation and $\pm 0{\cdot}05\ \mu$ on drum calibration.

The relative merits of variable slits and a small number of fixed slits were discussed. There appeared to be a preference for the latter in routine analysis, and they can be obtained, if required.

SPECTROSCOPIC LIGHT SOURCES

DR. H. KAISER (Institut für Spektrochimie und angewandte Spektroskopie, Dortmund) opened the session with an introductory talk on our incomplete knowledge of the complicated physical conditions obtaining in light sources used in analysis. Although we know, for example, that spark excitation gives higher accuracy and arc excitation gives higher sensitivity, such general rules are mainly of empirical derivation and we are still in an era of pre-scientific knowledge. We know that the so-called "arcs" and "sparks" are all arcs in their physical character. Discharge types can be specified in electrical terms and reproduced in any laboratory, but complications arise in applying them to the analysis of materials of different composition, metallurgical history, shape, surface condition and the many other variables which can affect the character of the discharge. The term "temperature" of the light source, which implies a state of equilibrium (which may not exist) is not always used in the correct sense, and the measurement of this parameter is very difficult.

MR. M. MILBOURN (Imperial Chemical Industries Ltd., Birmingham) described his experiences of "The behaviour of various metals in emission spectroscopy." Tests were made with the object of studying the transfer of metal to the vapour phase in the case of aluminium, copper, iron, lead, magnesium, nickel, tin, titanium and zinc, using a source unit developed by the British Non-ferrous Metals Research Association referred to as the B.N.F. "General Purpose" source unit. A graphite counter-electrode (point-plane discharge) was used with variations in polarity and electrical parameters, and the behaviour of each metal was found to be highly characteristic of that metal. The author observed that the further problems arising from the results of his tests were more involved than he had anticipated.

PROF. W. SEITH (Universität, Münster, Germany) questioned the advisability of selecting metals of commercial importance for these tests and suggested a systematic study of elements as grouped vertically or horizontally in the periodic table. M. J. ORSAG (Service de Recherche, Pechiney, France) mentioned that he had carried out similar extensive tests on metals, using a controlled but undamped d.c. arc with pilot spark ignition, and obtained broadly similar results. He had also studied impurity lines and had found that one of the most stable discharges was obtained between a globule of the metal and a large electrode of the same material. Dr. Kaiser (Dortmund) observed that polarity effects for different

metals could be accounted for by the fact that cathode excitation was largely electronic whereas anode excitation was thermal in character (so that the conductivity of the sample played a part). The spectrum background, which was heavy in some of the spectra shown, was emitted at the electrode surface and was due to electronic collisions.

DR. J. VAN CALKER (Universität, Münster, Germany) then presented his paper on "The problem of excitation in the spark." Measurement of the variation of line intensities with time, during a single spark, showed the parameters of the spark source to be fundamental in determining the components of an alloy. Effects of composition on line intensity/concentration curves could also be related to metallographic structure.

In reply to MR. E. H. S. VAN SOMEREN, the author said that the time scale was an abitrary scale obtained by numbering successive strokes in an oscillatory discharge.

DR. K. LANG (Technische Hochschule, Wien, Austria) presented a paper, of mainly theoretical importance, on "Line intensity distribution in gaseous discharges," describing interferometric measurements on spectra of discharges in neon by d.c. and 50c/s and 23Mc/s a.c. excitation. The intensity distributions of various lines at different pressures were compared with calculated intensities.

A "constant temperature d.c. arc" was used for the analysis of a variety of materials by DR. N. W. H. ADDINK (Philips Research Laboratories, Eindhoven, Netherlands). Complete combustion of a 5 mg sample, 90 mg carbon powder and an appropriate flux, in layers in a cavity in the anode, was obtained by an arc, taking 8 to 12 A, between specially shaped carbon electrodes, the estimated temperature of the discharge being about 7 000° C. Boric acid or borax was used as a flux and nickel powder was used to aid volatilization. Only the centre of the arc column was used in recording the spectra.

In reply to Dr. Menzies, the author said that the order of the layers in the arc crater would be varied according to the volatility of the sample under test. DR. F. X. MAYER (Institut der gerichtliche Medizin der Universität Wien, Austria) asked why nickel was selected; Dr. Addink thought that its alloying ability and high boiling point were the desirable qualities.

Mr. M. Milbourn confirmed that the author's method of using standard paper density scales[1] was useful in intensity determinations on faint spectrum lines.

The last paper in this session, "Sample preparation in the routine spectrographic analysis of aluminium and its alloys," by DR. F. ROHNER (Forschungsinstitut der Aluminium-Industrie, Switzerland), provided a topic which never fails to produce a lively discussion amongst metallurgical spectroscopists. A special type of aluminium mould was recommended, with the parting surface set at 50° to the vertical with no clamping, for chill casting pencil (rod) electrodes with a fine-grained homogeneous structure.

While agreeing that aluminium moulds were superior to copper moulds, M. J. Orsag (Service de Recherche, Pechiney, France) preferred to work with disk electrodes, as he claimed that they required no machining before sparking. A general discussion then ensued on size and shape of the electrode ends, effects of macro- and micro-segregation of constituents and other metallurgical and practical considerations. It was recognized that the choice of discharge parameters was entirely dependent on that of electrode shape, but no unanimity of opinion was reached on the optimum conditions for the analysis of aluminium alloys.

DIFFRACTION GRATINGS

DR. L. A. SAYCE (National Physical Laboratory, Teddington) reviewed the present position with regard to "The production of diffraction gratings" (Dr. R. C. Lord, Massachusetts Institute of Technology, U.S.A., in the Chair). Good quality gratings have hitherto been produced by reciprocating ruling engines constructed on broad principles laid down by Rowland some 70 years ago, and the speaker paid tribute to Johns Hopkins University which has maintained the lead which it established in this field. The increasing use of gratings in applied spectroscopy has intensified the demand beyond the present capacity to supply, and the N.P.L. is actively developing Sir Thomas Merton's method of constructing helical rulings (a screw-thread of unusual fineness and precision) from which high quality replicas can be provided, and in which the classical errors are avoided. Various interferometric and photometric tests have been devised to provide a more fundamental basis for the specification of gratings than the tests now in common use.

DR. A. H. S. HOLBOURN (Marischal College, Aberdeen) described a method of electronic control of ruling, based on Michelson fringes, using Kerr cells, which produced gratings free from periodic errors.

DR. D. RICHARDSON (Bausch and Lomb Optical Co., U.S.A.), in discussion, described modifications of technique with a view to producing concave grating replicas. He then presented his paper on "The use of echelles in spectroscopy." The echelle, which was developed in 1949 by DEAN G. R. HARRISON (M.I.T.), has properties intermediate between those of the reflexion echelon and the echelette grating. It may be used with either prism or grating cross dispersion to provide a spectrograph of moderate size with unusually high dispersion and resolving power, with considerable saving of space. Applications to various problems were described, such as the separation of practically coincident lines in the determination of boron and carbon in steel and the study of isotopes.

In answer to DR. A. H. GILLIESON (Atomic Energy Research Establishment, Harwell), the author said that the use of an echelle in convergent light would result in a loss of resolving power.

EMISSION SPECTROSCOPY

Attempts to determine the Curie point of nickel by spectrographic means were outlined by DR. J. M. LOPEZ DE AZCONA (Instituto Geologico y Minero de España, Madrid). The spectra were produced by means of a Feussner spark in a specially constructed furnace. Plotting the densities of various lines *versus* temperature, a density maximum was observed at 300° C and a minimum at 360° C, which suggested first a change in the nickel and then a magnetic transformation which occurs at 358° C.

Prof. W. Seith (Münster) suggested that if the vapour pressure of nickel varied in a comparable manner with the other quantities measured, it might partially account for the change in spectrum, but PROF. FISCHER (Vienna) said that the vapour pressure at these temperatures was too low to measure. In answer to the Chairman (M. J. POMEY, Regie Renault, Paris) the author proposed to continue this work with nickel–iron alloys.

Two papers were then presented on the important subject of the spectrographic determination of the major constituents of slags. MR. W. J. PRICE (British Cast Iron Research Association) used a controlled d.c. arc source. Known weights of the material to be analysed and an added internal standard were fused in borax, quenched, crushed and mixed

with graphite and briquetted. On the other hand, DR. F. BALDI (Centro Ricerche e Controlli, Acciaierie Ferriere Lombarde Falck, Italy) found that the best results were obtained by the use of pellets made of brass filings and the sample, subjected to controlled spark discharges. The mutual standard method was used for the oxide/silica ratios and the internal standard method for the metal oxide contents.

In the discussion M. P. MICHEL (Régie Renault, Paris) said that a pellet method for the analysis of slags had been published by R. Castro, who used metallic nickel as an internal standard, but MR. W. J. PRICE preferred to use an oxide; moreover, cobalt oxide was more soluble in borax than nickel oxide. DR. M. F. HASLER (A.R.L., U.S.A.) used much larger slag samples (0·5 gm) and a flux based on lithium salts. Dr. H. Kaiser (Dortmund) pelleted the slag/flux mixture with an equal volume of freshly precipitated copper powder and Mr. E. van Someren used silver powder.

Commenting on the variety of methods used, MR. A. ARGYLE (British Cast Iron Research Association) recommended the specification of the source units by oscilloscope measurements of duration and instantaneous current in the discharge.

DR. K. PFEILSTICKER (Chemisches Untersuchungsamt, Germany) described his technique for the analysis of biological material, using an adherent film, on the tip of each electrode, of a polymerized condensate of glucose, urea and glycocoll in a viscous aqueous solution.[2] Copper or aluminium served as arc electrode material; carbon was only successful with a series arc, and the choice depended on the type of material being analysed. The sample was completely volatilized during the exposure.

MR. W. MULD (Geological Survey of Sweden) presented a short paper on "Spectrochemical analysis of major constituents of minerals." Powder methods of analysis had been tried, including the use of rotating disks from pressed powders, but the author preferred solution methods with spark excitation. For the analysis of rocks, the sample was fused with a flux (1 : 5 sodium carbonate) and then dissolved in nitric or hydrochloric acid.

In reply to a question, the author stated that with the dilute silicate solutions employed the question of variable viscosity affecting the reproducibility of the results did not arise.

DIRECT READING SPECTROSCOPY

DR. M. F. HASLER (Applied Research Laboratories, Glendale, Calif., U.S.A.) described instrumental improvements in the A.R.L. Quantometer, e.g. sealed integrators, gold-plated rotary switches and a vibrating condenser, electrometer type amplifier of unusual design. An integrating sphere-type calibrating lamp, in connexion with a masking system at the receiver slits, allows the sensitivity of the multiplier phototubes to be checked with an accuracy of 0·1% and largely eliminates the need for frequent calibration with standard samples. He mentioned that his company proposed to establish a service centre ("A.R.L. Europe") in Switzerland.

DR. R. SCHMIDT (Algemene Kunstzyde Unie N.V., Netherlands) enquired as to the possibility of a flexible instrument for general analytical work, and Dr. Hasler replied that such an instrument was in course of construction. MR. H. R. CLAYTON (British Aluminium Company, Ltd., England) raised the question of maintenance costs (life of spare parts, air-conditioning, etc.) Dr. Hasler considered that air-conditioning was in the end more economical than frequent calibration checks.

M. J. ORSAG (Service de Recherche, Pechiney, France) related his experiences with the Radio-Cinéma direct reading spectrograph in industrial aluminium production. This versatile type of instrument was used for basic researches as well as for standardized routine analytical control. Its very short integrating time facilitated the study of spectral phenomena. Mr. M. Milbourn, in discussion, agreed that this equipment would be specially useful for investigational work.

Further discussion then diverted to questions concerning source units and metallurgical problems, such as third element effects.

INFRA-RED AND RAMAN SPECTROSCOPY

The principal speaker of this session, DR. H. W. THOMPSON (St. John's College, Oxford), reported on "New measurements in infra-red spectra with high resolving power" (DR. F. X. MAYER in the Chair). A spectrometer with echelette grating and photoconductive cells of the lead-telluride type, cooled with liquid air, permitted the study of fine structure, hitherto unresolved, and the detection of isotope bands in the spectra of simple molecules. Various examples were quoted. The high resolution obtained necessitated calibration of the spectra in the near infra-red with the iron arc, using higher order spectra, and a photomultiplier.

DR. H. TSCHAMLER (Universität, Wien, Austria) then described a systematic investigation of the infra-red spectra of aliphatic, aromatic and heterocyclic compounds with the object of providing a rapid qualitative determination of the $\equiv C-O-C\equiv$ grouping in different assemblages, for purposes of identification. He concluded that in simple cases it may be possible by observation of frequency shift to establish which type of structure is present. Dr. Thompson agreed that this was sound but quoted examples to show the difficulties which could arise in this kind of diagnosis. In a complex organic compound, the effect of other groups may be to shift the characteristic bands due to this group and even to modify their intensity. DR. H. W. DEINUM (Central Laboratory, State Mines, Netherlands) also cited a difficult case of identifying an unexpected infra-red spectrum of a long chain compound.

MME. C. CHERRIER (Soc. St. Gobain, Chauny et Cirey, Paris) gave details of apparatus for following the reactions of industrial syntheses in her paper "Chopped beam photoelectric gas analysis in industry." The analyser gives an instantaneous value of the concentration of a particular gas and this can be used to operate an alarm relay system.

M. J. FAVRE (Institut Français du Pétrole, Paris) presented a paper on applications of infra-red spectroscopy in petroleum analysis. Five types of olefins were estimated in cracking gasolines in fractions in the distillation range 20 to 100° C.

Two papers were then read on the direct recording of Raman spectra. MR. J. SKINNER (Hilger and Watts, Ltd., London) reported that instruments are now available for pen-recording as the spectrum is slowly scanned. Slow rates of scanning are required for high resolution and the photomultiplier should combine a high cathode sensitivity with low thermionic emission.

M. L. ROBERT (Institut Français du Pétrole, Paris) modified a Raman spectrograph to provide pen-recording by means of a photomultiplier with chopped radiation and a tuned amplifier. Various applications in petroleum analysis were studied, for example, the estimation of olefins and aromatics in gasolines, benzols and xylenols.

Dr. H. Kaiser queried the relative merits of Raman and infra-red spectroscopy, but Dr. A. C. Menzies observed that

it was more properly a question of which problems could be solved by each method. The Raman method is usually more suitable for substances containing water. Mr. L. Robert mentioned that for white mineral oils, Raman spectra of different products showed useful differences, but the infra-red spectra were the same.

Visits to Hilger and Watts Ltd. and Kodak Ltd. proved to be so popular that they had to be duplicated, and this was also the case of the alternative visits to Hatfield House and the Roman remains of Verulamium near St. Albans.

ACKNOWLEDGEMENTS

At the conclusion of the colloquium Mr. D. M. Smith, Chairman of the Industrial Spectroscopy Group of The Institute of Physics, thanked all those who had helped to make it a success by contributing papers or discussing them, mentioning particularly Mr. E. H. S. van Someren, the Organizing Secretary, M. W. Pasveer, who acted as interpreter, and the Institute's staff in London.

D. M. Smith

[A few copies of the summaries of the papers in English, French and German are still available from The Institute of Physics, 47 Belgrave Square, London, S.W.1.—Ed.]

REFERENCES

(1) *Spectrochim. Acta*, **4**, (1) pp. 36–42 (1950).
(2) *Spectrochim. Acta*, **4**, (2) pp. 100–115 (1950).

ORIGINAL CONTRIBUTIONS

A method for measuring the potential of a current-carrying electrode

By A. G. Milligan, M.Sc., A.R.I.C., Admiralty Engineering Laboratory, West Drayton, Middlesex

[*Paper received* 16 *May*, 1952]

Measurement of the potential of a current-carrying electrode is subject to error when the Luggin capillary of the reference electrode is situated in the path of the current through the electrolyte. This error can be avoided by siting the reference electrode behind a pin-hole through the main electrode, provided that no current flows through the hole. The method also permits the use of a reference electrode of moderate dimensions inserted directly into the cell electrolyte.

The potential of a current-polarized electrode is commonly measured against a reference electrode (e.g. a calomel electrode), enclosed, with its appropriate electrolyte, in a separate vessel which is furnished with a capillary extension, the end of which dips into the main cell electrolyte.(1) Owing to the flow of current through this electrolyte there is liable to be an ohmic p.d. between the tip of the capillary and the surface of the electrode under investigation, and this p.d. must be either eliminated or allowed for if it is not to be erroneously included in the measured electrode potential.

It is usually, if not eliminated, at least minimized by placing the capillary tip as close as possible to the electrode surface without actually touching it; but this cannot be regarded as a satisfactory method because the magnitude of the error remains unknown and may be greater than is desirable owing to the distortion of the lines of current flow, and consequently of the equipotential surfaces, caused by the presence of a glass tube in their path. For the same reason the current density close to the capillary tip may differ considerably from that on other parts of the electrode surface.

Azzam and Bockris have recently proposed the use of several auxiliary electrodes with their capillary tips at increasing distances from the electrode surface, and the extrapolation of their readings to zero distance.(2) Here, again, it may be objected that the current density, and hence the potential gradient, in the electrolyte will be less near the electrode, where the flow is unrestricted, than in the neighbourhood of the capillaries, where it is restricted by the glass tubes. The resulting error may be difficult to assess.

The purpose of this note is to describe a method to which these objections do not apply. A pin-hole is bored through the (usually plane) electrode, the back face of which is blanked off by an insulating wax or varnish. Since no current flows through the hole there is no potential gradient through it and the potential of the electrolyte immediately behind it is the same as that of the electrolyte round the front edge of the hole. Consequently an auxiliary electrode placed behind the pin-hole measures the potential of the electrolyte in close contact with the working face of the polarized electrode.

For the highest accuracy there ought to be an enclosed chamber of electrolyte behind the hole to ensure the total absence of current flow and potential gradient; but this will often be found unnecessary, since, even without it, the auxiliary electrode can usually be moved away from the pin-hole to a distance comparable with the dimensions of the main electrode with negligible effect upon the potentiometer reading. A theoretical objection which may be raised is that the presence of the hole must cause some distortion of the lines of current flow, resulting in a higher current density around the edge of the hole than elsewhere. If the hole is very small the effect upon the measured potential may be negligible and it can be reduced, probably to vanishing point, by rounding the sharp front edge of the hole. In any case the distortion of the current lines is much less than that caused by a glass capillary in the current path.

The method has been used successfully in this laboratory in the study of primary and secondary battery couples; but it is difficult to apply satisfactorily to very small-scale experiments in which the electrode under investigation may be much less than 1 cm^2 in area. It is of especial value when one desires to measure the potential of a polarized electrode against a reference electrode of the same material in the same electrolyte, because the results are unaffected by the finite dimensions of the reference electrode. I am informed that the method has been used by Piontelli and his co-workers in Italy, but I have been unable to trace a reference.

ACKNOWLEDGEMENTS

I am indebted to the Director of Electrical Engineering, Admiralty, for permission to publish this note.

REFERENCES

(1) Luggin. *Z. Phys. Chem.*, **32**, p. 208 (1900).
(2) Azzam and Bockris. *Nature*, **165**, p. 403 (1950).

Second-order transition points in high polymers

By K. L. Floyd, M.A.,* Research Centre, Dunlop Rubber Co. Ltd., Birmingham

[*Paper first received* 5 *June*, 1952, *and in final form* 12 *September*, 1952]

An optical method of measuring the second-order transition points of high polymers by the change in linear expansion is described. Various mixtures of Hycar OR15 and neoprene yield curves having two distinct and constant transition points. From these curves a relationship giving the composition of the mixture is derived. This may be of value in the analysis of elastomers.

The second-order transition point may be defined as the temperature at which a discontinuity occurs in the first derivative of some thermal property: for example, thermal expansion, heat capacity or thermal conductivity. If, instead of plotting expansion coefficient against temperature, dimension of sample is plotted against temperature a change in the slope of the graph replaces the discontinuity at the transition point, T_m.

In practice the transition spreads over several degrees and the change in slope is correspondingly gradual. It is therefore common practice to draw one straight line through the points lying below the transition region and another one through those above, the point of intersection giving the second-order transition temperature. Typical values which have been obtained by Boyer and Spencer[1] are

Unvulcanized natural rubber	− 73° C
G.R.S. (synthetic rubber)	− 61° C
Polyvinyl acetate	28° C
Polyvinyl chloride	75° C

The usually accepted explanation[1, 2] is that as the transition point is approached from below the polymer chains move further apart owing to increased thermal agitation. When the second-order point is reached the side groups in the hydrocarbon chain and whole segments of the chains (having up to 40 atoms per segment) can start to execute more or less free rotation about the long axis of the molecule. Since the high elasticity so characteristic of rubber is dependent on such rotation the second-order point theoretically marks the lower temperature limit of the rubber-like state. In practice, however, short range intermolecular forces so restrict the mobility of the molecules that a polymer does not become truly rubberlike until temperatures considerably above its transition point are reached.

METHOD

(i) *Principle.* It was decided to choose the linear expansion coefficient as the thermal property since, with a suitable design, the expansion could be made absolute and the apparatus then used for determining the coefficient of expansion for particular rubbers over quite small temperature ranges.

The small distances to be measured suggested an optical method and an instrument made by A. Hilger and Co. Ltd., the Angle Dekkor, seemed to be suitable for the purpose. This instrument measures small changes in angle between the axis of the instrument and a reflecting surface placed almost normal to this axis. The expanding rubber was therefore arranged to tilt a mirror onto which the Angle Dekkor was focused. This method is similar to that used by Roberts[3] for the determination of the expansion coefficient of metallic bismuth.

(ii) *Practical details.* After several designs of optical lever had been tried the arrangement shown in Fig. 1 was finally evolved.

A piece of 4 × 2 in channel girder 30 in long was used as the base plate. At one end a clamp, designed to give three way adjustment, supported the Dekkor. Near the other end a 6 in length of the girder was made water-tight. This section was filled with alcohol and housed the optical lever system. The required cooling was produced by solid carbon dioxide and alcohol in a surrounding tank.

In the optical lever system the sample support originally consisted of a mild steel block with a $\frac{1}{2}$ in high step cut in it. The raised part of the step has now been replaced by Invar columns to minimize the movement of the fixed legs of the optical lever. This lever consists of a brass plate $1 \times \frac{3}{8} \times \frac{3}{32}$ in supported by three gramophone needles spaced as shown in the inset in Fig. 1. The wide separation of the two legs which rest in grooves on the Invar columns ensures stability in that direction, while the $\frac{1}{8}$ in separation from the other leg gives the required magnification. Above the brass plate a $\frac{3}{4}$ in high cylinder of Tufnol carries a horizontal mirror of 1 cm diameter and a tube of copper foil 1 in long surrounds the upper part of the cylinder and projects $\frac{3}{4}$ in above the level of the mirror. This copper foil shield is surrounded by a heating coil wound on a copper tube of 1 in bore and of such a wattage that just sufficient heat is absorbed by the blackened foil to keep the mirror ice free as low as − 70° C. Finally a mirror placed above the optical lever at 45° enables the Dekkor to be used with its axis horizontal.

(iii) *Calibration.* To calibrate the Dekkor, a lever having a ratio of about 10 : 1 was supported by a knife edge on V-grooves. The single leg of the optical lever rested in a groove cut in the short weighted arm while the extremity of the long light arm pressed a small steel ball against a micrometer screw, providing point contacts. This arrangement yielded one division on the Dekkor scale equivalent to one division on the micrometer. After correcting for the arms of the lever being 20·6 cm and 2·03 cm the absolute value for one division on the Dekkor scale is $9{\cdot}8(5) \times 10^{-5}$ cm.

To check this result the separation of the legs was measured with a travelling microscope and found to be 0·342 cm; which gives $9{\cdot}98 \times 10^{-5}$ cm per Dekkor division. The value of $9{\cdot}9 \times 10^{-5}$ cm was therefore taken.

(iv) *Experimental procedure.* The small sample size, $\frac{3}{4} \times \frac{3}{8} \times \frac{1}{2}$ in, gives reasonable rigidity, a uniform temperature throughout the sample, and allows tests on new synthetic polymers of which there may be only a limited quantity available. A small piece of thin copper foil is placed on top of the sample to prevent the leg of the optical lever from sinking into the rubber, and the sample is then placed on the stepped block and stood in the central chamber. After positioning the optical lever, alcohol is added until it covers the top of the sample, but does not immerse the base

* Now with Thomas Hedley and Co. Ltd., West Thurrock, Grays, Essex.

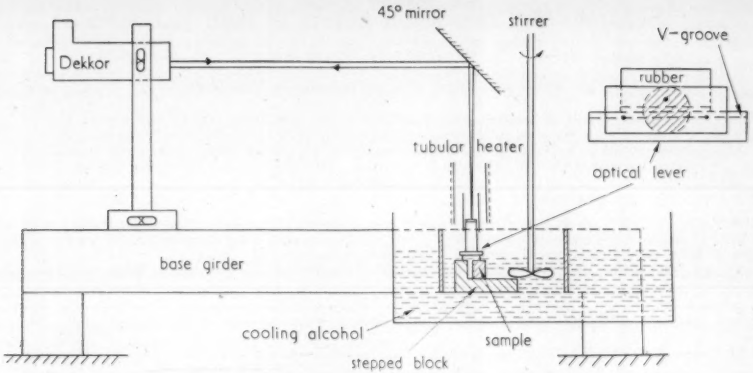

Fig. 1. The general arrangement of the present apparatus

of the optical lever. The electric heater is then lowered to surround the tubular foil of the lever and the heating current suitably adjusted.

Solid carbon dioxide is added to the alcohol in the outer bath and the temperature reduced to the lowest temperature required and maintained there for about an hour. Excess carbon dioxide is removed and the apparatus allowed to return to room temperature. Lagging ensures that this return is gradual and the liquid in the inner chamber is continually stirred. The temperature is noted for the observed Dekkor readings and to record the actual temperature of the sample the thermometer bulb is inserted in a block of rubber of similar shape to the sample and immersed in the alcohol close to the latter. It should be noted that graphs of second-order transition points obtained using the mild steel step are quite valid since the expansion of the step is uniform and continuous and does not therefore affect the temperature at which the transition occurs but merely alters the absolute value of length corresponding to the Dekkor reading.

RESULTS

Preliminary curves obtained from a 90/10 mixture of natural rubber and neoprene exhibited two transition regions confirming the work of Buchdahl and Nielsen.[2]

It was therefore decided to investigate the effect of varying the proportion of two polymers in a mixture, and because of its low transition point natural rubber was abandoned in favour of Hycar OR15. The polymers used, neoprene and Hycar OR15, have transition points at − 44° C and − 24° C respectively and so conveniently divide the temperature range readily available, namely, − 65° C to say 0° C. The results of the various proportions used are listed in Table 1 and the graphs are plotted in Fig. 2.

Table 1. *Transition points of various mixtures*

% neoprene	(T_m) *Hycar*	(T_n) *neoprene*
0	− 24	—
20	− 22	− 45·5
40	− 22·5	− 45
60	− 22	− 48
80	− 23·5	− 46
100	—	− 44

The following conclusions may be drawn from Fig. 2:

(1) There are two definite and distinct transitions for the mixtures.

(2) These transition temperatures appear to be constant within the experimental error estimated at ± 1° C and to coincide with the transition points for the pure polymers.

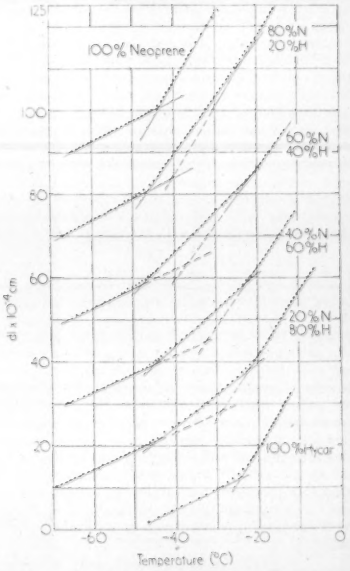

Fig. 2. Transition curves for (neoprene–Hycar) mixtures

(These observations confirm the expectation that for some mixtures at least there is no interaction between the components.[4]

(3) In the range $-24°$ C to $-44°$ C the slope increases with increasing percentage of neoprene, approaching the slope attained by 100% neoprene above its second-order point.

(4) By extrapolating (the slope above $-24°$ C) and (the slope below $-44°$ C) a temperature (T_{nh}) given by their intersection may be obtained.

If a graph of % of one component versus (T_{nh}) is plotted a straight line is obtained, as shown in Fig. 3 the equation being

$$T_{nh} = nT_h + (1 - n)T_n \qquad (1)$$

where n is the volume fraction of Hycar
T_h is the transition point of Hycar
T_n is the transition point for neoprene.

This linear relationship is analogous to that obtained for some copolymers in which the single transition point of the copolymer varies linearly with the fraction of one of the monomers in the copolymer.[5]

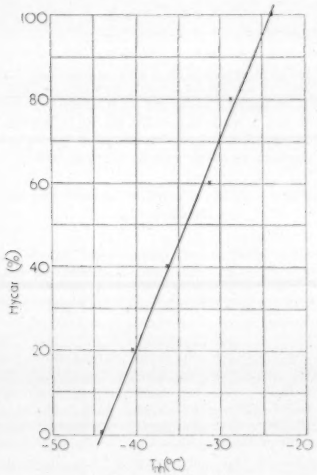

Fig. 3. Plot of percentage Hycar *versus* T_{nh}

An important application of this method may be in identifying an elastomer as either a mechanical mixture or as a copolymer and in determining its composition.

It is implicit in equation (1) that in a mixture the expansion coefficients of the constituents are additive. This yields, for the temperature range between the transition points,

$$a_{nh} = na_1 + (1 - n)a_2$$

where n is the volume fraction of Hycar
a_{nh} is the expansion coefficient of the mixture between transition points
a_1 is the expansion coefficient of Hycar below its transition point
and a_2 is the expansion coefficient of neoprene above its transition point.

From the graphs of 100% Hycar and 100% neoprene respectively,

$$a_1 = 55 \times 10^{-6} \text{ and } a_2 = 152 \times 10^{-6}$$

The coefficients calculated from these values are compared with those measured from the graph in Table 2.

Table 2. *Measured and predicted expansion coefficients*

% *Hycar*	*Measured* (a_{nh}) $\times 10^{-6}$	*Calculated* (a_{nh}) $\times 10^{-6}$
80	75	74
60	85	94
40	95	113
20	131	133

These differences would suggest that, although the transition temperatures can be determined to $\pm 1°$ C, the error in the expansion coefficients is of the order of $\pm 10\%$. This is the variation which previous work (e.g. on moduli determinations) has shown is to be expected from sample to sample in a given batch.

CONCLUSION

The apparatus described is sufficiently sensitive to detect a transition point of a polymer in a mixture when the polymer forms only 20% or even only 10% of the mixture. The linearity of the points is good and suggests an accuracy of $\pm 1°$ C for the second-order point.

Reproducibility of results is satisfactory, as is the general reliability. The main disadvantage is that readings must be taken continously for 2–3 hours as the sample warms up from say $-65°$ C to $-10°$ C. Automatic recording has been used in an interferometric method by R. N. Work[6] and could doubtless be effected in this case but the expense is unwarranted at present. A Speedomax temperature recorder by Leeds and Northrup Co. has, however, been modified so that the relevant temperature for a given Dekkor reading is plotted when a push button is depressed. By this means a plot of sample height against temperature is obtained directly.

ACKNOWLEDGEMENTS

The author wishes to thank the Technical Director (Birmingham), Dunlop Rubber Co. Ltd., for permission to publish this article, also Mr. E. F. Powell, Manager, Physical Research Division, and Mr. S. W. Gough for helpful suggestions.

REFERENCES

(1) Boyer, R. F., and Spencer, R. S. *Adv. Colloid Sci.*, Vol. II, p. 1 (New York: Interscience Publishers, 1946).
(2) Buchdahl, R., and Nielsen, L. E. *J. Appl. Phys.*, **21**, p. 482 (1950).
(3) Roberts, J. K. *Proc. Roy. Soc. A*, **106**, p. 385 (1924).
(4) Boyer, R. F., and Spencer, R. S. *J. Appl. Phys.*, **15**, p. 401 (1944).
(5) Nielsen, L. E., Pollard, R., and McIntyre, E. *J. Polymer Sci.*, **6**, p. 661 (1951).
(6) Work, R. N. *J. Res. Nat. Bur. Stand., Wash.*, **47**, 2, p. 80 (1951).

The use of extrapolation techniques with electrical network analogue solutions

By R. CULVER, B.Sc., B.E., A.M.I.E.Aust., Civil Engineering Dept., University of Adelaide, Australia

[*Paper first received* 1 *July, and in final form* 28 *July*, 1952]

The note outlines briefly simple numerical techniques which are used in finite difference mathematics to estimate the infinitesimal result from finite difference solutions taken with various network sizes. By virtue of the direct analogy between first order difference operators and electrical network voltages, these techniques are directly applicable to extrapolation procedures on characteristic values obtained from networks. In using these procedures the importance of selecting an extrapolation form consistent with the accuracy of the individual characteristic value determinations is emphasized.

The published works of Redshaw[1, 3] and Liebmann[2] have shown the use of electrical resistance networks in solving the Laplace and Poisson equations for various cases. Redshaw has developed the linear network for two and three dimensions, and Liebmann has shown a further three-dimensional network for axially symmetric systems. In the final values obtained from such techniques, there is always an error due to the finite approximation of the field. As the number of meshes is increased, so is the error decreased.[4] Under certain conditions, the desire for accuracy can lead to quite large networks being required. Liebmann has suggested the use of the Richardson "deferred approach to the limit" as a means of enhancing the accuracy obtained from these network solutions. The author has found that the characteristic values obtained can be considerably improved using these quite old techniques shown by Richardson and Gaunt[5, 6] originally in conjunction with finite difference solutions to certain physical problems.

EXTRAPOLATION PROCEDURE

If f is the true (infinitesimal) solution of a problem,

f_1 is a solution obtained, say, using a mesh size h_1, or better, using a mesh number n_1 (dimensionless) $n_1 = l/h_1$ where l = length of some defining region,

and f_2 is another solution obtained with a different mesh size h_2 having a mesh number n_2.

It can be shown that it is plausible to put for first order central differences (which is the difference operator used in setting up the electrical-finite difference analogy), where f_1 approaches monotonically its final value with increasing n

$$f = f_1 + \alpha h_1^2 + \beta h_1^4 + \gamma h_1^6 + \text{etc.} \tag{1}$$

and

$$f = f_2 + \alpha h_2^2 + \beta h_2^4 + \gamma h_2^6 + \text{etc.}$$

If now the first series term is taken as including the whole error, eliminating α between the two equations gives

$$f = (h_2^2 f_1 - h_1^2 f_2)/(h_2^2 - h_1^2) \tag{2}$$

or substituting mesh numbers as above

$$f = (n_2^2 f_2 - n_1^2 f_1)/(n_2^2 - n_1^2) \tag{3}$$

If now the first two series terms are taken as representing the whole error, then to eliminate α and β it will be necessary to have a further equation [as in equation (1) above] for another mesh size h_3, having a mesh number n_3.

Thus, with three equations for f, a final value obtains for

$$f = \frac{h_2^2 h_3^2 (h_2^2 - h_3^2) f_1 - h_1^2 h_3^2 (h_1^2 - h_3^2) f_2 + h_1^2 h_2^2 (h_1^2 - h_2^2) f_3}{h_1^4 (h_2^2 - h_3^2) - h_2^4 (h_1^2 - h_3^2) + h_3^4 (h_1^2 - h_2^2)} \tag{4}$$

and this may be substituted for in terms of mesh numbers n_i as previously, given

$$f = \frac{n_3^4 (n_2^2 - n_1^2) f_3 - n_2^4 (n_3^2 - n_1^2) f_2 - n_1^4 (n_3^2 - n_2^2) f_1}{n_1^2 n_2^2 (n_2^2 - n_1^2) - n_1^2 n_3^2 (n_3^2 - n_1^2) + n_2^2 n_3^2 (n_3^2 - n_2^2)} \tag{5}$$

It is noticed that all these formulae are homogeneous in n which allows a further convenience in expression and manipulation.

Equation (3) above becomes

$$f = a_2 f_2 - a_1 f_1 \tag{6}$$

and equation (4)

$$f = b_3 f_3 - b_2 f_2 + b_1 f_1 \tag{7}$$

where $a_1 = n_1^2/(n_2^2 - n_1^2)$ $a_2 = n_2^2/(n_2^2 - n_1^2)$

and similar expressions result for b_3, b_2 and b_1.

Tables 1 and 2 show values for a_1, b_1, b_2 and b_3. It is appreciated that for a 4 : 2 extrapolation, the a_1, a_2 values used are the same as those for a 2 : 1 extrapolation.

Table 1. *Values of constants* a_2 *and* a_1 *for use in equation* (6)

$n_2 : n_1$	a_2	a_1
2 : 1	1·33333	0·33333
3 : 2	1·800	0·800
4 : 3	2·28571	1·28571
5 : 3	1·56250	0·56250
5 : 4	2·77778	1·77778
6 : 5	3·27273	2·27273
7 : 4	1·48484	0·48484
7 : 5	2·04167	1·04167
7 : 6	3·76923	2·76923
8 : 5	1·64103	0·64103
8 : 7	4·26667	3·26667

Table 2. *Values of constants* b_3, b_2 *and* b_1 *for use in equation* (7)

$n_3 : n_2 : n_1$	b_3	b_2	b_1
3 : 2 : 1	2·02500	1·06667	0·04167
4 : 2 : 1	1·42222	0·44444	0·02222
4 : 3 : 2	3·04762	2·31429	0·26667
5 : 3 : 1	1·62760	0·63281	0·00521
5 : 4 : 3	4·34028	4·06349	0·72321
6 : 5 : 4	5·89091	6·31313	1·42222
7 : 5 : 3	2·50104	1·62760	0·12656
7 : 6 : 5	7·69551	9·06294	2·36742
8 : 7 : 6	9·75239	12·31282	3·56044

Approaches in finite difference solutions and in network solutions are not always monotonic and care is therefore

necessary to ensure that these extrapolation procedures are applied over values falling in monotonic sequence.

Salvadori[7] has shown in finite difference solutions various forms of approach as in Fig. 1. The author has found forms of approach as in (*a*), (*b*), (*c*) and (*d*), but so far in numerous

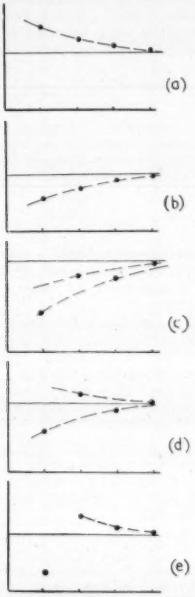

Fig. 1. Approaches to the limit shown by Salvadori.[7]

problems (apart from errors) has not had an approach as shown in Fig. 1(*e*) which is one mentioned by Salvadori. In this figure the dotted lines connect values which may be "improved" by using this extrapolation technique with appropriate values of n_i. It is immediately appreciated that this technique is readily applied to linear network systems, where all meshes of the network are of the same size, to yield excellent results. A problem may be evaluated on, say, an eight-mesh network, then on seven, and then, say, on six, and if the approach is monotonic [Fig. 1(*a*)] an 8 : 7 : 6 extrapolation, together with the 8 : 7 and 7 : 6 extrapolation will yield a more accurate final value. Should the approach be "oscillatory—one sided" [Fig. 1(*b*)], a further evaluation, say, on five meshes, will enable an 8 : 6 (i.e. 4 : 3) extrapolation and a 7 : 5 extrapolation to yield two improved final values.

It is appreciated that the final results from this technique depend critically on the values for the functions f_1, f_2 and f_3, etc., being accurately determined. A small error in one can seriously affect the final value obtained from an extrapolation involving its use.

This fact was forcibly shown in values obtained from a rough electrical network evaluation of a simple "eigenvalue" problem (in the buckling constant m of a beam under a particular loading condition). Salvadori, by finite differences, has shown solutions to this problem, and results of both evaluations are summarized in Table 3. The network solution is known to be in error as these values should be identical with the finite difference values. It is then of value to use these somewhat inaccurate values in the normal extrapolation procedures to see what error results.

Table 3. *Values of buckling constant m for various mesh sizes (n)*

No. of meshes (n)	*Values of m*		*Percentage error on finite difference*
	electrical	*finite difference*	
3	—	27·00	
4	27·54	27·49	+0·18
5	27·74	27·80	−0·22
6	27·96	27·96	0
7	28·14	28·05	+0·32

The approach in this case is monotonic (Fig. 2) and the following extrapolations can be made (Table 4), using equations (6) and (7).

Table 4. *Extrapolated values of m*

Extrapolation	*Final values of m*		*Percentage errors (theoretical)*	
	electrical	*finite difference*	*electrical*	*finite difference*
5 : 4	28·10	28·35	−0·8	+0·15
6 : 4 (3 : 2)	28·30	28·34	−0·05	+0·09
6 : 5	28·46	28·32	+0·5	+0·05
7 : 4	28·43	28·32	+0·4	+0·04
7 : 5	28·56	28·31	+0·9	0
7 : 6	28·64	28·30	+1·2	−0·04
6 : 5 : 4	28·75	28·30	+1·6	−0·04
7 : 6 : 5	28·82	28·27	+1·8	−0·14

The theoretical value obtained by infinite series solution is 28·31 and percentage errors of the various extrapolations are shown based on this value.

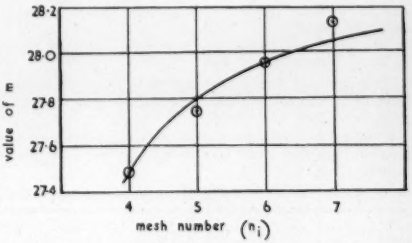

Fig. 2. Values of m (Table 3) shown thus:
—— = finite difference solution; ○ = electrical solution.

To fully utilize the accuracy improvement by this extrapolation technique it is seen that the appropriate f values should be of an accuracy such that their error is considerably less than that admitted in using the further βh^4 term in equation (1). This point is evidenced in the poorer values

obtained for the higher extrapolations using equation (7), and the two decimal place values for the finite difference values of m. It is of interest to use four decimal place figures from the finite difference evaluation for the 6 : 5 : 4 and the 7 : 6 : 5 extrapolation. These values yield a 6 : 5 : 4 extrapolation of 28·2964 and a 7 : 6 : 5 extrapolation of 28·3168. Comparing these values with those given in Table 4 the point emphasized previously is clearly shown.

ACCURACY

In the normal practical usage of these extrapolation techniques no idea can be gained of the accuracy of the final extrapolated result. The effect of resistance tolerance was investigated by Liebmann;(2) further errors will arise in the analogous system due to practical errors of measurement and errors incurred in drawing the analogy. (In the electrical network case the base resistances are made of much higher order than the network resistance to enable the network potential to be of insignificant order.) These errors are in addition to the error involved in using the finite difference approximation.

All errors but the last render the extrapolation technique less valuable as a means of improving the accuracy, especially where these errors are of a greater magnitude than the finite difference error function as indicated above. It is of interest to examine a set of values nominally falling in monotonic sequence to see how closely they fit the assumed approach form. This in itself is no guarantee of final accuracy whatever, but a guide to the order of magnitude only of the error likely to result.

Suppose a particular problem be solved on three network sizes [mesh numbers n_a, n_b, n_c $(n_a > n_b > n_c)$] giving solutions f_a, f_b and f_c

thus $$f = a_2 f_a - a_1 f_b$$

and $$f = a_2' f_a - a_1' f_c$$

If the extrapolation is ideal, each of these f values will be the same: equating gives

$$f_{a\ \text{computed}} = (a_1 f_b - a_1' f_c)/(a_2 - a_2') \qquad (8)$$

Thus it is seen that the f_a value can be computed from f_b and f_c. Dividing both sides of equation (8) by the actual value of f_a gives:

$$f_{a\ \text{computed}}/f_a = (a_1 f_b - a_1' f_c)/[(a_2 - a_2')f_a] \qquad (9)$$

If the approach is monotonic and the values fit the assumed form of approach, then this dimensionless ratio should be unity.

Using an additional series term requires, as a minimum, a solution using four mesh numbers n_a, n_b, n_c and n_d, where as before $n_a > n_b > n_c > n_d$.

Using equation (7) as previously,

$$f = b_3 f_a - b_2 f_b + b_1 f_c$$

and $$f = b_3' f_a - b_2' f_c + b_1' f_d$$

These equations yield

$$f_{a\ \text{computed}}/f_a = [b_2 f_b - f_c(b_1 + b_2') + b_1' f_d]/[(b_3 - b_3')f_a] \qquad (10)$$

and, as before, assuming that the approach form is monotonic and satisfies the form assumed, then this ratio should be unity.

The variation of these ratios from unity indicates the amount by which the values do not satisfy the assumed approach form. This technique purely uses values obtained from lower mesh numbers to anticipate the value obtained from a higher mesh number and then compares that value with the actual practically obtained value. It is appreciated that if this ratio could be established for $n_a >> n_b$, n_c, n_d, etc., then the method would be of value in anticipating final accuracy of extrapolated results. When n_a is only greater than n_b by an integer the method has some considerable value as is seen from its application to preceding results.

Table 5. *Values of ratio $f_{i\ comp}/f_{i\ act}$ for various extrapolations*

Mesh numbers used	*Ratio $f_{i\ comp}/f_{i\ act}$*	
	Finite difference	*Electrical solution*
6 : 5 , 6 : 4	1·00030	0·99601
7 : 6 , 7 : 5	1·00000	0·99831
7 : 6 , 7 : 4	1·00012	0·99677
7 : 5 , 7 : 4	1·00049	0·99197

Comparing these figures in Table 5 with those shown in Table 4 shows that the percentage variation of these figures from unity is a close guide to the order of accuracy of the final result.

In the case of the finite difference values an error of the order of 0·05% would be anticipated in the final extrapolated results and this is sensibly confirmed. From the much less accurate electrical mesh solution inspection of the ratio term in Table 5 would yield an expected error of the order of 0·5–1% which order is also confirmed in the tabulated values.

The author is conscious of the crudity of this approach, but feels it may serve as a useful guide to the final accuracy to be expected. It should be emphasized that this error anticipatory technique is applicable to values falling in monotonic sequence only.

CONCLUSION

It is appreciated that by using these extrapolation techniques, results of quite reasonable accuracy can be obtained from quite small mesh numbers. Care has to be taken to establish the exact form of approach to the limit requiring at least three mesh sizes to be used. Having established values falling in monotonic sequence the final values may be computed. The order of accuracy of the final extrapolated results may be estimated using a rather crude approach in the evaluation of equations (9) and (10) where appropriate. Techniques such as this are not confined to resistive networks only, but may be used to improve the values obtained from reactive network circuits where the mesh scale of the various units used lie in some suitable numerical ratio.

REFERENCES

(1) REDSHAW, S. C. *Proc. Inst. Mech. Engrs*, **159**, p. 55 (1948).

(2) LIEBMANN, G. *Brit. J. Appl. Phys.*, **1**, p. 92 (1950).

(3) REDSHAW, S. C. *Brit. J. Appl. Phys.*, **2**, p. 291 (1951).

(4) MILNE, W. E. *Numerical Calculus* (Princeton: University Press, 1949).

(5) RICHARDSON, L. F. *Philos. Trans A*, **210**, p. 307 (1911).

(6) RICHARDSON, L. F., and GAUNT, J. A. *Philos. Trans A*, **226**, p. 299 (1927).

(7) SALVADORI, M. G. *Proc. Amer. Soc. Civil Engrs*, **75**, p. 1441 (1949).

Stability and accuracy of numerical solutions of the heat flow equation

By P. H. PRICE, B.Sc., and M. R. SLACK, B.Eng., Department of Fuel Technology, University of Sheffield

[*Paper received* 2 *September*, 1952]

The merits of different finite difference representations of the heat flow equation and a convection boundary condition equation are discussed in terms of the stability and accuracy of the solutions they yield. A new method of deriving a condition for stability is given. This is applied to examples of heat conduction involving variable thermal diffusivity and heat transfer by convection at the surface. Some finite difference forms of this boundary condition impose stability criteria which are stricter than, or additional to, that required in the case of a prescribed surface temperature. A new finite difference representation of the surface heat flux equation is discussed.

The accuracy of the various finite difference schemes is investigated by comparing both their analytical and numerical solutions with analytical solutions of the differential equation of heat flow.

1. INTRODUCTION

This paper presents some aspects of the numerical analysis used in theoretical and practical investigations of the temperature variation in a steel ingot from casting to rolling.

A heating or cooling process is governed by the equation of heat flow, which for one dimension can be written

$$c\rho\frac{\partial\theta}{\partial t} = \frac{\partial}{\partial x}\left(\kappa\frac{\partial\theta}{\partial x}\right) \qquad (1)$$

where θ is the temperature at time t and distance x from the origin in a material of thermal conductivity κ, specific heat c and density ρ. For the case of constant thermal properties this can be written

$$\frac{\partial\theta}{\partial t} = D\frac{\partial^2\theta}{\partial x^2} \qquad (2)$$

where $D = \kappa/c\rho$ and is the thermal diffusivity of the conducting material.

Three methods employing finite differences for the solution of this equation have been used by Crank and Nicolson,[1] Richardson[2] and Schmidt.[3] The method given by Crank and Nicolson was actually used by Richardson to calculate his first step in the numerical integration. The difficulties encountered in the use of these methods arise in making the solutions stable and accurate. A stable solution is one in which the approximate solution, as given by the finite difference scheme, does not oscillate or "hunt" as it is developed. Accuracy is a measure of the closeness of the approximate solution to the true or analytical solution of the differential equation.

A method of investigating stability was used by von Neumann, and reported by Crank and Nicolson,[1] and by O'Brien, Hyman and Kaplan.[4] It showed that for the case of one dimensional flow with constant thermal properties and a boundary condition of prescribed surface temperature:

(i) Richardson's method is always unstable, though instability may not emerge in the first few steps of the solution.

(ii) Crank and Nicolson's method is stable under all conditions.

(iii) Schmidt's method is not stable under all conditions.

In this paper a further method of investigating stability is derived. This is used to show how various finite difference forms of the boundary condition equation affect the stability of the solution, and the results are compared with those obtained using von Neumann's method in a case where the latter may be applied.

The accuracy of various solutions is discussed by comparing analytical solutions of the differential equation with both analytical and numerical solutions obtained from the various difference schemes. The examples discussed involve only one space dimension, though the results of the investigations instanced on ingot temperatures have been derived for the case of two dimensional heat flow.

2. STABILITY OF THE SOLUTION APPLICABLE TO CONDUCTION WITHIN THE SOLID

Many types of boundary condition arise in industrial practice, the two considered here being a prescribed surface temperature and convection heat transfer between the surface and constant ambient temperature. More complicated conditions have been considered and will be reported upon later. For the case of prescribed surface temperature it is only necessary to consider the stability of the solutions obtained for the temperatures in the interior of the material, but for the heat flux boundary condition the stability of surface temperatures must also be ensured.

The example considered is that of a slab of conducting material (see the figure). The origin of the space dimension x

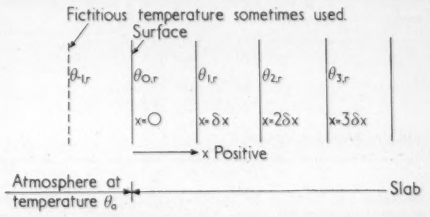

is at the left-hand surface and a number of points are taken in the slab at constant distances δx apart, δx being chosen so that the two extreme points lie on the surface of the material. One finite difference approximation to equation (2) is then

$$\theta_{m,r+1} = \theta_{m,r} + (\theta_{m+1,r} + \theta_{m-1,r} - 2\theta_{m,r})\delta t D(\theta_{m,r})/(\delta x)^2 \qquad (3)$$

where subscripts $m-1$, m, $m+1$, etc., refer to successive points δx apart in the space dimension, subscripts r, $r+1$, etc., refer to points δt apart in the time dimension and $D(\theta)$ denotes the thermal diffusivity at temperature θ.

The Schmidt solution of this difference scheme arises when D is independent of θ and $\delta t D/(\delta x)^2 = \frac{1}{2}$, so that

$$\theta_{m,r+1} = \tfrac{1}{2}(\theta_{m+1,r} + \theta_{m-1,r}) \tag{4}$$

The stability of the more general case of Schmidt's solution given by equation (3) may be investigated as follows.

Suppose that small errors $\Delta\theta_{m,r}$ are present at time $r\delta t$ and that their effect at time $(r+1)\delta t$ is denoted by $\Delta\theta_{m,r+1}$. Then taking differentials in equation (3)

$$\begin{aligned}\Delta\theta_{m,r+1} = {} & [\delta t D(\theta_{m,r})/(\delta x)^2](\Delta\theta^{*}_{m+1,r} + \Delta\theta_{m-1,r}) \\ & + [1 - 2\delta t D(\theta_{m,r})/(\delta x)^2 \\ & + (\theta_{m+1,r} + \theta_{m-1,r} - 2\theta_{m,r})\delta t D'(\theta_{m,r})/(\delta x)^2]\Delta\theta_{m,r}\end{aligned} \tag{5}$$

where $D'(\theta)$ is the derivative of diffusivity with respect to temperature.

This is of the form

$$\Delta\theta_{m,r+1} = P_{m,r}\Delta\theta_{m,r} + Q_{m,r}(\Delta\theta_{m+1,r} + \Delta\theta_{m-1,r}) \tag{6}$$

So

$$|\Delta\theta_{m,r+1}| \leqslant |P_{m,r}||\Delta\theta_{m,r}| + |Q_{m,r}|(|\Delta\theta_{m+1,r}| + |\Delta\theta_{m-1,r}|) \tag{7}$$

Let ϵ_r be the maximum value of $|\Delta\theta_{m,r}|$ as m varies and r remains constant. Then $\epsilon_{r+1} \leqslant \epsilon_r$ can be defined as the condition for stability. From equation (7)

$$|\Delta\theta_{m,r+1}| \leqslant |P_{m,r}|\epsilon_r + 2Q_{m,r}\epsilon_r$$

since Q must be positive. Therefore

$$\epsilon_{r+1} \leqslant |P_{m,r}|\epsilon_r + 2Q_{m,r}\epsilon_r$$

and a sufficient stability criterion is

$$|P_{m,r}| + 2Q_{m,r} \leqslant 1$$

Since the product

$$(\theta_{m+1,r} + \theta_{m-1,r} - 2\theta_{m,r})\delta t D'(\theta_{m,r})/(\delta x)^2$$

is usually small it may be neglected for the moment. This does not hold in the neighbourhood of a latent heat effect, where $D'(\theta)$ is large. Then if $1 \geqslant 2\,\delta t D(\theta_{m,r})/(\delta x)^2$

$$|P_{m,r}| + 2Q_{m,r} = 1$$

If $$1 \leqslant 2\,\delta t D(\theta_{m,r})/(\delta x)^2$$

$$|P_{m,r}| + 2Q_{m,r} = 4\delta t D(\theta_{m,r})/(\delta x)^2 - 1 \geqslant 1$$

and so stability is assured if

$$\delta t D(\theta_{m,r})/(\delta x)^2 \leqslant \tfrac{1}{2} \tag{8}$$

Equation (8) agrees with the corresponding result predicted by von Neumann for constant thermal properties, and shows that the Schmidt solution, obtained using equation (4), is always stable in the case of a prescribed surface temperature.

In the case of steel, $D'(\theta)$ is negative below the change point and positive above it. This means that calculations involving cooling below the change point or heating above it may be unstable, but this effect does not seem to be appreciable. In calculating cases taken from investigations of the heating and cooling of metallic masses, it has been found sufficient to take a value 0·8 or 0·9 of the δt given by equation (8) to allow for the term in $D'(\theta)$. In the ingot studies mentioned a vigilant attitude towards the possible occurrence of instability suggested that further reduction of δt might have been necessary, but the need did not arise.

3. STABILITY OF THE SOLUTION IN THE CASE OF A HEAT FLUX BOUNDARY CONDITION

Method I. The boundary condition assumed in this paper is

$$-\kappa\frac{\partial\theta_0}{\partial x} = h(\theta_A - \theta_0) \tag{9}$$

where θ_0 is the surface temperature, θ_A the ambient temperature and h is a coefficient of convection heat transfer. The methods associated with the various finite difference forms of equation (9) have been referred to for convenience in description by a series of Roman numerals. For brevity, the new method of deriving a condition for stability, already illustrated in Section 2, has been applied to the typical cases of Methods I, IV and VI. Only the results of the analysis in the case of the other methods have been quoted.

The boundary equation originally used by Schmidt is written in terms of a fictitious temperature $\theta_{-1,r}$ at a distance δx outside the body. This gives

$$\kappa(\theta_{-1,r} - \theta_{0,r})/\delta x = h(\theta_A - \theta_{0,r}) \tag{10}$$

and $$\theta_{0,r+1} = \tfrac{1}{2}(\theta_{-1,r} + \theta_{1,r})$$

This equation gives

$$\theta_{0,r+1} = \tfrac{1}{2}[\theta_{0,r}(1 - h\delta x/\kappa) + \theta_A h\delta x/\kappa + \theta_{1,r}] \tag{11}$$

Taking differentials in equation (11)

$$\Delta\theta_{0,r+1} = \tfrac{1}{2}(1 - h\delta x/\kappa)\Delta\theta_{0,r} + \tfrac{1}{2}\Delta\theta_{1,r}$$

A sufficient condition for stability is then

$$\tfrac{1}{2}|1 - h\delta x/\kappa| + \tfrac{1}{2} \leqslant 1$$

which is satisfied if $$h\delta x/\kappa \leqslant 2$$

The values of the finite differences in space and time must therefore be chosen to satisfy both this condition and the condition given in equation (8) for the interior of the slab.

For simplicity h and θ_A have been assumed constant, and this assumption has been made throughout the present paper. In the case of heat transfer between an ingot and its mould, θ_A was not constant and h was a complicated radiation coefficient, but accurate allowance was made for this in the work done on ingot cooling and reheating mentioned in Section 1.

Method II.[5] Schmidt's approximation, equation (10), is varied by taking

$$\kappa(\theta_{-1,r} - \theta_{1,r})/2\delta x = h(\theta_A - \theta_0)$$

and $$\theta_{0,r+1} = \theta_{0,r} + (\theta_{-1,r} + \theta_{1,r} - 2\theta_{0,r})\delta t D/(\delta x)^2$$

Eliminating $\theta_{-1,r}$ gives

$$\begin{aligned}\theta_{0,r+1} = {} & \theta_{0,r}[1 - (1 + h\delta x/\kappa)2\delta t D/(\delta x)^2] \\ & + \theta_{1,r}2\delta t D/(\delta x)^2 + \theta_A 2h\delta t D/\kappa\delta x\end{aligned}$$

and so $$\delta t \leqslant (\delta x)^2/D(2 + h\delta x/\kappa)$$

is a sufficient condition for stability. This result can also be obtained by applying von Neumann's method to the case

where δx = total thickness of the slab. A less severe condition holds if a smaller δx is chosen.

Method III.[6] For a case where $\delta t D/(\delta x)^2 = \frac{1}{3}$, Jaeger uses a boundary condition equation which reduces to

$$\theta_{0,r+1} = \left[\theta_{1,r} + \frac{h\delta x}{2\kappa}(2\theta_A - \theta_{0,r})\right] \Big/ \left(1 + \frac{h\delta x}{2\kappa}\right)$$

This gives a solution which is always stable.

Method IV. A simpler finite difference equation for convection transfer at the boundary of a conducting slab is obtained by writing

$$h(\theta_A - \theta_{0,r}) = \kappa(\theta_{0,r} - \theta_{1,r})/\delta x$$

which may be rewritten as

$$\theta_{0,r} = \left(\theta_{1,r} + \frac{h\delta x}{\kappa}\theta_A\right) \Big/ \left(1 + \frac{h\delta x}{\kappa}\right)$$

Taking differentials

$$\Delta\theta_{0,r} = \Delta\theta_{1,r} \Big/ \left(1 + \frac{h\delta x}{\kappa}\right)$$

So $|\Delta\theta_{0,r}|$ is always less than $|\Delta\theta_{1,r}|$ and therefore this equation for the boundary condition never causes instability.

Method V. A refinement of Method IV is the use of the equation

$$\frac{\partial\theta_{0,r}}{\partial x} = \frac{4\theta_{1,r} - 3\theta_{0,r} - \theta_{2,r}}{2\delta x}$$

instead of

$$\frac{\partial\theta_{0,r}}{\partial x} = \frac{\theta_{1,r} - \theta_{0,r}}{\delta x}$$

This gives the stability condition

$$h\delta x/\kappa > 1$$

Method VI. In this method the new surface equation is suggested:

$$\theta_{0r,} = \frac{\left[2\theta_{0,r-1} + \frac{\delta t D}{(\delta x)^2}\left(8\theta_{1,r} - \theta_{2,r} + \frac{6h\delta x}{\kappa}\theta_A\right)\right]}{\left[2 + \frac{\delta t D}{(\delta x)^2}\left(7 + \frac{6h\delta x}{\kappa}\right)\right]}$$

Taking differentials

$$\Delta\theta_{0,r} = \frac{\left[2\Delta\theta_{0,r-1} + \frac{\delta t D}{(\delta x)^2}(8\Delta\theta_{1,r} - \Delta\theta_{2,r})\right]}{\left[2 + \frac{\delta t D}{(\delta x)^2}\left(7 + \frac{6h\delta x}{\kappa}\right)\right]}$$

Therefore

$$|\Delta\theta_{0,r}| < \frac{\left[2\epsilon_{r-1} + \frac{9\delta t D}{(\delta x)^2}\epsilon'_r\right]}{\left[2 + \frac{\delta t D}{(\delta x)^2}\left(7 + \frac{6h\delta x}{\kappa}\right)\right]}$$

where ϵ'_r is the maximum value of $|\Delta\theta_{m,r}|$ at the internal points of the slab only. Then, since the stability condition for the equation within the solid must hold, $\epsilon'_r < \epsilon_{r-1}$,

and so

$$|\Delta\theta_{0,r}| < \epsilon_{r-1}\left[2 + \frac{9\delta t D}{(\delta x)^2}\right] \Big/ \left[2 + \frac{\delta t D}{(\delta x)^2}\left(7 + \frac{6h\delta x}{\kappa}\right)\right]$$

So the stability condition becomes

$$2 + \frac{9\delta t D}{(\delta x)^2} < 2 + \frac{\delta t D}{(\delta x)^2}\left(7 + \frac{6h\delta x}{\kappa}\right)$$

Therefore

$$9 < 7 + 6h\delta x/\kappa$$

and finally

$$h\delta x/\kappa > \tfrac{1}{3}$$

The stability conditions derived in this paper are sufficient but possibly more than necessary. In considering simple solutions of the heat flow equation, using the finite difference forms investigated here, stability criteria are required for the equation (3), and the equation associated with Methods I and II. In such cases the stability conditions here derived represent extreme or limiting cases of the necessary stability conditions.

For equations associated with Methods V and VI, it would appear that the conditions derived are unnecessary for the stability of the solutions, but they arise because of the strictness of the stability criterion ($\epsilon_{r+1} < \epsilon_r$) used.

4. ACCURACY

An attempt was made to relate the accuracy of the above methods to the approximations made in obtaining the equations. Only boundary condition equations which may be used with equation (3) for the interior of the slab are discussed, as distinct from the equations used in solutions of the Crank and Nicolson type. For different finite difference forms of the boundary condition equation Table 1 gives values of the corresponding error terms, that is:

$$\frac{\text{(Largest term ignored in construction of finite difference expression)}}{\text{(Surface heat flux)}}$$

Table 1. *Error terms in the different methods of representing the boundary condition equation*

Method	*Error term*
I	$\frac{\delta x}{2D}\frac{\partial\theta}{\partial t}\Big/\frac{\partial\theta}{\partial x}$
II	$\frac{(\delta x)^2}{6}\frac{\partial^3\theta}{\partial x^3}\Big/\frac{\partial\theta}{\partial x}$
III	$\frac{(\delta x)^2}{6}\frac{\partial^3\theta}{\partial x^3}\Big/\frac{\partial\theta}{\partial x}$
IV	$\frac{\delta x}{2D}\frac{\partial\theta}{\partial t}\Big/\frac{\partial\theta}{\partial x}$
V	$\frac{(\delta x)^2}{3}\frac{\partial^3\theta}{\partial x^3}\Big/\frac{\partial\theta}{\partial x}$
VI	$\frac{\delta x}{6D}\left[\delta t - \frac{(\delta x)^2}{3D}\right]\frac{\partial^2\theta}{\partial t^2}\Big/\frac{\partial\theta}{\partial x}$

Table 1 illustrates the principle of Method VI, where the difference equation was constructed to make the error term shown as small as possible. In general from Table 1 one would expect the order of accuracy of the different methods to be as follows:

(1) Method VI.
(2) Methods II and III.
(3) Method V.
(4) Methods I and IV.

The predicted errors for the various boundary equations shown in Table 1 were tested by comparing the solutions of a problem, as obtained by the various methods, with the analytical solution of the differential equation. For the interior mesh points the finite difference form of the type shown in equations (3) or (4) was used. The problem chosen, first treated by Crank and Nicolson[1] and later solved by Jaeger[6] is one in which a slab of thermal diffusivity 1 and thickness 2 initially at zero temperature is heated uniformly from both sides by convection.

$$h/\kappa = 4{\cdot}44 \text{ and } \theta_A = 3\,618/4{\cdot}44$$

Thus

$$\frac{\partial\theta}{\partial x} = 0 \text{ at } x = 1$$

$$\frac{\partial\theta}{\partial x} = 4{\cdot}44\theta - 3\,618 \text{ at } x = 0$$

Table 2 shows how the various stability criteria of Section 3 limit the values of the finite differences which may be chosen, and indicates the convenient values used which satisfied the required conditions.

Table 3 gives corresponding results obtained by the different methods at times 6/128 and 21/128 after the start of heating. They are compared with the analytical solution of the differential equation under these conditions. It is seen that the order of accuracy of the different methods, which is very pronounced, is:

(1) Method II, Method III and Method VI [Example (*b*)].
(2) Method VI [Example (*a*) and Method V (Example (*b*)].
(3) Method I.
(4) Method V [Example (*a*)].

It appears that the results agree well with the predictions.

Table 2. *Limiting conditions and chosen values of δx and δt*

Boundary equation	*Condition imposed on δx*	*Value of δx used*	*Value of δt to give stability to interior mesh points*	*Value of δt to give stability to boundary points*	*Value of δt chosen*
Method I	$\delta x \leqslant \frac{2\kappa}{h} = \frac{2}{4{\cdot}44}$	$\frac{1}{8}$	$\delta t \leqslant \frac{(\delta x)^2}{2D} = \frac{1}{128}$	—	$\frac{1}{128}$
Method II	—	$\frac{1}{8}$	$\delta t \leqslant \frac{(\delta x)^2}{2D} = \frac{1}{128}$	$\delta t \leqslant \frac{(\delta x)^2}{D(2 + h\delta x/\kappa)} = \frac{1}{64 \times 2{\cdot}555}$	$\frac{1}{256}$
Method III	—	$\frac{1}{8}$	$\delta t \leqslant \frac{(\delta x)^2}{2D} = \frac{1}{128}$	—	$\frac{1}{128}$
Method V	$\delta x \geqslant \frac{\kappa}{h} = \frac{1}{4{\cdot}44}$	$\frac{1}{4}$	$\delta t \leqslant \frac{(\delta x)^2}{2D} = \frac{1}{32}$	—	$\frac{1}{32}$ — (*a*) $\frac{1}{64}$ — (*b*)
Method VI	$\delta x \geqslant \frac{\kappa}{3h} = \frac{1}{3 \times 4{\cdot}44}$	$\frac{1}{8}$	$\delta t \leqslant \frac{(\delta x)^2}{2D} = \frac{1}{128}$	—	$\frac{1}{128}$ — (*a*) $\frac{1}{256}$ — (*b*)

Table 3. *Comparison of an analytical solution with corresponding solutions obtained by the different methods*

	$x =$	0	0·125	0·25	0·375	0·5	0·625	0·75	0·875	1·0
	Analytical	458	281	156	75	32	11	3	1	0
After	Method I (after 6 δt)	427	262	128	64	17	7	0	0	0
	Method II (after 12 δt)	463	285	155	74	30	10	3	1	0
Time	Method III (after 6 δt)	461	286	157	75	29	9	2	0	0
	Method V Example (*a*) (after 1·5 δt)			ACCURATE INTERPOLATION NOT POSSIBLE						
6	Method V Example (*b*) (after 3 δt)	455		147		22		0		0
$\frac{}{128}$	Method VI Example (*a*) (after 6 δt)	447	267	135	62	19	6	0	0	0
	Method VI Example (*b*) (after 12 δt)	454	275	147	68	27	9	3	1	0
	Analytical	586	466	359	269	196	137	98	77	68
	Method I (after 21 δt)	579	456	351	256	187	127	92	66	62
After	Method II (after 42 δt)	589	469	361	269	195	139	99	76	69
	Method III (after 21 δt)	589	468	362	269	195	138	99	75	68
time	Method V Example (*a*) (by interpolation at 5·25 δt)	576		345		176		75		45
21	Method V Example (*b*) (by interpolation									
$\frac{}{128}$	at 10·5 δt)	582		355		189		94		63
	Method VI Example (*a*) (after 21 δt)	586	464	356	263	189	131	93	69	63
	Method VI Example (*b*) (after 42 δt)	589	467	359	267	193	136	97	74	67

These solutions also emphasize the importance of using an analytical solution for a semi-infinite solid to obtain good values for the temperatures at time $t = \delta t$. This was not done in the above solutions and consequently some of them (Methods I, III, IV, V, and VI) were exceptionally inaccurate for small values of time.

Equation (3) applied in the interior of the slab has an error term of

$$\frac{1}{2}\left[\delta t - \frac{(\delta x)^2}{6D}\right]\frac{\partial^2\theta}{\partial t^2}\Big/\frac{\partial\theta}{\partial t} \qquad (12)$$

This is to be compared with the corresponding error term for the equations of Crank and Nicolson, which are always stable, namely

$$\frac{1}{12}\frac{(\delta x)^2}{D}\frac{\partial^2\theta}{\partial t^2}\Big/\frac{\partial\theta}{\partial t} \text{ within the solid} \qquad (13)$$

and

$$\frac{1}{2\delta x}\left[\delta t - \frac{(\delta x)^2}{D}\right]\frac{\partial\theta}{\partial t}\Big/\frac{\partial\theta}{\partial x} \text{ on the surface} \qquad (14)$$

For the case of prescribed surface temperature, expression (12) suggests that equation (3) might have advantages since the choice of δt and δx can make the expression equal to zero. For a heat flux boundary, however, the advantages of expression (12) might be outweighed by Crank and Nicolson's method where expression (14) can be made equal to zero.

Putting $\gamma = \delta t/(\delta x)^2$ the corresponding formal solutions of the finite difference equations are:

From equation (3),

(i) $t + x^2/2$

(ii) $t^2 + x^2t + x^4/12 + (\delta x)^2(\frac{1}{6} - \gamma)(a^2 - x^2)/2$.

By Crank and Nicolson's method,

(i) $t + x^2/2$

(ii) $t^2 + x^2t + x^4/12 + (\delta x)^2(a^2 - x^2)/12$

Thus, both solutions are correct for case (i) where surface temperature is linear in time. For case (ii), equation (3) is correct for $\gamma = \frac{1}{6}$ and the Crank and Nicolson solution is high by an amount independent of time. These conclusions conform with the characters of equations (12) and (13).

5. THE HEAT FLOW COMPUTOR[5]

This is an electrical analogue which uses a resistance capacity network. Von Neumann's technique shows that it is always stable, and the error terms in the difference equations are:

Within material $\frac{1}{12}\frac{(\delta x)^2}{D}\frac{\partial^2\theta}{\partial t^2}\Big/\frac{\partial\theta}{\partial t}$

Table 4. *Comparison of results of a problem as solved by Crank and Nicolson and by Method II*

	$x =$	0	0·125	0·25	0·375	0·5	0·625	0·75	0·875	1·0
After time	Crank and Nicolson's									
6	solution	459	283	156	76	33	12	4	1	0
128	Method II	463	285	155	74	30	10	3	1	0
After time	Crank and Nicolson's									
21	solution	587	468	361	269	194	138	98	75	66
128	Method II	589	469	361	269	195	139	99	76	69

Table 4 shows the solution of the previous problem obtained using Crank and Nicolson's equations and these are compared with results given in Table 2 for a solution obtained using the boundary condition equation of Method II with equation (3) for the temperatures in the interior of the slab. The values of δt used were 1/128 and 1/256 respectively. In both cases δx was the same, and similar times were required to compute the two solutions.

A further indication of accuracy in the case of prescribed surface temperature may be found by comparing the analytical solutions of the finite difference scheme of equation (3) and that of Crank and Nicolson, with the true solution for two simple cases.

For a region $-a \leqslant x \leqslant +a$ with unit diffusivity, if the surface temperatures for the two cases are given by:

(i) $t + a^2/2$

(ii) $t^2 + a^2t + a^4/12$

the final temperature distributions, independent of initial conditions are then

(i) $t + x^2/2$

(ii) $t^2 + x^2t + x^4/12$

For a boundary heat flux $\frac{(\delta x)^2}{6}\frac{\partial^3\theta}{\partial x^3}\Big/\frac{\partial\theta}{\partial x}$

The formal solutions of the two problems with prescribed surface temperature are:

(i) $t + x^2/2$

(ii) $t^2 + x^2t + x^4/12 + (\delta x)^2(a^2 - x^2)/12$

6. CONCLUSIONS

A new method of deriving a condition for stability has been presented, which can be applied directly to cases of heat flow involving variable diffusivity and complicated heat flux boundary conditions. The method might be expected to give over-strict conditions, but in cases where the comparison is possible, it has been found to agree with those of von Neumann.

Attention has been drawn to the possible adverse effects of heat flux boundary conditions on stability. In most cases, a restriction on δx is involved in addition to one on $\delta t/(\delta x)^2$, but in the case of Method II a stronger restriction is imposed on $\delta t/(\delta x)^2$ and no independent limitation is placed on δx.

The accuracy of six different methods of allowing for heat

flux boundary conditions has been discussed, including a new one which was expected to be an improvement on the others, and which has been shown to be as good as any of the other methods in the example considered.

It also appears that equation (3), used in conjunction with the boundary condition equation of Method II is as accurate as any other method. On a time and labour basis it was found from experience to be no more expensive than the method of Crank and Nicolson. This combination of equation (3) for the interior mesh points with the type of boundary equation of Method II was therefore used in a large range of ingot heating investigations, the results of which will be published shortly.

7. ACKNOWLEDGEMENTS

The authors wish to thank Professor R. J. Sarjant for the advice and encouragement he has given in the course of this work and Professor D. R. Hartree for his valuable criticisms.

REFERENCES

(1) CRANK, J., and NICOLSON, P. *Proc. Camb. Phil. Soc.*, **43**, p. 50 (1947).
(2) RICHARDSON, L. F. *Phil. Trans Roy. Soc.* (*A*), **210**, p. 307 (1910).
(3) SCHMIDT, E. *Föppls Festschrift*, p. 179 (Berlin: Springer, 1924). Abstr. in McAdams, W. H., *Heat Transmission*, p. 39 (New York: McGraw-Hill Book Co. Inc., 1942).
(4) O'BRIEN, G. G., HYMAN, M. A., KAPLAN, S. *J. Math. Phys.*, **24**, p. 223 (1951).
(5) EYRES, N. R., HARTREE, D. R., INGHAM, J., JACKSON, R., SARJANT, R. J., and WAGSTAFF, J. B. *Phil. Trans Roy. Soc.* (*A*), **240**, p. 1 (1946).
(6) JAEGER, J. C.: *Proc. Camb. Phil. Soc.*, **46**, p. 634 (1950).

The production of specimen mounting grids for the electron microscope*

By C. E. CHALLICE, B.Sc., Ph.D., A.Inst.P.,† and C. D. SUTTON, National Institute for Medical Research, Mill Hill, London, N.W.7

[*Paper received* 24 *June*, 1952]

A photographic etching technique has been used to produce specimen mounting grids for electron microscopy. The method may be used to produce grids of any desired shape or size.

In commercially produced grids for electron microscope specimen supports, the ratio of hole area : grid wire area is about 1 : 3. This means that three-quarters of the specimen is not available for examination in the microscope, a great disadvantage when examining tissue sections. Grids have been made by a simple modification of the photo-engraving process, and it has been found possible to reduce the proportion of specimen obscured by wire without unduly weakening the grid. In addition, the process enabled some experimental mesh designs to be tried. This process has the advantage over the electrodeposition method of Loening and Gresham,[1-4] in that no equipment not normally found in any electron microscope laboratory is used. Techniques similar to the one which we have used were employed in the production of gun sight graticules at the L.C.C. School of Photo-engraving.[5-7]

Several grid designs were drawn out, about six inches in diameter, and photographically reduced to 3 cm (Fig. 1); 350 prints were made, mounted on a board 20 × 30 in and photographed such that the size of the grid on the negative was that of the required electron microscope specimen support (Fig. 2). In this case it was found advantageous to make a second negative smaller than the standard $\frac{1}{4}$ in diameter to fit the Siemens electron microscope which takes a specimen of 3 mm diameter maximum.

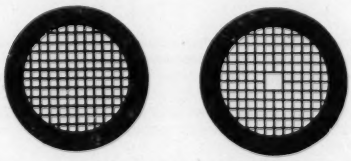

Fig. 1. Two typical grid designs

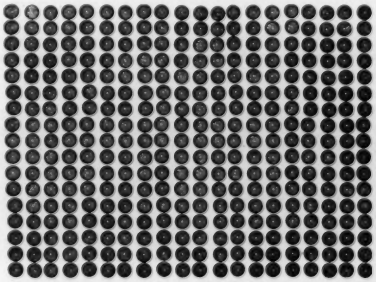

Fig. 2. Reproduction of a contact print from the master negative

The sensitized process engraving glue mixture which was used requires to be prepared some hours before use and this may not be kept for more than three days. The mixture was made up in the following proportions:

Process glue	1 part
Water	1 part
5% ammonium dichromate	1 part
0·880 ammonia	0·01 part

Copper foil 1/1000 in thick was supported on a glass plate

* This paper was read at the Bristol Conference of the Electron Microscopy group of The Institute of Physics, 17 September, 1952.
† Now at Wright–Fleming Institute of Microbiology, St. Mary's Hospital, London, W.2.

and secured by bending the edges over. The foil was coated with a thin and even layer of dichromated glue, by means of a "whirler," which was improvised from a drill brace, and a strip of metal bent to a Y-shape, the glass and foil being clipped to the arms of the Y and the stem held in the chuck.

The surface to be coated was cleaned under water by grinding with a piece of polishing charcoal. The dichromated glue was poured on to the metal, spread out, and the excess poured off and whirled, face down, at 600 r.p.m. and dried while being whirled at 150 r.p.m. over a hot plate, care being taken not to heat the foil above 50° C. The foil was then taken from the glass plate and any bent edges removed with a guillotine. To ensure good contact between negative and foil in the printing frame, a thin sheet of sponge rubber was placed behind the foil which was then exposed to ultra-violet light.* It was then developed in cold water for two minutes and stained in a 1% methyl violet solution.

After the foil had been dried the glue was "burnt in" by heating to 280° C on an electric hot plate set at medium heat. During this process the image becomes grey, as the dye is destroyed, then light yellow, red-brown and finally chocolate. The heating should be stopped at the red-brown stage. When cool, the back and edges were coated with a cellulose lacquer and allowed to dry. Finally, the foil was etched in a 20% aqueous solution of ferric chloride in the presence of a trace of hydrochloric acid, and during the etching it was found advisable to brush the foil gently with a camel hair brush to ensure an even etch. The last stages of the etching process were checked with a low power hand lens. The process was complete when the pattern of the grids could be seen in copper on a background of the cellulose film used as backing. This was removed with acetone, when the grids became free, and the glue washed off with warm dilute hydrochloric acid solution. By prolonging the etching it was found that the holes became rounded, but provided the narrowest parts of the grid wires were not less than one eighth of the width of the space, this was not found detrimental to the strength of the grid, while the added useful space was of considerable advantage. The most useful mesh was found to be about 100–150 wires per in. It was found possible by this method, once the negatives had been made, for one person to make 2000 grids in one hour. The whole process is closely allied to ordinary photographic engraving.

* Using a Hanovia sun lamp, at a distance of one foot for five minutes.

REFERENCES

(1) Loening, E. E. *Process Engravers' Monthly*, **57**, p. 266 (1950).
(2) Loening, E. E. *Process Engravers' Monthly*, **57**, p. 297 (1950).
(3) Loening, E. E., and Gresham, D. C. *Process Engravers' Monthly*, **57**, p. 358 (1950).
(4) Loening, E. E., and Gresham, D. C. *Brit. J. Phot.*, **98**, p. 612 (1951).
(5) Bull, A. J., and Cartwright, H. M. *Photogr. J.*, **87B**, p. 43 (1947).
(6) Smith, F. H. *Photogr. J.*, **88B**, p. 18 (1948).
(7) Cox, R. S., and Hallam, C. D. *Photogr. J.*, **88B**, p. 70 (1948).

Absorption and scattering of radiation by water sprays of large drops

By P. H. Thomas, M.A., Ph.D., Fire Research Station, Boreham Wood, Herts.

[*Paper received 5 September*, 1952]

An investigation of the efficiency of water sprays in the protection of buildings and fire-fighting personnel from heat radiation has resulted in a general theoretical study of the transmission of radiation through a layer of water spray of large drops. The treatment is based upon the work of Theissing(1) and takes account of multiple refractive scattering in dense sprays and extends the method to absorbing sprays.

The problem of the single drop is approached from the point of view of geometric optics, from which approximate expressions are derived for the absorption of a drop in terms of the absorption index for any given wavelength and for the angular distribution of radiation transmitted by a single drop. Since the absorption of thermal radiation depends markedly on the drop size it is found that the transmission of such radiation departs from the simple exponential extinction law when the drops and the quantities of water in the sprays are small. When the drops are less than about 0·005 cm in diameter, back reflexion by the spray may become significant.

This work was started in order to investigate the efficiency of water sprays in the protection of buildings and fire-fighting personnel from heat radiation. It was felt that the principles would have more general application and that a useful purpose would be served in presenting the theoretical analyses of scattering and absorption by water sprays for publication.

The reduction in radiation intensity due to a layer of particles is usually described by the extinction formula, known as the Lambert–Beer law which can be written as

$$T = \exp(-qNd) \qquad (1)$$

where T is the transmission of unit intensity,
q is the extinction or "total scattering" cross-section of a single particle,
N is the number of particles per unit volume,
d is the thickness of the layer.

This law is valid only when (*a*) the drops are totally absorbing, and (*b*) when, if they are not totally absorbing, the scattered radiation is excluded, i.e. the formula is restricted to the direction of propagation (Skinner and Boas-Traube(2)).

In the case of light scattering absorption is usually neglected. On the other hand, in the transmission of thermal radiation the drops may be almost totally absorbing if they are large enough. Because the absorption depends on the drop size as well as on the wavelengths of the radiation, no restriction is placed in this analysis on the absorption nor on the "density" of the spray. Since the drops are large, diffraction has been neglected but multiple refractive scattering has been taken into account. An infinite layer of spray is considered to be close to an infinite radiator parallel to the spray. Both the spray and the radiator are considered to be perpendicular to

the x axis such that the planes $x = o$ and $x = d$ are the boundaries of the spray (Fig. 1).

It is assumed throughout that the drops forming the spray are large compared with the wavelength of the incident radiation or, in other words, that we may neglect the energy from the panel which is of a wavelength greater than a certain fraction of the drop size. The arrangement of drops in the spray is assumed to be random and the distances between

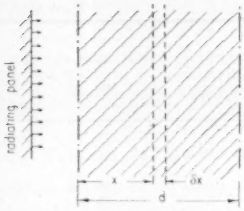

Fig. 1. Cross-section of spray and panel. Both the spray and panel are infinite in the zy directions

them are assumed large compared with the size of the drops so that phase interaction and interference phenomena may be neglected. The basis of the treatment used below is that the radiation passing through the spray is intercepted by water drops, which absorb some of it and scatter the remainder in all directions, some forwards and the rest backwards. The total radiation crossing any infinite section of the spray is then considered to be made up of two fluxes travelling in opposite directions. It is then possible to establish continuity equations between the fluxes (Schuster[3]).

A refinement introduced by Theissing[1] however, separates each major flux into components, according to the number of times the radiation has been scattered. Such a procedure is theoretically necessary because the ratio of the radiation scattered forwards to that scattered backwards is not necessarily unity as in Rayleigh scattering,[3] but depends on the drop size and on the number of scatterings the flux has already undergone. Hitherto absorption has been represented by an overall macroscopic index[1,3,4,5]. In this paper, however, absorption is expressed, more conveniently, by a fraction—the ratio of radiation absorbed by a drop to that incident upon it.

The first part of the paper deals with the evaluation of the forward and backward scattering fractions and the absorption fraction. In the second part these results are used in the general flux equations to evaluate the transmission, absorption and reflexion of the spray.

GENERAL THEORY OF THE ANGULAR DISTRIBUTION FUNCTIONS

Of the radiation incident upon a drop a fraction f is absorbed and a fraction $(1 - f)$ is scattered. This scattered radiation is distributed angularly. To describe this distribution, which depends on the number of scatterings m undergone by the radiation, a function $l_m(\phi)$ is introduced, so that the radiation scattered into a unit solid angle inclined at ϕ to the direction of propagation is a fraction $l_m(\phi)$ of the total scattered radiation of the mth order. From this definition

$$2\pi\int_0^{\pi} l_m(\phi)\sin\phi d\phi = 1 \tag{2}$$

Following Theissing we now define v_m and h_m as the fractions of radiation entering the forward and backward half-spaces respectively for the mth scattering.

Thus
$$v_m = 2\pi\int_0^{\pi/2} l_m(\phi)\sin\phi d\phi \tag{3}$$

and
$$h_m = 2\pi\int_{\pi/2}^{\pi} l_m(\phi)\sin\phi d\phi = 1 - v_m \tag{3a}$$

Since $l_m(\phi)$ is the scattering angular distribution function for a single drop it is clear that if the angular distribution of the radiation of order $(m-1)$ is independent of x then the angular distribution of the radiation of order m is also independent of x and is given by $l_m(\phi)$. It is assumed in this work that the angular distributions of the forward and backward m radiation can be so regarded.

If two further assumptions are made, simple recurrence relations may be found for $l_m(\phi)$. These assumptions are that a drop can be considered to be sufficiently distant from the edges of the spray to be totally surrounded by water, and that in the neighbourhood of a drop, the variation with x of the forward and backward fluxes may be neglected.

Then if $l^*(\gamma)$ is defined as the scattering function for the scattering from a pencil of rays we have

$$l_m(\phi) = \int_0^{2\pi} d\psi' \int_0^{\pi} l_{m-1}(\phi')l^*(\gamma)\sin\phi' d\phi' \tag{4}$$

where γ is the angle between the two vectors ϕ, ψ and ϕ', ψ' (in spherical angular co-ordinates). This equation is similar to that given by Hartel[4] except that $l^*(\gamma)$ is replaced by $l_1(\gamma)$. The difference is that in the case we are considering the incident radiation reaches a drop uniformly from all directions in one half-space.

Thus we have

$$l_1(\phi) = \frac{1}{2\pi}\int_0^{2\pi} d\psi \int_0^{\pi/2} l^*(\gamma)\sin\phi' d\phi' \tag{5}$$

(see also Ryde[5]).

Solutions to equations such as these are developed by expanding $l^*(\gamma)$ as a series of Legendre polynomials.[4]

Since $l^*(\gamma)$ satisfies an equation similar to equation (2) such an expression can be written as

$$l^*(\gamma) = \frac{1}{4\pi}\left[1 + \sum_1^{\infty} a_n P_n(\cos\gamma)\right] \tag{6}$$

i.e.
$$a_n = 2\pi(2n+1)\int_0^{\pi} l^*(\gamma)P_n(\cos\gamma)\sin\gamma d\gamma \tag{6a}$$

From elementary theory we now find[4]

$$l_m(\phi) = \frac{1}{4\pi}\left[1 + \sum_1^{\infty} \frac{(a_n)^m}{(2n+1)^{m-1}} p_n P_n(\cos\phi)\right] \tag{7}$$

where
$$p_n = \int_0^{\pi/2} P_n(\cos\theta)\sin\theta d\theta \tag{8}$$

Hence from equation (2)

$$v_m = 1 - h_m = \tfrac{1}{2}\left[1 + \sum_1^{\infty} \frac{(a_n)^m}{(2n+1)^{m-1}} p_n^2\right] \tag{9}$$

Where the incident radiation is from one direction only[4]

the expression for $I_m(\phi)$ is as in equation (7), except that the term p_n is excluded. Similarly the corresponding expression for v_m contains p_n to the first power only.

For large values of m, $I_m(\phi)$ approaches $1/4\pi$ and v_m approaches h_m approaches $\frac{1}{2}$. That is to say the scattering becomes progressively more diffuse. If the solid angle subtended by the radiator at a point in the spray is small the forward scattering is greater. The values of v_m and h_m then converge to the value $\frac{1}{2}$ more slowly.

THE EVALUATION OF f AND $I^*(\gamma)$ IN TERMS OF THE ABSORPTION INDEX FOR THE LIQUID DROP

In order to find v_m and h_m we require to know $I^*(\gamma)$. The fractional absorption f will also be required in evaluating the transmission of the spray. Both f and $I^*(\gamma)$ are established below by the methods of geometric optics.

(*a*) *The absorption fraction f.* If radiation falls on a spherical drop, the fraction absorbed from a parallel flux is clearly the same whatever the orientation of the radiation.

If the use of geometric optics is permissible for large drops we can superimpose any number of distributions of such fluxes to correspond with any given distribution of incident radiation without altering the value of f. We shall therefore consider a parallel flux of radiation. Fig. 2 is a section of a drop with radiation of intensity H incident on it, from one direction only.

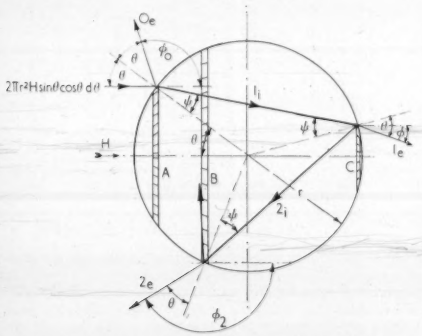

Fig. 2. This sketch shows the internal paths 1, 2, 3, etc., the external paths $O_e 1_e 2_e$, etc., and the emergent angles $\phi_0\phi_1\phi_2$, etc., for a pencil of radiation falling on an elementary area

The effect of absorption on the reflexion and transmission coefficients and the refractive index is neglected. The reflexion coefficient R_0 for a ray entering the denser medium of the drop is equal to the reflexion coefficient on emergence, where the angles of incidence and emergence are interchanged. Similarly, T_0 is the transmission coefficient for a ray making an angle θ with the outward normal to the drop surface, both when entering and leaving the drop. We then have

$$T_0 + R_0 = 1 \tag{10}$$

Let k be the absorption index such that the intensity falls by a fraction $\exp(-k)$ for unit absorbing path.

The energy flux just inside the elementary surface A for which the angle of incidence is everywhere equal to θ is given by

$$HT_0 2\pi r^2 \sin\theta\cos\theta\delta\theta$$

where H is the intensity of the parallel flux of radiation. The lengths of the internal paths 1_i, 2_i, 3_i are equal and given by $2r\cos\psi$. Hence the energy absorbed in path 1_i is

$$HT_0 2\pi r^2 \sin\theta\cos\theta[1 - \exp(-2kr\cos\psi)]\delta\theta$$

The intensity before reflexion at B is reduced by $\exp(-2kr\cos\psi)$ and after reflexion it is reduced by $R_0\exp(-2kr\cos\psi)$. Hence the total energy absorbed from that incident on A, putting $\alpha = -2kr\cos\psi$, is

$$\sum_0^\infty HT_0R_0^n 2\pi r^2 \sin\theta\cos\theta\,[1 - \exp(\alpha)][\exp(n\alpha)]d\theta$$

$$= HT_0 2\pi r^2 \sin\theta\cos\theta\,\frac{1 - \exp(\alpha)}{1 - R_0\exp(\alpha)}d\theta$$

Since the total incident energy is $\pi r^2 H$, the fraction absorbed is

$$f = \int_0^{\pi/2} T_0 \sin 2\theta\,\frac{1 - \exp(\alpha)}{1 - R_0\exp(\alpha)}d\theta \tag{11}$$

T_0 and R_0 for unpolarized radiation can be compounded from the values for plane and perpendicularly polarized radiation,

$$R_0 = \tfrac{1}{2}(R_\perp + R_\parallel) \tag{12}$$

where $R_\perp$ and $R_\parallel$ are given by Fresnel's formulae

i.e. $$R_\perp = [\sin^2(\theta - \psi)]/[\sin^2(\theta + \psi)] \tag{13}$$

and $$R_\parallel = [\tan^2(\theta - \psi)]/[\tan^2(\theta + \psi)] \tag{14}$$

where $\parallel$ and $\perp$ denote plane and perpendicular polarization. We also have the refractive law

$$\sin\theta = \eta\sin\psi \tag{15}$$

where η is the refractive index which is equal to 1·33 in the range considered, i.e. wavelengths less than 15 μ.

From the above formulae f has been evaluated by a series of graphical integrations as a function of kr and is shown in Fig. 3. For high values of kr, f reaches a limiting value of 0·95. This is only true if kr is large by virtue of r being large. If on the other hand k is large the reflexion coefficient R will

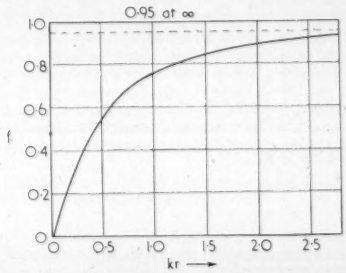

Fig. 3. The fraction f of the incident radiation absorbed by a drop as a function of the absorption index k and the radius r

be reduced, thus raising the value of f towards unity. In any case the error for large values of kr will not exceed 5%.

It is, of course, possible to establish a more approximate expression for f in the following manner. The reduction in intensity in an absorbing path p is $\exp(-kp)$ and the amount absorbed $1-\exp(-kp)$ for unit intensity. The mean absorbing path in a sphere must be of the order ϵr where ϵ lies between 1 and 2. A close approximation between this type of expression and the graph in Fig. 3 is obtained by putting

$$f = 0{\cdot}95[1 - \exp(-1{\cdot}75\,kr)] \tag{16}$$

The factor 0·95 represents a mean transmission coefficient for the incident and emergent surfaces of the drop.

Alternatively, if the surface of the drop is regarded as a radiator of diffuse flux, absorption by a sphere, as given by Nusselt[6] is

$$f = 1 + \frac{2\exp(-2kr)}{(2kr)} - \frac{2[1-\exp(-2kr)]}{(2kr)^2} \tag{17}$$

to which

$$f \simeq 1 - \exp(-1{\cdot}33kr) \tag{18}$$

is a reasonable approximation.

(*b*) *The scattering function* $I^*(\phi)$. From Fig. 2 we can write down the emergent angles for the emerging components of a ray incident on the elementary surface A.

$$\phi_0 = \pi - 2\theta \tag{19}$$

$$\phi_1 = 2(\theta - \psi) \tag{20}$$

$$\phi_s = 2\theta - 2s\psi + (s-1)\pi \tag{21}$$

Consider the emergent path O_e. The intensity/unit solid angle expressed as a fraction of the total incident parallel flux is

$$i_0(\phi_0) = \frac{2\pi r^2 H R_0 \sin\theta\cos\theta\delta\theta}{2\pi^2 r^2 H \sin\phi_0\delta\phi_0} \tag{22}$$

$$= R_0/4\pi \qquad \text{from (19)}$$

Similarly for the path 1_e

$$i_1(\phi_1) = \frac{T_0^2\exp(-2kr\cos\psi)\sin 2\theta}{2\pi\sin\phi_1}\frac{d\theta}{d\phi_1} \tag{23}$$

and in general

$$i_s(\phi_s) = \frac{T_0^2 R_0^{s-1}\exp(-2krs\cos\psi)\sin 2\theta}{2\pi\sin\phi_s}\left|\frac{d\theta}{d\phi_s}\right| \tag{24}$$

$(s = 2, 3, \text{etc.})$

where $||$ denotes the positive value. The components i_s ($s = 2, 3$, etc.) decrease rapidly with s except at certain angles where infinite values occur owing to the fact that for $s = 2, 3$, etc., $d\theta/d\phi_s$ becomes infinite at a certain angle $\bar{\phi}_s$. The total energy, however, in these components is finite and is less than 5% of the total (see Appendix I). When each component i_s has been evaluated separately as a function of the same angle we have

$$I^*(\phi) = \left[\sum_0^\infty i_s(\phi)\right]/(1-f) \tag{25}$$

$I^*(\phi)$ has been plotted in Fig. 4 for zero absorption. The methods of computation and the values of a_n and hence of v_m are given in Appendix I. The values of v_m and h_m are shown in Fig. 5 from which it is seen that the variation with kr is slight.

This treatment has been given by Wiener[7] and more recently by Shifrin[8] but without considering absorption. Shifrin's calculations cover both directions of polarization for values of s up to 10.

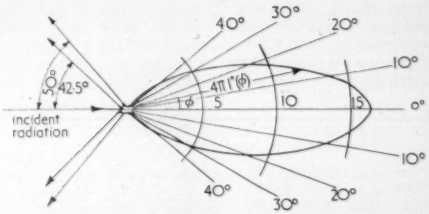

Fig. 4. $4\pi I^*(\phi)$ is shown for a non-absorbing drop. The high intensities in the backward direction occur at the first and second rainbow angles. Detailed numerical values for the function are given by Shifrin[8]

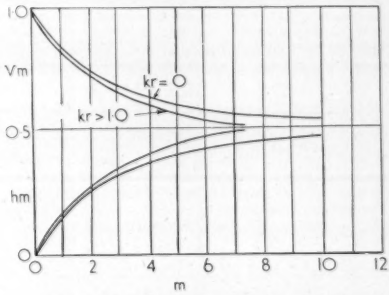

Fig. 5. The computed values of v_m and h_m

GENERAL THEORY OF THE RADIATION FLUXES

We now consider a spherical drop of radius r in the path of a radiation from an infinite plane radiator. It is shown in Appendix II that for this condition the amount of radiation intercepted is $2\pi r^2$ times the intensity. This result is obtained from a simple application of Lambert's cosine law and the inverse square law and is a reasonable assumption for drops whose diameter is greater than ten times the radiation wavelength. Hence, if the intensity of unscattered radiation is $Q_0(x)$ an amount $2\pi r^2 Q_0(x)$ is intercepted by each drop. If N is the number of drops/unit volume of spray, the number of drops in a layer of thickness δx is $N\delta x$ per unit area. Therefore the loss of intensity of unscattered radiation is

$$-\delta Q_0 = 2\pi r^2 Q_0 N\delta x$$

i.e.

$$\frac{1}{qN}\frac{dQ_0}{dx} + Q_0 = 0 \tag{26}$$

where

$$q = 2\pi r^2$$

If the total intensity incident on the spray at $x = o$ is denoted by I then

$$Q_0 = I \text{ at } x = o$$

Therefore

$$Q_0 = I\exp(-qNx) \tag{27}$$

For simplicity we shall also use $2\pi r^2$ for the value of the extinction cross-section q for the scattered fluxes, which are no longer plane waves. Consider the elementary layer δx. From the unscattered flux an amount $qNQ_0\delta x$ is intercepted. Of this $v_1(1-f)qNQ_0\delta x$ is scattered forwards and is the gross increment in Q_1, the once scattered forward radiation. Of Q_1, however, $qNQ_1\delta x$ is intercepted, so that the net gain in Q_1 is

$$\delta Q_1 = v_1(1-f)qNQ_0\delta x - qNQ_1\delta x$$

i.e.
$$\frac{1}{qN}\frac{dQ_1}{dx} + Q_1 = v_1(1-f)Q_0 \qquad (28)$$

Hence
$$Q_1 = v_1 I(1-f)qNx\exp(-qNx) \qquad (28a)$$

In general

$$\frac{1}{qN}\frac{dQ_m}{dx} + Q_m = v_m(1-f)Q_{m-1} + h_m(1-f)P_{m-1} \qquad (29)$$

where Q_m is the mth forward component, and P_m is the mth backward component.

Similarly

$$\frac{1}{qN}\frac{dP_m}{dx} - P_m = -h_m(1-f)Q_{m-1} - v_m(1-f)_{m-1} \qquad (30)$$

The boundary conditions are

$$Q_m = Q_m(0) = 0 \text{ at } x = o \quad m \neq o$$
$$P_m = P_m(d) = 0 \text{ at } x = d$$

The total emergent radiation is

$$\sum_0^\infty Q_m(d)$$

so that
$$T = \frac{1}{I}\sum_0^\infty Q_m(d) \qquad (31)$$

can be defined as the transmission of the spray, where I is the incident intensity at $x = 0$.

The reflectivity of the spray is, similarly

$$R = \frac{1}{I}\sum_0^\infty P_m(0) \qquad (32)$$

It is readily seen that the fraction of radiation absorbed by the spray is

$$A = 1 - T - R \qquad (33)$$

It is apparent from equations (29) and (30) that Q_m and P_m are proportional to $(1-f)^m$. The values of Q_m and P_m, taken from Theissing's paper,[1] which, but for the absence of the absorption term, gives equations identical with (29) and (30), must therefore be multiplied by $(1-f)^m$.

The analytic solutions for $Q_m(d)$ are given in Appendix III for $m \leqslant 3$.

Since for small values of qNd the series for T in equation (31) converges rapidly (i.e. for sprays in which N or d is small, only the first few orders of scattering need be considered) it is possible to use these expressions for $Q_m(d)$ to give T in terms of v_m and f.

For large values of qNd, however, the computation of the terms becomes too laborious and some simplifications are necessary.

We already have the result

$$T = \exp(-qNd)$$

from equation (27) for a spray in which each drop is totally absorbing. We shall therefore next consider the other extreme case of a non-absorbing spray.

Let
$$F = \sum_0^\infty Q_m$$
$$B = \sum_0^\infty P_m \quad (P_0 = 0)$$
$$y = qNx$$
$$D = qNd$$

From equations (29) and (30) we have

$$\frac{dB}{dy} = \frac{dF}{dy} = \tfrac{1}{2}(B-F) + \sum_0^\infty (v_{m+1} - \tfrac{1}{2})(Q_m - P_m) \qquad (34)$$

The solution to these equations is shown in Appendix IV to be

$$T(1 + D/2) = 1 + R_1 + \frac{1}{I}\sum_{m=1,2,3\ldots} R_m[P_{m-1}(0) - Q_{m-1}(D)] \qquad (35)$$

where

$$R_m = (v_m - \tfrac{1}{2})[1 + (2v_{m+1} - 1) + (2v_{m+1} - 1)(2v_{m+2} - 1) \text{ etc.}]$$

For large values of D, $(v_m - \tfrac{1}{2})Q_{m-1}(D)$ approaches zero for all values of m. Values of $P_m(0)$ for large values of D are given by Theissing. For $m \leqslant 5$ these are listed in Appendix III. The final result after substituting for v_1, v_2, etc., is

$$T \simeq 1{\cdot}60/(1 + D/2) \qquad (36)$$

If the incident radiation is a parallel flux the increased values of v_1, v_2, etc., lead to the result

$$T \simeq 2{\cdot}27/(1 + D/2)\dagger \qquad (37)$$

The solution to the general problem with arbitrary values of f and v_m is clearly most cumbersome. It is sufficient in this work to consider the case where the forward and backward scatterings are equal (i.e. $v_m = \frac{1}{2}$) and to compare the analytic result with the above results for the two special cases discussed above. In this way an approximate correction can be established.

If v_m is thus equal to $\frac{1}{2}$ in equations (29) and (30) we obtain the equations

$$\frac{dF}{dy} = -\tfrac{1}{2}(1+f)F + \tfrac{1}{2}(1-f)B \qquad (38)$$

$$\frac{dB}{dy} = -\tfrac{1}{2}(1+f)B - \tfrac{1}{2}(1-f)F \qquad (39)$$

where
$$F = I \text{ at } y = O$$

and
$$B = O \text{ and } F = TI \text{ at } y = D$$

We thus obtain the result

$$T = \sqrt{f}[\tfrac{1}{2}(1+f)\sinh D\sqrt{f} + \sqrt{f}\cosh D\sqrt{f}]^{-1} \qquad (40)$$

Clearly when $f = 1$ we have equation (1) again and as f approaches zero we have in the limit

$$T = 1/(1 + D/2) \qquad (41)$$

We can therefore say that the preferential forward scattering increases the spray transmission by an amount which increases

† For this case the value of q and consequently of D is reduced by 2 since the geometric extinction cross-section is then πr^2 not $2\pi r^2$.

with the parameter D. There is no increase when the drops are totally absorbing but when the absorption is zero the increase is greatest. For a near source this maximum increase is about 60% and for a distant source about 130%.

It must be mentioned that there is an error in Theissing's paper. To evaluate T for large values of D, a condition was introduced stating that the intensities of the forward and backward fluxes in the 90° direction were equal. The way that this was stated

$$\text{i.e.} \qquad \sum_0^\infty Q_m(d)\frac{I_m(90^\circ)}{v_m} = \sum_1^\infty P_m(0)\frac{I_m(90^\circ)}{h_m} \qquad (42)$$

leads to the incorrect result $T = \frac{1}{2}$ for large D and $f = 0$.

THE TRANSMISSION T FOR A GIVEN SPRAY

For small values of qNd, T is evaluated from equation (31). The results for various values of kr are shown in Fig. 6(a). The dotted curves show the relationship given by equation (40).

The curves in Fig. 6(b) are extrapolations of those in Fig. 6(a). They have been drawn so that the deviation from the values given by equation (40) increases as kr decreases. Clearly where the absolute value of T is small so also is the absolute error and this is of little concern here. The curve for kr equal to zero is asymptotic to equation (36).

$$\text{Now} \qquad qNd = 2\pi r^2 Nd = \frac{3}{2}\left(\frac{4\pi}{3}r^3N\right)\frac{d}{r}$$

$$= \frac{3}{2}V\frac{d}{r} \text{ or } \frac{C}{r} \qquad (43)$$

where V is the volume of water/unit volume of spray. T can then be plotted as a function of r for various values of C and k [Fig. 7 (a and b)].

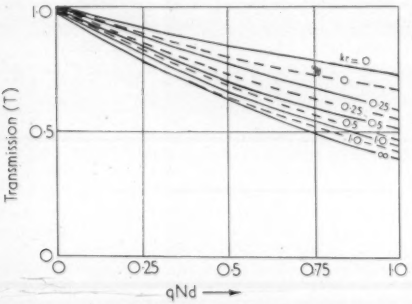

Fig. 6(a). The transmission T as a function of qNd. The full curves are based on computed values of Q_0, Q_1, Q_2 and Q_3 whilst the dotted curves are derived from the analytic expression for a diffuse flux

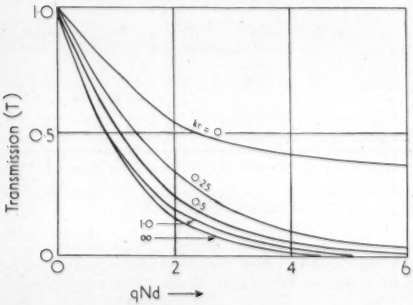

Fig. 6(b). The transmission T as a function of qNd for high values of qNd

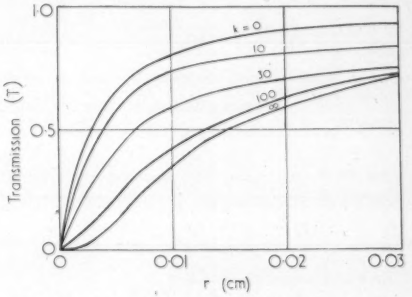

Fig. 7(a). The transmission T as a function of r for $C = 0{\cdot}01$. [Based on Fig. 6(b)]

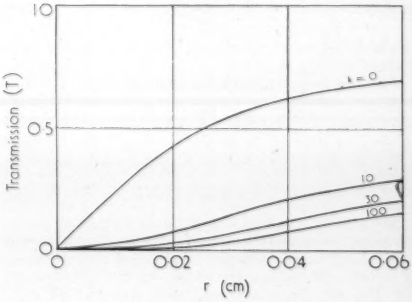

Fig. 7(b). The transmission T as a function of r for $C = 0{\cdot}1$. [Based on Fig. 6(b)]

Finally T has been plotted against r in Fig. 8 for $C = 0{\cdot}1$ and 0·01† taking into account the radiation spectrum from a panel at 1 000° C and using the values of k given in the International Critical Tables. Both curves follow those given in Fig. 7 (a and b) for a value of k approximately equal to 100 cm^{-1}. It will be seen in Fig. 7(a) that for values of r greater than about 0·015 cm there is little variation in T when k is increased beyond 100 cm^{-1}. The curves for

† Simple calculations suggest these to be suitable extreme values for conventional fire-fighting sprays.

$C = 0{\cdot}025$ cm and $C = 0{\cdot}05$ cm have therefore been drawn for this value of k.

If a drop is highly absorbing (i.e. kr is greater than about 3) equation (1) is valid. From this can be written

$$T = \exp(-C/r)$$

i.e.
$$T = \exp(-sd/2) \qquad (44)$$

where s is the surface of water/unit spray volume.

If in equation (16) the presence of the factor $0{\cdot}95$ is neglected, equation (44) can be compared with the full curves in Fig. 8. These approximate curves are shown dotted. Differences only arise when both the drop size and the water volume C are small.

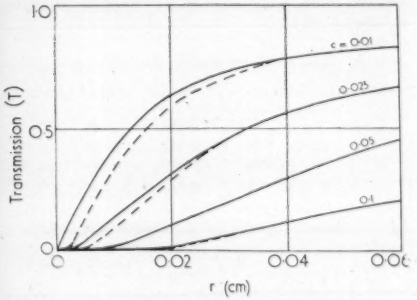

Fig. 8. The transmission T as a function of r for radiation from a black body at 1 000° C

THE ABSORPTION AND REFLEXION OF THE SPRAY

When the drops are small the transmission becomes small also. The radiation, however, is not all absorbed: some of it is reflected by the spray. This is most easily seen in Fig. 2 where f decreases as r decreases for a constant value of k.

For simplicity the case of diffuse scattering only is examined. We can then use equations (38) and (39) to evaluate A.

The radiation entering the spray is I, and that emerging is F_D at $y = D$, and B_0 at $y = 0$. Hence from equations (33), (38) and (39) we have

$$A = \frac{f \sinh D\sqrt{f} + \sqrt{f}(\cosh D\sqrt{f} - 1)}{\sqrt{f}\cosh D\sqrt{f} + \frac{1}{2}(1+f)\sinh D\sqrt{f}} \qquad (45)$$

Fig. 9 shows the relation between A and r for two values of R and three values of C. The marked dependence of A on k prevents the use of a mean value of 100 cm^{-1}. 500 cm^{-1} is probably nearer the best value.

The reflectivity R of the spray is given by B_0/I which is shown in Fig. 10. For very small drops, the above treatment becomes invalid and account must be taken of Mie scattering.

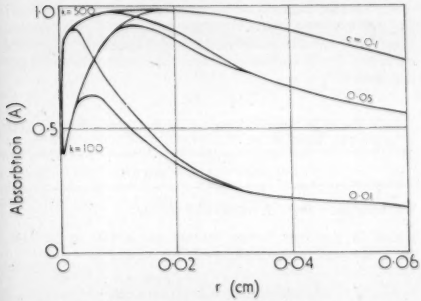

Fig. 9. The absorption A as a function of r for $k = 100$ and 500, and $C = 0{\cdot}01$, $0{\cdot}05$ and $0{\cdot}1$

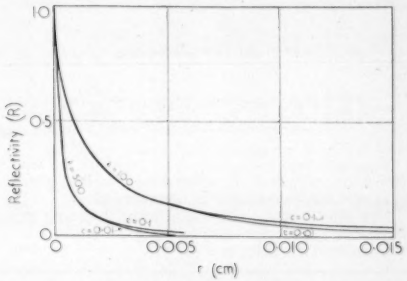

Fig. 10. The reflectivity R as a function of the drop size

It is of interest to note that the radiation absorbed per unit volume of water per unit intensity is given by

$$\frac{A}{Vd} = \frac{3}{2}\frac{A}{C}$$

This is a measure of the mean rate of radiative heat transfer.

CONCLUSIONS

This treatment of the problem of refractive scattering by large drops has shown that if there is no absorption the transmission of a thick layer of spray of large drops in front of a large radiator is about 60% greater than that evaluated on the assumption of equal forward and backward scattering. For a distant source the excess is over 100%.

Numerical results have been given for the transmission of thermal radiation. This is governed by the simple exponential law if the drops are large. When, however, the product (absorption index) (drop radius) falls below about 3, the absorption by the drops is incomplete and the spray transmits more than is predicted by the exponential law.

ACKNOWLEDGEMENTS

The work described in this paper forms part of the programme of the Joint Fire Research Organization of the Department of Scientific and Industrial Research and Fire Offices' Committee; the paper is published by permission of the Director of Fire Research.

REFERENCES

(1) THEISSING, H. H. *J. Opt. Soc. Amer.*, **40**, p. 232 (1950).
(2) SKINNER, D. J., and BOAS-TRAUBE, S. *Symposium on Particle Size Analysis*, p. 57. (London: Institute of Chemical Engineers and Society of Chemical Industry, 1947.)

(3) SCHUSTER, A. *Astrophys. J.*, **21**, p. 1 (1905).
(4) HARTEL, W. *Das Licht*, **10**, pp. 141, 165, 190, 214, 232 (1940).
(5) RYDE, J. W. *Proc. Roy. Soc. A*, **131**, p. 451 (1931).
(6) NUSSELT, W. *Forsch. Arb. Ing.-Wes.*, **264**, p. 41 (1923).
(7) WIENER, C. *Nova Acta Leop. Carol.*, **73**, p. 3 (1907).
(8) SHIFRIN, K. S. *Izv. Akad. Nauk. SSSR., Ser. Geogr. i. Geofiz.*, **14**, p. 128 (1950).

APPENDIX I

The computation of a_n and v_m. From equations (6*a*), (22), (24) and (25) we have

$$\frac{a_n}{2n+1}(1-f) = \tfrac{1}{2}\int_0^{\pi} R_0 P_n(\cos\phi)\sin\phi_0 d\phi_0 + \sum_{s=1}^{\infty}\int_0^{\pi} T^2 R^{s-1}\exp(-2krs\cos\psi)\sin 2\theta\left|\frac{d\theta}{d\phi_s}\right| P_n(\cos\phi_s)d\phi_s \quad (46)$$

Since each term in the series for v_m contains the term P_n [see equations (8) and (9)] which is zero for even values of n, a_n need only be evaluated for odd values of n.

Now the fraction r_s of the total radiation present in the component i_s is greatest when there is no absorption and for this condition it is given by

$$r_s = 2\pi\int_0^{\pi} i_s(\phi_s)\sin\phi_s d\phi_s = \int_0^{\pi/2} T^2 R^{s-1}\sin 2\theta d\theta \quad (47)$$

Moreover the sum of such fractions is

$$\sum_s^{\infty} r_s = \int_0^{\pi/2} T^2(R^{s-1} + R^s + \text{etc.})\sin 2\theta d\theta = \int_0^{\pi/2} TR^{s-1}\sin 2\theta d\theta \quad (48)$$

These integrals are obtained graphically and they show that even when there is no absorption only about 1·0% of the radiation is present in the components i_3, i_4, i_5, etc. Since r_2 is 4·1% it is reasonable to make the approximation that this radiation is emitted at the angle at which the intensity becomes infinite. This, the first rainbow angle, is found from equations (15) and (21) from which

$$\frac{d\theta}{d\phi_2} = \frac{1}{2}\left[1 - \frac{2\cos\theta}{\sqrt{(\eta^2 - \sin^2\theta)}}\right]^{-1} \quad (49)$$

From the value of θ that makes the denominator zero the corresponding values of ψ and ϕ are obtained. These are $\bar{\psi}_2 = 40{\cdot}5°$, and $\bar{\phi}_2 = 138°$.

It is also desirable to assume a mean value of ψ_1. This is chosen as that at which $T^2\sin 2\theta\dfrac{d\theta}{d\phi_1}P_1(\cos\phi_1)$ is a maximum. $\bar{\psi}_1$ is found to be 25°.

The series for a_n now becomes

$$\frac{a_n}{2n+1}(1-f) = c_n + \sum_{s=1}^{s=2}[\exp(-2s\cos\bar{\psi}_s)]^{kr}d_{s,n} \quad (50)$$

where
$$c_n = \tfrac{1}{2}\int_0^{\pi} R_0 P_n(\cos\phi_0)\sin\phi_0 d\phi_0 = -\int_0^{\pi/2} R_0 P_n(\cos 2\theta)\sin 2\theta d\theta \quad (51)$$

when n is odd;

where
$$d_{1,n} = \int_0^{\pi} T^2\sin 2\theta\frac{d\theta}{d\phi_1}P_n(\cos\phi_1)d\phi_1 \quad (52)$$

and
$$d_{2,n} = 0{\cdot}041P_n(\cos 138°) \quad (53)$$

c_n and $d_{1,n}$ are computed graphically for $n = 1$, 3, 5 and 7. Since f is a function of kr it is now possible to find a_n for any value of kr. The results from which v_m is computed are given in Tables 1 and 2.

Table 1. *Coefficients for determining a_n*

n	c_n	$d_{1,n}$	$d_{2,n}$
1	0·034	0·764	0·031
3	0·015	0·380	0·004
5	0·007	0·123	0·017
7	0·002	0·046	—

Table 2. *Coefficients for determining v_m*

n	$a_n/(2n+1)$					p_n
	$kr = 0$	0·25	0·5	1·0	∞	
1	0·77	0·76	0·75	0·68	0·68	0·500
3	0·40	0·39	0·38	0·34	0·30	−0·125
5	0·15	0·14	0·13	0·12	0·13	0·062
7	0·05	0·05	0·05	0·03	0·05	−0·039

APPENDIX II

The radiation intercepted by a large sphere. We shall consider a sphere of radius r at P, a perpendicular distance R from an infinite radiator. Although the result is true for all values of R it is sufficient to derive it here for the case where R is much greater than r.

Let i be the intensity of radiation emitted by the radiator per unit area per unit solid angle in the forward direction. Then from Lambert's cosine law and the inverse square law we have the well known result that the resultant intensity per unit area is

$$I = \pi i$$

Now the solid angle subtended by the sphere P at an area δs at P' (Fig. 11) is

$$\delta\omega = \frac{\pi r^2}{R^2}\cos^2\phi$$

We have also $\delta s = R^2\tan\phi\sec^2\phi\delta\phi\delta\psi$

Hence, by Lambert's cosine law and the inverse square law, the total radiation received by the sphere at P is

$$i\iint\cos\phi\delta s\delta\omega = 2\pi r^2 I\int_0^{\pi/2}\sin\phi d\phi = 2\pi r^2 I$$

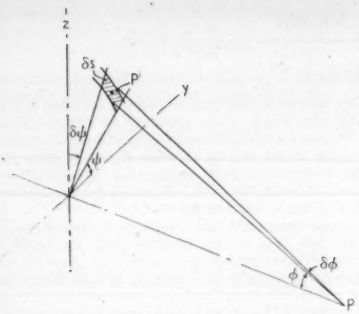

Fig. 11. The radiator is the whole of the zy plane

APPENDIX III

The analytic expressions for $Q_0(d)$, $Q_1(d)$, $Q_2(d)$ and $Q_3(d)$ evaluated from equations (29) and (30) are:

$$Q_0(d) = Ie^{-D}$$

$$Q_1(d) = I(1-f)v_1De^{-D}$$

$$Q_2(d) = I(1-f)^2 \left[\frac{h_1h_2}{2}De^{-D} + \frac{v_1v_2}{2}D^2e^{-D} - \frac{h_1h_2}{4}e^{-D}(1-e^{-D})\right]$$

$$Q_3(d) = I(1-f)^3\left[v_1v_2v_3\frac{D^3}{6}e^{-D} + \frac{v_3h_1h_2 + v_1h_2h_3}{2}\frac{D^2}{2}e^{-D} + \frac{v_1h_2h_3 + v_2h_1h_3}{4}De^{-D} + \frac{v_3h_1h_2 + v_2h_1h_3}{4}De^{-3D} - e^{-D}(1-e^{-2D})\left(\frac{v_3h_1h_2}{8} + \frac{v_2h_1h_3}{4} + \frac{v_1h_2h_3(2D+1)}{8}\right)\right]$$

where $D = qNd$.

These expressions were used to compute T for small values of D. For $D < 1$, the contribution of Q_3 is scarcely more than 1% of the total $Q_0 + Q_1 + Q_2 + Q_3$.

Values of $P_m(0)$, given by Theissing for a non-absorbing spray in which D is large are

$$P_1(0) \simeq I\frac{h_1}{2}$$

$$P_2(0) \simeq I\left(\frac{v_1h_2 + v_2h_1}{4}\right)$$

$$P_3(0) \simeq I\left(\frac{v_2^2h_2}{2} + \frac{h_2^2}{8}\right)$$

$$P_4(0) \simeq I\left(\frac{v_2^3h_3}{2} + \frac{3v_3h_3^2}{8}\right)$$

$$P_5(0) \simeq I\left(\frac{v_2^4h_4}{2} + \frac{3v_2^2h_4^2}{4} + \frac{h_4^2}{16}\right)$$

APPENDIX IV

From equations (34) we have immediately

$$F - B = \text{constant}$$

Since $B = O$ at $y = D$ and $F = TI$ at $y = D$

then
$$F - B = TI \tag{54}$$

Thus
$$\frac{dF}{dy} = -\frac{TI}{2} + \sum_{m=0}(v_{m+1} - \tfrac{1}{2})(Q_m - P_m) \tag{55}$$

i.e.
$$T(1 + D/2)I = I + \sum_{m=0}(v_{m+1} - \tfrac{1}{2})\int_0^D (Q_m - P_m)dy \tag{56}$$

Now from equations (29) and (30) we have

$$Q_m - P_m = (2v_m - 1)(Q_{m-1} - P_{m-1}) - \frac{dQ_m}{dy} - \frac{dP_m}{dy} \tag{57}$$

i.e.
$$\int_0^D (Q_m - P_m)dy = (2v_m - 1)\int_0^D (Q_{m-1} - P_{m-1})dy + P_m(0) - Q_m(D) \tag{58}$$

Repeated substitution of equation (58) into equation (56) yields the result

$$T(1 + D/2) = 1 + R_1 + \frac{1}{I}\sum_{m=1,2\ldots} R_m(P_{m-1}(0) - Q_{m-1}(D)$$

where

$$R_m = (v_m - \tfrac{1}{2})[1 + (2v_{m+1} - 1) + (2v_{m+1} - 1)(2v_{m+2} - 1) + \text{etc.}]$$

Correspondence

Ignition of wood by radiation

In a recent paper[1] Lawson and Simms have described experiments on the ignition of wood by radiation both with a pilot flame and without, i.e. spontaneous ignition. The authors have shown that the time, t, elapsing before ignition occurs is shorter the greater the intensity of radiation, I, and they have expressed their results in equations of the form $(I - I_0)t^x = A(K\rho s + B)$, where I_0 is the critical intensity for ignition after a very long time, x is $\frac{1}{2}$ and $\frac{4}{3}$ in the cases of pilot and spontaneous ignition respectively, and A and B are constants which also depend on whether the ignition is pilot or spontaneous. The underlying significance of such equations is not, however, clear to the writer, and it is suggested that a study of the total radiation energy required for ignition would give a clearer insight into the physical processes involved.

The total radiation energy falling on the wood specimens before ignition occurs is It cal/cm^2, and on estimating the corresponding values of I and t from Lawson and Simms, Figs. 1 and 2, it appears that the energy supplied increases as the time to ignition increases. Extrapolation of the energy time curves to zero time then gives the energy $(It)_0$ necessary for ignition when this is generated instantaneously in the wood surface, and an estimate of the values obtained for the different woods is given in the table below:

Wood	*Value of* $(It)_0$ *Pilot* cal/cm^2	*Spontaneous* cal/cm^2	*Mean value of* $(It)_0/\rho s$(° C.cm)
Fibre board	3	3	36·8
White wood	5	5	31·5
Cedar	4·5	4·5	36·8
Mahogany	6·5	6·5	34·2
Oak	8	7	36·2
Freijo	7·5	7	36·5
Iroko	9·5	—	38·8

No great accuracy can be claimed for the extrapolations, but it is clear that $(It)_0$ is very little different for pilot and spontaneous ignition, and that for each wood $(It)_0/\rho s$ is remarkably constant. ρs is of course proportional to the thermal capacity of that volume of wood the surface of which is actually heated under instantaneous conditions, and the constancy of energy/thermal capacity indicates that the temperature attained instantaneously is the same for each wood. The actual value of this temperature cannot be estimated without some assumption as to the thickness of the surface layer heated, but if, for example, the thickness were 0·5 mm, the temperature rise would be in the region of 720° C, a value at least of a reasonable order of magnitude.

When the energy necessary for ignition is supplied over a finite time, more energy will be needed than for instantaneous ignition as the processes of conduction in the wood will distribute the energy over a greater volume. The distribution of temperature in the wood specimen due to conduction will depend on the thermometric conductivity $(K/\rho s)$ and from the data given it will be seen that for fibre board $K/\rho s$ is 104 cm^2/sec, whereas for all the other woods it lies between 167 and 178 cm^2/sec. Consequently it would be expected that the energy necessary for ignition would increase less rapidly with increasing time to ignition for fibre board than for the other woods, which should all be similar. This is, in fact, the case for both pilot and spontaneous ignition, although the values of the rate of increase of energy with time are roughly twice as great for spontaneous ignition as for pilot ignition. A similar factor of 2 will be observed in the equations given by Lawson and Simms.

The experiments thus demonstrate that the ignition of wood by radiation is a process fundamentally the same as the ignition of gases by heated spheres[2] or wires,[3] and the ignition of solids by heated wires.[4] In each case it appears that a critical amount of energy is necessary for ignition, the energy required being least when generated instantaneously in a limited volume of the medium.

HARRY P. STOUT

31 Forthill Road,
Broughty Ferry,
Dundee.

REFERENCES

(1) LAWSON, D. I., and SIMMS, D. L. *Brit. J. Appl. Phys.*, **3**, p. 288 (1952).

(2) SILVER, R. S. *Phil. Mag.*, **23**, p. 633 (1937).

(3) JONES, E. L., and STOUT, H. P. Third symposium on combustion, flame, and explosion phenomena, p. 329 (Wisconsin: Williams and Wilkins Co., 1949).

(4) JONES, E. *Proc. Roy. Soc.*, *A*, **198**, p. 523 (1949).

Dr. Stout has made the assumption that when radiation falls on the surface of wood a layer of arbitrary thickness is heated and he has arrived at the expression $\left(\frac{It}{\rho s}\right)_{t\to 0} = \text{constant}$ as giving the minimum energy for ignition of various species of wood. It would appear to us that a more accurate expression would be $\left(\frac{I\sqrt{t}}{\rho s}\right)_{t\to 0} = \text{constant}$ and this is suggested by the following analysis.

If radiation of intensity I fall upon a surface of a semi-infinite solid, and if the cooling from the surface be Newtonian, then after a time t the surface temperature θ is given by[1]

$$\theta = \frac{I}{\Psi}(1 - e^{\beta^2} erfc\,\beta) \qquad (1)$$

where

$$\beta = \Psi\sqrt{\left(\frac{t}{K\rho s}\right)}$$

$$erfc\,\beta = \frac{2}{\sqrt{\pi}}\int_{\beta}^{\infty} e^{-\mu^2} d\mu$$

Ψ is the rate of loss of heat per unit area for each degree rise in temperature,
K is the thermal conductivity,
ρ is the density,
and s is the specific heat of the material.

The thermal constants occur as the function $K\rho s$ and not as $K/\rho s$ as surmised by Dr. Stout.

For small values of t, that is, for small values of β[1]

$$\theta = 2I\sqrt{\left(\frac{t}{\pi K\rho s}\right)}$$

If wood be regarded as an inert material and each species be assumed to ignite at a constant temperature, then

$$I\sqrt{\left(\frac{t}{\pi K\rho s}\right)} = \text{constant} \qquad (2)$$

This approximation is only true if the times at which ignition occurs are short enough ($\beta < 0{\cdot}12$ for an error less than 10%). The results available do not permit this hypothesis to be tested. However, another approximation may be made[1]

$$\theta = 2I\sqrt{\left(\frac{t}{\pi K\rho s}\right)}\left[1 - \frac{\Psi}{2}\sqrt{\left(\frac{\pi t}{K\rho s}\right)}\right] \qquad (3)$$

This formula may be used to an accuracy of 10% for $\beta < 0{\cdot}4$.

If expression (3) is valid, then the graph of $I\sqrt{t}$ plotted as a function of It should be linear. This is shown in Fig. 1.

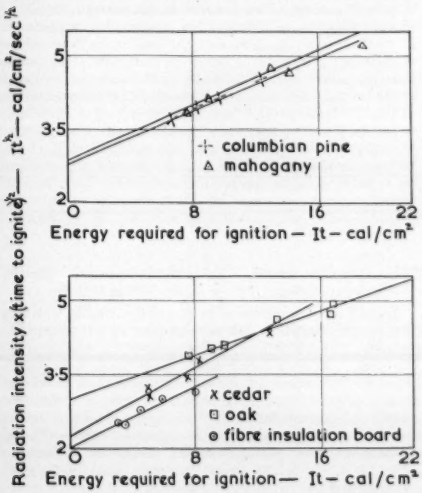

Fig. 1. Energy required for spontaneous ignition as a function of intensity of radiation × (time to ignite)$^{\frac{1}{2}}$.

From the slope of the lines and the intercepts on the $I\sqrt{t}$ axis, the ignition temperature of the materials may be computed.

The results for spontaneous ignition are shown in the following table:

Calculated values of ignition temperature θ and of $\theta\Psi$ for the spontaneous ignition of wood

Material	*Ignition temperature* θ °C	$\theta\Psi$ cal/cm²/sec
Fibre insulation board	600	0·78
Western red cedar	450	0·95
Columbian pine	420	0·93
African mahogany	380	1·0
Oak	350	1·0

The result for fibre insulation board appears to be high only because the approximation is not valid for the range of results available. It is interesting to note that for the other woods the rate of cooling $\theta\Psi$ at the temperature of ignition is roughly constant.

Since equation (3) is obeyed, it is probably legitimate to assume that equation (2) holds within its range. The thermal conductivity of wood in the direction perpendicular to the grain (the direction of heating in the experiments) is approximately proportional to the density.[2] Since the specific heat of wood is constant, it would be expected from expression (2) that the function $\left(\frac{I\sqrt{t}}{\rho s}\right)_{t\to 0}$ would be constant rather than Dr. Stout's expression $\left(\frac{It}{\rho s}\right)_{t\to 0}$.

Recently our work has been extended to higher intensities of radiation and correspondingly shorter times to ignite. In Fig. 2 these results are shown plotted: it may be seen that

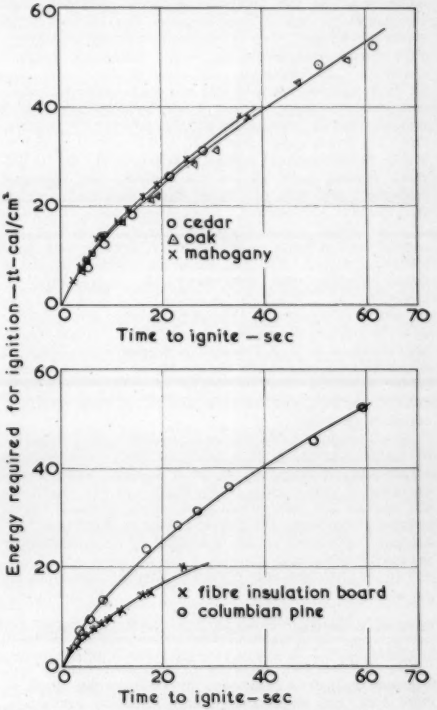

Fig. 2. Energy required for spontaneous ignition as a function of time taken to ignite

It tends to zero as t tends to zero as it should do if $\left(\frac{I\sqrt{t}}{\rho s}\right)_{t\to 0}$ were constant.

Finally, we would suggest that from these experiments the wood ignites when the surface reaches a fixed temperature rather than when it has received a fixed quantity of energy.

Fire Research Station, Boreham Wood, Herts.

D. I. LAWSON
D. L. SIMMS

REFERENCES

(1) LAWSON, D. I., FOX, L. L., and WEBSTER, C. T. *Dep. Sci. Industr. Res. and Fire Offices' Committee, Fire Res. Spec. Rep.* No. 1 (H.M. Stationery Office, 1952).
(2) MACLEAN, J. D. *Trans. Amer. Soc. Heat. Vent. Engrs*, **47**, p. 1184 (1941).

New books

Colour in theory and practice. Edited by H. D. MURRAY. (London: Chapman and Hall Ltd.) Pp. xiii + 360. Price 70s.

Colour is treated in this book under three main headings, physical and chemical aspects, physiological and psychophysical aspects, and light sources and colorimetry. The editor has had the assistance of seven specialists, each responsible for two or three chapters, and the very varied topics are all dealt with competently, although of necessity with considerable differences in the detail and depth of treatment. For example, the well-written twenty pages (P. Holliday) devoted to colour and chemical constitution—orbitals, conjugation, chromophores, auxochromes—can be no more than an introduction to a big subject. On the other hand, the sixteen-page account (R. G. Horner) of systems of colour description and specification (excluding the trichromatic system) gives all the main points and important references, and puts the reader *au courant* with a minor technological development. L. C. Thomson's contributions on the human visual apparatus, the visual process and normal and defective colour vision is again a very good introduction to a wide field, while the chapters devoted to colour-matching and colorimetry (R. G. Horner, R. Donaldson, G. T. Winch) are examples of the more meticulous treatment, all well done. Another major topic is the emission of radiation and the properties of all kinds of light source, ably discussed by V. J. Francis. A chapter on photoelectric effects (N. Laycock), five by the editor on miscellaneous colour questions, and appendices on colour terminology, colorimetric data, and the properties of colouring materials, complete the work.

This is something of a text-book, something of a collection of essays, something of a reference work, and, perhaps surprisingly, it turns out to be a mixture which people interested in colour from many angles will find interesting and useful. The book is well produced—a couple of figures referred to on pages 183 and 184 seem to have been lost, however. The editor should have made up his mind whether the luminous efficiency constant K has the value 621 (p. 32), 650 (p. 111) or 680 (the currently accepted value) lumens per watt.

W. S. STILES

Lightning protection. (Pennsylvania: The Franklin Institute.) Pp. 129. Price $1.

The "Philadelphia experiment" was first carried out, following Franklin's suggestion, by Dalibard near Paris in April 1752, and independently, and still more ingeniously, by Franklin himself with his kite about a month later. To celebrate the double centenary of its success and of his introduction of the lightning conductor, the Franklin Institute has devoted the May issue of its Journal to four contributions under the general title "Lightning protection." The first, by B. F. J. Schonland, deals all too shortly with the interlinked development of Franklin's experiments and ideas to their outstanding scientific and practical successes. The very slow decay of the prejudice against lightning rods, and of the erroneous ideas as to their purpose, contrast strangely with the immediate acclaim accorded to the success of the experiment. The second and by far the longest article by I. B. Cohen deals with this prejudice, and emphasizes the point made by Mr. Wedmore at the recent British Electrical Power Convention that research is not enough; habits of thought have to be changed for its successful application. In the third paper K. B. McEachron outlines the development of lightning protection of buildings and power installations since Franklin's day. The fourth, by H. Norinder, a pioneer in the cathode-ray oscillographic study of lightning effects, is entitled "Experimental lightning research." It is surprising, to say the least, in view of this broad title, that it contains no references to the several classic investigations of C. T. R. Wilson, Sir George Simpson, and Sir Edward Appleton and his collaborators, to whose studies, together with those of Schonland, we owe most of the knowledge gained since Franklin's day.

C. E. R. BRUCE

Magnetische werkstoffe. By FRANZ PAWLEK. (Berlin: Springer-Verlag.) Pp. vii + 303. Price DM 42.

Anyone actively interested in magnetism reading Pawlek's *Magnetische werkstoffe* will at once think of it in relation to Bozorth's *Ferromagnetism*, reviewed in this *Journal* in April this year. While the two books have much in common, there are differences in scope. Pawlek's book is almost entirely devoted to the metallurgical background of magnetic properties—current theories of coercive force, remanence and loss are very lightly treated, whilst applications are mentioned incidentally and testing omitted altogether. On the other hand, the author treats his main thesis with great thoroughness.

The three main divisions of the book deal with permanent magnet materials, soft magnetic materials and materials for high frequency work. The first two provide much information on composition, structure, texture and mechanical and thermal treatment of every important alloy, and there are no notable omissions. The introduction to the section on high-frequency materials could have included a fuller treatment of the requirements in this field and of the interpretation of test measurements, and the section on powder cores is slight, but the author gets into his stride again with the Fe–Ni–Cu alloys and the ferrites.

There are incidental references to magnetostriction throughout the text and one note on a series of Japanese nickel-based alloys which possess high magnetostriction coefficients. In a chapter on glass-sealing alloys and alloys with low temperature coefficients of expansion and elasticity, the author shows how the structural requirements of these alloys are related to

those of magnetic materials. The book ends with a chapter on non-magnetic ferrous alloys.

Pawlek's book is, of course, a compilation. But it is a good and objective compilation and as a work of reference it should find a place in the laboratory of every practitioner in magnetism. N. F. ASTBURY

The Auger effect. By E. H. S. BURHOP. (London: Cambridge University Press.) Pp. xiv + 188. Price 27*s*. 6*d*.

Books of this kind are just what are needed at a time when physics is developing fast. The author describes one phenomenon in physics, the Auger Effect, which has rather wide applications. By the Auger Effect he means all those transitions in which an excited inner shell of an atom, an excited nucleus or a nucleus interacting with a meson fall to a lower state by giving up its energy to an outer electron which is ejected. Dr. Burhop approaches the subject both as a theorist and an experimentalist; the theory, to which he has himself contributed much, is clearly explained and the results set out in tabular form. It is then applied to X-ray spectroscopy, to the internal conversion of gamma rays and to the capture of mesons, in which fields the experimental results are described and compared with theory.

The author claims that the book included all published papers till December 1950, and if this is when it went to press one wonders at its appearance only in May 1952. The editors of the series comment that book production is no longer a fairly rapid process, compared with the pre-war period. It is difficult to see why this should still be so; and though the production of the book is up to the high standard that one expects from the Cambridge University Press, it is regrettable that for this series of short and topical books rather quicker publication cannot be achieved.

N. F. MOTT

Cloud chamber photographs of the cosmic radiation. By G. D. ROCHESTER and J. G. WILSON. (London: Pergamon Press Ltd.) Pp. viii + 128. Price 70*s*.

This volume is a beautiful collection of 123 photographs of expansion chamber photographs, each of which is suitably annotated. It is a work which will not only be of value to the nuclear specialist, but will also be of great interest to a wider circle of physicists, many of whom may not have followed the subject since their university days. These events, collected and compiled by two well-known authorities in this field, have been taken from the work of various laboratories throughout the world, and suitable acknowledgements are made to this active co-operation without which a truly representative collection of photographs would not have been possible. The photographs are grouped in six sections starting with 26 plates illustrating the technical features of operation. Then follow sections on electron and cascade showers, slow mesons and nuclear disintegrations. Finally, save for one photograph of a heavy primary cosmic ray, the volume ends with 20 examples of the new V-particles first discovered in the Manchester laboratory and since verified in Pasadena. The latter are, of course, of very special interest at the present time in this advancing subject. The reproduction is good throughout the book. A. M. TYNDALL

Reports on progress in physics, Vol. XV, 1952. Edited by A. C. STICKLAND. (London: The Physical Society.) Pp. 338. Price 50*s*.

The present volume maintains the high standard of production set in previous volumes; but the extent to which previous knowledge is required for a profitable first reading varies considerably from article to article. Clearly, it is difficult to achieve uniformity of treatment when many experts report on a wide variety of subjects in a single volume; it is more difficult to induce the experts to meet the needs of the average physicist. These reports must be written by specialists *but not for specialists*; it is felt by the reviewer that it may be of value to ask Fellows of the Physical Society whether they now feel these reports are really meeting the needs of the average physicist.

In his own interest, a specialist is hardly likely to neglect the essential task of keeping up-to-date in his own field. He will do this either unaided himself or by making use of the more extensive library information and intelligence services available to-day. He is scarcely likely to await the appearance of a review article written by some other specialist in his particular field. He will be aware already of the new data presented, and his only interest will be, therefore, in the degree of emphasis given by the writer to this or that particular detail. For all other review articles in the volume he will be in the position of the general reader who wants to know what is happening in various branches of physics. As a general reader, he is not likely to fill his shelves with unreadable volumes merely to create an illusion of omniscience for all and sundry to admire.

The average physicist may not have a great deal of enthusiasm for a particular subject for which a report on progress is prepared; if, then, he finds new knowledge is clearly going to be hard won, he is easily self-persuaded to abandon the search: he moves on to the next report. It must be the job of the specialist to impart to the general reader some of his own enthusiasm for his subject, to make no rash assumptions in respect of specialized knowledge, to write less formally than usual, and to eschew any temptation to use a deal of mathematics.

To the reviewer, two reports in the present volume approach the ideal treatment sought: *viz*., the report by G. K. Batchelor of Trinity College, Cambridge, dealing with the advances during the last seventeen years in the study of turbulent motion and the report by R. Kompfner on travelling-wave tubes—dealing mainly with work carried out only during the last five or six years on new electron tubes which, operating in the microwave range of frequencies, amplify as a result of continuous interaction between an electron stream and a slow-travelling electromagnetic wave. It is, of course, true that some subjects present more difficulty in presentation than other subjects; but not all or even a great part of the difficulties in reading should be ascribed to the nature of the subject.

The range of work covered in these volumes is generally so wide that no one reviewer would claim to have adequate specialized knowledge for competent criticism of the subject-matter of all the reports presented. This volume is no exception. In addition to the two reports mentioned above, there are seven other reports. L. Kellner of the Imperial College of Science and Technology, London, surveys recent work on the mechanism and behaviour of hydrogen bond formation in molecules possessing a hydroxyl group or in molecules containing, for example, a CH linkage. K. I. Mayne of the Clarendon Laboratory, Oxford, discusses some recent theoretical work on design for second-order focusing in sector field mass spectrometers and reviews recent applications to geological studies and nuclear chemistry. A. E. Taylor of A.E.R.E., Harwell, reports on progress in recent experimental work in establishing more accurate range-energy relationships for alpha particles and protons. The

experimental results are compared with theoretical prediction. R. S. Christian of the Los Alamos Scientific Laboratory, New Mexico, undertakes a study of experimental data accumulated with the use of high-energy particle accelerators, the synchro-cyclotron and the linear accelerator, on high energy neutron-proton and proton-proton scattering. A Fairweather, F. F. Roberts and A. J. E. Welch of the Post Office Research Station, London, report on the preparation and the physical and chemical properties of ferrites—non-metallic ferromagnetic materials—from the point of view of the new knowledge which may result in studies of ferromagnetic and, to a lesser extent, of dielectric behaviour. G. V. Raynor of the University of Birmingham, in a review on the band structure of metals, considers to what extent recent work has improved the physicists' understanding of the fundamental nature of the metallic state. D. K. C. MacDonald and K. Sarginson of Oxford University are concerned in their review with galvanomagnetic effects (Hall field and magneto-resistance) in conductors.

An extensive list of references covering recent work is appended to each report. A useful and valuable addition to the present volume is a cumulative subject and author index for the whole series, Volumes I–XV. G. P. BARNARD

Progress in metal physics. Vol. 3. (London: Pergamon Press Ltd.) Pp. viii + 334. Price 48*s*.

The third volume of this series contains the following review articles. I. Crystallography of transformations by J. S. Bowles and C. S. Barrett. II. Properties of metals at low temperatures by D. K. C. MacDonald. III. Recent advances in the electron theory of metals by N. F. Mott. IV. Twinning by R. Clark and G. B. Craig. V. Ferromagnetism by Ursula M. Martius. VI. Quantitative X-ray diffraction observations on strained metal aggregates by G. B. Greenough. VII. Recrystallization and grain growth by J. E. Burke and D. Turnbull, and VIII. Structure of crystal boundaries by B. Chalmers. The book is well bound and printed, but there is a general tendency to include diagrams from published papers with so little explanation that they may be puzzling to many readers who are not acquainted with the originals.

According to the "Foreword to Volume I" of the series, which is reprinted in this volume, it is the purpose of these books to meet the increasing difficulty "for research workers in one part of the field to remain up to date in other branches," whilst in order "to make the series reasonably self-contained it is proposed that the necessary 'historical' background should be included the first time a particular subject is discussed." These intentions were admirably satisfied in the first volume, and reasonably so in the second, but the present volume is less satisfactory, and gives the impression that a lack of editorial control has allowed contributors to write as they please, with the result that some articles, whilst of great interest to those working on the same subject, are unattractive to those working in other fields. If the intentions of the "Foreword" are to be fulfilled, it must be realized that few authors with the necessary authority are able to write in the style required, and there are some places in this book where editorial revision was clearly needed. Further, the articles must be reasonably short, because few workers are prepared to read long papers on subjects which are not their own. The article by Burke and Turnbull occupies 70 pages, and for the present book would have been better at half this length. It may also be suggested that these volumes will be more useful if they deal mainly with real established progress in metal physics. The article by Mott is beautifully written, but some may feel that he has set a dangerous precedent by including original work, together with a detailed description of unpublished* work of a highly specialized nature by Friedel. Such work is hardly entitled to be called established progress, and if it be proved wrong its inclusion in these volumes may be harmful.

Of the articles published, those by MacDonald, Greenough, and (except for the point referred to above) Mott are excellent, and exactly what the volume requires. That by Bowles and Barrett is clearly written, and extremely interesting to the present reviewer, but many readers may think it too detailed. The paper by Clark and Craig is less successful; it does not satisfy the condition of giving the historical background, and lacks clarity in several places. The article by Martius is clear but rather superficial, and contains too many suggestions that original papers must be consulted. The paper on grain boundaries by Chalmers is clearly written, but is sometimes too much a series of abstracts, and is rather premature. It will be seen, therefore, that both the quality and scope of the articles in the present book are variable, and it is to be hoped that those responsible for these volumes will reconsider their nature, and return to the purpose of the original "Foreword."

W. HUME-ROTHERY

Advanced practical physics for students. By WORSNOP and FLINT. (London: Methuen and Co. Ltd.) Pp. vii + 760. Price 30*s*.

This well-known text-book was first published in 1923 and has established itself as a standard work. In the present edition—the ninth—the text has been thoroughly revised though the general form and character of the book remain essentially unchanged. Apart from numerous modifications of detail in the treatment of some of the experiments the main changes consist in the replacement of the introductory chapter on the calculus by one on errors of observations, and the inclusion of a number of new experiments particularly in the field of electronics and a.c. bridges. These changes and additions unquestionably improve the book. The discussion of errors is far more valuable than the chapter it replaces, and with regard to the new experiments the chief criticism is that there are not enough of them. It is, of course, only too easy to suggest additions to a book of this kind which must be kept to a reasonable size. Possibly some of the more elementary experiments could have been omitted and the theoretical work reduced. Several pages of half-tone illustrations of apparatus are included and it may be doubted whether these are really worth while.

The book originated in the experiments developed for the pass and honours degree course at King's College, London, and its appeal is primarily, though not exclusively, to students preparing for London degree examinations. In this field it admirably fulfils its purpose and will continue to be a most useful guide. The authors are to be congratulated on this improved edition, but at the same time one may venture to regret that more radical changes were not made in order to make the book more closely approach that comprehensive and authoritative work which is very much needed.

F. Y. POYNTON

* We understand that the paper has now been published.—Ed.

Notes and comments

Prizes for original contributions published in this Journal

We have pleasure in announcing that the Board of The Institute of Physics has accepted the offer of the Scientific Instrument Manufacturers' Association of Great Britain Ltd. of £50 *per annum* for the next three years from the Bowen Trust Fund for the purpose of providing prizes for the best original contributions relating to scientific instruments or their use published in either of the Institute's Journals. The Trust Fund was established by the late Mr. William Bowen, a Fellow of the Institute, and Governing Director of Bowen Instrument Co. Ltd. of Leeds.

The rules governing the award are as follows:

(1) Not more than three prizes *per annum* shall be awarded, none of which shall be less than £10 and the total of which shall not exceed £50.
(2) In awarding the prizes, due weight shall be given to each of the following: (i) Originality; (ii) Scientific value; (iii) Practical utility to instrument makers and users; (iv) Presentation, including the standard of presentation of the manuscript.
(3) Members and non-members of The Institute of Physics shall be equally eligible for prizes provided they were not more than 35 years of age on the date of the receipt of the manuscript in the editorial office (and not less than 21 years of age on that date). No member of the Board of The Institute of Physics or of the Prizes or Journals Committees shall be eligible.
(4) No article of which the substance has been previously published shall be eligible.
(5) The Board may withhold the award of prizes if, in its view, no paper of sufficient merit is presented.
(6) The decision of the Board of The Institute of Physics shall be final.

The prize-winners will be recommended to the Board by a Committee consisting of the Chairmen of the Advisory Committees of the *Journal of Scientific Instruments* and of the *British Journal of Applied Physics*, together with one member of the Board and the Editor.

It is interesting to recall that the Association is the direct descendant of the British Optical Instrument Manufacturers' Association (B.O.I.M.A.) which from 1930–1934 provided similar prizes.

Award of the Duddell Medal

At a meeting of the Physical Society held in London on 28 November last, the 29th (1952) Duddell Medal was presented to Mr. C. Waller of Ilford Ltd. The medal is awarded by the Society to "persons who have contributed to the advancement of knowledge by the invention or design of scientific instruments, or by the discovery of materials used in their construction."

Mr. Waller has been primarily responsible for the production of photographic plates sensitive to particles found in cosmic rays and which are also produced in the large machines used in nuclear research. Many of the remarkable advances in nucleonics have been brought about by the use of these special photographic emulsions. Not only has Mr. Waller devised and produced photographic plates of great reliability and uniformity for this work in nuclear physics, but he has also invented special plates for use in other branches of science.

City and Guilds of London Institute Insignia Award

The City and Guilds of London Institute is establishing an Insignia Award in Technology which will lay emphasis upon technical training based primarily upon practical experience, supplemented by theoretical study, as distinct from the more academic approach to training for which many educational facilities and inducements already exist. This new award is intended to be a mark of distinction for those who have combined with a sound practical training an adequate knowledge of the fundamental scientific principles of their industry, and who possess a capacity for leadership and administration. The holders must have had at least seven years' experience subsequent to their initial training. They will use the initials C.G.I.A. after their names. The standard of the Insignia Award will be well above that of any existing Full Technological Certificate awarded by the Institute. It is intended to introduce the award gradually as opportunity offers in the main branches of the chemical, constructional, electrical, mechanical and textile industries. The co-operation and assistance of representatives of industry will be sought in judging the eligibility of candidates, so that the Insignia Award will be indicative of exceptional competence and will ensure that persons receiving it will be recognized as being both trained and qualified to occupy posts of technical and executive responsibility in the class of work and in the branch of industry specified on the warrant they will receive.

Copies of the general regulations governing this new award scheme, together with notes for the guidance of candidates, will be sent on receipt of a stamped addressed foolscap envelope. Enquiries should be addressed to: The Director, Department of Technology (I.A.), 31 Brechin Place, South Kensington, London, S.W.7.

The Australian Radiophysics Laboratory

One of the Divisions of the Commonwealth Scientific and Industrial Research Organization is the Radiophysics Laboratory in Sydney. To enable the technical non-specialists to gain an idea of the wide range of the work carried out there under the direction of Dr. E. G. Bowen, a beautifully produced and illustrated 36-page brochure has just been published. It is a masterpiece of presentation which we should like to see followed by Government laboratories in this country. The work of the laboratory covers four main fields: radio astronomy, cloud and rain physics, automatic computation and the development of radio aids to navigation. A new solar radio spectroscope covering the range 40–240 Mc/s and a 32-element interferometer for use at decimetre wavelengths are described in the brochure, and a brief account is given of work on galactic and cosmic radio noise and on the ionosphere. The familiarity of the laboratory staff with wartime radar techniques led naturally to the work on cloud and rain physics, and this has been extended to investigations of techniques for the artificial stimulation of rain. The laboratory's electronic digital computer is intended primarily for the study of computing and programming techniques; it has been in operation for about a year.

International conference on the theory and applications of photography

To celebrate the centenary of The Royal Photographic Society an international conference on the science and applications of photography is to be held in London from 19 to 25 September, 1953. The conference will cover the following sections:

(i) Photographic science (including theory of latent image and development, sensitization, sensitometry, resolving power, granularity, properties of photographic materials).
(ii) Cinematography and colour photography.
(iii) Technique and applications of photography (including

industrial radiography, photomicrography, spectroscopy, aerial photography, photogrammetry, high-speed photography, nuclear track recording, and other physical, chemical and biological applications; also photocopying apparatus, processes, and manipulations).

(iv) Photomechanical processes.

(v) History, literature (including abstracting and documentation) and training in photography.

It is intended to have preprints available before the conference and publish the accepted papers as soon as possible afterwards. The suggested titles and an indication of the scope of papers to be presented should be submitted before 1 February, 1953, to the Honorary Secretary, The Royal Photographic Society Centenary Conference, 16 Princes Gate, London, S.W.7.

Atomic energy research reports

The second list of atomic energy research reports prepared by members of the staff of the Atomic Energy Research Establishment, Harwell, Berks. has been received. The list consists of eighteen reports all of which are available from H.M. Stationery Office, York House, Kingsway, London, W.C.2, at various prices ranging from 1*s.* 3*d.* to 4*s.* 6*d.*

Fuel research

The measurement of heat has been compared with the measurement of the flow of water using only vessels and pipes having holes of unknown sizes in them and these uncertain losses always make it difficult to balance heat equations. It is not therefore surprising that the Report for 1951 of the Director of the Government's Fuel Research Station* should record that the balances obtained in some of the first experiments made in the new calorimeter building "have not been very good." Some interesting work on domestic heaters has been commenced in this specially constructed building, among which is an investigation which showed that a 2 kW convective source of heat maintained a room 2° F higher than a reflector type of fire of the same power. It will be for the physicist to try to find out why!

Other items in this report which are likely to interest readers of this *Journal* are the intercomparison of Moll thermopiles between different laboratories, the testing of various types of domestic grates and stoves, tests on heat exchanges, the development of automatic instruments for measuring atmospheric pollution, adsorption on composite surfaces, infra-red spectrometry and the starting of radio-active tracer techniques in fuel research. In addition to these matters the Station has continued its important work on the chemical examination and carbonization of coal, on gasification and the production of oils and chemicals, on boilers and steam raising and on turbines.

Tables of the Bessel functions

To meet the continuing demand from nuclear technologists as well as from other design engineers and physicists, a publication of extensive tables of the Bessel functions $Y_0(x)$, $Y_1(x)$, $K_0(x)$ and $K_1(x)$ in the region between 0 and 1 has been re-issued with minor corrections. These tables, prepared by the National Bureau of Standards, are again available as a 60-page booklet from the Government Printing Office, Washington 25, D.C., price 40 cents. (Foreign remittances must be in U.S. exchange and should include an additional one-third of the publication price to cover mailing costs.)

* *Fuel Research*, 1951. (London: H.M. Stationery Office.) Price 2*s.* 6*d.*

Because of the frequent need for numerical values of the Bessel functions in many physics and engineering problems, the tables are computed at much closer intervals than are other existing tabulations of these functions, which enables the user to obtain almost the full accuracy of the table, over most of the range, by linear interpolation. Specifically, the tables give the values of $Y_0(x)$ and $Y_1(x)$ with first and second differences for $x = 0(\cdot 0001)0{\cdot}05(\cdot 001)1$ and the values of $K_0(x)$ and $K_1(x)$ with first and second differences for $x = 0(\cdot 0001)0{\cdot}03(\cdot 001)1$. To simplify interpolation in the table of $Y_0(x)$ and $Y_1(x)$ in the small region between 0 and 0·0050, auxiliary functions are tabulated at an interval of 0·0001. Similarly, auxiliary functions related to $K_0(x)$ and $K_1(x)$ are tabulated for $x = 0(\cdot 001)0{\cdot}030$.

The use of polyvinyl chloride in the manufacture of non-inflammable conveyor belts

We have received the first of a series of research papers issued by the National Coal Board Scientific Department. It is entitled *The use of p v c in the manufacture of non-inflammable conveyor belts*, by J. T. Barclay, and summarizes the advantages and characteristics of polyvinyl chloride, types of polyvinyl chloride conveyor belting, test procedure, results and manufacturing problems. An appendix is included which gives results of tests on many individual belts. Copies of this research paper are available from the National Coal Board, Hobart House, Grosvenor Place, London, S.W.1.

Journal of Scientific Instruments

Contents of the December issue

ORIGINAL CONTRIBUTIONS

Cameras for use with a fine focus X-ray tube. By J. W. Jeffery.
A big expansion helium liquefier. By A. J. Croft.
An accurate method of measuring frequency in the audio range. By A. F. B. Nickson.
A simplified method of calibrating infra-red spectrometers. By J. H. Towler and W. Guy.
An electron diffraction instrument. By R. S. Page and R. G. Garfitt.
A variable prism unit for range finders. By H. Asher.
A wide range oscillator of high stability. By D. E. Caro and L. U. Hibbard.

LABORATORY AND WORKSHOP NOTES

A high speed absorber for the determination of toxic substances in air. By J. C. Gage.
Extra high tension filter box for BF_3 proportional counters. By J. Sharpe.
Simple rotary vacuum seal. By A. G. Hayward.
Measurement of small forces, particularly in a vacuum. By G. C. Curtis.
An improved programme controller. By R. S. Bernhardt and A. J. Copson.
A method of preventing mercury from sticking to glass. By G. D. Archard.
Gas sample intake for mass spectrometer. By H. von Ubisch.
Solvent evaporator for rotary vacuum pump. By J. S. George.

CORRESPONDENCE

Universal mountings for X-ray goniometers. From K. A. Gross.
Colour matching filters for Macbeth illuminometer. From M. E. F. Howarth.
Simplified brightness temperature pyrometer using photoconductive cell. From E. C. Pyatt.
Unbonded wire resistance strain gauge accelerometers. From A. J. King.
Capillary depression in mercury barometers and manometers. From G. W. Thomson.
Decade counter tube. From L. T. Hinton.

NOTES AND COMMENTS

THIS JOURNAL is produced monthly by The Institute of Physics, in London. It deals with all branches of applied physics (including theory and technique). All rights reserved. Responsibility for the statements contained herein attaches only to the writers.
EDITORIAL MATTER. Communications concerning editorial matter should be addressed to the Editor, The Institute of Physics, 47 Belgrave Square, London, S.W.1. (*Telephone:* Sloane 9806.) Prospective authors are invited to prepare their scripts in accordance with the *Notes on the Preparation of Contributions*. (Price 2*s.* 6*d.* including postage.)
REPRODUCTION. The Institute of Physics is a signatory to The Royal Society's Fair Copying Declaration. Details may be obtained upon application from The Royal Society, London, W.1.
ADVERTISEMENTS. Communications concerning advertisements should be addressed to the agents, Messrs. Walter Judd Ltd., 47 Gresham Street, London, E.C.2. (*Telephone:* Monarch 7644.)
SUBSCRIPTION RATES. A new volume commences each January. The charge is £4 per volume ($11.50 U.S.A.), including index (post paid), payable in advance. Single parts, so far as available, may be purchased at 8*s.* each ($1.15 U.S.A.), post paid, cash with order. Orders should be sent to The Institute of Physics, 47 Belgrave Square, London, S.W.1, or to any Bookseller.